

NISTIR XXXX Draft

**Ongoing Face Recognition
Vendor Test (FRVT)
Part 1: Verification**

Patrick Grother
Mei Ngan
Kayee Hanaoka
*Information Access Division
Information Technology Laboratory*

This publication is available free of charge from:
<https://www.nist.gov/programs-projects/face-recognition-vendor-test-frvt-ongoing>

2019/04/12

ACKNOWLEDGMENTS

The authors are grateful to Wayne Salamon and Greg Fiumara at NIST for robust software infrastructure, particularly that which leverages [Berkeley DB Btrees](#) for storage of images and templates, and [Open MPI](#) for parallel execution of algorithms across our computers. Thanks also to Brian Cochran at NIST for providing highly available computers and network-attached storage.

DISCLAIMER

Specific hardware and software products identified in this report were used in order to perform the evaluations described in this document. In no case does identification of any commercial product, trade name, or vendor, imply recommendation or endorsement by the National Institute of Standards and Technology, nor does it imply that the products and equipment identified are necessarily the best available for the purpose.

FRVT STATUS

This report is a draft NIST Interagency Report, and is open for comment. It is the fifteenth edition of the report since the first was published in June 2017. Prior editions of this report are maintained on the FRVT website, and may contain useful information about older algorithms and datasets no longer used in FRVT.

This report will be updated as new algorithms are evaluated, as new datasets are added, and as new analyses are included. Comments and suggestions should be directed to frvt@nist.gov.

Changes since February 2019:

- ▷ This report adds results for 49 algorithms from 42 developers submitted in early March 2019.
- ▷ This report omits results for algorithms that we retired. We retired for three reasons: 1. The developer submitted a new algorithm, and we only list two. 2. The algorithm needs a GPU, and we no longer allow GPU-based algorithms. 3. Inoperable algorithms.
- ▷ Previous results for retired algorithms are available in older editions of this report linked [here](#).
- ▷ The mugshot database used from February 2017 to January 2019 has been replaced with an extract of the mugshot database documented in NIST Interagency Report 8238, November 2018. The new mugshot set is described in section 2.3 and is adopted because:
 - ▷▷ It has much better identity label integrity, so that false non-match rates are substantially lower than those reported in FRVT 1:1 reports to date - see Figure 21.
 - ▷▷ It includes images collected over a 17 year period such that ageing can be much better characterized - - see Figure 87.
- ▷ Using the new mugshot database, Figure 87 shows accuracy for demographic four groups identified in the biographic metadata that accompanies the data: black females, black males, white females and white males.
- ▷ The report adds Figure 4 with results for the twenty human-difficult pairs used in the May 2018 paper *Face recognition accuracy of forensic examiners, superrecognizers, and face recognition algorithms* by Phillips et al. [1].
- ▷ The report uses an update to the wild image database that corrects some ground truth labels.
- ▷ Some results for the child exploitation database are not complete. They are typically updated less frequently than for other image sets.

FRVT Status 2019-03-31: [FRVT](#) has been restructured into four tracks:

- ▷ [FRVT 1:1](#) - an ongoing evaluation of face verification algorithms [Open from June 3, 2019]
- ▷ [FRVT 1:N](#) - an ongoing evaluation of face identification algorithms [Open from June 3, 2019]. A revision to NIST Interagency Report 8238, on one-to-many recognition accuracy is in-preparation and is expected to be published in April 2019.
- ▷ [FRVT Morph](#) - an ongoing evaluation of face morph detection algorithms [Open now]
- ▷ [FRVT Quality](#) - an ongoing evaluation of face image quality assessment algorithms [Open from May 1, 2019. Open for comments until April 23, 2019.]

Contents

| | |
|--|-----------|
| ACKNOWLEDGMENTS | 1 |
| DISCLAIMER | 1 |
| 1 METRICS | 19 |
| 1.1 CORE ACCURACY | 19 |
| 2 DATASETS | 20 |
| 2.1 CHILD EXPLOITATION IMAGES | 20 |
| 2.2 VISA IMAGES | 20 |
| 2.3 MUGSHOT IMAGES | 20 |
| 2.4 WILD IMAGES | 21 |
| 3 RESULTS | 21 |
| 3.1 TEST GOALS | 21 |
| 3.2 TEST DESIGN | 22 |
| 3.3 FAILURE TO ENROL | 24 |
| 3.4 RECOGNITION ACCURACY | 26 |
| 3.5 GENUINE DISTRIBUTION STABILITY | 95 |
| 3.5.1 EFFECT OF BIRTH PLACE ON THE GENUINE DISTRIBUTION | 95 |
| 3.5.2 EFFECT OF AGEING | 105 |
| 3.5.3 EFFECT OF AGE ON GENUINE SUBJECTS | 113 |
| 3.6 IMPOSTOR DISTRIBUTION STABILITY | 124 |
| 3.6.1 EFFECT OF BIRTH PLACE ON THE IMPOSTOR DISTRIBUTION | 124 |
| 3.6.2 EFFECT OF AGE ON IMPOSTORS | 343 |

List of Tables

| | | |
|---|------------------------|----|
| 1 | ALGORITHM SUMMARY | 12 |
| 2 | ALGORITHM SUMMARY | 13 |
| 3 | ALGORITHM SUMMARY | 14 |
| 4 | FALSE NON-MATCH RATE | 15 |
| 5 | FALSE NON-MATCH RATE | 16 |
| 6 | FAILURE TO ENROL RATES | 24 |
| 7 | FAILURE TO ENROL RATES | 25 |

List of Figures

| | | |
|-----|--|----|
| 1 | PERFORMANCE SUMMARY: FNMR VS. TEMPLATE SIZE TRADEOFF | 17 |
| 2 | PERFORMANCE SUMMARY: FNMR VS. TEMPLATE TIME TRADEOFF | 18 |
| 3 | EXAMPLE IMAGES | 21 |
| (A) | VISA | 21 |
| (B) | MUGSHOT | 21 |
| (C) | WILD | 21 |
| 4 | PERFORMANCE ON 20 HUMAN-DIFFICULT PAIRS | 27 |
| 5 | ERROR TRADEOFF CHARACTERISTIC: VISA IMAGES | 28 |
| 6 | ERROR TRADEOFF CHARACTERISTIC: VISA IMAGES | 29 |
| 7 | ERROR TRADEOFF CHARACTERISTIC: VISA IMAGES | 30 |
| 8 | ERROR TRADEOFF CHARACTERISTIC: VISA IMAGES | 31 |
| 9 | ERROR TRADEOFF CHARACTERISTIC: VISA IMAGES | 32 |

| | | |
|----|---|----|
| 10 | ERROR TRADEOFF CHARACTERISTIC: VISA IMAGES | 33 |
| 11 | ERROR TRADEOFF CHARACTERISTIC: VISA IMAGES | 34 |
| 12 | ERROR TRADEOFF CHARACTERISTIC: VISA IMAGES | 35 |
| 13 | ERROR TRADEOFF CHARACTERISTIC: VISA IMAGES | 36 |
| 14 | ERROR TRADEOFF CHARACTERISTIC: VISA IMAGES | 37 |
| 15 | ERROR TRADEOFF CHARACTERISTIC: VISA IMAGES | 38 |
| 16 | ERROR TRADEOFF CHARACTERISTIC: MUGSHOT IMAGES | 39 |
| 17 | ERROR TRADEOFF CHARACTERISTIC: MUGSHOT IMAGES | 40 |
| 18 | ERROR TRADEOFF CHARACTERISTIC: MUGSHOT IMAGES | 41 |
| 19 | ERROR TRADEOFF CHARACTERISTIC: MUGSHOT IMAGES | 42 |
| 20 | ERROR TRADEOFF CHARACTERISTIC: MUGSHOT IMAGES | 43 |
| 21 | ERROR TRADEOFF CHARACTERISTIC: MUGSHOT IMAGES | 44 |
| 22 | ERROR TRADEOFF CHARACTERISTIC: WILD IMAGES | 45 |
| 23 | ERROR TRADEOFF CHARACTERISTIC: WILD IMAGES | 46 |
| 24 | ERROR TRADEOFF CHARACTERISTIC: WILD IMAGES | 47 |
| 25 | ERROR TRADEOFF CHARACTERISTIC: WILD IMAGES | 48 |
| 26 | ERROR TRADEOFF CHARACTERISTIC: WILD IMAGES | 49 |
| 27 | ERROR TRADEOFF CHARACTERISTICS: CHILD EXPLOITATION IMAGES | 50 |
| 28 | ERROR TRADEOFF CHARACTERISTICS: CHILD EXPLOITATION IMAGES | 51 |
| 29 | ERROR TRADEOFF CHARACTERISTICS: CHILD EXPLOITATION IMAGES | 52 |
| 30 | CMC CHARACTERISTICS: CHILD EXPLOITATION IMAGES | 53 |
| 31 | CMC CHARACTERISTICS: CHILD EXPLOITATION IMAGES | 54 |
| 32 | CMC CHARACTERISTICS: CHILD EXPLOITATION IMAGES | 55 |
| 33 | FALSE MATCH RATES WITHIN AND ACROSS DEMOGRAPHIC GROUPS | 56 |
| 34 | FALSE MATCH RATES WITHIN AND ACROSS DEMOGRAPHIC GROUPS | 57 |
| 35 | FALSE MATCH RATES WITHIN AND ACROSS DEMOGRAPHIC GROUPS | 58 |
| 36 | FALSE MATCH RATES WITHIN AND ACROSS DEMOGRAPHIC GROUPS | 59 |
| 37 | FALSE MATCH RATES WITHIN AND ACROSS DEMOGRAPHIC GROUPS | 60 |
| 38 | FALSE MATCH RATES WITHIN AND ACROSS DEMOGRAPHIC GROUPS | 61 |
| 39 | SEX AND RACE EFFECTS: MUGSHOT IMAGES | 62 |
| 40 | SEX AND RACE EFFECTS: MUGSHOT IMAGES | 63 |
| 41 | SEX AND RACE EFFECTS: MUGSHOT IMAGES | 64 |
| 42 | SEX AND RACE EFFECTS: MUGSHOT IMAGES | 65 |
| 43 | SEX AND RACE EFFECTS: MUGSHOT IMAGES | 66 |
| 44 | SEX AND RACE EFFECTS: MUGSHOT IMAGES | 67 |
| 45 | SEX EFFECTS: VISA IMAGES | 68 |
| 46 | SEX EFFECTS: VISA IMAGES | 69 |
| 47 | SEX EFFECTS: VISA IMAGES | 70 |
| 48 | SEX EFFECTS: VISA IMAGES | 71 |
| 49 | SEX EFFECTS: VISA IMAGES | 72 |
| 50 | SEX EFFECTS: VISA IMAGES | 73 |
| 51 | SEX EFFECTS: VISA IMAGES | 74 |
| 52 | SEX EFFECTS: VISA IMAGES | 75 |
| 53 | SEX EFFECTS: VISA IMAGES | 76 |
| 54 | FALSE MATCH RATE CALIBRATION: MUGSHOT IMAGES | 77 |
| 55 | FALSE MATCH RATE CALIBRATION: MUGSHOT IMAGES | 78 |
| 56 | FALSE MATCH RATE CALIBRATION: MUGSHOT IMAGES | 79 |
| 57 | FALSE MATCH RATE CALIBRATION: MUGSHOT IMAGES | 80 |
| 58 | FALSE MATCH RATE CALIBRATION: MUGSHOT IMAGES | 81 |
| 59 | FALSE MATCH RATE CALIBRATION: MUGSHOT IMAGES | 82 |
| 60 | FALSE MATCH RATE CALIBRATION: VISA IMAGES | 83 |
| 61 | FALSE MATCH RATE CALIBRATION: VISA IMAGES | 84 |
| 62 | FALSE MATCH RATE CALIBRATION: VISA IMAGES | 85 |
| 63 | FALSE MATCH RATE CALIBRATION: VISA IMAGES | 86 |
| 64 | FALSE MATCH RATE CALIBRATION: VISA IMAGES | 87 |
| 65 | FALSE MATCH RATE CALIBRATION: VISA IMAGES | 88 |
| 66 | FALSE MATCH RATE CALIBRATION: VISA IMAGES | 89 |

| | | |
|-----|---|-----|
| 67 | FALSE MATCH RATE CALIBRATION: VISA IMAGES | 90 |
| 68 | FALSE MATCH RATE CALIBRATION: VISA IMAGES | 91 |
| 69 | FALSE MATCH RATE CALIBRATION: VISA IMAGES | 92 |
| 70 | FALSE MATCH RATE CALIBRATION: VISA IMAGES | 93 |
| 71 | FALSE MATCH RATE CONCENTRATION: VISA IMAGES | 94 |
| 72 | EFFECT OF COUNTRY OF BIRTH ON FNMR | 96 |
| 73 | EFFECT OF COUNTRY OF BIRTH ON FNMR | 97 |
| 74 | EFFECT OF COUNTRY OF BIRTH ON FNMR | 98 |
| 75 | EFFECT OF COUNTRY OF BIRTH ON FNMR | 99 |
| 76 | EFFECT OF COUNTRY OF BIRTH ON FNMR | 100 |
| 77 | EFFECT OF COUNTRY OF BIRTH ON FNMR | 101 |
| 78 | EFFECT OF COUNTRY OF BIRTH ON FNMR | 102 |
| 79 | EFFECT OF COUNTRY OF BIRTH ON FNMR | 103 |
| 80 | EFFECT OF COUNTRY OF BIRTH ON FNMR | 104 |
| 81 | ERROR TRADEOFF CHARACTERISTIC: MUGSHOT IMAGES | 106 |
| 82 | ERROR TRADEOFF CHARACTERISTIC: MUGSHOT IMAGES | 107 |
| 83 | ERROR TRADEOFF CHARACTERISTIC: MUGSHOT IMAGES | 108 |
| 84 | ERROR TRADEOFF CHARACTERISTIC: MUGSHOT IMAGES | 109 |
| 85 | ERROR TRADEOFF CHARACTERISTIC: MUGSHOT IMAGES | 110 |
| 86 | ERROR TRADEOFF CHARACTERISTIC: MUGSHOT IMAGES | 111 |
| 87 | ERROR TRADEOFF CHARACTERISTIC: MUGSHOT IMAGES | 112 |
| 88 | EFFECT OF SUBJECT AGE ON FNMR | 114 |
| 89 | EFFECT OF SUBJECT AGE ON FNMR | 115 |
| 90 | EFFECT OF SUBJECT AGE ON FNMR | 116 |
| 91 | EFFECT OF SUBJECT AGE ON FNMR | 117 |
| 92 | EFFECT OF SUBJECT AGE ON FNMR | 118 |
| 93 | EFFECT OF SUBJECT AGE ON FNMR | 119 |
| 94 | EFFECT OF SUBJECT AGE ON FNMR | 120 |
| 95 | EFFECT OF SUBJECT AGE ON FNMR | 121 |
| 96 | EFFECT OF SUBJECT AGE ON FNMR | 122 |
| 97 | WORST CASE REGIONAL EFFECT FNMR | 125 |
| 98 | IMPOSTOR DISTRIBUTION SHIFTS FOR SELECT COUNTRY PAIRS | 127 |
| 99 | ALGORITHM 3DIVI-003 CROSS REGION FMR | 128 |
| 100 | ALGORITHM ALCHERA-000 CROSS REGION FMR | 129 |
| 101 | ALGORITHM ALCHERA-001 CROSS REGION FMR | 130 |
| 102 | ALGORITHM ALLGOVISION-000 CROSS REGION FMR | 131 |
| 103 | ALGORITHM AMPLIFIEDGROUP-001 CROSS REGION FMR | 132 |
| 104 | ALGORITHM ANKE-002 CROSS REGION FMR | 133 |
| 105 | ALGORITHM ANKE-003 CROSS REGION FMR | 134 |
| 106 | ALGORITHM ANYVISION-002 CROSS REGION FMR | 135 |
| 107 | ALGORITHM ANYVISION-004 CROSS REGION FMR | 136 |
| 108 | ALGORITHM AWARE-003 CROSS REGION FMR | 137 |
| 109 | ALGORITHM AWARE-004 CROSS REGION FMR | 138 |
| 110 | ALGORITHM AYONIX-000 CROSS REGION FMR | 139 |
| 111 | ALGORITHM BM-001 CROSS REGION FMR | 140 |
| 112 | ALGORITHM CAMVI-002 CROSS REGION FMR | 141 |
| 113 | ALGORITHM CAMVI-003 CROSS REGION FMR | 142 |
| 114 | ALGORITHM CEIEC-001 CROSS REGION FMR | 143 |
| 115 | ALGORITHM COGENT-002 CROSS REGION FMR | 144 |
| 116 | ALGORITHM COGENT-003 CROSS REGION FMR | 145 |
| 117 | ALGORITHM COGNITEC-000 CROSS REGION FMR | 146 |
| 118 | ALGORITHM COGNITEC-001 CROSS REGION FMR | 147 |
| 119 | ALGORITHM CYBEREXTRUDER-001 CROSS REGION FMR | 148 |
| 120 | ALGORITHM CYBEREXTRUDER-002 CROSS REGION FMR | 149 |
| 121 | ALGORITHM CYBERLINK-000 CROSS REGION FMR | 150 |
| 122 | ALGORITHM CYBERLINK-001 CROSS REGION FMR | 151 |

| | | |
|-----|--|-----|
| 123 | ALGORITHM DAHUA-001 CROSS REGION FMR | 152 |
| 124 | ALGORITHM DAHUA-002 CROSS REGION FMR | 153 |
| 125 | ALGORITHM DERMALOG-005 CROSS REGION FMR | 154 |
| 126 | ALGORITHM DERMALOG-006 CROSS REGION FMR | 155 |
| 127 | ALGORITHM DIGITALBARRIERS-002 CROSS REGION FMR | 156 |
| 128 | ALGORITHM EVERAI-001 CROSS REGION FMR | 157 |
| 129 | ALGORITHM EVERAI-002 CROSS REGION FMR | 158 |
| 130 | ALGORITHM GLORY-000 CROSS REGION FMR | 159 |
| 131 | ALGORITHM GLORY-001 CROSS REGION FMR | 160 |
| 132 | ALGORITHM GORILLA-001 CROSS REGION FMR | 161 |
| 133 | ALGORITHM GORILLA-002 CROSS REGION FMR | 162 |
| 134 | ALGORITHM HIK-001 CROSS REGION FMR | 163 |
| 135 | ALGORITHM HR-000 CROSS REGION FMR | 164 |
| 136 | ALGORITHM ID3-003 CROSS REGION FMR | 165 |
| 137 | ALGORITHM ID3-004 CROSS REGION FMR | 166 |
| 138 | ALGORITHM IDEMIA-003 CROSS REGION FMR | 167 |
| 139 | ALGORITHM IDEMIA-004 CROSS REGION FMR | 168 |
| 140 | ALGORITHM IIT-000 CROSS REGION FMR | 169 |
| 141 | ALGORITHM IMPERIAL-000 CROSS REGION FMR | 170 |
| 142 | ALGORITHM IMPERIAL-001 CROSS REGION FMR | 171 |
| 143 | ALGORITHM INCODE-002 CROSS REGION FMR | 172 |
| 144 | ALGORITHM INCODE-003 CROSS REGION FMR | 173 |
| 145 | ALGORITHM INNOVATRICS-004 CROSS REGION FMR | 174 |
| 146 | ALGORITHM INNOVATRICS-005 CROSS REGION FMR | 175 |
| 147 | ALGORITHM INTELLIVISION-001 CROSS REGION FMR | 176 |
| 148 | ALGORITHM ISITYOU-000 CROSS REGION FMR | 177 |
| 149 | ALGORITHM ISYSTEMS-001 CROSS REGION FMR | 178 |
| 150 | ALGORITHM ISYSTEMS-002 CROSS REGION FMR | 179 |
| 151 | ALGORITHM ITMO-005 CROSS REGION FMR | 180 |
| 152 | ALGORITHM ITMO-006 CROSS REGION FMR | 181 |
| 153 | ALGORITHM KAKAO-001 CROSS REGION FMR | 182 |
| 154 | ALGORITHM LOOKMAN-002 CROSS REGION FMR | 183 |
| 155 | ALGORITHM MEGVII-001 CROSS REGION FMR | 184 |
| 156 | ALGORITHM MEGVII-002 CROSS REGION FMR | 185 |
| 157 | ALGORITHM MEIYA-001 CROSS REGION FMR | 186 |
| 158 | ALGORITHM MICROFOCUS-001 CROSS REGION FMR | 187 |
| 159 | ALGORITHM MICROFOCUS-002 CROSS REGION FMR | 188 |
| 160 | ALGORITHM NEUROTECHNOLOGY-004 CROSS REGION FMR | 189 |
| 161 | ALGORITHM NEUROTECHNOLOGY-005 CROSS REGION FMR | 190 |
| 162 | ALGORITHM NODEFLUX-000 CROSS REGION FMR | 191 |
| 163 | ALGORITHM NODEFLUX-001 CROSS REGION FMR | 192 |
| 164 | ALGORITHM NTECHLAB-005 CROSS REGION FMR | 193 |
| 165 | ALGORITHM NTECHLAB-006 CROSS REGION FMR | 194 |
| 166 | ALGORITHM PSL-001 CROSS REGION FMR | 195 |
| 167 | ALGORITHM PSL-002 CROSS REGION FMR | 196 |
| 168 | ALGORITHM RANKONE-005 CROSS REGION FMR | 197 |
| 169 | ALGORITHM RANKONE-006 CROSS REGION FMR | 198 |
| 170 | ALGORITHM REALNETWORKS-001 CROSS REGION FMR | 199 |
| 171 | ALGORITHM REALNETWORKS-002 CROSS REGION FMR | 200 |
| 172 | ALGORITHM REMARKAI-000 CROSS REGION FMR | 201 |
| 173 | ALGORITHM REMARKAI-001 CROSS REGION FMR | 202 |
| 174 | ALGORITHM SAFFE-001 CROSS REGION FMR | 203 |
| 175 | ALGORITHM SAFFE-002 CROSS REGION FMR | 204 |
| 176 | ALGORITHM SENSETIME-001 CROSS REGION FMR | 205 |
| 177 | ALGORITHM SENSETIME-002 CROSS REGION FMR | 206 |
| 178 | ALGORITHM SHAMAN-000 CROSS REGION FMR | 207 |
| 179 | ALGORITHM SHAMAN-001 CROSS REGION FMR | 208 |

| | | |
|-----|--|-----|
| 180 | ALGORITHM SIAT-002 CROSS REGION FMR | 209 |
| 181 | ALGORITHM SIAT-004 CROSS REGION FMR | 210 |
| 182 | ALGORITHM SMILART-002 CROSS REGION FMR | 211 |
| 183 | ALGORITHM SMILART-003 CROSS REGION FMR | 212 |
| 184 | ALGORITHM SYNESIS-003 CROSS REGION FMR | 213 |
| 185 | ALGORITHM SYNESIS-004 CROSS REGION FMR | 214 |
| 186 | ALGORITHM TECH5-001 CROSS REGION FMR | 215 |
| 187 | ALGORITHM TECH5-002 CROSS REGION FMR | 216 |
| 188 | ALGORITHM TEVIAN-003 CROSS REGION FMR | 217 |
| 189 | ALGORITHM TEVIAN-004 CROSS REGION FMR | 218 |
| 190 | ALGORITHM TIGER-002 CROSS REGION FMR | 219 |
| 191 | ALGORITHM TIGER-003 CROSS REGION FMR | 220 |
| 192 | ALGORITHM TOSHIBA-002 CROSS REGION FMR | 221 |
| 193 | ALGORITHM TOSHIBA-003 CROSS REGION FMR | 222 |
| 194 | ALGORITHM VCOG-002 CROSS REGION FMR | 223 |
| 195 | ALGORITHM VD-001 CROSS REGION FMR | 224 |
| 196 | ALGORITHM VERIDAS-001 CROSS REGION FMR | 225 |
| 197 | ALGORITHM VERIDAS-002 CROSS REGION FMR | 226 |
| 198 | ALGORITHM VIGILANTSOLUTIONS-005 CROSS REGION FMR | 227 |
| 199 | ALGORITHM VIGILANTSOLUTIONS-006 CROSS REGION FMR | 228 |
| 200 | ALGORITHM VION-000 CROSS REGION FMR | 229 |
| 201 | ALGORITHM VISIONBOX-000 CROSS REGION FMR | 230 |
| 202 | ALGORITHM VISIONBOX-001 CROSS REGION FMR | 231 |
| 203 | ALGORITHM VISIONLABS-005 CROSS REGION FMR | 232 |
| 204 | ALGORITHM VISIONLABS-006 CROSS REGION FMR | 233 |
| 205 | ALGORITHM VOCORD-005 CROSS REGION FMR | 234 |
| 206 | ALGORITHM VOCORD-006 CROSS REGION FMR | 235 |
| 207 | ALGORITHM YISHENG-004 CROSS REGION FMR | 236 |
| 208 | ALGORITHM YITU-003 CROSS REGION FMR | 237 |
| 209 | ALGORITHM 3DIVI-003 CROSS COUNTRY FMR | 238 |
| 210 | ALGORITHM ALCHERA-000 CROSS COUNTRY FMR | 239 |
| 211 | ALGORITHM ALCHERA-001 CROSS COUNTRY FMR | 240 |
| 212 | ALGORITHM ALLGOVISION-000 CROSS COUNTRY FMR | 241 |
| 213 | ALGORITHM ANKE-002 CROSS COUNTRY FMR | 242 |
| 214 | ALGORITHM ANKE-003 CROSS COUNTRY FMR | 243 |
| 215 | ALGORITHM ANYVISION-002 CROSS COUNTRY FMR | 244 |
| 216 | ALGORITHM ANYVISION-004 CROSS COUNTRY FMR | 245 |
| 217 | ALGORITHM AWARE-003 CROSS COUNTRY FMR | 246 |
| 218 | ALGORITHM AWARE-004 CROSS COUNTRY FMR | 247 |
| 219 | ALGORITHM AYONIX-000 CROSS COUNTRY FMR | 248 |
| 220 | ALGORITHM BM-001 CROSS COUNTRY FMR | 249 |
| 221 | ALGORITHM CAMVI-002 CROSS COUNTRY FMR | 250 |
| 222 | ALGORITHM CAMVI-003 CROSS COUNTRY FMR | 251 |
| 223 | ALGORITHM CEIEC-001 CROSS COUNTRY FMR | 252 |
| 224 | ALGORITHM COGENT-002 CROSS COUNTRY FMR | 253 |
| 225 | ALGORITHM COGENT-003 CROSS COUNTRY FMR | 254 |
| 226 | ALGORITHM COGNITEC-000 CROSS COUNTRY FMR | 255 |
| 227 | ALGORITHM COGNITEC-001 CROSS COUNTRY FMR | 256 |
| 228 | ALGORITHM CYBEREXTRUDER-001 CROSS COUNTRY FMR | 257 |
| 229 | ALGORITHM CYBEREXTRUDER-002 CROSS COUNTRY FMR | 258 |
| 230 | ALGORITHM CYBERLINK-000 CROSS COUNTRY FMR | 259 |
| 231 | ALGORITHM CYBERLINK-001 CROSS COUNTRY FMR | 260 |
| 232 | ALGORITHM DAHUA-001 CROSS COUNTRY FMR | 261 |
| 233 | ALGORITHM DAHUA-002 CROSS COUNTRY FMR | 262 |
| 234 | ALGORITHM DERMALOG-005 CROSS COUNTRY FMR | 263 |
| 235 | ALGORITHM DERMALOG-006 CROSS COUNTRY FMR | 264 |
| 236 | ALGORITHM DIGITALBARRIERS-002 CROSS COUNTRY FMR | 265 |

| | | |
|-----|---|-----|
| 237 | ALGORITHM EVERAI-001 CROSS COUNTRY FMR | 266 |
| 238 | ALGORITHM EVERAI-002 CROSS COUNTRY FMR | 267 |
| 239 | ALGORITHM GLORY-000 CROSS COUNTRY FMR | 268 |
| 240 | ALGORITHM GLORY-001 CROSS COUNTRY FMR | 269 |
| 241 | ALGORITHM GORILLA-001 CROSS COUNTRY FMR | 270 |
| 242 | ALGORITHM GORILLA-002 CROSS COUNTRY FMR | 271 |
| 243 | ALGORITHM HIK-001 CROSS COUNTRY FMR | 272 |
| 244 | ALGORITHM HR-000 CROSS COUNTRY FMR | 273 |
| 245 | ALGORITHM ID3-003 CROSS COUNTRY FMR | 274 |
| 246 | ALGORITHM ID3-004 CROSS COUNTRY FMR | 275 |
| 247 | ALGORITHM IDEMIA-003 CROSS COUNTRY FMR | 276 |
| 248 | ALGORITHM IDEMIA-004 CROSS COUNTRY FMR | 277 |
| 249 | ALGORITHM IIT-000 CROSS COUNTRY FMR | 278 |
| 250 | ALGORITHM IMPERIAL-000 CROSS COUNTRY FMR | 279 |
| 251 | ALGORITHM IMPERIAL-001 CROSS COUNTRY FMR | 280 |
| 252 | ALGORITHM INCODE-002 CROSS COUNTRY FMR | 281 |
| 253 | ALGORITHM INCODE-003 CROSS COUNTRY FMR | 282 |
| 254 | ALGORITHM INNOVATRICES-004 CROSS COUNTRY FMR | 283 |
| 255 | ALGORITHM INNOVATRICES-005 CROSS COUNTRY FMR | 284 |
| 256 | ALGORITHM INTELLIVISION-001 CROSS COUNTRY FMR | 285 |
| 257 | ALGORITHM ISITYOU-000 CROSS COUNTRY FMR | 286 |
| 258 | ALGORITHM ISYSTEMS-001 CROSS COUNTRY FMR | 287 |
| 259 | ALGORITHM ISYSTEMS-002 CROSS COUNTRY FMR | 288 |
| 260 | ALGORITHM ITMO-005 CROSS COUNTRY FMR | 289 |
| 261 | ALGORITHM ITMO-006 CROSS COUNTRY FMR | 290 |
| 262 | ALGORITHM KAKAO-001 CROSS COUNTRY FMR | 291 |
| 263 | ALGORITHM LOOKMAN-002 CROSS COUNTRY FMR | 292 |
| 264 | ALGORITHM MEGVII-001 CROSS COUNTRY FMR | 293 |
| 265 | ALGORITHM MEGVII-002 CROSS COUNTRY FMR | 294 |
| 266 | ALGORITHM MEIYA-001 CROSS COUNTRY FMR | 295 |
| 267 | ALGORITHM MICROFOCUS-001 CROSS COUNTRY FMR | 296 |
| 268 | ALGORITHM MICROFOCUS-002 CROSS COUNTRY FMR | 297 |
| 269 | ALGORITHM NODEFLUX-001 CROSS COUNTRY FMR | 298 |
| 270 | ALGORITHM NTECHLAB-005 CROSS COUNTRY FMR | 299 |
| 271 | ALGORITHM NTECHLAB-006 CROSS COUNTRY FMR | 300 |
| 272 | ALGORITHM PSL-001 CROSS COUNTRY FMR | 301 |
| 273 | ALGORITHM PSL-002 CROSS COUNTRY FMR | 302 |
| 274 | ALGORITHM RANKONE-005 CROSS COUNTRY FMR | 303 |
| 275 | ALGORITHM RANKONE-006 CROSS COUNTRY FMR | 304 |
| 276 | ALGORITHM REALNETWORKS-001 CROSS COUNTRY FMR | 305 |
| 277 | ALGORITHM REALNETWORKS-002 CROSS COUNTRY FMR | 306 |
| 278 | ALGORITHM REMARKAI-000 CROSS COUNTRY FMR | 307 |
| 279 | ALGORITHM REMARKAI-001 CROSS COUNTRY FMR | 308 |
| 280 | ALGORITHM SAFFE-001 CROSS COUNTRY FMR | 309 |
| 281 | ALGORITHM SAFFE-002 CROSS COUNTRY FMR | 310 |
| 282 | ALGORITHM SENSETIME-001 CROSS COUNTRY FMR | 311 |
| 283 | ALGORITHM SENSETIME-002 CROSS COUNTRY FMR | 312 |
| 284 | ALGORITHM SHAMAN-000 CROSS COUNTRY FMR | 313 |
| 285 | ALGORITHM SHAMAN-001 CROSS COUNTRY FMR | 314 |
| 286 | ALGORITHM SIAT-002 CROSS COUNTRY FMR | 315 |
| 287 | ALGORITHM SIAT-004 CROSS COUNTRY FMR | 316 |
| 288 | ALGORITHM SMILART-002 CROSS COUNTRY FMR | 317 |
| 289 | ALGORITHM SMILART-003 CROSS COUNTRY FMR | 318 |
| 290 | ALGORITHM SYNESIS-003 CROSS COUNTRY FMR | 319 |
| 291 | ALGORITHM TECH5-001 CROSS COUNTRY FMR | 320 |
| 292 | ALGORITHM TECH5-002 CROSS COUNTRY FMR | 321 |
| 293 | ALGORITHM TEVIAN-003 CROSS COUNTRY FMR | 322 |

| | | |
|-----|--|-----|
| 294 | ALGORITHM TEVIAN-004 CROSS COUNTRY FMR | 323 |
| 295 | ALGORITHM TIGER-002 CROSS COUNTRY FMR | 324 |
| 296 | ALGORITHM TIGER-003 CROSS COUNTRY FMR | 325 |
| 297 | ALGORITHM TOSHIBA-002 CROSS COUNTRY FMR | 326 |
| 298 | ALGORITHM TOSHIBA-003 CROSS COUNTRY FMR | 327 |
| 299 | ALGORITHM VCOG-002 CROSS COUNTRY FMR | 328 |
| 300 | ALGORITHM VD-001 CROSS COUNTRY FMR | 329 |
| 301 | ALGORITHM VERIDAS-001 CROSS COUNTRY FMR | 330 |
| 302 | ALGORITHM VERIDAS-002 CROSS COUNTRY FMR | 331 |
| 303 | ALGORITHM VIGILANTSOLUTIONS-005 CROSS COUNTRY FMR | 332 |
| 304 | ALGORITHM VIGILANTSOLUTIONS-006 CROSS COUNTRY FMR | 333 |
| 305 | ALGORITHM VION-000 CROSS COUNTRY FMR | 334 |
| 306 | ALGORITHM VISIONBOX-000 CROSS COUNTRY FMR | 335 |
| 307 | ALGORITHM VISIONBOX-001 CROSS COUNTRY FMR | 336 |
| 308 | ALGORITHM VISIONLABS-005 CROSS COUNTRY FMR | 337 |
| 309 | ALGORITHM VISIONLABS-006 CROSS COUNTRY FMR | 338 |
| 310 | ALGORITHM VOCORD-005 CROSS COUNTRY FMR | 339 |
| 311 | ALGORITHM YISHENG-004 CROSS COUNTRY FMR | 340 |
| 312 | ALGORITHM YITU-003 CROSS COUNTRY FMR | 341 |
| 313 | IMPOSTOR COUNTS FOR CROSS COUNTRY FMR CALCULATIONS | 342 |
| 314 | ALGORITHM 3DIVI-003 CROSS AGE FMR | 344 |
| 315 | ALGORITHM ALCHERA-000 CROSS AGE FMR | 345 |
| 316 | ALGORITHM ALCHERA-001 CROSS AGE FMR | 346 |
| 317 | ALGORITHM ALLGOVISION-000 CROSS AGE FMR | 347 |
| 318 | ALGORITHM AMPLIFIEDGROUP-001 CROSS AGE FMR | 348 |
| 319 | ALGORITHM ANKE-002 CROSS AGE FMR | 349 |
| 320 | ALGORITHM ANKE-003 CROSS AGE FMR | 350 |
| 321 | ALGORITHM ANYVISION-002 CROSS AGE FMR | 351 |
| 322 | ALGORITHM ANYVISION-004 CROSS AGE FMR | 352 |
| 323 | ALGORITHM AWARE-003 CROSS AGE FMR | 353 |
| 324 | ALGORITHM AWARE-004 CROSS AGE FMR | 354 |
| 325 | ALGORITHM AYONIX-000 CROSS AGE FMR | 355 |
| 326 | ALGORITHM BM-001 CROSS AGE FMR | 356 |
| 327 | ALGORITHM CAMVI-002 CROSS AGE FMR | 357 |
| 328 | ALGORITHM CAMVI-003 CROSS AGE FMR | 358 |
| 329 | ALGORITHM CEIEC-001 CROSS AGE FMR | 359 |
| 330 | ALGORITHM COGENT-002 CROSS AGE FMR | 360 |
| 331 | ALGORITHM COGENT-003 CROSS AGE FMR | 361 |
| 332 | ALGORITHM COGNITEC-000 CROSS AGE FMR | 362 |
| 333 | ALGORITHM COGNITEC-001 CROSS AGE FMR | 363 |
| 334 | ALGORITHM CYBEREXTRUDER-001 CROSS AGE FMR | 364 |
| 335 | ALGORITHM CYBEREXTRUDER-002 CROSS AGE FMR | 365 |
| 336 | ALGORITHM CYBERLINK-000 CROSS AGE FMR | 366 |
| 337 | ALGORITHM CYBERLINK-001 CROSS AGE FMR | 367 |
| 338 | ALGORITHM DAHUA-001 CROSS AGE FMR | 368 |
| 339 | ALGORITHM DAHUA-002 CROSS AGE FMR | 369 |
| 340 | ALGORITHM DERMALOG-005 CROSS AGE FMR | 370 |
| 341 | ALGORITHM DERMALOG-006 CROSS AGE FMR | 371 |
| 342 | ALGORITHM DIGITALBARRIERS-002 CROSS AGE FMR | 372 |
| 343 | ALGORITHM EVERAI-001 CROSS AGE FMR | 373 |
| 344 | ALGORITHM EVERAI-002 CROSS AGE FMR | 374 |
| 345 | ALGORITHM GLORY-001 CROSS AGE FMR | 375 |
| 346 | ALGORITHM GORILLA-001 CROSS AGE FMR | 376 |
| 347 | ALGORITHM GORILLA-002 CROSS AGE FMR | 377 |
| 348 | ALGORITHM HIK-001 CROSS AGE FMR | 378 |
| 349 | ALGORITHM HR-000 CROSS AGE FMR | 379 |
| 350 | ALGORITHM ID3-003 CROSS AGE FMR | 380 |

| | | |
|-----|---|-----|
| 351 | ALGORITHM ID3-004 CROSS AGE FMR | 381 |
| 352 | ALGORITHM IDEMIA-003 CROSS AGE FMR | 382 |
| 353 | ALGORITHM IDEMIA-004 CROSS AGE FMR | 383 |
| 354 | ALGORITHM IIT-000 CROSS AGE FMR | 384 |
| 355 | ALGORITHM IMPERIAL-000 CROSS AGE FMR | 385 |
| 356 | ALGORITHM IMPERIAL-001 CROSS AGE FMR | 386 |
| 357 | ALGORITHM INCODE-002 CROSS AGE FMR | 387 |
| 358 | ALGORITHM INCODE-003 CROSS AGE FMR | 388 |
| 359 | ALGORITHM INNOVATRICS-004 CROSS AGE FMR | 389 |
| 360 | ALGORITHM INNOVATRICS-005 CROSS AGE FMR | 390 |
| 361 | ALGORITHM INTELLIVISION-001 CROSS AGE FMR | 391 |
| 362 | ALGORITHM ISITYOU-000 CROSS AGE FMR | 392 |
| 363 | ALGORITHM ISYSTEMS-001 CROSS AGE FMR | 393 |
| 364 | ALGORITHM ISYSTEMS-002 CROSS AGE FMR | 394 |
| 365 | ALGORITHM ITMO-005 CROSS AGE FMR | 395 |
| 366 | ALGORITHM ITMO-006 CROSS AGE FMR | 396 |
| 367 | ALGORITHM KAKAO-001 CROSS AGE FMR | 397 |
| 368 | ALGORITHM LOOKMAN-002 CROSS AGE FMR | 398 |
| 369 | ALGORITHM MEGVII-001 CROSS AGE FMR | 399 |
| 370 | ALGORITHM MEGVII-002 CROSS AGE FMR | 400 |
| 371 | ALGORITHM MEIYA-001 CROSS AGE FMR | 401 |
| 372 | ALGORITHM MICROFOCUS-001 CROSS AGE FMR | 402 |
| 373 | ALGORITHM MICROFOCUS-002 CROSS AGE FMR | 403 |
| 374 | ALGORITHM NEUROTECHNOLOGY-004 CROSS AGE FMR | 404 |
| 375 | ALGORITHM NODEFLUX-001 CROSS AGE FMR | 405 |
| 376 | ALGORITHM NTECHLAB-005 CROSS AGE FMR | 406 |
| 377 | ALGORITHM NTECHLAB-006 CROSS AGE FMR | 407 |
| 378 | ALGORITHM PSL-001 CROSS AGE FMR | 408 |
| 379 | ALGORITHM PSL-002 CROSS AGE FMR | 409 |
| 380 | ALGORITHM RANKONE-005 CROSS AGE FMR | 410 |
| 381 | ALGORITHM RANKONE-006 CROSS AGE FMR | 411 |
| 382 | ALGORITHM REALNETWORKS-001 CROSS AGE FMR | 412 |
| 383 | ALGORITHM REALNETWORKS-002 CROSS AGE FMR | 413 |
| 384 | ALGORITHM REMARKAI-000 CROSS AGE FMR | 414 |
| 385 | ALGORITHM REMARKAI-001 CROSS AGE FMR | 415 |
| 386 | ALGORITHM SAFFE-001 CROSS AGE FMR | 416 |
| 387 | ALGORITHM SAFFE-002 CROSS AGE FMR | 417 |
| 388 | ALGORITHM SENSETIME-001 CROSS AGE FMR | 418 |
| 389 | ALGORITHM SENSETIME-002 CROSS AGE FMR | 419 |
| 390 | ALGORITHM SHAMAN-000 CROSS AGE FMR | 420 |
| 391 | ALGORITHM SHAMAN-001 CROSS AGE FMR | 421 |
| 392 | ALGORITHM SIAT-002 CROSS AGE FMR | 422 |
| 393 | ALGORITHM SIAT-004 CROSS AGE FMR | 423 |
| 394 | ALGORITHM SMILART-002 CROSS AGE FMR | 424 |
| 395 | ALGORITHM SMILART-003 CROSS AGE FMR | 425 |
| 396 | ALGORITHM SYNESIS-003 CROSS AGE FMR | 426 |
| 397 | ALGORITHM SYNESIS-004 CROSS AGE FMR | 427 |
| 398 | ALGORITHM TECH5-001 CROSS AGE FMR | 428 |
| 399 | ALGORITHM TECH5-002 CROSS AGE FMR | 429 |
| 400 | ALGORITHM TEVIAN-003 CROSS AGE FMR | 430 |
| 401 | ALGORITHM TEVIAN-004 CROSS AGE FMR | 431 |
| 402 | ALGORITHM TIGER-002 CROSS AGE FMR | 432 |
| 403 | ALGORITHM TIGER-003 CROSS AGE FMR | 433 |
| 404 | ALGORITHM TOSHIBA-002 CROSS AGE FMR | 434 |
| 405 | ALGORITHM TOSHIBA-003 CROSS AGE FMR | 435 |
| 406 | ALGORITHM VCOG-002 CROSS AGE FMR | 436 |
| 407 | ALGORITHM VD-001 CROSS AGE FMR | 437 |

| | | |
|-----|---|-----|
| 408 | ALGORITHM VERIDAS-001 CROSS AGE FMR | 438 |
| 409 | ALGORITHM VERIDAS-002 CROSS AGE FMR | 439 |
| 410 | ALGORITHM VIGILANTSOLUTIONS-005 CROSS AGE FMR | 440 |
| 411 | ALGORITHM VIGILANTSOLUTIONS-006 CROSS AGE FMR | 441 |
| 412 | ALGORITHM VION-000 CROSS AGE FMR | 442 |
| 413 | ALGORITHM VISIONBOX-000 CROSS AGE FMR | 443 |
| 414 | ALGORITHM VISIONBOX-001 CROSS AGE FMR | 444 |
| 415 | ALGORITHM VISIONLABS-005 CROSS AGE FMR | 445 |
| 416 | ALGORITHM VISIONLABS-006 CROSS AGE FMR | 446 |
| 417 | ALGORITHM VOCORD-005 CROSS AGE FMR | 447 |
| 418 | ALGORITHM VOCORD-006 CROSS AGE FMR | 448 |
| 419 | ALGORITHM YISHENG-004 CROSS AGE FMR | 449 |
| 420 | ALGORITHM YITU-003 CROSS AGE FMR | 450 |

| | Developer | Short | Seq. | Validation | Config ¹ | Template | | | GPU | Comparison Time (ns) ³ | |
|----|---------------------------------------|----------------|------|------------|---------------------|-------------------------|-------------------------|----|-----------------------------|-----------------------------------|--|
| | Name | Name | Num. | Date | Data (KB) | Size (B) | Time (ms) ² | | Genuine | Impostor | |
| 1 | 3DiVi | 3divi | 003 | 2018-10-09 | 191636 | ¹⁰¹ 4096 ± 0 | ⁷³ 650 ± 90 | No | ²⁵ 627 ± 11 | ²⁷ 623 ± 32 | |
| 2 | Alchera | alchera | 000 | 2019-03-01 | 258450 | ⁶¹ 2048 ± 0 | ⁶⁷ 587 ± 13 | No | ⁷⁶ 3189 ± 32 | ⁷⁷ 3031 ± 142 | |
| 3 | Alchera | alchera | 000 | 2019-03-01 | 174013 | ⁵⁸ 2048 ± 0 | ⁷⁰ 627 ± 11 | No | ⁷⁹ 3342 ± 81 | ⁷⁸ 3243 ± 47 | |
| 4 | AllGoVision | allgovision | 000 | 2019-03-01 | 172509 | ⁵⁷ 2048 ± 0 | ⁴⁵ 384 ± 8 | No | ¹⁰⁴ 29903 ± 406 | ¹⁰⁵ 29735 ± 194 | |
| 5 | Amplified Group | amplifiedgroup | 001 | 2019-03-01 | 0 | ²³ 866 ± 2 | ⁵⁹ 3 ± 0 | No | ¹⁰⁷ 57803 ± 4210 | ¹⁰⁷ 56365 ± 1196 | |
| 6 | Anke Investments | anke | 002 | 2018-10-19 | 798686 | ⁹⁰ 2072 ± 0 | ⁵² 419 ± 30 | No | ¹⁸ 501 ± 17 | ¹⁹ 492 ± 17 | |
| 7 | Anke Investments | anke | 003 | 2019-02-27 | 340160 | ⁸⁸ 2056 ± 0 | ⁹⁵ 811 ± 23 | No | ¹² 425 ± 28 | ¹⁴ 437 ± 32 | |
| 8 | AnyVision | anyvision | 002 | 2018-01-31 | 662659 | ²⁸ 1024 ± 0 | ¹⁹ 248 ± 0 | No | ¹⁰⁸ 74069 ± 188 | ¹⁰⁸ 74019 ± 198 | |
| 9 | AnyVision | anyvision | 004 | 2018-06-15 | 401001 | ³¹ 1024 ± 0 | ³⁸ 355 ± 1 | No | ⁶¹ 1891 ± 51 | ⁵⁹ 1829 ± 85 | |
| 10 | Aware | aware | 003 | 2018-10-19 | 377729 | ⁹⁶ 1024 ± 0 | ⁹² 783 ± 10 | No | ⁵⁰ 1392 ± 42 | ⁵⁴ 1334 ± 80 | |
| 11 | Aware | aware | 004 | 2019-03-01 | 427829 | ⁹² 2084 ± 0 | ¹⁰⁷ 900 ± 10 | No | ⁴⁷ 1279 ± 50 | ⁵³ 1287 ± 100 | |
| 12 | Ayonix | ayonix | 000 | 2017-06-22 | 58505 | ³³ 1036 ± 0 | ¹ 18 ± 2 | No | ²⁴ 621 ± 23 | ²⁶ 620 ± 26 | |
| 13 | Bitmain | bitmain | 001 | 2018-10-17 | 287734 | ¹ 64 ± 0 | ⁵⁴ 444 ± 88 | No | ⁶⁰ 1887 ± 31 | ⁶¹ 1877 ± 26 | |
| 14 | Camvi Technologies | camvitech | 002 | 2018-10-19 | 236278 | ²⁶ 1024 ± 0 | ⁸¹ 677 ± 7 | No | ²³ 612 ± 26 | ²⁴ 603 ± 20 | |
| 15 | Camvi Technologies | camvitech | 003 | 2019-03-01 | 285657 | ²⁵ 1024 ± 0 | ⁸⁷ 750 ± 3 | No | ²¹ 571 ± 23 | ²³ 565 ± 26 | |
| 16 | China Electronics Import-Export Corp | ceiec | 001 | 2019-03-01 | 159618 | ²⁷ 1024 ± 0 | ³² 314 ± 3 | No | ¹⁰² 22831 ± 108 | ¹⁰² 22813 ± 120 | |
| 17 | Gemalto Cogent | cogent | 002 | 2018-10-19 | 696959 | ⁴⁷ 1979 ± 0 | ¹⁰⁸ 941 ± 0 | No | ⁹⁷ 14394 ± 134 | ⁹⁷ 14385 ± 176 | |
| 18 | Gemalto Cogent | cogent | 003 | 2019-03-01 | 698290 | ²⁴ 973 ± 0 | ¹⁰⁸ 952 ± 0 | No | ⁹⁴ 12496 ± 75 | ⁹⁴ 11822 ± 163 | |
| 19 | Cognitec Systems GmbH | cognitec | 000 | 2018-10-19 | 474759 | ⁷⁶ 2052 ± 0 | ¹⁷ 224 ± 1 | No | ⁸² 3835 ± 108 | ⁸² 3782 ± 83 | |
| 20 | Cognitec Systems GmbH | cognitec | 001 | 2019-03-01 | 476809 | ⁷² 2052 ± 0 | ²⁸ 297 ± 17 | No | ⁸⁴ 4253 ± 59 | ⁸⁴ 4102 ± 167 | |
| 21 | Cyberextruder | cyberex | 001 | 2017-08-02 | 121211 | ⁷ 256 ± 0 | ¹⁰⁶ 893 ± 25 | No | ⁴⁰ 1083 ± 16 | ⁴⁴ 1079 ± 19 | |
| 22 | Cyberextruder | cyberex | 002 | 2018-01-30 | 168909 | ⁵² 2048 ± 0 | ⁵⁹ 532 ± 6 | No | ⁵⁹ 1803 ± 14 | ⁵⁸ 1779 ± 22 | |
| 23 | Cyberlink Corp | cyberlink | 000 | 2019-03-01 | 221801 | ⁷³ 2052 ± 0 | ³⁷ 338 ± 6 | No | ⁶⁷ 2102 ± 40 | ⁶⁸ 2093 ± 32 | |
| 24 | Cyberline Corp | cyberlink | 001 | 2019-03-01 | 222009 | ⁸¹ 2052 ± 0 | ⁵³ 425 ± 29 | No | ⁶⁵ 2051 ± 32 | ⁶⁶ 2060 ± 31 | |
| 25 | Dahua Technology Co. Ltd | dahua | 001 | 2018-10-19 | 283642 | ⁶⁹ 2048 ± 0 | ⁴⁰ 363 ± 6 | No | ⁷ 367 ± 10 | ⁹ 354 ± 16 | |
| 26 | Dahua Technology Co. Ltd | dahua | 002 | 2019-03-01 | 526452 | ⁵⁹ 2048 ± 0 | ⁷¹ 628 ± 7 | No | ¹⁴ 461 ± 23 | ¹⁶ 454 ± 20 | |
| 27 | Dermalog | dermalog | 005 | 2018-02-02 | 0 | ³ 128 ± 0 | ⁷ 130 ± 11 | No | ¹⁷ 499 ± 22 | ²⁰ 500 ± 22 | |
| 28 | Dermalog | dermalog | 006 | 2018-10-18 | 0 | ² 128 ± 0 | ⁵⁸ 532 ± 12 | No | ¹⁹ 506 ± 23 | ¹⁷ 459 ± 23 | |
| 29 | Digital Barriers | barriers | 002 | 2019-03-01 | 83002 | ⁸³ 2056 ± 0 | ¹⁵ 209 ± 11 | No | ⁹⁶ 13409 ± 228 | ⁹⁶ 13267 ± 206 | |
| 30 | Ever AI | everai | 001 | 2018-10-19 | 449149 | ⁵³ 2048 ± 0 | ⁸² 701 ± 1 | No | ⁹ 395 ± 11 | ¹² 404 ± 23 | |
| 31 | Ever AI | everai | 002 | 2019-03-01 | 561727 | ¹⁰³ 4096 ± 0 | ⁸⁸ 758 ± 0 | No | ²⁷ 644 ± 14 | ²⁸ 624 ± 35 | |
| 32 | Glory Ltd | glory | 000 | 2018-06-06 | 0 | ¹⁵ 418 ± 0 | ¹⁰ 165 ± 2 | No | ⁸⁹ 7003 ± 84 | ⁸⁸ 6978 ± 71 | |
| 33 | Glory Ltd | glory | 001 | 2018-06-08 | 0 | ⁴⁴ 1726 ± 0 | ⁴⁷ 393 ± 2 | No | ⁹³ 9607 ± 128 | ⁹³ 9539 ± 182 | |
| 34 | Gorilla Technology | gorilla | 001 | 2018-05-25 | 93768 | ⁹⁴ 2156 ± 0 | ⁹ 160 ± 14 | No | ⁸⁰ 3429 ± 145 | ⁸¹ 3288 ± 51 | |
| 35 | Gorilla Technology | gorilla | 002 | 2018-10-17 | 93869 | ³⁶ 1132 ± 0 | ³⁵ 322 ± 14 | No | ⁷⁵ 2715 ± 68 | ⁷⁶ 2585 ± 84 | |
| 36 | Hikvision | hik | 001 | 2019-03-01 | 667866 | ³⁹ 1408 ± 0 | ⁷⁴ 651 ± 0 | No | ¹⁶ 488 ± 19 | ¹⁸ 477 ± 22 | |
| 37 | Hengrui AI Technology Ltd | hr | 000 | 2019-03-01 | 284600 | ⁸⁹ 2057 ± 0 | ⁶⁸ 600 ± 2 | No | ⁹⁸ 16747 ± 238 | ⁹⁸ 16627 ± 220 | |
| 38 | ID3 Technology | id3 | 003 | 2018-10-05 | 265951 | ¹¹ 264 ± 0 | ³³ 316 ± 19 | No | ⁴⁹ 1330 ± 25 | ⁵⁵ 1354 ± 28 | |
| 39 | ID3 Technology | id3 | 004 | 2019-03-01 | 171526 | ¹² 264 ± 0 | ⁶² 541 ± 11 | No | ⁴² 1135 ± 23 | ⁴⁸ 1156 ± 32 | |
| 40 | Idemia | Idemia | 003 | 2018-10-19 | 427244 | ¹⁴ 352 ± 0 | ⁴¹ 368 ± 6 | No | ⁸⁸ 6654 ± 75 | ⁸⁵ 4835 ± 90 | |
| 41 | Idemia | Idemia | 004 | 2019-03-01 | 406924 | ¹³ 352 ± 0 | ³⁰ 306 ± 5 | No | ⁸⁶ 5592 ± 518 | ⁸⁷ 5533 ± 426 | |
| 42 | Institute of Information Technologies | ittvision | 000 | 2019-03-01 | 237317 | ³² 1024 ± 0 | ¹⁴ 197 ± 8 | No | ⁵³ 1537 ± 81 | ⁵² 1282 ± 20 | |
| 43 | Imperial College London | imperial | 000 | 2019-03-01 | 370120 | ⁶⁸ 2048 ± 0 | ⁷⁷ 669 ± 1 | No | ⁶⁸ 2130 ± 32 | ⁶⁵ 2052 ± 100 | |
| 44 | Imperial College London | imperial | 001 | 2019-03-01 | 370260 | ⁶⁵ 2048 ± 0 | ⁷⁹ 671 ± 0 | No | ⁶⁶ 2090 ± 28 | ⁶⁷ 2062 ± 74 | |

Notes

| | |
|---|---|
| 1 | The configuration size does not capture static data included in libraries. We do not count these because some algorithms include common ancillary libraries for image processing (e.g. openCV) or numerical computation (e.g. blas). |
| 2 | The median template creation times are measured on Intel®Xeon®CPU E5-2630 v4 @ 2.20GHz processors or, for GPU-enabled implementations, NVidia Tesla K40. |
| 3 | The comparison durations, in nanoseconds, are estimated using std::chrono::high_resolution_clock which on the machine in (2) counts 1ns clock ticks. Precision is somewhat worse than that however. The ± value is the median absolute deviation times 1.48 for Normal consistency. |

Table 1: Summary of algorithms and properties included in this report. The red superscripts give ranking for the quantity in that column.

| | Developer | Short | Seq. | Validation | Config ¹ | Template | | GPU | Comparison Time (ns) ³ | |
|----|--|---------------|------|------------|---------------------|--------------------------|------------------------|-----|-----------------------------------|------------------------------|
| | Name | Name | Num. | Date | Data (KB) | Size (B) | Time (ms) ² | | Genuine | Impostor |
| 45 | Incode Technologies Inc | incode | 002 | 2018-10-18 | 73239 | ⁵⁵ 2048 ± 0 | ²⁵ 281 ± 15 | No | ⁵⁴ 1544 ± 38 | ⁵⁶ 1488 ± 69 |
| 46 | Incode Technologies Inc | incode | 003 | 2019-03-01 | 170632 | ¹⁰² 4096 ± 0 | ⁴⁴ 384 ± 11 | No | ⁶² 1928 ± 44 | ⁶⁰ 1876 ± 81 |
| 47 | Innovatrics | innova | 004 | 2018-10-19 | 0 | ³⁴ 1076 ± 0 | ⁴⁶ 391 ± 0 | No | ⁹² 8573 ± 274 | ⁹¹ 7929 ± 244 |
| 48 | Innovatrics | innova | 005 | 2019-03-01 | 0 | ³⁵ 1076 ± 0 | ⁶⁵ 577 ± 1 | No | ⁹⁹ 16880 ± 194 | ⁹⁹ 17232 ± 385 |
| 49 | Intellivision | intellivision | 001 | 2017-10-10 | 43692 | ⁸⁶ 2056 ± 0 | ² 62 ± 2 | No | ⁷³ 2573 ± 91 | ⁷⁵ 2544 ± 38 |
| 50 | Is It You | isityou | 000 | 2017-06-26 | 48010 | ¹⁰⁹ 19200 ± 0 | ⁶ 113 ± 5 | No | ¹⁰⁹ 237517 ± 1318 | ¹⁰⁹ 237374 ± 1279 |
| 51 | Innovation Systems | isystems | 001 | 2018-06-12 | 274621 | ⁴⁸ 2048 ± 0 | ²⁶ 291 ± 9 | No | ²⁰ 557 ± 16 | ²² 564 ± 22 |
| 52 | Innovation Systems | isystems | 002 | 2018-10-18 | 358984 | ⁵⁴ 2048 ± 0 | ⁹⁸ 822 ± 8 | No | ³¹ 749 ± 31 | ²⁹ 632 ± 28 |
| 53 | ITMO University | itmo | 005 | 2018-10-19 | 482155 | ¹⁰⁸ 4173 ± 0 | ⁸⁹ 759 ± 1 | No | ⁹⁵ 13214 ± 164 | ⁹⁵ 12576 ± 257 |
| 54 | ITMO University | itmo | 006 | 2019-03-01 | 599187 | ⁹³ 2121 ± 0 | ⁹⁶ 814 ± 1 | No | ¹⁰³ 26154 ± 148 | ¹⁰³ 26217 ± 260 |
| 55 | Kakao Corp | kakao | 001 | 2019-03-01 | 107616 | ³⁰ 1024 ± 0 | ⁴³ 379 ± 1 | No | ³⁷ 930 ± 22 | ⁴¹ 948 ± 38 |
| 56 | Lookman Electroplast Industries | lookman | 002 | 2018-06-13 | 138200 | ²⁰ 548 ± 0 | ¹¹ 173 ± 1 | No | ²² 610 ± 19 | ²⁵ 612 ± 22 |
| 57 | Megvii/Face++ | megvii | 001 | 2018-06-15 | 1361523 | ⁶⁷ 2048 ± 0 | ⁶⁴ 543 ± 0 | No | ⁸⁵ 5228 ± 32 | ⁸⁶ 5252 ± 60 |
| 58 | Megvii/Face++ | megvii | 002 | 2018-10-19 | 1809564 | ¹⁰⁶ 4100 ± 0 | ⁷² 644 ± 0 | No | ¹⁰⁶ 50630 ± 183 | ¹⁰⁶ 47591 ± 716 |
| 59 | Xiamen Meiya Pico Information Co. Ltd | meiyea | 001 | 2019-03-01 | 280055 | ⁷¹ 2049 ± 0 | ⁶⁹ 622 ± 12 | No | ⁹¹ 8356 ± 615 | ⁹² 8134 ± 97 |
| 60 | MicroFocus | microfocus | 001 | 2018-06-13 | 104524 | ¹⁰ 256 ± 0 | ²² 264 ± 18 | No | ¹ 215 ± 8 | ¹ 217 ± 10 |
| 61 | MicroFocus | microfocus | 002 | 2018-10-17 | 96288 | ⁶ 256 ± 0 | ²¹ 259 ± 18 | No | ⁵ 337 ± 34 | ² 230 ± 25 |
| 62 | Neurotechnology | neurotech | 004 | 2018-10-19 | 293384 | ⁹ 256 ± 0 | ⁵⁰ 401 ± 0 | No | ² 219 ± 8 | ³ 231 ± 13 |
| 63 | Neurotechnology | neurotech | 005 | 2019-03-01 | 270450 | ⁸ 256 ± 0 | ⁴⁹ 399 ± 0 | No | ³ 238 ± 10 | ⁴ 237 ± 7 |
| 64 | Nodeflux | nodeflux | 000 | 2019-03-01 | 347079 | ⁵¹ 2048 ± 0 | ⁶³ 542 ± 1 | No | ⁷⁸ 3283 ± 51 | ⁸⁰ 3285 ± 56 |
| 65 | Nodeflux | nodeflux | 001 | 2019-03-01 | 262553 | ⁵⁰ 2048 ± 0 | ¹⁸ 247 ± 1 | No | ⁷⁷ 3242 ± 81 | ⁷⁹ 3255 ± 93 |
| 66 | N-Tech Lab | ntech | 005 | 2018-10-19 | 1726214 | ⁴⁶ 1940 ± 0 | ⁸³ 712 ± 1 | No | ³⁶ 882 ± 42 | ³⁹ 880 ± 29 |
| 67 | N-Tech Lab | ntech | 006 | 2019-03-01 | 7901590 | ⁹⁵ 2600 ± 0 | ⁸⁶ 749 ± 1 | No | ³⁹ 1055 ± 93 | ³⁸ 844 ± 48 |
| 68 | Panasonic R+D Center Singapore | psl | 001 | 2018-10-12 | 382035 | ⁸⁷ 2056 ± 0 | ⁹³ 785 ± 16 | No | ⁴ 298 ± 13 | ⁵ 292 ± 14 |
| 69 | Panasonic R+D Center Singapore | psl | 002 | 2019-02-28 | 804934 | ⁷⁸ 2052 ± 0 | ¹⁰⁵ 888 ± 9 | No | ⁵⁵ 1590 ± 48 | ⁴⁵ 1133 ± 78 |
| 70 | Rank One Computing | rankone | 005 | 2018-10-09 | 0 | ⁴ 133 ± 0 | ³ 71 ± 2 | No | ¹⁰ 403 ± 10 | ⁷ 337 ± 19 |
| 71 | Rank One Computing | rankone | 006 | 2019-02-27 | 0 | ⁵ 165 ± 0 | ¹⁶ 210 ± 1 | No | ¹³ 443 ± 26 | ¹¹ 395 ± 22 |
| 72 | Realnetworks Inc | realnetworks | 001 | 2018-10-19 | 99044 | ¹⁰⁵ 4100 ± 0 | ⁸ 144 ± 2 | No | ⁷¹ 2500 ± 47 | ⁷³ 2420 ± 34 |
| 73 | Realnetworks Inc | realnetworks | 002 | 2019-02-28 | 95328 | ⁴⁵ 1848 ± 0 | ²⁰ 250 ± 2 | No | ⁴⁸ 1285 ± 17 | ⁵⁰ 1247 ± 42 |
| 74 | KanKan Ai | remarkai | 000 | 2019-03-01 | 240152 | ⁴⁹ 2048 ± 0 | ⁹⁹ 829 ± 7 | No | ³⁴ 873 ± 4 | ³⁷ 835 ± 35 |
| 75 | KanKan Ai | remarkai | 001 | 2019-03-01 | 241857 | ⁸² 2052 ± 0 | ¹⁰⁰ 831 ± 6 | No | ⁴⁴ 1229 ± 20 | ³⁶ 805 ± 56 |
| 76 | Saffe Ltd | saffe | 001 | 2018-10-19 | 85973 | ³⁸ 1280 ± 0 | ²⁴ 281 ± 1 | No | ⁴⁶ 1274 ± 19 | ⁵¹ 1277 ± 26 |
| 77 | Saffe Ltd | saffe | 002 | 2019-03-01 | 260622 | ⁶⁰ 2048 ± 0 | ⁹⁷ 817 ± 11 | No | ³⁰ 717 ± 7 | ³² 714 ± 29 |
| 78 | Sensetime Group Ltd | sensetime | 002 | 2018-10-19 | 531783 | ⁷⁴ 2052 ± 0 | ⁸⁴ 725 ± 3 | No | ⁷² 2546 ± 102 | ⁷¹ 2371 ± 45 |
| 79 | Sensetime Group Ltd | sensetime | 002 | 2018-10-19 | 531783 | ⁷⁵ 2052 ± 0 | ⁹⁴ 797 ± 3 | No | ⁷⁴ 2713 ± 90 | ⁷⁰ 2301 ± 25 |
| 80 | Shaman Software | shaman | 000 | 2017-12-05 | 0 | ⁹⁹ 4096 ± 0 | ⁷⁵ 653 ± 16 | No | ⁸ 380 ± 25 | ¹⁰ 379 ± 31 |
| 81 | Shaman Software | shaman | 001 | 2018-01-13 | 0 | ⁹⁸ 4096 ± 0 | ²⁷ 294 ± 2 | No | ²⁶ 635 ± 19 | ¹⁵ 441 ± 25 |
| 82 | Shenzhen Inst. Adv. Integrated Tech. CAS | SIAT | 002 | 2018-06-13 | 486842 | ⁷⁹ 2052 ± 0 | ⁶⁶ 579 ± 0 | No | ³² 769 ± 13 | ³⁴ 750 ± 13 |
| 83 | Shenzhen Inst. Adv. Integrated Tech. CAS | SIAT | 004 | 2019-03-01 | 940063 | ¹⁰⁷ 4100 ± 0 | ⁷⁸ 670 ± 0 | No | ⁸³ 4013 ± 45 | ⁸³ 3782 ± 173 |
| 84 | Smilart | smilart | 002 | 2018-02-06 | 111826 | ²⁹ 1024 ± 0 | ¹² 176 ± 16 | No | ¹⁰¹ 18784 ± 136 | ¹⁰¹ 18795 ± 151 |
| 85 | Smilart | smilart | 003 | 2018-06-18 | 67339 | ¹⁰ 512 ± 0 | ¹³ 180 ± 12 | No | ⁵¹ 1395 ± 74 | ⁴² 1027 ± 66 |
| 86 | Synesis | synesis | 003 | 2018-10-19 | 256748 | ¹⁰⁰ 4096 ± 0 | ⁴ 90 ± 0 | No | ⁹⁰ 7118 ± 121 | ⁹⁰ 7162 ± 100 |
| 87 | Synesis | synesis | 004 | 2019-03-01 | 270628 | ⁶⁶ 2048 ± 0 | ⁸⁵ 735 ± 15 | No | ¹¹ 424 ± 14 | ¹³ 430 ± 22 |
| 88 | Tech5 SA | tech5 | 001 | 2018-10-19 | 636346 | ¹⁰⁴ 4096 ± 0 | ⁵⁷ 522 ± 5 | No | ⁴¹ 1087 ± 34 | ³⁵ 799 ± 44 |

| Notes | |
|-------|---|
| 1 | The configuration size does not capture static data included in libraries. We do not count these because some algorithms include common ancilliary libraries for image processing (e.g. openCV) or numerical computation (e.g. blas). |
| 2 | The median template creation times are measured on Intel®Xeon®CPU E5-2630 v4 @ 2.20GHz processors or, for GPU-enabled implementations, NVidia Tesla K40. |
| 3 | The comparison durations, in nanoseconds, are estimated using std::chrono::high_resolution_clock which on the machine in (2) counts 1ns clock ticks. Precision is somewhat worse than that however. The ± value is the median absolute deviation times 1.48 for Normal consistency. |

Table 2: Summary of algorithms and properties included in this report. The red superscripts give ranking for the quantity in that column.

| | Developer | Short | Seq. | Validation | Config ¹ | Template | | GPU | Comparison Time (ns) ³ | |
|-----|---|------------|------|------------|---------------------|--------------------------|-------------------------|-----|-----------------------------------|------------------------------|
| | Name | Name | Num. | Date | Data (KB) | Size (B) | Time (ms) ² | | Genuine | Impostor |
| 89 | Tech5 SA | tech5 | 002 | 2019-03-01 | 1150887 | ³⁷ 1280 ± 0 | ⁹¹ 780 ± 10 | No | ⁵² 1406 ± 120 | ⁴³ 1048 ± 57 |
| 90 | Tevian | tevia | 003 | 2018-10-19 | 791725 | ⁷⁰ 2049 ± 0 | ⁵¹ 404 ± 15 | No | ⁶ 350 ± 11 | ⁸ 338 ± 25 |
| 91 | Tevian | tevia | 004 | 2019-03-01 | 863474 | ⁶² 2048 ± 0 | ⁵⁶ 506 ± 30 | No | ¹⁵ 474 ± 31 | ⁶ 326 ± 20 |
| 92 | TigerIT Americas LLC | tiger | 002 | 2018-06-13 | 341638 | ⁸⁴ 2056 ± 0 | ⁴⁸ 393 ± 20 | No | ⁶⁹ 2135 ± 29 | ⁶⁹ 2137 ± 38 |
| 93 | TigerIT Americas LLC | tiger | 003 | 2018-10-16 | 426164 | ⁸⁵ 2056 ± 0 | ⁵⁵ 458 ± 21 | No | ⁶⁴ 2031 ± 35 | ⁶⁴ 2029 ± 38 |
| 94 | Toshiba | toshiba | 002 | 2018-10-19 | 813606 | ⁴² 1560 ± 0 | ⁶¹ 541 ± 0 | No | ⁸¹ 3521 ± 369 | ⁷⁴ 2449 ± 124 |
| 95 | Toshiba | toshiba | 003 | 2019-03-01 | 984125 | ⁴³ 1560 ± 0 | ⁶⁰ 540 ± 0 | No | ⁷⁰ 2390 ± 41 | ⁷² 2407 ± 81 |
| 96 | VCognition | vcog | 002 | 2017-06-12 | 3229434 | ¹¹⁰ 61504 ± 5 | ³⁹ 357 ± 25 | No | ¹¹⁰ 296154 ± 3077 | ¹¹⁰ 296436 ± 4183 |
| 97 | Visidon | visidon | 001 | 2019-02-26 | 170262 | ⁷⁷ 2052 ± 0 | ³⁴ 316 ± 6 | No | ⁴⁵ 1258 ± 38 | ⁴⁶ 1148 ± 109 |
| 98 | Veridas Digital Authentication Solutions S.L. | veridas | 001 | 2019-03-01 | 196540 | ⁶⁴ 2048 ± 0 | ⁸⁰ 671 ± 21 | No | ⁸⁷ 5748 ± 20 | ⁸⁹ 7111 ± 148 |
| 99 | Veridas Digital Authentication Solutions S.L. | veridas | 000 | 2019-03-01 | 193466 | ¹⁹ 512 ± 0 | ⁷⁶ 669 ± 20 | No | ⁵⁷ 1733 ± 81 | ⁶² 1934 ± 44 |
| 100 | Vigilant Solutions | vigilant | 005 | 2018-10-11 | 343048 | ⁴⁰ 1548 ± 0 | ¹⁰¹ 837 ± 13 | No | ³⁵ 874 ± 22 | ³⁰ 637 ± 16 |
| 101 | Vigilant Solutions | vigilant | 006 | 2019-03-01 | 343048 | ⁴¹ 1548 ± 0 | ¹⁰² 841 ± 8 | No | ³⁸ 939 ± 32 | ³¹ 711 ± 37 |
| 102 | Beijing Vion Technology Inc | vion | 000 | 2018-10-19 | 228219 | ⁸⁰ 2052 ± 0 | ³⁶ 333 ± 1 | No | ¹⁰⁵ 39839 ± 3561 | ¹⁰⁴ 26830 ± 2241 |
| 103 | Vision-Box | visionbox | 000 | 2019-02-26 | 176501 | ⁶³ 2048 ± 0 | ²⁹ 304 ± 7 | No | ⁵⁶ 1648 ± 57 | ⁴⁹ 1192 ± 42 |
| 104 | Vision-Box | visionbox | 001 | 2019-03-01 | 256869 | ⁵⁶ 2048 ± 0 | ¹¹⁰ 983 ± 7 | No | ⁴³ 1161 ± 22 | ⁴⁷ 1154 ± 20 |
| 105 | VisionLabs | visionlabs | 005 | 2018-10-19 | 369602 | ¹⁷ 512 ± 0 | ³¹ 313 ± 0 | No | ³³ 848 ± 26 | ⁴⁰ 889 ± 37 |
| 106 | VisionLabs | visionlabs | 006 | 2019-03-01 | 353044 | ¹⁸ 512 ± 0 | ²³ 270 ± 0 | No | ²⁹ 698 ± 19 | ³³ 734 ± 28 |
| 107 | Vocord | vocord | 005 | 2018-10-19 | 1060445 | ²¹ 768 ± 0 | ⁹⁰ 771 ± 1 | No | ⁵⁸ 1768 ± 48 | ⁵⁷ 1713 ± 77 |
| 108 | Vocord | vocord | 006 | 2019-03-01 | 559457 | ²² 768 ± 0 | ¹⁰⁴ 886 ± 1 | No | ⁶³ 2020 ± 72 | ⁶³ 1969 ± 62 |
| 109 | Zhuhai Yisheng Electronics Technology | yisheng | 004 | 2018-06-12 | 486351 | ⁹⁷ 3704 ± 0 | ⁴² 378 ± 12 | No | ²⁸ 693 ± 137 | ²¹ 526 ± 34 |
| 110 | Shanghai Yitu Technology | yitu | 003 | 2019-03-01 | 1525719 | ⁹¹ 2082 ± 0 | ¹⁰³ 860 ± 0 | No | ¹⁰⁰ 18305 ± 71 | ¹⁰⁰ 18286 ± 62 |

| Notes | |
|-------|---|
| 1 | The configuration size does not capture static data included in libraries. We do not count these because some algorithms include common ancillary libraries for image processing (e.g. openCV) or numerical computation (e.g. blas). |
| 2 | The median template creation times are measured on Intel®Xeon®CPU E5-2630 v4 @ 2.20GHz processors or, for GPU-enabled implementations, NVidia Tesla K40. |
| 3 | The comparison durations, in nanoseconds, are estimated using std::chrono::high_resolution_clock which on the machine in (2) counts 1ns clock ticks. Precision is somewhat worse than that however. The ± value is the median absolute deviation times 1.48 for Normal consistency. |

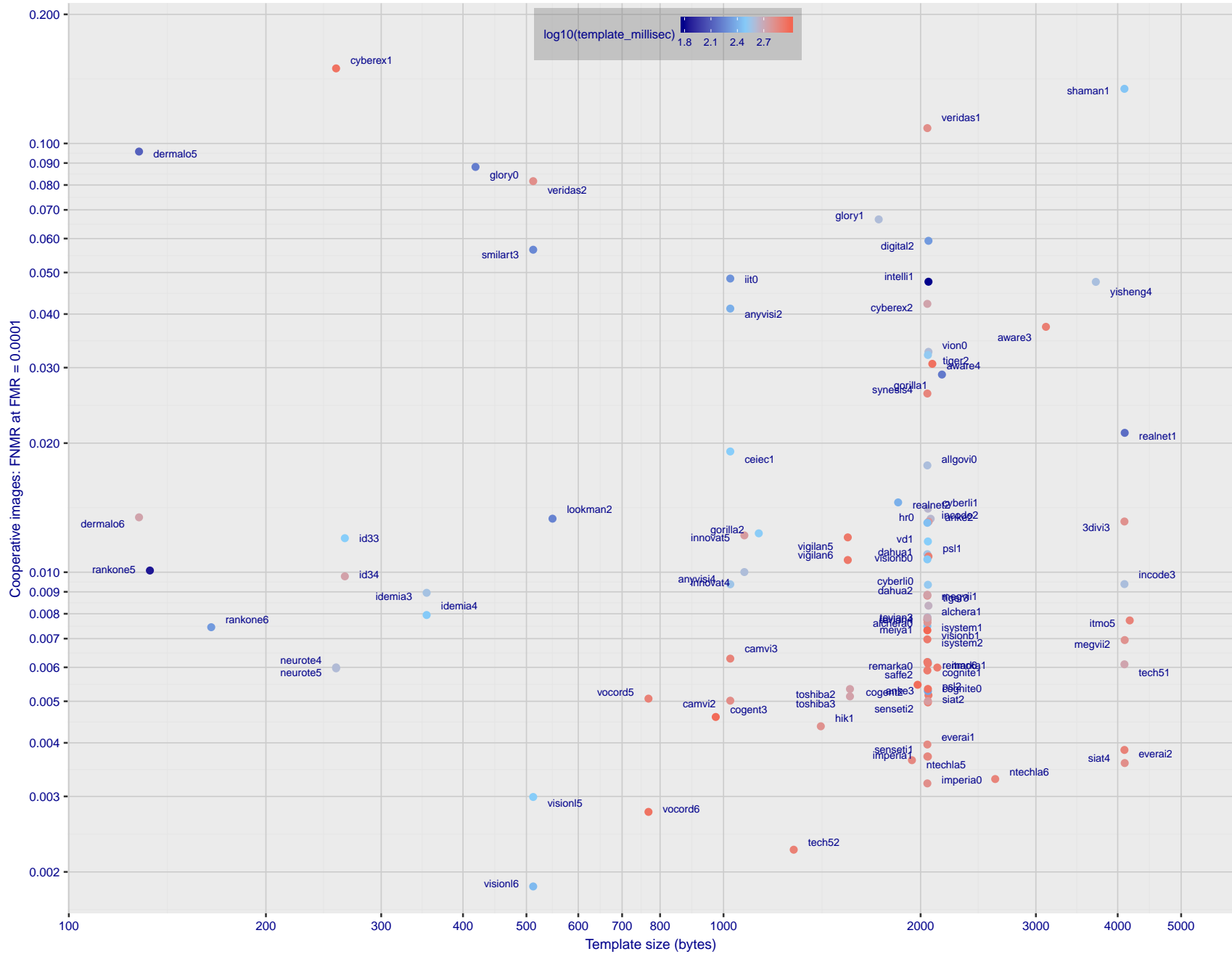
Table 3: Summary of algorithms and properties included in this report. The red superscripts give ranking for the quantity in that column.

| | Algorithm | FALSE NON-MATCH RATE (FNMR) | | | | | | | | | | | |
|-----|---------------------|-----------------------------|-----|--------|-----|--------|-----|-----------------------------|-----|--------|-----|-----------|----|
| | | CONSTRAINED, COOPERATIVE | | | | | | LESS CONSTRAINED, NON-COOP. | | | | | |
| | | VISAMC | | VISA | | VISA | | MUGSHOT | | WILD | | CHILD EXP | |
| FMR | 0.0001 | 1E-06 | | 0.0001 | | 1E-05 | | 0.0001 | | 0.01 | | | |
| 1 | 3divi-003 | 0.0318 | 69 | 0.0588 | 70 | 0.0097 | 60 | 0.0389 | 68 | 0.0867 | 71 | 0.536 | 15 |
| 2 | alchera-000 | 0.0165 | 43 | 0.0243 | 33 | 0.0086 | 55 | 0.0125 | 32 | 0.0370 | 29 | - | - |
| 3 | alchera-001 | 0.0183 | 47 | 0.0299 | 46 | 0.0078 | 50 | 0.0142 | 38 | 0.0372 | 30 | - | - |
| 4 | allgovision-000 | 0.0346 | 71 | 0.0527 | 66 | 0.0210 | 78 | 0.0232 | 58 | 0.0607 | 63 | - | - |
| 5 | amplifiedgroup-001 | 0.5034 | 102 | 0.5848 | 102 | 0.2999 | 103 | 0.6973 | 100 | 0.4250 | 93 | - | - |
| 6 | anke-002 | 0.0402 | 73 | 0.0759 | 76 | 0.0136 | 70 | 0.0271 | 61 | 0.0664 | 65 | 0.440 | 5 |
| 7 | anke-003 | 0.0131 | 31 | 0.0213 | 28 | 0.0056 | 35 | 0.0094 | 13 | 0.0302 | 14 | - | - |
| 8 | anyvision-002 | 0.0660 | 79 | 0.0898 | 78 | 0.0387 | 84 | 0.0928 | 83 | 0.2227 | 85 | 0.696 | 31 |
| 9 | anyvision-004 | 0.0267 | 62 | 0.0385 | 57 | 0.0081 | 51 | 0.0258 | 60 | 0.0470 | 45 | 0.463 | 7 |
| 10 | aware-003 | 0.0793 | 81 | 0.1161 | 82 | 0.0288 | 82 | 0.1028 | 84 | 0.3180 | 90 | 0.851 | 46 |
| 11 | aware-004 | 0.0690 | 80 | 0.0949 | 80 | 0.0257 | 80 | 0.0837 | 80 | 0.0516 | 54 | - | - |
| 12 | ayonix-000 | 0.4351 | 99 | 0.4872 | 97 | 0.2299 | 100 | 0.6150 | 98 | 0.3635 | 91 | 0.843 | 45 |
| 13 | bm-001 | 0.7431 | 105 | 0.9494 | 107 | 0.6188 | 106 | 0.9586 | 104 | 0.9935 | 98 | 0.884 | 49 |
| 14 | camvi-002 | 0.0125 | 26 | 0.0221 | 31 | 0.0049 | 29 | 0.0089 | 11 | 0.0288 | 9 | 0.576 | 18 |
| 15 | camvi-003 | 0.0184 | 48 | 0.0320 | 50 | 0.0062 | 38 | 0.0134 | 36 | 0.0300 | 12 | - | - |
| 16 | ceiec-001 | 0.0328 | 70 | 0.0475 | 64 | 0.0163 | 73 | 0.0295 | 64 | 0.0847 | 68 | - | - |
| 17 | cogent-002 | 0.0148 | 38 | 0.0321 | 51 | 0.0044 | 22 | 0.0095 | 14 | 0.0562 | 59 | 0.634 | 26 |
| 18 | cogent-003 | 0.0091 | 13 | 0.0188 | 25 | 0.0032 | 12 | 0.0098 | 17 | 0.0406 | 33 | - | - |
| 19 | cognitec-000 | 0.0116 | 21 | 0.0177 | 21 | 0.0036 | 15 | 0.0118 | 29 | 0.0953 | 75 | 0.837 | 43 |
| 20 | cognitec-001 | 0.0126 | 27 | 0.0185 | 24 | 0.0047 | 26 | 0.0120 | 31 | 0.0598 | 62 | - | - |
| 21 | cyberextruder-001 | 0.1972 | 91 | 0.2547 | 89 | 0.0755 | 93 | 0.4686 | 96 | 0.1747 | 82 | 0.780 | 39 |
| 22 | cyberextruder-002 | 0.0811 | 82 | 0.1336 | 84 | 0.0265 | 81 | 0.1465 | 89 | 0.1000 | 76 | 0.610 | 22 |
| 23 | cyberlink-000 | 0.0181 | 45 | 0.0274 | 41 | 0.0106 | 65 | 0.0125 | 33 | 0.1864 | 83 | - | - |
| 24 | cyberlink-001 | 0.0131 | 30 | 0.0210 | 27 | 0.0050 | 30 | 0.0439 | 73 | 0.0318 | 21 | - | - |
| 25 | dahua-001 | 0.0250 | 58 | 0.0466 | 63 | 0.0108 | 66 | 0.0228 | 56 | 0.0457 | 42 | 0.504 | 12 |
| 26 | dahua-002 | 0.0129 | 28 | 0.0157 | 18 | 0.0090 | 57 | 0.0116 | 28 | 0.0323 | 23 | - | - |
| 27 | dermalog-005 | 0.1526 | 88 | 0.1823 | 85 | 0.0658 | 91 | 0.2580 | 93 | 0.0855 | 70 | 0.684 | 29 |
| 28 | dermalog-006 | 0.0253 | 59 | 0.0369 | 56 | 0.0172 | 76 | 0.0171 | 46 | 0.0623 | 64 | 0.585 | 20 |
| 29 | digitalbarriers-002 | 0.3360 | 96 | 0.3690 | 94 | 0.0968 | 95 | 0.0877 | 81 | 0.0436 | 37 | - | - |
| 30 | everai-001 | 0.0085 | 10 | 0.0156 | 16 | 0.0038 | 19 | 0.0072 | 6 | 0.0287 | 8 | - | - |
| 31 | everai-002 | 0.0104 | 18 | 0.0159 | 19 | 0.0041 | 21 | 0.0063 | 3 | 0.0294 | 10 | - | - |
| 32 | glory-000 | 0.1094 | 84 | 0.1286 | 83 | 0.0514 | 88 | 0.2179 | 91 | 0.4762 | 95 | 0.894 | 50 |
| 33 | glory-001 | 0.0902 | 83 | 0.1082 | 81 | 0.0410 | 85 | 0.1642 | 90 | 0.4261 | 94 | 0.883 | 48 |
| 34 | gorilla-001 | 0.0488 | 76 | 0.0756 | 73 | 0.0155 | 72 | 0.1218 | 88 | 0.0564 | 60 | 0.835 | 42 |
| 35 | gorilla-002 | 0.0256 | 60 | 0.0413 | 58 | 0.0076 | 49 | 0.0478 | 76 | 0.0507 | 52 | 0.616 | 23 |
| 36 | hik-001 | 0.0096 | 17 | 0.0125 | 10 | 0.0036 | 17 | 0.0093 | 12 | 0.0271 | 1 | - | - |
| 37 | hr-000 | 0.0265 | 61 | 0.0434 | 59 | 0.0112 | 68 | 0.0340 | 66 | 0.1902 | 84 | - | - |
| 38 | id3-003 | 0.0361 | 72 | 0.0757 | 75 | 0.0104 | 64 | 0.0292 | 63 | 0.0848 | 69 | 0.586 | 21 |
| 39 | id3-004 | 0.0198 | 50 | 0.0344 | 52 | 0.0084 | 53 | 0.0238 | 59 | - | - | - | - |
| 40 | idemia-003 | 0.0222 | 52 | 0.0316 | 49 | 0.0082 | 52 | 0.0188 | 48 | 0.0578 | 61 | 0.617 | 24 |
| 41 | idemia-004 | 0.0160 | 42 | 0.0244 | 35 | 0.0065 | 39 | 0.0199 | 51 | 0.0309 | 18 | - | - |
| 42 | iit-000 | 0.1516 | 87 | 0.1981 | 86 | 0.0620 | 90 | 0.0828 | 79 | - | - | - | - |
| 43 | imperial-000 | 0.0067 | 6 | 0.0108 | 8 | 0.0022 | 6 | 0.0080 | 7 | 0.0281 | 4 | - | - |
| 44 | imperial-001 | 0.0094 | 16 | 0.0154 | 14 | 0.0033 | 13 | 0.0072 | 5 | 0.0276 | 3 | - | - |
| 45 | incode-002 | 0.0293 | 64 | 0.0548 | 69 | 0.0096 | 59 | 0.0436 | 72 | 0.0498 | 49 | 0.583 | 19 |
| 46 | incode-003 | 0.0142 | 34 | 0.0249 | 37 | 0.0054 | 33 | 0.0448 | 74 | 0.0318 | 20 | - | - |
| 47 | innovatrics-004 | 0.0194 | 49 | 0.0292 | 43 | 0.0068 | 45 | 0.0344 | 67 | 0.0454 | 40 | 0.465 | 8 |
| 48 | innovatrics-005 | 0.0230 | 54 | 0.0353 | 54 | 0.0085 | 54 | 0.0398 | 70 | 0.0301 | 13 | - | - |
| 49 | intellivision-001 | 0.1335 | 86 | 0.2205 | 87 | 0.0417 | 86 | 0.1090 | 86 | 0.2445 | 86 | 0.777 | 38 |
| 50 | isityou-000 | 0.5682 | 103 | 0.7033 | 103 | 0.4145 | 104 | 1.0000 | 106 | 1.0000 | 102 | 1.000 | 58 |
| 51 | isystems-001 | 0.0149 | 39 | 0.0245 | 36 | 0.0067 | 44 | 0.0138 | 37 | 0.0524 | 57 | 0.515 | 13 |
| 52 | isystems-002 | 0.0118 | 22 | 0.0182 | 23 | 0.0066 | 40 | 0.0111 | 24 | 0.0516 | 55 | 0.488 | 10 |
| 53 | itmo-005 | 0.0182 | 46 | 0.0345 | 53 | 0.0067 | 43 | 0.0181 | 47 | 0.0433 | 36 | 0.481 | 9 |
| 54 | itmo-006 | 0.0125 | 24 | 0.0220 | 30 | 0.0046 | 24 | 0.0149 | 40 | 0.0329 | 25 | - | - |
| 55 | kakao-001 | 0.4553 | 101 | 0.5532 | 101 | 0.2034 | 99 | 0.6580 | 99 | 1.0000 | 109 | - | - |
| 56 | lookman-002 | 0.0297 | 65 | 0.0547 | 68 | 0.0102 | 63 | 0.0339 | 65 | 0.2640 | 89 | - | - |
| 57 | megvii-001 | 0.0157 | 40 | 0.0244 | 34 | 0.0045 | 23 | 0.0392 | 69 | 0.0916 | 73 | 0.442 | 6 |
| 58 | megvii-002 | 0.0104 | 19 | 0.0145 | 13 | 0.0036 | 16 | 0.0225 | 54 | 0.0692 | 66 | 0.301 | 1 |

Table 4: FNMR is the proportion of mated comparisons below a threshold set to achieve the FMR given in the header on the fourth row. FMR is the proportion of impostor comparisons at or above that threshold. The light grey values give rank over all algorithms in that column. The green column applies to “matched-covariates” i.e. impostors of the same sex, age group, and country of birth. The pink column uses only same-sex impostors; All others are zero effort. The pink column includes effects of extended ageing, and is the most important. Missing entries for visa, mugshot and wild images generally mean the algorithm did not run to completion. For child exploitation, missing entries arise because NIST executes those runs only infrequently.

| | | FALSE NON-MATCH RATE (FNMR) | | | | | | | | | | | |
|-----------|-----------------------|-----------------------------|-----|--------|-----|--------|-----------------------------|---------|-----|--------|-----|-----------|----|
| Algorithm | | CONSTRAINED, COOPERATIVE | | | | | LESS CONSTRAINED, NON-COOP. | | | | | | |
| Name | | VISAMC | | VISA | | VISA | | MUGSHOT | | WILD | | CHILD EXP | |
| FMR | | 0.0001 | | 1E-06 | | 0.0001 | | 1E-05 | | 0.0001 | | 0.01 | |
| 59 | meiya-001 | 0.0171 | 44 | 0.0275 | 42 | 0.0066 | 41 | 0.0159 | 43 | 0.0363 | 28 | - | - |
| 60 | microfocus-001 | 0.4482 | 100 | 0.5524 | 100 | 0.2309 | 101 | 0.7256 | 101 | 0.2567 | 88 | 0.689 | 30 |
| 61 | microfocus-002 | 0.3605 | 97 | 0.5057 | 98 | 0.1566 | 98 | 0.5783 | 97 | 0.1582 | 81 | 0.652 | 27 |
| 62 | neurotechnology-004 | 0.0146 | 36 | 0.0297 | 44 | 0.0051 | 32 | 0.0107 | 20 | 0.0467 | 44 | 0.654 | 28 |
| 63 | neurotechnology-005 | 0.0141 | 33 | 0.0300 | 47 | 0.0051 | 31 | 0.0108 | 22 | 0.0332 | 26 | - | - |
| 64 | nodeflux-000 | 1.0000 | 109 | 1.0000 | 109 | 1.0000 | 109 | 1.0000 | 107 | 1.0000 | 104 | - | - |
| 65 | nodeflux-001 | 1.0000 | 110 | 1.0000 | 110 | 1.0000 | 110 | 1.0000 | 108 | 1.0000 | 105 | - | - |
| 66 | ntechlab-005 | 0.0093 | 15 | 0.0145 | 12 | 0.0024 | 7 | 0.0131 | 35 | 0.0466 | 43 | 0.333 | 2 |
| 67 | ntechlab-006 | 0.0078 | 9 | 0.0111 | 9 | 0.0021 | 5 | 0.0112 | 26 | 0.0275 | 2 | - | - |
| 68 | psl-001 | 0.0549 | 77 | 0.0927 | 79 | 0.0198 | 77 | 0.0096 | 15 | 0.0431 | 35 | 0.624 | 25 |
| 69 | psl-002 | 0.0107 | 20 | 0.0180 | 22 | 0.0048 | 28 | 0.0089 | 10 | 0.0295 | 11 | - | - |
| 70 | rankone-005 | 0.0405 | 74 | 0.0757 | 74 | 0.0100 | 62 | 0.0170 | 45 | 0.0786 | 67 | 0.716 | 36 |
| 71 | rankone-006 | 0.0242 | 55 | 0.0460 | 62 | 0.0070 | 47 | 0.0119 | 30 | 0.0538 | 58 | - | - |
| 72 | realnetworks-001 | 0.0315 | 68 | 0.0455 | 61 | 0.0116 | 69 | 0.0920 | 82 | 0.0500 | 50 | 0.545 | 16 |
| 73 | realnetworks-002 | 0.0248 | 57 | 0.0358 | 55 | 0.0099 | 61 | 0.0513 | 77 | 0.0334 | 27 | - | - |
| 74 | remarkai-000 | 0.0147 | 37 | 0.0257 | 39 | 0.0062 | 37 | 0.0102 | 18 | 0.0304 | 15 | - | - |
| 75 | remarkai-001 | 0.0144 | 35 | 0.0256 | 38 | 0.0061 | 36 | 0.0102 | 19 | 0.0308 | 17 | - | - |
| 76 | saife-001 | 0.4339 | 98 | 0.5261 | 99 | 0.2340 | 102 | 0.7539 | 102 | 0.3887 | 92 | 0.897 | 51 |
| 77 | saife-002 | 0.0119 | 23 | 0.0206 | 26 | 0.0054 | 34 | 0.0107 | 21 | 0.0308 | 16 | - | - |
| 78 | sensetime-001 | 0.0063 | 5 | 0.0092 | 4 | 0.0030 | 11 | 0.0130 | 34 | 1.0000 | 101 | 0.700 | 32 |
| 79 | sensetime-002 | 0.0068 | 8 | 0.0098 | 5 | 0.0035 | 14 | 0.0143 | 39 | 0.9999 | 99 | 0.531 | 14 |
| 80 | shaman-000 | 0.9297 | 108 | 0.9774 | 108 | 0.9128 | 108 | 0.9990 | 105 | 0.9575 | 97 | 0.962 | 54 |
| 81 | shaman-001 | 0.3346 | 95 | 0.4616 | 95 | 0.1360 | 97 | 0.2368 | 92 | 0.1498 | 80 | 0.899 | 52 |
| 82 | siat-002 | 0.0091 | 14 | 0.0126 | 11 | 0.0039 | 20 | 0.0109 | 23 | 0.0520 | 56 | 0.428 | 4 |
| 83 | siat-004 | 0.0067 | 7 | 0.0099 | 6 | 0.0028 | 9 | 0.0152 | 42 | 1.0000 | 100 | - | - |
| 84 | smilart-002 | 0.2440 | 94 | 0.3532 | 93 | 0.0821 | 94 | - | - | - | - | 0.700 | 33 |
| 85 | smilart-003 | 0.6944 | 104 | 0.8836 | 104 | 0.1088 | 96 | 0.0695 | 78 | 0.1190 | 77 | - | - |
| 86 | synesis-003 | 0.8375 | 107 | 0.8857 | 105 | 0.7320 | 107 | 0.8548 | 103 | 0.6504 | 96 | 0.797 | 41 |
| 87 | synesis-004 | 0.0310 | 66 | 0.0480 | 65 | 0.0166 | 75 | 0.0476 | 75 | 0.1319 | 78 | - | - |
| 88 | tech5-001 | 0.0130 | 29 | 0.0176 | 20 | 0.0037 | 18 | 0.0218 | 53 | 0.0938 | 74 | 0.838 | 44 |
| 89 | tech5-002 | 0.0046 | 3 | 0.0063 | 2 | 0.0009 | 2 | 0.0113 | 27 | 0.0310 | 19 | - | - |
| 90 | tevian-003 | 0.0217 | 51 | 0.0298 | 45 | 0.0067 | 42 | 0.0230 | 57 | 0.0456 | 41 | 0.504 | 11 |
| 91 | tevian-004 | 0.0228 | 53 | 0.0304 | 48 | 0.0069 | 46 | 0.0226 | 55 | 0.0394 | 32 | - | - |
| 92 | tiger-002 | 0.0658 | 78 | 0.0889 | 77 | 0.0227 | 79 | 0.1083 | 85 | 0.0512 | 53 | 0.786 | 40 |
| 93 | tiger-003 | 0.0313 | 67 | 0.0602 | 72 | 0.0087 | 56 | 0.0188 | 49 | 0.0482 | 47 | 0.561 | 17 |
| 94 | toshiba-002 | 0.0134 | 32 | 0.0222 | 32 | 0.0048 | 27 | 0.0097 | 16 | - | - | 0.710 | 34 |
| 95 | toshiba-003 | 0.0125 | 25 | 0.0214 | 29 | 0.0047 | 25 | 0.0085 | 9 | 0.0282 | 5 | - | - |
| 96 | vcog-002 | 0.7522 | 106 | 0.9033 | 106 | 0.5040 | 105 | - | - | - | - | 0.752 | 37 |
| 97 | vd-001 | 0.0243 | 56 | 0.0452 | 60 | 0.0093 | 58 | 0.0271 | 62 | 0.1389 | 79 | - | - |
| 98 | veridas-001 | 0.1998 | 93 | 0.2724 | 90 | 0.0742 | 92 | 0.2987 | 95 | 0.0501 | 51 | - | - |
| 99 | veridas-002 | 0.1733 | 90 | 0.2257 | 88 | 0.0528 | 89 | 0.2617 | 94 | 0.0450 | 39 | - | - |
| 100 | vigilantsolutions-005 | 0.1613 | 89 | 0.4702 | 96 | 0.0166 | 74 | 0.0163 | 44 | 0.0497 | 48 | 0.979 | 55 |
| 101 | vigilantsolutions-006 | 0.1264 | 85 | 0.3221 | 91 | 0.0136 | 71 | 0.0150 | 41 | 0.0321 | 22 | - | - |
| 102 | vion-000 | 0.0419 | 75 | 0.0590 | 71 | 0.0288 | 83 | 0.0422 | 71 | 0.2479 | 87 | 0.876 | 47 |
| 103 | visionbox-000 | 0.0293 | 63 | 0.0541 | 67 | 0.0110 | 67 | 0.0197 | 50 | 0.0476 | 46 | - | - |
| 104 | visionbox-001 | 0.0159 | 41 | 0.0270 | 40 | 0.0072 | 48 | 0.0111 | 25 | 0.0389 | 31 | - | - |
| 105 | visionlabs-005 | 0.0088 | 11 | 0.0156 | 17 | 0.0029 | 10 | 0.0048 | 2 | 0.0422 | 34 | 0.368 | 3 |
| 106 | visionlabs-006 | 0.0037 | 2 | 0.0066 | 3 | 0.0012 | 3 | 0.0041 | 1 | 0.0285 | 7 | - | - |
| 107 | vocord-005 | 0.0089 | 12 | 0.0155 | 15 | 0.0025 | 8 | 0.0216 | 52 | 0.0444 | 38 | 0.906 | 53 |
| 108 | vocord-006 | 0.0062 | 4 | 0.0102 | 7 | 0.0016 | 4 | 0.0082 | 8 | 0.0282 | 6 | - | - |
| 109 | yisheng-004 | 0.1988 | 92 | 0.3329 | 92 | 0.0475 | 87 | 0.1147 | 87 | 0.0908 | 72 | 0.715 | 35 |
| 110 | yitu-003 | 0.0015 | 1 | 0.0026 | 1 | 0.0003 | 1 | 0.0066 | 4 | 0.0325 | 24 | - | - |

Table 5: FNMR is the proportion of mated comparisons below a threshold set to achieve the FMR given in the header on the fourth row. FMR is the proportion of impostor comparisons at or above that threshold. The light grey values give rank over all algorithms in that column. The green column applies to “matched-covariates” i.e. impostors of the same sex, age group, and country of birth. The pink column uses only same-sex impostors; All others are zero effort. The pink column includes effects of extended ageing, and is the most important. Missing entries for visa, mugshot and wild images generally mean the algorithm did not run to completion. For child exploitation, missing entries arise because NIST executes those runs only infrequently.



FNMR(T)
FMR(T)
"False non-match rate"
"False match rate"

Figure 1: The points show false non-match rates (FNMR) versus the size of the encoded template. FNMR is the geometric mean of FNMR values for visa and mugshot images (from Figs. 15 and 21) at a false match rate (FMR) of 0.0001. The color of the points encodes template generation time - which spans at least one order of magnitude. Durations are measured on a single core of a c. 2016 Intel Xeon CPU E5-2630 v4 running at 2.20GHz. Algorithms with poor FNMR are omitted.

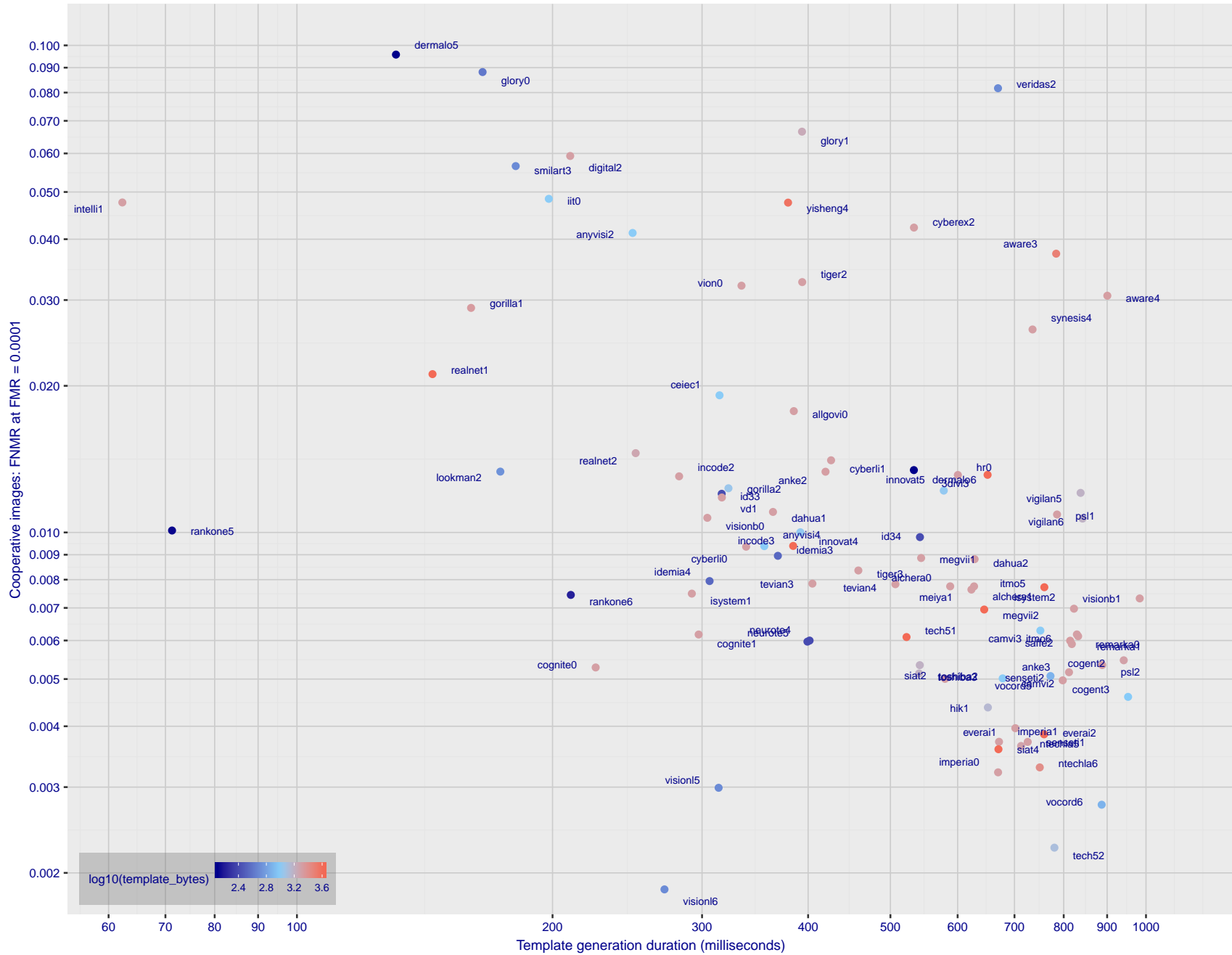


Figure 2: The points show false non-match rates (FNMR) versus the duration of the template generation operation. FNMR is the geometric mean of FNMR values for visa and mugshot images (from Figs. 15 and 21) at a false match rate (FMR) of 0.0001. Template generation time is a median estimated over 640 x 480 pixel portraits. It is measured on a single core of a c. 2016 Intel Xeon CPU E5-2630 v4 running at 2.20GHz. The color of the points encodes template size - which span two orders of magnitude. Algorithms with poor FNMR are omitted.

1 Metrics

1.1 Core accuracy

Given a vector of N genuine scores, u , the false non-match rate (FNMR) is computed as the proportion below some threshold, T :

$$\text{FNMR}(T) = 1 - \frac{1}{N} \sum_{i=1}^N H(u_i - T) \quad (1)$$

where $H(x)$ is the unit step function, and $H(0)$ taken to be 1.

Similarly, given a vector of N impostor scores, v , the false match rate (FMR) is computed as the proportion above T :

$$\text{FMR}(T) = \frac{1}{N} \sum_{i=1}^N H(v_i - T) \quad (2)$$

The threshold, T , can take on any value. We typically generate a set of thresholds from quantiles of the observed impostor scores, v , as follows. Given some interesting false match rate range, $[\text{FMR}_L, \text{FMR}_U]$, we form a vector of K thresholds corresponding to FMR measurements evenly spaced on a logarithmic scale

$$T_k = Q_v(1 - \text{FMR}_k) \quad (3)$$

where Q is the quantile function, and FMR_k comes from

$$\log_{10} \text{FMR}_k = \log_{10} \text{FMR}_L + \frac{k}{K} [\log_{10} \text{FMR}_U - \log_{10} \text{FMR}_L] \quad (4)$$

Error tradeoff characteristics are plots of $\text{FNMR}(T)$ vs. $\text{FMR}(T)$. These are plotted with $\text{FMR}_U \rightarrow 1$ and FMR_L as low as is sustained by the number of impostor comparisons, N . This is somewhat higher than the “rule of three” limit $3/N$ because samples are not independent, due to re-use of images.

2 Datasets

2.1 Child exploitation images

- ▷ The number of images is on the order of 10^4 .
- ▷ The number of subjects is on the order of 10^3 .
- ▷ The number of subjects with two images on the order of 10^3 .
- ▷ The images are operational. They are taken from ongoing investigations of child exploitation crimes. The images are arbitrarily unconstrained. Pose varies considerably around all three axes, including subject lying down. Resolution varies very widely. Faces can be occluded by other objects, including hair and hands. Lighting varies, although the images are intended for human viewing. Mis-focus is rare. Images are given to the algorithm without any cropping; faces may occupy widely varying areas.
- ▷ The images are usually large from contemporary cameras. The mean interocular distance (IOD) is 70 pixels.
- ▷ The images are of subjects from several countries, due to the global production of this imagery.
- ▷ The images are of children, from infancy to late adolescence.
- ▷ All of the images are live capture, none are scanned. Many have been cropped.
- ▷ When these images are input to the algorithm, they are labelled as being of type "EXPLOITATION" - see Table 4 of the FRVT API.

2.2 Visa images

- ▷ The number of images is on the order of 10^5 .
- ▷ The number of subjects is on the order of 10^5 .
- ▷ The number of subjects with two images on the order of 10^4 .
- ▷ The images have geometry in reasonable conformance with the ISO/IEC 19794-5 Full Frontal image type. Pose is generally excellent.
- ▷ The images are of size 252x300 pixels. The mean interocular distance (IOD) is 69 pixels.
- ▷ The images are of subjects from greater than 100 countries, with significant imbalance due to visa issuance patterns.
- ▷ The images are of subjects of all ages, including children, again with imbalance due to visa issuance demand.
- ▷ Many of the images are live capture. A substantial number of the images are photographs of paper photographs.
- ▷ When these images are input to the algorithm, they are labelled as being of type "ISO" - see Table 4 of the FRVT API.

2.3 Mugshot images

- ▷ The number of images is on the order of 10^6 .
- ▷ The number of subjects is on the order of 10^6 .
- ▷ The number of subjects with two images on the order of 10^6 .

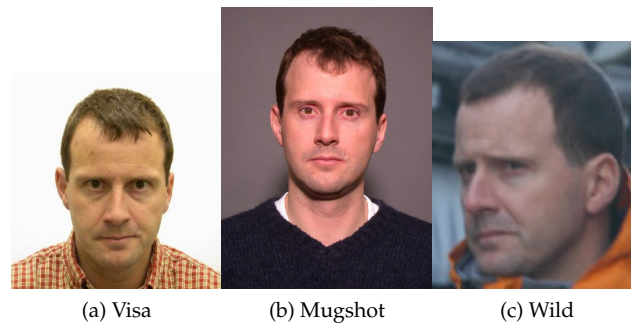


Figure 3: The figure gives simulated samples of image types used in this report.

- ▷ The images have geometry in reasonable conformance with the ISO/IEC 19794-5 Full Frontal image type.
- ▷ The images are of variable sizes. The median IOD is 104 pixels. The mean IOD is 123 pixels.
- ▷ The images are of subjects from the United States.
- ▷ The images are of adults.
- ▷ The images are all live capture.
- ▷ When these images are input to the algorithm, they are labelled as being of type "mugshot" - see Table 4 of the FRVT API.

2.4 Wild images

- ▷ The number of images is on the order of 10^5 .
- ▷ The number of subjects is on the order of 10^3 .
- ▷ The number of subjects with two images on the order of 10^3 .
- ▷ The images include many photojournalism-style images. Images are given to the algorithm using a variable but generally tight crop of the head. Resolution varies very widely. The images are very unconstrained, with wide yaw and pitch pose variation. Faces can be occluded, including hair and hands.
- ▷ The images are of adults.
- ▷ All of the images are live capture, none are scanned.
- ▷ When these images are input to the algorithm, they are labelled as being of type "WILD" - see Table 4 of the FRVT API.

3 Results

3.1 Test goals

- ▷ To state overall accuracy.
- ▷ To compare algorithms.

3.2 Test design

Method: For visa images:

- ▷ The comparisons are of visa photos against visa photos.
- ▷ The number of genuine comparisons is on the order of 10^4 .
- ▷ The number of impostor comparisons is on the order of 10^{10} .
- ▷ The comparisons are fully zero-effort, meaning impostors are paired without attention to sex, age or other covariates. However, later analysis is conducted on subsets.
- ▷ The number of persons is on the order of 10^5 .
- ▷ The number of images used to make 1 template is 1.
- ▷ The number of templates used to make each comparison score is two corresponding to simple one-to-one verification.

For mugshot images:

- ▷ The comparisons are of mugshot photos against mugshot photos.
- ▷ The number of genuine comparisons is on the order of 10^6 .
- ▷ The number of impostor comparisons is on the order of 10^8 .
- ▷ The impostors are paired by sex, but not by age or other covariates.
- ▷ The number of persons is on the order of 10^6 .
- ▷ The number of images used to make 1 template is 1.
- ▷ The number of templates used to make each comparison score is two corresponding to simple one-to-one verification.

Method: For wild images:

- ▷ The comparisons are of wild photos against wild photos.
- ▷ The number of genuine comparisons is on the order of 10^6 .
- ▷ The number of impostor comparisons is on the order of 10^7 .
- ▷ The comparisons are fully zero-effort, meaning impostors are paired without attention to sex, age or other covariates.
- ▷ The number of persons is on the order of 10^4 .
- ▷ The number of images used to make 1 template is 1.
- ▷ The number of templates used to make each comparison score is two corresponding to simple one-to-one verification.

For child exploitation images:

- ▷ The comparisons are of unconstrained child exploitation photos against others of the same type.

- ▷ The number of genuine comparisons is on the order of 10^4 .
- ▷ The number of impostor comparisons is on the order of 10^7 .
- ▷ The comparisons are fully zero-effort, meaning impostors are paired without attention to sex, age or other covariates.
- ▷ The number of persons is on the order of 10^3 .
- ▷ The number of images used to make 1 template is 1.
- ▷ The number of templates used to make each comparison score is two corresponding to simple one-to-one verification.
- ▷ We produce two performance statements. First, is a DET as used for visa and mugshot images. The second is a cumulative match characteristic (CMC) summarizing a simulated one-to-many search process. This is done as follows.
 - We regard M enrollment templates as items in a gallery.
 - These M templates come from $M > N$ individuals, because multiple images of a subject are present in the gallery under separate identifiers.
 - We regard the verification templates as search templates.
 - For each search we compute the rank of the highest scoring mate.
 - This process should properly be conducted with a 1:N algorithm, such as those tested in NIST IR 8009. We use the 1:1 algorithms in a simulated 1:N mode here to a) better reflect what a child exploitation analyst does, and b) to do show algorithm efficacy is better than that revealed in the verification DETs.

3.3 Failure to enrol

| Algorithm Name | Failure to Enrol Rate ¹ | | | | | | | |
|---------------------|------------------------------------|-----|---------|-----|--------|-----|--------|-----|
| | CHILD-EXPLOIT | | MUGSHOT | | VISA | | WILD | |
| 3divi-003 | 0.1806 | 41 | 0.0007 | 75 | 0.0006 | 67 | 0.0294 | 85 |
| alchera-000 | - | 110 | 0.0004 | 63 | 0.0014 | 93 | 0.0038 | 53 |
| alchera-001 | - | 110 | 0.0004 | 62 | 0.0014 | 92 | 0.0038 | 52 |
| algovision-000 | - | 110 | 0.0026 | 96 | 0.0052 | 107 | 0.0131 | 77 |
| amplifiedgroup-001 | - | 110 | 0.0189 | 110 | 0.0279 | 113 | 0.1390 | 104 |
| anke-002 | 0.1371 | 35 | 0.0004 | 60 | 0.0009 | 77 | 0.0094 | 70 |
| anke-003 | - | 110 | 0.0001 | 35 | 0.0004 | 46 | 0.0006 | 32 |
| anyvision-002 | 0.4866 | 57 | 0.0070 | 104 | 0.0090 | 109 | 0.1146 | 98 |
| anyvision-004 | 0.1660 | 38 | 0.0001 | 43 | 0.0004 | 51 | 0.0080 | 65 |
| aware-003 | 0.3314 | 52 | 0.0016 | 91 | 0.0013 | 89 | 0.0745 | 97 |
| aware-004 | - | 110 | 0.0002 | 45 | 0.0005 | 58 | 0.0014 | 43 |
| ayonix-000 | 0.0000 | 4 | 0.0113 | 107 | 0.0137 | 111 | 0.1194 | 99 |
| bm-001 | 0.0000 | 8 | 0.0000 | 19 | 0.0000 | 14 | 0.0000 | 11 |
| camvi-002 | 0.0000 | 5 | 0.0000 | 3 | 0.0000 | 3 | 0.0000 | 2 |
| camvi-003 | - | 110 | 0.0000 | 2 | 0.0000 | 2 | 0.0000 | 1 |
| ceiec-001 | - | 110 | 0.0029 | 99 | 0.0023 | 99 | 0.0068 | 61 |
| cogent-002 | 0.2096 | 43 | 0.0002 | 44 | 0.0004 | 55 | 0.0063 | 59 |
| cogent-003 | - | 110 | 0.0001 | 34 | 0.0004 | 49 | 0.0009 | 41 |
| cognitec-000 | 0.6342 | 60 | 0.0007 | 76 | 0.0007 | 73 | 0.0388 | 90 |
| cognitec-001 | - | 110 | 0.0008 | 80 | 0.0010 | 78 | 0.0185 | 81 |
| cyberextruder-001 | 0.5338 | 58 | 0.0024 | 94 | 0.0029 | 102 | 0.0597 | 95 |
| cyberextruder-002 | 0.2672 | 50 | 0.0027 | 97 | 0.0028 | 101 | 0.0335 | 89 |
| cyberlink-000 | - | 110 | 0.0006 | 73 | 0.0008 | 74 | 0.1374 | 102 |
| cyberlink-001 | - | 110 | 0.0073 | 105 | 0.0005 | 59 | 0.0008 | 37 |
| dahua-001 | 0.0000 | 14 | 0.0000 | 17 | 0.0000 | 19 | 0.0000 | 16 |
| dahua-002 | - | 110 | 0.0024 | 95 | 0.0022 | 97 | 0.0009 | 39 |
| dermalog-005 | 0.1796 | 39 | 0.0013 | 88 | 0.0041 | 104 | 0.0163 | 79 |
| dermalog-006 | 0.1797 | 40 | 0.0013 | 87 | 0.0041 | 105 | 0.0163 | 80 |
| digitalbarriers-002 | - | 110 | 0.0028 | 98 | 0.0027 | 100 | 0.0071 | 62 |
| everai-001 | - | 110 | 0.0004 | 65 | 0.0004 | 54 | 0.0006 | 36 |
| everai-002 | - | 110 | 0.0002 | 47 | 0.0004 | 34 | 0.0004 | 29 |
| glory-000 | 0.0000 | 7 | 0.0053 | 102 | 0.0013 | 90 | 0.1565 | 105 |
| glory-001 | 0.0000 | 10 | 0.0051 | 101 | 0.0010 | 79 | 0.1651 | 106 |
| gorilla-001 | 0.1347 | 32 | 0.0003 | 56 | 0.0004 | 57 | 0.0117 | 73 |
| gorilla-002 | 0.1347 | 33 | 0.0003 | 55 | 0.0004 | 56 | 0.0117 | 72 |
| hik-001 | - | 110 | 0.0000 | 7 | 0.0000 | 8 | 0.0000 | 6 |
| hr-000 | - | 110 | 0.0003 | 52 | 0.0008 | 75 | 0.0034 | 51 |
| id3-003 | 0.3032 | 51 | 0.0016 | 92 | 0.0011 | 87 | 0.0317 | 87 |
| id3-004 | - | 110 | 0.0015 | 90 | 0.0011 | 88 | - | 110 |
| idemia-003 | 0.0481 | 20 | 0.0000 | 23 | 0.0004 | 36 | 0.0042 | 56 |
| idemia-004 | - | 110 | 0.0000 | 26 | 0.0004 | 39 | 0.0003 | 27 |
| iiit-000 | - | 110 | 0.0007 | 74 | 0.0011 | 83 | - | 110 |
| imperial-000 | - | 110 | 0.0000 | 16 | 0.0000 | 18 | 0.0000 | 15 |
| imperial-001 | - | 110 | 0.0000 | 13 | 0.0000 | 15 | 0.0000 | 12 |
| incode-002 | 0.2202 | 44 | 0.0004 | 67 | 0.0007 | 70 | 0.0081 | 66 |
| incode-003 | - | 110 | 0.0004 | 66 | 0.0007 | 69 | 0.0014 | 42 |
| innovatrics-004 | 0.1170 | 31 | 0.0000 | 29 | 0.0004 | 53 | 0.0041 | 55 |
| innovatrics-005 | - | 110 | 0.0000 | 30 | 0.0004 | 52 | 0.0006 | 31 |
| intellivision-001 | 0.5495 | 59 | 0.0048 | 100 | 0.0042 | 106 | 0.1358 | 101 |
| isityou-000 | 0.4714 | 56 | 0.0023 | 93 | 0.0010 | 80 | 0.0663 | 96 |
| isystems-001 | 0.1421 | 36 | 0.0010 | 82 | 0.0007 | 71 | 0.0128 | 75 |
| isystems-002 | 0.1421 | 37 | 0.0010 | 83 | 0.0007 | 72 | 0.0128 | 76 |
| itmo-005 | 0.1353 | 34 | 0.0005 | 70 | 0.0002 | 23 | 0.0075 | 63 |
| itmo-006 | - | 110 | 0.0004 | 68 | 0.0004 | 50 | 0.0006 | 35 |
| kakao-001 | - | 110 | 0.0002 | 48 | 0.0005 | 60 | 0.0310 | 86 |
| lookman-002 | - | 110 | 0.0000 | 6 | 0.0000 | 7 | 0.0000 | 5 |

Table 6: FTE is the proportion of failed template generation attempts. Failures can occur because the software throws an exception, or because the software electively refuses to process the input image. This would typically occur if a face is not detected. FTE is measured as the number of function calls that give EITHER a non-zero error code OR that give a “small” template. This is defined as one whose size is less than 0.3 times the median template size for that algorithm. This second rule is needed because some algorithms incorrectly fail to return a non-zero error code when template generation fails.

¹The effects of FTE are included in the accuracy results of this report by regarding any template comparison involving a failed template to produce a low similarity score. Thus higher FTE results in higher FNMR and lower FMR.

| Algorithm Name | Failure to Enrol Rate ¹ | | | | | | | |
|-----------------------|------------------------------------|-----|---------|-----|--------|-----|--------|-----|
| | CHILD-EXPLOIT | | MUGSHOT | | VISA | | WILD | |
| megvii-001 | 0.0274 | 18 | 0.0007 | 77 | 0.0004 | 41 | 0.0152 | 78 |
| megvii-002 | 0.0274 | 17 | 0.0054 | 103 | 0.0004 | 40 | 0.0126 | 74 |
| meiya-001 | - | 110 | 0.0004 | 69 | 0.0010 | 81 | 0.0025 | 46 |
| microfocus-001 | 0.0791 | 30 | 0.0008 | 79 | 0.0016 | 95 | 0.0220 | 84 |
| microfocus-002 | 0.0791 | 29 | 0.0008 | 78 | 0.0016 | 94 | 0.0220 | 83 |
| neurotechnology-004 | 0.0055 | 15 | 0.0000 | 22 | 0.0001 | 22 | 0.0026 | 47 |
| neurotechnology-005 | - | 110 | 0.0004 | 59 | 0.0004 | 44 | 0.0018 | 44 |
| nodeflux-000 | - | 110 | 0.0001 | 37 | 0.0002 | 25 | 0.0003 | 24 |
| nodeflux-001 | - | 110 | 0.0001 | 36 | 0.0002 | 24 | 0.0003 | 23 |
| ntechlab-005 | 0.0315 | 19 | 0.0000 | 21 | 0.0004 | 38 | 0.0032 | 50 |
| ntechlab-006 | - | 110 | 0.0000 | 20 | 0.0004 | 33 | 0.0003 | 22 |
| psl-001 | 0.0000 | 11 | 0.0000 | 14 | 0.0000 | 16 | 0.0000 | 13 |
| psl-002 | - | 110 | 0.0000 | 12 | 0.0000 | 13 | 0.0000 | 10 |
| rankone-005 | 0.0000 | 3 | 0.0000 | 10 | 0.0000 | 11 | 0.0000 | 8 |
| rankone-006 | - | 110 | 0.0000 | 11 | 0.0000 | 12 | 0.0000 | 9 |
| realnetworks-001 | 0.0076 | 16 | 0.0004 | 58 | 0.0003 | 28 | 0.0064 | 60 |
| realnetworks-002 | - | 110 | 0.0004 | 57 | 0.0003 | 27 | 0.0004 | 28 |
| remarkai-000 | - | 110 | 0.0000 | 5 | 0.0000 | 5 | 0.0000 | 19 |
| remarkai-001 | - | 110 | 0.0000 | 18 | 0.0000 | 20 | 0.0000 | 20 |
| saffe-001 | 0.0000 | 12 | 0.0000 | 15 | 0.0000 | 17 | 0.0000 | 14 |
| saffe-002 | - | 110 | 0.0000 | 9 | 0.0000 | 10 | 0.0000 | 7 |
| sensetime-001 | 0.0631 | 28 | 0.0000 | 25 | 0.0004 | 45 | 0.0003 | 25 |
| sensetime-002 | 0.3345 | 53 | 0.0011 | 84 | 0.0005 | 65 | 0.0218 | 82 |
| shaman-000 | 0.0000 | 6 | 0.0000 | 4 | 0.0000 | 4 | 0.0000 | 3 |
| shaman-001 | 0.0000 | 1 | 0.0000 | 1 | 0.0000 | 1 | 0.0000 | 17 |
| siat-002 | 0.0616 | 25 | 0.0000 | 28 | 0.0004 | 48 | 0.0048 | 57 |
| siat-004 | - | 110 | 0.0000 | 27 | 0.0004 | 47 | 0.0003 | 26 |
| smilart-002 | 0.2422 | 46 | 0.0003 | 54 | 0.0011 | 84 | 0.0575 | 94 |
| smilart-003 | - | 110 | 0.0014 | 89 | 0.0013 | 91 | 0.0555 | 93 |
| synesis-003 | 0.4572 | 55 | 0.0102 | 106 | 0.1184 | 114 | 0.1209 | 100 |
| synesis-004 | - | 110 | 0.0164 | 109 | 0.0035 | 103 | 0.0485 | 92 |
| tech5-001 | 0.0000 | 2 | 0.0004 | 61 | 0.0003 | 30 | 0.0409 | 91 |
| tech5-002 | - | 110 | 0.0001 | 33 | 0.0003 | 26 | 0.0000 | 18 |
| tevan-003 | 0.2430 | 48 | 0.0003 | 50 | 0.0005 | 66 | 0.0076 | 64 |
| tevan-004 | - | 110 | 0.0002 | 46 | 0.0005 | 64 | 0.0057 | 58 |
| tiger-002 | 0.0619 | 26 | 0.0001 | 38 | 0.0004 | 42 | 0.0082 | 67 |
| tiger-003 | 0.0619 | 27 | 0.0001 | 39 | 0.0004 | 43 | 0.0082 | 68 |
| toshiba-002 | 0.0000 | 13 | 0.0000 | 8 | 0.0000 | 9 | - | 110 |
| toshiba-003 | - | 110 | 0.0001 | 40 | 0.0001 | 21 | 0.0002 | 21 |
| vd-001 | - | 110 | 0.0004 | 64 | 0.0009 | 76 | 0.0024 | 45 |
| veridas-001 | - | 110 | 0.0001 | 41 | 0.0005 | 62 | 0.0006 | 33 |
| veridas-002 | - | 110 | 0.0001 | 42 | 0.0005 | 63 | 0.0006 | 34 |
| vigilantsolutions-005 | 0.2538 | 49 | 0.0001 | 31 | 0.0004 | 35 | 0.0041 | 54 |
| vigilantsolutions-006 | - | 110 | 0.0001 | 32 | 0.0004 | 37 | 0.0005 | 30 |
| vion-000 | 0.6388 | 61 | 0.0130 | 108 | 0.0078 | 108 | 0.1389 | 103 |
| visionbox-000 | - | 110 | 0.0005 | 72 | 0.0011 | 86 | 0.0028 | 49 |
| visionbox-001 | - | 110 | 0.0005 | 71 | 0.0011 | 85 | 0.0028 | 48 |
| visionlabs-005 | 0.1875 | 42 | 0.0002 | 49 | 0.0023 | 98 | 0.0085 | 69 |
| visionlabs-006 | - | 110 | 0.0003 | 53 | 0.0005 | 61 | 0.0009 | 40 |
| vocord-005 | 0.0000 | 9 | 0.0013 | 86 | 0.0003 | 32 | 0.0102 | 71 |
| vocord-006 | - | 110 | 0.0003 | 51 | 0.0003 | 31 | 0.0008 | 38 |
| yisheng-004 | 0.4279 | 54 | 0.0013 | 85 | 0.0006 | 68 | 0.0321 | 88 |
| ytu-003 | - | 110 | 0.0009 | 81 | 0.0000 | 6 | 0.0000 | 4 |

Table 7: FTE is the proportion of failed template generation attempts. Failures can occur because the software throws an exception, or because the software electively refuses to process the input image. This would typically occur if a face is not detected. FTE is measured as the number of function calls that give EITHER a non-zero error code OR that give a “small” template. This is defined as one whose size is less than 0.3 times the median template size for that algorithm. This second rule is needed because some algorithms incorrectly fail to return a non-zero error code when template generation fails.

¹The effects of FTE are included in the accuracy results of this report by regarding any template comparison involving a failed template to produce a low similarity score. Thus higher FTE results in higher FNMR and lower FMR.

3.4 Recognition accuracy

Core algorithm accuracy is stated via:

▷ **Cooperative subjects**

- The summary table of Figure 5;
- The visa image DETs of Figure 15;
- The mugshot DETs of Figure 21;
- The mugshot ageing profiles of Figure 87;
- The human-difficult pairs of Figure 4

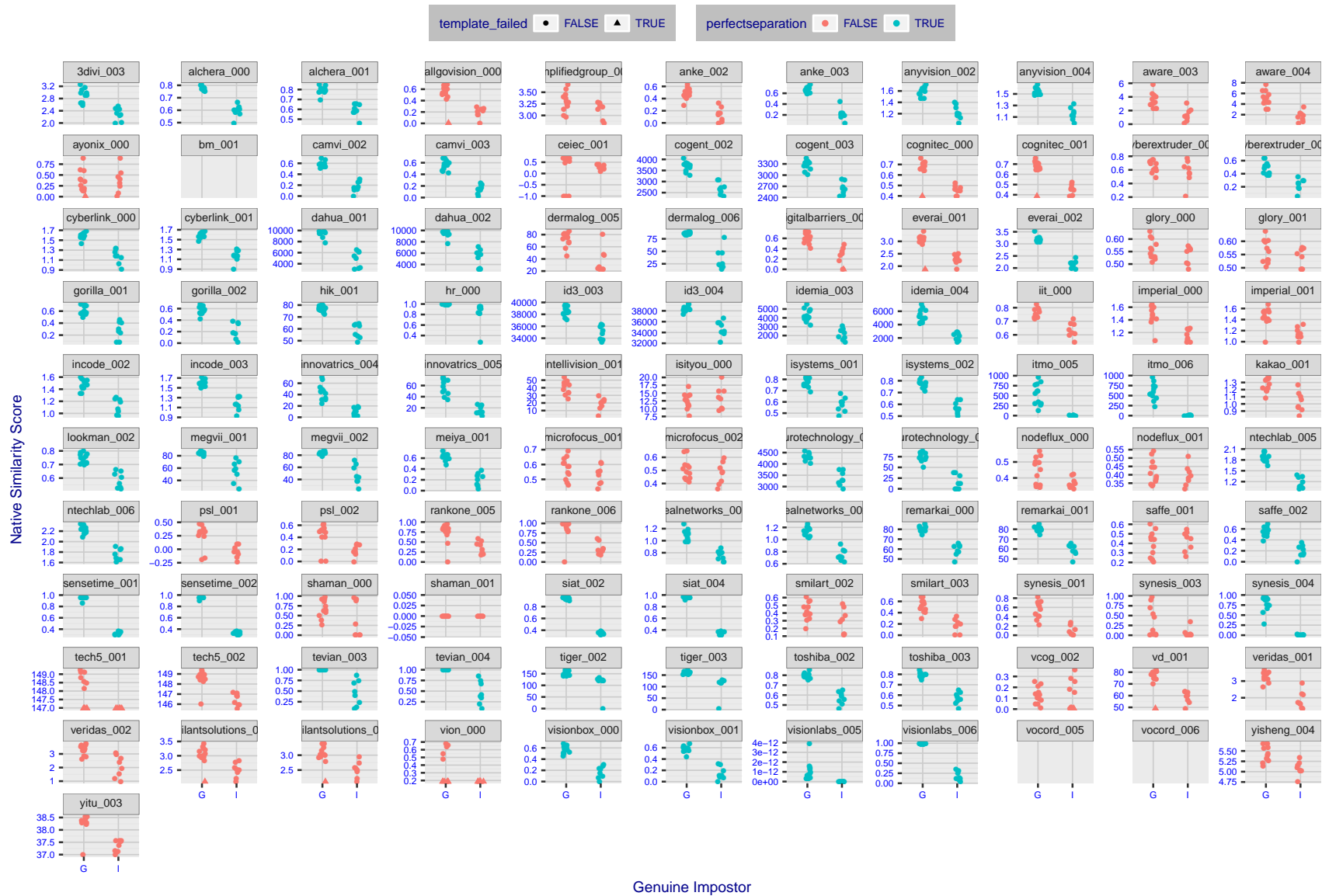
▷ **Non-cooperative subjects**

- The photojournalism DET of Figure 26
- The child-exploitation DET of Figure 29;
- The child-exploitation CMC of Figure 31.

Figure 70 shows dependence of false match rate on algorithm score threshold. This allows a deployer to set a threshold to target a particular false match rate appropriate to the security objectives of the application.

Figure 59 likewise shows FMR(T) but for mugshots, and specially four subsets of the population.

Note that in both the mugshot and visa sets false match rates vary with the ethnicity, age, and sex, of the enrollee and impostor - see section 3.6. For example figure 38 summarizes FMR for impostors paired from four groups black females, black males, white females, white males.



FNMR(T)
FMR(T)
"False non-match rate"
"False match rate"

Figure 4: The Figure shows, in blue, algorithms that correctly separate the 12 genuine and 8 impostor pairs used in the May 2018 paper [Face recognition accuracy of forensic examiners, superrecognizers, and face recognition algorithms \(Phillips et al. \[1\]\)](#). In red are algorithms that are imperfect. Some algorithms fail only because they failed to make a template e.g. due to face detection failure (shown as a triangle). Others fail because the pairs were selected for that study because they had been difficult for three leading algorithms used in FRVT 2006. Caution: Given the small sample size (n=20) the figure may change substantially if larger or different sets were used.

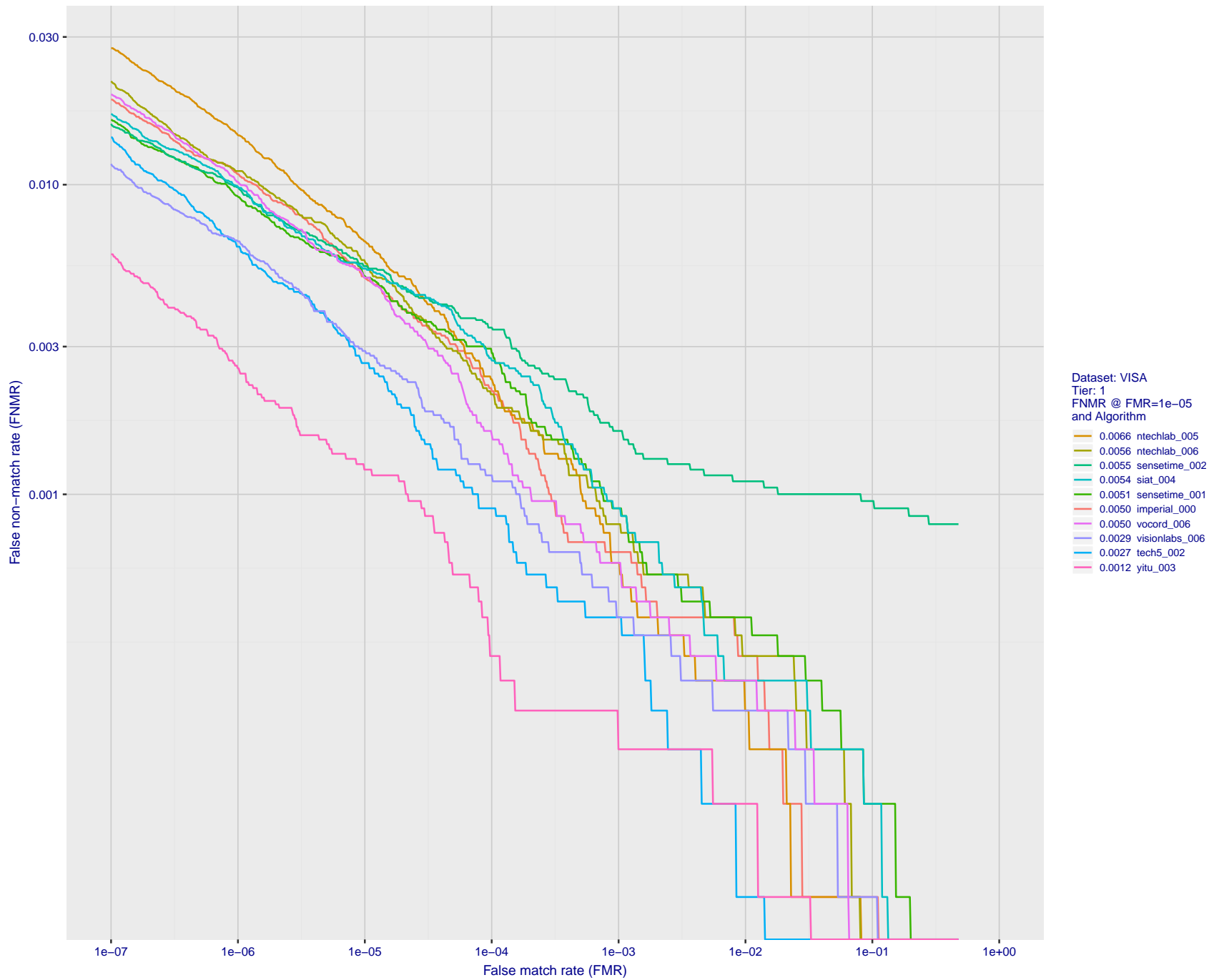


Figure 5: For the visa images, detection error tradeoff (DET) characteristics showing false non-match rate vs. false match rate plotted parametrically on threshold, T . The scales are logarithmic in order to show many decades of FMR.

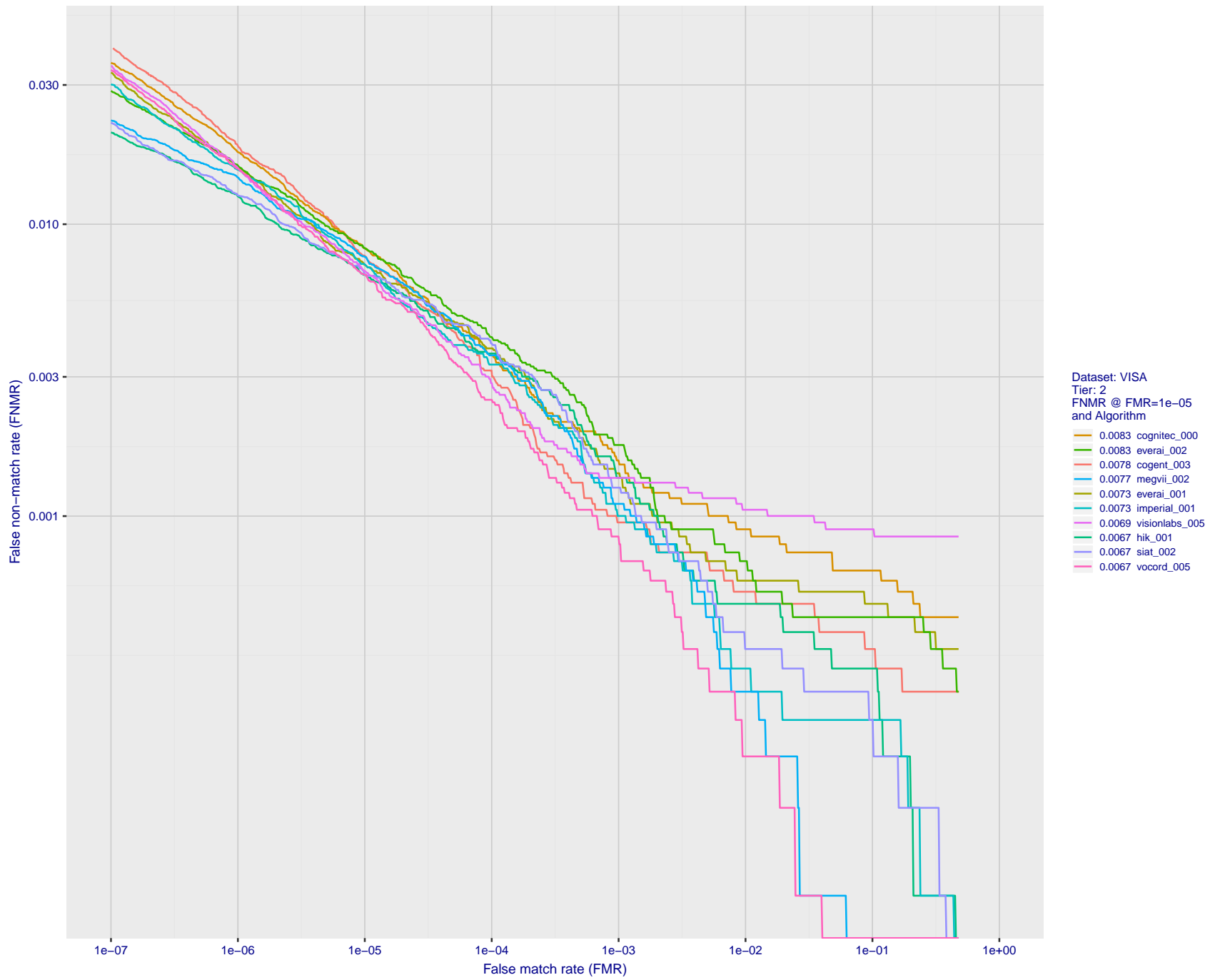


Figure 6: For the visa images, detection error tradeoff (DET) characteristics showing false non-match rate vs. false match rate plotted parametrically on threshold, T . The scales are logarithmic in order to show many decades of FMR.

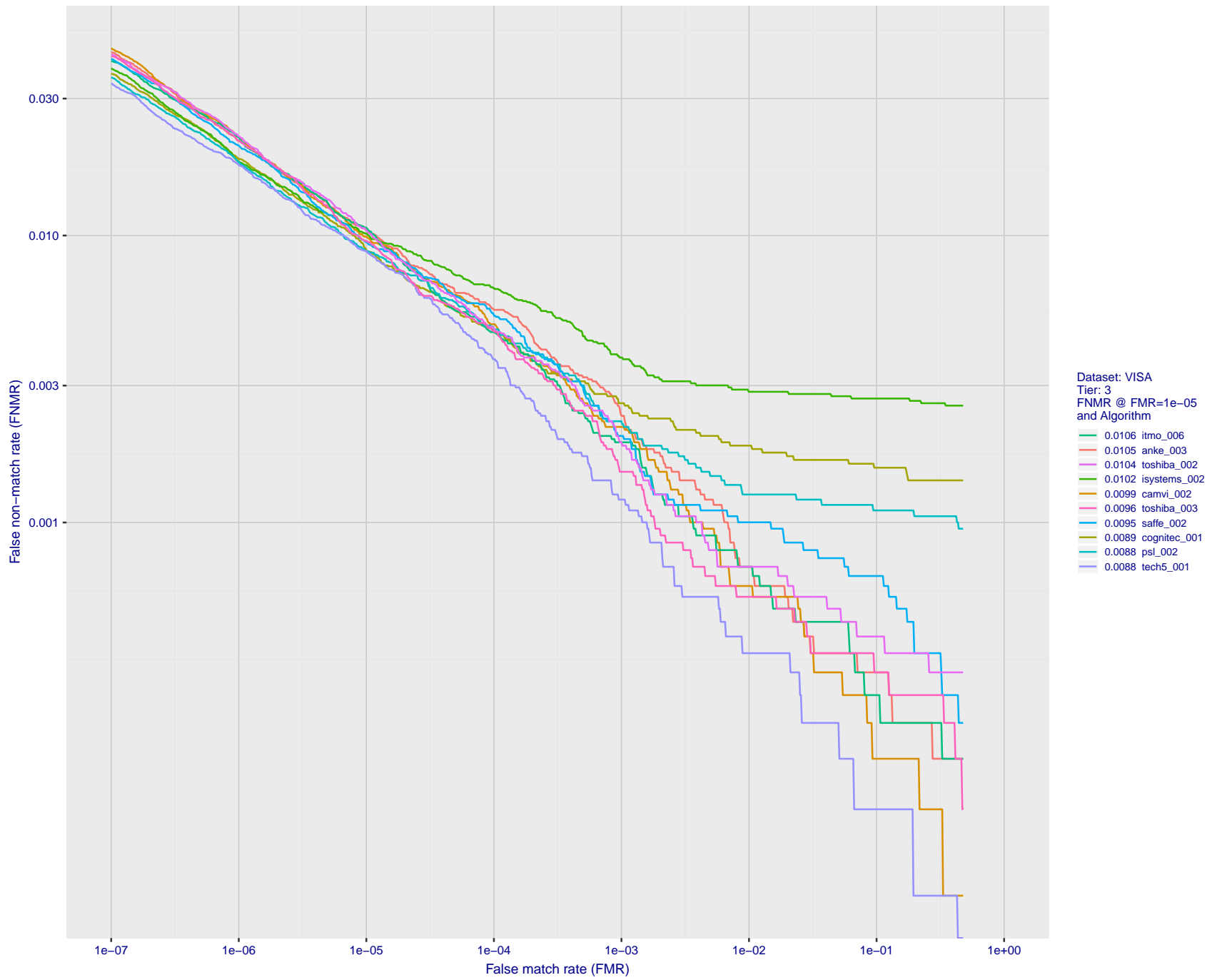


Figure 7: For the visa images, detection error tradeoff (DET) characteristics showing false non-match rate vs. false match rate plotted parametrically on threshold, T . The scales are logarithmic in order to show many decades of FMR.

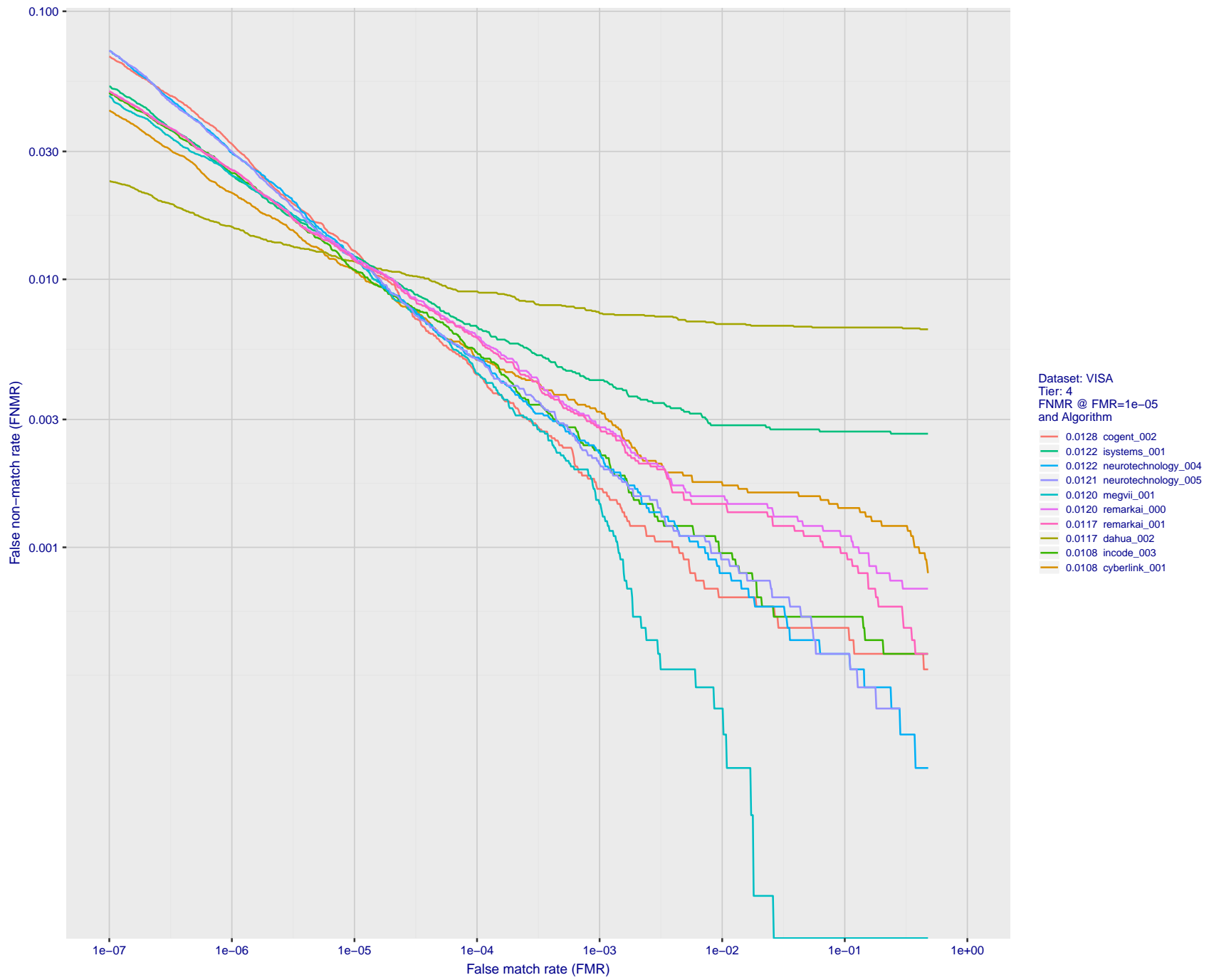


Figure 8: For the visa images, detection error tradeoff (DET) characteristics showing false non-match rate vs. false match rate plotted parametrically on threshold, T . The scales are logarithmic in order to show many decades of FMR.

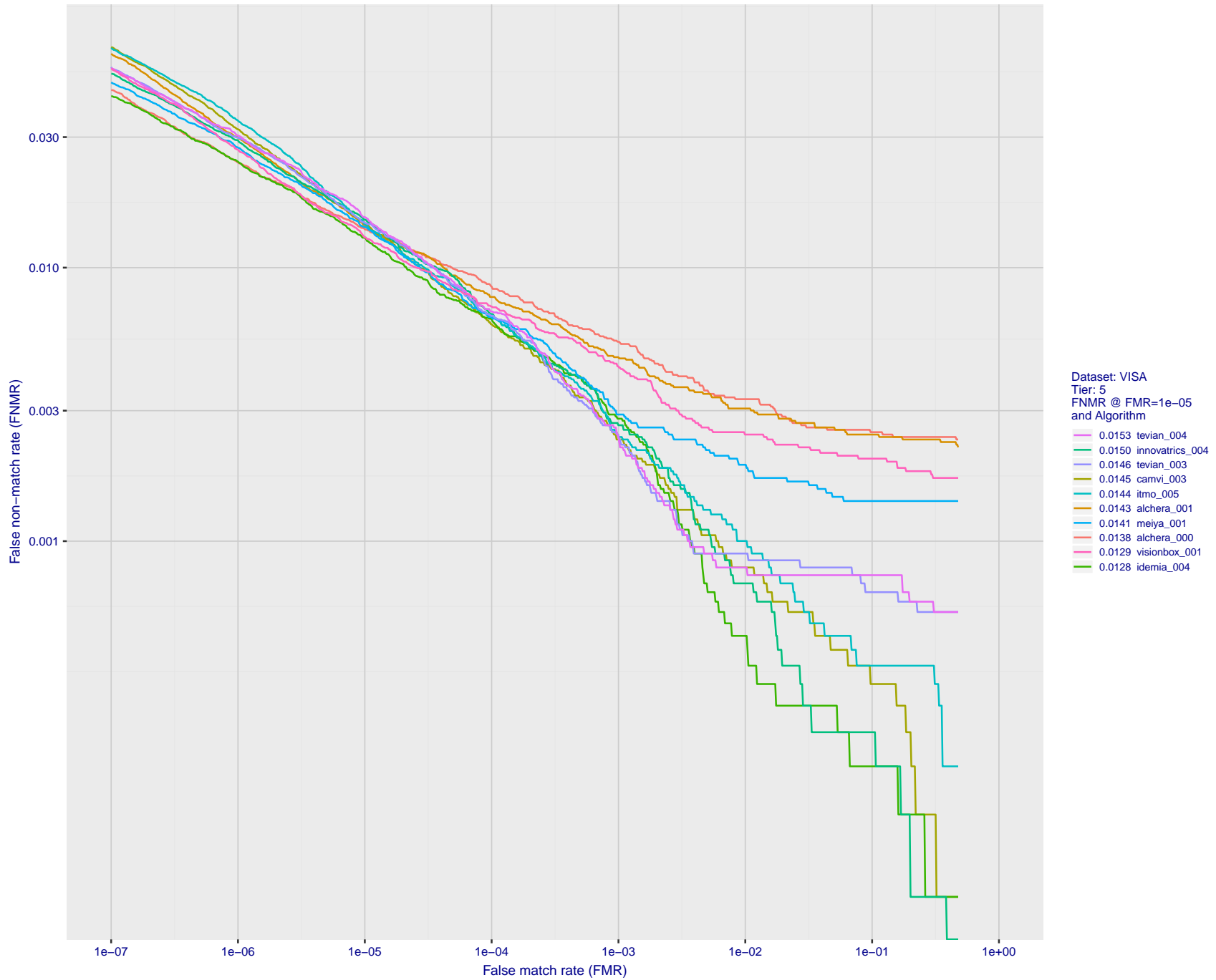


Figure 9: For the visa images, detection error tradeoff (DET) characteristics showing false non-match rate vs. false match rate plotted parametrically on threshold, T . The scales are logarithmic in order to show many decades of FMR.

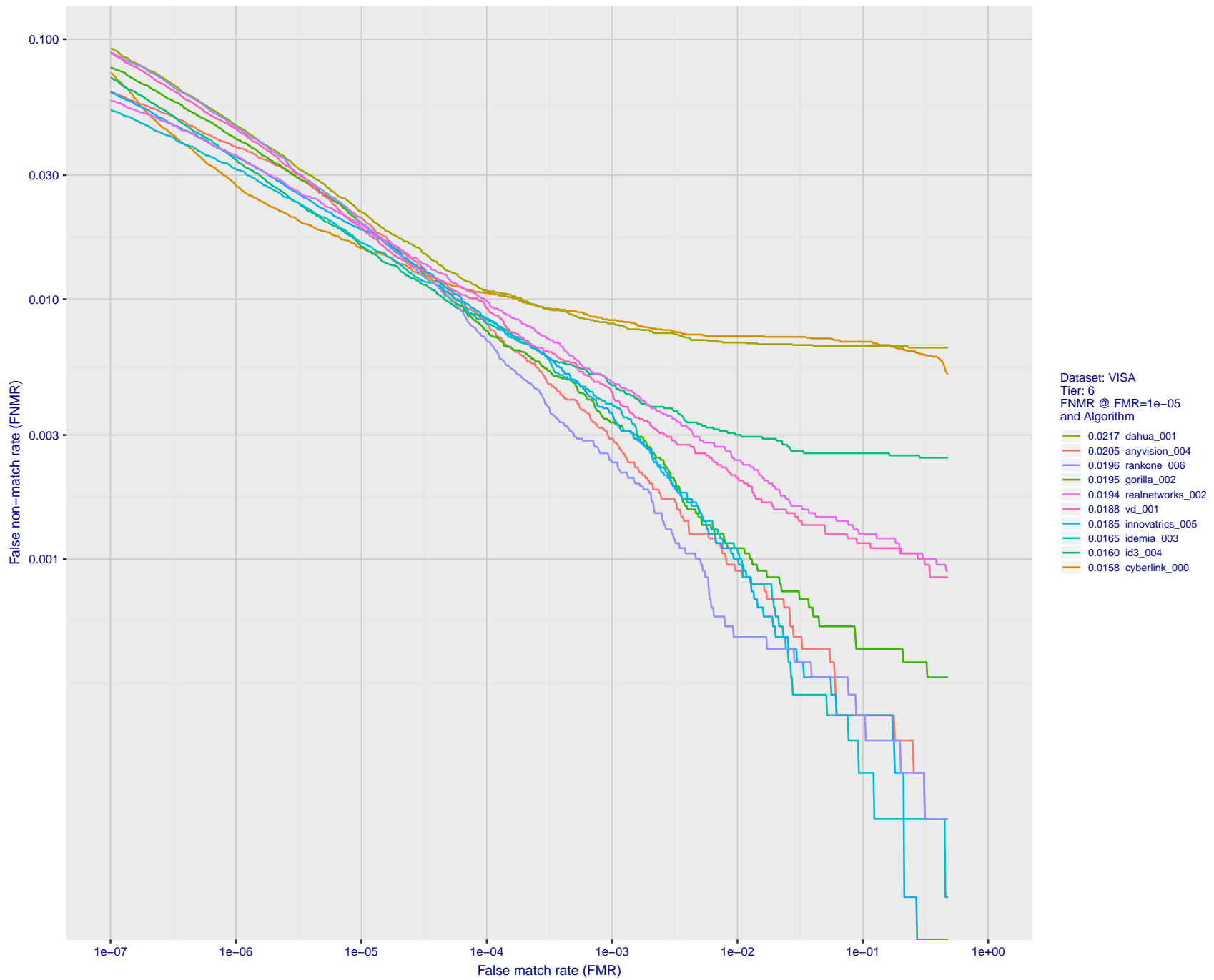


Figure 10: For the visa images, detection error tradeoff (DET) characteristics showing false non-match rate vs. false match rate plotted parametrically on threshold, T . The scales are logarithmic in order to show many decades of FMR.

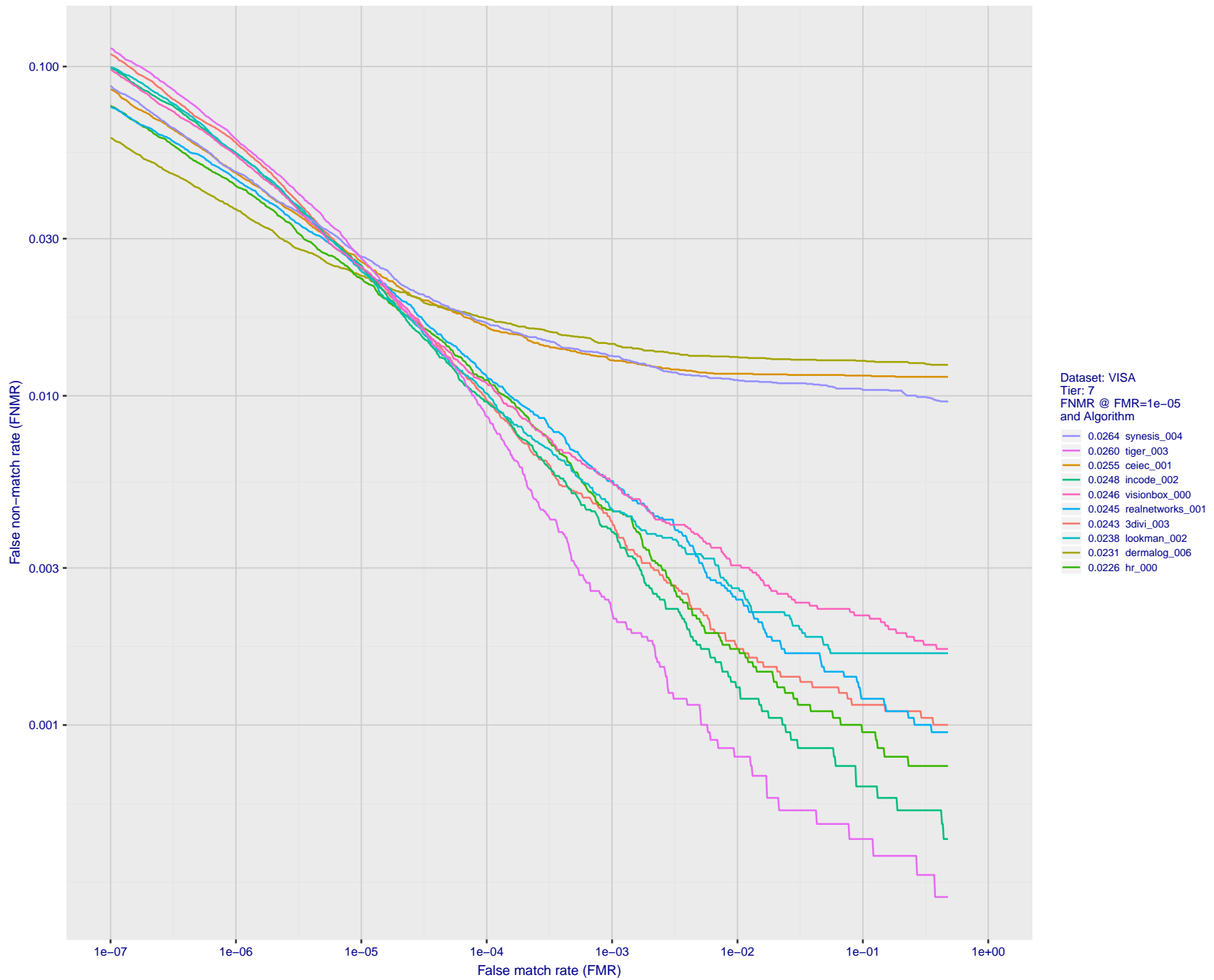


Figure 11: For the visa images, detection error tradeoff (DET) characteristics showing false non-match rate vs. false match rate plotted parametrically on threshold, T . The scales are logarithmic in order to show many decades of FMR.

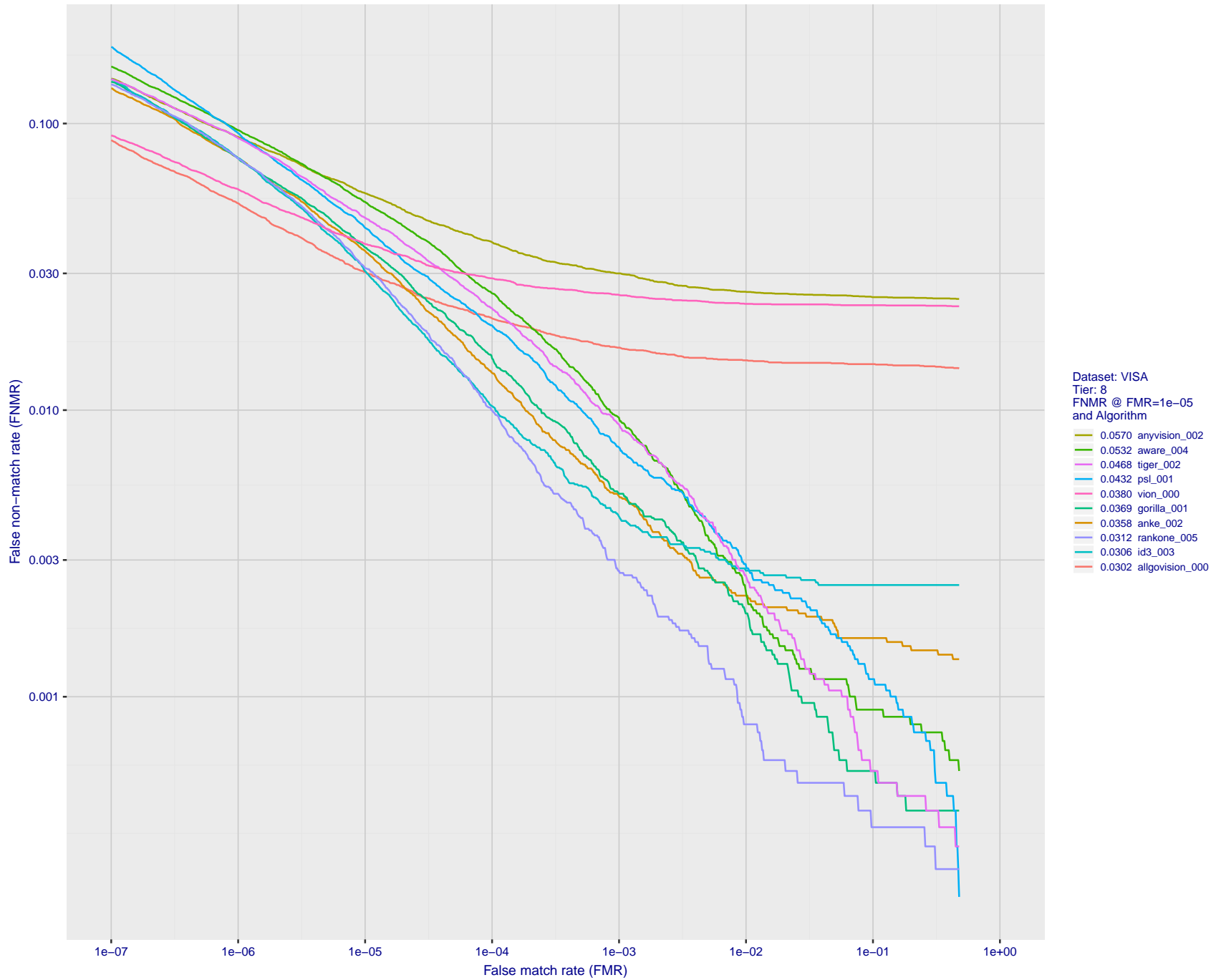


Figure 12: For the visa images, detection error tradeoff (DET) characteristics showing false non-match rate vs. false match rate plotted parametrically on threshold, T . The scales are logarithmic in order to show many decades of FMR.

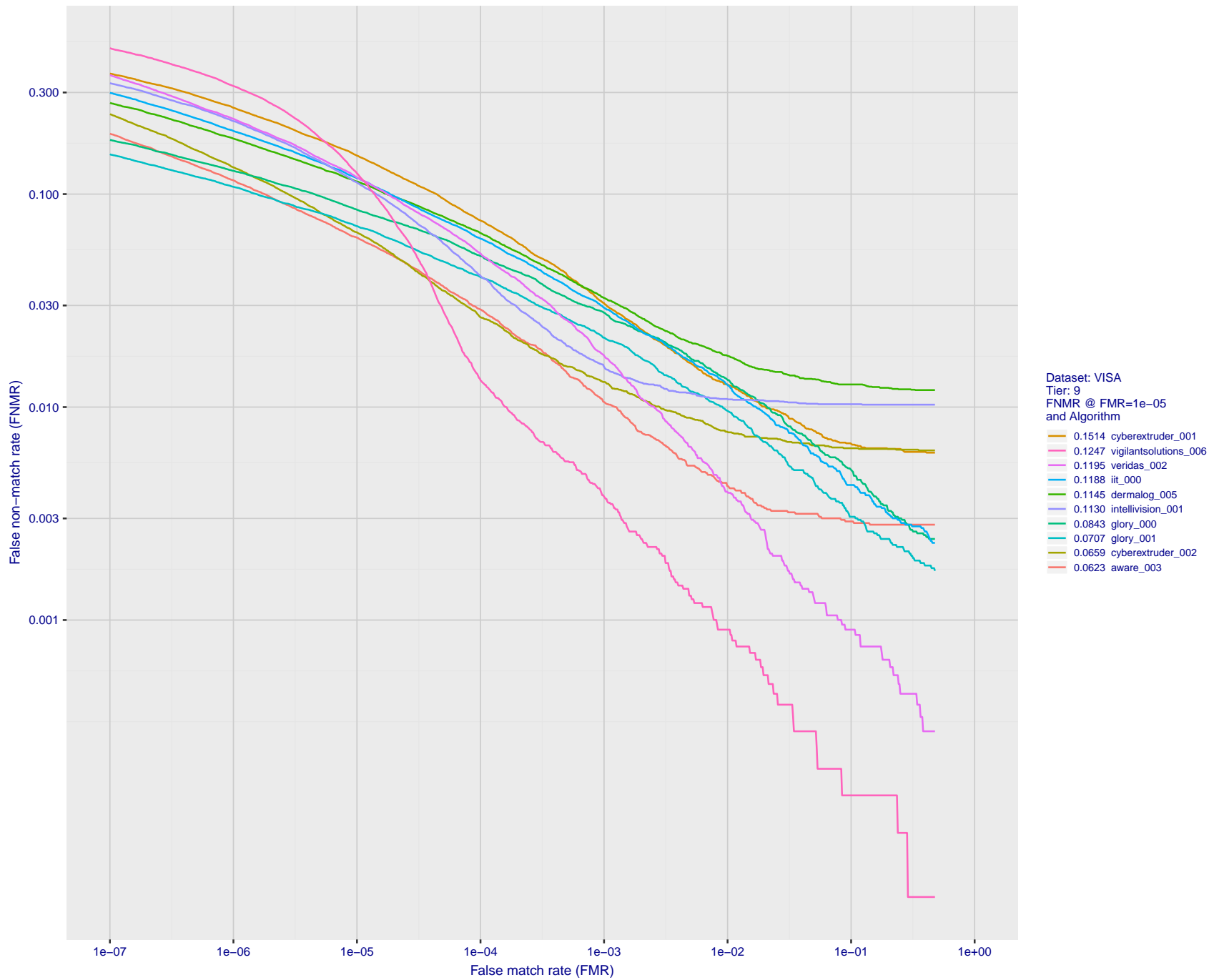


Figure 13: For the visa images, detection error tradeoff (DET) characteristics showing false non-match rate vs. false match rate plotted parametrically on threshold, T . The scales are logarithmic in order to show many decades of FMR.

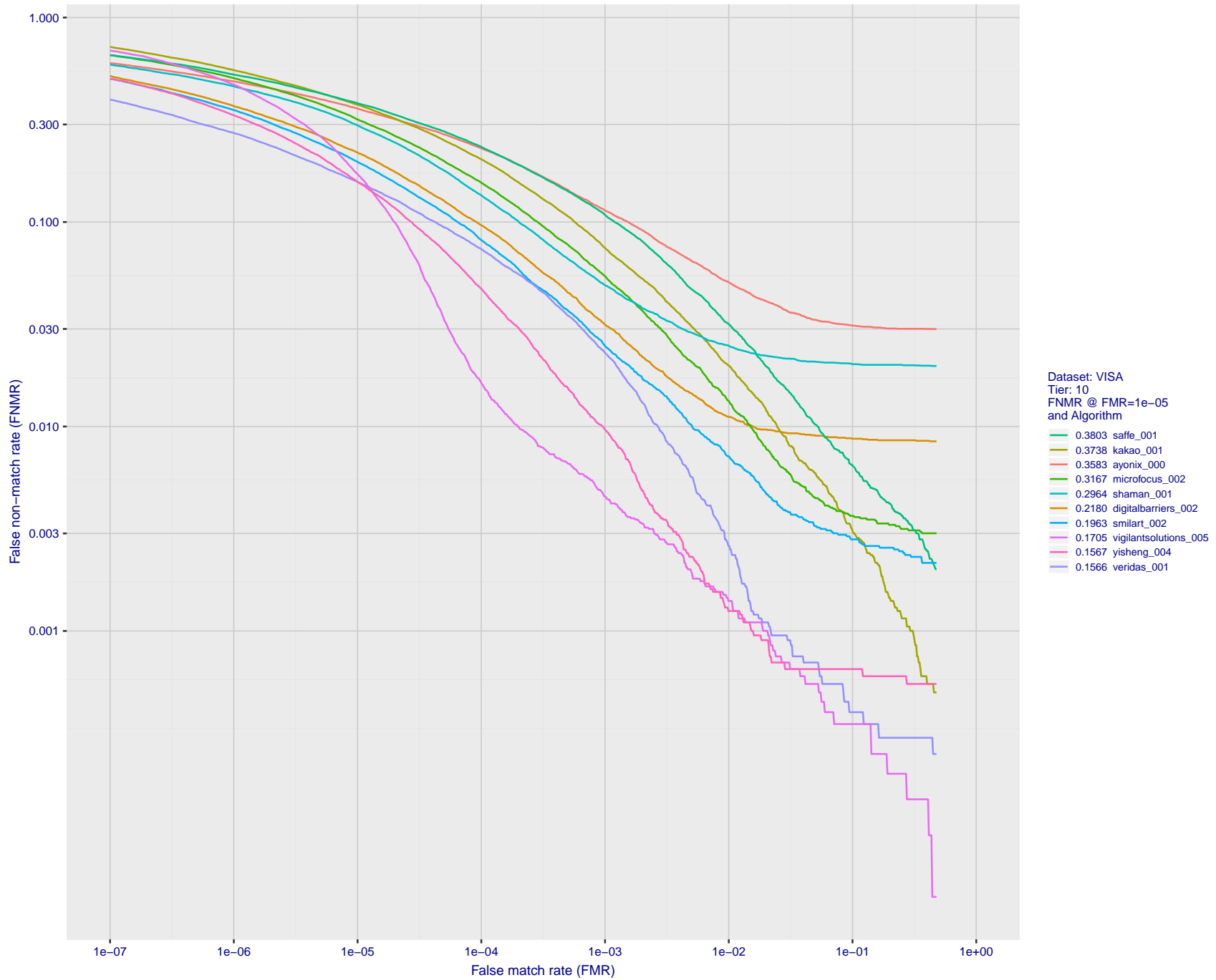
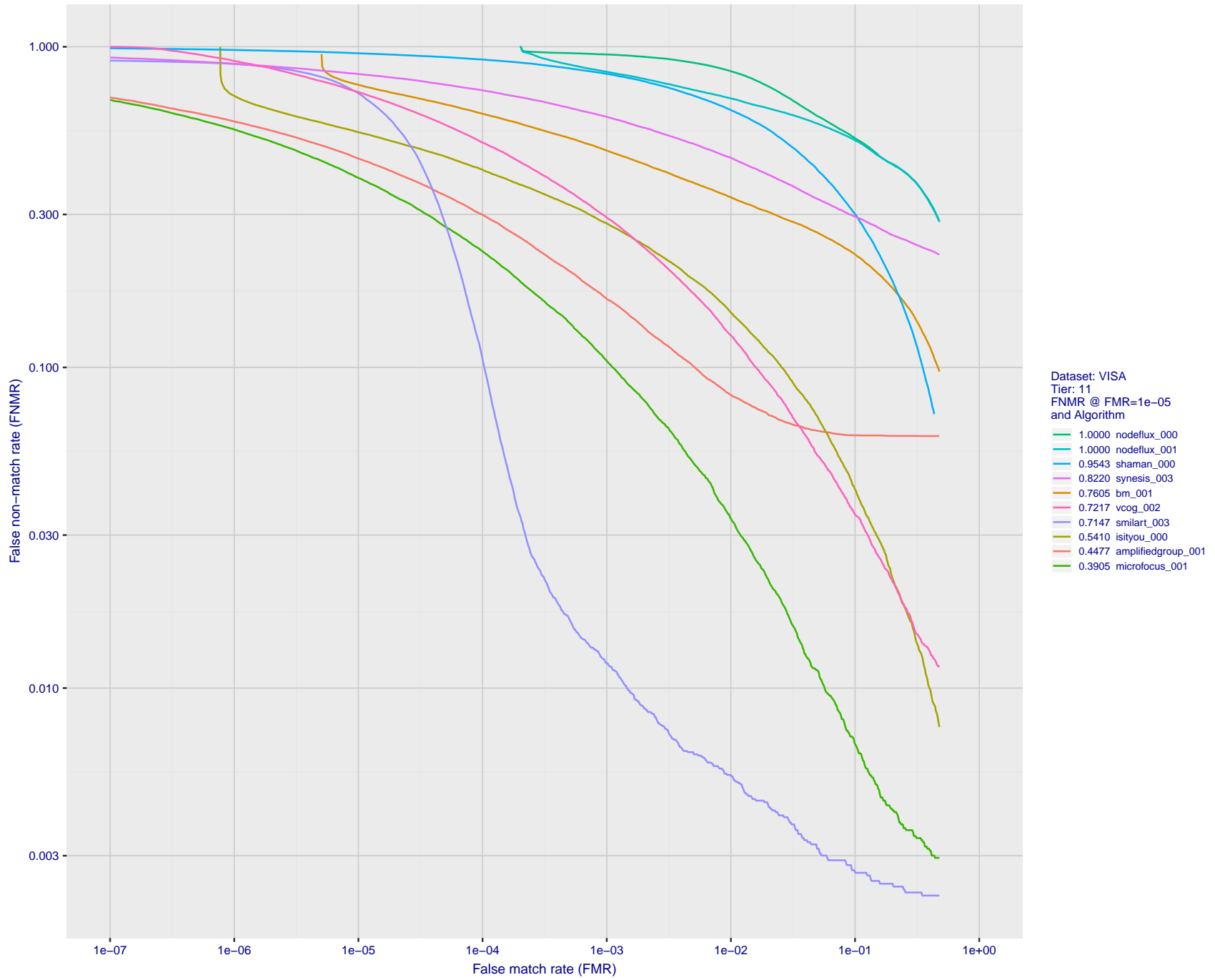


Figure 14: For the visa images, detection error tradeoff (DET) characteristics showing false non-match rate vs. false match rate plotted parametrically on threshold, T . The scales are logarithmic in order to show many decades of FMR.



FNMR(T)
FMR(T)
"False non-match rate"
"False match rate"

Figure 15: For the visa images, detection error tradeoff (DET) characteristics showing false non-match rate vs. false match rate plotted parametrically on threshold, T . The scales are logarithmic in order to show many decades of FMR.

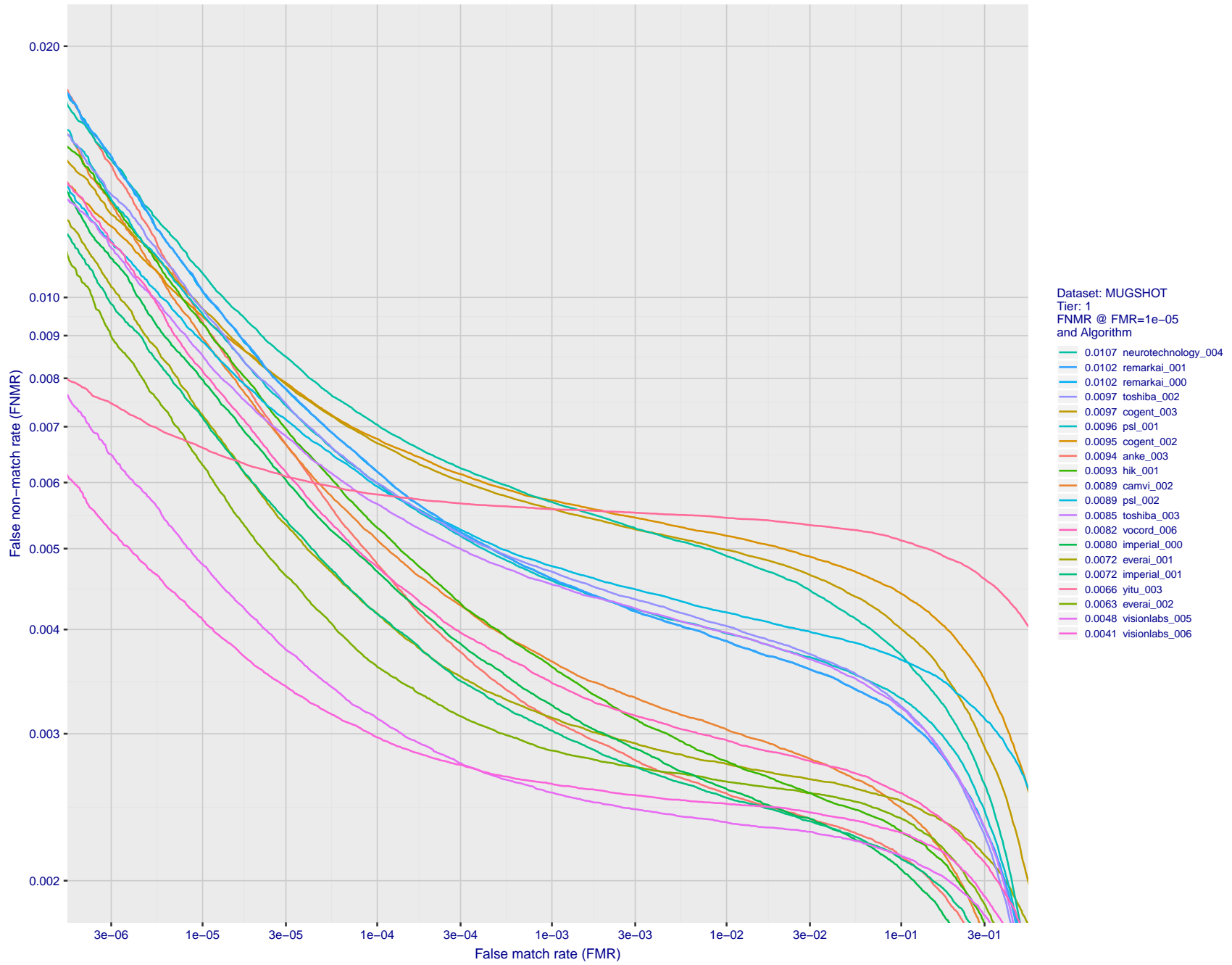


Figure 16: For the mugshot images, detection error tradeoff (DET) characteristics showing false non-match rate vs. false match rate plotted parametrically on threshold, T . The scales are logarithmic in order to show decades of FMR.

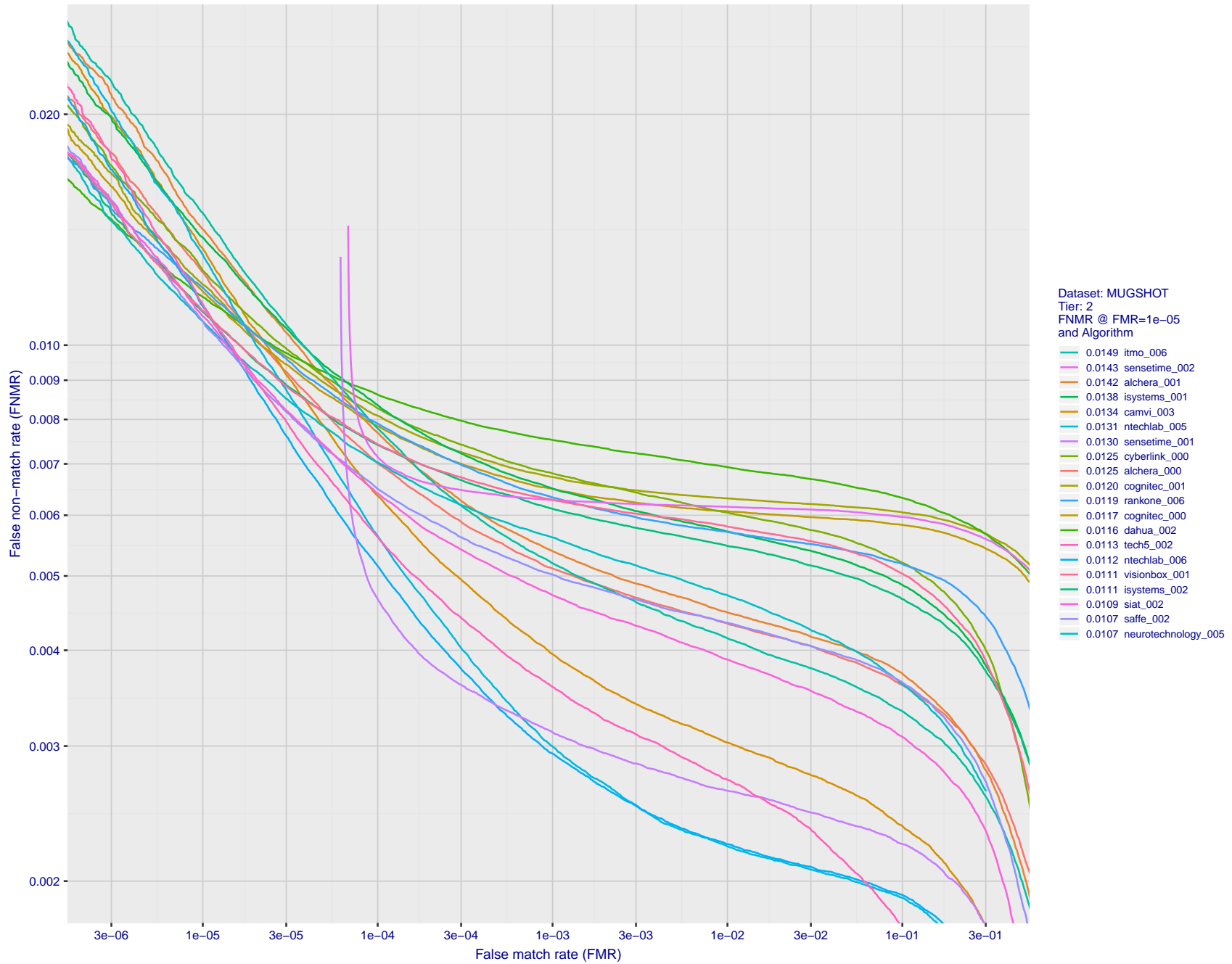


Figure 17: For the mugshot images, detection error tradeoff (DET) characteristics showing false non-match rate vs. false match rate plotted parametrically on threshold, T . The scales are logarithmic in order to show decades of FMR.

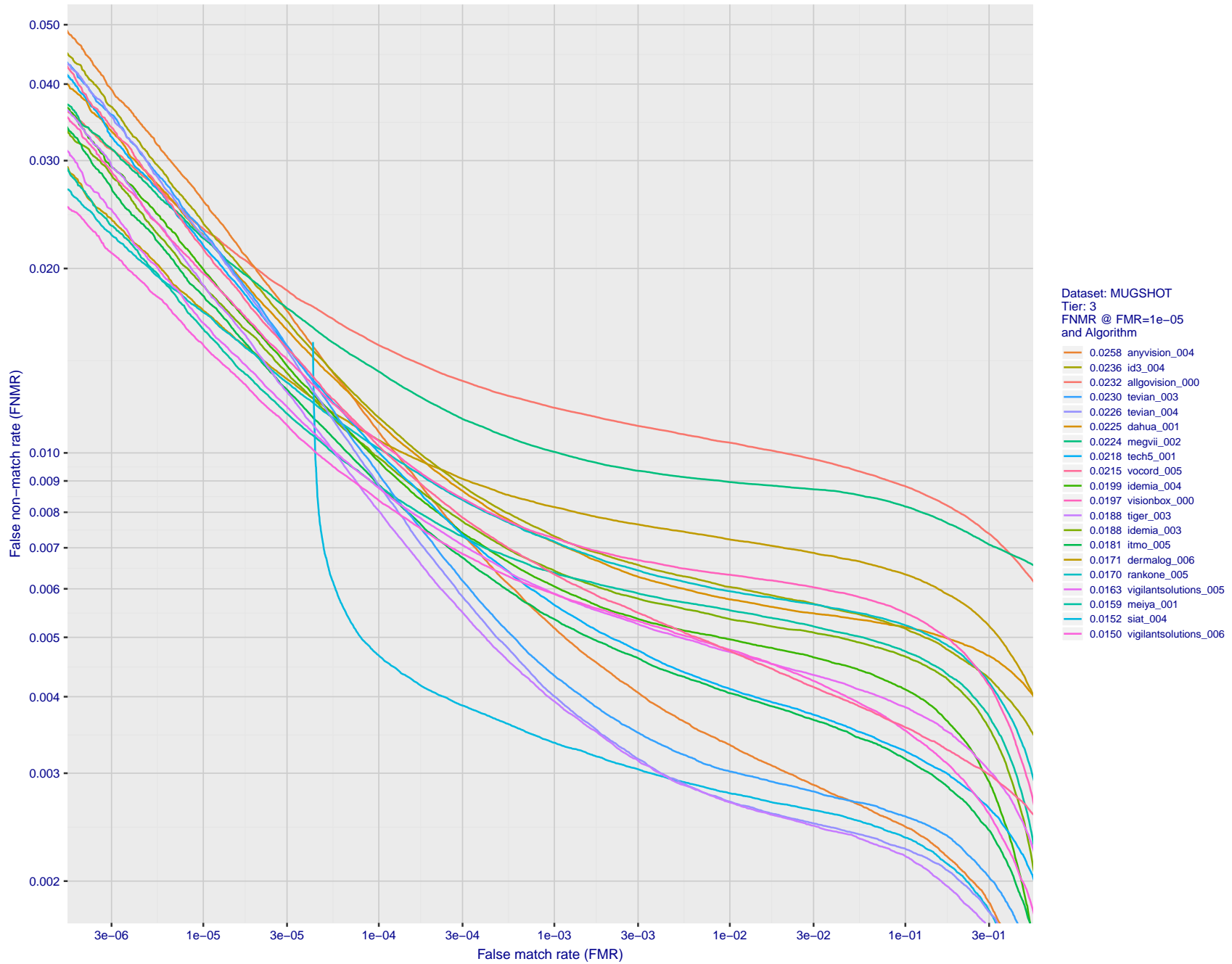


Figure 18: For the mugshot images, detection error tradeoff (DET) characteristics showing false non-match rate vs. false match rate plotted parametrically on threshold, T . The scales are logarithmic in order to show decades of FMR.

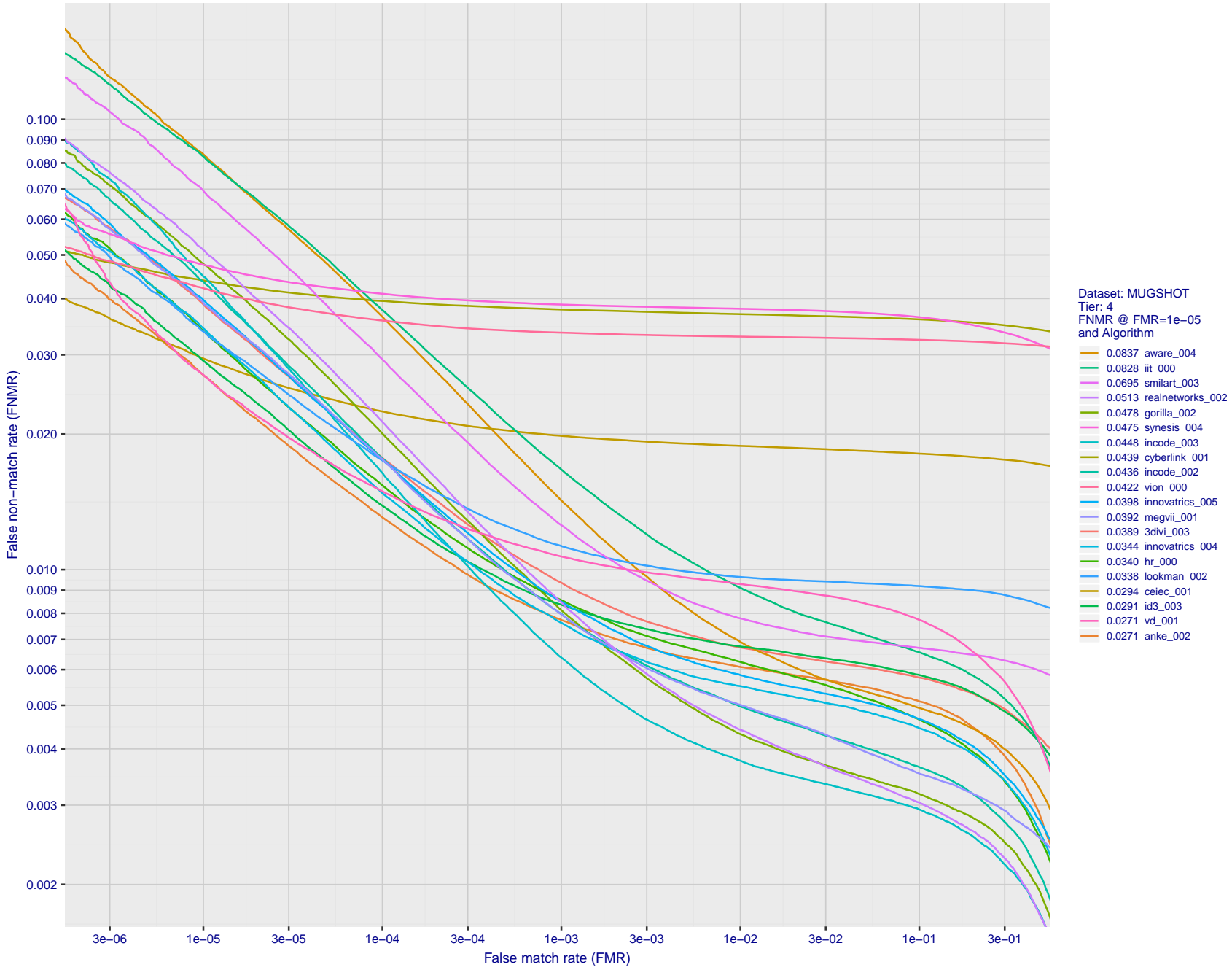


Figure 19: For the mugshot images, detection error tradeoff (DET) characteristics showing false non-match rate vs. false match rate plotted parametrically on threshold, T . The scales are logarithmic in order to show decades of FMR.

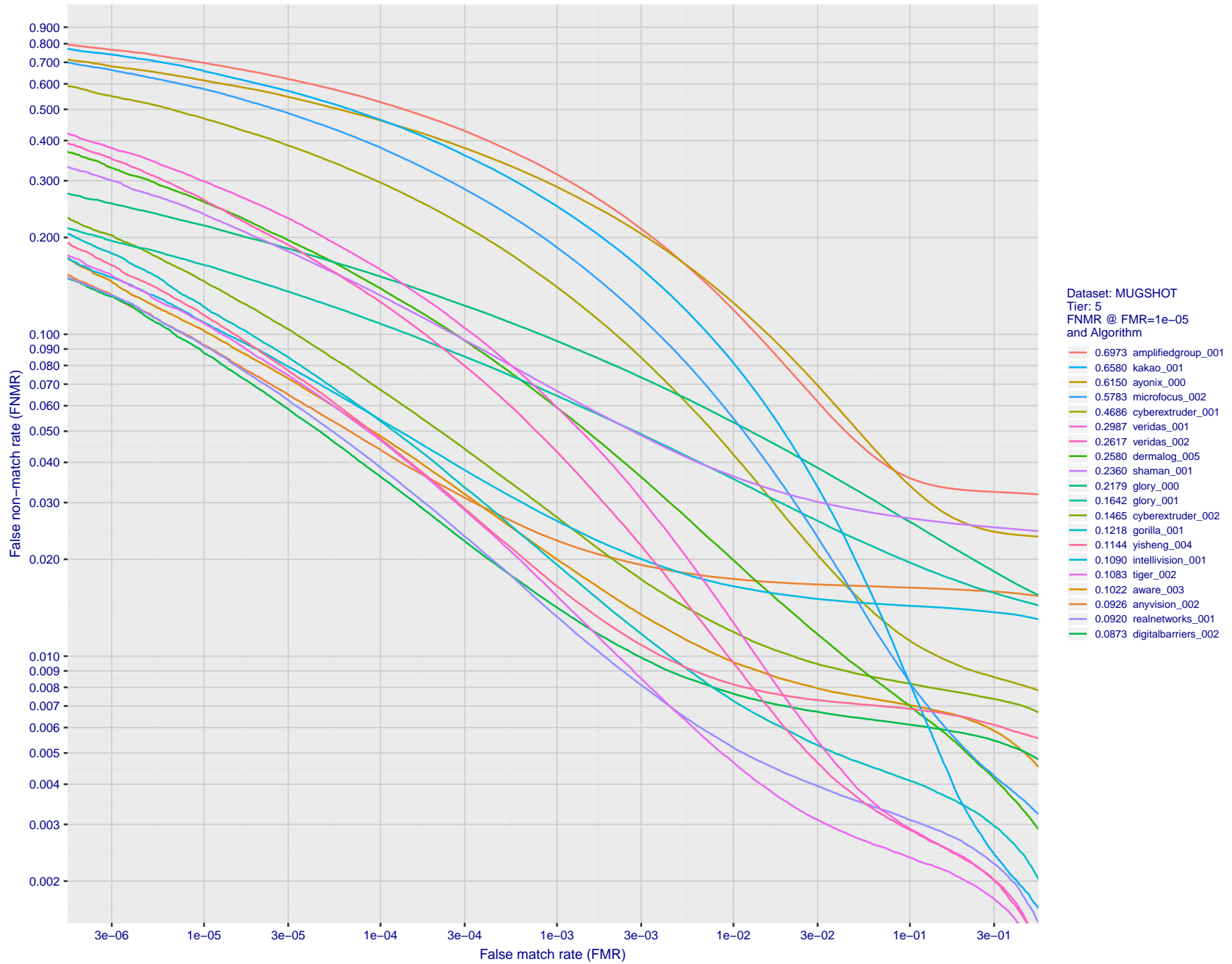


Figure 20: For the mugshot images, detection error tradeoff (DET) characteristics showing false non-match rate vs. false match rate plotted parametrically on threshold, T . The scales are logarithmic in order to show decades of FMR.

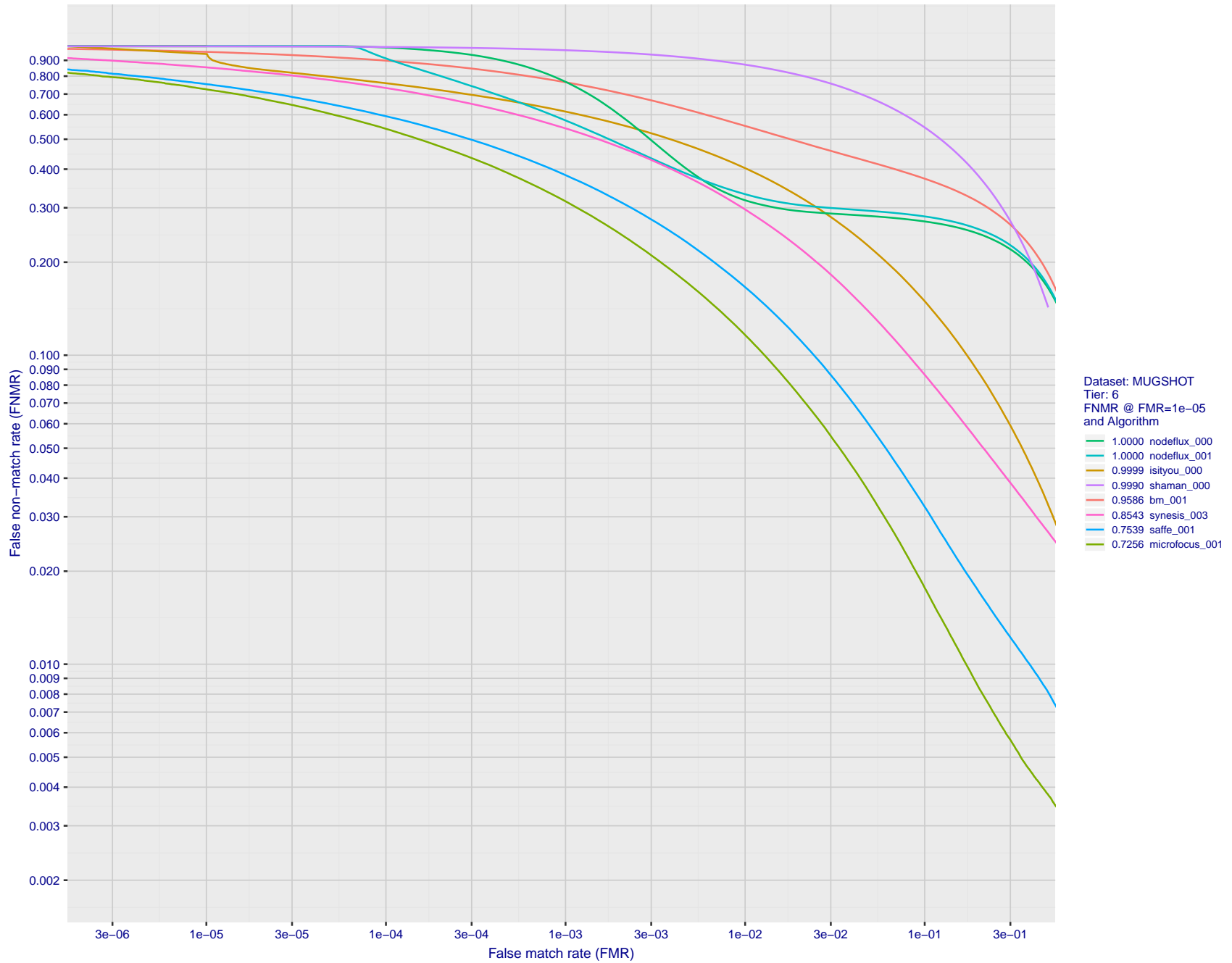
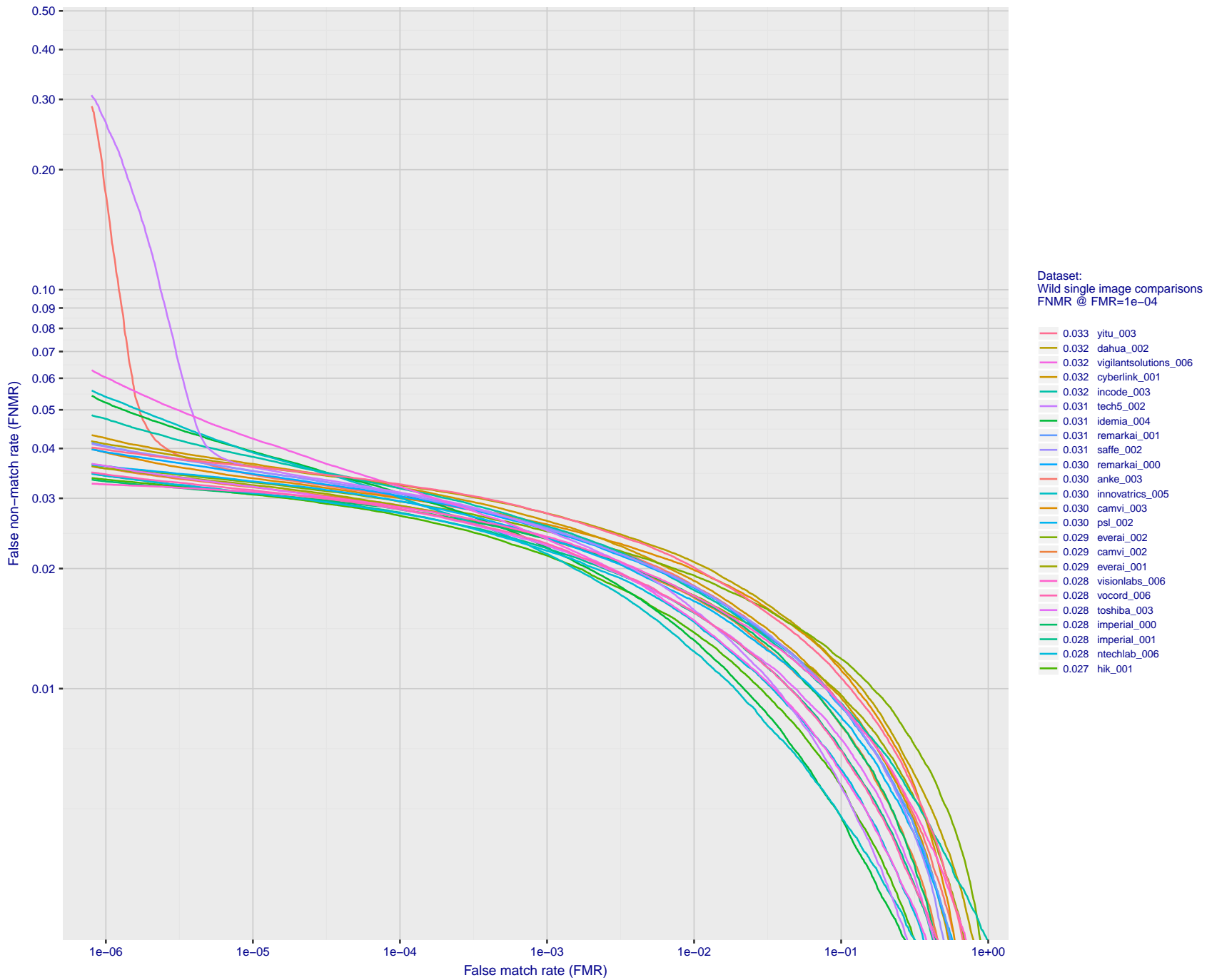
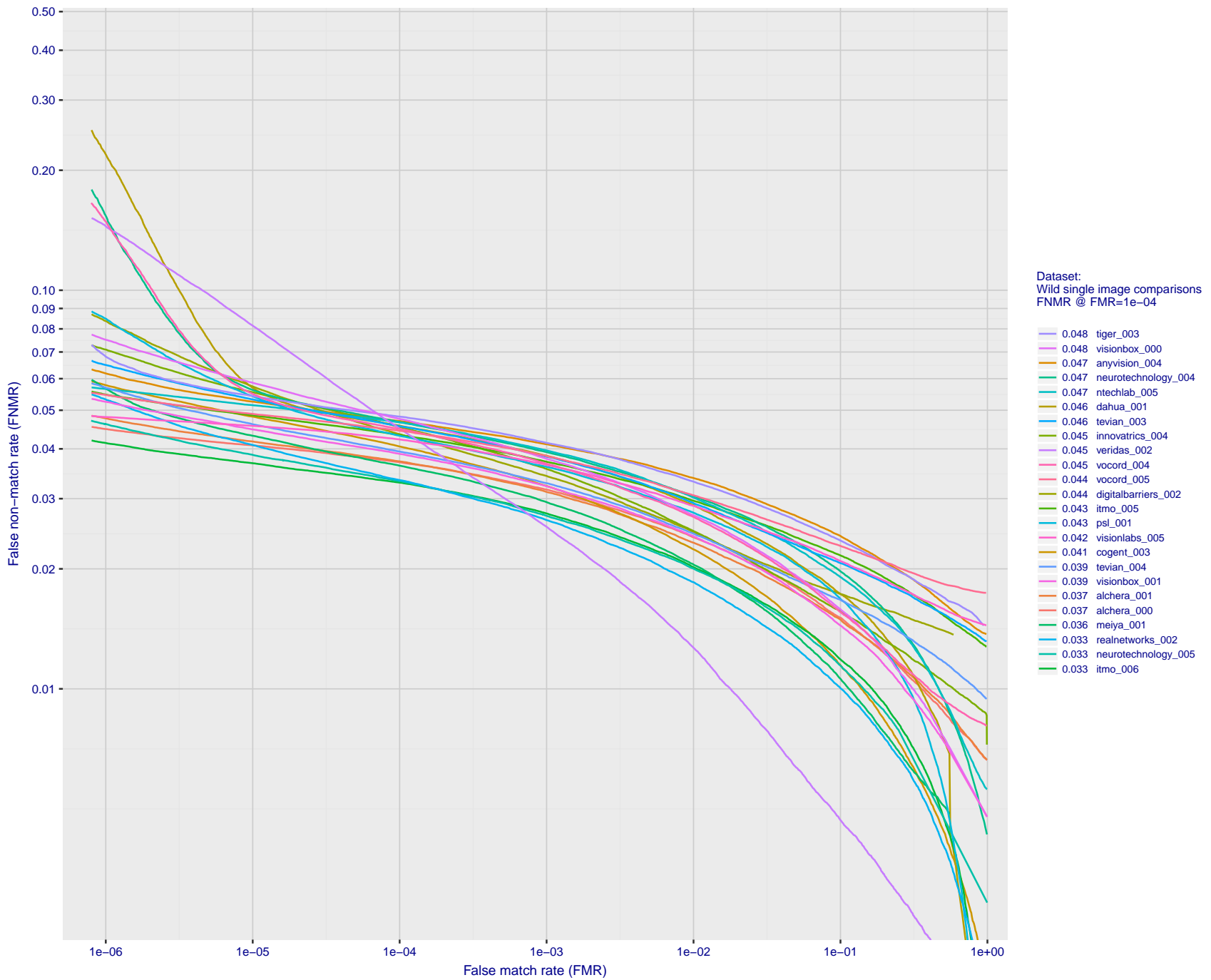


Figure 21: For the mugshot images, detection error tradeoff (DET) characteristics showing false non-match rate vs. false match rate plotted parametrically on threshold, T . The scales are logarithmic in order to show decades of FMR.



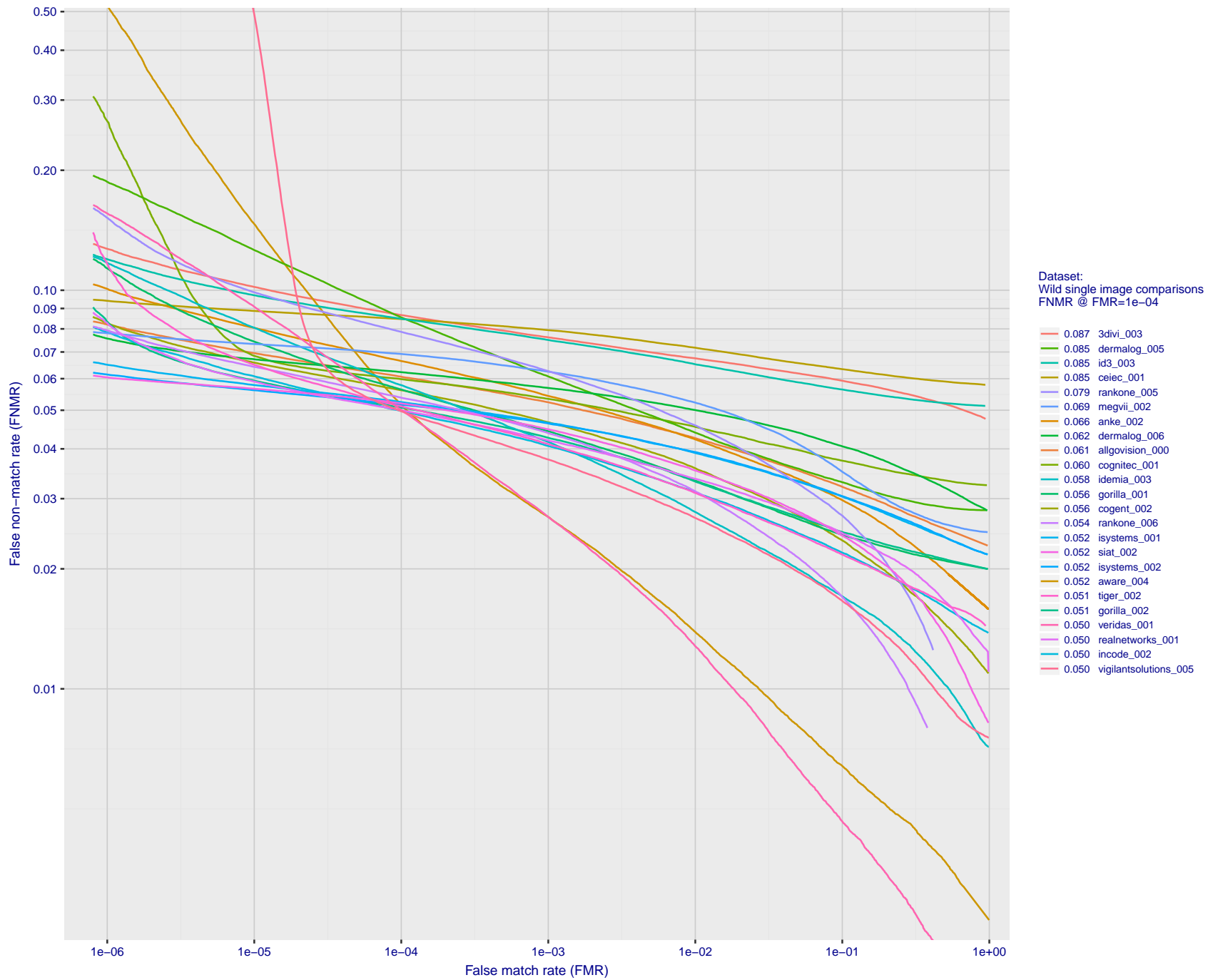
FNMR(T)
FMR(T)
"False non-match rate"
"False match rate"

Figure 22: For the 2018 wild image comparisons, detection error tradeoff (DET) characteristics showing false non-match rate vs. false match rate plotted parametrically on threshold, T . The scales are logarithmic in order to show several decades of FMR.



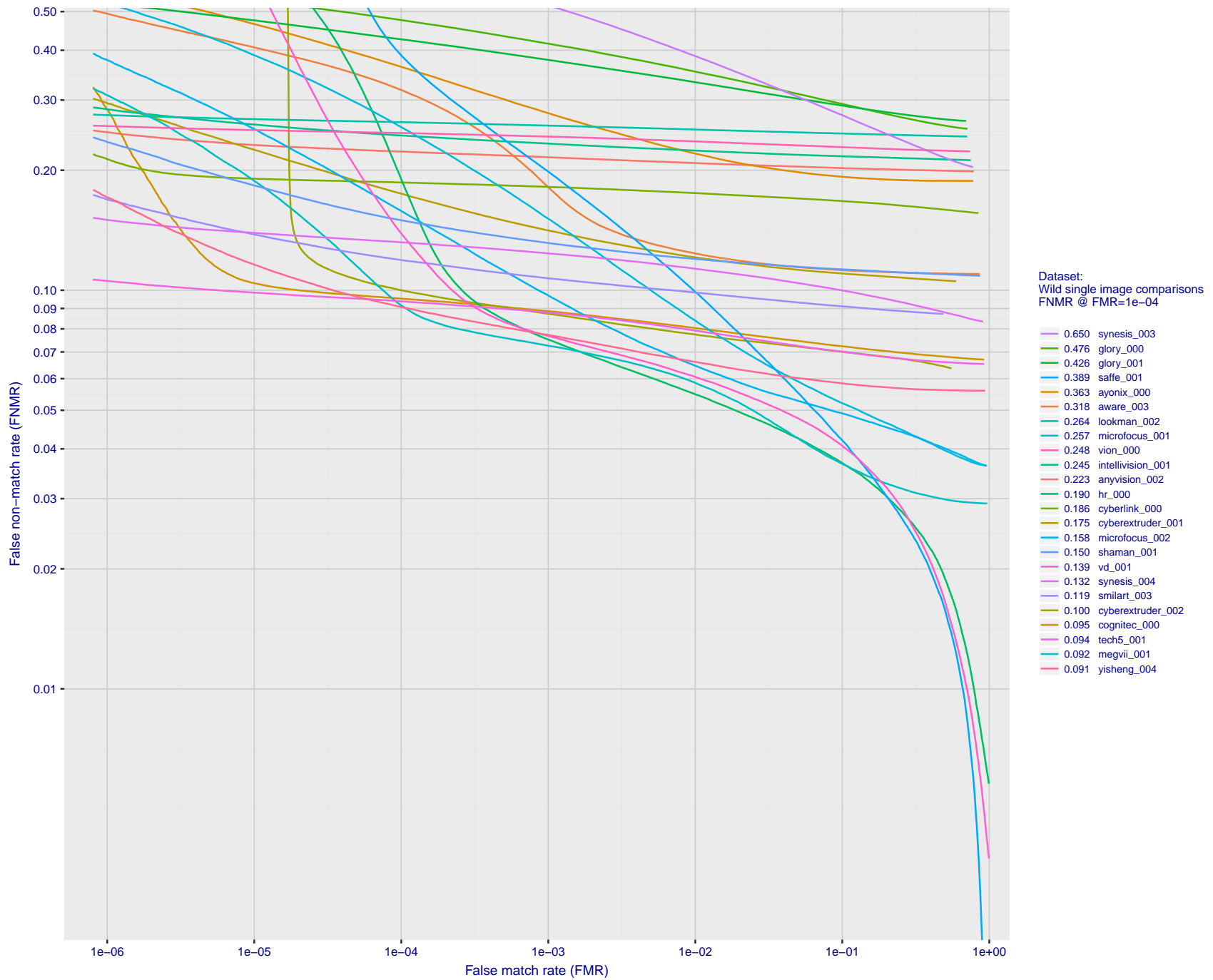
FNMR(T)
FMR(T)
"False non-match rate"
"False match rate"

Figure 23: For the 2018 wild image comparisons, detection error tradeoff (DET) characteristics showing false non-match rate vs. false match rate plotted parametrically on threshold, T . The scales are logarithmic in order to show several decades of FMR.



FNMR(T)
FMR(T)
"False non-match rate"
"False match rate"

Figure 24: For the 2018 wild image comparisons, detection error tradeoff (DET) characteristics showing false non-match rate vs. false match rate plotted parametrically on threshold, T. The scales are logarithmic in order to show several decades of FMR.



FNMR(T)
FMR(T)
"False non-match rate"
"False match rate"

Figure 25: For the 2018 wild image comparisons, detection error tradeoff (DET) characteristics showing false non-match rate vs. false match rate plotted parametrically on threshold, T . The scales are logarithmic in order to show several decades of FMR.

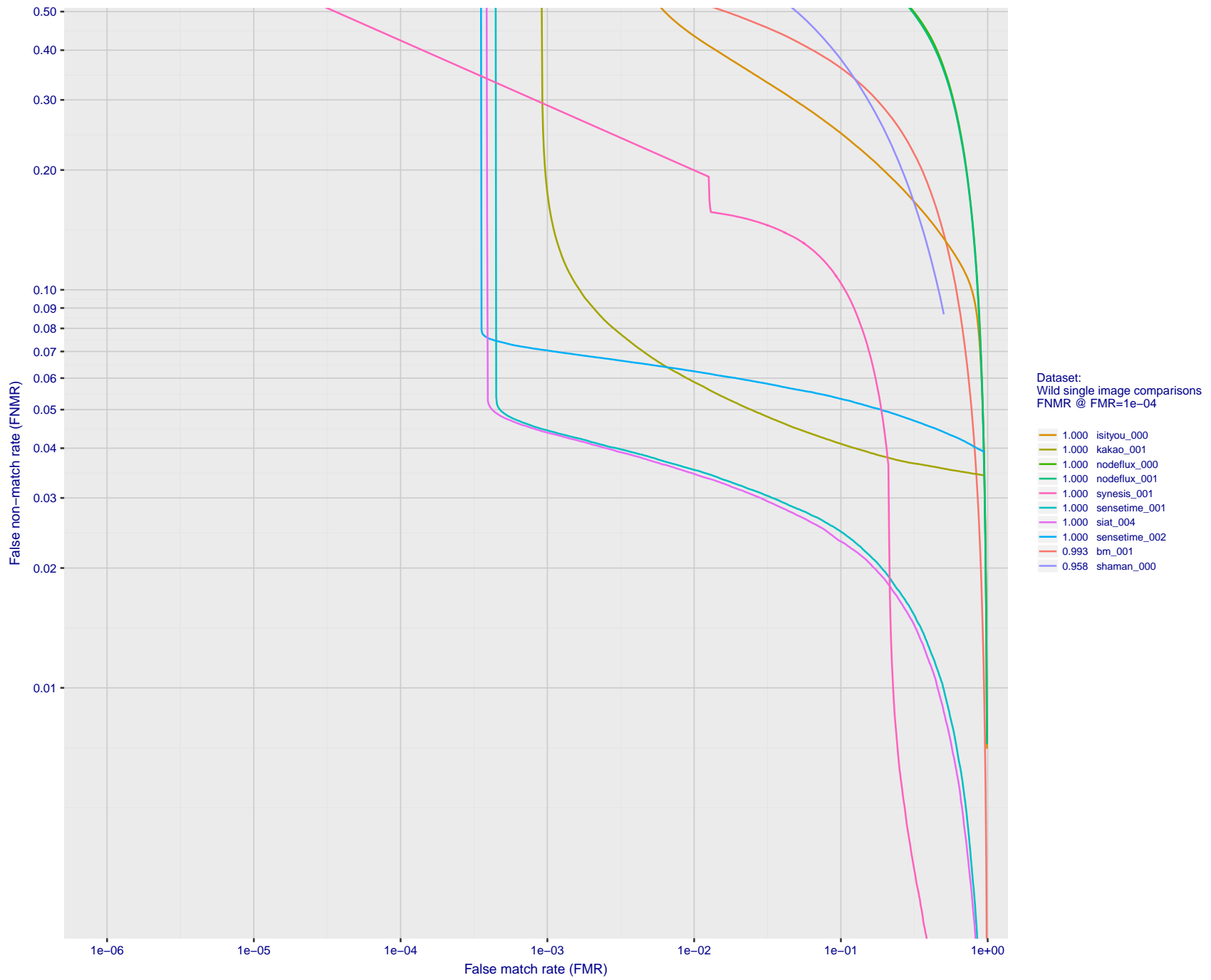


Figure 26: For the 2018 wild image comparisons, detection error tradeoff (DET) characteristics showing false non-match rate vs. false match rate plotted parametrically on threshold, T . The scales are logarithmic in order to show several decades of FMR.

2019 / 04 / 12 09:22:53

FNMR(T)
FMR(T)
"False non-match rate"
"False match rate"

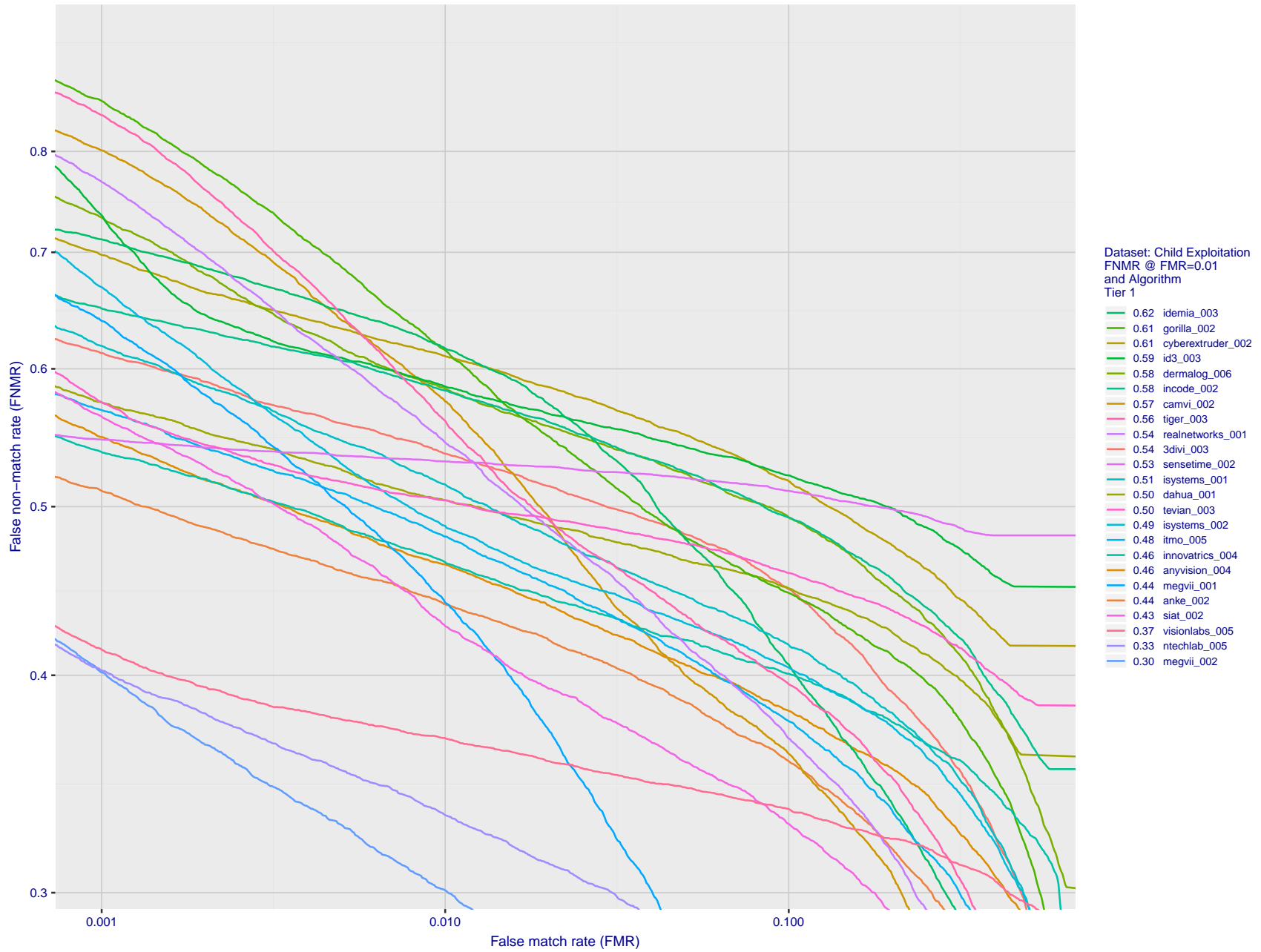


Figure 27: For child exploitation images, detection error tradeoff (DET) characteristics showing false non-match rate vs. false match rate plotted parametrically on threshold, T . The scales are logarithmic in order to show many decades of FMR. Accuracy is poor because many images have adverse quality characteristics, and because detection and enrollment fails.

FNMR(T)
FMR(T)
"False non-match rate"
"False match rate"

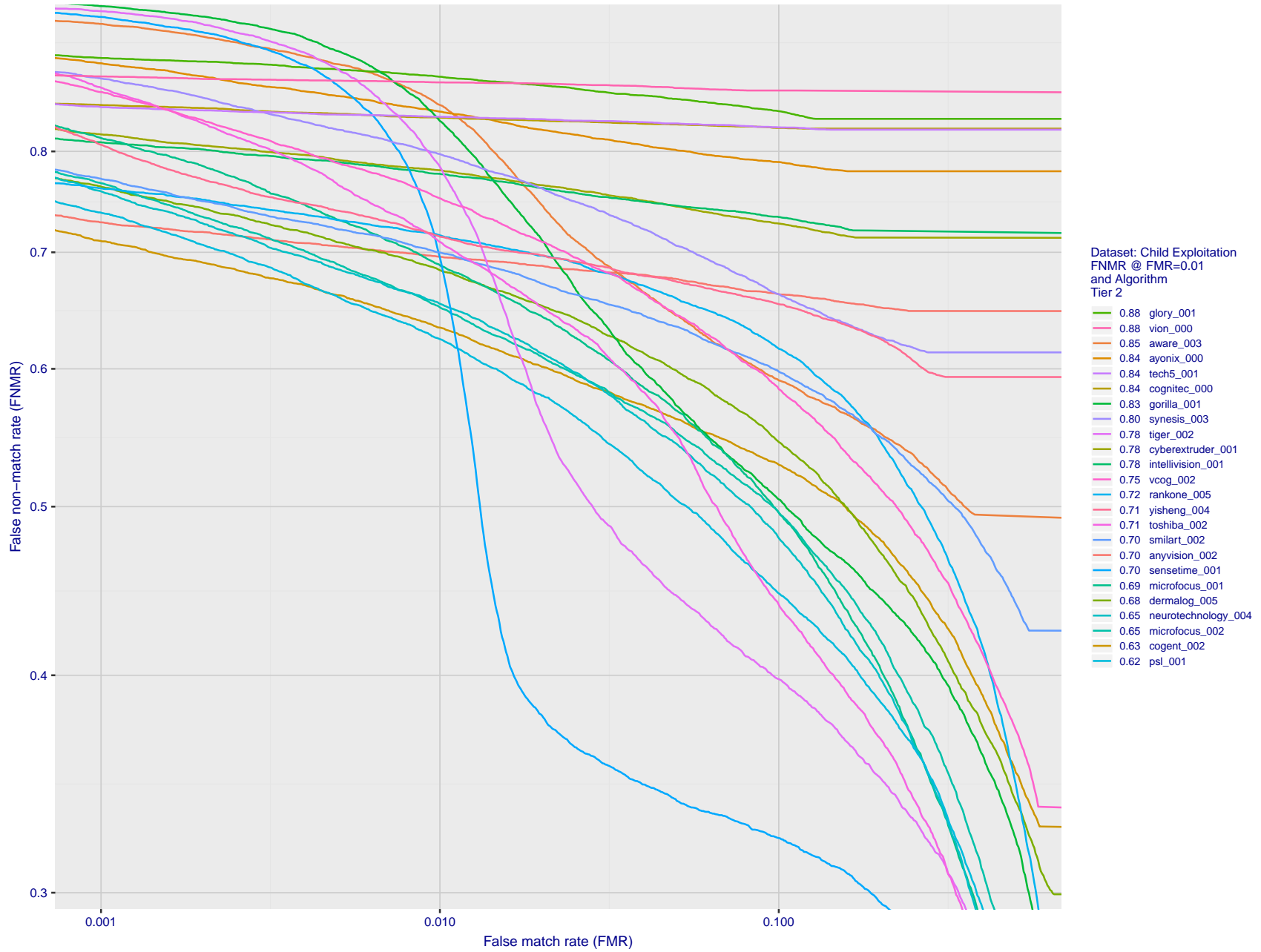
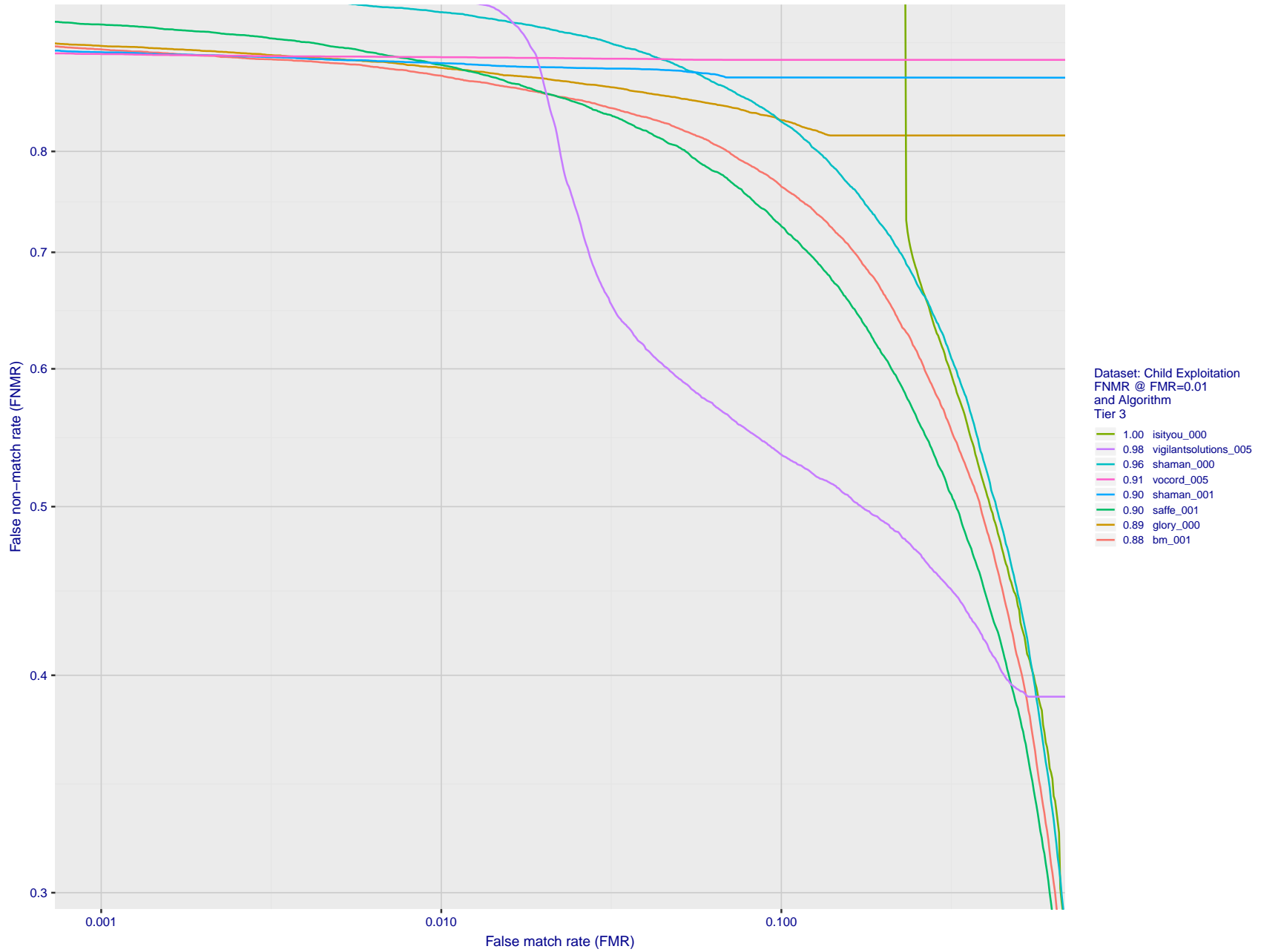


Figure 28: For child exploitation images, detection error tradeoff (DET) characteristics showing false non-match rate vs. false match rate plotted parametrically on threshold, T . The scales are logarithmic in order to show many decades of FMR. Accuracy is poor because many images have adverse quality characteristics, and because detection and enrollment fails.

FNMR(T)
FMR(T)
"False non-match rate"
"False match rate"



FNMR(T)
FMR(T)
"False non-match rate"
"False match rate"

Figure 29: For child exploitation images, detection error tradeoff (DET) characteristics showing false non-match rate vs. false match rate plotted parametrically on threshold, T . The scales are logarithmic in order to show many decades of FMR. Accuracy is poor because many images have adverse quality characteristics, and because detection and enrollment fails.

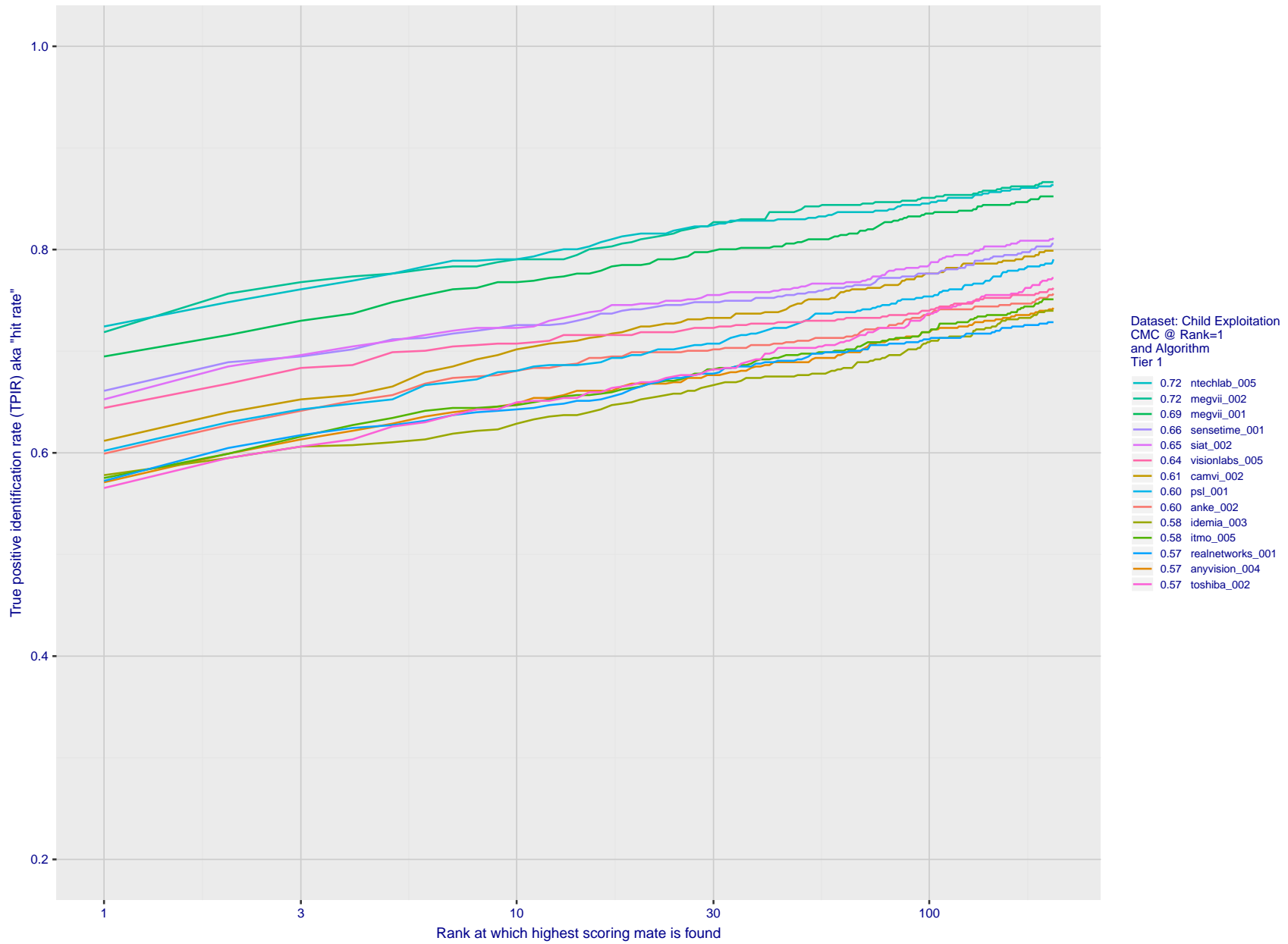


Figure 30: For child exploitation images, cumulative match characteristics (CMC) showing true positive identification rate vs. rank. This is simulation of a one-to-many search experiment - see discussion in section 3.2. The scales are logarithmic in order to show the effect of long candidate lists. Accuracy is poor but much improved relative to the 1:1 DETs of Fig. 29 because a search can succeed if any of a subject's several enrolled images matches the search image with a high score.

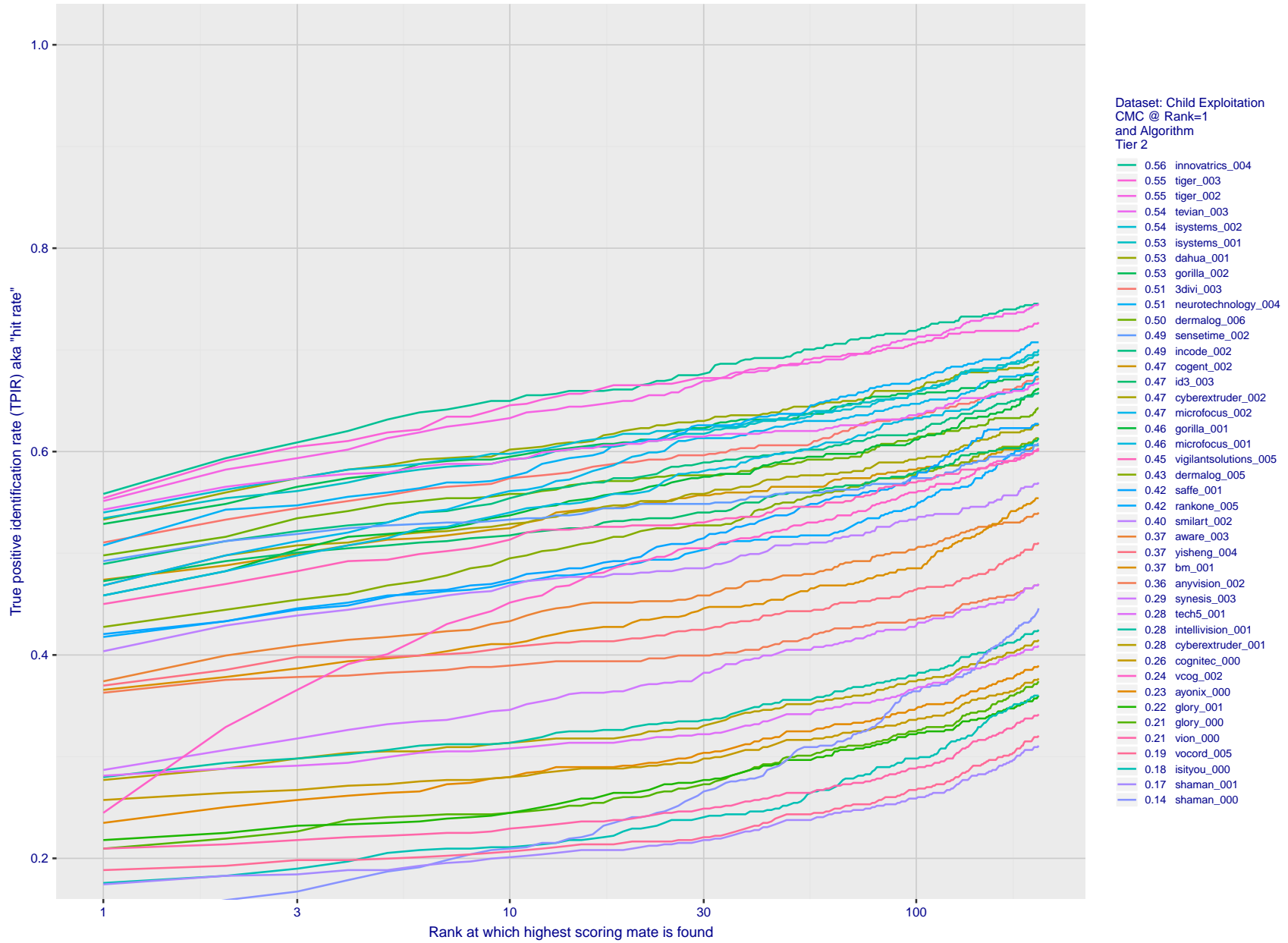


Figure 31: For child exploitation images, cumulative match characteristics (CMC) showing true positive identification rate vs. rank. This is simulation of a one-to-many search experiment - see discussion in section 3.2. The scales are logarithmic in order to show the effect of long candidate lists. Accuracy is poor but much improved relative to the 1:1 DETs of Fig. 29 because a search can succeed if any of a subject's several enrolled images matches the search image with a high score.

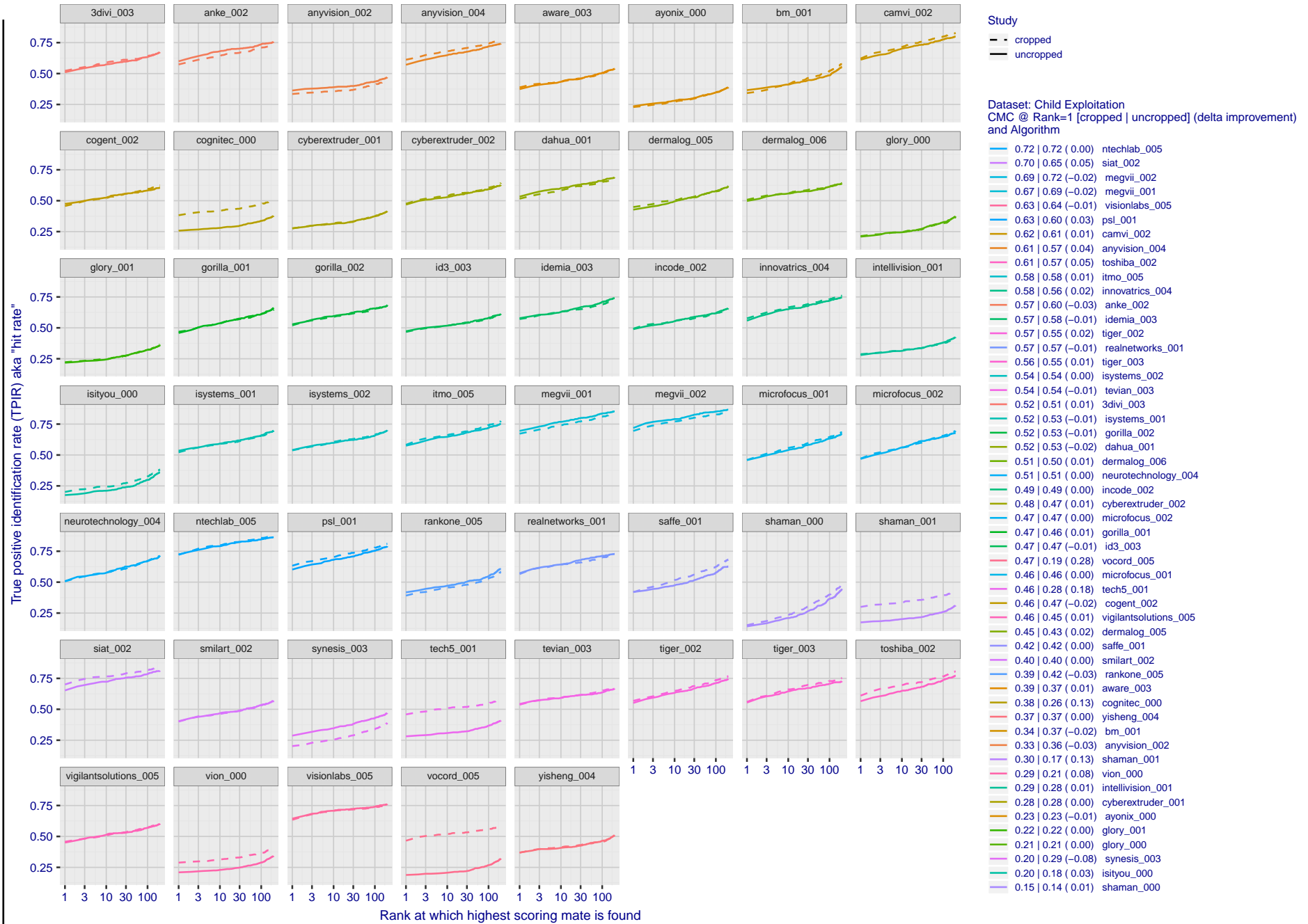


Figure 32: For child exploitation images, cumulative match characteristics (CMC) showing true positive identification rate vs. rank for two cases: 1. Whole image provided to the algorithm; 2. Human annotated rectangular region, cropped and provided to the algorithm. The difference between the traces is associated with detection of difficult faces, and fine localization.

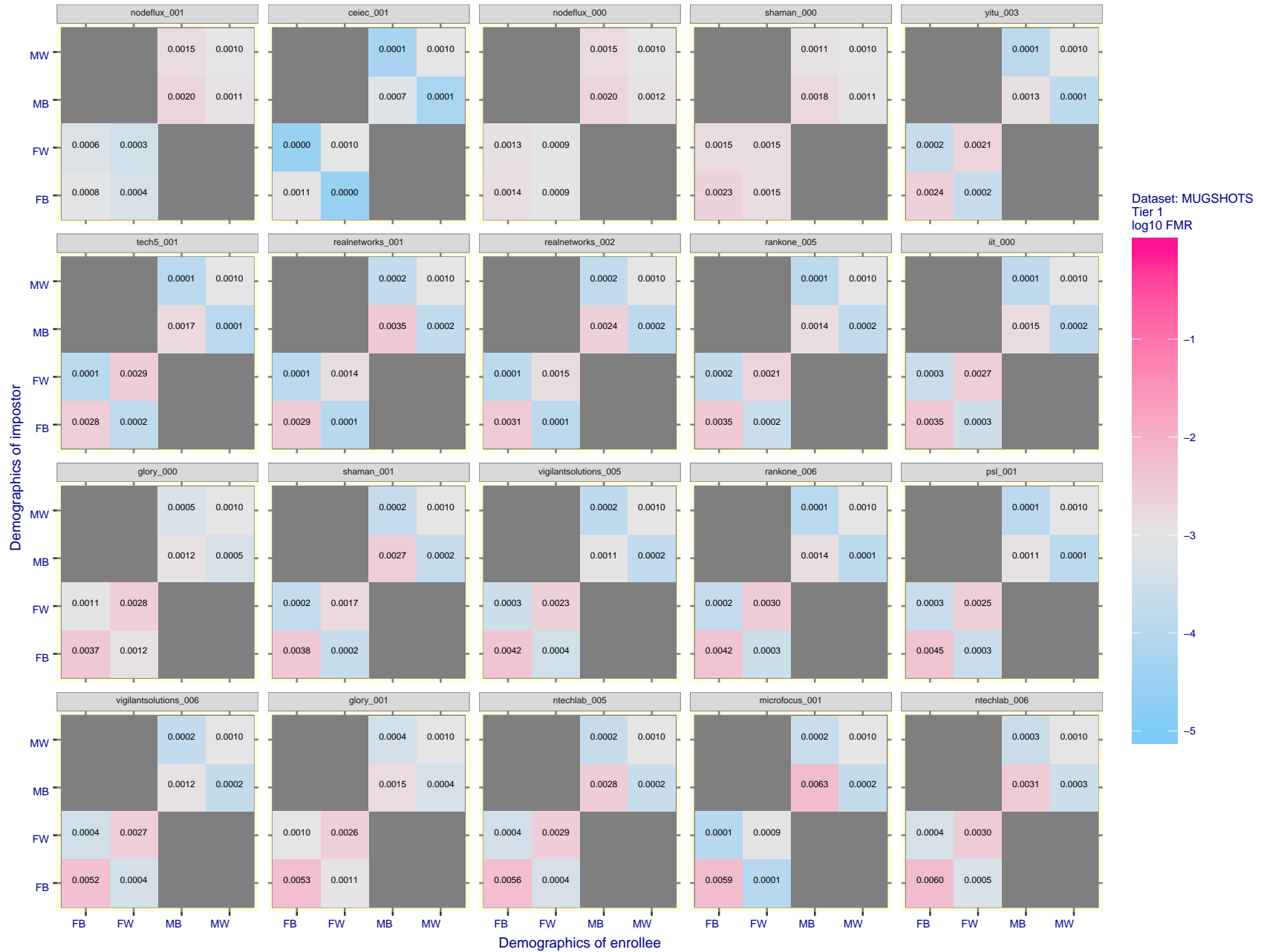


Figure 33: For the mugshot images, FMR for same-sex impostor pairs of images annotated with codes for black female, black male, white female, white male. The threshold is set for each algorithm to give FMR = 0.001 for white males which is the demographic that usually gives the lowest FMR. This means the top right box is the same color in all panels. The panels are sorted over multiple pages in order of FMR on black females, which is the demographic that usually gives the highest FMR.

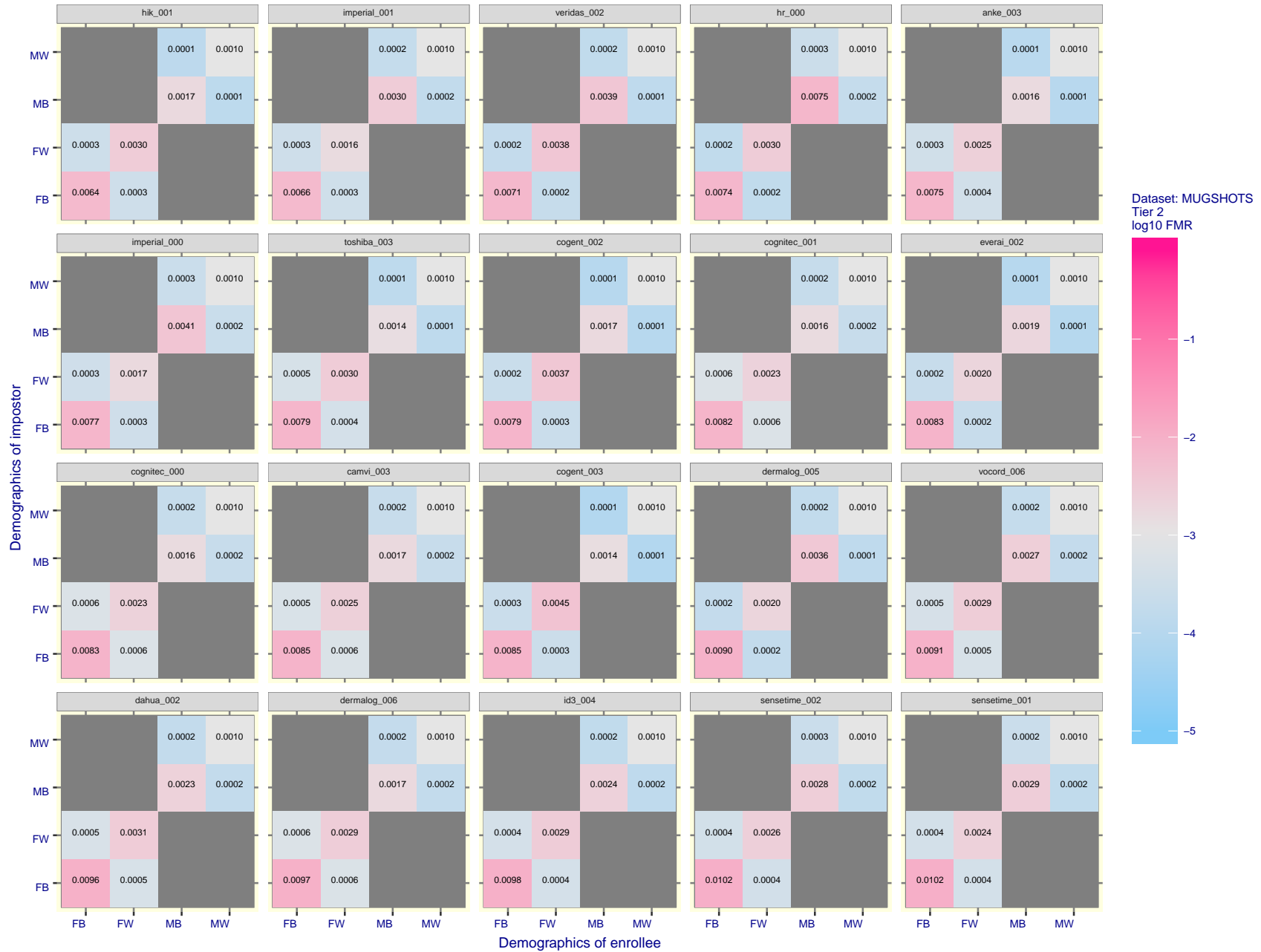


Figure 34: For the mugshot images, FMR for same-sex impostor pairs of images annotated with codes for black female, black male, white female, white male. The threshold is set for each algorithm to give FMR = 0.001 for white males which is the demographic that usually gives the lowest FMR. This means the top right box is the same color in all panels. The panels are sorted over multiple pages in order of FMR on black females, which is the demographic that usually gives the highest FMR.

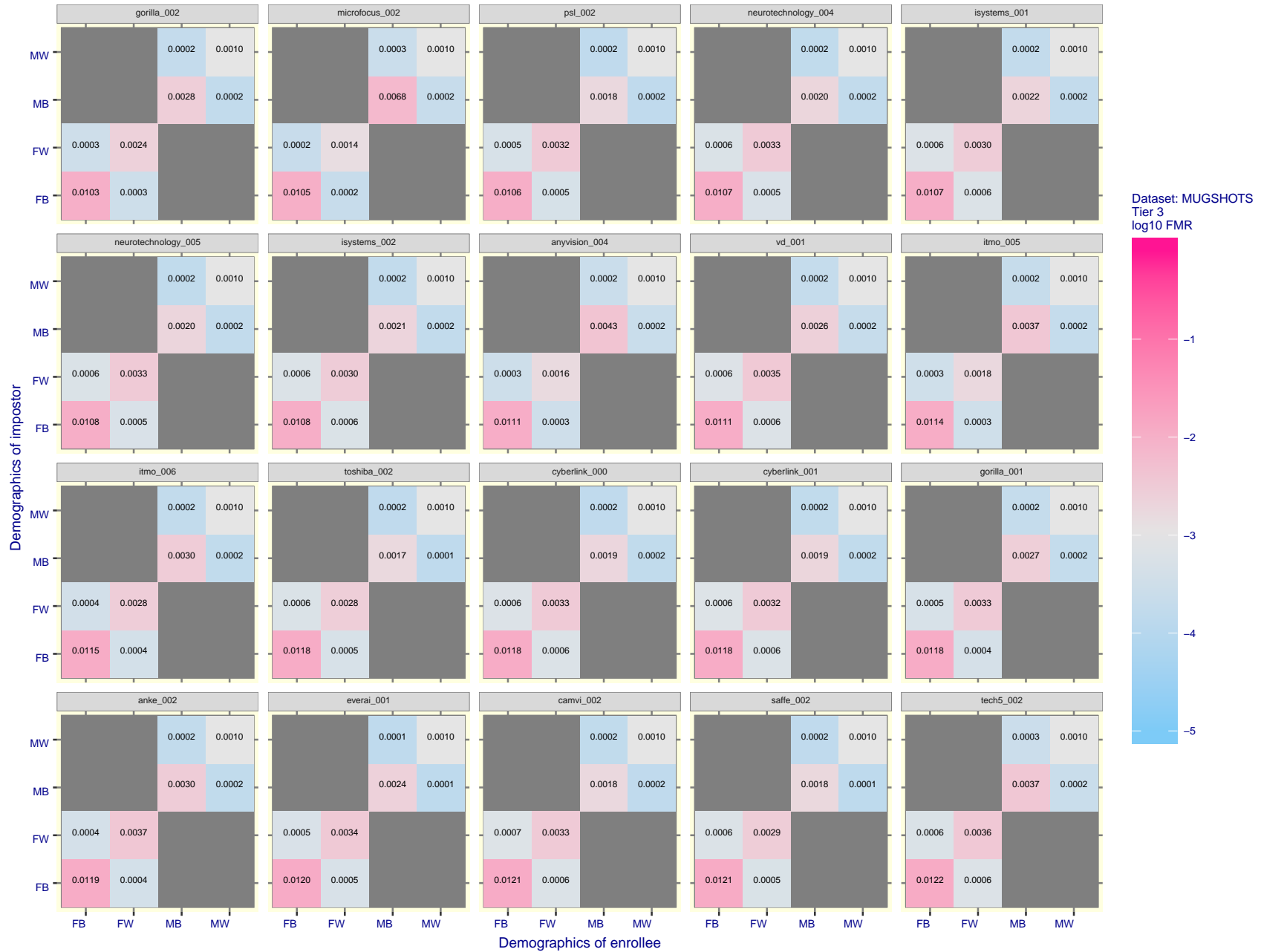


Figure 35: For the mugshot images, FMR for same-sex impostor pairs of images annotated with codes for black female, black male, white female, white male. The threshold is set for each algorithm to give FMR = 0.001 for white males which is the demographic that usually gives the lowest FMR. This means the top right box is the same color in all panels. The panels are sorted over multiple pages in order of FMR on black females, which is the demographic that usually gives the highest FMR.

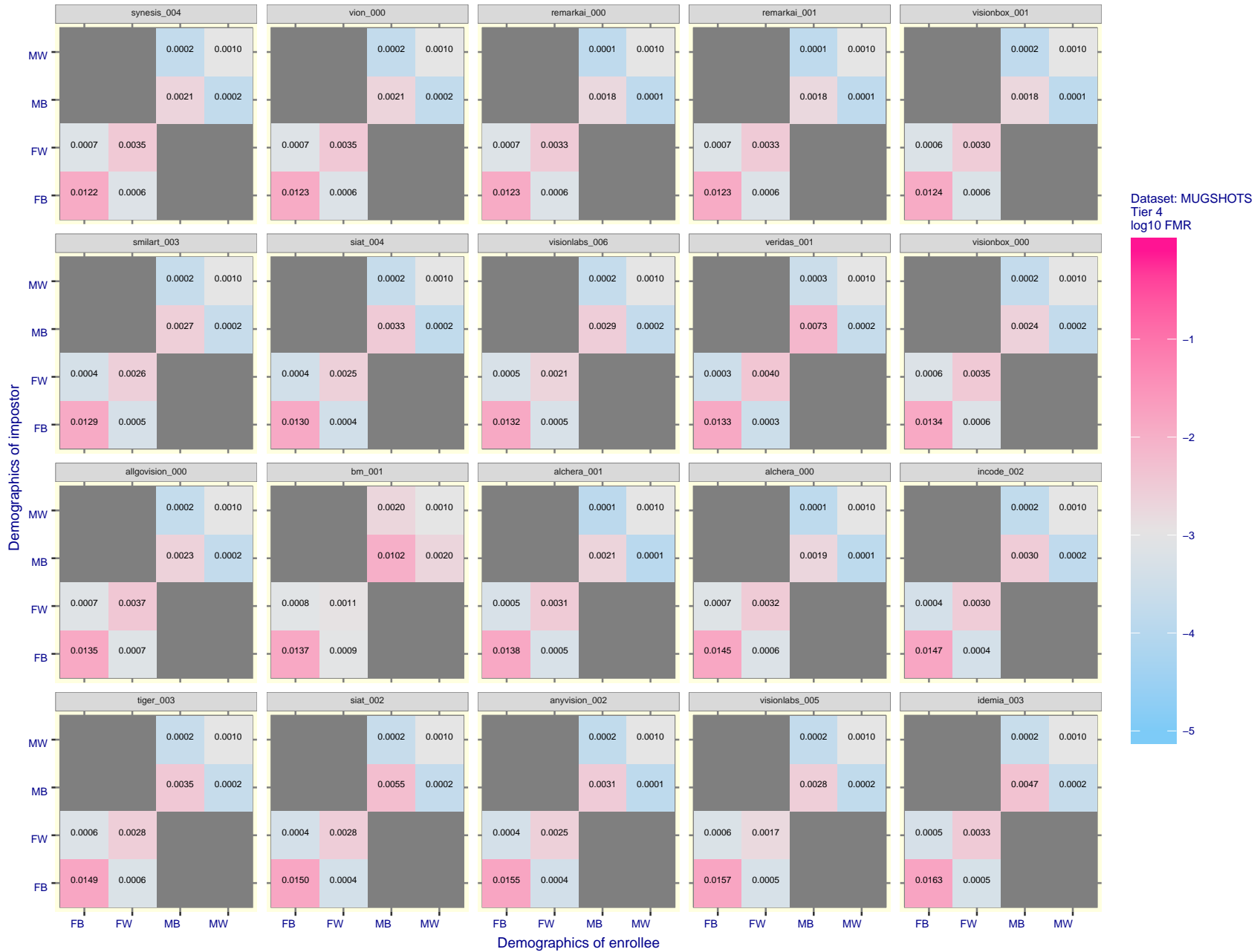


Figure 36: For the mugshot images, FMR for same-sex impostor pairs of images annotated with codes for black female, black male, white female, white male. The threshold is set for each algorithm to give FMR = 0.001 for white males which is the demographic that usually gives the lowest FMR. This means the top right box is the same color in all panels. The panels are sorted over multiple pages in order of FMR on black females, which is the demographic that usually gives the highest FMR.

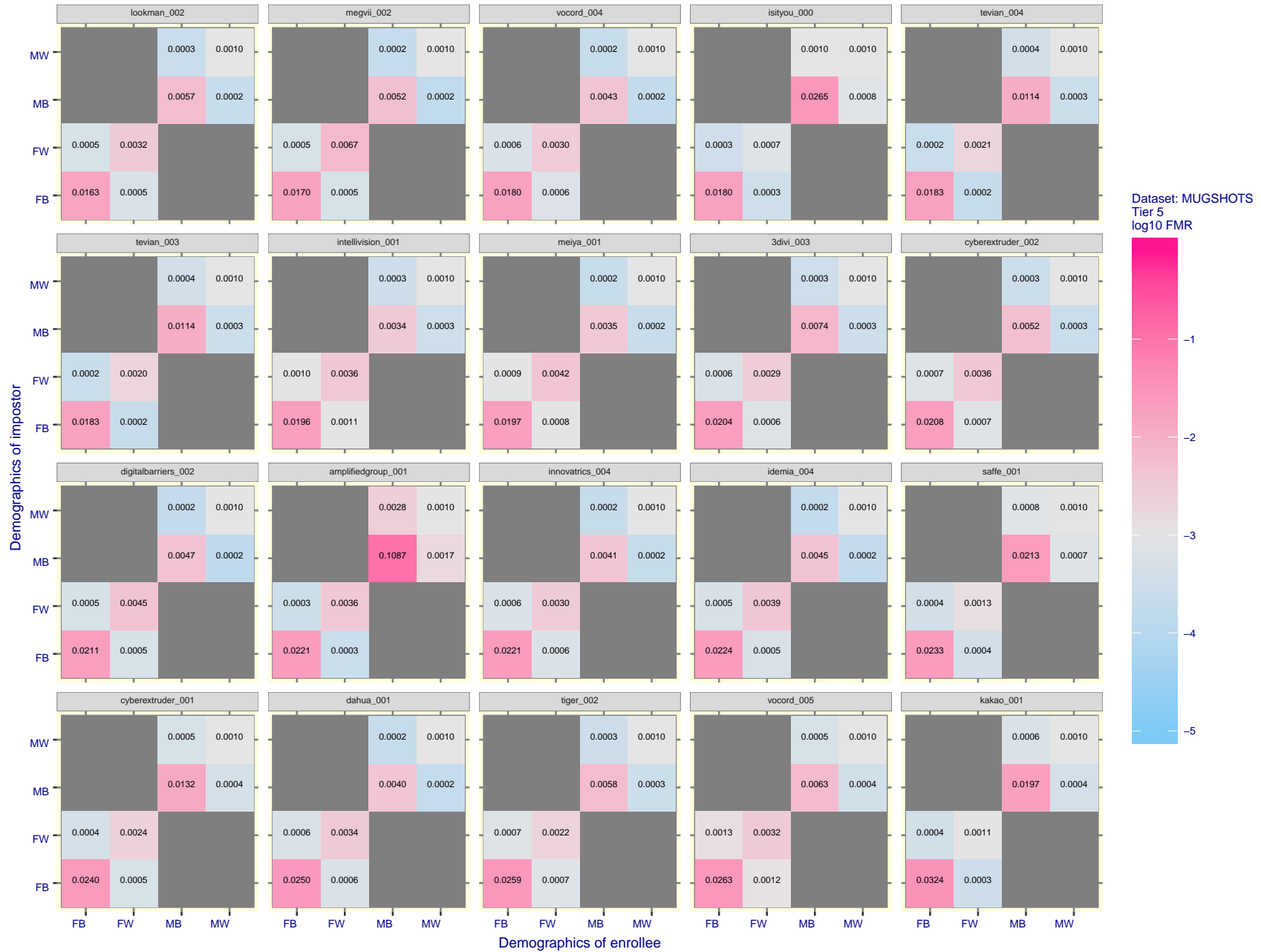


Figure 37: For the mugshot images, FMR for same-sex impostor pairs of images annotated with codes for black female, black male, white female, white male. The threshold is set for each algorithm to give FMR = 0.001 for white males which is the demographic that usually gives the lowest FMR. This means the top right box is the same color in all panels. The panels are sorted over multiple pages in order of FMR on black females, which is the demographic that usually gives the highest FMR.

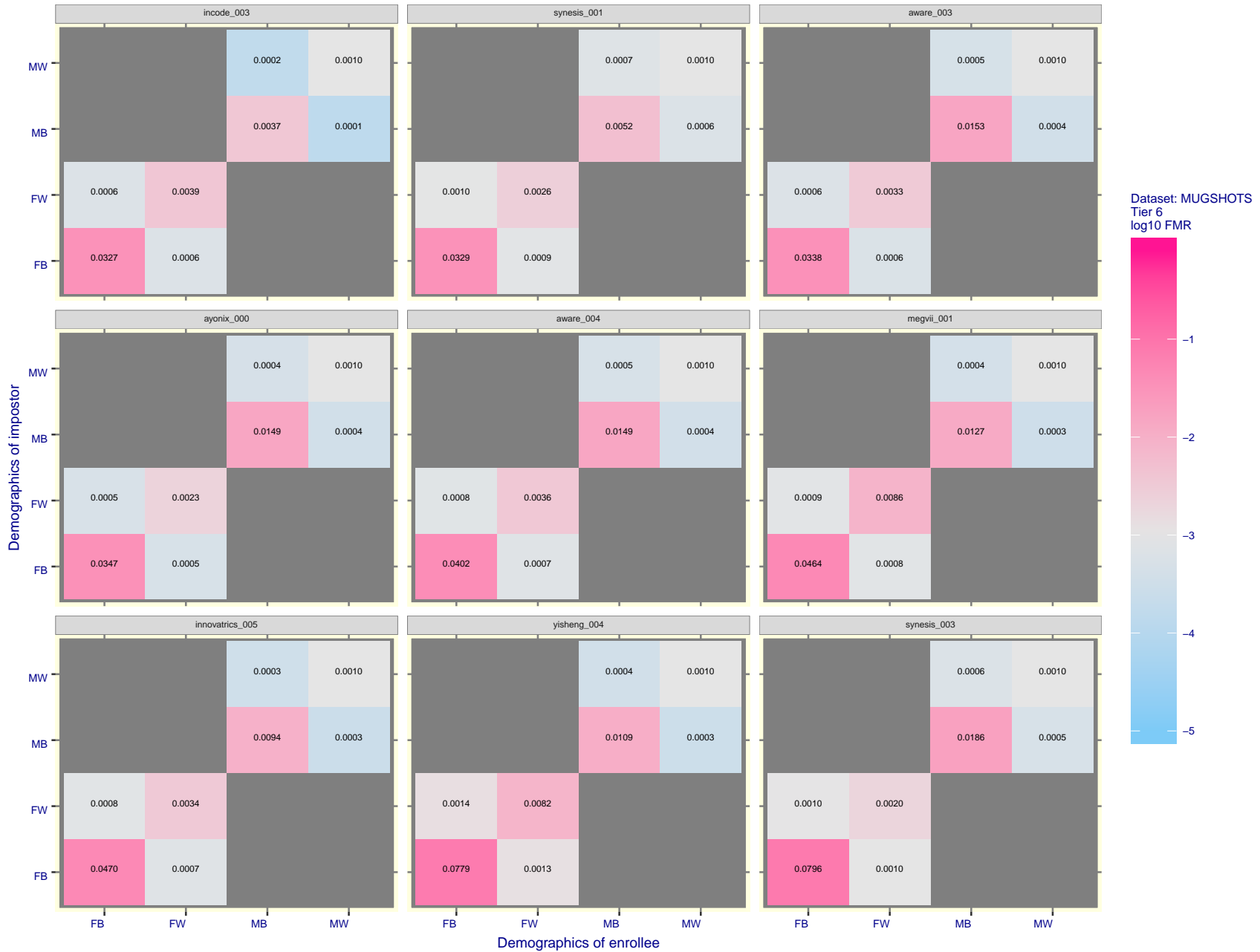


Figure 38: For the mugshot images, FMR for same-sex impostor pairs of images annotated with codes for black female, black male, white female, white male. The threshold is set for each algorithm to give $FMR = 0.001$ for white males which is the demographic that usually gives the lowest FMR. This means the top right box is the same color in all panels. The panels are sorted over multiple pages in order of FMR on black females, which is the demographic that usually gives the highest FMR.

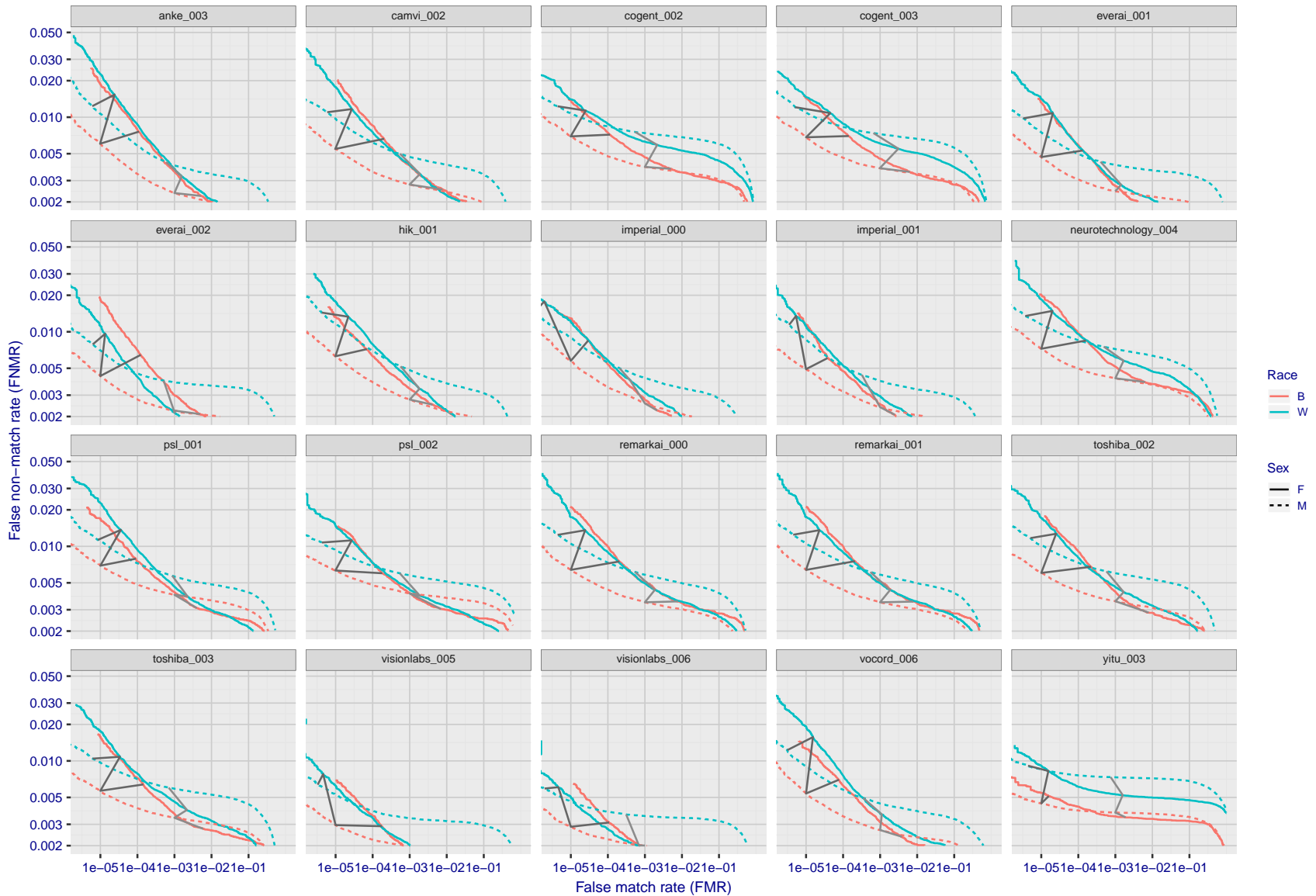
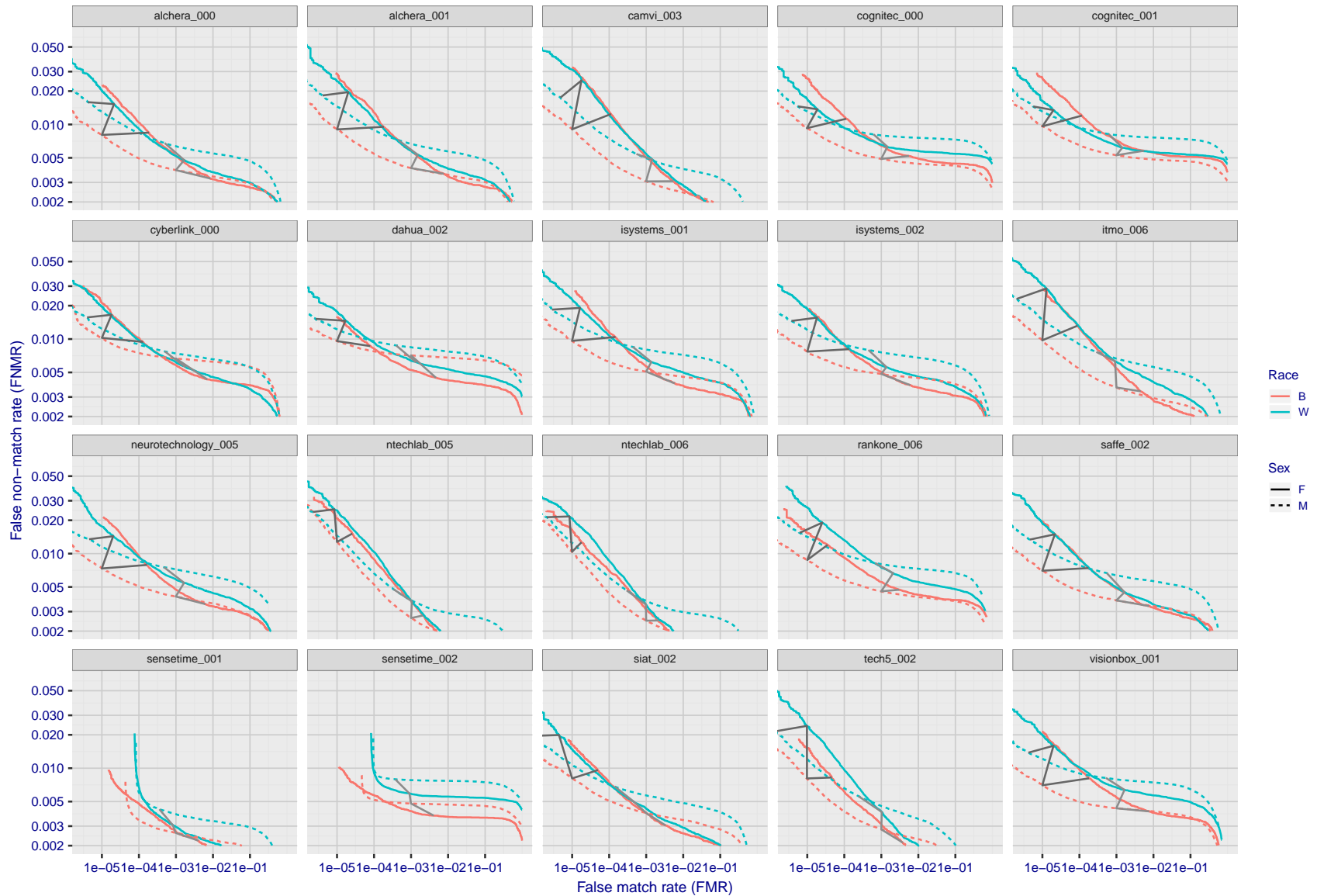


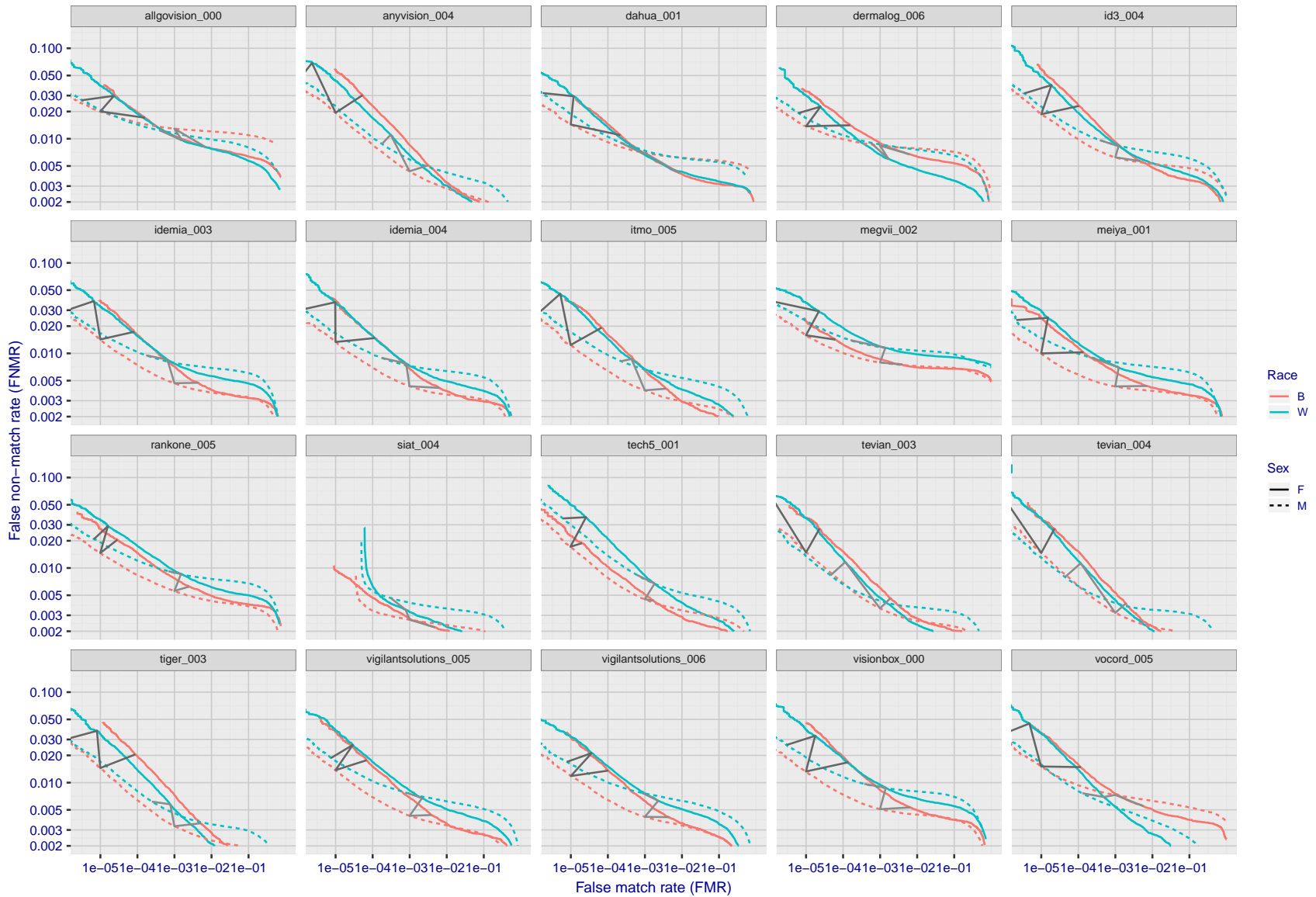
Figure 39: For the mugshot images, error tradeoff characteristics for white females, black females, black males and white males. The Z-shaped grey lines correspond to fixed thresholds, showing both FNMR and FMR vary at one T value. Note: Many of the plots will naively be read as saying women gives worse error rates than men because the solid traces lie above the dotted ones. However, this is misleading and incomplete: The grey lines show the traces reveal horizontal shifts. Thus for the cogent-003 algorithm FNMR for men is higher than for women at a fixed threshold but, at the same time, FMR is higher for women - see Figure 59. As access control systems almost always operate at a fixed threshold, the naive interpretation is incorrect.

FNMR(T)
FMR(T)
"False non-match rate"
"False match rate"



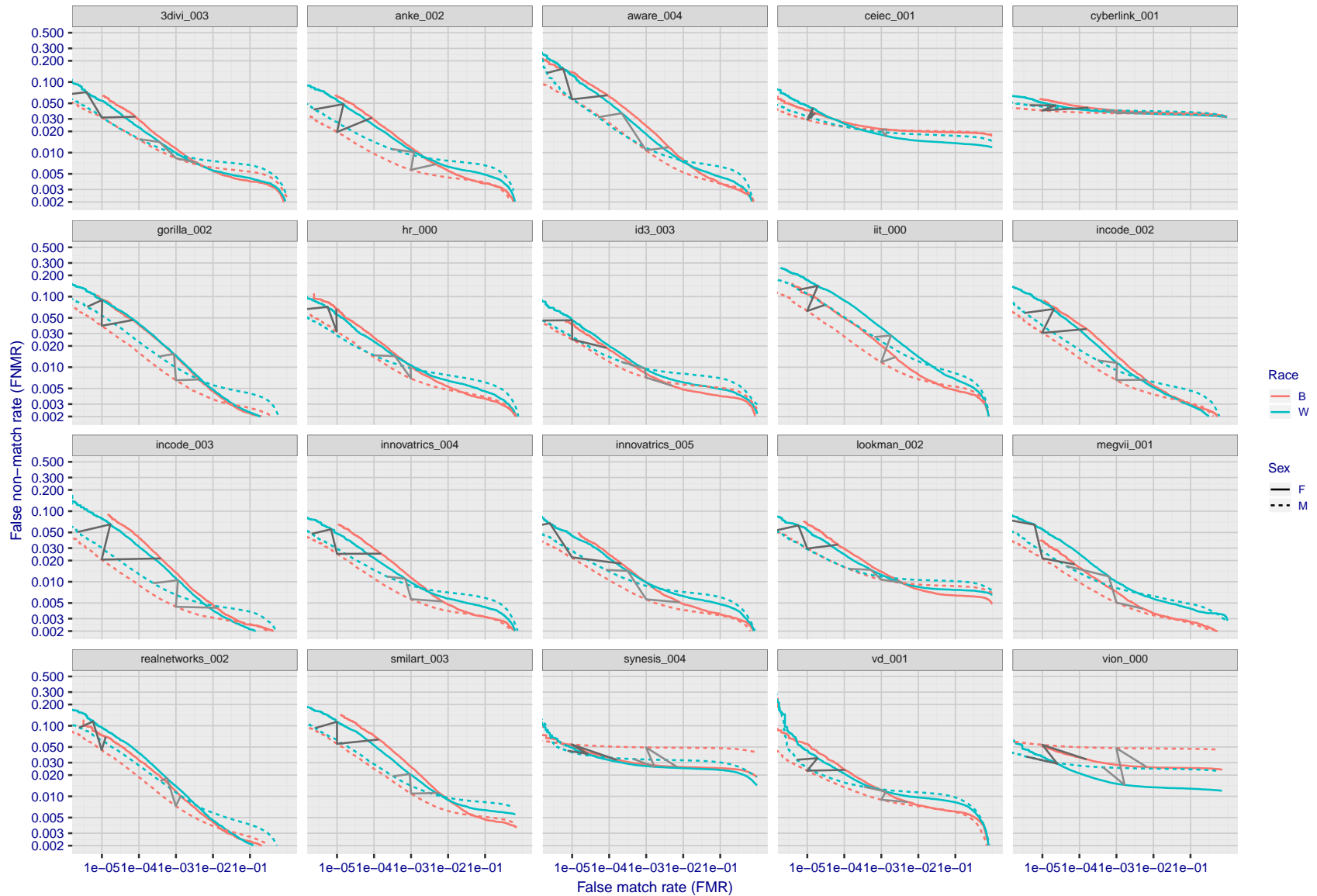
FNMR(T)
FMR(T)
"False non-match rate"
"False match rate"

Figure 40: For the mugshot images, error tradeoff characteristics for white females, black females, black males and white males. The Z-shaped grey lines correspond to fixed thresholds, showing both FNMR and FMR vary at one T value. Note: Many of the plots will naively be read as saying women gives worse error rates than men because the solid traces lie above the dotted ones. However, this is misleading and incomplete: The grey lines show the traces reveal horizontal shifts. Thus for the cogent-003 algorithm FNMR for men is higher than for women at a fixed threshold but, at the same time, FMR is higher for women - see Figure 59. As access control systems almost always operate at a fixed threshold, the naive interpretation is incorrect.



FNMR(T)
FMR(T)
"False non-match rate"
"False match rate"

Figure 41: For the mugshot images, error tradeoff characteristics for white females, black females, black males and white males. The Z-shaped grey lines correspond to fixed thresholds, showing both FNMR and FMR vary at one T value. Note: Many of the plots will naively be read as saying women gives worse error rates than men because the solid traces lie above the dotted ones. However, this is misleading and incomplete: The grey lines show the traces reveal horizontal shifts. Thus for the cogent-003 algorithm FNMR for men is higher than for women at a fixed threshold but, at the same time, FMR is higher for women - see Figure 59. As access control systems almost always operate at a fixed threshold, the naive interpretation is incorrect.



FNMR(T)
FMR(T)
"False non-match rate"
"False match rate"

Figure 42: For the mugshot images, error tradeoff characteristics for white females, black females, black males and white males. The Z-shaped grey lines correspond to fixed thresholds, showing both FNMR and FMR vary at one T value. Note: Many of the plots will naively be read as saying women gives worse error rates than men because the solid traces lie above the dotted ones. However, this is misleading and incomplete: The grey lines show the traces reveal horizontal shifts. Thus for the cogent-003 algorithm FNMR for men is higher than for women at a fixed threshold but, at the same time, FMR is higher for women - see Figure 59. As access control systems almost always operate at a fixed threshold, the naive interpretation is incorrect.

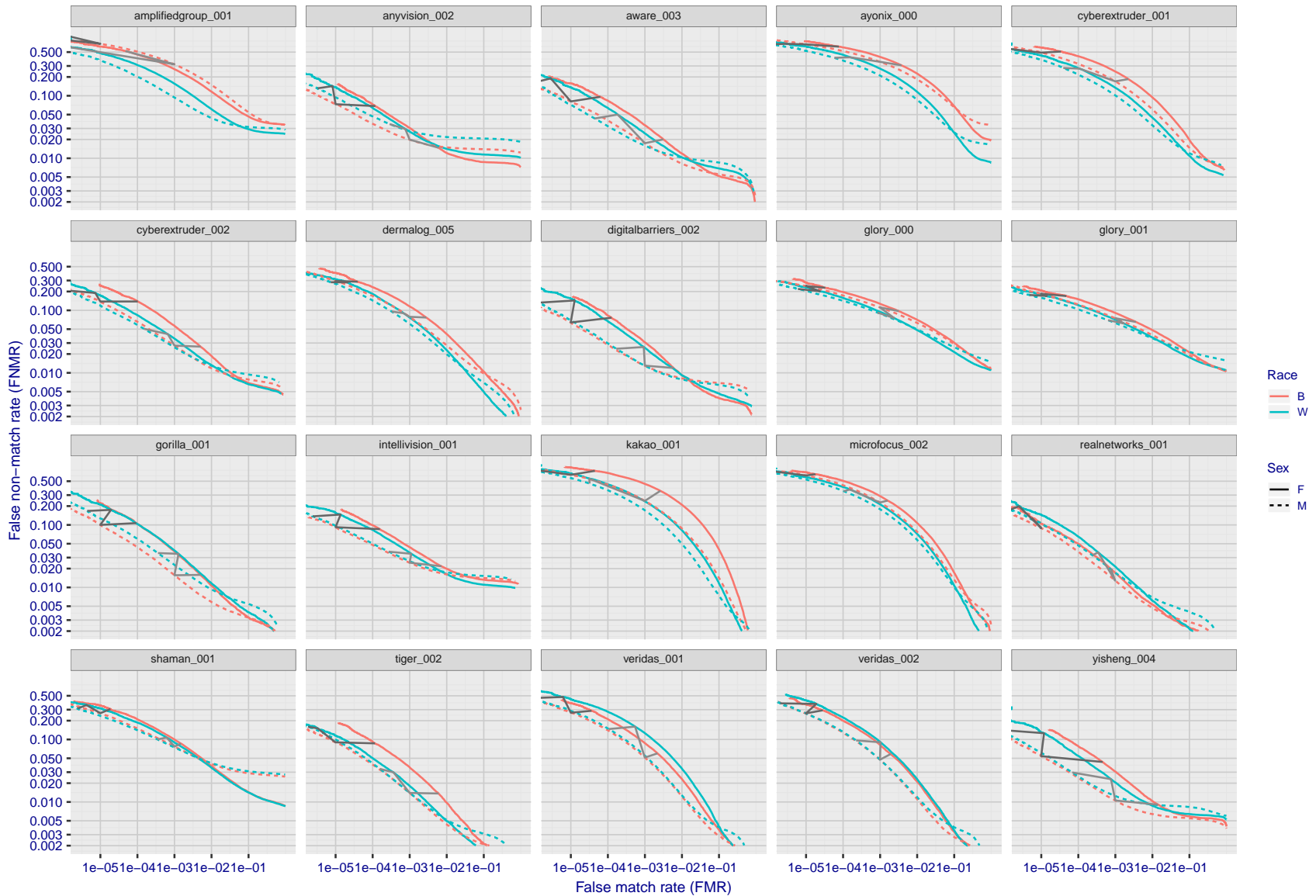


Figure 43: For the mugshot images, error tradeoff characteristics for white females, black females, black males and white males. The Z-shaped grey lines correspond to fixed thresholds, showing both FNMR and FMR vary at one T value. Note: Many of the plots will naively be read as saying women gives worse error rates than men because the solid traces lie above the dotted ones. However, this is misleading and incomplete: The grey lines show the traces reveal horizontal shifts. Thus for the cogent-003 algorithm FNMR for men is higher than for women at a fixed threshold but, at the same time, FMR is higher for women - see Figure 59. As access control systems almost always operate at a fixed threshold, the naive interpretation is incorrect.

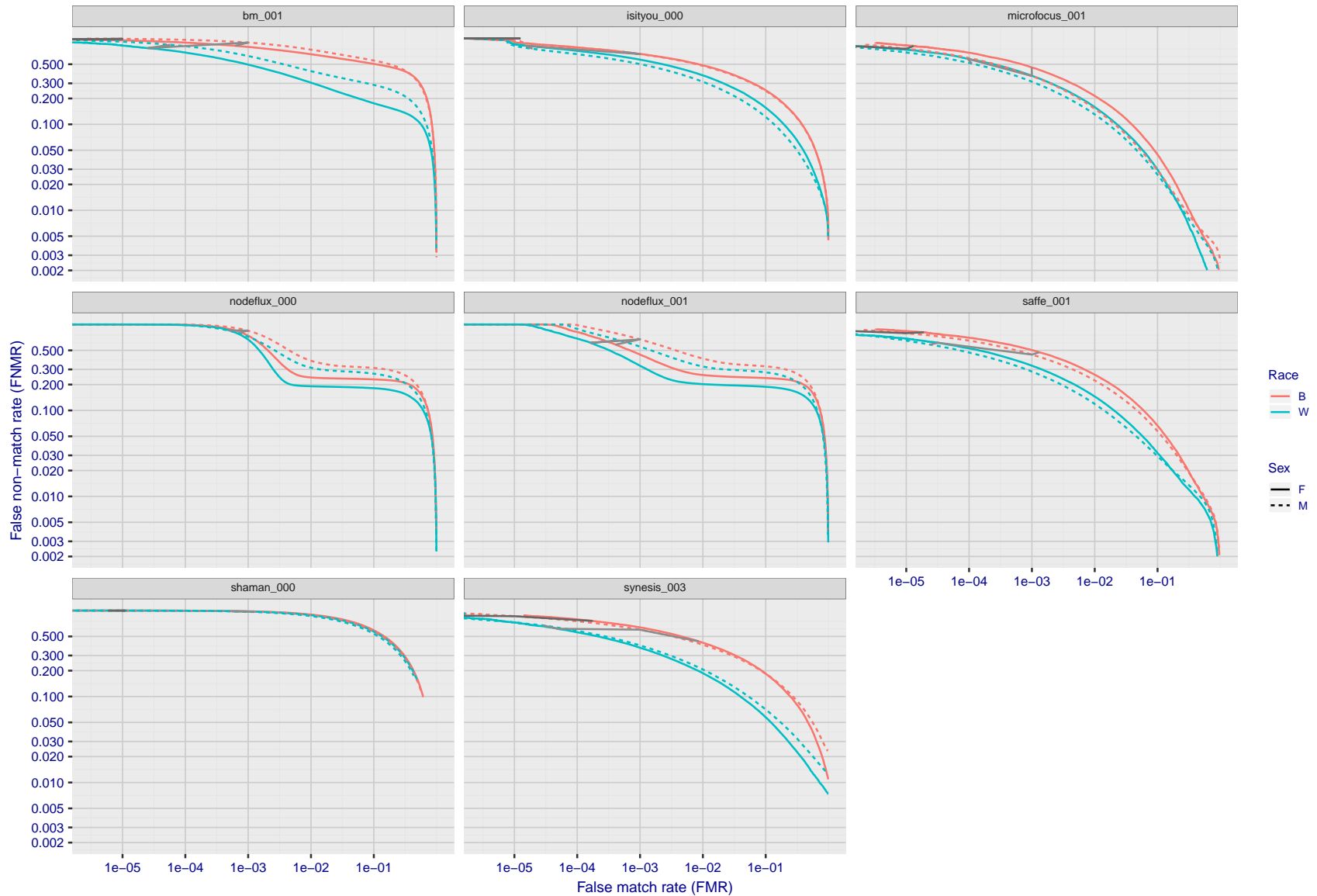
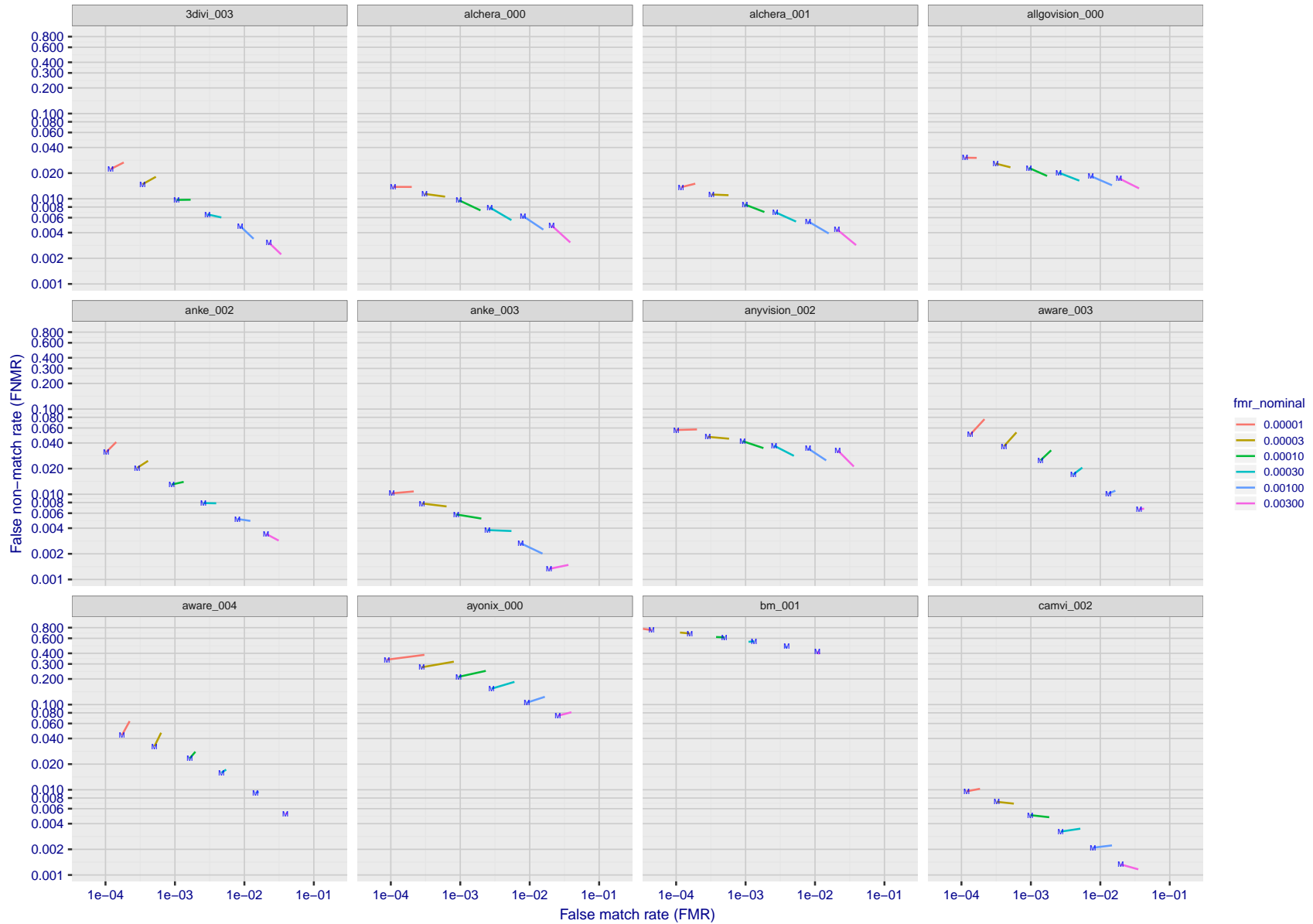


Figure 44: For the mugshot images, error tradeoff characteristics for white females, black females, black males and white males. The Z-shaped grey lines correspond to fixed thresholds, showing both FNMR and FMR vary at one T value. Note: Many of the plots will naively be read as saying women gives worse error rates than men because the solid traces lie above the dotted ones. However, this is misleading and incomplete: The grey lines show the traces reveal horizontal shifts. Thus for the cogent-003 algorithm FNMR for men is higher than for women at a fixed threshold but, at the same time, FMR is higher for women - see Figure 59. As access control systems almost always operate at a fixed threshold, the naive interpretation is incorrect.



FNMR(T)
FMR(T)
"False non-match rate"
"False match rate"

Figure 45: For the visa images, FNMR and FMR at six operating points along the DET characteristic. At each point a line is drawn between $(FMR, FNMR)_{MALE}$ and $(FMR, FNMR)_{FEMALE}$ showing how which sex has lower FMR and/or FNMR. The "M" label denotes male, the other end of the line corresponds to female. The six operating thresholds are selected to give the nominal false match rates given in the legend, and are computed over all impostor pairs regardless of age, sex, and place of birth. The plotted FMR values are broadly an order of magnitude larger than the nominal rates because FMR is computed over demographically-matched impostor pairs i.e individuals of the same sex, from the same geographic region (see section 3.6.1), and the same age group (see section 3.6.2).

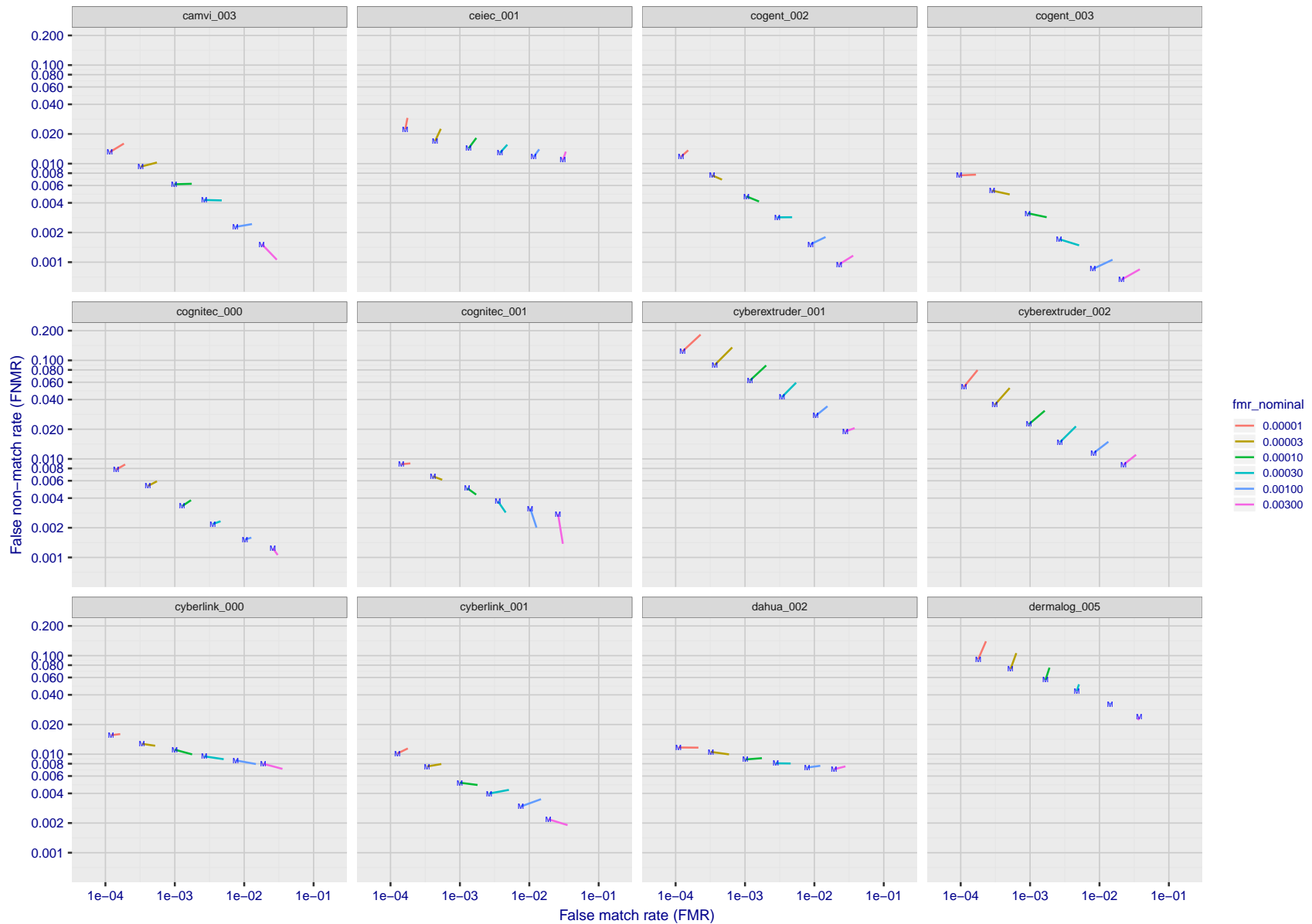
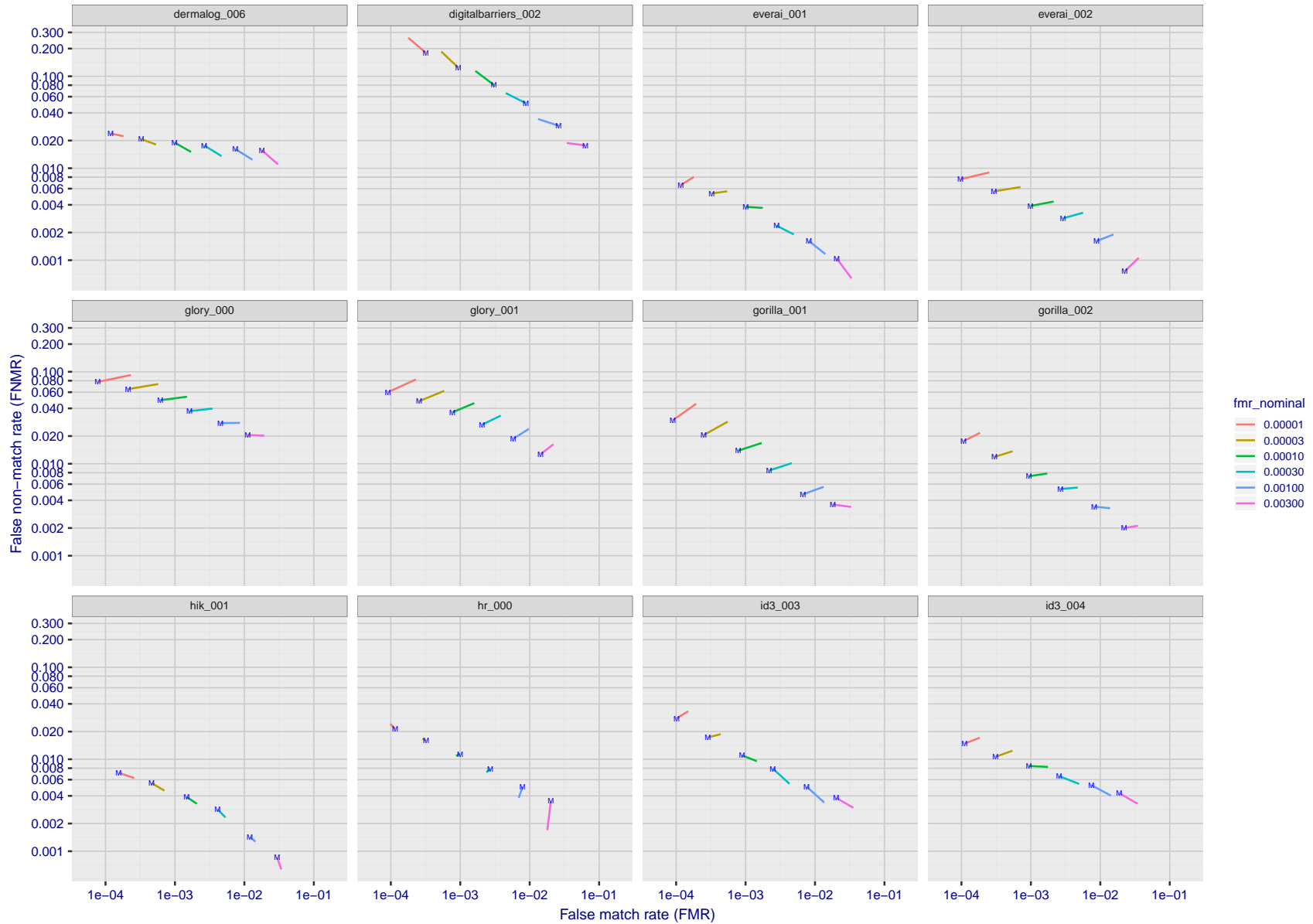


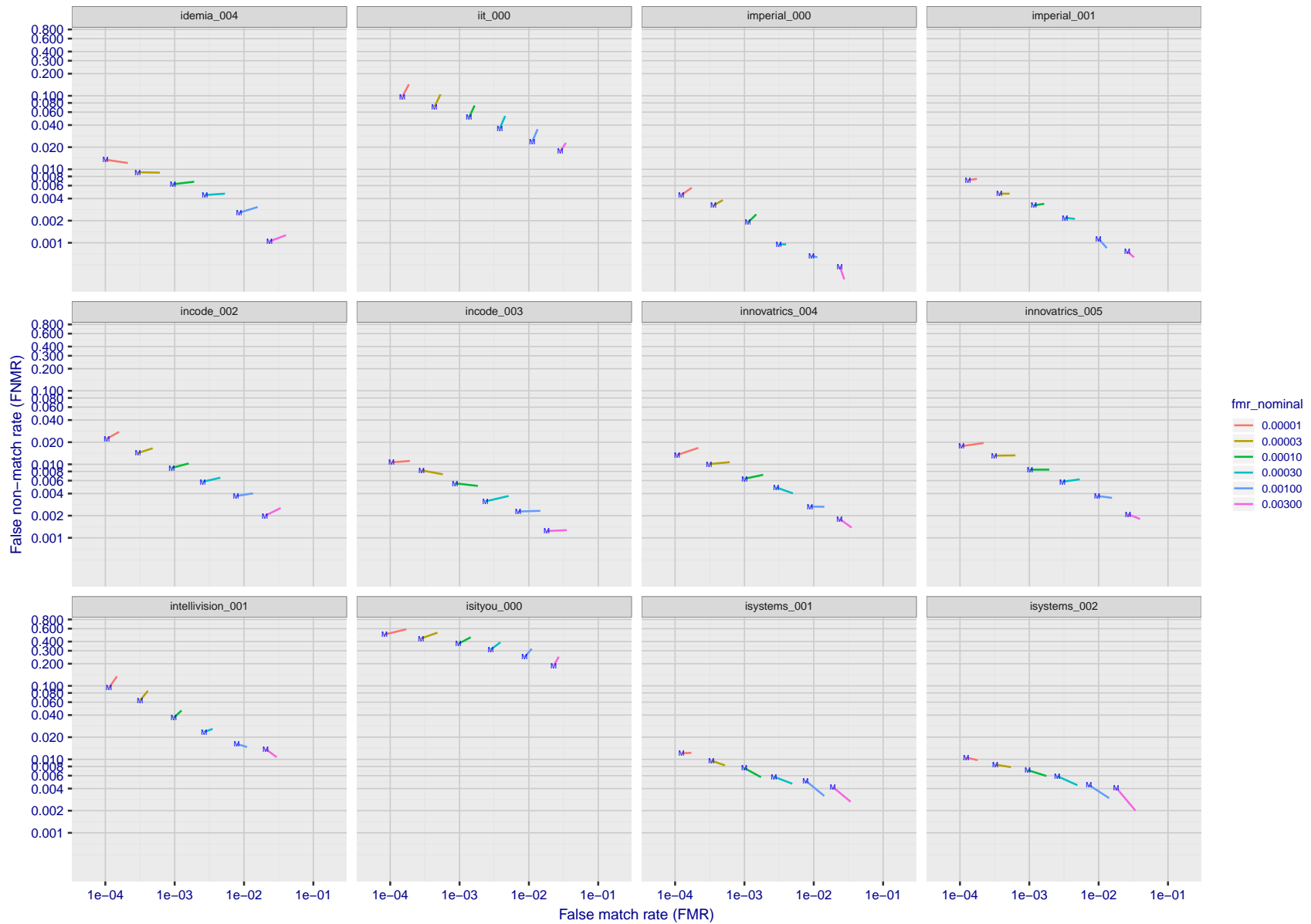
Figure 46: For the visa images, FNMR and FMR at six operating points along the DET characteristic. At each point a line is drawn between $(FMR, FNMR)_{MALE}$ and $(FMR, FNMR)_{FEMALE}$ showing how which sex has lower FMR and/or FNMR. The "M" label denotes male, the other end of the line corresponds to female. The six operating thresholds are selected to give the nominal false match rates given in the legend, and are computed over all impostor pairs regardless of age, sex, and place of birth. The plotted FMR values are broadly an order of magnitude larger than the nominal rates because FMR is computed over demographically-matched impostor pairs i.e individuals of the same sex, from the same geographic region (see section 3.6.1), and the same age group (see section 3.6.2).

FNMR(T)
FMR(T)
"False non-match rate"
"False match rate"



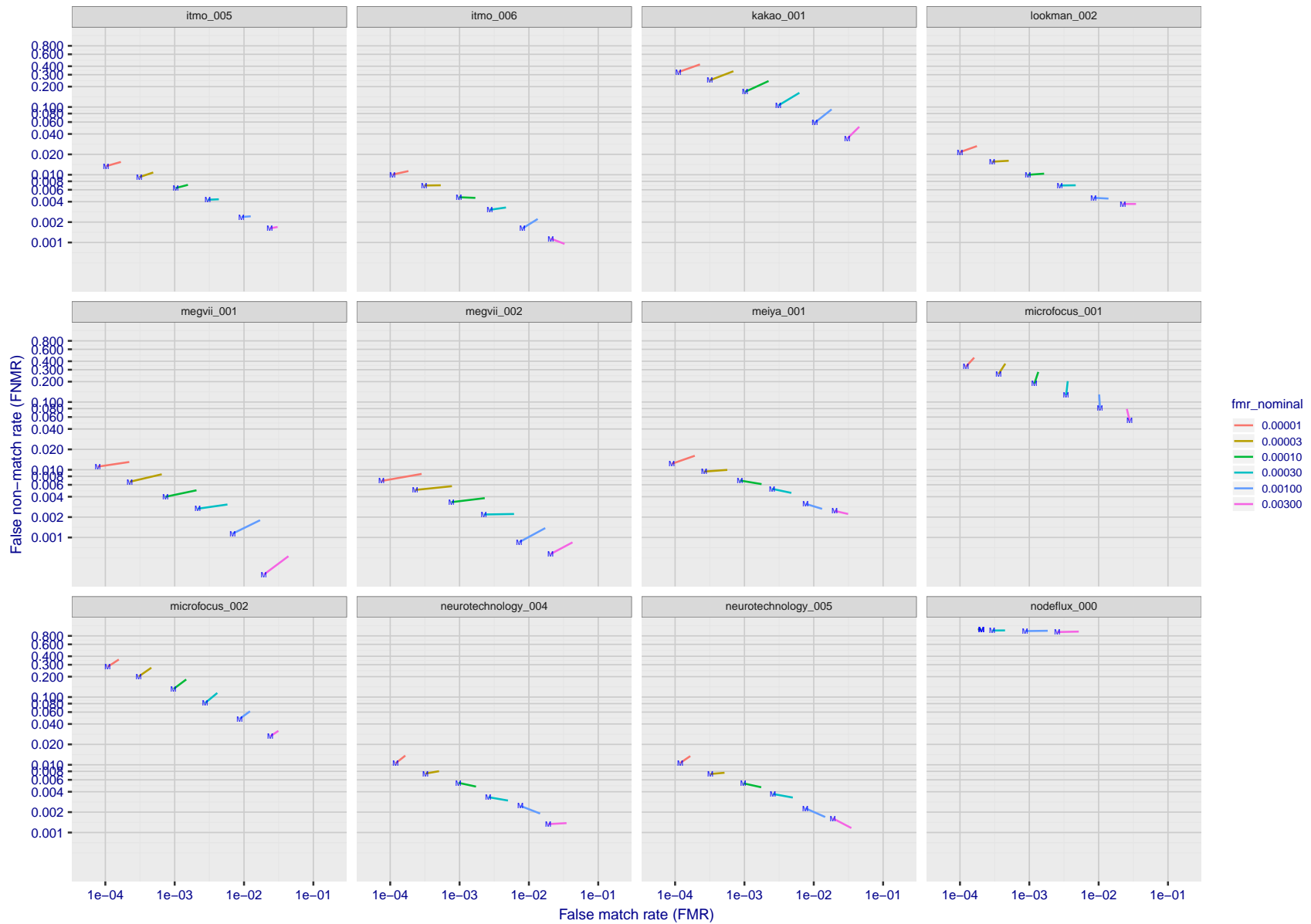
FNMR(T)
FMR(T)
"False non-match rate"
"False match rate"

Figure 47: For the visa images, FNMR and FMR at six operating points along the DET characteristic. At each point a line is drawn between $(FMR, FNMR)_{MALE}$ and $(FMR, FNMR)_{FEMALE}$ showing how which sex has lower FMR and/or FNMR. The "M" label denotes male, the other end of the line corresponds to female. The six operating thresholds are selected to give the nominal false match rates given in the legend, and are computed over all impostor pairs regardless of age, sex, and place of birth. The plotted FMR values are broadly an order of magnitude larger than the nominal rates because FMR is computed over demographically-matched impostor pairs i.e individuals of the same sex, from the same geographic region (see section 3.6.1), and the same age group (see section 3.6.2).



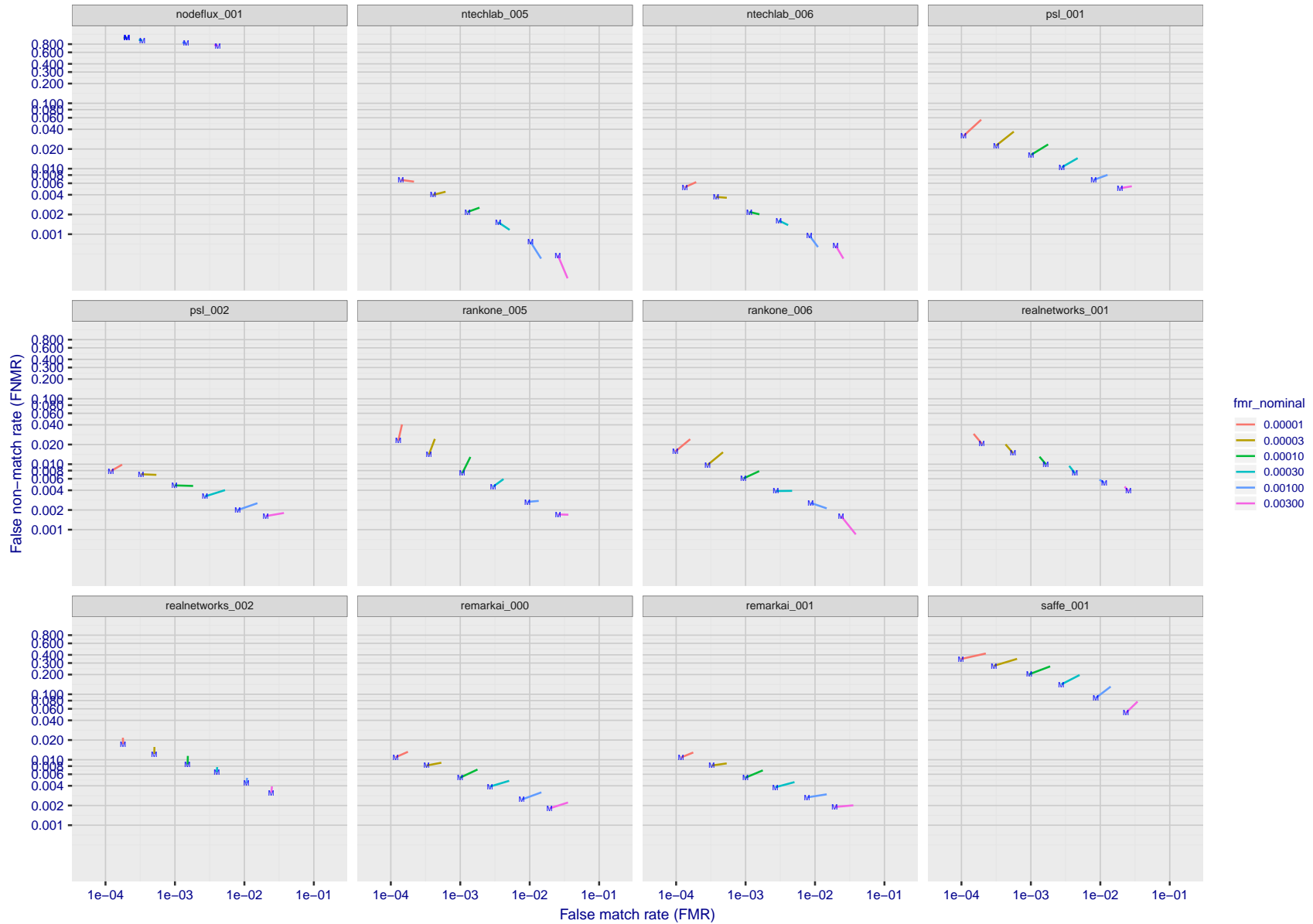
FNMR(T)
FMR(T)
"False non-match rate"
"False match rate"

Figure 48: For the visa images, FNMR and FMR at six operating points along the DET characteristic. At each point a line is drawn between $(FMR, FNMR)_{MALE}$ and $(FMR, FNMR)_{FEMALE}$ showing how which sex has lower FMR and/or FNMR. The "M" label denotes male, the other end of the line corresponds to female. The six operating thresholds are selected to give the nominal false match rates given in the legend, and are computed over all impostor pairs regardless of age, sex, and place of birth. The plotted FMR values are broadly an order of magnitude larger than the nominal rates because FMR is computed over demographically-matched impostor pairs i.e individuals of the same sex, from the same geographic region (see section 3.6.1), and the same age group (see section 3.6.2).



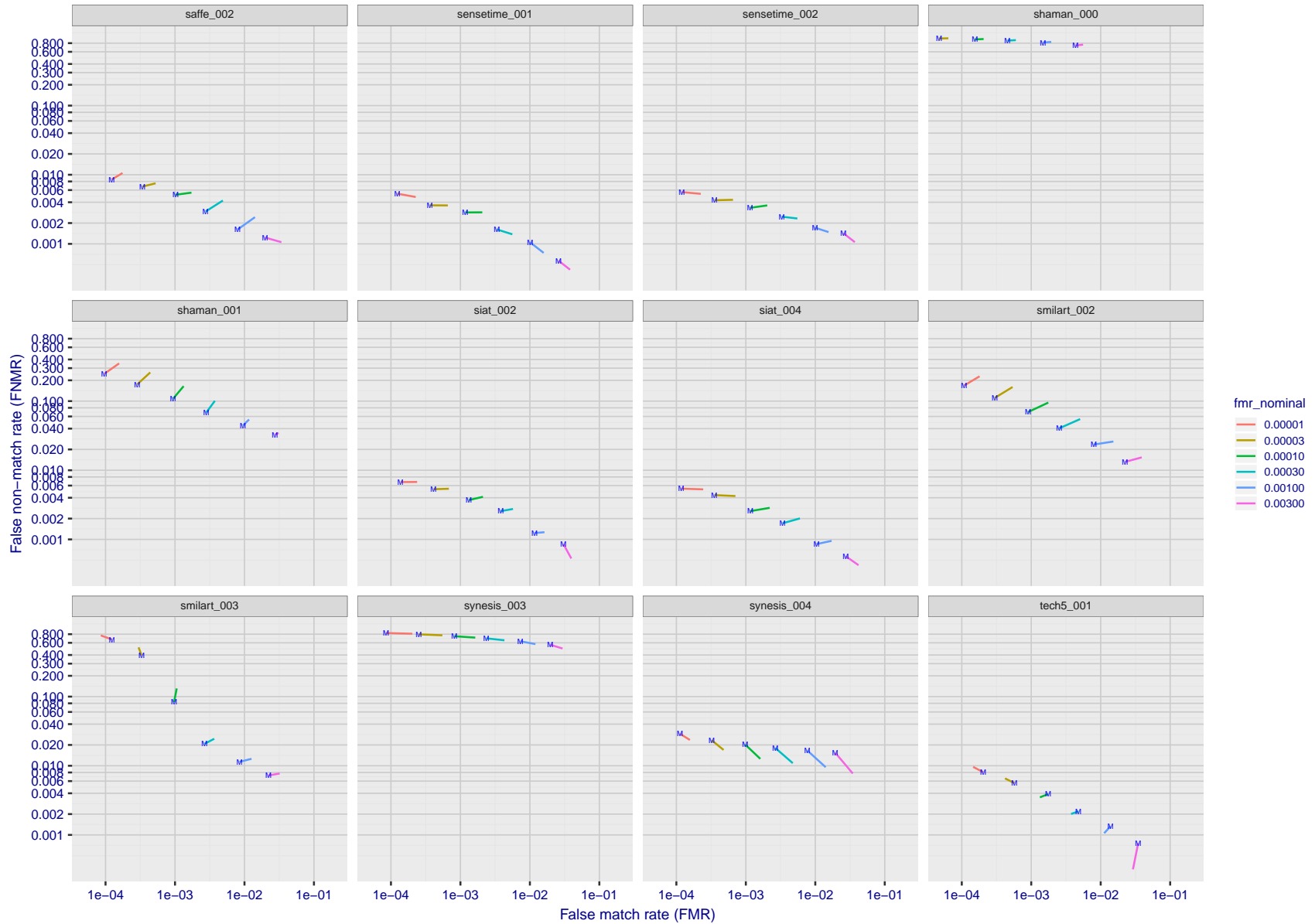
FNMR(T)
FMR(T)
"False non-match rate"
"False match rate"

Figure 49: For the visa images, FNMR and FMR at six operating points along the DET characteristic. At each point a line is drawn between $(FMR, FNMR)_{MALE}$ and $(FMR, FNMR)_{FEMALE}$ showing how which sex has lower FMR and/or FNMR. The "M" label denotes male, the other end of the line corresponds to female. The six operating thresholds are selected to give the nominal false match rates given in the legend, and are computed over all impostor pairs regardless of age, sex, and place of birth. The plotted FMR values are broadly an order of magnitude larger than the nominal rates because FMR is computed over demographically-matched impostor pairs i.e individuals of the same sex, from the same geographic region (see section 3.6.1), and the same age group (see section 3.6.2).



FNMR(T)
 FMR(T)
 "False non-match rate"
 "False match rate"

Figure 50: For the visa images, FNMR and FMR at six operating points along the DET characteristic. At each point a line is drawn between $(FMR, FNMR)_{MALE}$ and $(FMR, FNMR)_{FEMALE}$ showing how which sex has lower FMR and/or FNMR. The "M" label denotes male, the other end of the line corresponds to female. The six operating thresholds are selected to give the nominal false match rates given in the legend, and are computed over all impostor pairs regardless of age, sex, and place of birth. The plotted FMR values are broadly an order of magnitude larger than the nominal rates because FMR is computed over demographically-matched impostor pairs i.e individuals of the same sex, from the same geographic region (see section 3.6.1), and the same age group (see section 3.6.2).



FNMR(T)
FMR(T)
"False non-match rate"
"False match rate"

Figure 51: For the visa images, FNMR and FMR at six operating points along the DET characteristic. At each point a line is drawn between $(FMR, FNMR)_{MALE}$ and $(FMR, FNMR)_{FEMALE}$ showing how which sex has lower FMR and/or FNMR. The "M" label denotes male, the other end of the line corresponds to female. The six operating thresholds are selected to give the nominal false match rates given in the legend, and are computed over all impostor pairs regardless of age, sex, and place of birth. The plotted FMR values are broadly an order of magnitude larger than the nominal rates because FMR is computed over demographically-matched impostor pairs i.e individuals of the same sex, from the same geographic region (see section 3.6.1), and the same age group (see section 3.6.2).

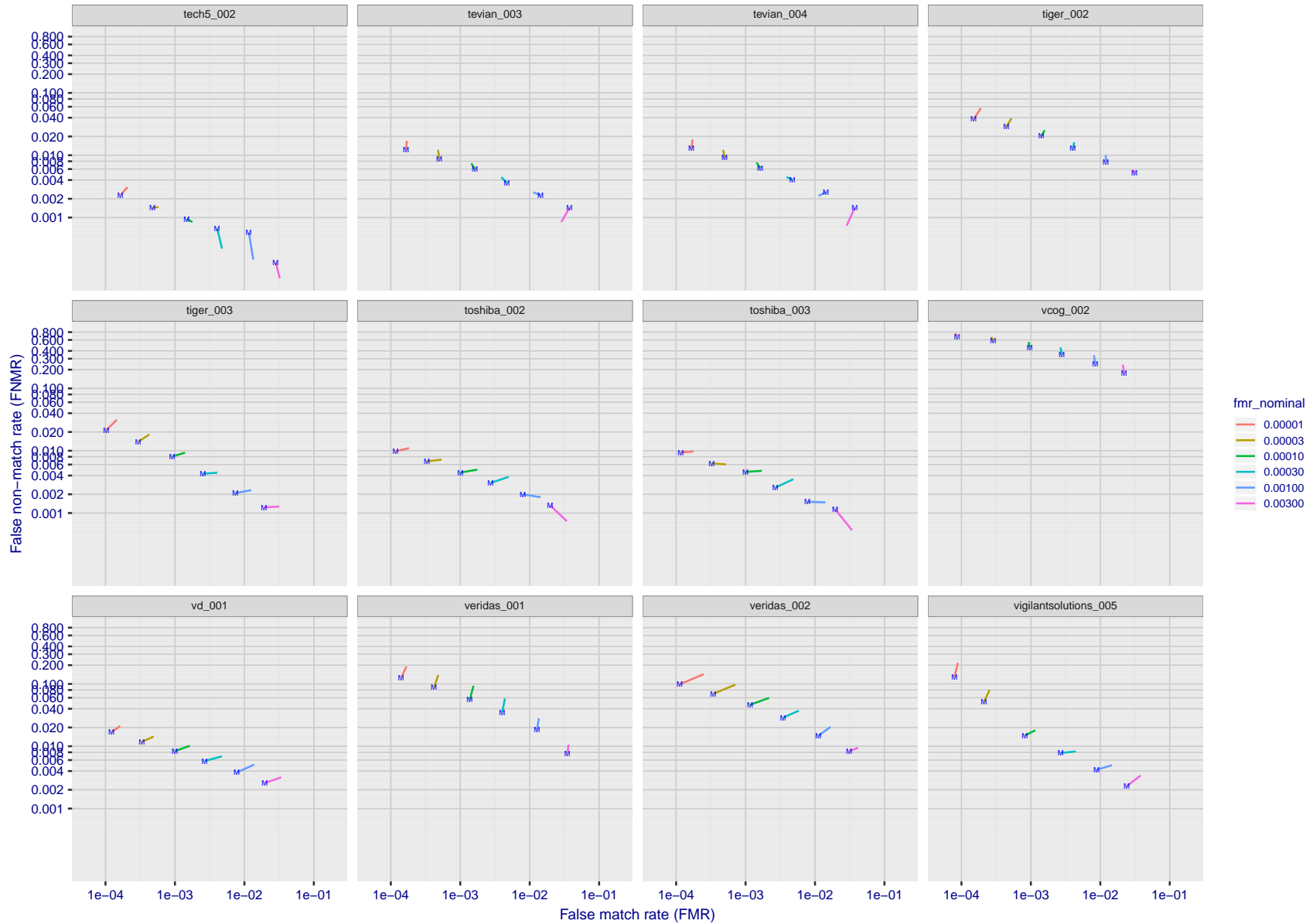
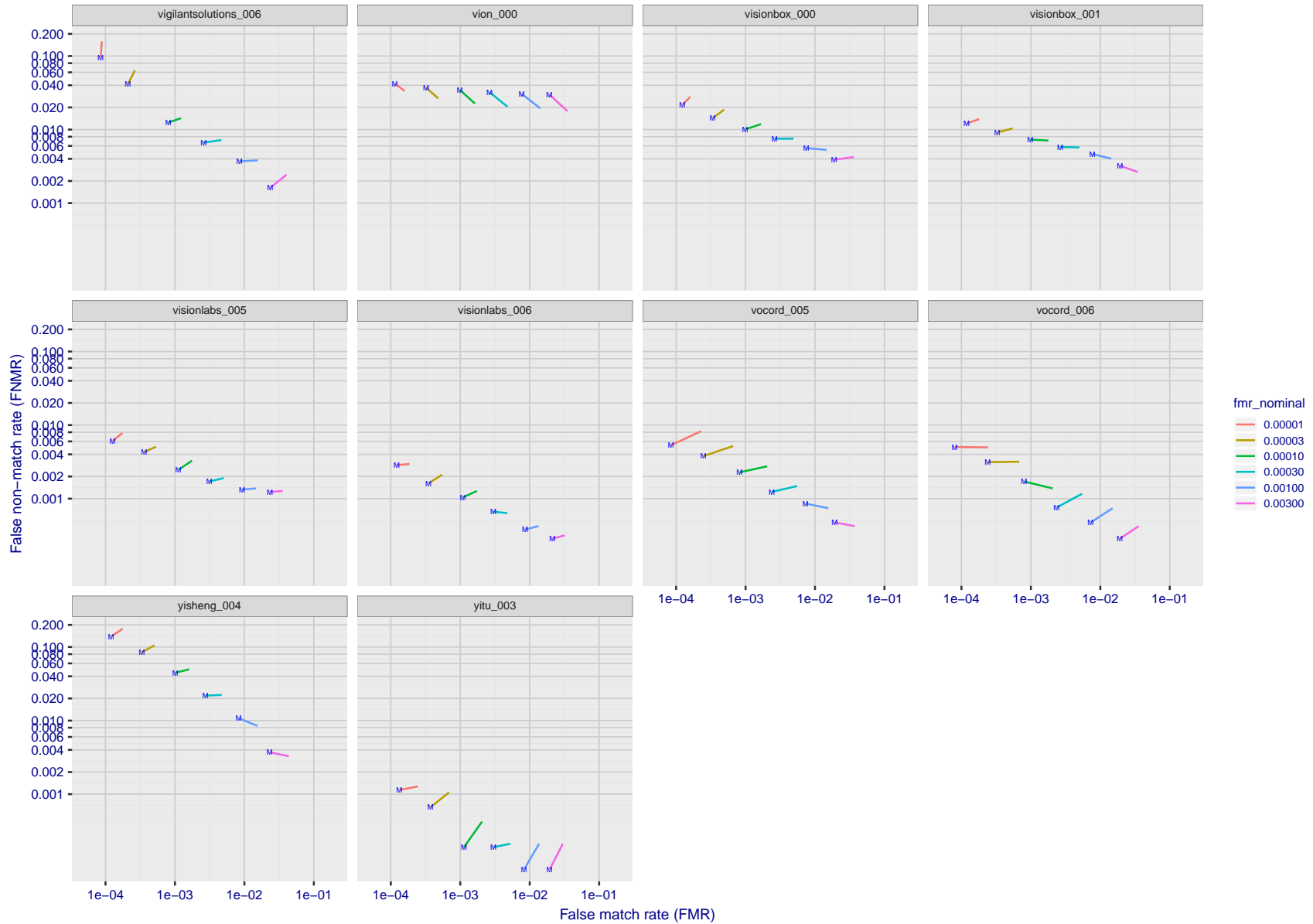


Figure 52: For the visa images, FNMR and FMR at six operating points along the DET characteristic. At each point a line is drawn between $(FMR, FNMR)_{MALE}$ and $(FMR, FNMR)_{FEMALE}$ showing how which sex has lower FMR and/or FNMR. The "M" label denotes male, the other end of the line corresponds to female. The six operating thresholds are selected to give the nominal false match rates given in the legend, and are computed over all impostor pairs regardless of age, sex, and place of birth. The plotted FMR values are broadly an order of magnitude larger than the nominal rates because FMR is computed over demographically-matched impostor pairs i.e individuals of the same sex, from the same geographic region (see section 3.6.1), and the same age group (see section 3.6.2).



FNMR(T)
FMR(T)
"False non-match rate"
"False match rate"

Figure 53: For the visa images, FNMR and FMR at six operating points along the DET characteristic. At each point a line is drawn between $(FMR, FNMR)_{MALE}$ and $(FMR, FNMR)_{FEMALE}$ showing how which sex has lower FMR and/or FNMR. The "M" label denotes male, the other end of the line corresponds to female. The six operating thresholds are selected to give the nominal false match rates given in the legend, and are computed over all impostor pairs regardless of age, sex, and place of birth. The plotted FMR values are broadly an order of magnitude larger than the nominal rates because FMR is computed over demographically-matched impostor pairs i.e individuals of the same sex, from the same geographic region (see section 3.6.1), and the same age group (see section 3.6.2).

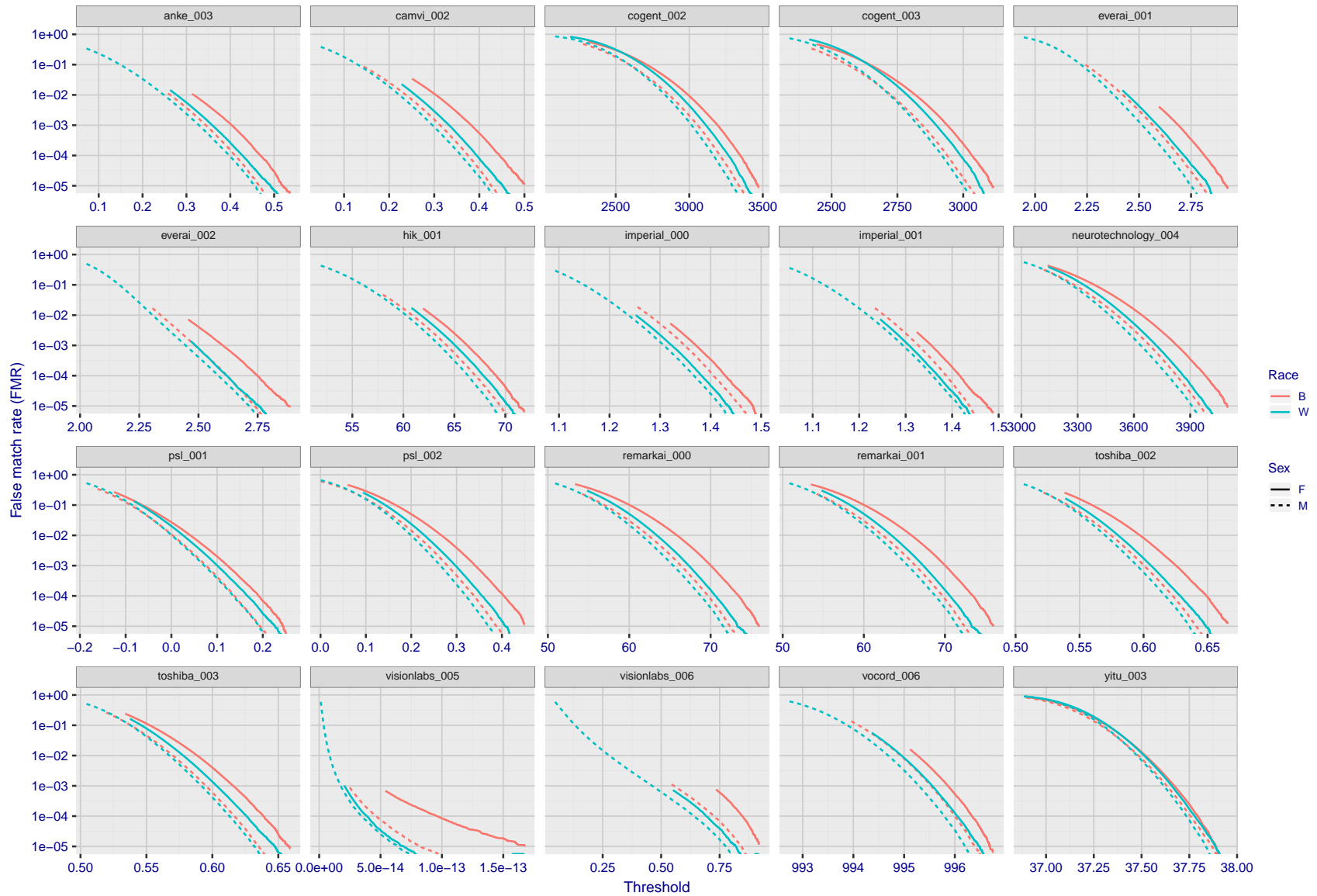
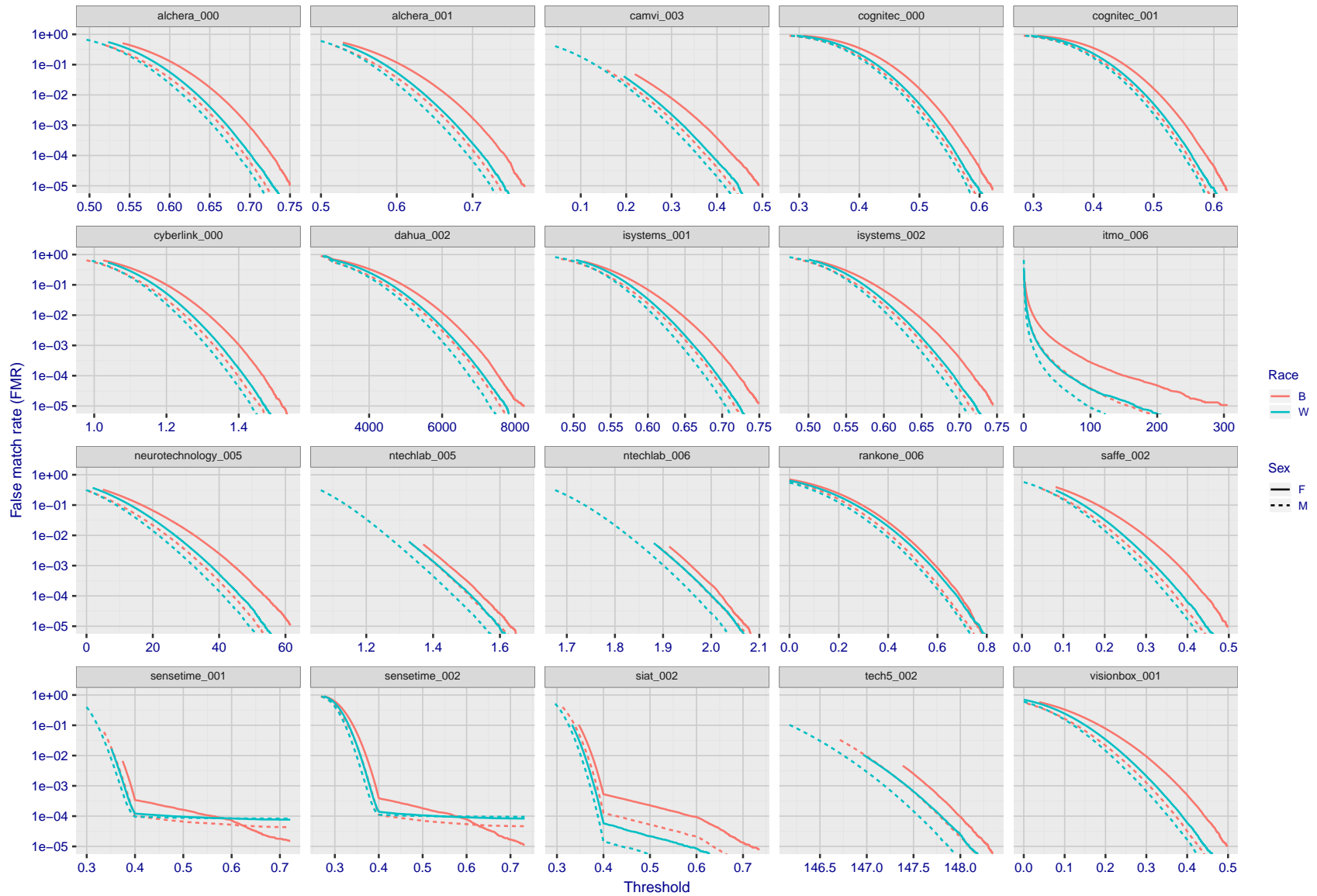
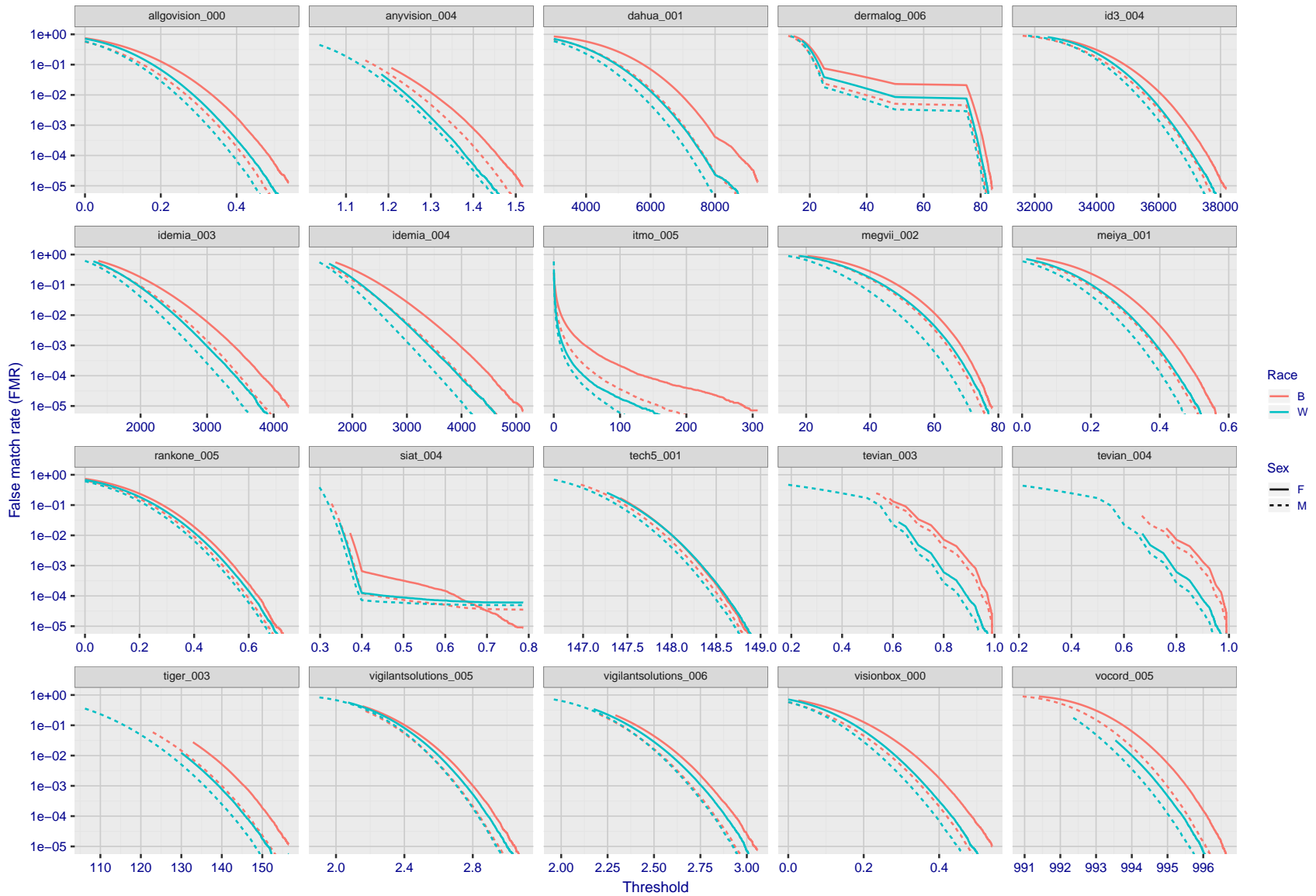


Figure 54: For the mugshot images, the false match calibration curves show false match rate vs. threshold. Separate curves appear for white females, black females, black males and white males.



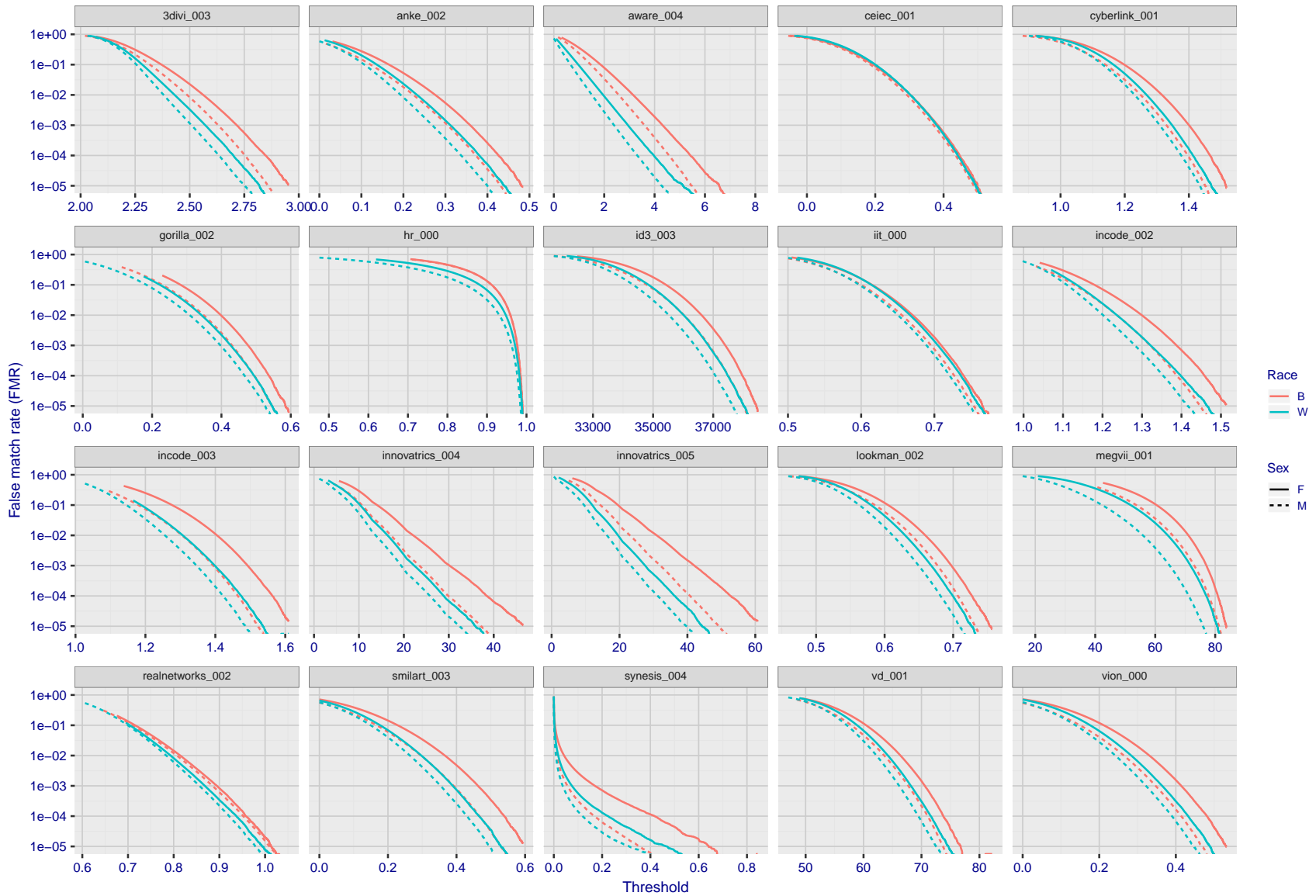
FNMR(T)
FMR(T)
"False non-match rate"
"False match rate"

Figure 55: For the mugshot images, the false match calibration curves show false match rate vs. threshold. Separate curves appear for white females, black females, black males and white males.



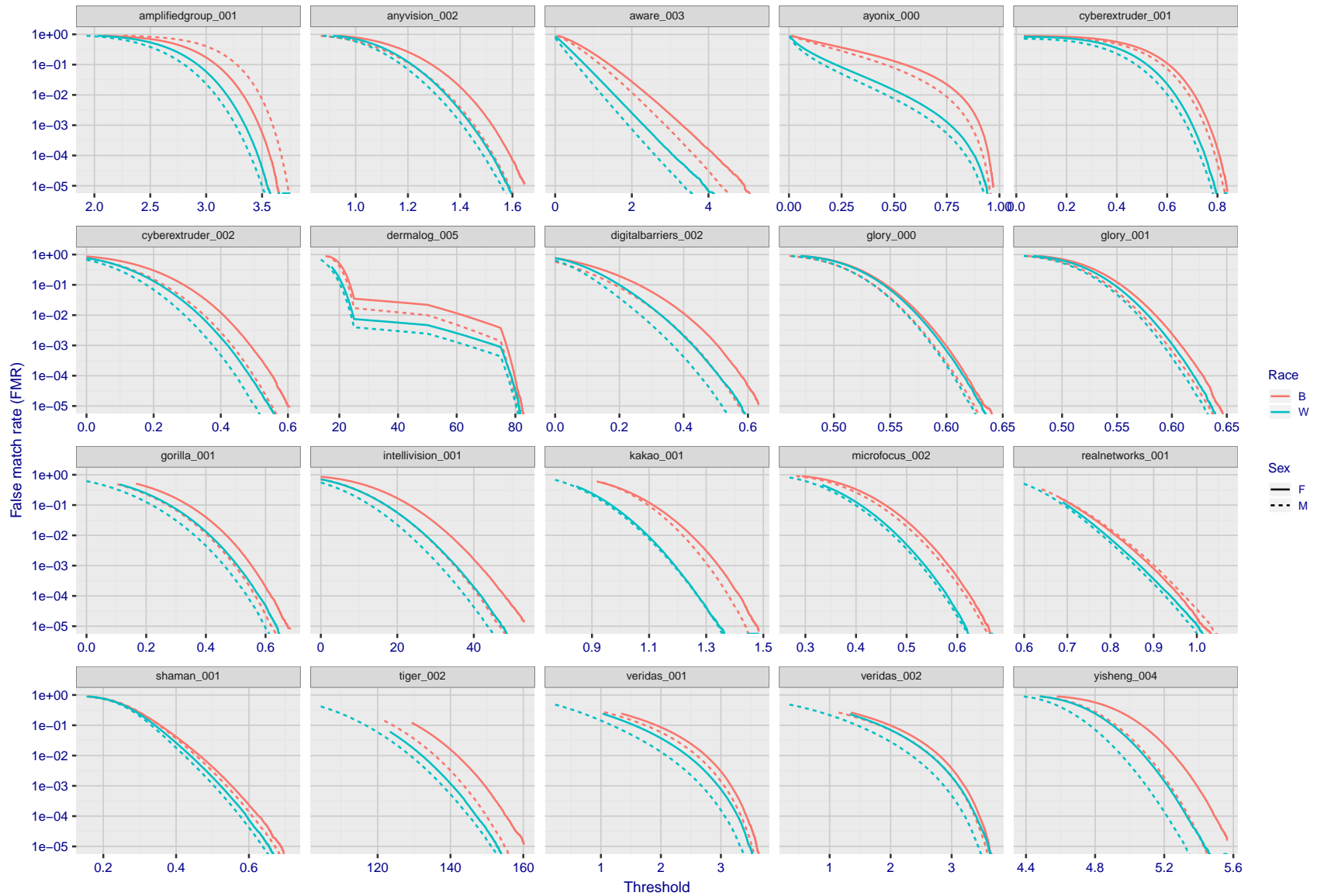
FNMR(T)
FMR(T)
"False non-match rate"
"False match rate"

Figure 56: For the mugshot images, the false match calibration curves show false match rate vs. threshold. Separate curves appear for white females, black females, black males and white males.



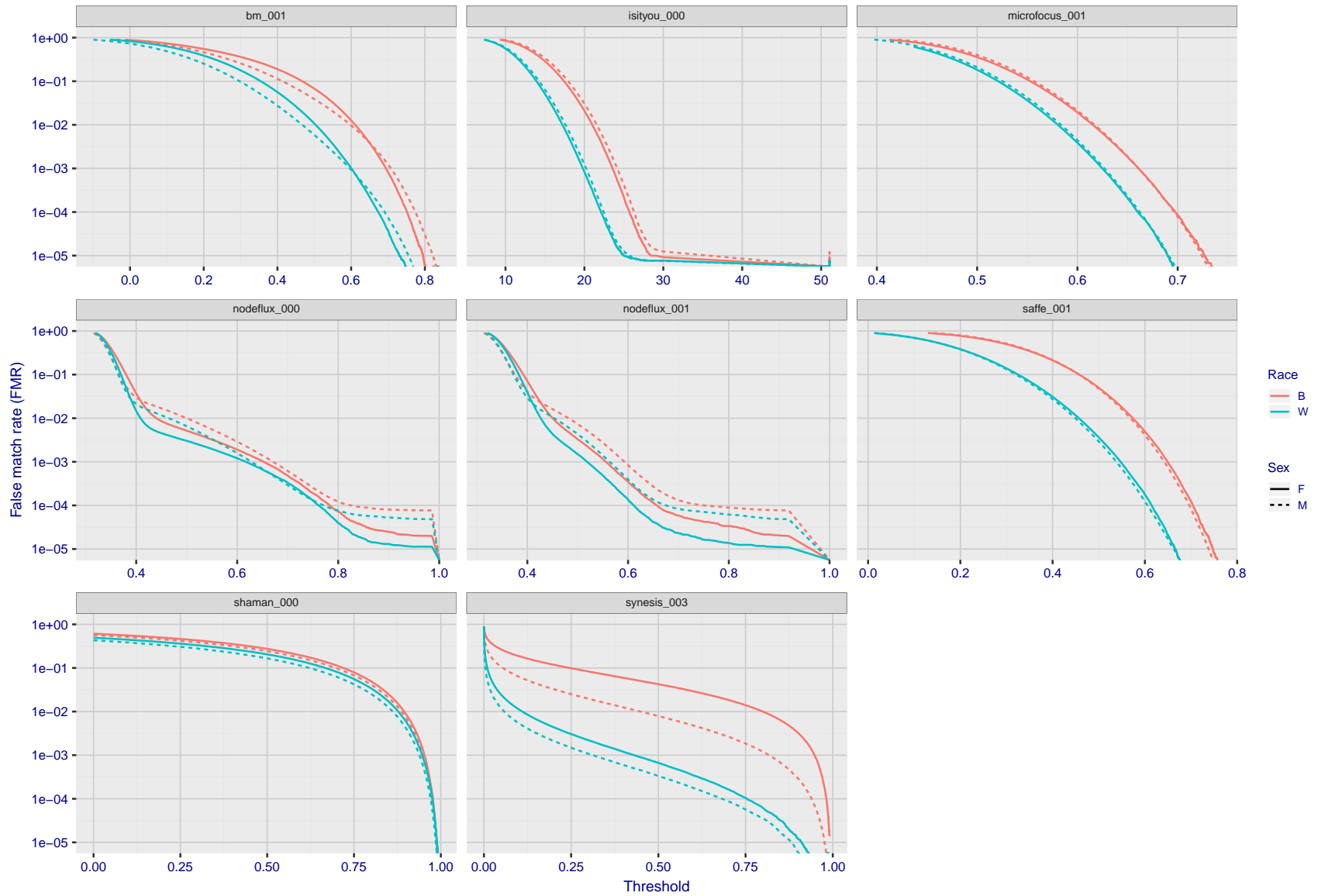
FNMR(T)
FMR(T)
"False non-match rate"
"False match rate"

Figure 57: For the mugshot images, the false match calibration curves show false match rate vs. threshold. Separate curves appear for white females, black females, black males and white males.



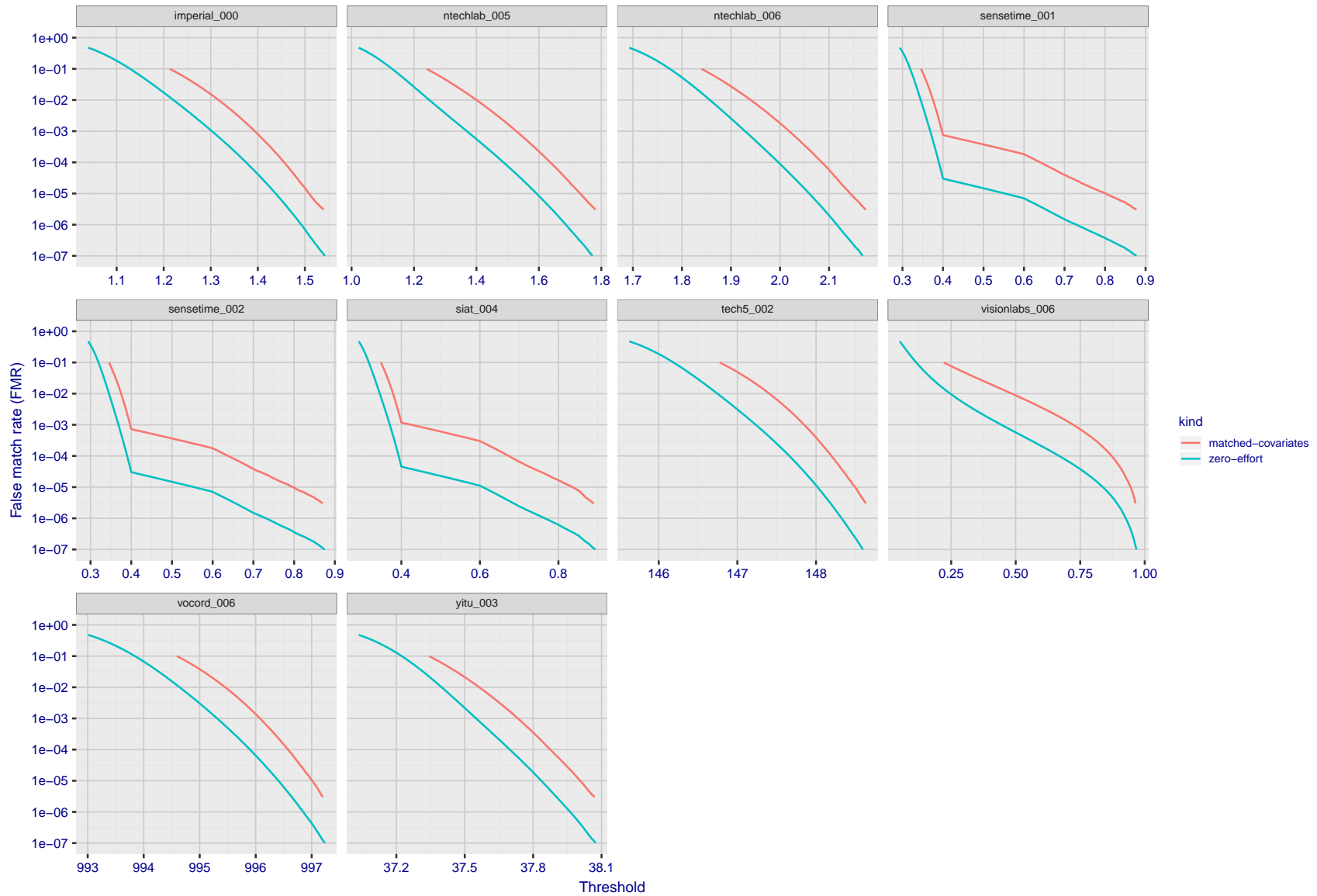
FNMR(T)
FMR(T)
"False non-match rate"
"False match rate"

Figure 58: For the mugshot images, the false match calibration curves show false match rate vs. threshold. Separate curves appear for white females, black females, black males and white males.



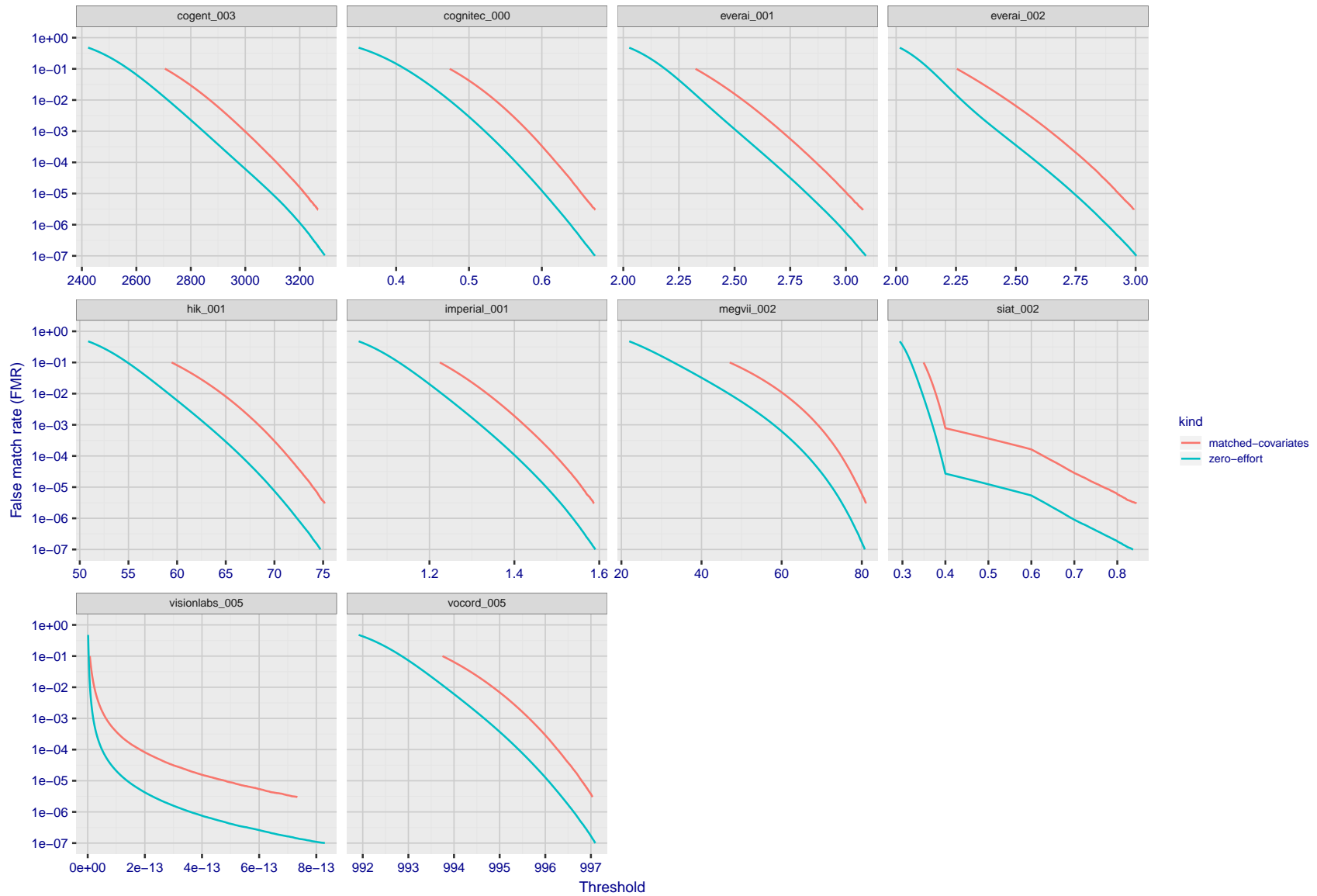
FNMR(T)
FMR(T)
"False non-match rate"
"False match rate"

Figure 59: For the mugshot images, the false match calibration curves show false match rate vs. threshold. Separate curves appear for white females, black females, black males and white males.



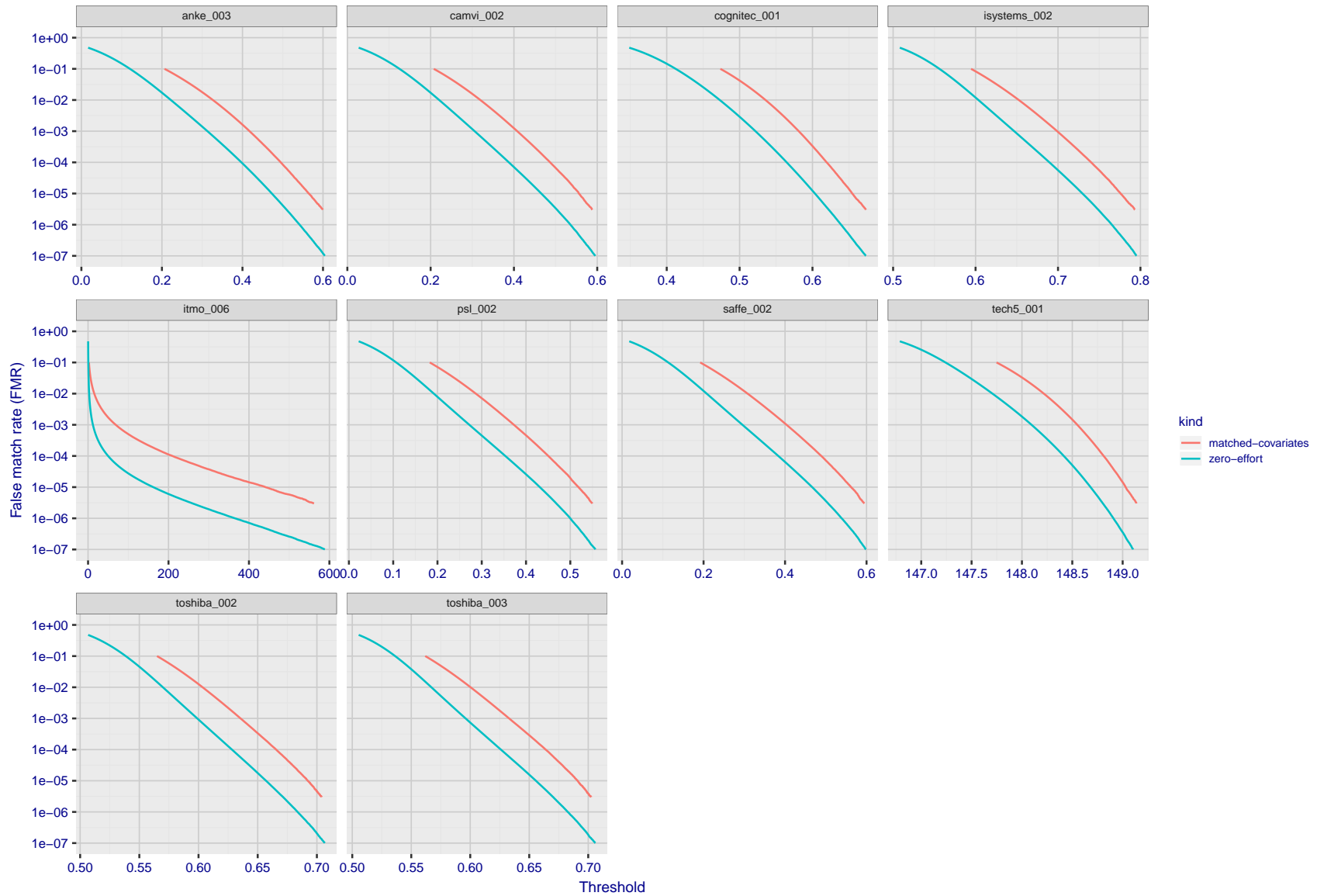
FNMR(T)
FMR(T)
"False non-match rate"
"False match rate"

Figure 60: For the visa images, the false match calibration curves show FMR vs. threshold, T . The blue (lower) curves are for zero-effort impostors (i.e. comparing all images against all). The red (upper) curves are for persons of the same-sex, same-age, and same national-origin. This shows that FMR is underestimated (by a factor of 10 or more) by using a zero-effort impostor calculation to calibrate T . As shown later (sec. 3.6), FMR is higher for demographic-matched impostors.



FNMR(T)
FMR(T)
"False non-match rate"
"False match rate"

Figure 61: For the visa images, the false match calibration curves show FMR vs. threshold, T . The blue (lower) curves are for zero-effort impostors (i.e. comparing all images against all). The red (upper) curves are for persons of the same-sex, same-age, and same national-origin. This shows that FMR is underestimated (by a factor of 10 or more) by using a zero-effort impostor calculation to calibrate T . As shown later (sec. 3.6), FMR is higher for demographic-matched impostors.



FNMRR(T)
 FMR(T)
 "False non-match rate"
 "False match rate"

Figure 62: For the visa images, the false match calibration curves show FMR vs. threshold, T . The blue (lower) curves are for zero-effort impostors (i.e. comparing all images against all). The red (upper) curves are for persons of the same-sex, same-age, and same national-origin. This shows that FMR is underestimated (by a factor of 10 or more) by using a zero-effort impostor calculation to calibrate T . As shown later (sec. 3.6), FMR is higher for demographic-matched impostors.

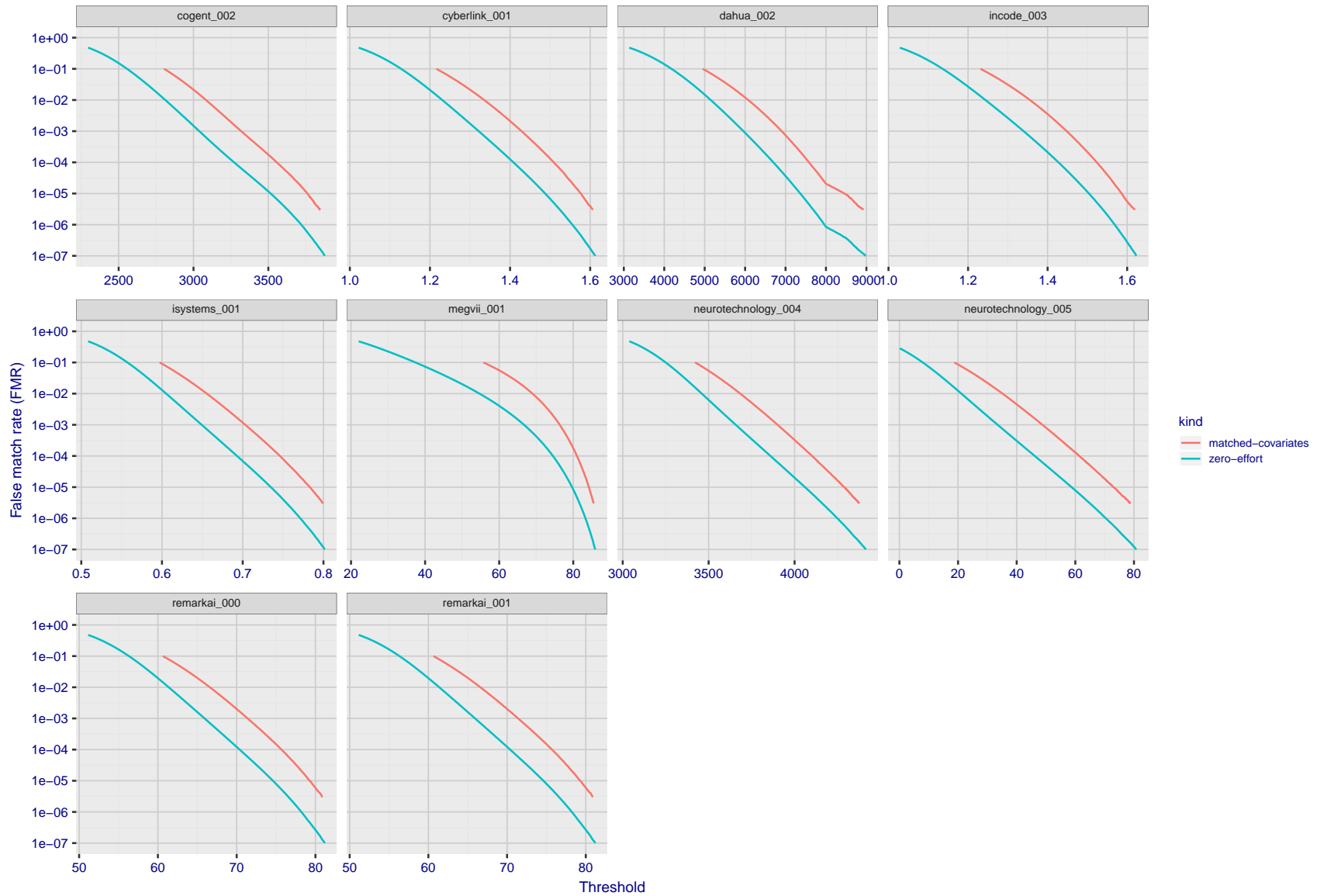


Figure 63: For the visa images, the false match calibration curves show FMR vs. threshold, T . The blue (lower) curves are for zero-effort impostors (i.e. comparing all images against all). The red (upper) curves are for persons of the same-sex, same-age, and same national-origin. This shows that FMR is underestimated (by a factor of 10 or more) by using a zero-effort impostor calculation to calibrate T . As shown later (sec. 3.6), FMR is higher for demographic-matched impostors.

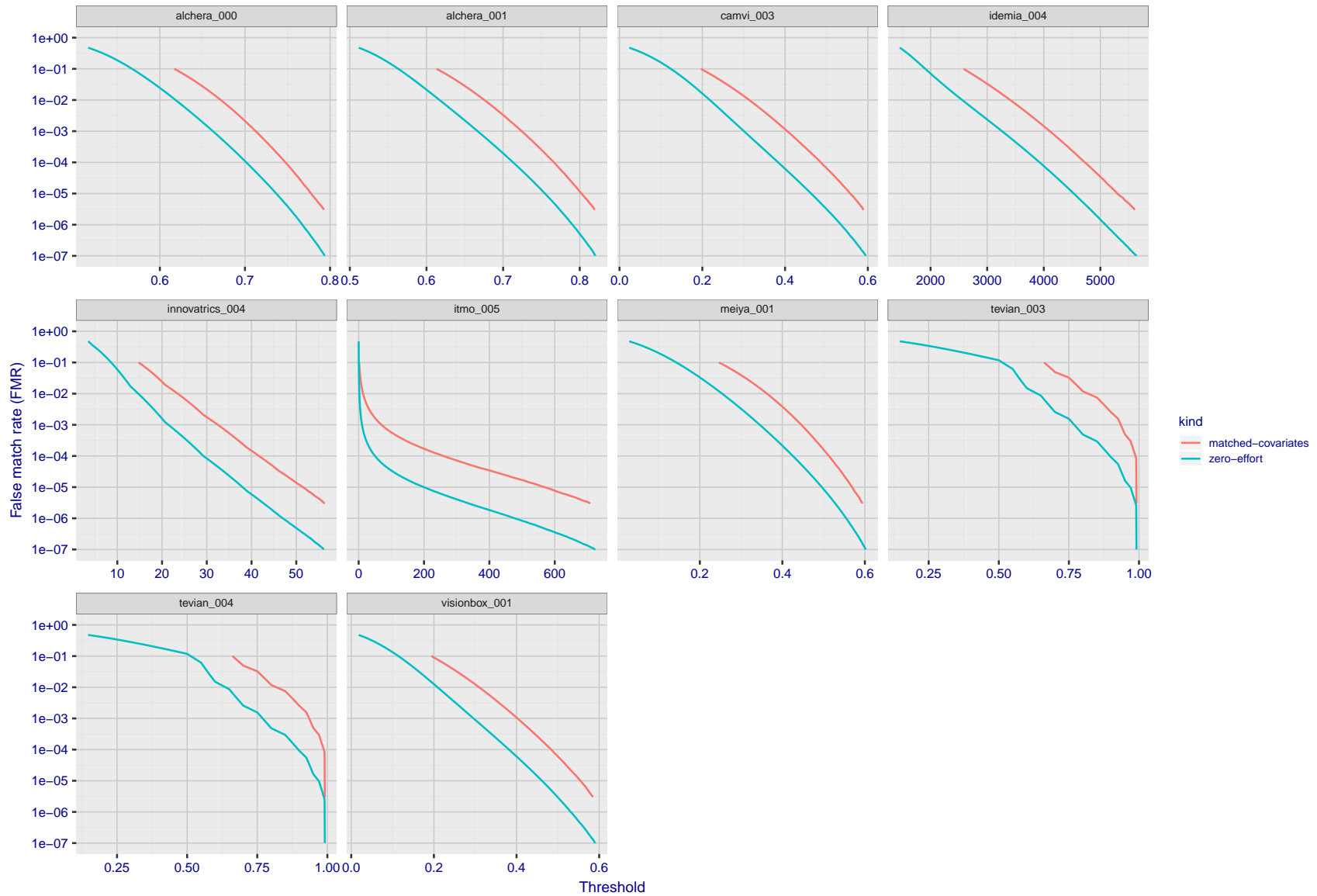
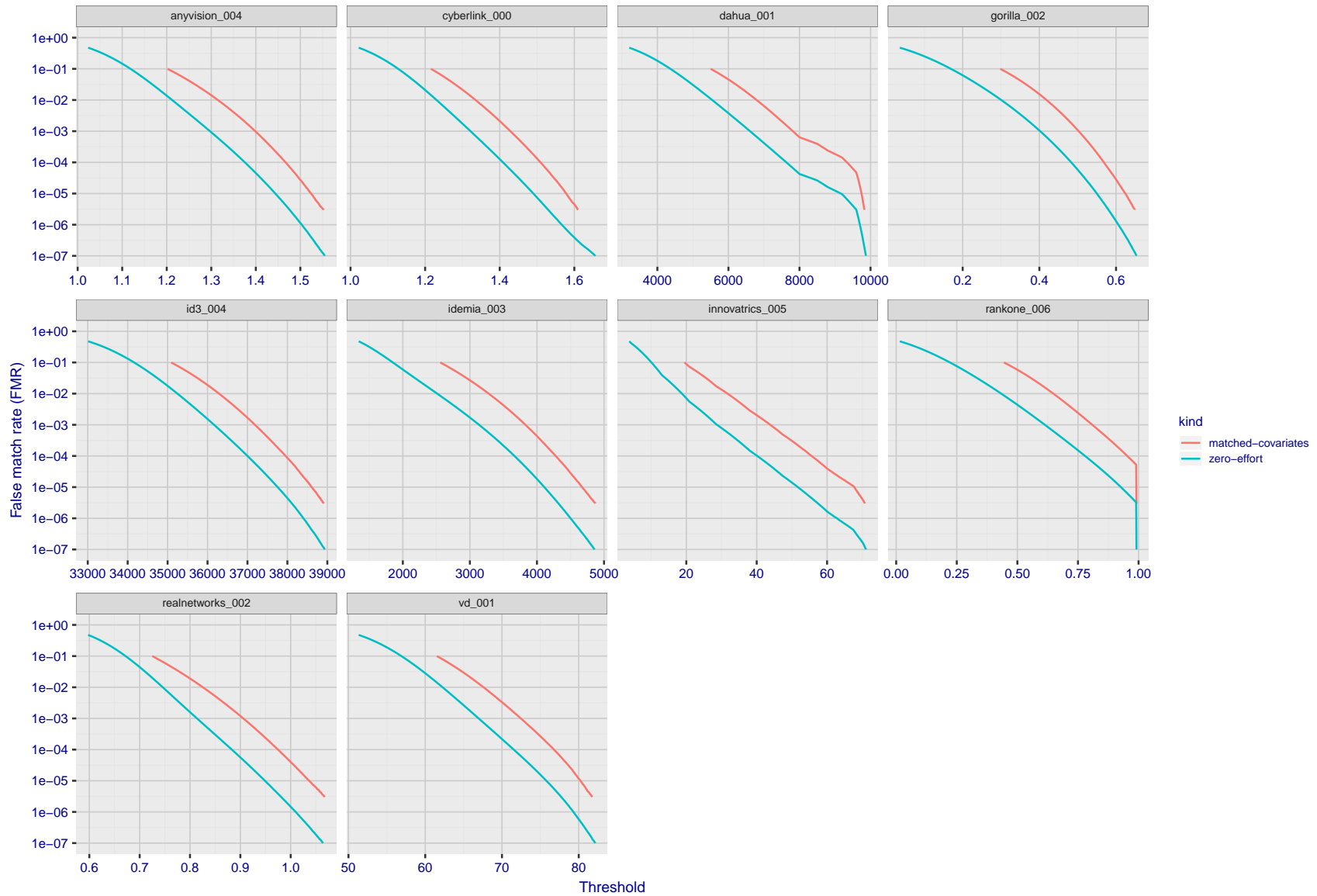


Figure 64: For the visa images, the false match calibration curves show FMR vs. threshold, T . The blue (lower) curves are for zero-effort impostors (i.e. comparing all images against all). The red (upper) curves are for persons of the same-sex, same-age, and same national-origin. This shows that FMR is underestimated (by a factor of 10 or more) by using a zero-effort impostor calculation to calibrate T . As shown later (sec. 3.6), FMR is higher for demographic-matched impostors.



FNMR(T)
FMR(T)
"False non-match rate"
"False match rate"

Figure 65: For the visa images, the false match calibration curves show FMR vs. threshold, T . The blue (lower) curves are for zero-effort impostors (i.e. comparing all images against all). The red (upper) curves are for persons of the same-sex, same-age, and same national-origin. This shows that FMR is underestimated (by a factor of 10 or more) by using a zero-effort impostor calculation to calibrate T . As shown later (sec. 3.6), FMR is higher for demographic-matched impostors.

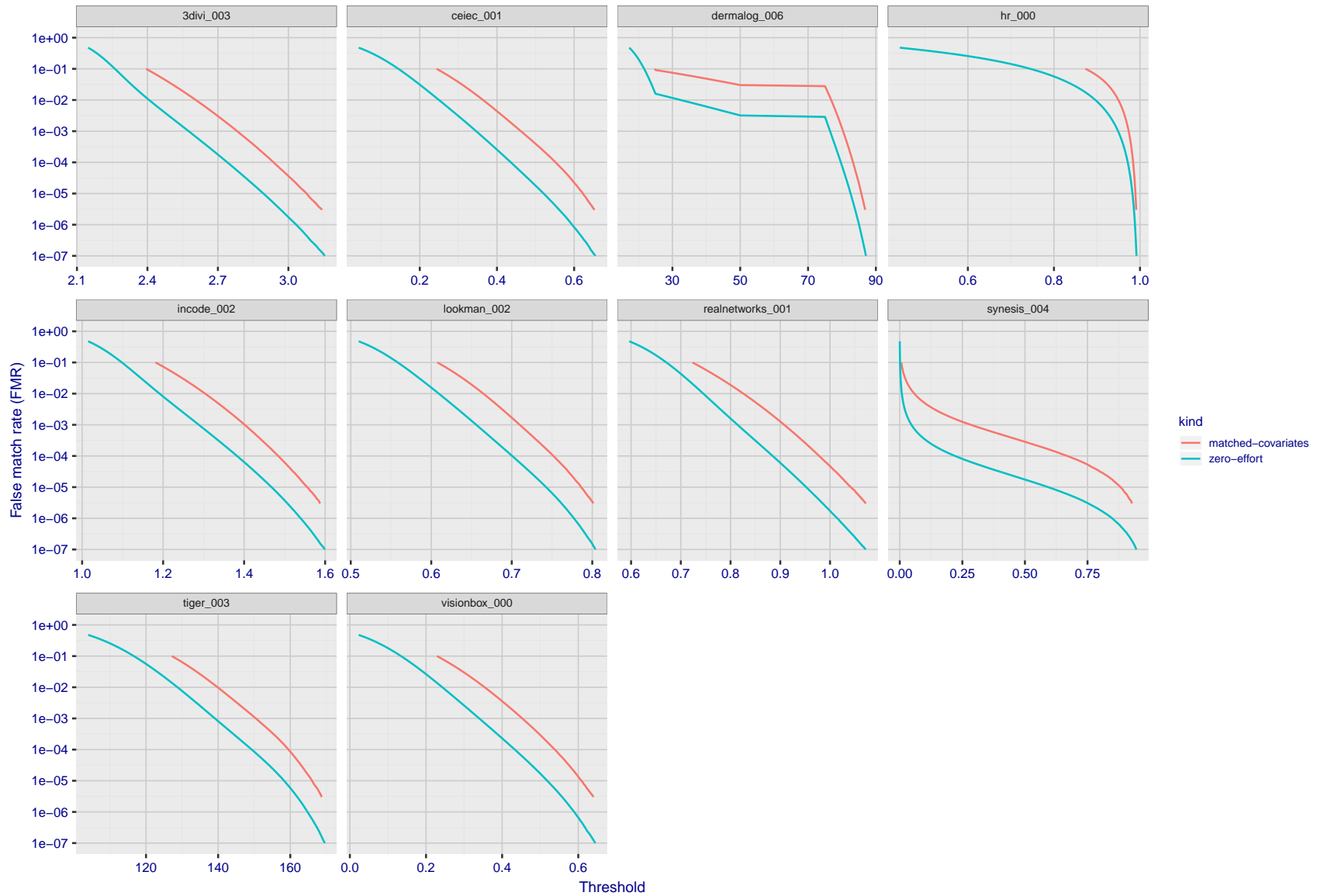
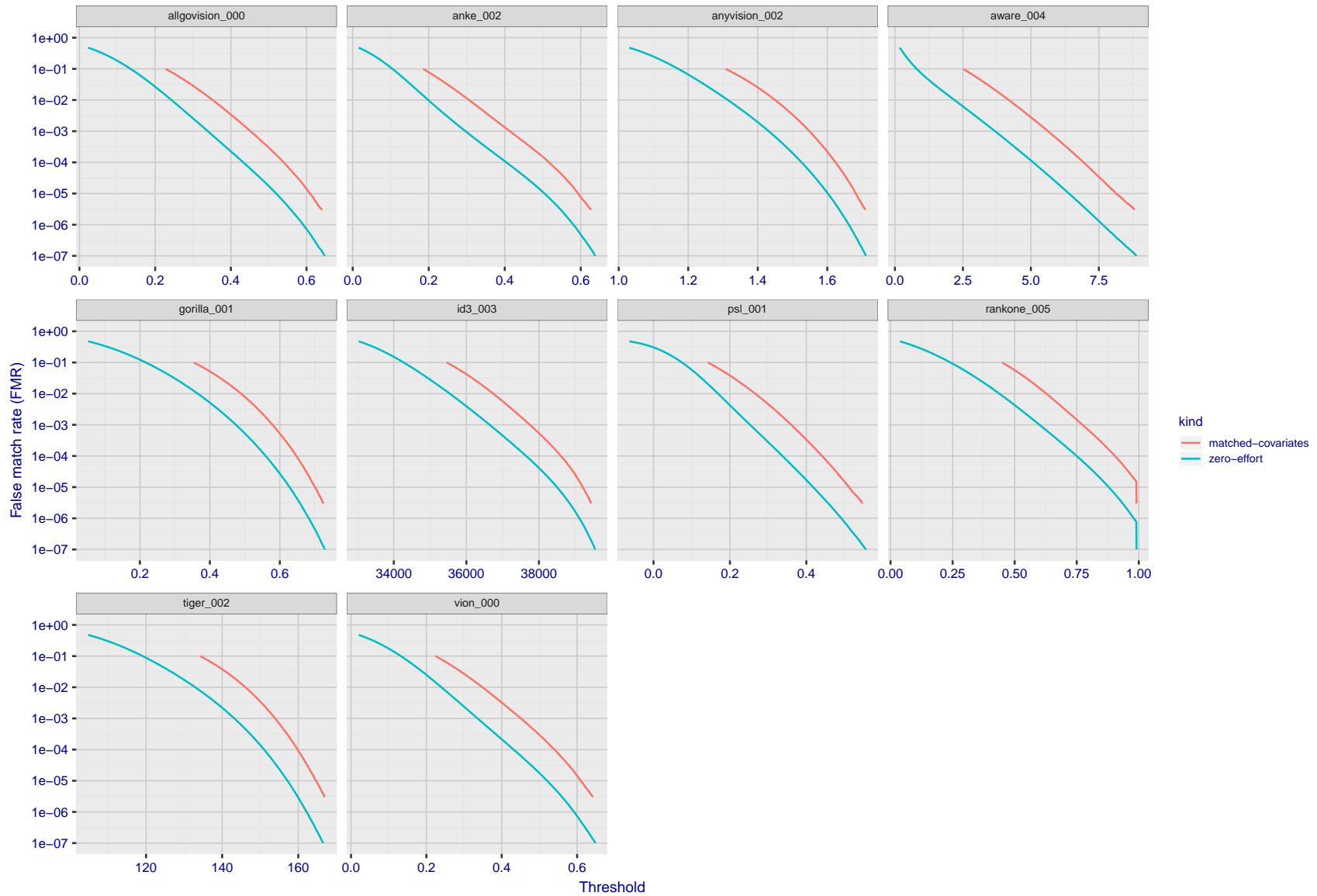
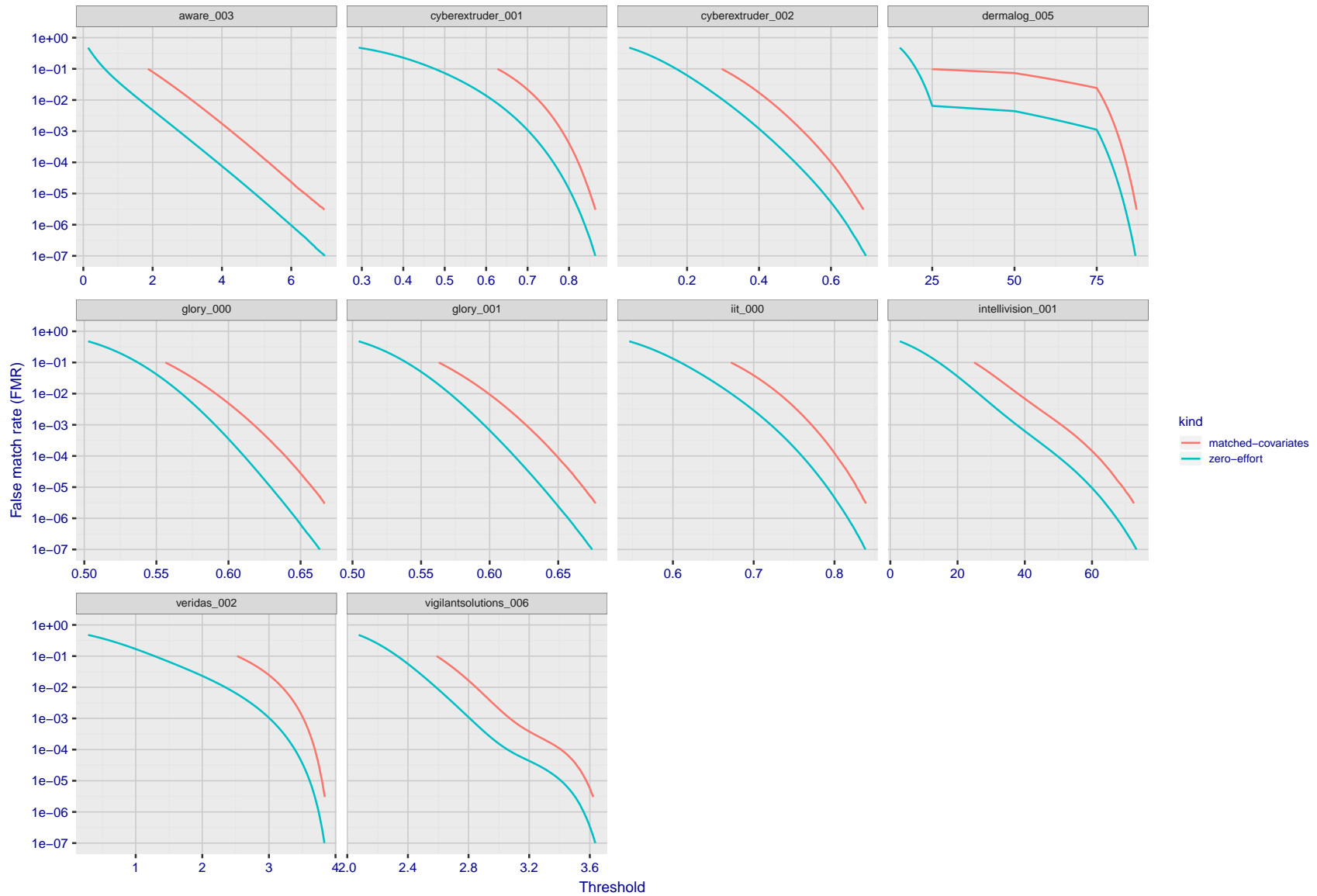


Figure 66: For the visa images, the false match calibration curves show FMR vs. threshold, T . The blue (lower) curves are for zero-effort impostors (i.e. comparing all images against all). The red (upper) curves are for persons of the same-sex, same-age, and same national-origin. This shows that FMR is underestimated (by a factor of 10 or more) by using a zero-effort impostor calculation to calibrate T . As shown later (sec. 3.6), FMR is higher for demographic-matched impostors.



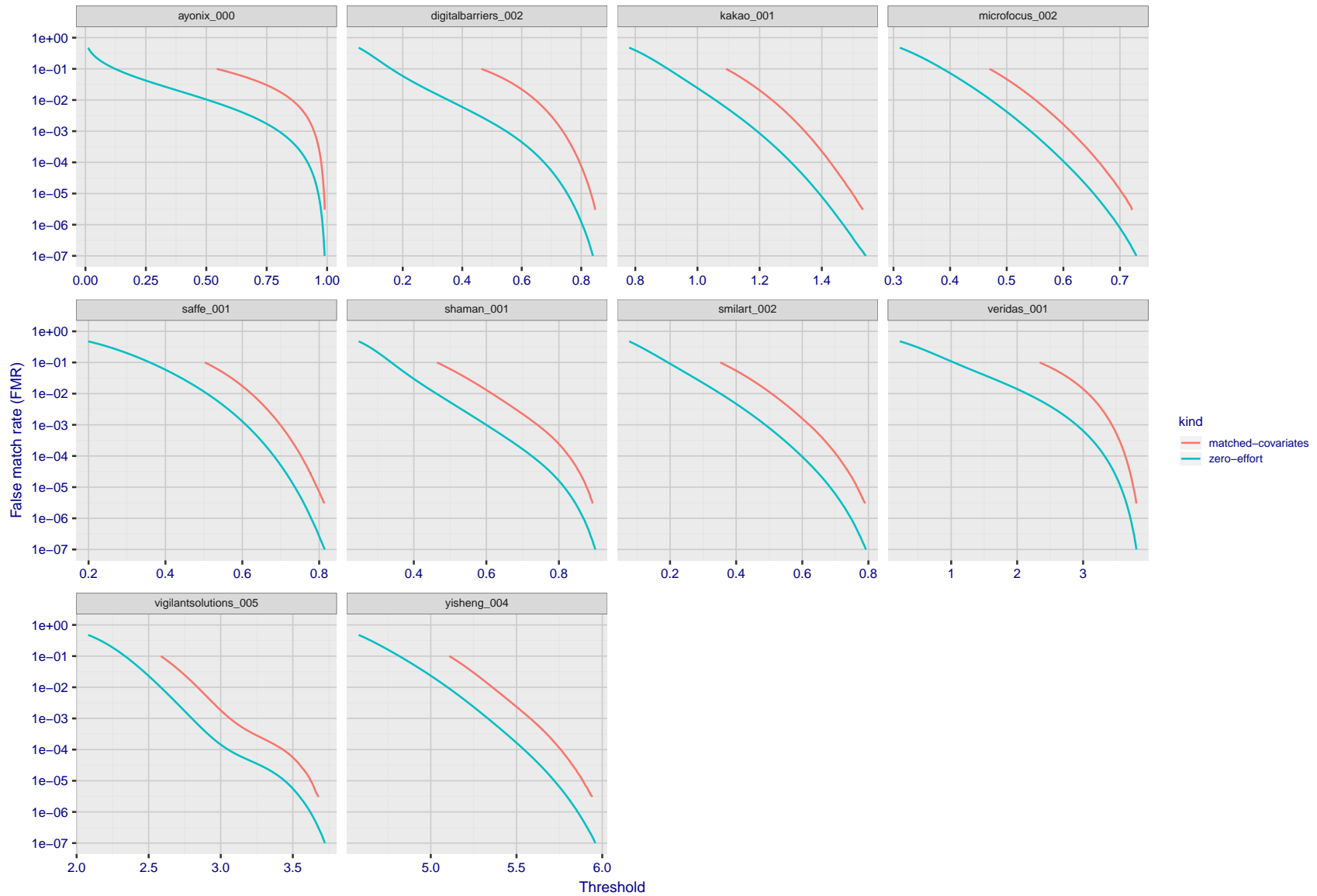
FNMR(T)
 FMR(T)
 "False non-match rate"
 "False match rate"

Figure 67: For the visa images, the false match calibration curves show FMR vs. threshold, T . The blue (lower) curves are for zero-effort impostors (i.e. comparing all images against all). The red (upper) curves are for persons of the same-sex, same-age, and same national-origin. This shows that FMR is underestimated (by a factor of 10 or more) by using a zero-effort impostor calculation to calibrate T . As shown later (sec. 3.6), FMR is higher for demographic-matched impostors.



FNMR(T)
 FMR(T)
 "False non-match rate"
 "False match rate"

Figure 68: For the visa images, the false match calibration curves show FMR vs. threshold, T . The blue (lower) curves are for zero-effort impostors (i.e. comparing all images against all). The red (upper) curves are for persons of the same-sex, same-age, and same national-origin. This shows that FMR is underestimated (by a factor of 10 or more) by using a zero-effort impostor calculation to calibrate T . As shown later (sec. 3.6), FMR is higher for demographic-matched impostors.



FNMR(T)
FMR(T)
"False non-match rate"
"False match rate"

Figure 69: For the visa images, the false match calibration curves show FMR vs. threshold, T . The blue (lower) curves are for zero-effort impostors (i.e. comparing all images against all). The red (upper) curves are for persons of the same-sex, same-age, and same national-origin. This shows that FMR is underestimated (by a factor of 10 or more) by using a zero-effort impostor calculation to calibrate T . As shown later (sec. 3.6), FMR is higher for demographic-matched impostors.

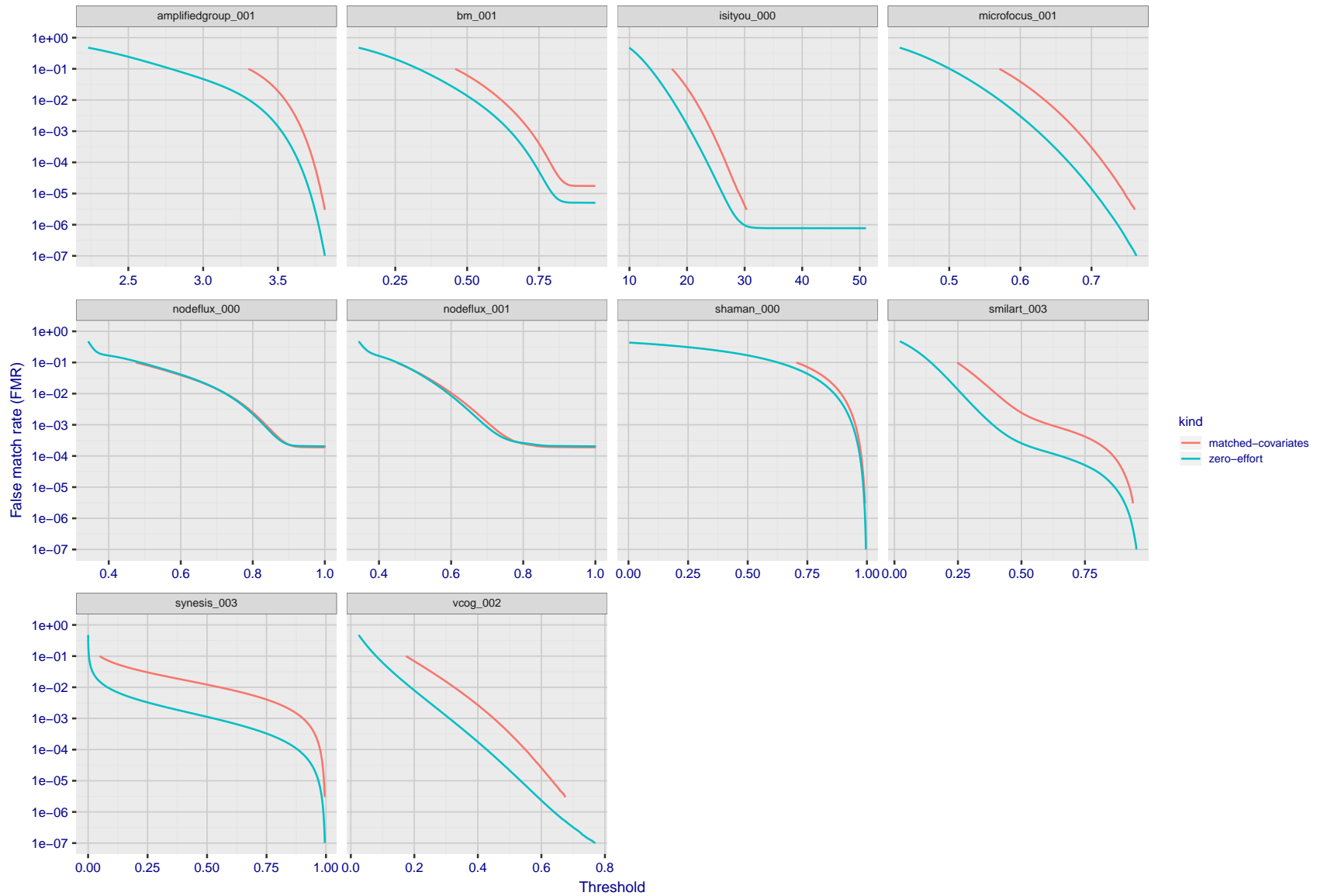


Figure 70: For the visa images, the false match calibration curves show FMR vs. threshold, T . The blue (lower) curves are for zero-effort impostors (i.e. comparing all images against all). The red (upper) curves are for persons of the same-sex, same-age, and same national-origin. This shows that FMR is underestimated (by a factor of 10 or more) by using a zero-effort impostor calculation to calibrate T . As shown later (sec. 3.6), FMR is higher for demographic-matched impostors.

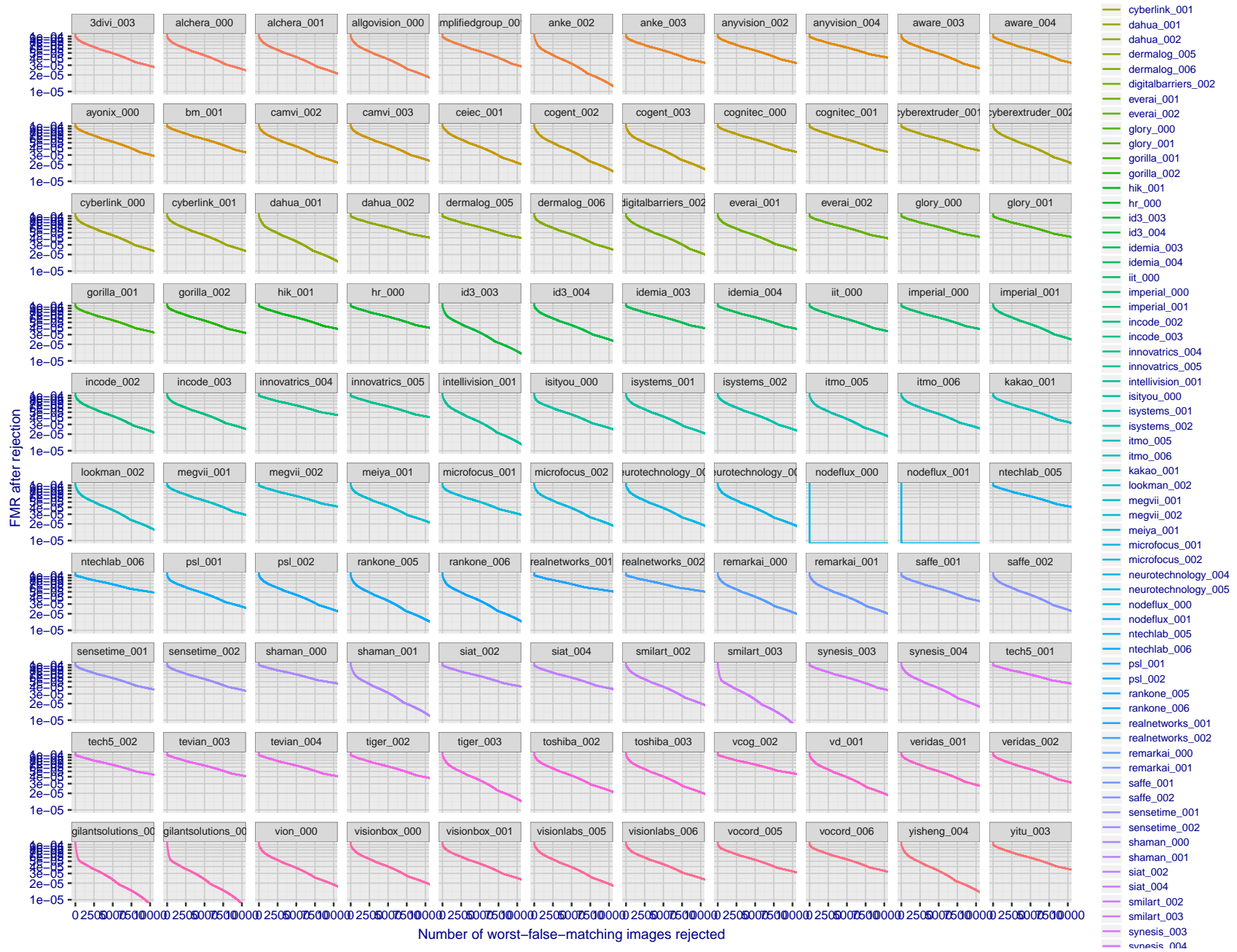


Figure 71: For the visa images, the curves show how false matches are concentrated in certain images. Specifically each line plots $FMR(k)$ with k the number of images rejected in decreasing order of how many false matches that image was involved in. $FMR(0) = 10^{-4}$. In terms of the biometric zoo, the most “wolf-ish” images are rejected first i.e. those enrollment or verification images most often involved in false matches. A flatter response is considered superior. A steeply descending response indicates that certain kinds of images false match against others, e.g. if hypothetically images of men with particular mustaches would falsely match others.

3.5 Genuine distribution stability

3.5.1 Effect of birth place on the genuine distribution

Background: Both skin tone and bone structure vary geographically. Prior studies have reported variations in FNMR and FMR.

Goal: To measure false non-match rate (FNMR) variation with country of birth.

Methods: Thresholds are determined that give $FMR = \{0.001, 0.0001\}$ over the entire impostor set. Then FNMR is measured over 1000 bootstrap replications of the genuine scores. Only those countries with at least 140 individuals are included in the analysis.

Results: Figure 80 shows FNMR by country of birth for the two thresholds.

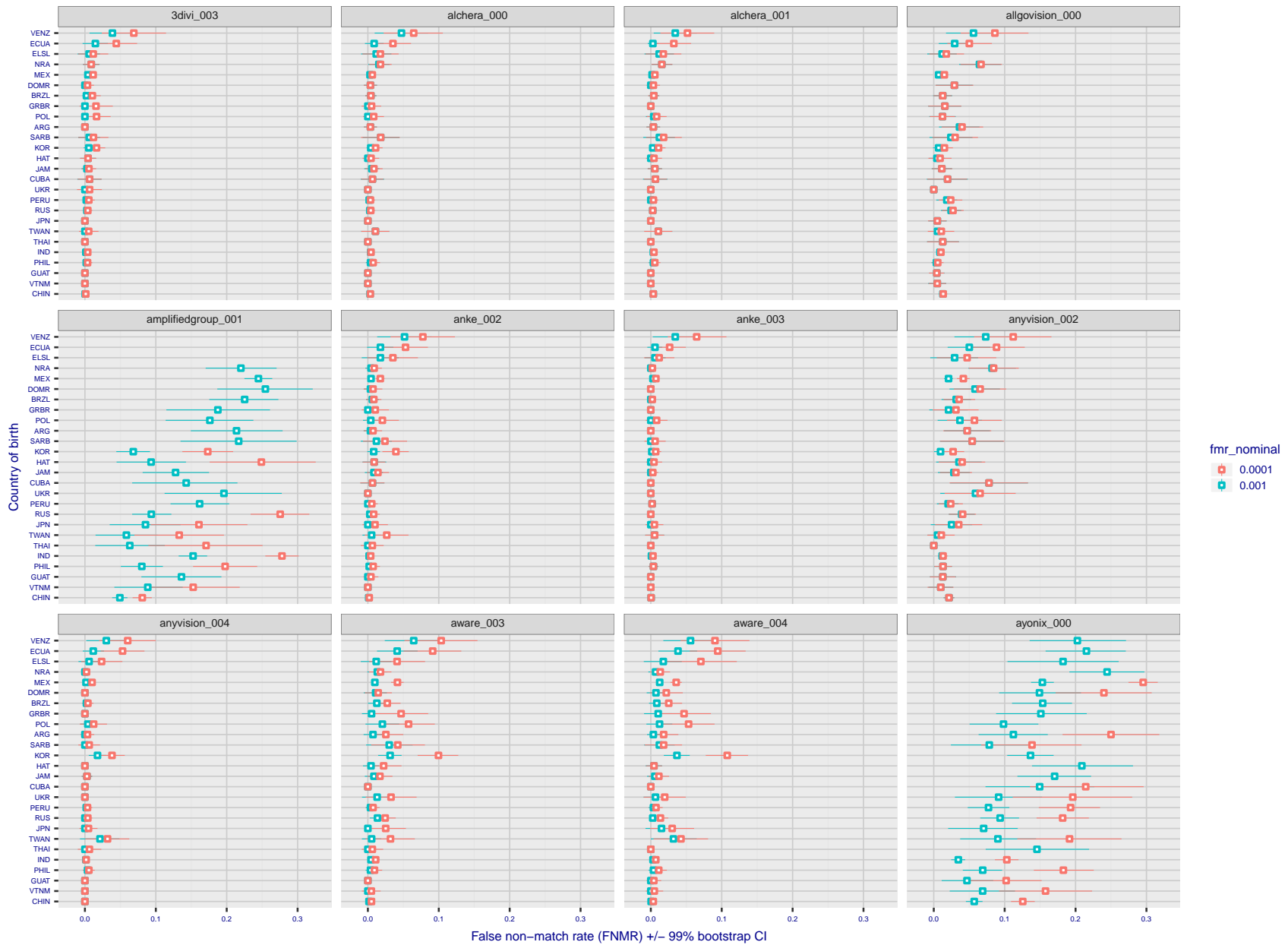
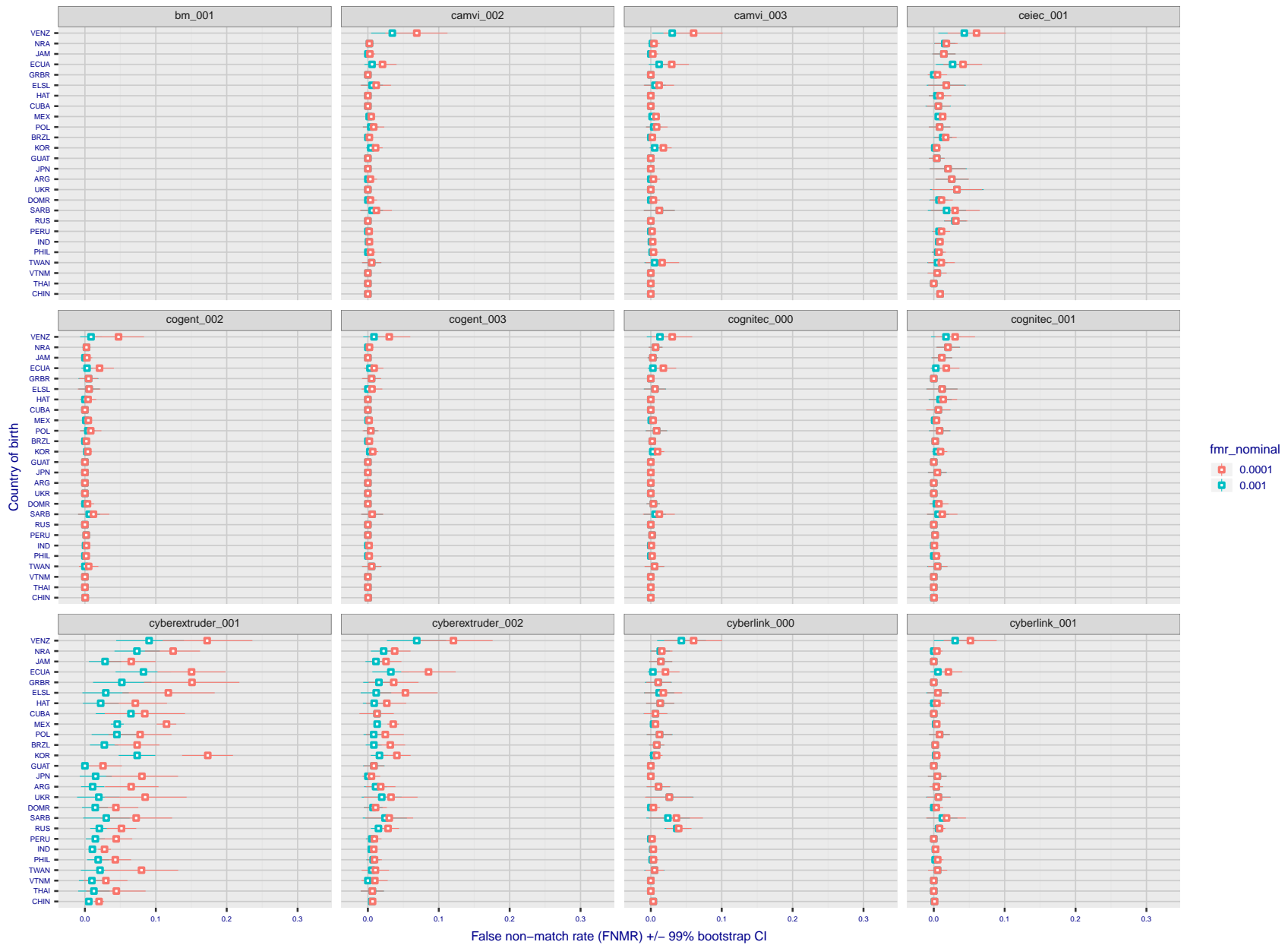


Figure 72: For the visa images, the dots show FNMR by country of birth for two globally set operating thresholds corresponding to $FMR = \{0.001, 0.0001\}$ computed over all on the order of 10^{10} impostor scores. The FMR in each bin will vary also - see subsequent impostor heatmaps in sec. 3.6.1. The figures shows an order of magnitude variation in FNMR across country of birth; these effects are likely due quality variations, then demographics like age and race. The error rates in some cases are zero, and in others the DET is flat so the error rates at the two thresholds are identical. The lines span 1% and 99% of bootstrap replicated FNMR estimates.

FNMR(T)
FMR(T)
"False non-match rate"
"False match rate"



FNMR(T)
FMR(T)
"False non-match rate"
"False match rate"

Figure 73: For the visa images, the dots show FNMR by country of birth for two globally set operating thresholds corresponding to $FMR = \{0.001, 0.0001\}$ computed over all on the order of 10^{10} impostor scores. The FMR in each bin will vary also - see subsequent impostor heatmaps in sec. 3.6.1. The figures shows an order of magnitude variation in FNMR across country of birth; these effects are likely due quality variations, then demographics like age and race. The error rates in some cases are zero, and in others the DET is flat so the error rates at the two thresholds are identical. The lines span 1% and 99% of bootstrap replicated FNMR estimates.

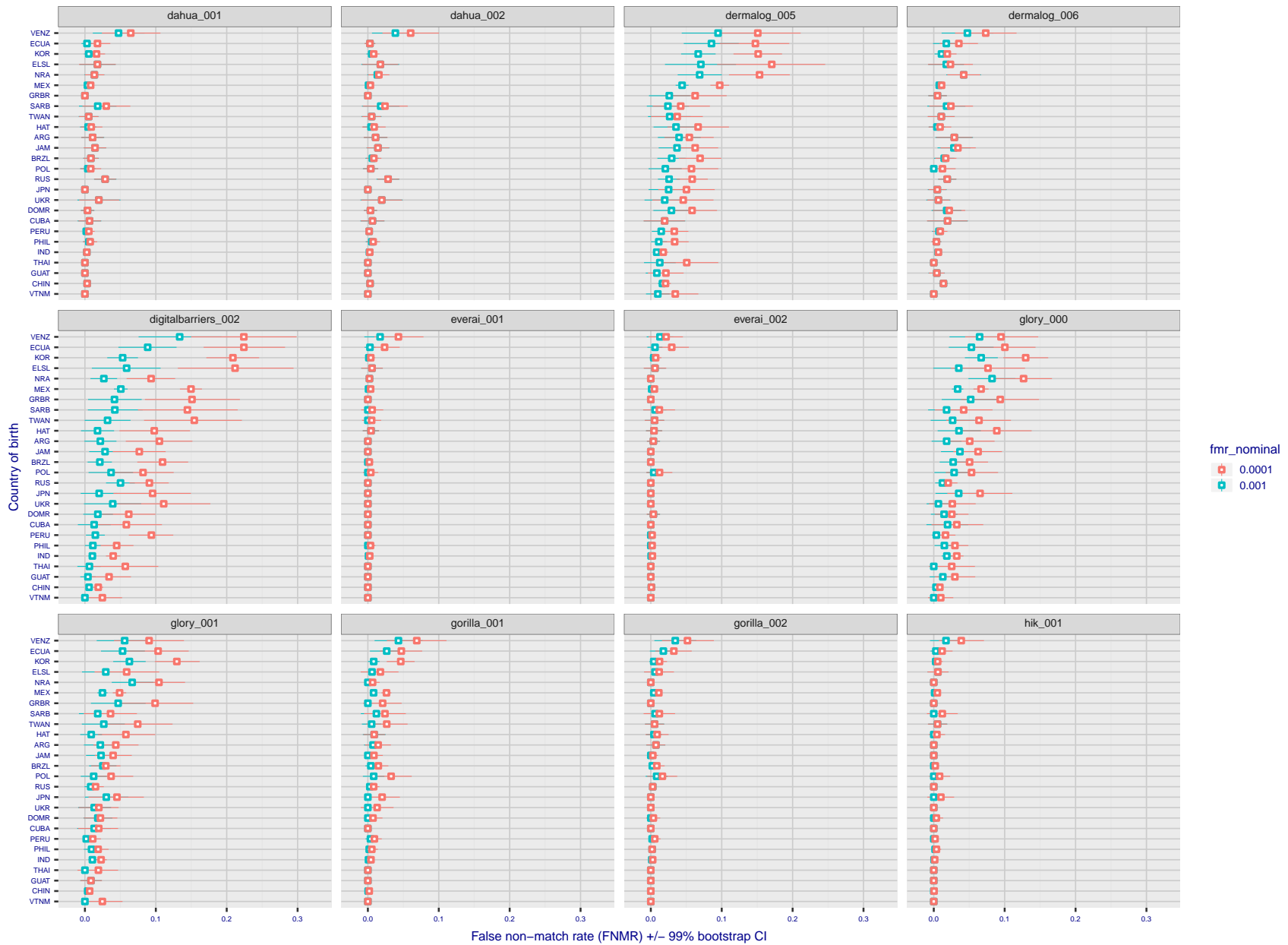
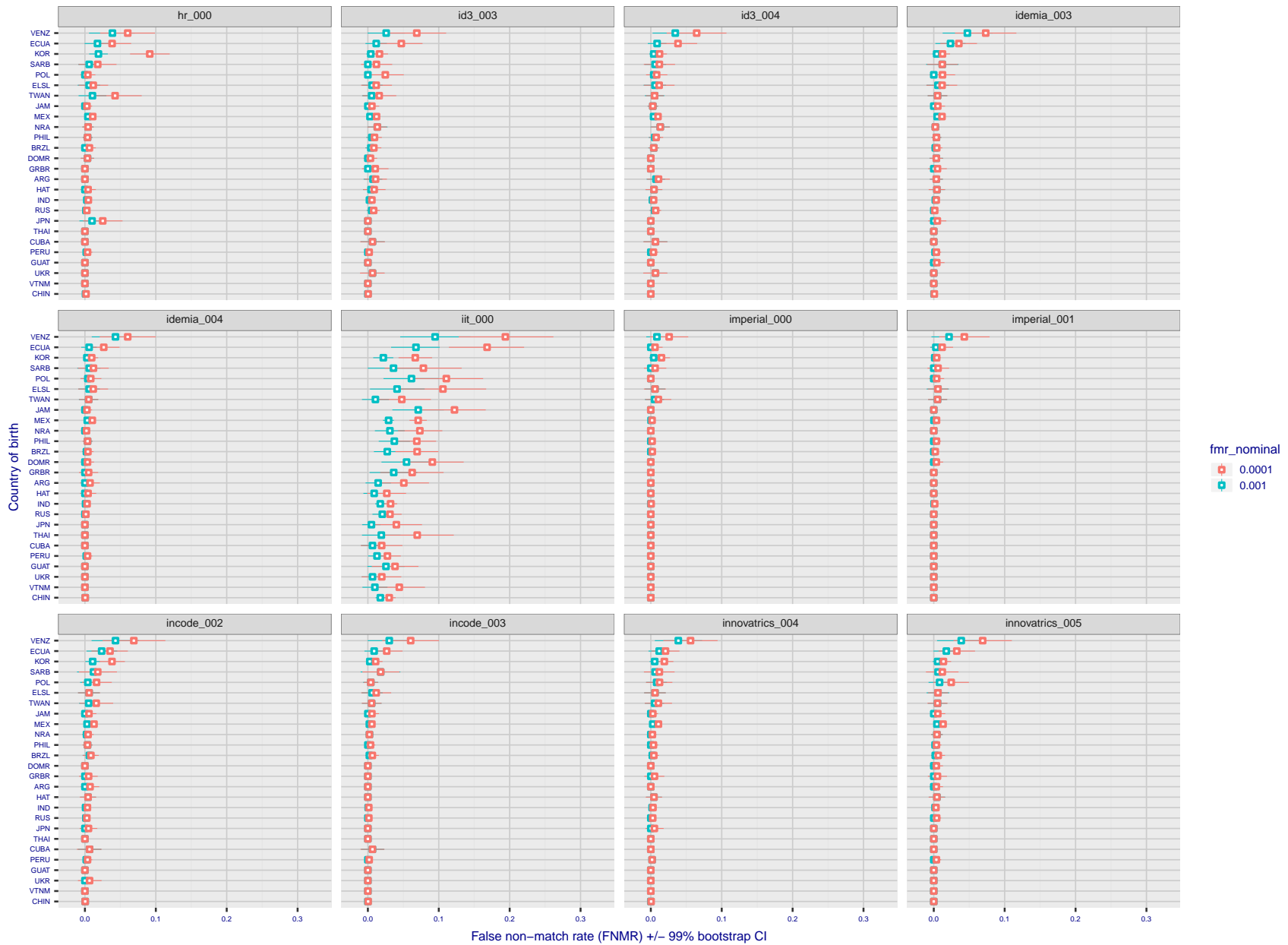


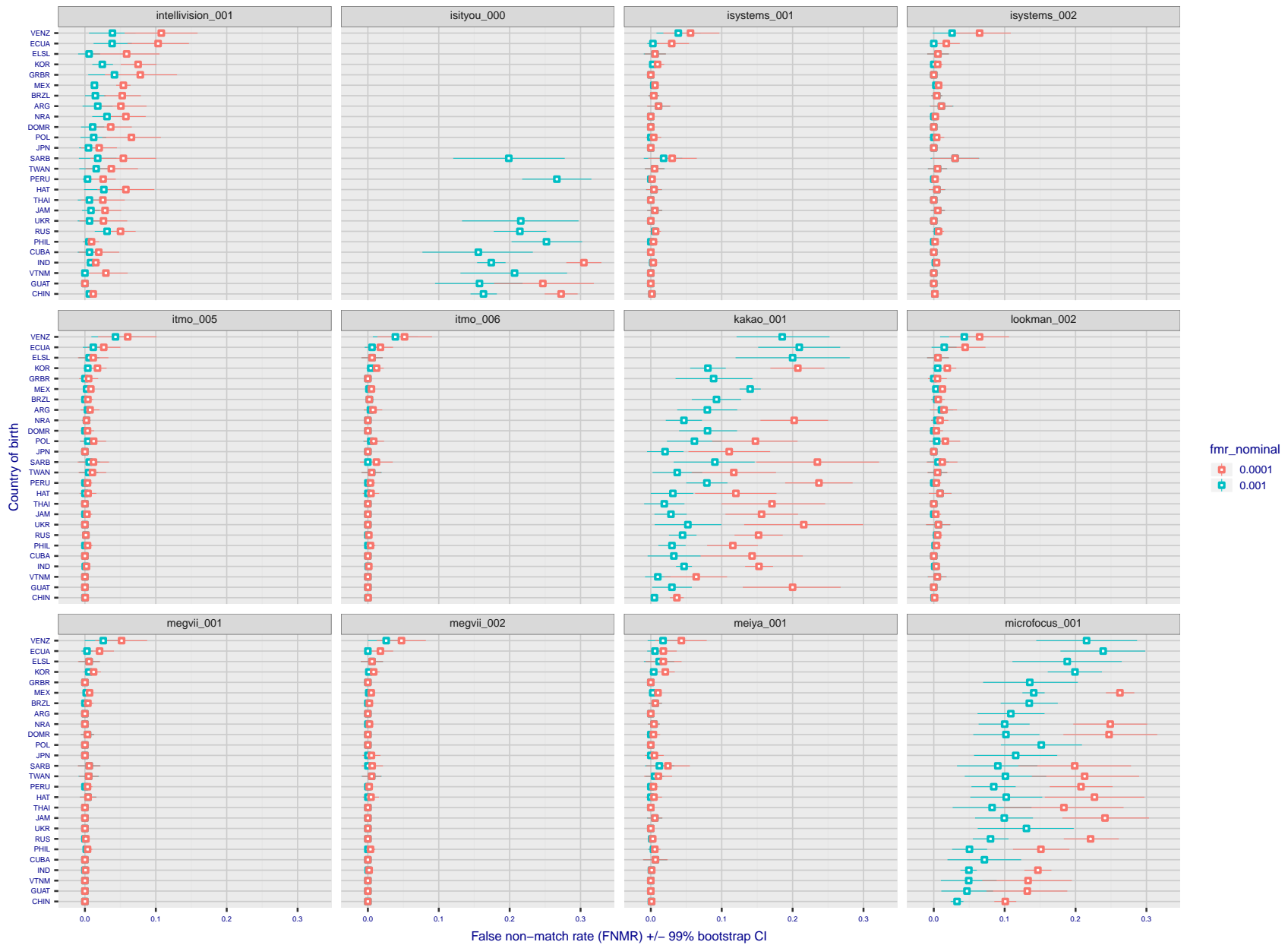
Figure 74: For the visa images, the dots show FNMR by country of birth for two globally set operating thresholds corresponding to $FMR = \{0.001, 0.0001\}$ computed over all on the order of 10^{10} impostor scores. The FMR in each bin will vary also - see subsequent impostor heatmaps in sec. 3.6.1. The figures shows an order of magnitude variation in FNMR across country of birth; these effects are likely due quality variations, then demographics like age and race. The error rates in some cases are zero, and in others the DET is flat so the error rates at the two thresholds are identical. The lines span 1% and 99% of bootstrap replicated FNMR estimates.

FNMR(T)
FMR(T)
"False non-match rate"
"False match rate"



FNMR(T)
FMR(T)
"False non-match rate"
"False match rate"

Figure 75: For the visa images, the dots show FNMR by country of birth for two globally set operating thresholds corresponding to $FMR = \{0.001, 0.0001\}$ computed over all on the order of 10^{10} impostor scores. The FMR in each bin will vary also - see subsequent impostor heatmaps in sec. 3.6.1. The figures shows an order of magnitude variation in FNMR across country of birth; these effects are likely due quality variations, then demographics like age and race. The error rates in some cases are zero, and in others the DET is flat so the error rates at the two thresholds are identical. The lines span 1% and 99% of bootstrap replicated FNMR estimates.



FNMR(T)
FMR(T)
"False non-match rate"
"False match rate"

Figure 76: For the visa images, the dots show FNMR by country of birth for two globally set operating thresholds corresponding to $FMR = \{0.001, 0.0001\}$ computed over all on the order of 10^{10} impostor scores. The FMR in each bin will vary also - see subsequent impostor heatmaps in sec. 3.6.1. The figures shows an order of magnitude variation in FNMR across country of birth; these effects are likely due quality variations, then demographics like age and race. The error rates in some cases are zero, and in others the DET is flat so the error rates at the two thresholds are identical. The lines span 1% and 99% of bootstrap replicated FNMR estimates.

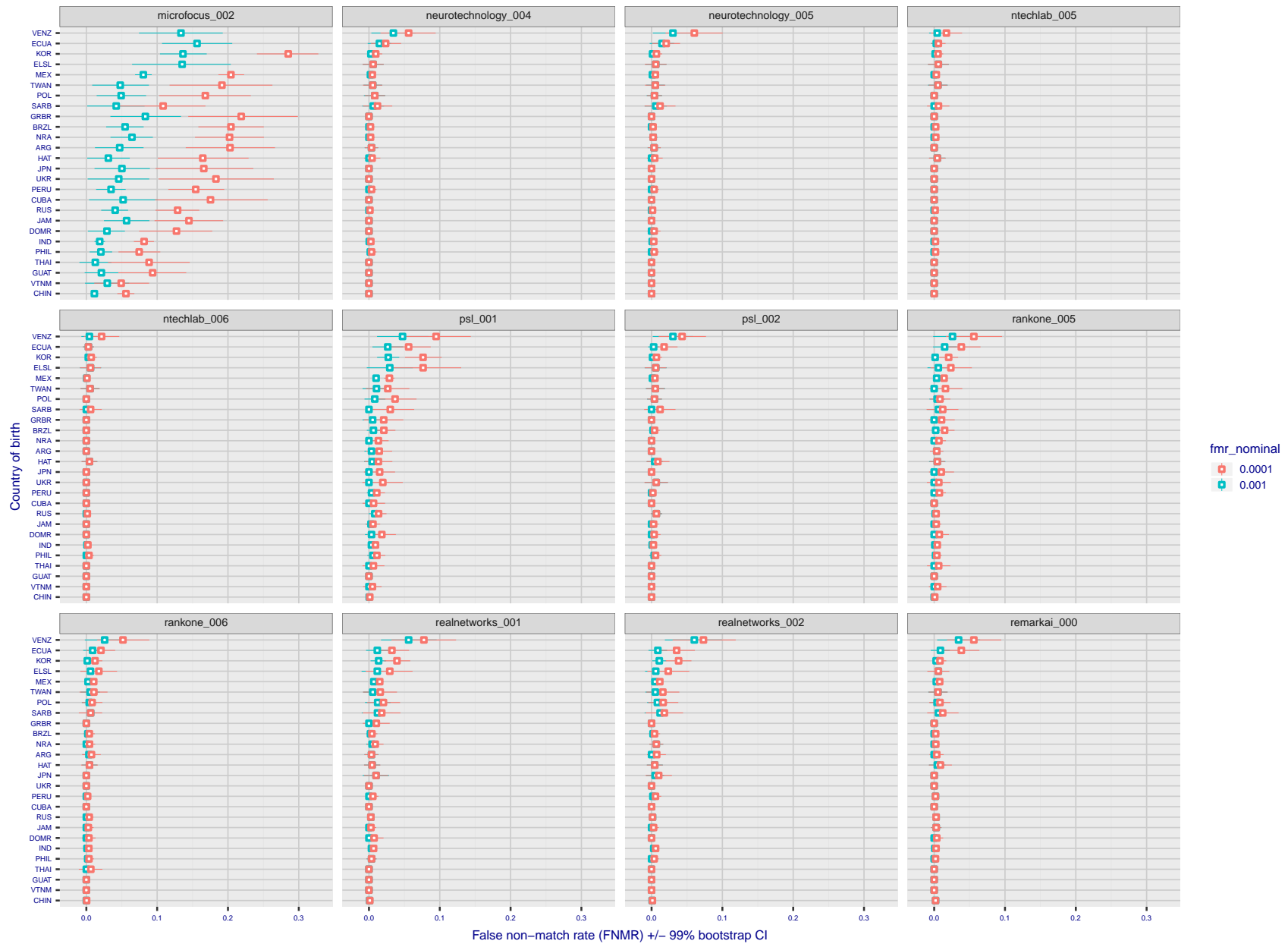
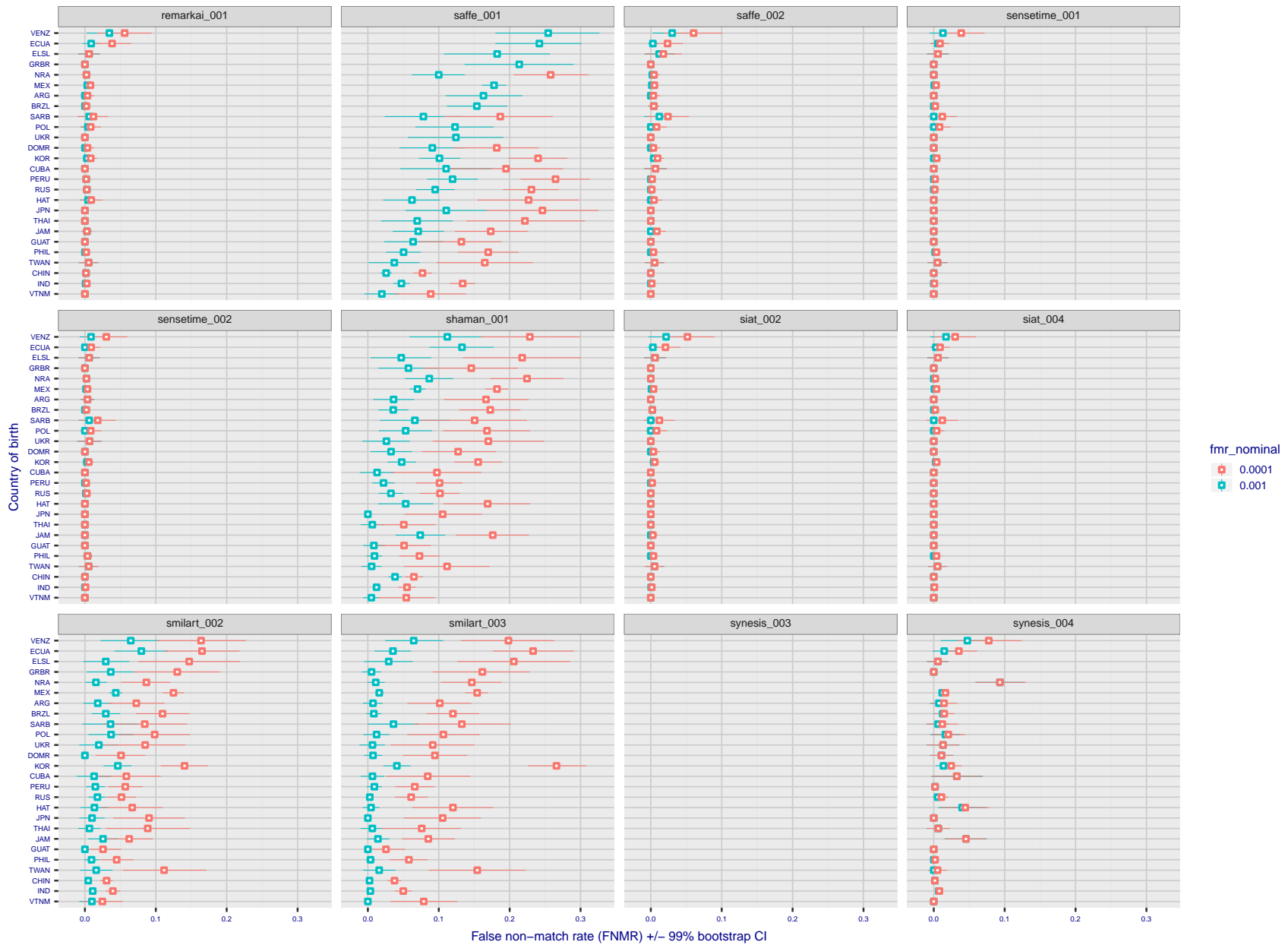


Figure 77: For the visa images, the dots show FNMR by country of birth for two globally set operating thresholds corresponding to $FMR = \{0.001, 0.0001\}$ computed over all on the order of 10^{10} impostor scores. The FMR in each bin will vary also - see subsequent impostor heatmaps in sec. 3.6.1. The figures shows an order of magnitude variation in FNMR across country of birth; these effects are likely due quality variations, then demographics like age and race. The error rates in some cases are zero, and in others the DET is flat so the error rates at the two thresholds are identical. The lines span 1% and 99% of bootstrap replicated FNMR estimates.



FNMR(T)
FMR(T)
"False non-match rate"
"False match rate"

Figure 78: For the visa images, the dots show FNMR by country of birth for two globally set operating thresholds corresponding to $FMR = \{0.001, 0.0001\}$ computed over all on the order of 10^{10} impostor scores. The FMR in each bin will vary also - see subsequent impostor heatmaps in sec. 3.6.1. The figures shows an order of magnitude variation in FNMR across country of birth; these effects are likely due quality variations, then demographics like age and race. The error rates in some cases are zero, and in others the DET is flat so the error rates at the two thresholds are identical. The lines span 1% and 99% of bootstrap replicated FNMR estimates.

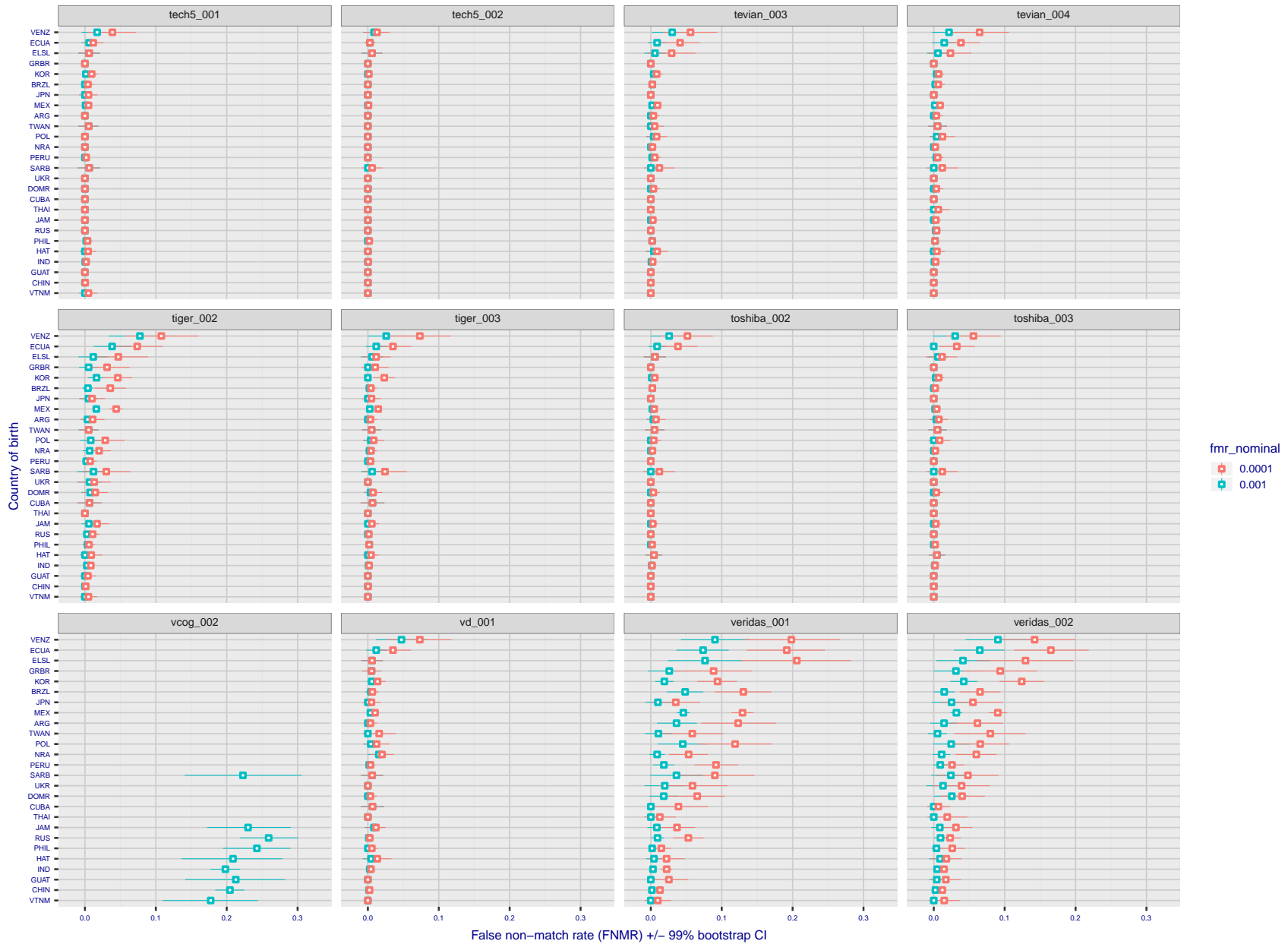


Figure 79: For the visa images, the dots show FNMR by country of birth for two globally set operating thresholds corresponding to $FMR = \{0.001, 0.0001\}$ computed over all on the order of 10^{10} impostor scores. The FMR in each bin will vary also - see subsequent impostor heatmaps in sec. 3.6.1. The figures shows an order of magnitude variation in FNMR across country of birth; these effects are likely due quality variations, then demographics like age and race. The error rates in some cases are zero, and in others the DET is flat so the error rates at the two thresholds are identical. The lines span 1% and 99% of bootstrap replicated FNMR estimates.

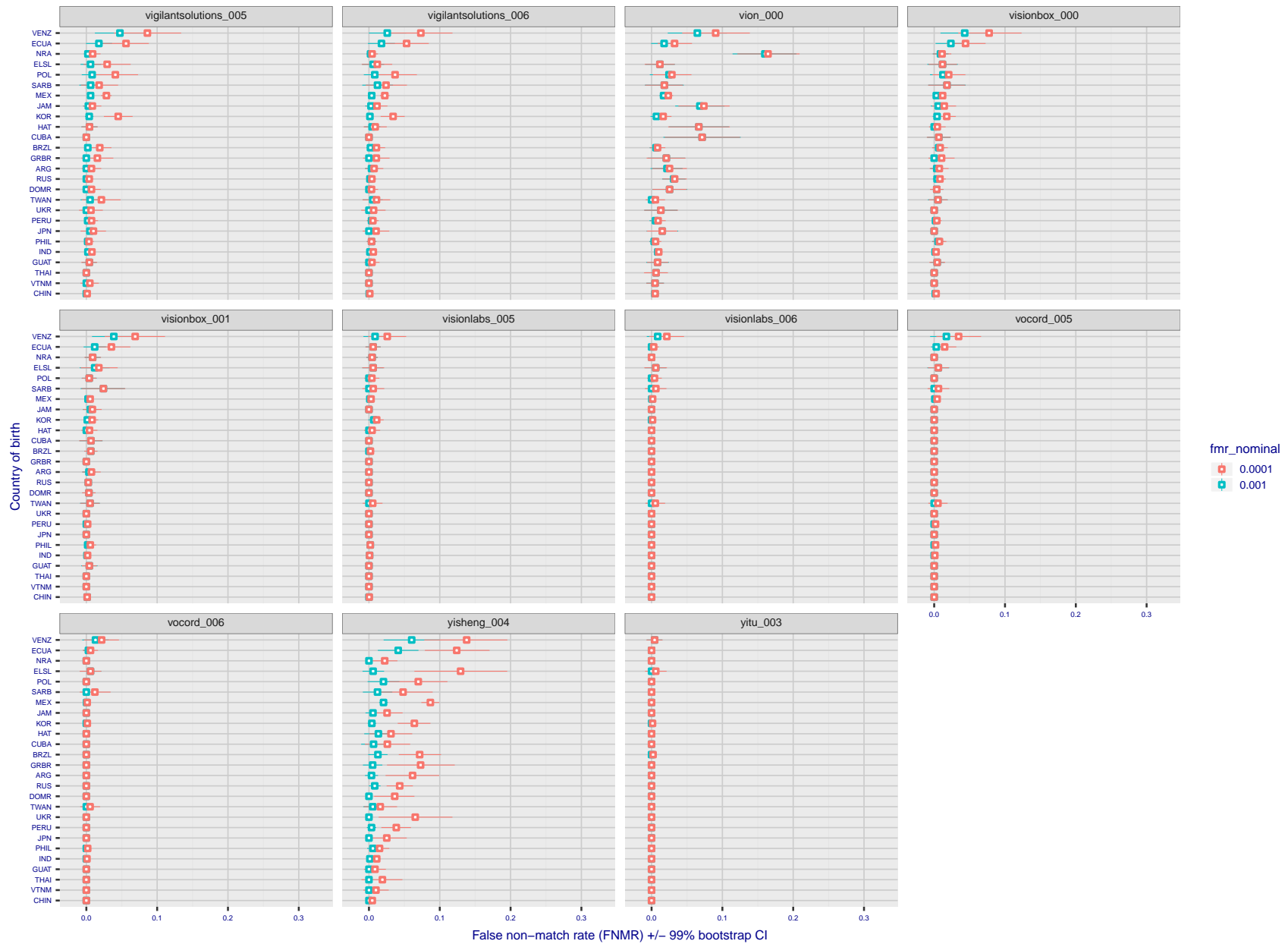


Figure 80: For the visa images, the dots show FNMR by country of birth for two globally set operating thresholds corresponding to $FMR = \{0.001, 0.0001\}$ computed over all on the order of 10^{10} impostor scores. The FMR in each bin will vary also - see subsequent impostor heatmaps in sec. 3.6.1. The figures shows an order of magnitude variation in FNMR across country of birth; these effects are likely due quality variations, then demographics like age and race. The error rates in some cases are zero, and in others the DET is flat so the error rates at the two thresholds are identical. The lines span 1% and 99% of bootstrap replicated FNMR estimates.

Caveats: The results may not relate to subject-specific properties. Instead they could reflect image-specific quality differences, which could occur due to collection protocol or software processing variations.

3.5.2 Effect of ageing

Background: Faces change appearance throughout life. This change gradually reduces similarity of a new image to an earlier image. Face recognition algorithms give reduced similarity scores and more frequent false rejections.

Goal: To quantify false non-match rates (FNMR) as a function of elapsed time in an adult population.

Methods: Using the mugshot images, a threshold is set to give $FMR = 0.00001$ over the entire impostor set. Then FNMR is measured over 1000 bootstrap replications of the genuine scores.

Results: For the visa images, Figure 87 shows how false non-match rates for genuine users, as a function of age group.

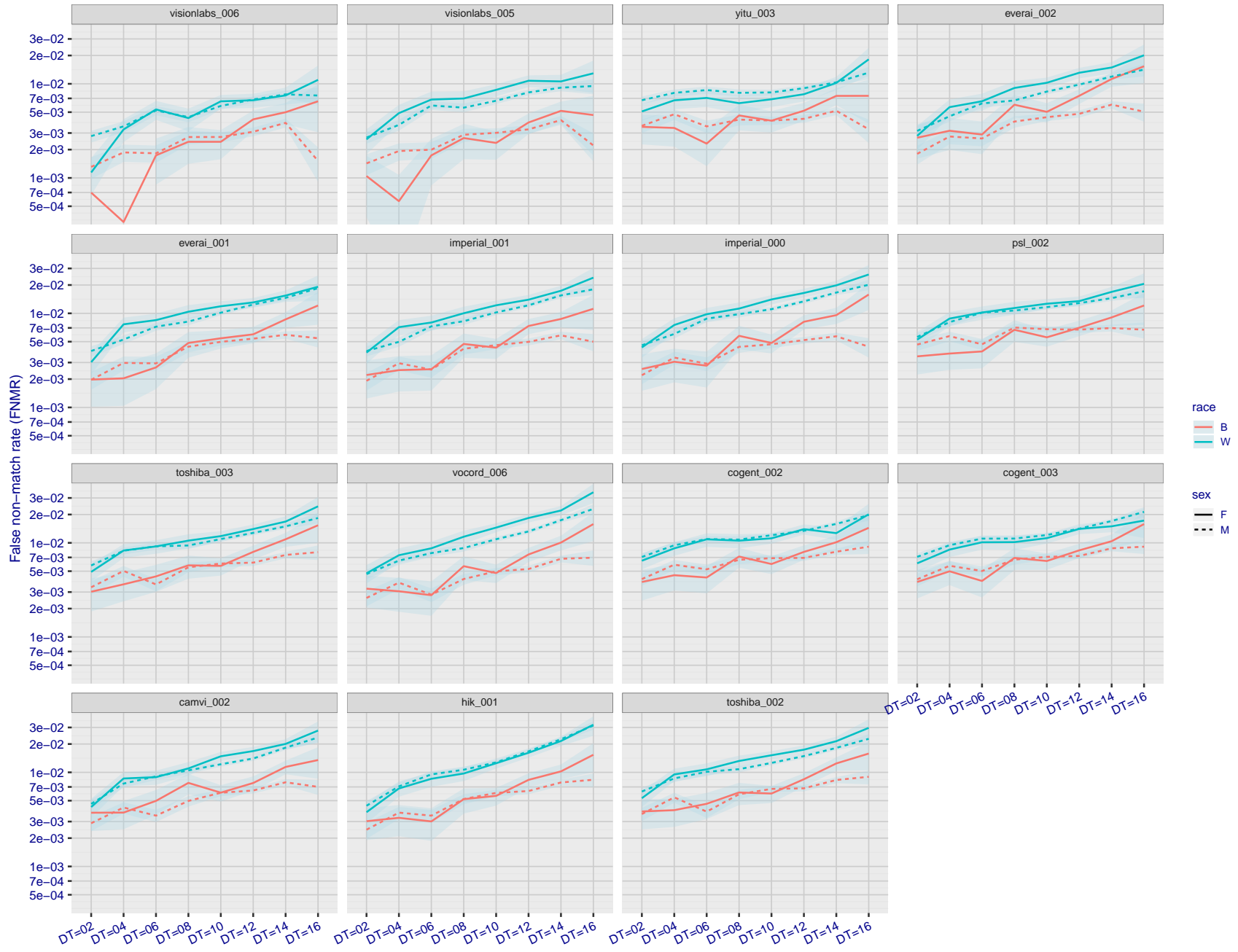


Figure 81: For the mugshot images, FNMR as a function of elapsed time between initial enrollment and second verification images. The panels appear most accurate first, and vertical scale changes on each page. The four traces correspond to images annotated with codes for black female, black male, white female, white male. The threshold is fixed for each algorithm to give FMR = 0.00001 over all (10^8) impostor comparisons. For short time-lapses, the most accurate algorithms give very few errors (FNMR < 0.001) so that the uncertainty estimates are high.

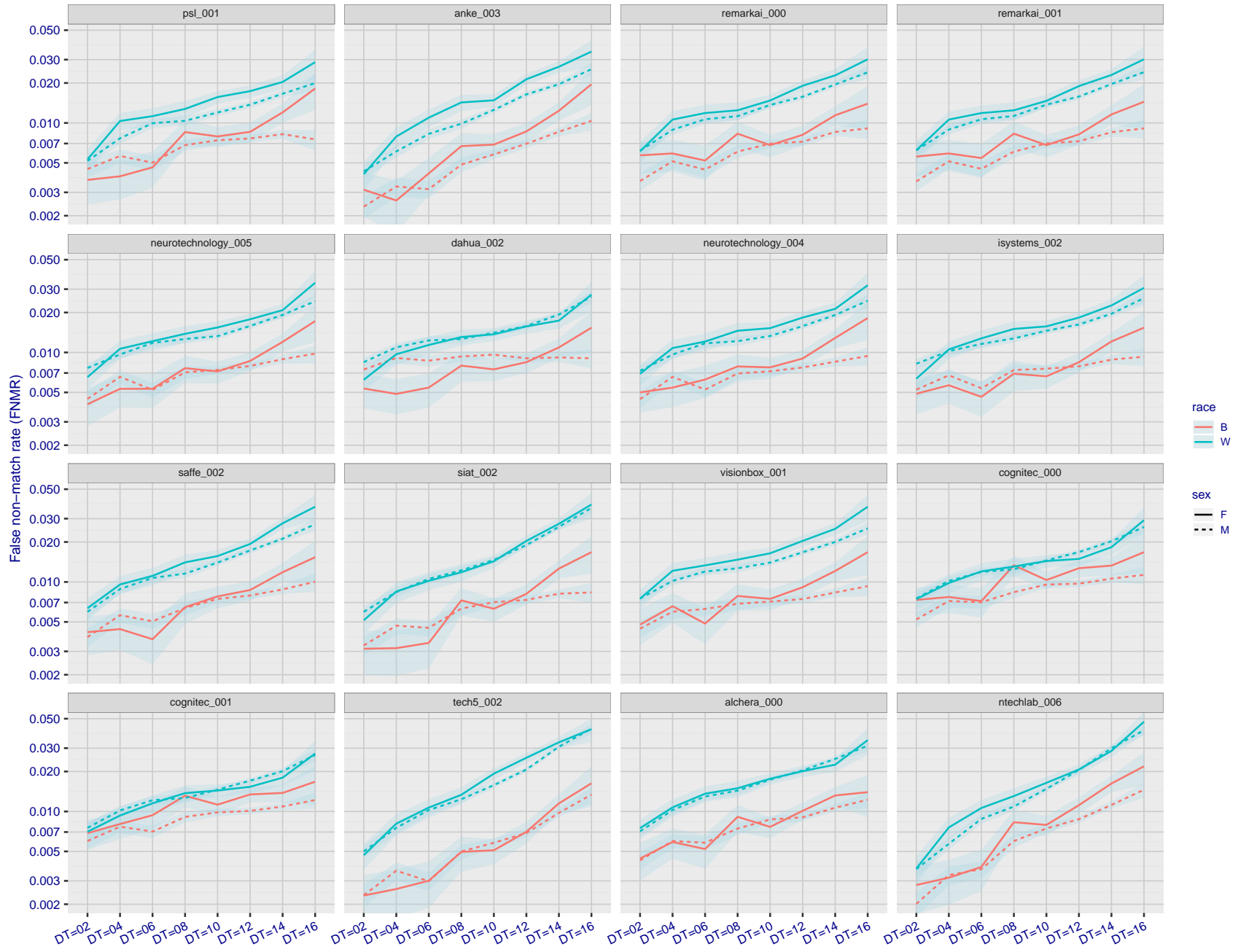


Figure 82: For the mugshot images, FNMR as a function of elapsed time between initial enrollment and second verification images. The panels appear most accurate first, and vertical scale changes on each page. The four traces correspond to images annotated with codes for black female, black male, white female, white male. The threshold is fixed for each algorithm to give FMR = 0.00001 over all (10^8) impostor comparisons. For short time-lapses, the most accurate algorithms give very few errors (FNMR < 0.001) so that the uncertainty estimates are high.

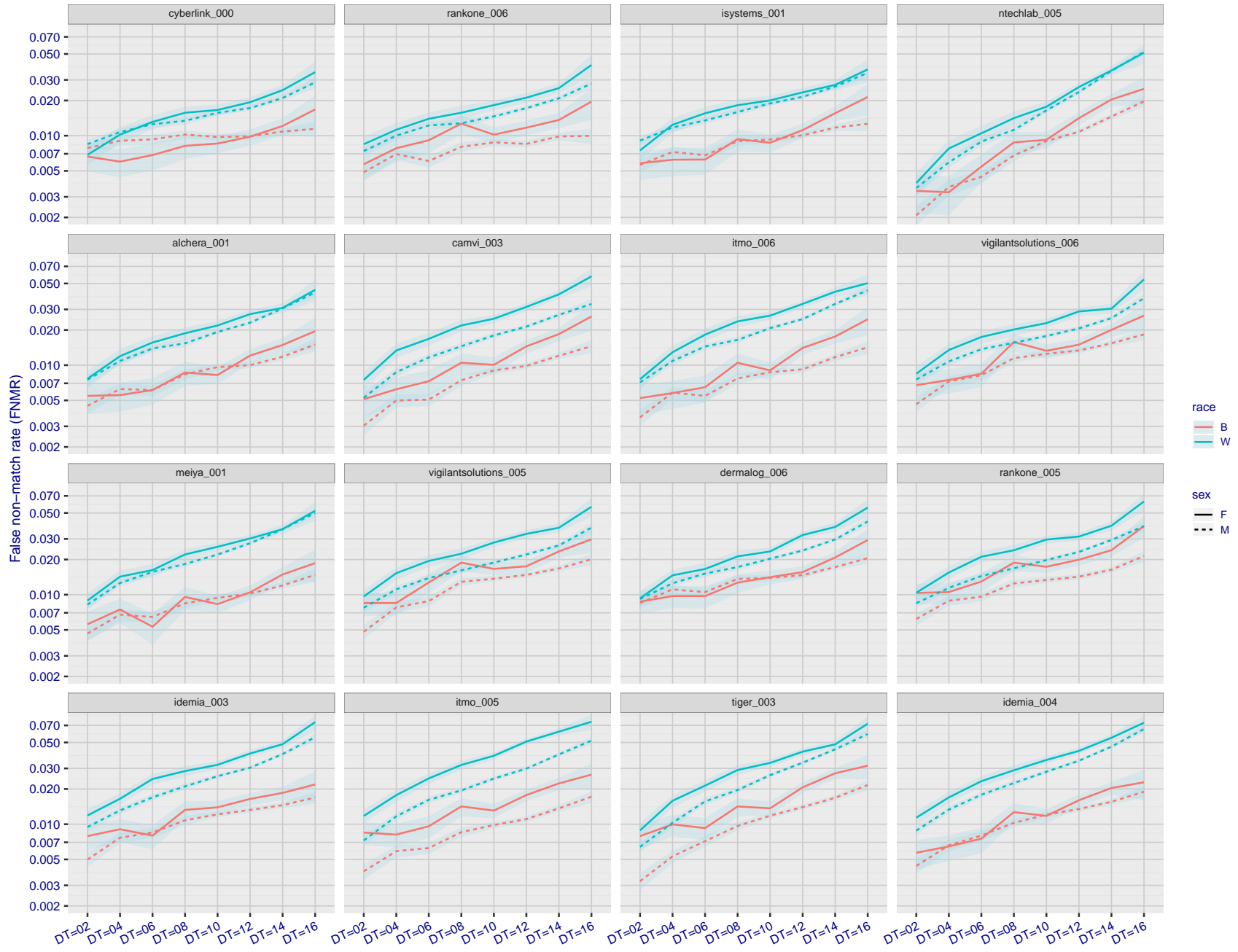
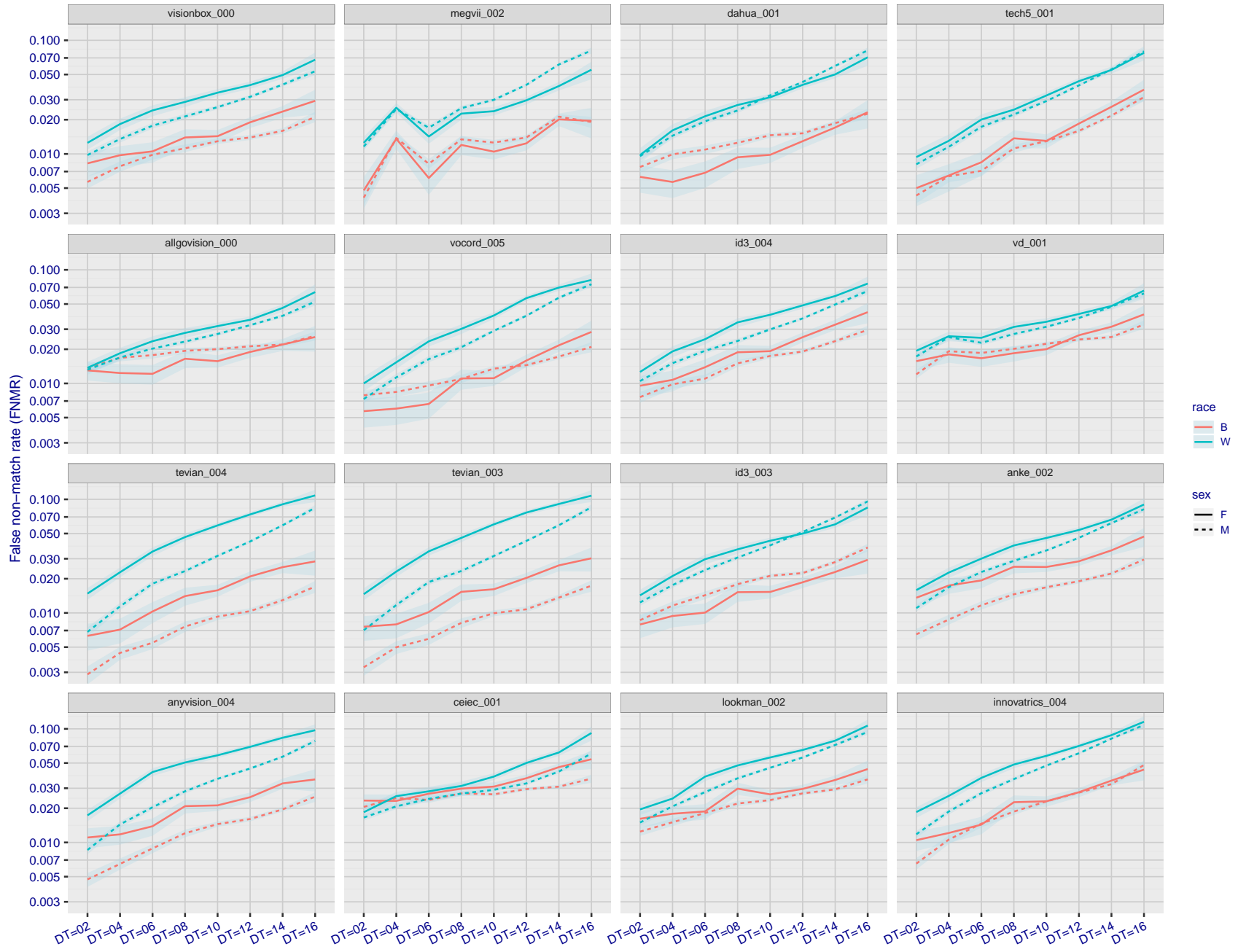


Figure 83: For the mugshot images, FNMR as a function of elapsed time between initial enrollment and second verification images. The panels appear most accurate first, and vertical scale changes on each page. The four traces correspond to images annotated with codes for black female, black male, white female, white male. The threshold is fixed for each algorithm to give FMR = 0.00001 over all (10^8) impostor comparisons. For short time-lapses, the most accurate algorithms give very few errors (FNMR < 0.001) so that the uncertainty estimates are high.



FNMR(T)
FMR(T)
"False non-match rate"
"False match rate"

Figure 84: For the mugshot images, FNMR as a function of elapsed time between initial enrollment and second verification images. The panels appear most accurate first, and vertical scale changes on each page. The four traces correspond to images annotated with codes for black female, black male, white female, white male. The threshold is fixed for each algorithm to give FMR = 0.00001 over all (10^8) impostor comparisons. For short time-lapses, the most accurate algorithms give very few errors (FNMR < 0.001) so that the uncertainty estimates are high.

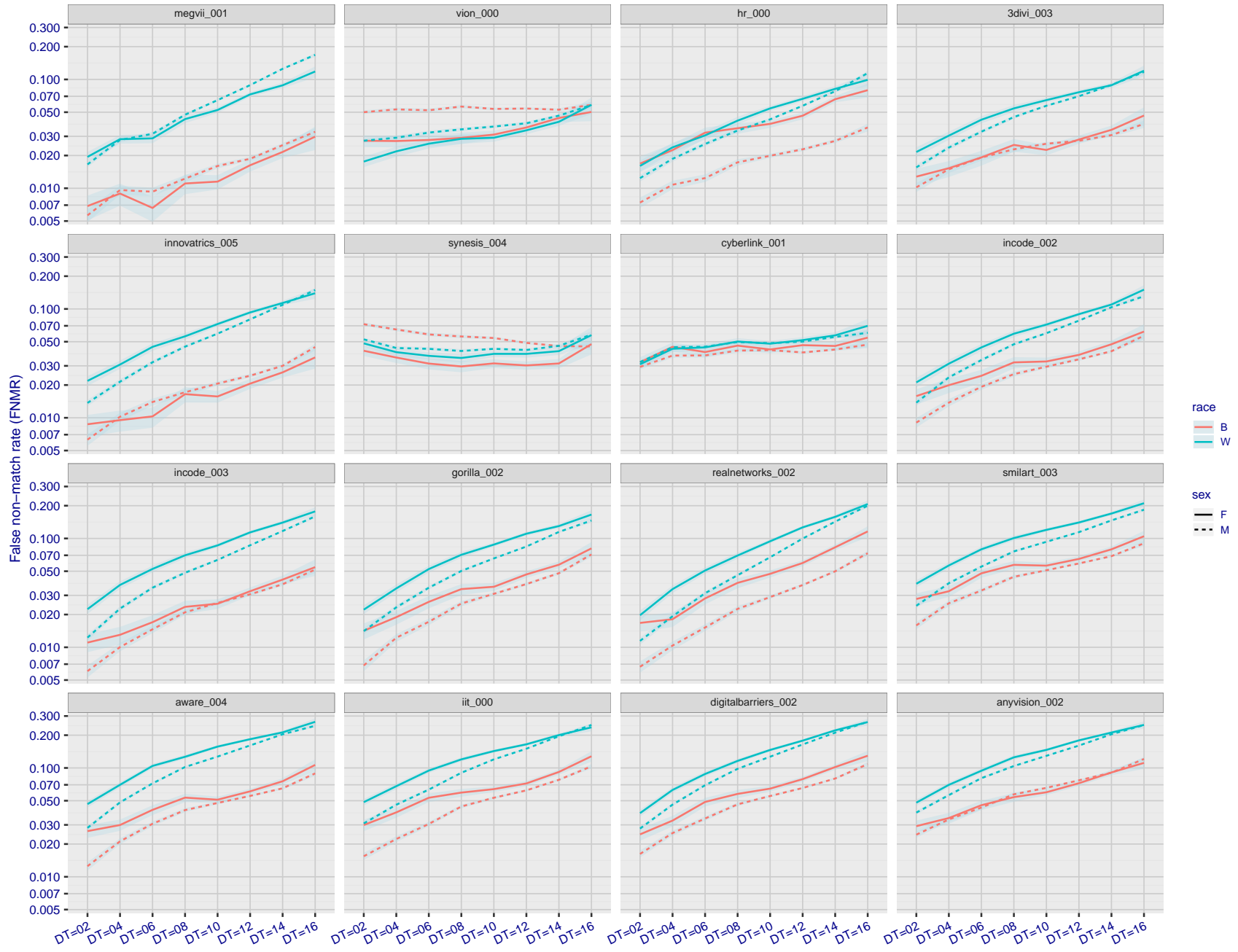
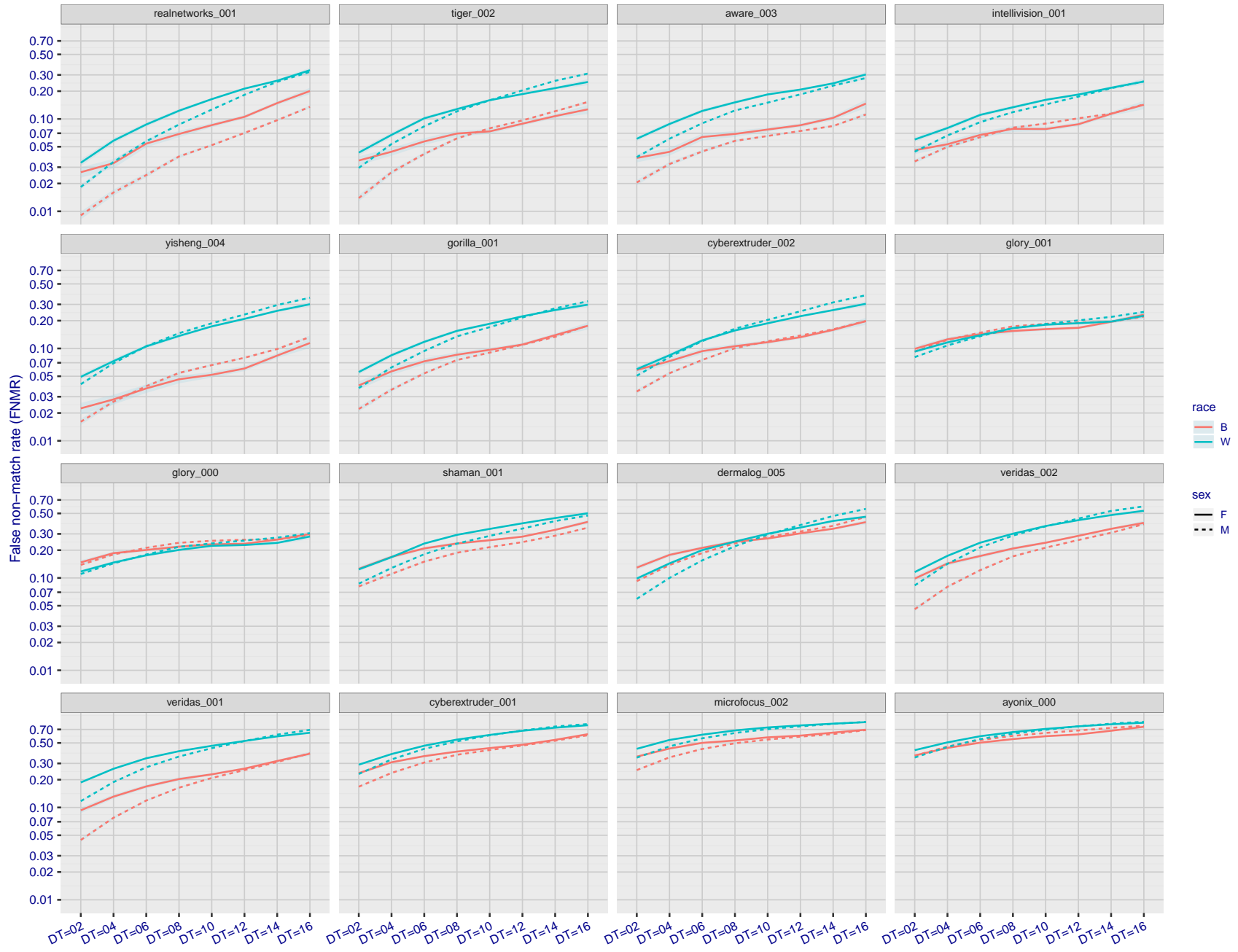


Figure 85: For the mugshot images, FNMR as a function of elapsed time between initial enrollment and second verification images. The panels appear most accurate first, and vertical scale changes on each page. The four traces correspond to images annotated with codes for black female, black male, white female, white male. The threshold is fixed for each algorithm to give FMR = 0.00001 over all (10^8) impostor comparisons. For short time-lapses, the most accurate algorithms give very few errors (FNMR < 0.001) so that the uncertainty estimates are high.



FNMR(T)
FMR(T)
"False non-match rate"
"False match rate"

Figure 86: For the mugshot images, FNMR as a function of elapsed time between initial enrollment and second verification images. The panels appear most accurate first, and vertical scale changes on each page. The four traces correspond to images annotated with codes for black female, black male, white female, white male. The threshold is fixed for each algorithm to give FMR = 0.00001 over all (10^8) impostor comparisons. For short time-lapses, the most accurate algorithms give very few errors (FNMR < 0.001) so that the uncertainty estimates are high.

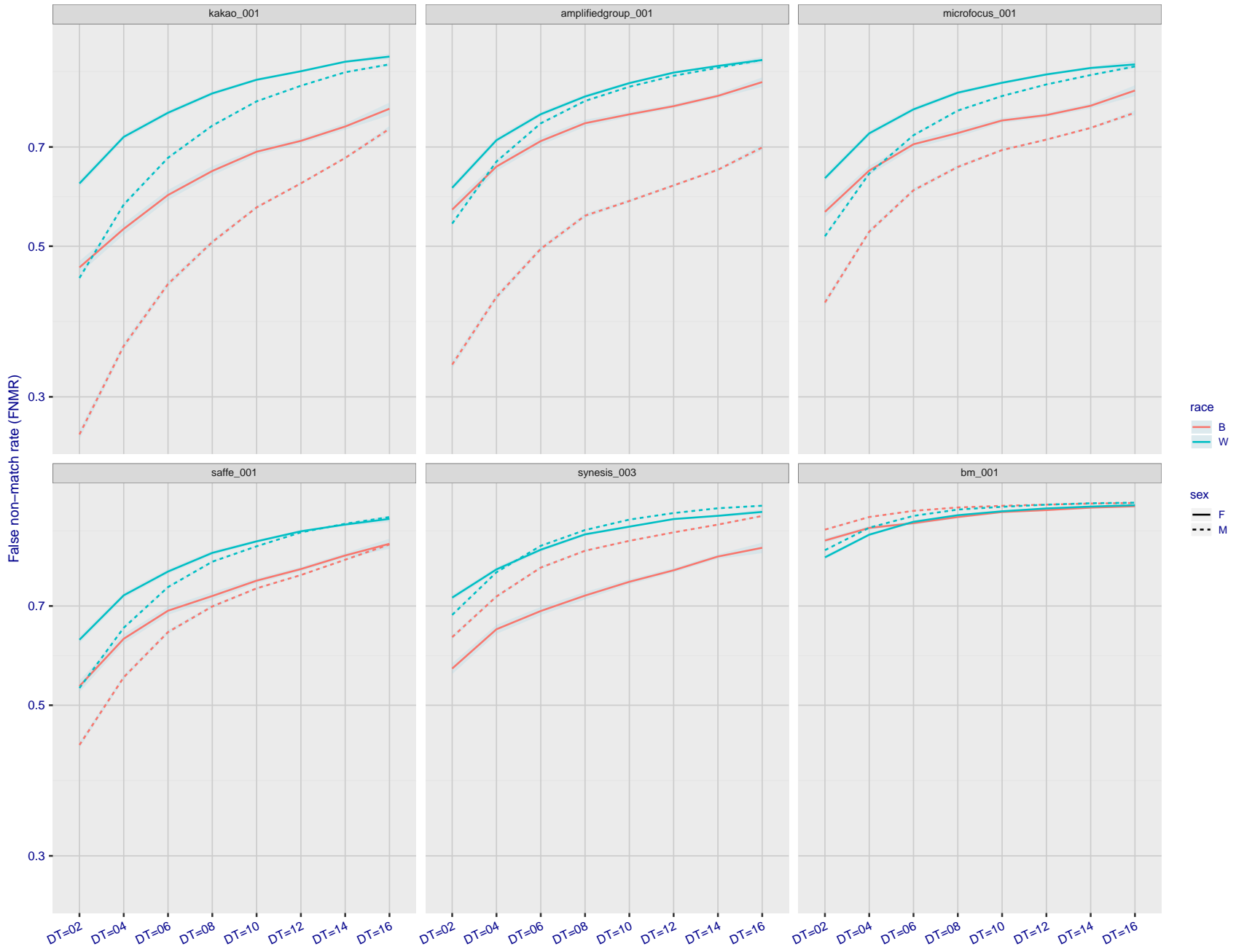


Figure 87: For the mugshot images, FNMR as a function of elapsed time between initial enrollment and second verification images. The panels appear most accurate first, and vertical scale changes on each page. The four traces correspond to images annotated with codes for black female, black male, white female, white male. The threshold is fixed for each algorithm to give FMR = 0.00001 over all (10^8) impostor comparisons. For short time-lapses, the most accurate algorithms give very few errors (FNMR < 0.001) so that the uncertainty estimates are high.

3.5.3 Effect of age on genuine subjects

Background: Faces change appearance throughout life. Face recognition algorithms have previously been reported to give better accuracy on older individuals (See NIST IR 8009).

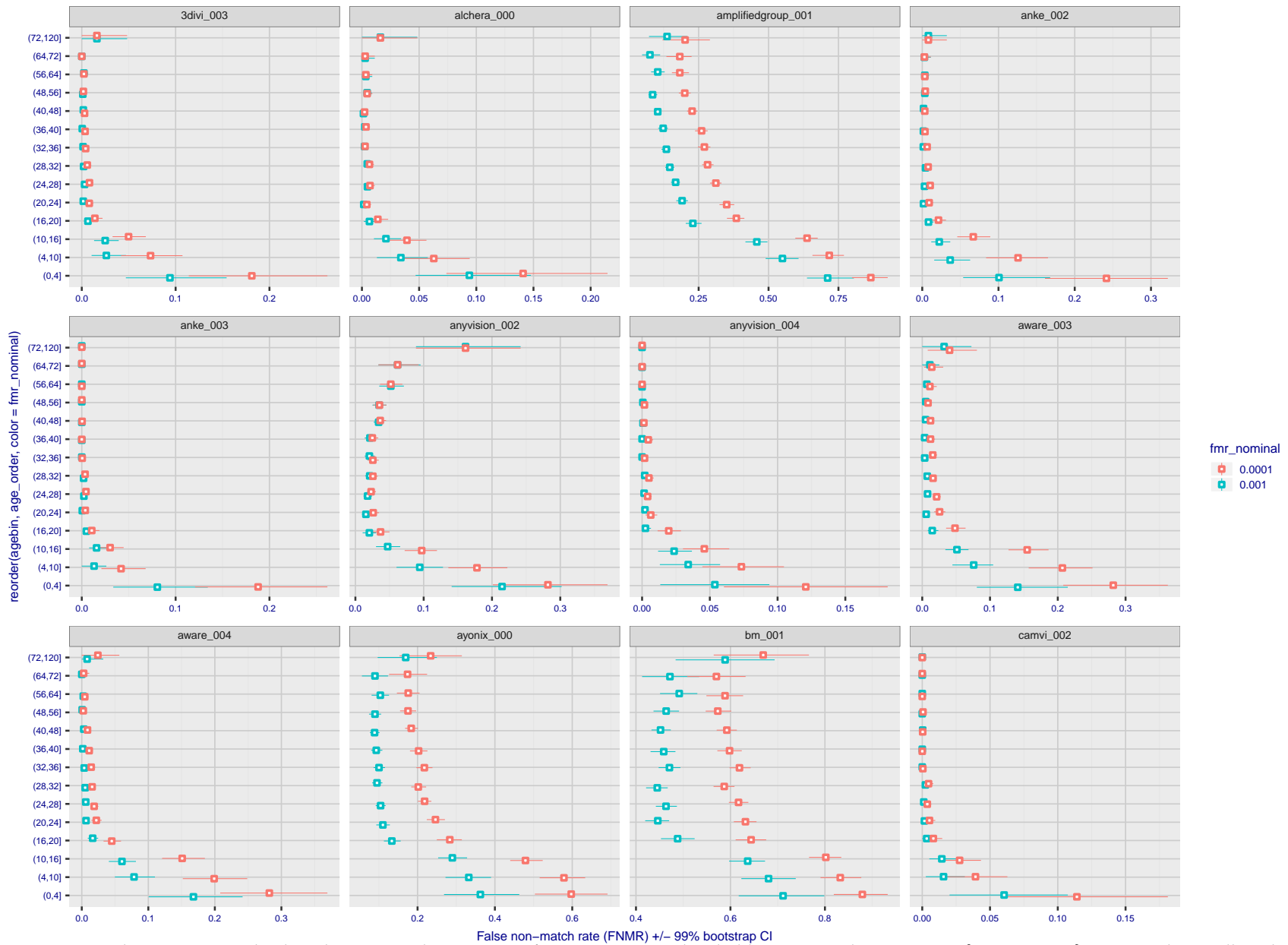
Goal: To quantify false non-match rates (FNMR) as a function of age, without an ageing component.

Methods: Using the visa images, which span fewer than five years, thresholds are determined that give FMR = 0.001 and 0.0001 over the entire impostor set. Then FNMR is measured over 1000 bootstrap replications of the genuine scores.

Results: For the visa images, Figure 96 shows how false non-match rates for genuine users, as a function of age group.

The notable aspects are:

- ▷ Younger subjects give considerably higher FNMR. This is likely due to rapid growth and change in facial appearance.
- ▷ FNMR trends down throughout life. The last bin, AGE > 72, contains fewer than 140 mated pairs, and may be affected by small sample size.



FNMR(T)
FMR(T)
"False non-match rate"
"False match rate"

Figure 88: For the visa images, the dots show FNMR by age group for two operating thresholds corresponding to $FMR = \{0.001, 0.0001\}$ computed over all on the order of 10^{10} impostor scores. The FMR in each bin will vary also - see subsequent impostor heatmaps in sec. 3.6.2. Given a pair of face images taken at different times, we assign the comparison to the bin that is the arithmetic average of the subject's ages. This plot shows only the effect of age, not ageing. The number of comparisons in each bin is generally in the thousands, however the first and last bins are computed over 149 and 124 respectively. The error rates in some (adult) cases are zero, and in others the DET is flat so the error rates at the two thresholds are identical. The lines span 1% and 99% of bootstrap replicated FNMR estimates.

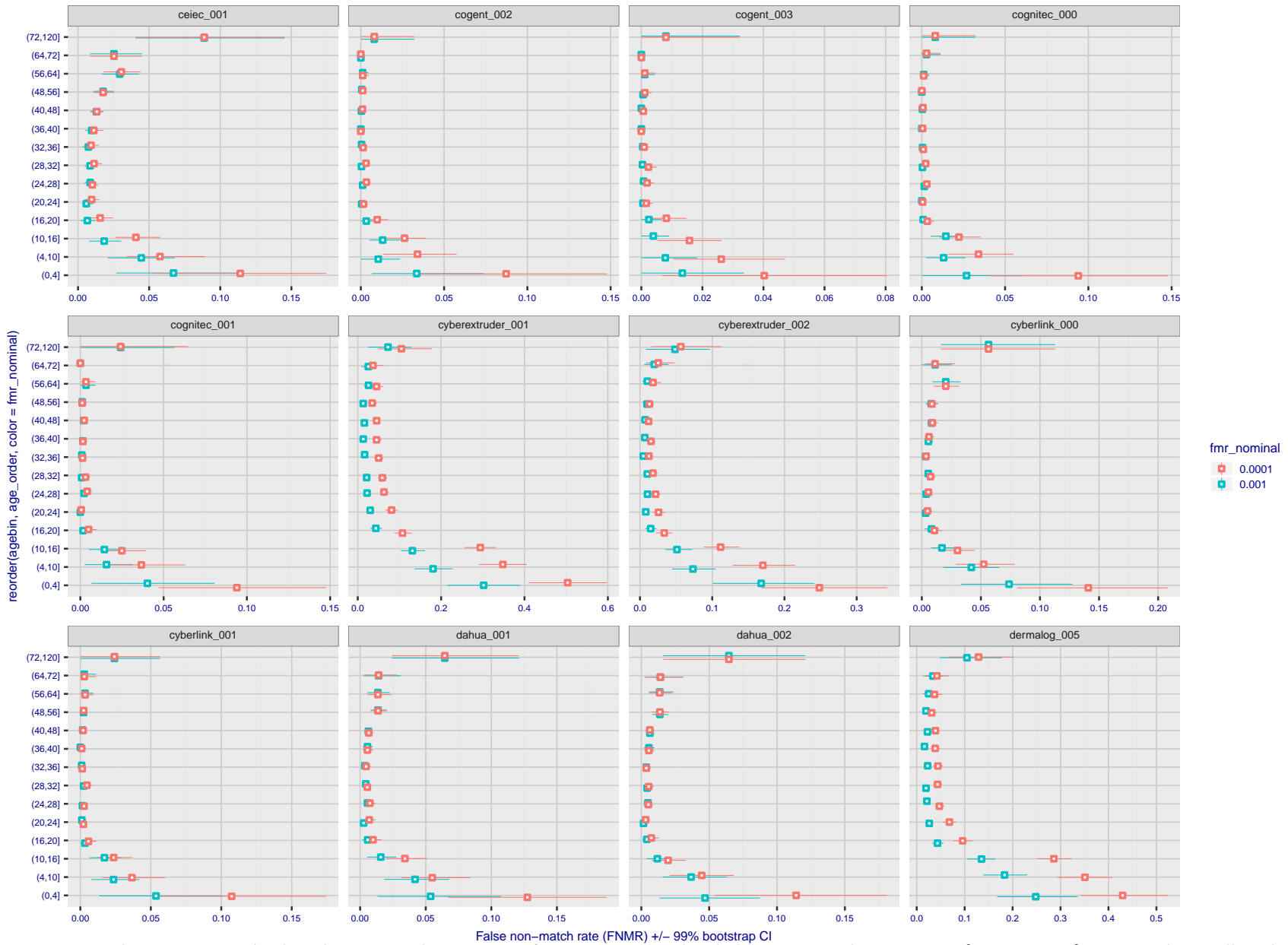


Figure 89: For the visa images, the dots show FNMR by age group for two operating thresholds corresponding to $FMR = \{0.001, 0.0001\}$ computed over all on the order of 10^{10} impostor scores. The FMR in each bin will vary also - see subsequent impostor heatmaps in sec. 3.6.2. Given a pair of face images taken at different times, we assign the comparison to the bin that is the arithmetic average of the subject's ages. This plot shows only the effect of age, not ageing. The number of comparisons in each bin is generally in the thousands, however the first and last bins are computed over 149 and 124 respectively. The error rates in some (adult) cases are zero, and in others the DET is flat so the error rates at the two thresholds are identical. The lines span 1% and 99% of bootstrap replicated FNMR estimates.



FNMR(T)
FMR(T)
"False non-match rate"
"False match rate"

Figure 90: For the visa images, the dots show FNMR by age group for two operating thresholds corresponding to $FMR = \{0.001, 0.0001\}$ computed over all on the order of 10^{10} impostor scores. The FMR in each bin will vary also - see subsequent impostor heatmaps in sec. 3.6.2. Given a pair of face images taken at different times, we assign the comparison to the bin that is the arithmetic average of the subject's ages. This plot shows only the effect of age, not ageing. The number of comparisons in each bin is generally in the thousands, however the first and last bins are computed over 149 and 124 respectively. The error rates in some (adult) cases are zero, and in others the DET is flat so the error rates at the two thresholds are identical. The lines span 1% and 99% of bootstrap replicated FNMR estimates.

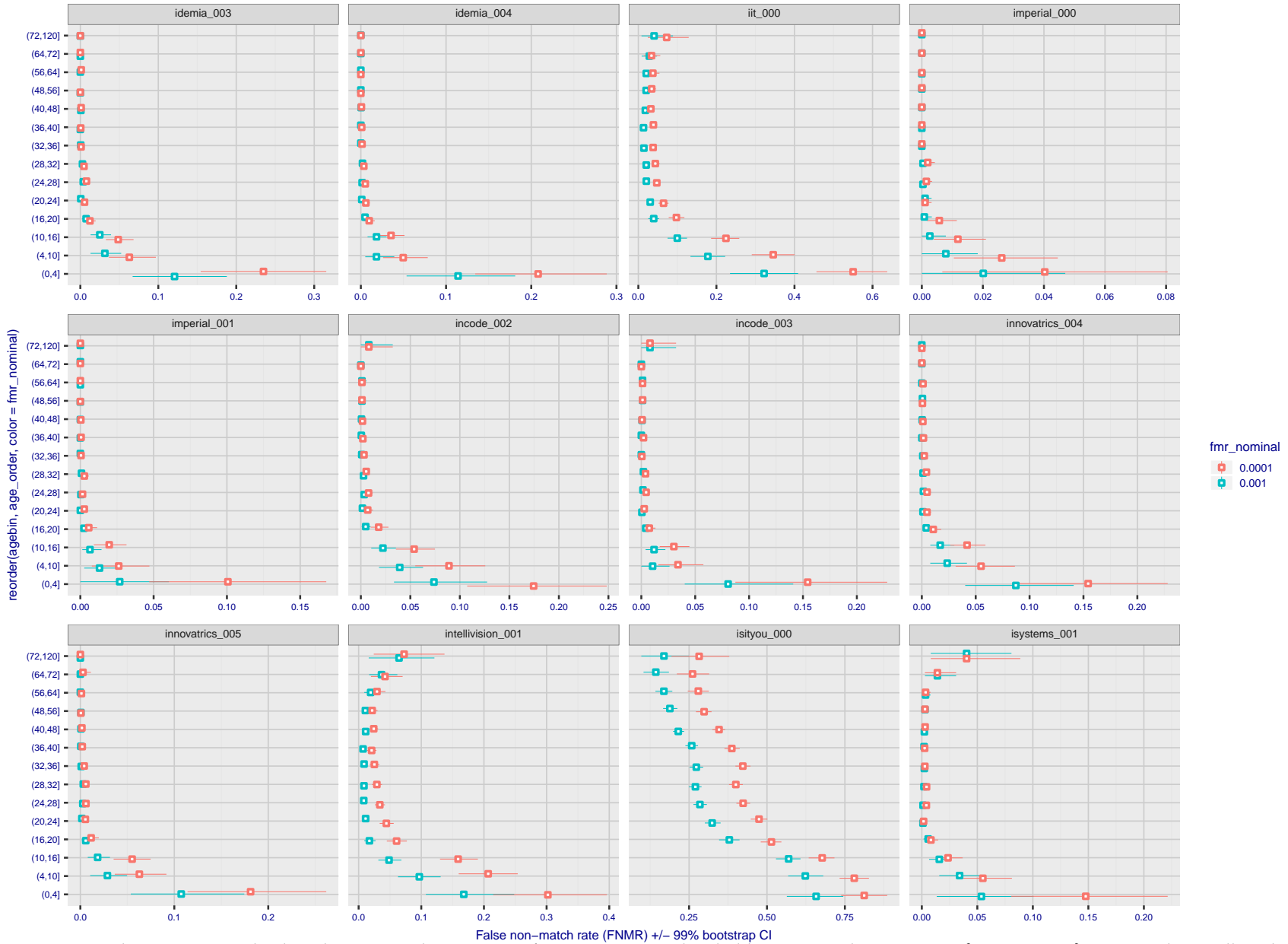
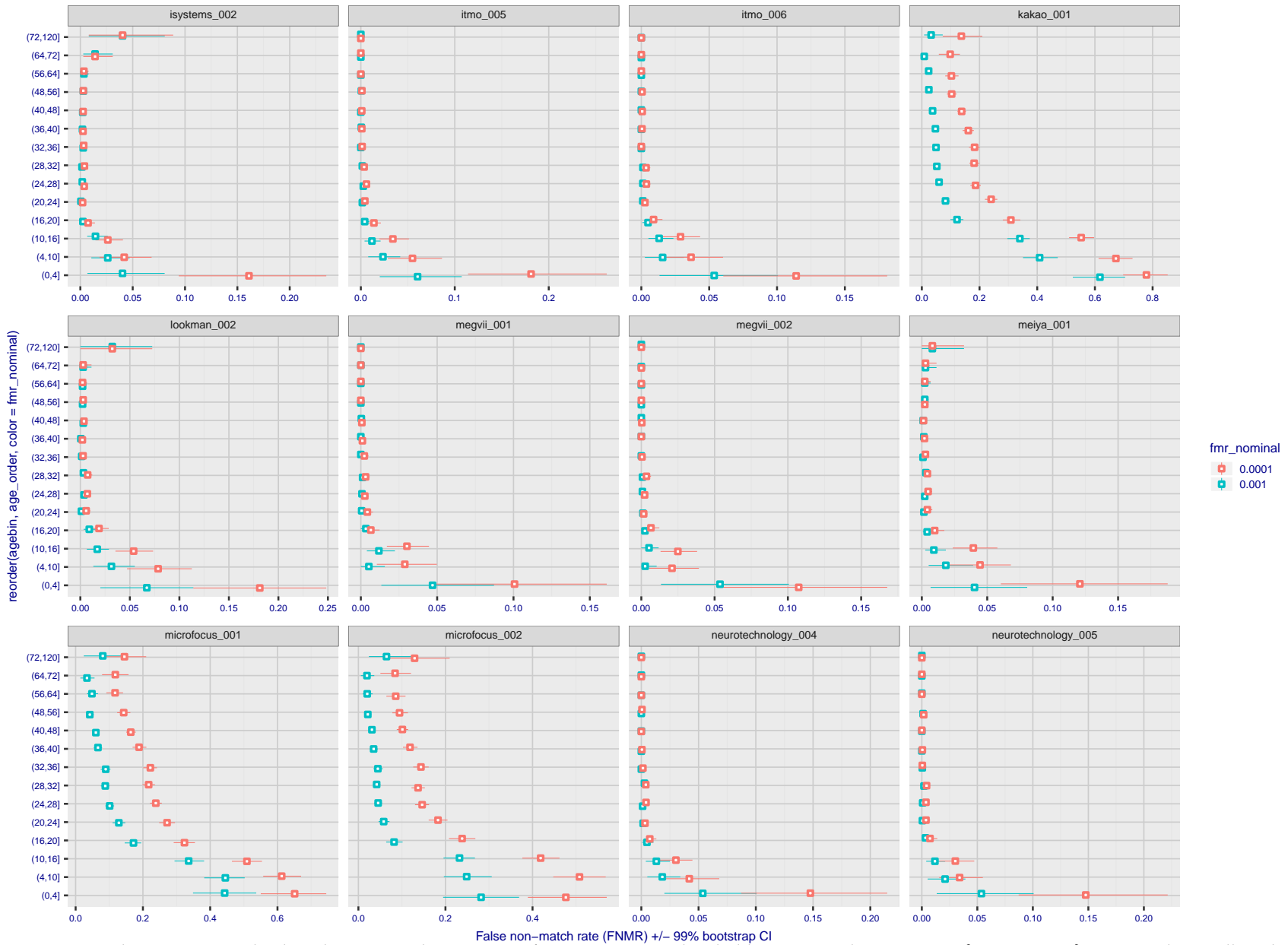


Figure 91: For the visa images, the dots show FNMR by age group for two operating thresholds corresponding to $FMR = \{0.001, 0.0001\}$ computed over all on the order of 10^{10} impostor scores. The FMR in each bin will vary also - see subsequent impostor heatmaps in sec. 3.6.2. Given a pair of face images taken at different times, we assign the comparison to the bin that is the arithmetic average of the subject's ages. This plot shows only the effect of age, not ageing. The number of comparisons in each bin is generally in the thousands, however the first and last bins are computed over 149 and 124 respectively. The error rates in some (adult) cases are zero, and in others the DET is flat so the error rates at the two thresholds are identical. The lines span 1% and 99% of bootstrap replicated FNMR estimates.



FNMR(T)
FMR(T)
"False non-match rate"
"False match rate"

Figure 92: For the visa images, the dots show FNMR by age group for two operating thresholds corresponding to $FMR = \{0.001, 0.0001\}$ computed over all on the order of 10^{10} impostor scores. The FMR in each bin will vary also - see subsequent impostor heatmaps in sec. 3.6.2. Given a pair of face images taken at different times, we assign the comparison to the bin that is the arithmetic average of the subject's ages. This plot shows only the effect of age, not ageing. The number of comparisons in each bin is generally in the thousands, however the first and last bins are computed over 149 and 124 respectively. The error rates in some (adult) cases are zero, and in others the DET is flat so the error rates at the two thresholds are identical. The lines span 1% and 99% of bootstrap replicated FNMR estimates.



Figure 93: For the visa images, the dots show FNMR by age group for two operating thresholds corresponding to $FMR = \{0.001, 0.0001\}$ computed over all on the order of 10^{10} impostor scores. The FMR in each bin will vary also - see subsequent impostor heatmaps in sec. 3.6.2. Given a pair of face images taken at different times, we assign the comparison to the bin that is the arithmetic average of the subject's ages. This plot shows only the effect of age, not ageing. The number of comparisons in each bin is generally in the thousands, however the first and last bins are computed over 149 and 124 respectively. The error rates in some (adult) cases are zero, and in others the DET is flat so the error rates at the two thresholds are identical. The lines span 1% and 99% of bootstrap replicated FNMR estimates.

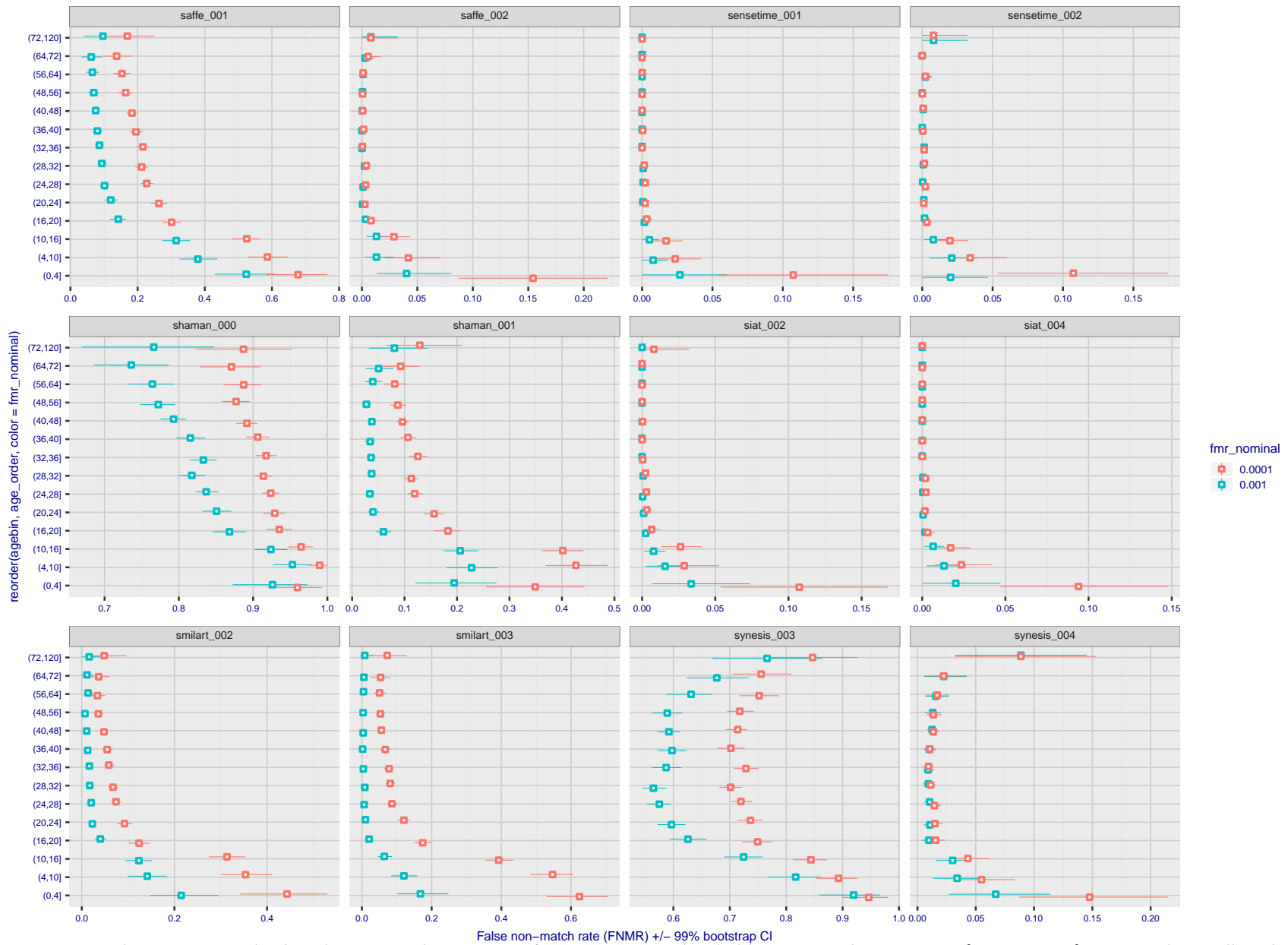
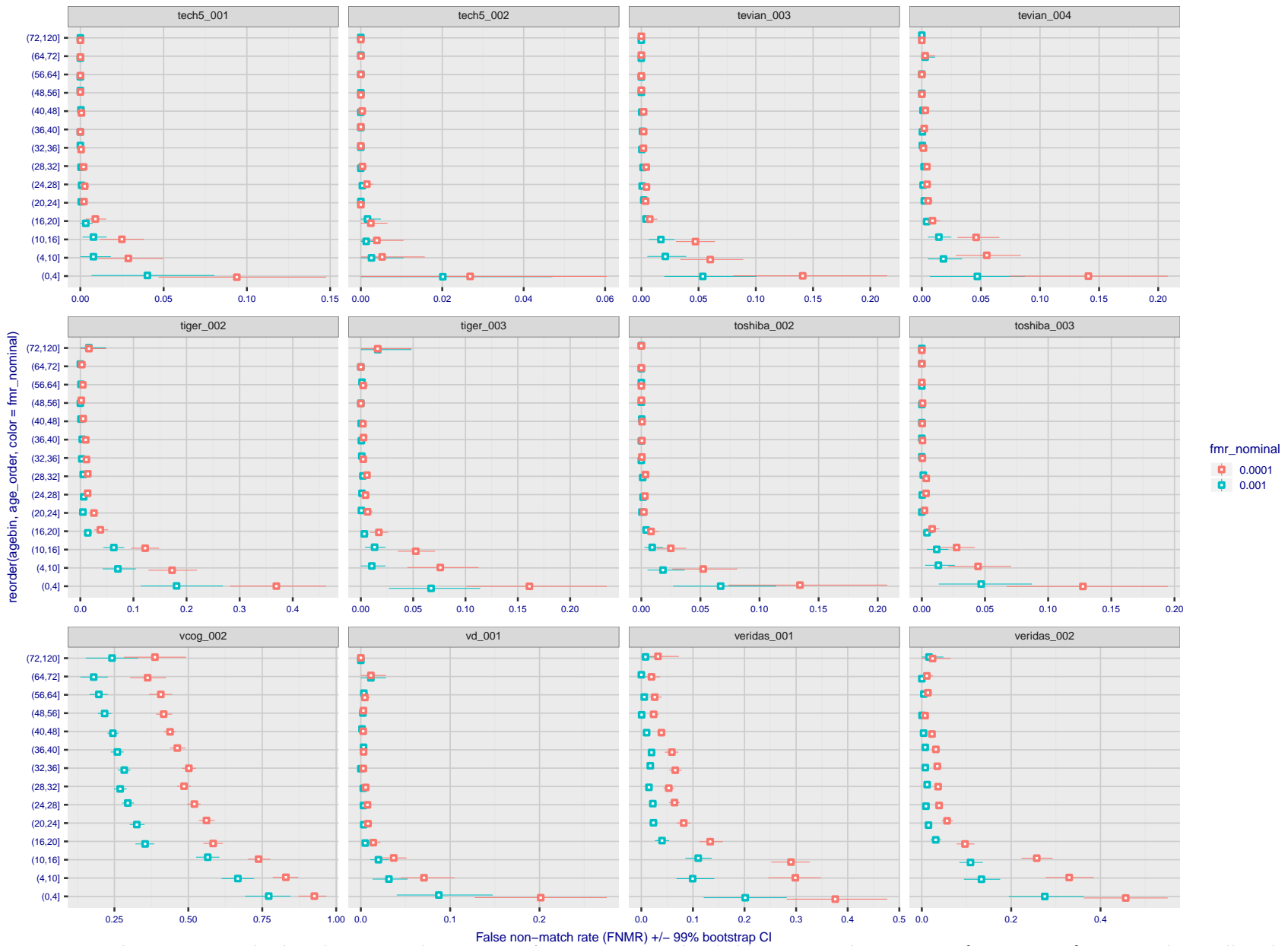
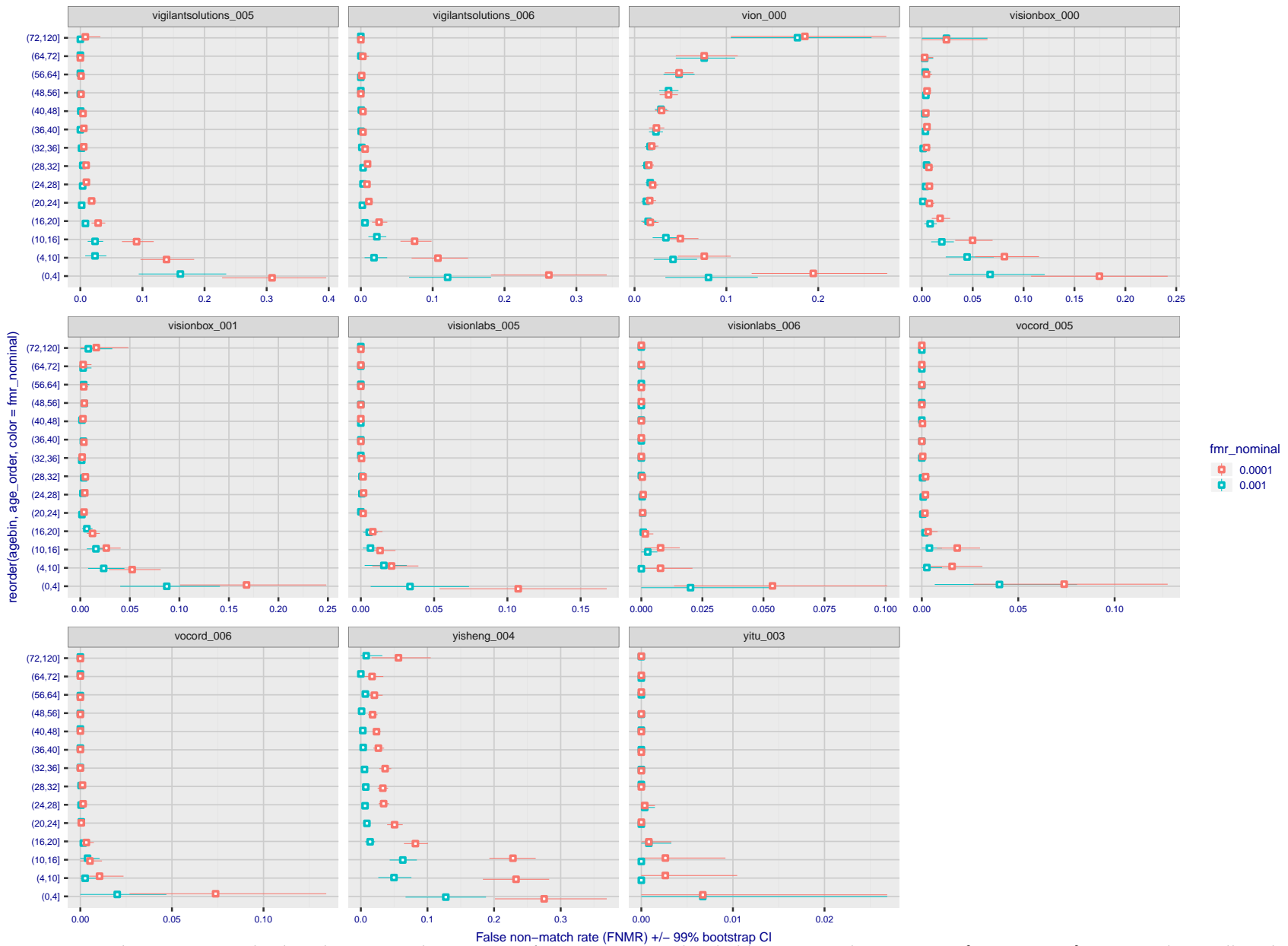


Figure 94: For the visa images, the dots show FNMR by age group for two operating thresholds corresponding to $FMR = \{0.001, 0.0001\}$ computed over all on the order of 10^{10} impostor scores. The FMR in each bin will vary also - see subsequent impostor heatmaps in sec. 3.6.2. Given a pair of face images taken at different times, we assign the comparison to the bin that is the arithmetic average of the subject's ages. This plot shows only the effect of age, not ageing. The number of comparisons in each bin is generally in the thousands, however the first and last bins are computed over 149 and 124 respectively. The error rates in some (adult) cases are zero, and in others the DET is flat so the error rates at the two thresholds are identical. The lines span 1% and 99% of bootstrap replicated FNMR estimates.



FNMR(T)
FMR(T)
"False non-match rate"
"False match rate"

Figure 95: For the visa images, the dots show FNMR by age group for two operating thresholds corresponding to $FMR = \{0.001, 0.0001\}$ computed over all on the order of 10^{10} impostor scores. The FMR in each bin will vary also - see subsequent impostor heatmaps in sec. 3.6.2. Given a pair of face images taken at different times, we assign the comparison to the bin that is the arithmetic average of the subject's ages. This plot shows only the effect of age, not ageing. The number of comparisons in each bin is generally in the thousands, however the first and last bins are computed over 149 and 124 respectively. The error rates in some (adult) cases are zero, and in others the DET is flat so the error rates at the two thresholds are identical. The lines span 1% and 99% of bootstrap replicated FNMR estimates.



FNMR(T)
FMR(T)
"False non-match rate"
"False match rate"

Figure 96: For the visa images, the dots show FNMR by age group for two operating thresholds corresponding to $FMR = \{0.001, 0.0001\}$ computed over all on the order of 10^{10} impostor scores. The FMR in each bin will vary also - see subsequent impostor heatmaps in sec. 3.6.2. Given a pair of face images taken at different times, we assign the comparison to the bin that is the arithmetic average of the subject's ages. This plot shows only the effect of age, not ageing. The number of comparisons in each bin is generally in the thousands, however the first and last bins are computed over 149 and 124 respectively. The error rates in some (adult) cases are zero, and in others the DET is flat so the error rates at the two thresholds are identical. The lines span 1% and 99% of bootstrap replicated FNMR estimates.

Caveats: None.

3.6 Impostor distribution stability

3.6.1 Effect of birth place on the impostor distribution

Background: Facial appearance varies geographically, both in terms of skin tone, cranio-facial structure and size. This section addresses whether false match rates vary intra- and inter-regionally.

Goals:

- ▷ To show the effect of birth region of the impostor and enrollee on false match rates.
- ▷ To determine whether some algorithms give better impostor distribution stability.

Methods:

- ▷ For the visa images, NIST defined 10 regions: Sub-Saharan Africa, South Asia, Polynesia, North Africa, Middle East, Europe, East Asia, Central and South America, Central Asia, and the Caribbean.
- ▷ For the visa images, NIST mapped each country of birth to a region. There is some arbitrariness to this. For example, Egypt could reasonably be assigned to the Middle East instead of North Africa. An alternative methodology could, for example, assign the Philippines to *both* Polynesia and East Asia.
- ▷ FMR is computed for cases where all face images of impostors born in region r_2 are compared with enrolled face images of persons born in region r_1 .

$$\text{FMR}(r_1, r_2, T) = \frac{\sum_{i=1}^{N_{r_1, r_2}} H(s_i - T)}{N_{r_1, r_2}} \quad (5)$$

where the same threshold, T , is used in all cells, and H is the unit step function. The threshold is set to give $\text{FMR}(T) = 0.001$ over the entire set of visa image impostor comparisons.

- ▷ This analysis is then repeated by country-pair, but only for those country pairs where both have at least 1000 images available. The countries¹ appear in the axes of graphs that follow.
- ▷ The mean number of impostor scores in any cross-region bin is 33 million. The smallest number of impostor scores in any bin is 135000, for Central Asia - North Africa. While these counts are large enough to support reasonable significance, the number of individual faces is much smaller, on the order of $N^{0.5}$.
- ▷ The numbers of impostor scores in any cross-country bin is shown in Figure 313.

Results: Subsequent figures show heatmaps that use color to represent the base-10 logarithm of the false match rate. Red colors indicate high (bad) false match rates. Dark colors indicate benign false match rates. There are two series of graphs corresponding to aggregated geographical regions, and to countries. The notable observations are:

- ▷ The on-diagonal elements correspond to within-region impostors. FMR is generally above the nominal value of $\text{FMR} = 0.001$. Particularly there is usually higher FMR in, Sub-Saharan Africa, South Asia, and the Caribbean. Europe and Central Asia, on the other hand, usually give FMR closer to the nominal value.
- ▷ The off-diagonal elements correspond to across-region impostors. The highest FMR is produced between the Caribbean and Sub-Saharan Africa.
- ▷ Algorithms vary.

¹These are Argentina, Australia, Brazil, Chile, China, Costa Rica, Cuba, Czech Republic, Dominican Republic, Ecuador, Egypt, El Salvador, Germany, Ghana, Great Britain, Greece, Guatemala, Haiti, Hong Kong, Honduras, Indonesia, India, Israel, Jamaica, Japan, Kenya, Korea, Lebanon, Mexico, Malaysia, Nepal, Nigeria, Peru, Philippines, Pakistan, Poland, Romania, Russia, South Africa, Saudi Arabia, Thailand, Trinidad, Turkey, Taiwan, Ukraine, Venezuela, and Vietnam.

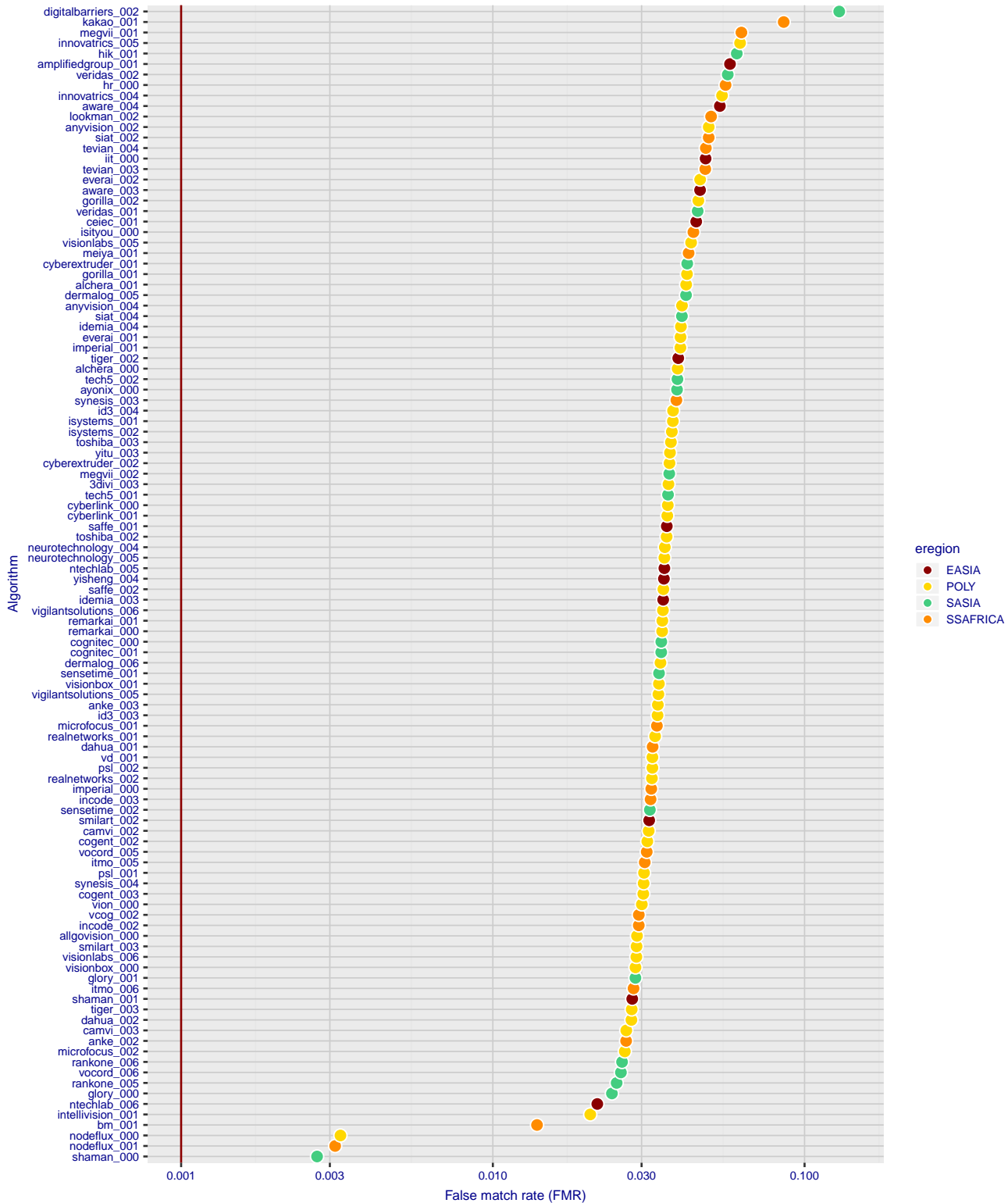


Figure 97: For the visa images, the dots show FMR for impostor comparisons of individuals of the same sex and same age group for the region of the world that gives the worst (highest) FMR when the threshold is set to give FMR = 0.001 (red vertical line) over all on the order of 10^{10} impostor scores i.e. zero-effort. The shift of the dots to right shows massive increases in FMR when impostors have the same sex, age, and region of birth. The color code indicates which region gives the worst case FMR. If the observed variation is due to the prevalence of one kind of images in the training imagery, then algorithms developed on one kind of data might be expected to give higher FMR on other kinds.

- ▷ We computed the same quantities for a global FMR = 0.0001. The effects are similar.

Caveats:

- ▷ The effects of variable impostor rates on one-to-many identification systems may well differ from what's implied by these one-to-one verification results. Two reasons for this are a) the enrollment galleries are usually imbalanced across countries of birth, age and sex; b) one-to-many identification algorithms often implement techniques aimed at stabilizing the impostor distribution. Further research is necessary.
- ▷ In principle, the effects seen in this subsection could be due to differences in the image capture process. We consider this unlikely since the effects are maintained across geography - e.g. Caribbean vs. Africa, or Japan vs. China.

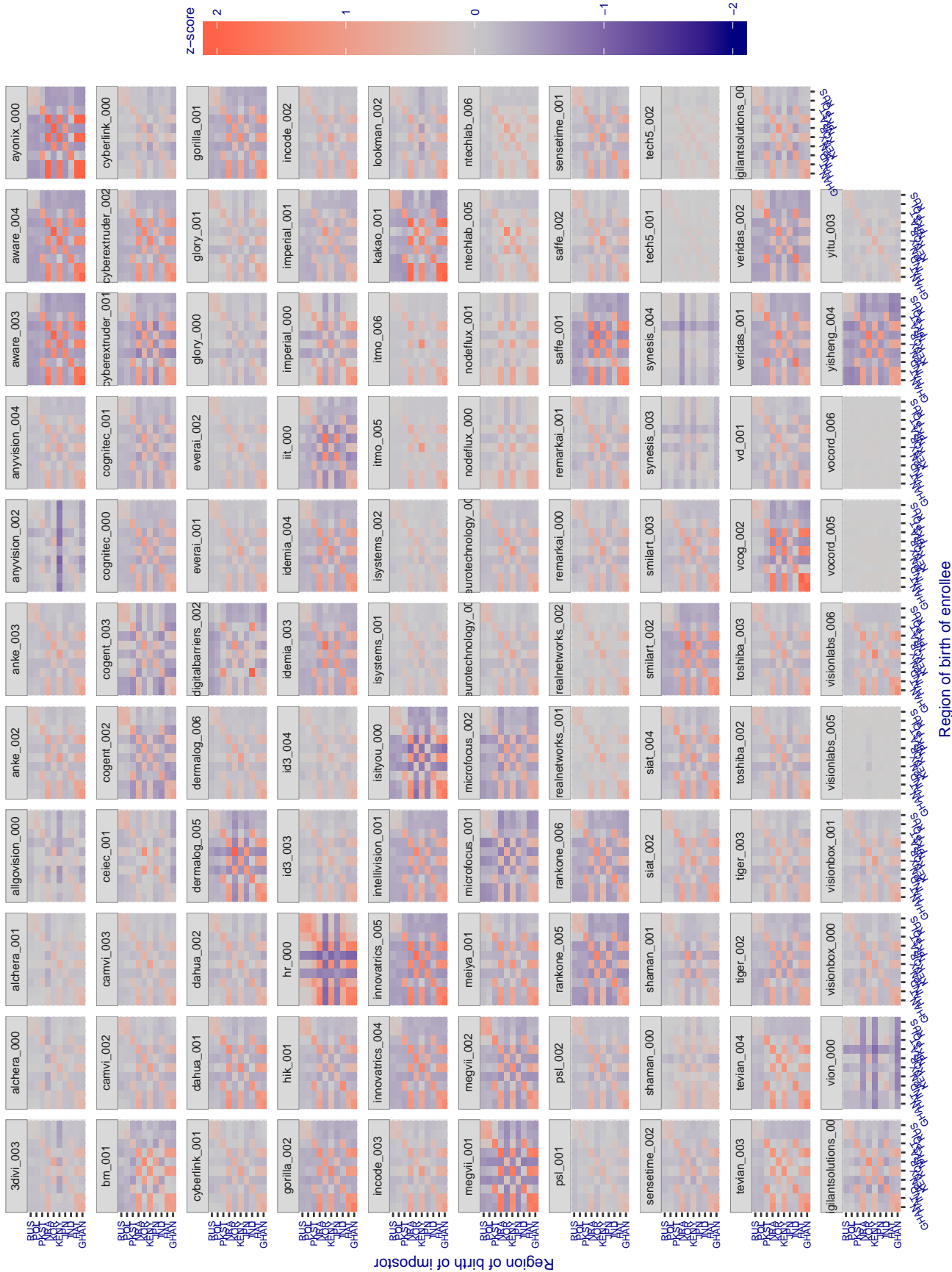


Figure 98: For visa images, the heatmap shows how the mean of the impostor distribution for the country pair (a,b) is shifted relative to the mean of the global impostor distribution, expressed as a number of standard deviations of the global impostor distribution. This statistic is designed to show shifts in the entire impostor distribution, not just tail effects that manifest as the anomalously high (or low) false match rates that appear in the subsequent figures. The countries are chosen to show that skin tone alone does not explain impostor distribution shifts. The reduced shift in Asian populations with the Yitu and TongYiTrans algorithms, is accompanied by positive shifts in the European populations. This reversal relative to most other algorithms, may derive from use of nationally weighted training sets. The Visionlabs algorithm appears most insensitive to country effects. The figure is computed from same-sex and same-age impostor pairs.

Cross region FMR at threshold $T = 2.740$ for algorithm 3divi_003, giving $FMR(T) = 0.0001$ globally.

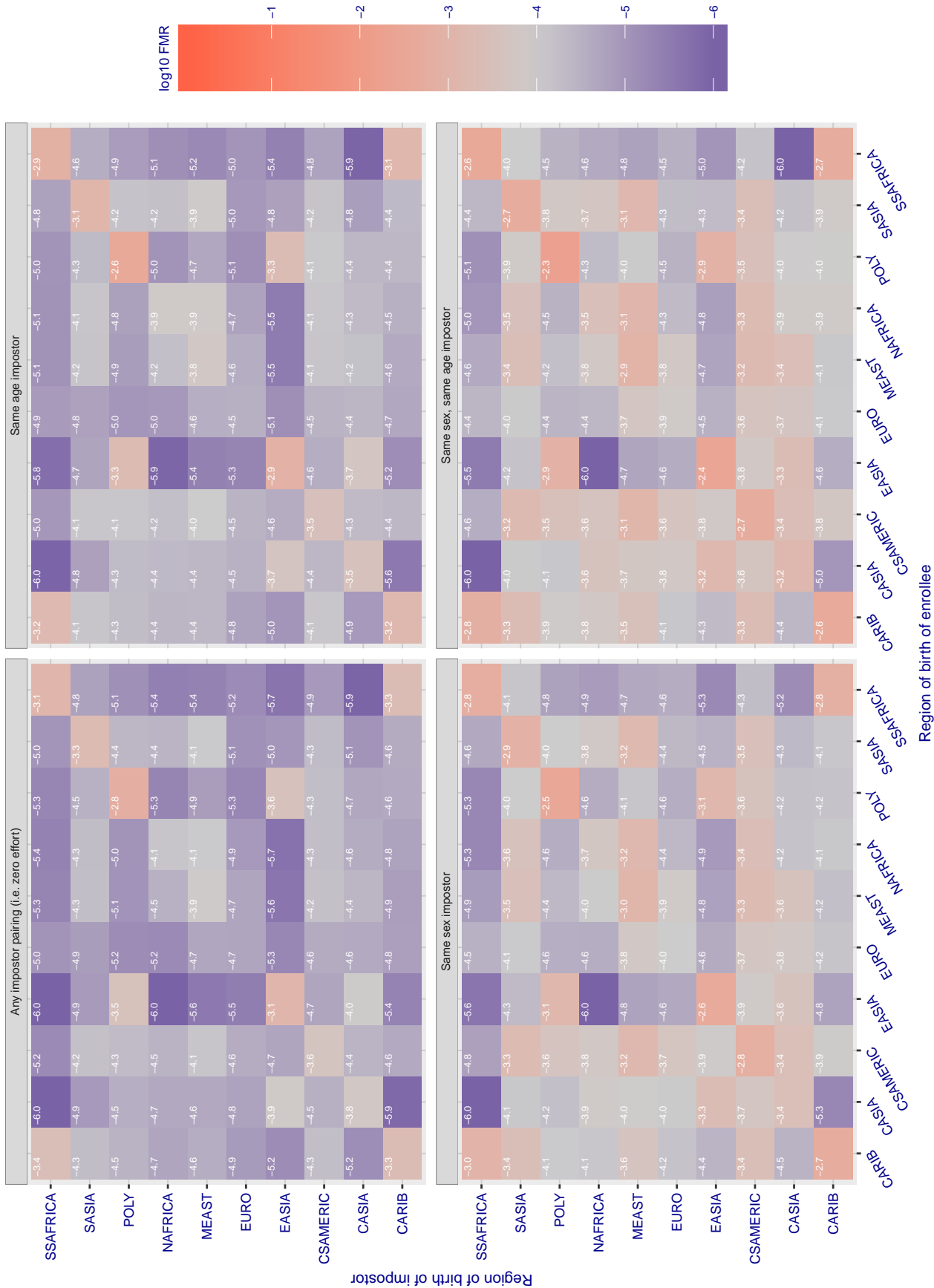


Figure 99: For algorithm 3divi-003 operating on visa images, the heatmap shows false match rates observed over impostor comparisons of faces from different individuals who were born in the given region pair. False matches are counted against a recognition threshold fixed globally to give the target FMR in the plot title, computed over all on the order of 10^{10} impostor comparisons. If text appears in each box it give the same quantity as that coded by the color. Grey indicates FMR is at the intended FMR target level. Light red colors present a security vulnerability to, for example, a passport gate. Each +1 increase in $\log_{10} FMR$ corresponds to a factor of 10 increase in FMR. The matrix is not quite symmetric because images in the enrollment and verification sets are different.

Cross region FMR at threshold $T = 0.702$ for algorithm alchera_000, giving $FMR(T) = 0.0001$ globally.

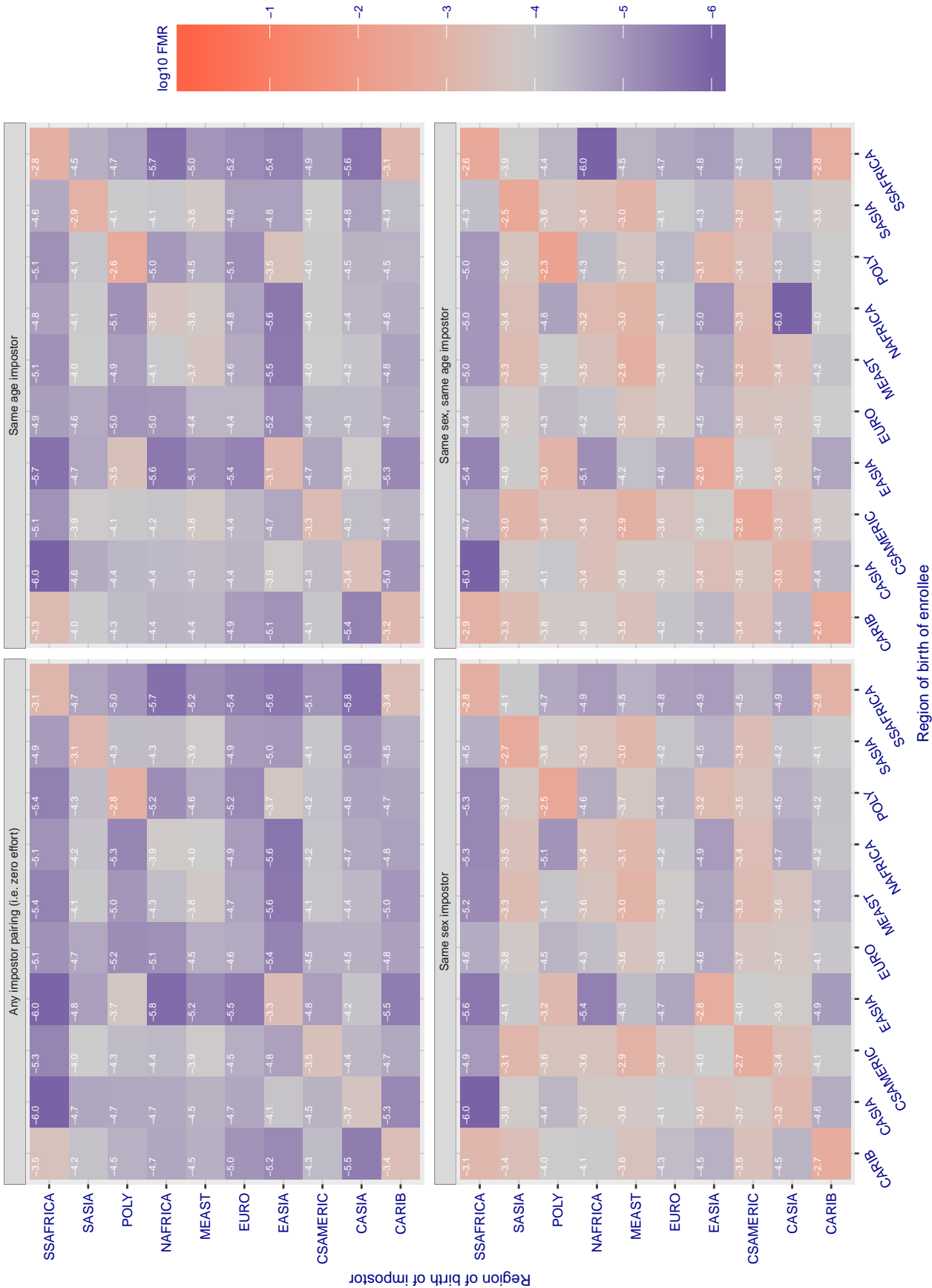


Figure 100: For algorithm alchera-000 operating on visa images, the heatmap shows false match rates observed over impostor comparisons of faces from different individuals who were born in the given region pair. False matches are counted against a recognition threshold fixed globally to give the target FMR in the plot title, computed over all on the order of 10^{10} impostor comparisons. If text appears in each box it give the same quantity as that coded by the color. Grey indicates FMR is at the intended FMR target level. Light red colors present a security vulnerability to, for example, a passport gate. Each +1 increase in \log_{10} FMR corresponds to a factor of 10 increase in FMR. The matrix is not quite symmetric because images in the enrollment and verification sets are different.

Cross region FMR at threshold $T = 0.713$ for algorithm alchera_001, giving $FMR(T) = 0.0001$ globally.

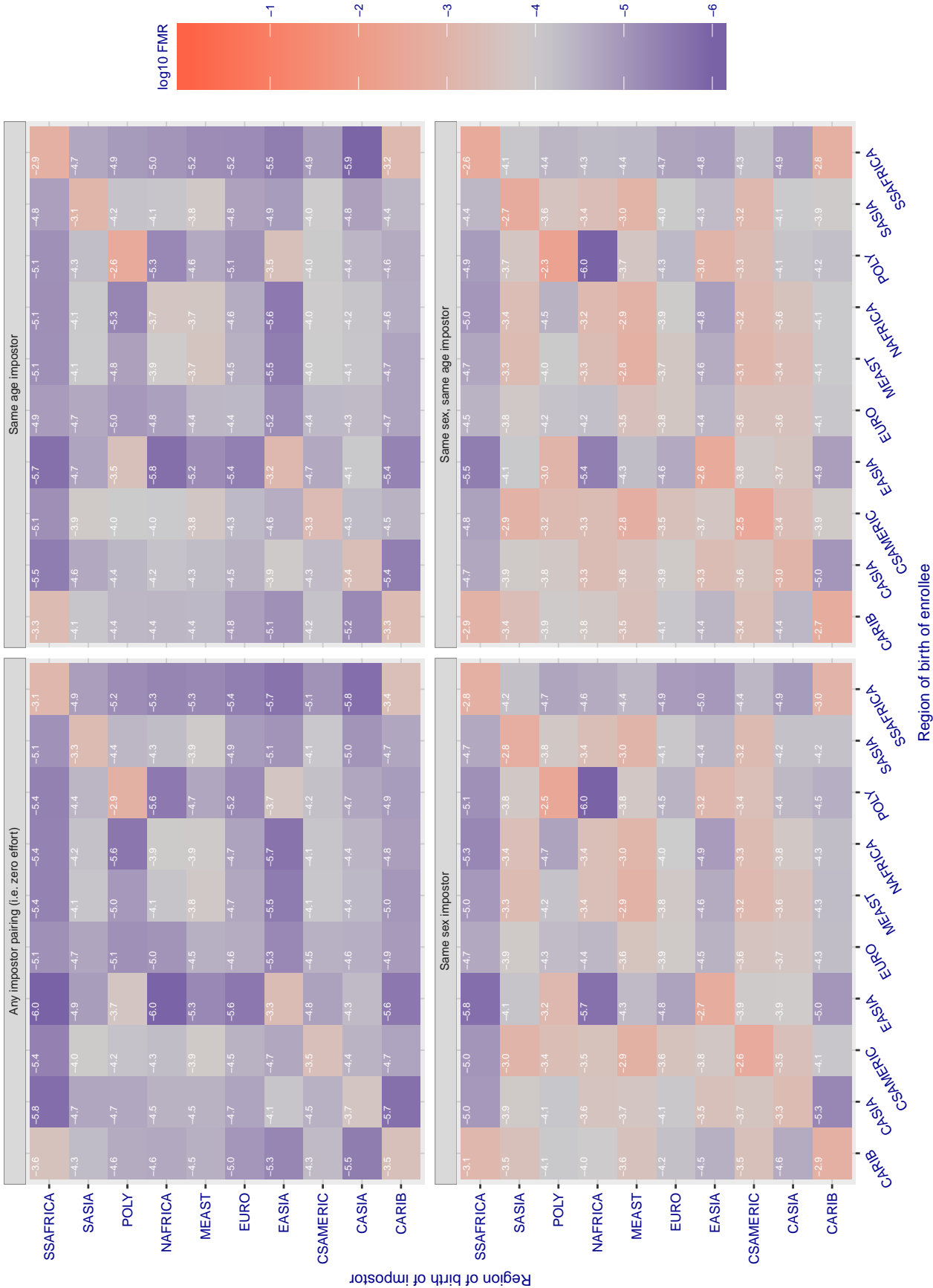


Figure 101: For algorithm alchera-001 operating on visa images, the heatmap shows false match rates observed over impostor comparisons of faces from different individuals who were born in the given region pair. False matches are counted against a recognition threshold fixed globally to give the target FMR in the plot title, computed over all on the order of 10^{10} impostor comparisons. If text appears in each box it give the same quantity as that coded by the color. Grey indicates FMR is at the intended FMR target level. Light red colors present a security vulnerability to, for example, a passport gate. Each +1 increase in \log_{10} FMR corresponds to a factor of 10 increase in FMR. The matrix is not quite symmetric because images in the enrollment and verification sets are different.

Cross region FMR at threshold $T = 0.433$ for algorithm allgvision_000, giving $FMR(T) = 0.0001$ globally.

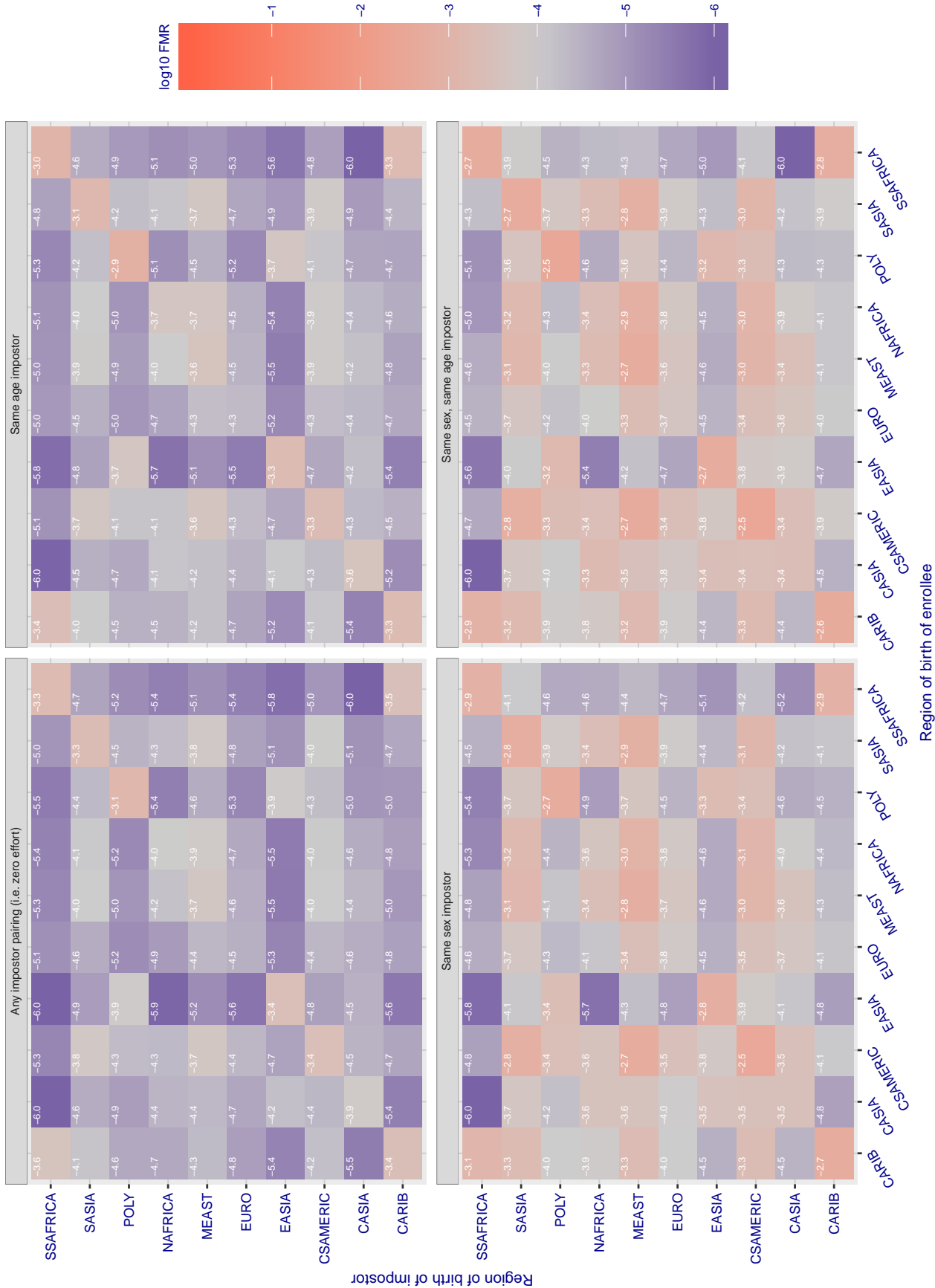


Figure 102: For algorithm allgvision-000 operating on visa images, the heatmap shows false match rates observed over impostor comparisons of faces from different individuals who were born in the given region pair. False matches are counted against a recognition threshold fixed globally to give the target FMR in the plot title, computed over all on the order of 10^{10} impostor comparisons. If text appears in each box it give the same quantity as that coded by the color. Grey indicates FMR is at the intended FMR target level. Light red colors present a security vulnerability to, for example, a passport gate. Each +1 increase in \log_{10} FMR corresponds to a factor of 10 increase in FMR. The matrix is not quite symmetric because images in the enrollment and verification sets are different.

Cross region FMR at threshold $T = 3.640$ for algorithm amplifiedgroup_001, giving $FMR(T) = 0.0001$ globally.

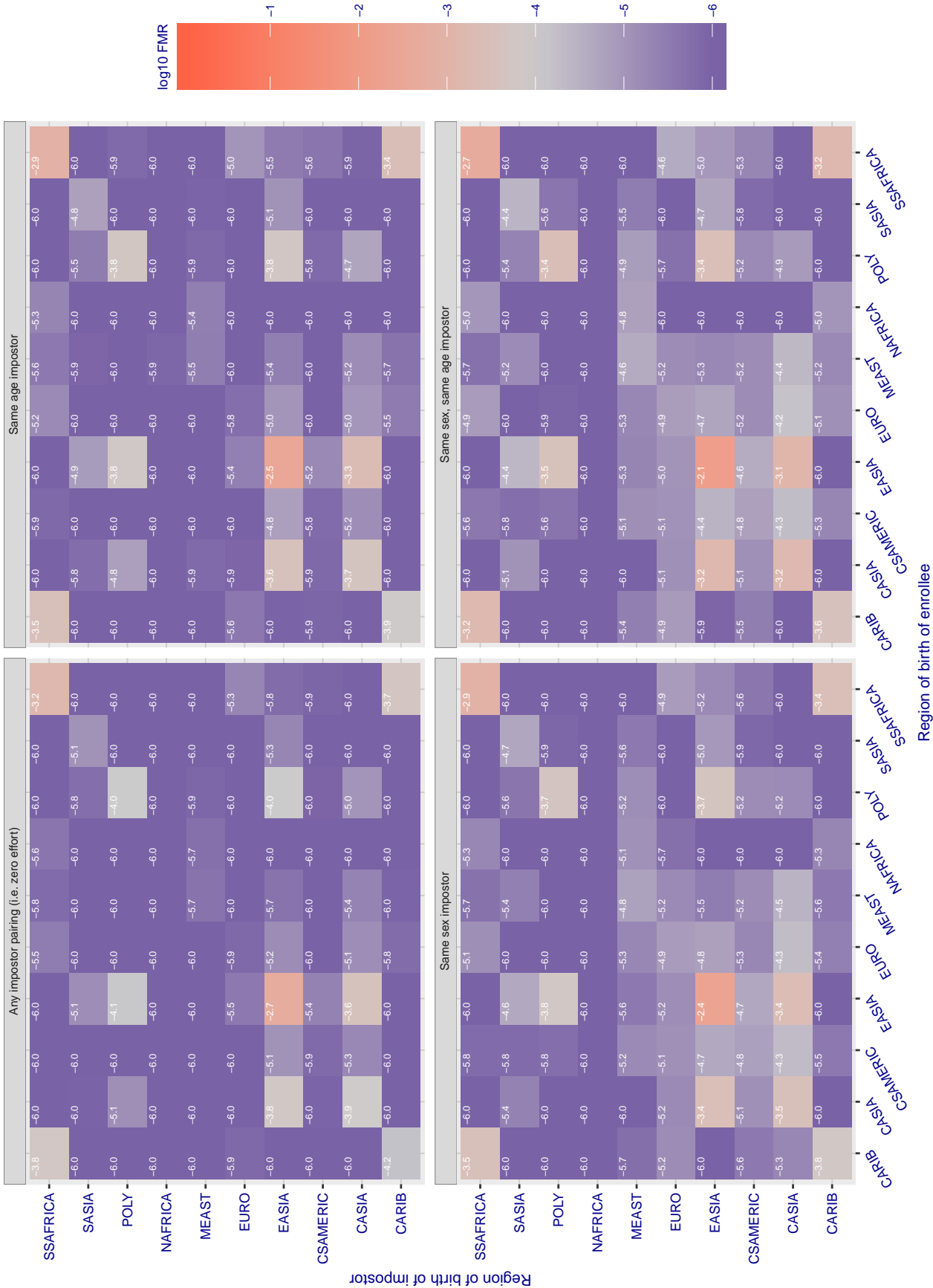


Figure 103: For algorithm amplifiedgroup-001 operating on visa images, the heatmap shows false match rates observed over impostor comparisons of faces from different individuals who were born in the given region pair. False matches are counted against a recognition threshold fixed globally to give the target FMR in the plot title, computed over all on the order of 10^{10} impostor comparisons. If text appears in each box it give the same quantity as that coded by the color. Grey indicates FMR is at the intended FMR target level. Light red colors present a security vulnerability to, for example, a passport gate. Each +1 increase in \log_{10} FMR corresponds to a factor of 10 increase in FMR. The matrix is not quite symmetric because images in the enrollment and verification sets are different.

Cross region FMR at threshold $T = 0.404$ for algorithm anke_002, giving $FMR(T) = 0.0001$ globally.

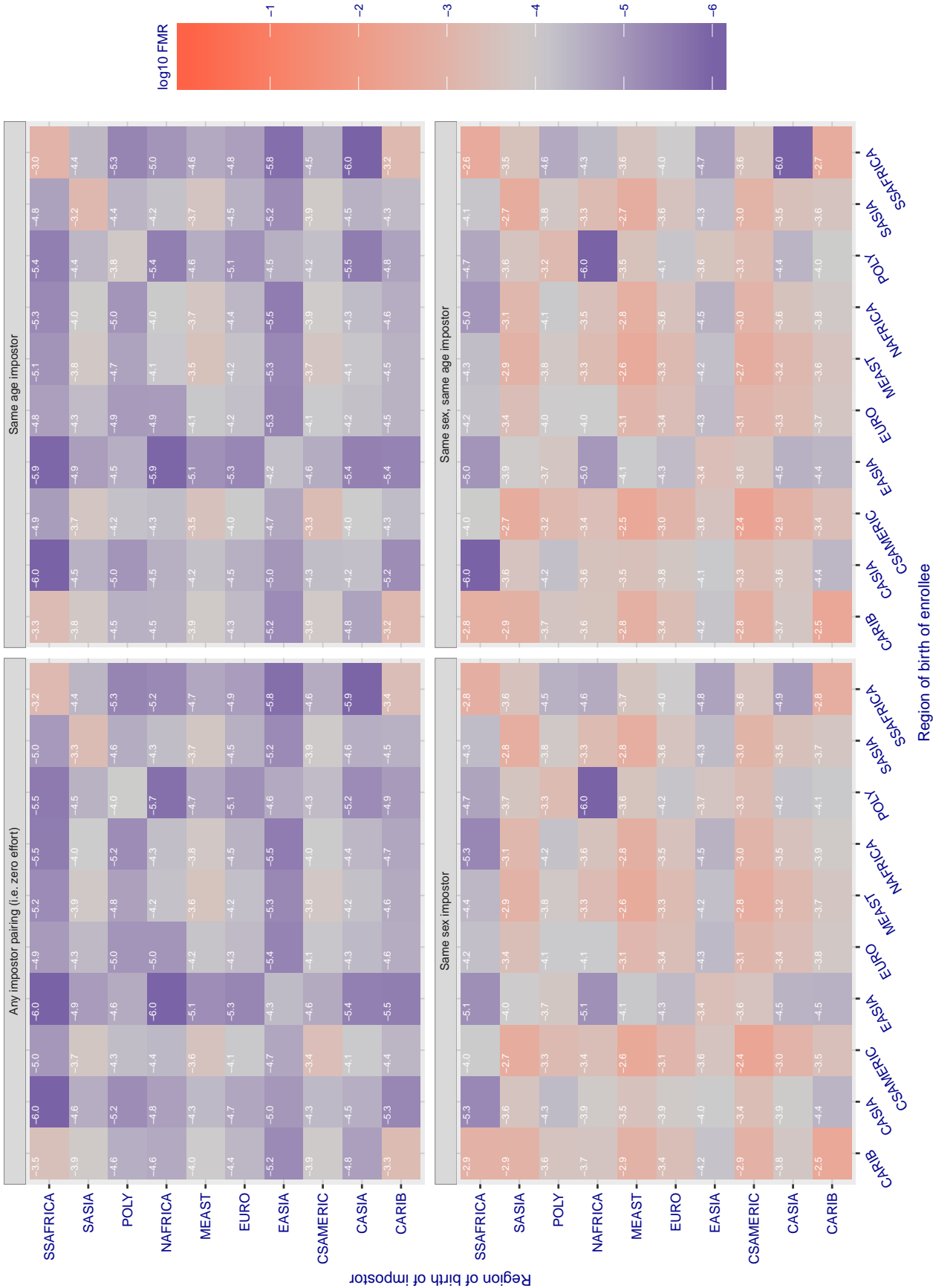


Figure 104: For algorithm anke-002 operating on visa images, the heatmap shows false match rates observed over impostor comparisons of faces from different individuals who were born in the given region pair. False matches are counted against a recognition threshold fixed globally to give the target FMR in the plot title, computed over all on the order of 10^{10} impostor comparisons. If text appears in each box it give the same quantity as that coded by the color. Grey indicates FMR is at the intended FMR target level. Light red colors present a security vulnerability to, for example, a passport gate. Each +1 increase in \log_{10} FMR corresponds to a factor of 10 increase in FMR. The matrix is not quite symmetric because images in the enrollment and verification sets are different.

Cross region FMR at threshold $T = 0.397$ for algorithm anke_003, giving $FMR(T) = 0.0001$ globally.

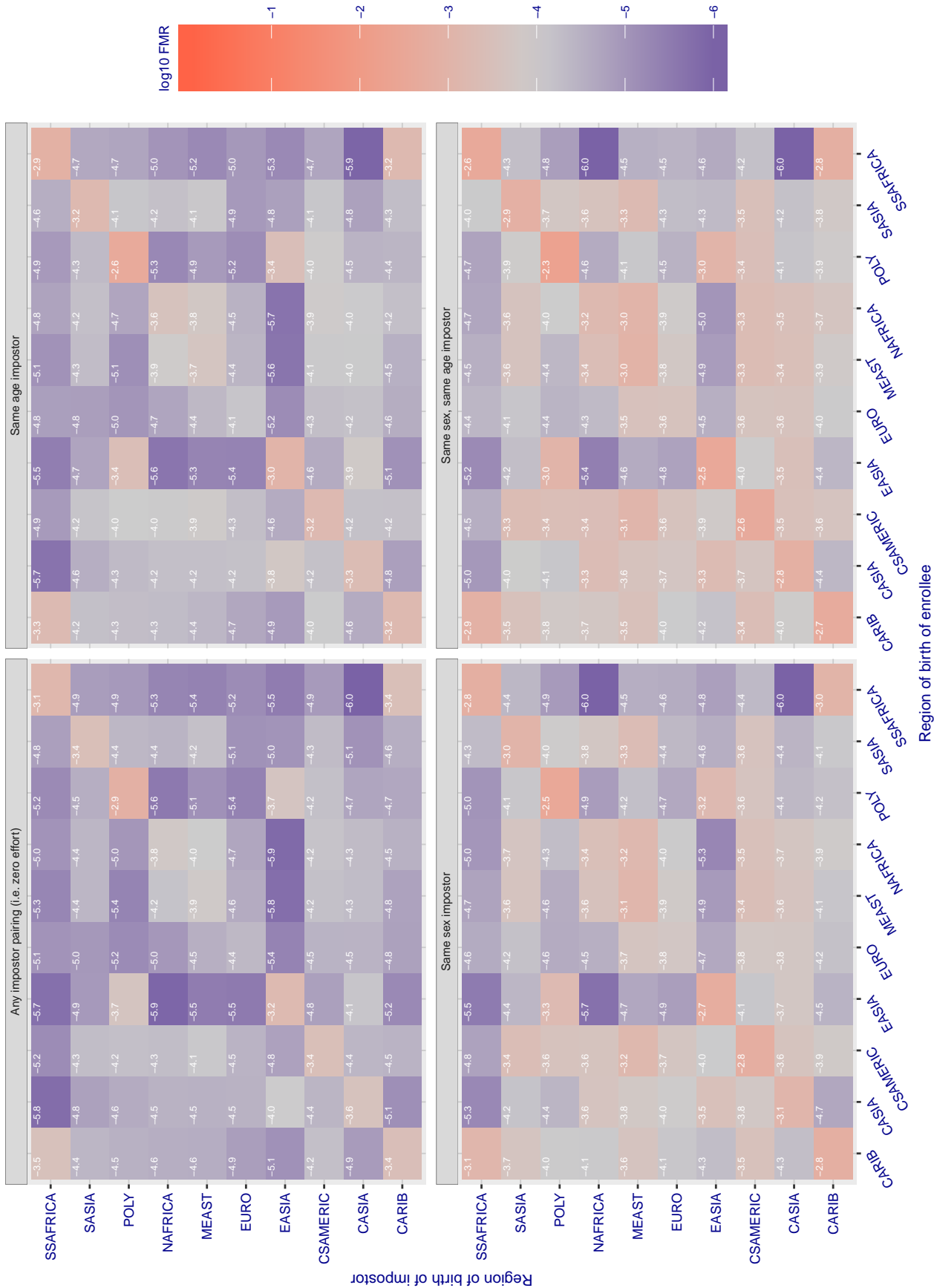


Figure 105: For algorithm anke-003 operating on visa images, the heatmap shows false match rates observed over impostor comparisons of faces from different individuals who were born in the given region pair. False matches are counted against a recognition threshold fixed globally to give the target FMR in the plot title, computed over all on the order of 10^{10} impostor comparisons. If text appears in each box it give the same quantity as that coded by the color. Grey indicates FMR is at the intended FMR target level. Light red colors present a security vulnerability to, for example, a passport gate. Each +1 increase in $\log_{10} FMR$ corresponds to a factor of 10 increase in FMR. The matrix is not quite symmetric because images in the enrollment and verification sets are different.

Cross region FMR at threshold $T = 1.526$ for algorithm anyvision_002, giving FMR(T) = 0.0001 globally.

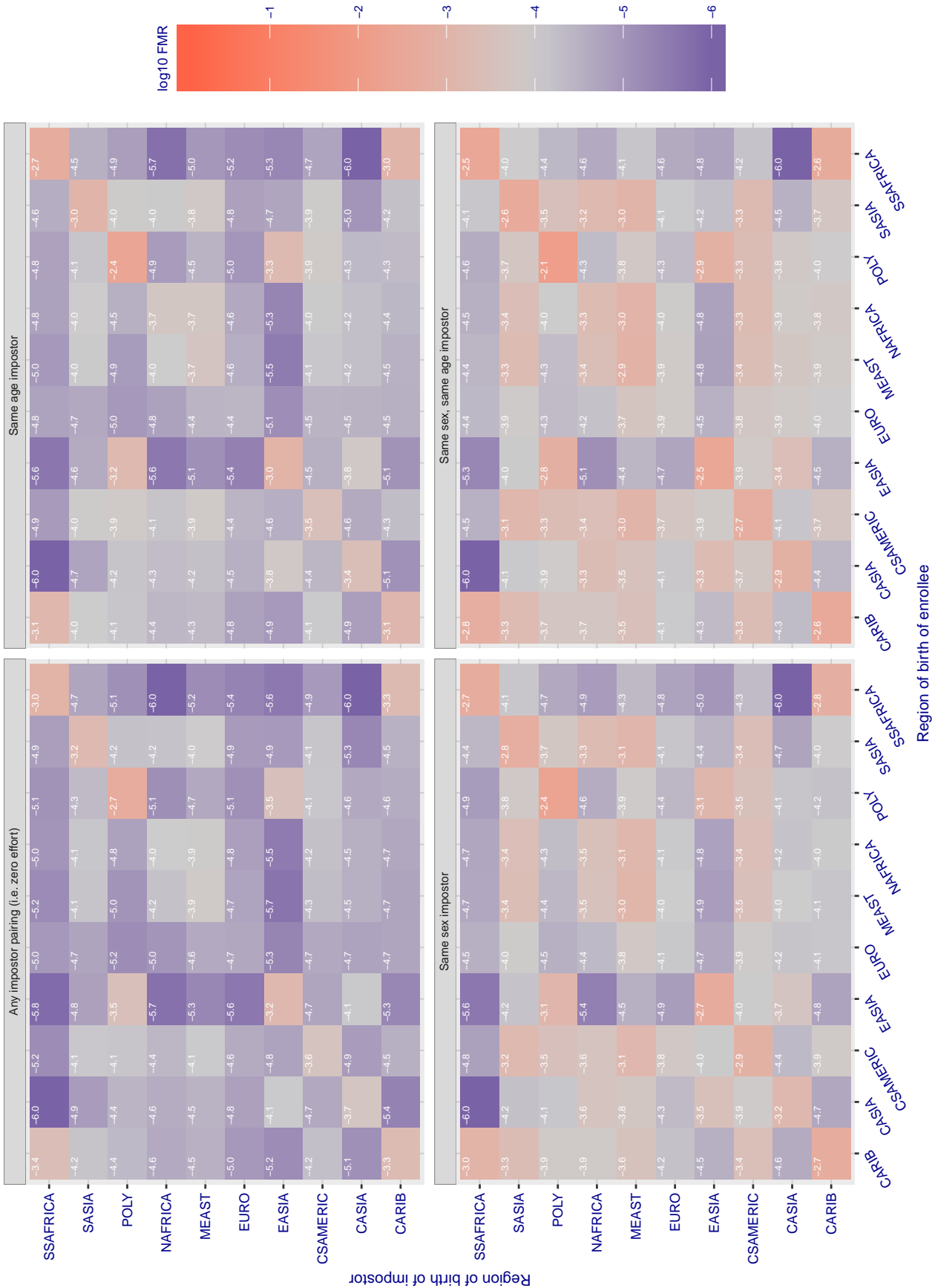


Figure 106: For algorithm anyvision-002 operating on visa images, the heatmap shows false match rates observed over impostor comparisons of faces from different individuals who were born in the given region pair. False matches are counted against a recognition threshold fixed globally to give the target FMR in the plot title, computed over all on the order of 10^{10} impostor comparisons. If text appears in each box it give the same quantity as that coded by the color. Grey indicates FMR is at the intended FMR target level. Light red colors present a security vulnerability to, for example, a passport gate. Each +1 increase in \log_{10} FMR corresponds to a factor of 10 increase in FMR. The matrix is not quite symmetric because images in the enrollment and verification sets are different.

Cross region FMR at threshold $T = 1.375$ for algorithm anyvision_004, giving FMR(T) = 0.0001 globally.

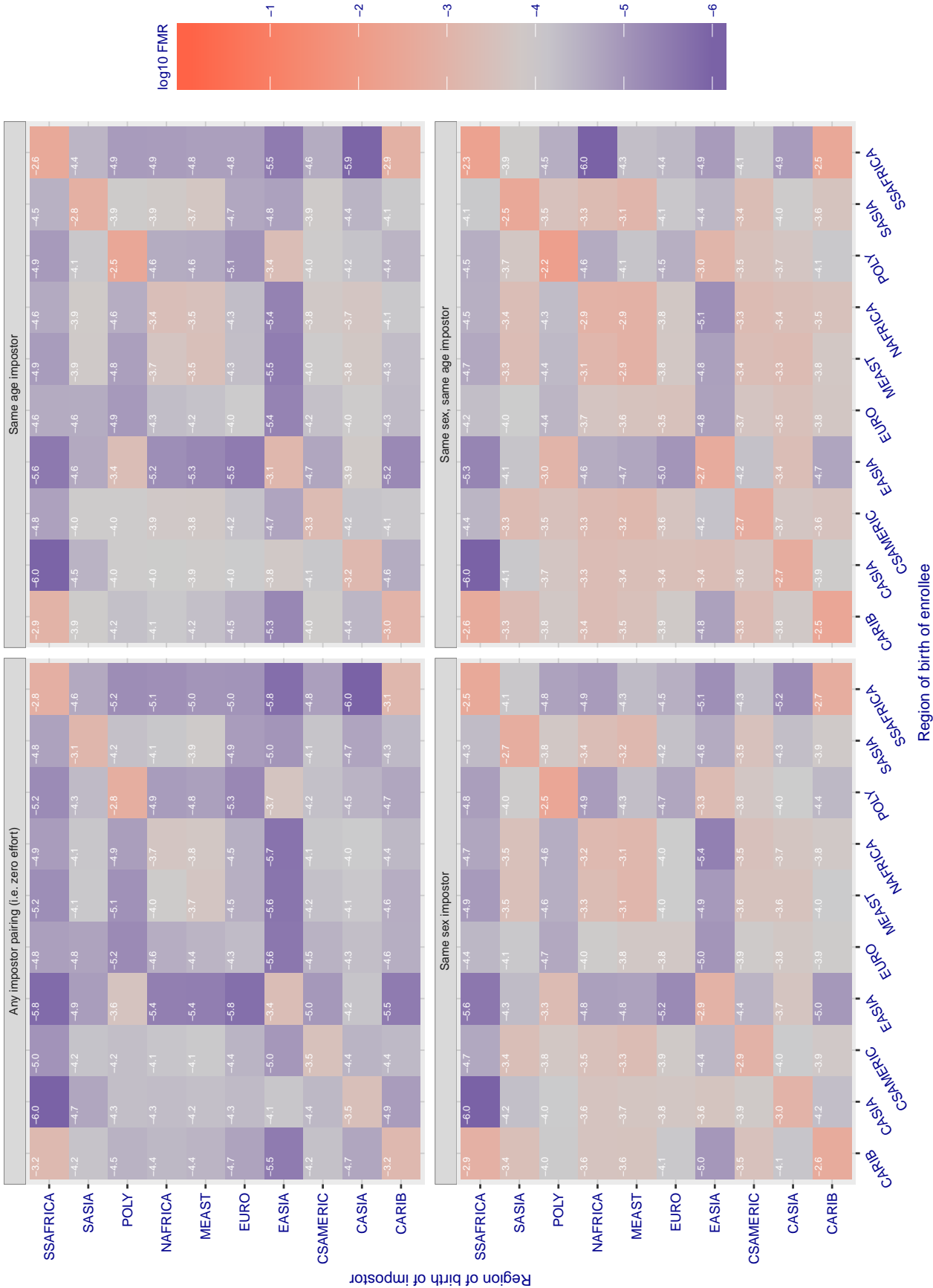


Figure 107: For algorithm anyvision-004 operating on visa images, the heatmap shows false match rates observed over impostor comparisons of faces from different individuals who were born in the given region pair. False matches are counted against a recognition threshold fixed globally to give the target FMR in the plot title, computed over all on the order of 10^{10} impostor comparisons. If text appears in each box it give the same quantity as that coded by the color. Grey indicates FMR is at the intended FMR target level. Light red colors present a security vulnerability to, for example, a passport gate. Each +1 increase in log10 FMR corresponds to a factor of 10 increase in FMR. The matrix is not quite symmetric because images in the enrollment and verification sets are different.

Cross region FMR at threshold $T = 3.868$ for algorithm aware_003, giving $FMR(T) = 0.0001$ globally.

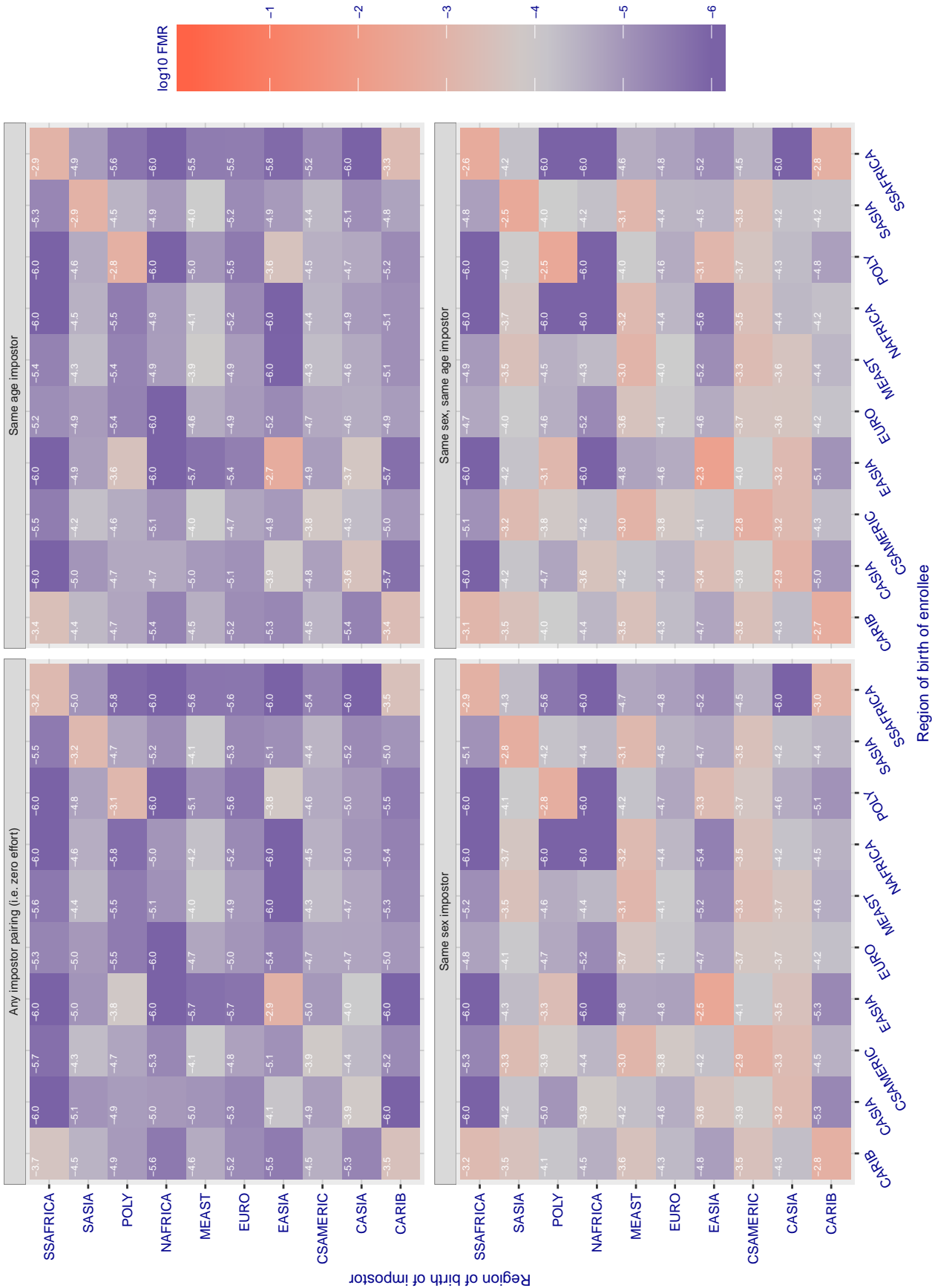


Figure 108: For algorithm aware-003 operating on visa images, the heatmap shows false match rates observed over impostor comparisons of faces from different individuals who were born in the given region pair. False matches are counted against a recognition threshold fixed globally to give the target FMR in the plot title, computed over all on the order of 10^{10} impostor comparisons. If text appears in each box it give the same quantity as that coded by the color. Grey indicates FMR is at the intended FMR target level. Light red colors present a security vulnerability to, for example, a passport gate. Each +1 increase in \log_{10} FMR corresponds to a factor of 10 increase in FMR. The matrix is not quite symmetric because images in the enrollment and verification sets are different.

Cross region FMR at threshold $T = 5.084$ for algorithm aware_004, giving $FMR(T) = 0.0001$ globally.

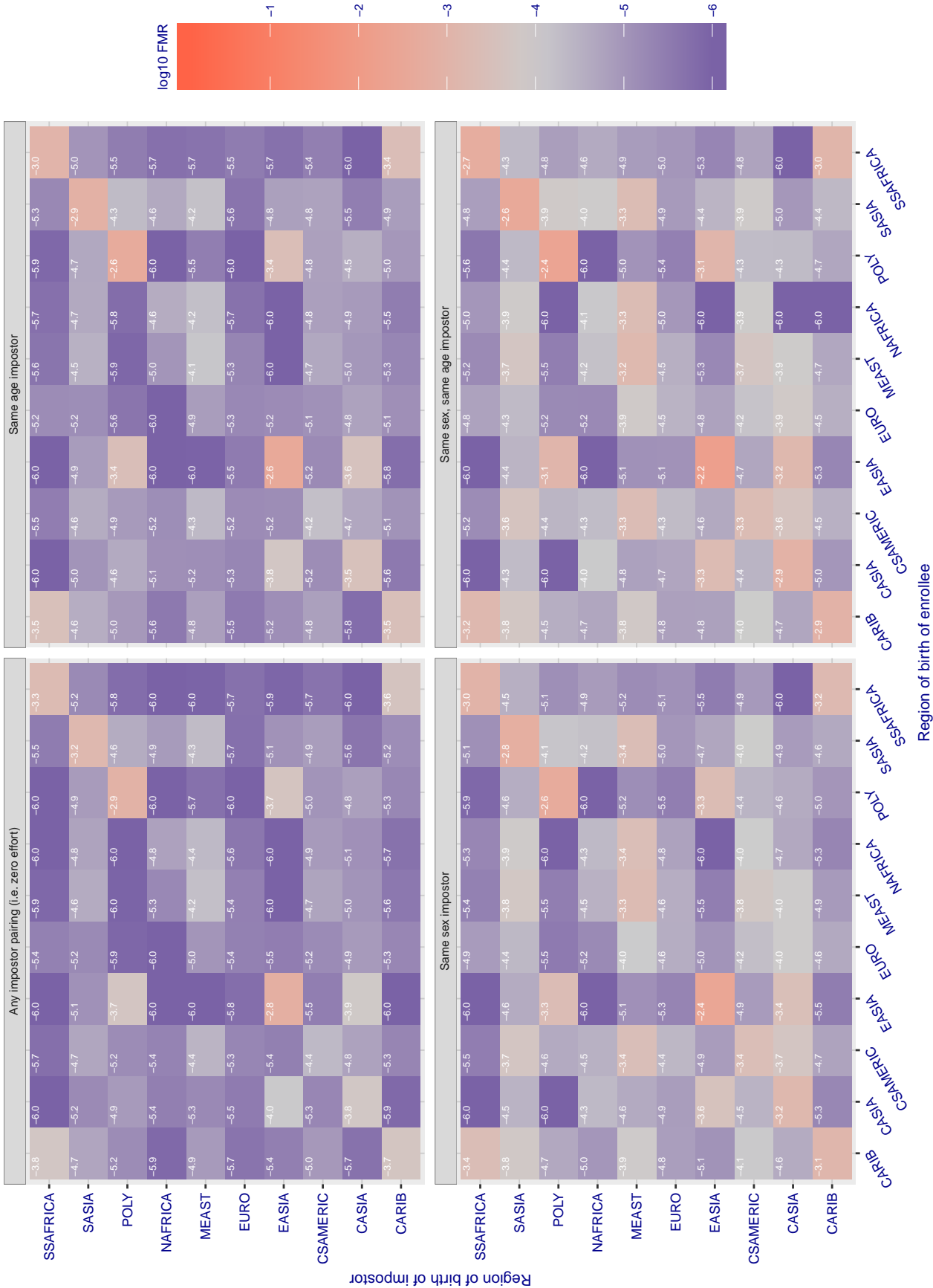


Figure 109: For algorithm aware-004 operating on visa images, the heatmap shows false match rates observed over impostor comparisons of faces from different individuals who were born in the given region pair. False matches are counted against a recognition threshold fixed globally to give the target FMR in the plot title, computed over all on the order of 10^{10} impostor comparisons. If text appears in each box it give the same quantity as that coded by the color. Grey indicates FMR is at the intended FMR target level. Light red colors present a security vulnerability to, for example, a passport gate. Each +1 increase in \log_{10} FMR corresponds to a factor of 10 increase in FMR. The matrix is not quite symmetric because images in the enrollment and verification sets are different.

Cross region FMR at threshold $T = 0.919$ for algorithm ayonix_000, giving $FMR(T) = 0.0001$ globally.

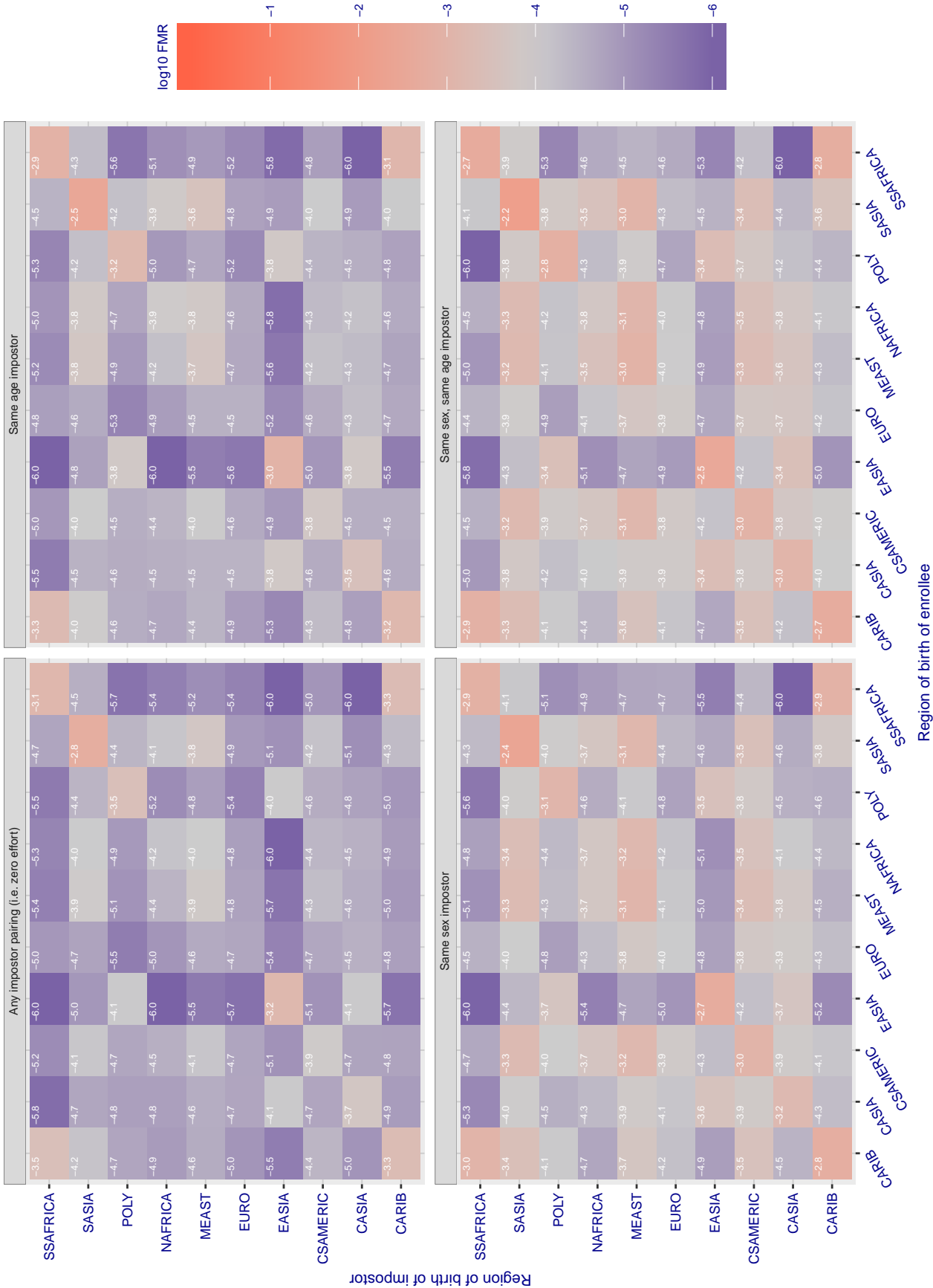


Figure 110: For algorithm ayonix-000 operating on visa images, the heatmap shows false match rates observed over impostor comparisons of faces from different individuals who were born in the given region pair. False matches are counted against a recognition threshold fixed globally to give the target FMR in the plot title, computed over all on the order of 10^{10} impostor comparisons. If text appears in each box it give the same quantity as that coded by the color. Grey indicates FMR is at the intended FMR target level. Light red colors present a security vulnerability to, for example, a passport gate. Each +1 increase in \log_{10} FMR corresponds to a factor of 10 increase in FMR. The matrix is not quite symmetric because images in the enrollment and verification sets are different.

Cross region FMR at threshold $T = 0.731$ for algorithm bm_001 , giving $FMR(T) = 0.0001$ globally.

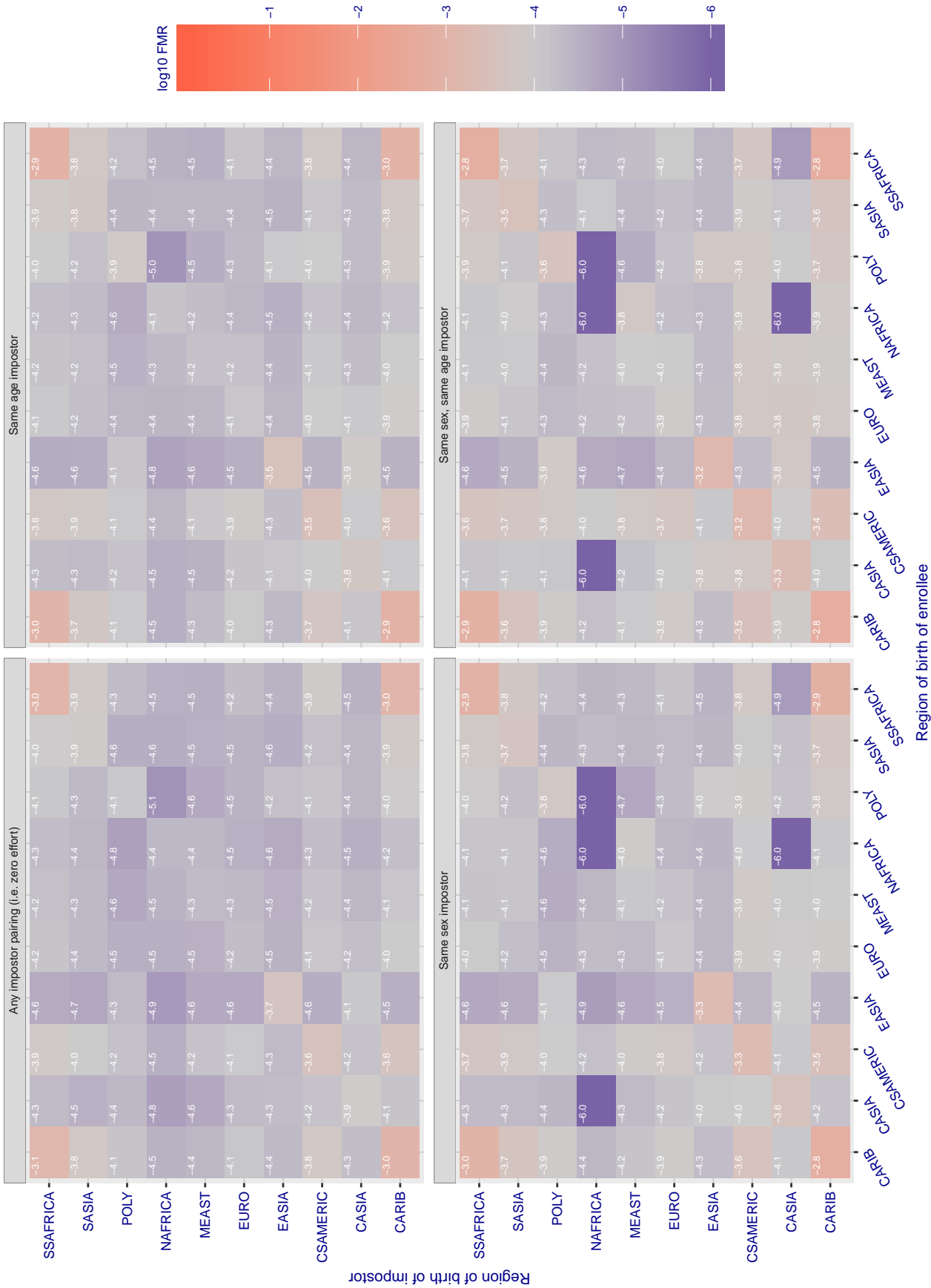


Figure 111: For algorithm $bm-001$ operating on visa images, the heatmap shows false match rates observed over impostor comparisons of faces from different individuals who were born in the given region pair. False matches are counted against a recognition threshold fixed globally to give the target FMR in the plot title, computed over all on the order of 10^{10} impostor comparisons. If text appears in each box it give the same quantity as that coded by the color. Grey indicates FMR is at the intended FMR target level. Light red colors present a security vulnerability to, for example, a passport gate. Each +1 increase in \log_{10} FMR corresponds to a factor of 10 increase in FMR. The matrix is not quite symmetric because images in the enrollment and verification sets are different.

Cross region FMR at threshold $T = 0.388$ for algorithm camvi_002, giving $FMR(T) = 0.0001$ globally.

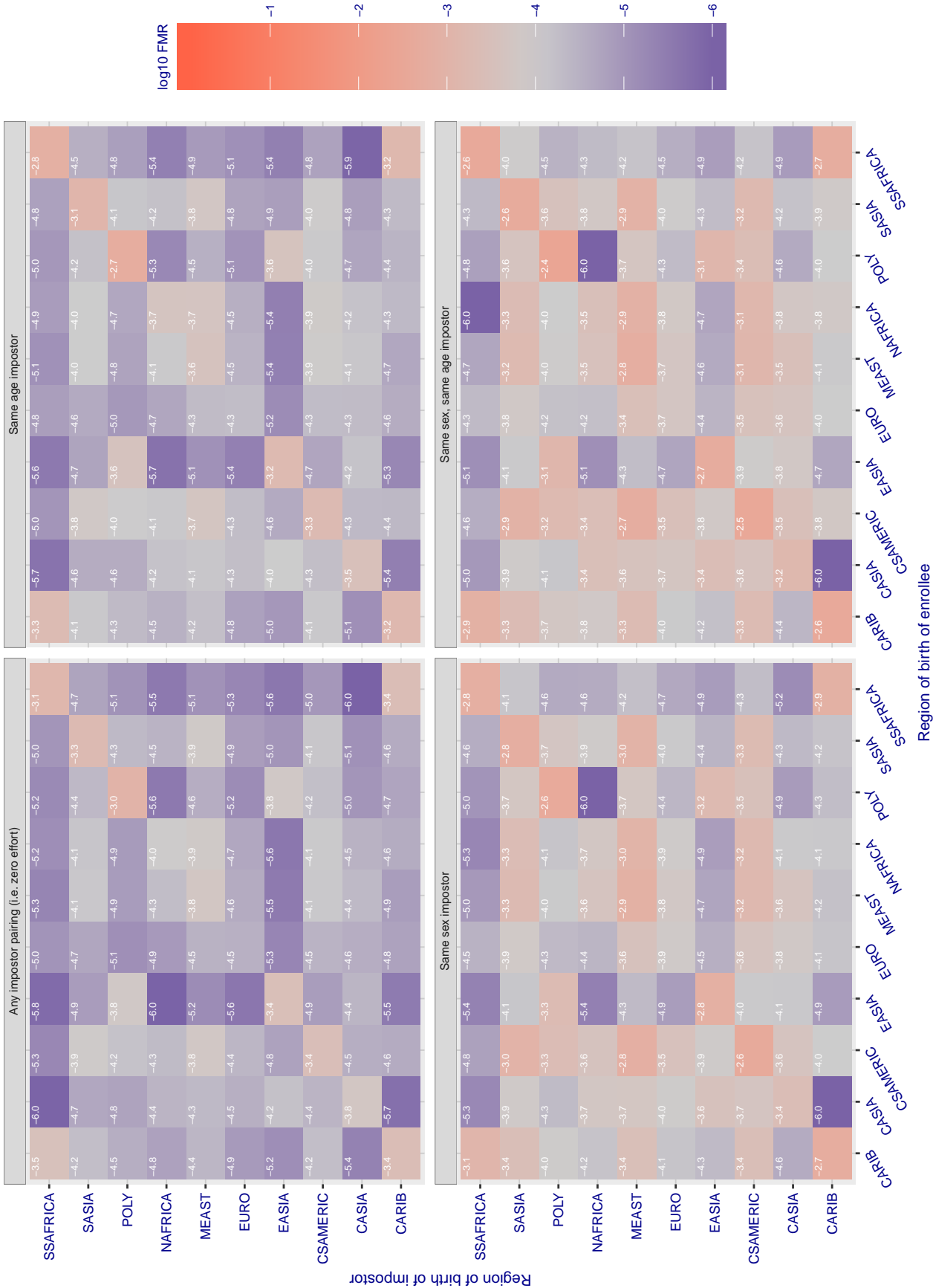


Figure 112: For algorithm camvi-002 operating on visa images, the heatmap shows false match rates observed over impostor comparisons of faces from different individuals who were born in the given region pair. False matches are counted against a recognition threshold fixed globally to give the target FMR in the plot title, computed over all on the order of 10^{10} impostor comparisons. If text appears in each box it give the same quantity as that coded by the color. Grey indicates FMR is at the intended FMR target level. Light red colors present a security vulnerability to, for example, a passport gate. Each +1 increase in \log_{10} FMR corresponds to a factor of 10 increase in FMR. The matrix is not quite symmetric because images in the enrollment and verification sets are different.

Cross region FMR at threshold $T = 0.383$ for algorithm camvi_003, giving $FMR(T) = 0.0001$ globally.

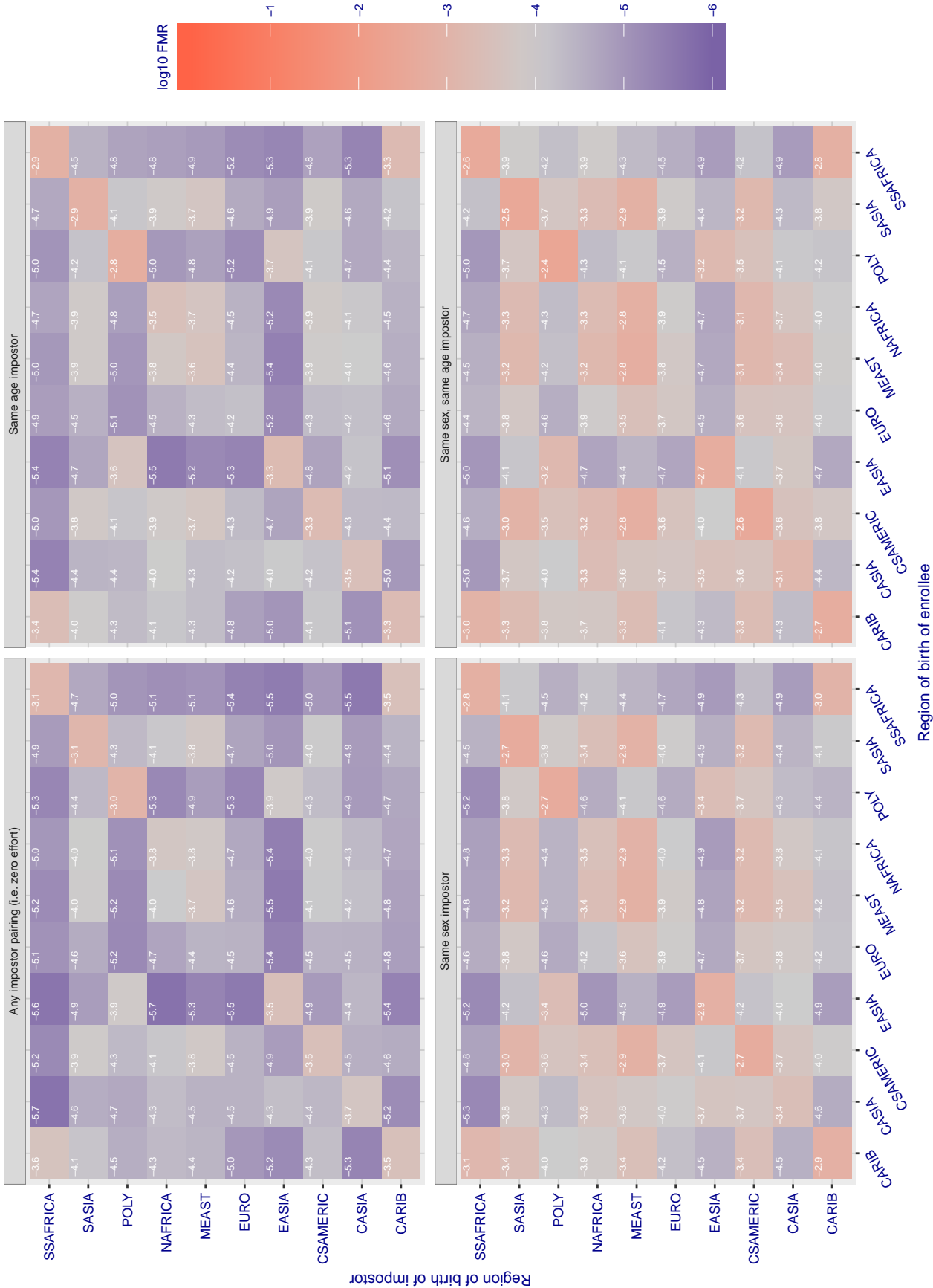


Figure 113: For algorithm camvi-003 operating on visa images, the heatmap shows false match rates observed over impostor comparisons of faces from different individuals who were born in the given region pair. False matches are counted against a recognition threshold fixed globally to give the target FMR in the plot title, computed over all on the order of 10^{10} impostor comparisons. If text appears in each box it give the same quantity as that coded by the color. Grey indicates FMR is at the intended FMR target level. Light red colors present a security vulnerability to, for example, a passport gate. Each +1 increase in \log_{10} FMR corresponds to a factor of 10 increase in FMR. The matrix is not quite symmetric because images in the enrollment and verification sets are different.

Cross region FMR at threshold $T = 0.436$ for algorithm ceiec_001, giving $FMR(T) = 0.0001$ globally.

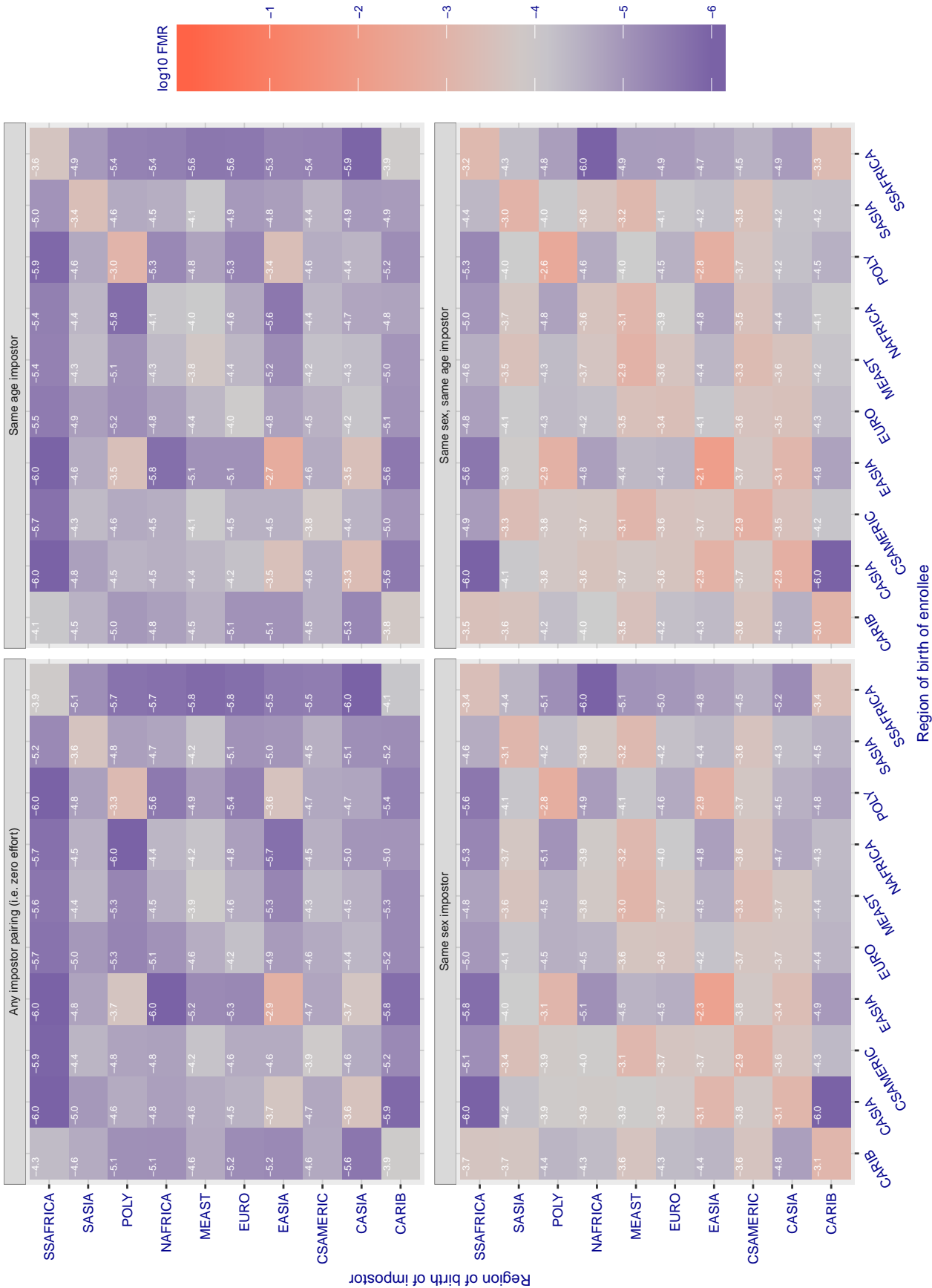


Figure 114: For algorithm ceiec-001 operating on visa images, the heatmap shows false match rates observed over impostor comparisons of faces from different individuals who were born in the given region pair. False matches are counted against a recognition threshold fixed globally to give the target FMR in the plot title, computed over all on the order of 10^{10} impostor comparisons. If text appears in each box it give the same quantity as that coded by the color. Grey indicates FMR is at the intended FMR target level. Light red colors present a security vulnerability to, for example, a passport gate. Each +1 increase in \log_{10} FMR corresponds to a factor of 10 increase in FMR. The matrix is not quite symmetric because images in the enrollment and verification sets are different.

Cross region FMR at threshold $T = 3271.000$ for algorithm cogent_002, giving $FMR(T) = 0.0001$ globally.

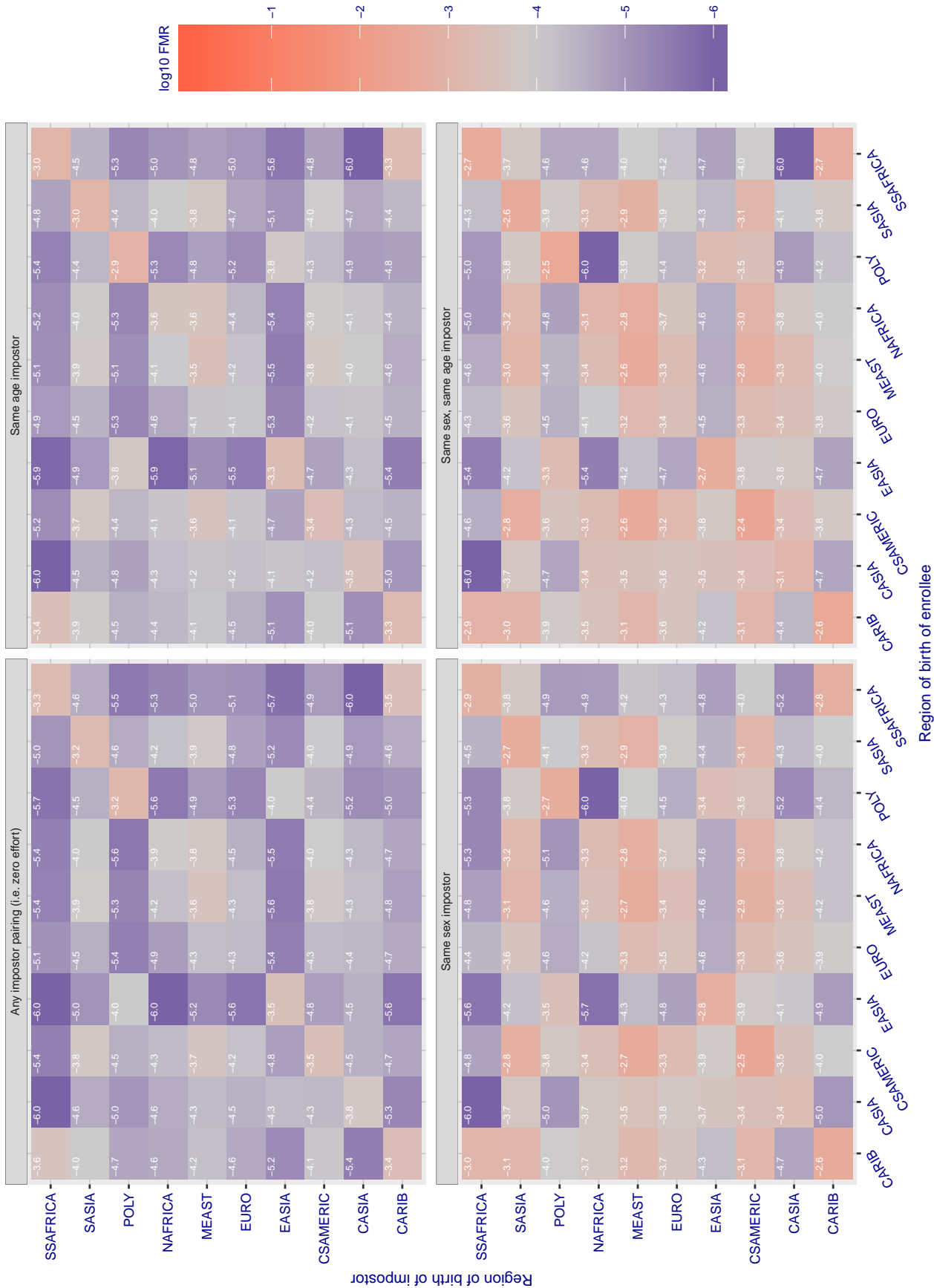


Figure 115: For algorithm cogent-002 operating on visa images, the heatmap shows false match rates observed over impostor comparisons of faces from different individuals who were born in the given region pair. False matches are counted against a recognition threshold fixed globally to give the target FMR in the plot title, computed over all on the order of 10^{10} impostor comparisons. If text appears in each box it give the same quantity as that coded by the color. Grey indicates FMR is at the intended FMR target level. Light red colors present a security vulnerability to, for example, a passport gate. Each +1 increase in $\log_{10} FMR$ corresponds to a factor of 10 increase in FMR. The matrix is not quite symmetric because images in the enrollment and verification sets are different.

Cross region FMR at threshold $T = 2972.000$ for algorithm cogent_003, giving $FMR(T) = 0.0001$ globally.

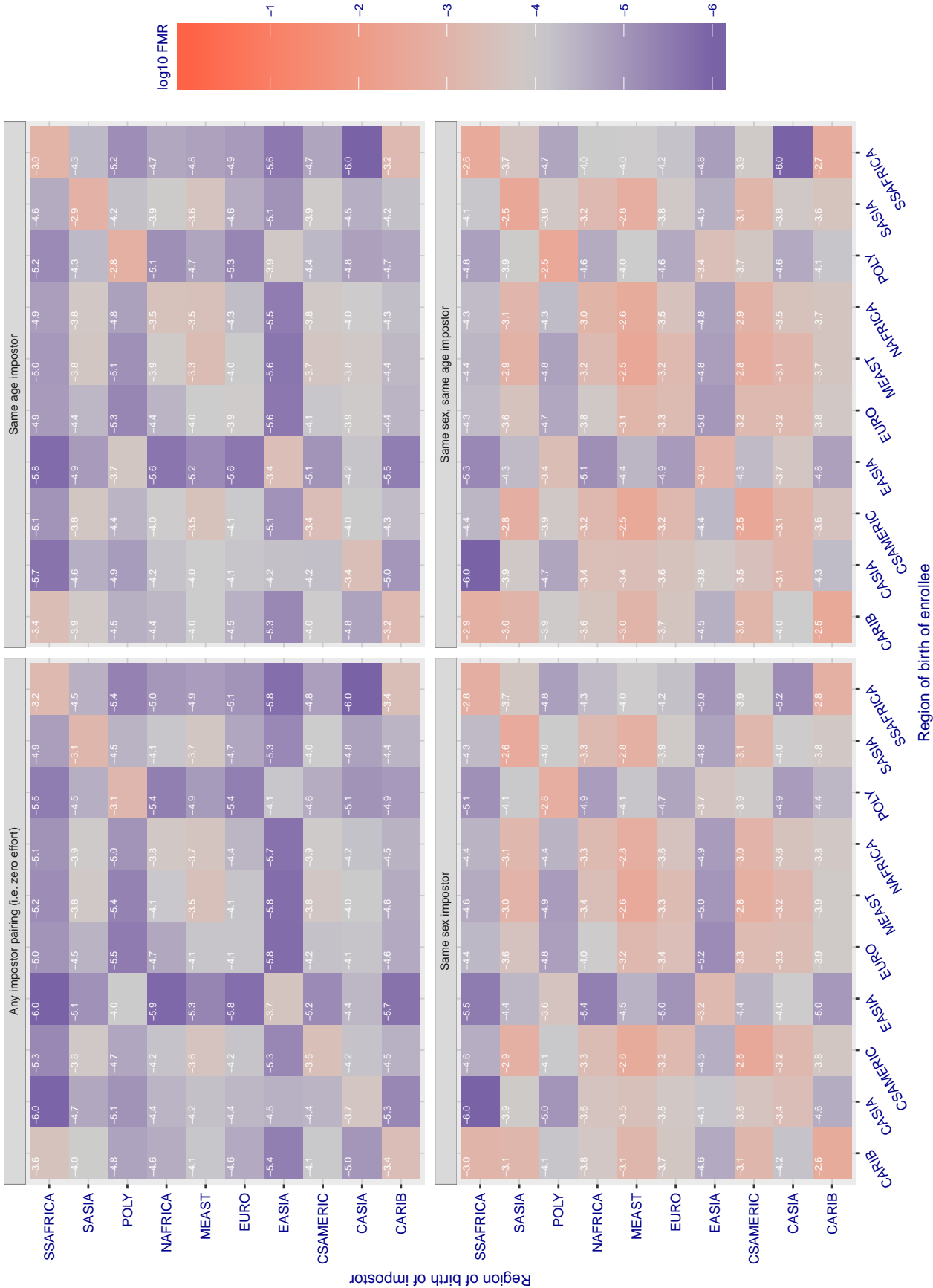


Figure 116: For algorithm cogent-003 operating on visa images, the heatmap shows false match rates observed over impostor comparisons of faces from different individuals who were born in the given region pair. False matches are counted against a recognition threshold fixed globally to give the target FMR in the plot title, computed over all on the order of 10^{10} impostor comparisons. If text appears in each box it give the same quantity as that coded by the color. Grey indicates FMR is at the intended FMR target level. Light red colors present a security vulnerability to, for example, a passport gate. Each +1 increase in \log_{10} FMR corresponds to a factor of 10 increase in FMR. The matrix is not quite symmetric because images in the enrollment and verification sets are different.

Cross region FMR at threshold $T = 0.565$ for algorithm `cognitec_000`, giving $FMR(T) = 0.0001$ globally.

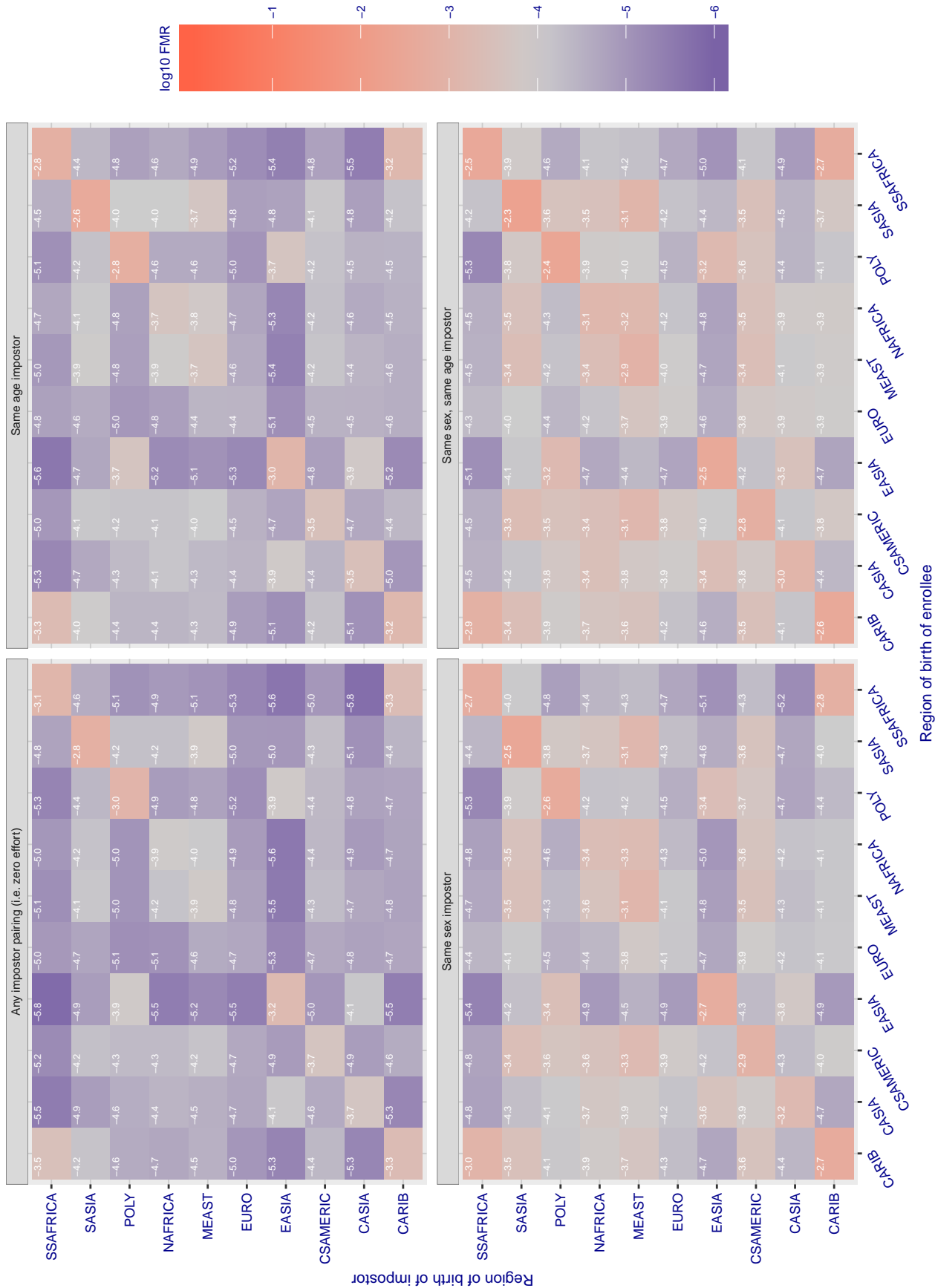


Figure 117: For algorithm `cognitec-000` operating on visa images, the heatmap shows false match rates observed over impostor comparisons of faces from different individuals who were born in the given region pair. False matches are counted against a recognition threshold fixed globally to give the target FMR in the plot title, computed over all on the order of 10^{10} impostor comparisons. If text appears in each box it give the same quantity as that coded by the color. Grey indicates FMR is at the intended FMR target level. Light red colors present a security vulnerability to, for example, a passport gate. Each +1 increase in \log_{10} FMR corresponds to a factor of 10 increase in FMR. The matrix is not quite symmetric because images in the enrollment and verification sets are different.

Cross region FMR at threshold $T = 0.565$ for algorithm *cognitec_001*, giving $FMR(T) = 0.0001$ globally.

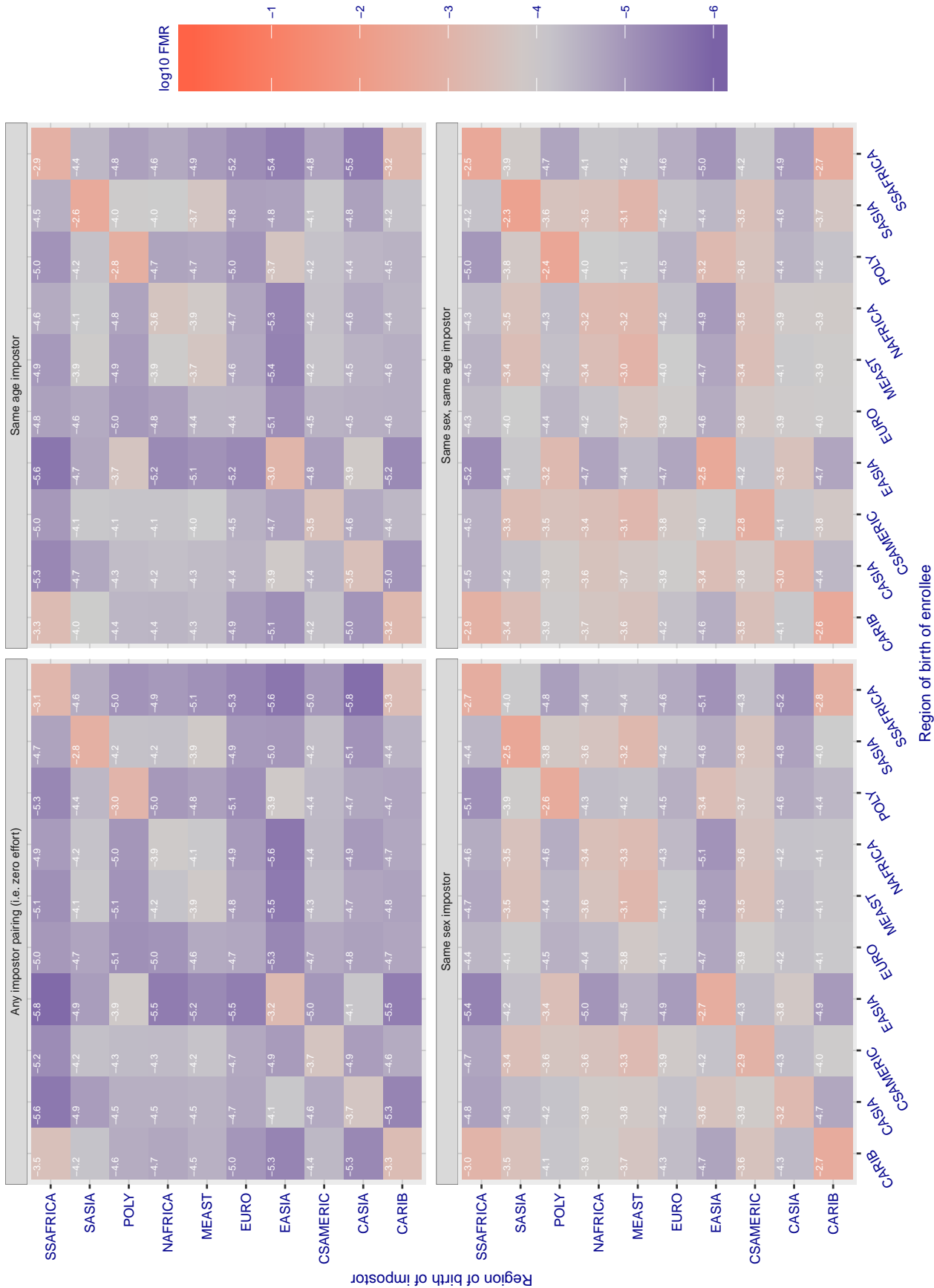


Figure 118: For algorithm *cognitec-001* operating on visa images, the heatmap shows false match rates observed over impostor comparisons of faces from different individuals who were born in the given region pair. False matches are counted against a recognition threshold fixed globally to give the target FMR in the plot title, computed over all on the order of 10^{10} impostor comparisons. If text appears in each box it give the same quantity as that coded by the color. Grey indicates FMR is at the intended FMR target level. Light red colors present a security vulnerability to, for example, a passport gate. Each +1 increase in \log_{10} FMR corresponds to a factor of 10 increase in FMR. The matrix is not quite symmetric because images in the enrollment and verification sets are different.

Cross region FMR at threshold $T = 0.762$ for algorithm cyberextruder_001, giving $FMR(T) = 0.0001$ globally.

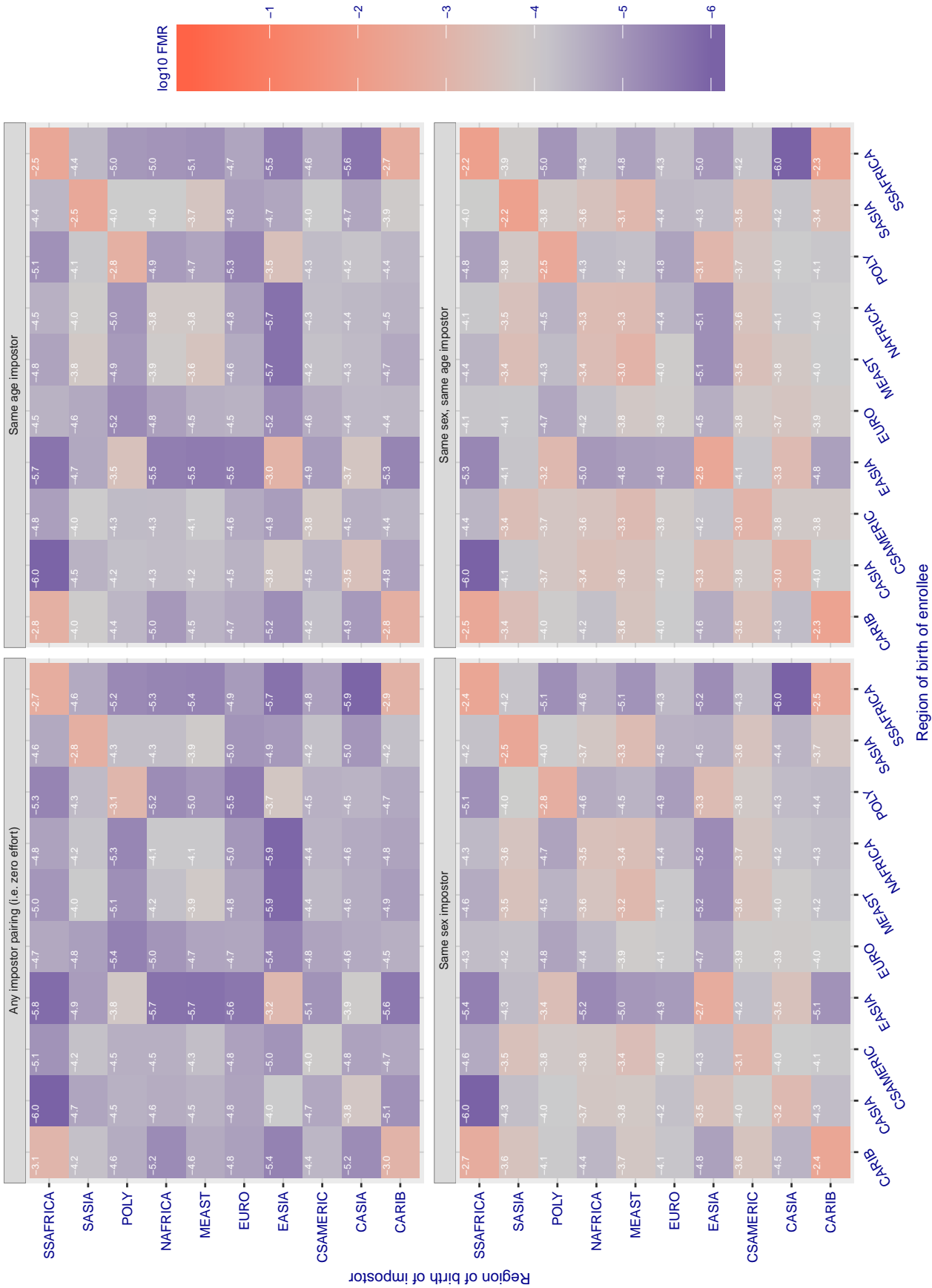


Figure 119: For algorithm cyberextruder-001 operating on visa images, the heatmap shows false match rates observed over impostor comparisons of faces from different individuals who were born in the given region pair. False matches are counted against a recognition threshold fixed globally to give the target FMR in the plot title, computed over all on the order of 10^{10} impostor comparisons. If text appears in each box it give the same quantity as that coded by the color. Grey indicates FMR is at the intended FMR target level. Light red colors present a security vulnerability to, for example, a passport gate. Each +1 increase in \log_{10} FMR corresponds to a factor of 10 increase in FMR. The matrix is not quite symmetric because images in the enrollment and verification sets are different.

Cross region FMR at threshold T = 0.500 for algorithm cyberextruder_002, giving FMR(T) = 0.0001 globally.

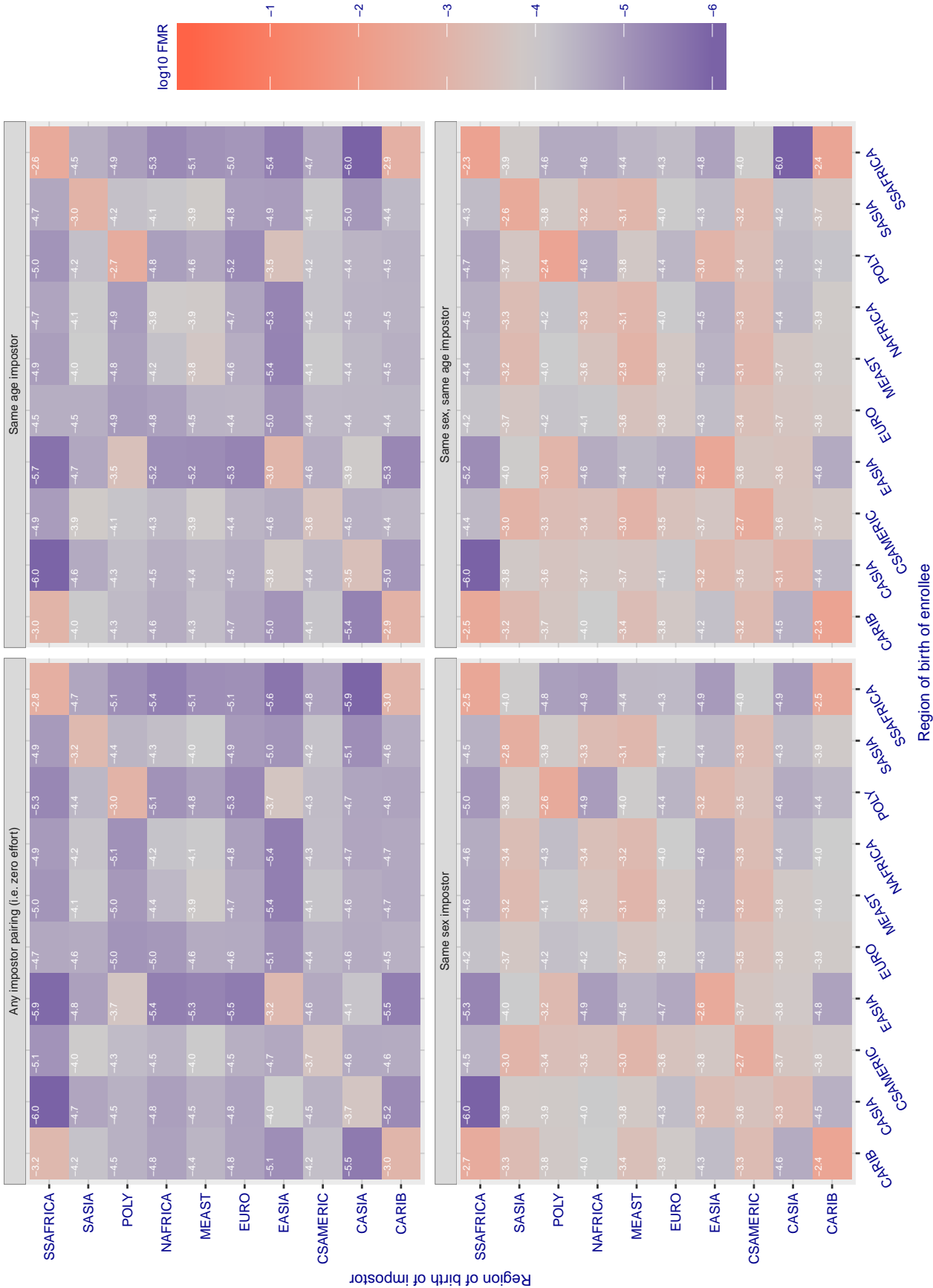


Figure 120: For algorithm cyberextruder-002 operating on visa images, the heatmap shows false match rates observed over impostor comparisons of faces from different individuals who were born in the given region pair. False matches are counted against a recognition threshold fixed globally to give the target FMR in the plot title, computed over all on the order of 10^{10} impostor comparisons. If text appears in each box it give the same quantity as that coded by the color. Grey indicates FMR is at the intended FMR target level. Light red colors present a security vulnerability to, for example, a passport gate. Each +1 increase in \log_{10} FMR corresponds to a factor of 10 increase in FMR. The matrix is not quite symmetric because images in the enrollment and verification sets are different.

Cross region FMR at threshold $T = 1.409$ for algorithm cyberlink_000, giving $FMR(T) = 0.0001$ globally.

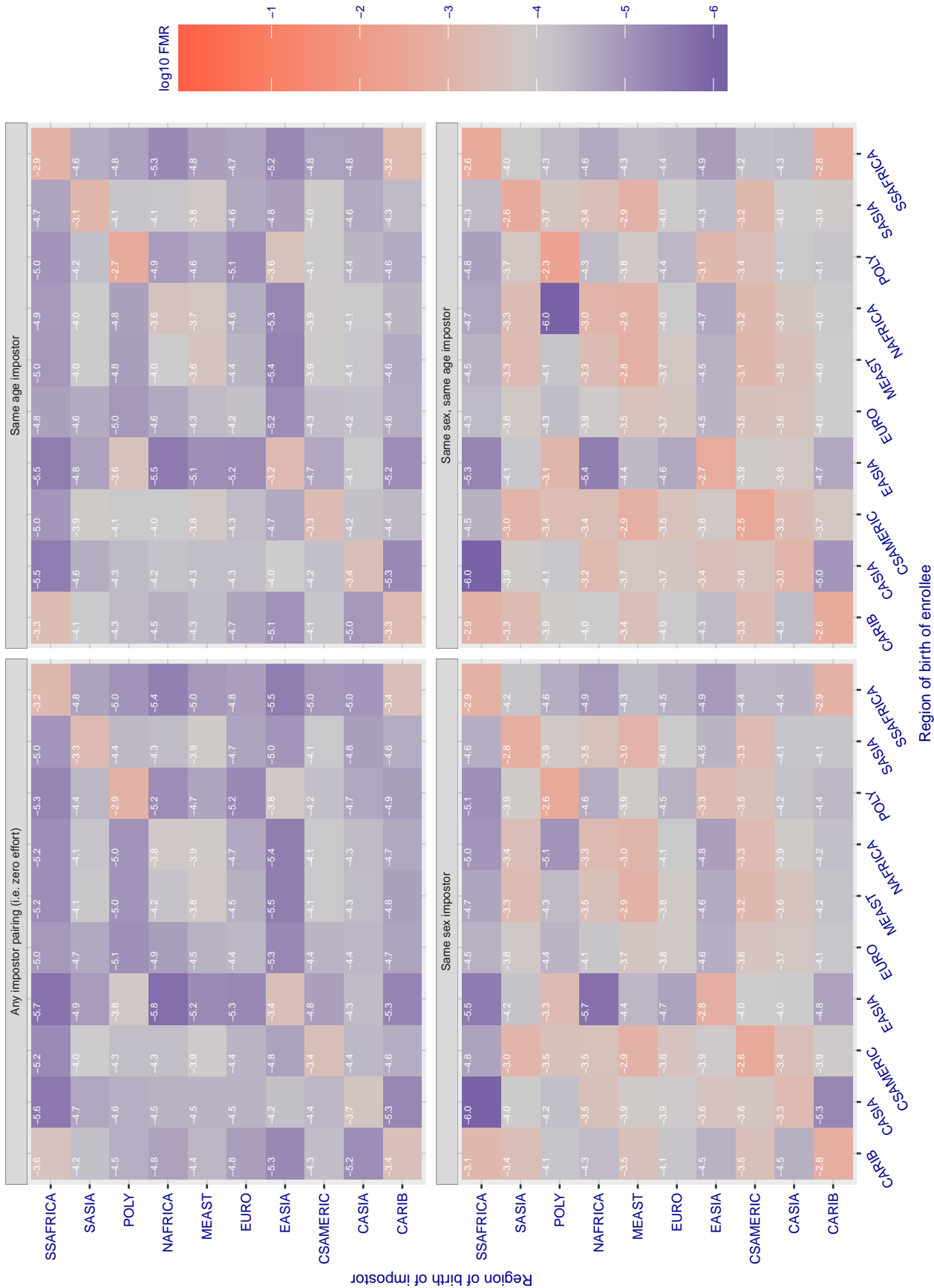


Figure 121: For algorithm cyberlink-000 operating on visa images, the heatmap shows false match rates observed over impostor comparisons of faces from different individuals who were born in the given region pair. False matches are counted against a recognition threshold fixed globally to give the target FMR in the plot title, computed over all on the order of 10^{10} impostor comparisons. If text appears in each box it give the same quantity as that coded by the color. Grey indicates FMR is at the intended FMR target level. Light red colors present a security vulnerability to, for example, a passport gate. Each +1 increase in \log_{10} FMR corresponds to a factor of 10 increase in FMR. The matrix is not quite symmetric because images in the enrollment and verification sets are different.

Cross region FMR at threshold $T = 1.408$ for algorithm cyberlink_001, giving $FMR(T) = 0.0001$ globally.

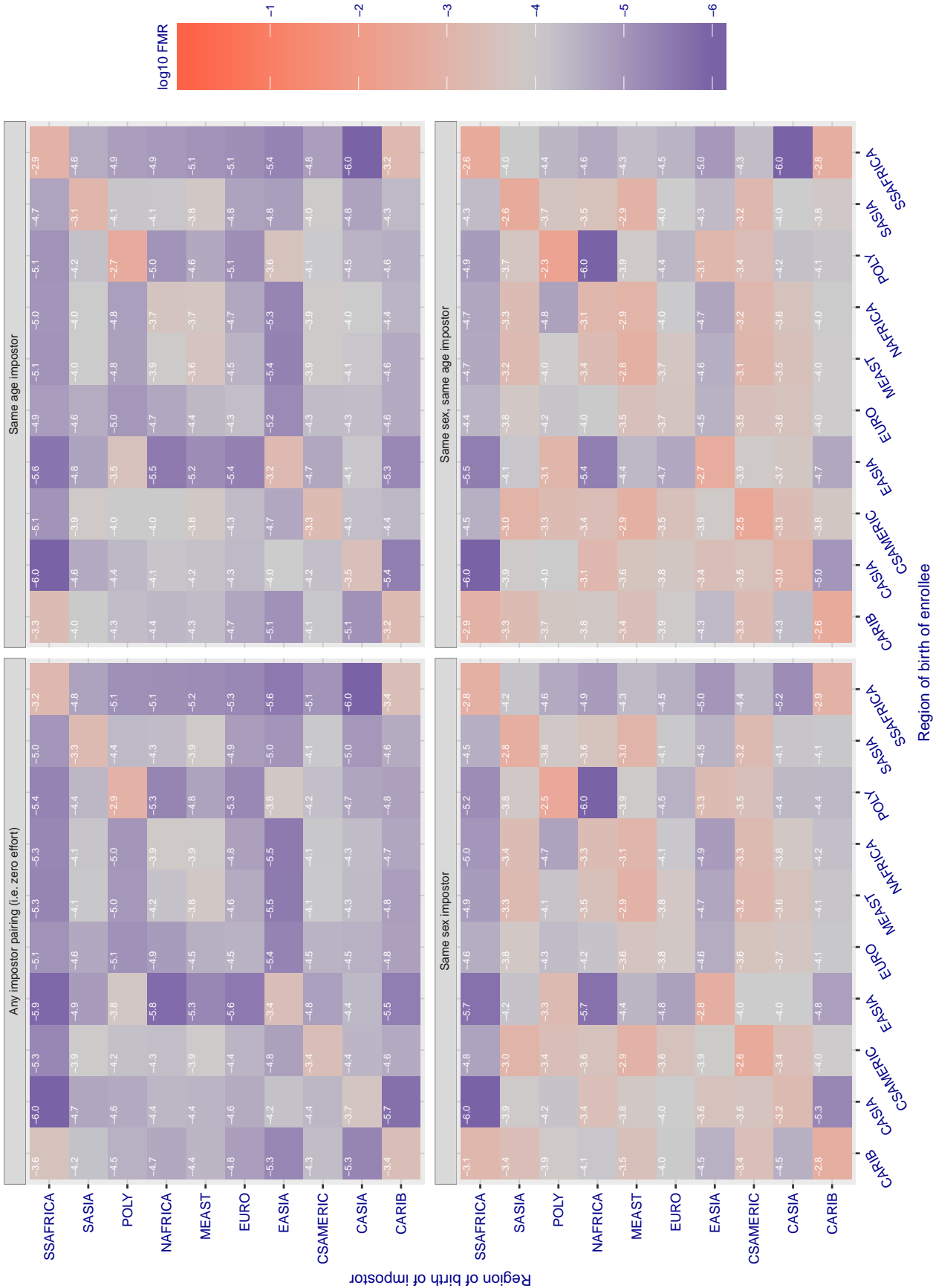


Figure 122: For algorithm cyberlink-001 operating on visa images, the heatmap shows false match rates observed over impostor comparisons of faces from different individuals who were born in the given region pair. False matches are counted against a recognition threshold fixed globally to give the target FMR in the plot title, computed over all on the order of 10^{10} impostor comparisons. If text appears in each box it give the same quantity as that coded by the color. Grey indicates FMR is at the intended FMR target level. Light red colors present a security vulnerability to, for example, a passport gate. Each +1 increase in \log_{10} FMR corresponds to a factor of 10 increase in FMR. The matrix is not quite symmetric because images in the enrollment and verification sets are different.

Cross region FMR at threshold $T = 7630.000$ for algorithm dahua_001, giving $FMR(T) = 0.0001$ globally.

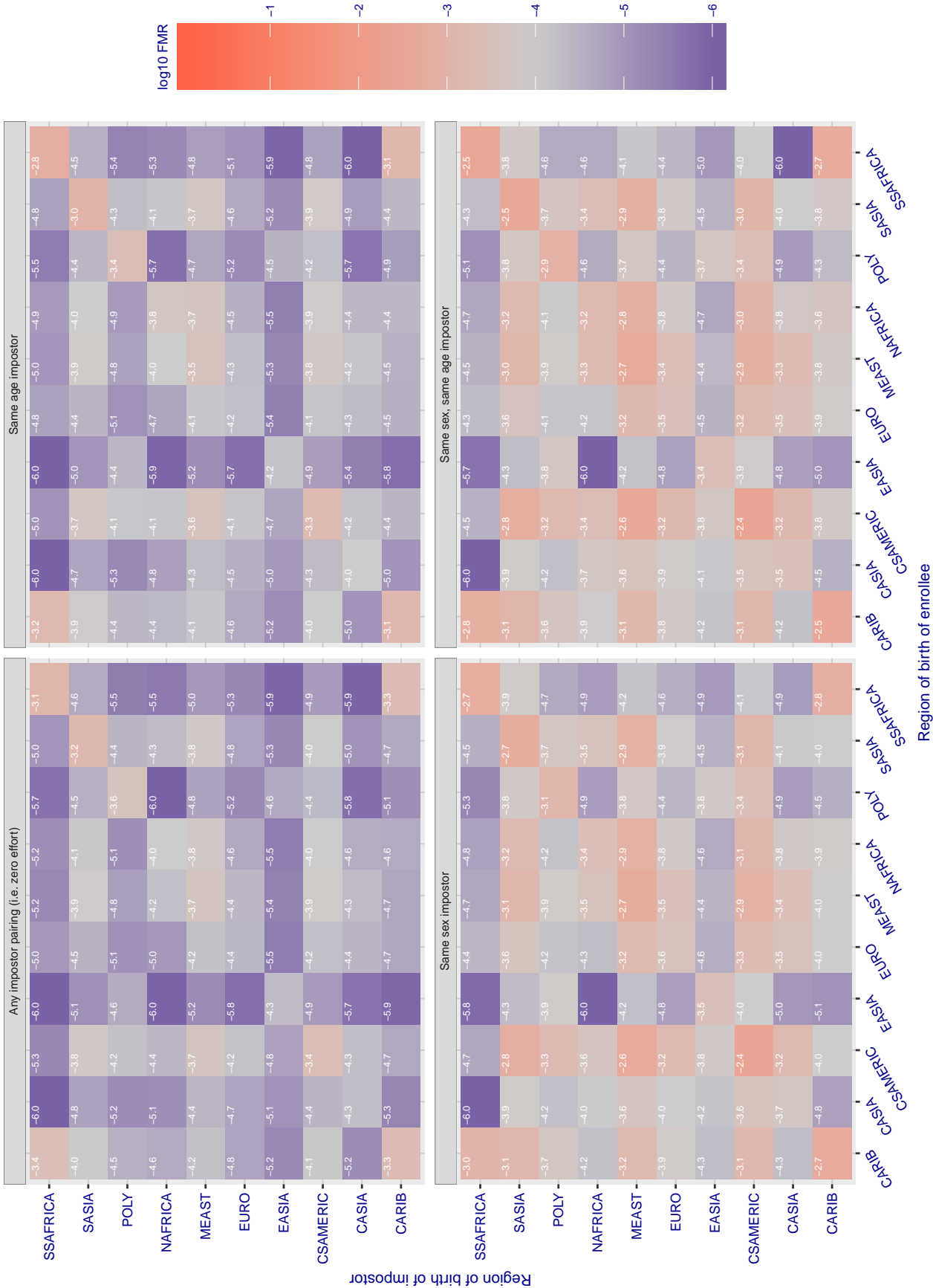


Figure 123: For algorithm dahua-001 operating on visa images, the heatmap shows false match rates observed over impostor comparisons of faces from different individuals who were born in the given region pair. False matches are counted against a recognition threshold fixed globally to give the target FMR in the plot title, computed over all on the order of 10^{10} impostor comparisons. If text appears in each box it give the same quantity as that coded by the color. Grey indicates FMR is at the intended FMR target level. Light red colors present a security vulnerability to, for example, a passport gate. Each +1 increase in \log_{10} FMR corresponds to a factor of 10 increase in FMR. The matrix is not quite symmetric because images in the enrollment and verification sets are different.

Cross region FMR at threshold $T = 6696.000$ for algorithm dahua_002, giving $FMR(T) = 0.0001$ globally.

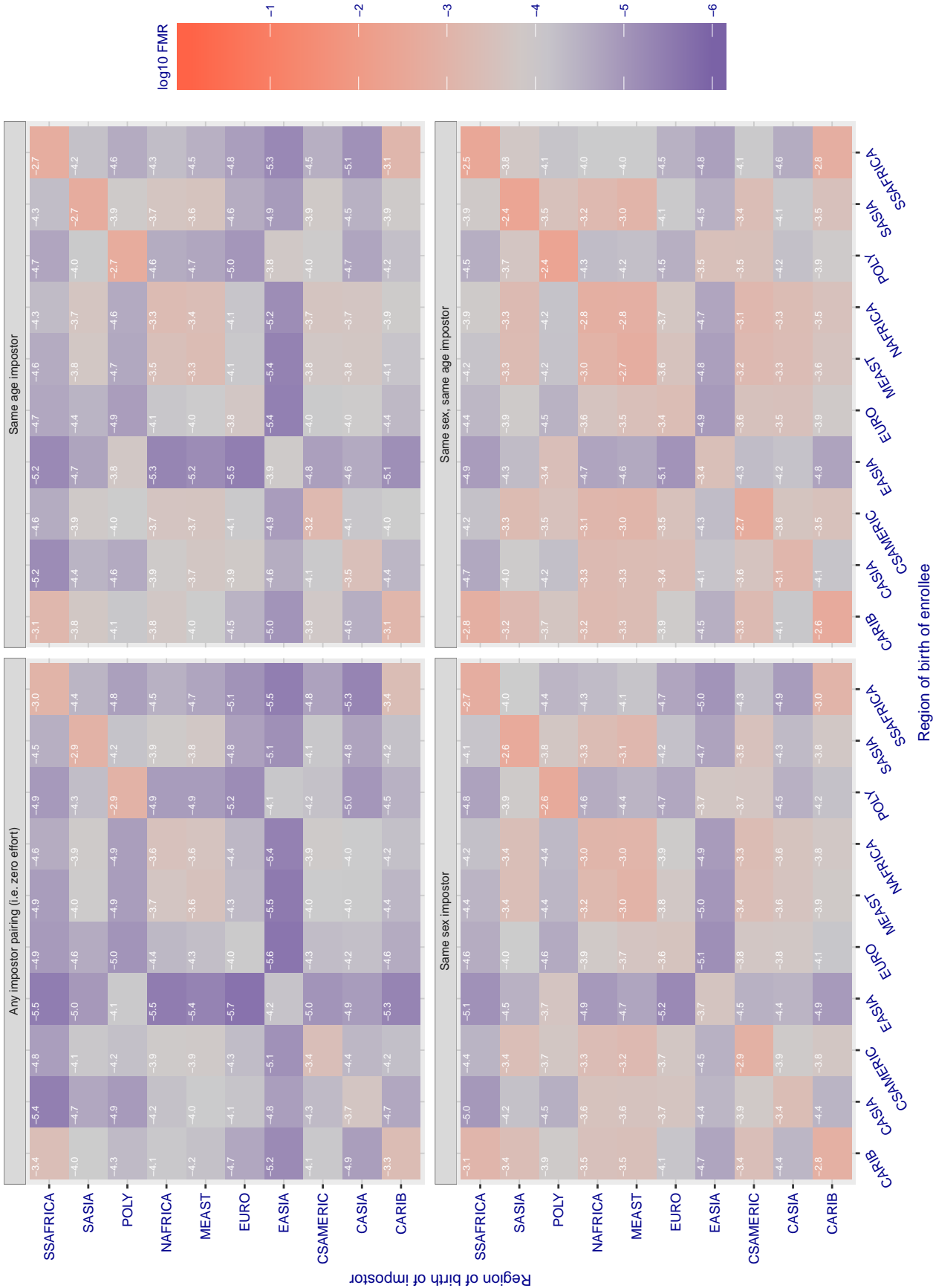


Figure 124: For algorithm dahua-002 operating on visa images, the heatmap shows false match rates observed over impostor comparisons of faces from different individuals who were born in the given region pair. False matches are counted against a recognition threshold fixed globally to give the target FMR in the plot title, computed over all on the order of 10^{10} impostor comparisons. If text appears in each box it give the same quantity as that coded by the color. Grey indicates FMR is at the intended FMR target level. Light red colors present a security vulnerability to, for example, a passport gate. Each +1 increase in \log_{10} FMR corresponds to a factor of 10 increase in FMR. The matrix is not quite symmetric because images in the enrollment and verification sets are different.

Cross region FMR at threshold $T = 79.344$ for algorithm dermalog_005, giving $FMR(T) = 0.0001$ globally.

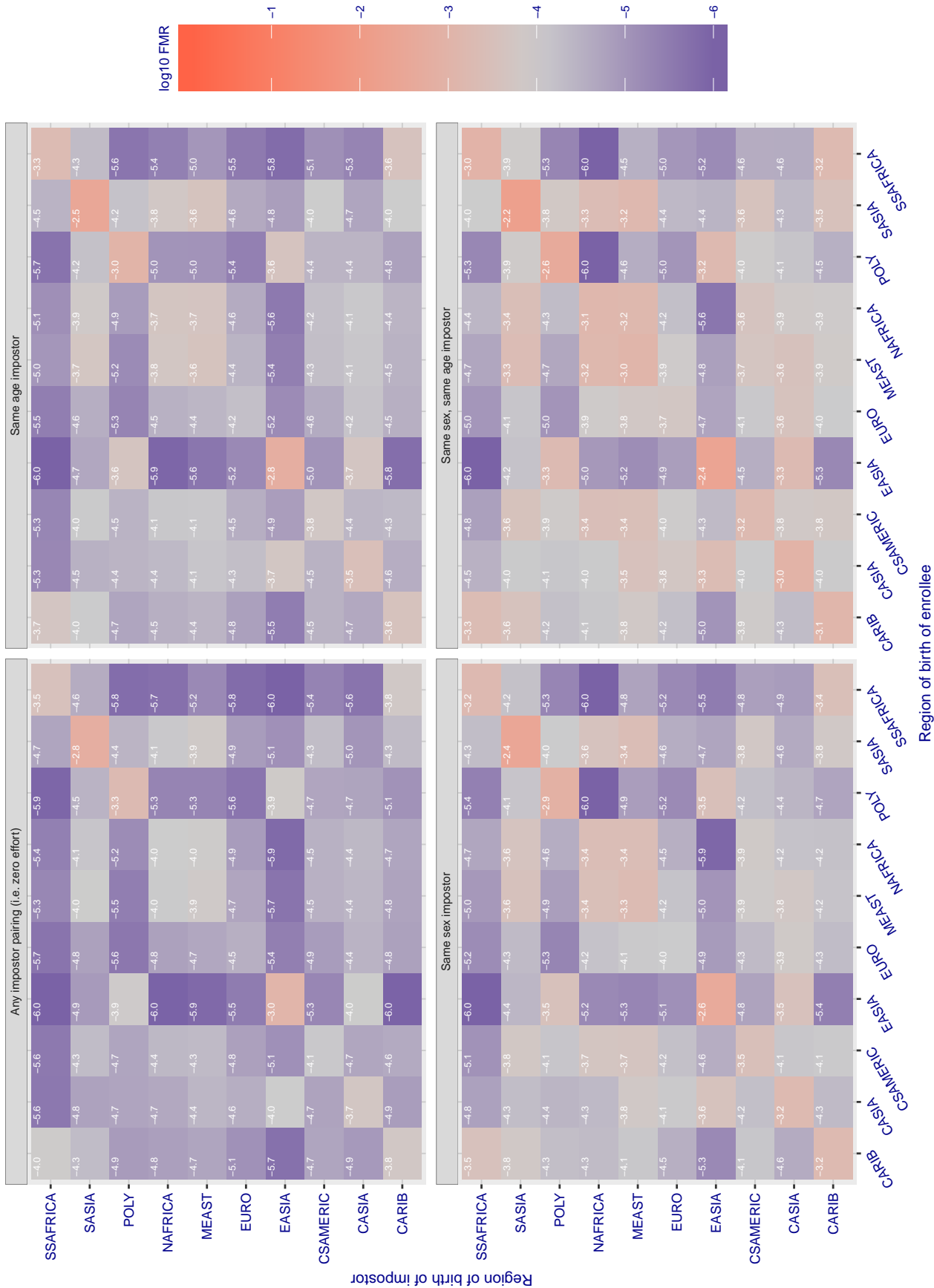


Figure 125: For algorithm dermalog-005 operating on visa images, the heatmap shows false match rates observed over impostor comparisons of faces from different individuals who were born in the given region pair. False matches are counted against a recognition threshold fixed globally to give the target FMR in the plot title, computed over all on the order of 10^{10} impostor comparisons. If text appears in each box it give the same quantity as that coded by the color. Grey indicates FMR is at the intended FMR target level. Light red colors present a security vulnerability to, for example, a passport gate. Each +1 increase in \log_{10} FMR corresponds to a factor of 10 increase in FMR. The matrix is not quite symmetric because images in the enrollment and verification sets are different.

Cross region FMR at threshold T = 79.670 for algorithm dermalog_006, giving FMR(T) = 0.0001 globally.

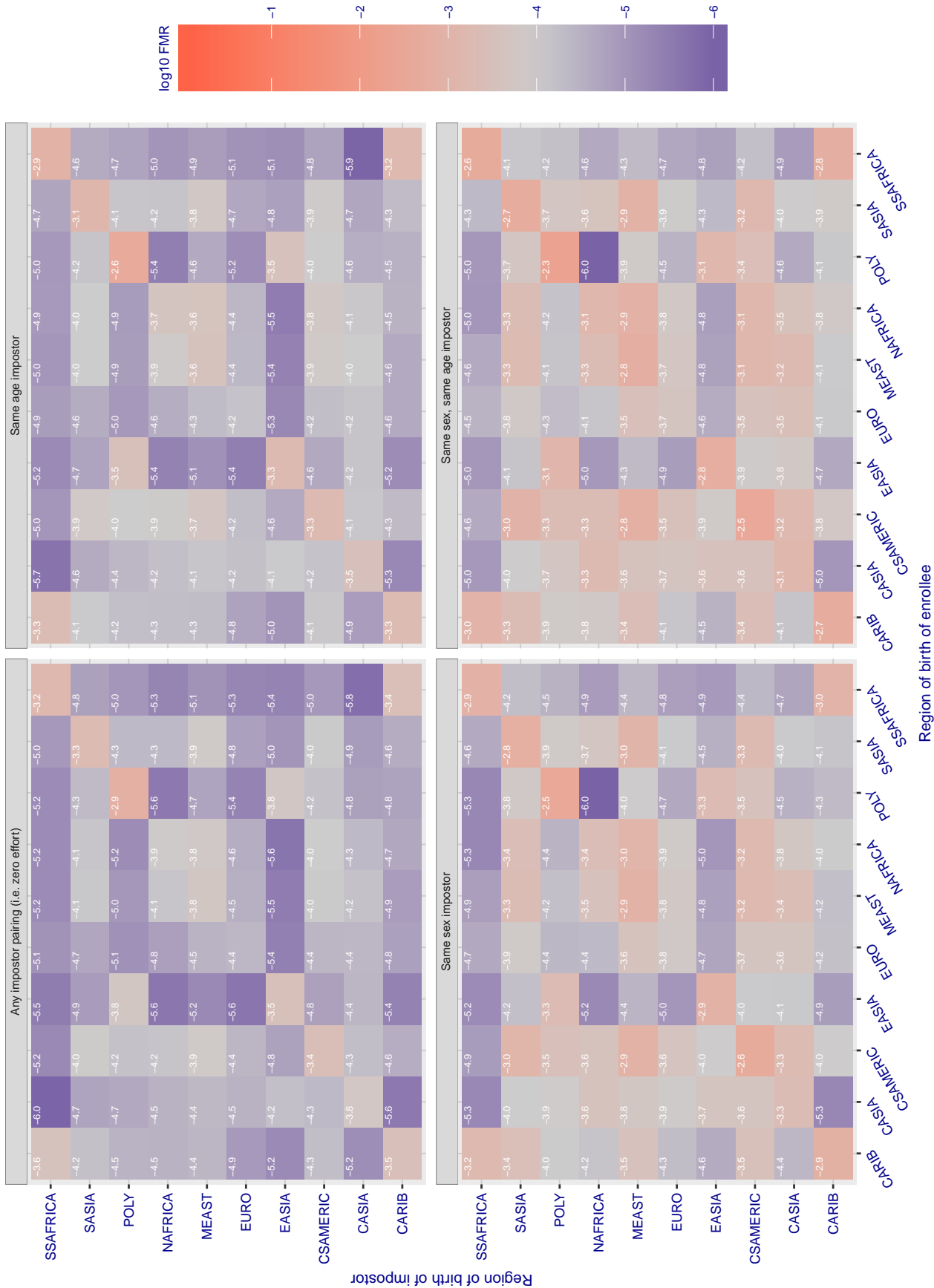


Figure 126: For algorithm dermalog-006 operating on visa images, the heatmap shows false match rates observed over impostor comparisons of faces from different individuals who were born in the given region pair. False matches are counted against a recognition threshold fixed globally to give the target FMR in the plot title, computed over all on the order of 10^{10} impostor comparisons. If text appears in each box it give the same quantity as that coded by the color. Grey indicates FMR is at the intended FMR target level. Light red colors present a security vulnerability to, for example, a passport gate. Each +1 increase in \log_{10} FMR corresponds to a factor of 10 increase in FMR. The matrix is not quite symmetric because images in the enrollment and verification sets are different.

Cross region FMR at threshold T = 0.675 for algorithm digitalbarriers_002, giving FMR(T) = 0.0001 globally.

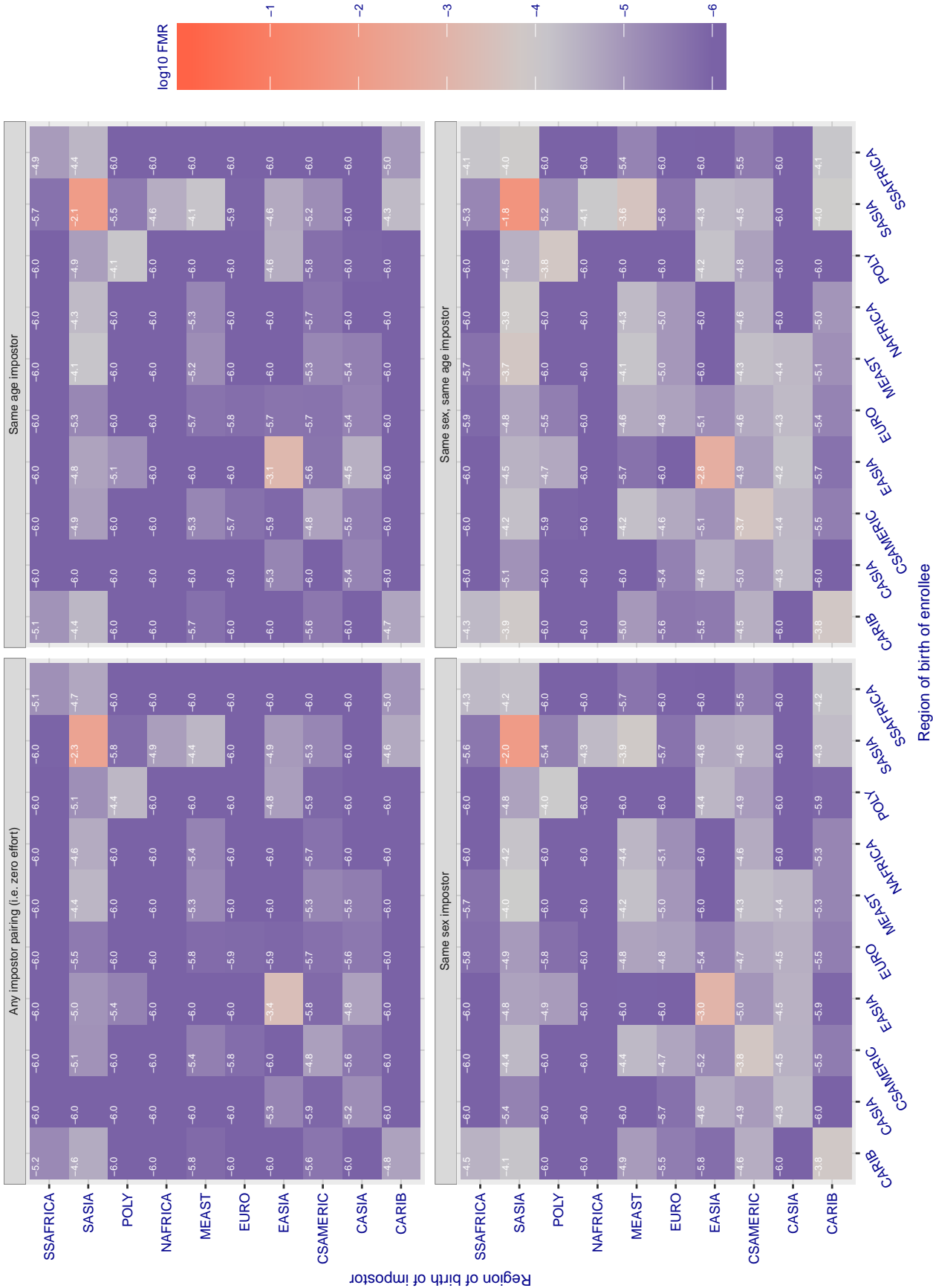


Figure 127: For algorithm digitalbarriers-002 operating on visa images, the heatmap shows false match rates observed over impostor comparisons of faces from different individuals who were born in the given region pair. False matches are counted against a recognition threshold fixed globally to give the target FMR in the plot title, computed over all on the order of 10^{10} impostor comparisons. If text appears in each box it give the same quantity as that coded by the color. Grey indicates FMR is at the intended FMR target level. Light red colors present a security vulnerability to, for example, a passport gate. Each +1 increase in \log_{10} FMR corresponds to a factor of 10 increase in FMR. The matrix is not quite symmetric because images in the enrollment and verification sets are different.

Cross region FMR at threshold $T = 2.672$ for algorithm everai_001, giving $FMR(T) = 0.0001$ globally.

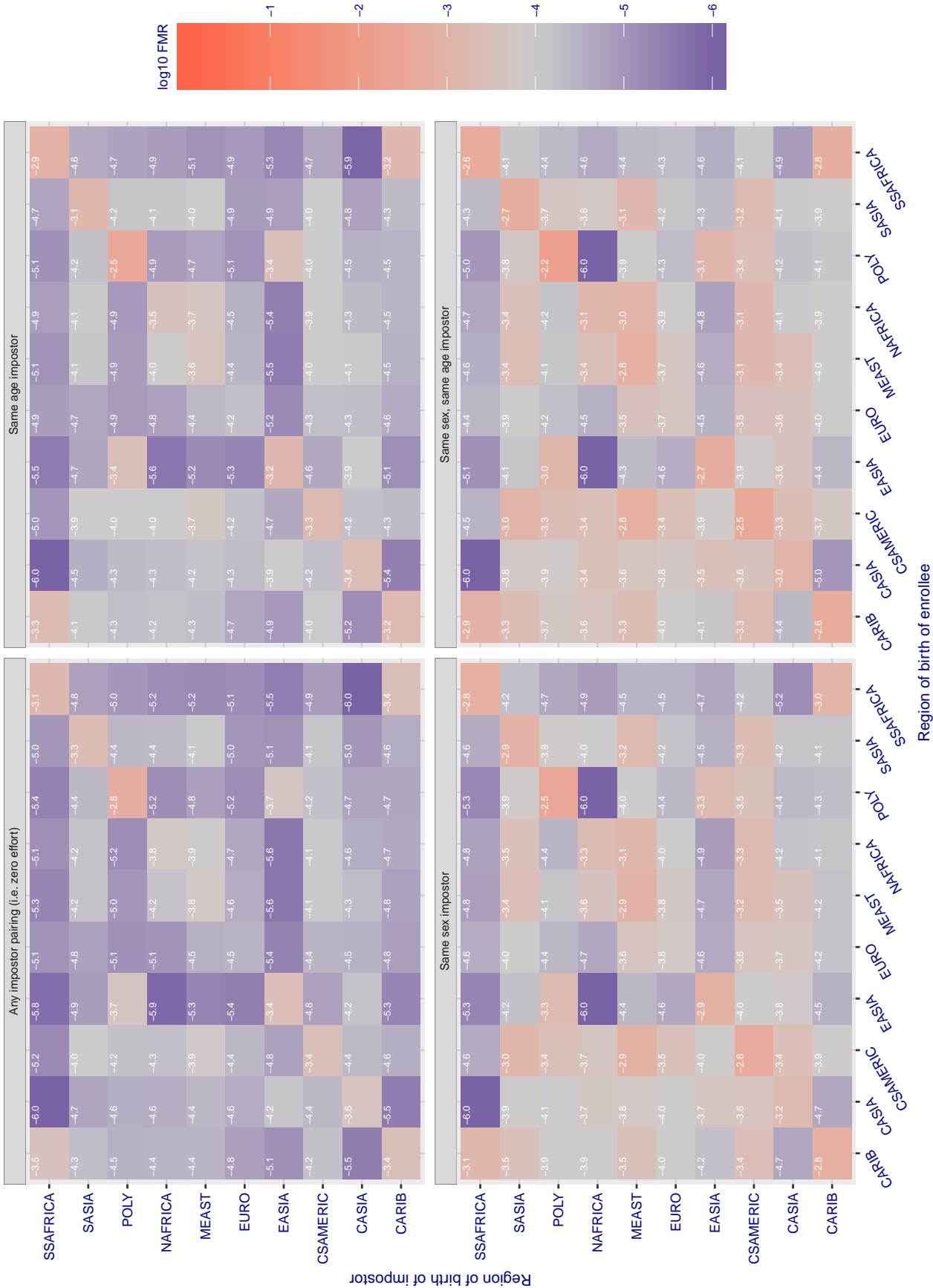


Figure 128: For algorithm everai-001 operating on visa images, the heatmap shows false match rates observed over impostor comparisons of faces from different individuals who were born in the given region pair. False matches are counted against a recognition threshold fixed globally to give the target FMR in the plot title, computed over all on the order of 10^{10} impostor comparisons. If text appears in each box it give the same quantity as that coded by the color. Grey indicates FMR is at the intended FMR target level. Light red colors present a security vulnerability to, for example, a passport gate. Each +1 increase in \log_{10} FMR corresponds to a factor of 10 increase in FMR. The matrix is not quite symmetric because images in the enrollment and verification sets are different.

Cross region FMR at threshold $T = 2.589$ for algorithm everai_002, giving $FMR(T) = 0.0001$ globally.

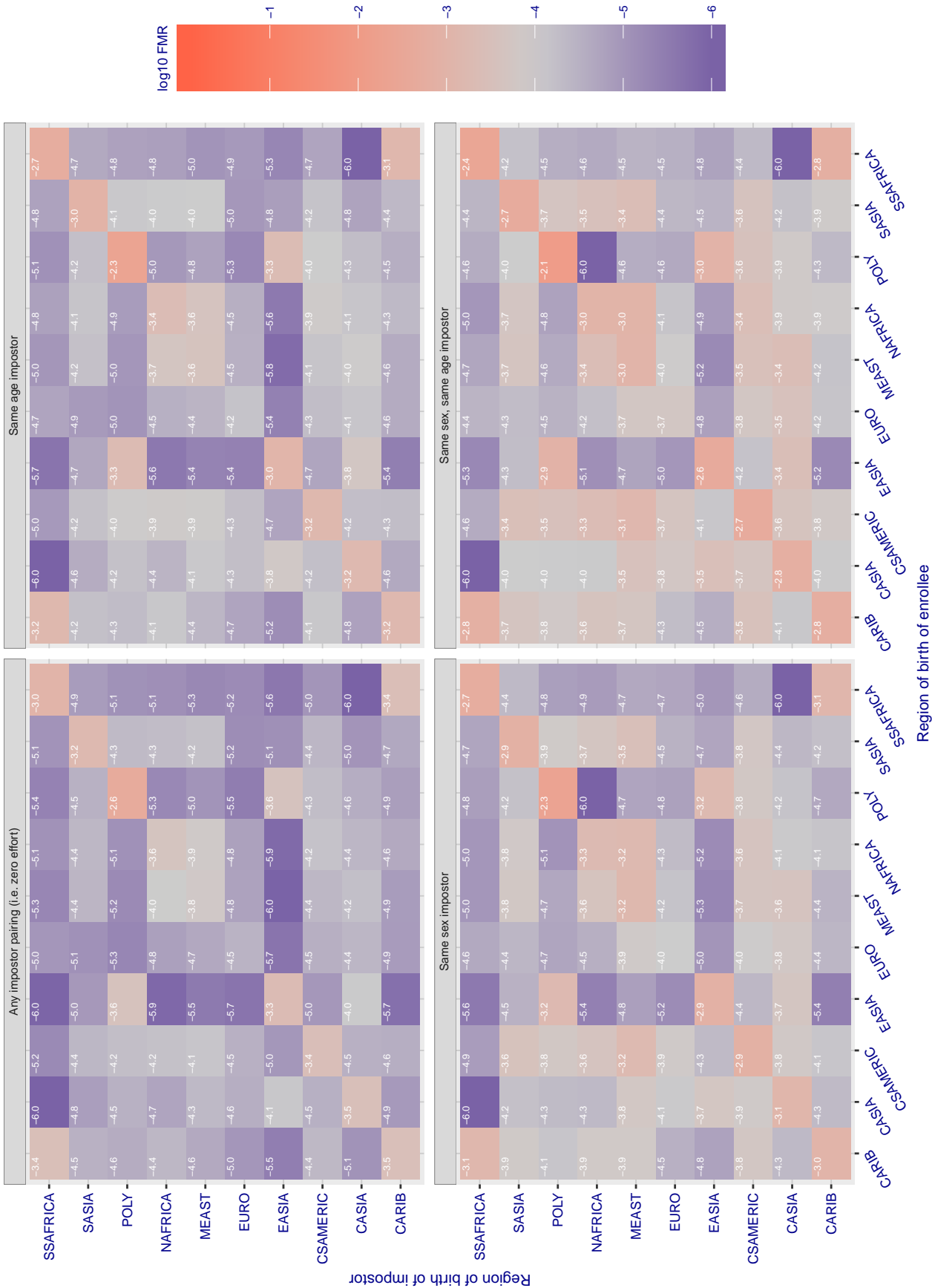


Figure 129: For algorithm everai-002 operating on visa images, the heatmap shows false match rates observed over impostor comparisons of faces from different individuals who were born in the given region pair. False matches are counted against a recognition threshold fixed globally to give the target FMR in the plot title, computed over all on the order of 10^{10} impostor comparisons. If text appears in each box it give the same quantity as that coded by the color. Grey indicates FMR is at the intended FMR target level. Light red colors present a security vulnerability to, for example, a passport gate. Each +1 increase in \log_{10} FMR corresponds to a factor of 10 increase in FMR. The matrix is not quite symmetric because images in the enrollment and verification sets are different.

Cross region FMR at threshold $T = 0.611$ for algorithm glory_000, giving $FMR(T) = 0.0001$ globally.

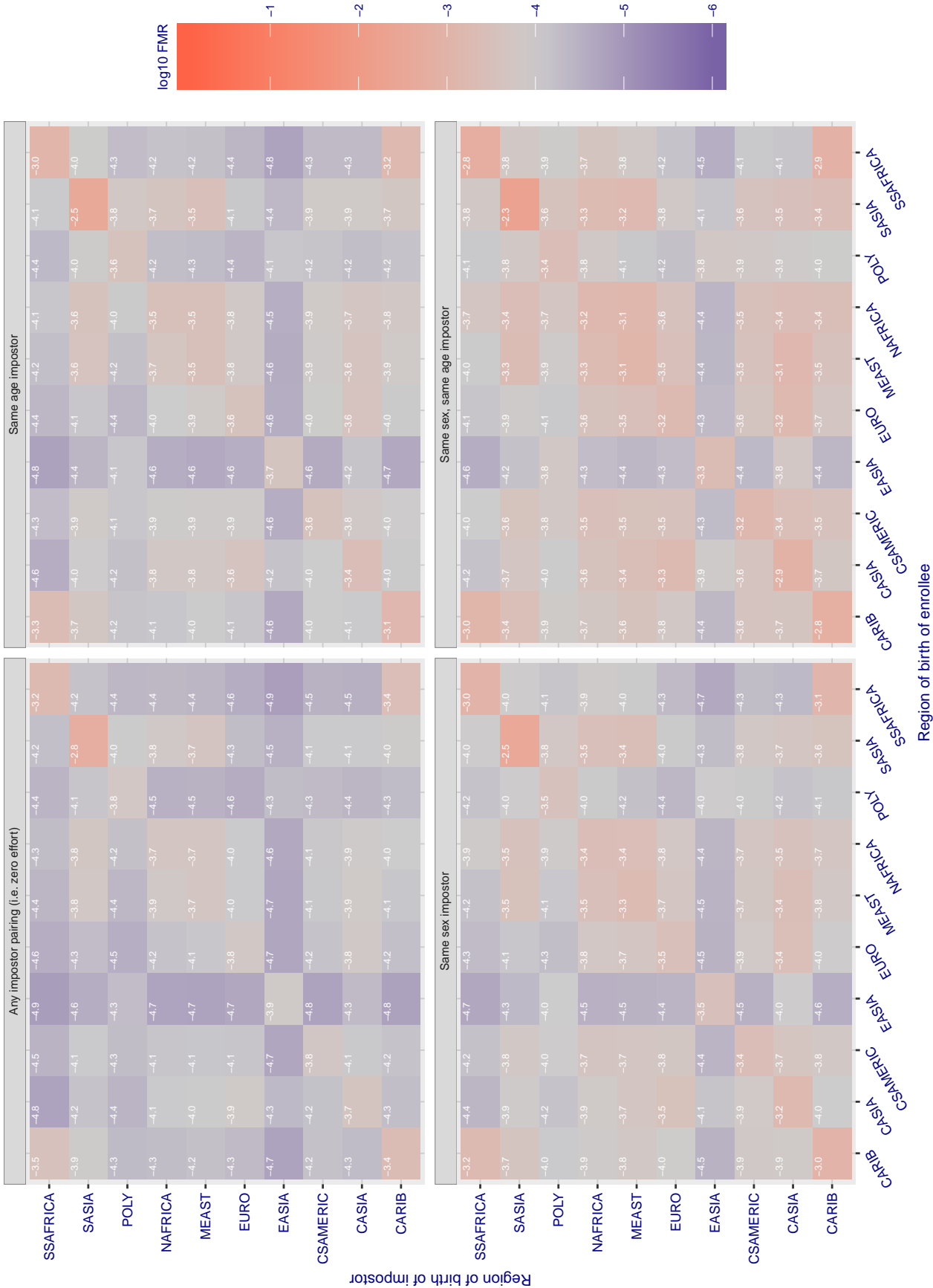


Figure 130: For algorithm glory-000 operating on visa images, the heatmap shows false match rates observed over impostor comparisons of faces from different individuals who were born in the given region pair. False matches are counted against a recognition threshold fixed globally to give the target FMR in the plot title, computed over all on the order of 10^{10} impostor comparisons. If text appears in each box it give the same quantity as that coded by the color. Grey indicates FMR is at the intended FMR target level. Light red colors present a security vulnerability to, for example, a passport gate. Each +1 increase in \log_{10} FMR corresponds to a factor of 10 increase in FMR. The matrix is not quite symmetric because images in the enrollment and verification sets are different.

Cross region FMR at threshold $T = 0.618$ for algorithm glory_001, giving $FMR(T) = 0.0001$ globally.

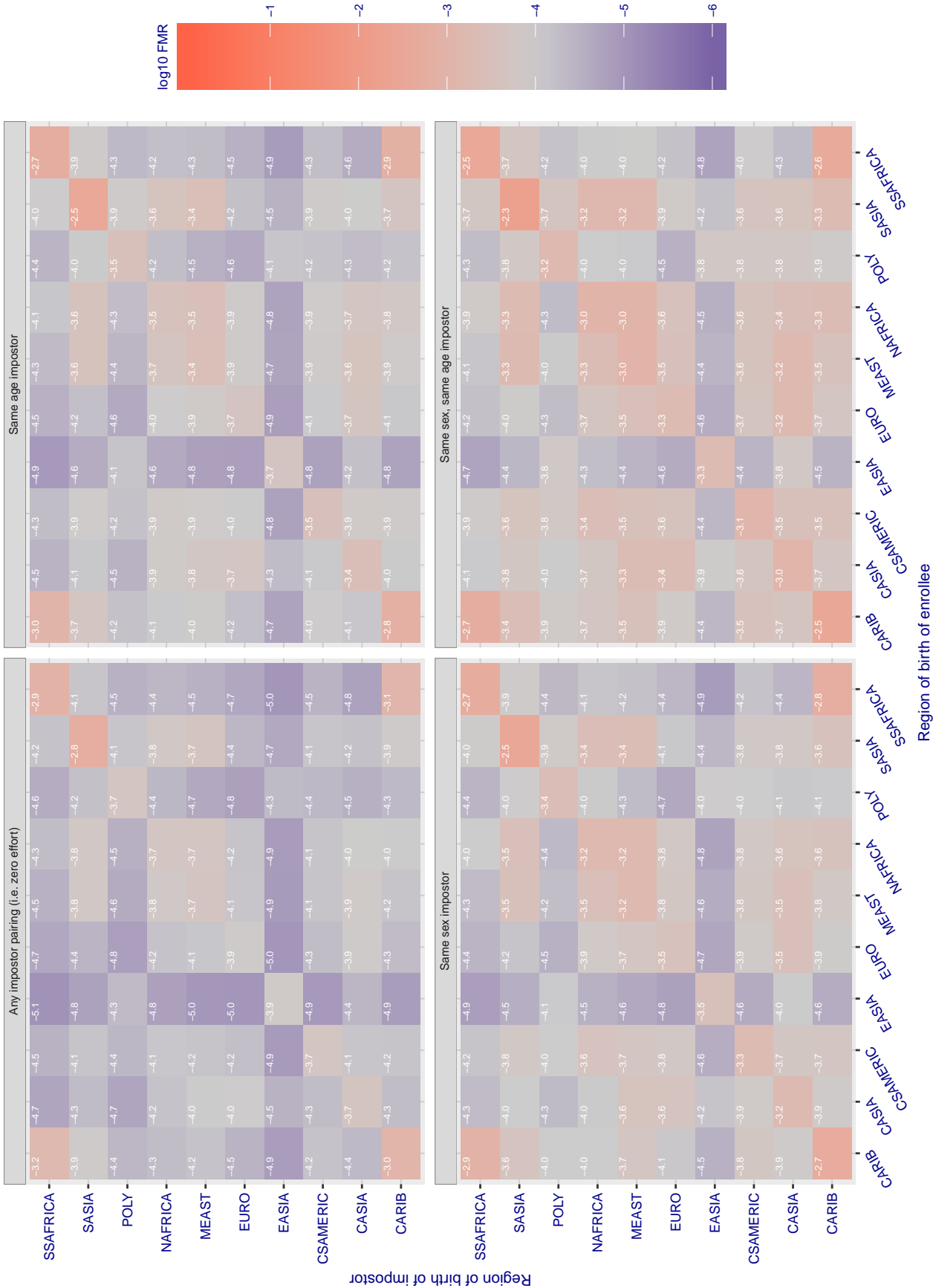


Figure 131: For algorithm glory-001 operating on visa images, the heatmap shows false match rates observed over impostor comparisons of faces from different individuals who were born in the given region pair. False matches are counted against a recognition threshold fixed globally to give the target FMR in the plot title, computed over all on the order of 10^{10} impostor comparisons. If text appears in each box it give the same quantity as that coded by the color. Grey indicates FMR is at the intended FMR target level. Light red colors present a security vulnerability to, for example, a passport gate. Each +1 increase in \log_{10} FMR corresponds to a factor of 10 increase in FMR. The matrix is not quite symmetric because images in the enrollment and verification sets are different.

Cross region FMR at threshold $T = 0.559$ for algorithm gorilla_001, giving $FMR(T) = 0.0001$ globally.

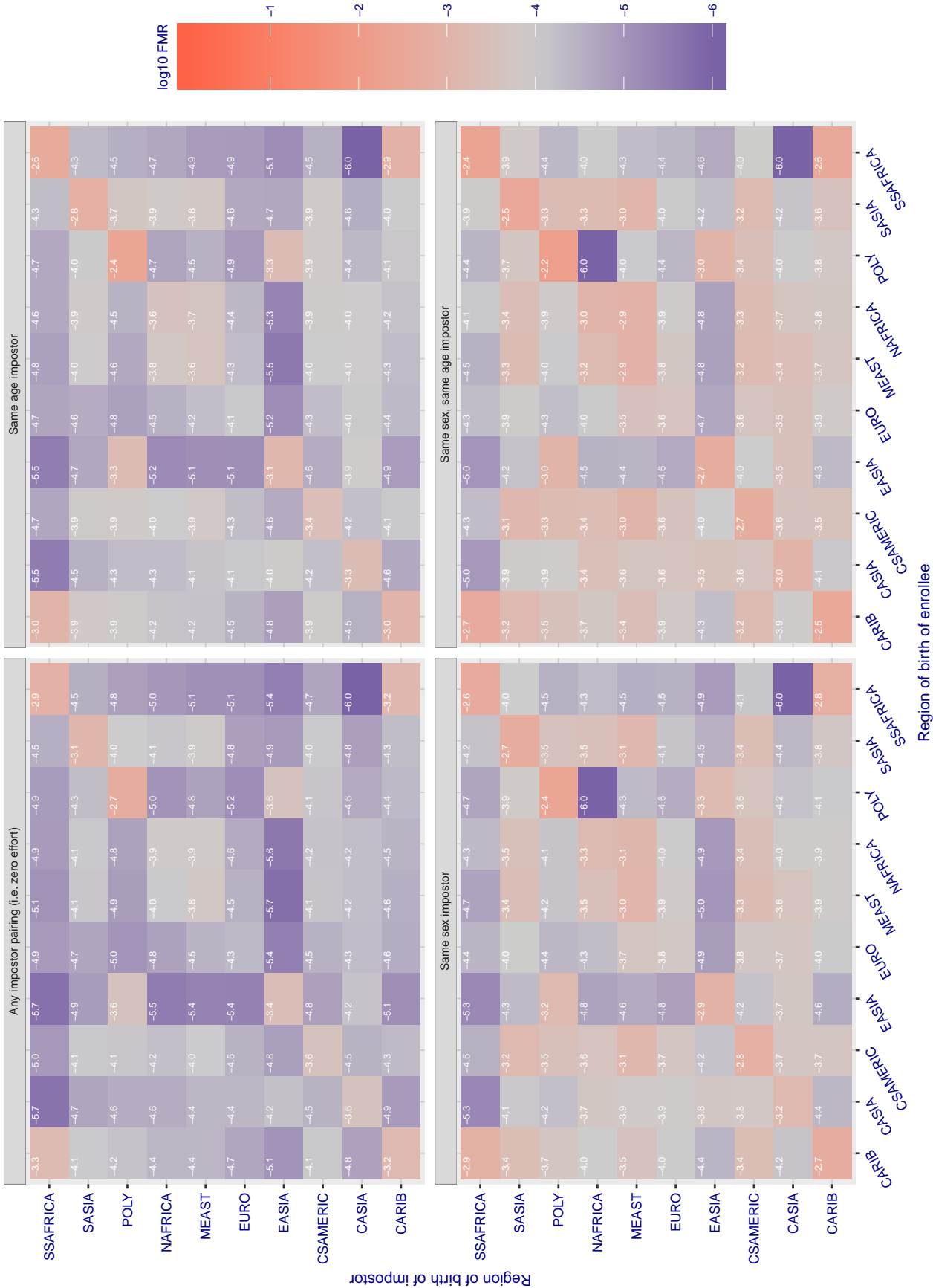


Figure 132: For algorithm gorilla-001 operating on visa images, the heatmap shows false match rates observed over impostor comparisons of faces from different individuals who were born in the given region pair. False matches are counted against a recognition threshold fixed globally to give the target FMR in the plot title, computed over all on the order of 10^{10} impostor comparisons. If text appears in each box it give the same quantity as that coded by the color. Grey indicates FMR is at the intended FMR target level. Light red colors present a security vulnerability to, for example, a passport gate. Each +1 increase in \log_{10} FMR corresponds to a factor of 10 increase in FMR. The matrix is not quite symmetric because images in the enrollment and verification sets are different.

Cross region FMR at threshold $T = 0.483$ for algorithm gorilla_002, giving $FMR(T) = 0.0001$ globally.

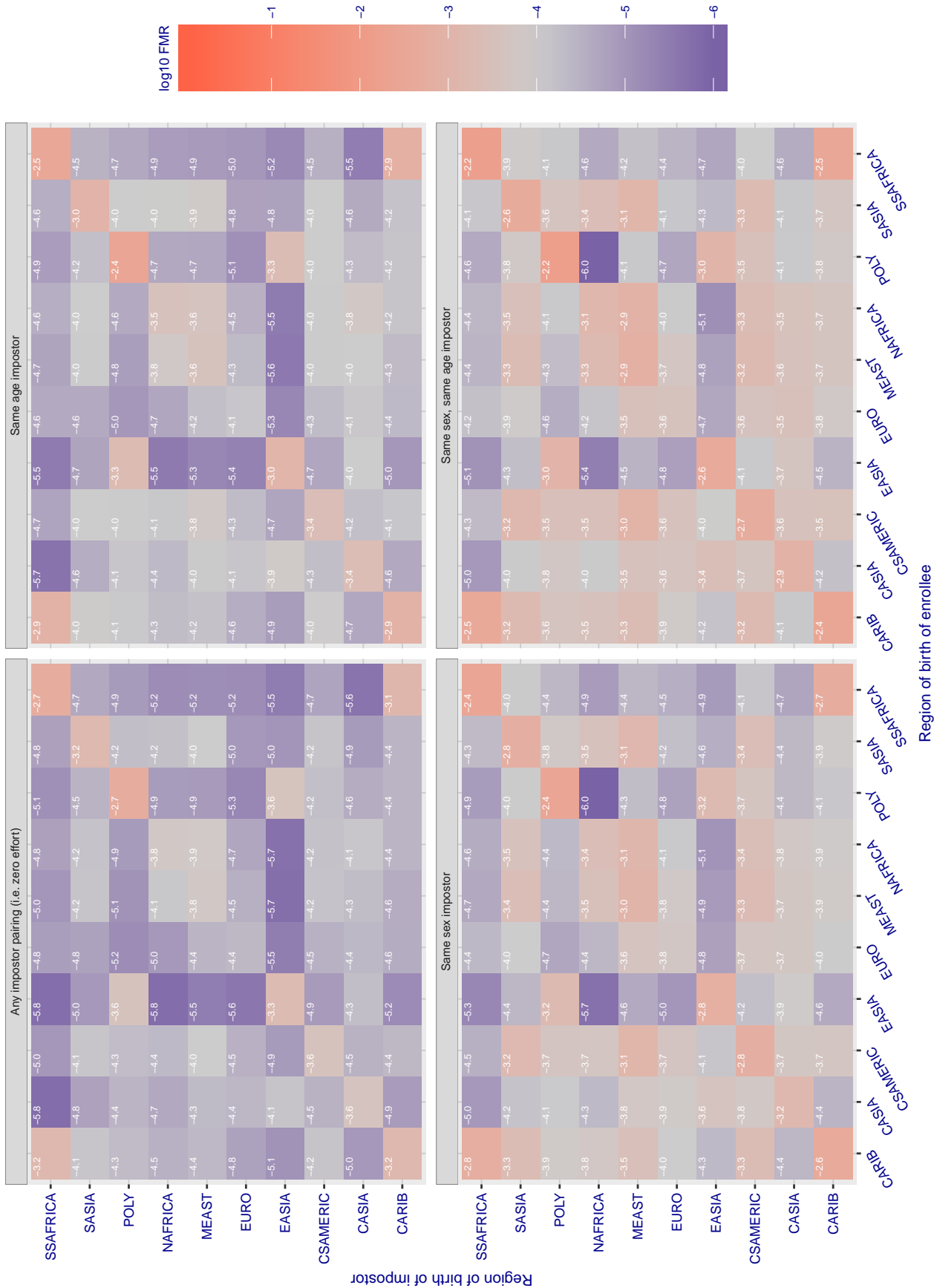


Figure 133: For algorithm gorilla-002 operating on visa images, the heatmap shows false match rates observed over impostor comparisons of faces from different individuals who were born in the given region pair. False matches are counted against a recognition threshold fixed globally to give the target FMR in the plot title, computed over all on the order of 10^{10} impostor comparisons. If text appears in each box it give the same quantity as that coded by the color. Grey indicates FMR is at the intended FMR target level. Light red colors present a security vulnerability to, for example, a passport gate. Each +1 increase in $\log_{10} FMR$ corresponds to a factor of 10 increase in FMR. The matrix is not quite symmetric because images in the enrollment and verification sets are different.

Cross region FMR at threshold T = 66.565 for algorithm hik_001, giving FMR(T) = 0.0001 globally.

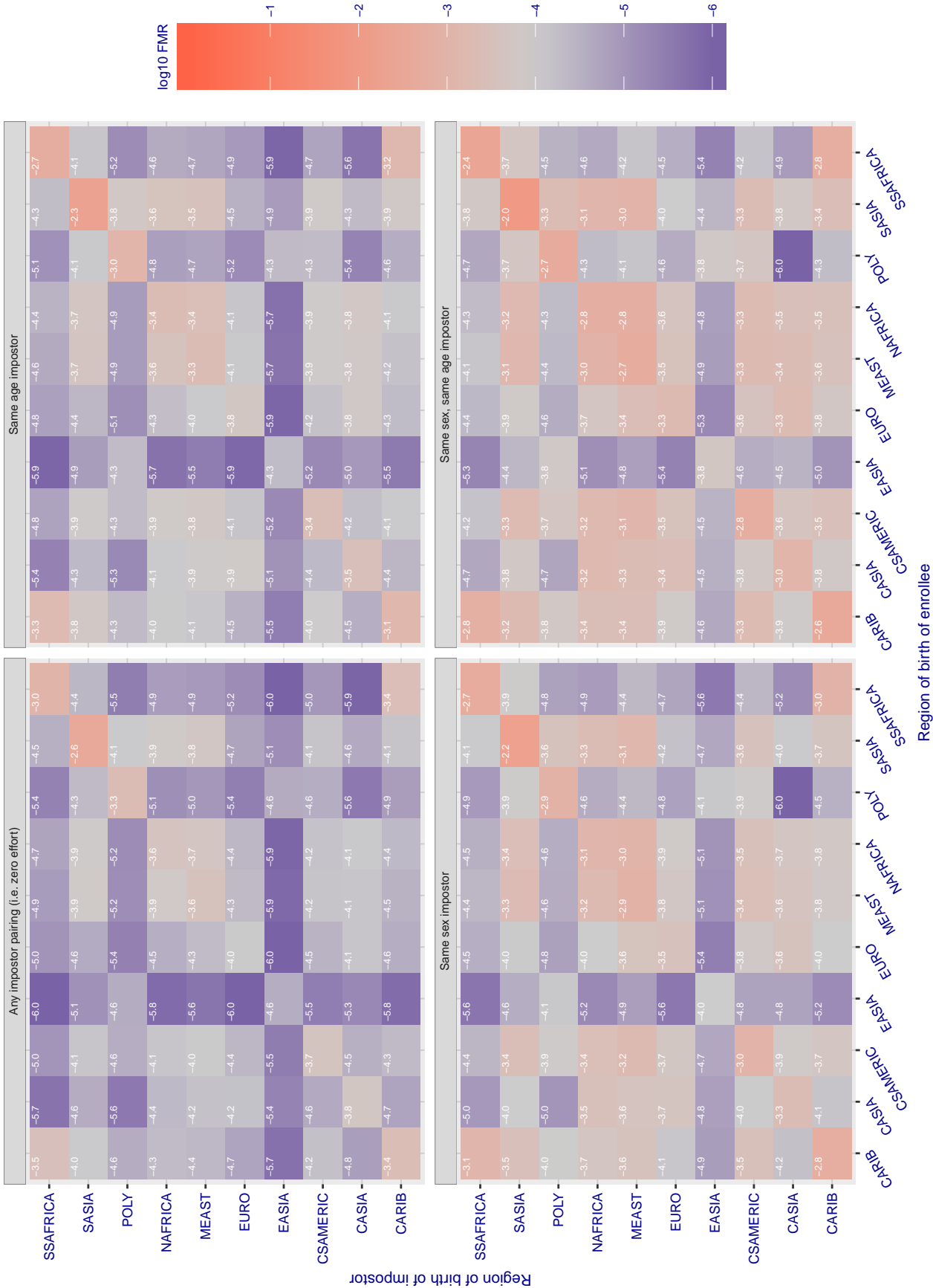


Figure 134: For algorithm hik-001 operating on visa images, the heatmap shows false match rates observed over impostor comparisons of faces from different individuals who were born in the given region pair. False matches are counted against a recognition threshold fixed globally to give the target FMR in the plot title, computed over all on the order of 10^{10} impostor comparisons. If text appears in each box it give the same quantity as that coded by the color. Grey indicates FMR is at the intended FMR target level. Light red colors present a security vulnerability to, for example, a passport gate. Each +1 increase in \log_{10} FMR corresponds to a factor of 10 increase in FMR. The matrix is not quite symmetric because images in the enrollment and verification sets are different.

Cross region FMR at threshold $T = 0.971$ for algorithm hr_000, giving $FMR(T) = 0.0001$ globally.

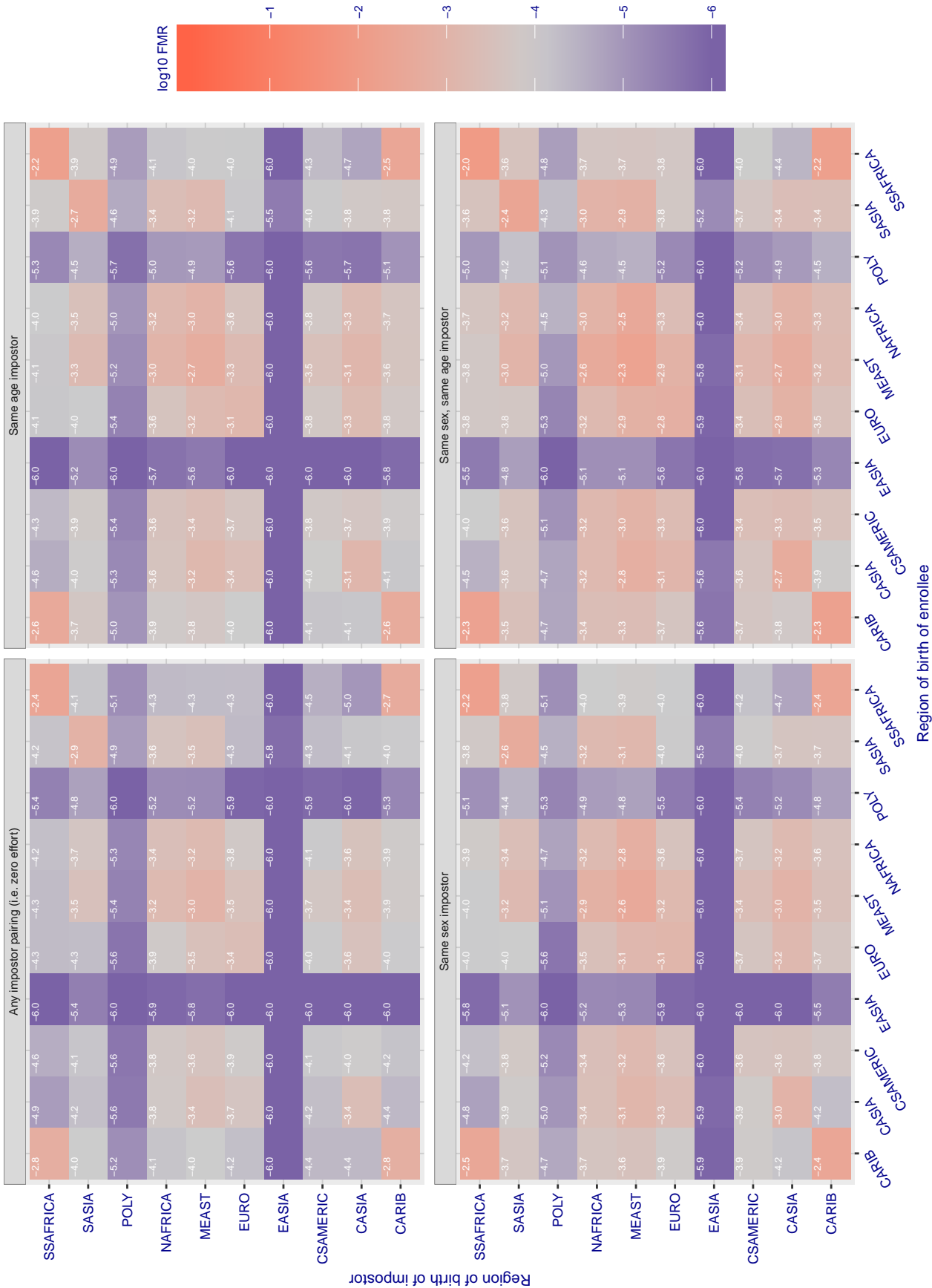


Figure 135: For algorithm hr-000 operating on visa images, the heatmap shows false match rates observed over impostor comparisons of faces from different individuals who were born in the given region pair. False matches are counted against a recognition threshold fixed globally to give the target FMR in the plot title, computed over all on the order of 10^{10} impostor comparisons. If text appears in each box it give the same quantity as that coded by the color. Grey indicates FMR is at the intended FMR target level. Light red colors present a security vulnerability to, for example, a passport gate. Each +1 increase in \log_{10} FMR corresponds to a factor of 10 increase in FMR. The matrix is not quite symmetric because images in the enrollment and verification sets are different.

Cross region FMR at threshold T = 37645.000 for algorithm id3_003, giving FMR(T) = 0.0001 globally.

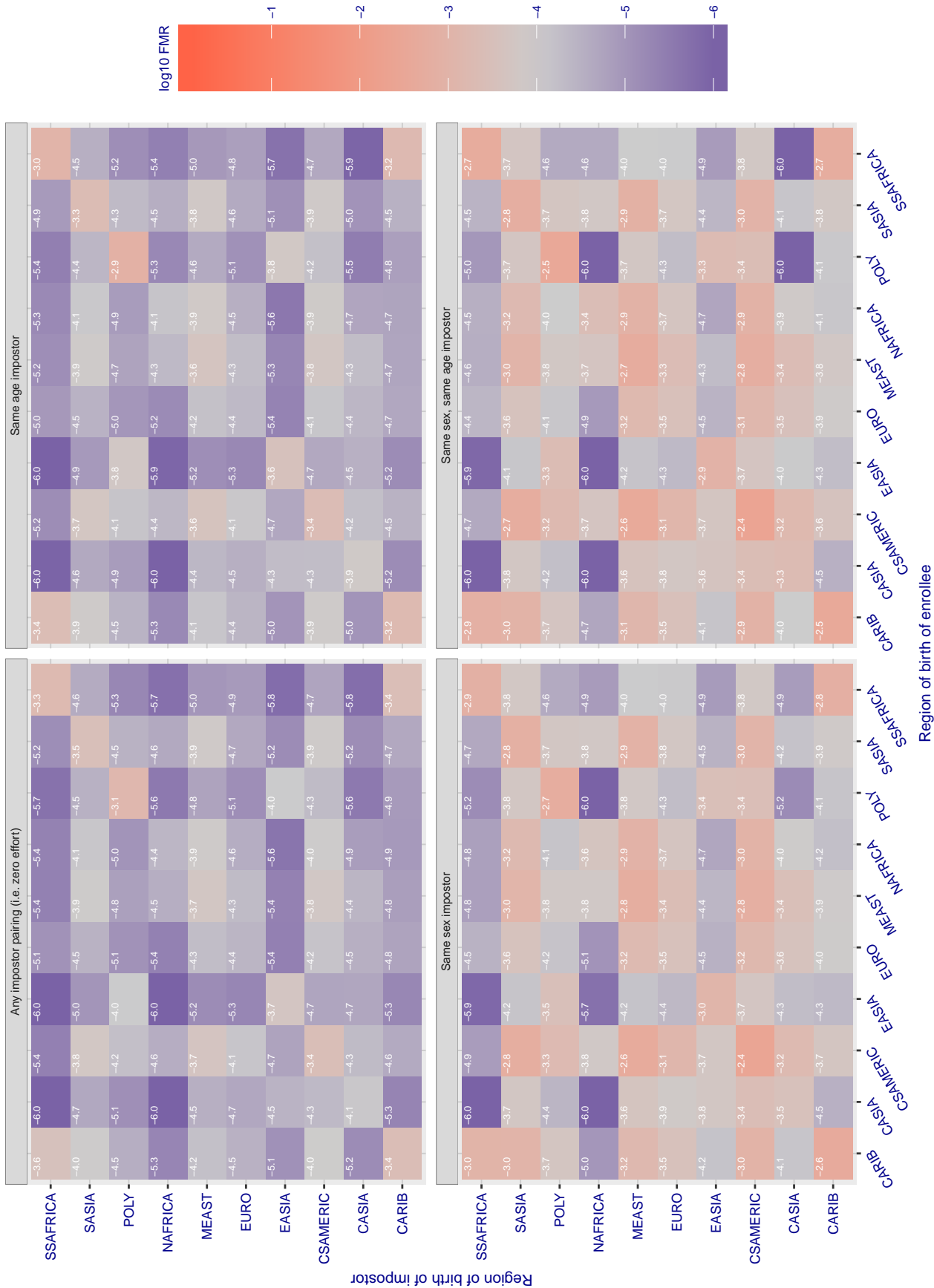


Figure 136: For algorithm id3-003 operating on visa images, the heatmap shows false match rates observed over impostor comparisons of faces from different individuals who were born in the given region pair. False matches are counted against a recognition threshold fixed globally to give the target FMR in the plot title, computed over all on the order of 10^{10} impostor comparisons. If text appears in each box it give the same quantity as that coded by the color. Grey indicates FMR is at the intended FMR target level. Light red colors present a security vulnerability to, for example, a passport gate. Each +1 increase in \log_{10} FMR corresponds to a factor of 10 increase in FMR. The matrix is not quite symmetric because images in the enrollment and verification sets are different.

Cross region FMR at threshold T = 37001.000 for algorithm id3_004, giving FMR(T) = 0.0001 globally.

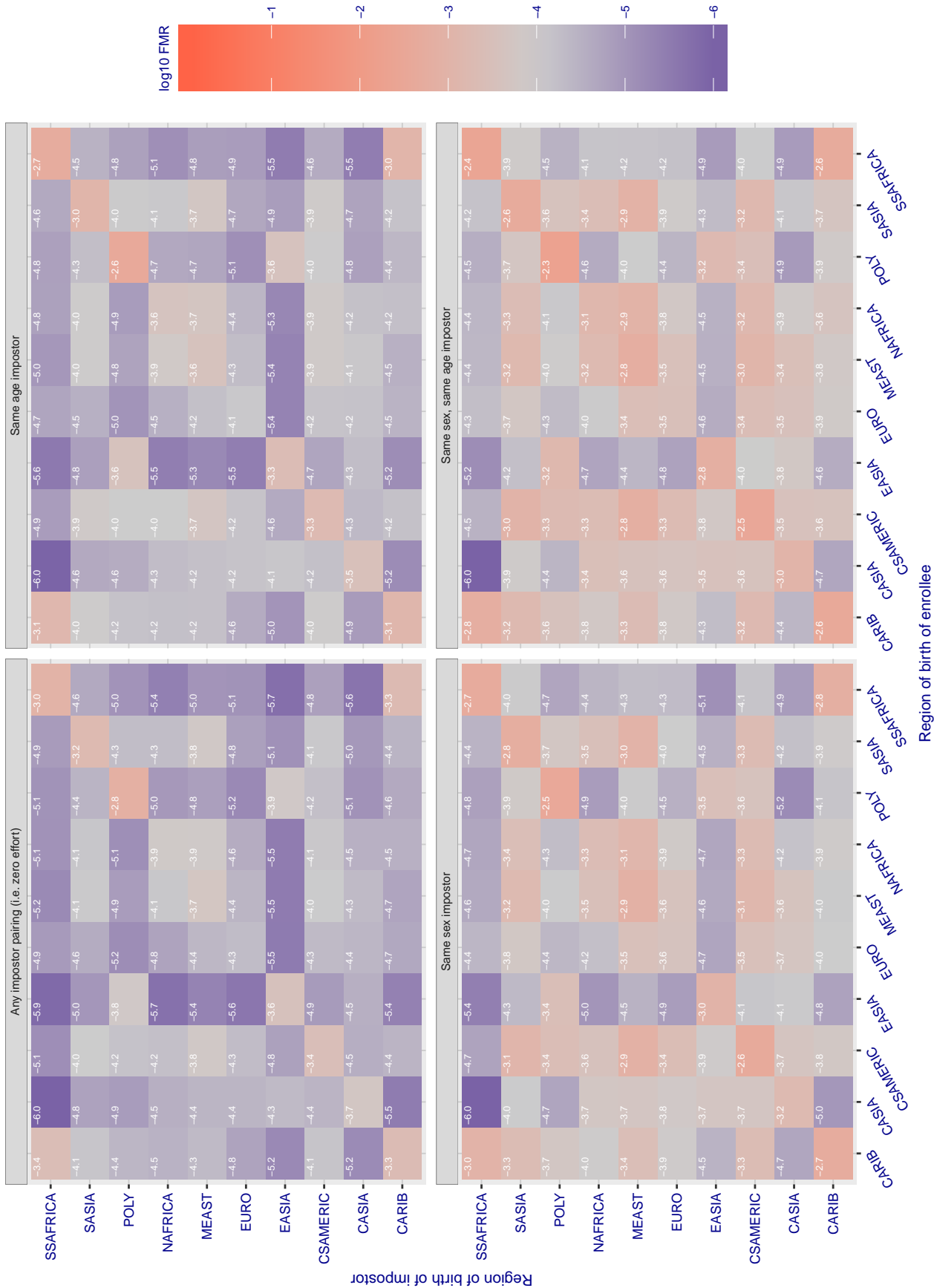


Figure 137: For algorithm id3-004 operating on visa images, the heatmap shows false match rates observed over impostor comparisons of faces from different individuals who were born in the given region pair. False matches are counted against a recognition threshold fixed globally to give the target FMR in the plot title, computed over all on the order of 10^{10} impostor comparisons. If text appears in each box it give the same quantity as that coded by the color. Grey indicates FMR is at the intended FMR target level. Light red colors present a security vulnerability to, for example, a passport gate. Each +1 increase in \log_{10} FMR corresponds to a factor of 10 increase in FMR. The matrix is not quite symmetric because images in the enrollment and verification sets are different.

Cross region FMR at threshold $T = 3664.380$ for algorithm `idemia_003`, giving $FMR(T) = 0.0001$ globally.

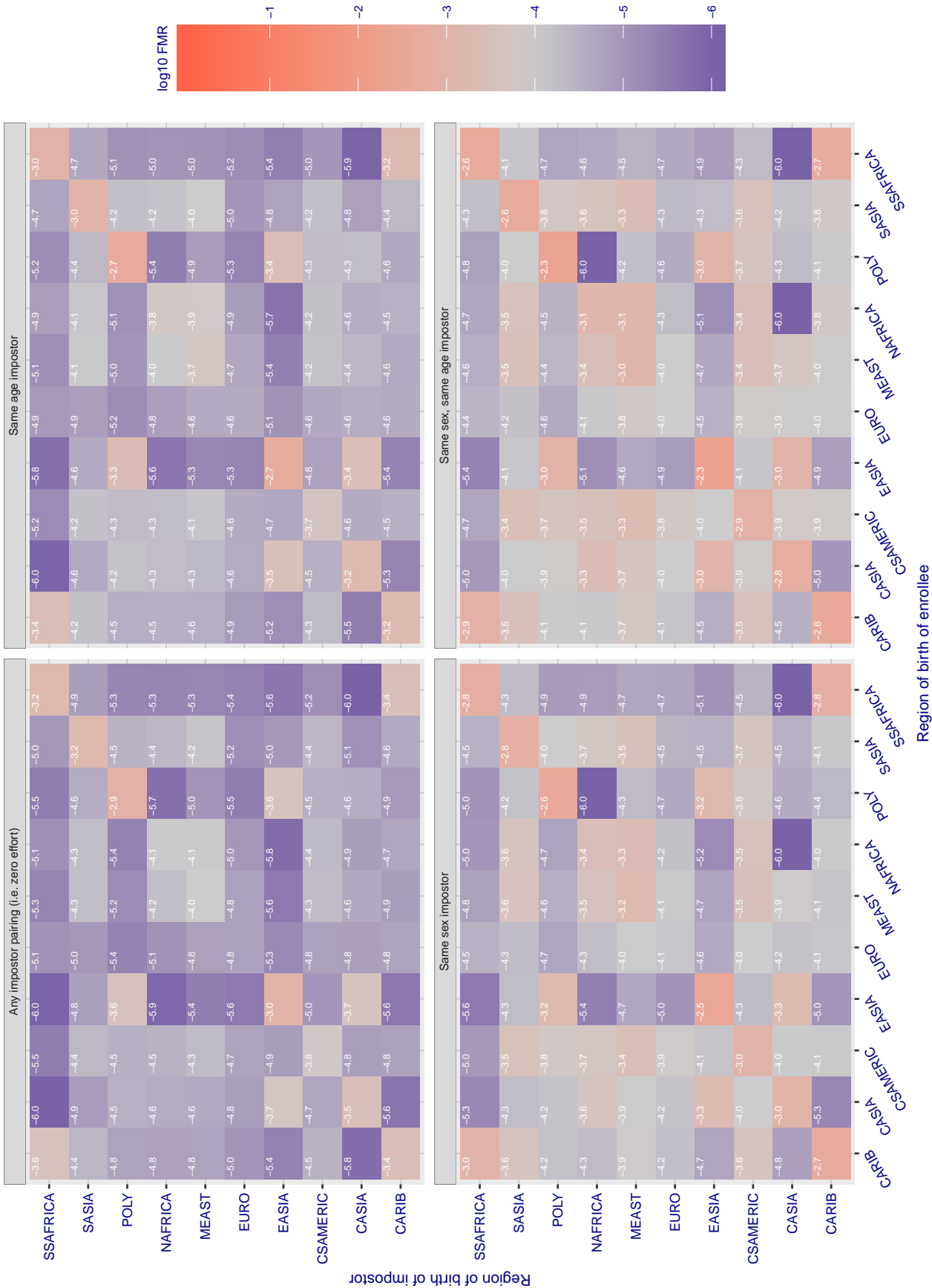


Figure 138: For algorithm `idemia-003` operating on visa images, the heatmap shows false match rates observed over impostor comparisons of faces from different individuals who were born in the given region pair. False matches are counted against a recognition threshold fixed globally to give the target FMR in the plot title, computed over all on the order of 10^{10} impostor comparisons. If text appears in each box it give the same quantity as that coded by the color. Grey indicates FMR is at the intended FMR target level. Light red colors present a security vulnerability to, for example, a passport gate. Each +1 increase in \log_{10} FMR corresponds to a factor of 10 increase in FMR. The matrix is not quite symmetric because images in the enrollment and verification sets are different.

Cross region FMR at threshold T = 3925.463 for algorithm idemia_004, giving FMR(T) = 0.0001 globally.

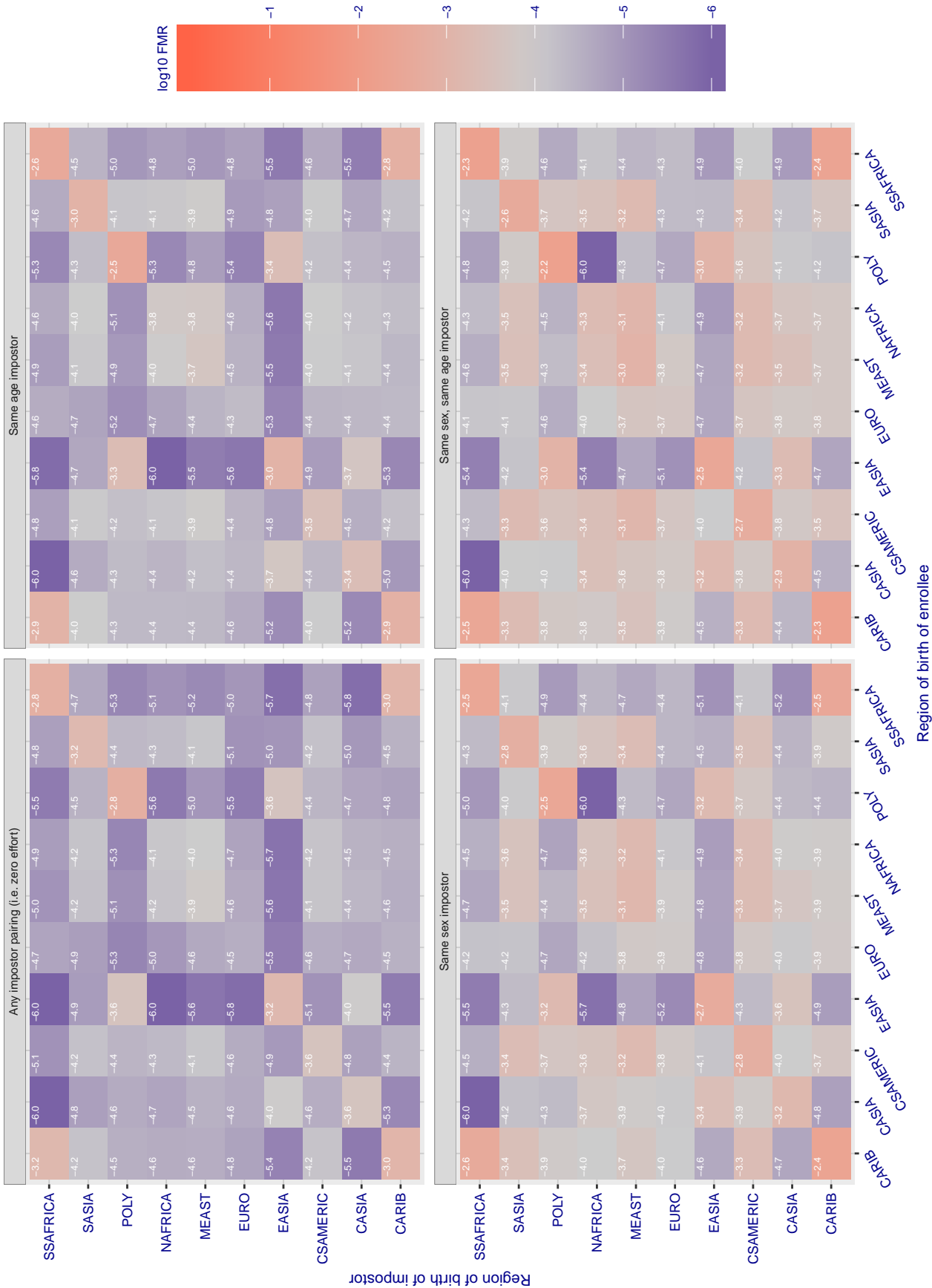


Figure 139: For algorithm idemia-004 operating on visa images, the heatmap shows false match rates observed over impostor comparisons of faces from different individuals who were born in the given region pair. False matches are counted against a recognition threshold fixed globally to give the target FMR in the plot title, computed over all on the order of 10¹⁰ impostor comparisons. If text appears in each box it give the same quantity as that coded by the color. Grey indicates FMR is at the intended FMR target level. Light red colors present a security vulnerability to, for example, a passport gate. Each +1 increase in log10 FMR corresponds to a factor of 10 increase in FMR. The matrix is not quite symmetric because images in the enrollment and verification sets are different.

Cross region FMR at threshold $T = 0.760$ for algorithm it_000 , giving $FMR(T) = 0.0001$ globally.

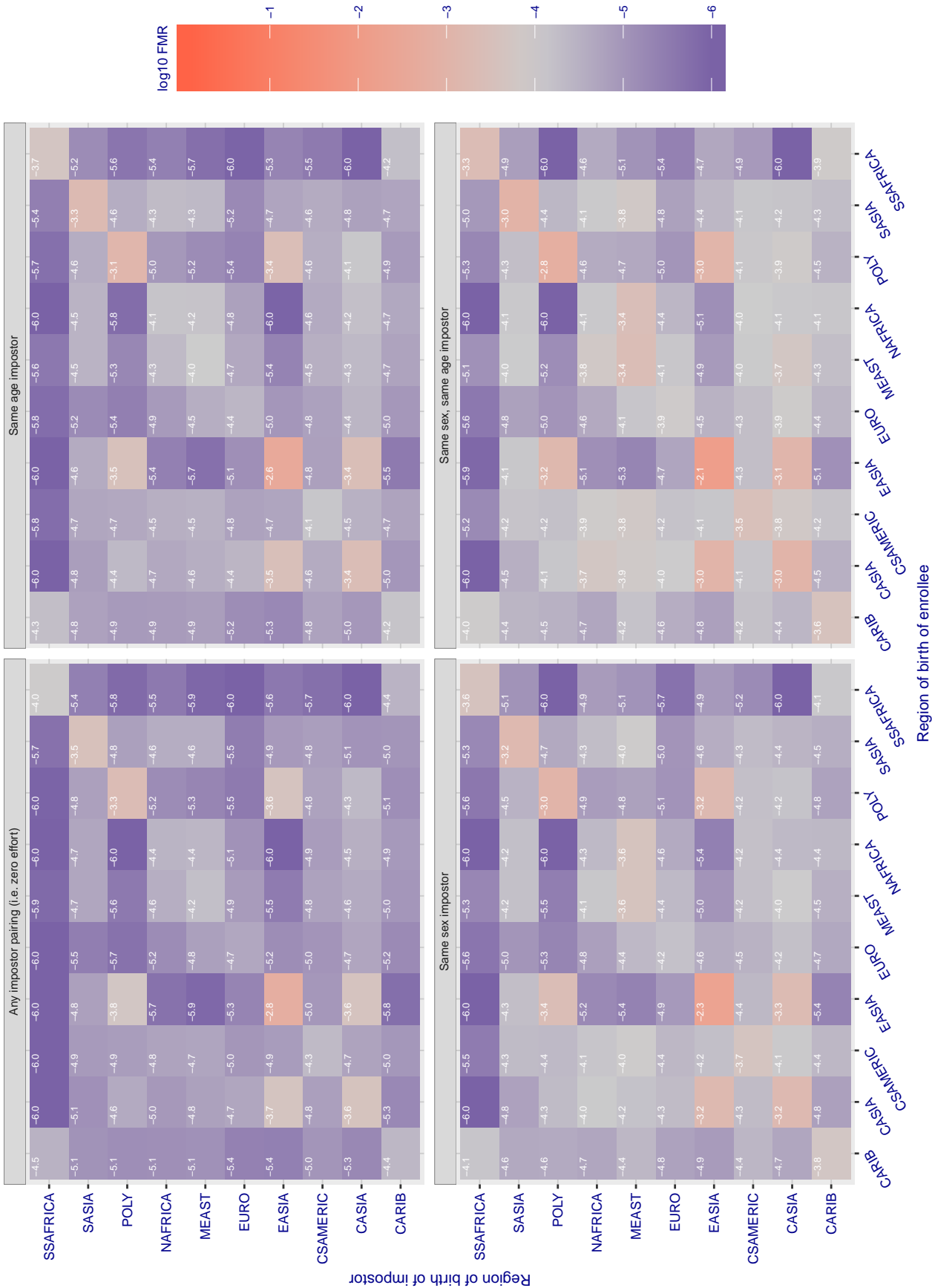


Figure 140: For algorithm $it-000$ operating on visa images, the heatmap shows false match rates observed over impostor comparisons of faces from different individuals who were born in the given region pair. False matches are counted against a recognition threshold fixed globally to give the target FMR in the plot title, computed over all on the order of 10^{10} impostor comparisons. If text appears in each box it give the same quantity as that coded by the color. Grey indicates FMR is at the intended FMR target level. Light red colors present a security vulnerability to, for example, a passport gate. Each +1 increase in $\log_{10} FMR$ corresponds to a factor of 10 increase in FMR. The matrix is not quite symmetric because images in the enrollment and verification sets are different.

Cross region FMR at threshold $T = 1.375$ for algorithm imperial_000, giving $FMR(T) = 0.0001$ globally.

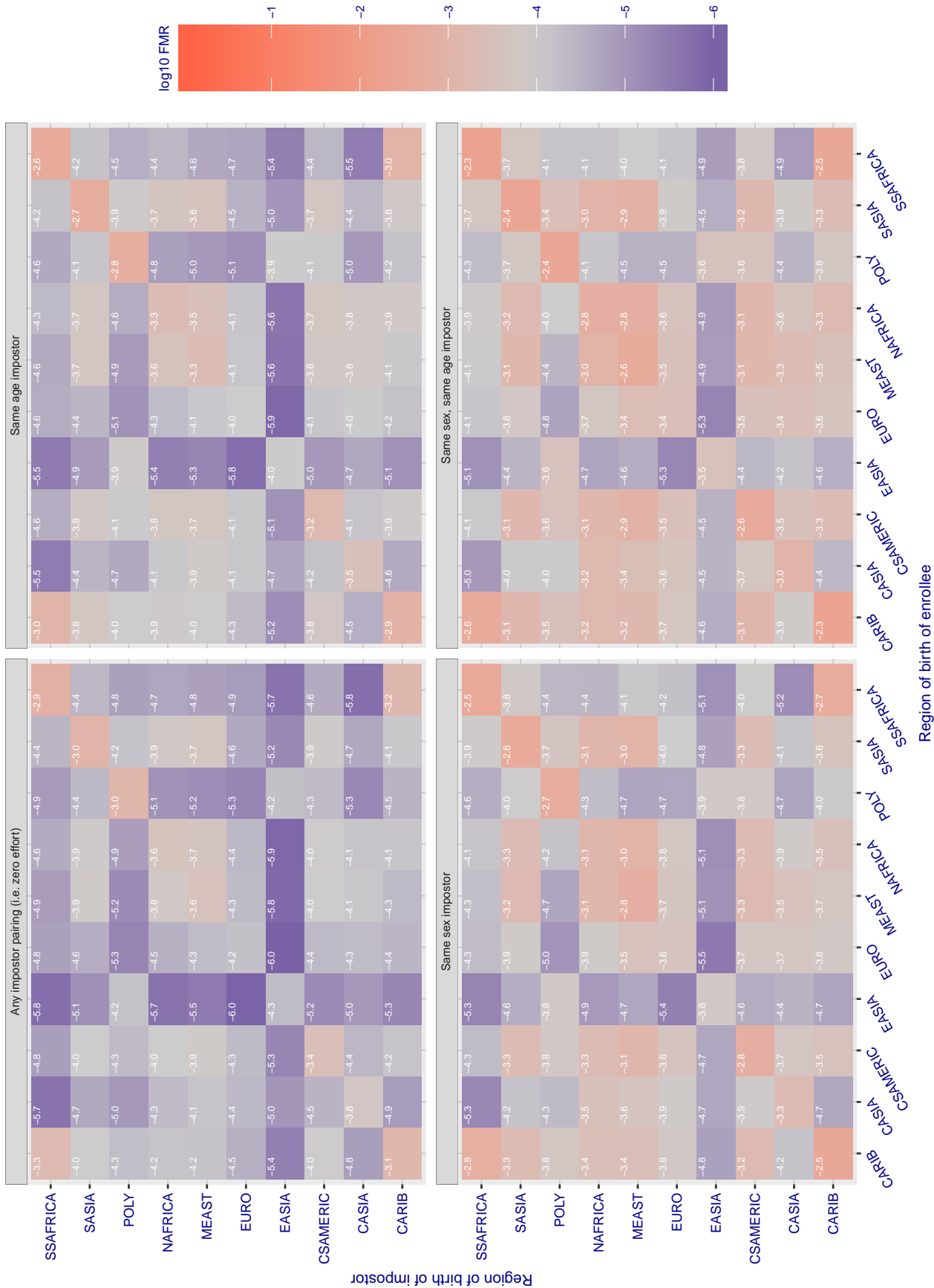


Figure 141: For algorithm imperial-000 operating on visa images, the heatmap shows false match rates observed over impostor comparisons of faces from different individuals who were born in the given region pair. False matches are counted against a recognition threshold fixed globally to give the target FMR in the plot title, computed over all on the order of 10^{10} impostor comparisons. If text appears in each box it give the same quantity as that coded by the color. Grey indicates FMR is at the intended FMR target level. Light red colors present a security vulnerability to, for example, a passport gate. Each +1 increase in $\log_{10} FMR$ corresponds to a factor of 10 increase in FMR. The matrix is not quite symmetric because images in the enrollment and verification sets are different.

Cross region FMR at threshold $T = 1.402$ for algorithm imperial_001, giving $FMR(T) = 0.0001$ globally.

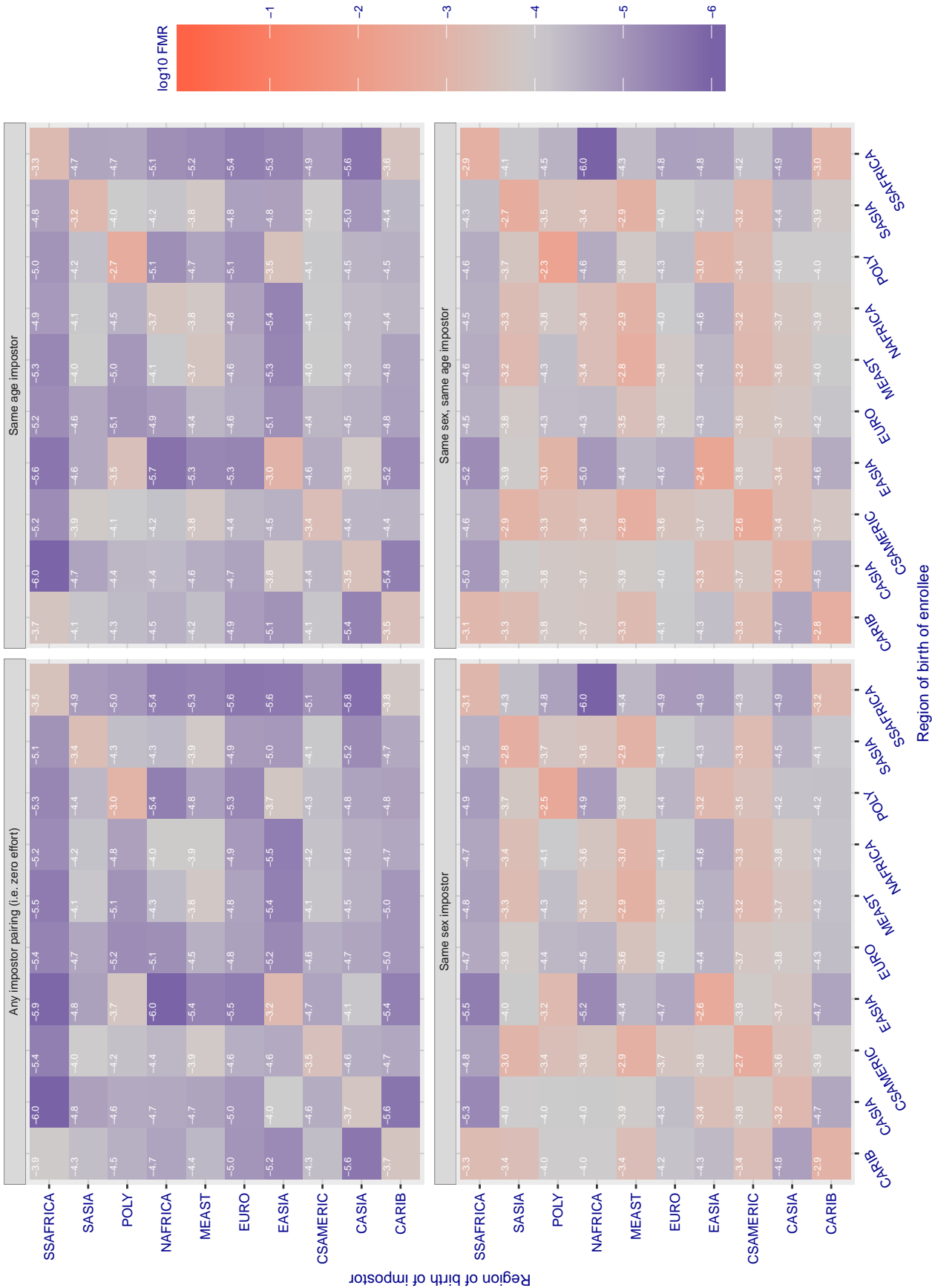


Figure 142: For algorithm imperial-001 operating on visa images, the heatmap shows false match rates observed over impostor comparisons of faces from different individuals who were born in the given region pair. False matches are counted against a recognition threshold fixed globally to give the target FMR in the plot title, computed over all on the order of 10^{10} impostor comparisons. If text appears in each box it give the same quantity as that coded by the color. Grey indicates FMR is at the intended FMR target level. Light red colors present a security vulnerability to, for example, a passport gate. Each +1 increase in \log_{10} FMR corresponds to a factor of 10 increase in FMR. The matrix is not quite symmetric because images in the enrollment and verification sets are different.

Cross region FMR at threshold $T = 1.382$ for algorithm `incde_002`, giving $FMR(T) = 0.0001$ globally.

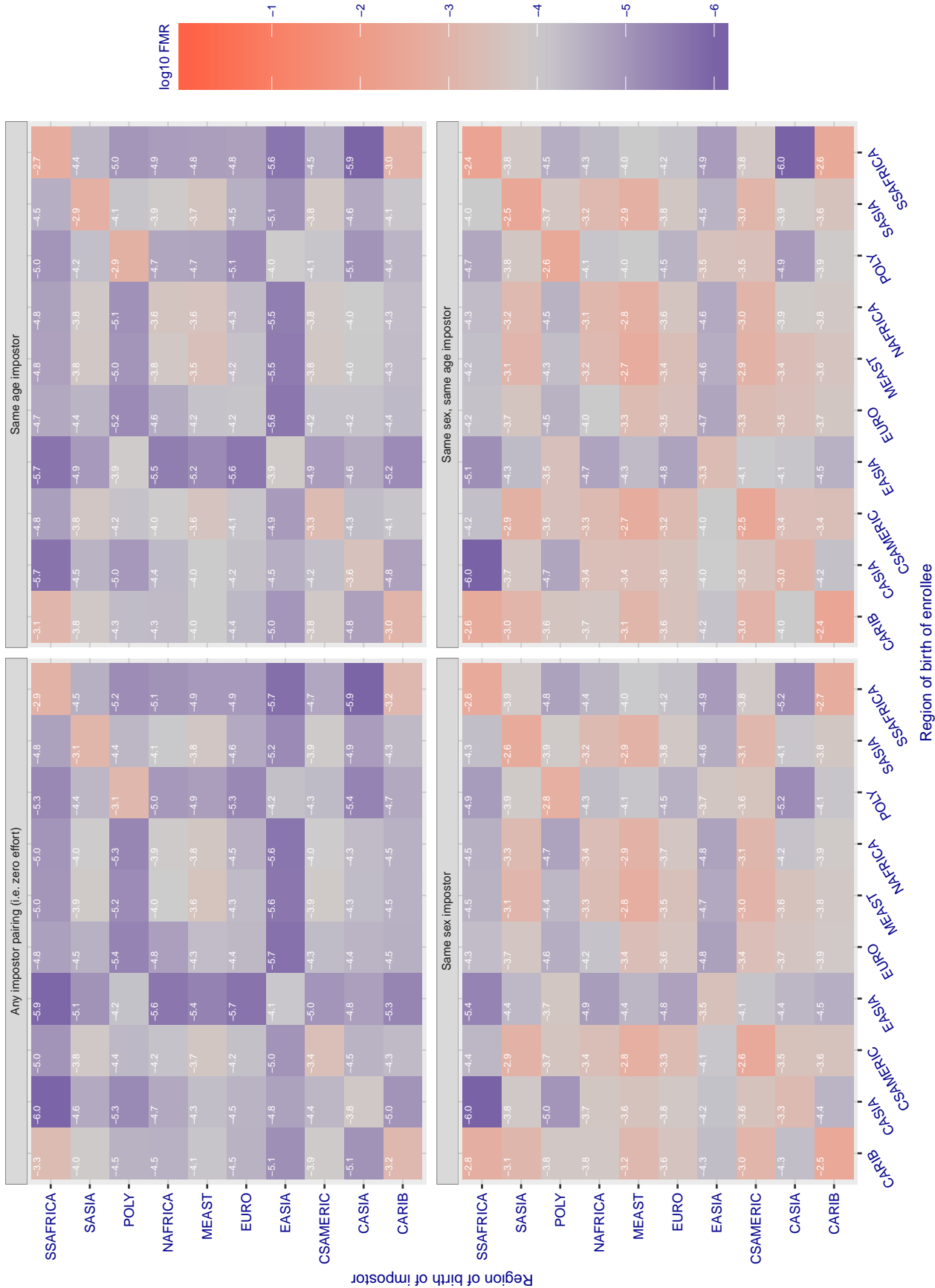


Figure 143: For algorithm `incde-002` operating on visa images, the heatmap shows false match rates observed over impostor comparisons of faces from different individuals who were born in the given region pair. False matches are counted against a recognition threshold fixed globally to give the target FMR in the plot title, computed over all on the order of 10^{10} impostor comparisons. If text appears in each box it give the same quantity as that coded by the color. Grey indicates FMR is at the intended FMR target level. Light red colors present a security vulnerability to, for example, a passport gate. Each +1 increase in \log_{10} FMR corresponds to a factor of 10 increase in FMR. The matrix is not quite symmetric because images in the enrollment and verification sets are different.

Cross region FMR at threshold $T = 1.427$ for algorithm `incde_003`, giving $FMR(T) = 0.0001$ globally.

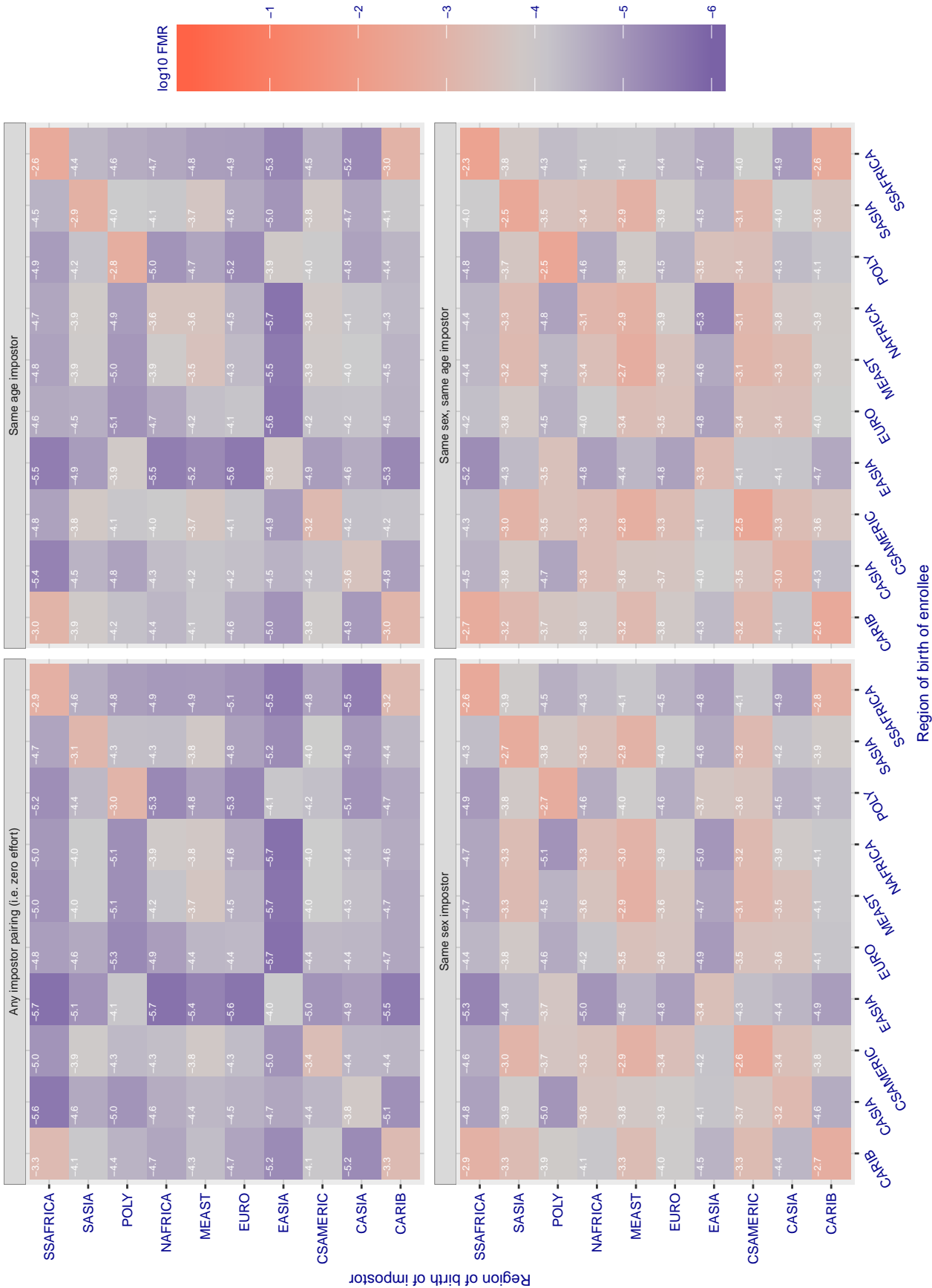


Figure 144: For algorithm `incde-003` operating on visa images, the heatmap shows false match rates observed over impostor comparisons of faces from different individuals who were born in the given region pair. False matches are counted against a recognition threshold fixed globally to give the target FMR in the plot title, computed over all on the order of 10^{10} impostor comparisons. If text appears in each box it give the same quantity as that coded by the color. Grey indicates FMR is at the intended FMR target level. Light red colors present a security vulnerability to, for example, a passport gate. Each +1 increase in \log_{10} FMR corresponds to a factor of 10 increase in FMR. The matrix is not quite symmetric because images in the enrollment and verification sets are different.

Cross region FMR at threshold $T = 29.232$ for algorithm innovatrics_004, giving $FMR(T) = 0.0001$ globally.

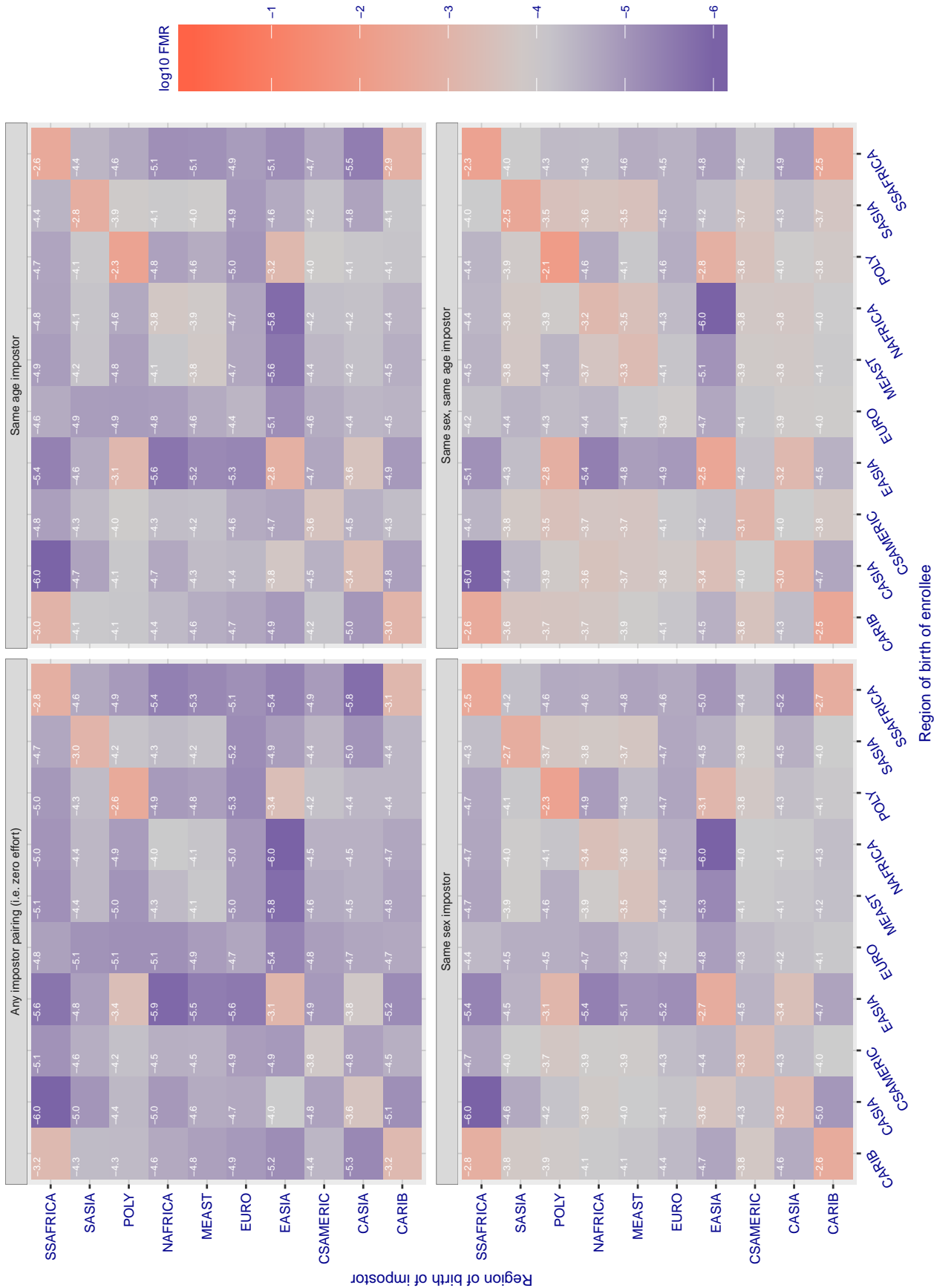


Figure 145: For algorithm innovatrics-004 operating on visa images, the heatmap shows false match rates observed over impostor comparisons of faces from different individuals who were born in the given region pair. False matches are counted against a recognition threshold fixed globally to give the target FMR in the plot title, computed over all on the order of 10^{10} impostor comparisons. If text appears in each box it give the same quantity as that coded by the color. Grey indicates FMR is at the intended FMR target level. Light red colors present a security vulnerability to, for example, a passport gate. Each +1 increase in \log_{10} FMR corresponds to a factor of 10 increase in FMR. The matrix is not quite symmetric because images in the enrollment and verification sets are different.

Cross region FMR at threshold $T = 40.157$ for algorithm innovatrics_005, giving $FMR(T) = 0.0001$ globally.

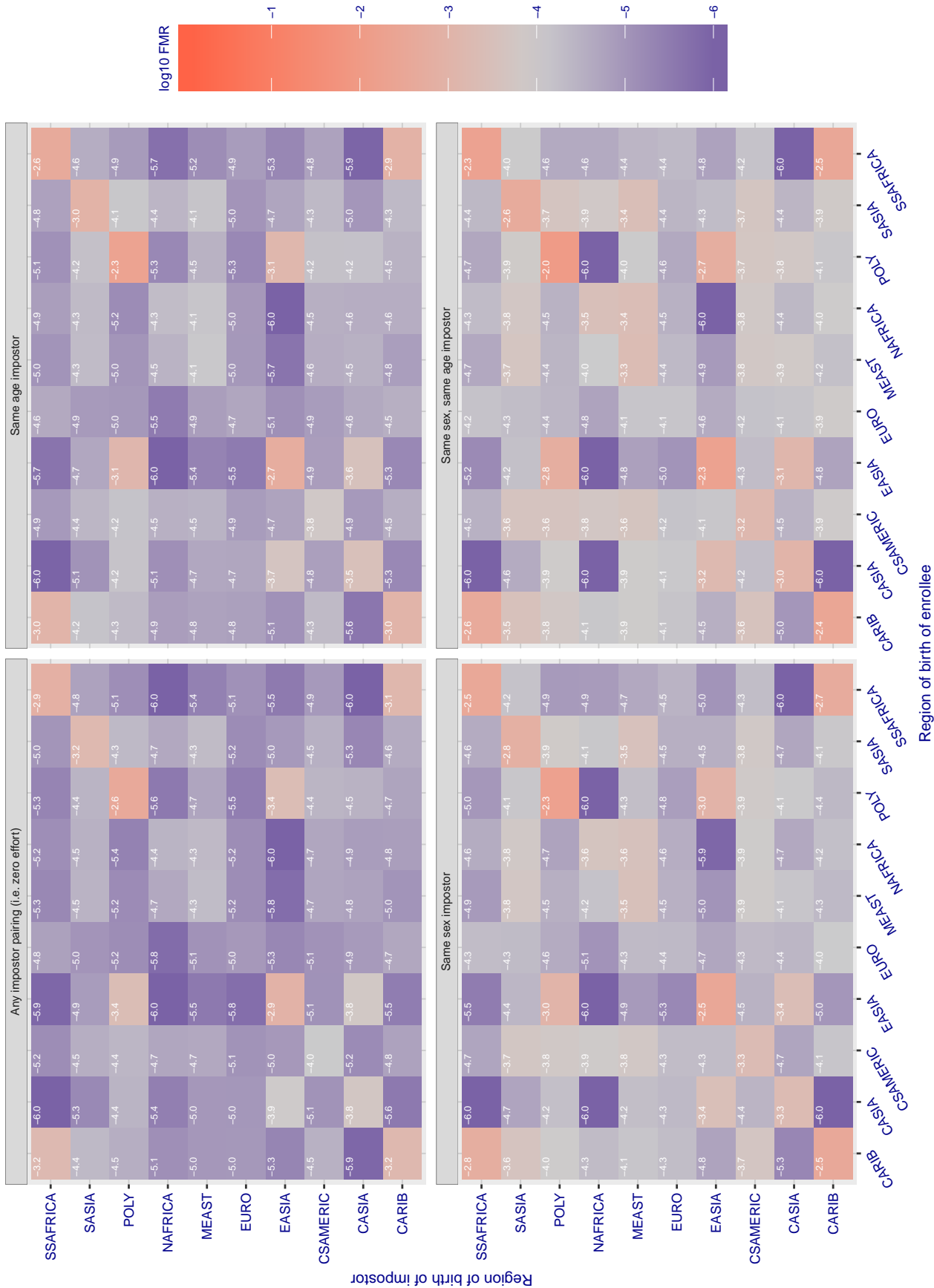


Figure 146: For algorithm innovatrics-005 operating on visa images, the heatmap shows false match rates observed over impostor comparisons of faces from different individuals who were born in the given region pair. False matches are counted against a recognition threshold fixed globally to give the target FMR in the plot title, computed over all on the order of 10^{10} impostor comparisons. If text appears in each box it give the same quantity as that coded by the color. Grey indicates FMR is at the intended FMR target level. Light red colors present a security vulnerability to, for example, a passport gate. Each +1 increase in \log_{10} FMR corresponds to a factor of 10 increase in FMR. The matrix is not quite symmetric because images in the enrollment and verification sets are different.

Cross region FMR at threshold $T = 49.664$ for algorithm intellivision_001, giving $FMR(T) = 0.0001$ globally.

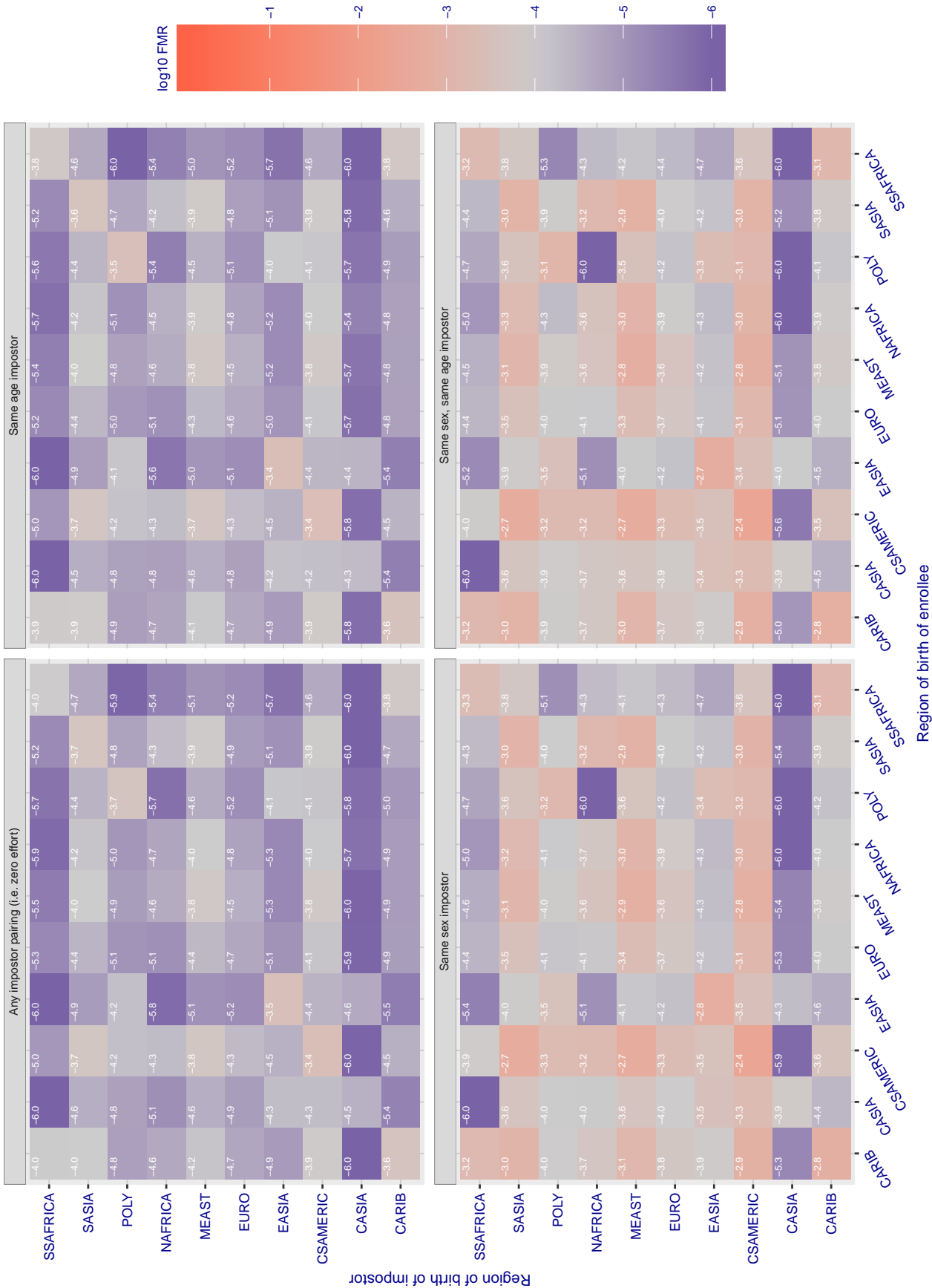


Figure 147: For algorithm intellivision-001 operating on visa images, the heatmap shows false match rates observed over impostor comparisons of faces from different individuals who were born in the given region pair. False matches are counted against a recognition threshold fixed globally to give the target FMR in the plot title, computed over all on the order of 10^{10} impostor comparisons. If text appears in each box it give the same quantity as that coded by the color. Grey indicates FMR is at the intended FMR target level. Light red colors present a security vulnerability to, for example, a passport gate. Each +1 increase in \log_{10} FMR corresponds to a factor of 10 increase in FMR. The matrix is not quite symmetric because images in the enrollment and verification sets are different.

Cross region FMR at threshold T = 23.498 for algorithm isityou_000, giving FMR(T) = 0.0001 globally.

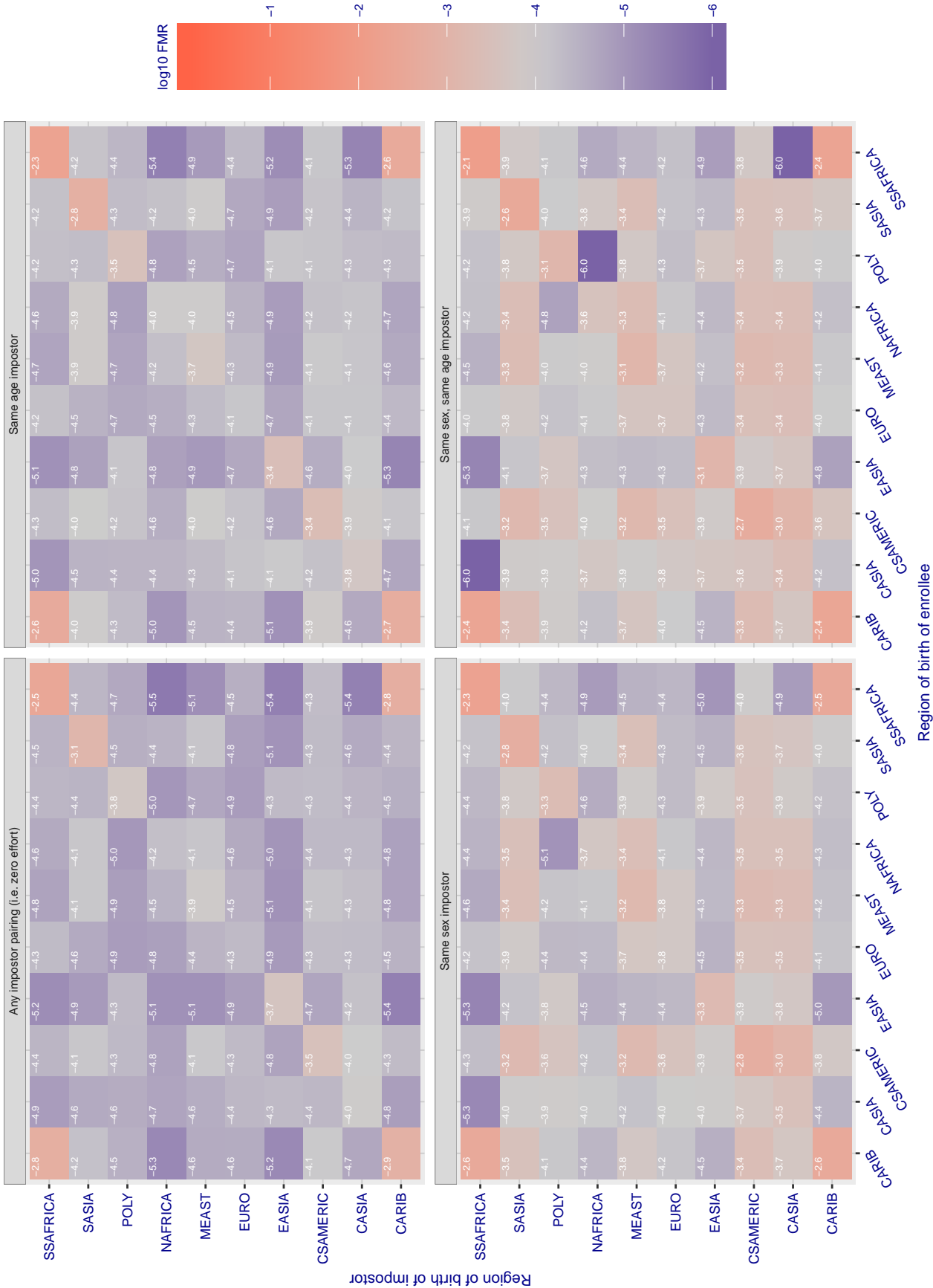


Figure 148: For algorithm isityou-000 operating on visa images, the heatmap shows false match rates observed over impostor comparisons of faces from different individuals who were born in the given region pair. False matches are counted against a recognition threshold fixed globally to give the target FMR in the plot title, computed over all on the order of 10¹⁰ impostor comparisons. If text appears in each box it give the same quantity as that coded by the color. Grey indicates FMR is at the intended FMR target level. Light red colors present a security vulnerability to, for example, a passport gate. Each +1 increase in log10 FMR corresponds to a factor of 10 increase in FMR. The matrix is not quite symmetric because images in the enrollment and verification sets are different.

Cross region FMR at threshold $T = 0.693$ for algorithm isystems_001, giving $FMR(T) = 0.0001$ globally.

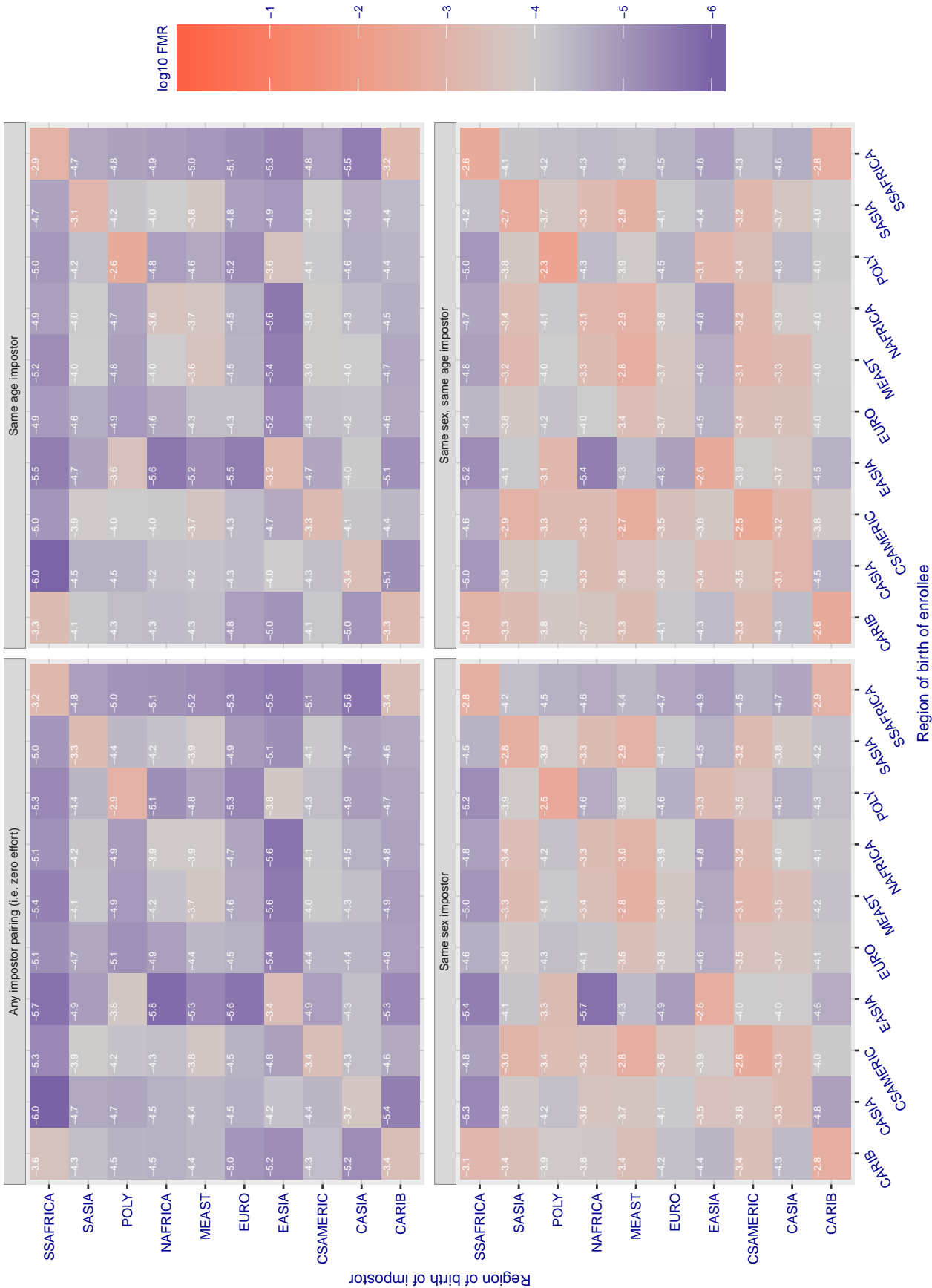


Figure 149: For algorithm isystems-001 operating on visa images, the heatmap shows false match rates observed over impostor comparisons of faces from different individuals who were born in the given region pair. False matches are counted against a recognition threshold fixed globally to give the target FMR in the plot title, computed over all on the order of 10^{10} impostor comparisons. If text appears in each box it give the same quantity as that coded by the color. Grey indicates FMR is at the intended FMR target level. Light red colors present a security vulnerability to, for example, a passport gate. Each +1 increase in \log_{10} FMR corresponds to a factor of 10 increase in FMR. The matrix is not quite symmetric because images in the enrollment and verification sets are different.

Cross region FMR at threshold T = 0.690 for algorithm isystems_002, giving FMR(T) = 0.0001 globally.

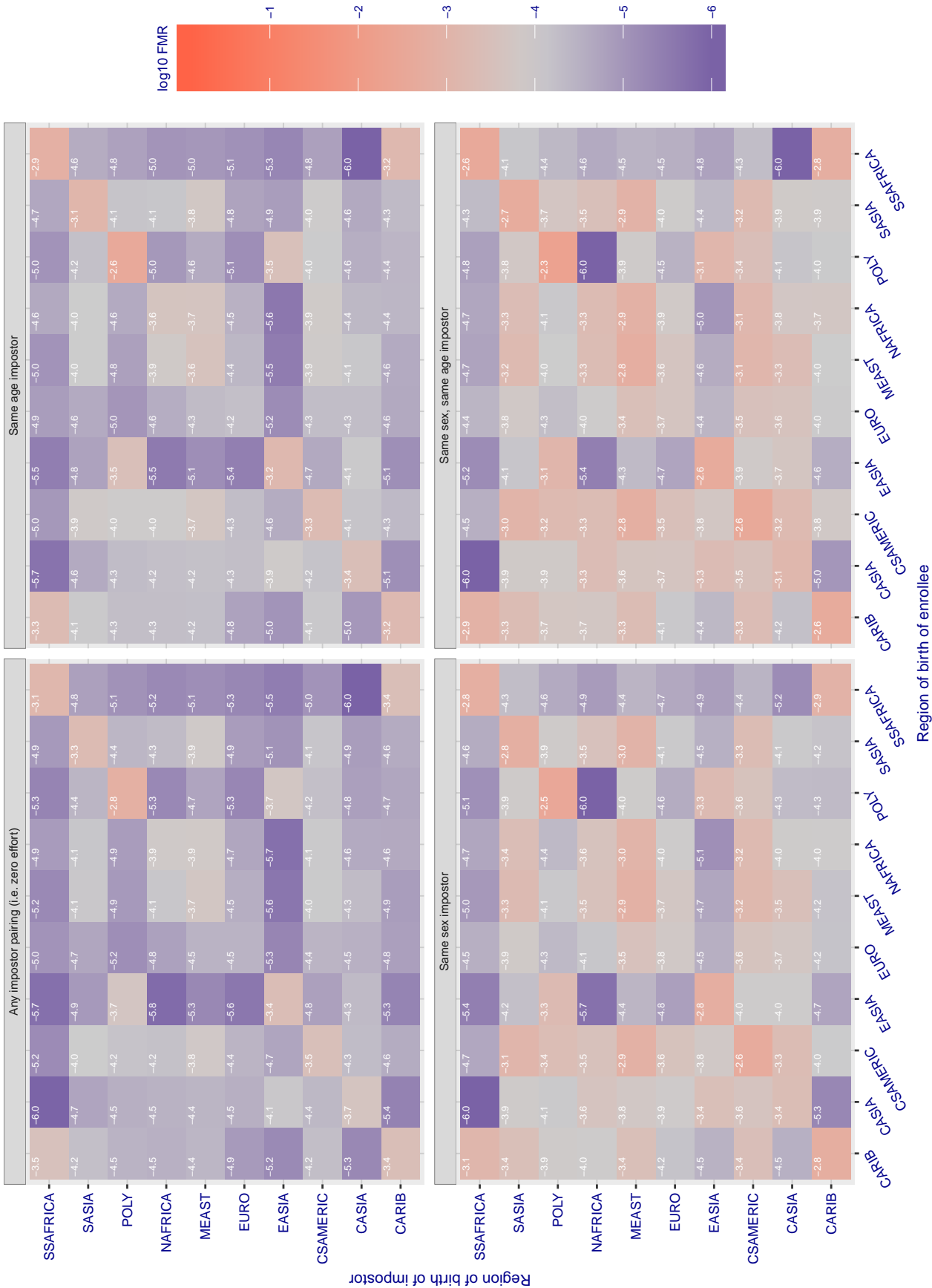


Figure 150: For algorithm isystems-002 operating on visa images, the heatmap shows false match rates observed over impostor comparisons of faces from different individuals who were born in the given region pair. False matches are counted against a recognition threshold fixed globally to give the target FMR in the plot title, computed over all on the order of 10¹⁰ impostor comparisons. If text appears in each box it give the same quantity as that coded by the color. Grey indicates FMR is at the intended FMR target level. Light red colors present a security vulnerability to, for example, a passport gate. Each +1 increase in log10 FMR corresponds to a factor of 10 increase in FMR. The matrix is not quite symmetric because images in the enrollment and verification sets are different.

Cross region FMR at threshold $T = 49.879$ for algorithm itmo_005, giving $FMR(T) = 0.0001$ globally.

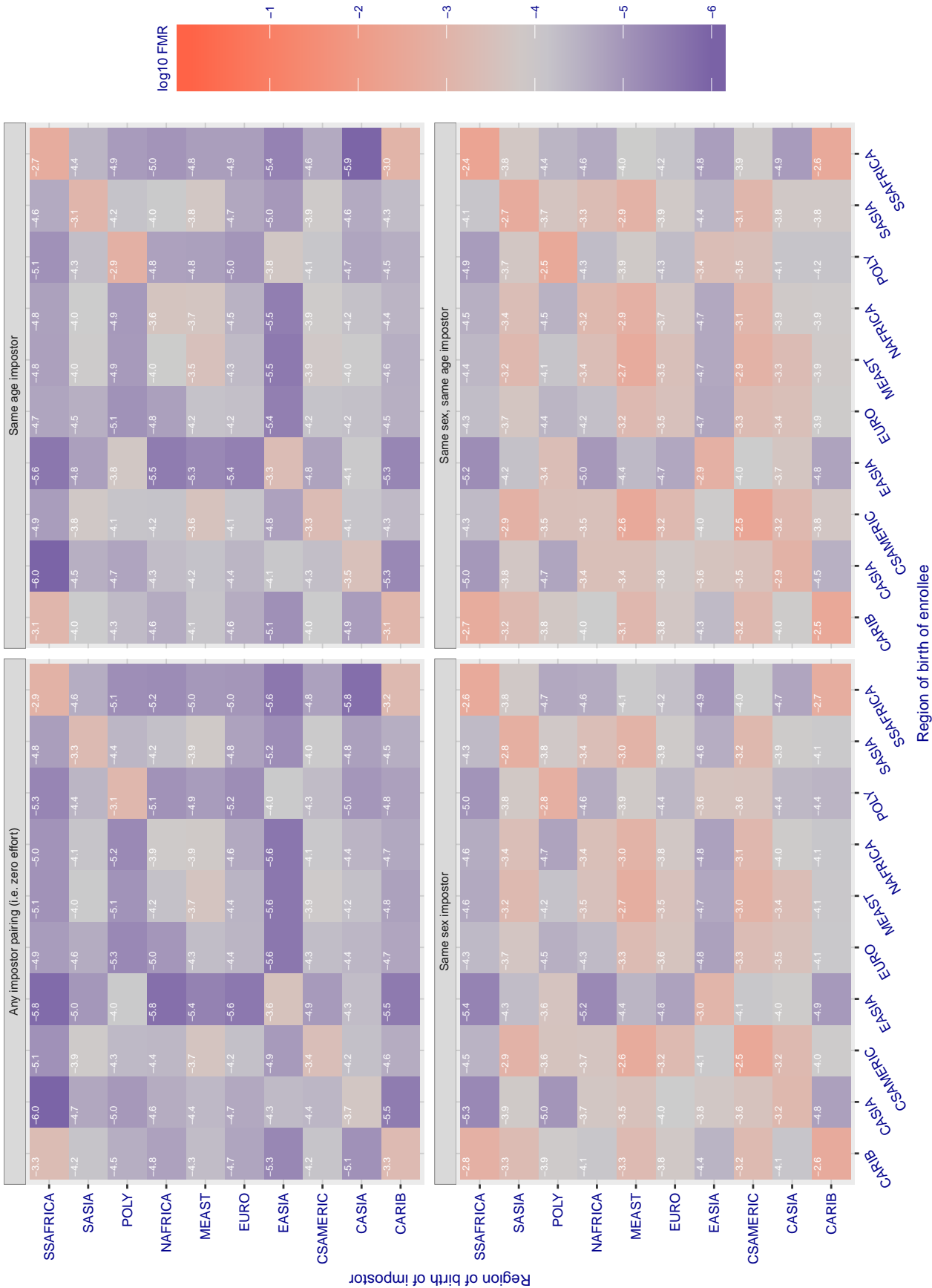


Figure 151: For algorithm itmo-005 operating on visa images, the heatmap shows false match rates observed over impostor comparisons of faces from different individuals who were born in the given region pair. False matches are counted against a recognition threshold fixed globally to give the target FMR in the plot title, computed over all on the order of 10^{10} impostor comparisons. If text appears in each box it give the same quantity as that coded by the color. Grey indicates FMR is at the intended FMR target level. Light red colors present a security vulnerability to, for example, a passport gate. Each +1 increase in $\log_{10} FMR$ corresponds to a factor of 10 increase in FMR. The matrix is not quite symmetric because images in the enrollment and verification sets are different.

Cross region FMR at threshold $T = 49.789$ for algorithm itmo_006, giving $FMR(T) = 0.0001$ globally.

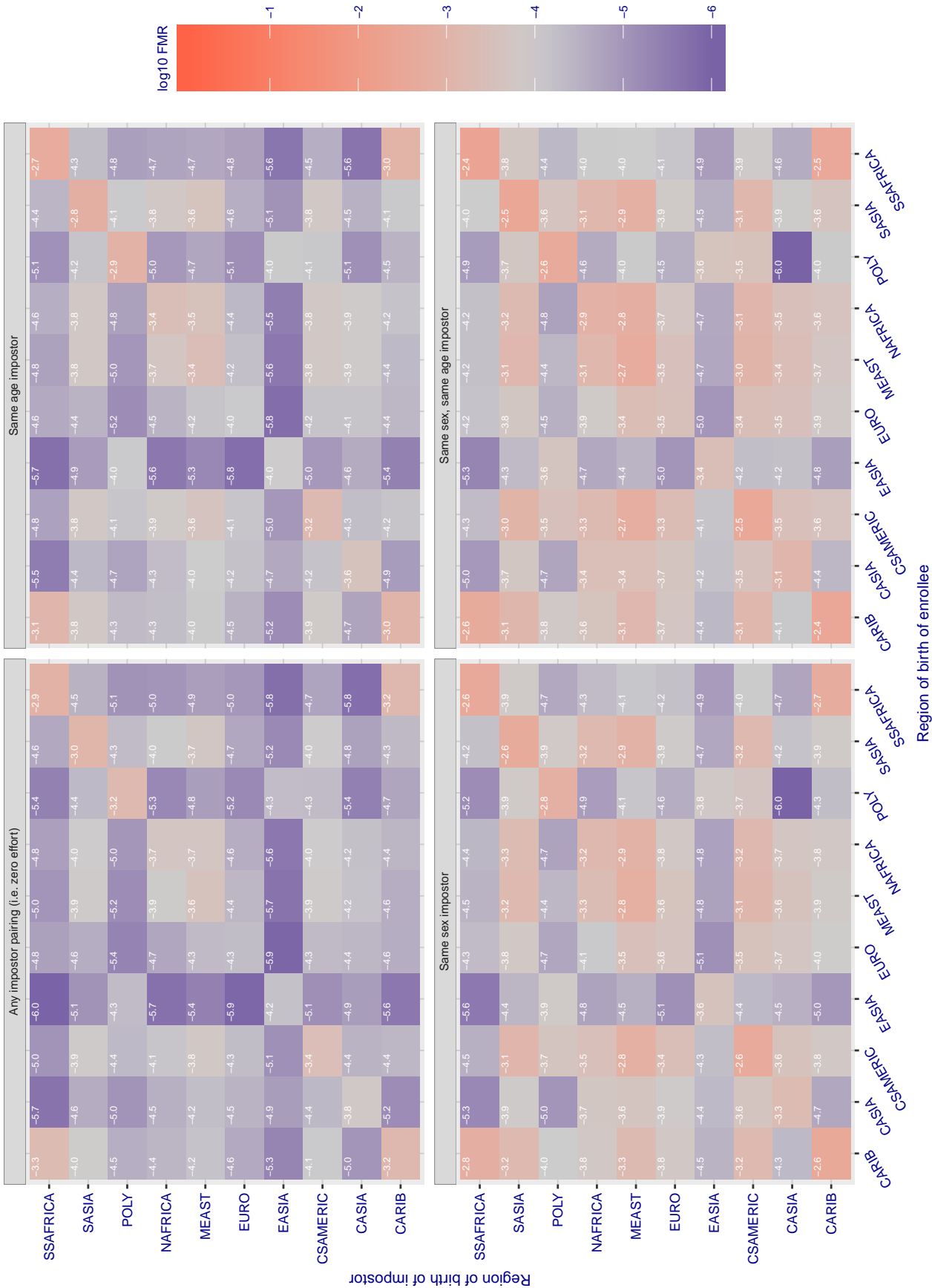


Figure 152: For algorithm itmo-006 operating on visa images, the heatmap shows false match rates observed over impostor comparisons of faces from different individuals who were born in the given region pair. False matches are counted against a recognition threshold fixed globally to give the target FMR in the plot title, computed over all on the order of 10^{10} impostor comparisons. If text appears in each box it give the same quantity as that coded by the color. Grey indicates FMR is at the intended FMR target level. Light red colors present a security vulnerability to, for example, a passport gate. Each +1 increase in \log_{10} FMR corresponds to a factor of 10 increase in FMR. The matrix is not quite symmetric because images in the enrollment and verification sets are different.

Cross region FMR at threshold $T = 1.301$ for algorithm kakao_001, giving $FMR(T) = 0.0001$ globally.

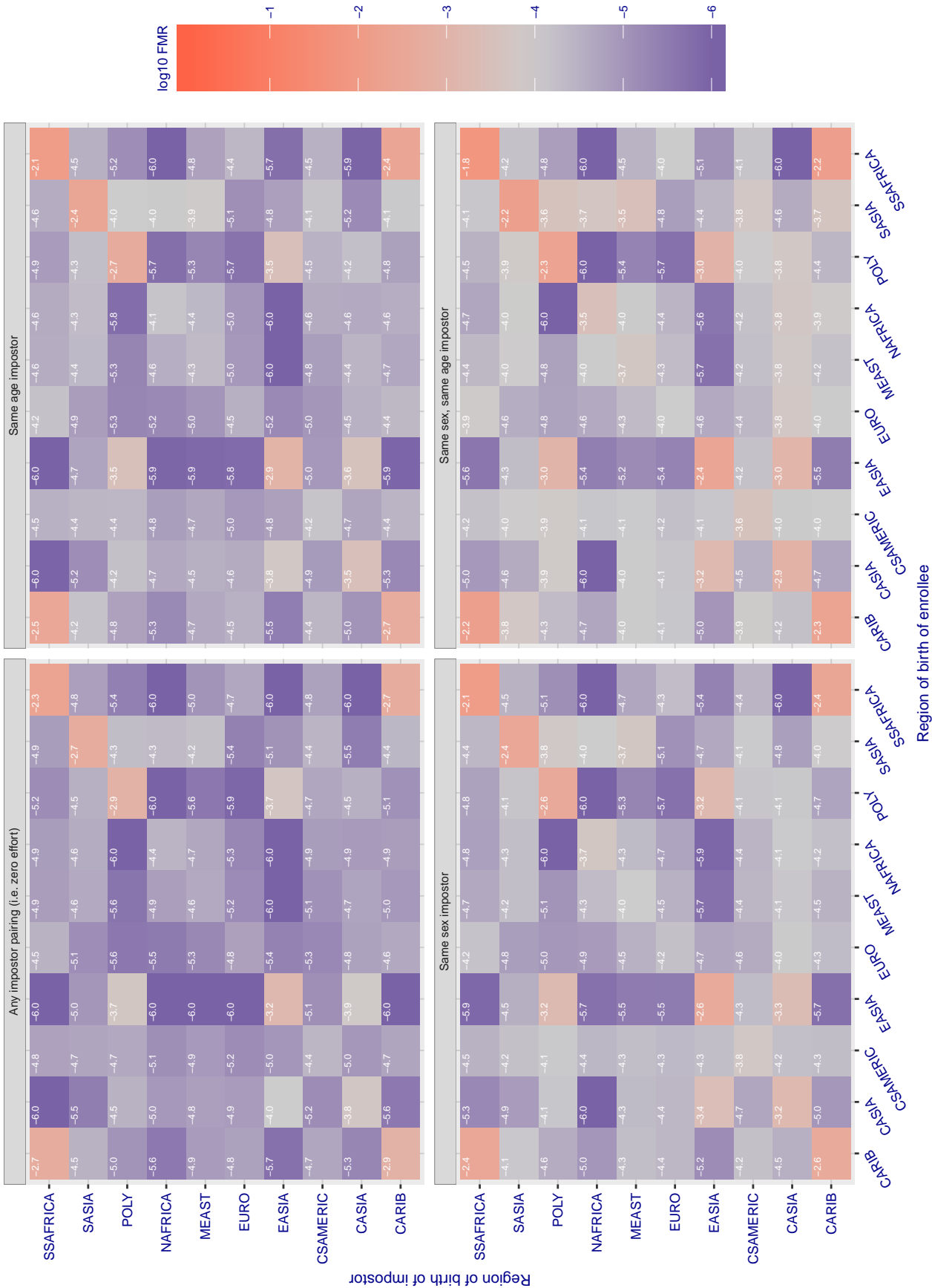


Figure 153: For algorithm kakao-001 operating on visa images, the heatmap shows false match rates observed over impostor comparisons of faces from different individuals who were born in the given region pair. False matches are counted against a recognition threshold fixed globally to give the target FMR in the plot title, computed over all on the order of 10^{10} impostor comparisons. If text appears in each box it give the same quantity as that coded by the color. Grey indicates FMR is at the intended FMR target level. Light red colors present a security vulnerability to, for example, a passport gate. Each +1 increase in \log_{10} FMR corresponds to a factor of 10 increase in FMR. The matrix is not quite symmetric because images in the enrollment and verification sets are different.

Cross region FMR at threshold $T = 0.701$ for algorithm lookman_002, giving $FMR(T) = 0.0001$ globally.

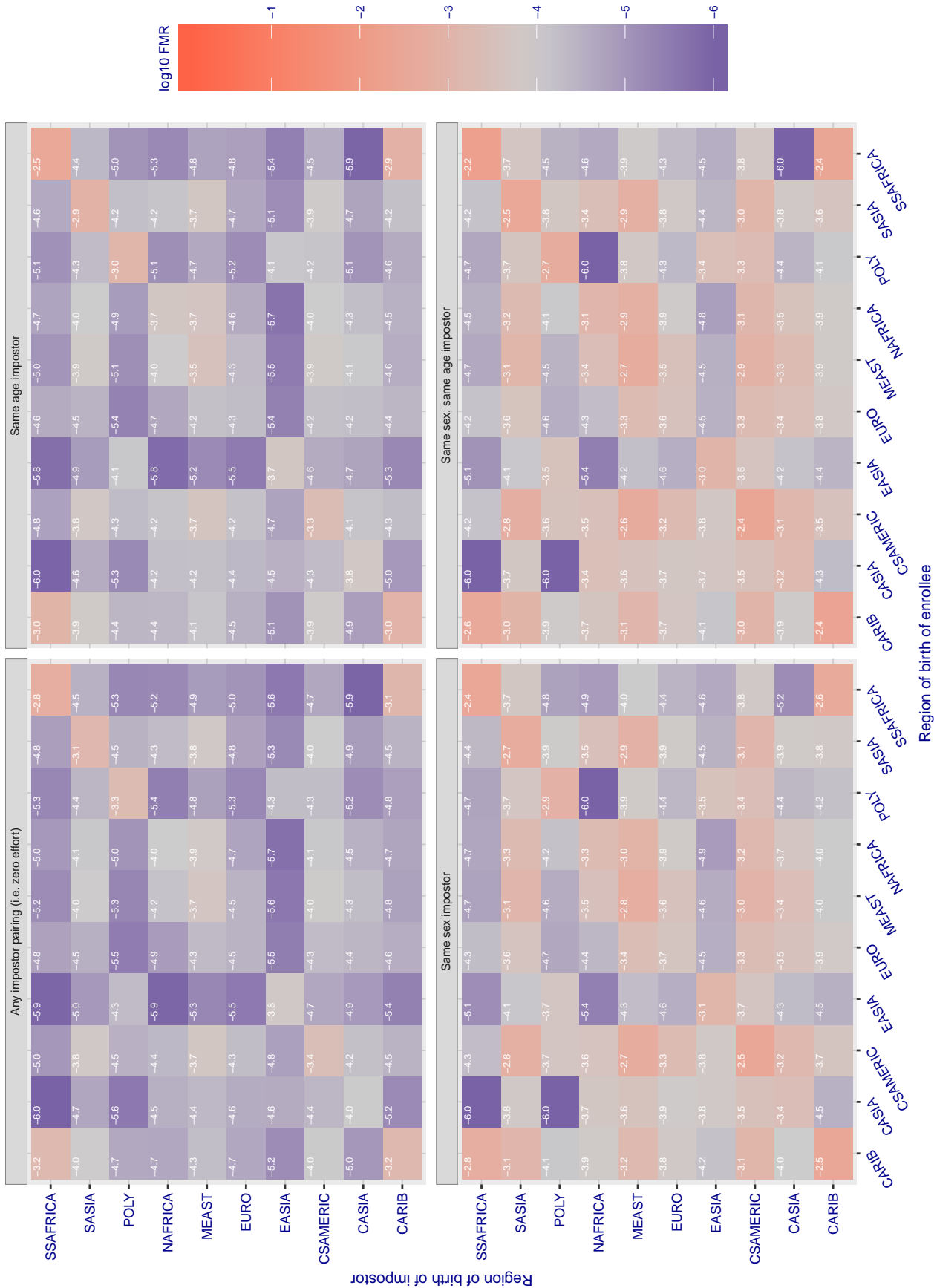


Figure 154: For algorithm lookman-002 operating on visa images, the heatmap shows false match rates observed over impostor comparisons of faces from different individuals who were born in the given region pair. False matches are counted against a recognition threshold fixed globally to give the target FMR in the plot title, computed over all on the order of 10^{10} impostor comparisons. If text appears in each box it give the same quantity as that coded by the color. Grey indicates FMR is at the intended FMR target level. Light red colors present a security vulnerability to, for example, a passport gate. Each +1 increase in \log_{10} FMR corresponds to a factor of 10 increase in FMR. The matrix is not quite symmetric because images in the enrollment and verification sets are different.

Cross region FMR at threshold $T = 74.511$ for algorithm megvii_001, giving $FMR(T) = 0.0001$ globally.

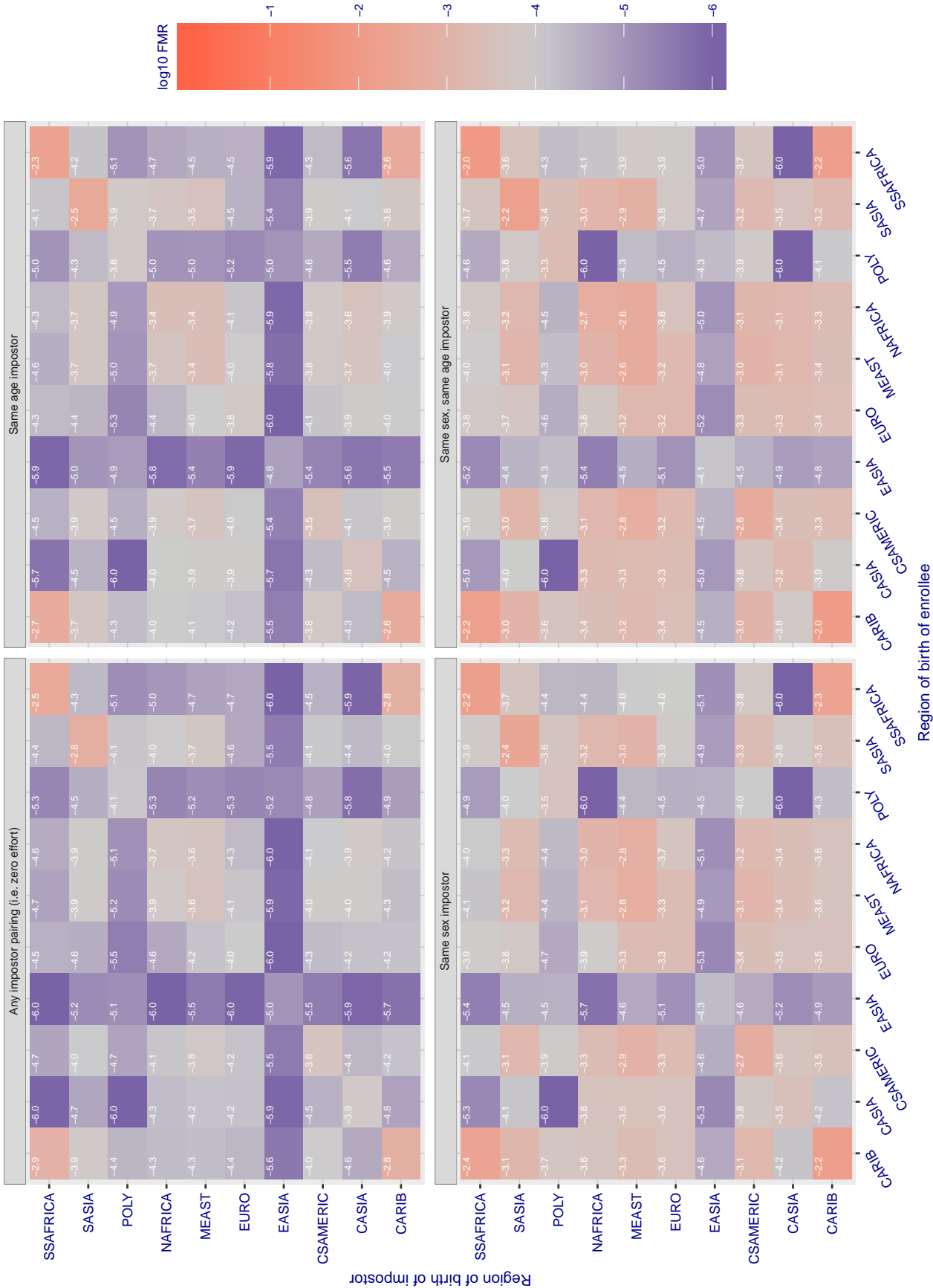


Figure 155: For algorithm megvii-001 operating on visa images, the heatmap shows false match rates observed over impostor comparisons of faces from different individuals who were born in the given region pair. False matches are counted against a recognition threshold fixed globally to give the target FMR in the plot title, computed over all on the order of 10^{10} impostor comparisons. If text appears in each box it give the same quantity as that coded by the color. Grey indicates FMR is at the intended FMR target level. Light red colors present a security vulnerability to, for example, a passport gate. Each +1 increase in \log_{10} FMR corresponds to a factor of 10 increase in FMR. The matrix is not quite symmetric because images in the enrollment and verification sets are different.

Cross region FMR at threshold $T = 66.384$ for algorithm megvii_002, giving $FMR(T) = 0.0001$ globally.

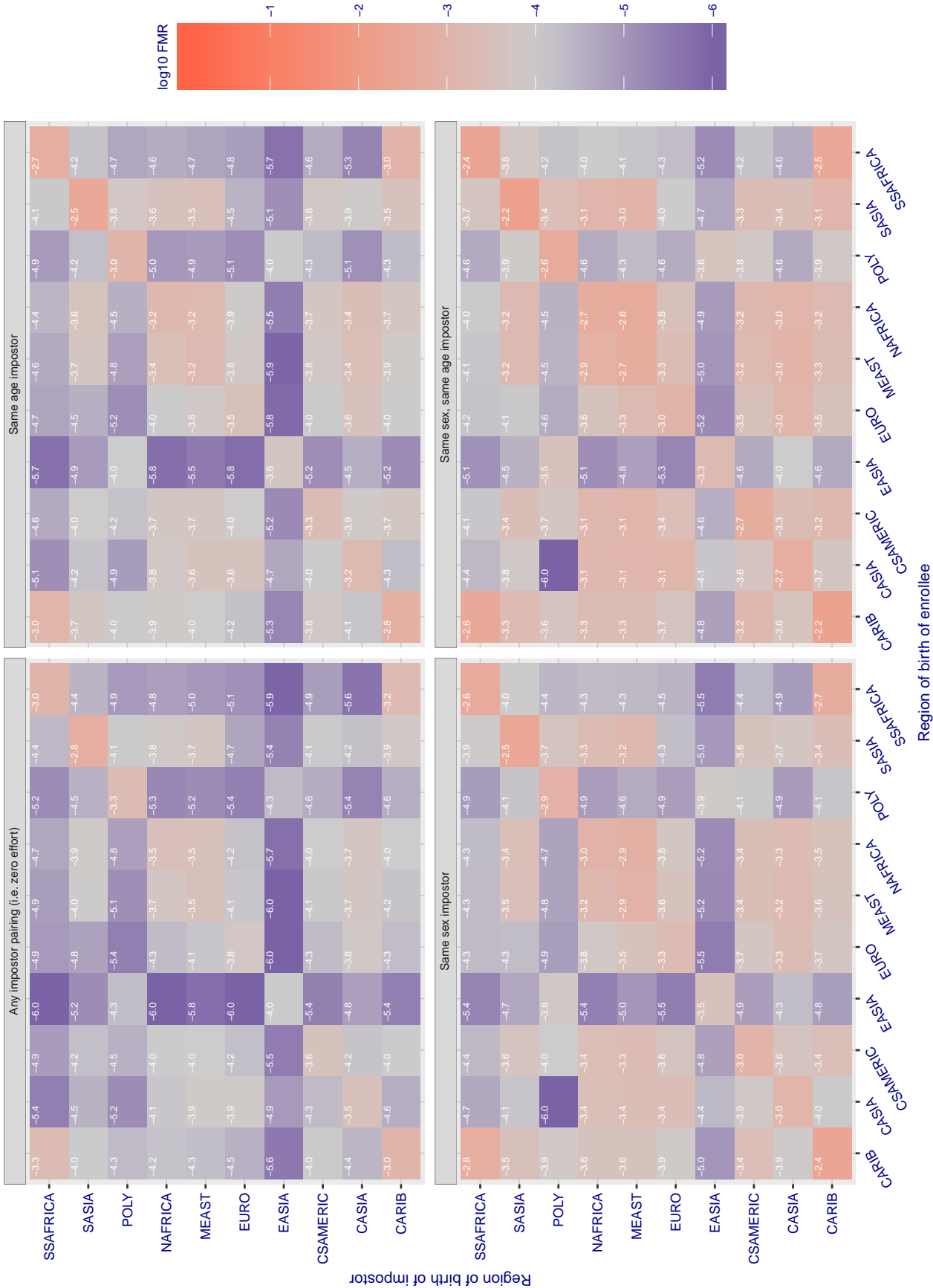


Figure 156: For algorithm megvii-002 operating on visa images, the heatmap shows false match rates observed over impostor comparisons of faces from different individuals who were born in the given region pair. False matches are counted against a recognition threshold fixed globally to give the target FMR in the plot title, computed over all on the order of 10^{10} impostor comparisons. If text appears in each box it give the same quantity as that coded by the color. Grey indicates FMR is at the intended FMR target level. Light red colors present a security vulnerability to, for example, a passport gate. Each +1 increase in \log_{10} FMR corresponds to a factor of 10 increase in FMR. The matrix is not quite symmetric because images in the enrollment and verification sets are different.

Cross region FMR at threshold $T = 0.425$ for algorithm meiya_001, giving $FMR(T) = 0.0001$ globally.

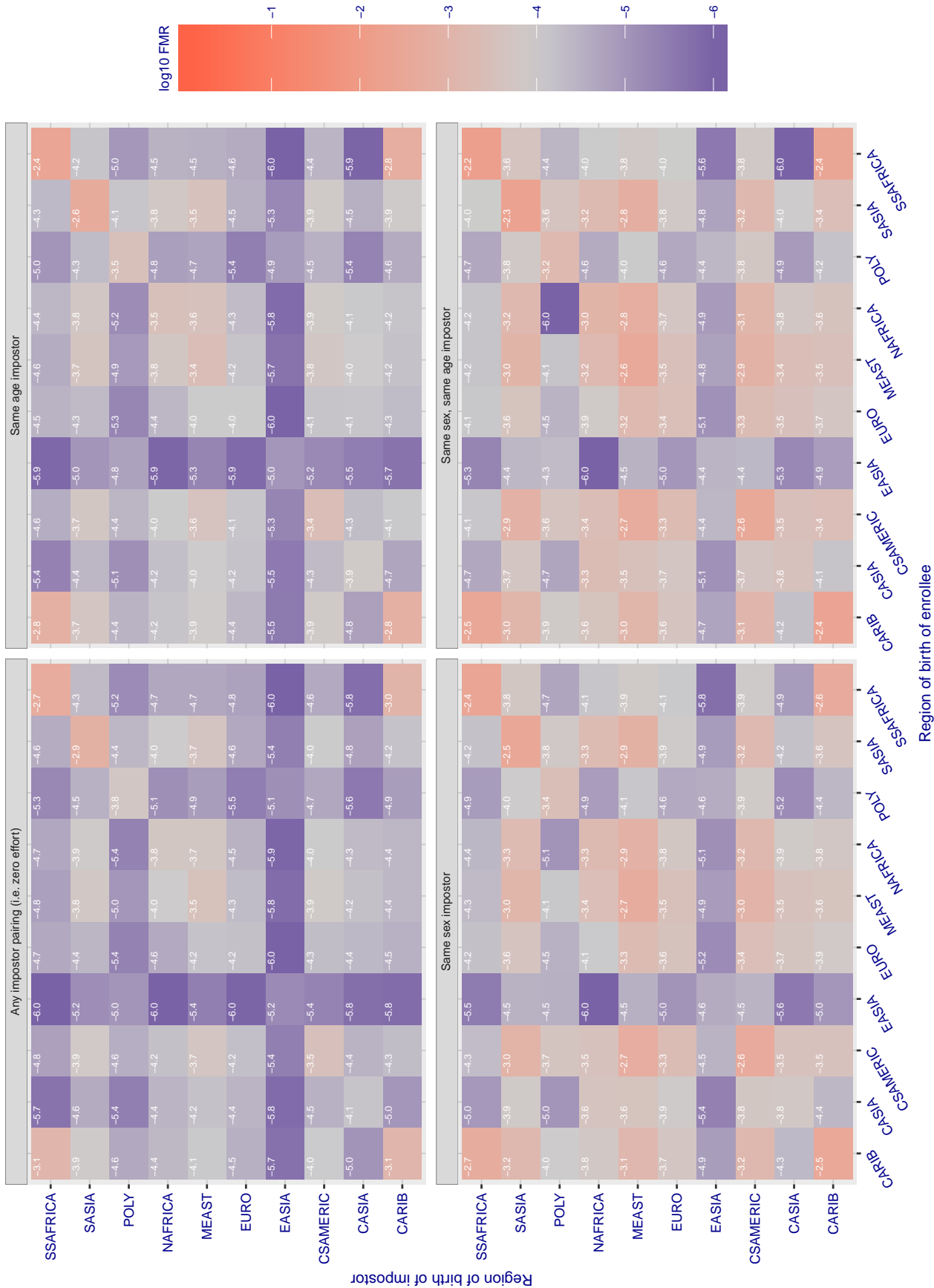


Figure 157: For algorithm meiya-001 operating on visa images, the heatmap shows false match rates observed over impostor comparisons of faces from different individuals who were born in the given region pair. False matches are counted against a recognition threshold fixed globally to give the target FMR in the plot title, computed over all on the order of 10^{10} impostor comparisons. If text appears in each box it give the same quantity as that coded by the color. Grey indicates FMR is at the intended FMR target level. Light red colors present a security vulnerability to, for example, a passport gate. Each +1 increase in \log_{10} FMR corresponds to a factor of 10 increase in FMR. The matrix is not quite symmetric because images in the enrollment and verification sets are different.

Cross region FMR at threshold $T = 0.668$ for algorithm microfocus_001, giving $FMR(T) = 0.0001$ globally.

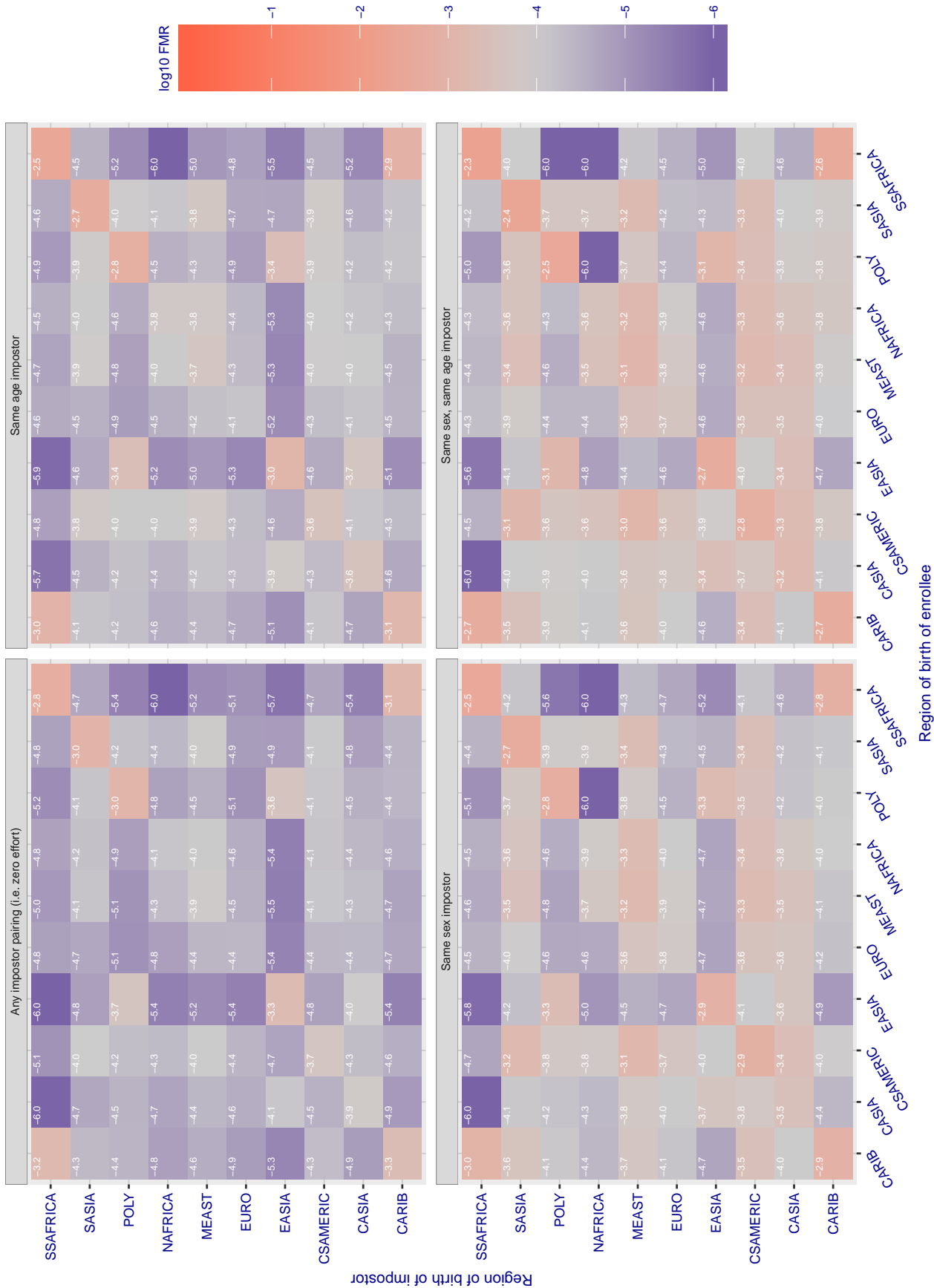


Figure 158: For algorithm microfocus-001 operating on visa images, the heatmap shows false match rates observed over impostor comparisons of faces from different individuals who were born in the given region pair. False matches are counted against a recognition threshold fixed globally to give the target FMR in the plot title, computed over all on the order of 10^{10} impostor comparisons. If text appears in each box it give the same quantity as that coded by the color. Grey indicates FMR is at the intended FMR target level. Light red colors present a security vulnerability to, for example, a passport gate. Each +1 increase in \log_{10} FMR corresponds to a factor of 10 increase in FMR. The matrix is not quite symmetric because images in the enrollment and verification sets are different.

Cross region FMR at threshold $T = 0.602$ for algorithm microfocus_002, giving $FMR(T) = 0.0001$ globally.

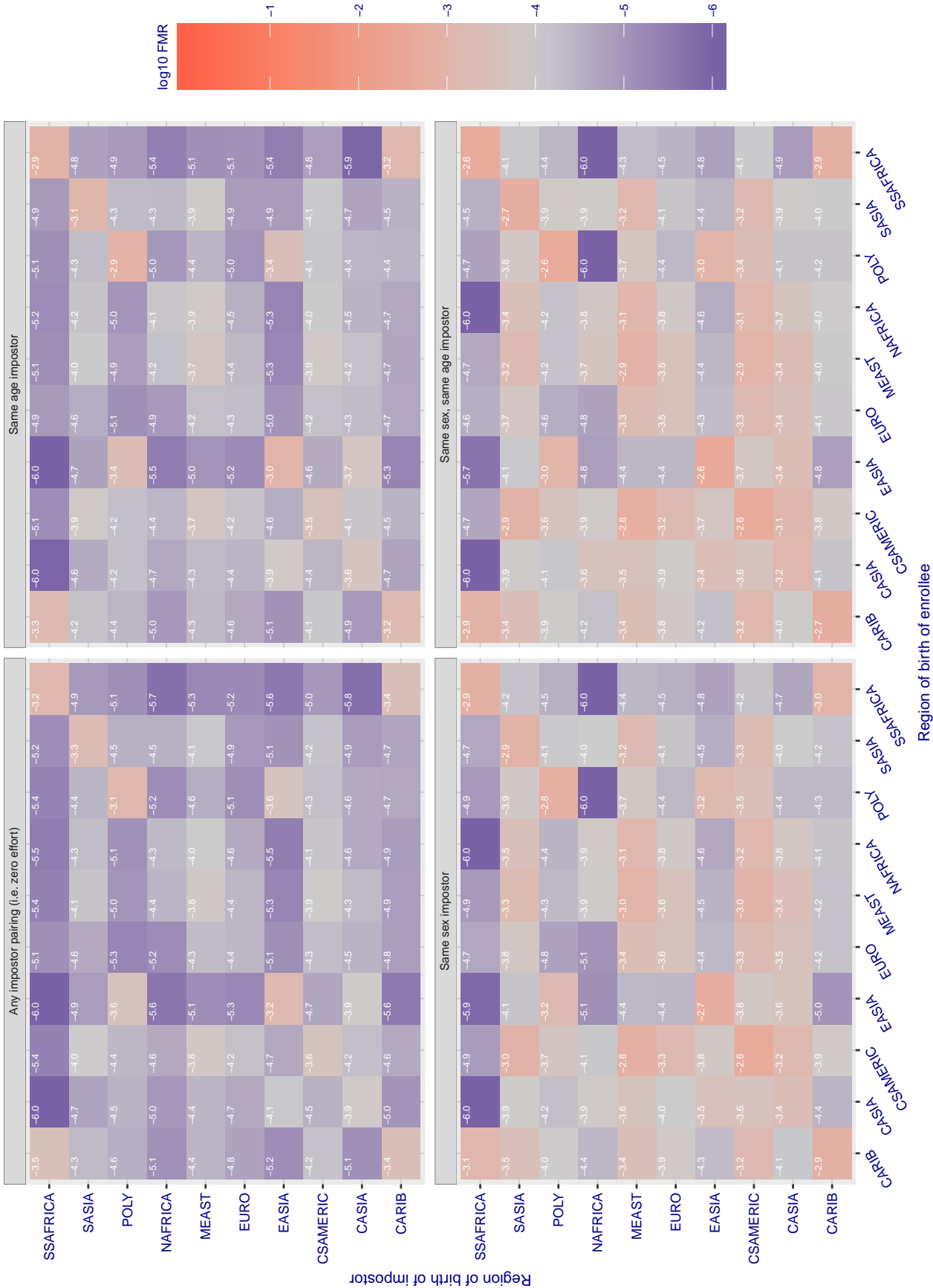


Figure 159: For algorithm microfocus-002 operating on visa images, the heatmap shows false match rates observed over impostor comparisons of faces from different individuals who were born in the given region pair. False matches are counted against a recognition threshold fixed globally to give the target FMR in the plot title, computed over all on the order of 10^{10} impostor comparisons. If text appears in each box it give the same quantity as that coded by the color. Grey indicates FMR is at the intended FMR target level. Light red colors present a security vulnerability to, for example, a passport gate. Each +1 increase in $\log_{10} FMR$ corresponds to a factor of 10 increase in FMR. The matrix is not quite symmetric because images in the enrollment and verification sets are different.

Cross region FMR at threshold $T = 3859.000$ for algorithm neurotechnology_004, giving $FMR(T) = 0.0001$ globally.

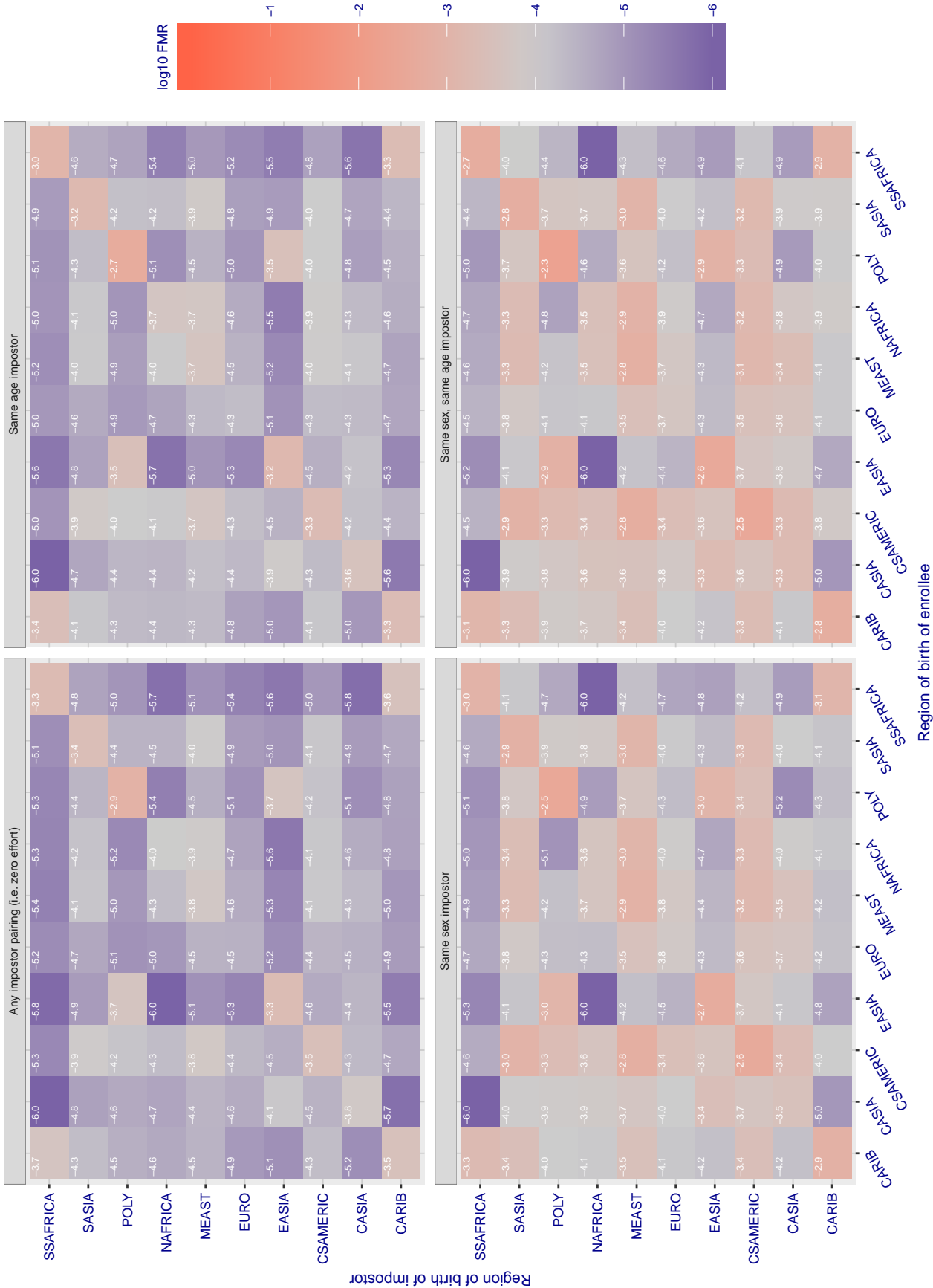


Figure 160: For algorithm neurotechnology-004 operating on visa images, the heatmap shows false match rates observed over impostor comparisons of faces from different individuals who were born in the given region pair. False matches are counted against a recognition threshold fixed globally to give the target FMR in the plot title, computed over all on the order of $10^{1.0}$ impostor comparisons. If text appears in each box it give the same quantity as that coded by the color. Grey indicates FMR is at the intended FMR target level. Light red colors present a security vulnerability to, for example, a passport gate. Each +1 increase in log10 FMR corresponds to a factor of 10 increase in FMR. The matrix is not quite symmetric because images in the enrollment and verification sets are different.

Cross region FMR at threshold $T = 46.101$ for algorithm neurotechnology_005, giving $FMR(T) = 0.0001$ globally.

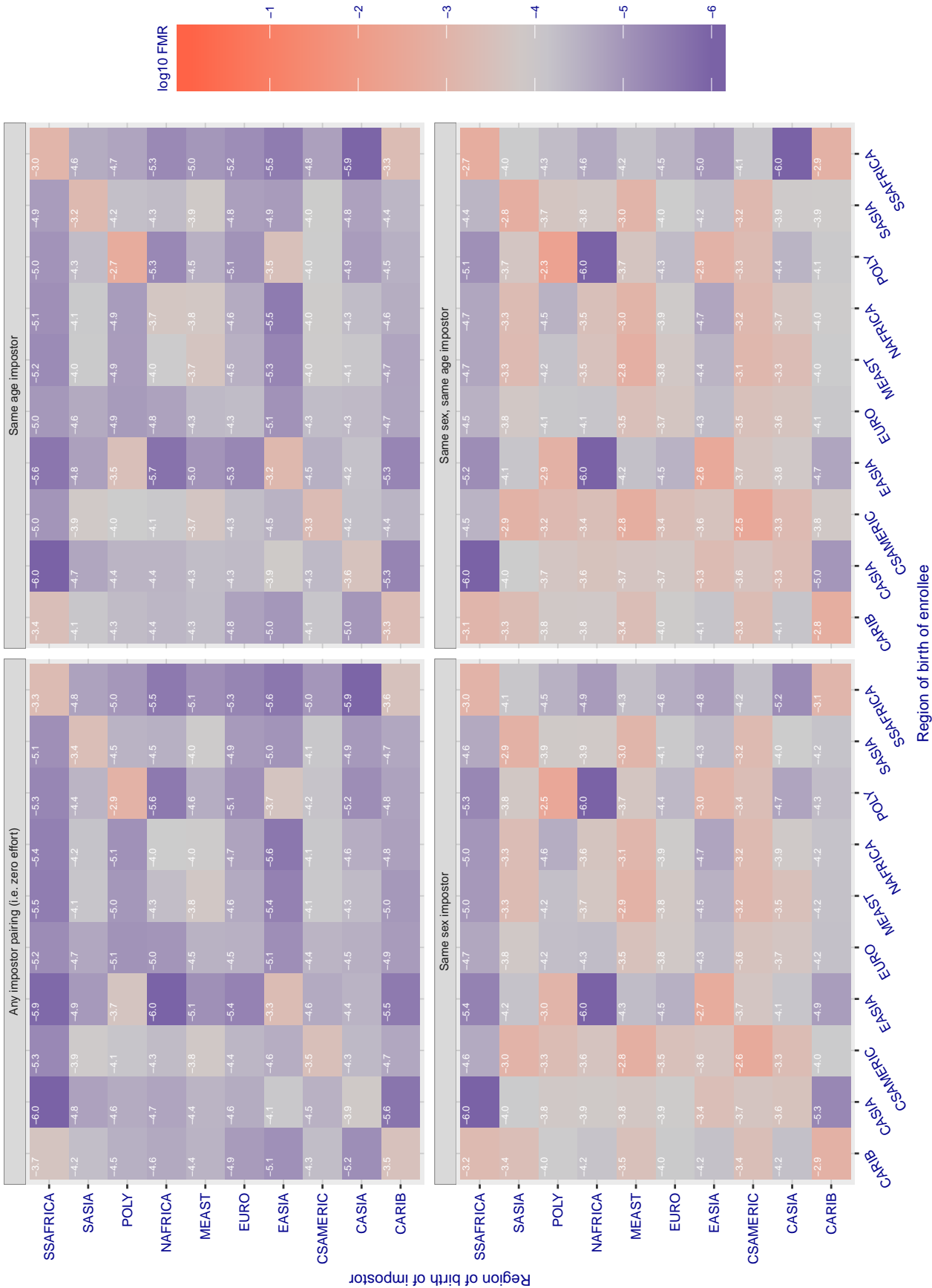


Figure 161: For algorithm neurotechnology-005 operating on visa images, the heatmap shows false match rates observed over impostor comparisons of faces from different individuals who were born in the given region pair. False matches are counted against a recognition threshold fixed globally to give the target FMR in the plot title, computed over all on the order of $10^{1.0}$ impostor comparisons. If text appears in each box it give the same quantity as that coded by the color. Grey indicates FMR is at the intended FMR target level. Light red colors present a security vulnerability to, for example, a passport gate. Each +1 increase in \log_{10} FMR corresponds to a factor of 10 increase in FMR. The matrix is not quite symmetric because images in the enrollment and verification sets are different.

Cross region FMR at threshold $T = 1.000$ for algorithm `nodeflux_000`, giving $FMR(T) = 0.0001$ globally.

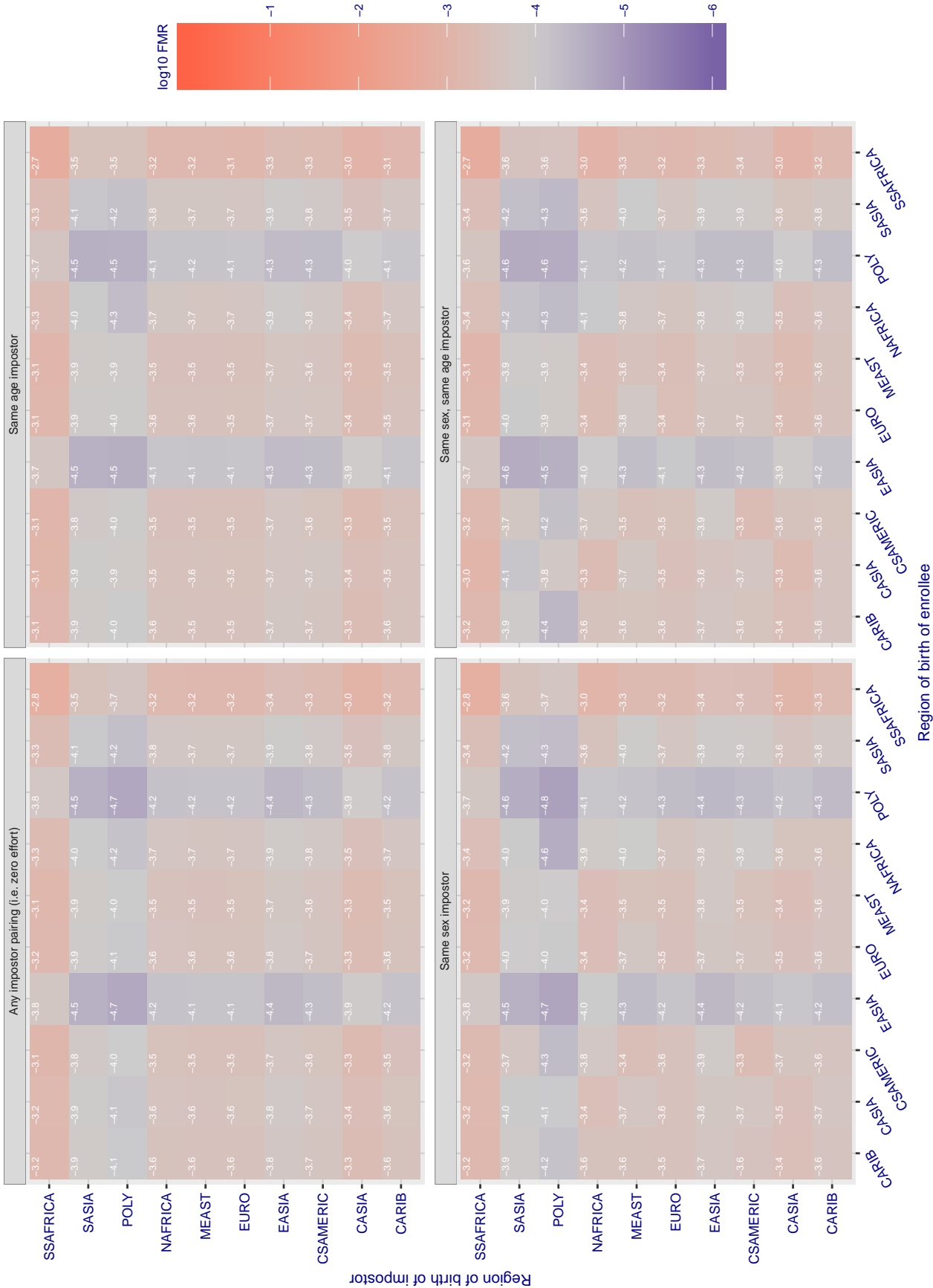


Figure 162: For algorithm `nodeflux-000` operating on visa images, the heatmap shows false match rates observed over impostor comparisons of faces from different individuals who were born in the given region pair. False matches are counted against a recognition threshold fixed globally to give the target FMR in the plot title, computed over all on the order of 10^{10} impostor comparisons. If text appears in each box it give the same quantity as that coded by the color. Grey indicates FMR is at the intended FMR target level. Light red colors present a security vulnerability to, for example, a passport gate. Each +1 increase in \log_{10} FMR corresponds to a factor of 10 increase in FMR. The matrix is not quite symmetric because images in the enrollment and verification sets are different.

Cross region FMR at threshold $T = 1.000$ for algorithm `nodeflux_001`, giving $FMR(T) = 0.0001$ globally.

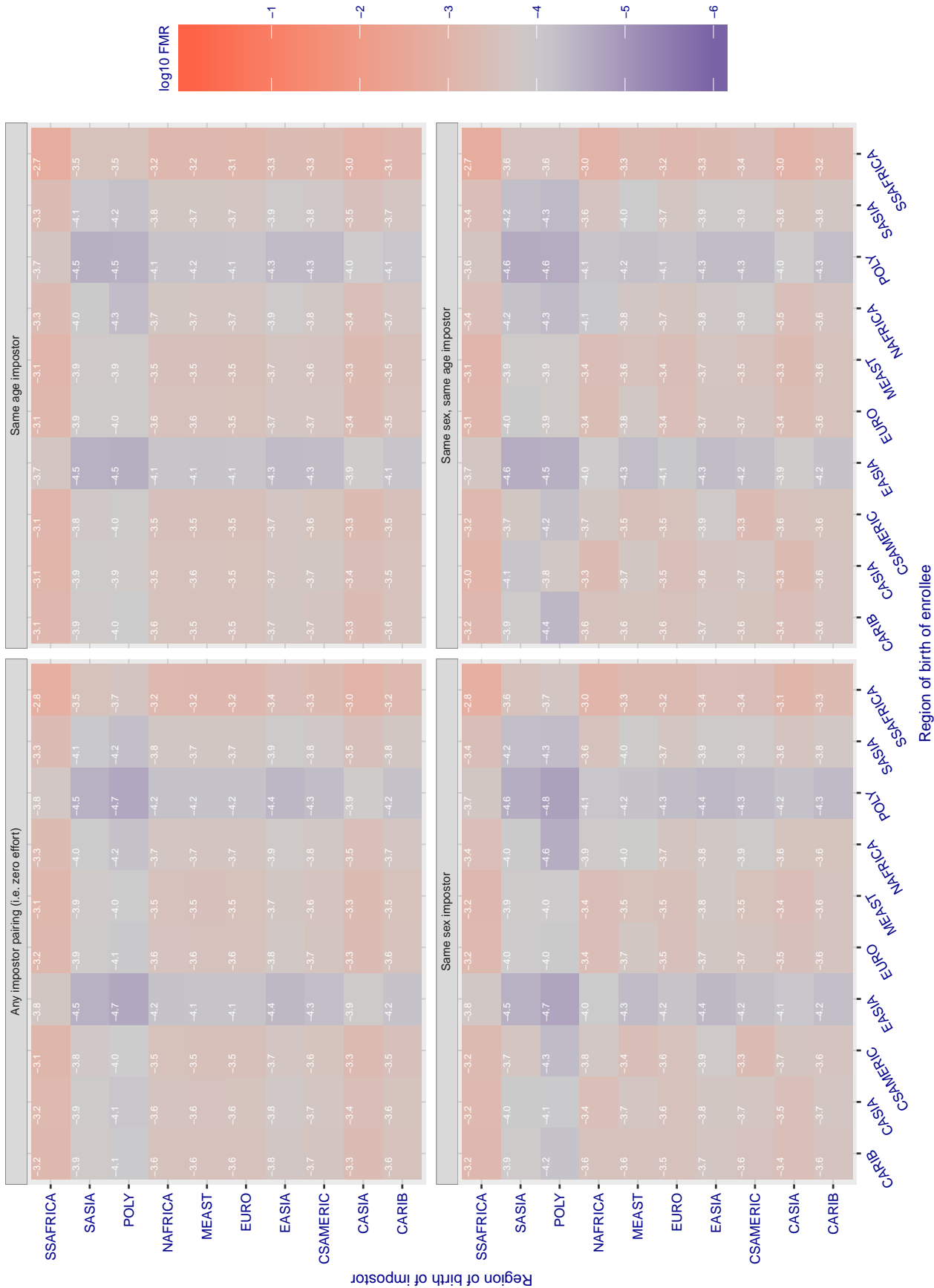


Figure 163: For algorithm `nodeflux-001` operating on visa images, the heatmap shows false match rates observed over impostor comparisons of faces from different individuals who were born in the given region pair. False matches are counted against a recognition threshold fixed globally to give the target FMR in the plot title, computed over all on the order of 10^{10} impostor comparisons. If text appears in each box it give the same quantity as that coded by the color. Grey indicates FMR is at the intended FMR target level. Light red colors present a security vulnerability to, for example, a passport gate. Each +1 increase in \log_{10} FMR corresponds to a factor of 10 increase in FMR. The matrix is not quite symmetric because images in the enrollment and verification sets are different.

Cross region FMR at threshold T = 1.487 for algorithm ntechlab_005, giving FMR(T) = 0.0001 globally.

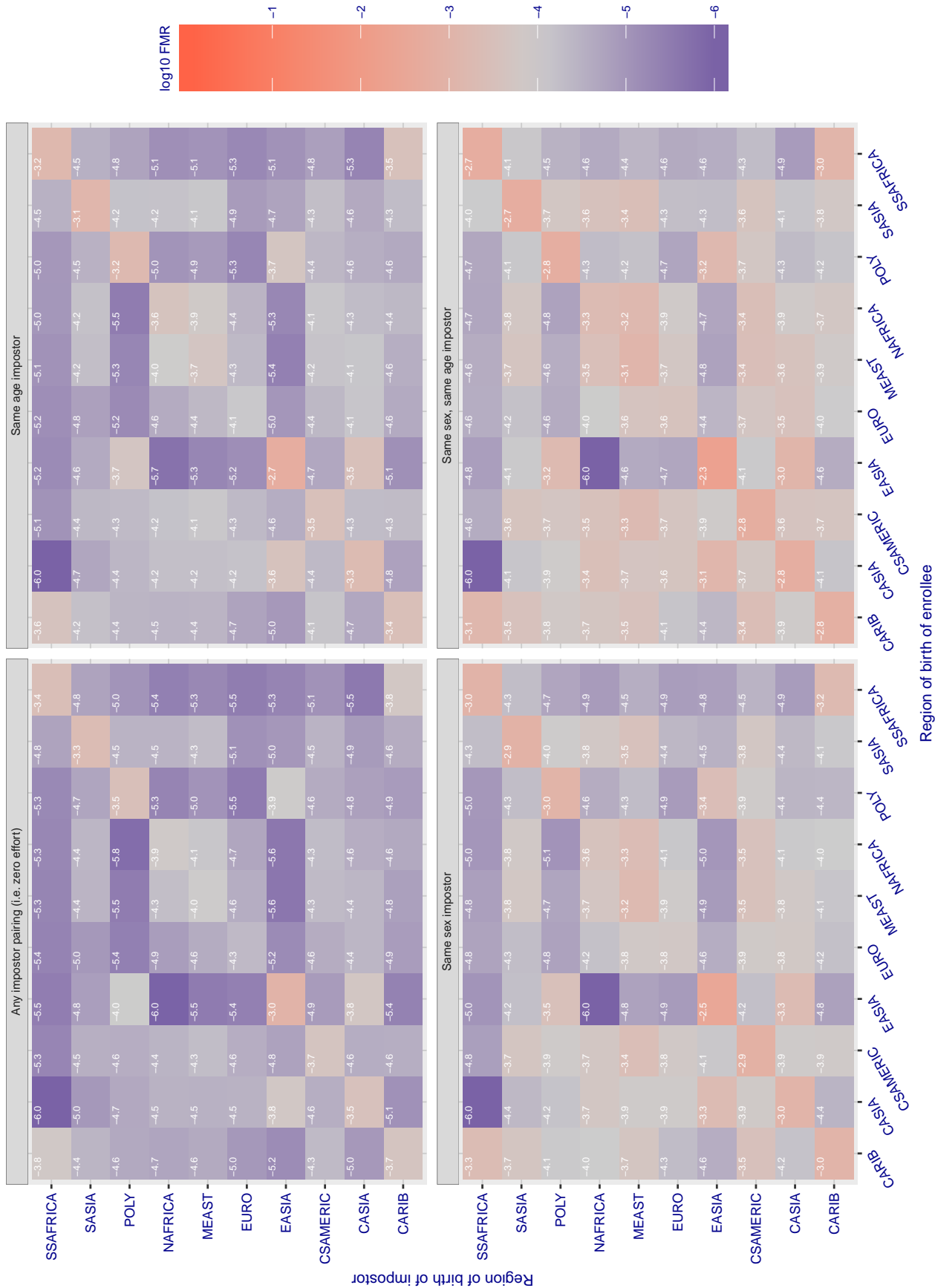


Figure 164: For algorithm ntechlab-005 operating on visa images, the heatmap shows false match rates observed over impostor comparisons of faces from different individuals who were born in the given region pair. False matches are counted against a recognition threshold fixed globally to give the target FMR in the plot title, computed over all on the order of 10¹⁰ impostor comparisons. If text appears in each box it give the same quantity as that coded by the color. Grey indicates FMR is at the intended FMR target level. Light red colors present a security vulnerability to, for example, a passport gate. Each +1 increase in log10 FMR corresponds to a factor of 10 increase in FMR. The matrix is not quite symmetric because images in the enrollment and verification sets are different.

Cross region FMR at threshold $T = 1.997$ for algorithm ntechlab_006, giving $FMR(T) = 0.0001$ globally.

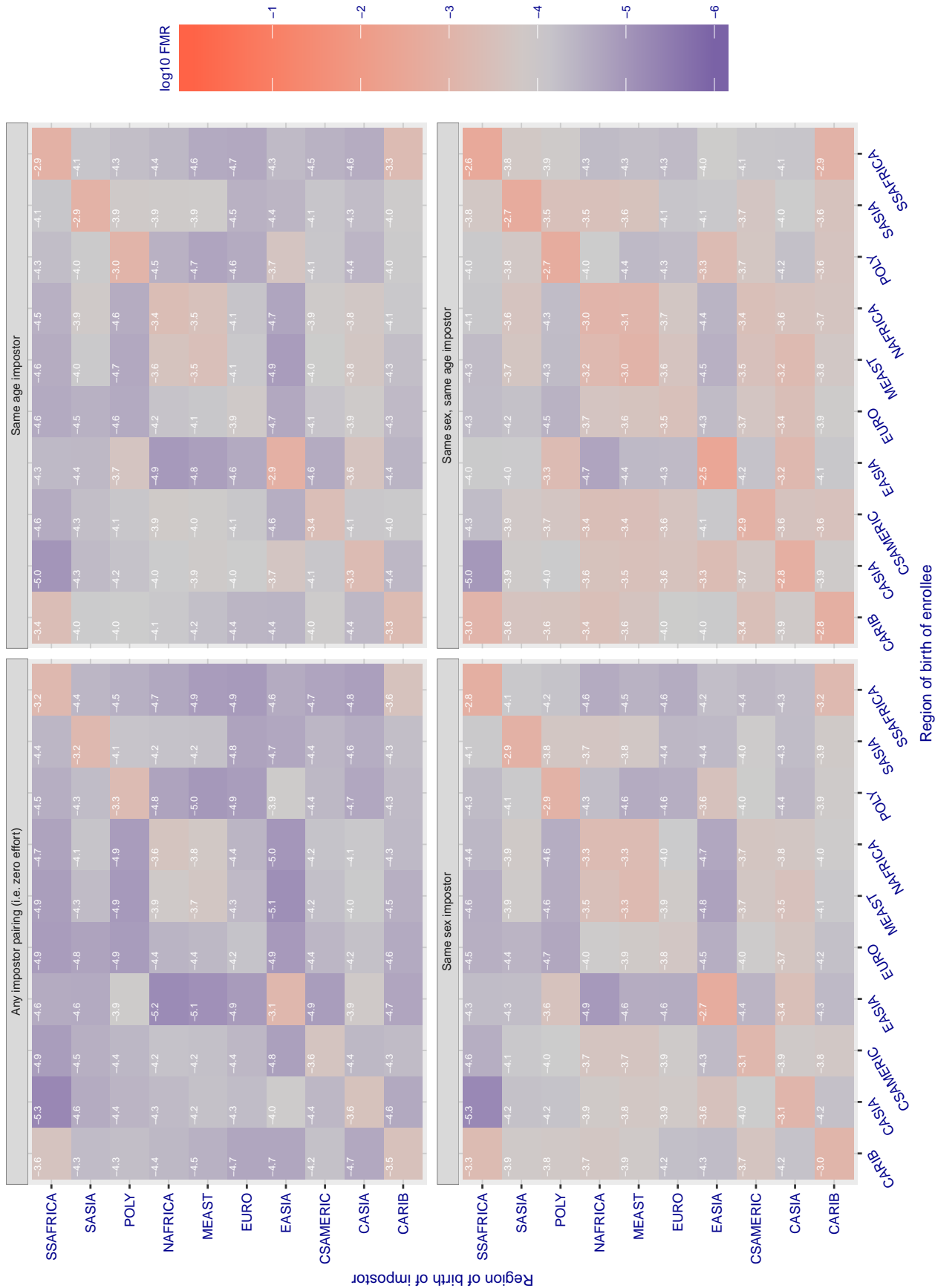


Figure 165: For algorithm ntechlab-006 operating on visa images, the heatmap shows false match rates observed over impostor comparisons of faces from different individuals who were born in the given region pair. False matches are counted against a recognition threshold fixed globally to give the target FMR in the plot title, computed over all on the order of 10^{10} impostor comparisons. If text appears in each box it give the same quantity as that coded by the color. Grey indicates FMR is at the intended FMR target level. Light red colors present a security vulnerability to, for example, a passport gate. Each +1 increase in \log_{10} FMR corresponds to a factor of 10 increase in FMR. The matrix is not quite symmetric because images in the enrollment and verification sets are different.

Cross region FMR at threshold $T = 0.337$ for algorithm `psl_001`, giving $FMR(T) = 0.0001$ globally.

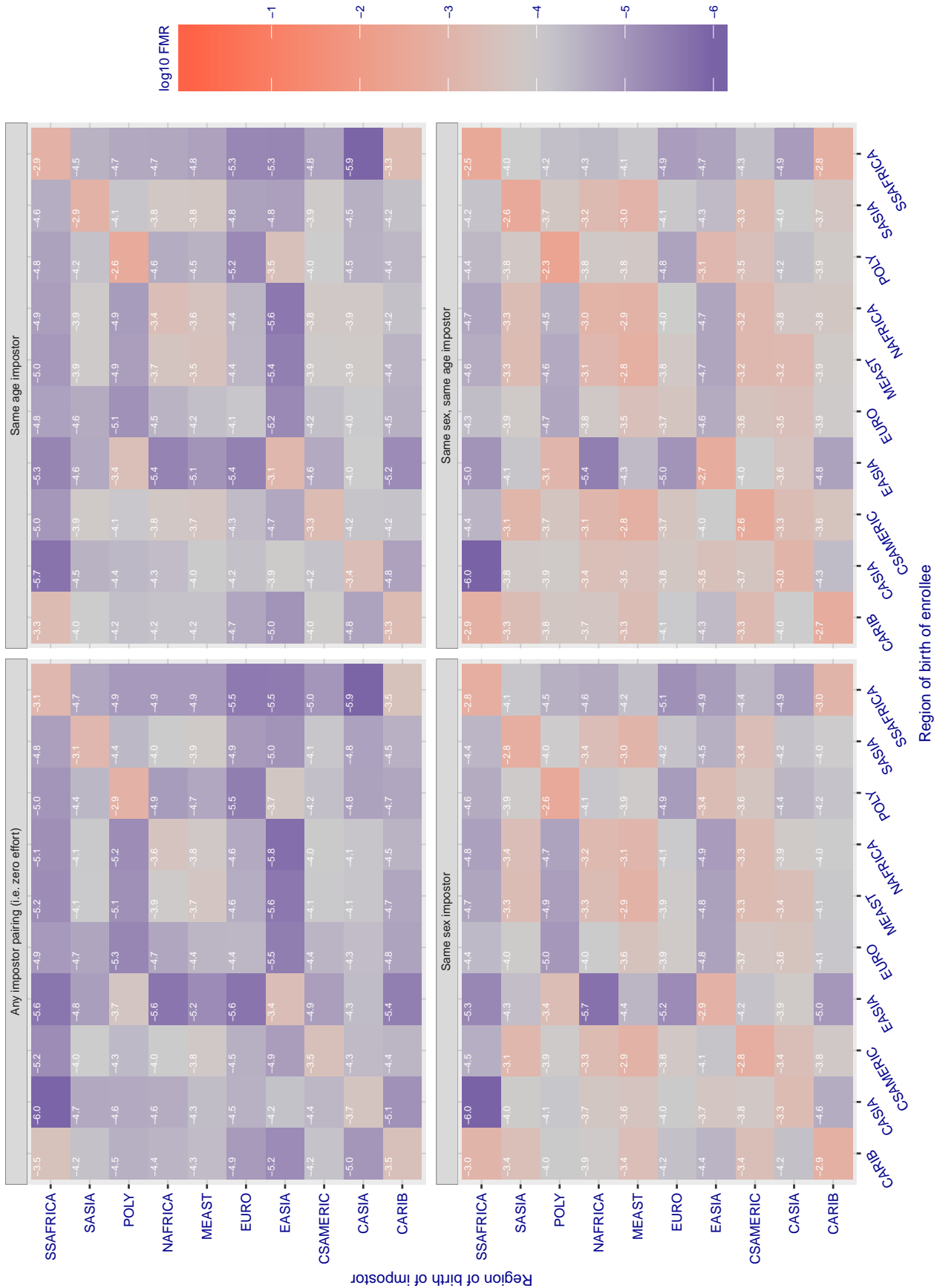


Figure 166: For algorithm `psl-001` operating on visa images, the heatmap shows false match rates observed over impostor comparisons of faces from different individuals who were born in the given region pair. False matches are counted against a recognition threshold fixed globally to give the target FMR in the plot title, computed over all on the order of 10^{10} impostor comparisons. If text appears in each box it give the same quantity as that coded by the color. Grey indicates FMR is at the intended FMR target level. Light red colors present a security vulnerability to, for example, a passport gate. Each +1 increase in $\log_{10} FMR$ corresponds to a factor of 10 increase in FMR. The matrix is not quite symmetric because images in the enrollment and verification sets are different.

Cross region FMR at threshold $T = 0.353$ for algorithm `psl_002`, giving $FMR(T) = 0.0001$ globally.

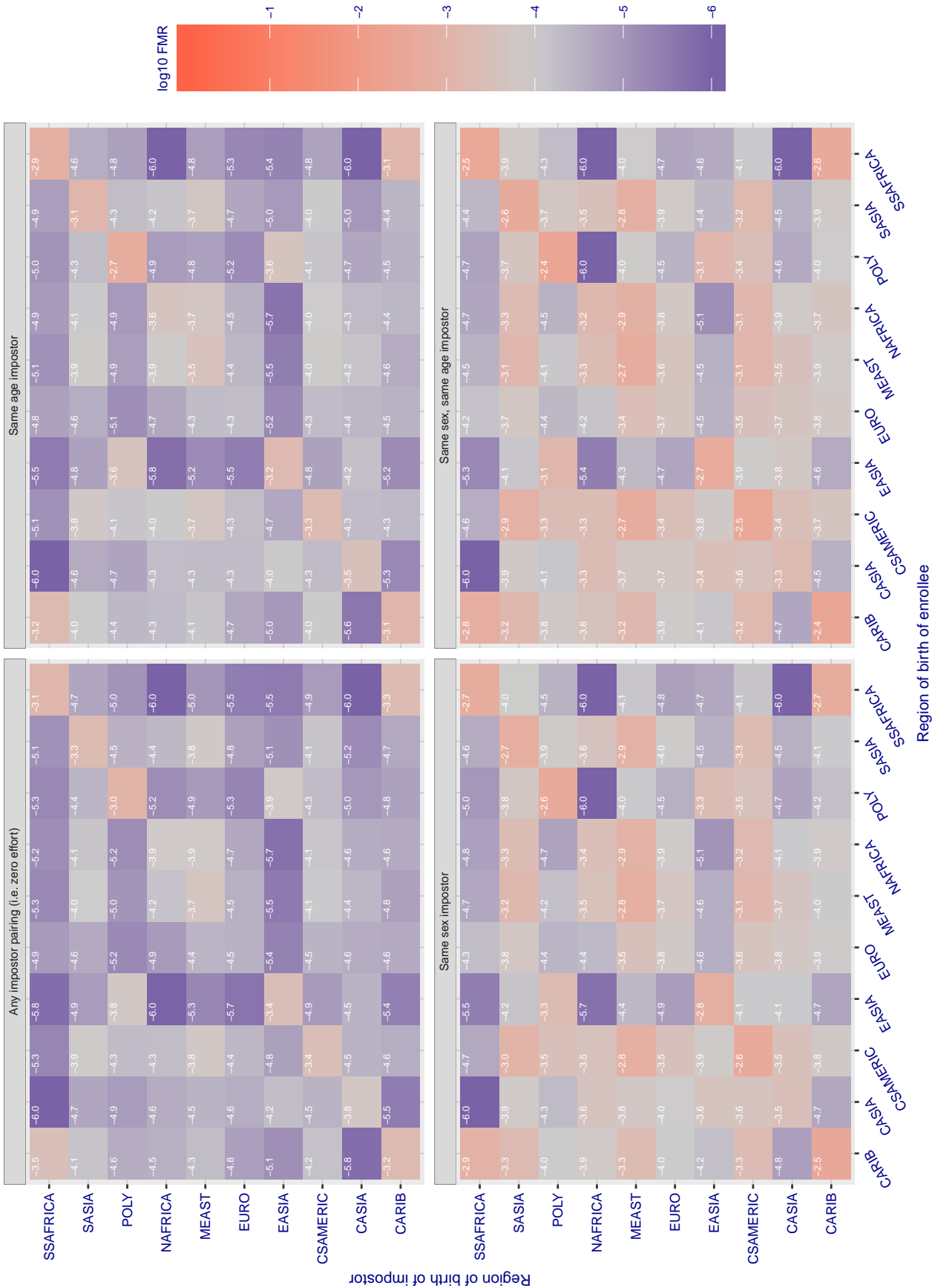


Figure 167: For algorithm `psl-002` operating on visa images, the heatmap shows false match rates observed over impostor comparisons of faces from different individuals who were born in the given region pair. False matches are counted against a recognition threshold fixed globally to give the target FMR in the plot title, computed over all on the order of 10^{10} impostor comparisons. If text appears in each box it give the same quantity as that coded by the color. Grey indicates FMR is at the intended FMR target level. Light red colors present a security vulnerability to, for example, a passport gate. Each +1 increase in \log_{10} FMR corresponds to a factor of 10 increase in FMR. The matrix is not quite symmetric because images in the enrollment and verification sets are different.

Cross region FMR at threshold $T = 0.750$ for algorithm `rankone_005`, giving $FMR(T) = 0.0001$ globally.

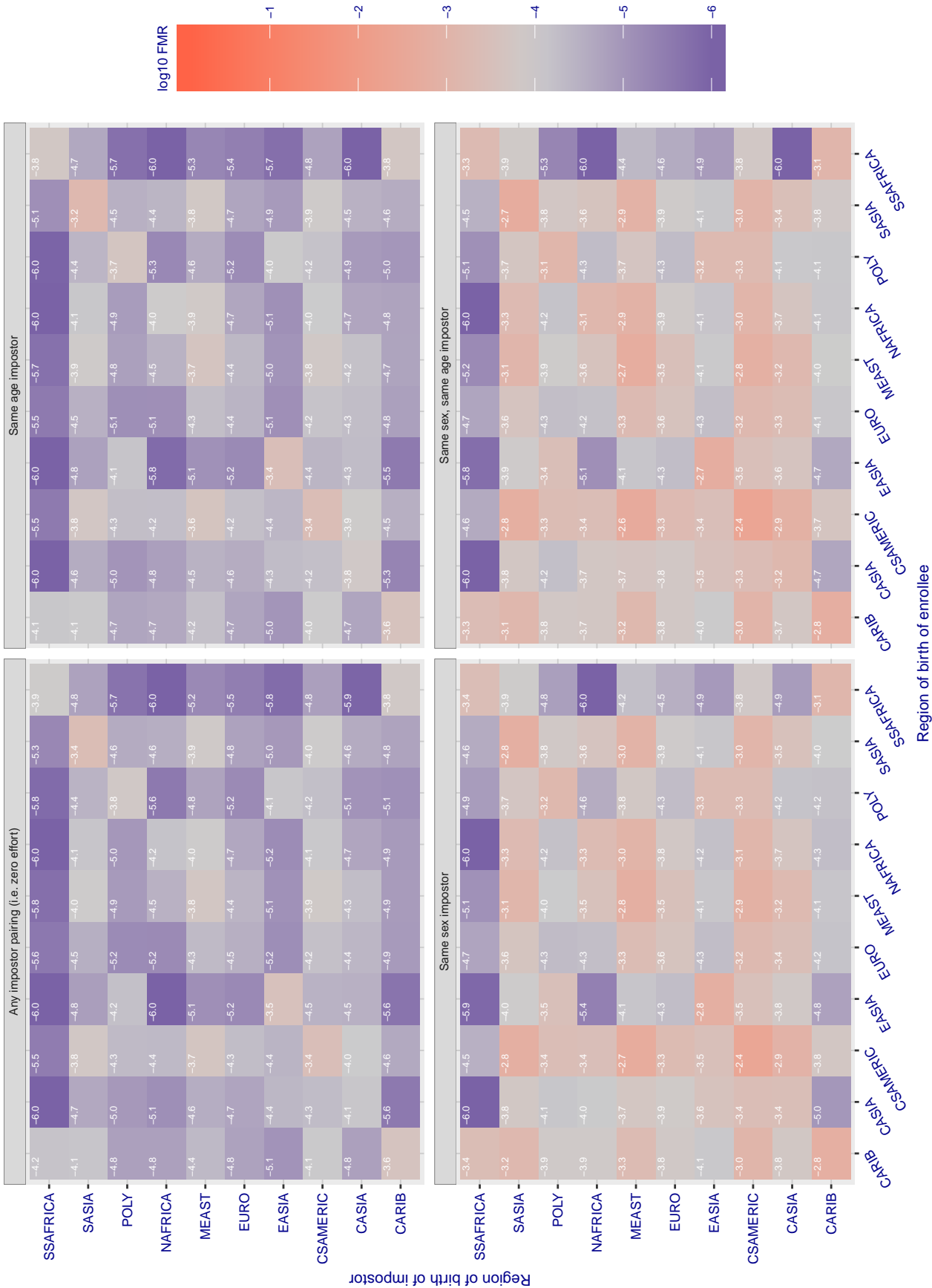


Figure 168: For algorithm `rankone-005` operating on visa images, the heatmap shows false match rates observed over impostor comparisons of faces from different individuals who were born in the given region pair. False matches are counted against a recognition threshold fixed globally to give the target FMR in the plot title, computed over all on the order of 10^{10} impostor comparisons. If text appears in each box it give the same quantity as that coded by the color. Grey indicates FMR is at the intended FMR target level. Light red colors present a security vulnerability to, for example, a passport gate. Each +1 increase in \log_{10} FMR corresponds to a factor of 10 increase in FMR. The matrix is not quite symmetric because images in the enrollment and verification sets are different.

Cross region FMR at threshold $T = 0.779$ for algorithm rankone_006, giving $FMR(T) = 0.0001$ globally.

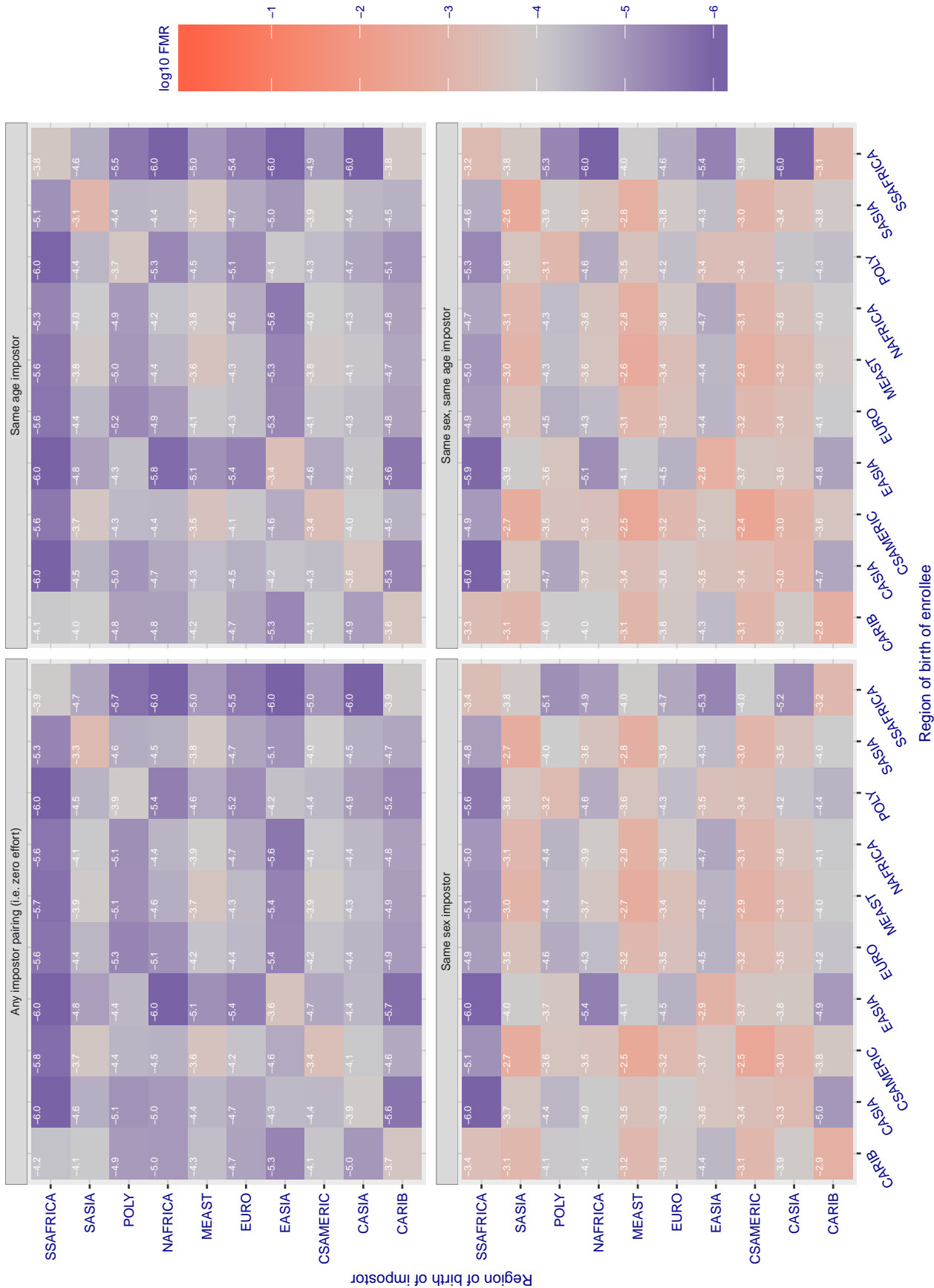


Figure 169: For algorithm rankone-006 operating on visa images, the heatmap shows false match rates observed over impostor comparisons of faces from different individuals who were born in the given region pair. False matches are counted against a recognition threshold fixed globally to give the target FMR in the plot title, computed over all on the order of 10^{10} impostor comparisons. If text appears in each box it give the same quantity as that coded by the color. Grey indicates FMR is at the intended FMR target level. Light red colors present a security vulnerability to, for example, a passport gate. Each +1 increase in \log_{10} FMR corresponds to a factor of 10 increase in FMR. The matrix is not quite symmetric because images in the enrollment and verification sets are different.

Cross region FMR at threshold $T = 0.885$ for algorithm realnetworks_001, giving $FMR(T) = 0.0001$ globally.

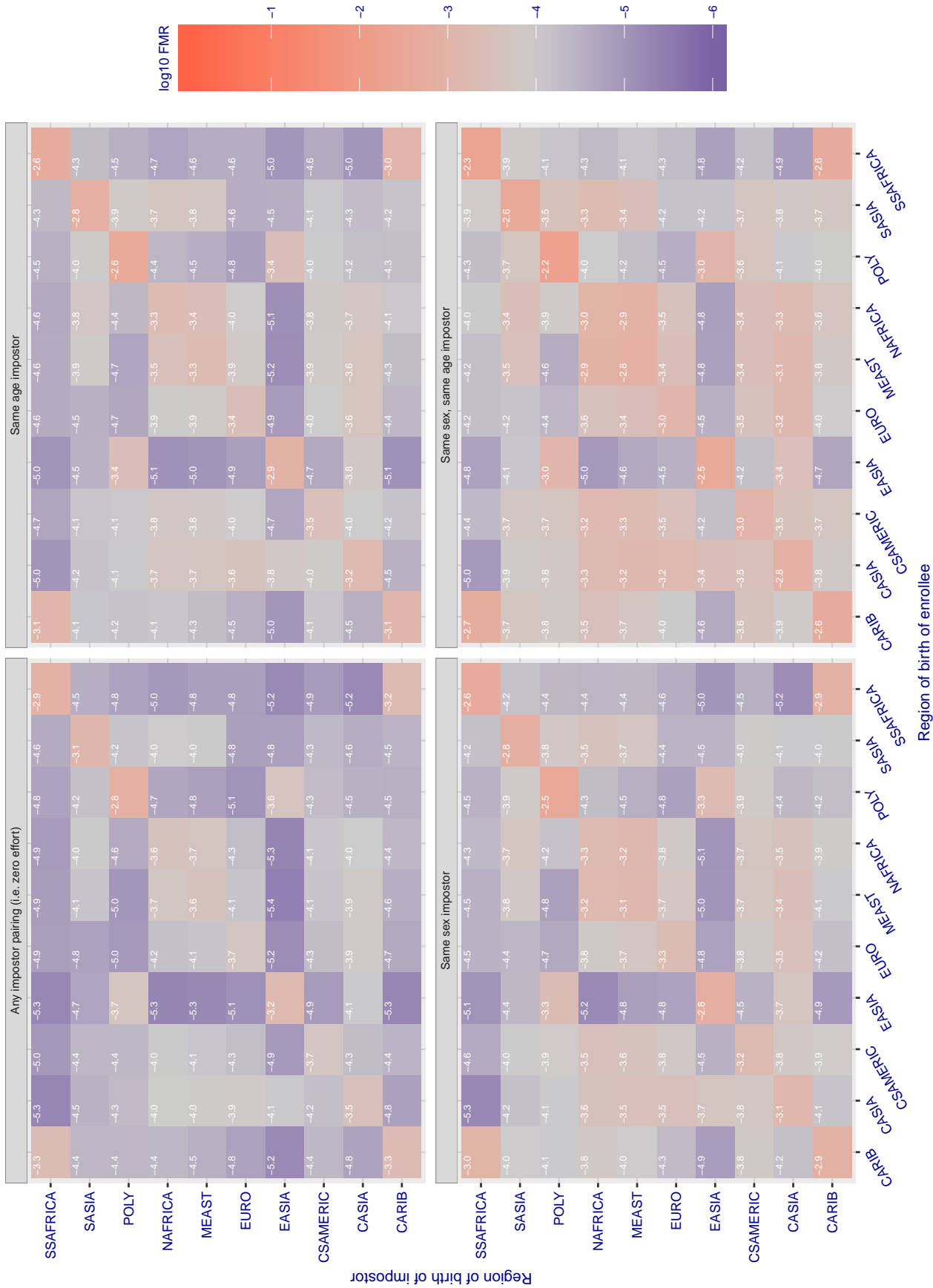


Figure 170: For algorithm realnetworks-001 operating on visa images, the heatmap shows false match rates observed over impostor comparisons of faces from different individuals who were born in the given region pair. False matches are counted against a recognition threshold fixed globally to give the target FMR in the plot title, computed over all on the order of 10^{10} impostor comparisons. If text appears in each box it give the same quantity as that coded by the color. Grey indicates FMR is at the intended FMR target level. Light red colors present a security vulnerability to, for example, a passport gate. Each +1 increase in $\log_{10} FMR$ corresponds to a factor of 10 increase in FMR. The matrix is not quite symmetric because images in the enrollment and verification sets are different.

Cross region FMR at threshold $T = 0.883$ for algorithm realnetworks_002, giving $FMR(T) = 0.0001$ globally.

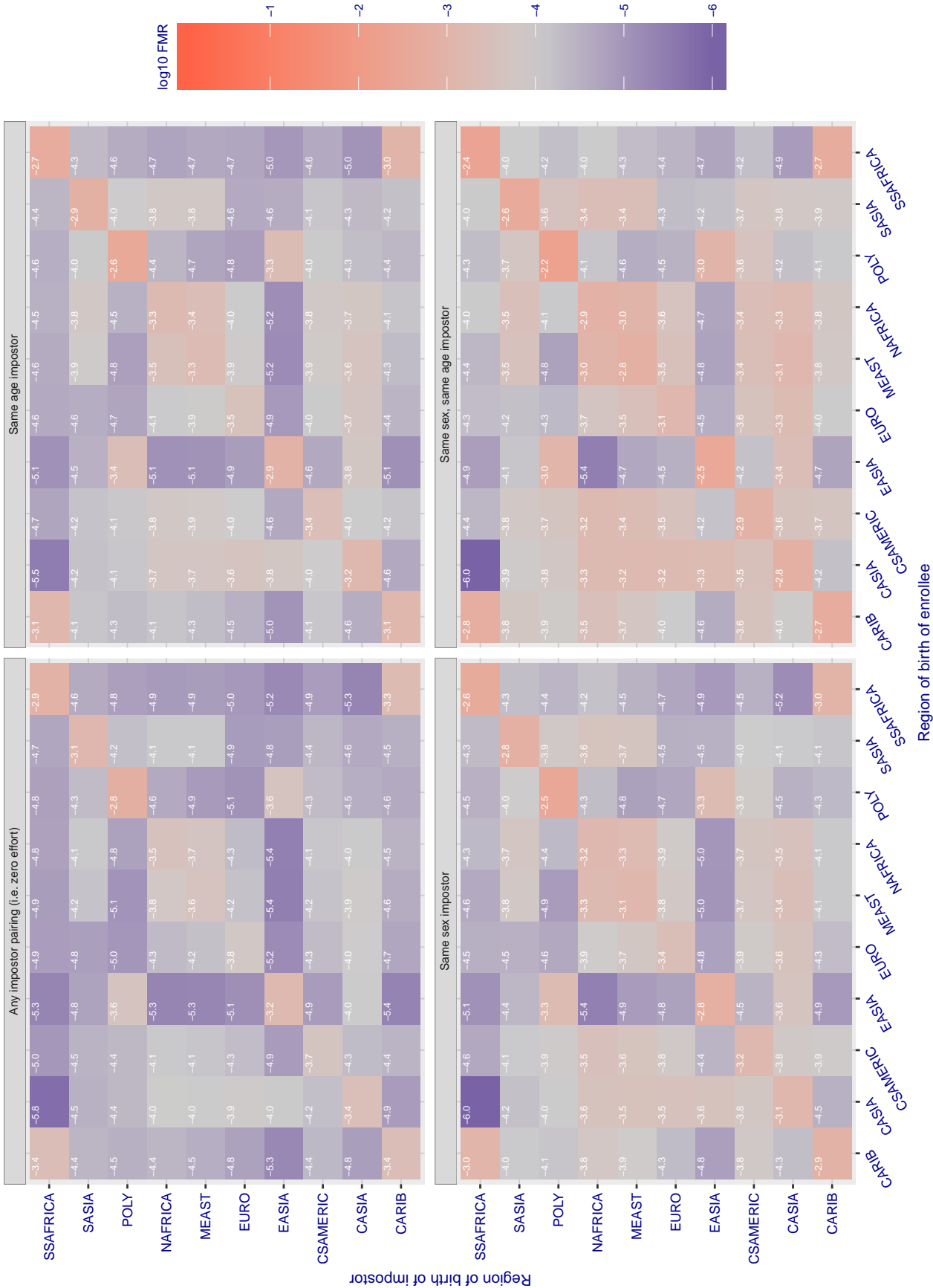


Figure 171: For algorithm realnetworks-002 operating on visa images, the heatmap shows false match rates observed over impostor comparisons of faces from different individuals who were born in the given region pair. False matches are counted against a recognition threshold fixed globally to give the target FMR in the plot title, computed over all on the order of 10^{10} impostor comparisons. If text appears in each box it give the same quantity as that coded by the color. Grey indicates FMR is at the intended FMR target level. Light red colors present a security vulnerability to, for example, a passport gate. Each +1 increase in \log_{10} FMR corresponds to a factor of 10 increase in FMR. The matrix is not quite symmetric because images in the enrollment and verification sets are different.

Cross region FMR at threshold $T = 70.373$ for algorithm remarkai_000, giving $FMR(T) = 0.0001$ globally.

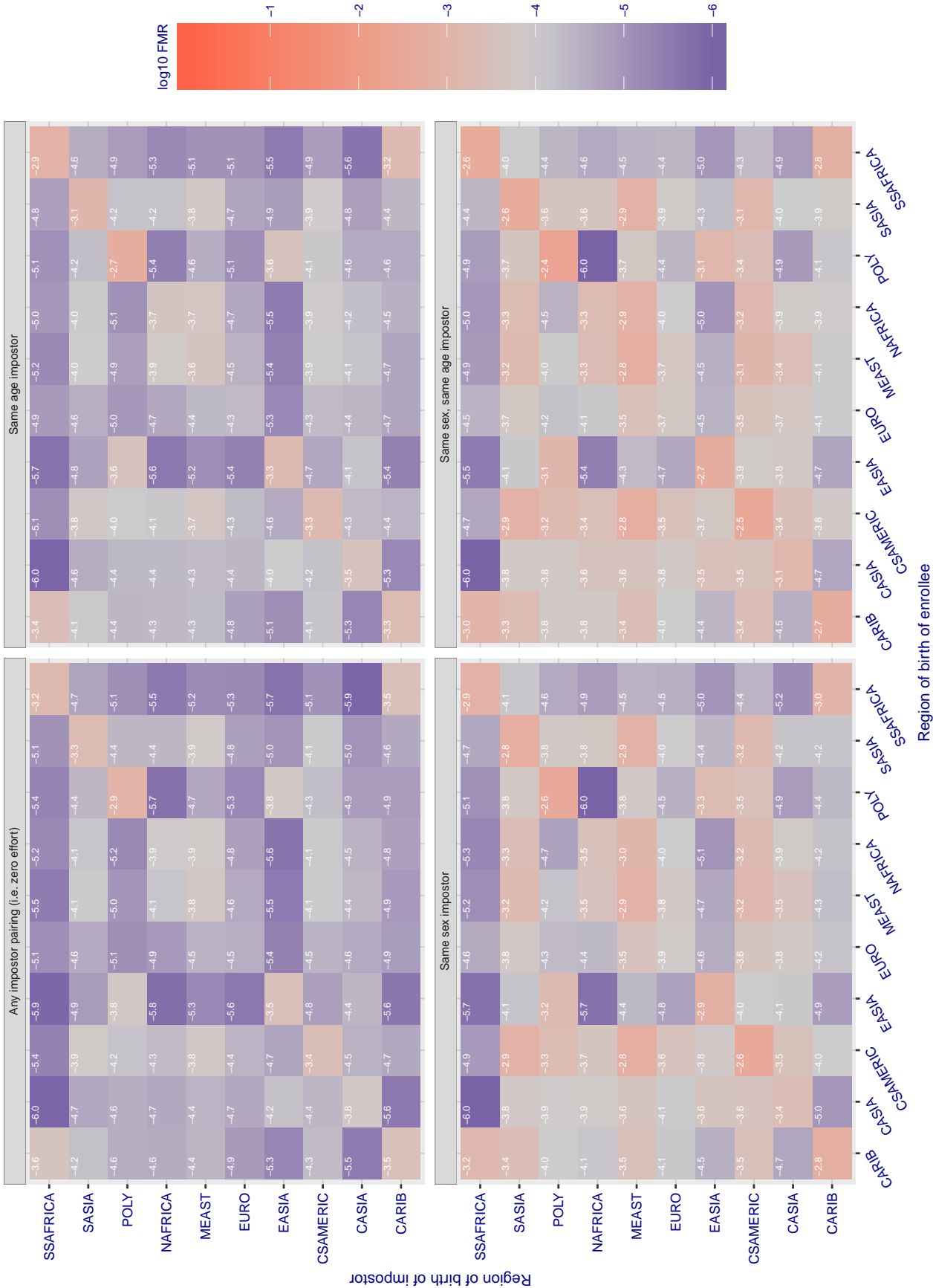


Figure 172: For algorithm remarkai-000 operating on visa images, the heatmap shows false match rates observed over impostor comparisons of faces from different individuals who were born in the given region pair. False matches are counted against a recognition threshold fixed globally to give the target FMR in the plot title, computed over all on the order of 10^{10} impostor comparisons. If text appears in each box it give the same quantity as that coded by the color. Grey indicates FMR is at the intended FMR target level. Light red colors present a security vulnerability to, for example, a passport gate. Each +1 increase in \log_{10} FMR corresponds to a factor of 10 increase in FMR. The matrix is not quite symmetric because images in the enrollment and verification sets are different.

Cross region FMR at threshold $T = 70.384$ for algorithm remarkai_001, giving $FMR(T) = 0.0001$ globally.

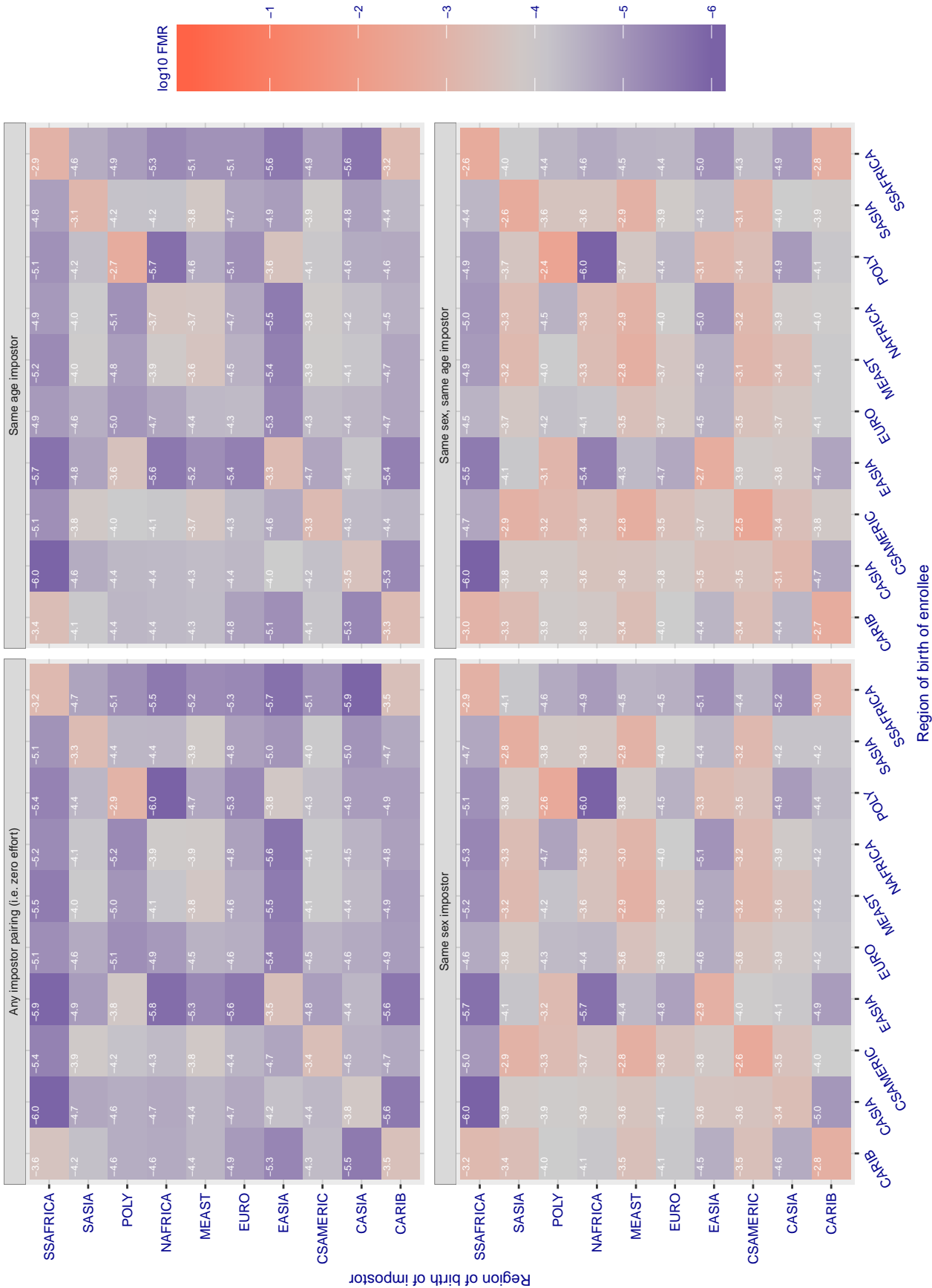


Figure 173: For algorithm remarkai-001 operating on visa images, the heatmap shows false match rates observed over impostor comparisons of faces from different individuals who were born in the given region pair. False matches are counted against a recognition threshold fixed globally to give the target FMR in the plot title, computed over all on the order of 10^{10} impostor comparisons. If text appears in each box it give the same quantity as that coded by the color. Grey indicates FMR is at the intended FMR target level. Light red colors present a security vulnerability to, for example, a passport gate. Each +1 increase in \log_{10} FMR corresponds to a factor of 10 increase in FMR. The matrix is not quite symmetric because images in the enrollment and verification sets are different.

Cross region FMR at threshold $T = 0.682$ for algorithm safe_001, giving $FMR(T) = 0.0001$ globally.

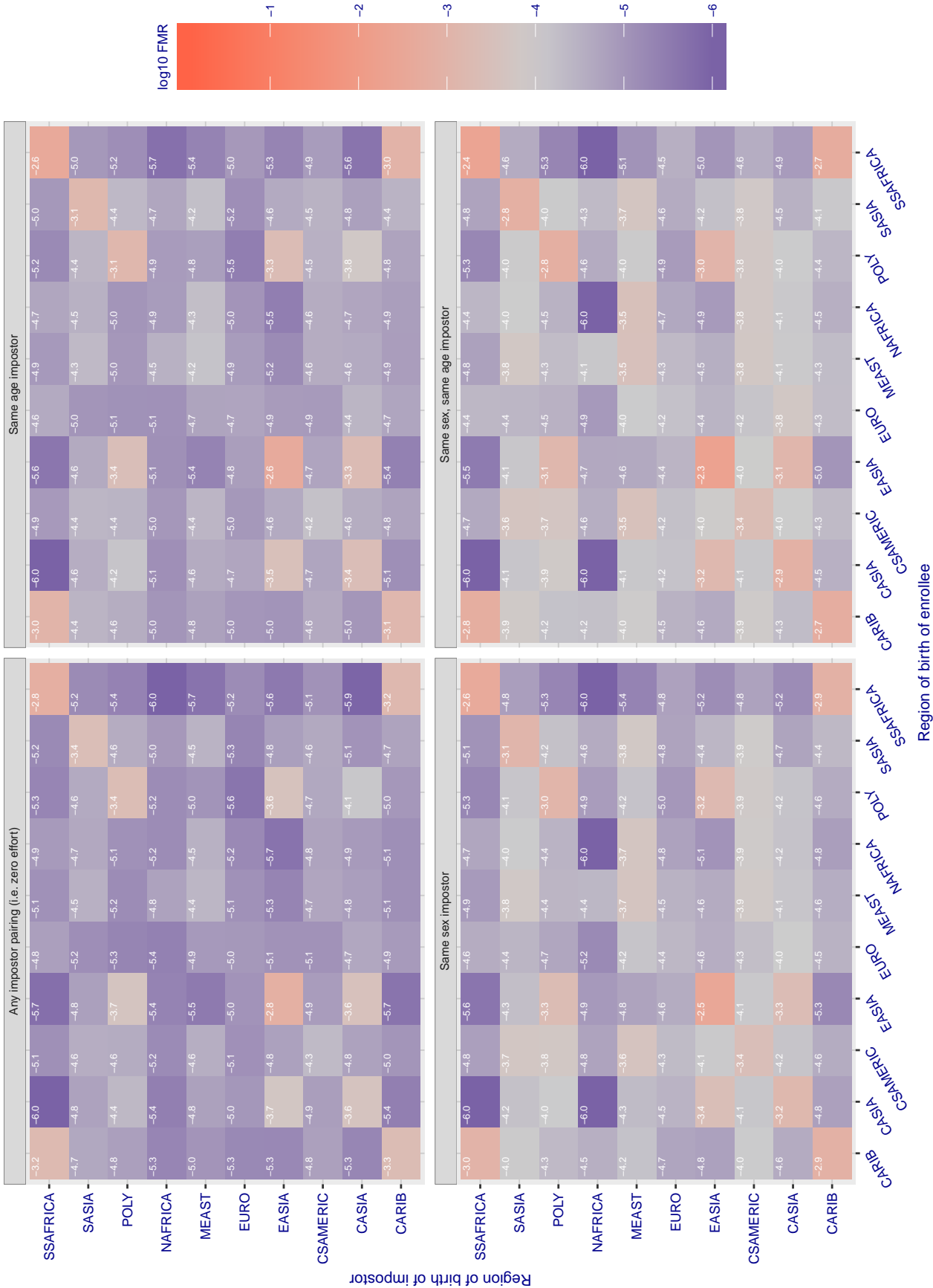


Figure 174: For algorithm safe-001 operating on visa images, the heatmap shows false match rates observed over impostor comparisons of faces from different individuals who were born in the given region pair. False matches are counted against a recognition threshold fixed globally to give the target FMR in the plot title, computed over all on the order of 10^{10} impostor comparisons. If text appears in each box it give the same quantity as that coded by the color. Grey indicates FMR is at the intended FMR target level. Light red colors present a security vulnerability to, for example, a passport gate. Each +1 increase in \log_{10} FMR corresponds to a factor of 10 increase in FMR. The matrix is not quite symmetric because images in the enrollment and verification sets are different.

Cross region FMR at threshold $T = 0.383$ for algorithm safe_002, giving $FMR(T) = 0.0001$ globally.

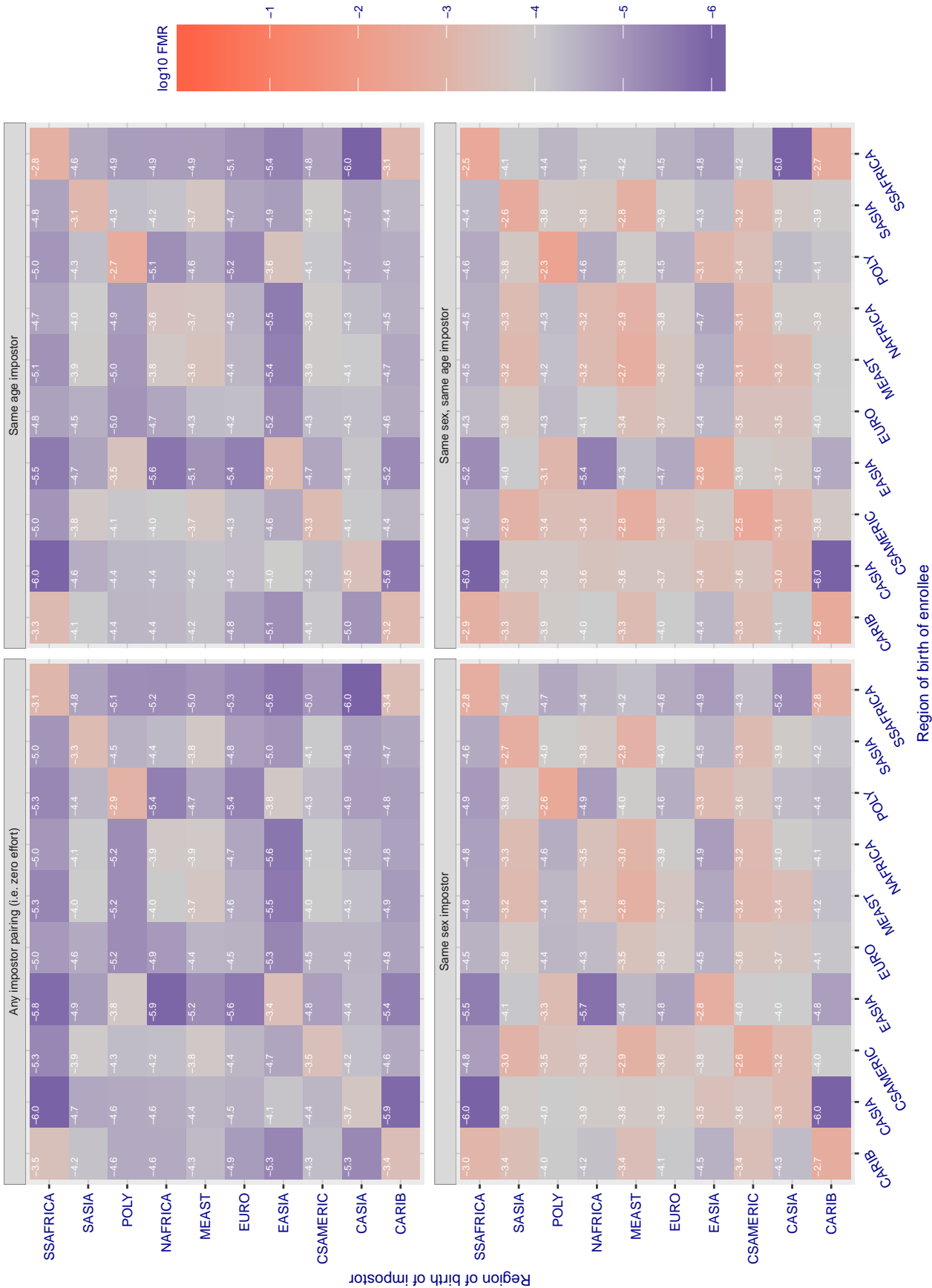


Figure 175: For algorithm safe-002 operating on visa images, the heatmap shows false match rates observed over impostor comparisons of faces from different individuals who were born in the given region pair. False matches are counted against a recognition threshold fixed globally to give the target FMR in the plot title, computed over all on the order of 10^{10} impostor comparisons. If text appears in each box it give the same quantity as that coded by the color. Grey indicates FMR is at the intended FMR target level. Light red colors present a security vulnerability to, for example, a passport gate. Each +1 increase in \log_{10} FMR corresponds to a factor of 10 increase in FMR. The matrix is not quite symmetric because images in the enrollment and verification sets are different.

Cross region FMR at threshold $T = 0.390$ for algorithm `sensetime_001`, giving $FMR(T) = 0.0001$ globally.

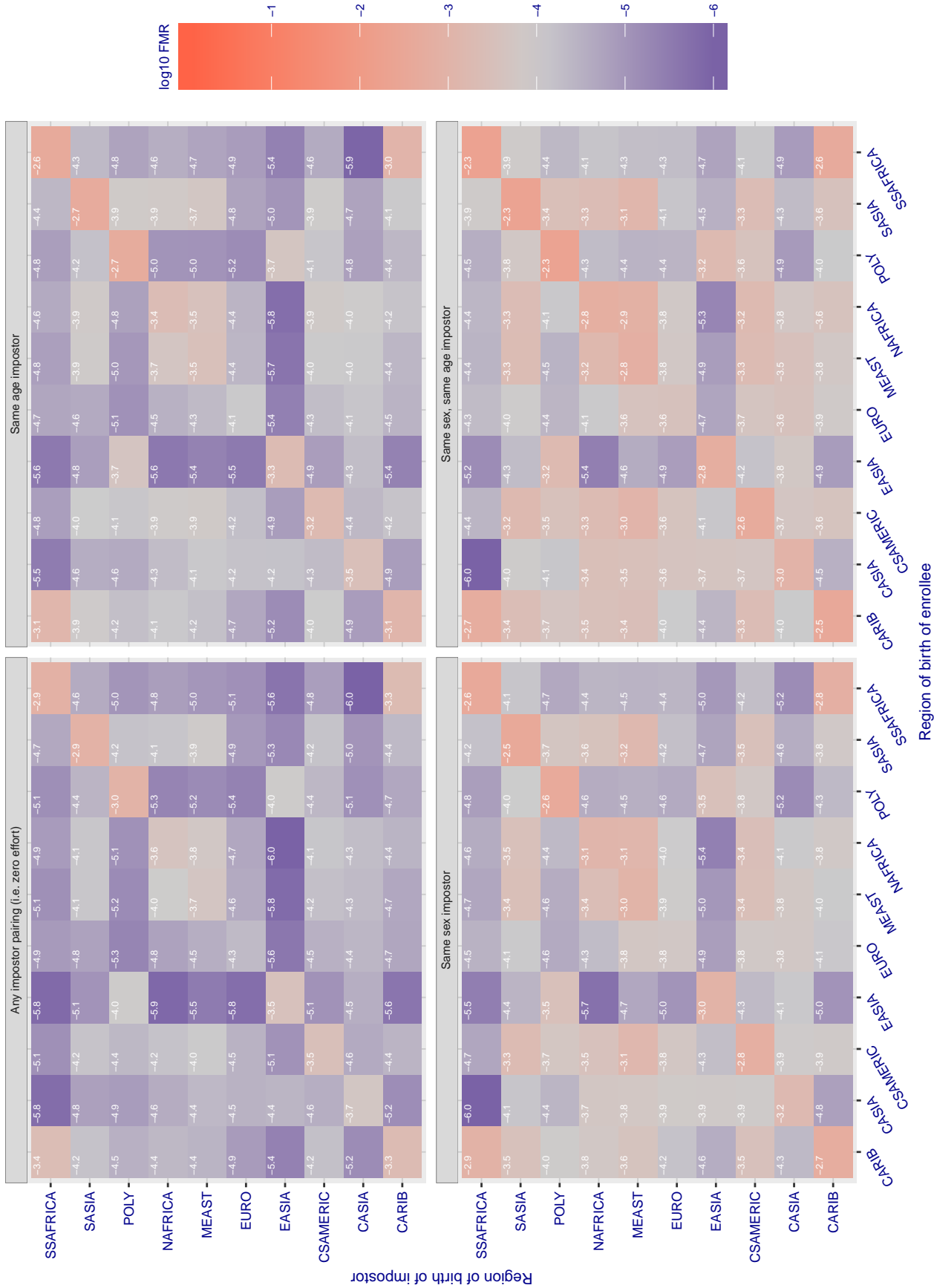


Figure 176: For algorithm `sensetime-001` operating on visa images, the heatmap shows false match rates observed over impostor comparisons of faces from different individuals who were born in the given region pair. False matches are counted against a recognition threshold fixed globally to give the target FMR in the plot title, computed over all on the order of 10^{10} impostor comparisons. If text appears in each box it give the same quantity as that coded by the color. Grey indicates FMR is at the intended FMR target level. Light red colors present a security vulnerability to, for example, a passport gate. Each +1 increase in \log_{10} FMR corresponds to a factor of 10 increase in FMR. The matrix is not quite symmetric because images in the enrollment and verification sets are different.

Cross region FMR at threshold $T = 0.390$ for algorithm `sensetime_002`, giving $FMR(T) = 0.0001$ globally.

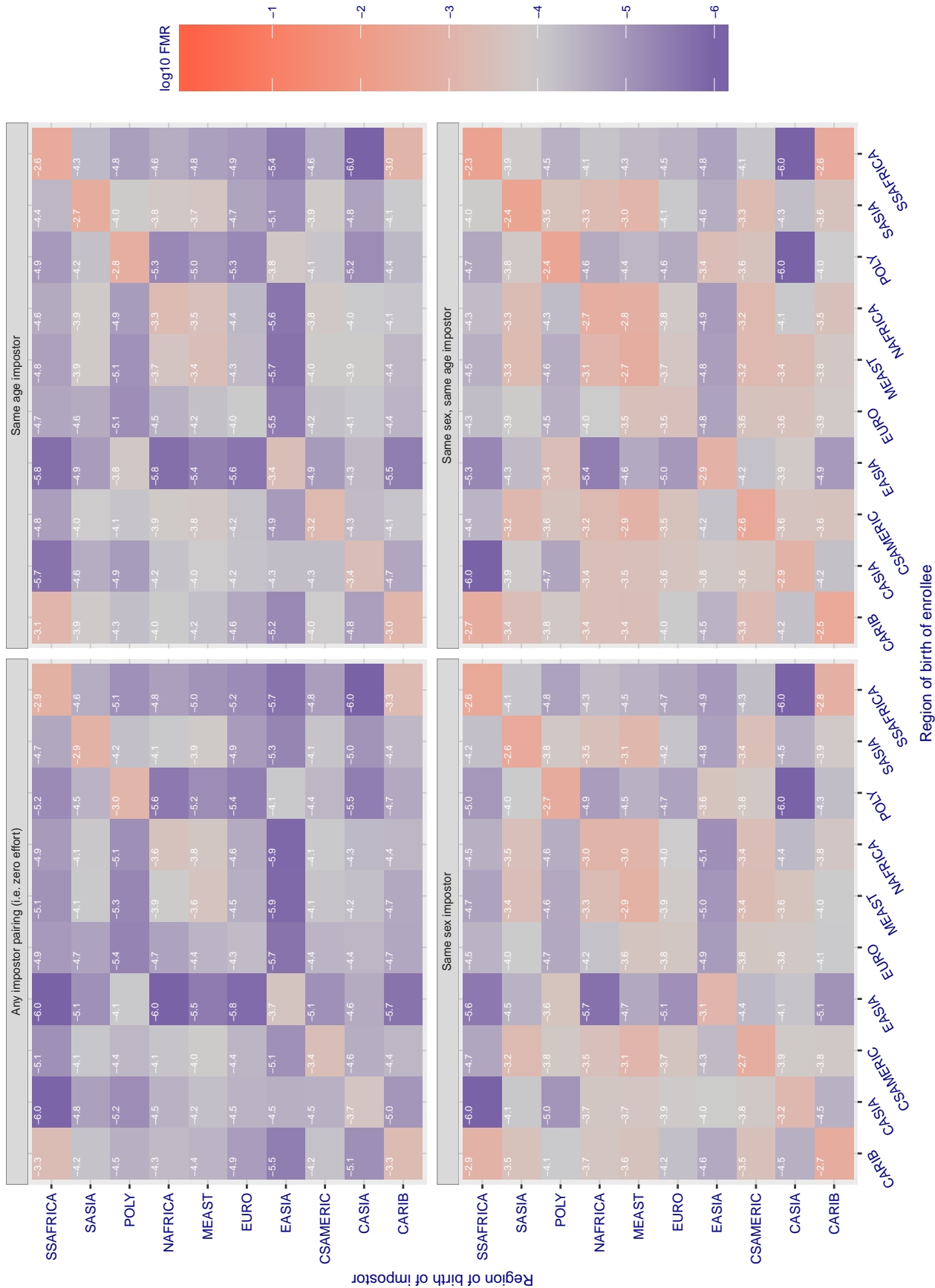


Figure 177: For algorithm `sensetime-002` operating on visa images, the heatmap shows false match rates observed over impostor comparisons of faces from different individuals who were born in the given region pair. False matches are counted against a recognition threshold fixed globally to give the target FMR in the plot title, computed over all on the order of 10^{10} impostor comparisons. If text appears in each box it give the same quantity as that coded by the color. Grey indicates FMR is at the intended FMR target level. Light red colors present a security vulnerability to, for example, a passport gate. Each +1 increase in \log_{10} FMR corresponds to a factor of 10 increase in FMR. The matrix is not quite symmetric because images in the enrollment and verification sets are different.

Cross region FMR at threshold $T = 0.970$ for algorithm shaman_000, giving $FMR(T) = 0.0001$ globally.

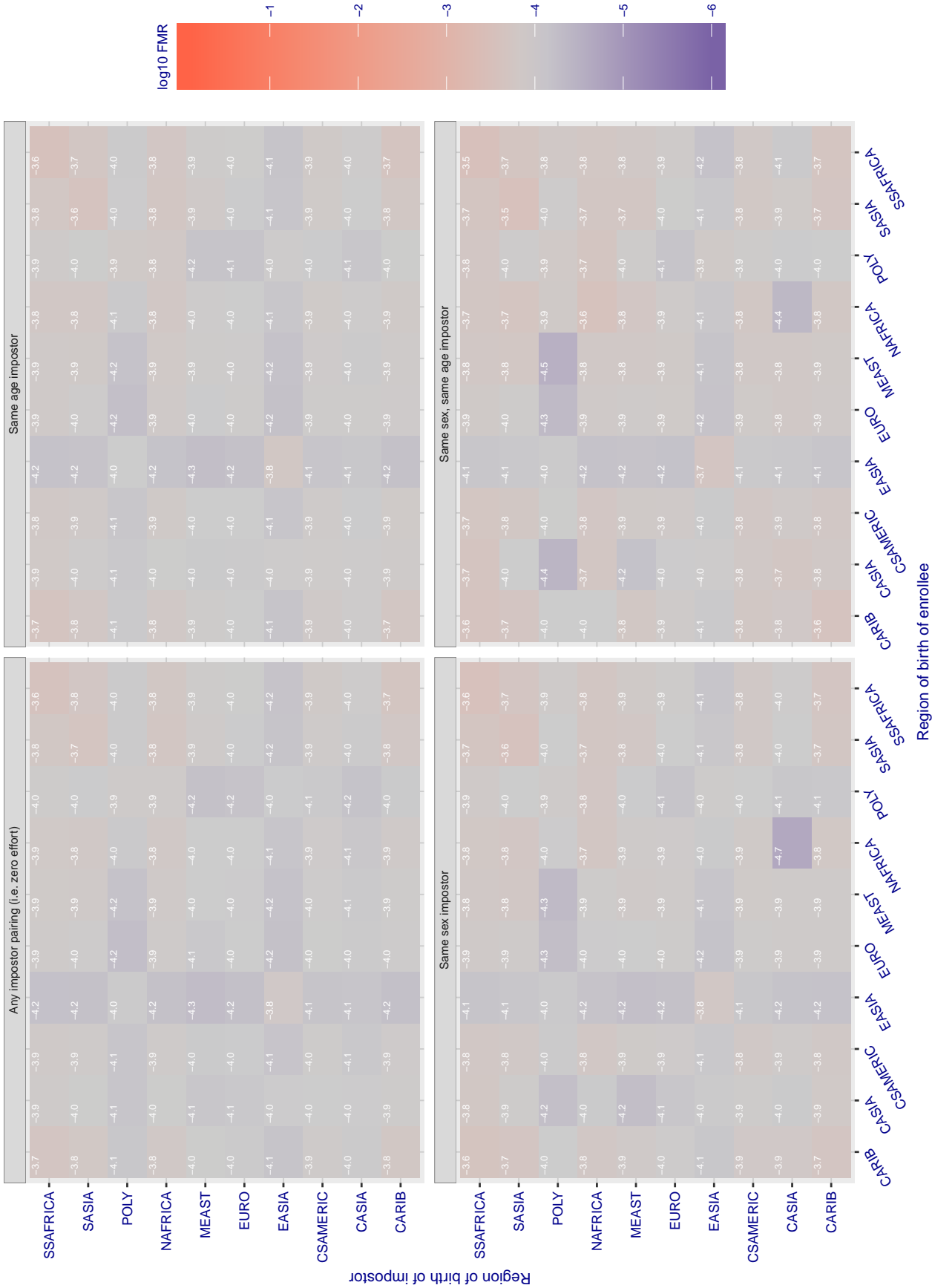


Figure 178: For algorithm shaman-000 operating on visa images, the heatmap shows false match rates observed over impostor comparisons of faces from different individuals who were born in the given region pair. False matches are counted against a recognition threshold fixed globally to give the target FMR in the plot title, computed over all on the order of 10^{10} impostor comparisons. If text appears in each box it give the same quantity as that coded by the color. Grey indicates FMR is at the intended FMR target level. Light red colors present a security vulnerability to, for example, a passport gate. Each +1 increase in \log_{10} FMR corresponds to a factor of 10 increase in FMR. The matrix is not quite symmetric because images in the enrollment and verification sets are different.

Cross region FMR at threshold $T = 0.725$ for algorithm shaman_001, giving $FMR(T) = 0.0001$ globally.

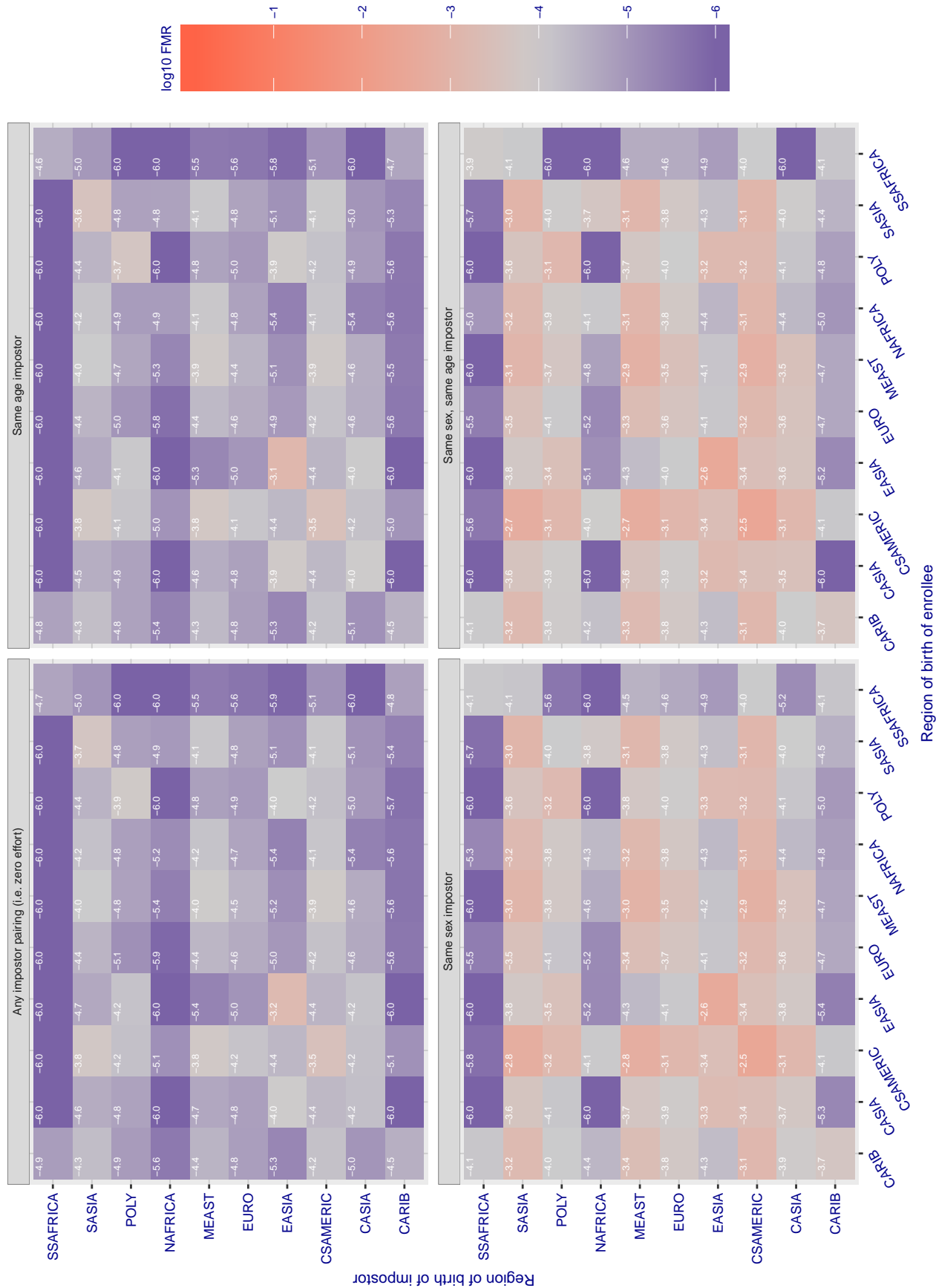


Figure 179: For algorithm shaman-001 operating on visa images, the heatmap shows false match rates observed over impostor comparisons of faces from different individuals who were born in the given region pair. False matches are counted against a recognition threshold fixed globally to give the target FMR in the plot title, computed over all on the order of 10^{10} impostor comparisons. If text appears in each box it give the same quantity as that coded by the color. Grey indicates FMR is at the intended FMR target level. Light red colors present a security vulnerability to, for example, a passport gate. Each +1 increase in \log_{10} FMR corresponds to a factor of 10 increase in FMR. The matrix is not quite symmetric because images in the enrollment and verification sets are different.

Cross region FMR at threshold $T = 0.390$ for algorithm `siat_002`, giving $FMR(T) = 0.0001$ globally.

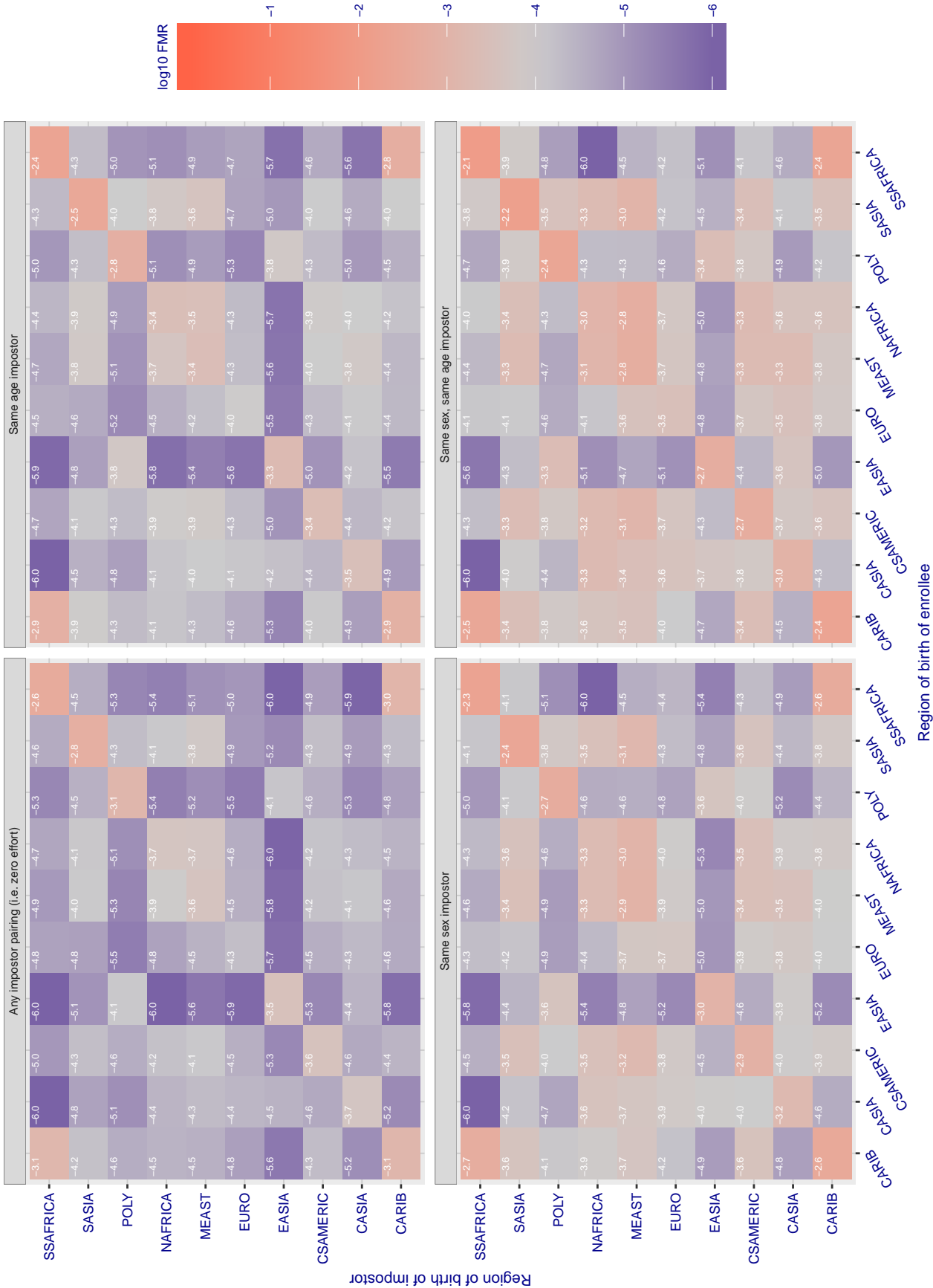


Figure 180: For algorithm `siat-002` operating on visa images, the heatmap shows false match rates observed over impostor comparisons of faces from different individuals who were born in the given region pair. False matches are counted against a recognition threshold fixed globally to give the target FMR in the plot title, computed over all on the order of 10^{10} impostor comparisons. If text appears in each box it give the same quantity as that coded by the color. Grey indicates FMR is at the intended FMR target level. Light red colors present a security vulnerability to, for example, a passport gate. Each +1 increase in \log_{10} FMR corresponds to a factor of 10 increase in FMR. The matrix is not quite symmetric because images in the enrollment and verification sets are different.

Cross region FMR at threshold $T = 0.393$ for algorithm `siat_004`, giving $FMR(T) = 0.0001$ globally.

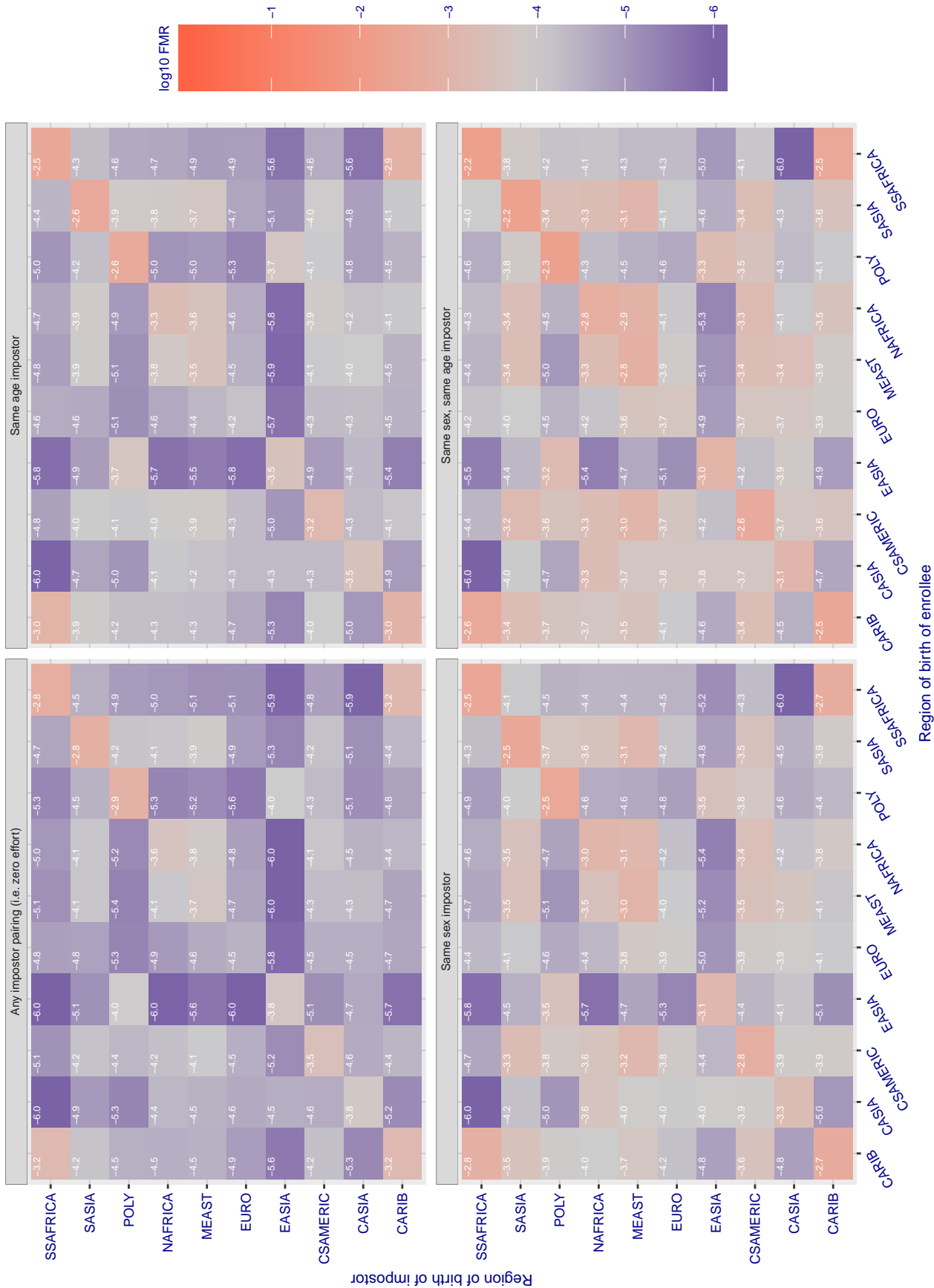


Figure 181: For algorithm `siat-004` operating on visa images, the heatmap shows false match rates observed over impostor comparisons of faces from different individuals who were born in the given region pair. False matches are counted against a recognition threshold fixed globally to give the target FMR in the plot title, computed over all on the order of 10^{10} impostor comparisons. If text appears in each box it give the same quantity as that coded by the color. Grey indicates FMR is at the intended FMR target level. Light red colors present a security vulnerability to, for example, a passport gate. Each +1 increase in \log_{10} FMR corresponds to a factor of 10 increase in FMR. The matrix is not quite symmetric because images in the enrollment and verification sets are different.

Cross region FMR at threshold $T = 0.598$ for algorithm `smilart_002`, giving $FMR(T) = 0.0001$ globally.

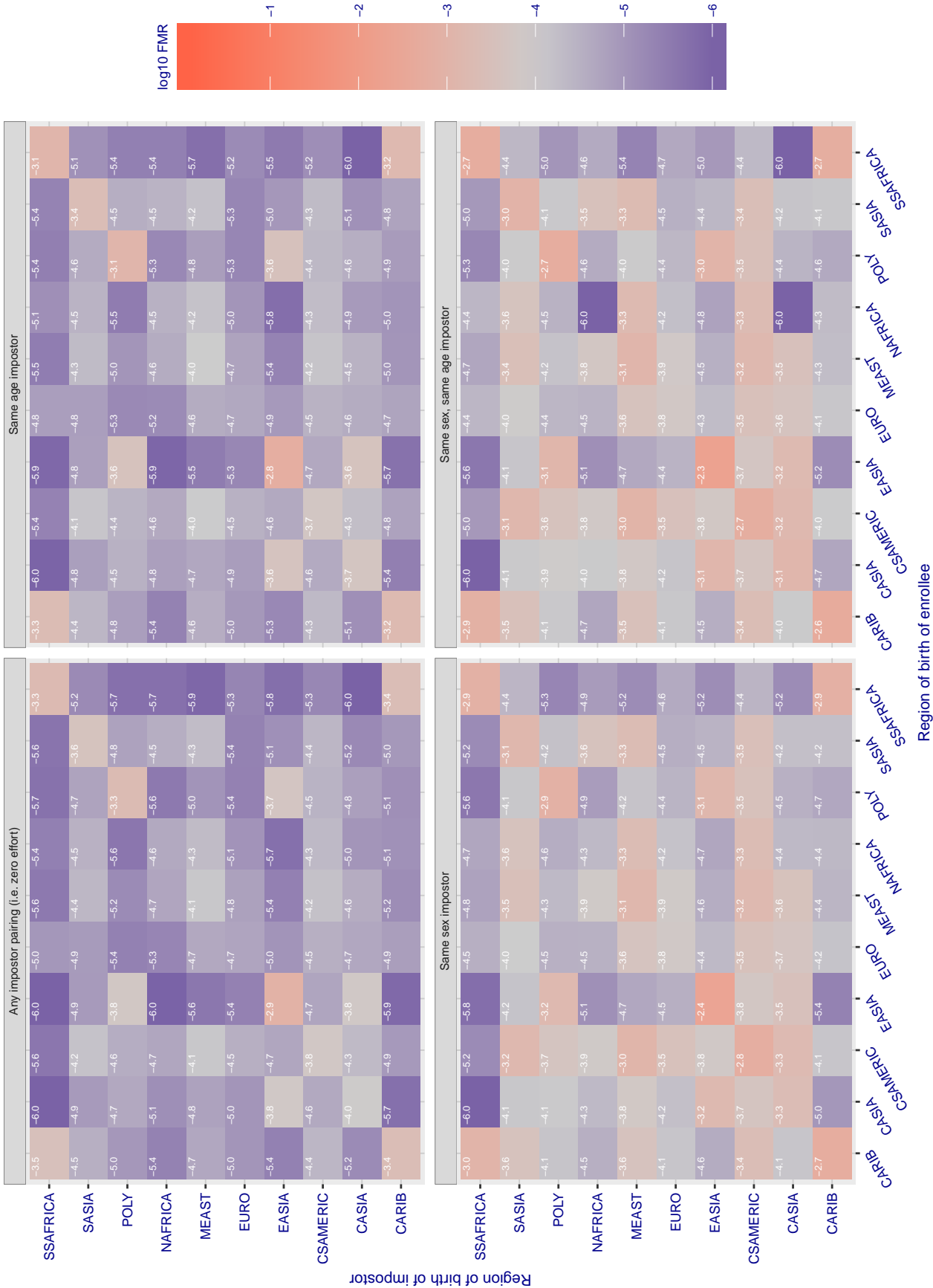


Figure 182: For algorithm `smilart-002` operating on visa images, the heatmap shows false match rates observed over impostor comparisons of faces from different individuals who were born in the given region pair. False matches are counted against a recognition threshold fixed globally to give the target FMR in the plot title, computed over all on the order of 10^{10} impostor comparisons. If text appears in each box it give the same quantity as that coded by the color. Grey indicates FMR is at the intended FMR target level. Light red colors present a security vulnerability to, for example, a passport gate. Each +1 increase in \log_{10} FMR corresponds to a factor of 10 increase in FMR. The matrix is not quite symmetric because images in the enrollment and verification sets are different.

Cross region FMR at threshold $T = 0.654$ for algorithm `smilart_003`, giving $FMR(T) = 0.0001$ globally.

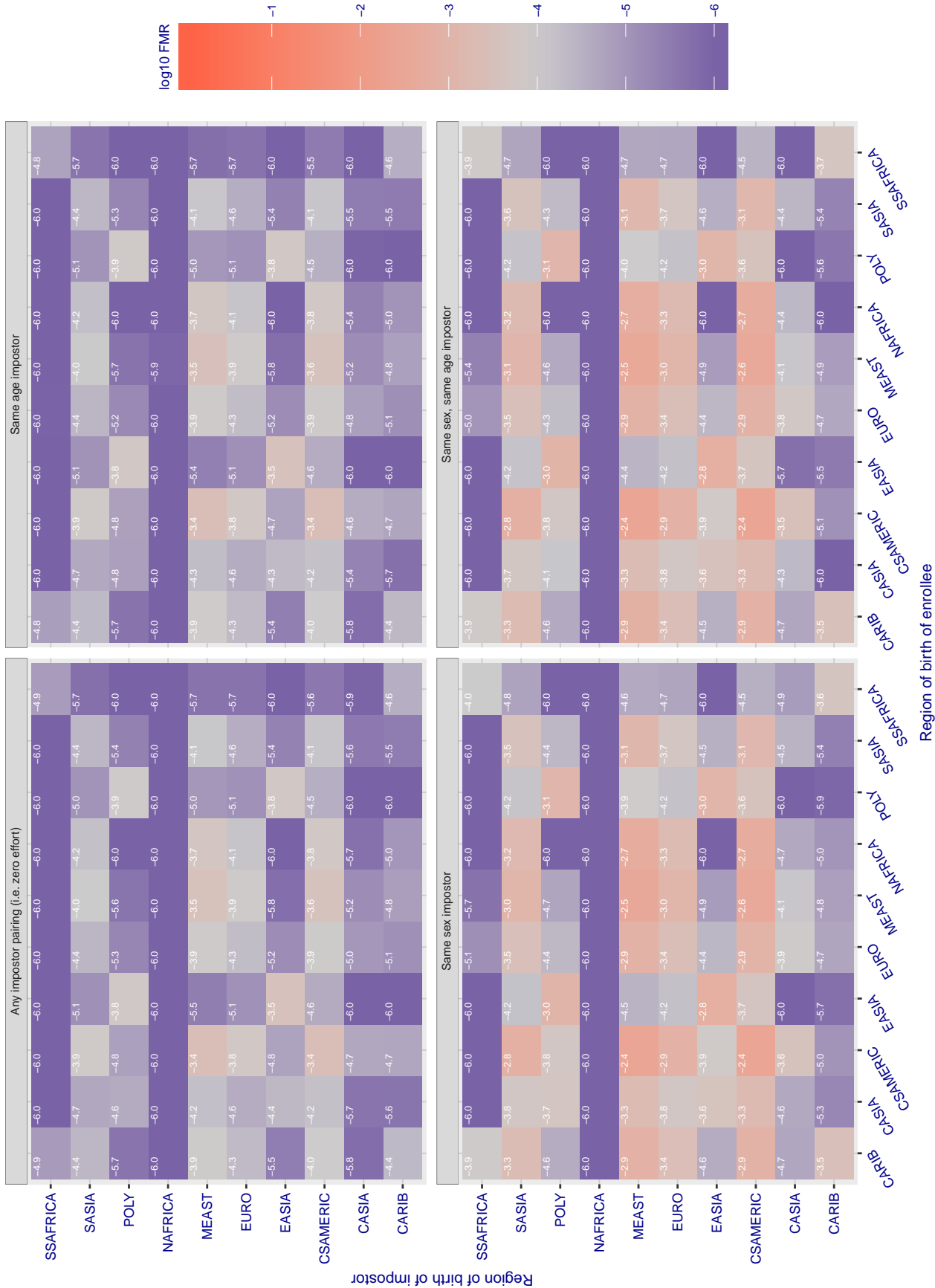


Figure 183: For algorithm `smilart-003` operating on visa images, the heatmap shows false match rates observed over impostor comparisons of faces from different individuals who were born in the given region pair. False matches are counted against a recognition threshold fixed globally to give the target FMR in the plot title, computed over all on the order of 10^{10} impostor comparisons. If text appears in each box it give the same quantity as that coded by the color. Grey indicates FMR is at the intended FMR target level. Light red colors present a security vulnerability to, for example, a passport gate. Each +1 increase in \log_{10} FMR corresponds to a factor of 10 increase in FMR. The matrix is not quite symmetric because images in the enrollment and verification sets are different.

Cross region FMR at threshold $T = 0.881$ for algorithm synthesis_003, giving $FMR(T) = 0.0001$ globally.

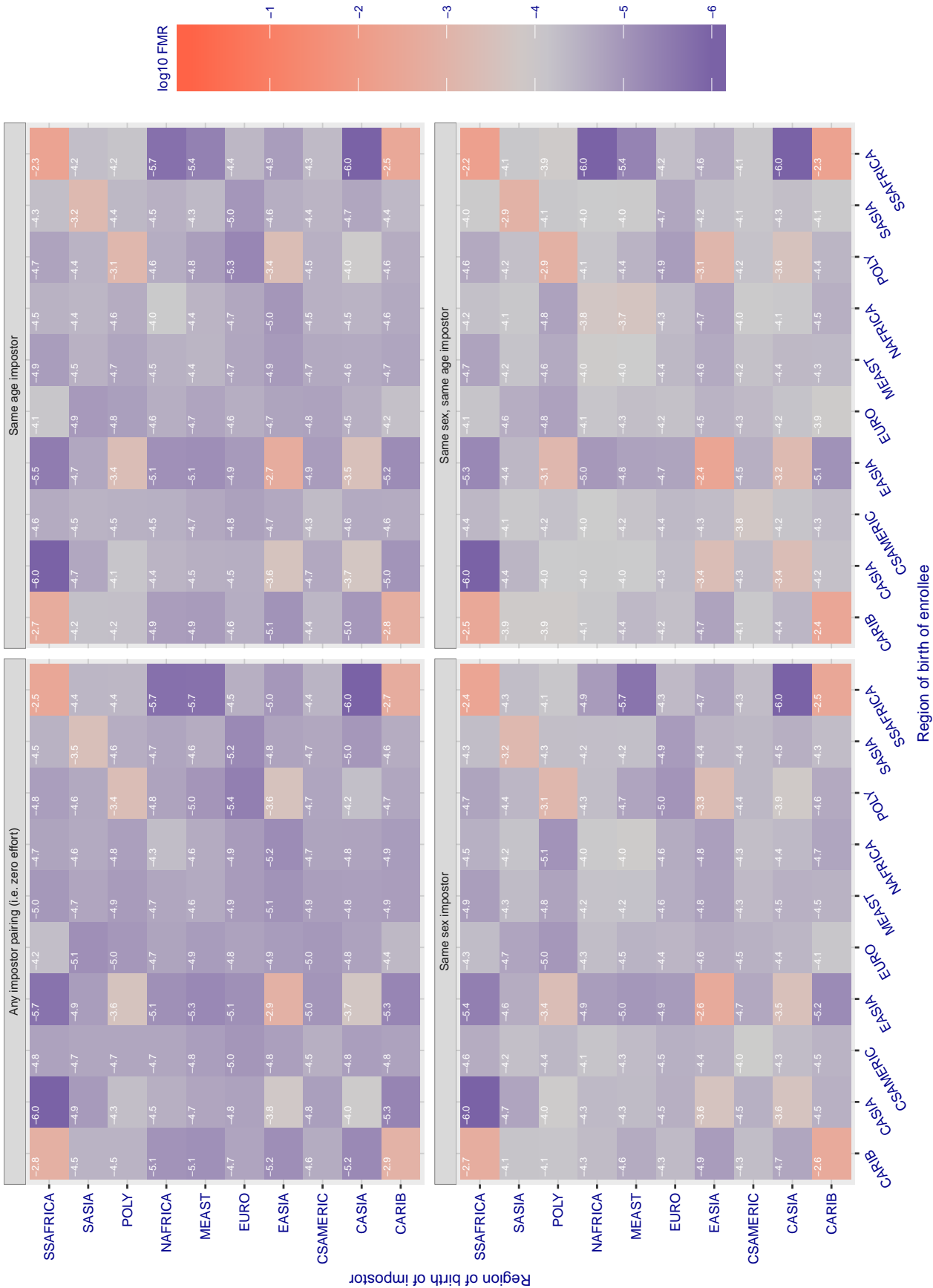


Figure 184: For algorithm synthesis-003 operating on visa images, the heatmap shows false match rates observed over impostor comparisons of faces from different individuals who were born in the given region pair. False matches are counted against a recognition threshold fixed globally to give the target FMR in the plot title, computed over all on the order of 10^{10} impostor comparisons. If text appears in each box it give the same quantity as that coded by the color. Grey indicates FMR is at the intended FMR target level. Light red colors present a security vulnerability to, for example, a passport gate. Each +1 increase in log10 FMR corresponds to a factor of 10 increase in FMR. The matrix is not quite symmetric because images in the enrollment and verification sets are different.

Cross region FMR at threshold $T = 0.221$ for algorithm synthesis_004, giving $FMR(T) = 0.0001$ globally.

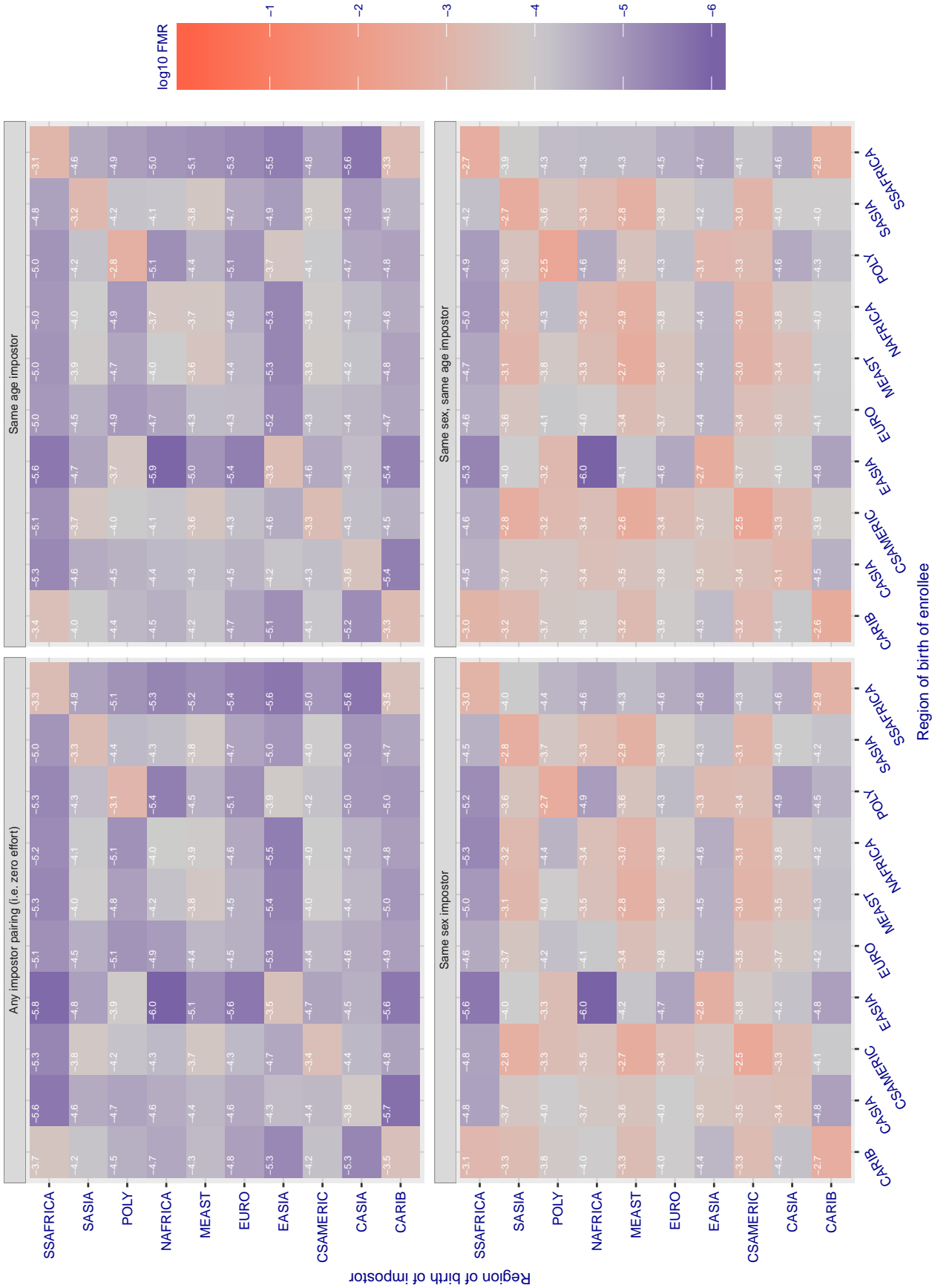


Figure 185: For algorithm synthesis-004 operating on visa images, the heatmap shows false match rates observed over impostor comparisons of faces from different individuals who were born in the given region pair. False matches are counted against a recognition threshold fixed globally to give the target FMR in the plot title, computed over all on the order of 10^{10} impostor comparisons. If text appears in each box it give the same quantity as that coded by the color. Grey indicates FMR is at the intended FMR target level. Light red colors present a security vulnerability to, for example, a passport gate. Each +1 increase in \log_{10} FMR corresponds to a factor of 10 increase in FMR. The matrix is not quite symmetric because images in the enrollment and verification sets are different.

Cross region FMR at threshold T = 148.416 for algorithm tech5_001, giving FMR(T) = 0.0001 globally.

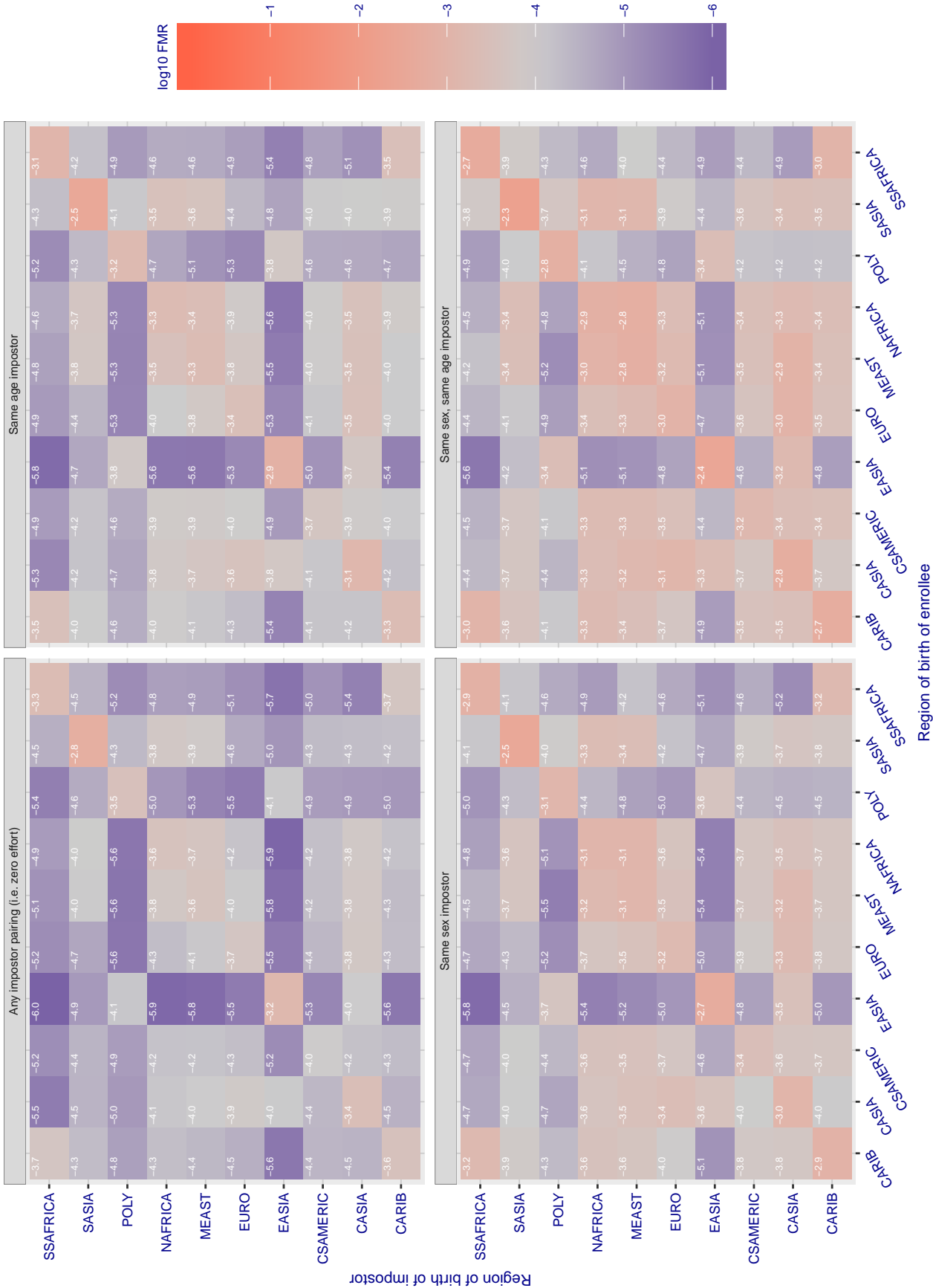


Figure 186: For algorithm tech5-001 operating on visa images, the heatmap shows false match rates observed over impostor comparisons of faces from different individuals who were born in the given region pair. False matches are counted against a recognition threshold fixed globally to give the target FMR in the plot title, computed over all on the order of 10^{10} impostor comparisons. If text appears in each box it give the same quantity as that coded by the color. Grey indicates FMR is at the intended FMR target level. Light red colors present a security vulnerability to, for example, a passport gate. Each +1 increase in \log_{10} FMR corresponds to a factor of 10 increase in FMR. The matrix is not quite symmetric because images in the enrollment and verification sets are different.

Cross region FMR at threshold $T = 147.661$ for algorithm tech5_002, giving $FMR(T) = 0.0001$ globally.

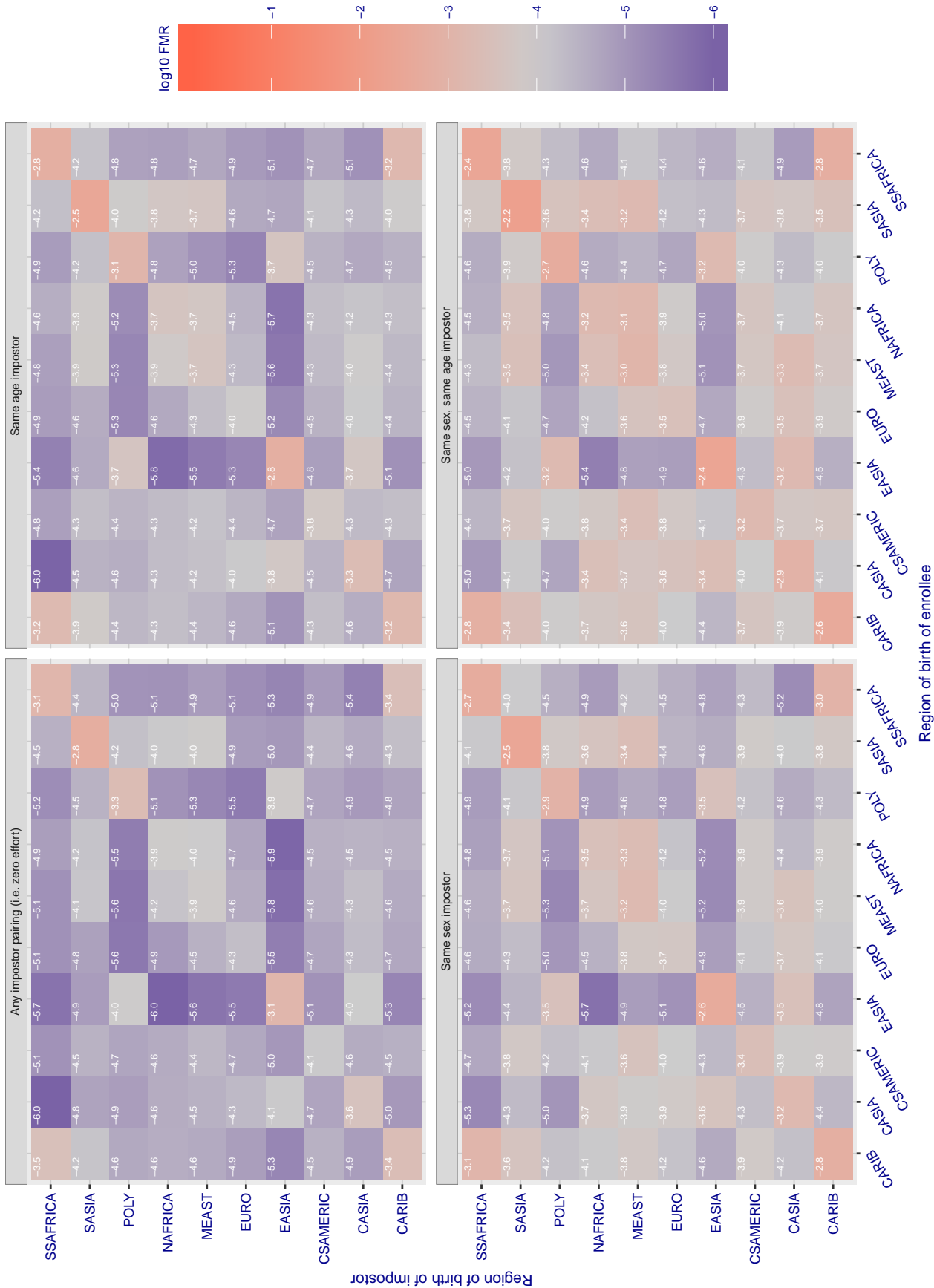


Figure 187: For algorithm tech5-002 operating on visa images, the heatmap shows false match rates observed over impostor comparisons of faces from different individuals who were born in the given region pair. False matches are counted against a recognition threshold fixed globally to give the target FMR in the plot title, computed over all on the order of 10^{10} impostor comparisons. If text appears in each box it give the same quantity as that coded by the color. Grey indicates FMR is at the intended FMR target level. Light red colors present a security vulnerability to, for example, a passport gate. Each +1 increase in log10 FMR corresponds to a factor of 10 increase in FMR. The matrix is not quite symmetric because images in the enrollment and verification sets are different.

Cross region FMR at threshold $T = 0.896$ for algorithm `tevian_003`, giving $FMR(T) = 0.0001$ globally.

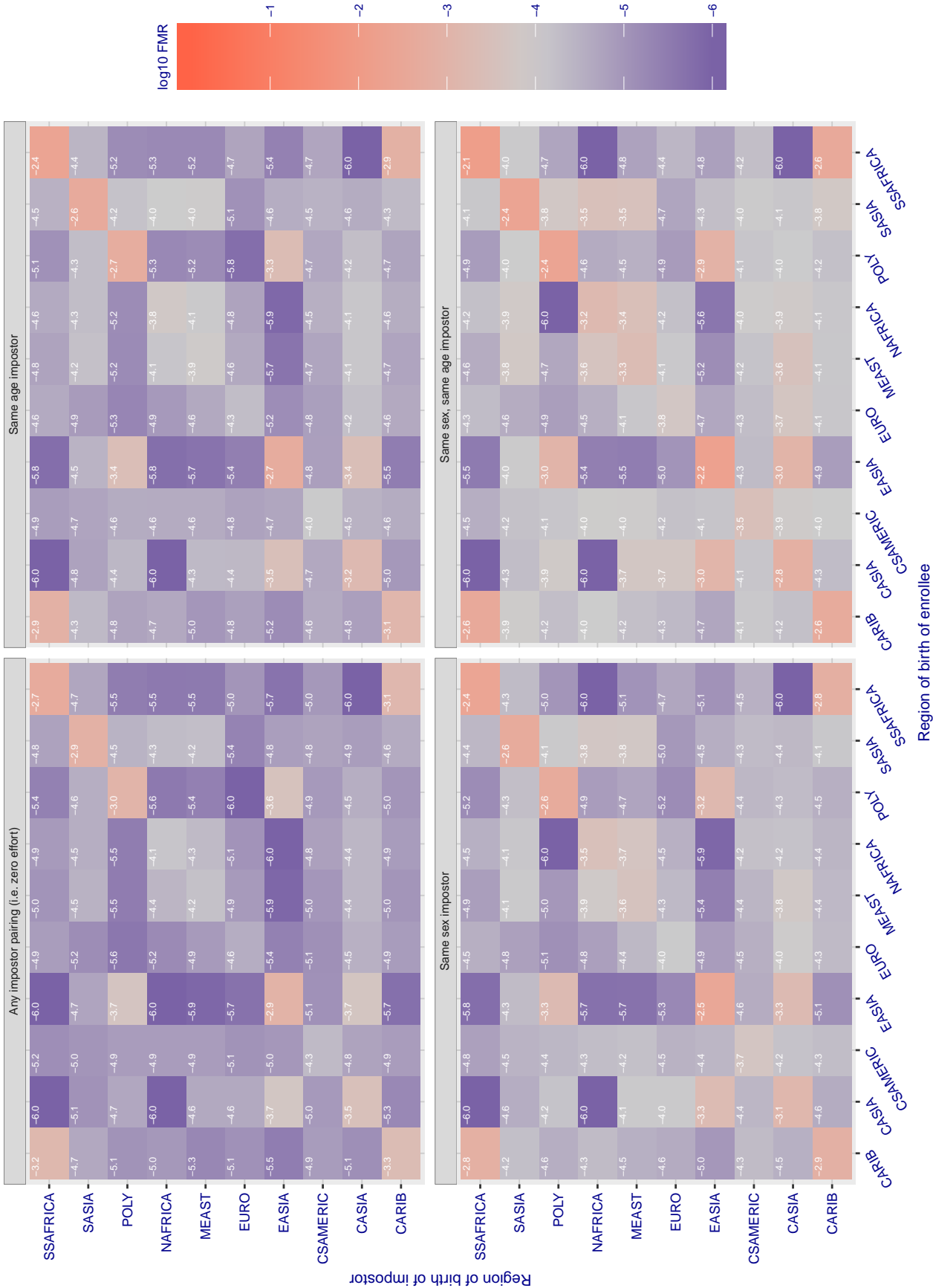


Figure 188: For algorithm `tevian-003` operating on visa images, the heatmap shows false match rates observed over impostor comparisons of faces from different individuals who were born in the given region pair. False matches are counted against a recognition threshold fixed globally to give the target FMR in the plot title, computed over all on the order of 10^{10} impostor comparisons. If text appears in each box it give the same quantity as that coded by the color. Grey indicates FMR is at the intended FMR target level. Light red colors present a security vulnerability to, for example, a passport gate. Each +1 increase in \log_{10} FMR corresponds to a factor of 10 increase in FMR. The matrix is not quite symmetric because images in the enrollment and verification sets are different.

Cross region FMR at threshold $T = 0.896$ for algorithm `tevia_004`, giving $FMR(T) = 0.0001$ globally.

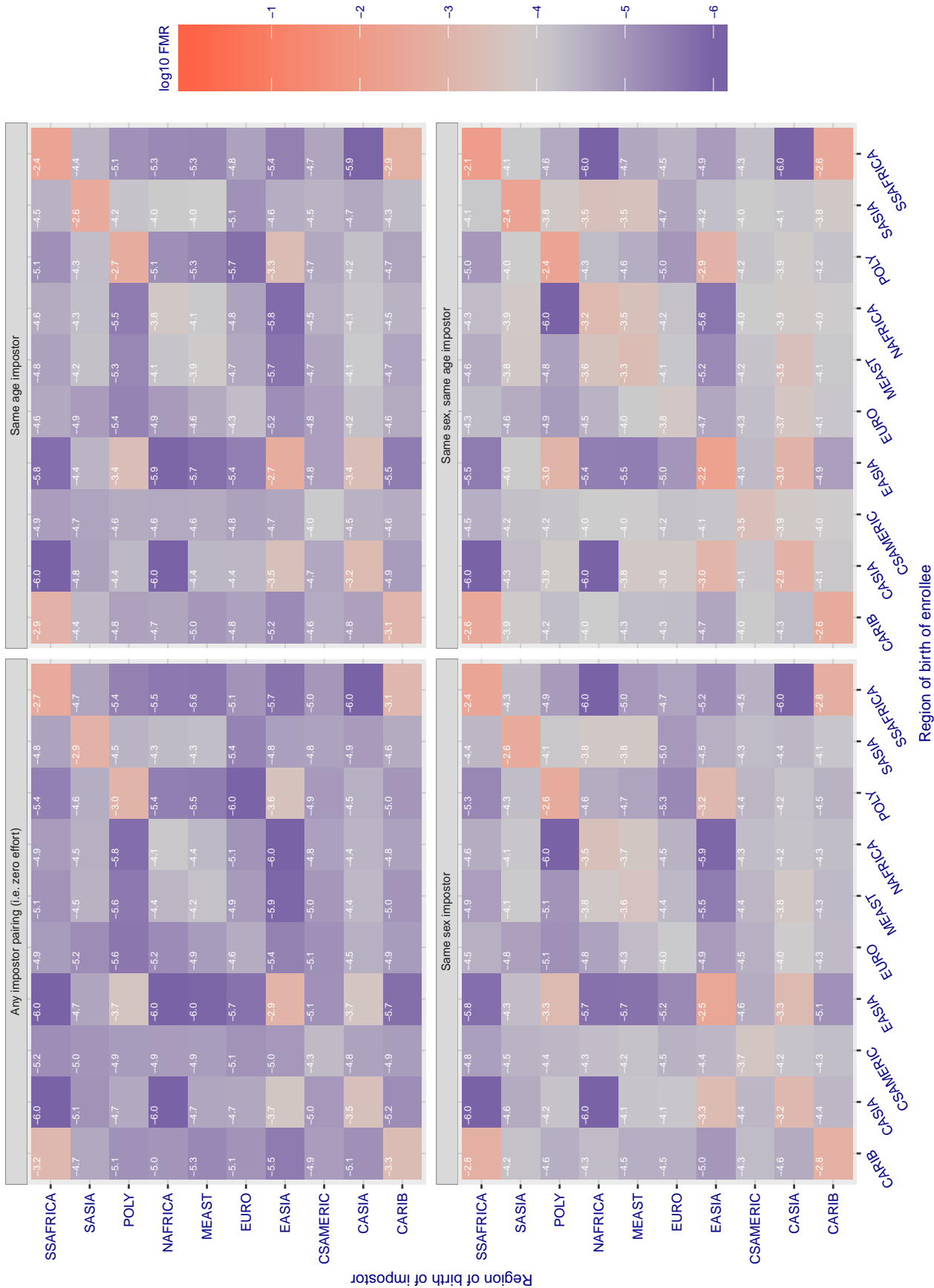


Figure 189: For algorithm `tevia-004` operating on visa images, the heatmap shows false match rates observed over impostor comparisons of faces from different individuals who were born in the given region pair. False matches are counted against a recognition threshold fixed globally to give the target FMR in the plot title, computed over all on the order of 10^{10} impostor comparisons. If text appears in each box it give the same quantity as that coded by the color. Grey indicates FMR is at the intended FMR target level. Light red colors present a security vulnerability to, for example, a passport gate. Each +1 increase in \log_{10} FMR corresponds to a factor of 10 increase in FMR. The matrix is not quite symmetric because images in the enrollment and verification sets are different.

Cross region FMR at threshold $T = 151.011$ for algorithm tiger_002, giving $FMR(T) = 0.0001$ globally.

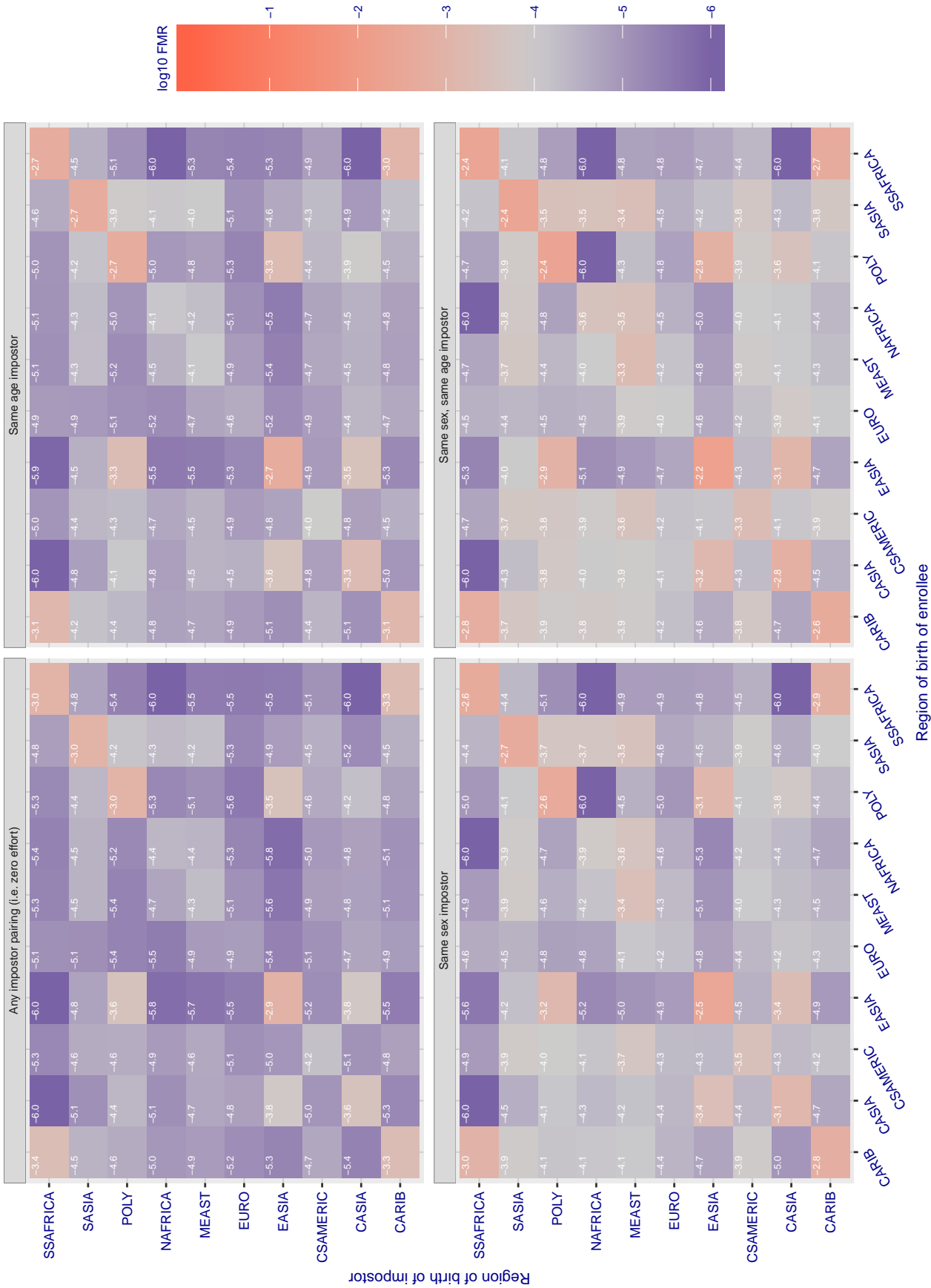


Figure 190: For algorithm tiger-002 operating on visa images, the heatmap shows false match rates observed over impostor comparisons of faces from different individuals who were born in the given region pair. False matches are counted against a recognition threshold fixed globally to give the target FMR in the plot title, computed over all on the order of 10^{10} impostor comparisons. If text appears in each box it give the same quantity as that coded by the color. Grey indicates FMR is at the intended FMR target level. Light red colors present a security vulnerability to, for example, a passport gate. Each +1 increase in \log_{10} FMR corresponds to a factor of 10 increase in FMR. The matrix is not quite symmetric because images in the enrollment and verification sets are different.

Cross region FMR at threshold $T = 149.313$ for algorithm tiger_003, giving $FMR(T) = 0.0001$ globally.

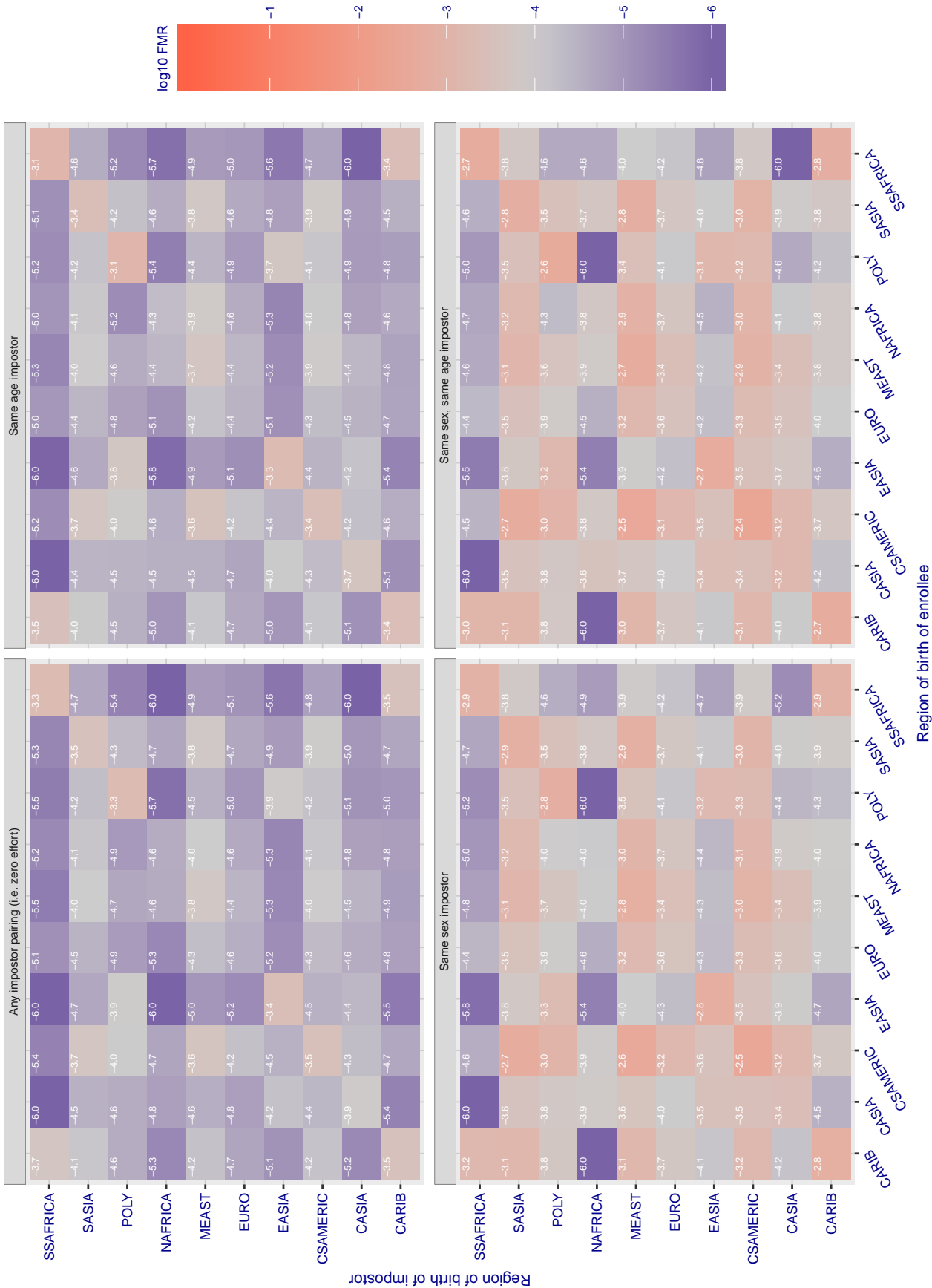


Figure 191: For algorithm tiger-003 operating on visa images, the heatmap shows false match rates observed over impostor comparisons of faces from different individuals who were born in the given region pair. False matches are counted against a recognition threshold fixed globally to give the target FMR in the plot title, computed over all on the order of 10^{10} impostor comparisons. If text appears in each box it give the same quantity as that coded by the color. Grey indicates FMR is at the intended FMR target level. Light red colors present a security vulnerability to, for example, a passport gate. Each +1 increase in \log_{10} FMR corresponds to a factor of 10 increase in FMR. The matrix is not quite symmetric because images in the enrollment and verification sets are different.

Cross region FMR at threshold $T = 0.628$ for algorithm toshiba_002, giving $FMR(T) = 0.0001$ globally.

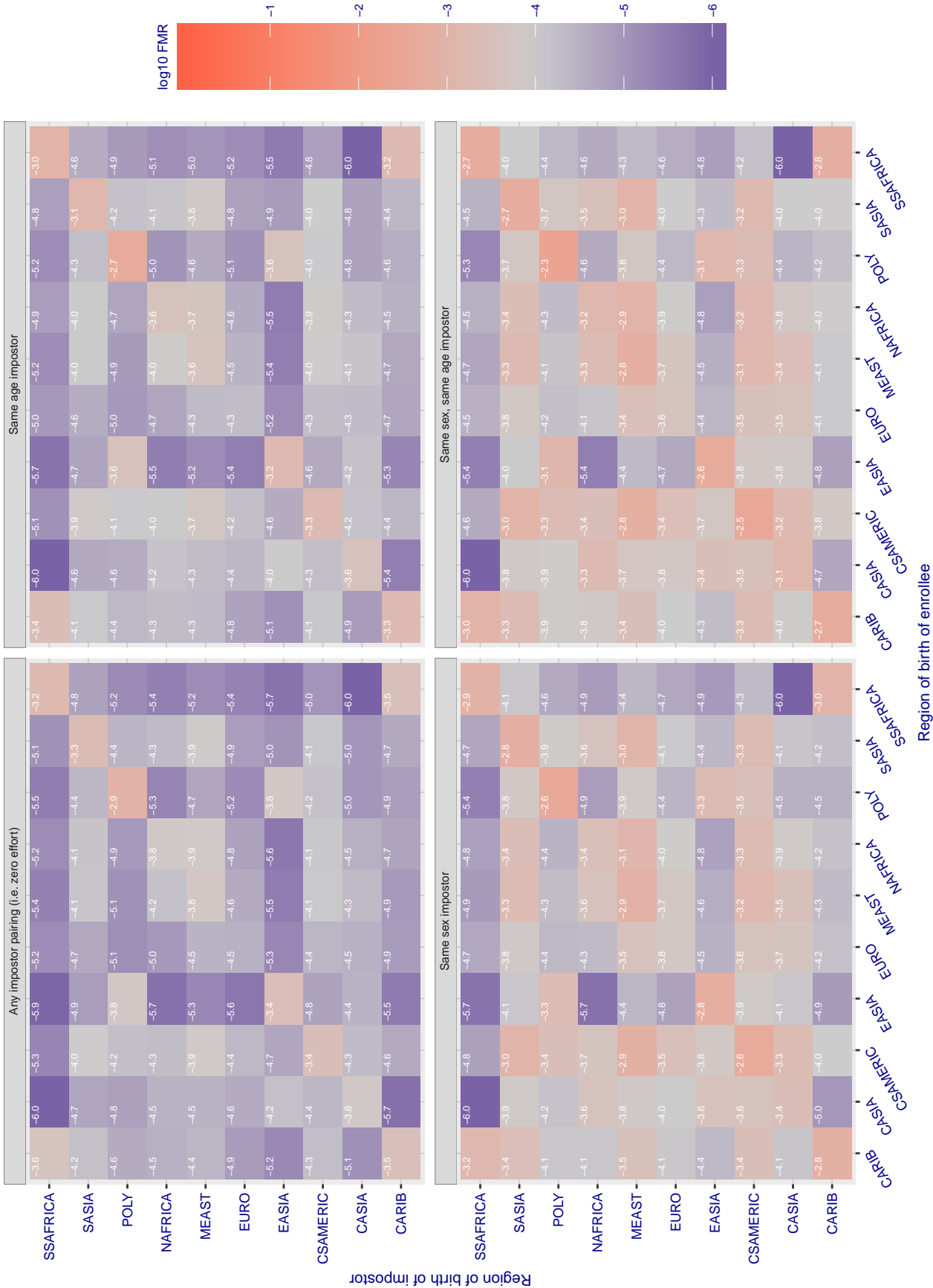


Figure 192: For algorithm toshiba-002 operating on visa images, the heatmap shows false match rates observed over impostor comparisons of faces from different individuals who were born in the given region pair. False matches are counted against a recognition threshold fixed globally to give the target FMR in the plot title, computed over all on the order of 10^{10} impostor comparisons. If text appears in each box it give the same quantity as that coded by the color. Grey indicates FMR is at the intended FMR target level. Light red colors present a security vulnerability to, for example, a passport gate. Each +1 increase in \log_{10} FMR corresponds to a factor of 10 increase in FMR. The matrix is not quite symmetric because images in the enrollment and verification sets are different.

Cross region FMR at threshold $T = 0.626$ for algorithm toshiba_003, giving $FMR(T) = 0.0001$ globally.

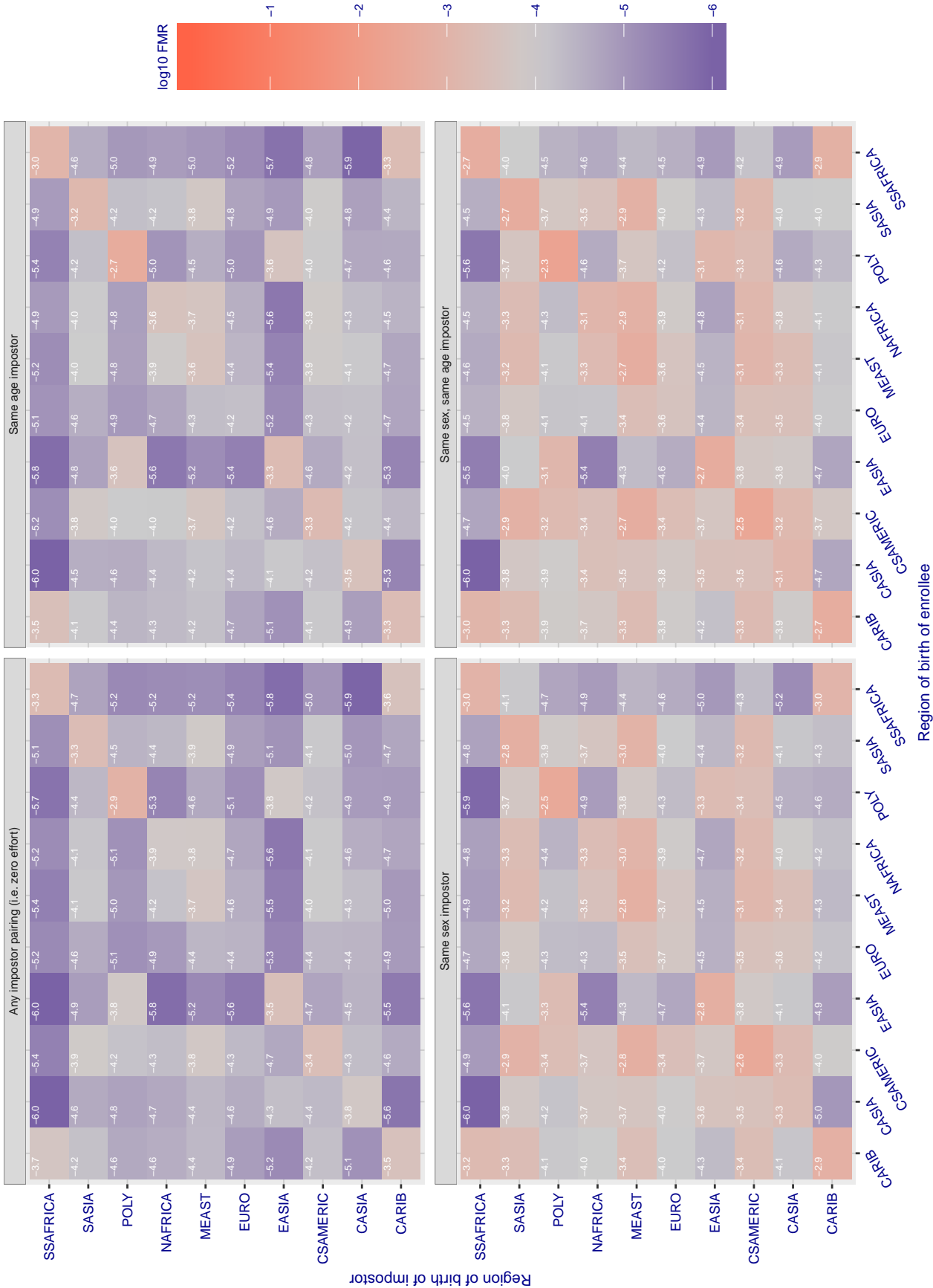


Figure 193: For algorithm toshiba-003 operating on visa images, the heatmap shows false match rates observed over impostor comparisons of faces from different individuals who were born in the given region pair. False matches are counted against a recognition threshold fixed globally to give the target FMR in the plot title, computed over all on the order of 10^{10} impostor comparisons. If text appears in each box it give the same quantity as that coded by the color. Grey indicates FMR is at the intended FMR target level. Light red colors present a security vulnerability to, for example, a passport gate. Each +1 increase in \log_{10} FMR corresponds to a factor of 10 increase in FMR. The matrix is not quite symmetric because images in the enrollment and verification sets are different.

Cross region FMR at threshold $T = 0.428$ for algorithm vcog_002, giving $FMR(T) = 0.0001$ globally.

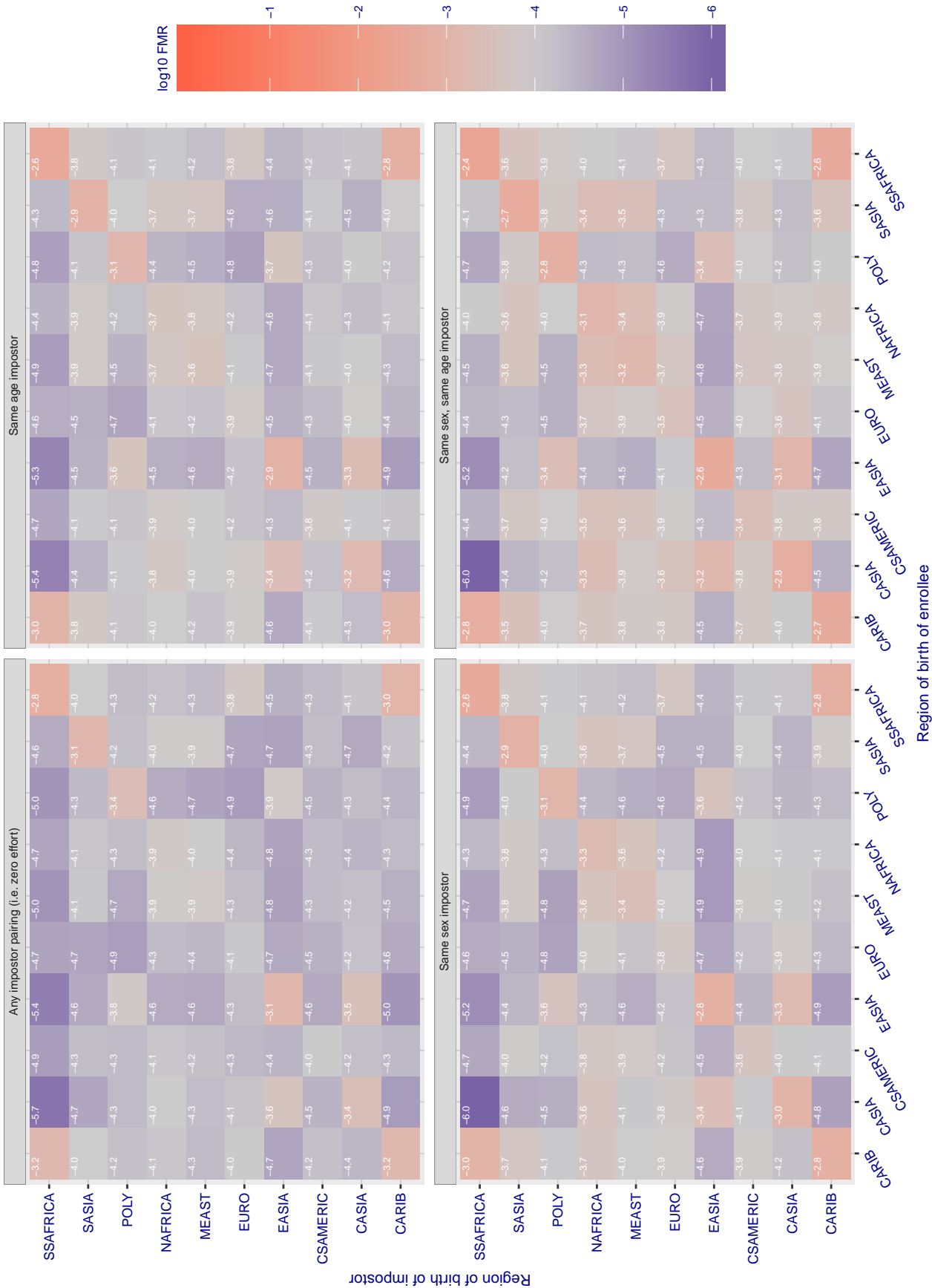


Figure 194: For algorithm vcog-002 operating on visa images, the heatmap shows false match rates observed over impostor comparisons of faces from different individuals who were born in the given region pair. False matches are counted against a recognition threshold fixed globally to give the target FMR in the plot title, computed over all on the order of 10^{10} impostor comparisons. If text appears in each box it give the same quantity as that coded by the color. Grey indicates FMR is at the intended FMR target level. Light red colors present a security vulnerability to, for example, a passport gate. Each +1 increase in \log_{10} FMR corresponds to a factor of 10 increase in FMR. The matrix is not quite symmetric because images in the enrollment and verification sets are different.

Cross region FMR at threshold $T = 71.529$ for algorithm vd_001, giving $FMR(T) = 0.0001$ globally.

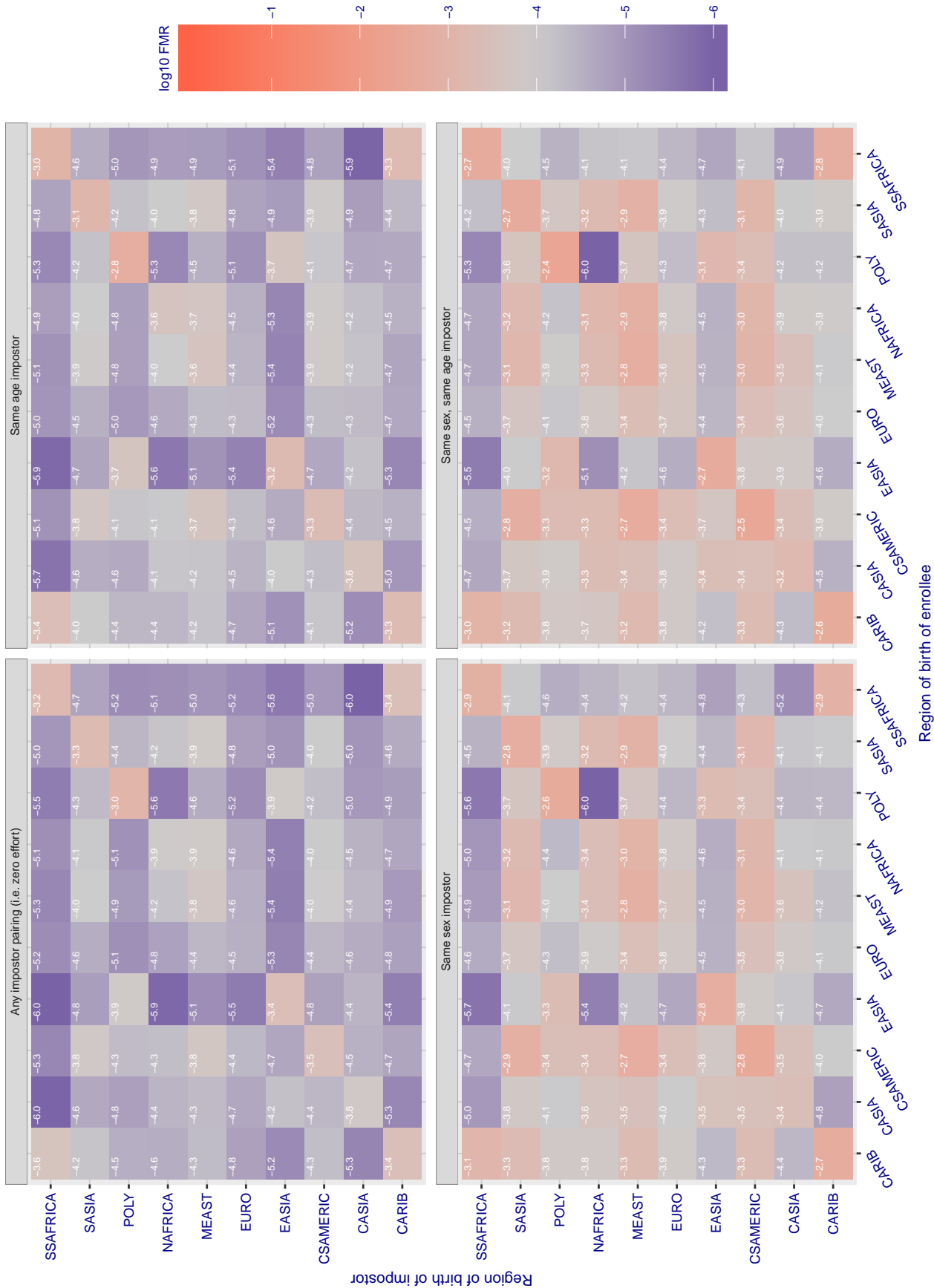


Figure 195: For algorithm vd-001 operating on visa images, the heatmap shows false match rates observed over impostor comparisons of faces from different individuals who were born in the given region pair. False matches are counted against a recognition threshold fixed globally to give the target FMR in the plot title, computed over all on the order of 10^{10} impostor comparisons. If text appears in each box it give the same quantity as that coded by the color. Grey indicates FMR is at the intended FMR target level. Light red colors present a security vulnerability to, for example, a passport gate. Each +1 increase in \log_{10} FMR corresponds to a factor of 10 increase in FMR. The matrix is not quite symmetric because images in the enrollment and verification sets are different.

Cross region FMR at threshold $T = 3.325$ for algorithm veridas_001, giving $FMR(T) = 0.0001$ globally.

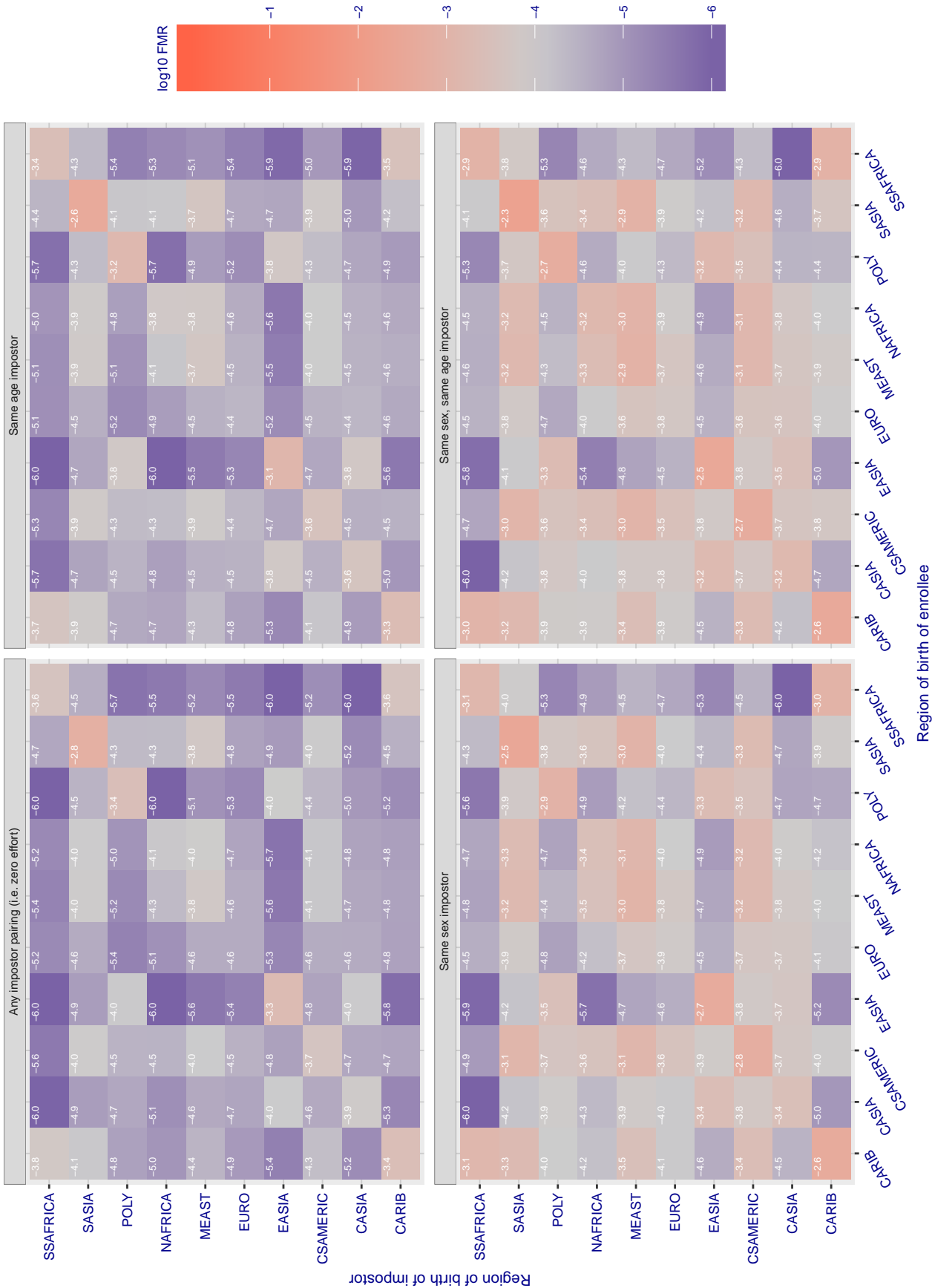


Figure 196: For algorithm veridas-001 operating on visa images, the heatmap shows false match rates observed over impostor comparisons of faces from different individuals who were born in the given region pair. False matches are counted against a recognition threshold fixed globally to give the target FMR in the plot title, computed over all on the order of 10^{10} impostor comparisons. If text appears in each box it give the same quantity as that coded by the color. Grey indicates FMR is at the intended FMR target level. Light red colors present a security vulnerability to, for example, a passport gate. Each +1 increase in \log_{10} FMR corresponds to a factor of 10 increase in FMR. The matrix is not quite symmetric because images in the enrollment and verification sets are different.

Cross region FMR at threshold $T = 3.389$ for algorithm veridas_002, giving $FMR(T) = 0.0001$ globally.

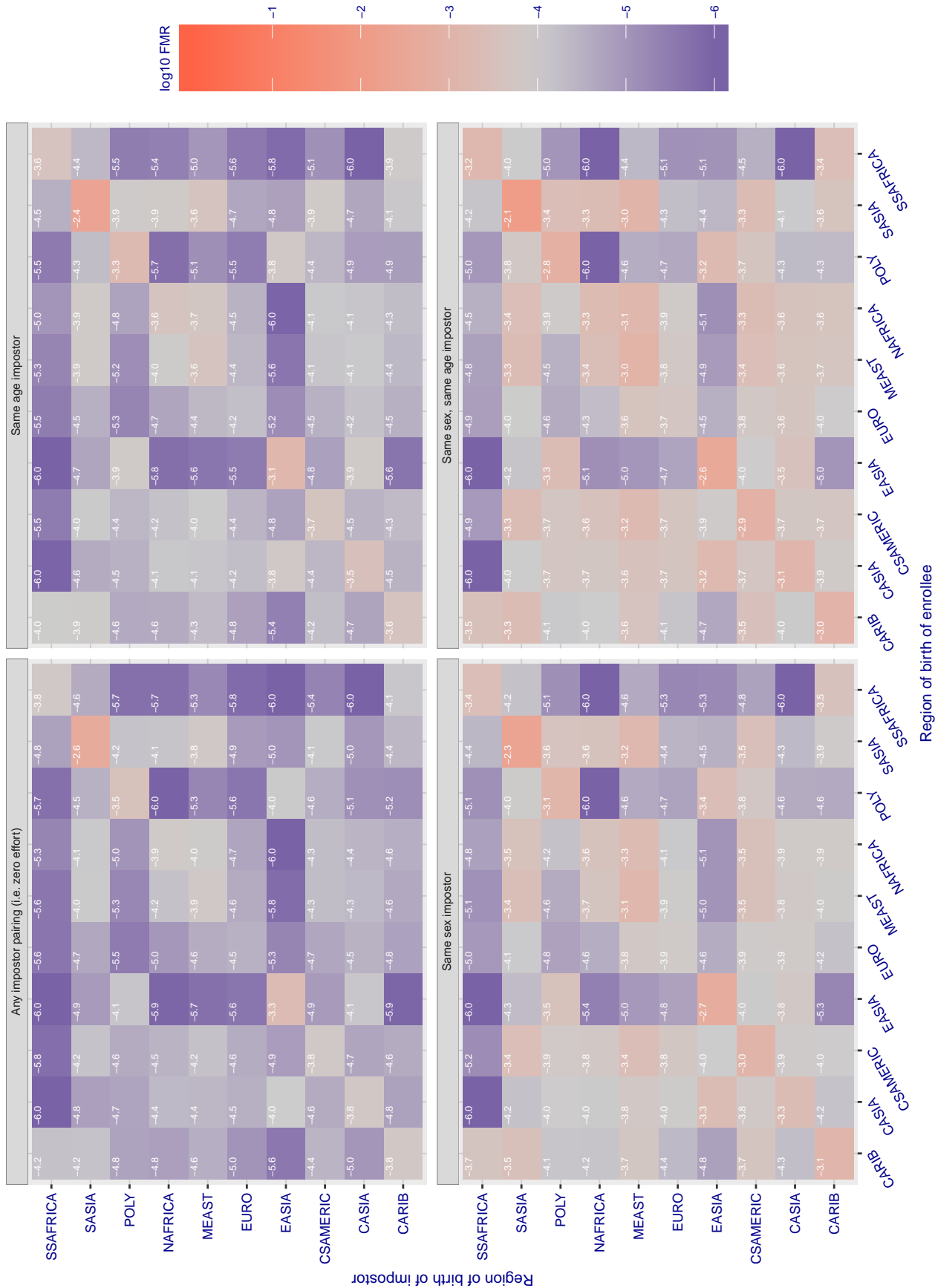


Figure 197: For algorithm veridas-002 operating on visa images, the heatmap shows false match rates observed over impostor comparisons of faces from different individuals who were born in the given region pair. False matches are counted against a recognition threshold fixed globally to give the target FMR in the plot title, computed over all on the order of 10^{10} impostor comparisons. If text appears in each box it give the same quantity as that coded by the color. Grey indicates FMR is at the intended FMR target level. Light red colors present a security vulnerability to, for example, a passport gate. Each +1 increase in \log_{10} FMR corresponds to a factor of 10 increase in FMR. The matrix is not quite symmetric because images in the enrollment and verification sets are different.

Cross region FMR at threshold $T = 3.051$ for algorithm *vigilantsolutions_005*, giving $FMR(T) = 0.0001$ globally.

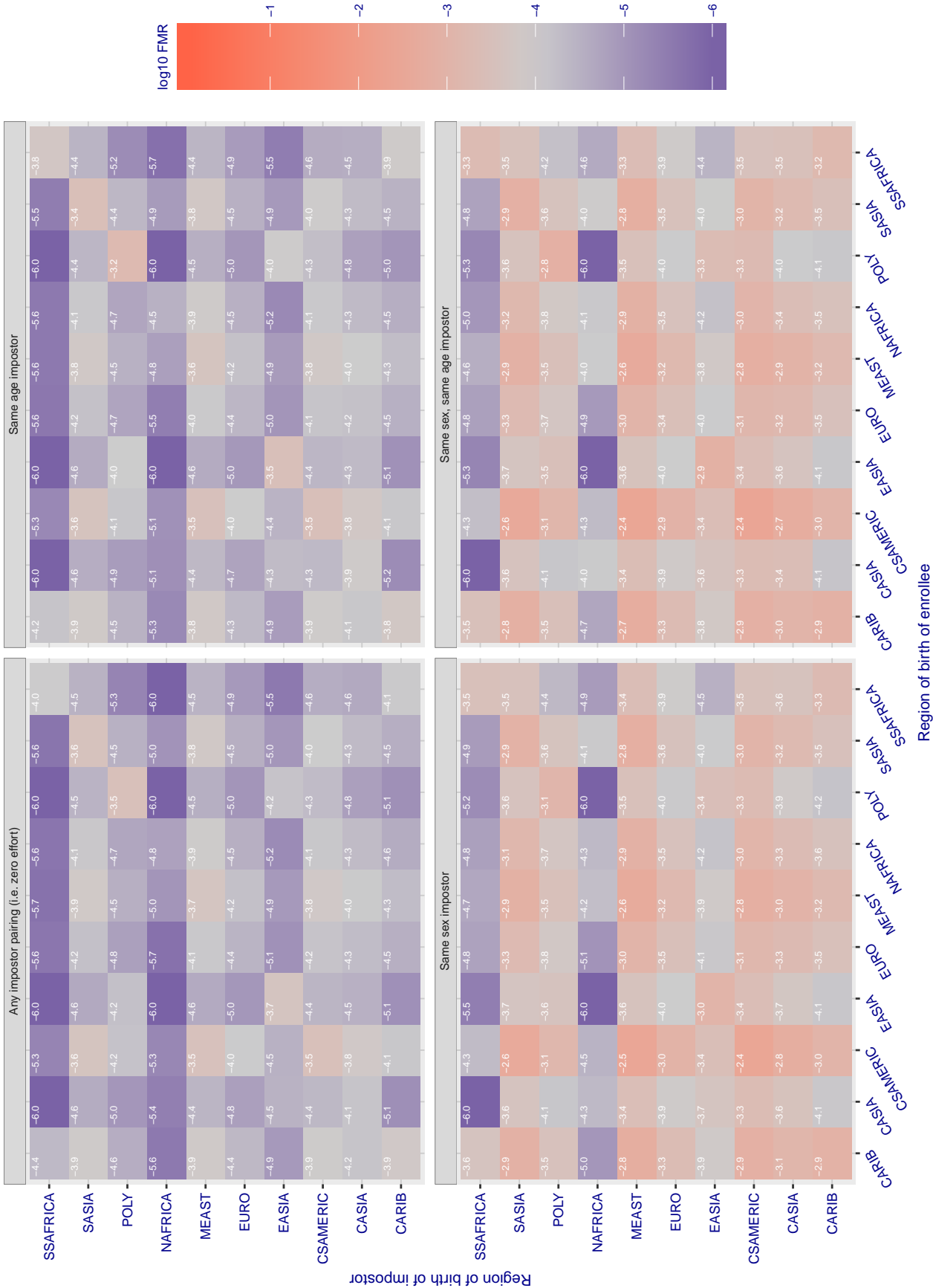


Figure 198: For algorithm *vigilantsolutions-005* operating on visa images, the heatmap shows false match rates observed over impostor comparisons of faces from different individuals who were born in the given region pair. False matches are counted against a recognition threshold fixed globally to give the target FMR in the plot title, computed over all on the order of 10^{10} impostor comparisons. If text appears in each box it give the same quantity as that coded by the color. Grey indicates FMR is at the intended FMR target level. Light red colors present a security vulnerability to, for example, a passport gate. Each +1 increase in \log_{10} FMR corresponds to a factor of 10 increase in FMR. The matrix is not quite symmetric because images in the enrollment and verification sets are different.

Cross region FMR at threshold $T = 3.057$ for algorithm *vigilantsolutions_006*, giving $FMR(T) = 0.0001$ globally.

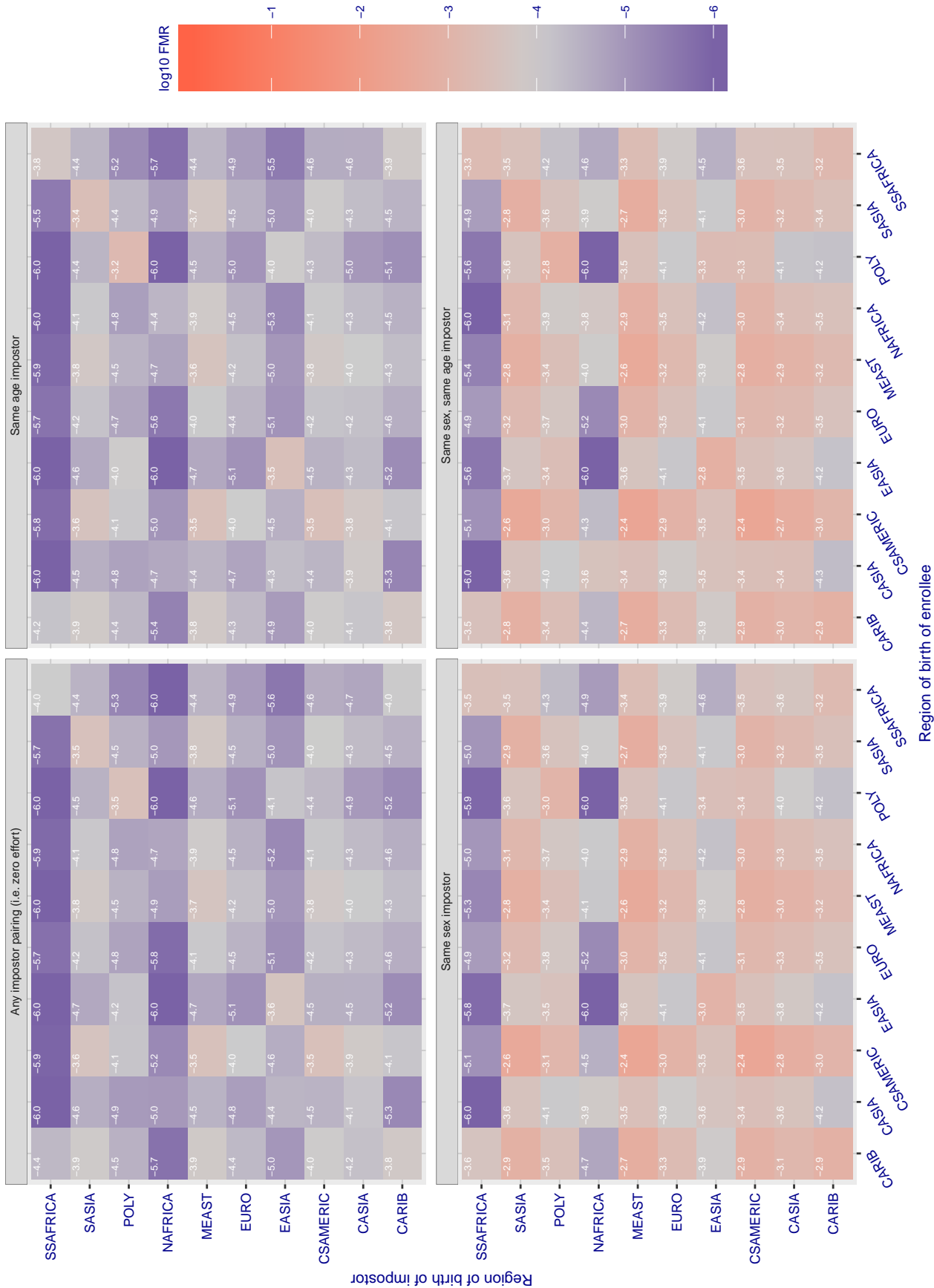


Figure 199: For algorithm *vigilantsolutions-006* operating on visa images, the heatmap shows false match rates observed over impostor comparisons of faces from different individuals who were born in the given region pair. False matches are counted against a recognition threshold fixed globally to give the target FMR in the plot title, computed over all on the order of 10^{10} impostor comparisons. If text appears in each box it give the same quantity as that coded by the color. Grey indicates FMR is at the intended FMR target level. Light red colors present a security vulnerability to, for example, a passport gate. Each +1 increase in \log_{10} FMR corresponds to a factor of 10 increase in FMR. The matrix is not quite symmetric because images in the enrollment and verification sets are different.

Cross region FMR at threshold $T = 0.432$ for algorithm vion_{000} , giving $\text{FMR}(T) = 0.0001$ globally.

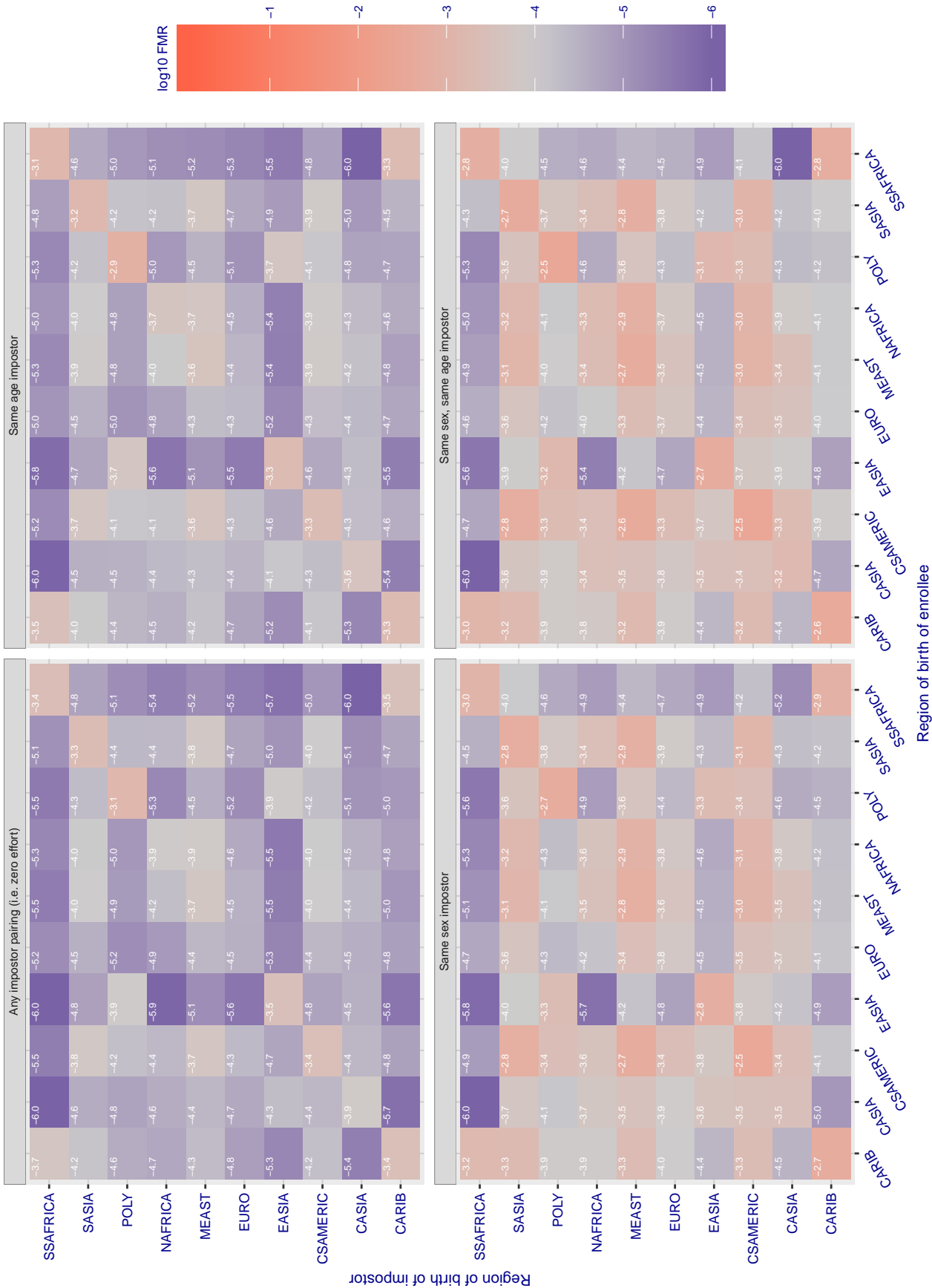


Figure 200: For algorithm vion_{000} operating on visa images, the heatmap shows false match rates observed over impostor comparisons of faces from different individuals who were born in the given region pair. False matches are counted against a recognition threshold fixed globally to give the target FMR in the plot title, computed over all on the order of 10^{10} impostor comparisons. If text appears in each box it give the same quantity as that coded by the color. Grey indicates FMR is at the intended FMR target level. Light red colors present a security vulnerability to, for example, a passport gate. Each +1 increase in \log_{10} FMR corresponds to a factor of 10 increase in FMR. The matrix is not quite symmetric because images in the enrollment and verification sets are different.

Cross region FMR at threshold $T = 0.433$ for algorithm visionbox_000, giving $FMR(T) = 0.0001$ globally.

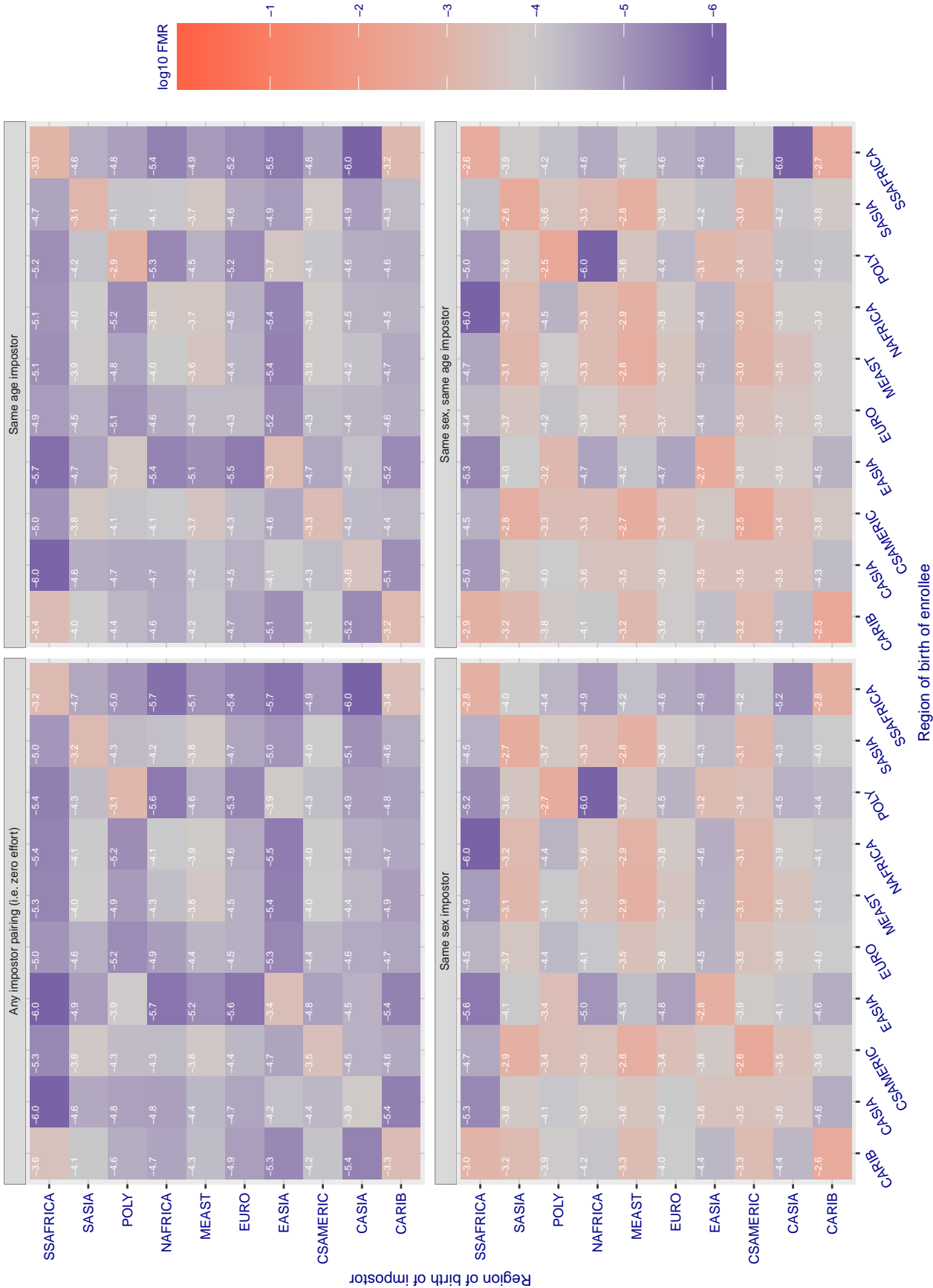


Figure 201: For algorithm visionbox-000 operating on visa images, the heatmap shows false match rates observed over impostor comparisons of faces from different individuals who were born in the given region pair. False matches are counted against a recognition threshold fixed globally to give the target FMR in the plot title, computed over all on the order of 10^{10} impostor comparisons. If text appears in each box it give the same quantity as that coded by the color. Grey indicates FMR is at the intended FMR target level. Light red colors present a security vulnerability to, for example, a passport gate. Each +1 increase in \log_{10} FMR corresponds to a factor of 10 increase in FMR. The matrix is not quite symmetric because images in the enrollment and verification sets are different.

Cross region FMR at threshold $T = 0.382$ for algorithm visionbox_001, giving $FMR(T) = 0.0001$ globally.

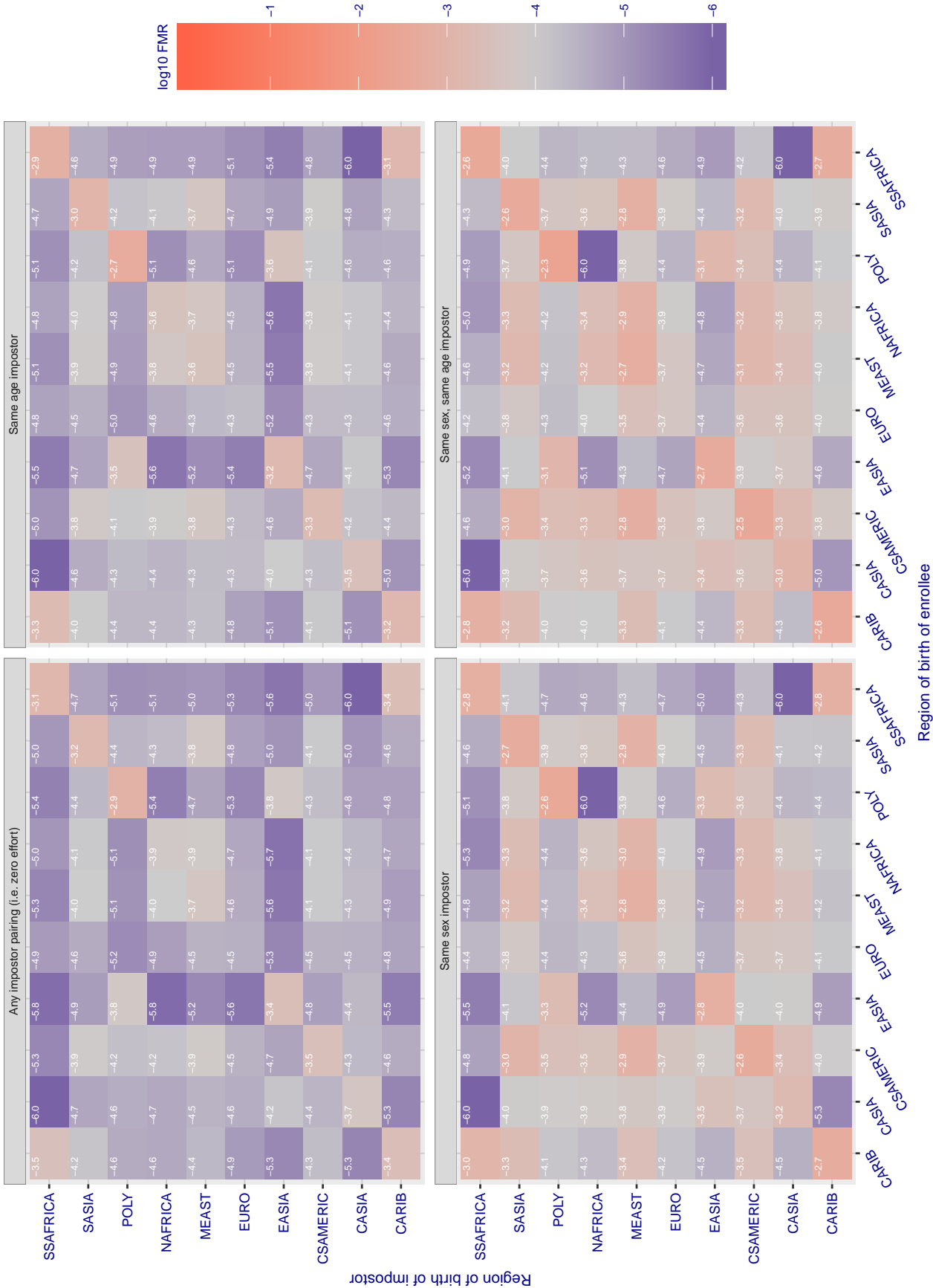


Figure 202: For algorithm visionbox-001 operating on visa images, the heatmap shows false match rates observed over impostor comparisons of faces from different individuals who were born in the given region pair. False matches are counted against a recognition threshold fixed globally to give the target FMR in the plot title, computed over all on the order of 10^{10} impostor comparisons. If text appears in each box it give the same quantity as that coded by the color. Grey indicates FMR is at the intended FMR target level. Light red colors present a security vulnerability to, for example, a passport gate. Each +1 increase in \log_{10} FMR corresponds to a factor of 10 increase in FMR. The matrix is not quite symmetric because images in the enrollment and verification sets are different.

Cross region FMR at threshold $T = 0.000$ for algorithm visionlabs_005, giving $FMR(T) = 0.0001$ globally.

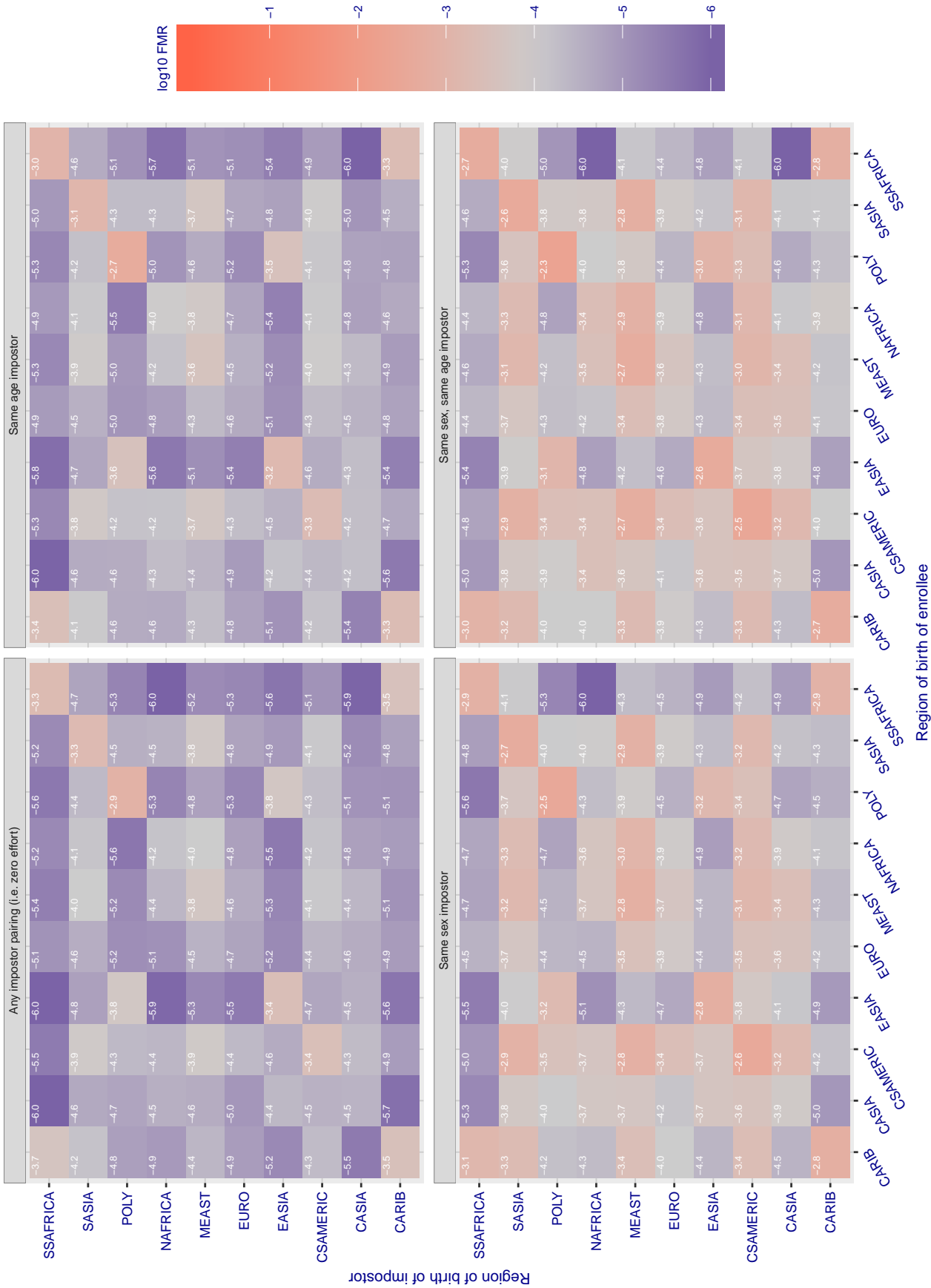


Figure 203: For algorithm visionlabs-005 operating on visa images, the heatmap shows false match rates observed over impostor comparisons of faces from different individuals who were born in the given region pair. False matches are counted against a recognition threshold fixed globally to give the target FMR in the plot title, computed over all on the order of 10^{10} impostor comparisons. If text appears in each box it give the same quantity as that coded by the color. Grey indicates FMR is at the intended FMR target level. Light red colors present a security vulnerability to, for example, a passport gate. Each +1 increase in \log_{10} FMR corresponds to a factor of 10 increase in FMR. The matrix is not quite symmetric because images in the enrollment and verification sets are different.

Cross region FMR at threshold $T = 0.669$ for algorithm visionlabs_006, giving $FMR(T) = 0.0001$ globally.

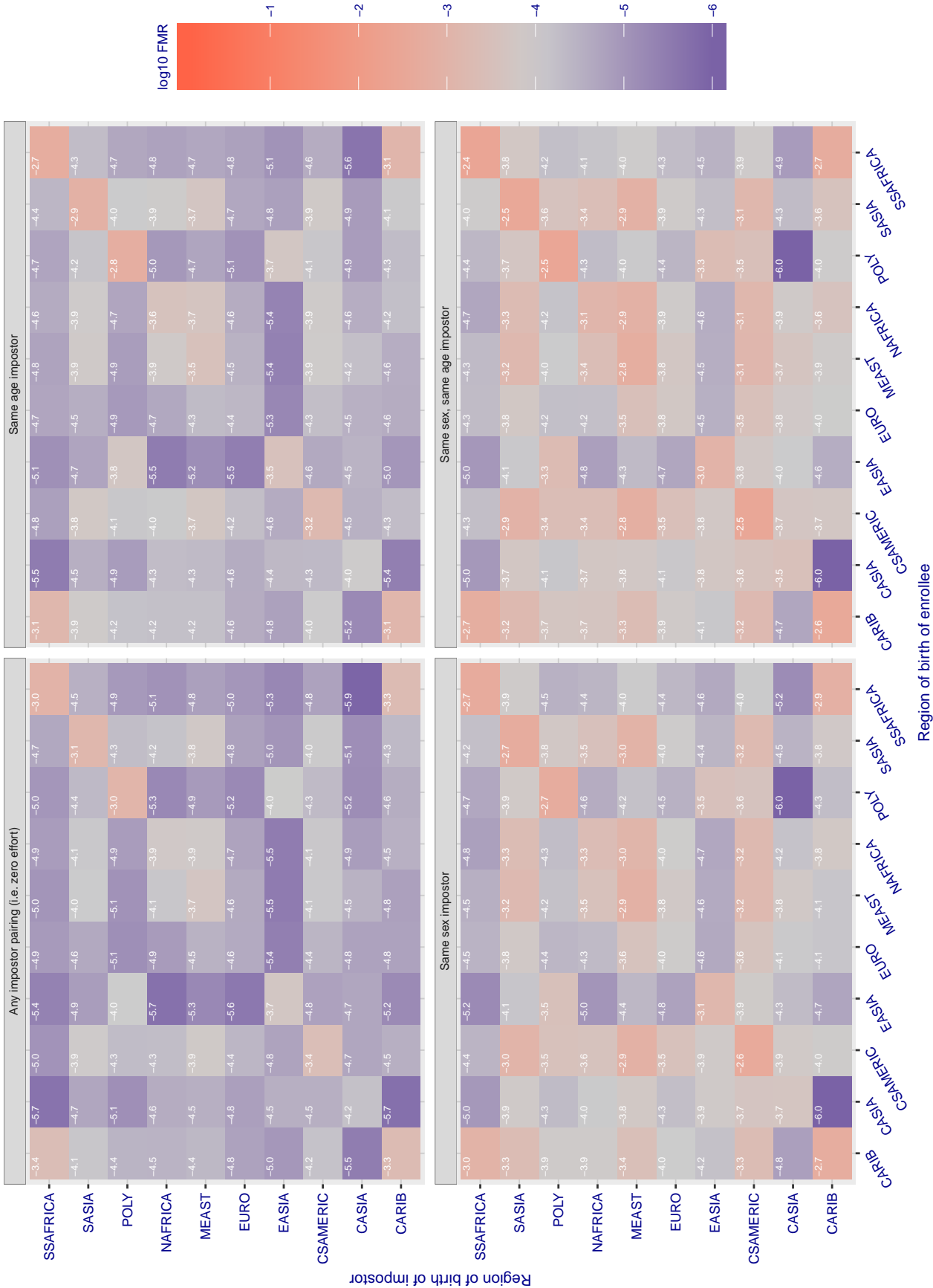


Figure 204: For algorithm visionlabs-006 operating on visa images, the heatmap shows false match rates observed over impostor comparisons of faces from different individuals who were born in the given region pair. False matches are counted against a recognition threshold fixed globally to give the target FMR in the plot title, computed over all on the order of 10^{10} impostor comparisons. If text appears in each box it give the same quantity as that coded by the color. Grey indicates FMR is at the intended FMR target level. Light red colors present a security vulnerability to, for example, a passport gate. Each +1 increase in \log_{10} FMR corresponds to a factor of 10 increase in FMR. The matrix is not quite symmetric because images in the enrollment and verification sets are different.

Cross region FMR at threshold T = 995.416 for algorithm vocord_005, giving FMR(T) = 0.0001 globally.

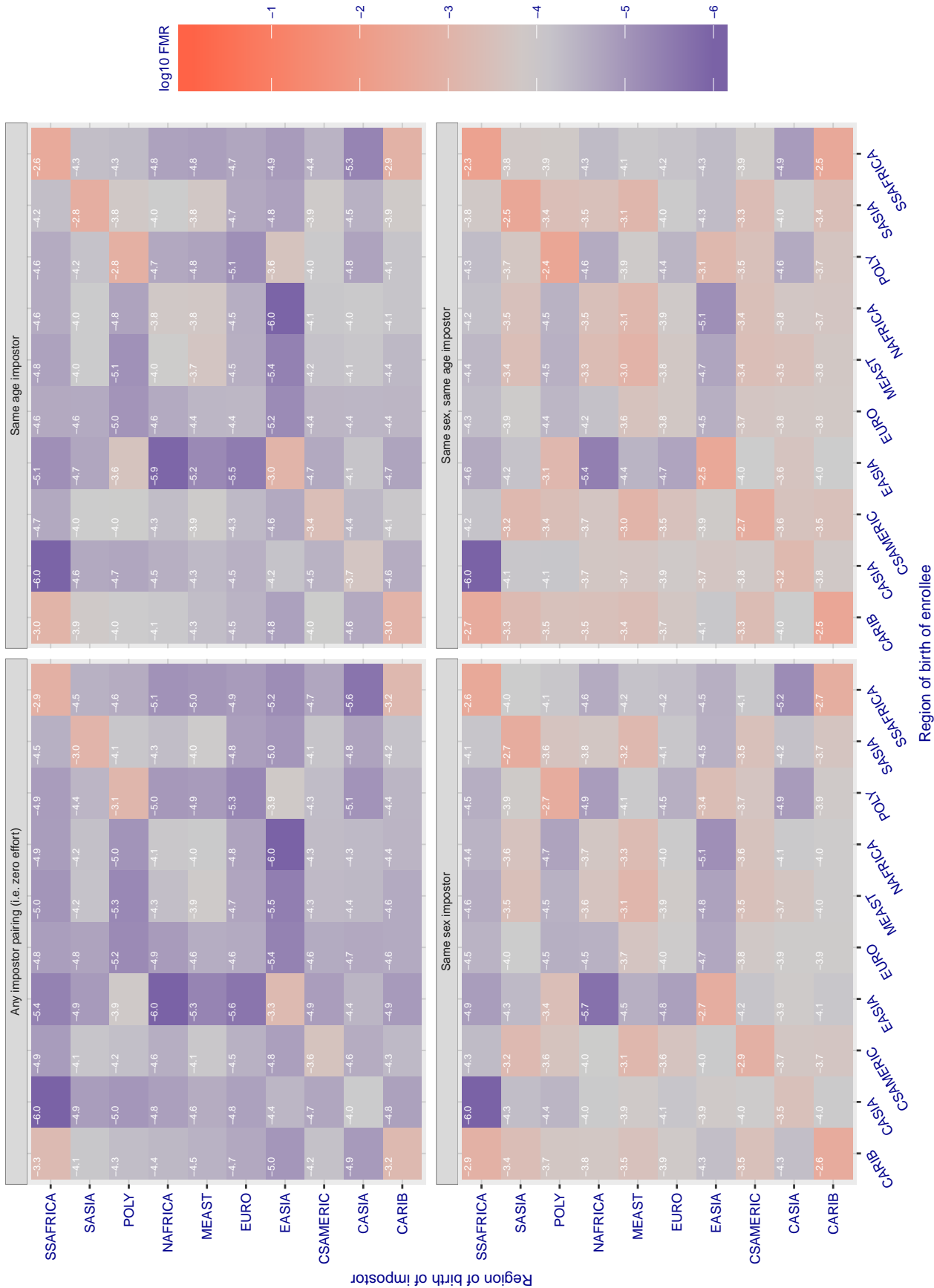


Figure 205: For algorithm vocord-005 operating on visa images, the heatmap shows false match rates observed over impostor comparisons of faces from different individuals who were born in the given region pair. False matches are counted against a recognition threshold fixed globally to give the target FMR in the plot title, computed over all on the order of 10¹⁰ impostor comparisons. If text appears in each box it give the same quantity as that coded by the color. Grey indicates FMR is at the intended FMR target level. Light red colors present a security vulnerability to, for example, a passport gate. Each +1 increase in log10 FMR corresponds to a factor of 10 increase in FMR. The matrix is not quite symmetric because images in the enrollment and verification sets are different.

Cross region FMR at threshold T = 995.898 for algorithm vocord_006, giving FMR(T) = 0.0001 globally.

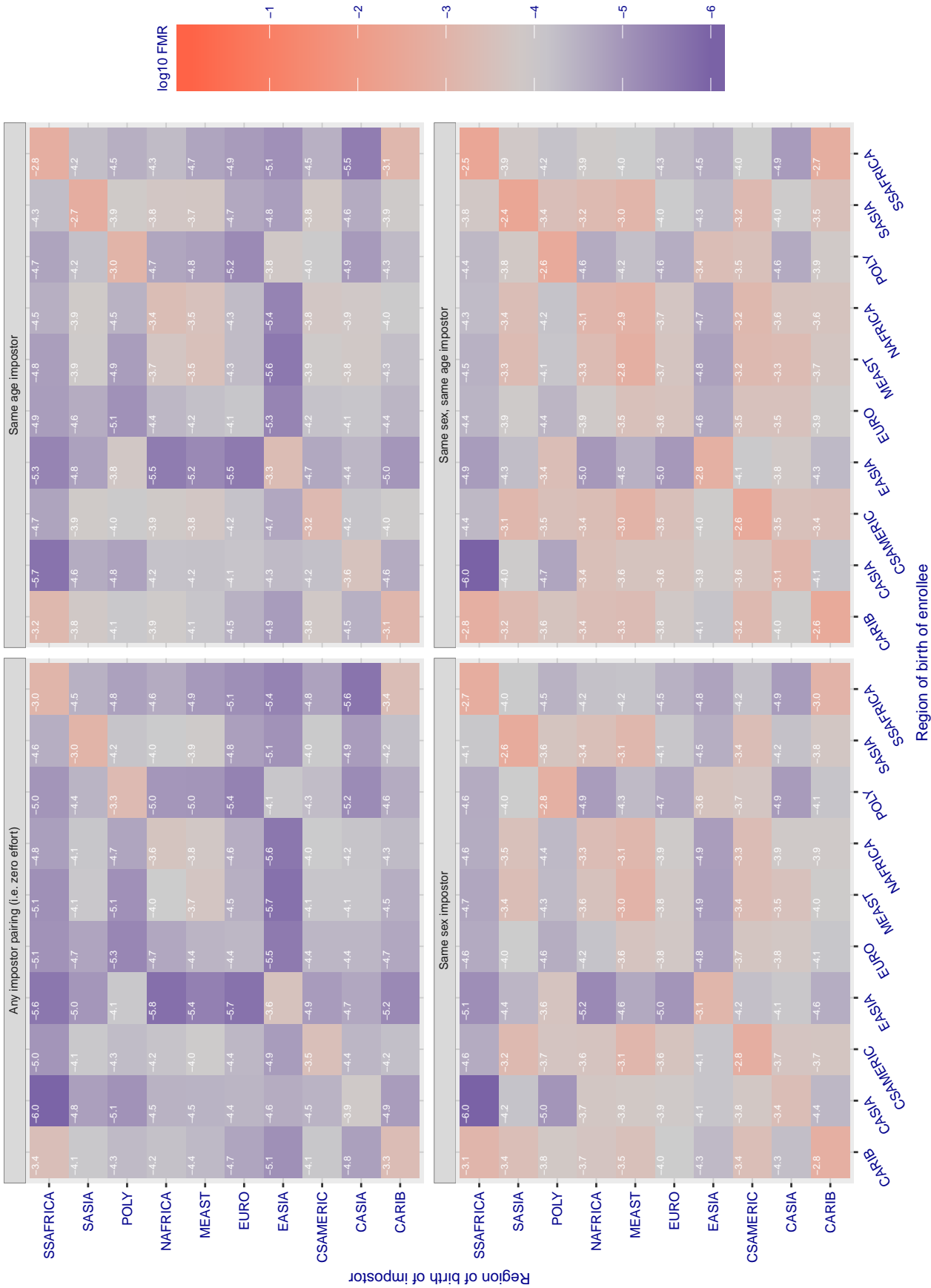


Figure 206: For algorithm vocord-006 operating on visa images, the heatmap shows false match rates observed over impostor comparisons of faces from different individuals who were born in the given region pair. False matches are counted against a recognition threshold fixed globally to give the target FMR in the plot title, computed over all on the order of 10^{10} impostor comparisons. If text appears in each box it give the same quantity as that coded by the color. Grey indicates FMR is at the intended FMR target level. Light red colors present a security vulnerability to, for example, a passport gate. Each +1 increase in \log_{10} FMR corresponds to a factor of 10 increase in FMR. The matrix is not quite symmetric because images in the enrollment and verification sets are different.

Cross region FMR at threshold $T = 5.544$ for algorithm yisheng_004, giving $FMR(T) = 0.0001$ globally.

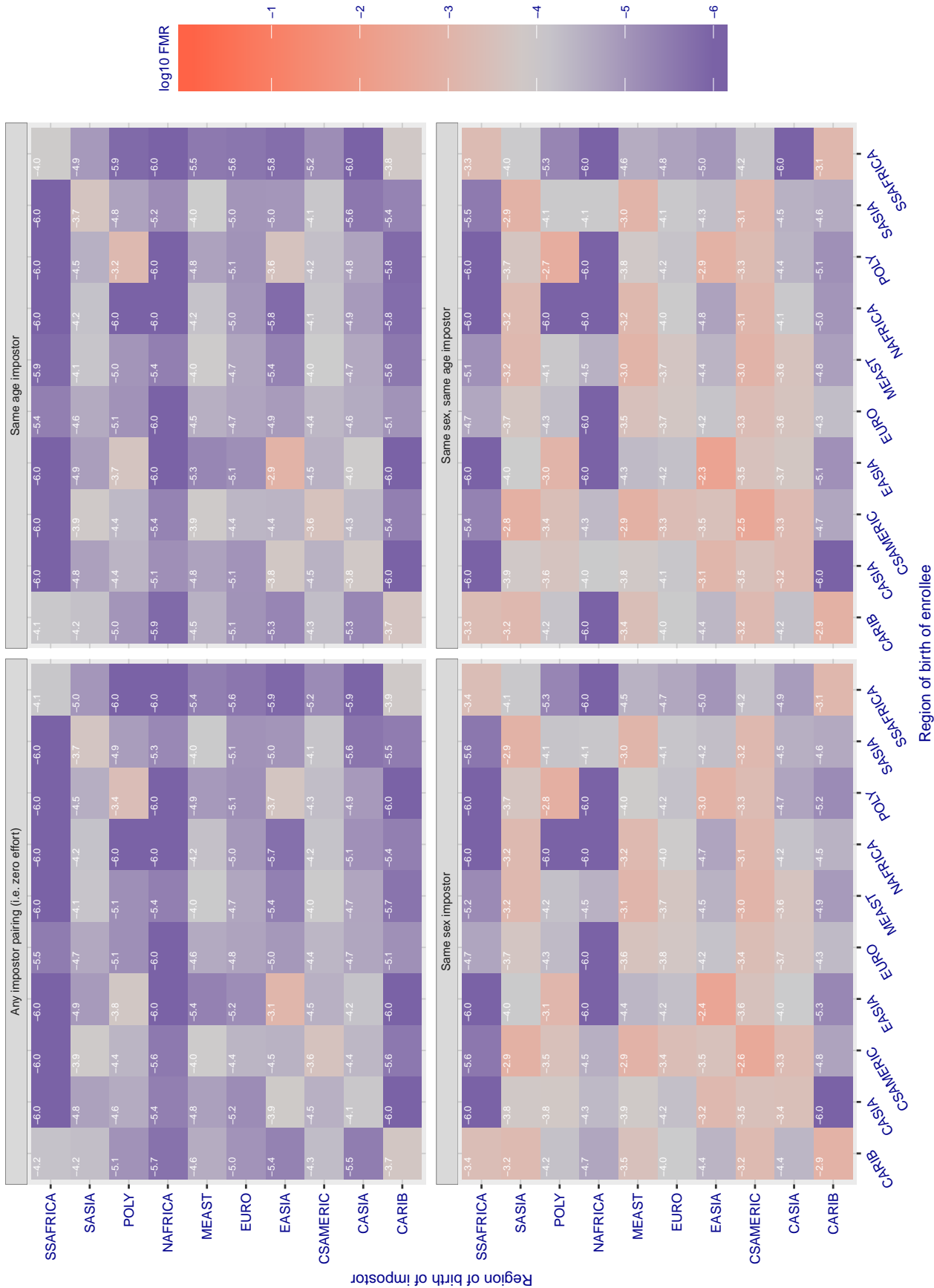


Figure 207: For algorithm yisheng-004 operating on visa images, the heatmap shows false match rates observed over impostor comparisons of faces from different individuals who were born in the given region pair. False matches are counted against a recognition threshold fixed globally to give the target FMR in the plot title, computed over all on the order of 10^{10} impostor comparisons. If text appears in each box it give the same quantity as that coded by the color. Grey indicates FMR is at the intended FMR target level. Light red colors present a security vulnerability to, for example, a passport gate. Each +1 increase in \log_{10} FMR corresponds to a factor of 10 increase in FMR. The matrix is not quite symmetric because images in the enrollment and verification sets are different.

Cross region FMR at threshold $T = 37.698$ for algorithm yitu_003, giving $FMR(T) = 0.0001$ globally.

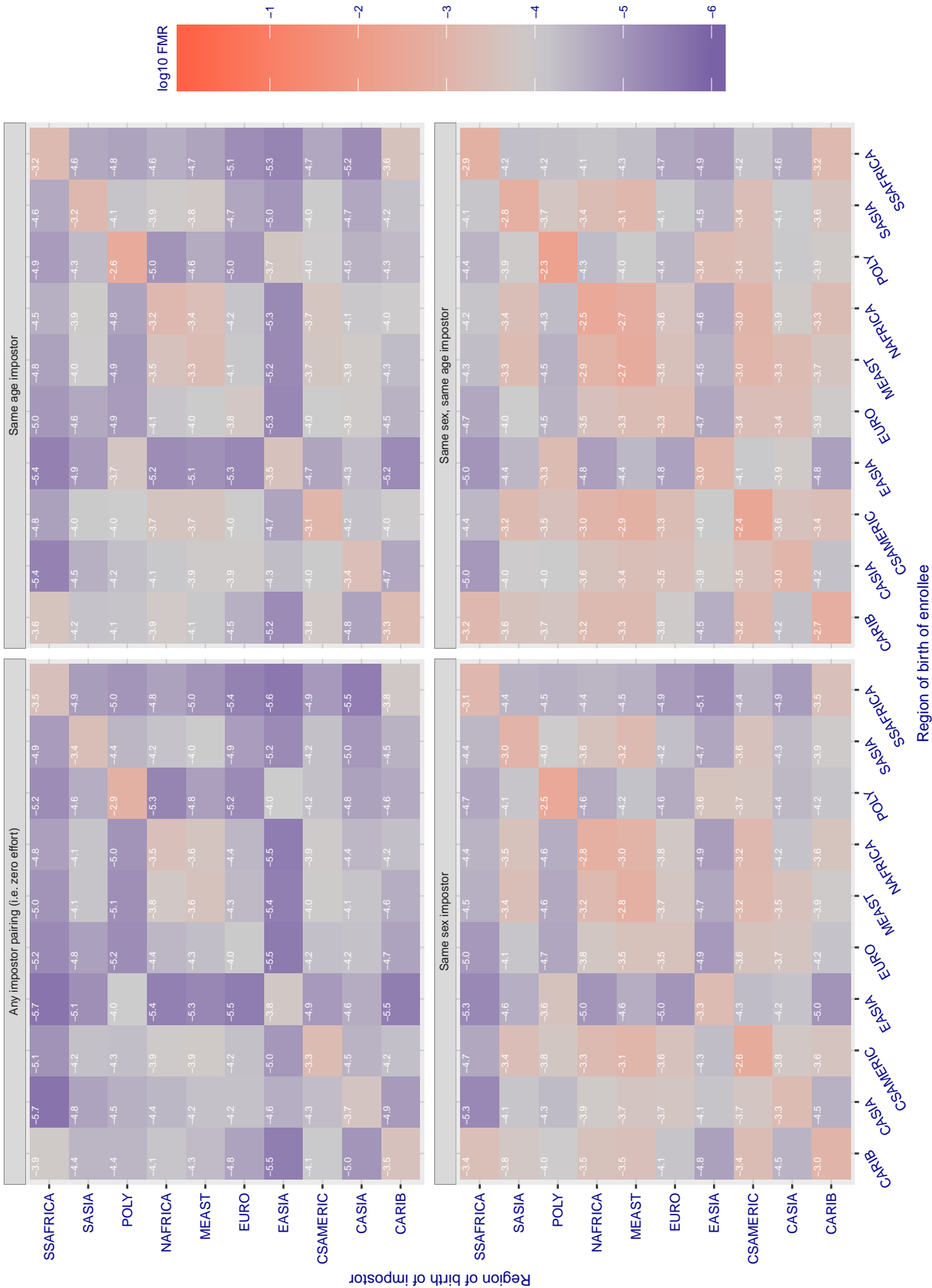


Figure 208: For algorithm yitu-003 operating on visa images, the heatmap shows false match rates observed over impostor comparisons of faces from different individuals who were born in the given region pair. False matches are counted against a recognition threshold fixed globally to give the target FMR in the plot title, computed over all on the order of 10^{10} impostor comparisons. If text appears in each box it give the same quantity as that coded by the color. Grey indicates FMR is at the intended FMR target level. Light red colors present a security vulnerability to, for example, a passport gate. Each +1 increase in $\log_{10} FMR$ corresponds to a factor of 10 increase in FMR. The matrix is not quite symmetric because images in the enrollment and verification sets are different.

Cross country FMR at threshold $T = 2.575$ for algorithm 3divi_003, giving $FMR(T) = 0.001$ globally.

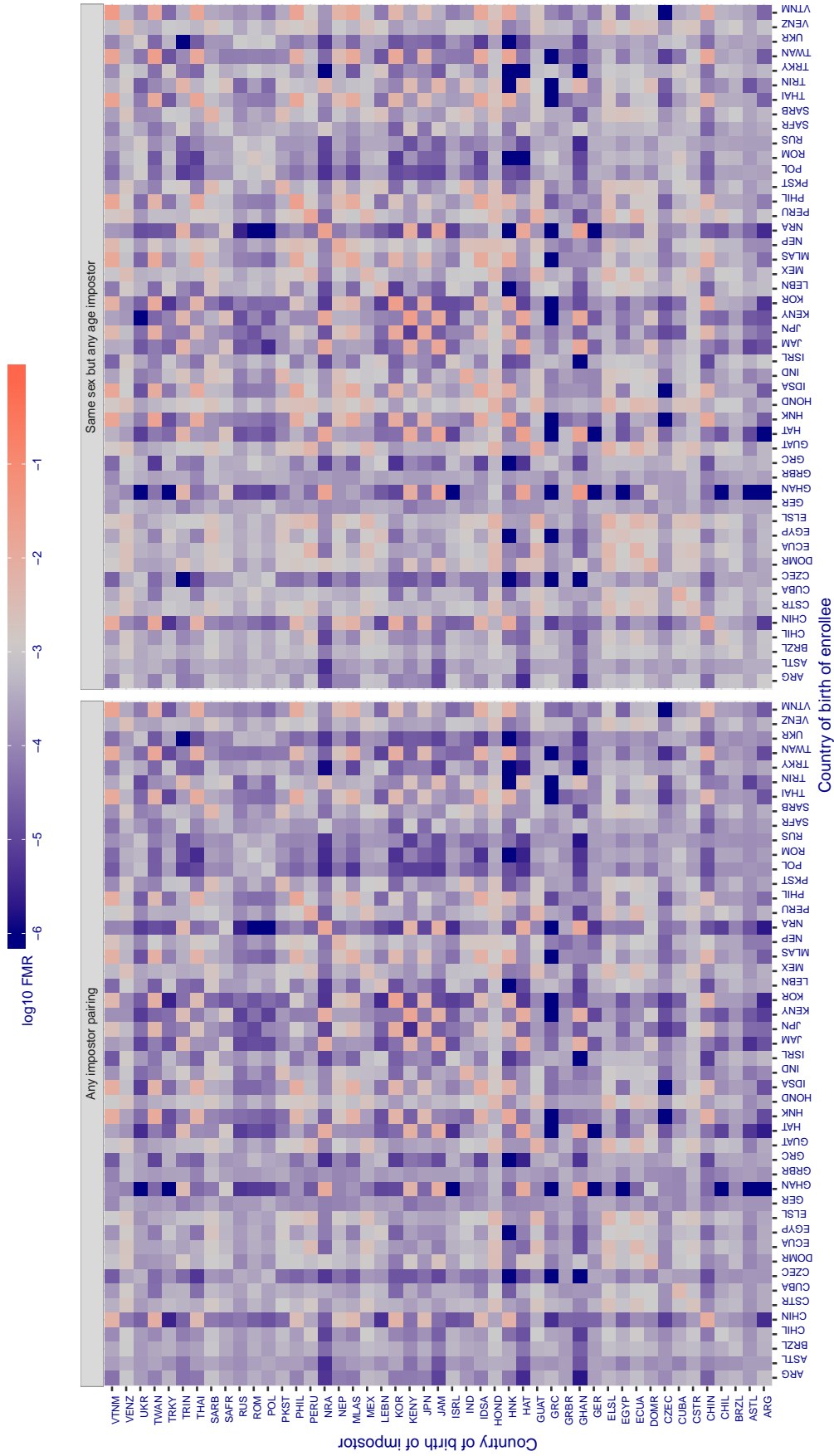


Figure 209: For algorithm 3divi-003 operating on visa images, the heatmap shows false match rates observed over impostor comparisons of faces from different individuals who were born in the given country pair. False matches are counted against a recognition threshold fixed globally to give the target FMR in the plot title, computed over all on the order of 10^{10} impostor comparisons. If text appears in each box it give the same quantity as that coded by the color. Grey indicates FMR is at the intended FMR target level. Light red colors present a security vulnerability to, for example, a passport gate. Each +1 increase in \log_{10} FMR corresponds to a factor of 10 increase in FMR. The matrix is not quite symmetric because images in the enrollment and verification sets are different.

Cross country FMR at threshold $T = 0.662$ for algorithm alchera_000, giving $FMR(T) = 0.001$ globally.

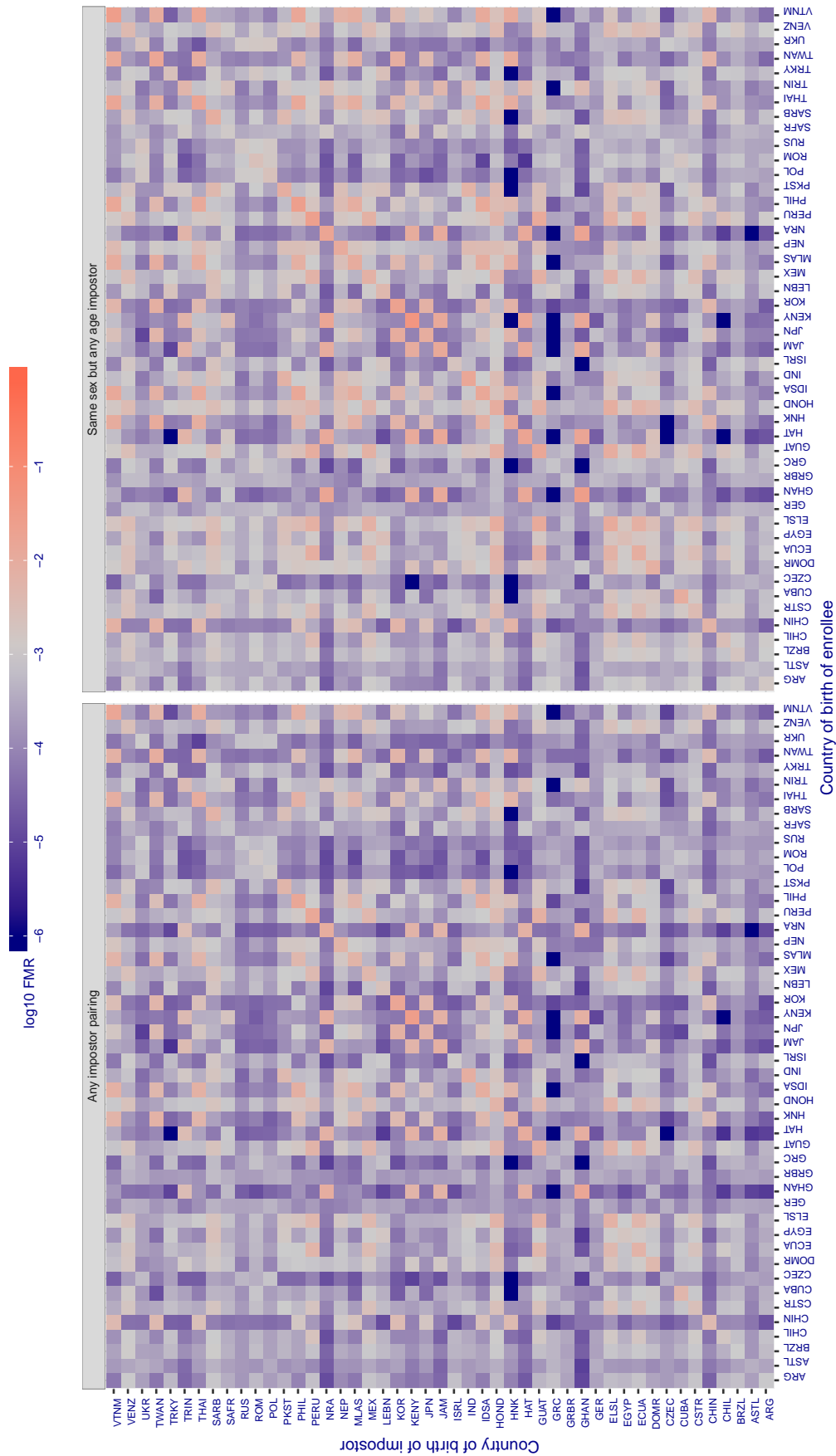


Figure 210: For algorithm alchera-000 operating on visa images, the heatmap shows false match rates observed over impostor comparisons of faces from different individuals who were born in the given country pair. False matches are counted against a recognition threshold fixed globally to give the target FMR in the plot title, computed over all on the order of 10^{10} impostor comparisons. If text appears in each box it give the same quantity as that coded by the color. Grey indicates FMR is at the intended FMR target level. Light red colors present a security vulnerability to, for example, a passport gate. Each +1 increase in $\log_{10} FMR$ corresponds to a factor of 10 increase in FMR. The matrix is not quite symmetric because images in the enrollment and verification sets are different.

Cross country FMR at threshold $T = 0.667$ for algorithm alchera_001, giving $FMR(T) = 0.001$ globally.

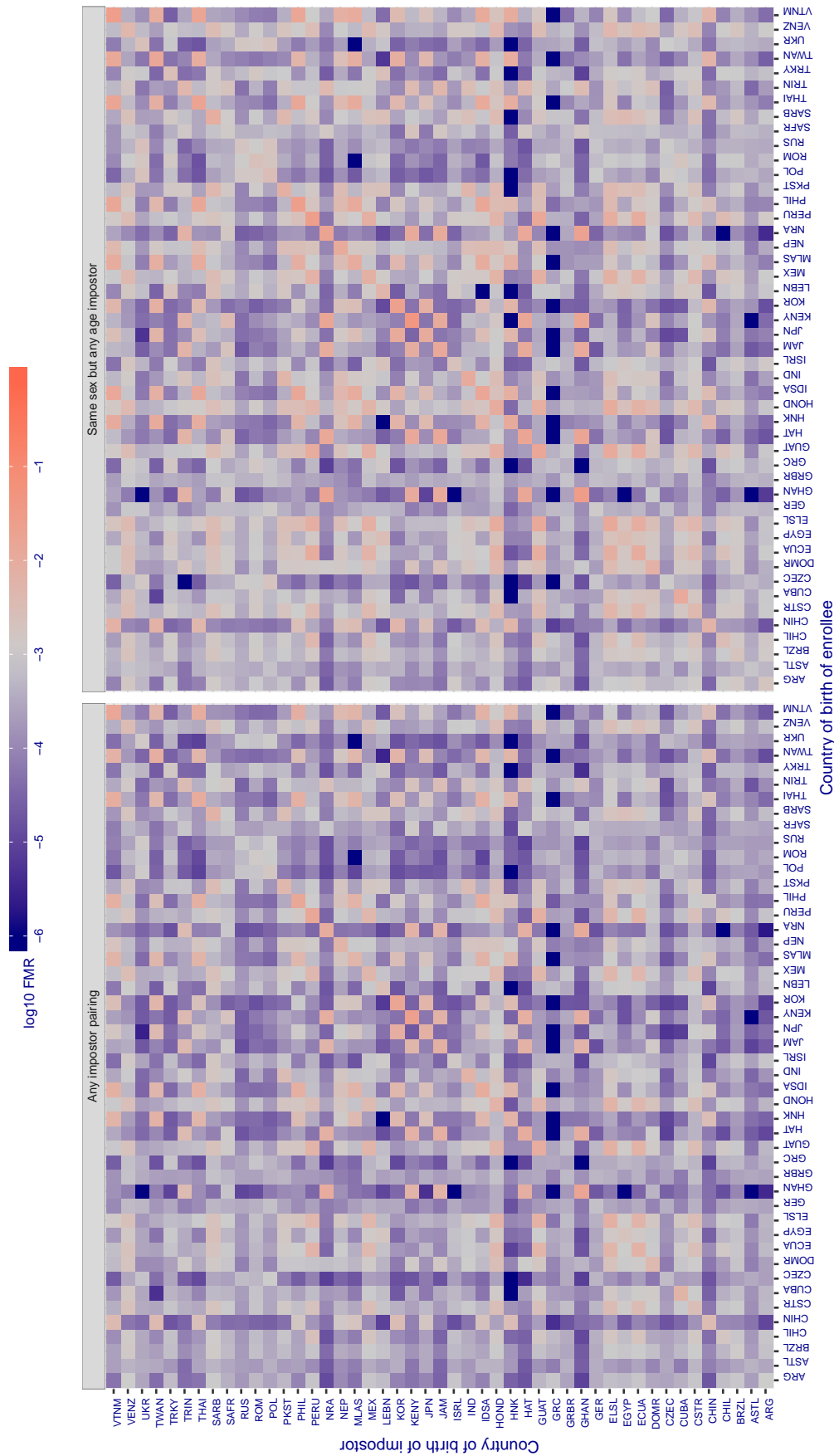


Figure 211: For algorithm alchera-001 operating on visa images, the heatmap shows false match rates observed over impostor comparisons of faces from different individuals who were born in the given country pair. False matches are counted against a recognition threshold fixed globally to give the target FMR in the plot title, computed over all on the order of 10^{10} impostor comparisons. If text appears in each box it give the same quantity as that coded by the color. Grey indicates FMR is at the intended FMR target level. Light red colors present a security vulnerability to, for example, a passport gate. Each +1 increase in \log_{10} FMR corresponds to a factor of 10 increase in FMR. The matrix is not quite symmetric because images in the enrollment and verification sets are different.

Cross country FMR at threshold $T = 0.339$ for algorithm allgvision_000, giving $FMR(T) = 0.001$ globally.

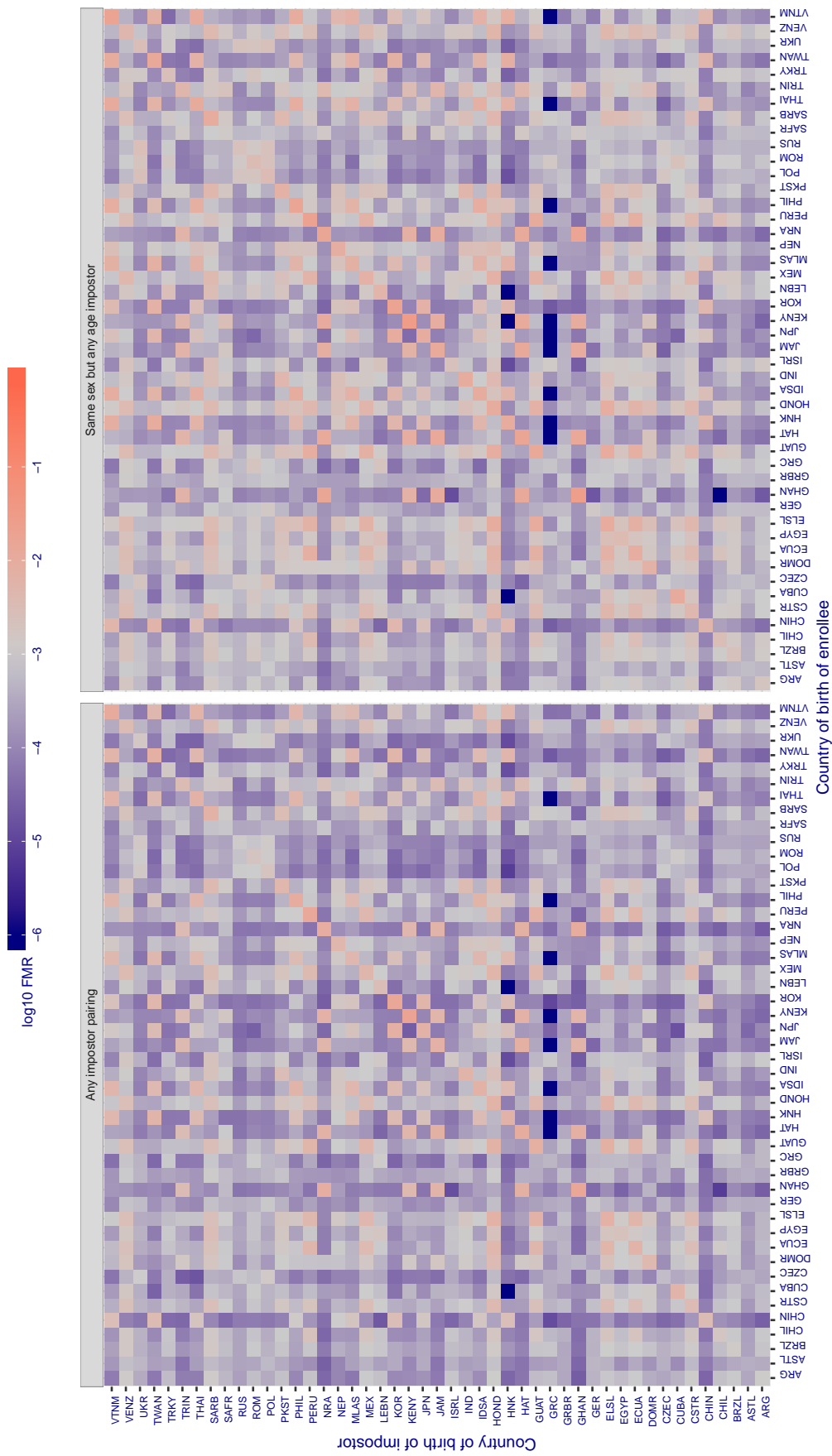


Figure 212: For algorithm allgvision-000 operating on visa images, the heatmap shows false match rates observed over impostor comparisons of faces from different individuals who were born in the given country pair. False matches are counted against a recognition threshold fixed globally to give the target FMR in the plot title, computed over all on the order of 10^{10} impostor comparisons. If text appears in each box it give the same quantity as that coded by the color. Grey indicates FMR is at the intended FMR target level. Light red colors present a security vulnerability to, for example, a passport gate. Each +1 increase in log10 FMR corresponds to a factor of 10 increase in FMR. The matrix is not quite symmetric because images in the enrollment and verification sets are different.

Cross country FMR at threshold $T = 0.297$ for algorithm anke_002, giving $FMR(T) = 0.001$ globally.

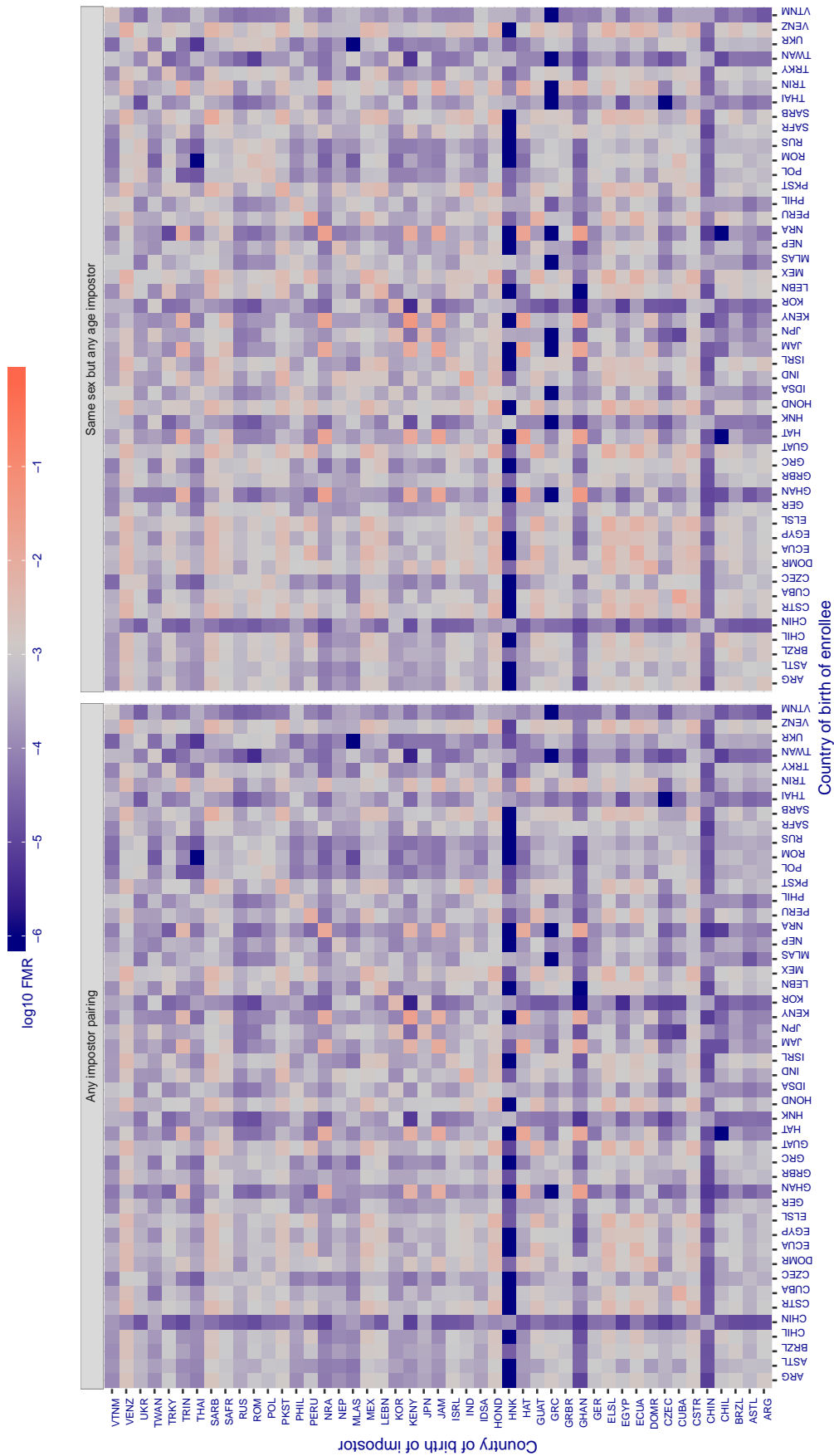


Figure 213: For algorithm anke-002 operating on visa images, the heatmap shows false match rates observed over impostor comparisons of faces from different individuals who were born in the given country pair. False matches are counted against a recognition threshold fixed globally to give the target FMR in the plot title, computed over all on the order of 10^{10} impostor comparisons. If text appears in each box it give the same quantity as that coded by the color. Grey indicates FMR is at the intended FMR target level. Light red colors present a security vulnerability to, for example, a passport gate. Each +1 increase in \log_{10} FMR corresponds to a factor of 10 increase in FMR. The matrix is not quite symmetric because images in the enrollment and verification sets are different.

Cross country FMR at threshold $T = 0.313$ for algorithm anke_003, giving $FMR(T) = 0.001$ globally.

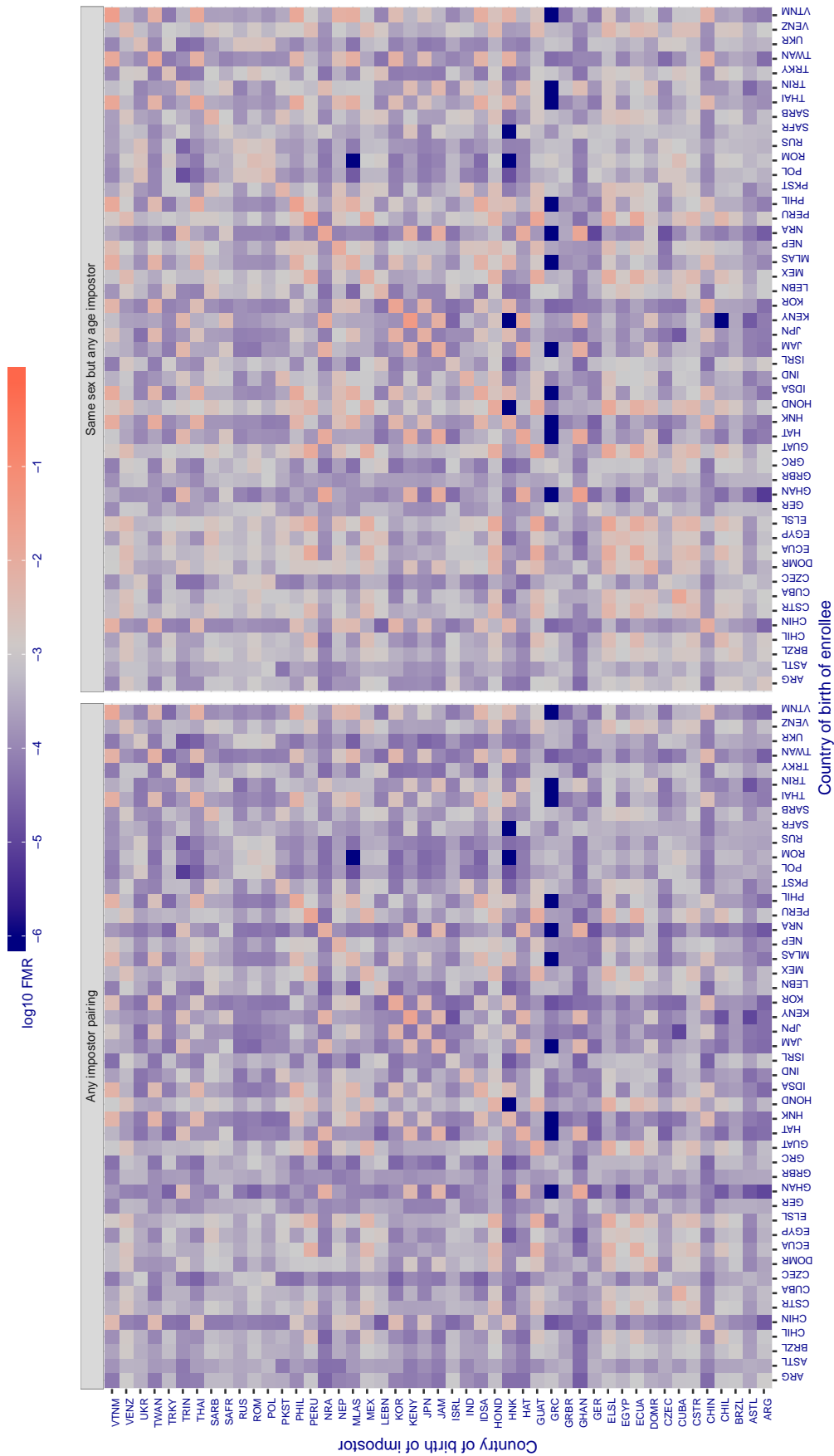


Figure 214: For algorithm anke-003 operating on visa images, the heatmap shows false match rates observed over impostor comparisons of faces from different individuals who were born in the given country pair. False matches are counted against a recognition threshold fixed globally to give the target FMR in the plot title, computed over all on the order of 10^{10} impostor comparisons. If text appears in each box it give the same quantity as that coded by the color. Grey indicates FMR is at the intended FMR target level. Light red colors present a security vulnerability to, for example, a passport gate. Each +1 increase in \log_{10} FMR corresponds to a factor of 10 increase in FMR. The matrix is not quite symmetric because images in the enrollment and verification sets are different.

Cross country FMR at threshold $T = 1.431$ for algorithm anyvision_002, giving $FMR(T) = 0.001$ globally.

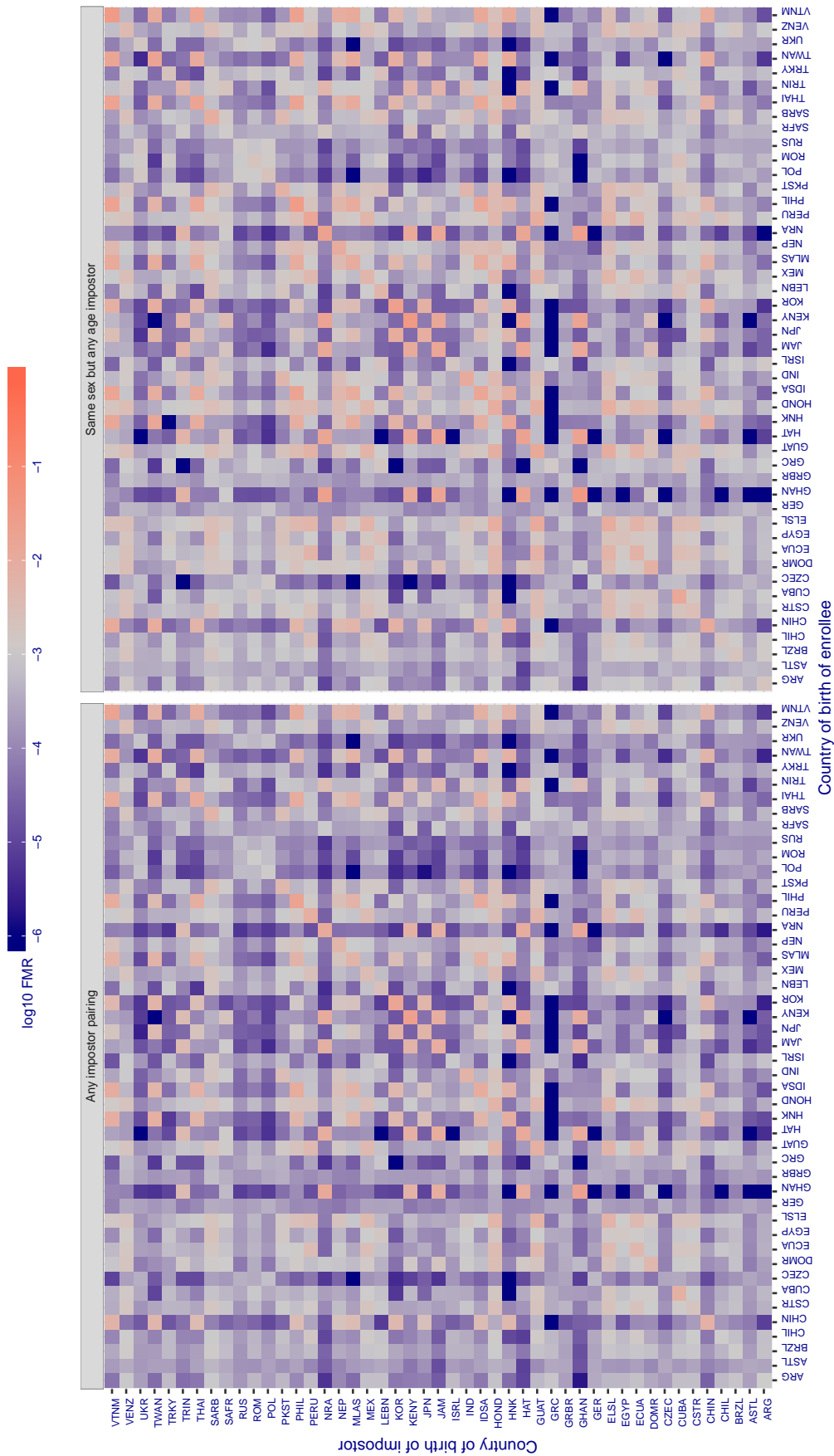


Figure 215: For algorithm anyvision-002 operating on visa images, the heatmap shows false match rates observed over impostor comparisons of faces from different individuals who were born in the given country pair. False matches are counted against a recognition threshold fixed globally to give the target FMR in the plot title, computed over all on the order of 10^{10} impostor comparisons. If text appears in each box it give the same quantity as that coded by the color. Grey indicates FMR is at the intended FMR target level. Light red colors present a security vulnerability to, for example, a passport gate. Each +1 increase in \log_{10} FMR corresponds to a factor of 10 increase in FMR. The matrix is not quite symmetric because images in the enrollment and verification sets are different.

Cross country FMR at threshold $T = 1.297$ for algorithm anyvision_004, giving $FMR(T) = 0.001$ globally.

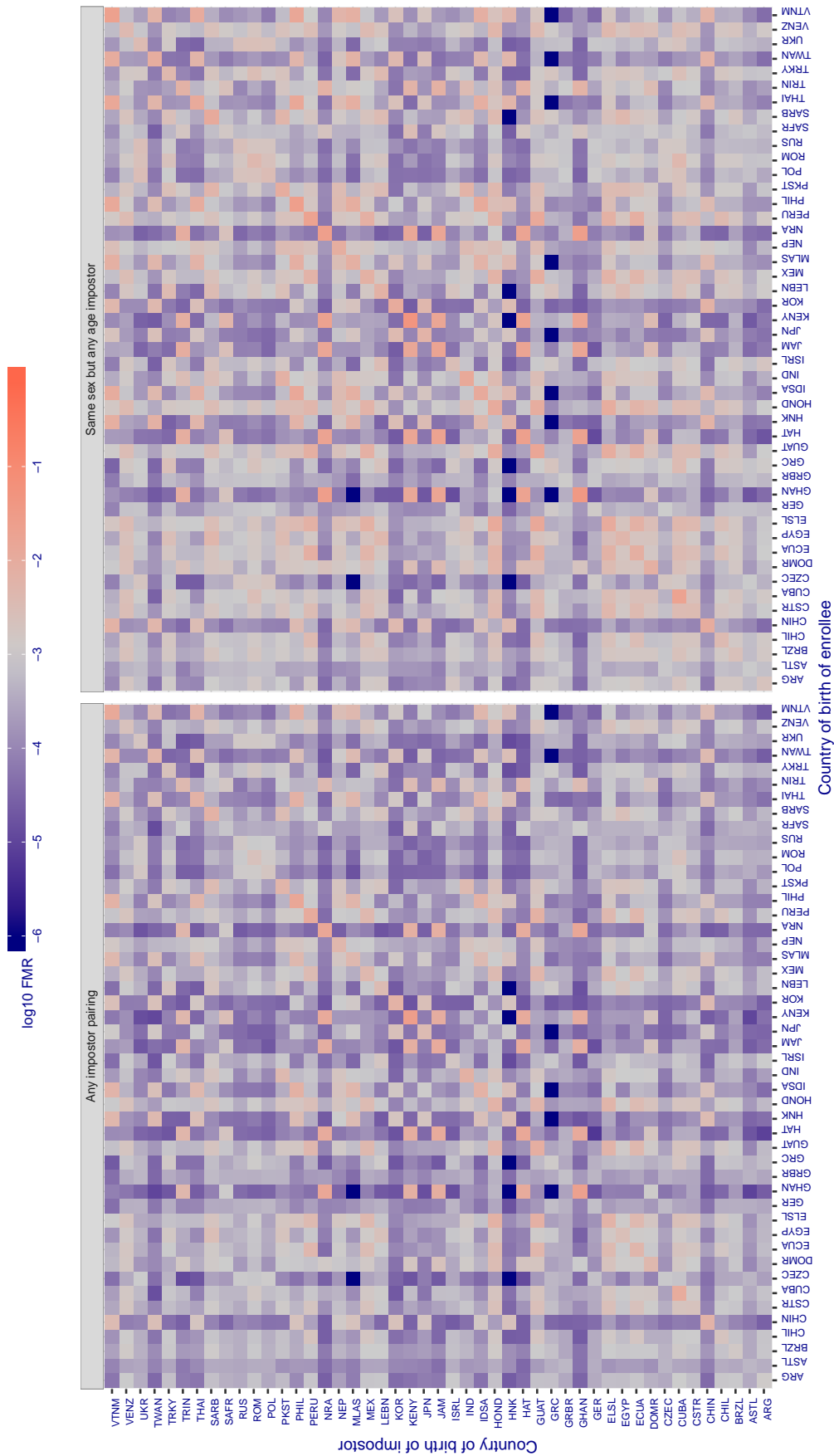


Figure 216: For algorithm anyvision-004 operating on visa images, the heatmap shows false match rates observed over impostor comparisons of faces from different individuals who were born in the given country pair. False matches are counted against a recognition threshold fixed globally to give the target FMR in the plot title, computed over all on the order of 10^{10} impostor comparisons. If text appears in each box it give the same quantity as that coded by the color. Grey indicates FMR is at the intended FMR target level. Light red colors present a security vulnerability to, for example, a passport gate. Each +1 increase in \log_{10} FMR corresponds to a factor of 10 increase in FMR. The matrix is not quite symmetric because images in the enrollment and verification sets are different.

Cross country FMR at threshold $T = 2.758$ for algorithm aware_003, giving $FMR(T) = 0.001$ globally.

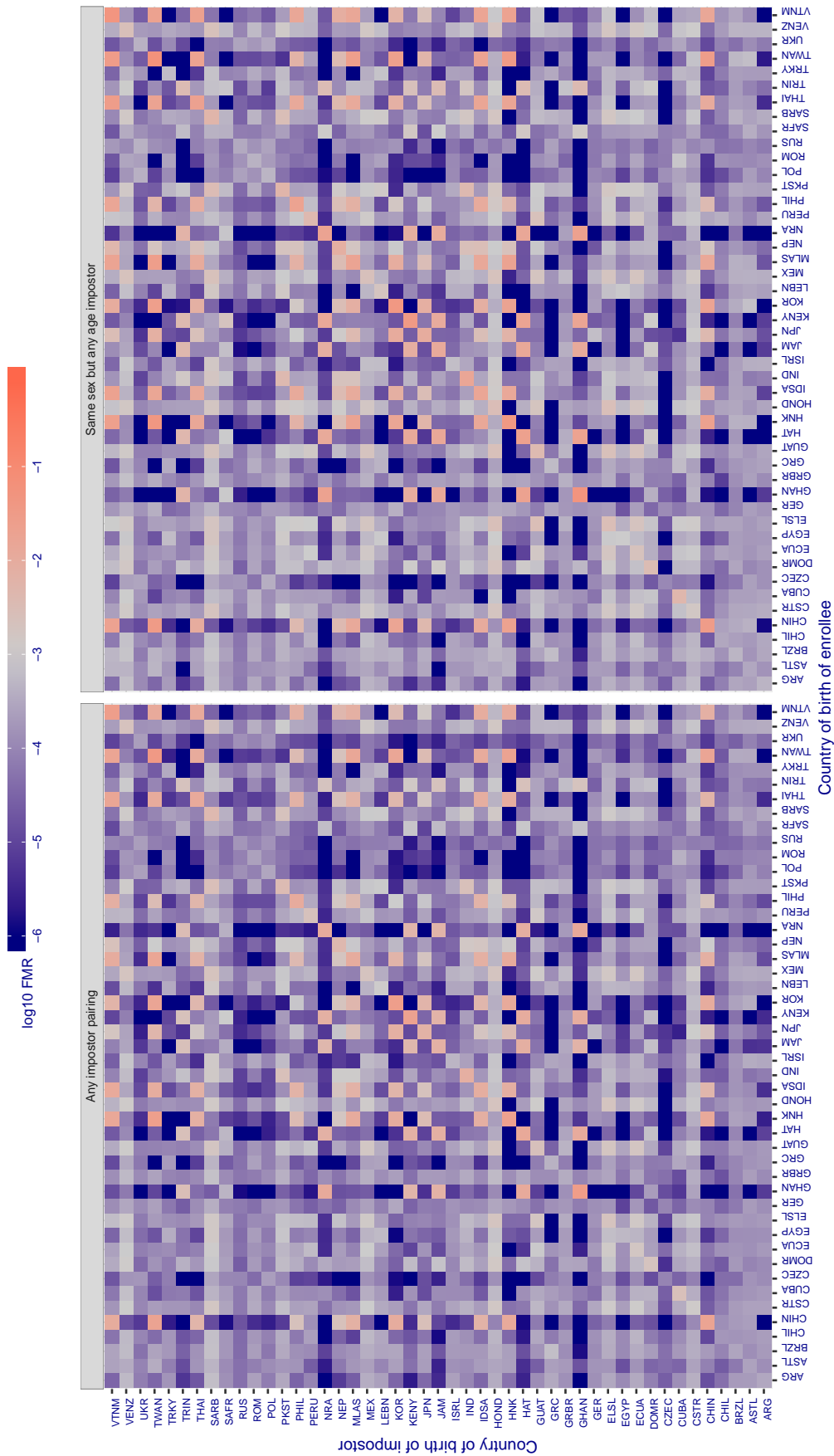


Figure 217: For algorithm aware-003 operating on visa images, the heatmap shows false match rates observed over impostor comparisons of faces from different individuals who were born in the given country pair. False matches are counted against a recognition threshold fixed globally to give the target FMR in the plot title, computed over all on the order of 10^{10} impostor comparisons. If text appears in each box it give the same quantity as that coded by the color. Grey indicates FMR is at the intended FMR target level. Light red colors present a security vulnerability to, for example, a passport gate. Each +1 increase in $\log_{10} FMR$ corresponds to a factor of 10 increase in FMR. The matrix is not quite symmetric because images in the enrollment and verification sets are different.

Cross country FMR at threshold $T = 3.681$ for algorithm aware_004, giving $FMR(T) = 0.001$ globally.

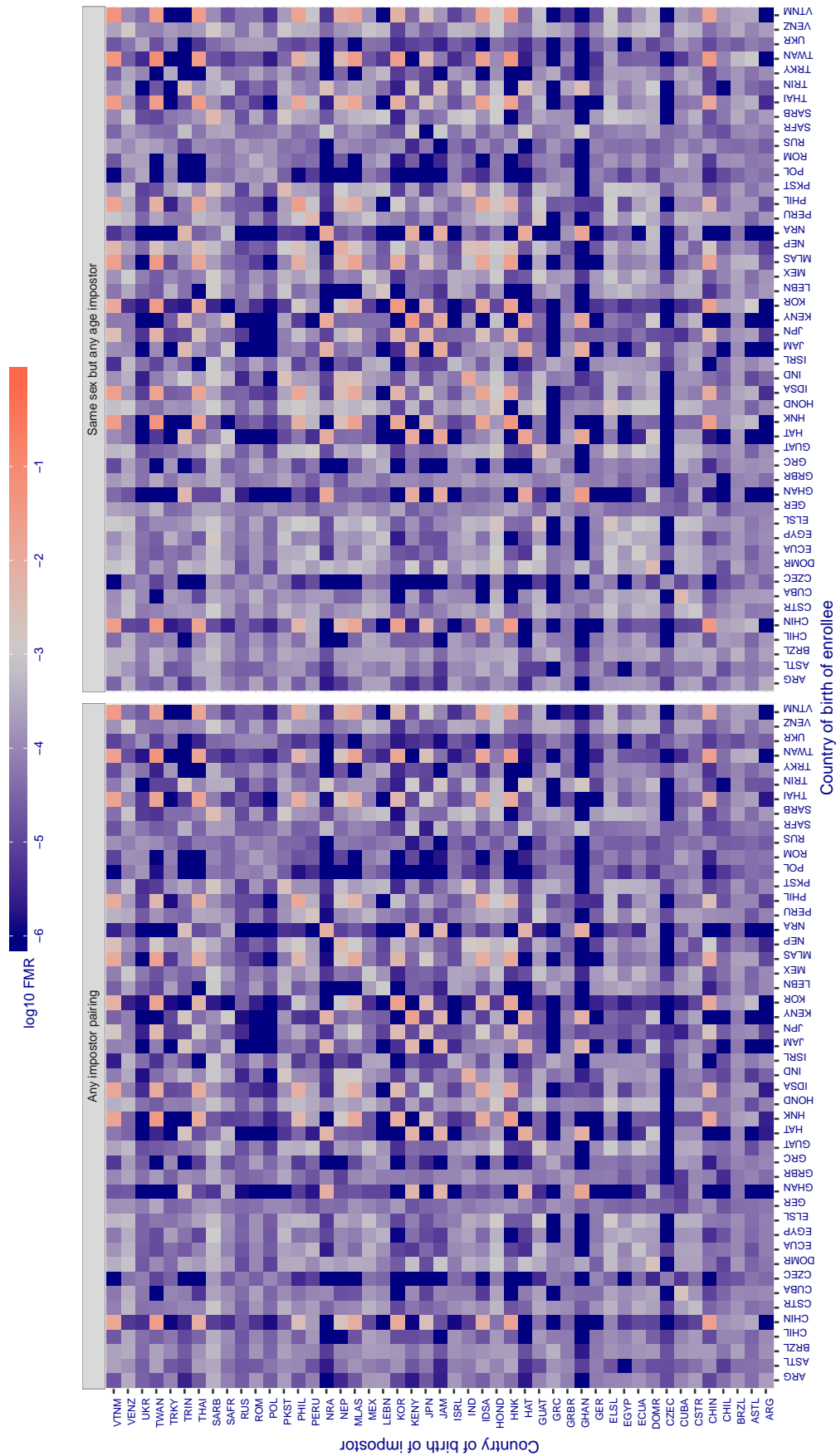


Figure 218: For algorithm aware-004 operating on visa images, the heatmap shows false match rates observed over impostor comparisons of faces from different individuals who were born in the given country pair. False matches are counted against a recognition threshold fixed globally to give the target FMR in the plot title, computed over all on the order of 10^{10} impostor comparisons. If text appears in each box it give the same quantity as that coded by the color. Grey indicates FMR is at the intended FMR target level. Light red colors present a security vulnerability to, for example, a passport gate. Each +1 increase in \log_{10} FMR corresponds to a factor of 10 increase in FMR. The matrix is not quite symmetric because images in the enrollment and verification sets are different.

Cross country FMR at threshold $T = 0.800$ for algorithm ayonix_000, giving $FMR(T) = 0.001$ globally.

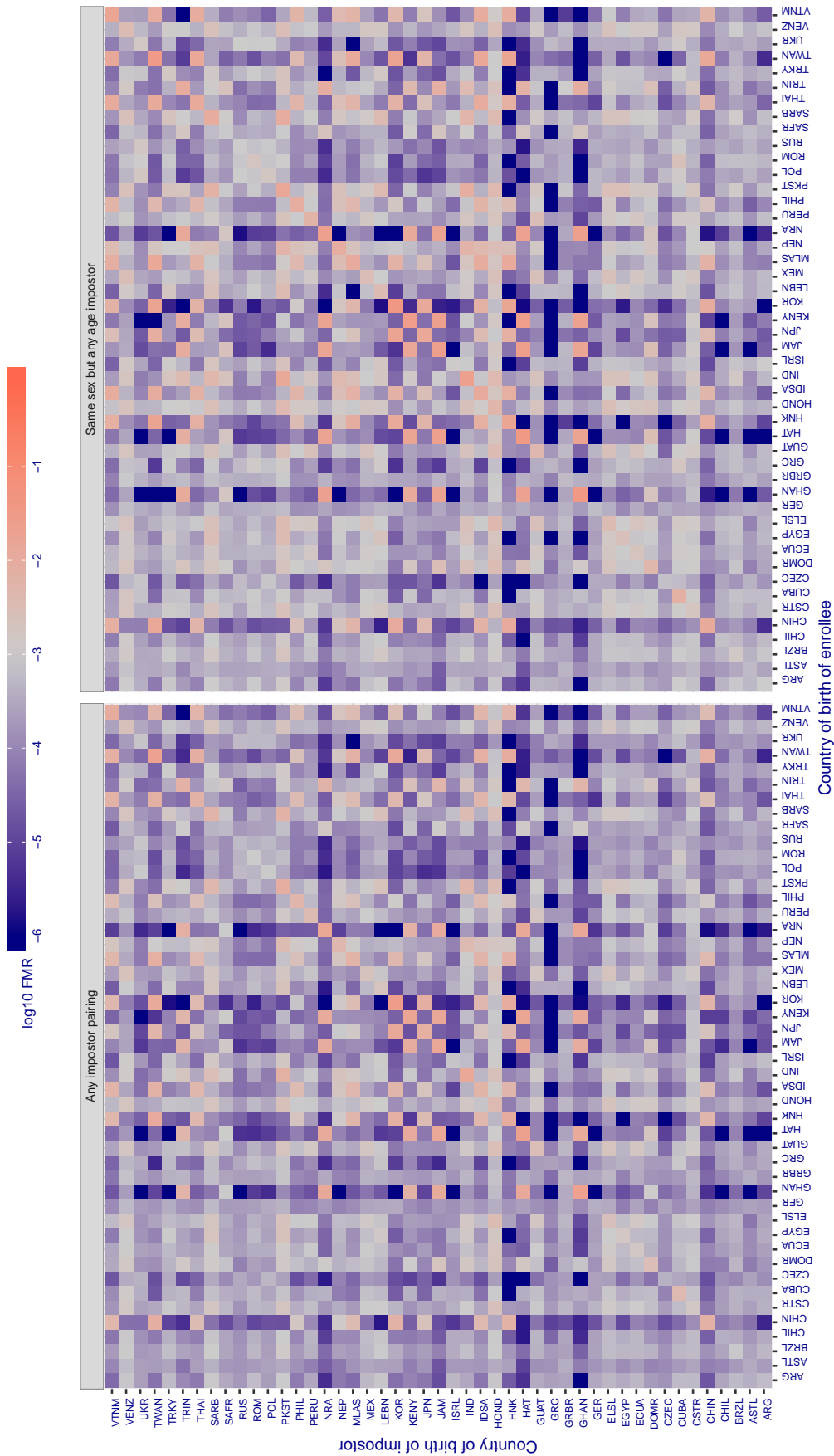


Figure 219: For algorithm ayonix-000 operating on visa images, the heatmap shows false match rates observed over impostor comparisons of faces from different individuals who were born in the given country pair. False matches are counted against a recognition threshold fixed globally to give the target FMR in the plot title, computed over all on the order of 10^{10} impostor comparisons. If text appears in each box it give the same quantity as that coded by the color. Grey indicates FMR is at the intended FMR target level. Light red colors present a security vulnerability to, for example, a passport gate. Each +1 increase in $\log_{10} FMR$ corresponds to a factor of 10 increase in FMR. The matrix is not quite symmetric because images in the enrollment and verification sets are different.

Cross country FMR at threshold $T = 0.649$ for algorithm `bm_001`, giving $FMR(T) = 0.001$ globally.

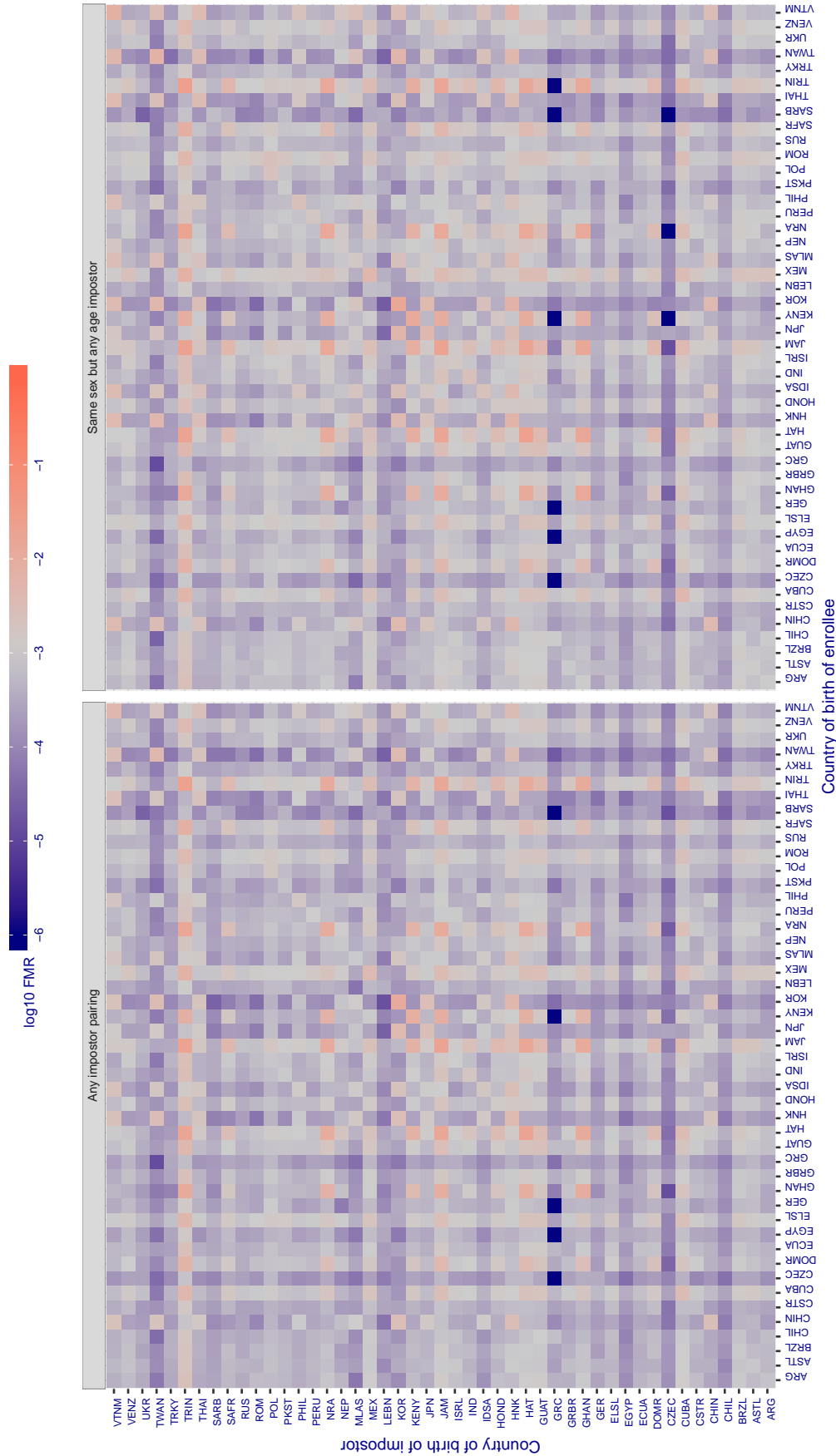


Figure 220: For algorithm `bm-001` operating on visa images, the heatmap shows false match rates observed over impostor comparisons of faces from different individuals who were born in the given country pair. False matches are counted against a recognition threshold fixed globally to give the target FMR in the plot title, computed over all on the order of 10^{10} impostor comparisons. If text appears in each box it give the same quantity as that coded by the color. Grey indicates FMR is at the intended FMR target level. Light red colors present a security vulnerability to, for example, a passport gate. Each +1 increase in \log_{10} FMR corresponds to a factor of 10 increase in FMR. The matrix is not quite symmetric because images in the enrollment and verification sets are different.

Cross country FMR at threshold $T = 0.306$ for algorithm camvi_002, giving $FMR(T) = 0.001$ globally.

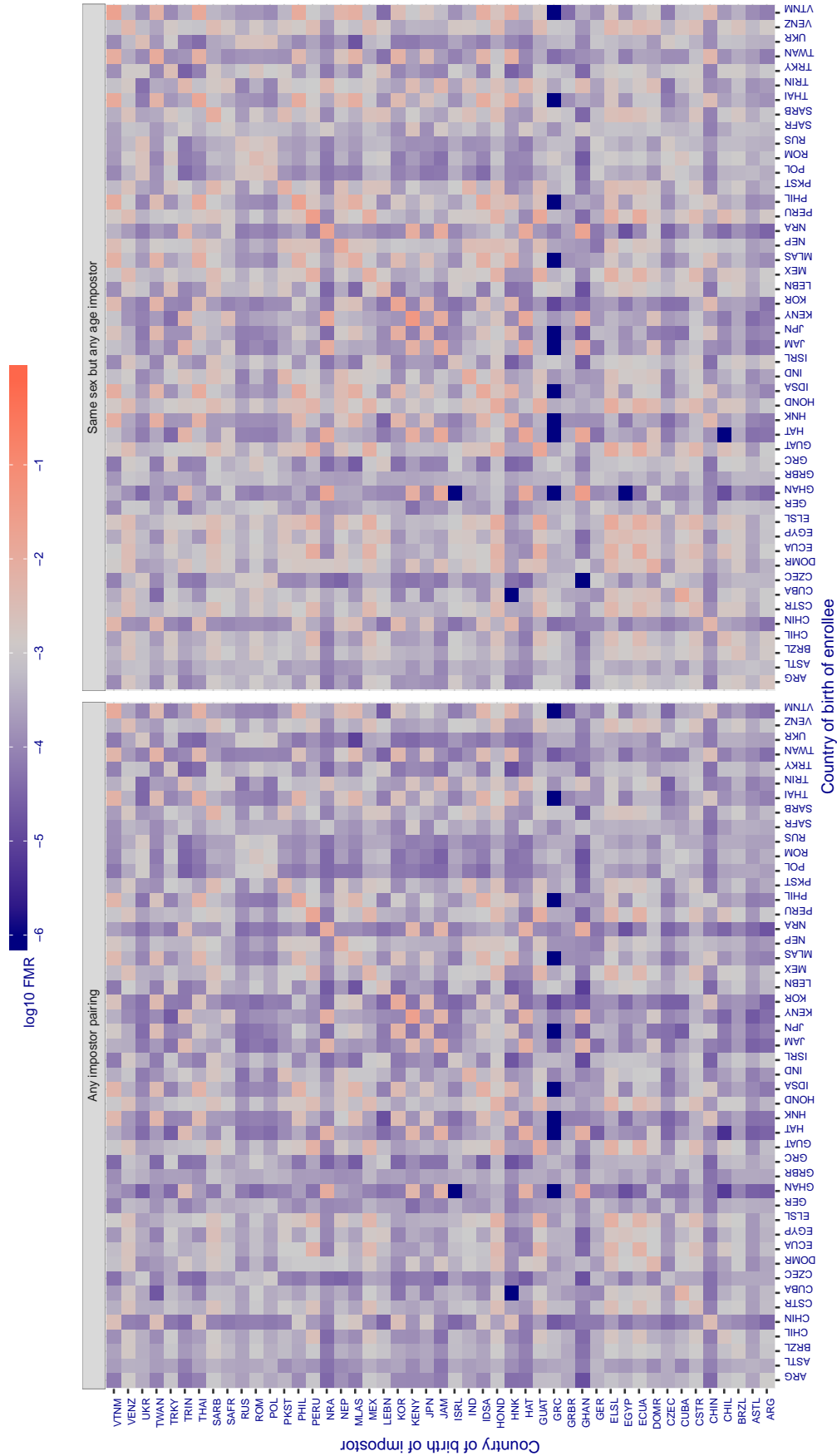


Figure 221: For algorithm camvi-002 operating on visa images, the heatmap shows false match rates observed over impostor comparisons of faces from different individuals who were born in the given country pair. False matches are counted against a recognition threshold fixed globally to give the target FMR in the plot title, computed over all on the order of 10^{10} impostor comparisons. If text appears in each box it give the same quantity as that coded by the color. Grey indicates FMR is at the intended FMR target level. Light red colors present a security vulnerability to, for example, a passport gate. Each +1 increase in \log_{10} FMR corresponds to a factor of 10 increase in FMR. The matrix is not quite symmetric because images in the enrollment and verification sets are different.

Cross country FMR at threshold $T = 0.301$ for algorithm camvi_003, giving $FMR(T) = 0.001$ globally.

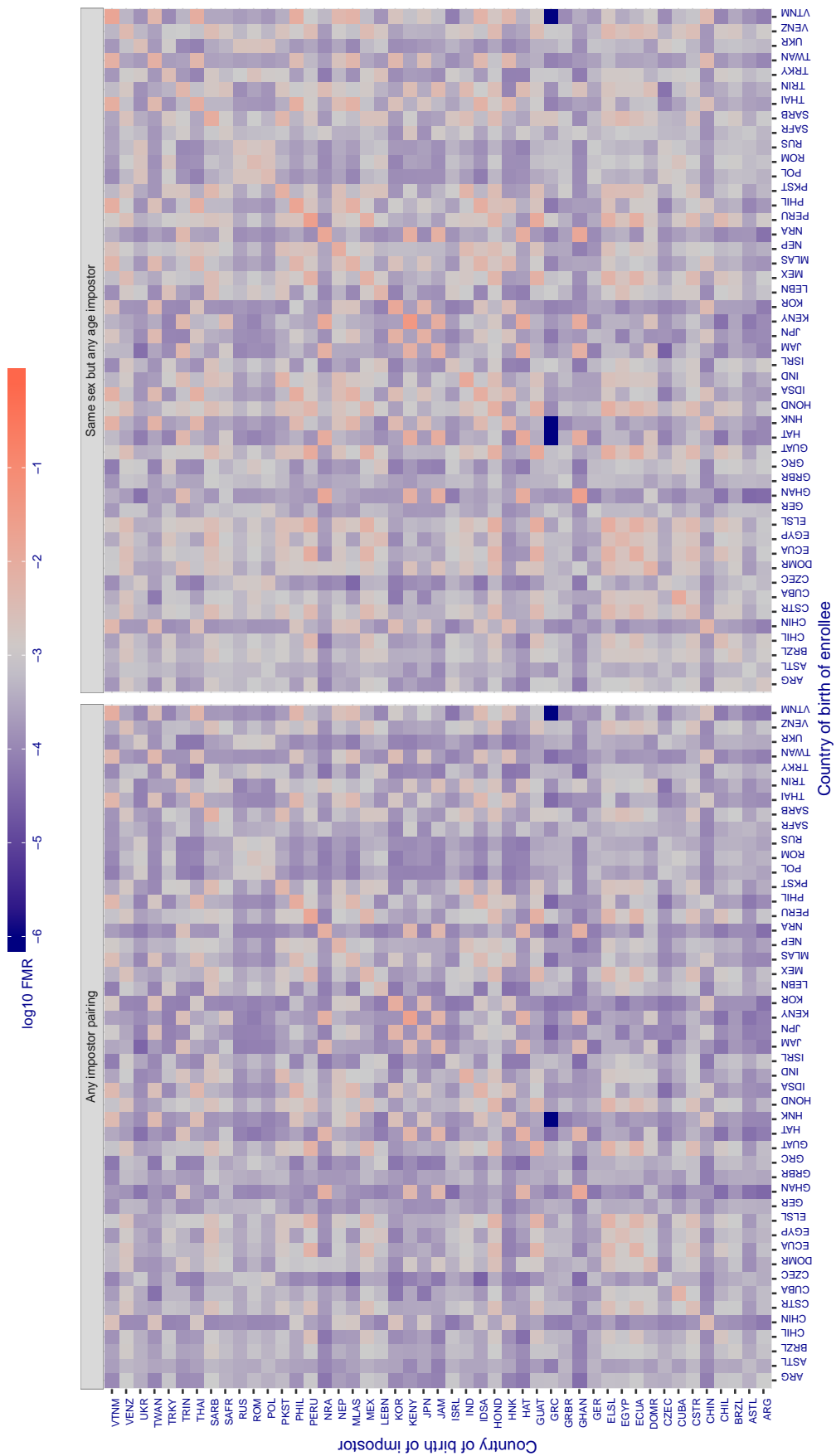


Figure 222: For algorithm camvi-003 operating on visa images, the heatmap shows false match rates observed over impostor comparisons of faces from different individuals who were born in the given country pair. False matches are counted against a recognition threshold fixed globally to give the target FMR in the plot title, computed over all on the order of 10^{10} impostor comparisons. If text appears in each box it give the same quantity as that coded by the color. Grey indicates FMR is at the intended FMR target level. Light red colors present a security vulnerability to, for example, a passport gate. Each +1 increase in \log_{10} FMR corresponds to a factor of 10 increase in FMR. The matrix is not quite symmetric because images in the enrollment and verification sets are different.

Cross country FMR at threshold $T = 0.346$ for algorithm ceiec_001, giving $FMR(T) = 0.001$ globally.

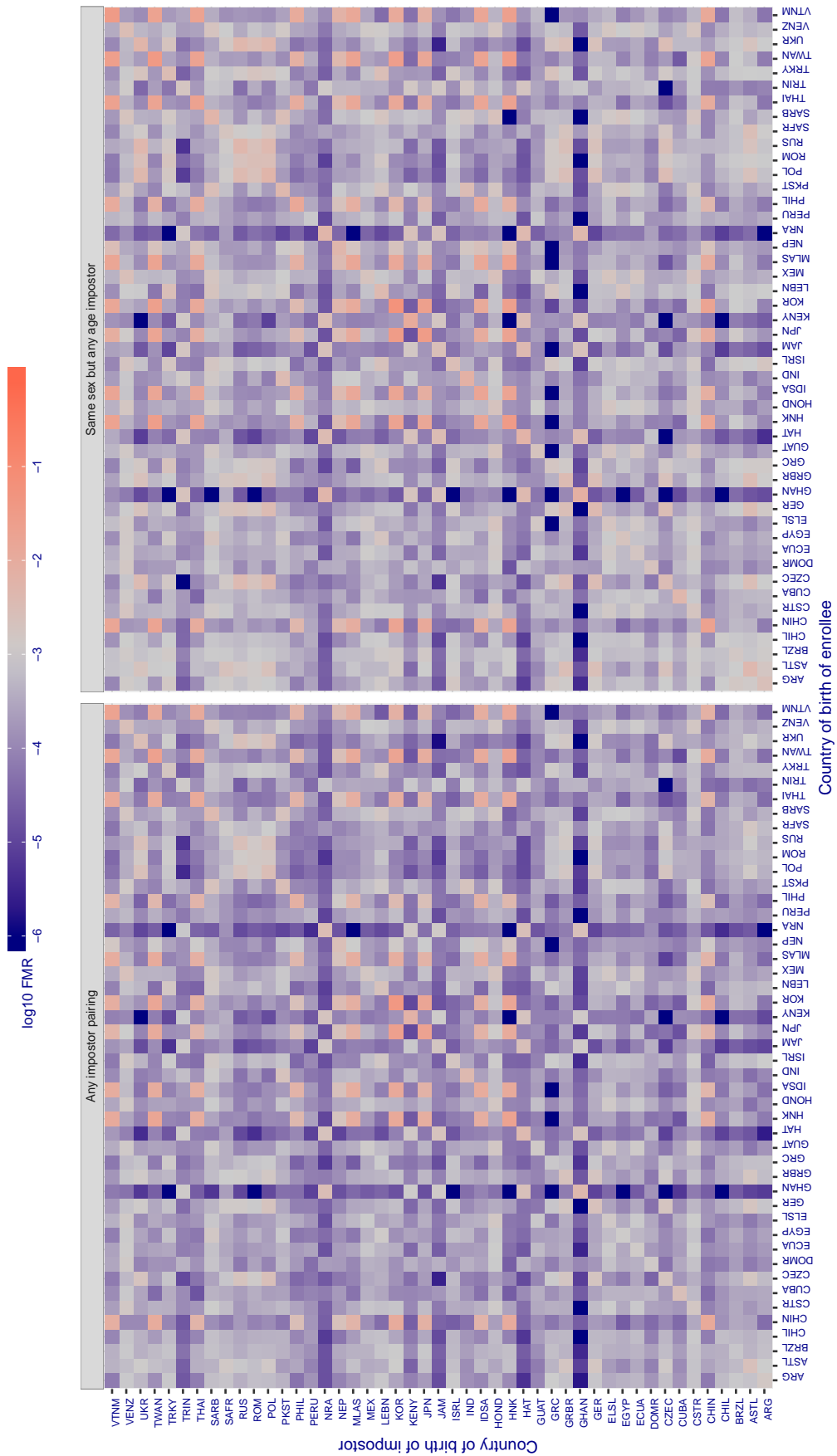


Figure 223: For algorithm ceiec-001 operating on visa images, the heatmap shows false match rates observed over impostor comparisons of faces from different individuals who were born in the given country pair. False matches are counted against a recognition threshold fixed globally to give the target FMR in the plot title, computed over all on the order of 10^{10} impostor comparisons. If text appears in each box it give the same quantity as that coded by the color. Grey indicates FMR is at the intended FMR target level. Light red colors present a security vulnerability to, for example, a passport gate. Each +1 increase in \log_{10} FMR corresponds to a factor of 10 increase in FMR. The matrix is not quite symmetric because images in the enrollment and verification sets are different.

Cross country FMR at threshold $T = 3038.000$ for algorithm cogent_002, giving $FMR(T) = 0.001$ globally.

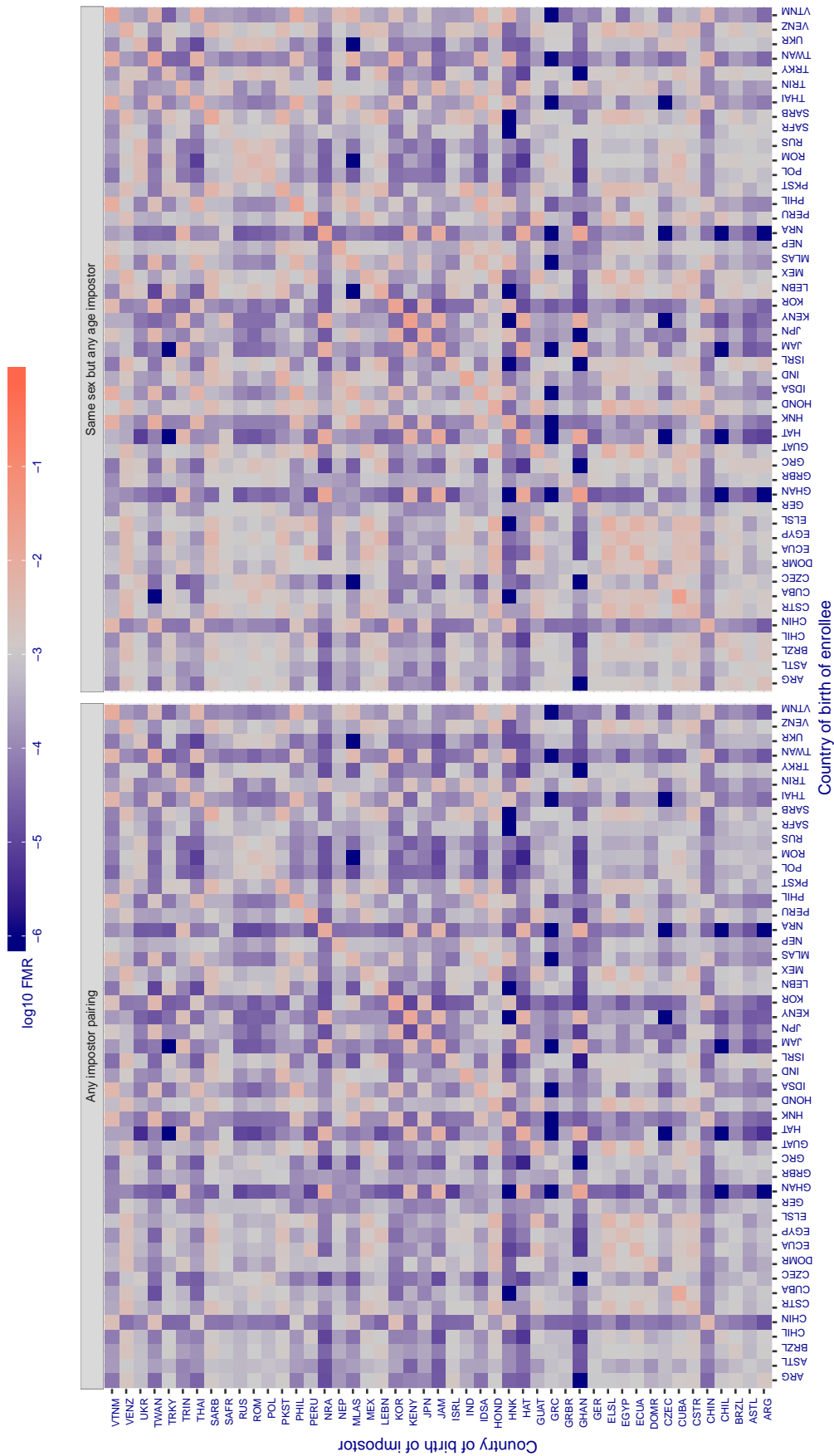


Figure 224: For algorithm cogent-002 operating on visa images, the heatmap shows false match rates observed over impostor comparisons of faces from different individuals who were born in the given country pair. False matches are counted against a recognition threshold fixed globally to give the target FMR in the plot title, computed over all on the order of 10^{10} impostor comparisons. If text appears in each box it give the same quantity as that coded by the color. Grey indicates FMR is at the intended FMR target level. Light red colors present a security vulnerability to, for example, a passport gate. Each +1 increase in \log_{10} FMR corresponds to a factor of 10 increase in FMR. The matrix is not quite symmetric because images in the enrollment and verification sets are different.

Cross country FMR at threshold $T = 2845.000$ for algorithm cogent_003, giving $FMR(T) = 0.001$ globally.

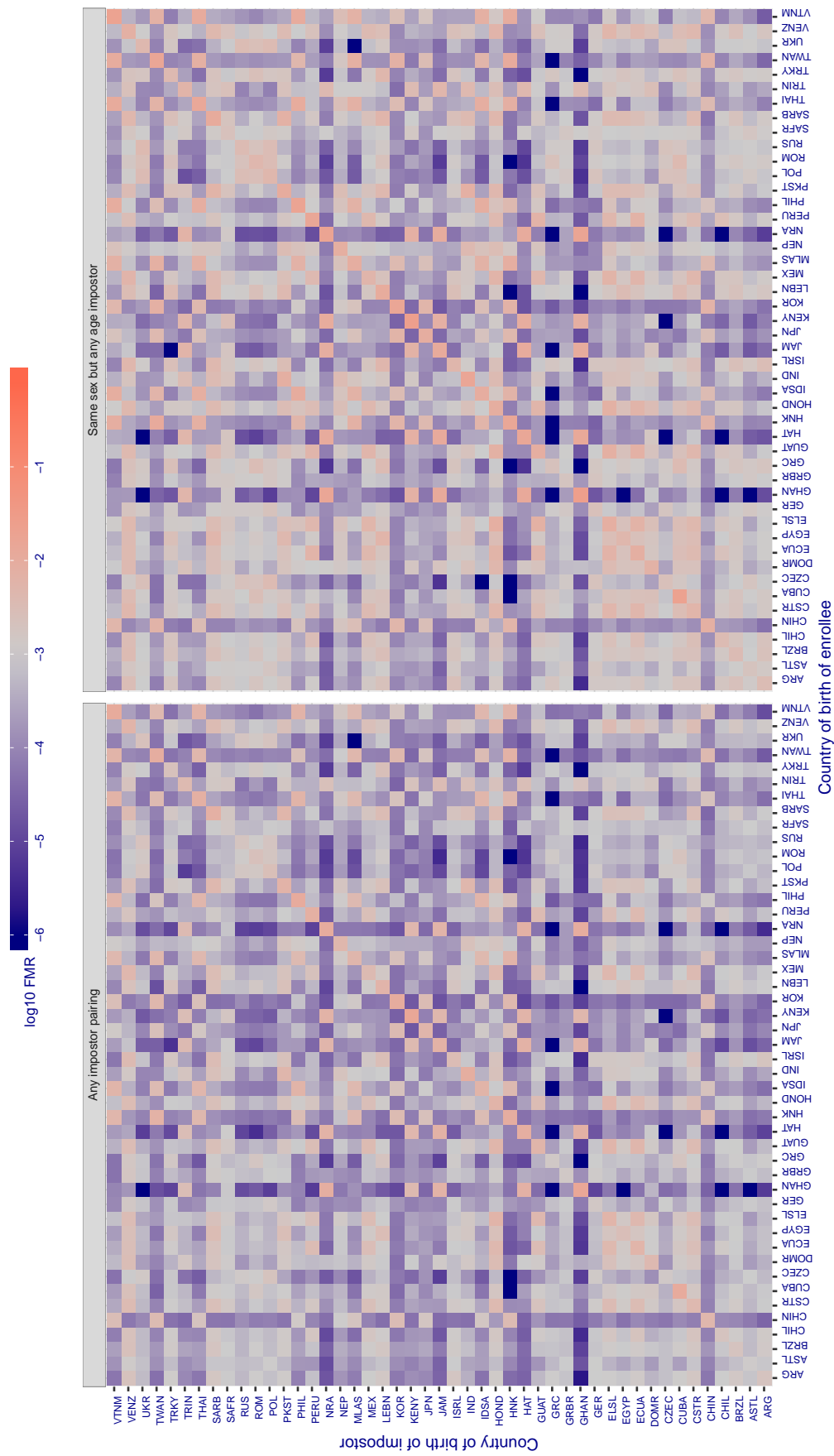


Figure 225: For algorithm cogent-003 operating on visa images, the heatmap shows false match rates observed over impostor comparisons of faces from different individuals who were born in the given country pair. False matches are counted against a recognition threshold fixed globally to give the target FMR in the plot title, computed over all on the order of 10^{10} impostor comparisons. If text appears in each box it give the same quantity as that coded by the color. Grey indicates FMR is at the intended FMR target level. Light red colors present a security vulnerability to, for example, a passport gate. Each +1 increase in \log_{10} FMR corresponds to a factor of 10 increase in FMR. The matrix is not quite symmetric because images in the enrollment and verification sets are different.

Cross country FMR at threshold $T = 0.522$ for algorithm `cognitec_000`, giving $FMR(T) = 0.001$ globally.

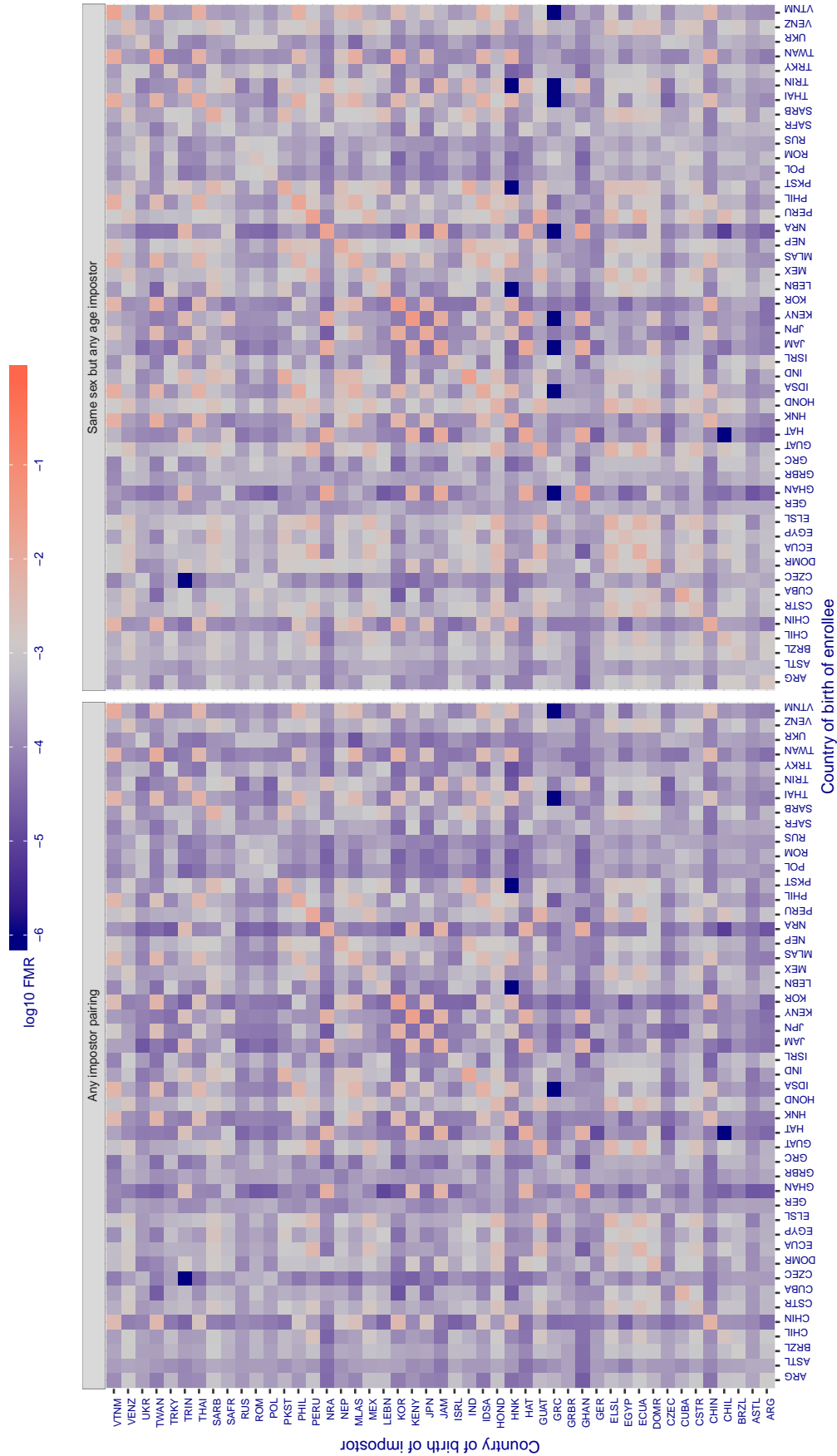


Figure 226: For algorithm `cognitec-000` operating on visa images, the heatmap shows false match rates observed over impostor comparisons of faces from different individuals who were born in the given country pair. False matches are counted against a recognition threshold fixed globally to give the target FMR in the plot title, computed over all on the order of 10^{10} impostor comparisons. If text appears in each box it give the same quantity as that coded by the color. Grey indicates FMR is at the intended FMR target level. Light red colors present a security vulnerability to, for example, a passport gate. Each +1 increase in \log_{10} FMR corresponds to a factor of 10 increase in FMR. The matrix is not quite symmetric because images in the enrollment and verification sets are different.

Cross country FMR at threshold $T = 0.522$ for algorithm `cognitec_001`, giving $FMR(T) = 0.001$ globally.

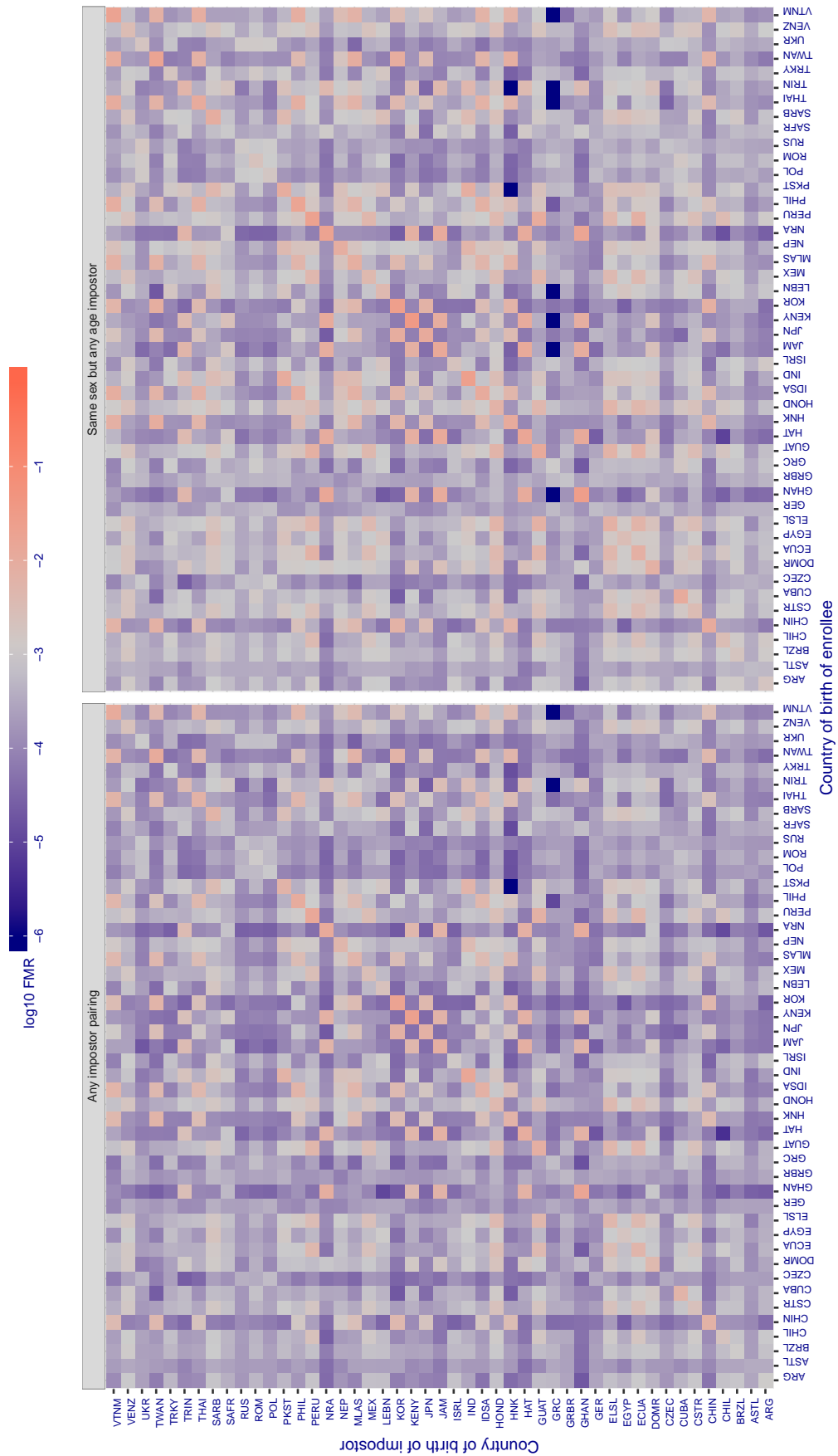


Figure 227: For algorithm `cognitec-001` operating on visa images, the heatmap shows false match rates observed over impostor comparisons of faces from different individuals who were born in the given country pair. False matches are counted against a recognition threshold fixed globally to give the target FMR in the plot title, computed over all on the order of 10^{10} impostor comparisons. If text appears in each box it give the same quantity as that coded by the color. Grey indicates FMR is at the intended FMR target level. Light red colors present a security vulnerability to, for example, a passport gate. Each +1 increase in \log_{10} FMR corresponds to a factor of 10 increase in FMR. The matrix is not quite symmetric because images in the enrollment and verification sets are different.

Cross country FMR at threshold $T = 0.702$ for algorithm cyberextruder_001, giving $FMR(T) = 0.001$ globally.

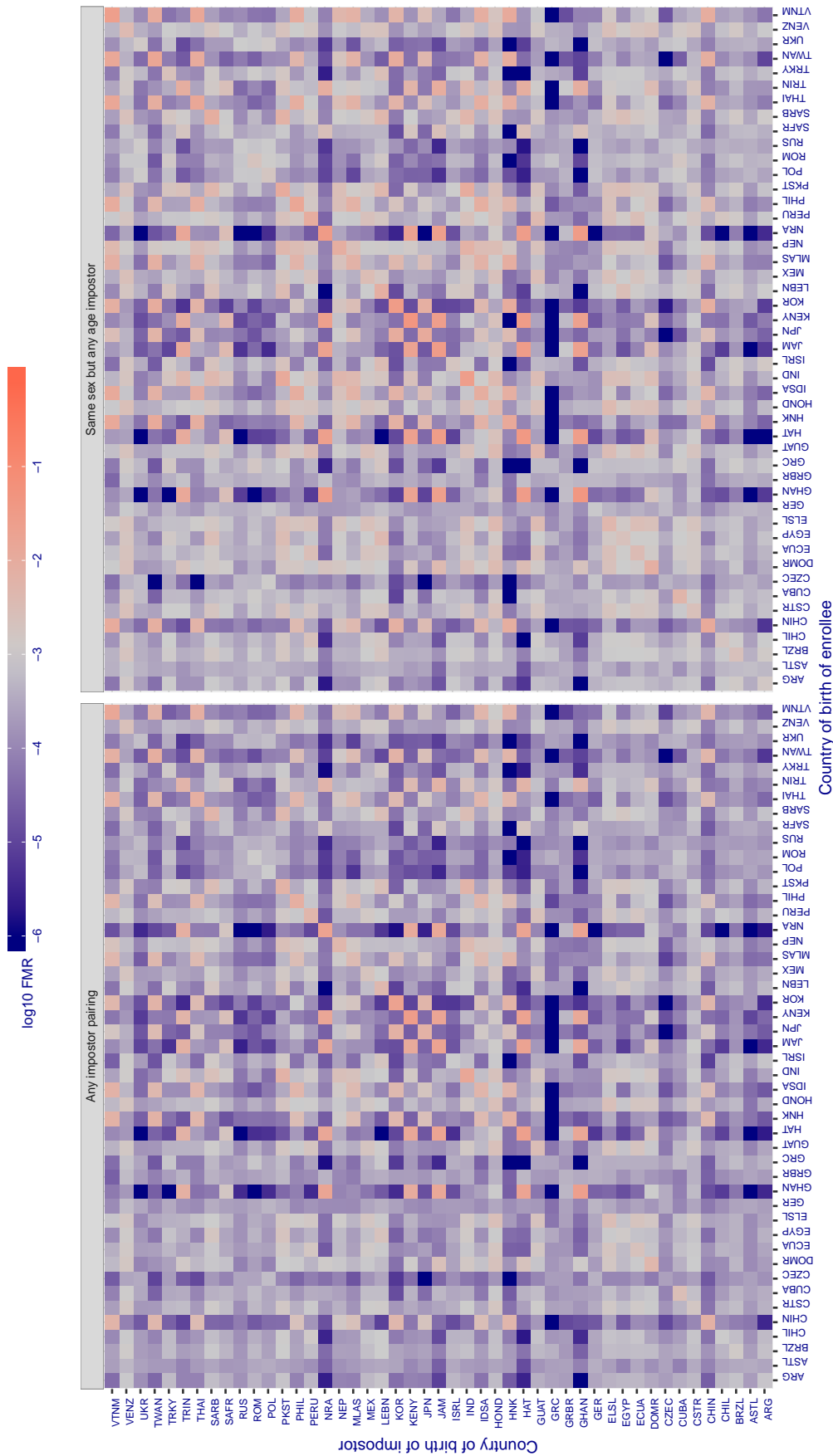


Figure 228: For algorithm cyberextruder-001 operating on visa images, the heatmap shows false match rates observed over impostor comparisons of faces from different individuals who were born in the given country pair. False matches are counted against a recognition threshold fixed globally to give the target FMR in the plot title, computed over all on the order of 10^{10} impostor comparisons. If text appears in each box it give the same quantity as that coded by the color. Grey indicates FMR is at the intended FMR target level. Light red colors present a security vulnerability to, for example, a passport gate. Each +1 increase in \log_{10} FMR corresponds to a factor of 10 increase in FMR. The matrix is not quite symmetric because images in the enrollment and verification sets are different.

Cross country FMR at threshold $T = 0.408$ for algorithm cyberextruder_002, giving $FMR(T) = 0.001$ globally.

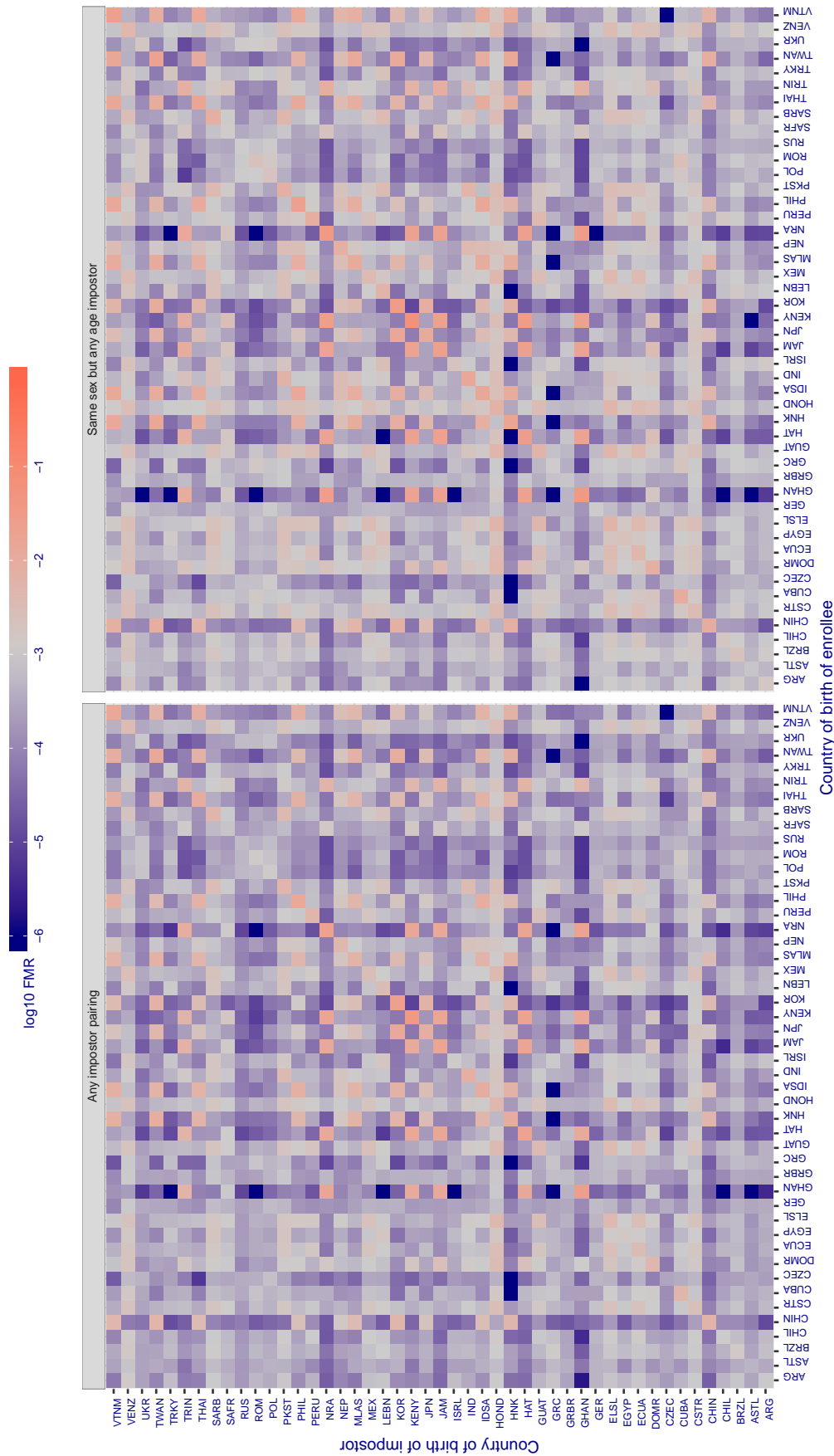


Figure 229: For algorithm cyberextruder-002 operating on visa images, the heatmap shows false match rates observed over impostor comparisons of faces from different individuals who were born in the given country pair. False matches are counted against a recognition threshold fixed globally to give the target FMR in the plot title, computed over all on the order of 10^{10} impostor comparisons. If text appears in each box it give the same quantity as that coded by the color. Grey indicates FMR is at the intended FMR target level. Light red colors present a security vulnerability to, for example, a passport gate. Each +1 increase in \log_{10} FMR corresponds to a factor of 10 increase in FMR. The matrix is not quite symmetric because images in the enrollment and verification sets are different.

Cross country FMR at threshold $T = 1.322$ for algorithm cyberlink_000, giving $FMR(T) = 0.001$ globally.

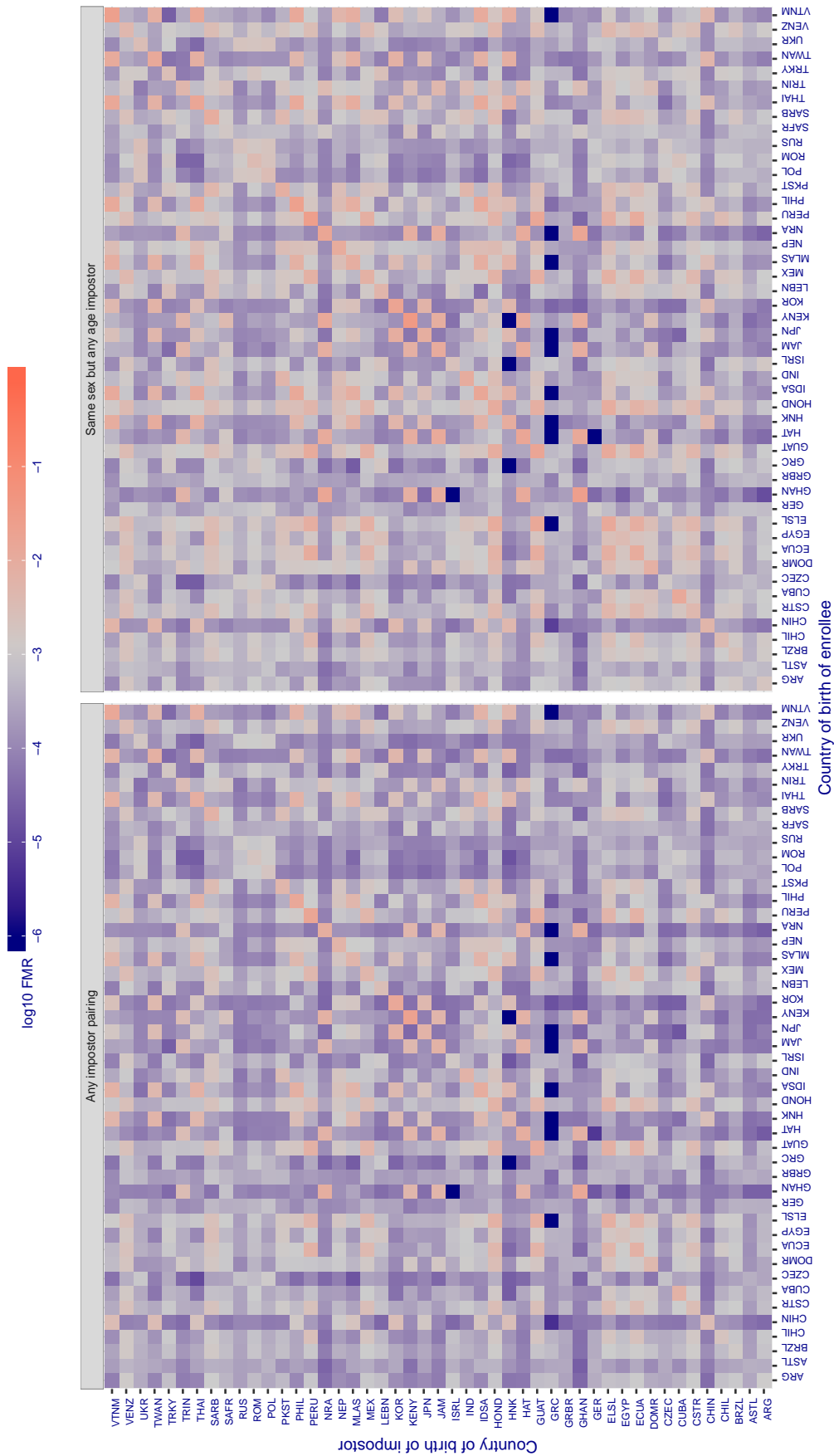


Figure 230: For algorithm cyberlink-000 operating on visa images, the heatmap shows false match rates observed over impostor comparisons of faces from different individuals who were born in the given country pair. False matches are counted against a recognition threshold fixed globally to give the target FMR in the plot title, computed over all on the order of 10^{10} impostor comparisons. If text appears in each box it give the same quantity as that coded by the color. Grey indicates FMR is at the intended FMR target level. Light red colors present a security vulnerability to, for example, a passport gate. Each +1 increase in $\log_{10} FMR$ corresponds to a factor of 10 increase in FMR. The matrix is not quite symmetric because images in the enrollment and verification sets are different.

Cross country FMR at threshold $T = 1.322$ for algorithm cyberlink_001, giving $FMR(T) = 0.001$ globally.

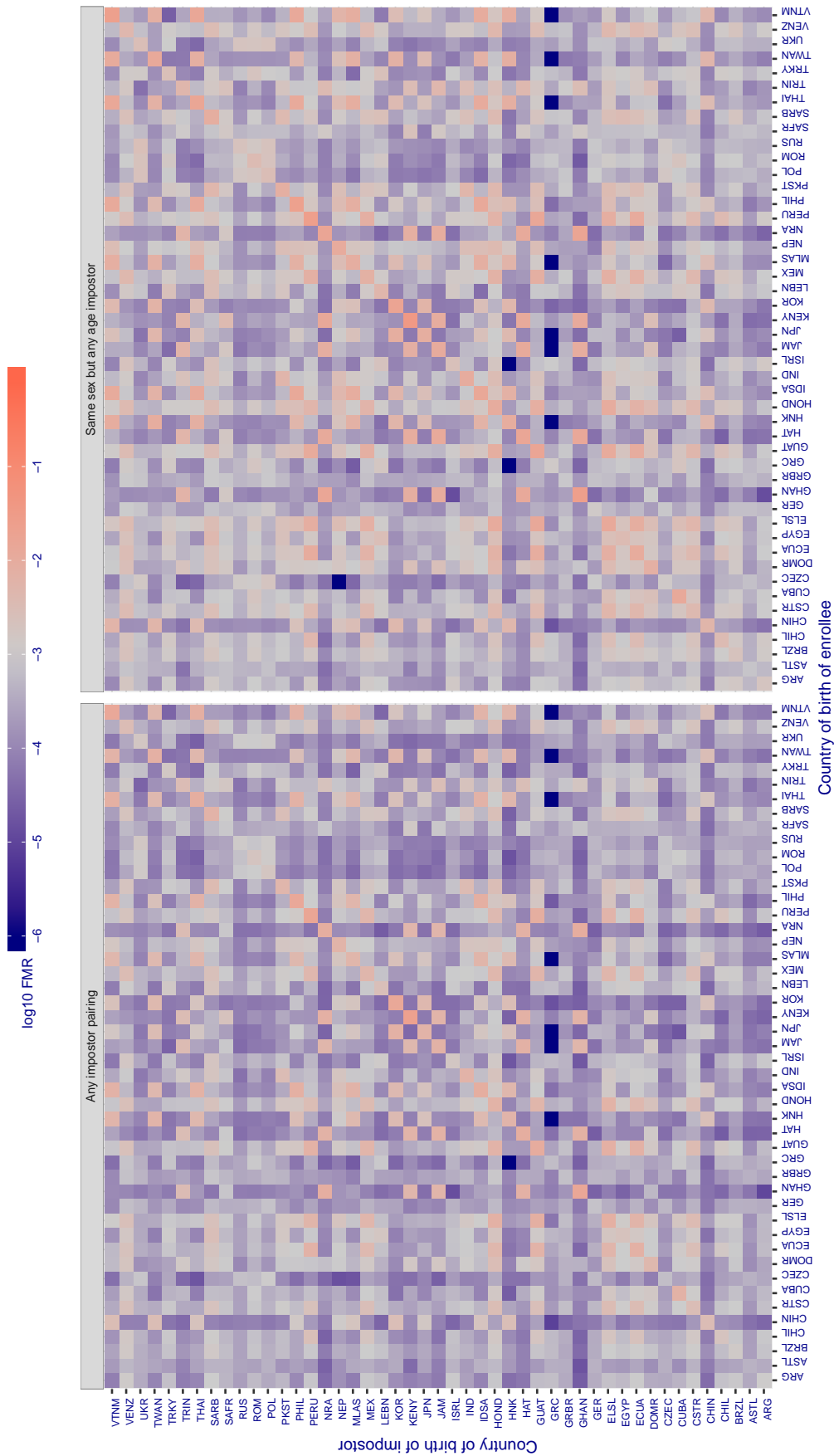


Figure 231: For algorithm cyberlink-001 operating on visa images, the heatmap shows false match rates observed over impostor comparisons of faces from different individuals who were born in the given country pair. False matches are counted against a recognition threshold fixed globally to give the target FMR in the plot title, computed over all on the order of 10^{10} impostor comparisons. If text appears in each box it give the same quantity as that coded by the color. Grey indicates FMR is at the intended FMR target level. Light red colors present a security vulnerability to, for example, a passport gate. Each +1 increase in \log_{10} FMR corresponds to a factor of 10 increase in FMR. The matrix is not quite symmetric because images in the enrollment and verification sets are different.

Cross country FMR at threshold $T = 6606.000$ for algorithm dahua_001, giving $FMR(T) = 0.001$ globally.

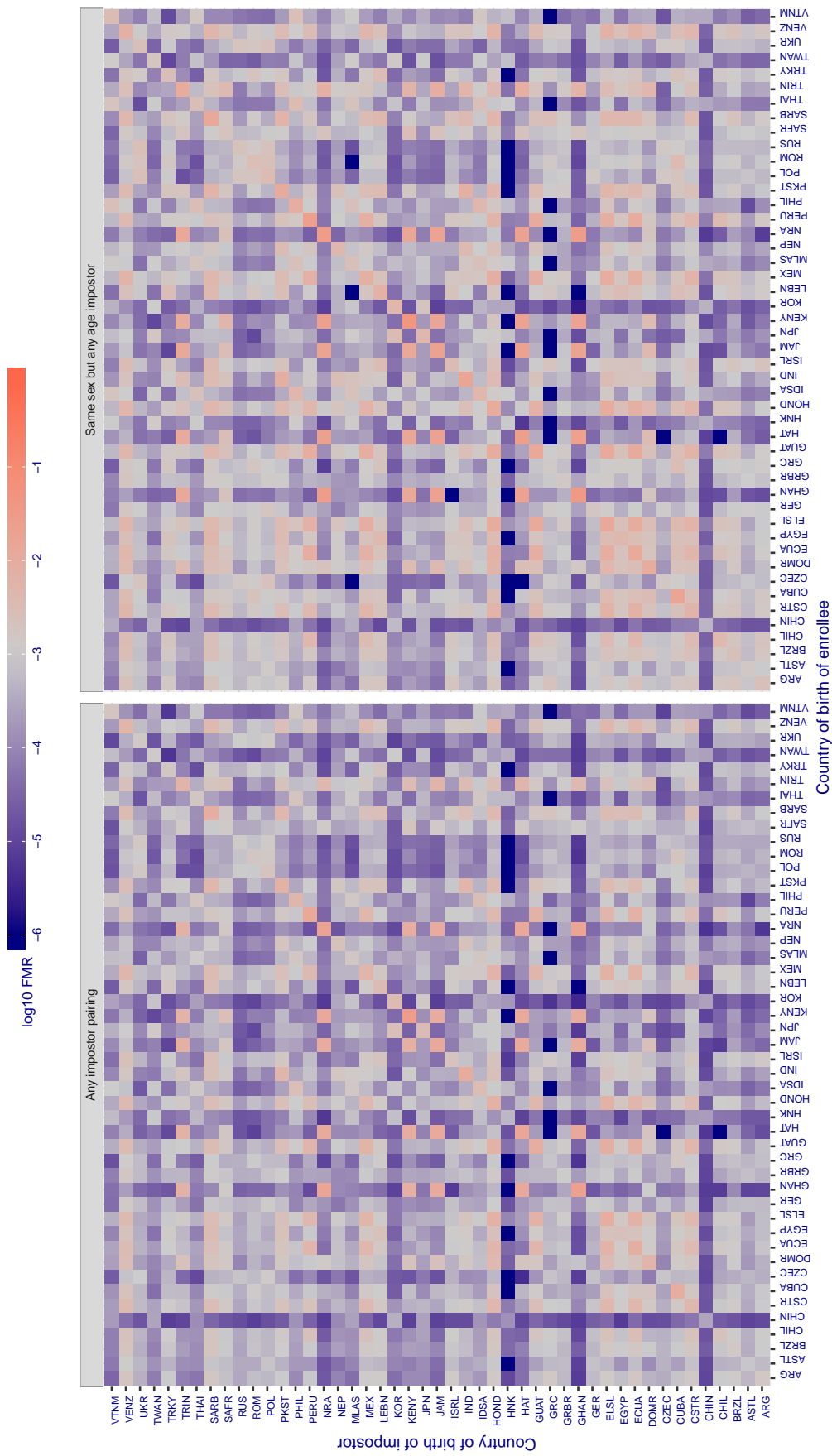


Figure 232: For algorithm dahua-001 operating on visa images, the heatmap shows false match rates observed over impostor comparisons of faces from different individuals who were born in the given country pair. False matches are counted against a recognition threshold fixed globally to give the target FMR in the plot title, computed over all on the order of 10^{10} impostor comparisons. If text appears in each box it give the same quantity as that coded by the color. Grey indicates FMR is at the intended FMR target level. Light red colors present a security vulnerability to, for example, a passport gate. Each +1 increase in $\log_{10} FMR$ corresponds to a factor of 10 increase in FMR. The matrix is not quite symmetric because images in the enrollment and verification sets are different.

Cross country FMR at threshold $T = 5958.000$ for algorithm dahua_002, giving $FMR(T) = 0.001$ globally.

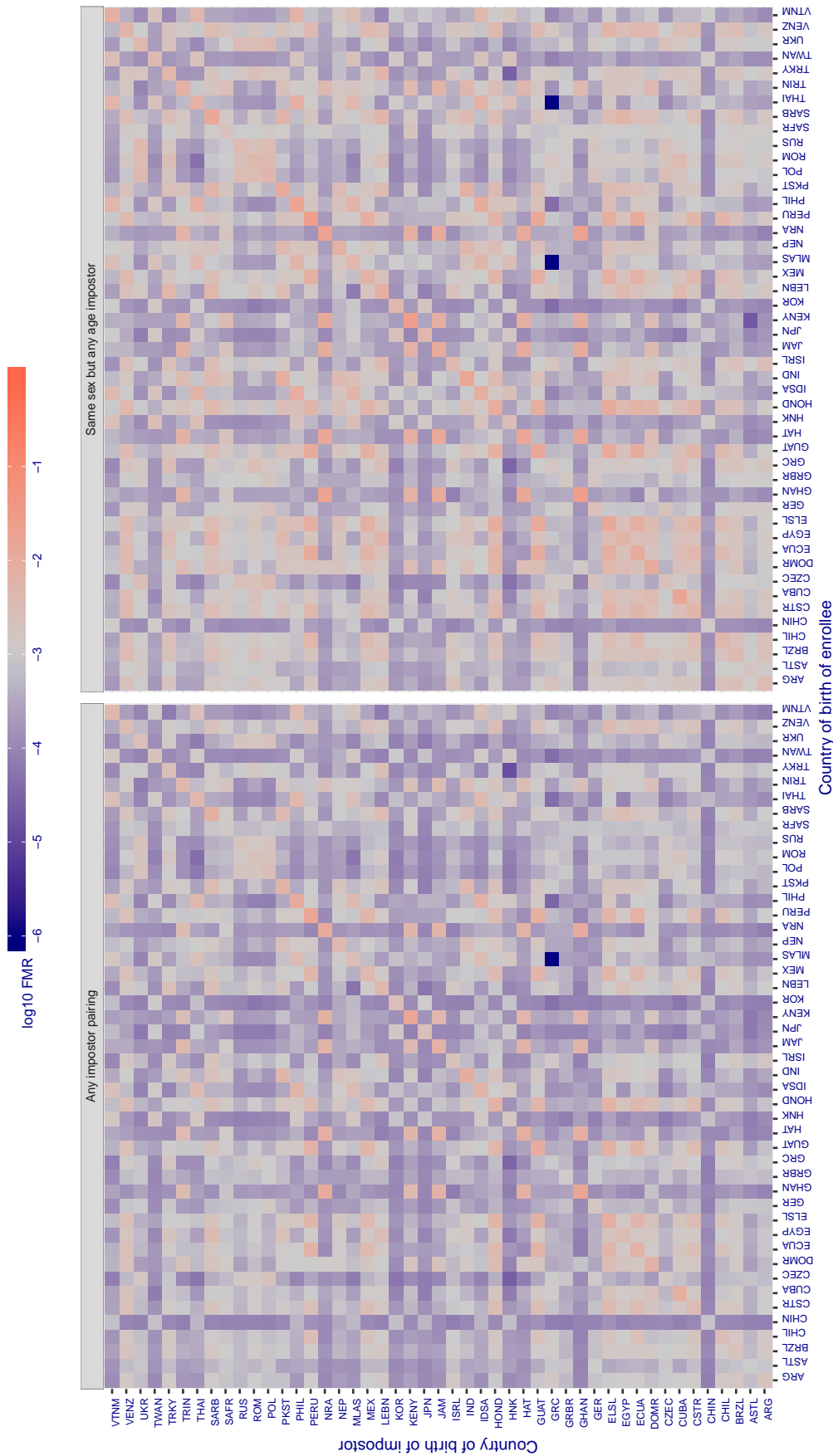


Figure 233: For algorithm dahua-002 operating on visa images, the heatmap shows false match rates observed over impostor comparisons of faces from different individuals who were born in the given country pair. False matches are counted against a recognition threshold fixed globally to give the target FMR in the plot title, computed over all on the order of 10^{10} impostor comparisons. If text appears in each box it give the same quantity as that coded by the color. Grey indicates FMR is at the intended FMR target level. Light red colors present a security vulnerability to, for example, a passport gate. Each +1 increase in $\log_{10} FMR$ corresponds to a factor of 10 increase in FMR. The matrix is not quite symmetric because images in the enrollment and verification sets are different.

Cross country FMR at threshold $T = 75.231$ for algorithm dermalog_005, giving $FMR(T) = 0.001$ globally.

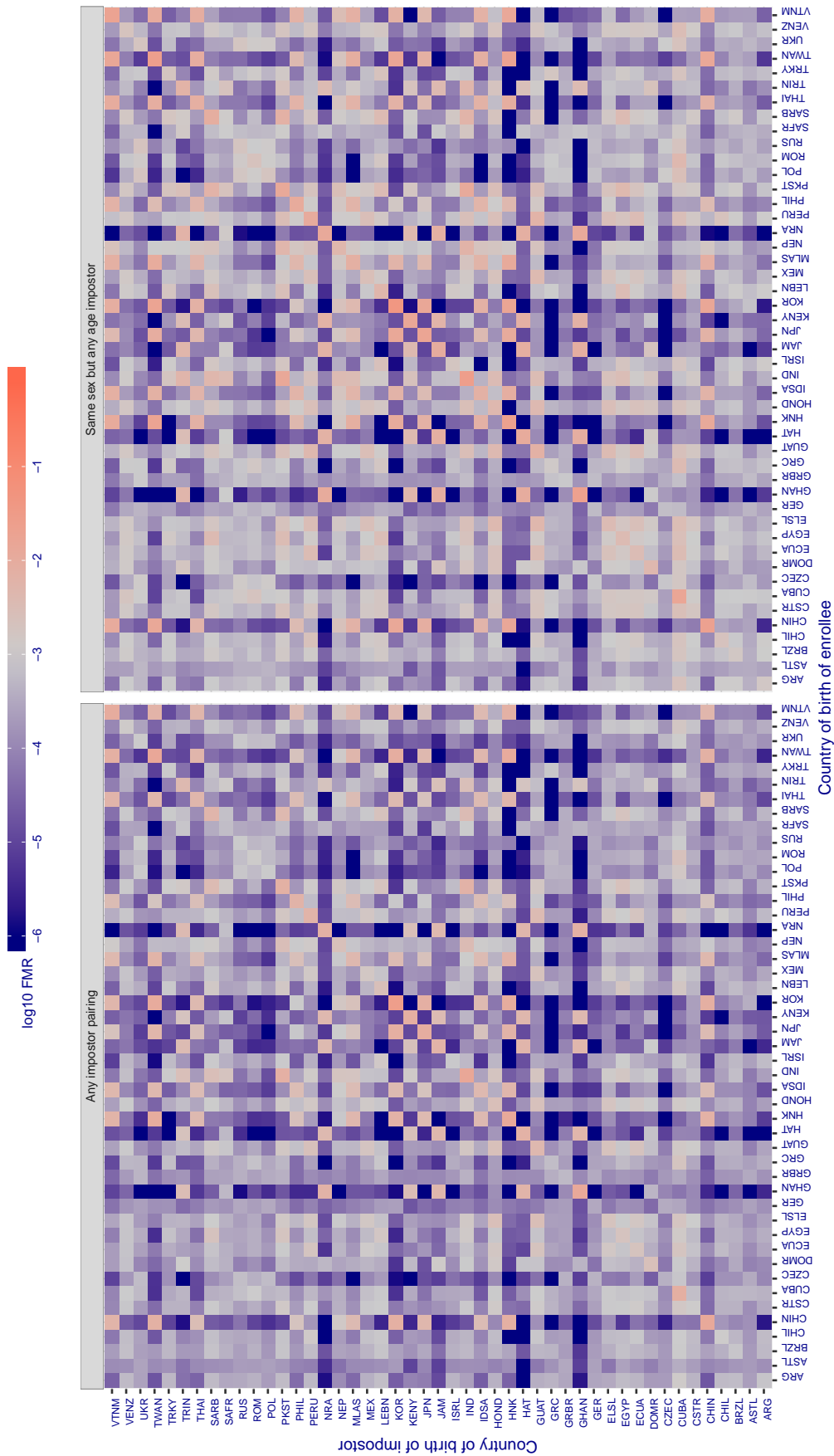


Figure 234: For algorithm dermalog-005 operating on visa images, the heatmap shows false match rates observed over impostor comparisons of faces from different individuals who were born in the given country pair. False matches are counted against a recognition threshold fixed globally to give the target FMR in the plot title, computed over all on the order of 10^{10} impostor comparisons. If text appears in each box it give the same quantity as that coded by the color. Grey indicates FMR is at the intended FMR target level. Light red colors present a security vulnerability to, for example, a passport gate. Each +1 increase in \log_{10} FMR corresponds to a factor of 10 increase in FMR. The matrix is not quite symmetric because images in the enrollment and verification sets are different.

Cross country FMR at threshold $T = 76.496$ for algorithm dermalog_006, giving $FMR(T) = 0.001$ globally.

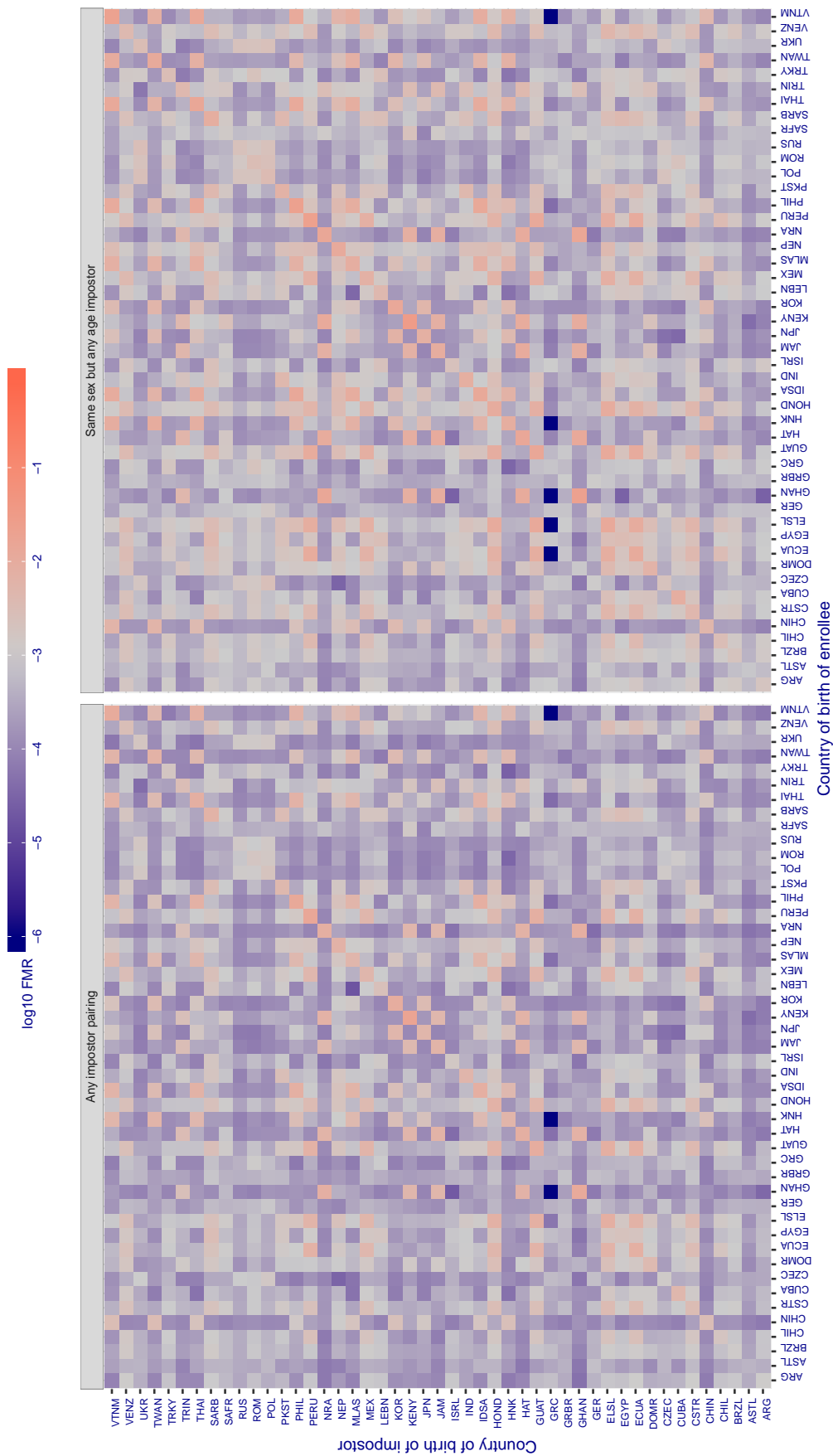


Figure 235: For algorithm dermalog-006 operating on visa images, the heatmap shows false match rates observed over impostor comparisons of faces from different individuals who were born in the given country pair. False matches are counted against a recognition threshold fixed globally to give the target FMR in the plot title, computed over all on the order of 10^{10} impostor comparisons. If text appears in each box it give the same quantity as that coded by the color. Grey indicates FMR is at the intended FMR target level. Light red colors present a security vulnerability to, for example, a passport gate. Each +1 increase in \log_{10} FMR corresponds to a factor of 10 increase in FMR. The matrix is not quite symmetric because images in the enrollment and verification sets are different.

Cross country FMR at threshold $T = 0.547$ for algorithm digitalbarriers_002, giving $FMR(T) = 0.001$ globally.

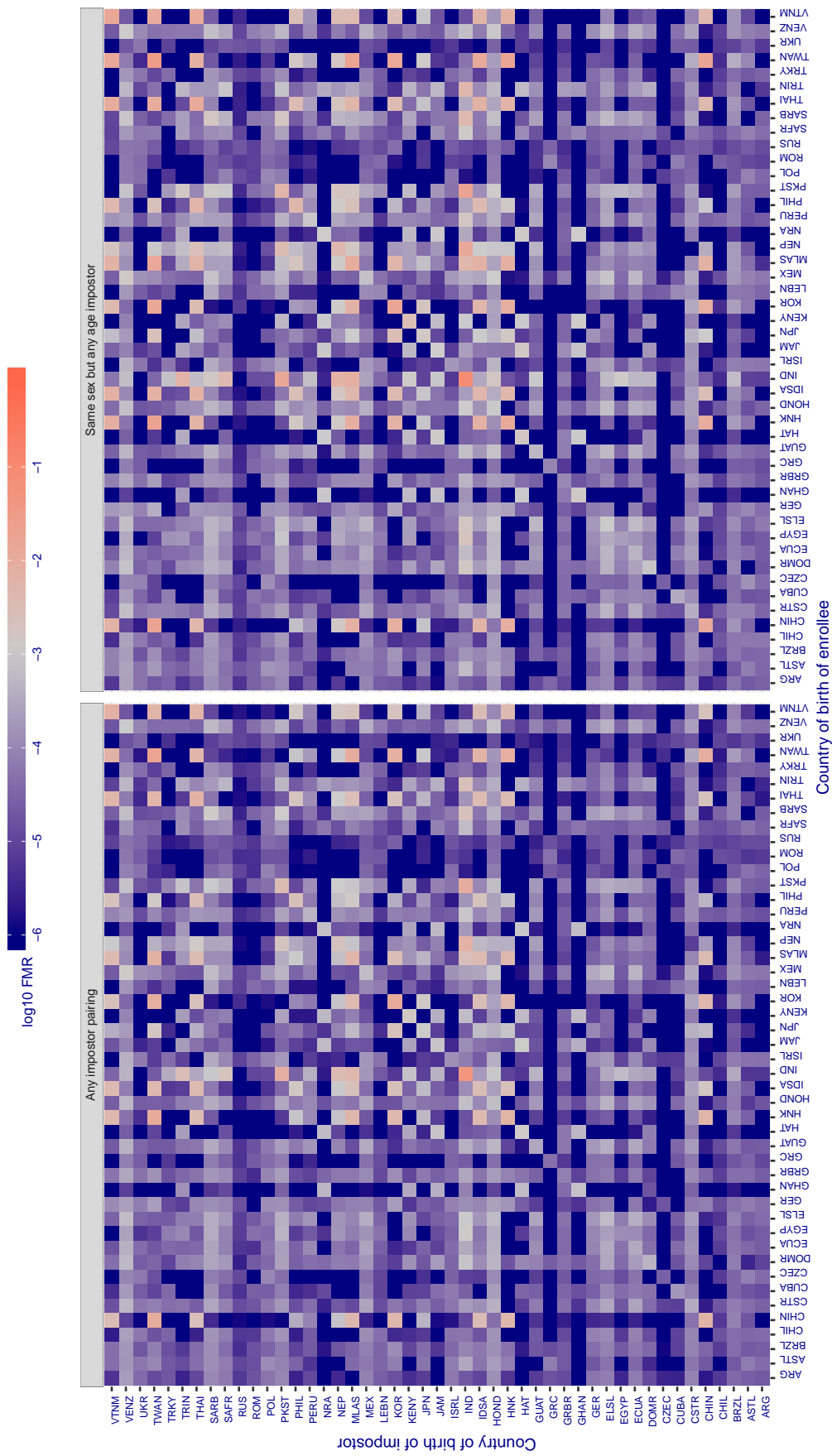


Figure 236: For algorithm digitalbarriers-002 operating on visa images, the heatmap shows false match rates observed over impostor comparisons of faces from different individuals who were born in the given country pair. False matches are counted against a recognition threshold fixed globally to give the target FMR in the plot title, computed over all on the order of 10^{10} impostor comparisons. If text appears in each box it give the same quantity as that coded by the color. Grey indicates FMR is at the intended FMR target level. Light red colors present a security vulnerability to, for example, a passport gate. Each +1 increase in \log_{10} FMR corresponds to a factor of 10 increase in FMR. The matrix is not quite symmetric because images in the enrollment and verification sets are different.

Cross country FMR at threshold $T = 2.510$ for algorithm everai_001, giving $FMR(T) = 0.001$ globally.

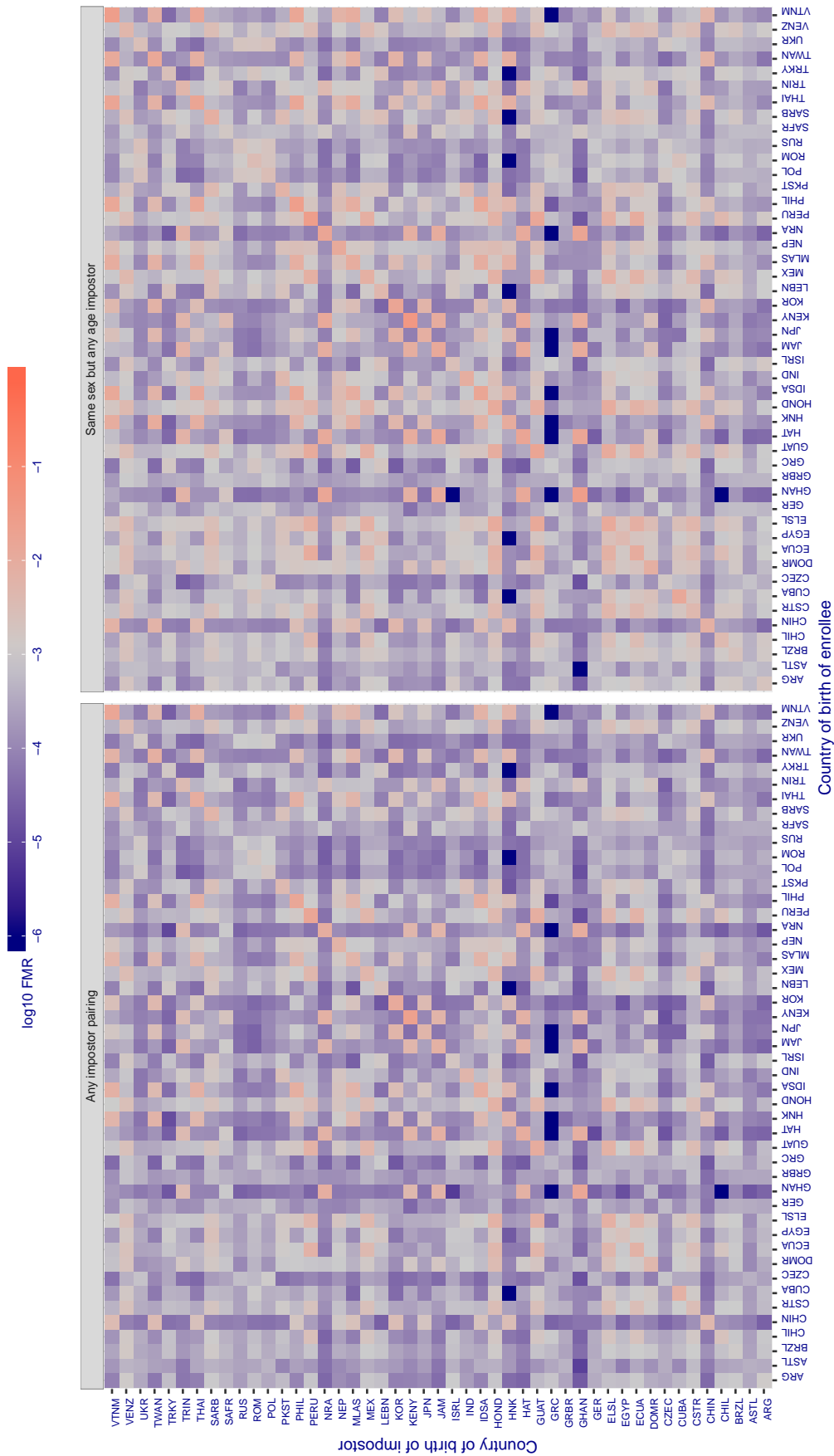


Figure 237: For algorithm everai-001 operating on visa images, the heatmap shows false match rates observed over impostor comparisons of faces from different individuals who were born in the given country pair. False matches are counted against a recognition threshold fixed globally to give the target FMR in the plot title, computed over all on the order of 10^{10} impostor comparisons. If text appears in each box it give the same quantity as that coded by the color. Grey indicates FMR is at the intended FMR target level. Light red colors present a security vulnerability to, for example, a passport gate. Each +1 increase in \log_{10} FMR corresponds to a factor of 10 increase in FMR. The matrix is not quite symmetric because images in the enrollment and verification sets are different.

Cross country FMR at threshold $T = 2.426$ for algorithm everai_002, giving $FMR(T) = 0.001$ globally.

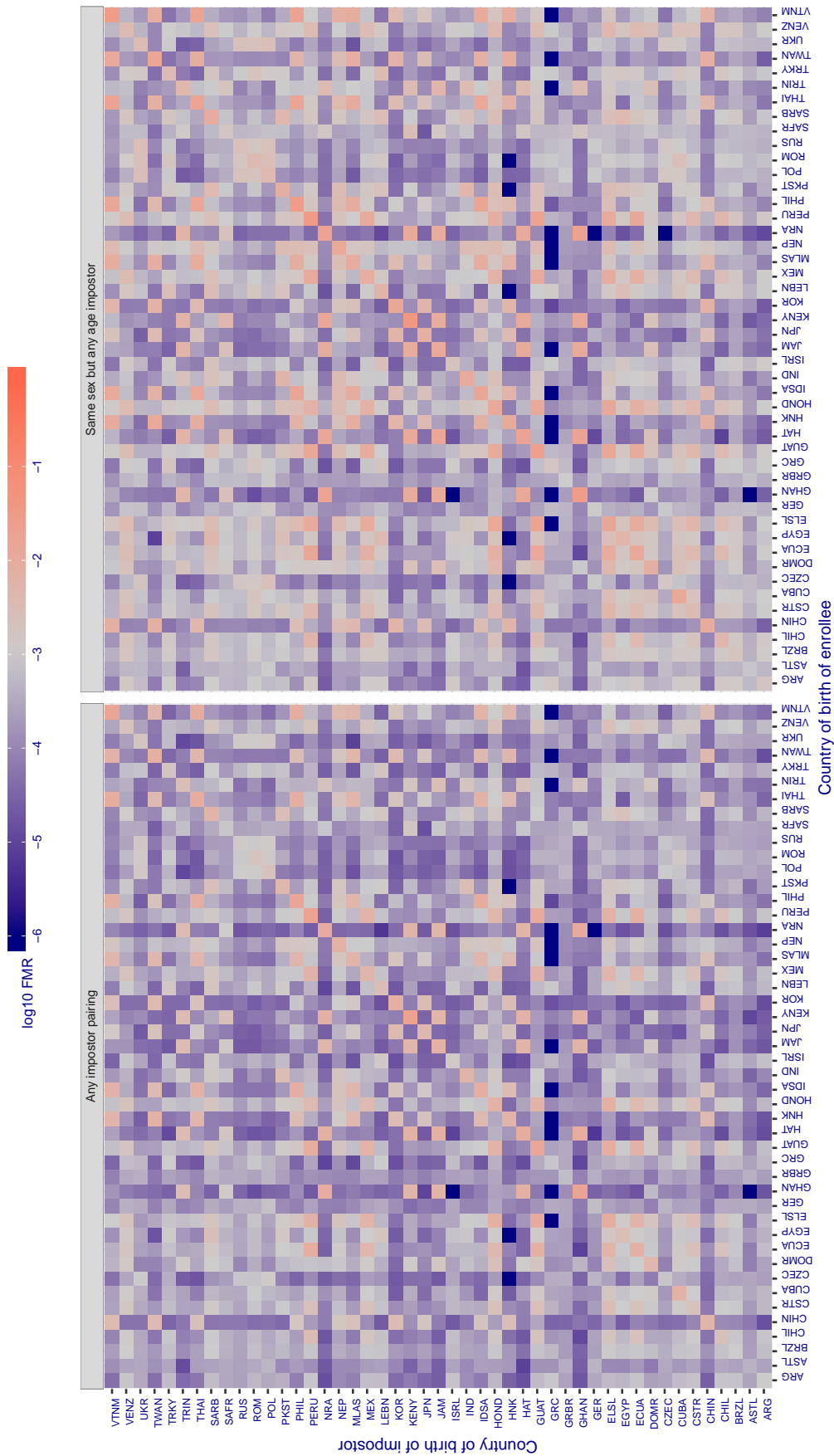


Figure 238: For algorithm everai-002 operating on visa images, the heatmap shows false match rates observed over impostor comparisons of faces from different individuals who were born in the given country pair. False matches are counted against a recognition threshold fixed globally to give the target FMR in the plot title, computed over all on the order of 10^{10} impostor comparisons. If text appears in each box it give the same quantity as that coded by the color. Grey indicates FMR is at the intended FMR target level. Light red colors present a security vulnerability to, for example, a passport gate. Each +1 increase in \log_{10} FMR corresponds to a factor of 10 increase in FMR. The matrix is not quite symmetric because images in the enrollment and verification sets are different.

Cross country FMR at threshold $T = 0.591$ for algorithm glory_000, giving $FMR(T) = 0.001$ globally.

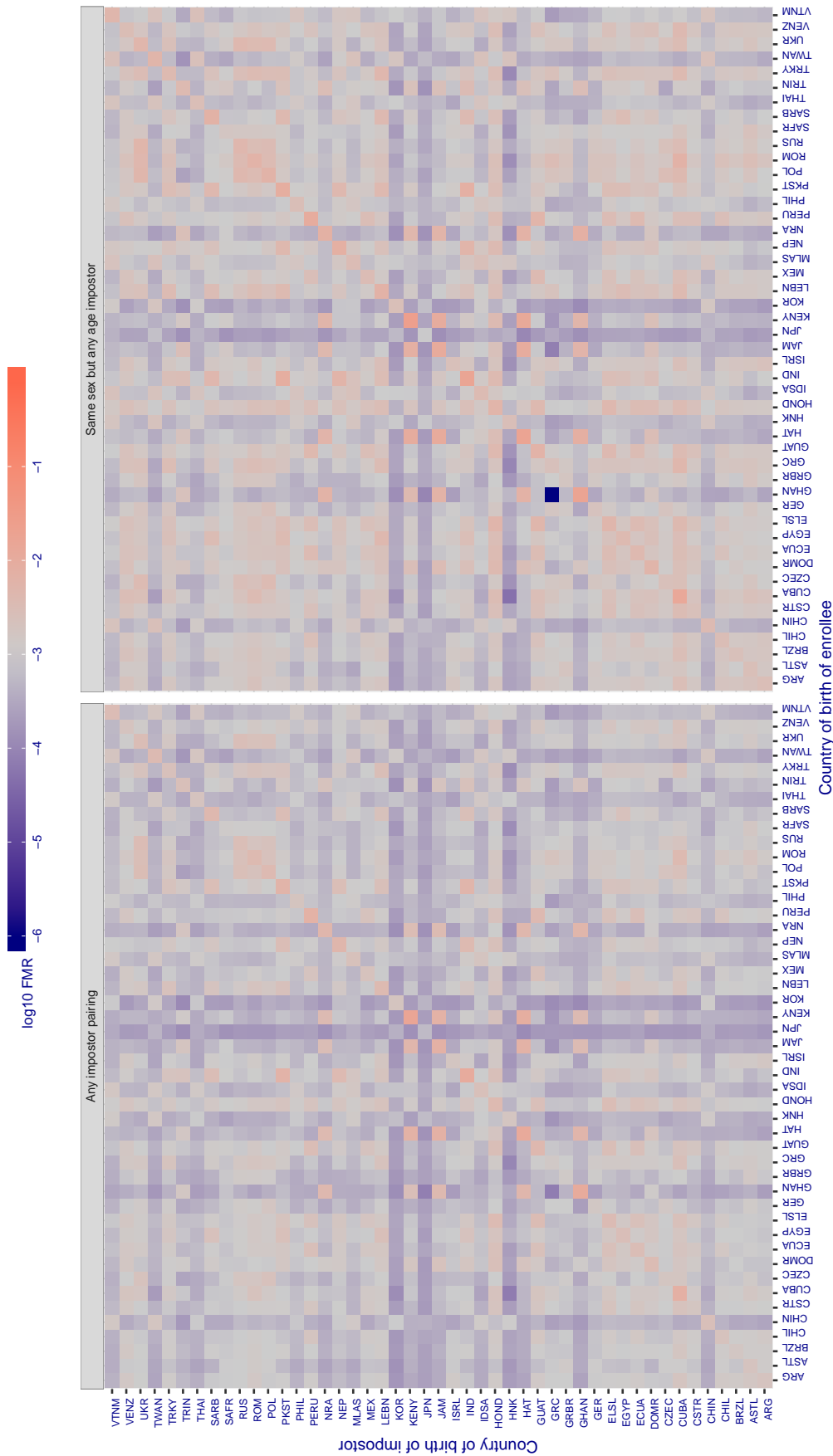


Figure 239: For algorithm glory-000 operating on visa images, the heatmap shows false match rates observed over impostor comparisons of faces from different individuals who were born in the given country pair. False matches are counted against a recognition threshold fixed globally to give the target FMR in the plot title, computed over all on the order of 10^{10} impostor comparisons. If text appears in each box it give the same quantity as that coded by the color. Grey indicates FMR is at the intended FMR target level. Light red colors present a security vulnerability to, for example, a passport gate. Each +1 increase in log10 FMR corresponds to a factor of 10 increase in FMR. The matrix is not quite symmetric because images in the enrollment and verification sets are different.

Cross country FMR at threshold $T = 0.596$ for algorithm glory_001, giving $FMR(T) = 0.001$ globally.

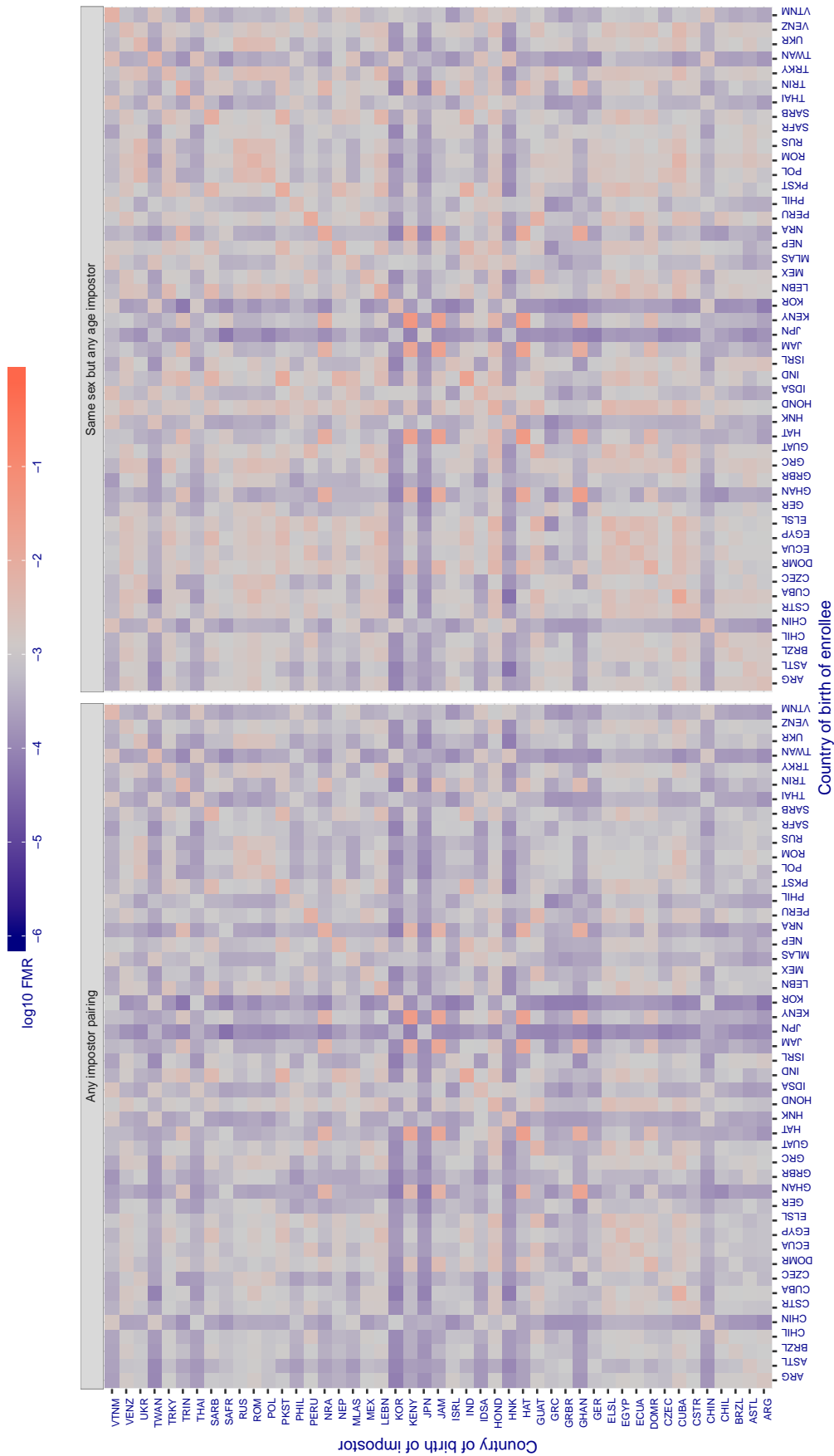


Figure 240: For algorithm glory-001 operating on visa images, the heatmap shows false match rates observed over impostor comparisons of faces from different individuals who were born in the given country pair. False matches are counted against a recognition threshold fixed globally to give the target FMR in the plot title, computed over all on the order of 10^{10} impostor comparisons. If text appears in each box it give the same quantity as that coded by the color. Grey indicates FMR is at the intended FMR target level. Light red colors present a security vulnerability to, for example, a passport gate. Each +1 increase in \log_{10} FMR corresponds to a factor of 10 increase in FMR. The matrix is not quite symmetric because images in the enrollment and verification sets are different.

Cross country FMR at threshold $T = 0.474$ for algorithm gorilla_001, giving $FMR(T) = 0.001$ globally.

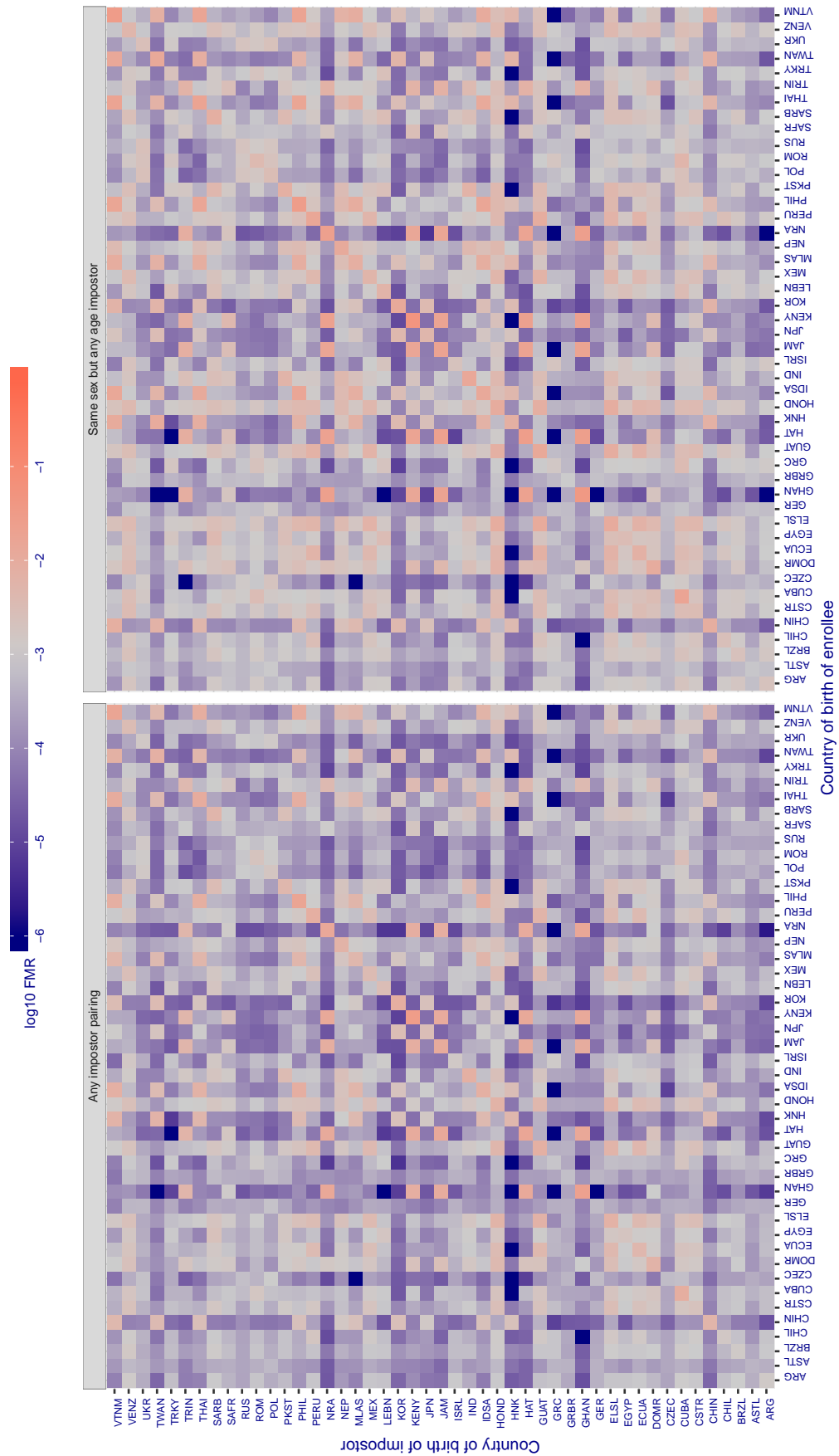


Figure 241: For algorithm gorilla-001 operating on visa images, the heatmap shows false match rates observed over impostor comparisons of faces from different individuals who were born in the given country pair. False matches are counted against a recognition threshold fixed globally to give the target FMR in the plot title, computed over all on the order of 10^{10} impostor comparisons. If text appears in each box it give the same quantity as that coded by the color. Grey indicates FMR is at the intended FMR target level. Light red colors present a security vulnerability to, for example, a passport gate. Each +1 increase in $\log_{10} FMR$ corresponds to a factor of 10 increase in FMR. The matrix is not quite symmetric because images in the enrollment and verification sets are different.

Cross country FMR at threshold $T = 0.402$ for algorithm gorilla_002, giving $FMR(T) = 0.001$ globally.

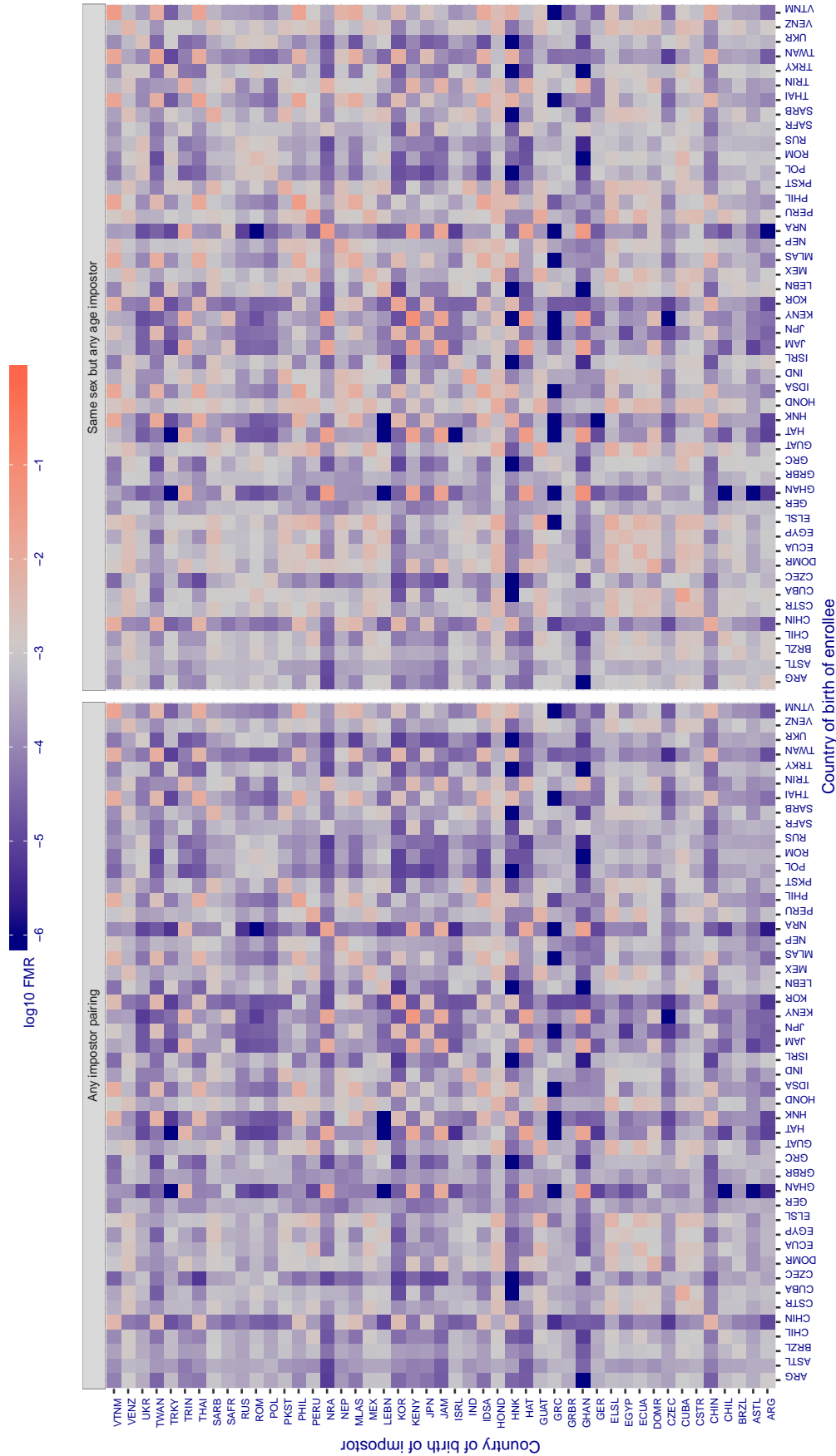


Figure 242: For algorithm gorilla-002 operating on visa images, the heatmap shows false match rates observed over impostor comparisons of faces from different individuals who were born in the given country pair. False matches are counted against a recognition threshold fixed globally to give the target FMR in the plot title, computed over all on the order of 10^{10} impostor comparisons. If text appears in each box it give the same quantity as that coded by the color. Grey indicates FMR is at the intended FMR target level. Light red colors present a security vulnerability to, for example, a passport gate. Each +1 increase in \log_{10} FMR corresponds to a factor of 10 increase in FMR. The matrix is not quite symmetric because images in the enrollment and verification sets are different.

Cross country FMR at threshold $T = 63.025$ for algorithm hik_001, giving $FMR(T) = 0.001$ globally.

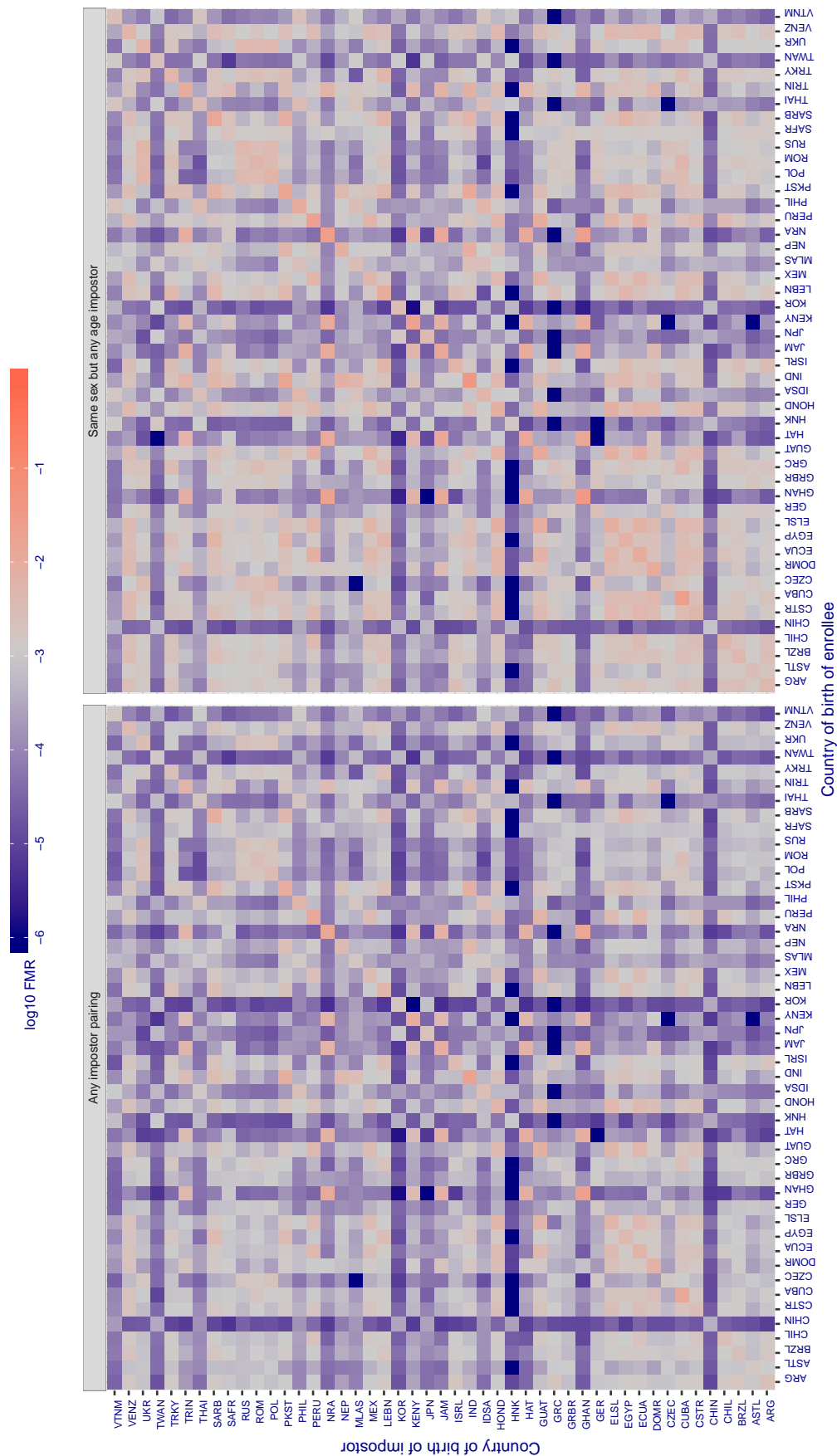


Figure 243: For algorithm hik-001 operating on visa images, the heatmap shows false match rates observed over impostor comparisons of faces from different individuals who were born in the given country pair. False matches are counted against a recognition threshold fixed globally to give the target FMR in the plot title, computed over all on the order of 10^{10} impostor comparisons. If text appears in each box it give the same quantity as that coded by the color. Grey indicates FMR is at the intended FMR target level. Light red colors present a security vulnerability to, for example, a passport gate. Each +1 increase in \log_{10} FMR corresponds to a factor of 10 increase in FMR. The matrix is not quite symmetric because images in the enrollment and verification sets are different.

Cross country FMR at threshold $T = 0.949$ for algorithm hr_000, giving $FMR(T) = 0.001$ globally.

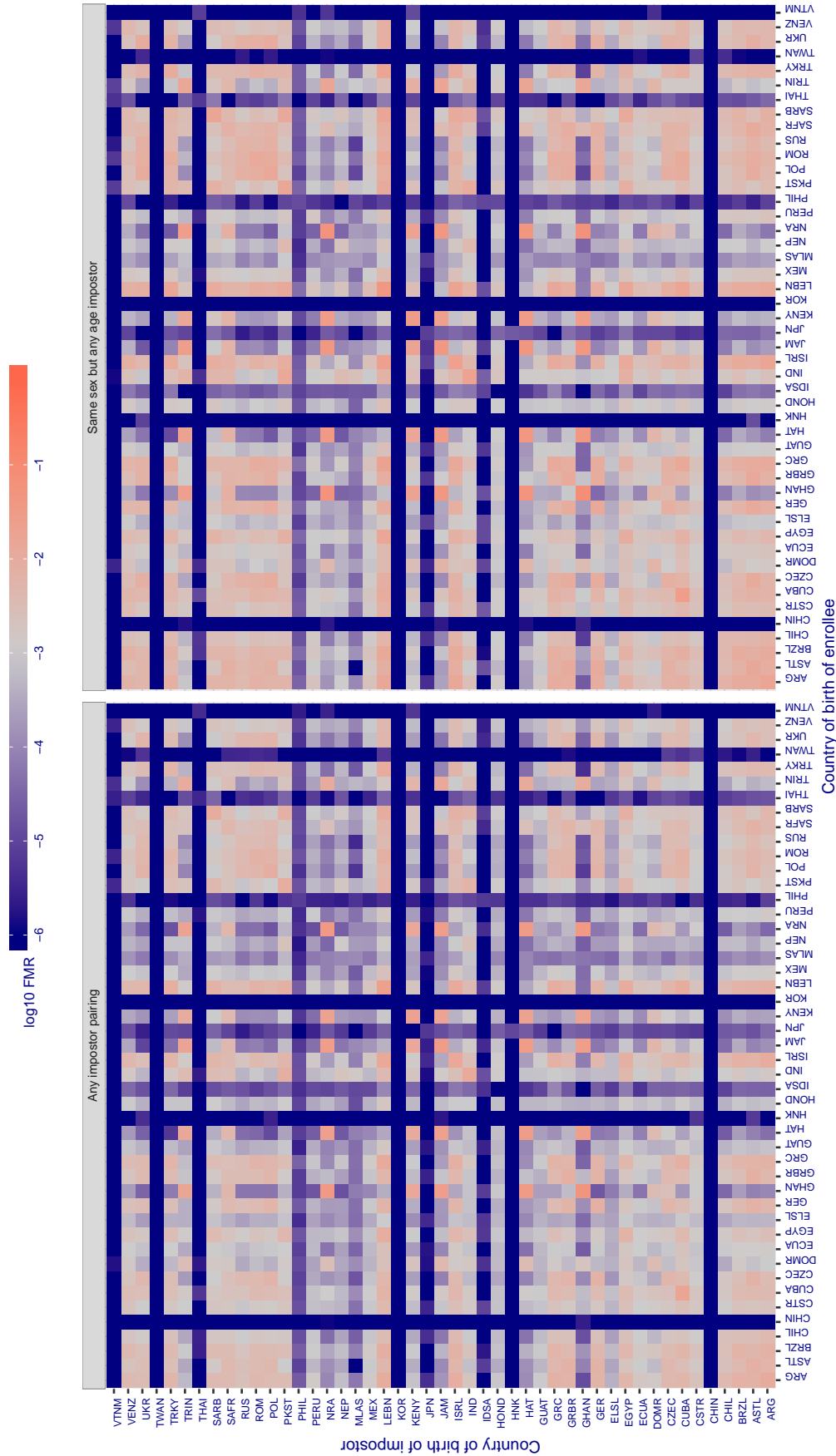


Figure 244: For algorithm hr-000 operating on visa images, the heatmap shows false match rates observed over impostor comparisons of faces from different individuals who were born in the given country pair. False matches are counted against a recognition threshold fixed globally to give the target FMR in the plot title, computed over all on the order of 10^{10} impostor comparisons. If text appears in each box it give the same quantity as that coded by the color. Grey indicates FMR is at the intended FMR target level. Light red colors present a security vulnerability to, for example, a passport gate. Each +1 increase in \log_{10} FMR corresponds to a factor of 10 increase in FMR. The matrix is not quite symmetric because images in the enrollment and verification sets are different.

Cross country FMR at threshold $T = 36641.000$ for algorithm `id3_003`, giving $FMR(T) = 0.001$ globally.

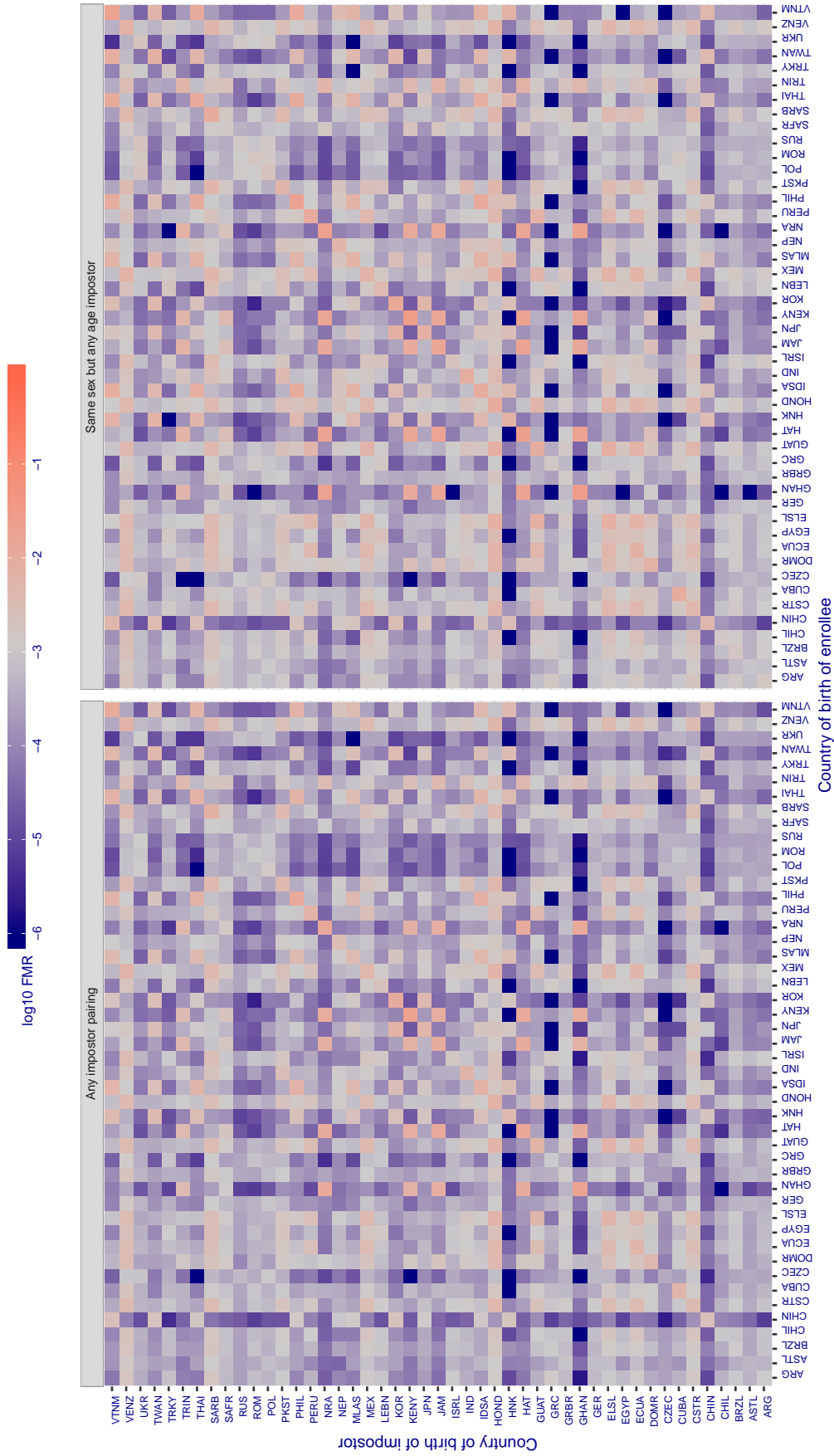


Figure 245: For algorithm `id3-003` operating on visa images, the heatmap shows false match rates observed over impostor comparisons of faces from different individuals who were born in the given country pair. False matches are counted against a recognition threshold fixed globally to give the target FMR in the plot title, computed over all on the order of 10^{10} impostor comparisons. If text appears in each box it give the same quantity as that coded by the color. Grey indicates FMR is at the intended FMR target level. Light red colors present a security vulnerability to, for example, a passport gate. Each +1 increase in $\log_{10} FMR$ corresponds to a factor of 10 increase in FMR. The matrix is not quite symmetric because images in the enrollment and verification sets are different.

Cross country FMR at threshold $T = 36163.000$ for algorithm `id3_004`, giving $FMR(T) = 0.001$ globally.

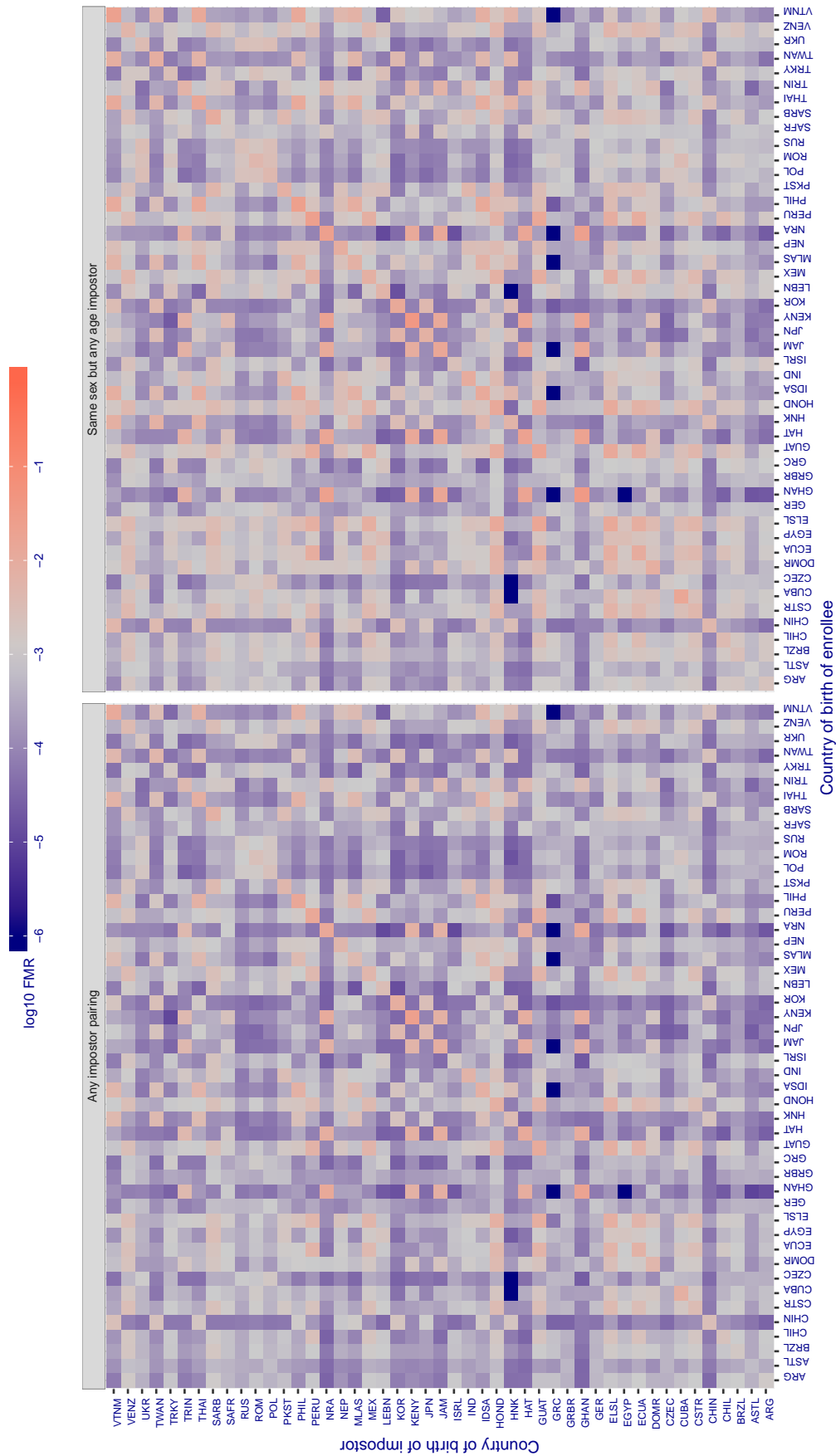


Figure 246: For algorithm `id3-004` operating on visa images, the heatmap shows false match rates observed over impostor comparisons of faces from different individuals who were born in the given country pair. False matches are counted against a recognition threshold fixed globally to give the target FMR in the plot title, computed over all on the order of 10^{10} impostor comparisons. If text appears in each box it give the same quantity as that coded by the color. Grey indicates FMR is at the intended FMR target level. Light red colors present a security vulnerability to, for example, a passport gate. Each +1 increase in \log_{10} FMR corresponds to a factor of 10 increase in FMR. The matrix is not quite symmetric because images in the enrollment and verification sets are different.

Cross country FMR at threshold $T = 3136.629$ for algorithm idemia_003, giving $FMR(T) = 0.001$ globally.

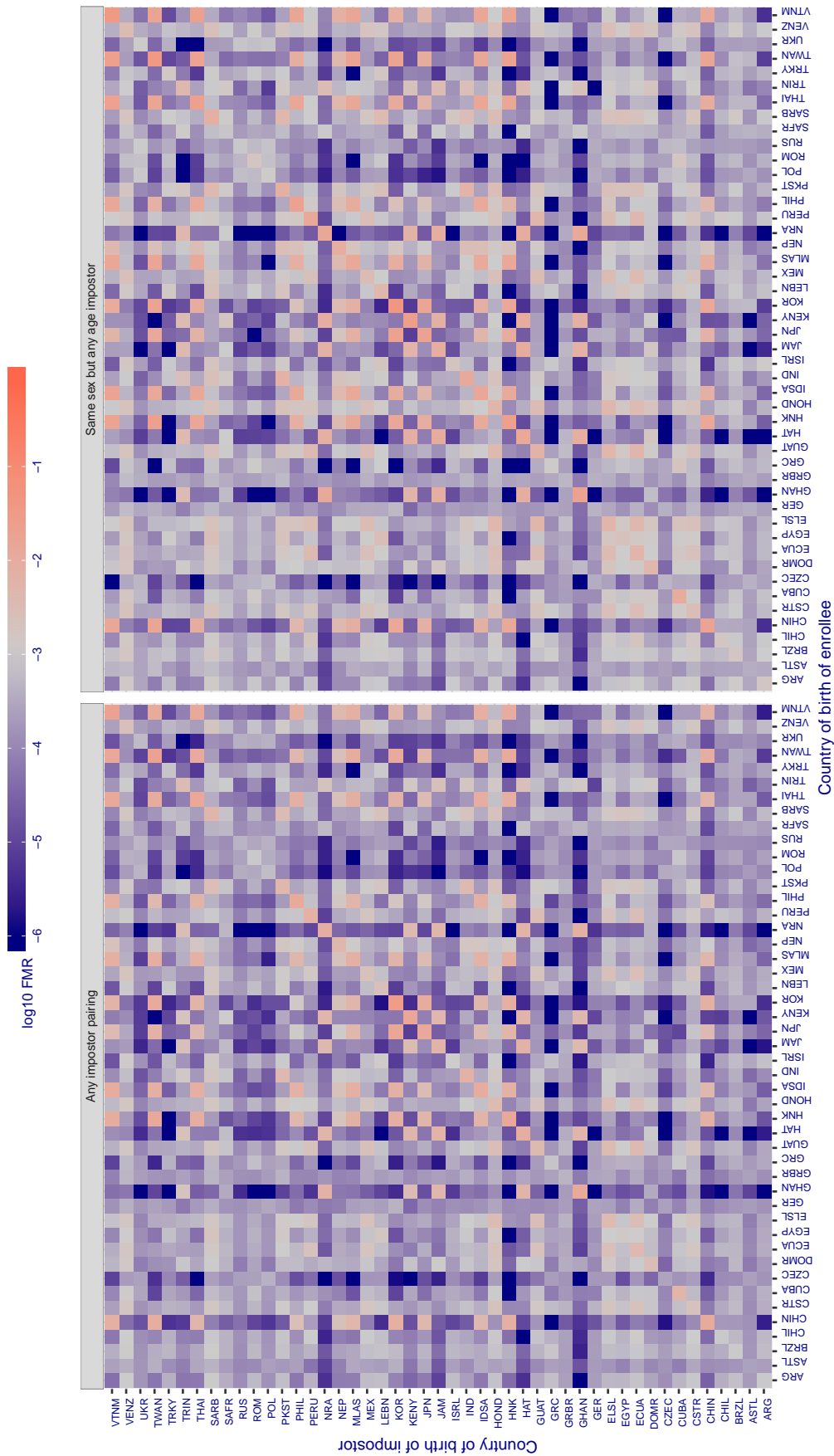


Figure 247: For algorithm idemia-003 operating on visa images, the heatmap shows false match rates observed over impostor comparisons of faces from different individuals who were born in the given country pair. False matches are counted against a recognition threshold fixed globally to give the target FMR in the plot title, computed over all on the order of 10^{10} impostor comparisons. If text appears in each box it give the same quantity as that coded by the color. Grey indicates FMR is at the intended FMR target level. Light red colors present a security vulnerability to, for example, a passport gate. Each +1 increase in $\log_{10} FMR$ corresponds to a factor of 10 increase in FMR. The matrix is not quite symmetric because images in the enrollment and verification sets are different.

Cross country FMR at threshold $T = 3261.090$ for algorithm idemia_004, giving $FMR(T) = 0.001$ globally.

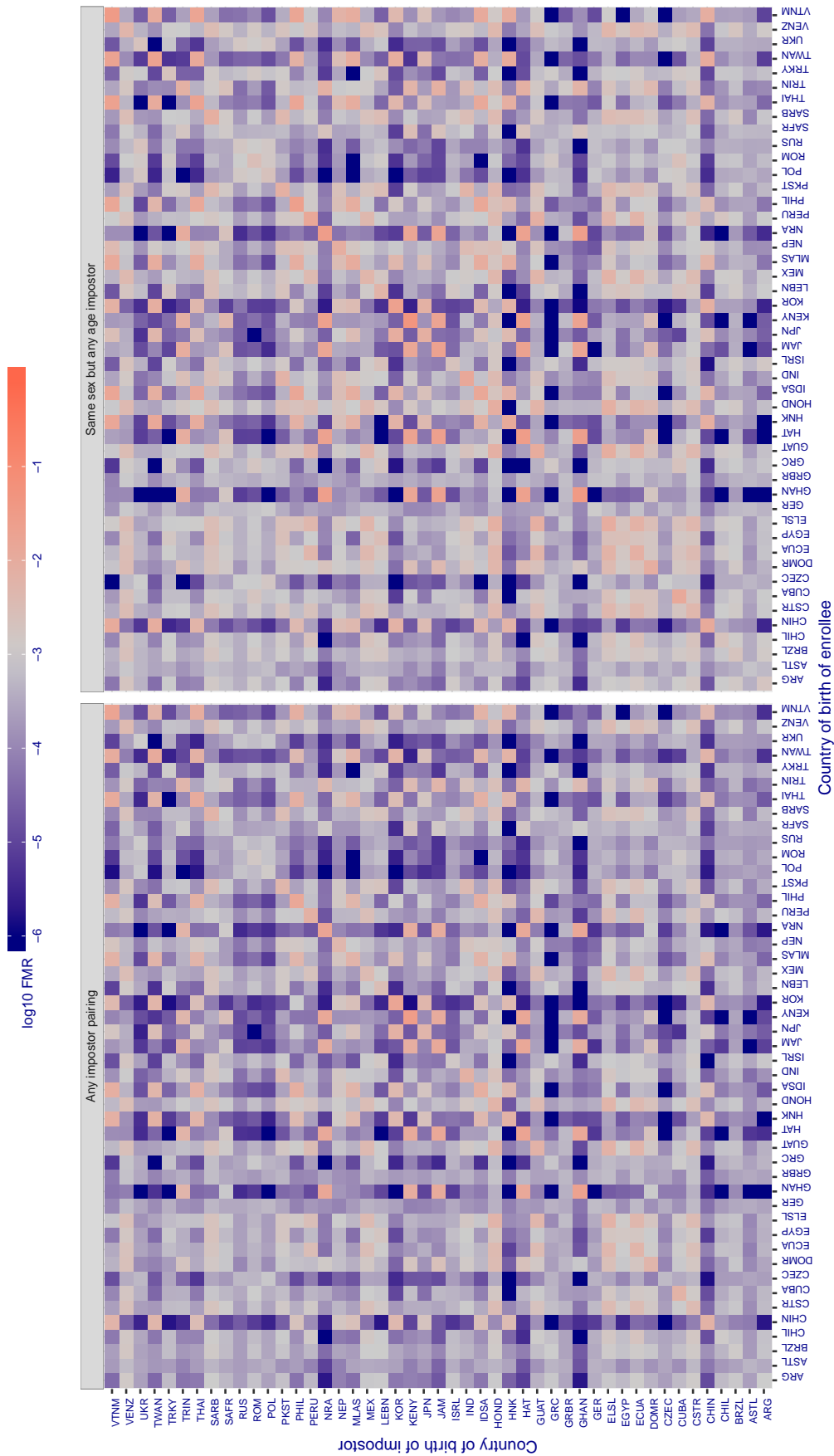


Figure 248: For algorithm idemia-004 operating on visa images, the heatmap shows false match rates observed over impostor comparisons of faces from different individuals who were born in the given country pair. False matches are counted against a recognition threshold fixed globally to give the target FMR in the plot title, computed over all on the order of 10^{10} impostor comparisons. If text appears in each box it give the same quantity as that coded by the color. Grey indicates FMR is at the intended FMR target level. Light red colors present a security vulnerability to, for example, a passport gate. Each +1 increase in \log_{10} FMR corresponds to a factor of 10 increase in FMR. The matrix is not quite symmetric because images in the enrollment and verification sets are different.

Cross country FMR at threshold $T = 0.721$ for algorithm iit_000, giving $FMR(T) = 0.001$ globally.

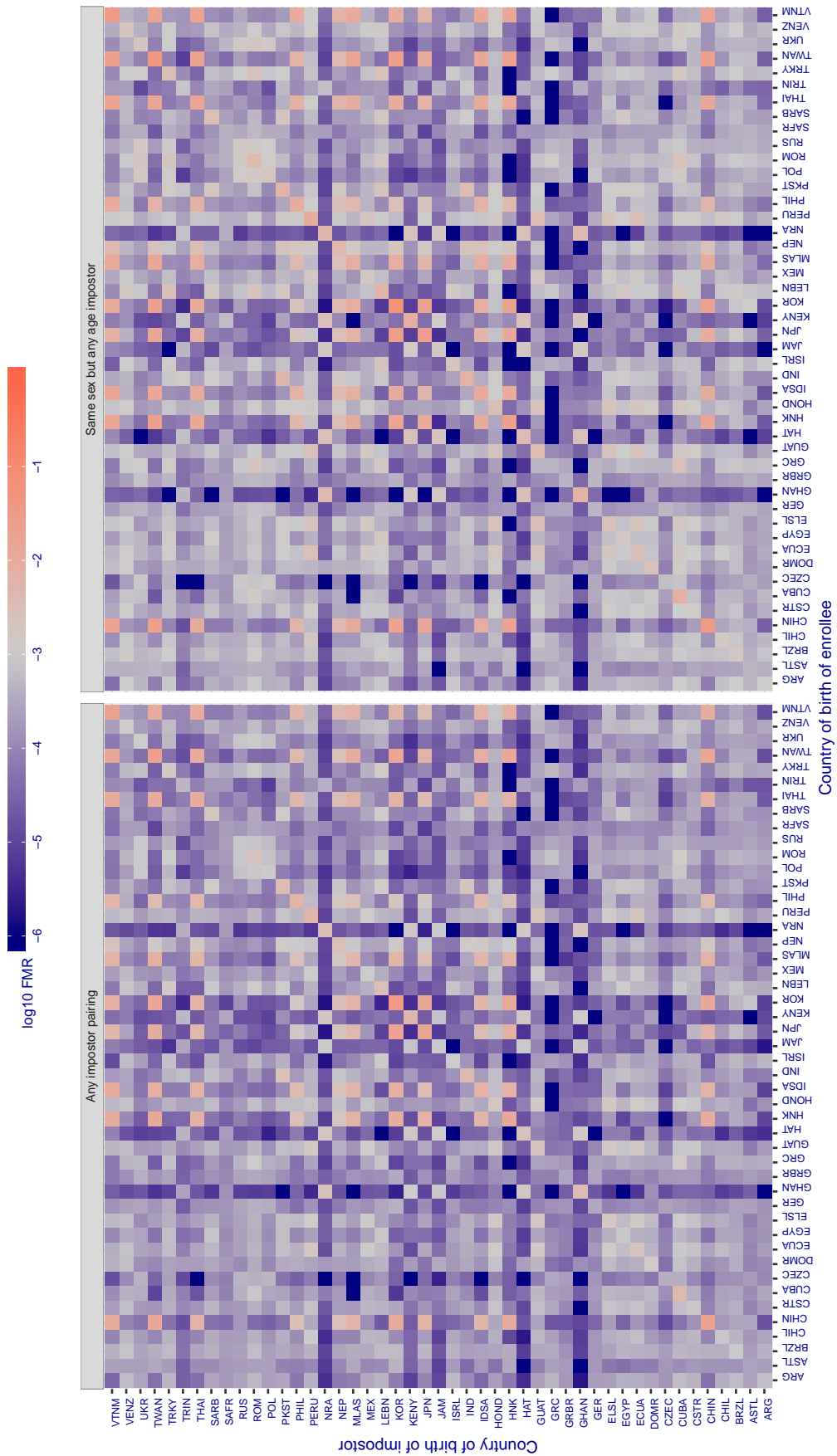


Figure 249: For algorithm iit-000 operating on visa images, the heatmap shows false match rates observed over impostor comparisons of faces from different individuals who were born in the given country pair. False matches are counted against a recognition threshold fixed globally to give the target FMR in the plot title, computed over all on the order of 10^{10} impostor comparisons. If text appears in each box it give the same quantity as that coded by the color. Grey indicates FMR is at the intended FMR target level. Light red colors present a security vulnerability to, for example, a passport gate. Each +1 increase in \log_{10} FMR corresponds to a factor of 10 increase in FMR. The matrix is not quite symmetric because images in the enrollment and verification sets are different.

Cross country FMR at threshold $T = 1.302$ for algorithm imperial_000, giving $FMR(T) = 0.001$ globally.

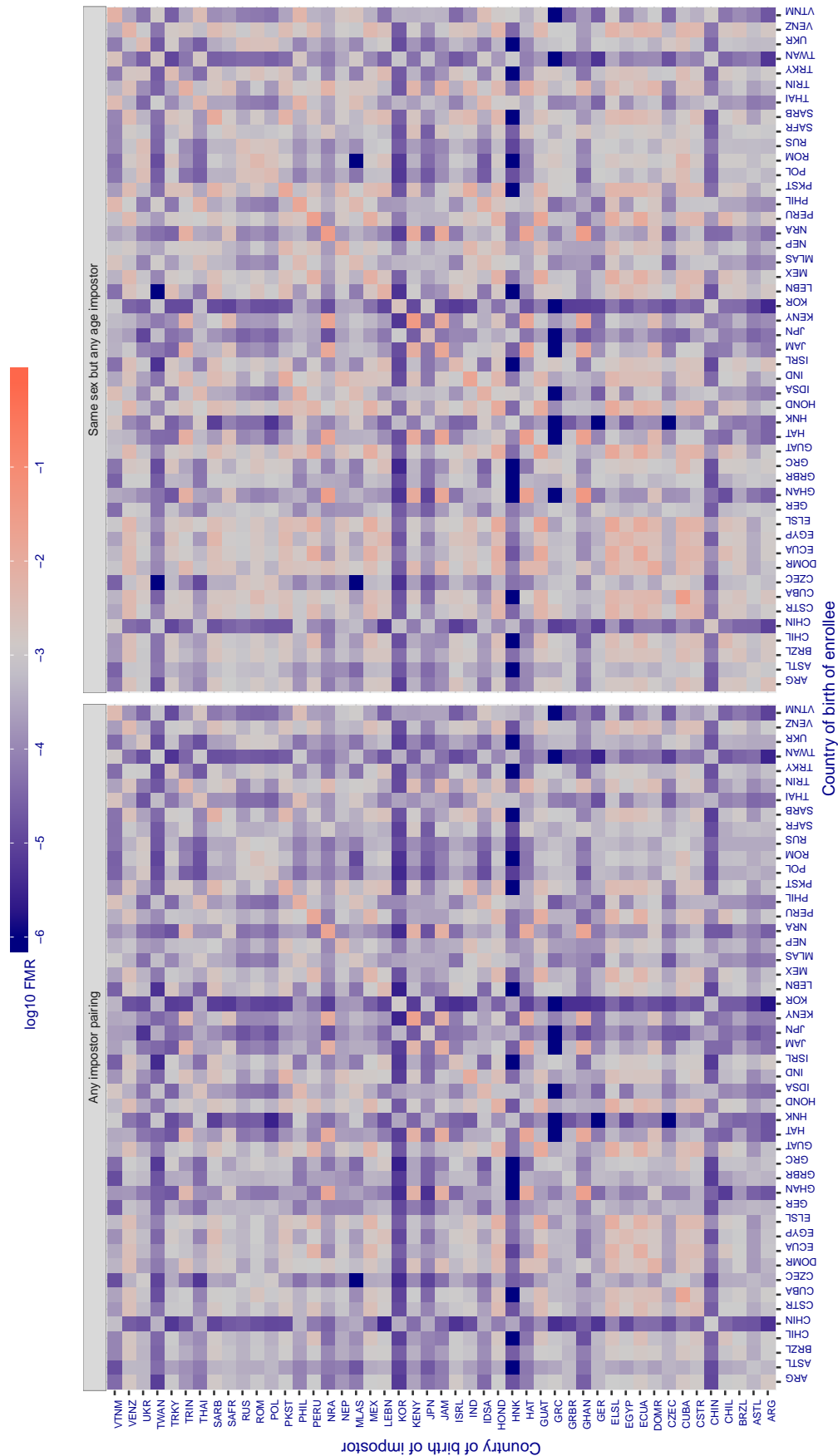


Figure 250: For algorithm imperial-000 operating on visa images, the heatmap shows false match rates observed over impostor comparisons of faces from different individuals who were born in the given country pair. False matches are counted against a recognition threshold fixed globally to give the target FMR in the plot title, computed over all on the order of 10^{10} impostor comparisons. If text appears in each box it give the same quantity as that coded by the color. Grey indicates FMR is at the intended FMR target level. Light red colors present a security vulnerability to, for example, a passport gate. Each +1 increase in $\log_{10} FMR$ corresponds to a factor of 10 increase in FMR. The matrix is not quite symmetric because images in the enrollment and verification sets are different.

Cross country FMR at threshold $T = 1.320$ for algorithm imperial_001, giving $FMR(T) = 0.001$ globally.

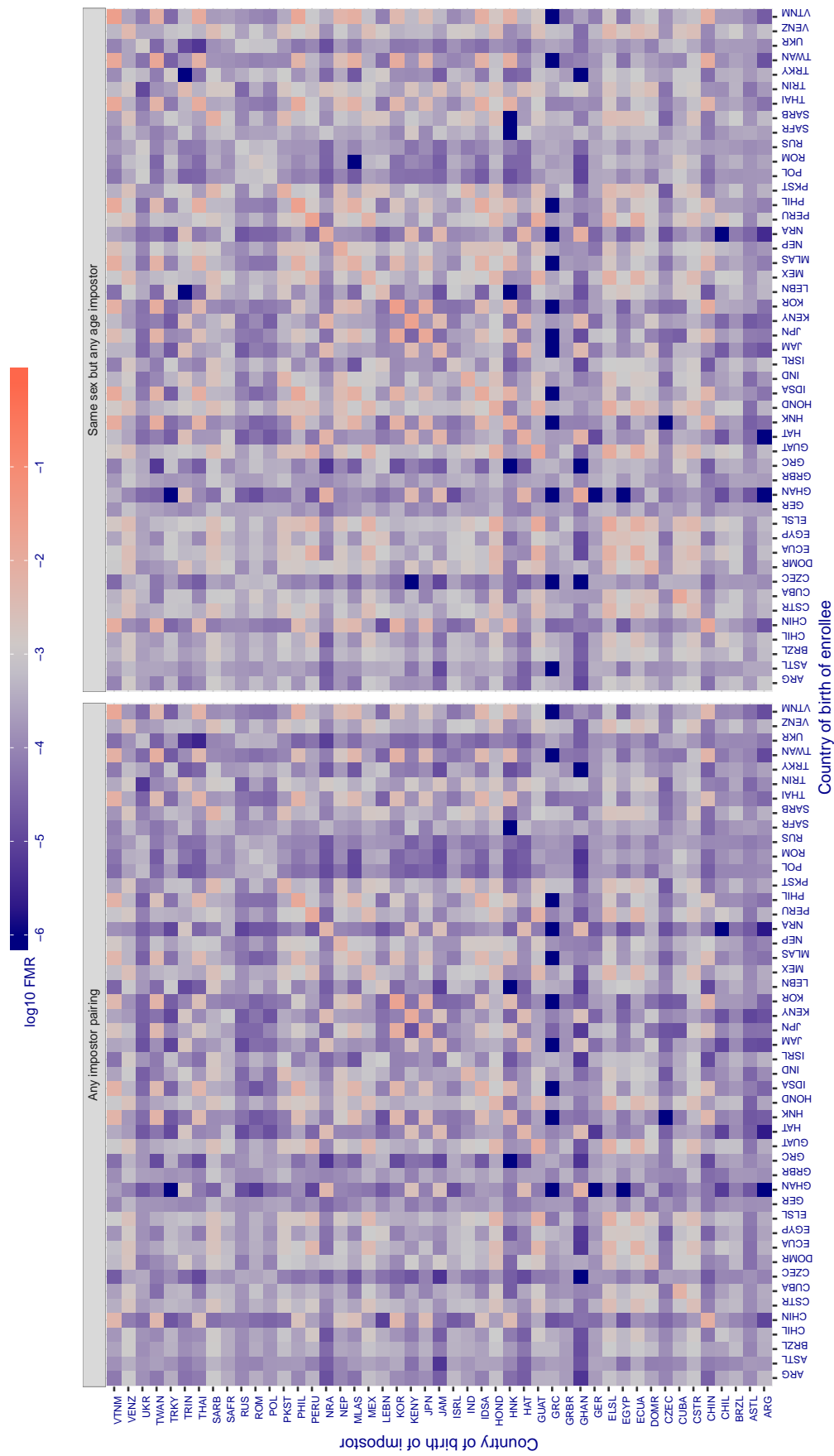


Figure 251: For algorithm imperial-001 operating on visa images, the heatmap shows false match rates observed over impostor comparisons of faces from different individuals who were born in the given country pair. False matches are counted against a recognition threshold fixed globally to give the target FMR in the plot title, computed over all on the order of 10^{10} impostor comparisons. If text appears in each box it give the same quantity as that coded by the color. Grey indicates FMR is at the intended FMR target level. Light red colors present a security vulnerability to, for example, a passport gate. Each +1 increase in \log_{10} FMR corresponds to a factor of 10 increase in FMR. The matrix is not quite symmetric because images in the enrollment and verification sets are different.

Cross country FMR at threshold $T = 1.288$ for algorithm `incode_002`, giving $FMR(T) = 0.001$ globally.

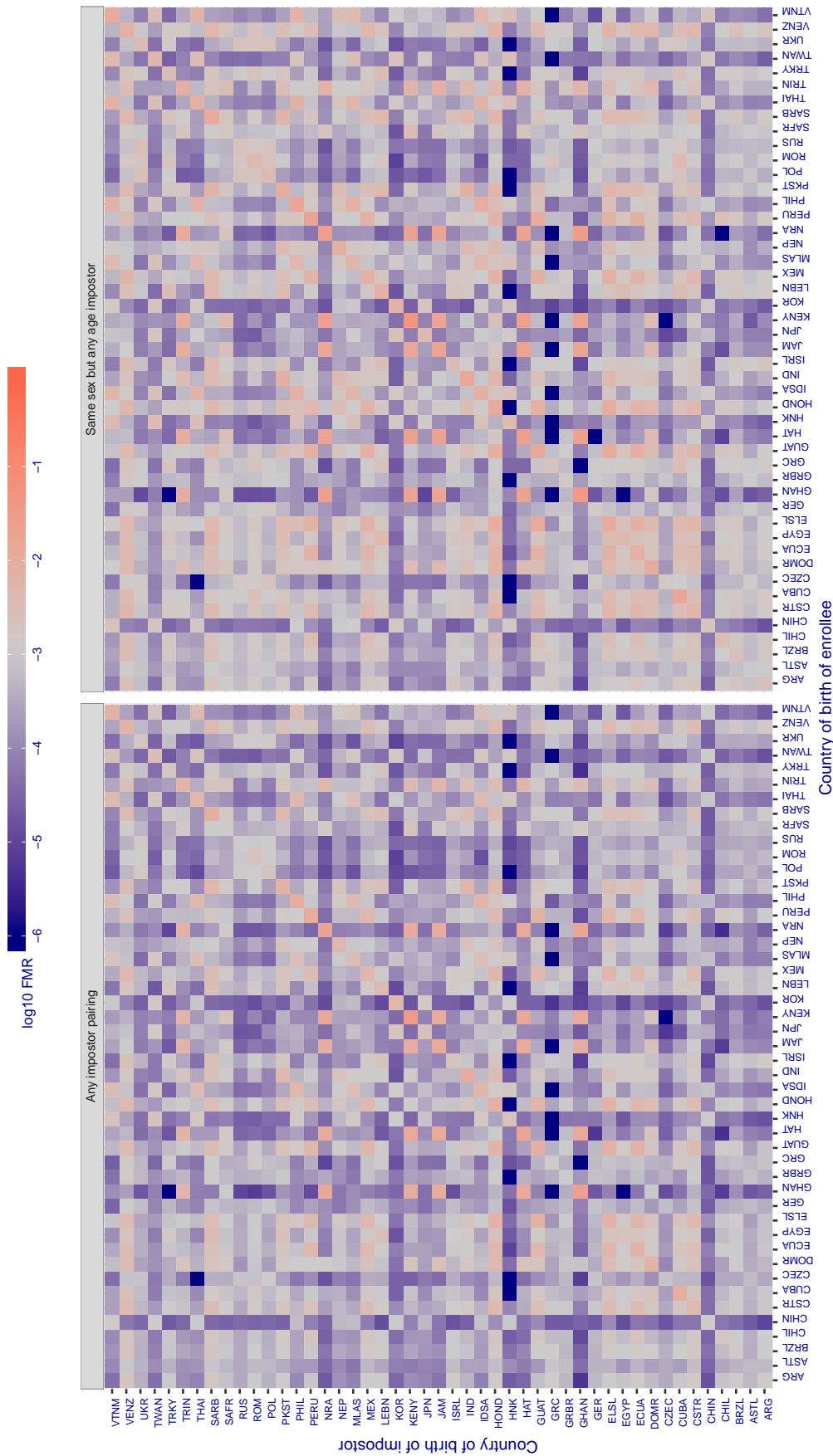


Figure 252: For algorithm `incode-002` operating on visa images, the heatmap shows false match rates observed over impostor comparisons of faces from different individuals who were born in the given country pair. False matches are counted against a recognition threshold fixed globally to give the target FMR in the plot title, computed over all on the order of 10^{10} impostor comparisons. If text appears in each box it give the same quantity as that coded by the color. Grey indicates FMR is at the intended FMR target level. Light red colors present a security vulnerability to, for example, a passport gate. Each +1 increase in \log_{10} FMR corresponds to a factor of 10 increase in FMR. The matrix is not quite symmetric because images in the enrollment and verification sets are different.

Cross country FMR at threshold $T = 1.340$ for algorithm incode_003, giving $FMR(T) = 0.001$ globally.

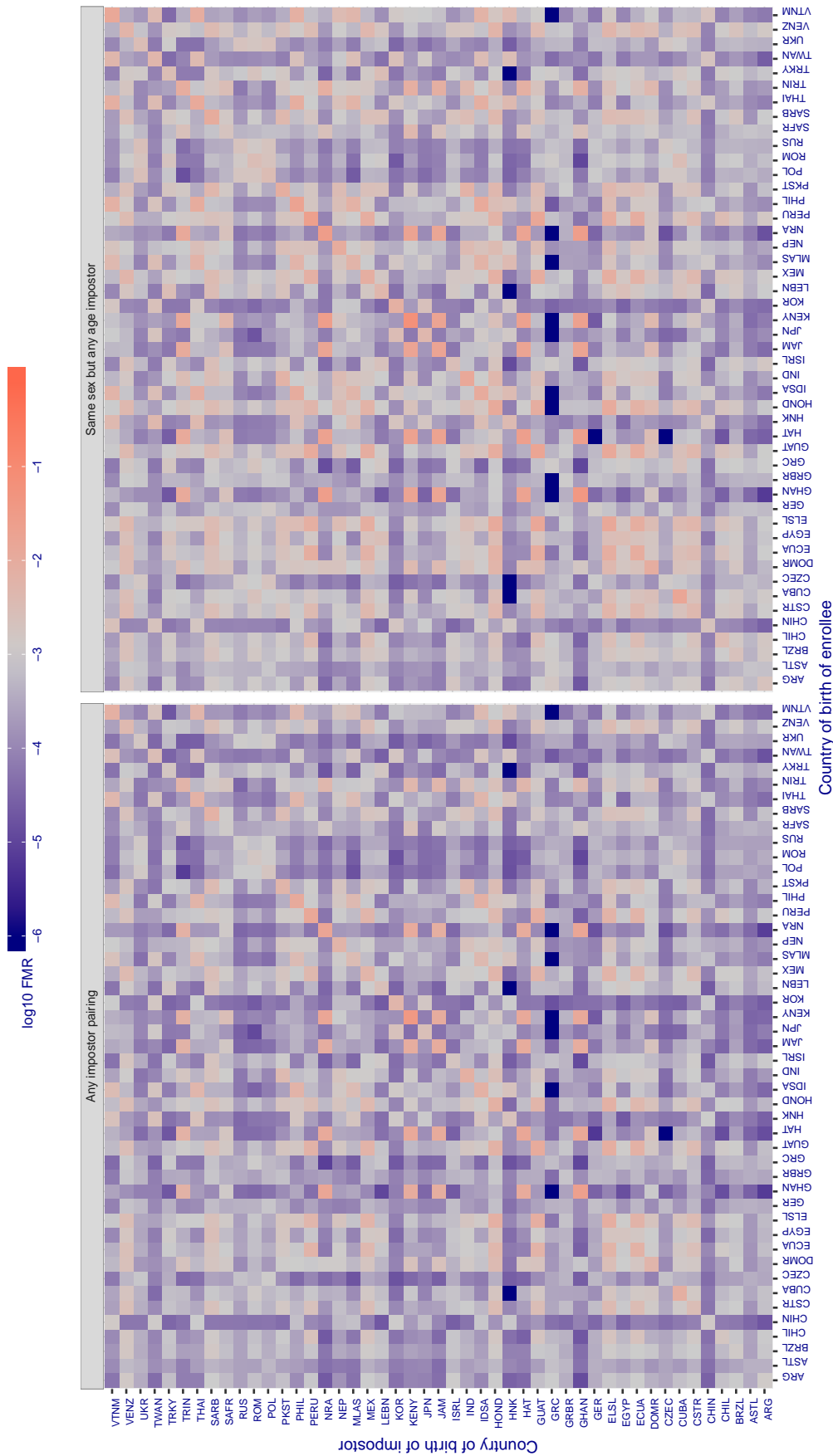


Figure 253: For algorithm incode-003 operating on visa images, the heatmap shows false match rates observed over impostor comparisons of faces from different individuals who were born in the given country pair. False matches are counted against a recognition threshold fixed globally to give the target FMR in the plot title, computed over all on the order of 10^{10} impostor comparisons. If text appears in each box it give the same quantity as that coded by the color. Grey indicates FMR is at the intended FMR target level. Light red colors present a security vulnerability to, for example, a passport gate. Each +1 increase in \log_{10} FMR corresponds to a factor of 10 increase in FMR. The matrix is not quite symmetric because images in the enrollment and verification sets are different.

Cross country FMR at threshold $T = 21.422$ for algorithm innovatrics_004, giving $FMR(T) = 0.001$ globally.

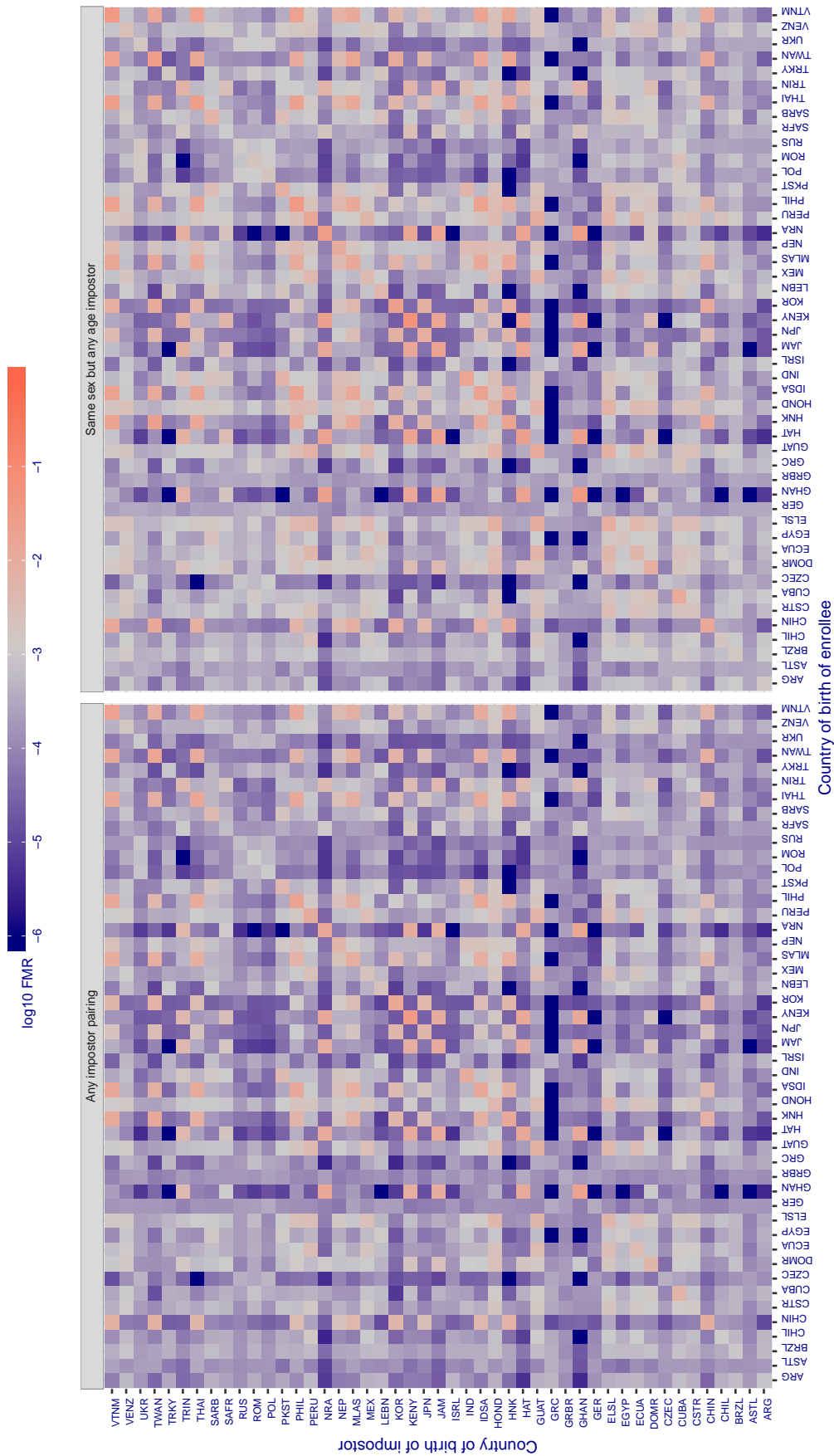


Figure 254: For algorithm innovatrics-004 operating on visa images, the heatmap shows false match rates observed over impostor comparisons of faces from different individuals who were born in the given country pair. False matches are counted against a recognition threshold fixed globally to give the target FMR in the plot title, computed over all on the order of 10^{10} impostor comparisons. If text appears in each box it give the same quantity as that coded by the color. Grey indicates FMR is at the intended FMR target level. Light red colors present a security vulnerability to, for example, a passport gate. Each +1 increase in $\log_{10} FMR$ corresponds to a factor of 10 increase in FMR. The matrix is not quite symmetric because images in the enrollment and verification sets are different.

Cross country FMR at threshold $T = 28.706$ for algorithm innovatrics_005, giving $FMR(T) = 0.001$ globally.

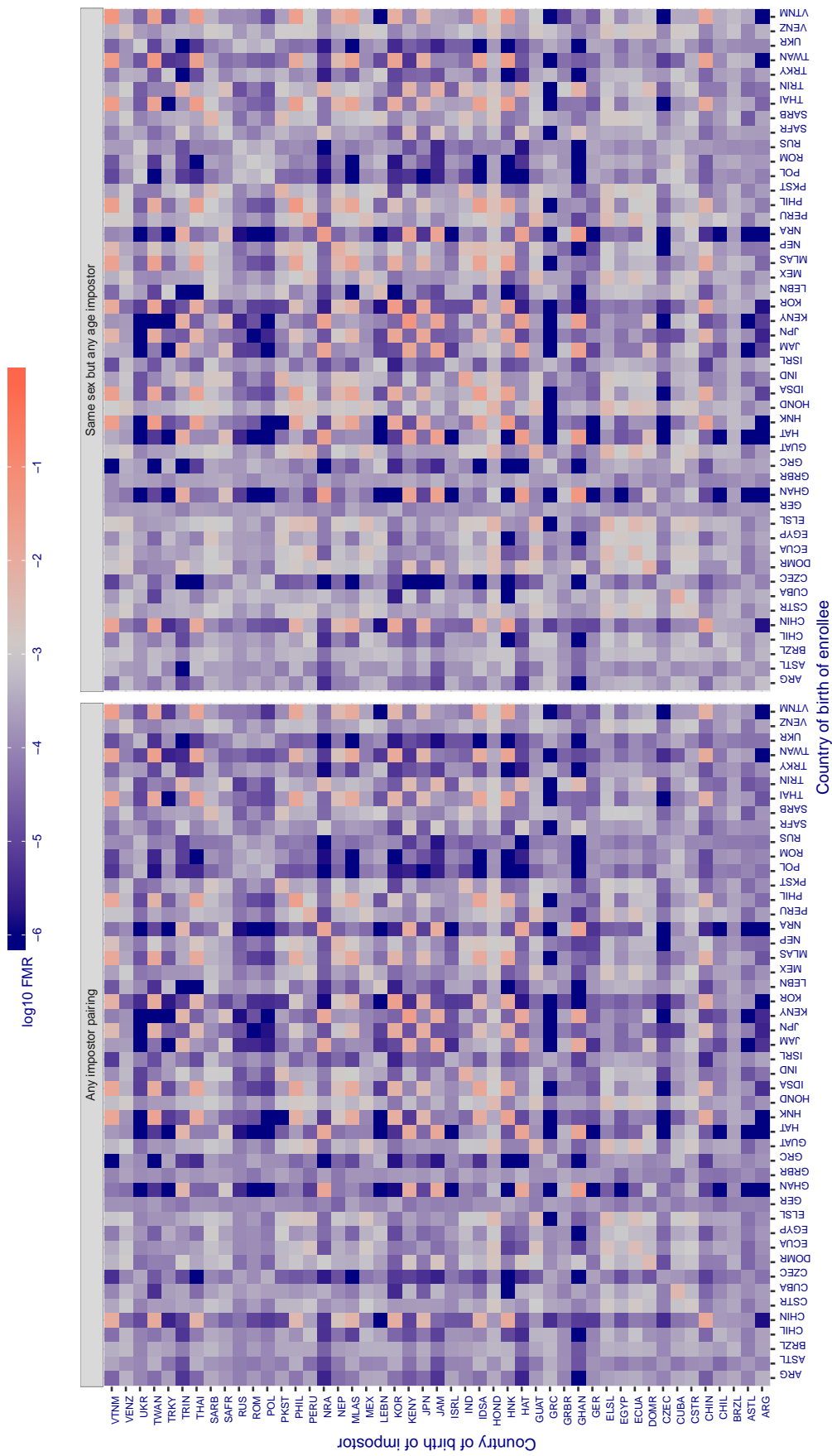


Figure 255: For algorithm innovatrics-005 operating on visa images, the heatmap shows false match rates observed over impostor comparisons of faces from different individuals who were born in the given country pair. False matches are counted against a recognition threshold fixed globally to give the target FMR in the plot title, computed over all on the order of 10^{10} impostor comparisons. If text appears in each box it give the same quantity as that coded by the color. Grey indicates FMR is at the intended FMR target level. Light red colors present a security vulnerability to, for example, a passport gate. Each +1 increase in \log_{10} FMR corresponds to a factor of 10 increase in FMR. The matrix is not quite symmetric because images in the enrollment and verification sets are different.

Cross country FMR at threshold $T = 37.554$ for algorithm `intellivision_001`, giving $FMR(T) = 0.001$ globally.

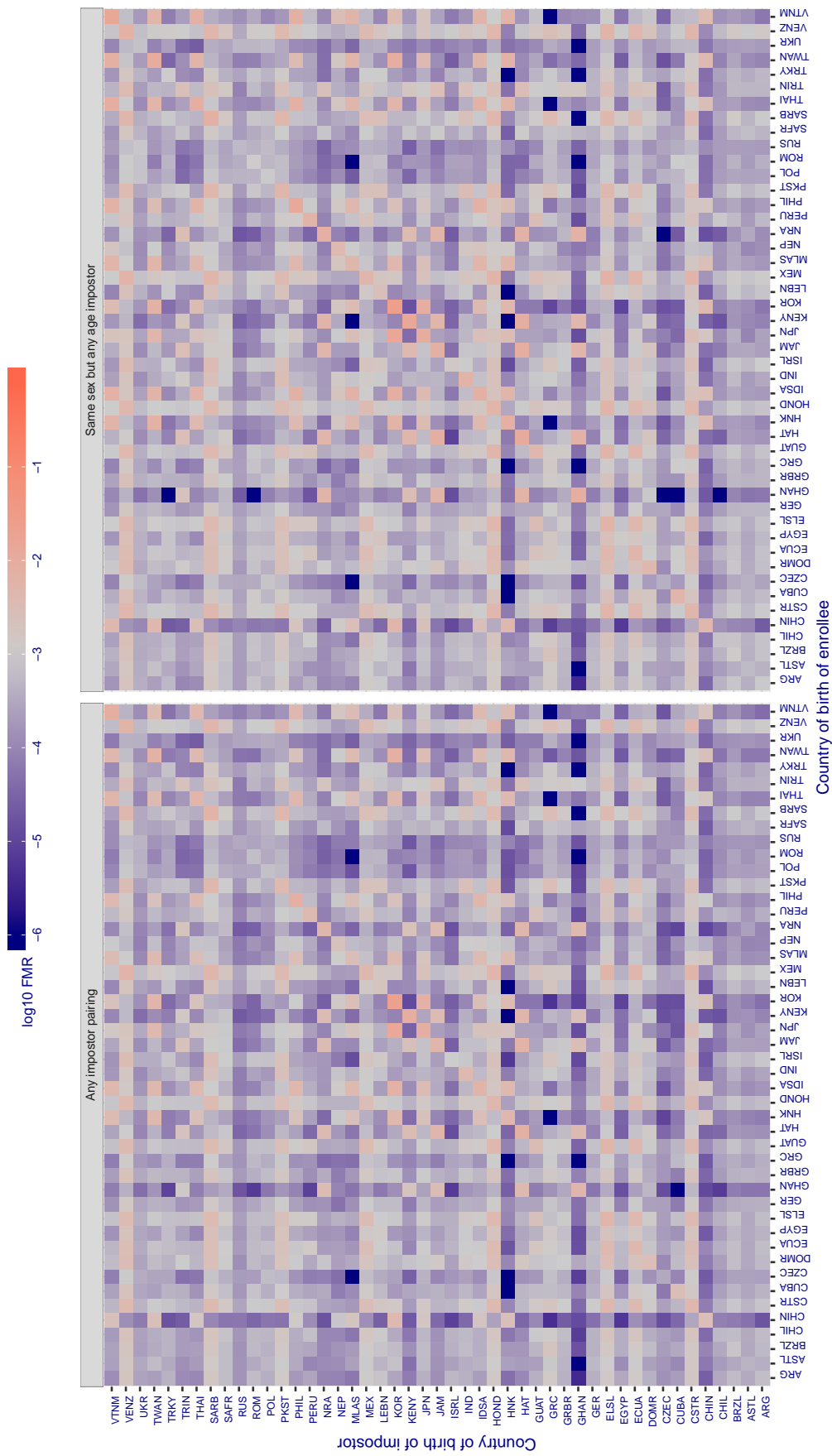


Figure 256: For algorithm `intellivision-001` operating on visa images, the heatmap shows false match rates observed over impostor comparisons of faces from different individuals who were born in the given country pair. False matches are counted against a recognition threshold fixed globally to give the target FMR in the plot title, computed over all on the order of 10^{10} impostor comparisons. If text appears in each box it give the same quantity as that coded by the color. Grey indicates FMR is at the intended FMR target level. Light red colors present a security vulnerability to, for example, a passport gate. Each +1 increase in $\log_{10} FMR$ corresponds to a factor of 10 increase in FMR. The matrix is not quite symmetric because images in the enrollment and verification sets are different.

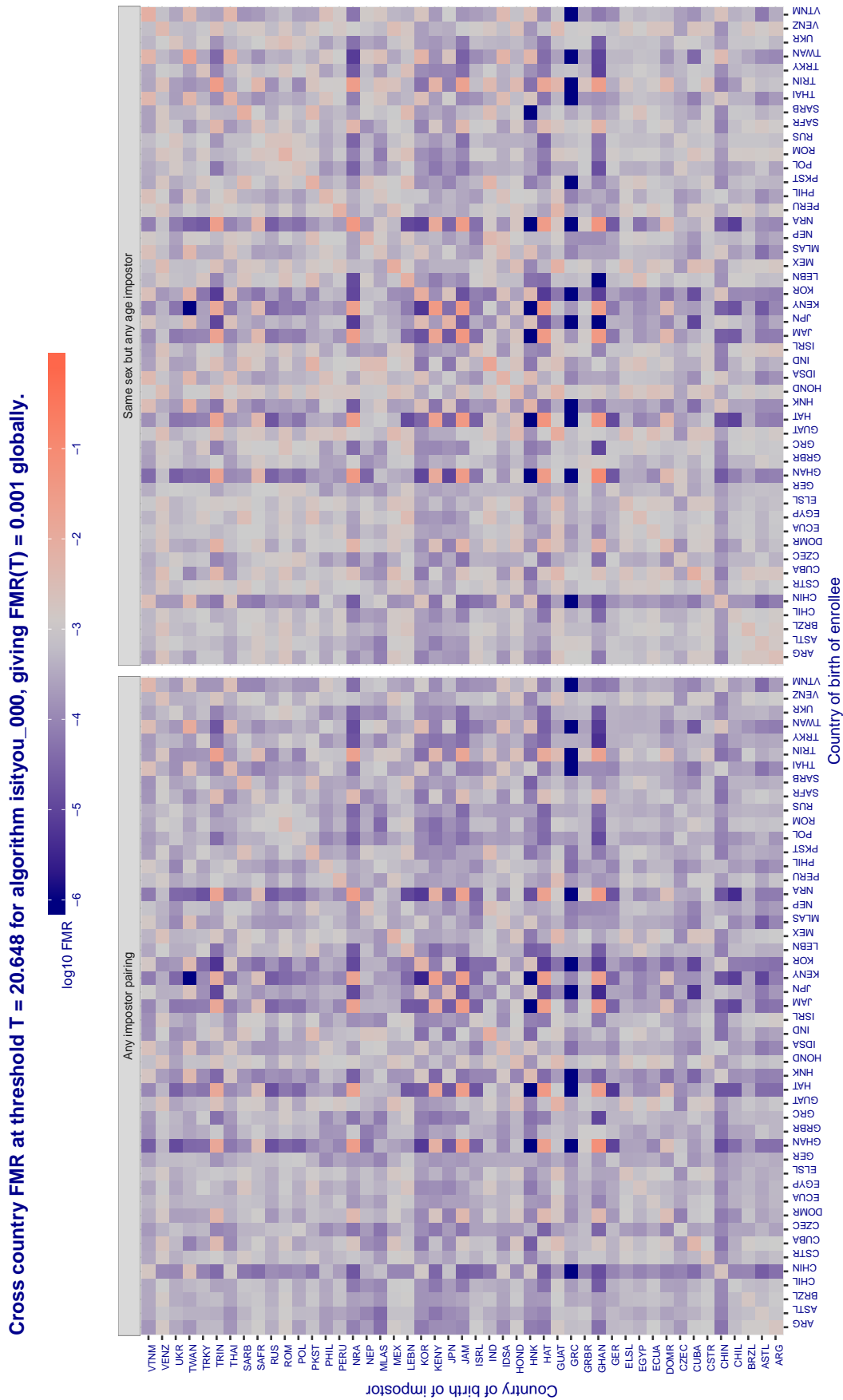


Figure 257: For algorithm isityou-000 operating on visa images, the heatmap shows false match rates observed over impostor comparisons of faces from different individuals who were born in the given country pair. False matches are counted against a recognition threshold fixed globally to give the target FMR in the plot title, computed over all on the order of 10^{10} impostor comparisons. If text appears in each box it give the same quantity as that coded by the color. Grey indicates FMR is at the intended FMR target level. Light red colors present a security vulnerability to, for example, a passport gate. Each +1 increase in \log_{10} FMR corresponds to a factor of 10 increase in FMR. The matrix is not quite symmetric because images in the enrollment and verification sets are different.

Cross country FMR at threshold $T = 0.649$ for algorithm isystems_001, giving $FMR(T) = 0.001$ globally.

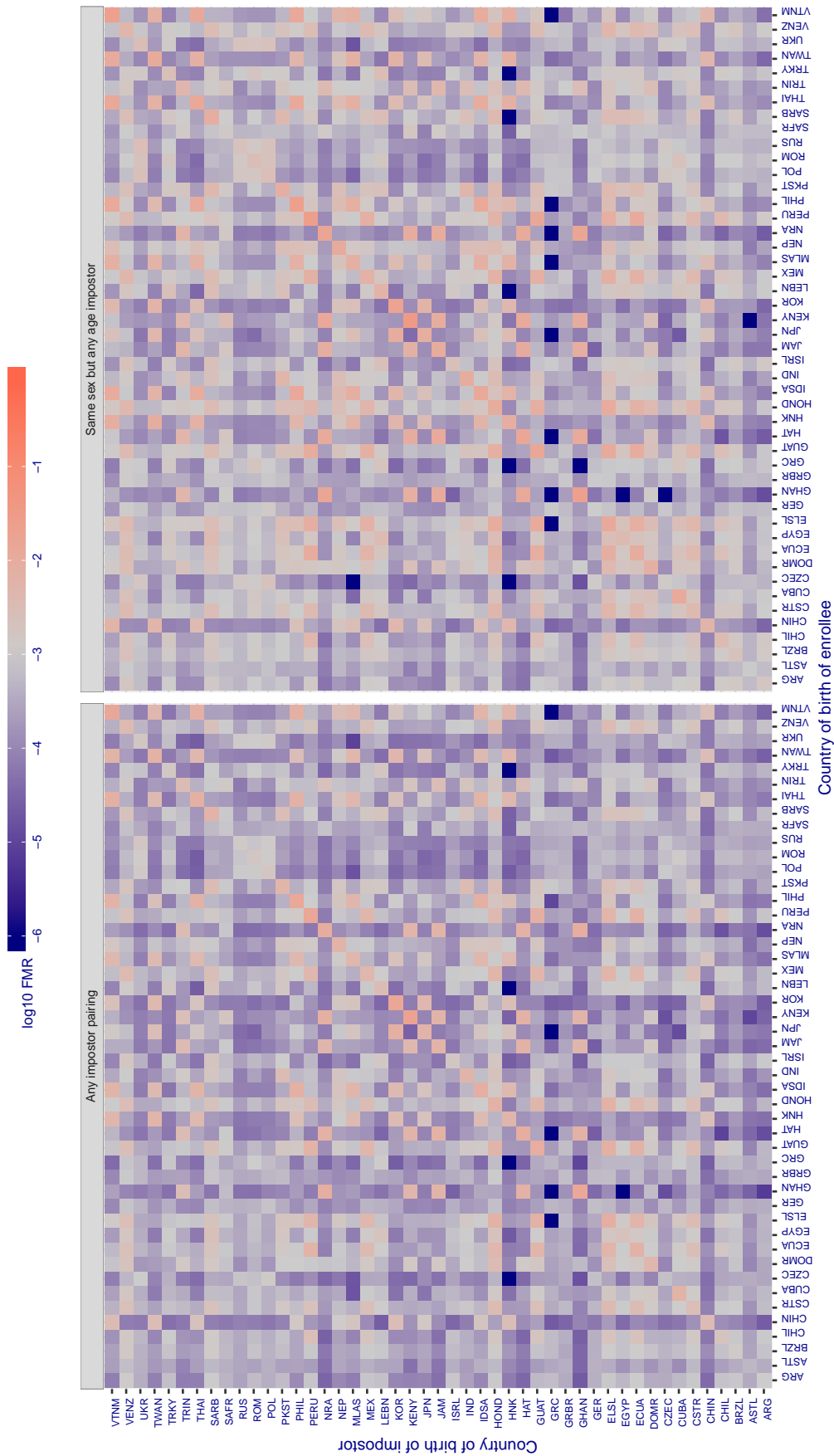


Figure 258: For algorithm isystems-001 operating on visa images, the heatmap shows false match rates observed over impostor comparisons of faces from different individuals who were born in the given country pair. False matches are counted against a recognition threshold fixed globally to give the target FMR in the plot title, computed over all on the order of 10^{10} impostor comparisons. If text appears in each box it give the same quantity as that coded by the color. Grey indicates FMR is at the intended FMR target level. Light red colors present a security vulnerability to, for example, a passport gate. Each +1 increase in \log_{10} FMR corresponds to a factor of 10 increase in FMR. The matrix is not quite symmetric because images in the enrollment and verification sets are different.

Cross country FMR at threshold $T = 0.647$ for algorithm isystems_002, giving $FMR(T) = 0.001$ globally.

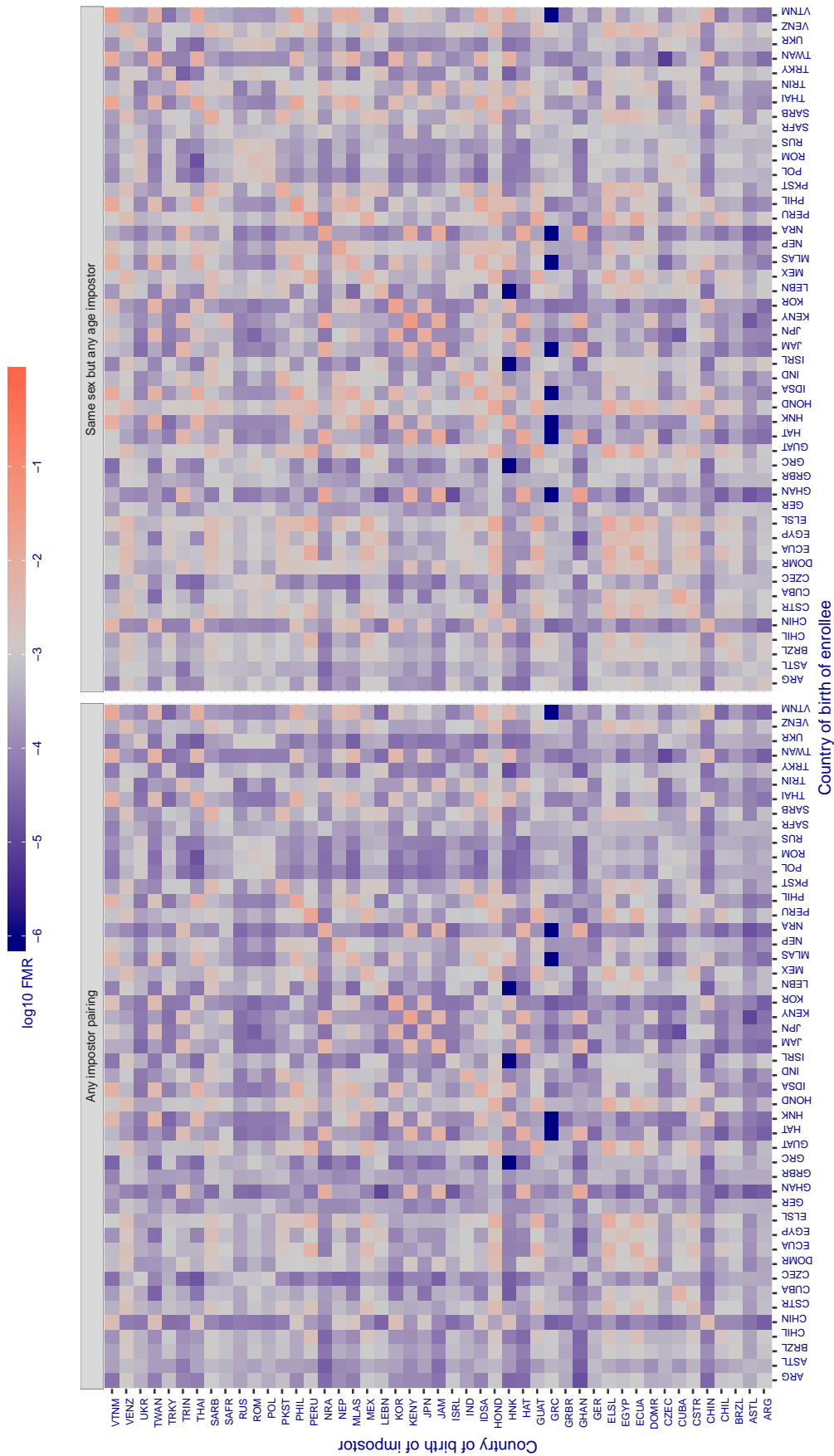


Figure 259: For algorithm isystems-002 operating on visa images, the heatmap shows false match rates observed over impostor comparisons of faces from different individuals who were born in the given country pair. False matches are counted against a recognition threshold fixed globally to give the target FMR in the plot title, computed over all on the order of 10^{10} impostor comparisons. If text appears in each box it give the same quantity as that coded by the color. Grey indicates FMR is at the intended FMR target level. Light red colors present a security vulnerability to, for example, a passport gate. Each +1 increase in \log_{10} FMR corresponds to a factor of 10 increase in FMR. The matrix is not quite symmetric because images in the enrollment and verification sets are different.

Cross country FMR at threshold $T = 10.316$ for algorithm itmo_005, giving $FMR(T) = 0.001$ globally.

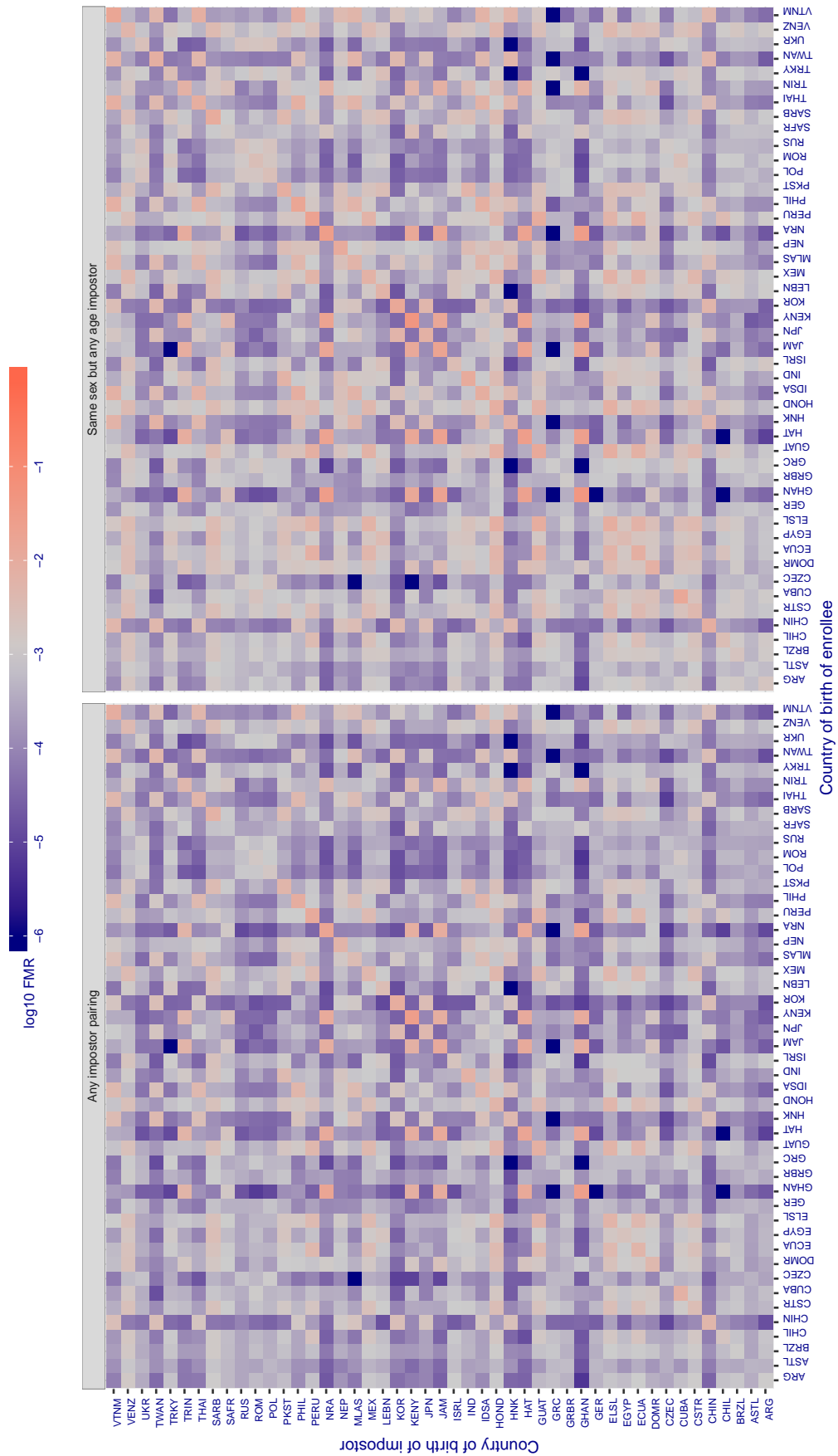


Figure 260: For algorithm itmo-005 operating on visa images, the heatmap shows false match rates observed over impostor comparisons of faces from different individuals who were born in the given country pair. False matches are counted against a recognition threshold fixed globally to give the target FMR in the plot title, computed over all on the order of 10^{10} impostor comparisons. If text appears in each box it give the same quantity as that coded by the color. Grey indicates FMR is at the intended FMR target level. Light red colors present a security vulnerability to, for example, a passport gate. Each +1 increase in log10 FMR corresponds to a factor of 10 increase in FMR. The matrix is not quite symmetric because images in the enrollment and verification sets are different.

Cross country FMR at threshold $T = 12.030$ for algorithm itmo_006, giving $FMR(T) = 0.001$ globally.

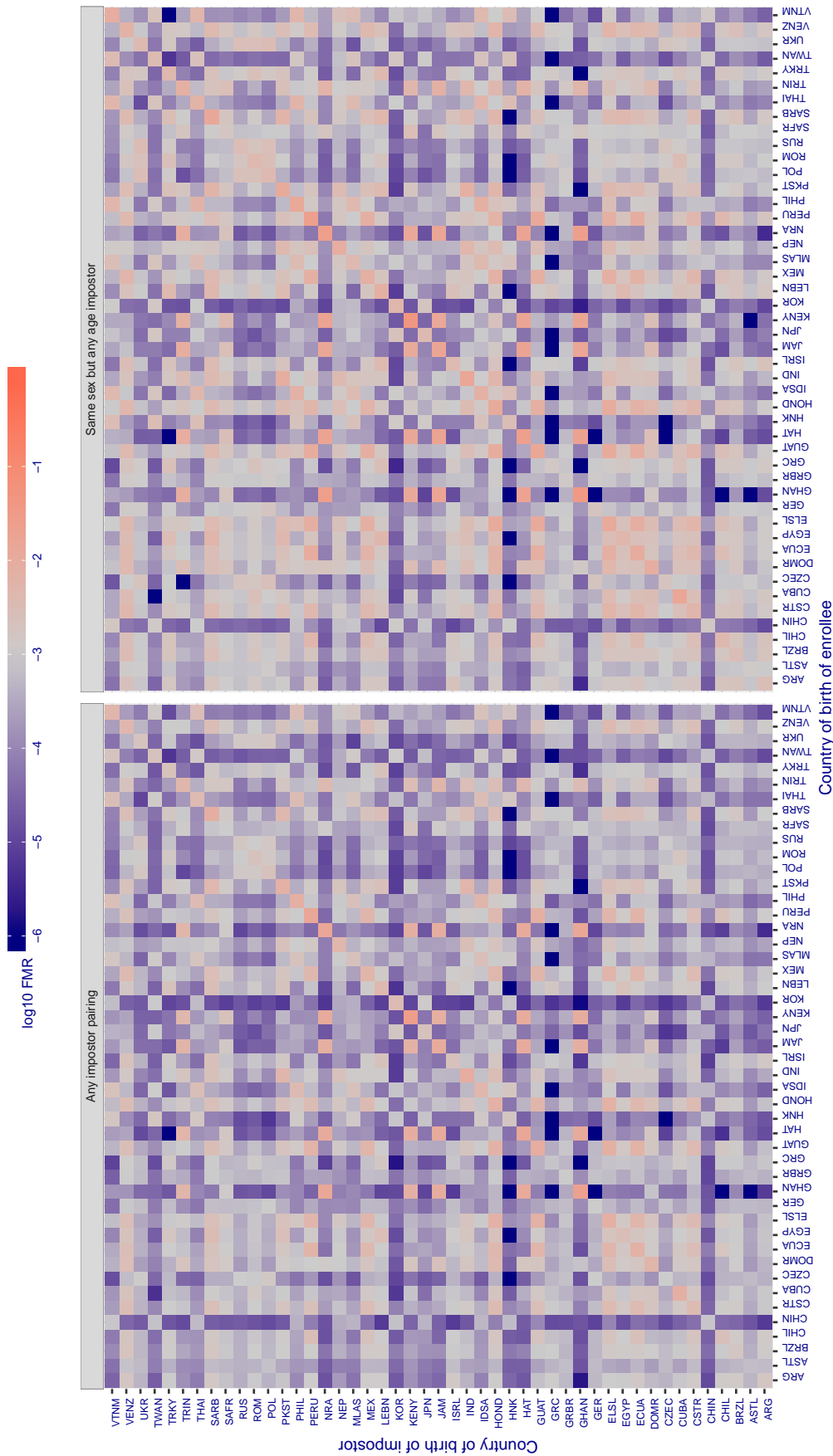


Figure 261: For algorithm itmo-006 operating on visa images, the heatmap shows false match rates observed over impostor comparisons of faces from different individuals who were born in the given country pair. False matches are counted against a recognition threshold fixed globally to give the target FMR in the plot title, computed over all on the order of 10^{10} impostor comparisons. If text appears in each box it give the same quantity as that coded by the color. Grey indicates FMR is at the intended FMR target level. Light red colors present a security vulnerability to, for example, a passport gate. Each +1 increase in log10 FMR corresponds to a factor of 10 increase in FMR. The matrix is not quite symmetric because images in the enrollment and verification sets are different.

Cross country FMR at threshold $T = 1.192$ for algorithm kakao_001, giving $FMR(T) = 0.001$ globally.

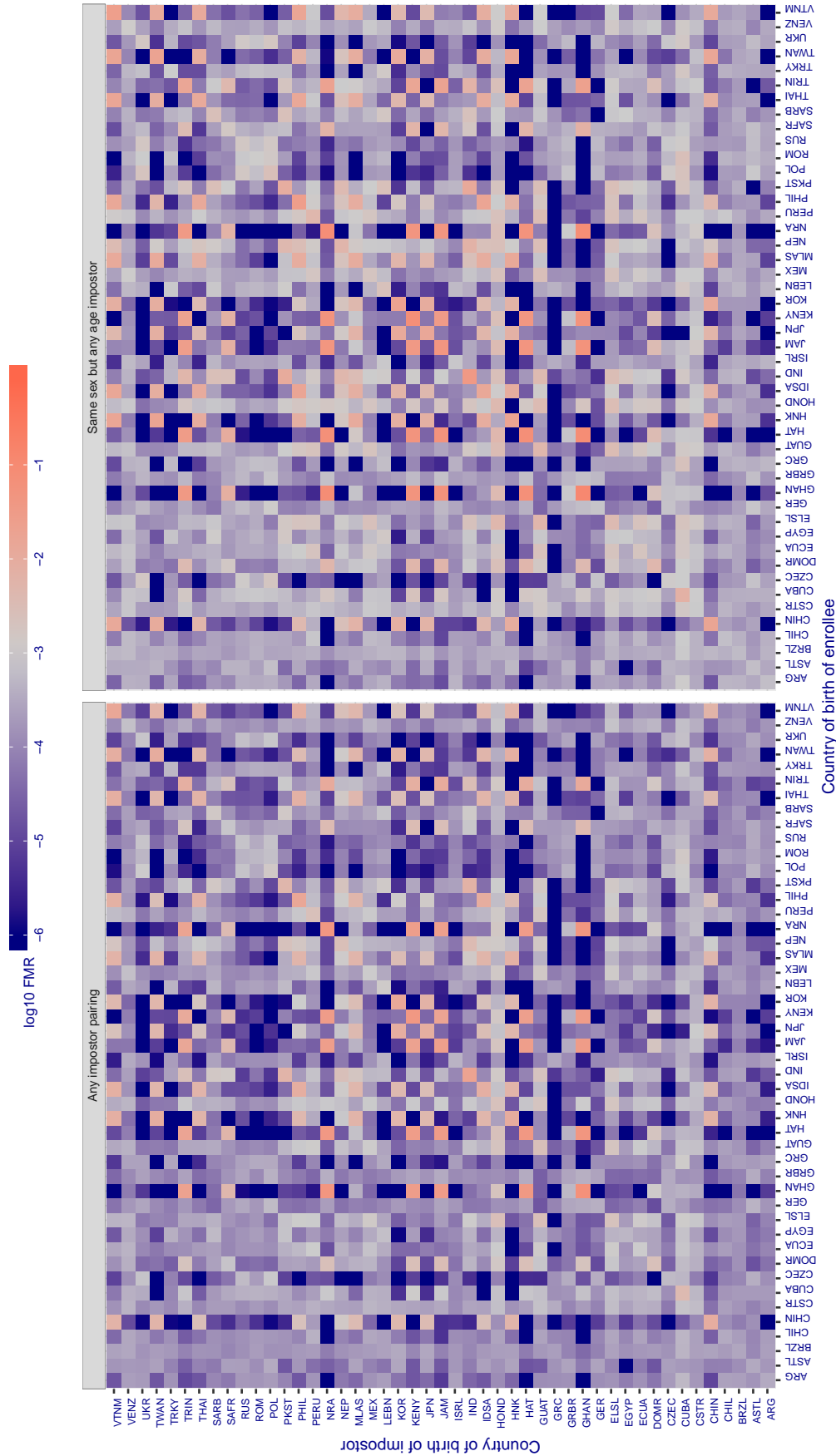


Figure 262: For algorithm kakao-001 operating on visa images, the heatmap shows false match rates observed over impostor comparisons of faces from different individuals who were born in the given country pair. False matches are counted against a recognition threshold fixed globally to give the target FMR in the plot title, computed over all on the order of 10^{10} impostor comparisons. If text appears in each box it give the same quantity as that coded by the color. Grey indicates FMR is at the intended FMR target level. Light red colors present a security vulnerability to, for example, a passport gate. Each +1 increase in \log_{10} FMR corresponds to a factor of 10 increase in FMR. The matrix is not quite symmetric because images in the enrollment and verification sets are different.

Cross country FMR at threshold $T = 0.656$ for algorithm lookman_002, giving $FMR(T) = 0.001$ globally.

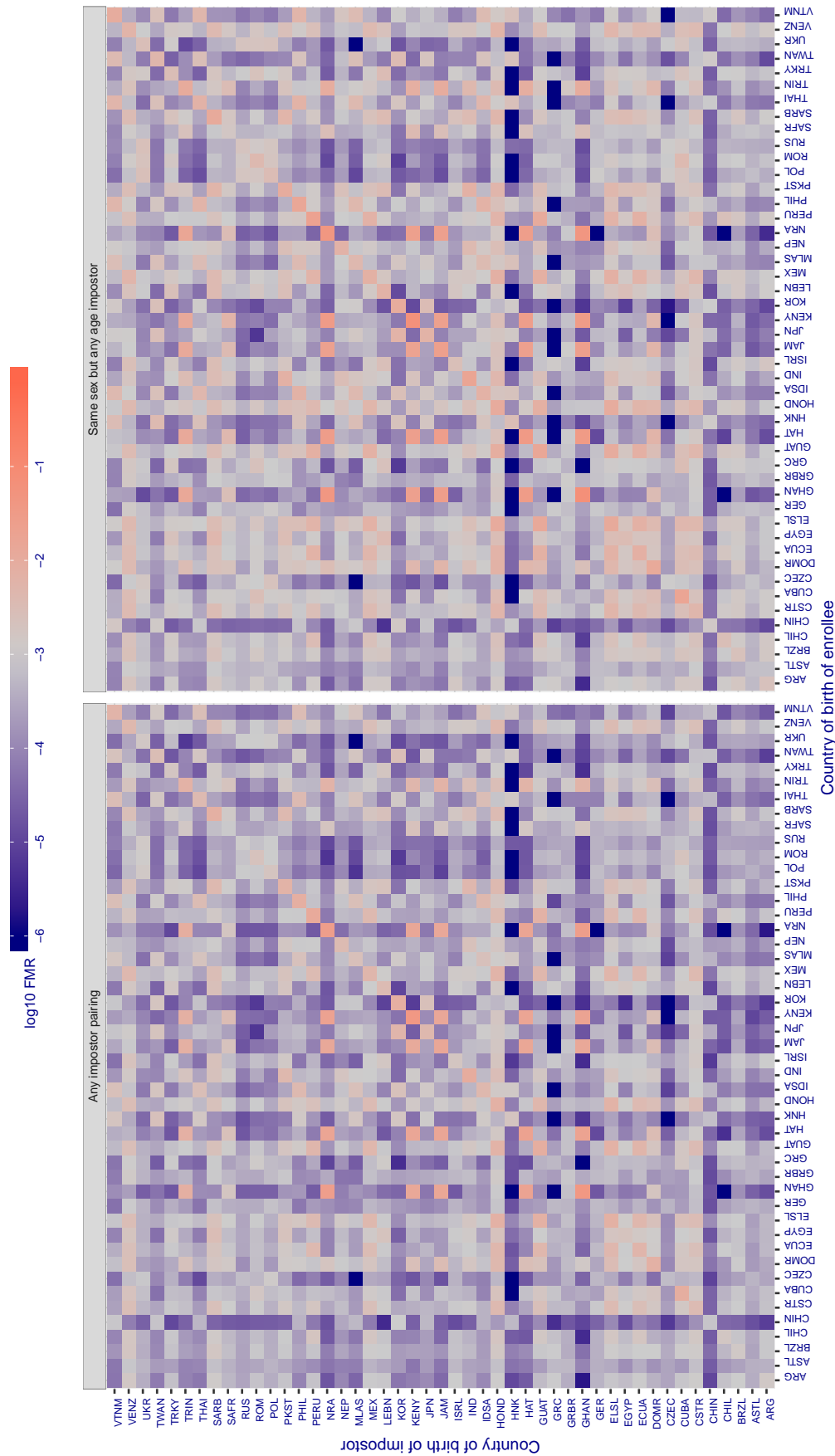


Figure 263: For algorithm lookman-002 operating on visa images, the heatmap shows false match rates observed over impostor comparisons of faces from different individuals who were born in the given country pair. False matches are counted against a recognition threshold fixed globally to give the target FMR in the plot title, computed over all on the order of 10^{10} impostor comparisons. If text appears in each box it give the same quantity as that coded by the color. Grey indicates FMR is at the intended FMR target level. Light red colors present a security vulnerability to, for example, a passport gate. Each +1 increase in \log_{10} FMR corresponds to a factor of 10 increase in FMR. The matrix is not quite symmetric because images in the enrollment and verification sets are different.

Cross country FMR at threshold $T = 66.706$ for algorithm megvii_001, giving $FMR(T) = 0.001$ globally.

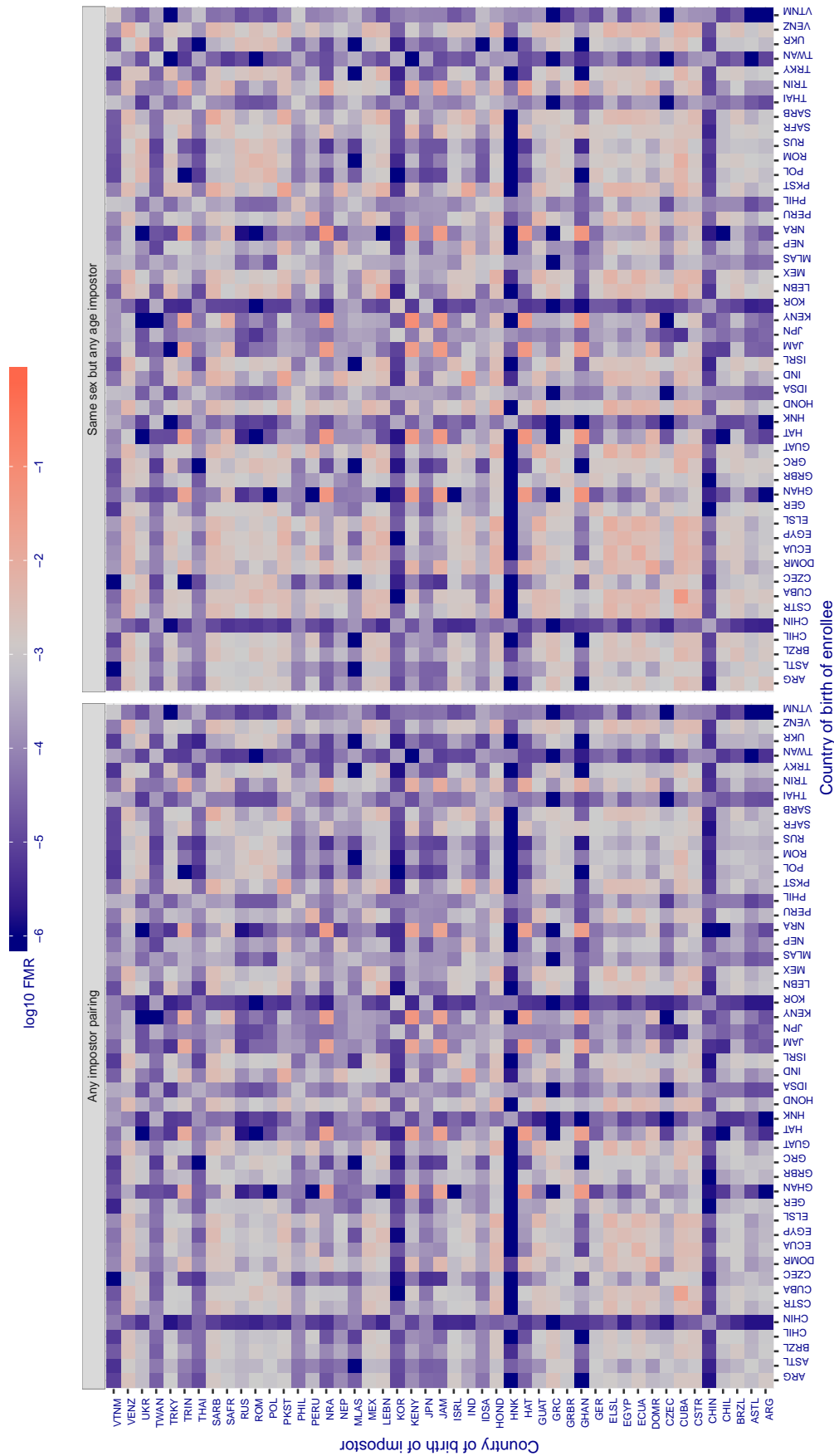


Figure 264: For algorithm megvii-001 operating on visa images, the heatmap shows false match rates observed over impostor comparisons of faces from different individuals who were born in the given country pair. False matches are counted against a recognition threshold fixed globally to give the target FMR in the plot title, computed over all on the order of 10^{10} impostor comparisons. If text appears in each box it give the same quantity as that coded by the color. Grey indicates FMR is at the intended FMR target level. Light red colors present a security vulnerability to, for example, a passport gate. Each +1 increase in log10 FMR corresponds to a factor of 10 increase in FMR. The matrix is not quite symmetric because images in the enrollment and verification sets are different.

Cross country FMR at threshold $T = 58.026$ for algorithm megvii_002, giving $FMR(T) = 0.001$ globally.

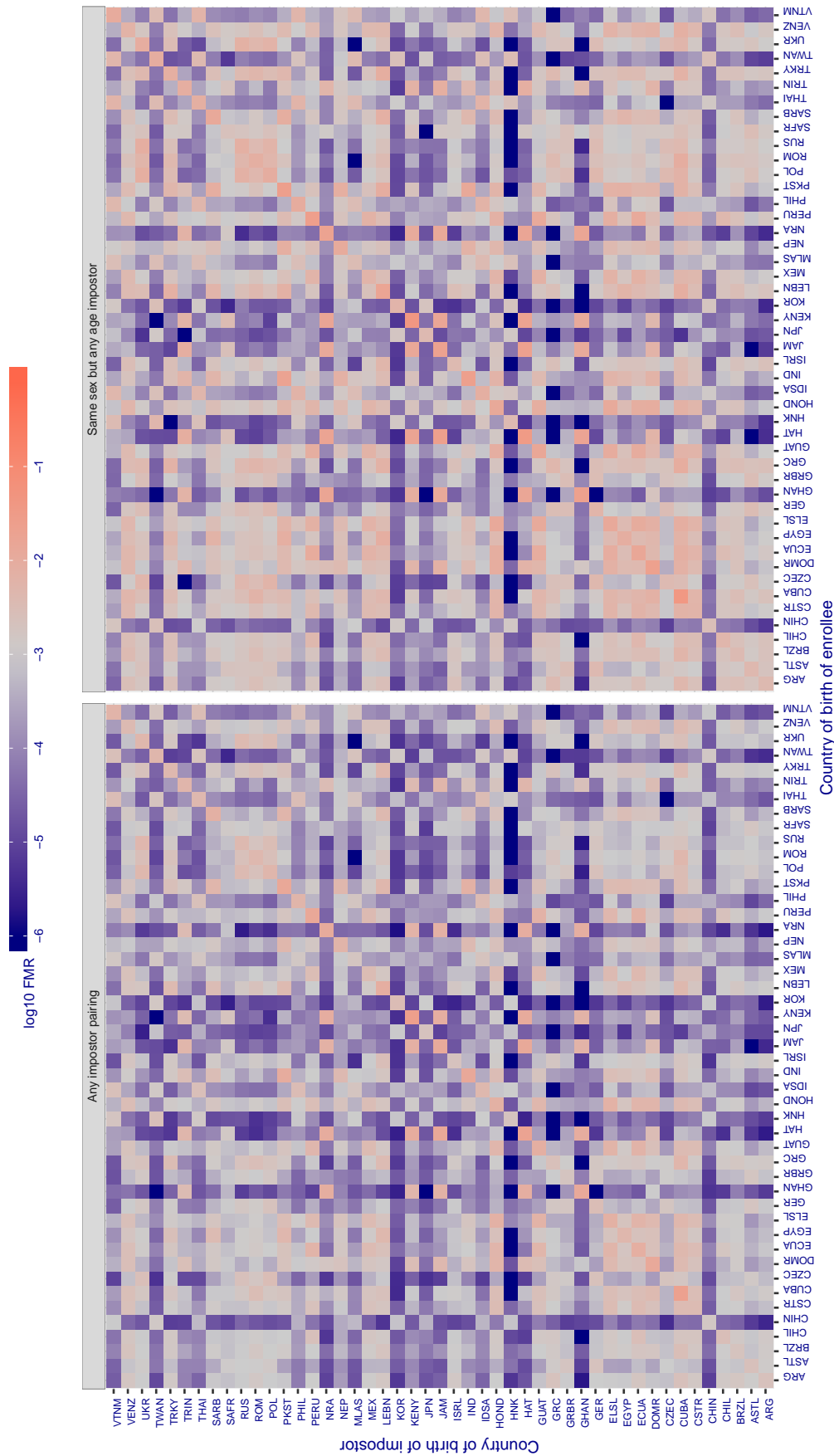


Figure 265: For algorithm megvii-002 operating on visa images, the heatmap shows false match rates observed over impostor comparisons of faces from different individuals who were born in the given country pair. False matches are counted against a recognition threshold fixed globally to give the target FMR in the plot title, computed over all on the order of 10^{10} impostor comparisons. If text appears in each box it give the same quantity as that coded by the color. Grey indicates FMR is at the intended FMR target level. Light red colors present a security vulnerability to, for example, a passport gate. Each +1 increase in $\log_{10} FMR$ corresponds to a factor of 10 increase in FMR. The matrix is not quite symmetric because images in the enrollment and verification sets are different.

Cross country FMR at threshold $T = 0.345$ for algorithm meiya_001, giving $FMR(T) = 0.001$ globally.

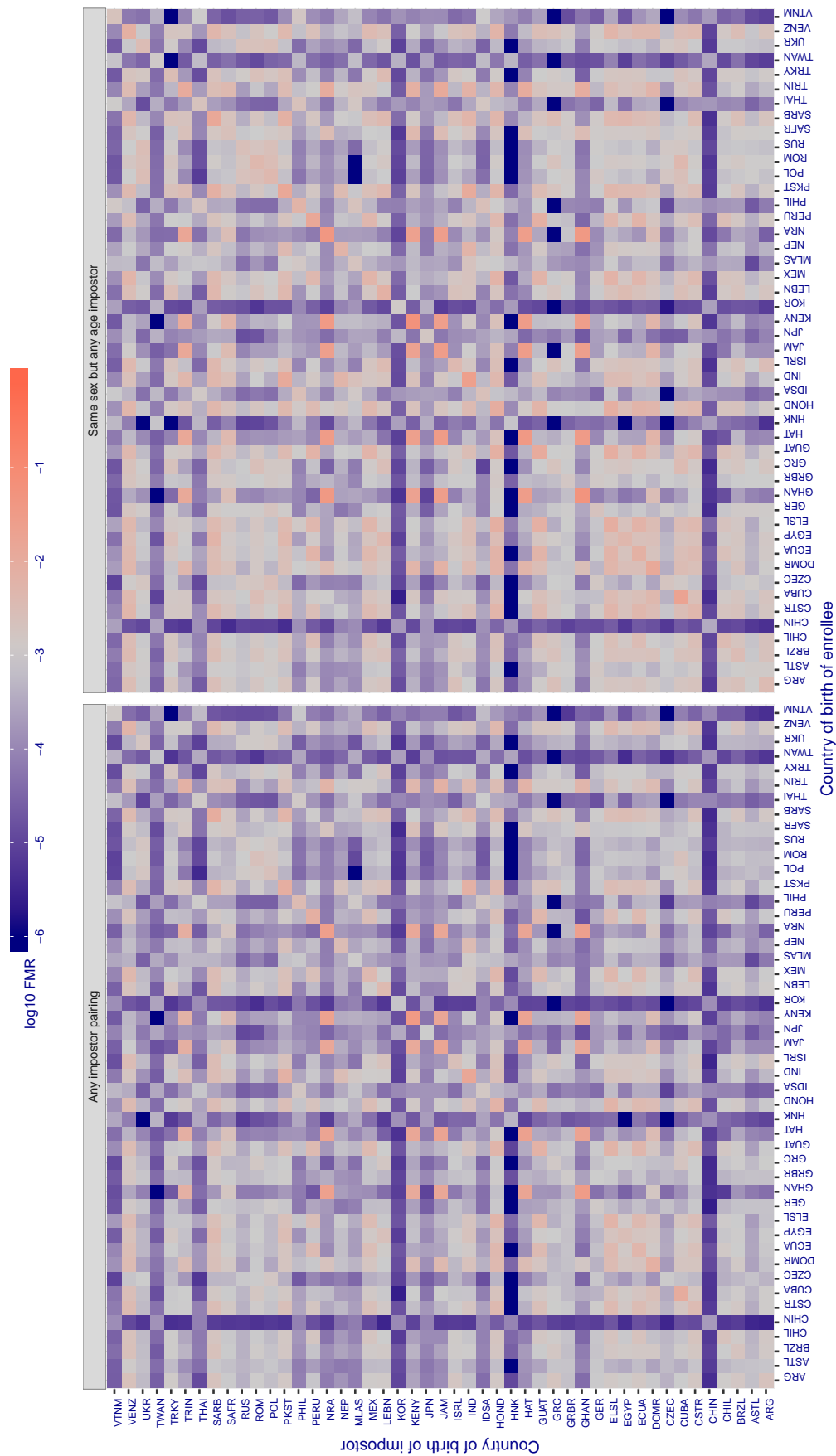


Figure 266: For algorithm meiya-001 operating on visa images, the heatmap shows false match rates observed over impostor comparisons of faces from different individuals who were born in the given country pair. False matches are counted against a recognition threshold fixed globally to give the target FMR in the plot title, computed over all on the order of 10^{10} impostor comparisons. If text appears in each box it give the same quantity as that coded by the color. Grey indicates FMR is at the intended FMR target level. Light red colors present a security vulnerability to, for example, a passport gate. Each +1 increase in \log_{10} FMR corresponds to a factor of 10 increase in FMR. The matrix is not quite symmetric because images in the enrollment and verification sets are different.

Cross country FMR at threshold $T = 0.624$ for algorithm microfocus_001, giving $FMR(T) = 0.001$ globally.

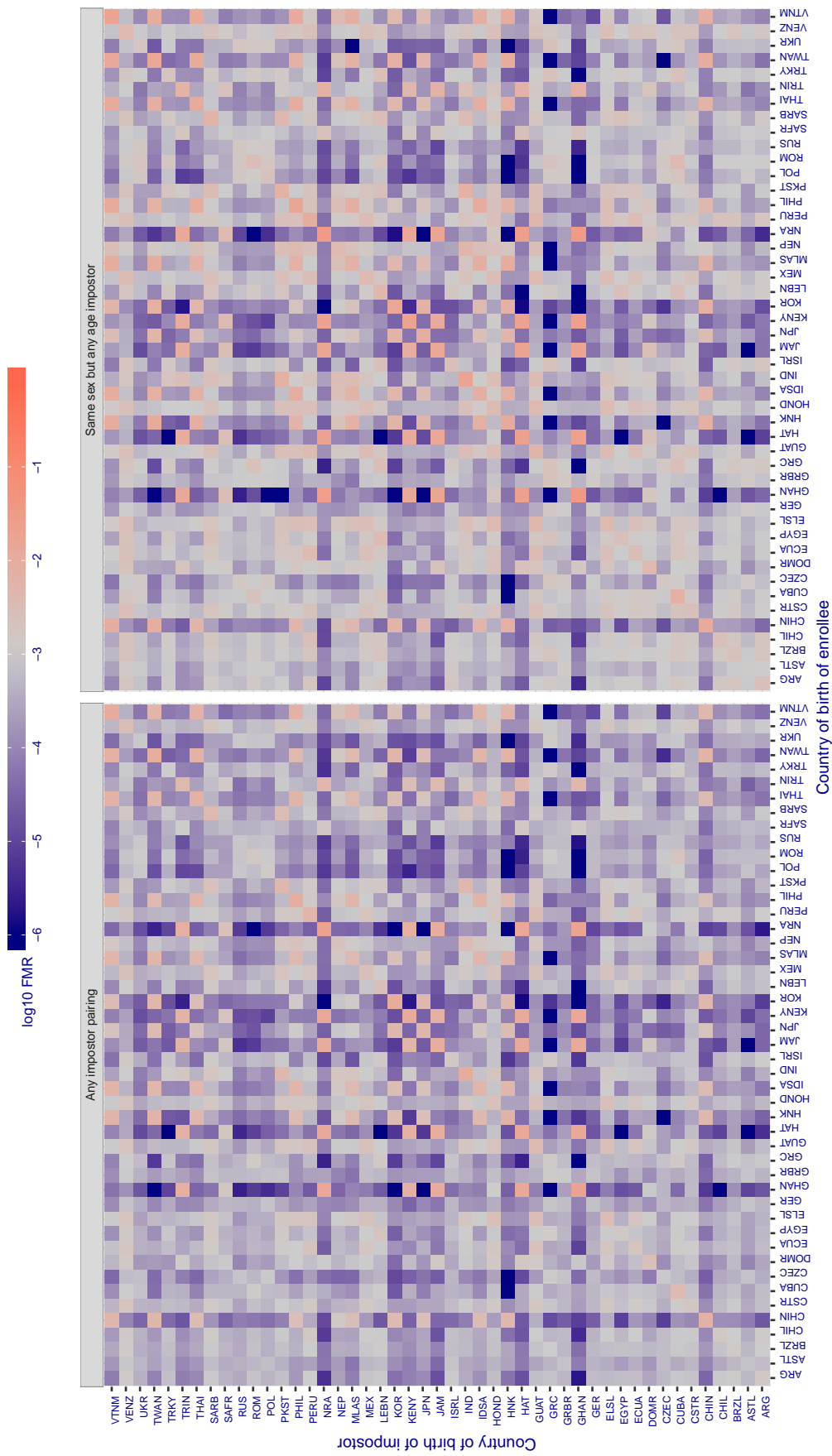


Figure 267: For algorithm microfocus-001 operating on visa images, the heatmap shows false match rates observed over impostor comparisons of faces from different individuals who were born in the given country pair. False matches are counted against a recognition threshold fixed globally to give the target FMR in the plot title, computed over all on the order of 10^{10} impostor comparisons. If text appears in each box it give the same quantity as that coded by the color. Grey indicates FMR is at the intended FMR target level. Light red colors present a security vulnerability to, for example, a passport gate. Each +1 increase in \log_{10} FMR corresponds to a factor of 10 increase in FMR. The matrix is not quite symmetric because images in the enrollment and verification sets are different.

Cross country FMR at threshold $T = 0.542$ for algorithm microfocus_002, giving $FMR(T) = 0.001$ globally.

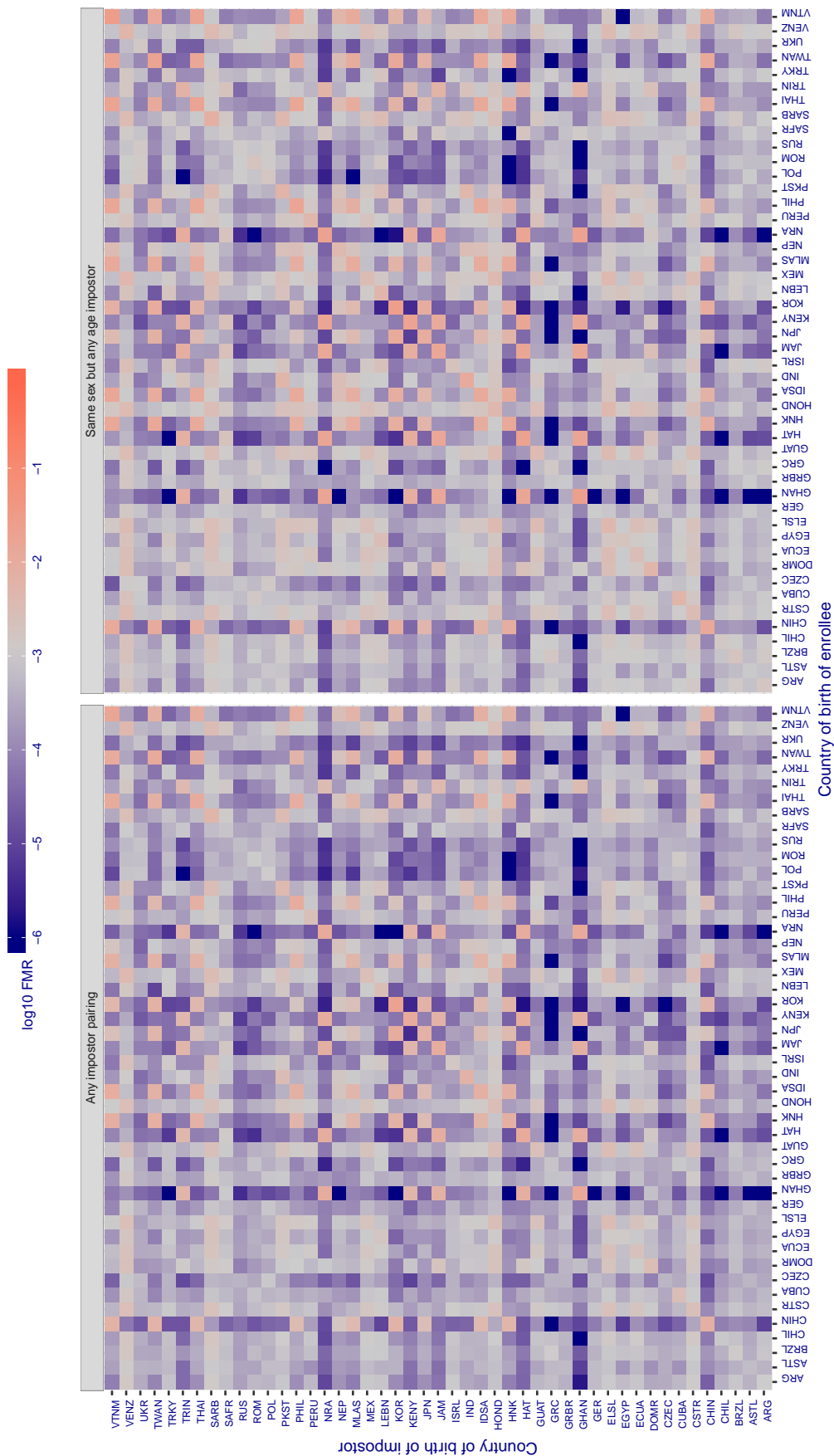


Figure 268: For algorithm microfocus-002 operating on visa images, the heatmap shows false match rates observed over impostor comparisons of faces from different individuals who were born in the given country pair. False matches are counted against a recognition threshold fixed globally to give the target FMR in the plot title, computed over all on the order of 10^{10} impostor comparisons. If text appears in each box it give the same quantity as that coded by the color. Grey indicates FMR is at the intended FMR target level. Light red colors present a security vulnerability to, for example, a passport gate. Each +1 increase in \log_{10} FMR corresponds to a factor of 10 increase in FMR. The matrix is not quite symmetric because images in the enrollment and verification sets are different.

Cross country FMR at threshold $T = 0.693$ for algorithm `nodeflux_001`, giving $FMR(T) = 0.001$ globally.

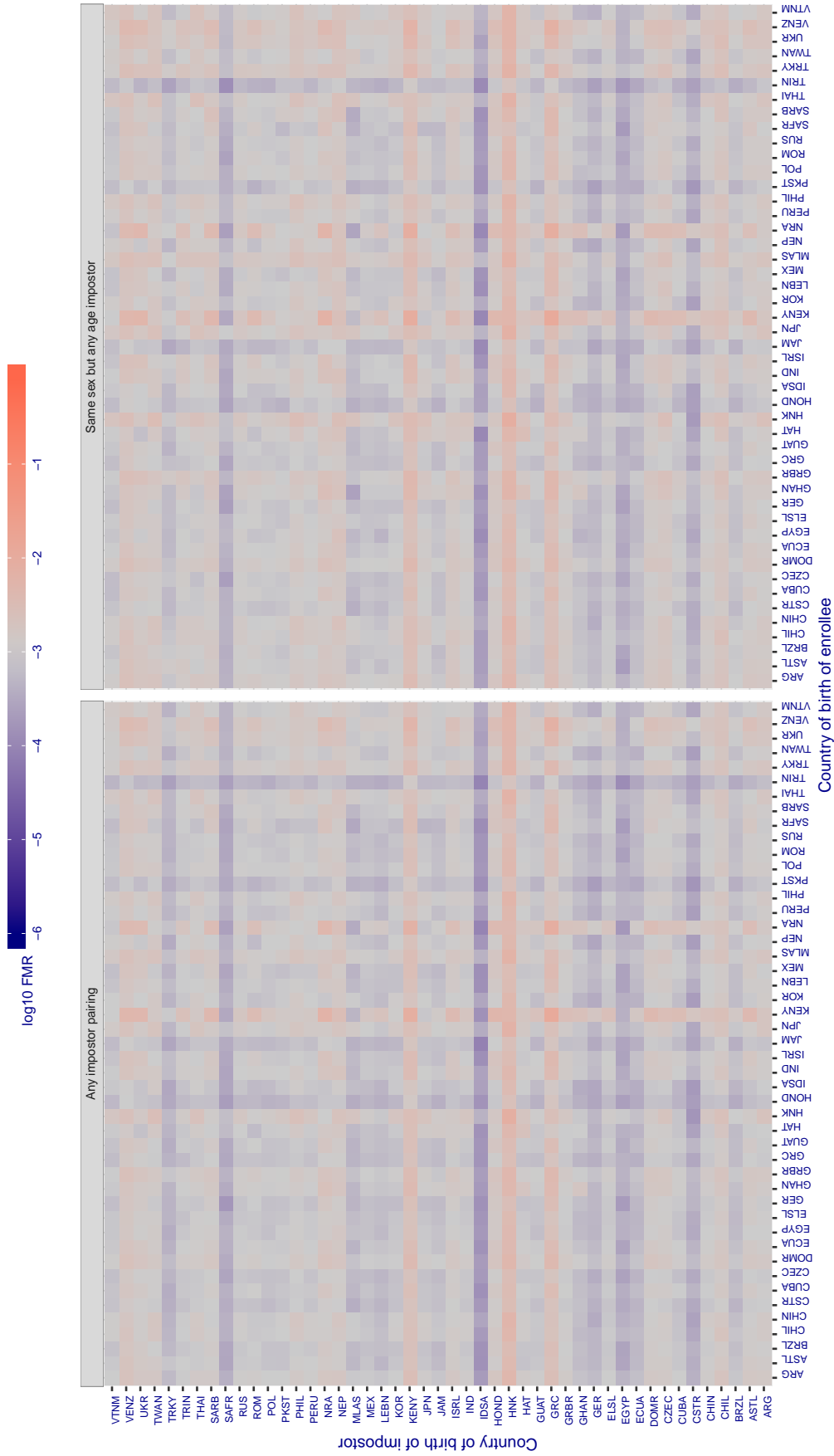


Figure 269: For algorithm `nodeflux-001` operating on visa images, the heatmap shows false match rates observed over impostor comparisons of faces from different individuals who were born in the given country pair. False matches are counted against a recognition threshold fixed globally to give the target FMR in the plot title, computed over all on the order of 10^{10} impostor comparisons. If text appears in each box it give the same quantity as that coded by the color. Grey indicates FMR is at the intended FMR target level. Light red colors present a security vulnerability to, for example, a passport gate. Each +1 increase in $\log_{10} FMR$ corresponds to a factor of 10 increase in FMR. The matrix is not quite symmetric because images in the enrollment and verification sets are different.

Cross country FMR at threshold $T = 1.369$ for algorithm ntechlab_005, giving $FMR(T) = 0.001$ globally.

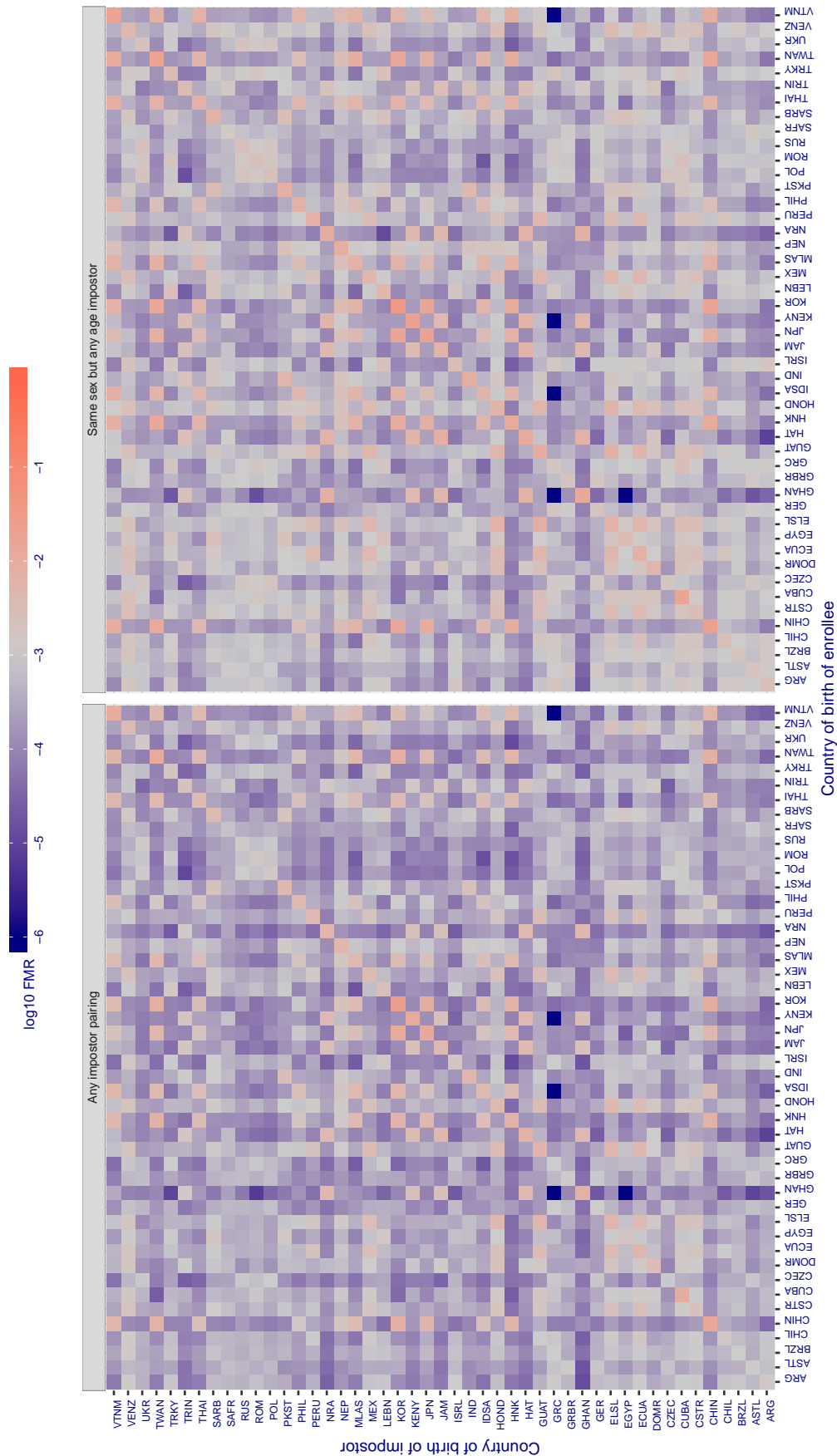


Figure 270: For algorithm ntechlab-005 operating on visa images, the heatmap shows false match rates observed over impostor comparisons of faces from different individuals who were born in the given country pair. False matches are counted against a recognition threshold fixed globally to give the target FMR in the plot title, computed over all on the order of 10^{10} impostor comparisons. If text appears in each box it give the same quantity as that coded by the color. Grey indicates FMR is at the intended FMR target level. Light red colors present a security vulnerability to, for example, a passport gate. Each +1 increase in log10 FMR corresponds to a factor of 10 increase in FMR. The matrix is not quite symmetric because images in the enrollment and verification sets are different.

Cross country FMR at threshold $T = 1.929$ for algorithm ntechlab_006, giving $FMR(T) = 0.001$ globally.

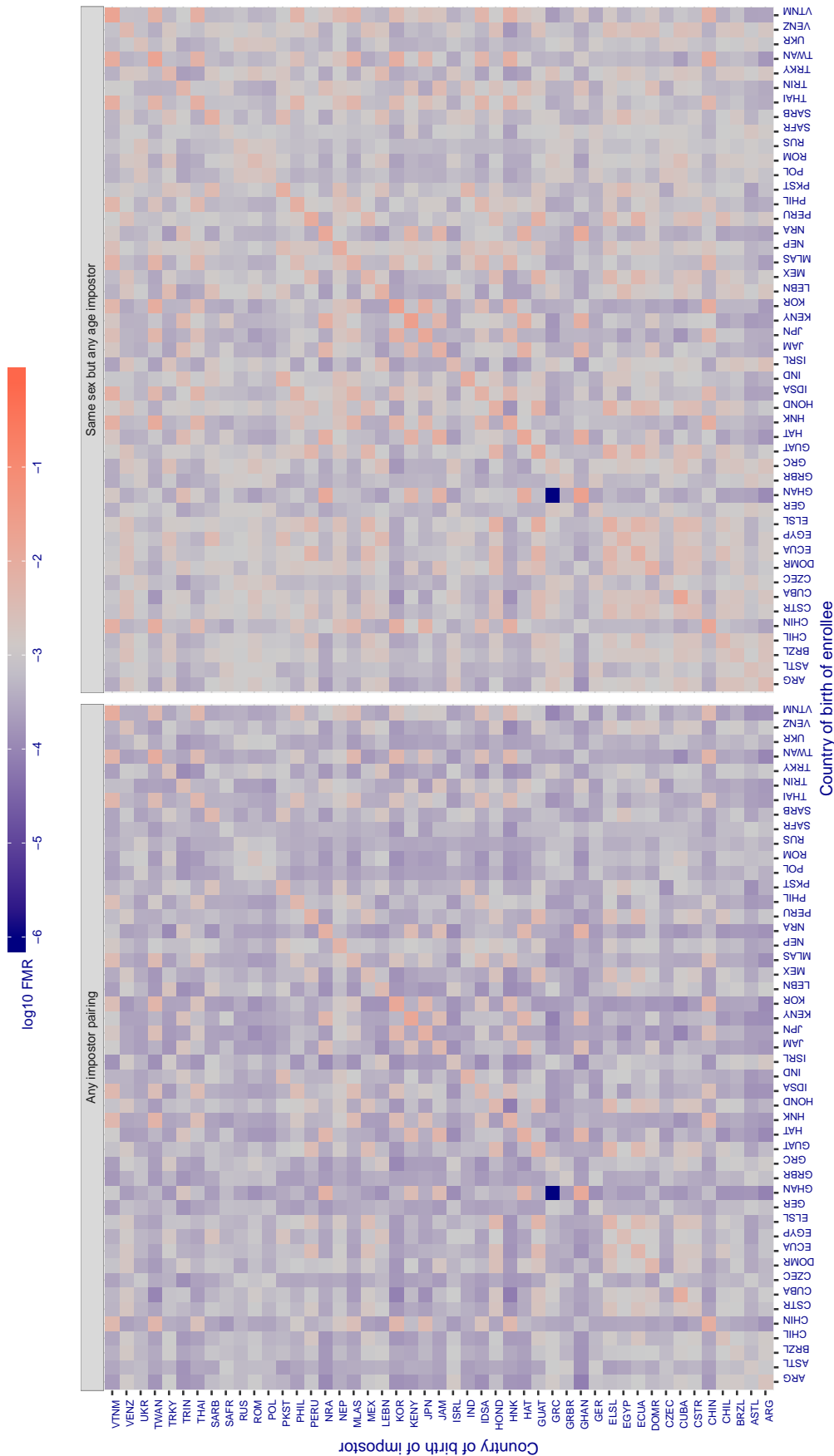


Figure 271: For algorithm ntechlab-006 operating on visa images, the heatmap shows false match rates observed over impostor comparisons of faces from different individuals who were born in the given country pair. False matches are counted against a recognition threshold fixed globally to give the target FMR in the plot title, computed over all on the order of 10^{10} impostor comparisons. If text appears in each box it give the same quantity as that coded by the color. Grey indicates FMR is at the intended FMR target level. Light red colors present a security vulnerability to, for example, a passport gate. Each +1 increase in \log_{10} FMR corresponds to a factor of 10 increase in FMR. The matrix is not quite symmetric because images in the enrollment and verification sets are different.

Cross country FMR at threshold $T = 0.253$ for algorithm psl_{001} , giving $FMR(T) = 0.001$ globally.

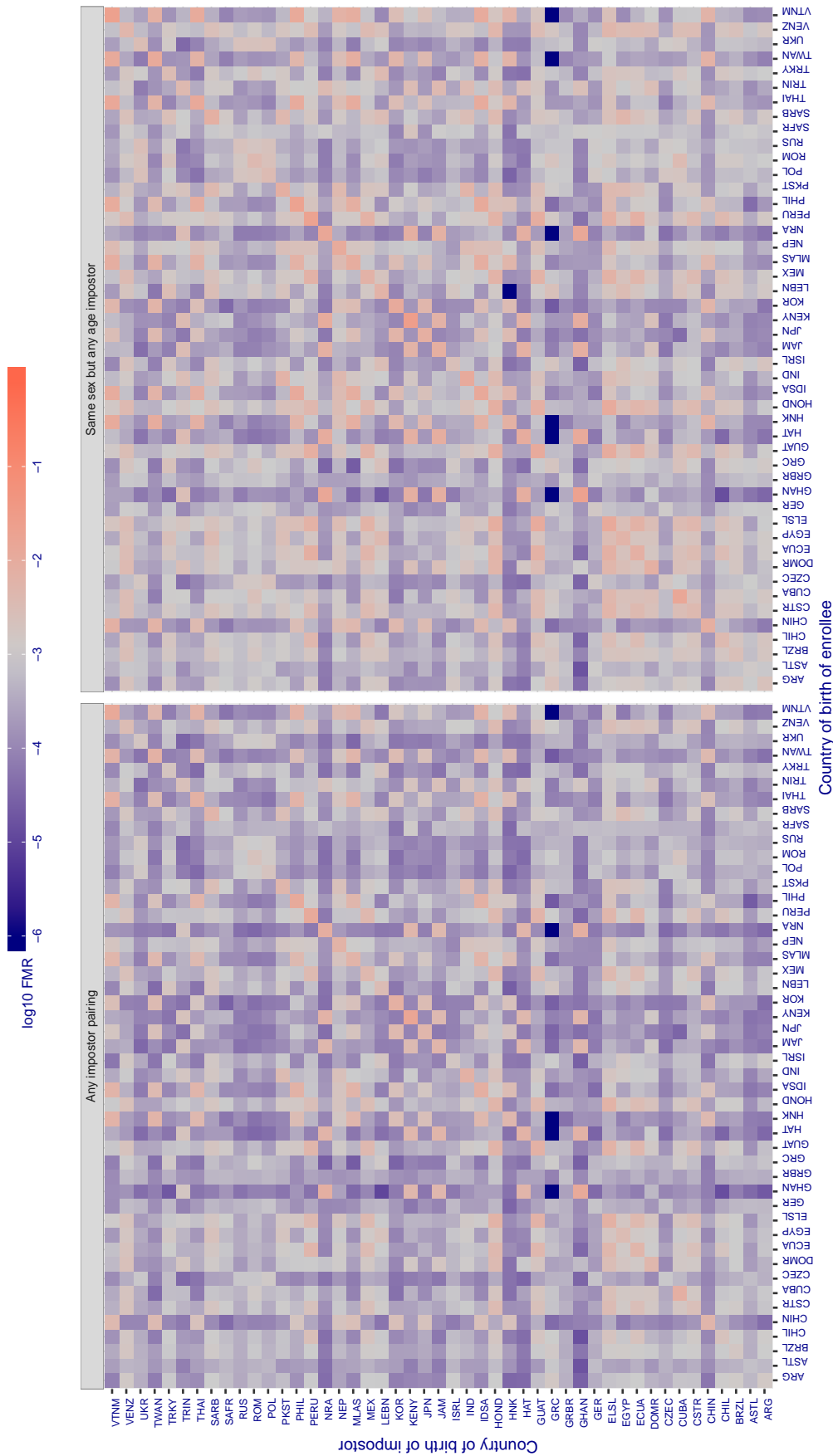


Figure 272: For algorithm psl_{001} operating on visa images, the heatmap shows false match rates observed over impostor comparisons of faces from different individuals who were born in the given country pair. False matches are counted against a recognition threshold fixed globally to give the target FMR in the plot title, computed over all on the order of 10^{10} impostor comparisons. If text appears in each box it give the same quantity as that coded by the color. Grey indicates FMR is at the intended FMR target level. Light red colors present a security vulnerability to, for example, a passport gate. Each +1 increase in \log_{10} FMR corresponds to a factor of 10 increase in FMR. The matrix is not quite symmetric because images in the enrollment and verification sets are different.

Cross country FMR at threshold $T = 0.272$ for algorithm psl_{002} , giving $FMR(T) = 0.001$ globally.

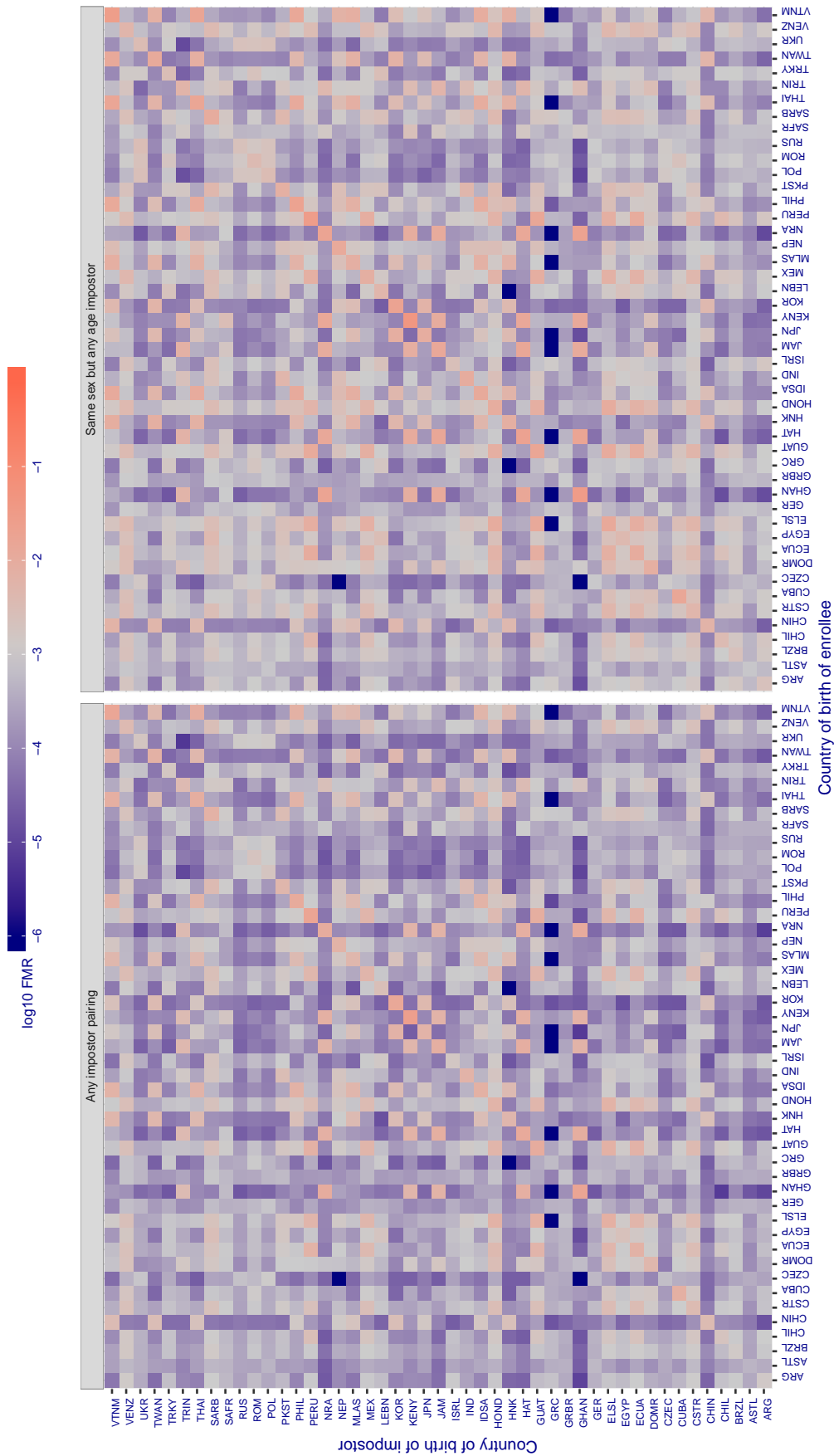


Figure 273: For algorithm psl_{002} operating on visa images, the heatmap shows false match rates observed over impostor comparisons of faces from different individuals who were born in the given country pair. False matches are counted against a recognition threshold fixed globally to give the target FMR in the plot title, computed over all on the order of 10^{10} impostor comparisons. If text appears in each box it give the same quantity as that coded by the color. Grey indicates FMR is at the intended FMR target level. Light red colors present a security vulnerability to, for example, a passport gate. Each +1 increase in $\log_{10} FMR$ corresponds to a factor of 10 increase in FMR. The matrix is not quite symmetric because images in the enrollment and verification sets are different.

Cross country FMR at threshold $T = 0.600$ for algorithm rankone_{005} , giving $\text{FMR}(T) = 0.001$ globally.

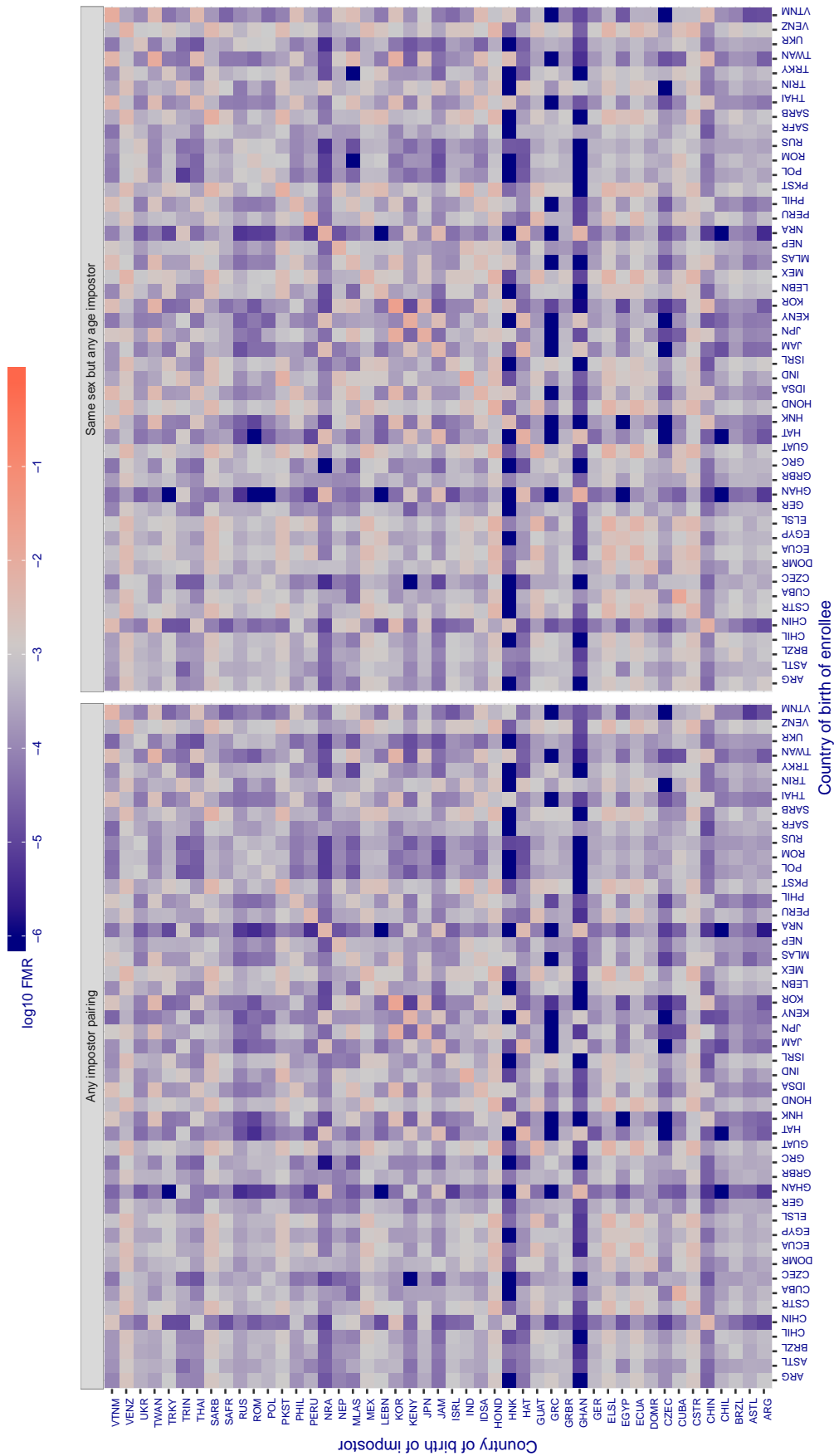


Figure 274: For algorithm rankone_{005} operating on visa images, the heatmap shows false match rates observed over impostor comparisons of faces from different individuals who were born in the given country pair. False matches are counted against a recognition threshold fixed globally to give the target FMR in the plot title, computed over all on the order of 10^{10} impostor comparisons. If text appears in each box it give the same quantity as that coded by the color. Grey indicates FMR is at the intended FMR target level. Light red colors present a security vulnerability to, for example, a passport gate. Each +1 increase in \log_{10} FMR corresponds to a factor of 10 increase in FMR. The matrix is not quite symmetric because images in the enrollment and verification sets are different.

Cross country FMR at threshold $T = 0.613$ for algorithm `rankone_006`, giving $FMR(T) = 0.001$ globally.

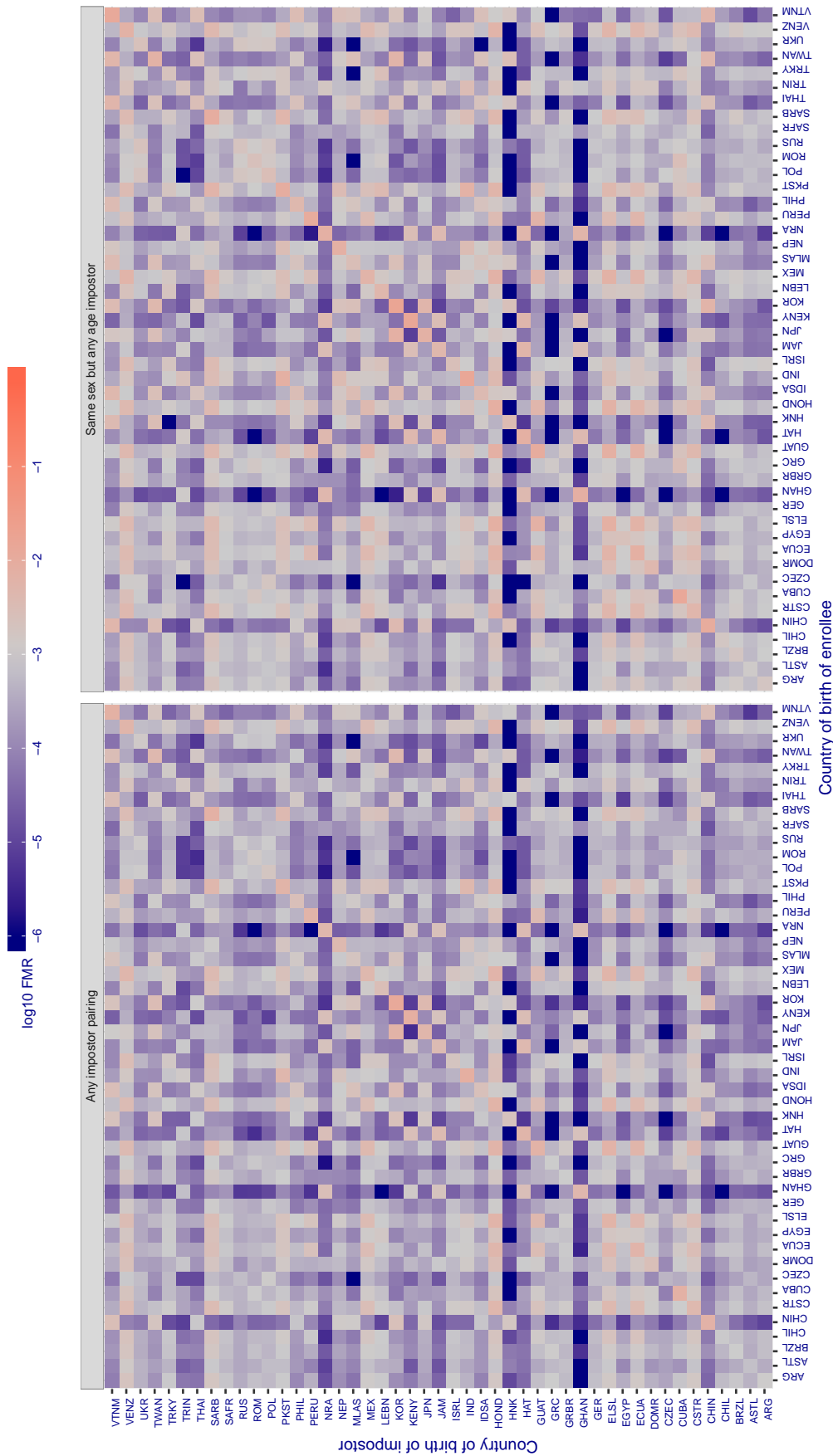


Figure 275: For algorithm `rankone-006` operating on visa images, the heatmap shows false match rates observed over impostor comparisons of faces from different individuals who were born in the given country pair. False matches are counted against a recognition threshold fixed globally to give the target FMR in the plot title, computed over all on the order of 10^{10} impostor comparisons. If text appears in each box it give the same quantity as that coded by the color. Grey indicates FMR is at the intended FMR target level. Light red colors present a security vulnerability to, for example, a passport gate. Each +1 increase in \log_{10} FMR corresponds to a factor of 10 increase in FMR. The matrix is not quite symmetric because images in the enrollment and verification sets are different.

Cross country FMR at threshold $T = 0.814$ for algorithm realnetworks_001, giving $FMR(T) = 0.001$ globally.

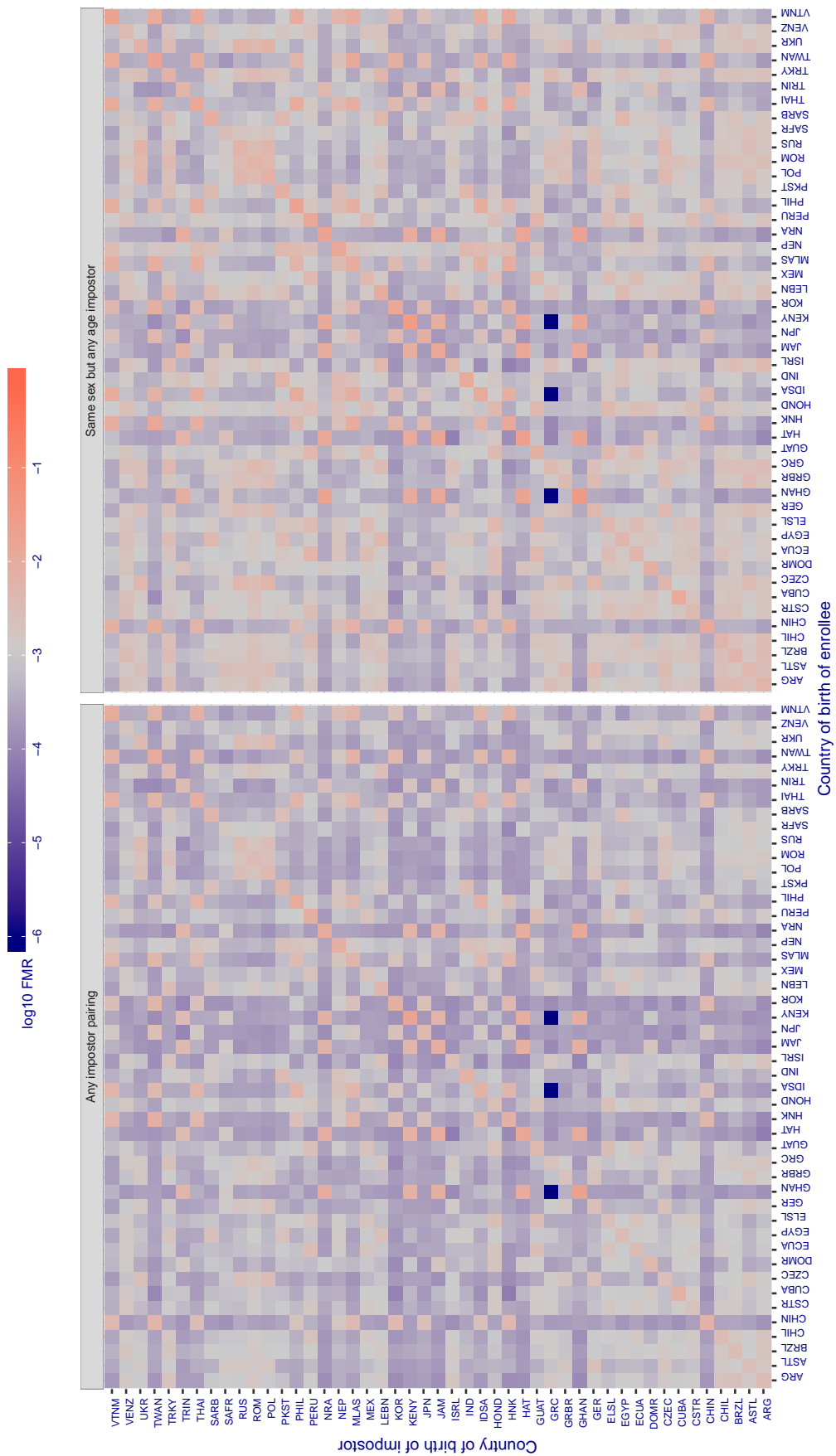


Figure 276: For algorithm realnetworks-001 operating on visa images, the heatmap shows false match rates observed over impostor comparisons of faces from different individuals who were born in the given country pair. False matches are counted against a recognition threshold fixed globally to give the target FMR in the plot title, computed over all on the order of 10^{10} impostor comparisons. If text appears in each box it give the same quantity as that coded by the color. Grey indicates FMR is at the intended FMR target level. Light red colors present a security vulnerability to, for example, a passport gate. Each +1 increase in \log_{10} FMR corresponds to a factor of 10 increase in FMR. The matrix is not quite symmetric because images in the enrollment and verification sets are different.

Cross country FMR at threshold $T = 0.814$ for algorithm realnetworks_002, giving $FMR(T) = 0.001$ globally.

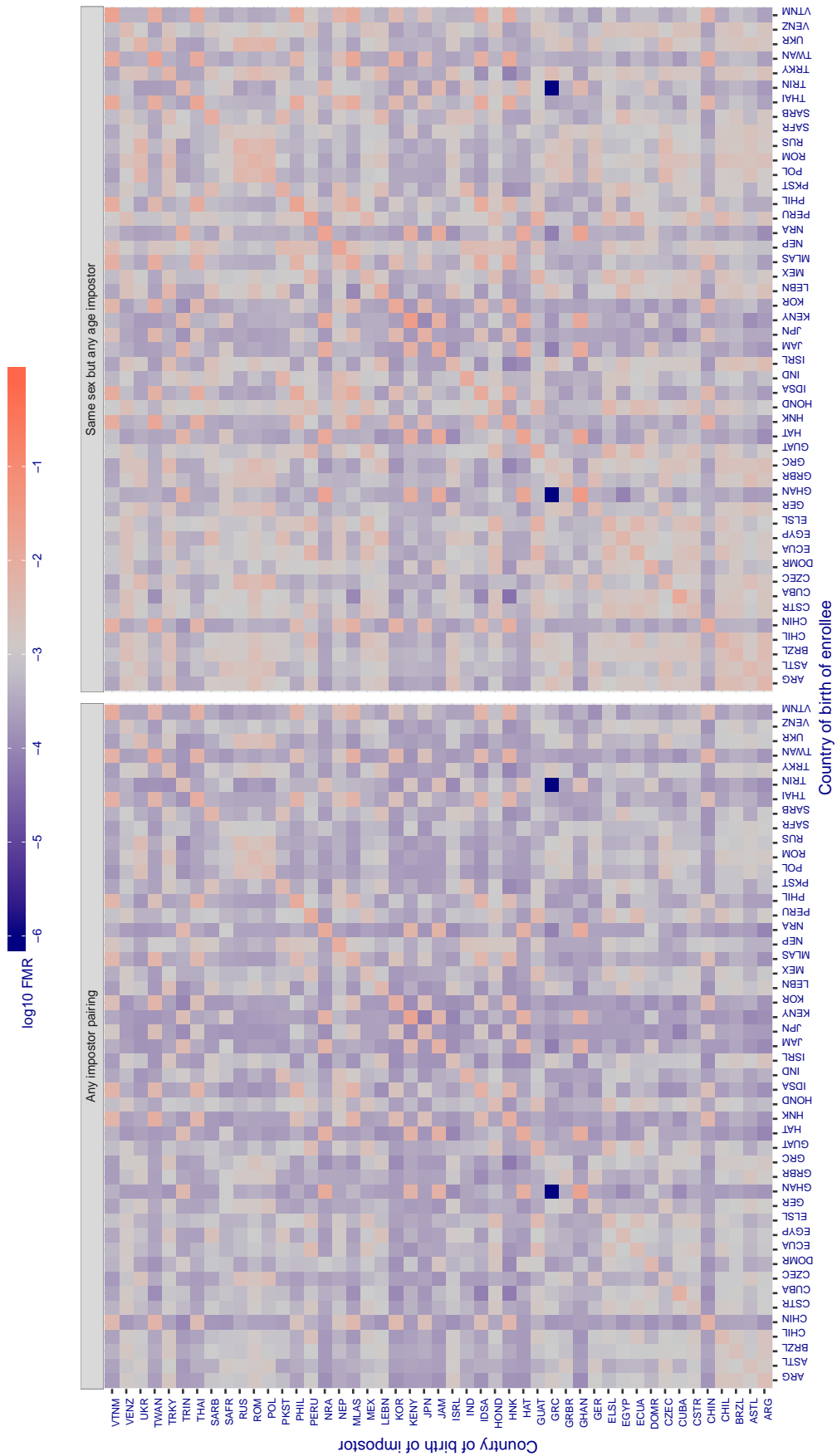


Figure 277: For algorithm realnetworks-002 operating on visa images, the heatmap shows false match rates observed over impostor comparisons of faces from different individuals who were born in the given country pair. False matches are counted against a recognition threshold fixed globally to give the target FMR in the plot title, computed over all on the order of 10^{10} impostor comparisons. If text appears in each box it give the same quantity as that coded by the color. Grey indicates FMR is at the intended FMR target level. Light red colors present a security vulnerability to, for example, a passport gate. Each +1 increase in \log_{10} FMR corresponds to a factor of 10 increase in FMR. The matrix is not quite symmetric because images in the enrollment and verification sets are different.

Cross country FMR at threshold $T = 65.920$ for algorithm remarkai_000, giving $FMR(T) = 0.001$ globally.

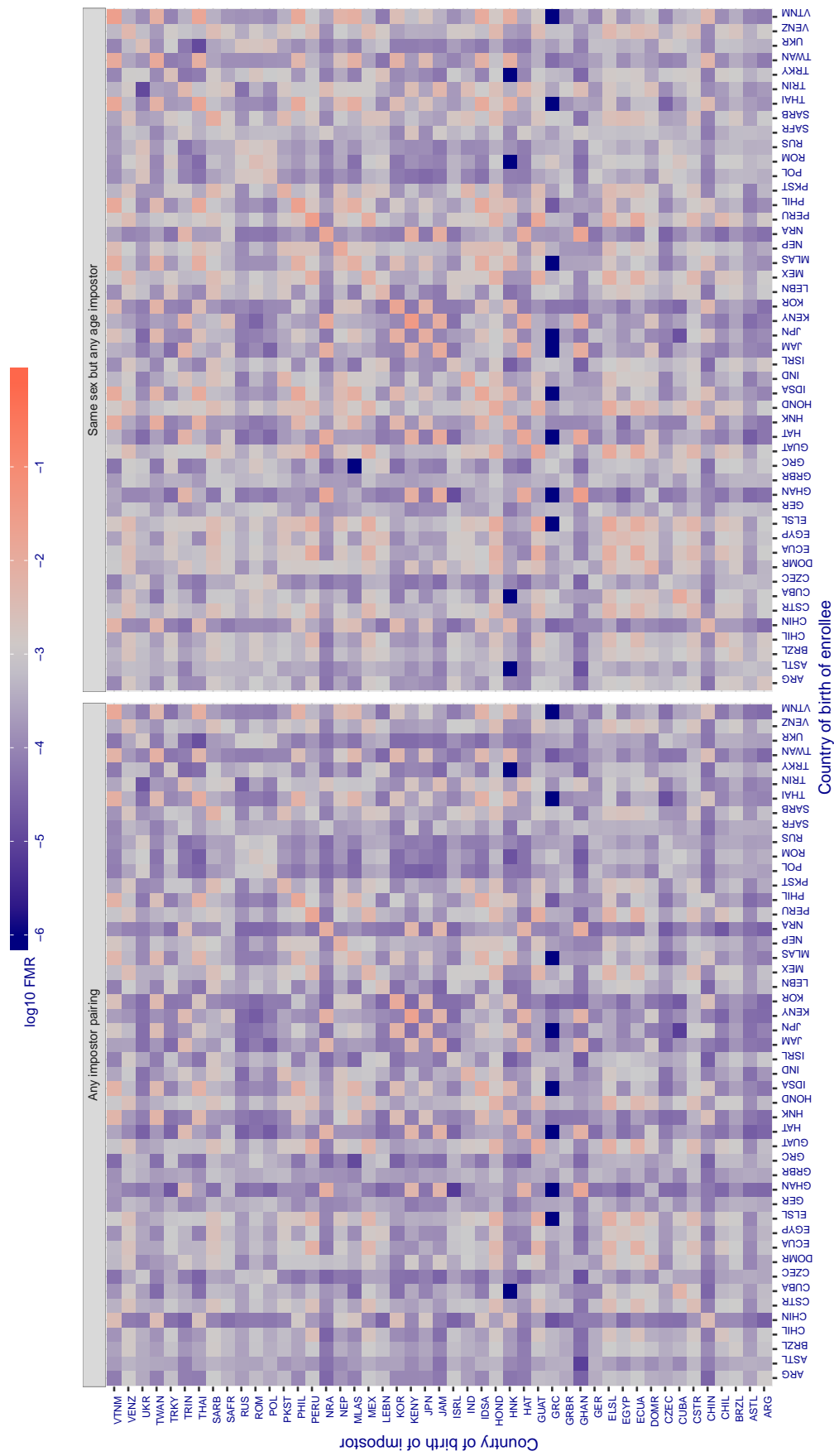


Figure 278: For algorithm remarkai-000 operating on visa images, the heatmap shows false match rates observed over impostor comparisons of faces from different individuals who were born in the given country pair. False matches are counted against a recognition threshold fixed globally to give the target FMR in the plot title, computed over all on the order of 10^{10} impostor comparisons. If text appears in each box it give the same quantity as that coded by the color. Grey indicates FMR is at the intended FMR target level. Light red colors present a security vulnerability to, for example, a passport gate. Each +1 increase in \log_{10} FMR corresponds to a factor of 10 increase in FMR. The matrix is not quite symmetric because images in the enrollment and verification sets are different.

Cross country FMR at threshold $T = 65.928$ for algorithm remarkai_001, giving $FMR(T) = 0.001$ globally.

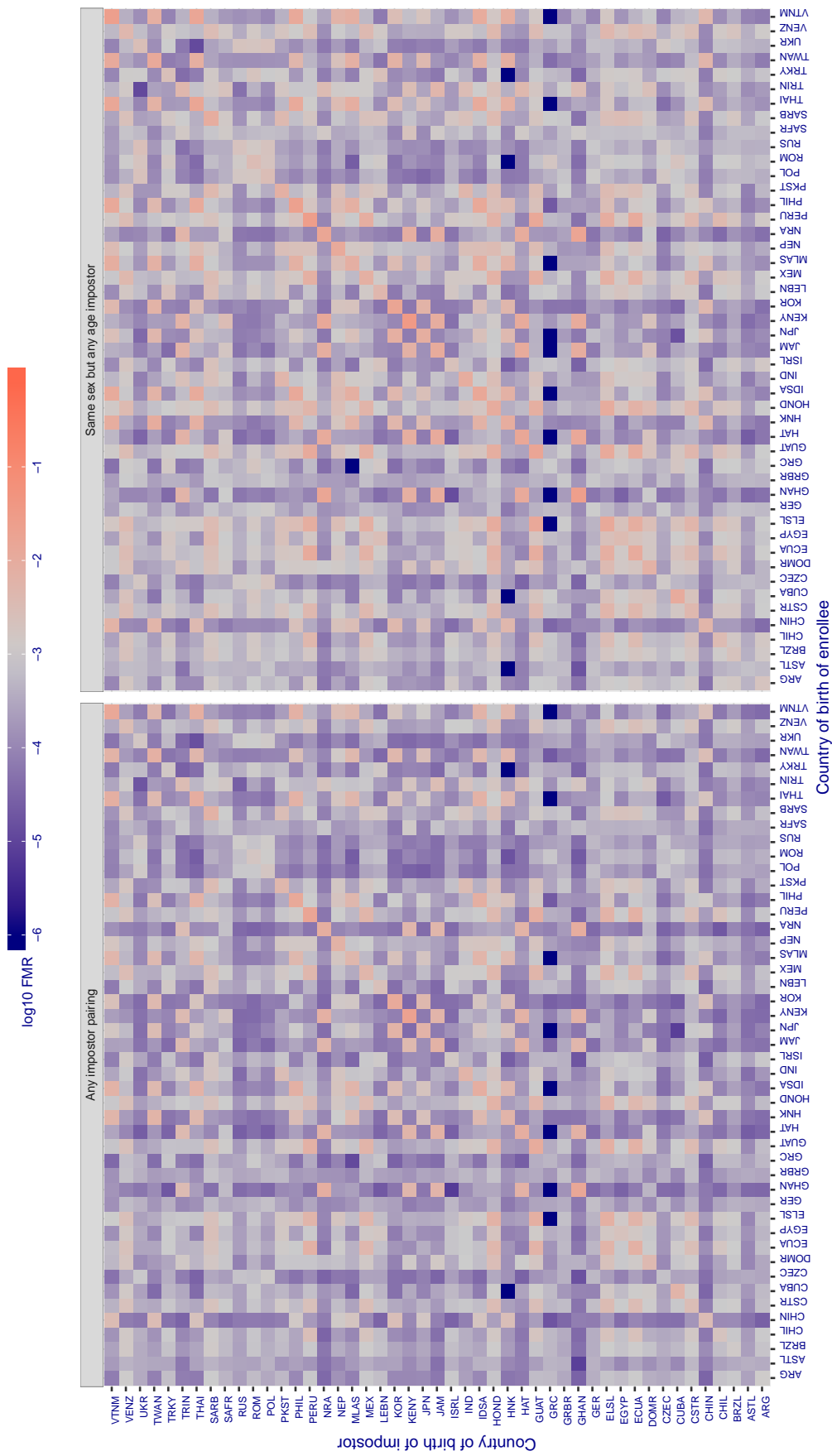


Figure 279: For algorithm remarkai-001 operating on visa images, the heatmap shows false match rates observed over impostor comparisons of faces from different individuals who were born in the given country pair. False matches are counted against a recognition threshold fixed globally to give the target FMR in the plot title, computed over all on the order of 10^{10} impostor comparisons. If text appears in each box it give the same quantity as that coded by the color. Grey indicates FMR is at the intended FMR target level. Light red colors present a security vulnerability to, for example, a passport gate. Each +1 increase in \log_{10} FMR corresponds to a factor of 10 increase in FMR. The matrix is not quite symmetric because images in the enrollment and verification sets are different.

Cross country FMR at threshold $T = 0.609$ for algorithm safe_001, giving $FMR(T) = 0.001$ globally.

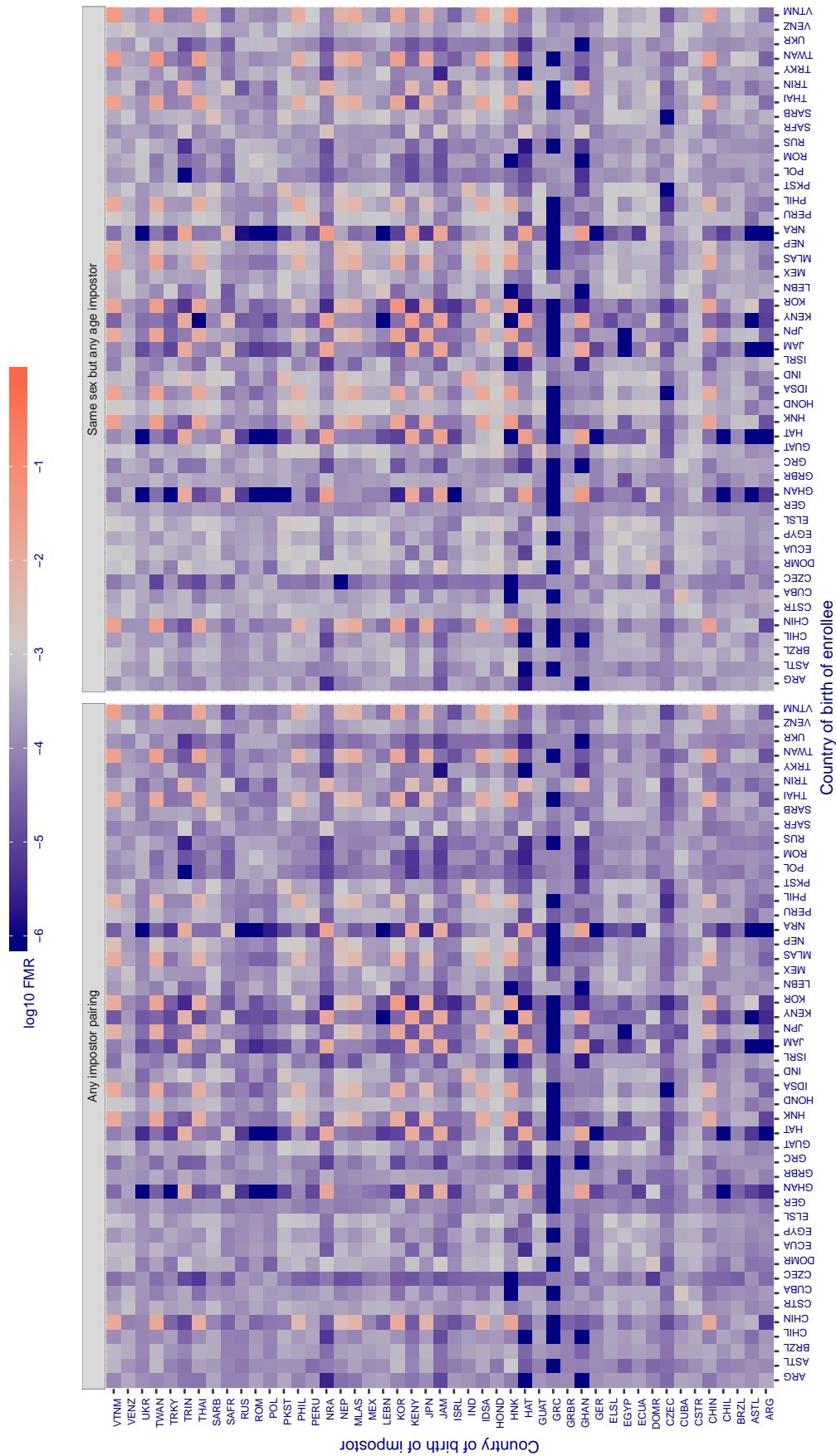


Figure 280: For algorithm safe-001 operating on visa images, the heatmap shows false match rates observed over impostor comparisons of faces from different individuals who were born in the given country pair. False matches are counted against a recognition threshold fixed globally to give the target FMR in the plot title, computed over all on the order of 10^{10} impostor comparisons. If text appears in each box it give the same quantity as that coded by the color. Grey indicates FMR is at the intended FMR target level. Light red colors present a security vulnerability to, for example, a passport gate. Each +1 increase in \log_{10} FMR corresponds to a factor of 10 increase in FMR. The matrix is not quite symmetric because images in the enrollment and verification sets are different.

Cross country FMR at threshold $T = 0.295$ for algorithm safe_002, giving $FMR(T) = 0.001$ globally.

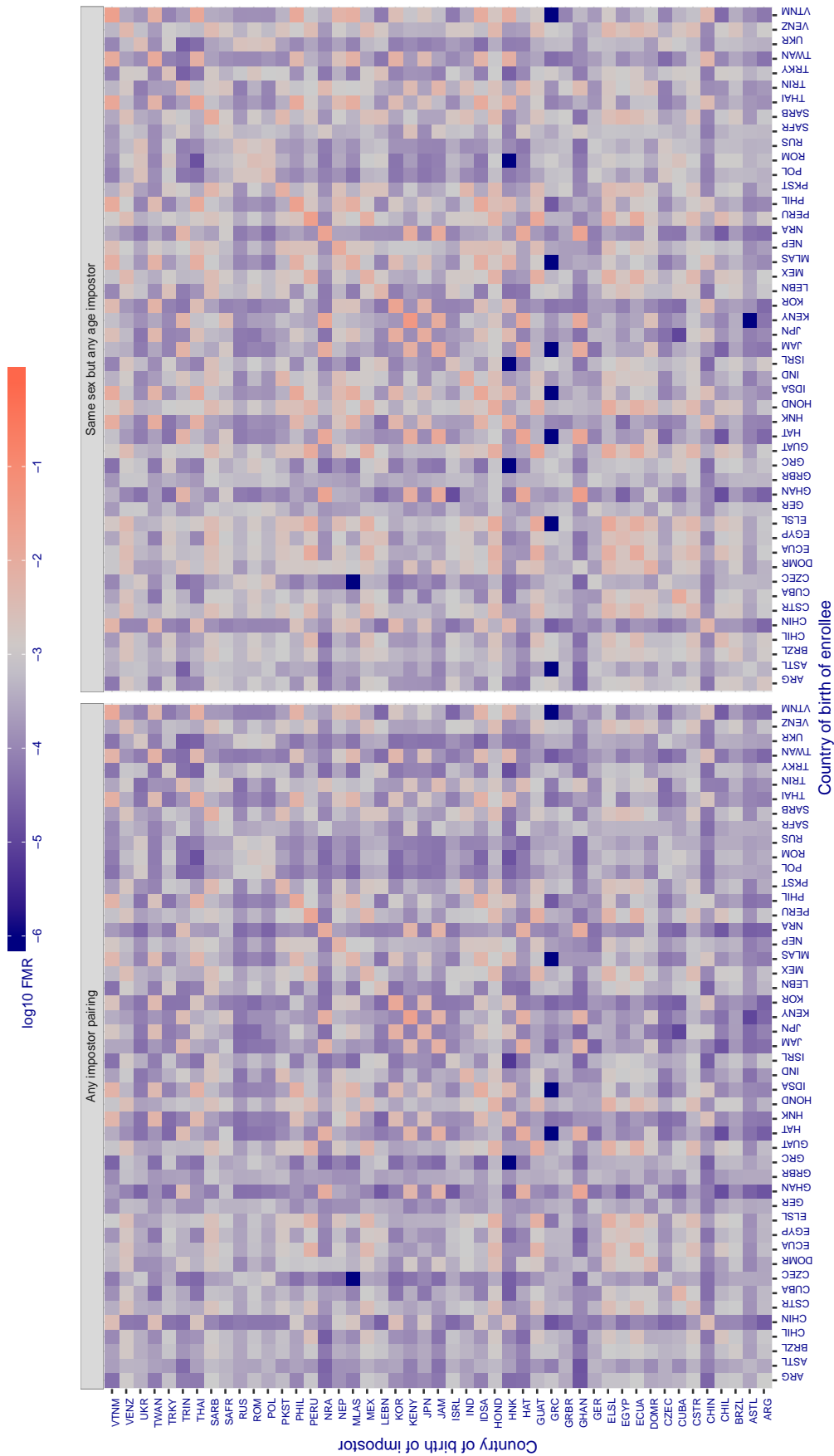


Figure 281: For algorithm safe-002 operating on visa images, the heatmap shows false match rates observed over impostor comparisons of faces from different individuals who were born in the given country pair. False matches are counted against a recognition threshold fixed globally to give the target FMR in the plot title, computed over all on the order of 10^{10} impostor comparisons. If text appears in each box it give the same quantity as that coded by the color. Grey indicates FMR is at the intended FMR target level. Light red colors present a security vulnerability to, for example, a passport gate. Each +1 increase in $\log_{10} FMR$ corresponds to a factor of 10 increase in FMR. The matrix is not quite symmetric because images in the enrollment and verification sets are different.

Cross country FMR at threshold $T = 0.368$ for algorithm `sensetime_001`, giving $FMR(T) = 0.001$ globally.

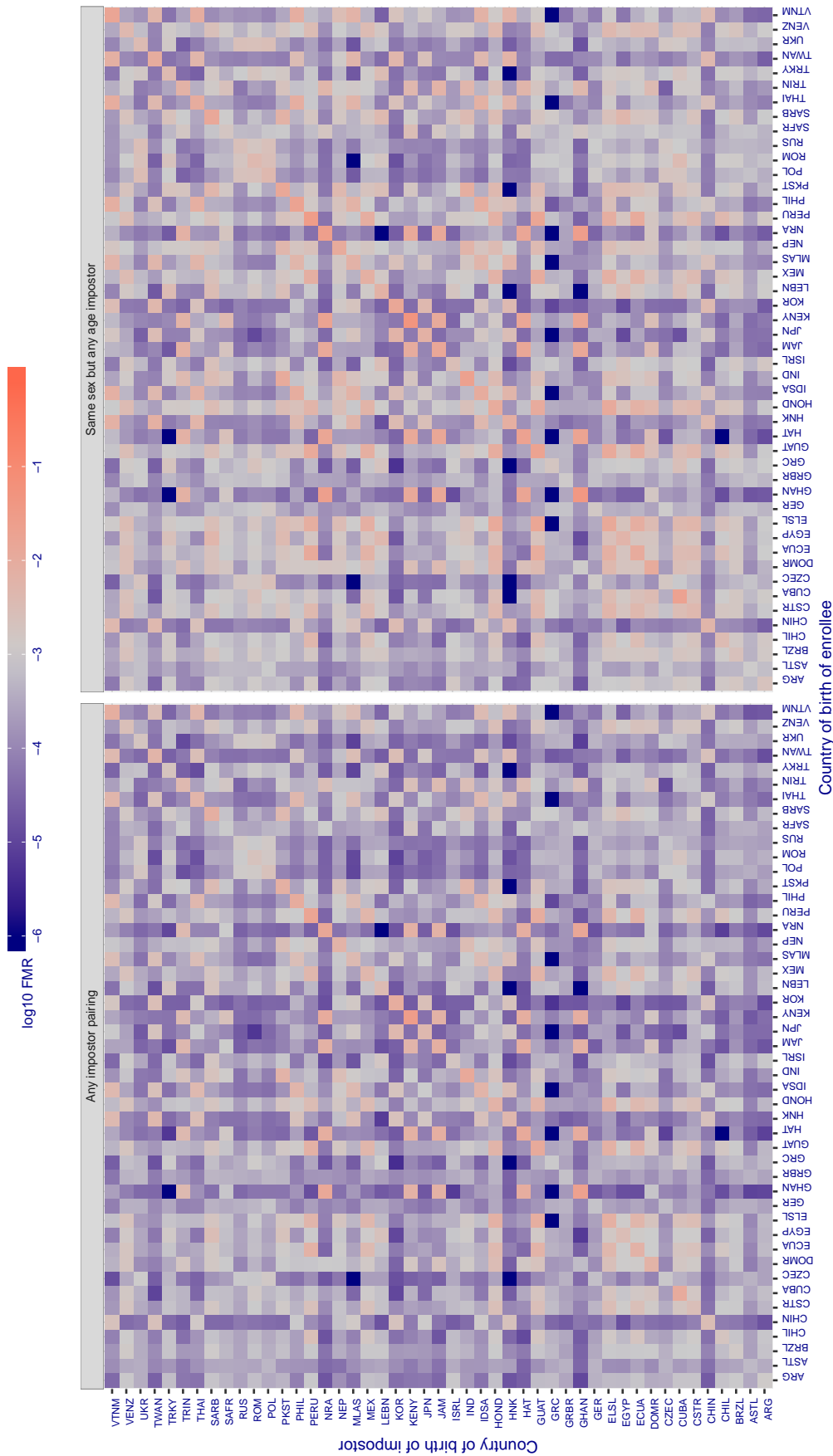


Figure 282: For algorithm `sensetime-001` operating on visa images, the heatmap shows false match rates observed over impostor comparisons of faces from different individuals who were born in the given country pair. False matches are counted against a recognition threshold fixed globally to give the target FMR in the plot title, computed over all on the order of 10^{10} impostor comparisons. If text appears in each box it give the same quantity as that coded by the color. Grey indicates FMR is at the intended FMR target level. Light red colors present a security vulnerability to, for example, a passport gate. Each +1 increase in \log_{10} FMR corresponds to a factor of 10 increase in FMR. The matrix is not quite symmetric because images in the enrollment and verification sets are different.

Cross country FMR at threshold $T = 0.369$ for algorithm `sensetime_002`, giving $FMR(T) = 0.001$ globally.

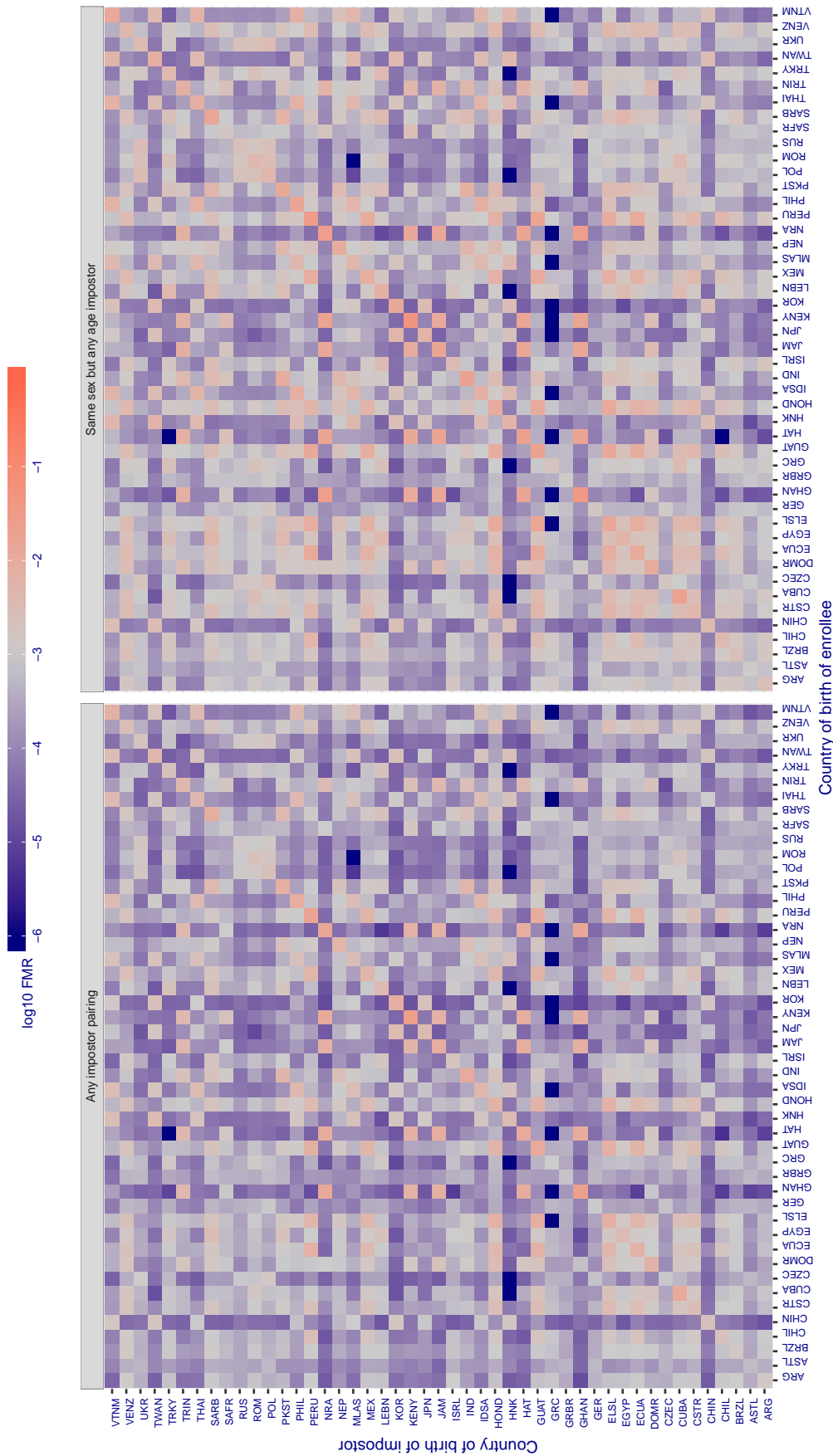


Figure 283: For algorithm `sensetime-002` operating on visa images, the heatmap shows false match rates observed over impostor comparisons of faces from different individuals who were born in the given country pair. False matches are counted against a recognition threshold fixed globally to give the target FMR in the plot title, computed over all on the order of 10^{10} impostor comparisons. If text appears in each box it give the same quantity as that coded by the color. Grey indicates FMR is at the intended FMR target level. Light red colors present a security vulnerability to, for example, a passport gate. Each +1 increase in \log_{10} FMR corresponds to a factor of 10 increase in FMR. The matrix is not quite symmetric because images in the enrollment and verification sets are different.

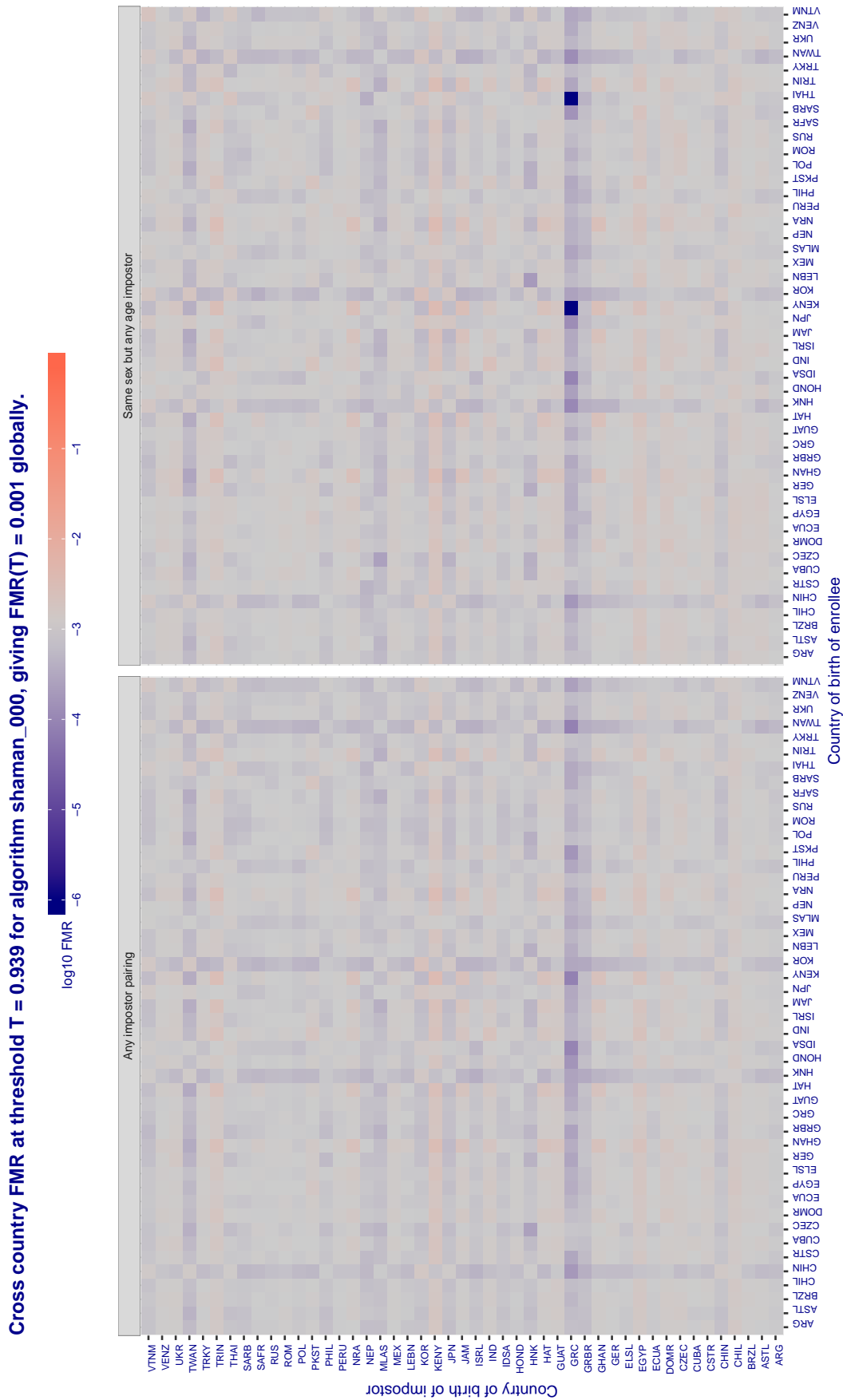


Figure 284: For algorithm shaman-000 operating on visa images, the heatmap shows false match rates observed over impostor comparisons of faces from different individuals who were born in the given country pair. False matches are counted against a recognition threshold fixed globally to give the target FMR in the plot title, computed over all on the order of 10^{10} impostor comparisons. If text appears in each box it give the same quantity as that coded by the color. Grey indicates FMR is at the intended FMR target level. Light red colors present a security vulnerability to, for example, a passport gate. Each +1 increase in \log_{10} FMR corresponds to a factor of 10 increase in FMR. The matrix is not quite symmetric because images in the enrollment and verification sets are different.

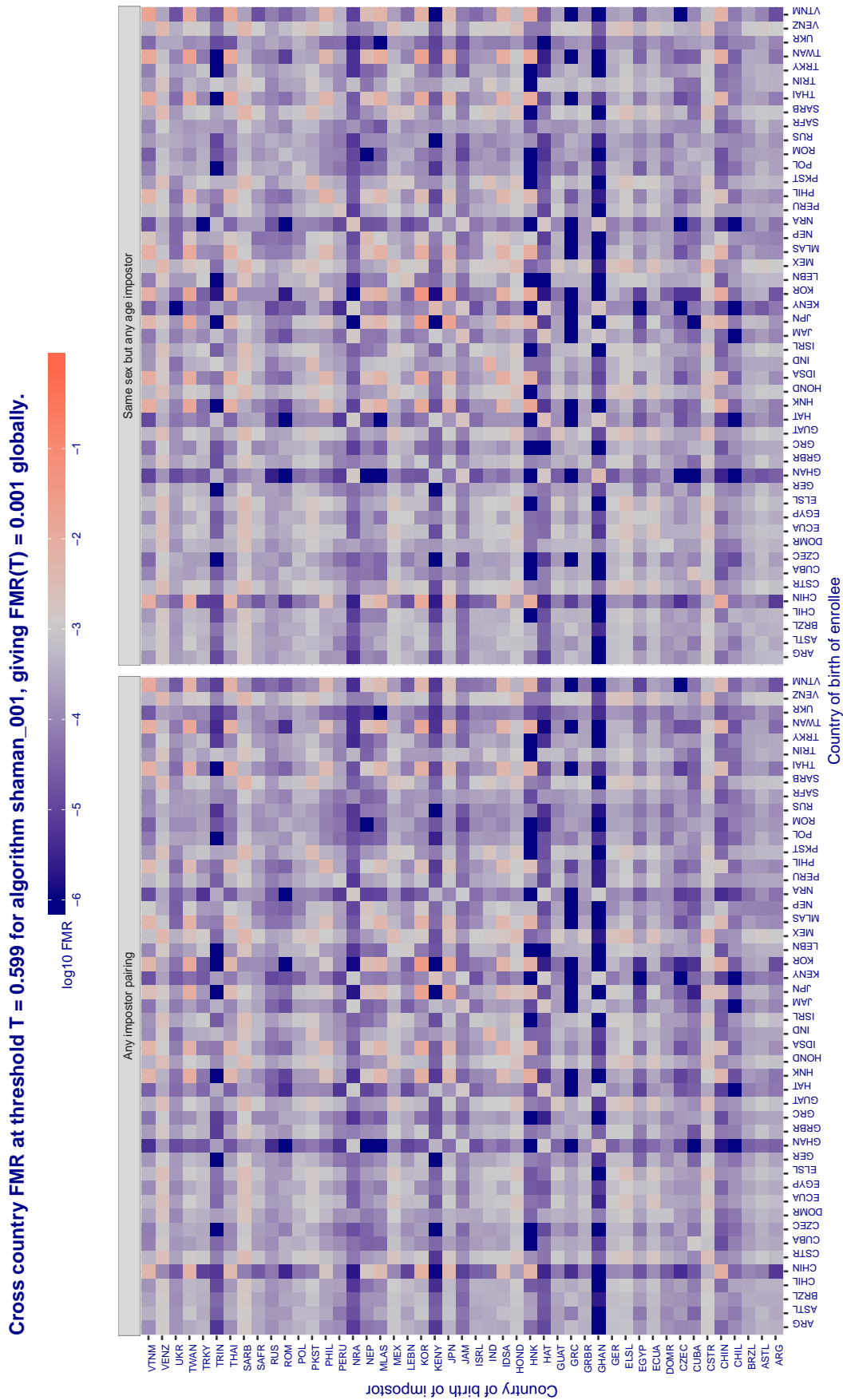


Figure 285: For algorithm shaman-001 operating on visa images, the heatmap shows false match rates observed over impostor comparisons of faces from different individuals who were born in the given country pair. False matches are counted against a recognition threshold fixed globally to give the target FMR in the plot title, computed over all on the order of 10^{10} impostor comparisons. If text appears in each box it give the same quantity as that coded by the color. Grey indicates FMR is at the intended FMR target level. Light red colors present a security vulnerability to, for example, a passport gate. Each +1 increase in $\log_{10} FMR$ corresponds to a factor of 10 increase in FMR. The matrix is not quite symmetric because images in the enrollment and verification sets are different.

Cross country FMR at threshold $T = 0.370$ for algorithm `siat_002`, giving $FMR(T) = 0.001$ globally.

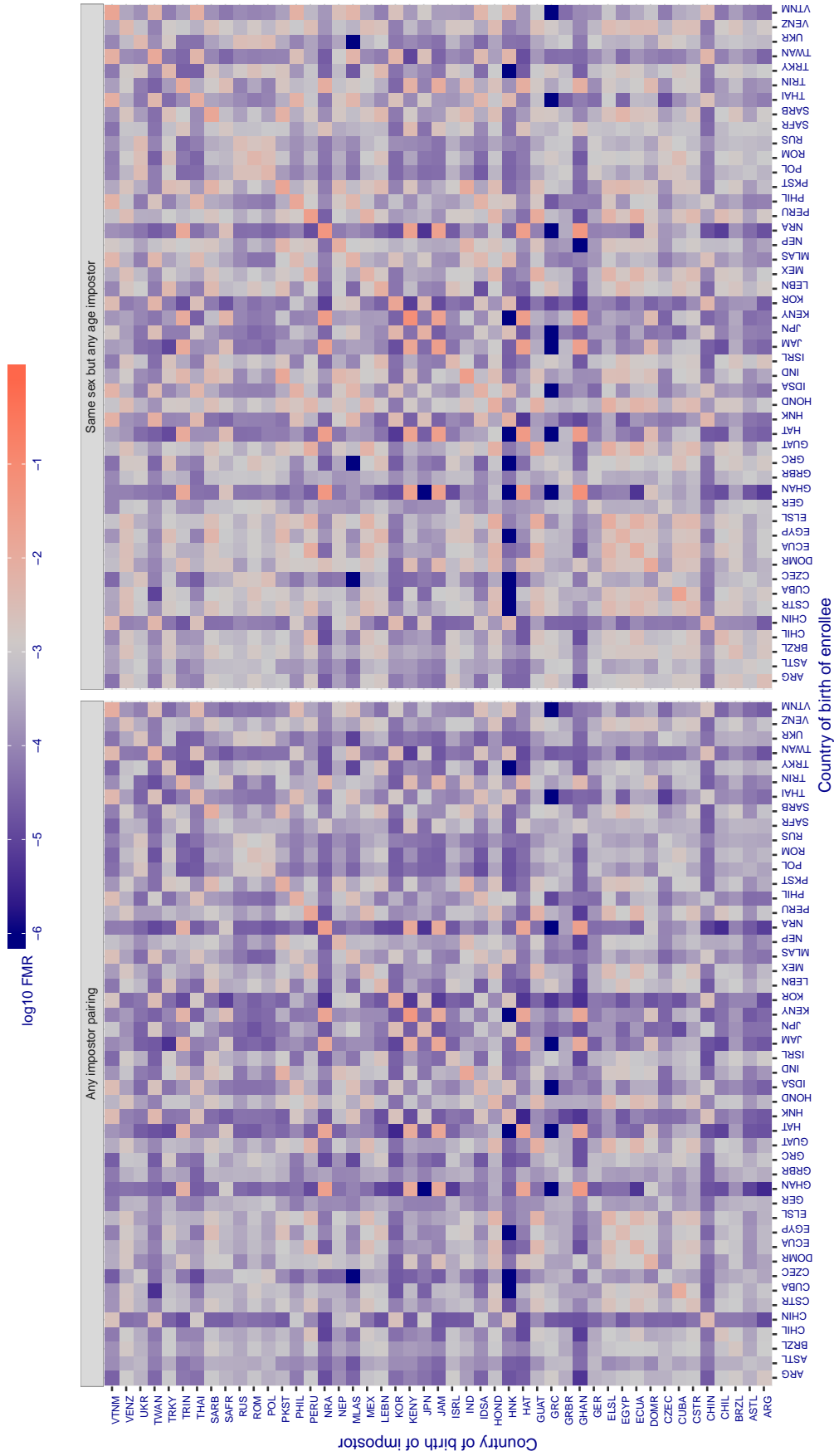


Figure 286: For algorithm `siat-002` operating on visa images, the heatmap shows false match rates observed over impostor comparisons of faces from different individuals who were born in the given country pair. False matches are counted against a recognition threshold fixed globally to give the target FMR in the plot title, computed over all on the order of 10^{10} impostor comparisons. If text appears in each box it give the same quantity as that coded by the color. Grey indicates FMR is at the intended FMR target level. Light red colors present a security vulnerability to, for example, a passport gate. Each +1 increase in \log_{10} FMR corresponds to a factor of 10 increase in FMR. The matrix is not quite symmetric because images in the enrollment and verification sets are different.

Cross country FMR at threshold $T = 0.371$ for algorithm `siat_004`, giving $FMR(T) = 0.001$ globally.

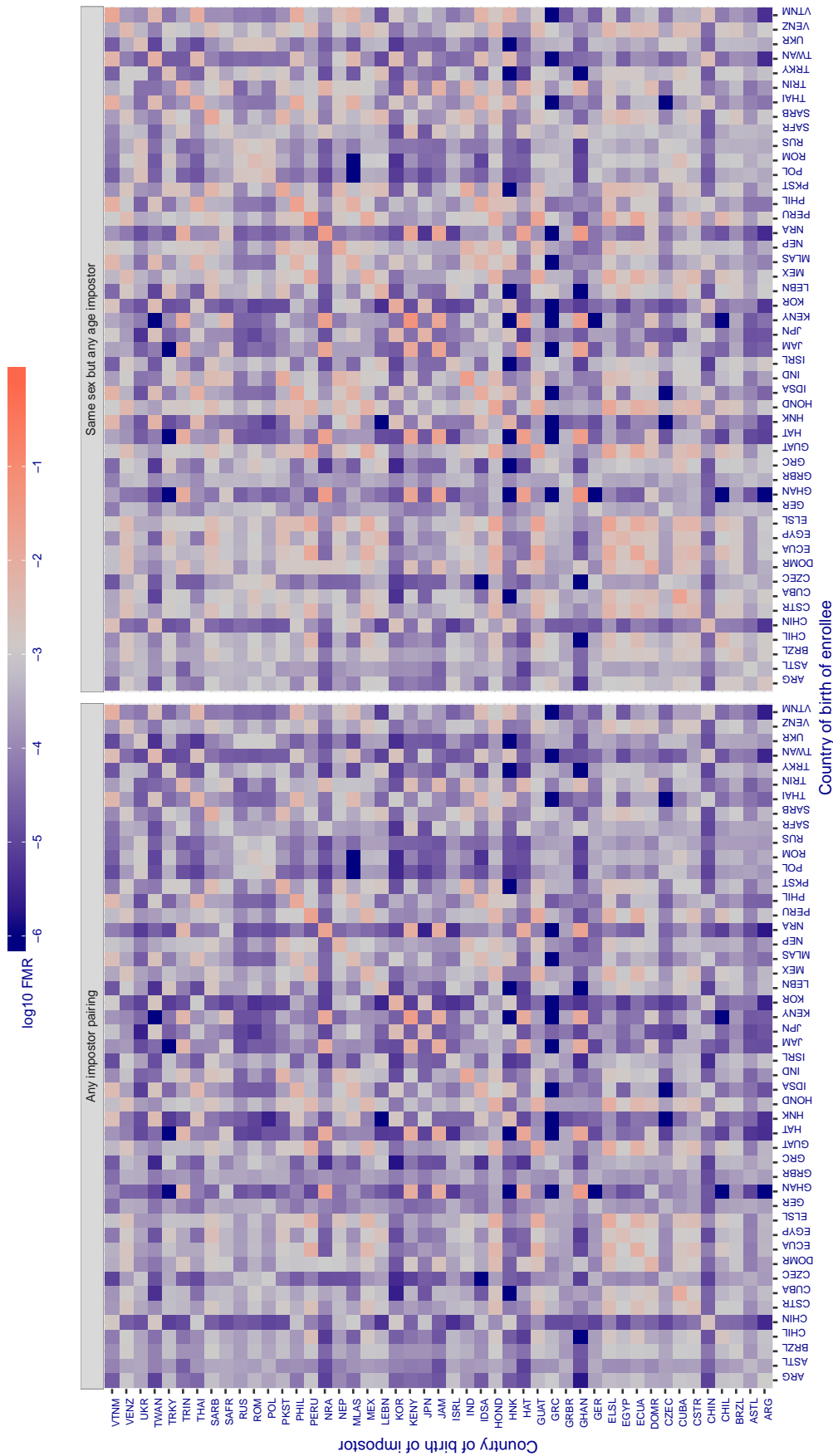


Figure 287: For algorithm `siat-004` operating on visa images, the heatmap shows false match rates observed over impostor comparisons of faces from different individuals who were born in the given country pair. False matches are counted against a recognition threshold fixed globally to give the target FMR in the plot title, computed over all on the order of 10^{10} impostor comparisons. If text appears in each box it give the same quantity as that coded by the color. Grey indicates FMR is at the intended FMR target level. Light red colors present a security vulnerability to, for example, a passport gate. Each $+1$ increase in $\log_{10} FMR$ corresponds to a factor of 10 increase in FMR. The matrix is not quite symmetric because images in the enrollment and verification sets are different.

Cross country FMR at threshold $T = 0.488$ for algorithm `smilart_002`, giving $FMR(T) = 0.001$ globally.

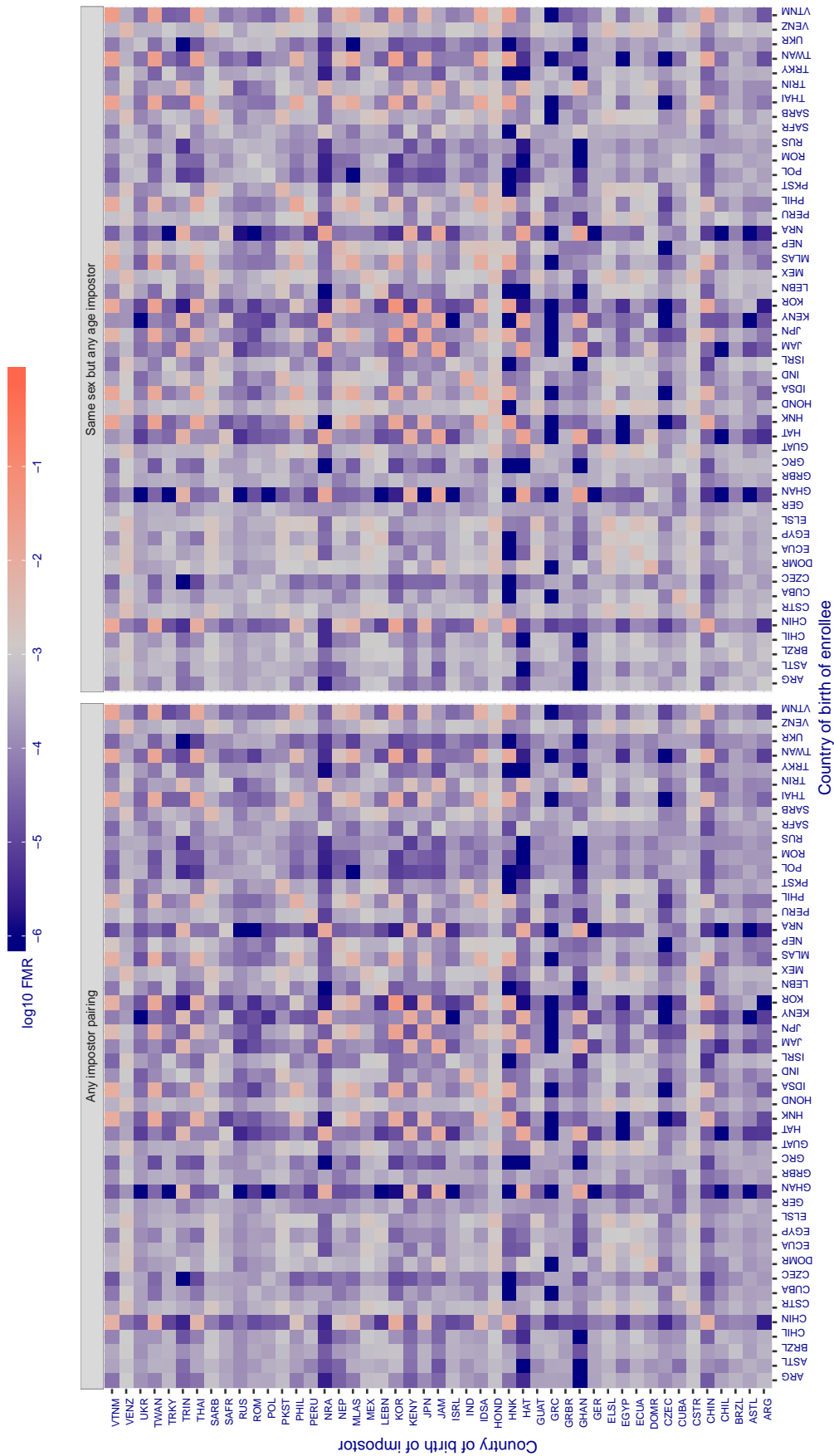


Figure 288: For algorithm `smilart-002` operating on visa images, the heatmap shows false match rates observed over impostor comparisons of faces from different individuals who were born in the given country pair. False matches are counted against a recognition threshold fixed globally to give the target FMR in the plot title, computed over all on the order of 10^{10} impostor comparisons. If text appears in each box it give the same quantity as that coded by the color. Grey indicates FMR is at the intended FMR target level. Light red colors present a security vulnerability to, for example, a passport gate. Each +1 increase in $\log_{10} FMR$ corresponds to a factor of 10 increase in FMR. The matrix is not quite symmetric because images in the enrollment and verification sets are different.

Cross country FMR at threshold $T = 0.388$ for algorithm `smilart_003`, giving $FMR(T) = 0.001$ globally.

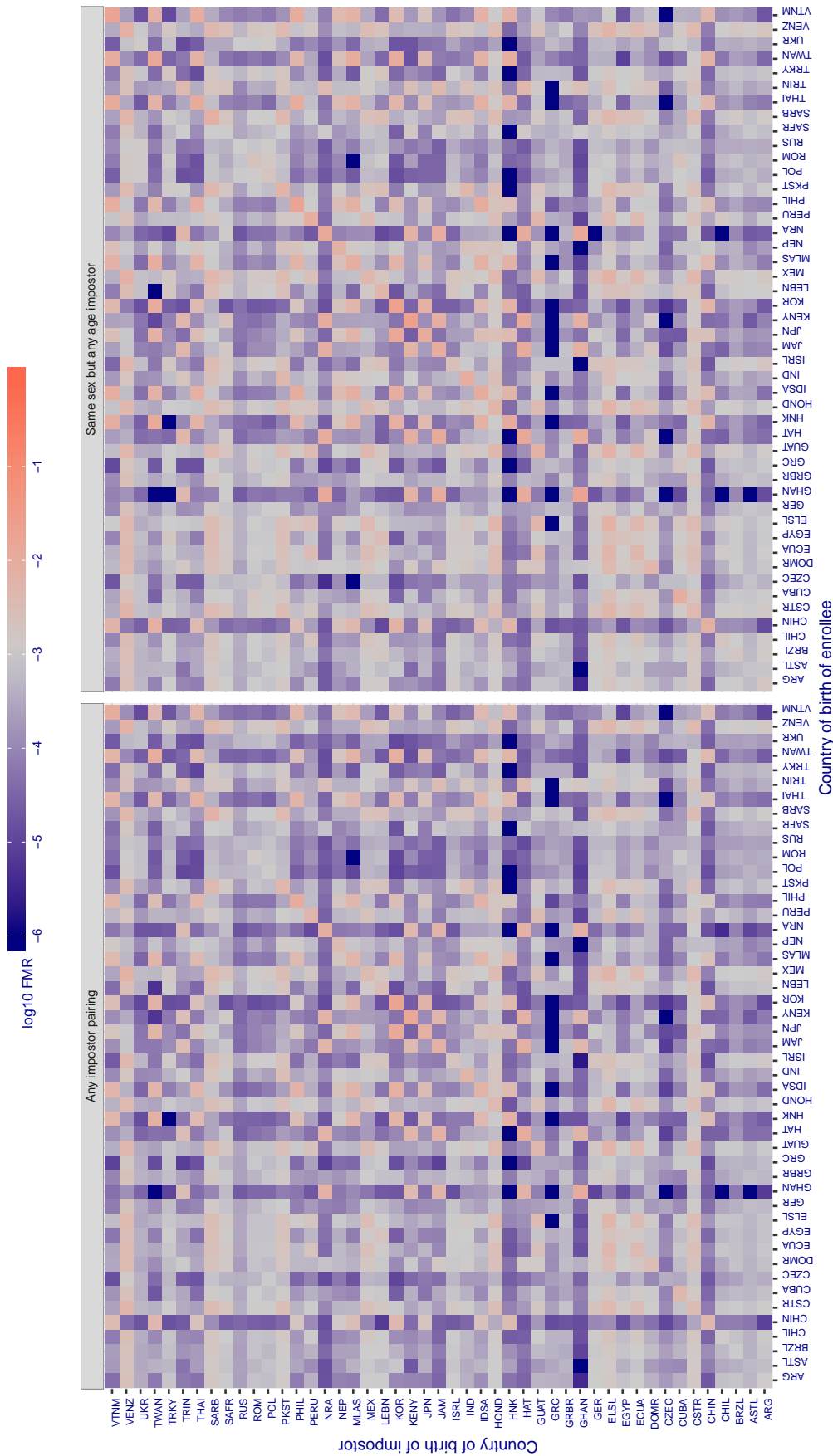


Figure 289: For algorithm `smilart-003` operating on visa images, the heatmap shows false match rates observed over impostor comparisons of faces from different individuals who were born in the given country pair. False matches are counted against a recognition threshold fixed globally to give the target FMR in the plot title, computed over all on the order of 10^{10} impostor comparisons. If text appears in each box it give the same quantity as that coded by the color. Grey indicates FMR is at the intended FMR target level. Light red colors present a security vulnerability to, for example, a passport gate. Each +1 increase in \log_{10} FMR corresponds to a factor of 10 increase in FMR. The matrix is not quite symmetric because images in the enrollment and verification sets are different.

Cross country FMR at threshold $T = 0.528$ for algorithm synthesis_003, giving $FMR(T) = 0.001$ globally.

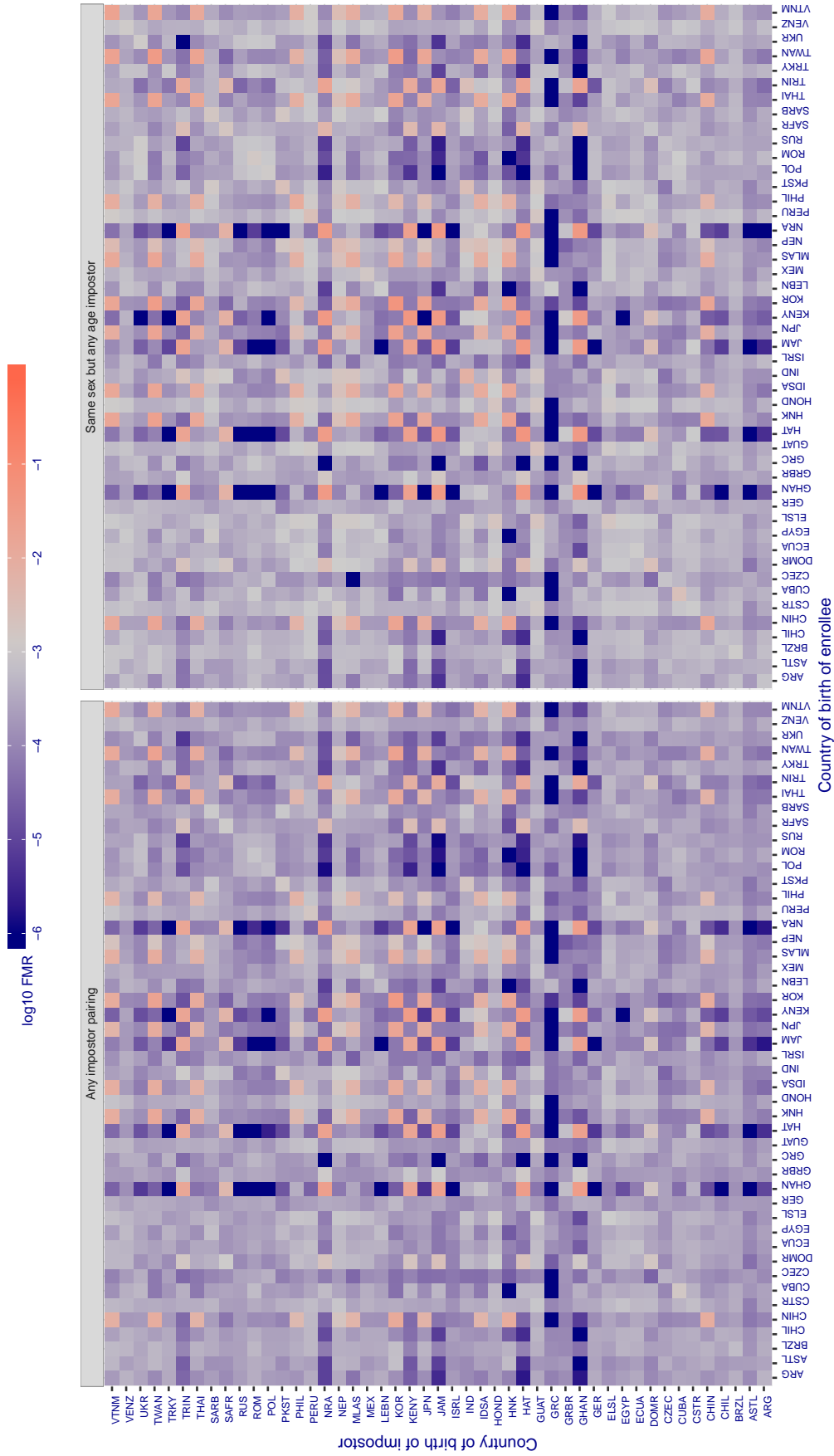


Figure 290: For algorithm synthesis-003 operating on visa images, the heatmap shows false match rates observed over impostor comparisons of faces from different individuals who were born in the given country pair. False matches are counted against a recognition threshold fixed globally to give the target FMR in the plot title, computed over all on the order of 10^{10} impostor comparisons. If text appears in each box it give the same quantity as that coded by the color. Grey indicates FMR is at the intended FMR target level. Light red colors present a security vulnerability to, for example, a passport gate. Each +1 increase in \log_{10} FMR corresponds to a factor of 10 increase in FMR. The matrix is not quite symmetric because images in the enrollment and verification sets are different.

Cross country FMR at threshold $T = 148.095$ for algorithm tech5_001, giving $FMR(T) = 0.001$ globally.

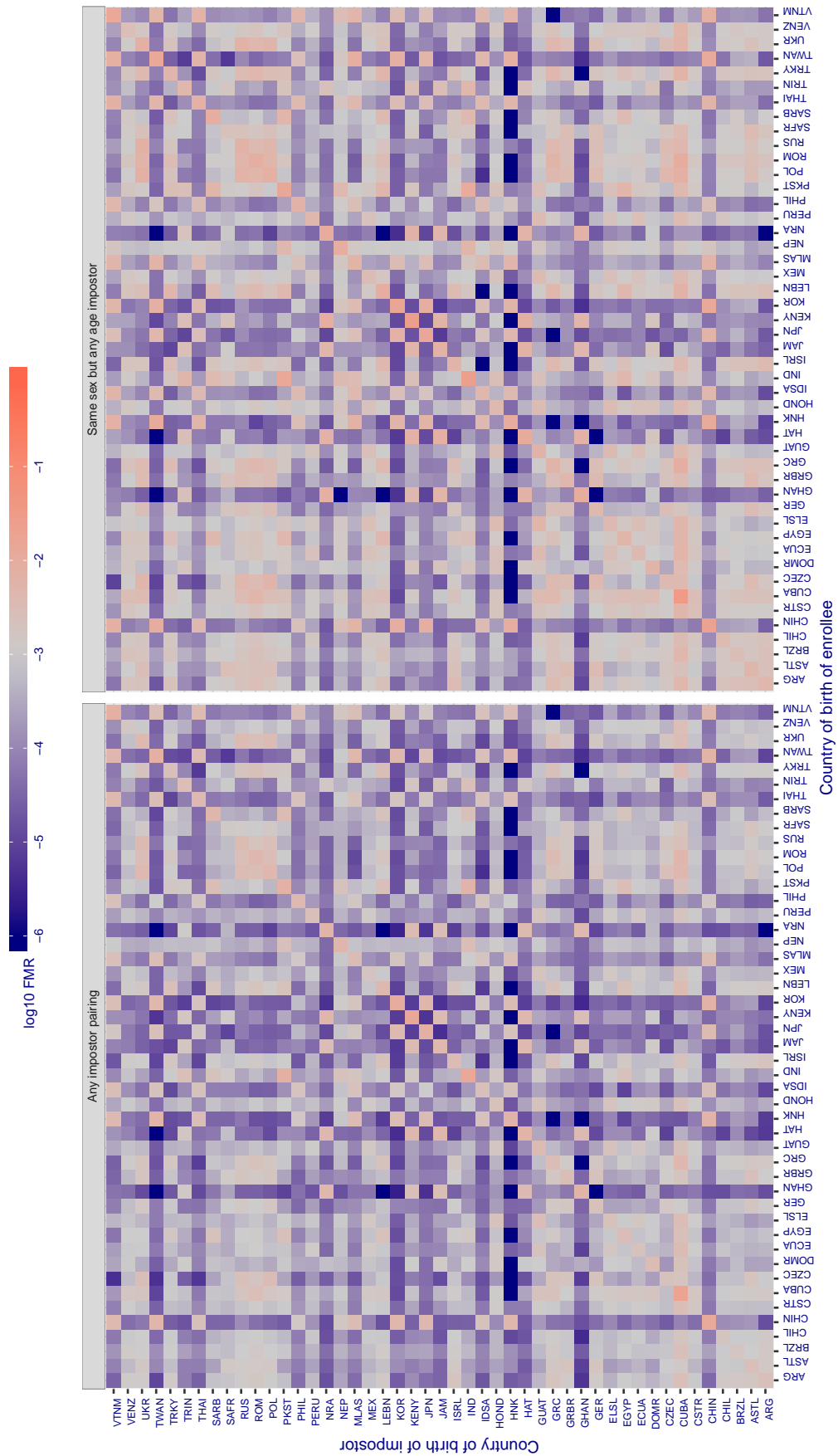


Figure 291: For algorithm tech5-001 operating on visa images, the heatmap shows false match rates observed over impostor comparisons of faces from different individuals who were born in the given country pair. False matches are counted against a recognition threshold fixed globally to give the target FMR in the plot title, computed over all on the order of 10^{10} impostor comparisons. If text appears in each box it give the same quantity as that coded by the color. Grey indicates FMR is at the intended FMR target level. Light red colors present a security vulnerability to, for example, a passport gate. Each +1 increase in \log_{10} FMR corresponds to a factor of 10 increase in FMR. The matrix is not quite symmetric because images in the enrollment and verification sets are different.

Cross country FMR at threshold $T = 147.234$ for algorithm tech5_002, giving $FMR(T) = 0.001$ globally.

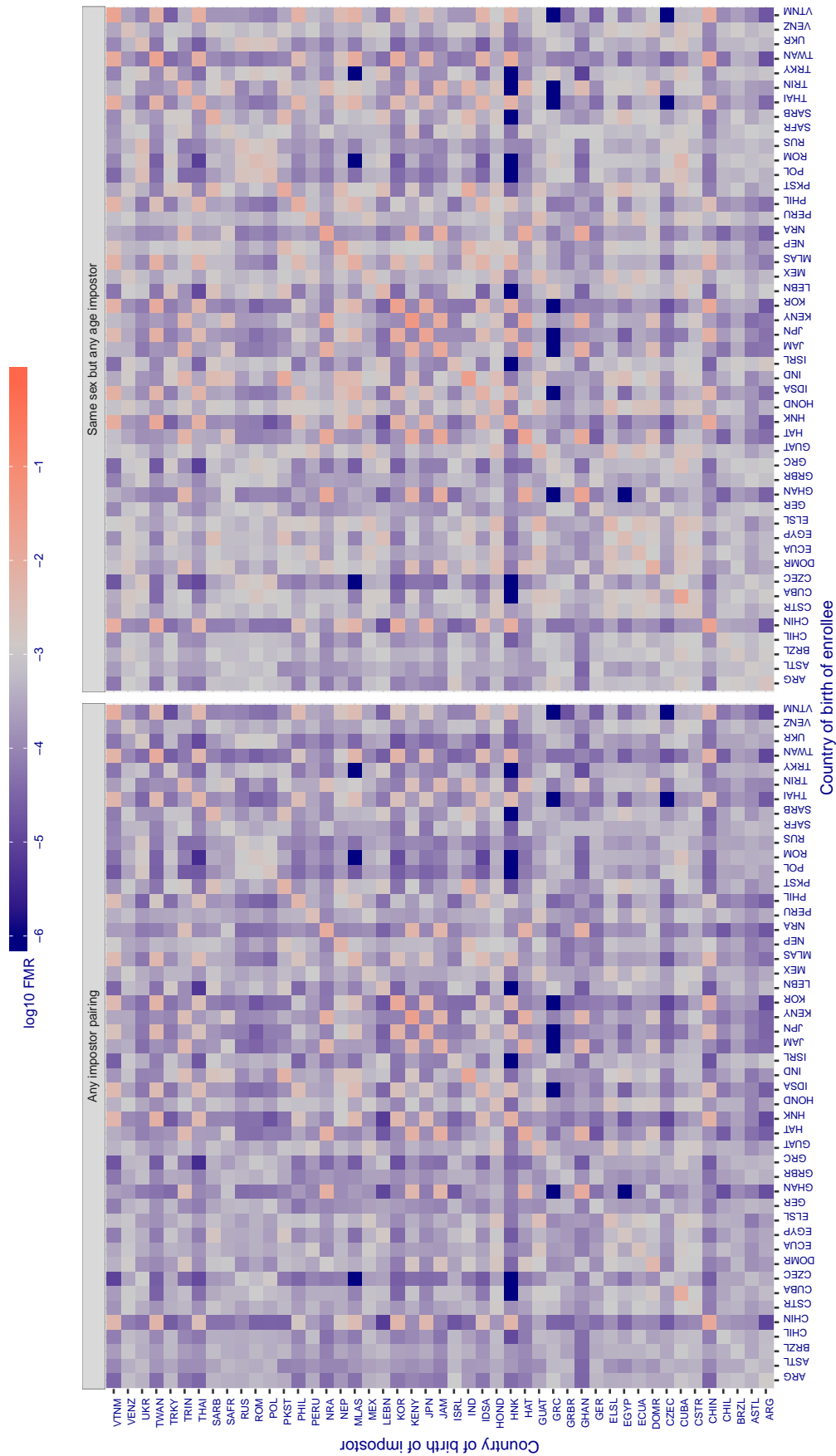


Figure 292: For algorithm tech5-002 operating on visa images, the heatmap shows false match rates observed over impostor comparisons of faces from different individuals who were born in the given country pair. False matches are counted against a recognition threshold fixed globally to give the target FMR in the plot title, computed over all on the order of 10^{10} impostor comparisons. If text appears in each box it give the same quantity as that coded by the color. Grey indicates FMR is at the intended FMR target level. Light red colors present a security vulnerability to, for example, a passport gate. Each +1 increase in \log_{10} FMR corresponds to a factor of 10 increase in FMR. The matrix is not quite symmetric because images in the enrollment and verification sets are different.

Cross country FMR at threshold $T = 0.769$ for algorithm `tevian_003`, giving $FMR(T) = 0.001$ globally.

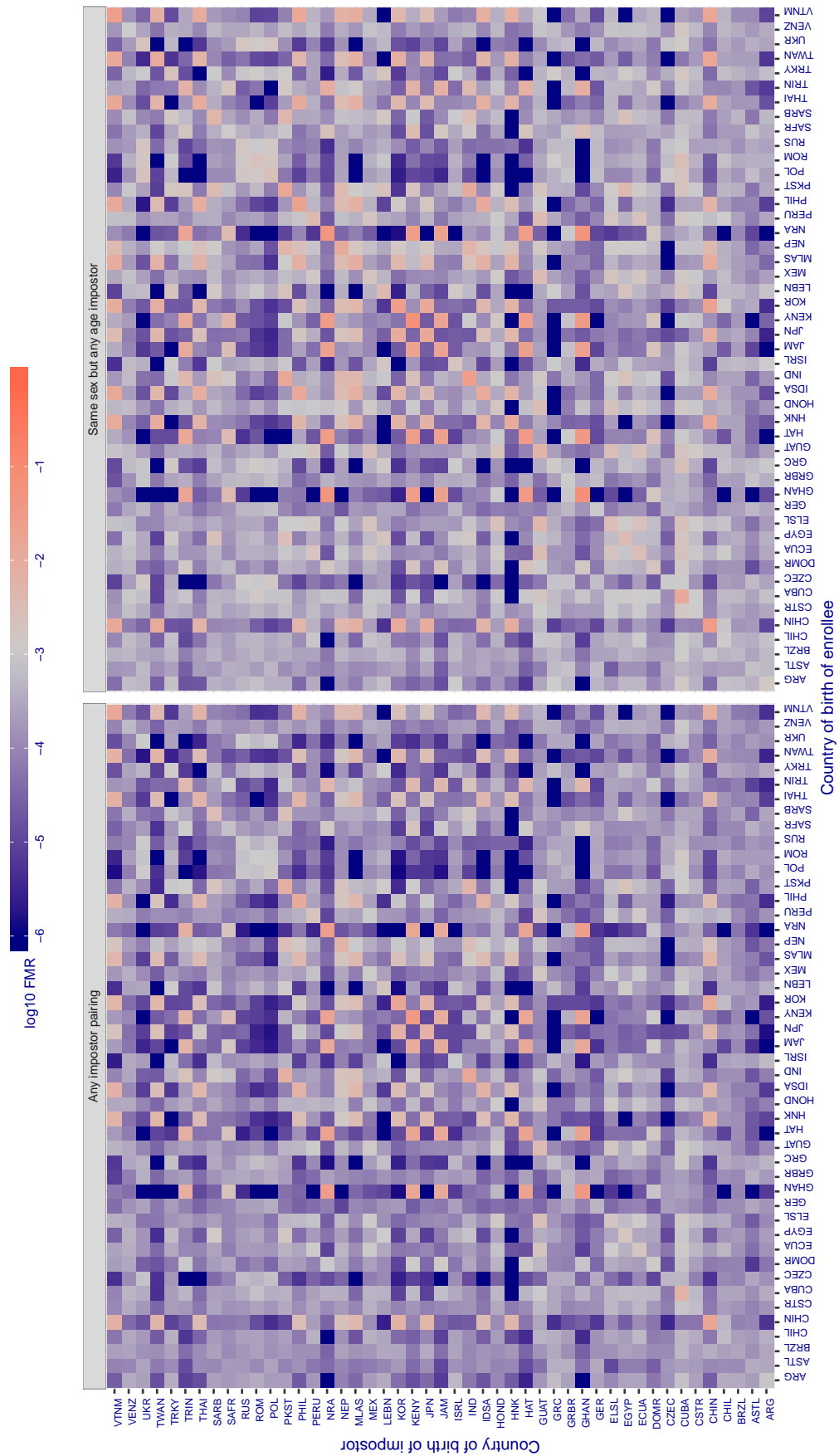


Figure 293: For algorithm `tevian-003` operating on visa images, the heatmap shows false match rates observed over impostor comparisons of faces from different individuals who were born in the given country pair. False matches are counted against a recognition threshold fixed globally to give the target FMR in the plot title, computed over all on the order of 10^{10} impostor comparisons. If text appears in each box it give the same quantity as that coded by the color. Grey indicates FMR is at the intended FMR target level. Light red colors present a security vulnerability to, for example, a passport gate. Each +1 increase in \log_{10} FMR corresponds to a factor of 10 increase in FMR. The matrix is not quite symmetric because images in the enrollment and verification sets are different.

Cross country FMR at threshold $T = 0.769$ for algorithm `tevian_004`, giving $FMR(T) = 0.001$ globally.

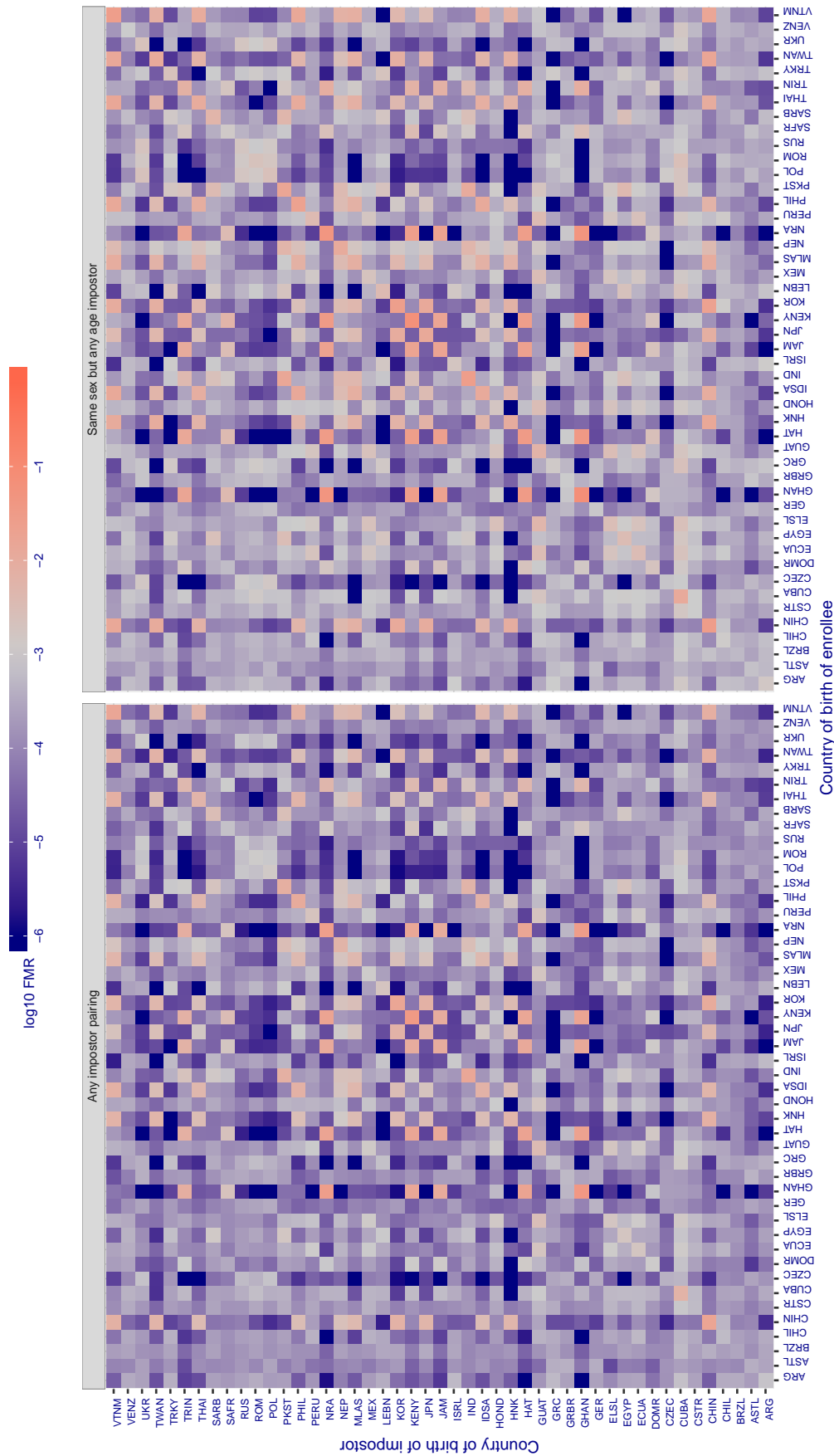


Figure 294: For algorithm `tevian-004` operating on visa images, the heatmap shows false match rates observed over impostor comparisons of faces from different individuals who were born in the given country pair. False matches are counted against a recognition threshold fixed globally to give the target FMR in the plot title, computed over all on the order of 10^{10} impostor comparisons. If text appears in each box it give the same quantity as that coded by the color. Grey indicates FMR is at the intended FMR target level. Light red colors present a security vulnerability to, for example, a passport gate. Each +1 increase in \log_{10} FMR corresponds to a factor of 10 increase in FMR. The matrix is not quite symmetric because images in the enrollment and verification sets are different.

Cross country FMR at threshold $T = 143.194$ for algorithm tiger_002, giving $FMR(T) = 0.001$ globally.

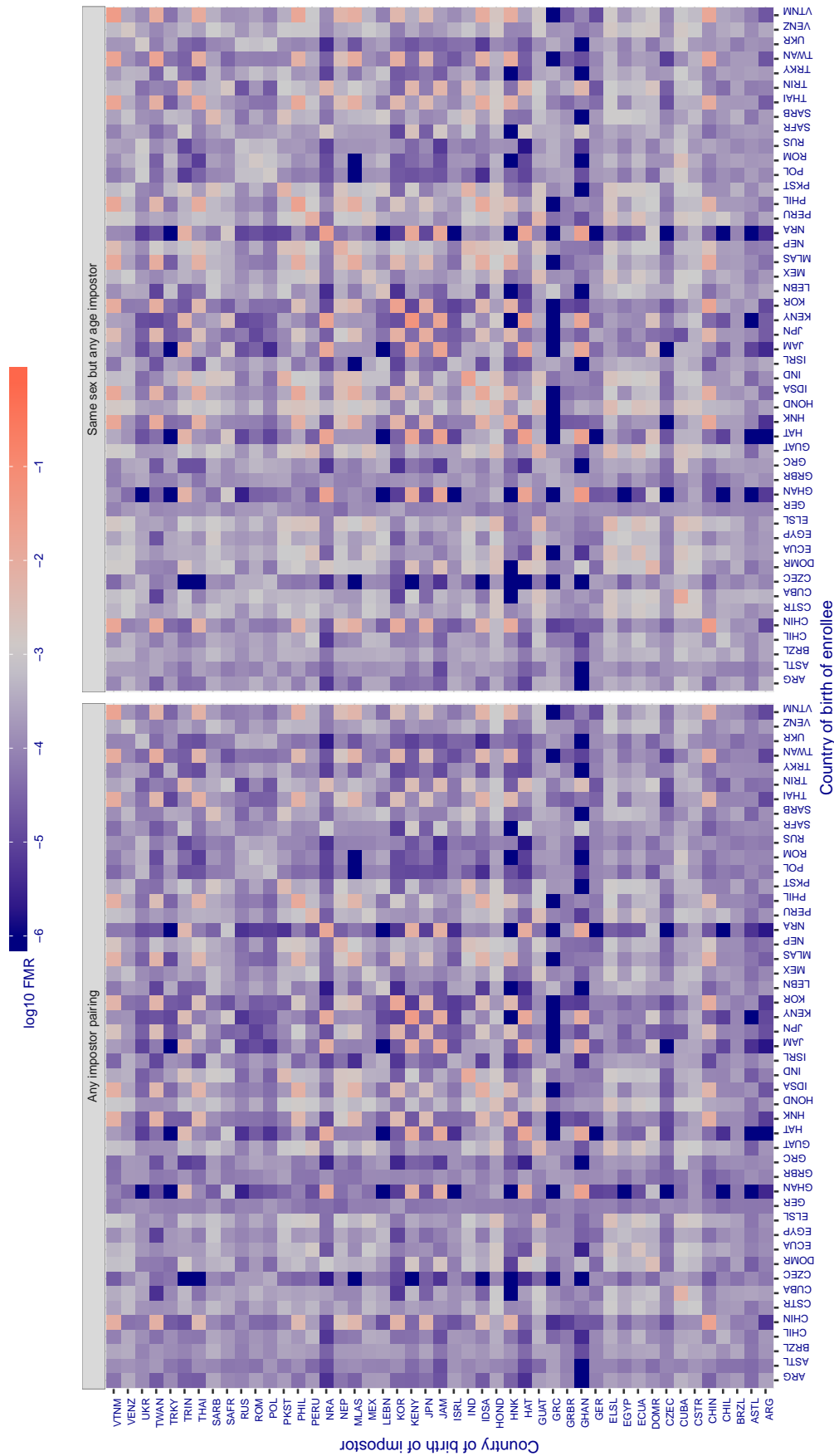


Figure 295: For algorithm tiger-002 operating on visa images, the heatmap shows false match rates observed over impostor comparisons of faces from different individuals who were born in the given country pair. False matches are counted against a recognition threshold fixed globally to give the target FMR in the plot title, computed over all on the order of 10^{10} impostor comparisons. If text appears in each box it give the same quantity as that coded by the color. Grey indicates FMR is at the intended FMR target level. Light red colors present a security vulnerability to, for example, a passport gate. Each +1 increase in \log_{10} FMR corresponds to a factor of 10 increase in FMR. The matrix is not quite symmetric because images in the enrollment and verification sets are different.

Cross country FMR at threshold $T = 139.101$ for algorithm tiger_003, giving $FMR(T) = 0.001$ globally.

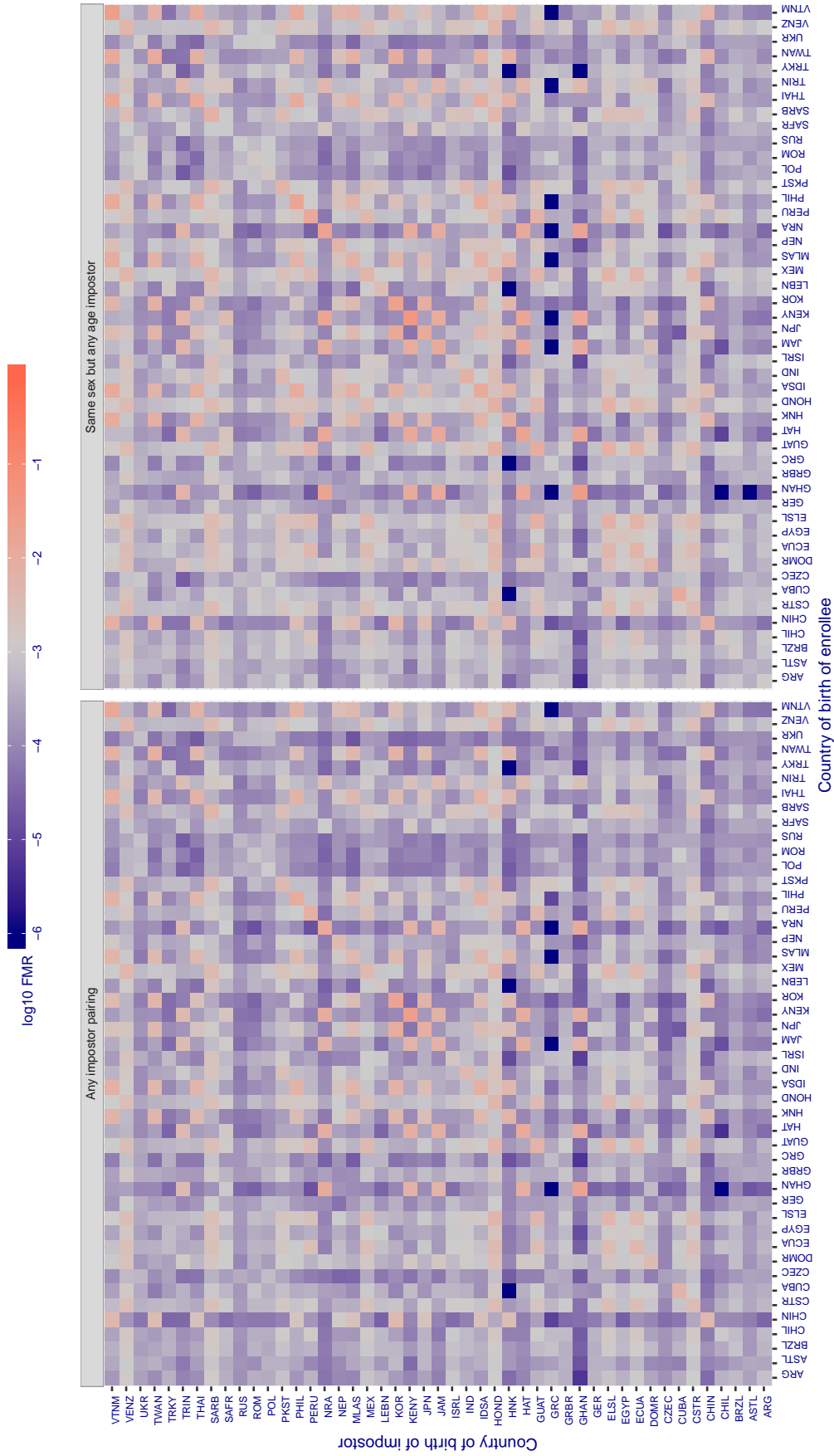


Figure 296: For algorithm tiger-003 operating on visa images, the heatmap shows false match rates observed over impostor comparisons of faces from different individuals who were born in the given country pair. False matches are counted against a recognition threshold fixed globally to give the target FMR in the plot title, computed over all on the order of 10^{10} impostor comparisons. If text appears in each box it give the same quantity as that coded by the color. Grey indicates FMR is at the intended FMR target level. Light red colors present a security vulnerability to, for example, a passport gate. Each +1 increase in \log_{10} FMR corresponds to a factor of 10 increase in FMR. The matrix is not quite symmetric because images in the enrollment and verification sets are different.

Cross country FMR at threshold $T = 0.599$ for algorithm toshiba_002, giving $FMR(T) = 0.001$ globally.

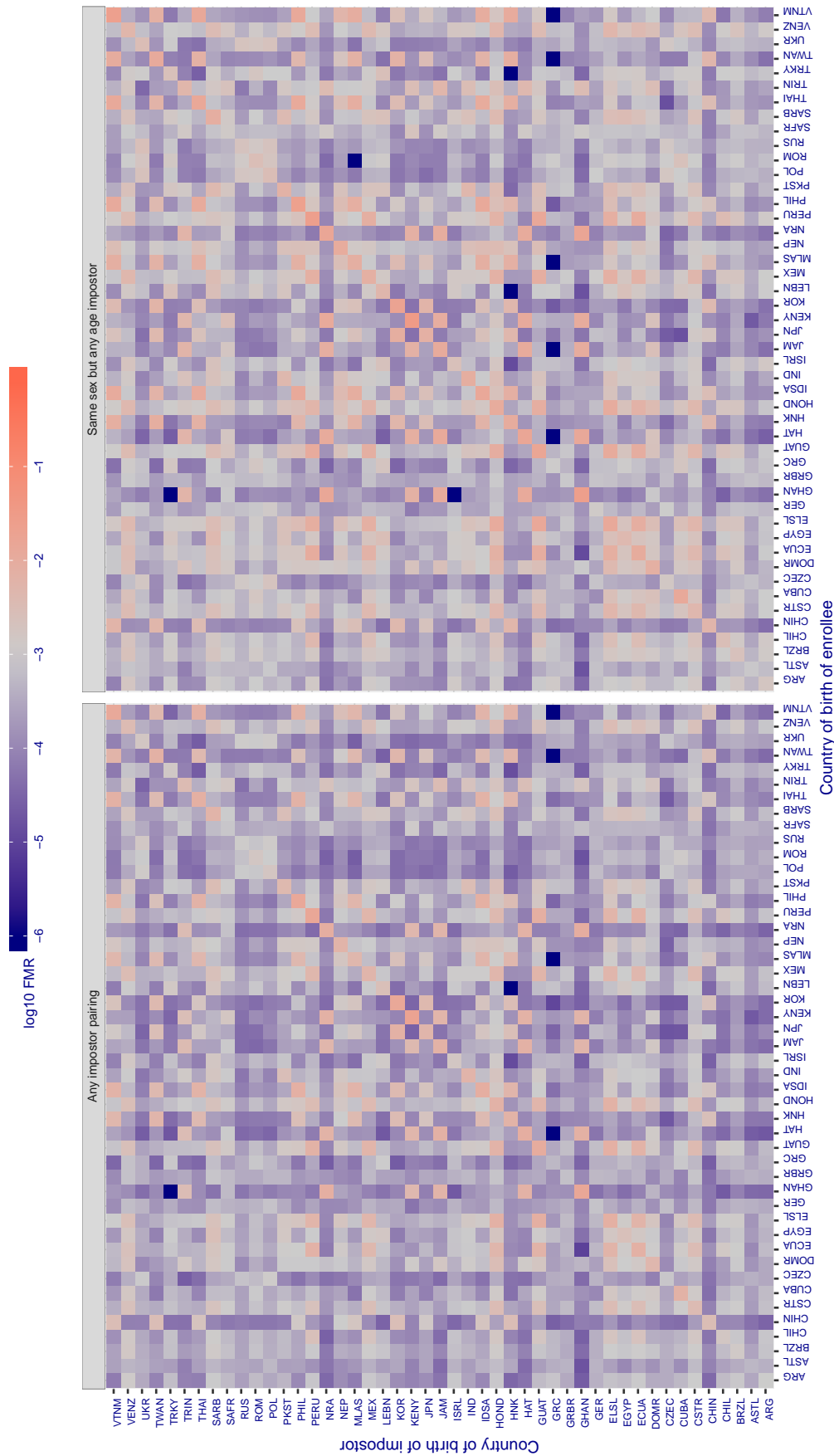


Figure 297: For algorithm toshiba-002 operating on visa images, the heatmap shows false match rates observed over impostor comparisons of faces from different individuals who were born in the given country pair. False matches are counted against a recognition threshold fixed globally to give the target FMR in the plot title, computed over all on the order of 10^{10} impostor comparisons. If text appears in each box it give the same quantity as that coded by the color. Grey indicates FMR is at the intended FMR target level. Light red colors present a security vulnerability to, for example, a passport gate. Each +1 increase in \log_{10} FMR corresponds to a factor of 10 increase in FMR. The matrix is not quite symmetric because images in the enrollment and verification sets are different.

Cross country FMR at threshold $T = 0.596$ for algorithm toshiba_003, giving $FMR(T) = 0.001$ globally.

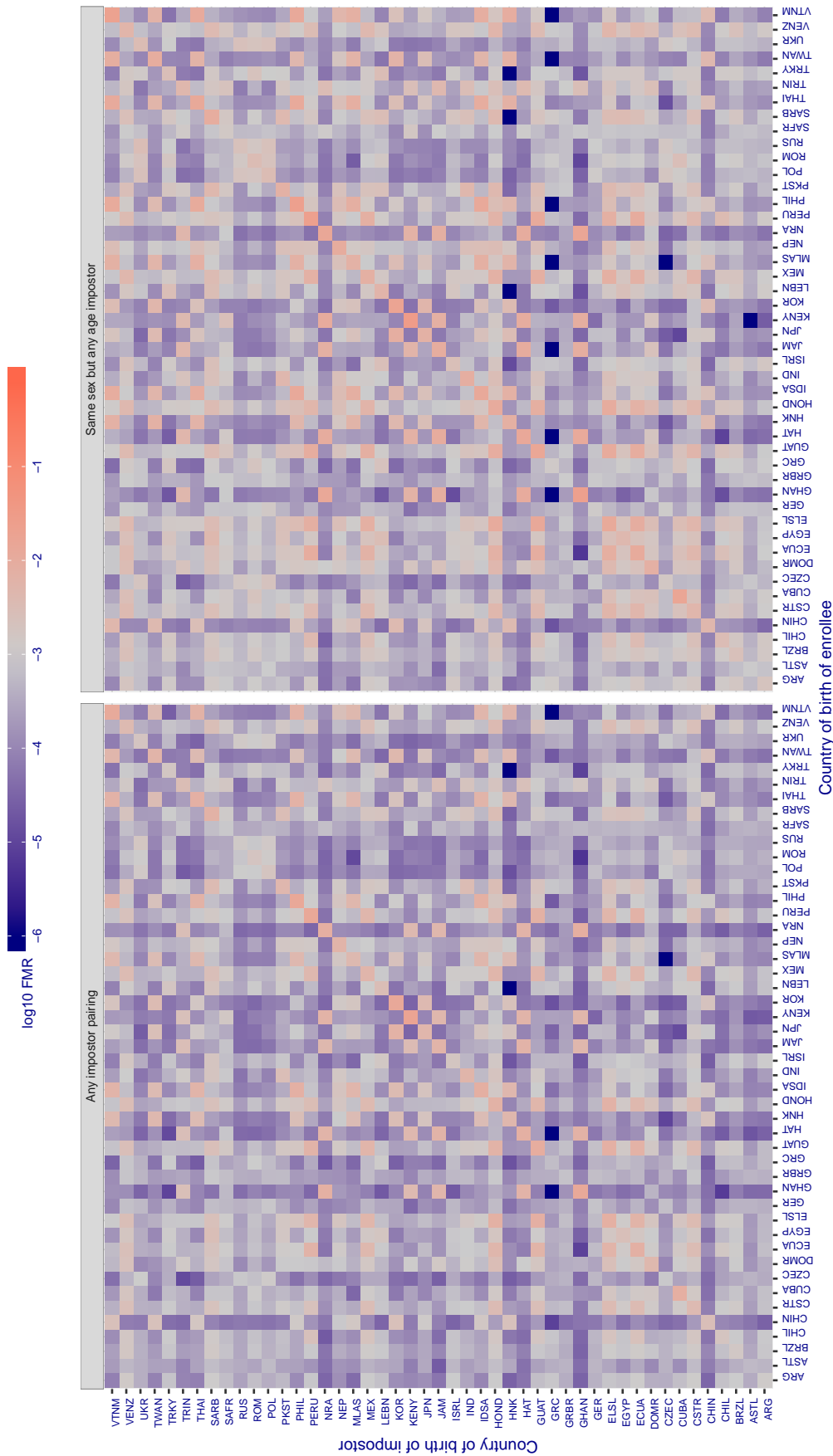


Figure 298: For algorithm toshiba-003 operating on visa images, the heatmap shows false match rates observed over impostor comparisons of faces from different individuals who were born in the given country pair. False matches are counted against a recognition threshold fixed globally to give the target FMR in the plot title, computed over all on the order of 10^{10} impostor comparisons. If text appears in each box it give the same quantity as that coded by the color. Grey indicates FMR is at the intended FMR target level. Light red colors present a security vulnerability to, for example, a passport gate. Each +1 increase in \log_{10} FMR corresponds to a factor of 10 increase in FMR. The matrix is not quite symmetric because images in the enrollment and verification sets are different.

Cross country FMR at threshold $T = 0.310$ for algorithm vcog_002, giving $FMR(T) = 0.001$ globally.

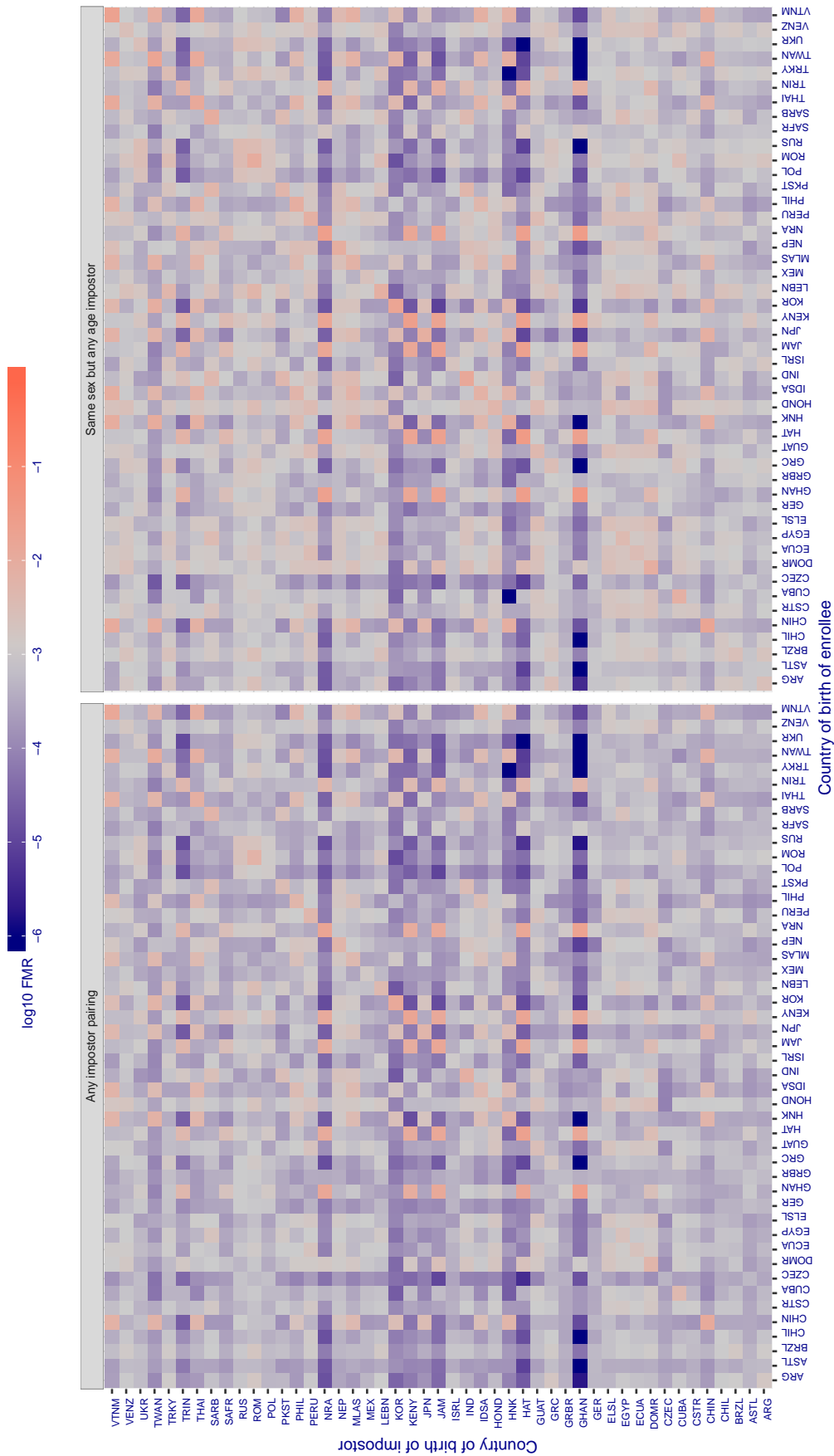


Figure 299: For algorithm vcog-002 operating on visa images, the heatmap shows false match rates observed over impostor comparisons of faces from different individuals who were born in the given country pair. False matches are counted against a recognition threshold fixed globally to give the target FMR in the plot title, computed over all on the order of 10^{10} impostor comparisons. If text appears in each box it give the same quantity as that coded by the color. Grey indicates FMR is at the intended FMR target level. Light red colors present a security vulnerability to, for example, a passport gate. Each +1 increase in \log_{10} FMR corresponds to a factor of 10 increase in FMR. The matrix is not quite symmetric because images in the enrollment and verification sets are different.

Cross country FMR at threshold $T = 66.962$ for algorithm `vd_001`, giving $FMR(T) = 0.001$ globally.

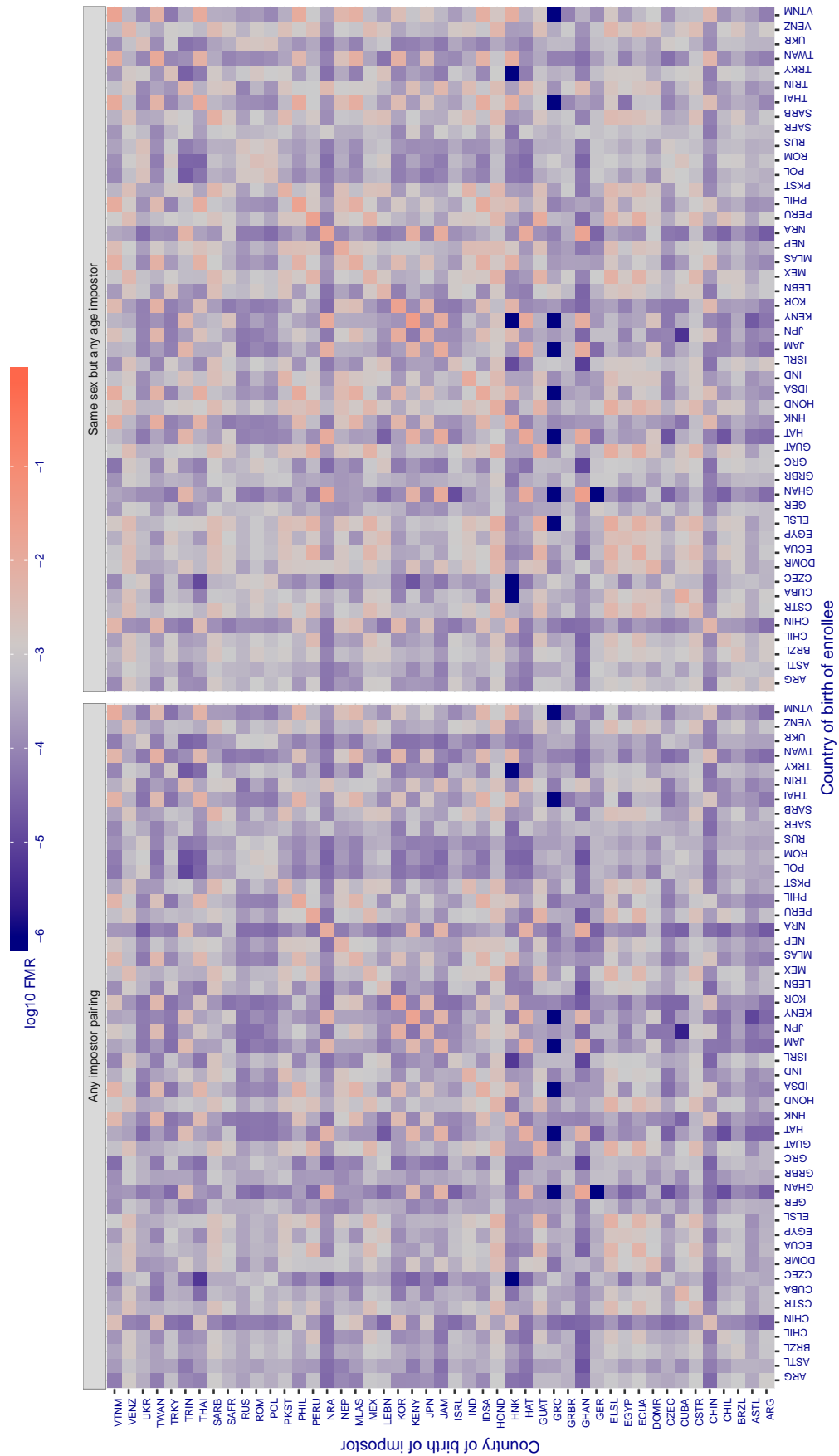


Figure 300: For algorithm `vd-001` operating on visa images, the heatmap shows false match rates observed over impostor comparisons of faces from different individuals who were born in the given country pair. False matches are counted against a recognition threshold fixed globally to give the target FMR in the plot title, computed over all on the order of 10^{10} impostor comparisons. If text appears in each box it give the same quantity as that coded by the color. Grey indicates FMR is at the intended FMR target level. Light red colors present a security vulnerability to, for example, a passport gate. Each $+1$ increase in \log_{10} FMR corresponds to a factor of 10 increase in FMR. The matrix is not quite symmetric because images in the enrollment and verification sets are different.

Cross country FMR at threshold $T = 2.897$ for algorithm veridas_001, giving $FMR(T) = 0.001$ globally.

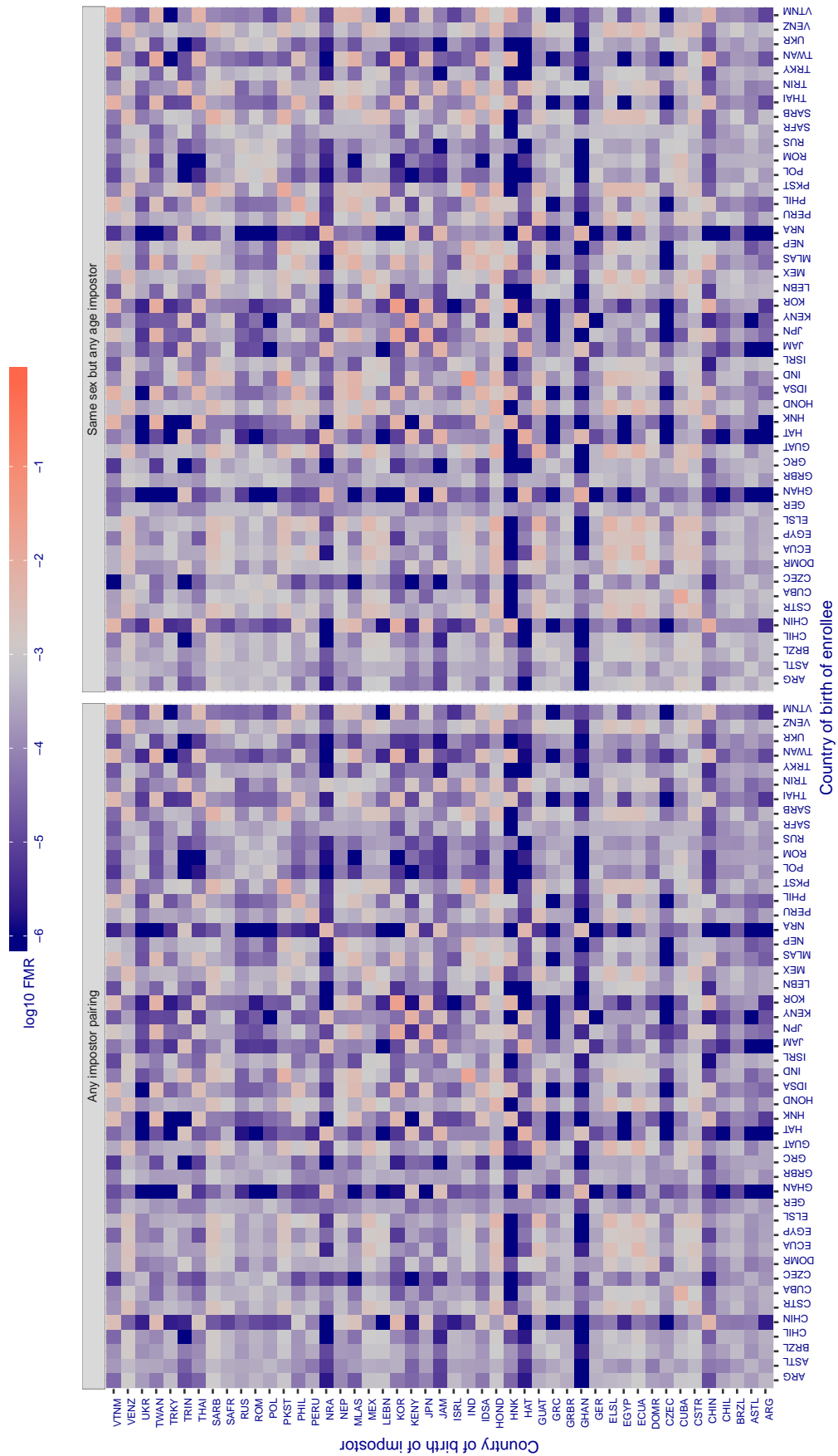


Figure 301: For algorithm veridas-001 operating on visa images, the heatmap shows false match rates observed over impostor comparisons of faces from different individuals who were born in the given country pair. False matches are counted against a recognition threshold fixed globally to give the target FMR in the plot title, computed over all on the order of 10^{10} impostor comparisons. If text appears in each box it give the same quantity as that coded by the color. Grey indicates FMR is at the intended FMR target level. Light red colors present a security vulnerability to, for example, a passport gate. Each +1 increase in $\log_{10} FMR$ corresponds to a factor of 10 increase in FMR. The matrix is not quite symmetric because images in the enrollment and verification sets are different.

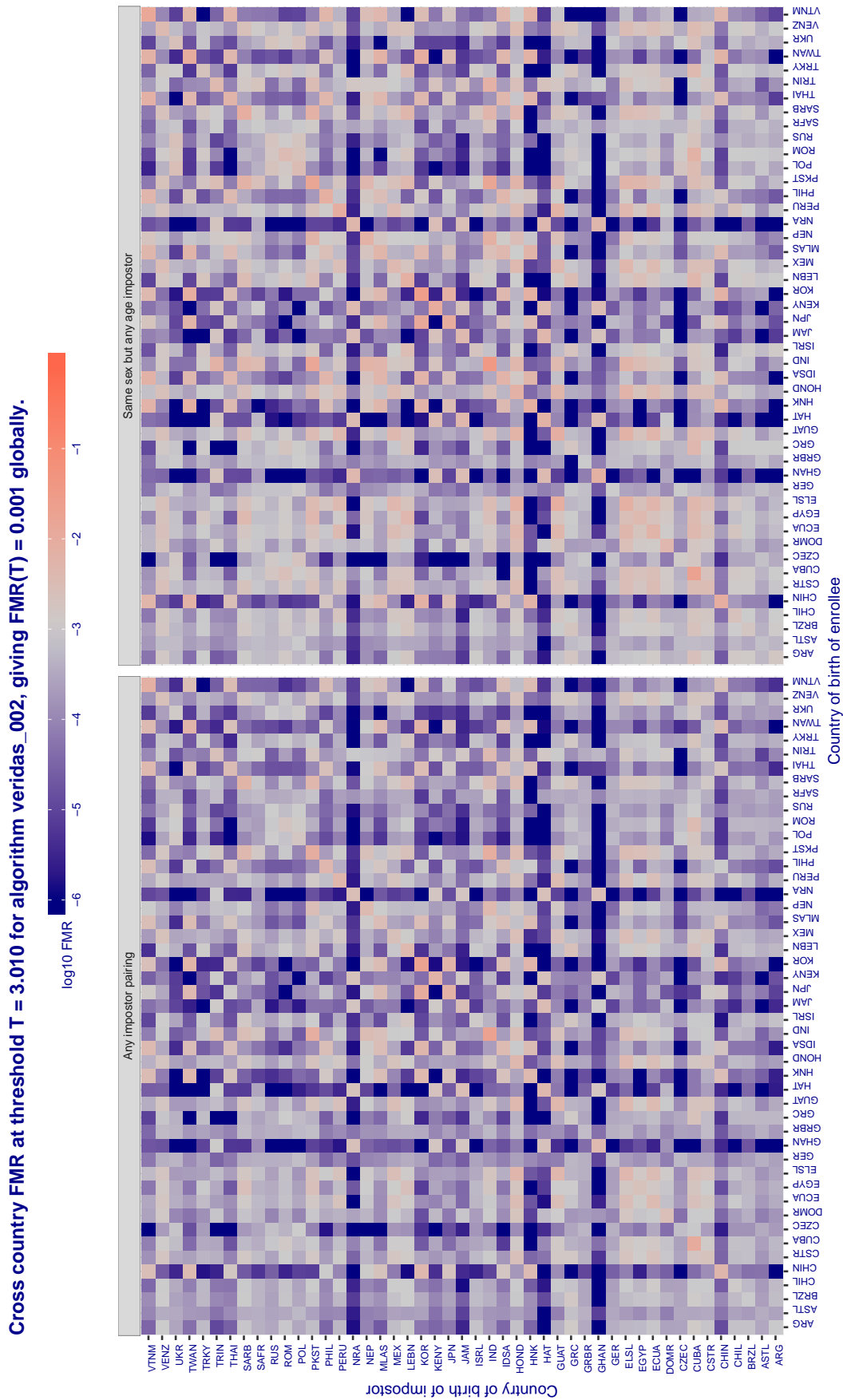


Figure 302: For algorithm veridas-002 operating on visa images, the heatmap shows false match rates observed over impostor comparisons of faces from different individuals who were born in the given country pair. False matches are counted against a recognition threshold fixed globally to give the target FMR in the plot title, computed over all on the order of 10^{10} impostor comparisons. If text appears in each box it give the same quantity as that coded by the color. Grey indicates FMR is at the intended FMR target level. Light red colors present a security vulnerability to, for example, a passport gate. Each +1 increase in \log_{10} FMR corresponds to a factor of 10 increase in FMR. The matrix is not quite symmetric because images in the enrollment and verification sets are different.

Cross country FMR at threshold $T = 2.800$ for algorithm `vigilantsolutions_005`, giving $FMR(T) = 0.001$ globally.

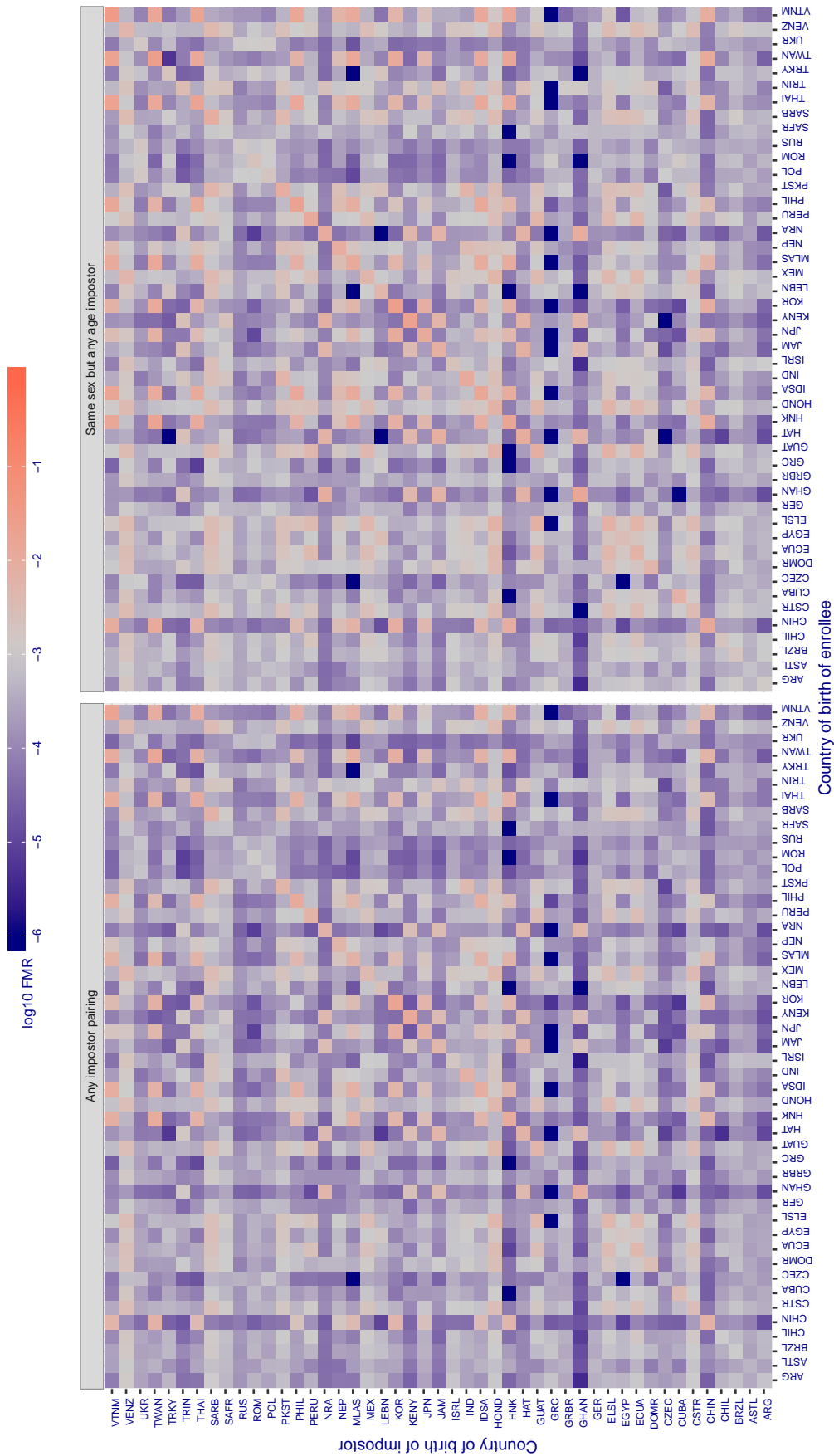


Figure 303: For algorithm `vigilantsolutions-005` operating on visa images, the heatmap shows false match rates observed over impostor comparisons of faces from different individuals who were born in the given country pair. False matches are counted against a recognition threshold fixed globally to give the target FMR in the plot title, computed over all on the order of 10^{10} impostor comparisons. If text appears in each box it give the same quantity as that coded by the color. Grey indicates FMR is at the intended FMR target level. Light red colors present a security vulnerability to, for example, a passport gate. Each +1 increase in \log_{10} FMR corresponds to a factor of 10 increase in FMR. The matrix is not quite symmetric because images in the enrollment and verification sets are different.

Cross country FMR at threshold $T = 2.809$ for algorithm `vigilantsolutions_006`, giving $FMR(T) = 0.001$ globally.

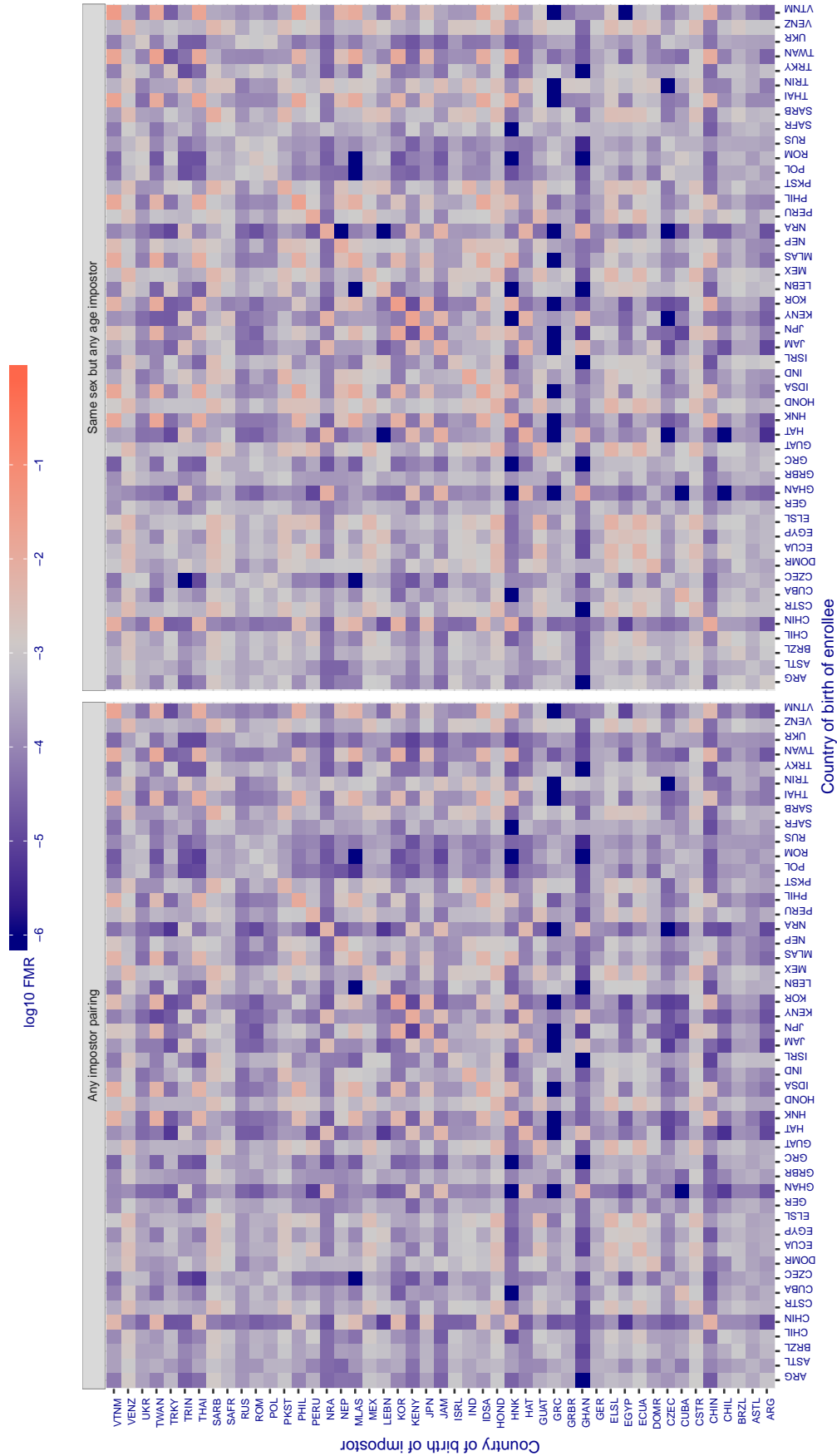


Figure 304: For algorithm `vigilantsolutions-006` operating on visa images, the heatmap shows false match rates observed over impostor comparisons of faces from different individuals who were born in the given country pair. False matches are counted against a recognition threshold fixed globally to give the target FMR in the plot title, computed over all on the order of 10^{10} impostor comparisons. If text appears in each box it give the same quantity as that coded by the color. Grey indicates FMR is at the intended FMR target level. Light red colors present a security vulnerability to, for example, a passport gate. Each +1 increase in \log_{10} FMR corresponds to a factor of 10 increase in FMR. The matrix is not quite symmetric because images in the enrollment and verification sets are different.

Cross country FMR at threshold $T = 0.336$ for algorithm vion_{000} , giving $\text{FMR}(T) = 0.001$ globally.

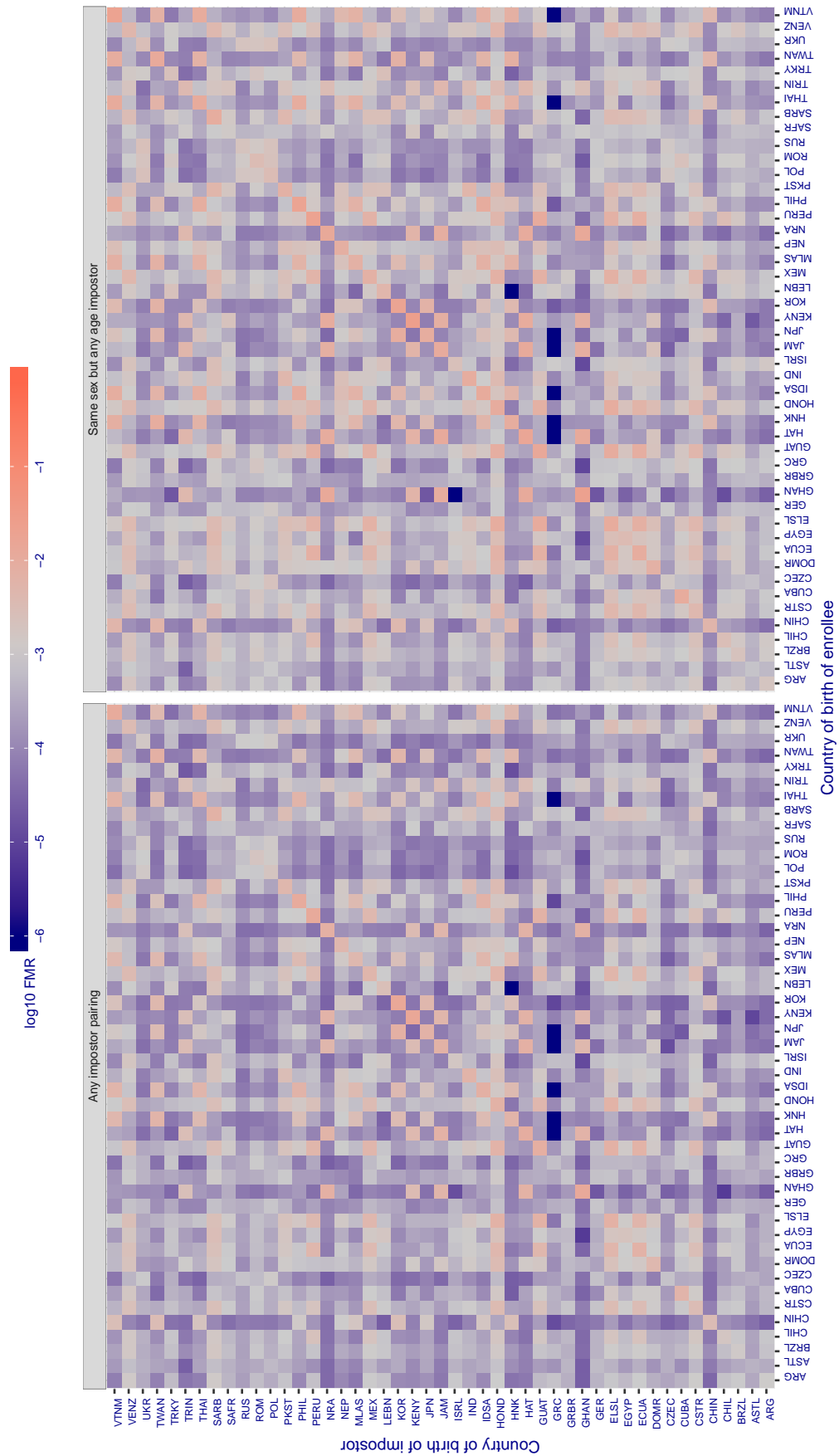


Figure 305: For algorithm vion_{000} operating on visa images, the heatmap shows false match rates observed over impostor comparisons of faces from different individuals who were born in the given country pair. False matches are counted against a recognition threshold fixed globally to give the target FMR in the plot title, computed over all on the order of 10^{10} impostor comparisons. If text appears in each box it give the same quantity as that coded by the color. Grey indicates FMR is at the intended FMR target level. Light red colors present a security vulnerability to, for example, a passport gate. Each +1 increase in \log_{10} FMR corresponds to a factor of 10 increase in FMR. The matrix is not quite symmetric because images in the enrollment and verification sets are different.

Cross country FMR at threshold $T = 0.340$ for algorithm visionbox_000, giving $FMR(T) = 0.001$ globally.

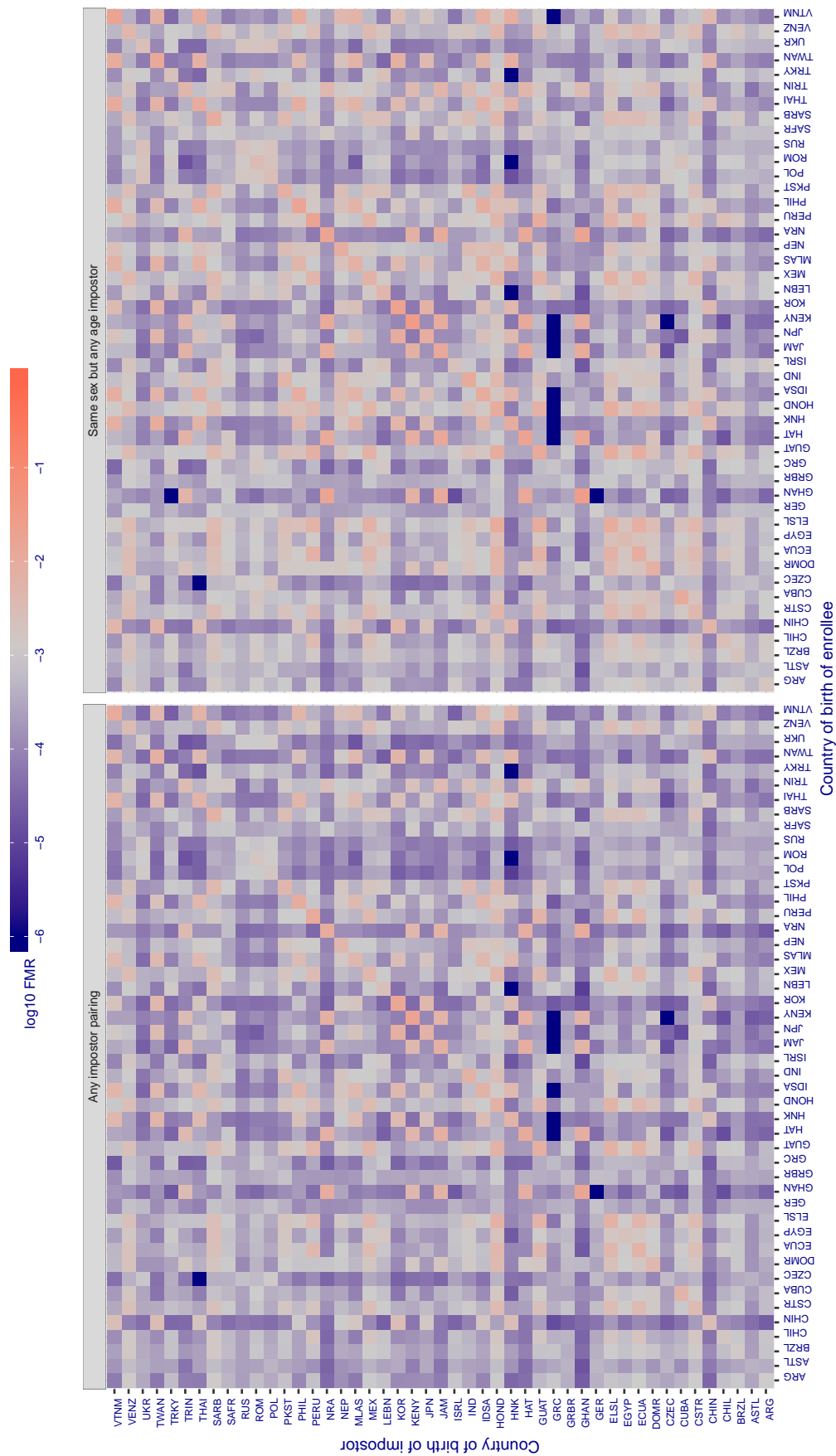


Figure 306: For algorithm visionbox-000 operating on visa images, the heatmap shows false match rates observed over impostor comparisons of faces from different individuals who were born in the given country pair. False matches are counted against a recognition threshold fixed globally to give the target FMR in the plot title, computed over all on the order of 10^{10} impostor comparisons. If text appears in each box it give the same quantity as that coded by the color. Grey indicates FMR is at the intended FMR target level. Light red colors present a security vulnerability to, for example, a passport gate. Each +1 increase in log10 FMR corresponds to a factor of 10 increase in FMR. The matrix is not quite symmetric because images in the enrollment and verification sets are different.

Cross country FMR at threshold $T = 0.296$ for algorithm visionbox_001, giving $FMR(T) = 0.001$ globally.

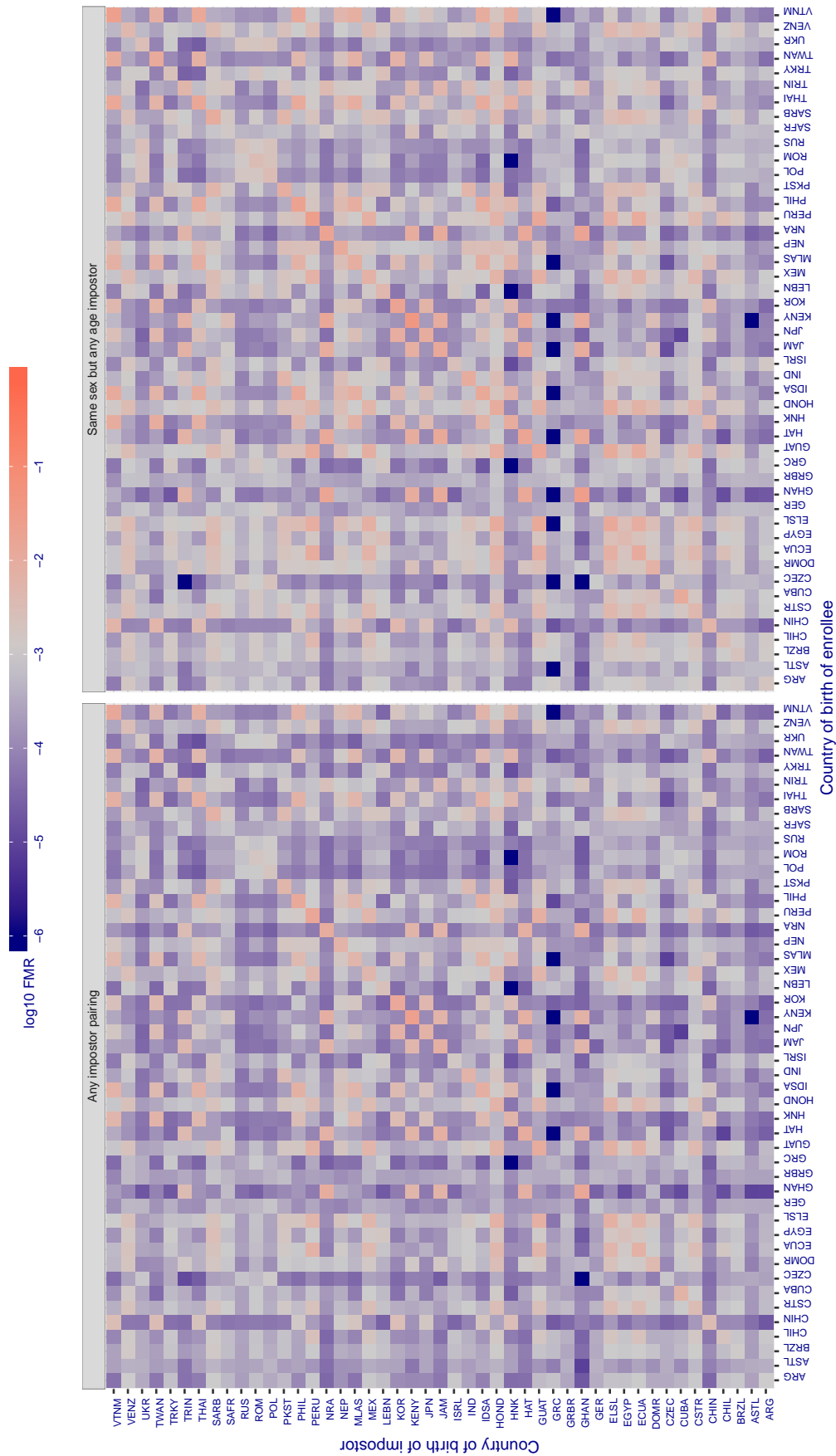


Figure 307: For algorithm visionbox-001 operating on visa images, the heatmap shows false match rates observed over impostor comparisons of faces from different individuals who were born in the given country pair. False matches are counted against a recognition threshold fixed globally to give the target FMR in the plot title, computed over all on the order of 10^{10} impostor comparisons. If text appears in each box it give the same quantity as that coded by the color. Grey indicates FMR is at the intended FMR target level. Light red colors present a security vulnerability to, for example, a passport gate. Each +1 increase in \log_{10} FMR corresponds to a factor of 10 increase in FMR. The matrix is not quite symmetric because images in the enrollment and verification sets are different.

Cross country FMR at threshold $T = 0.000$ for algorithm visionlabs_005, giving $FMR(T) = 0.001$ globally.

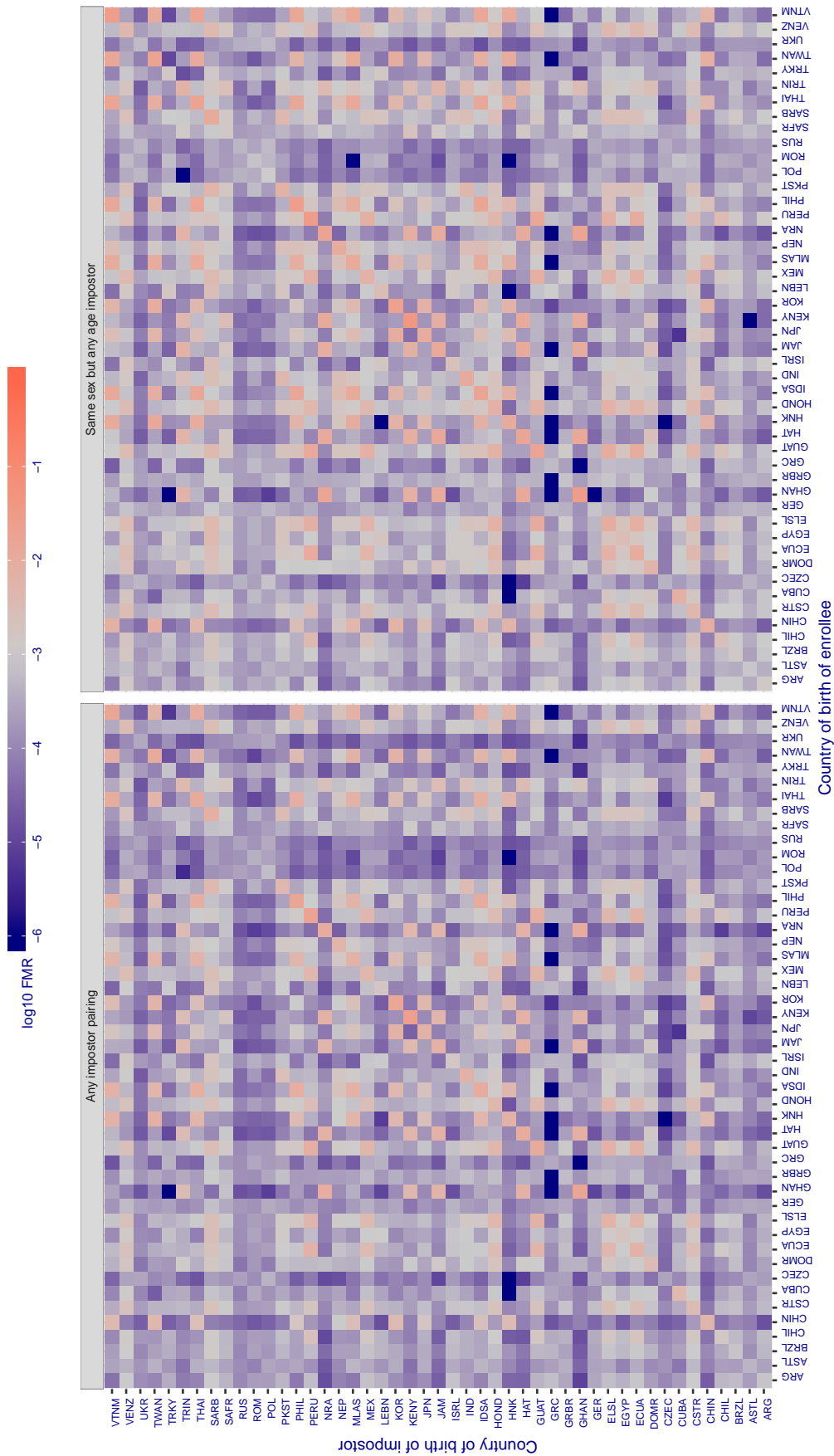


Figure 308: For algorithm visionlabs-005 operating on visa images, the heatmap shows false match rates observed over impostor comparisons of faces from different individuals who were born in the given country pair. False matches are counted against a recognition threshold fixed globally to give the target FMR in the plot title, computed over all on the order of 10^{10} impostor comparisons. If text appears in each box it give the same quantity as that coded by the color. Grey indicates FMR is at the intended FMR target level. Light red colors present a security vulnerability to, for example, a passport gate. Each +1 increase in log10 FMR corresponds to a factor of 10 increase in FMR. The matrix is not quite symmetric because images in the enrollment and verification sets are different.

Cross country FMR at threshold $T = 0.444$ for algorithm visionlabs_006, giving $FMR(T) = 0.001$ globally.

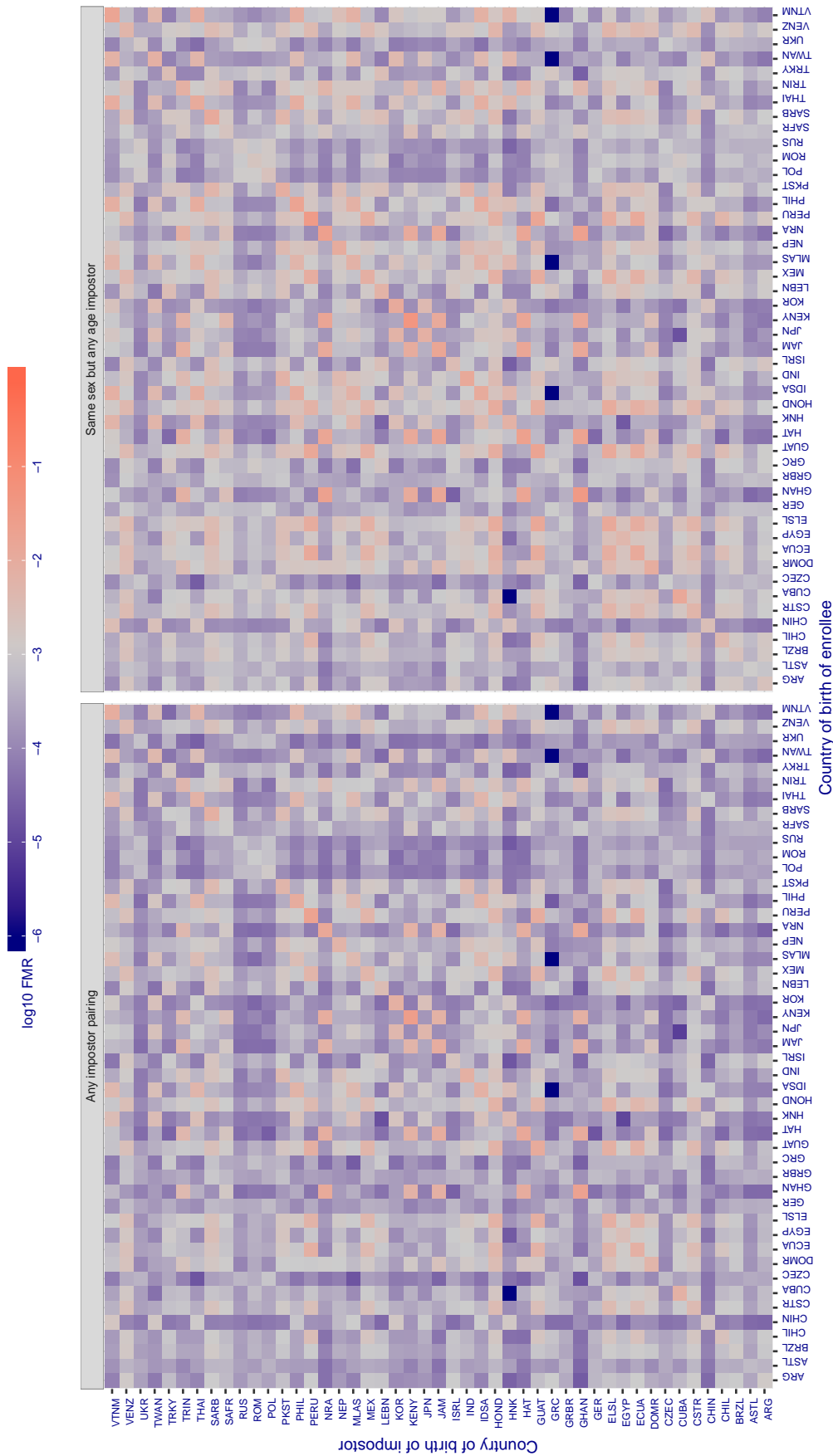


Figure 309: For algorithm visionlabs-006 operating on visa images, the heatmap shows false match rates observed over impostor comparisons of faces from different individuals who were born in the given country pair. False matches are counted against a recognition threshold fixed globally to give the target FMR in the plot title, computed over all on the order of 10^{10} impostor comparisons. If text appears in each box it give the same quantity as that coded by the color. Grey indicates FMR is at the intended FMR target level. Light red colors present a security vulnerability to, for example, a passport gate. Each +1 increase in $\log_{10} FMR$ corresponds to a factor of 10 increase in FMR. The matrix is not quite symmetric because images in the enrollment and verification sets are different.

Cross country FMR at threshold $T = 994.662$ for algorithm vocord_005, giving $FMR(T) = 0.001$ globally.

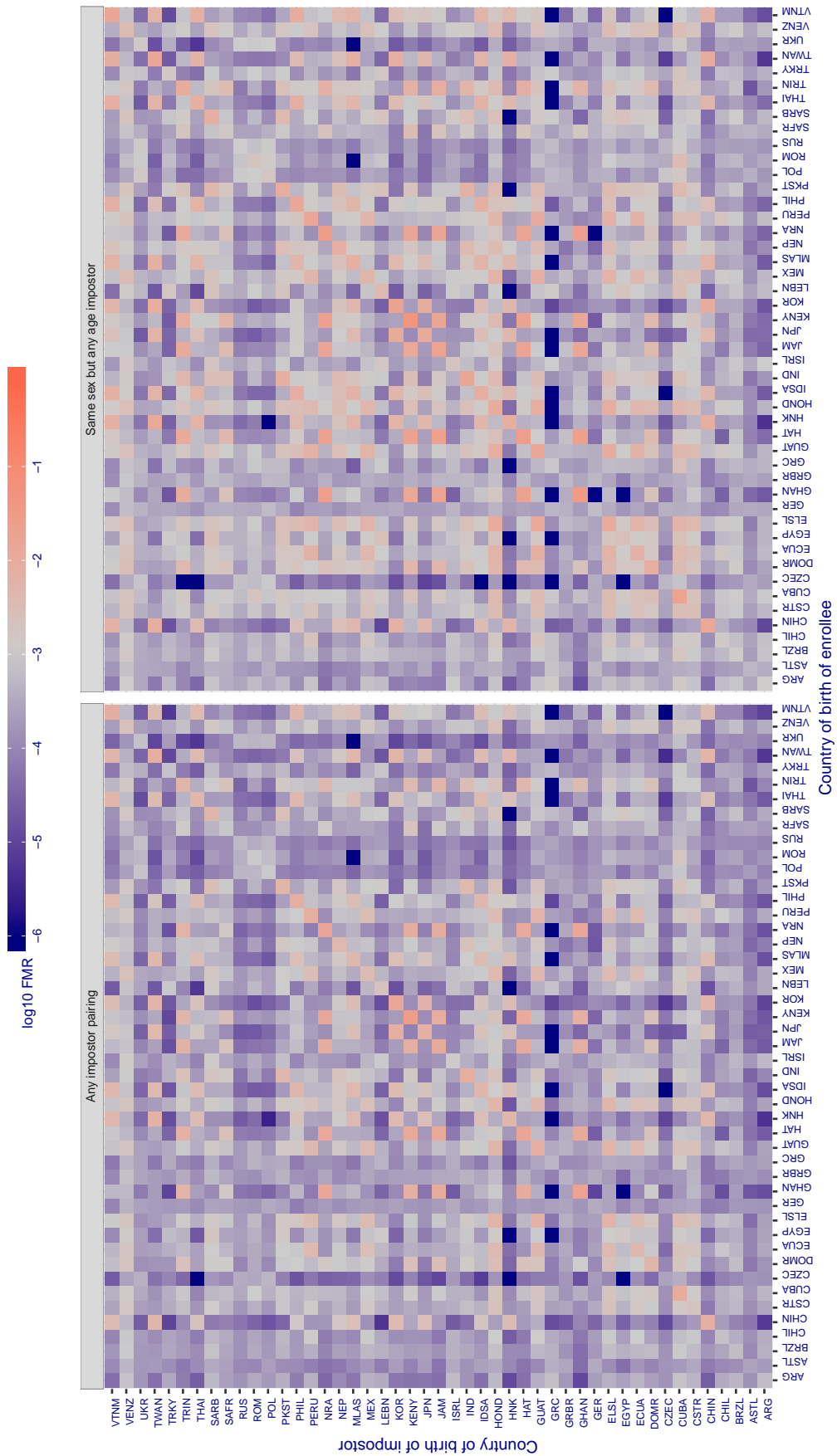


Figure 310: For algorithm vocord-005 operating on visa images, the heatmap shows false match rates observed over impostor comparisons of faces from different individuals who were born in the given country pair. False matches are counted against a recognition threshold fixed globally to give the target FMR in the plot title, computed over all on the order of 10^{10} impostor comparisons. If text appears in each box it give the same quantity as that coded by the color. Grey indicates FMR is at the intended FMR target level. Light red colors present a security vulnerability to, for example, a passport gate. Each +1 increase in \log_{10} FMR corresponds to a factor of 10 increase in FMR. The matrix is not quite symmetric because images in the enrollment and verification sets are different.

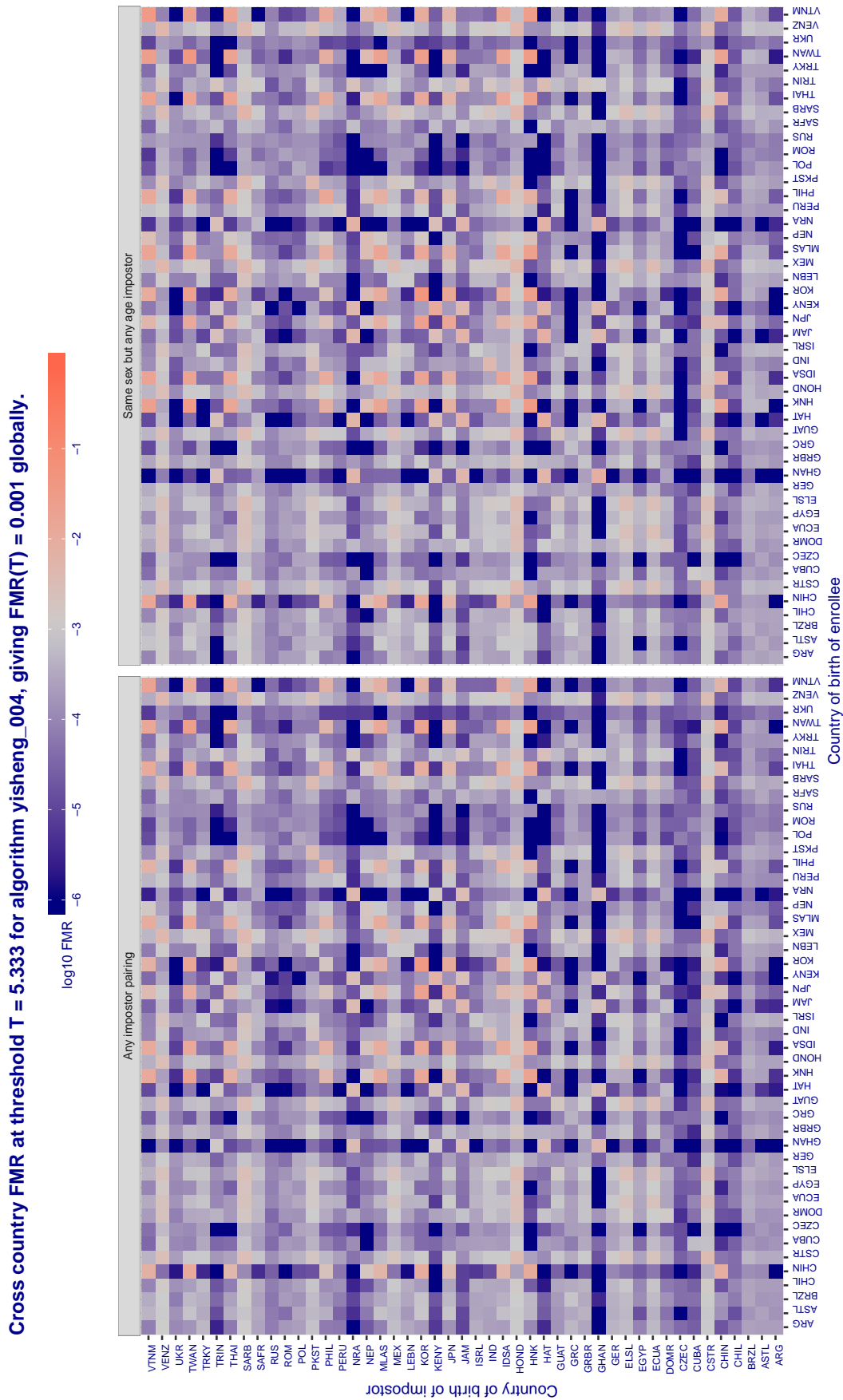


Figure 311: For algorithm yisheng-004 operating on visa images, the heatmap shows false match rates observed over impostor comparisons of faces from different individuals who were born in the given country pair. False matches are counted against a recognition threshold fixed globally to give the target FMR in the plot title, computed over all on the order of 10^{10} impostor comparisons. If text appears in each box it give the same quantity as that coded by the color. Grey indicates FMR is at the intended FMR target level. Light red colors present a security vulnerability to, for example, a passport gate. Each +1 increase in \log_{10} FMR corresponds to a factor of 10 increase in FMR. The matrix is not quite symmetric because images in the enrollment and verification sets are different.

Cross country FMR at threshold $T = 37.550$ for algorithm yitu_003, giving $FMR(T) = 0.001$ globally.

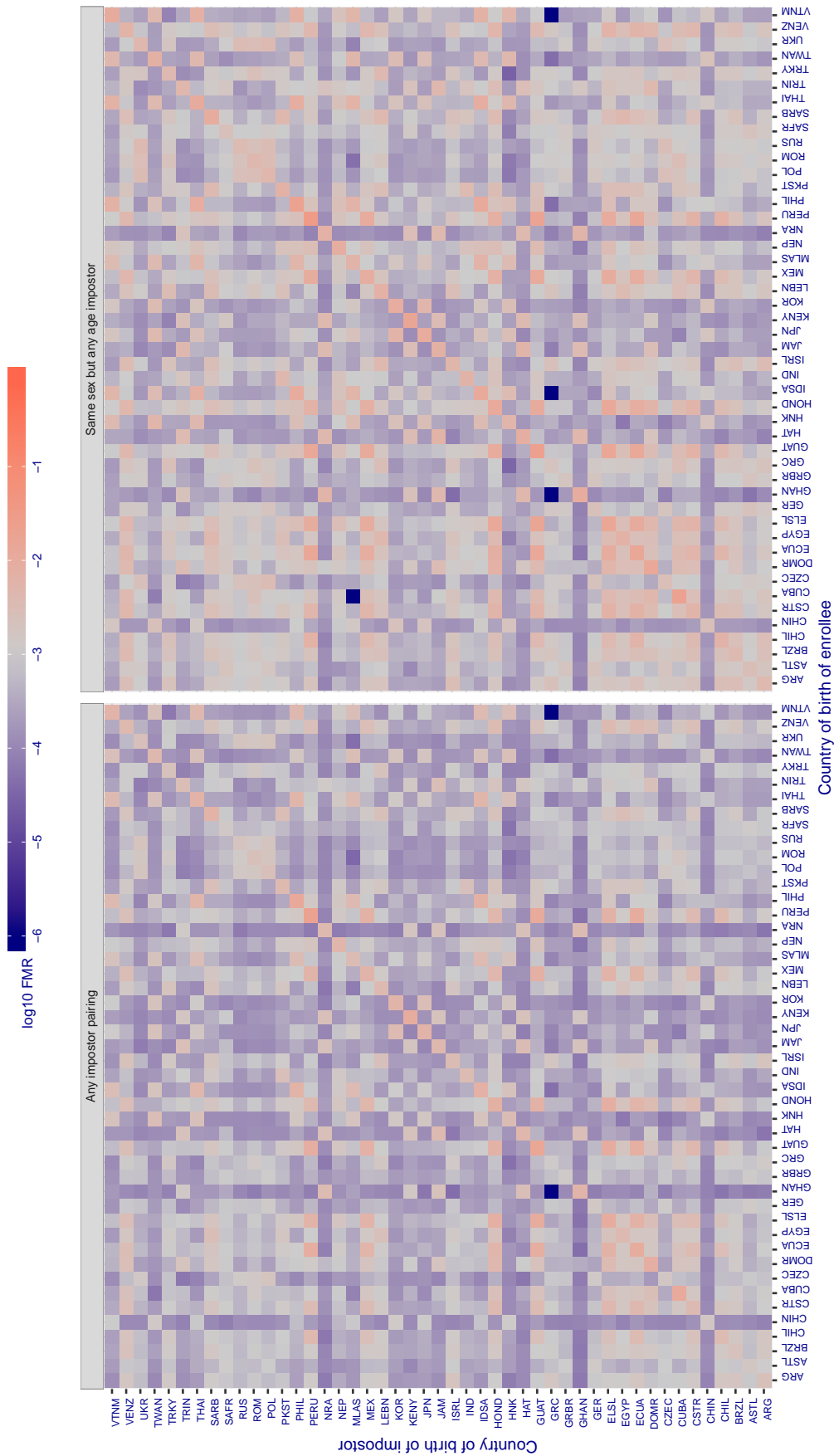


Figure 312: For algorithm yitu-003 operating on visa images, the heatmap shows false match rates observed over impostor comparisons of faces from different individuals who were born in the given country pair. False matches are counted against a recognition threshold fixed globally to give the target FMR in the plot title, computed over all on the order of 10^{10} impostor comparisons. If text appears in each box it give the same quantity as that coded by the color. Grey indicates FMR is at the intended FMR target level. Light red colors present a security vulnerability to, for example, a passport gate. Each +1 increase in \log_{10} FMR corresponds to a factor of 10 increase in FMR. The matrix is not quite symmetric because images in the enrollment and verification sets are different.

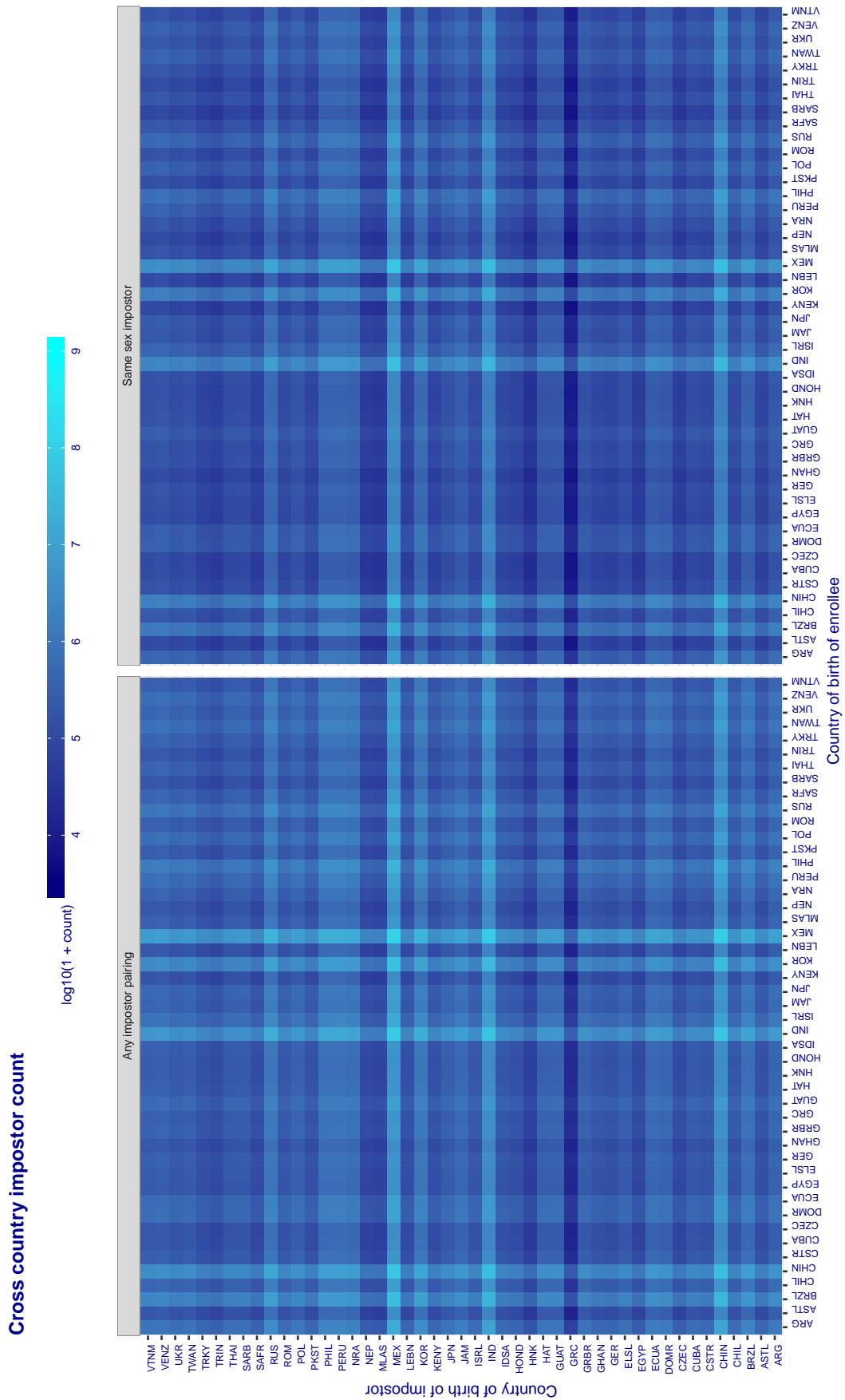


Figure 313: For visa images, the heatmap shows the count of impostor comparisons of faces from different individuals who were born in the given country pair.

3.6.2 Effect of age on impostors

Background: This section shows the effect of age on the impostor distribution. The ideal behaviour is that the age of the enrollee and the impostor would not affect impostor scores. This would support FMR stability over sub-populations.

Goals:

- ▷ To show the effect of relative ages of the impostor and enrollee on false match rates.
- ▷ To determine whether some algorithms have better impostor distribution stability.

Methods:

- ▷ Define 14 age group bins, spanning 0 to over 100 years old.
- ▷ Compute FMR over all impostor comparisons for which the subjects in the enrollee and impostor images have ages in two bins.
- ▷ Compute FMR over all impostor comparisons for which the subjects are additionally of the same sex, and born in the same geographic region.

Results:

The notable aspects are:

- ▷ Diagonal dominance: Impostors are more likely to be matched against their same age group.
- ▷ Same sex and same region impostors are more successful. On the diagonal, an impostor is more likely to succeed by posing as someone of the same sex. If $\Delta \log_{10} \text{FMR} = 0.2$, then same-sex same-region FMR exceeds the all-pairs FMR by factor of $10^{0.2} = 1.6$.
- ▷ Young children impostors give elevated FMR against young children. Older adult impostor give elevated FMR against older adults. These effects are quite large, for example if $\Delta \log_{10} \text{FMR} = 1.0$ larger than a 32 year old, then these groups have higher FMR by a factor of $10^1 = 10$. This would imply an FMR above 0.01 for a nominal (global) FMR = 0.001.
- ▷ Algorithms vary.
- ▷ We computed the same quantities for a global FMR = 0.0001. The effects are similar.

Note the calculations in this section include impostors paired across all countries of birth.

Cross age FMR at threshold $T = 2.740$ for algorithm 3divi_003, giving $FMR(T) = 0.0001$ globally.

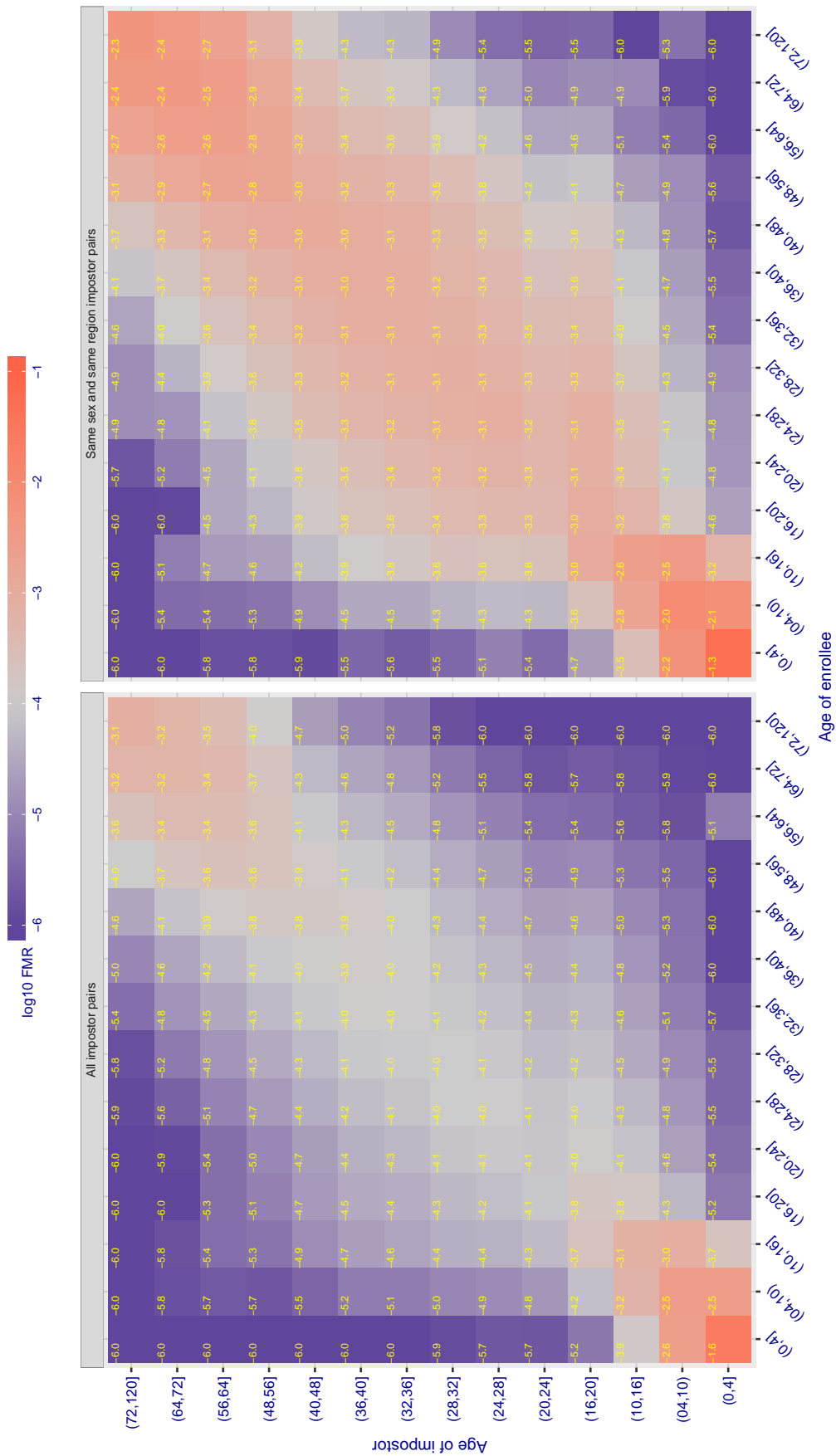


Figure 314: For algorithm 3divi-003 operating on visa images, the heatmap shows false match observed over impostor comparisons of faces from different individuals who have the given age pair. False matches are counted against a recognition threshold fixed globally to give $FMR = 0.001$ over all on the order of 10^{10} impostor comparisons. The text in each box gives the same quantity as that coded by the color. Light colors present a security vulnerability to, for example, a passport gate.

Cross age FMR at threshold $T = 0.702$ for algorithm alchera_000, giving $FMR(T) = 0.0001$ globally.

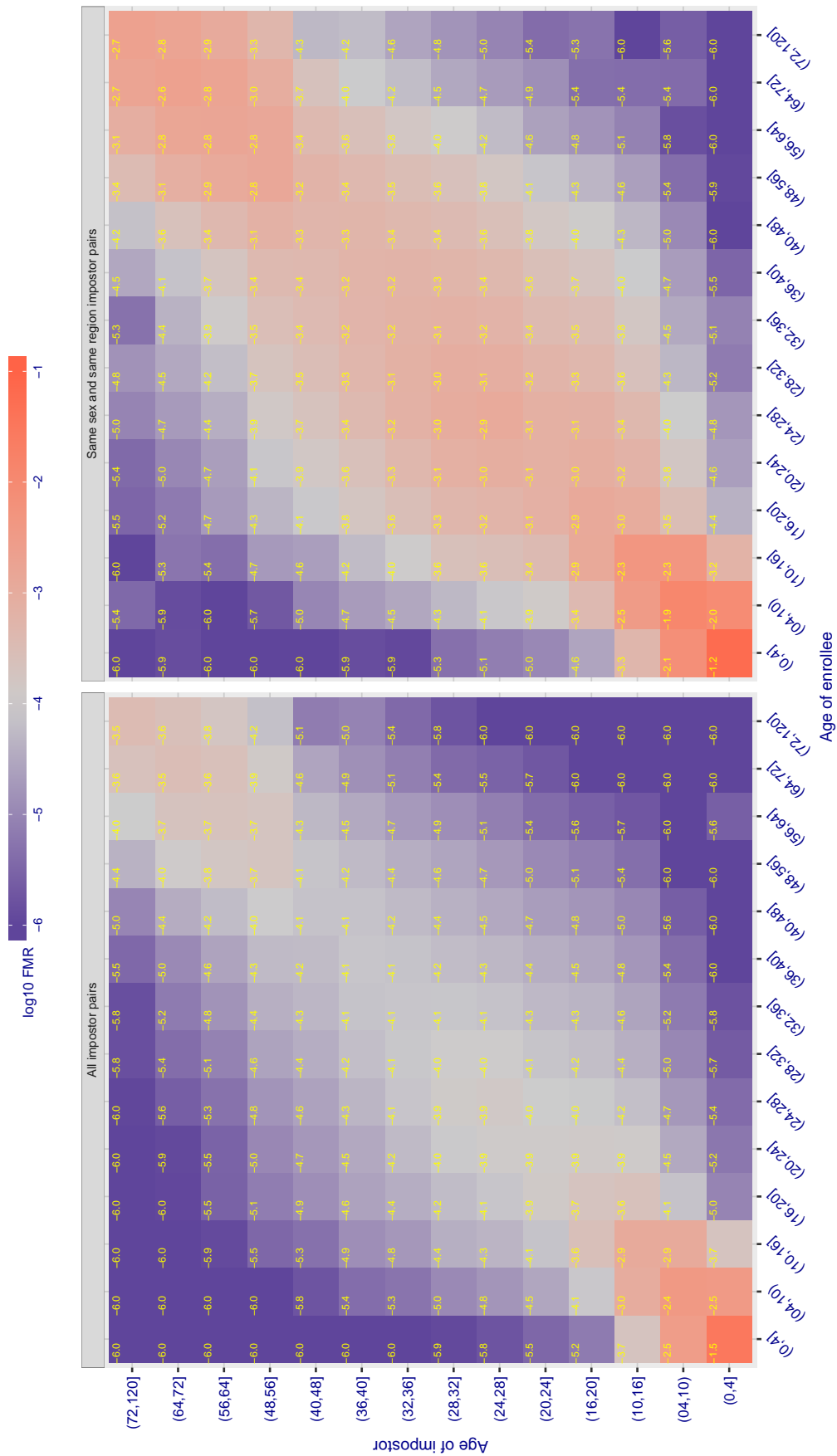


Figure 315: For algorithm alchera-000 operating on visa images, the heatmap shows false match observed over impostor comparisons of faces from different individuals who have the given age pair. False matches are counted against a recognition threshold fixed globally to give $FMR = 0.001$ over all on the order of 10^{10} impostor comparisons. The text in each box gives the same quantity as that coded by the color. Light colors present a security vulnerability to, for example, a passport gate.

Cross age FMR at threshold $T = 0.713$ for algorithm alchera_001, giving $FMR(T) = 0.0001$ globally.

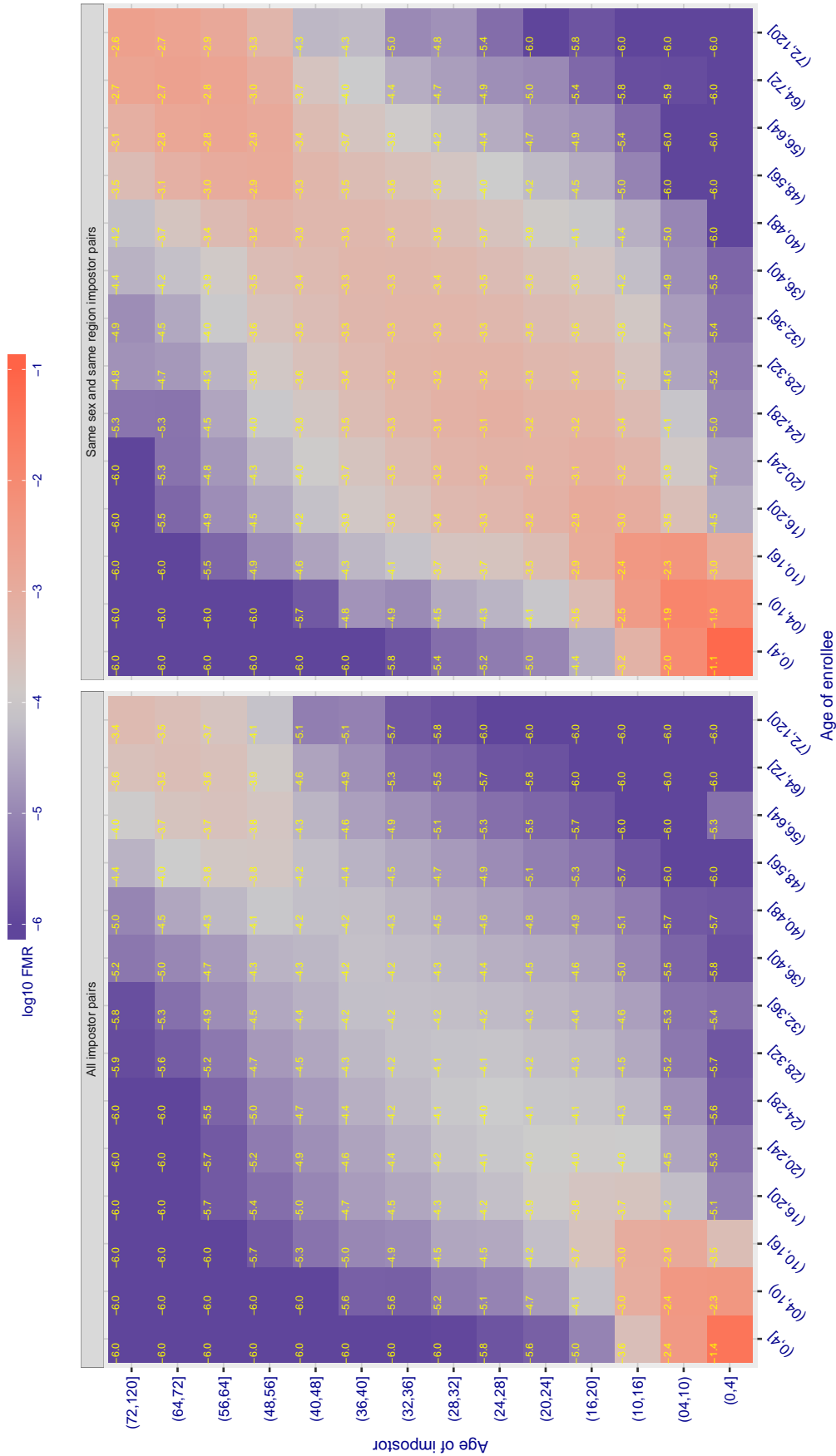


Figure 316: For algorithm alchera-001 operating on visa images, the heatmap shows false match observed over impostor comparisons of faces from different individuals who have the given age pair. False matches are counted against a recognition threshold fixed globally to give $FMR = 0.001$ over all on the order of 10^{10} impostor comparisons. The text in each box gives the same quantity as that coded by the color. Light colors present a security vulnerability to, for example, a passport gate.

Cross age FMR at threshold $T = 0.433$ for algorithm allgvision_000, giving $FMR(T) = 0.0001$ globally.

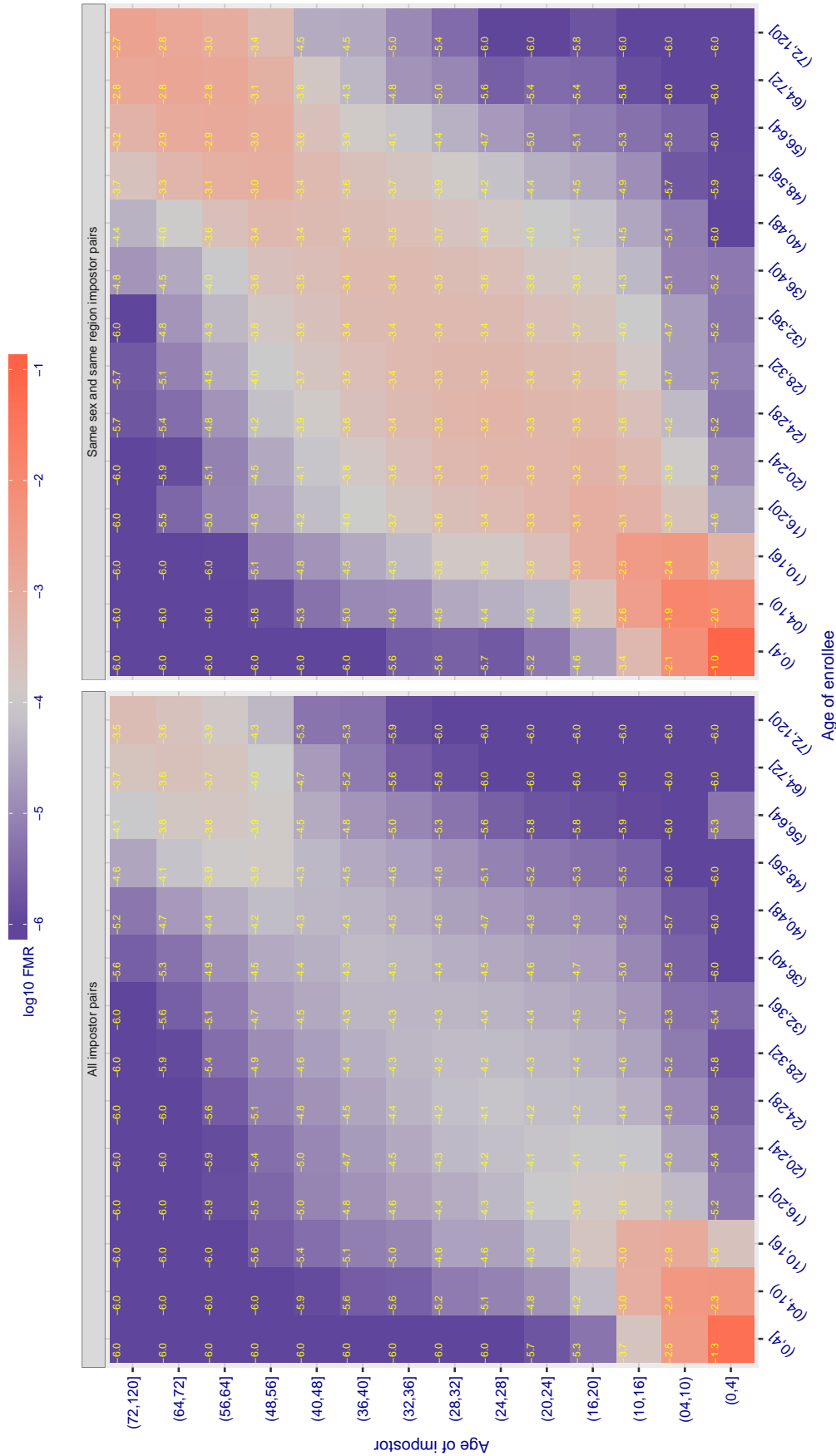


Figure 317: For algorithm allgvision-000 operating on visa images, the heatmap shows false match observed over impostor comparisons of faces from different individuals who have the given age pair. False matches are counted against a recognition threshold fixed globally to give $FMR = 0.0001$ over all on the order of 10^{10} impostor comparisons. The text in each box gives the same quantity as that coded by the color. Light colors present a security vulnerability to, for example, a passport gate.

Cross age FMR at threshold $T = 3.640$ for algorithm amplifiedgroup_001, giving $FMR(T) = 0.0001$ globally.

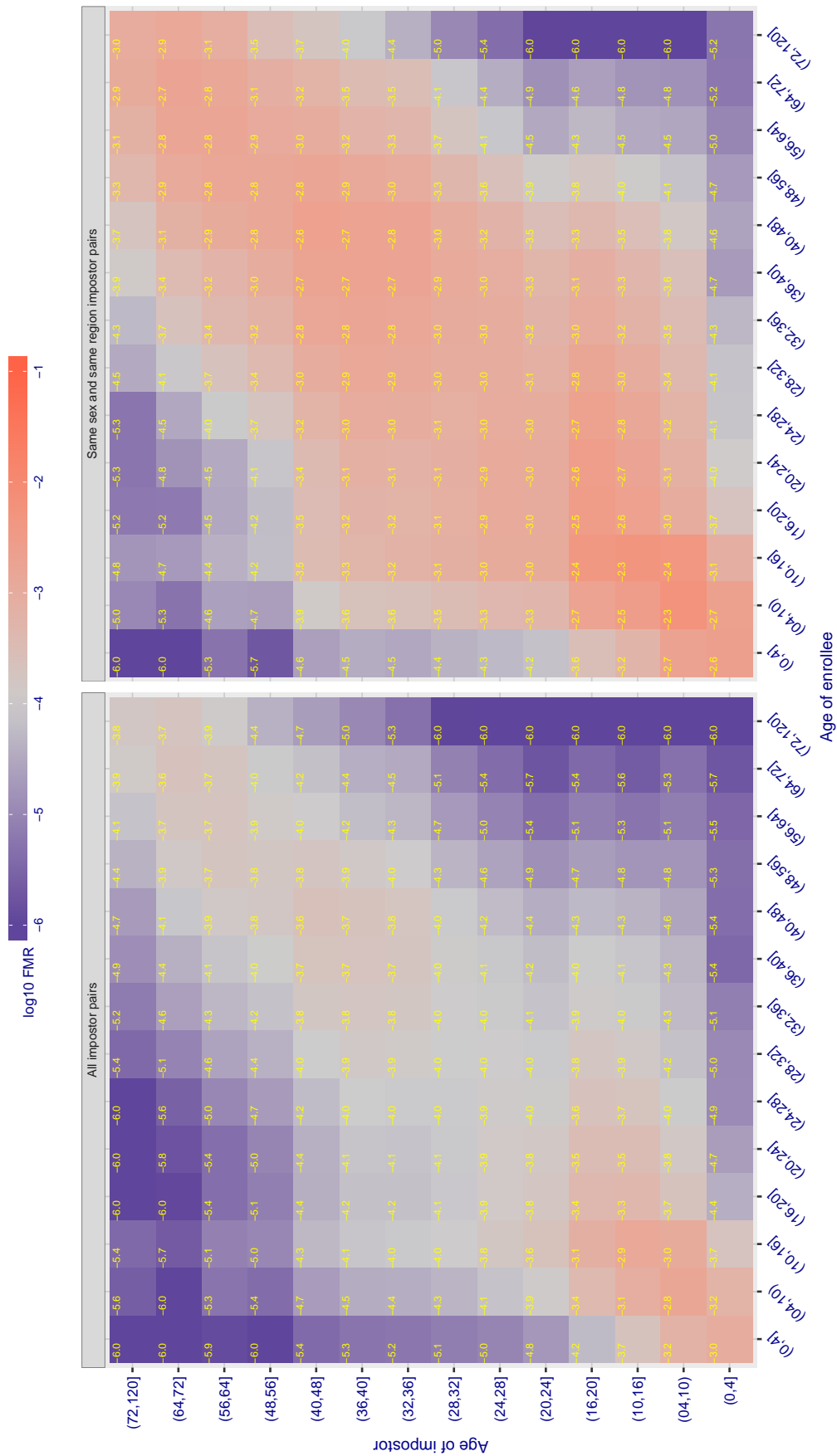


Figure 318: For algorithm amplifiedgroup-001 operating on visa images, the heatmap shows false match observed over impostor comparisons of faces from different individuals who have the given age pair. False matches are counted against a recognition threshold fixed globally to give $FMR = 0.001$ over all on the order of 10^{10} impostor comparisons. The text in each box gives the same quantity as that coded by the color. Light colors present a security vulnerability to, for example, a passport gate.

Cross age FMR at threshold $T = 0.404$ for algorithm anke_002, giving $FMR(T) = 0.0001$ globally.

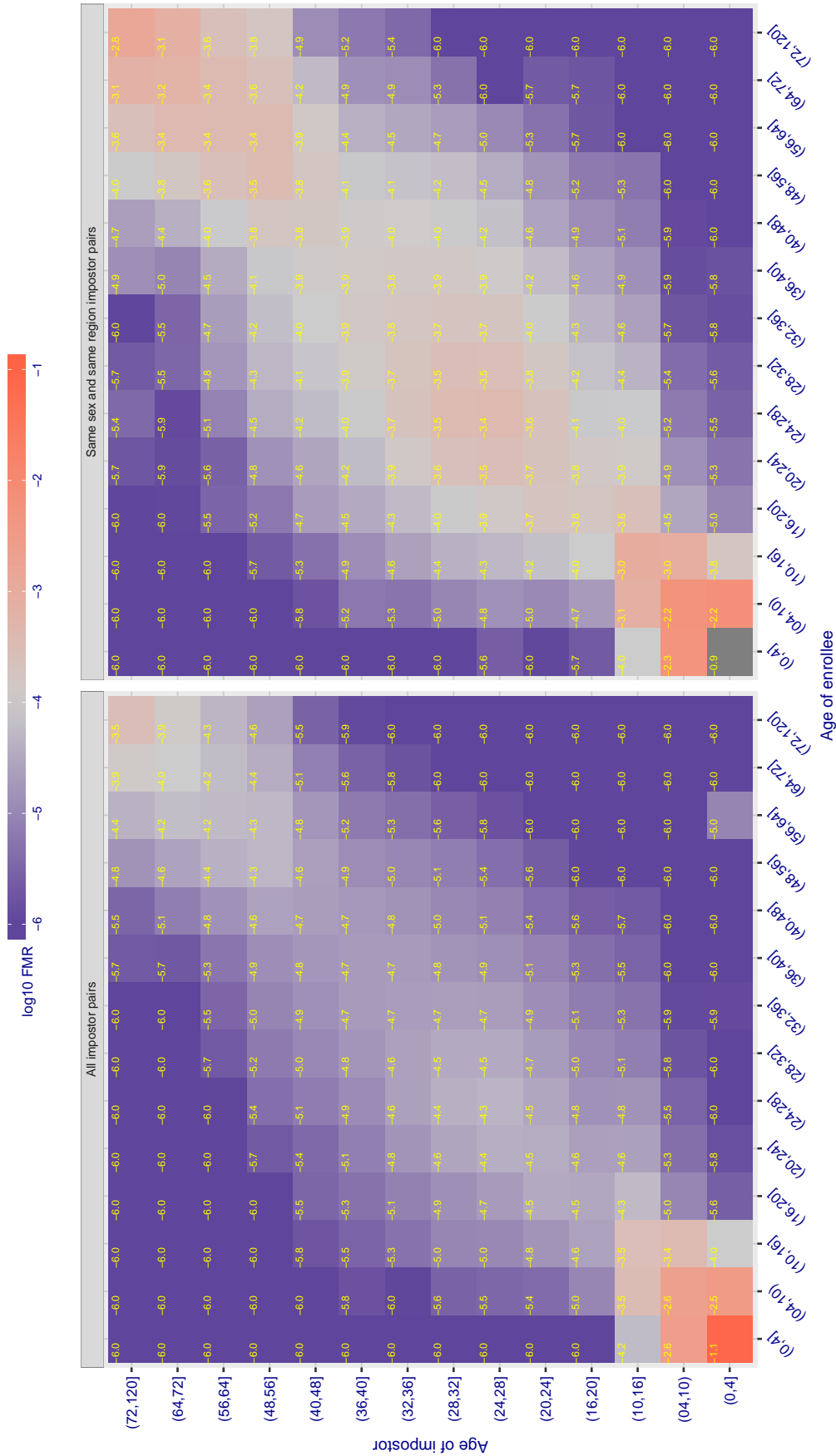


Figure 319: For algorithm anke-002 operating on visa images, the heatmap shows false match observed over impostor comparisons of faces from different individuals who have the given age pair. False matches are counted against a recognition threshold fixed globally to give $FMR = 0.001$ over all on the order of 10^{10} impostor comparisons. The text in each box gives the same quantity as that coded by the color. Light colors present a security vulnerability to, for example, a passport gate.

Cross age FMR at threshold $T = 0.397$ for algorithm anke_003, giving $FMR(T) = 0.0001$ globally.

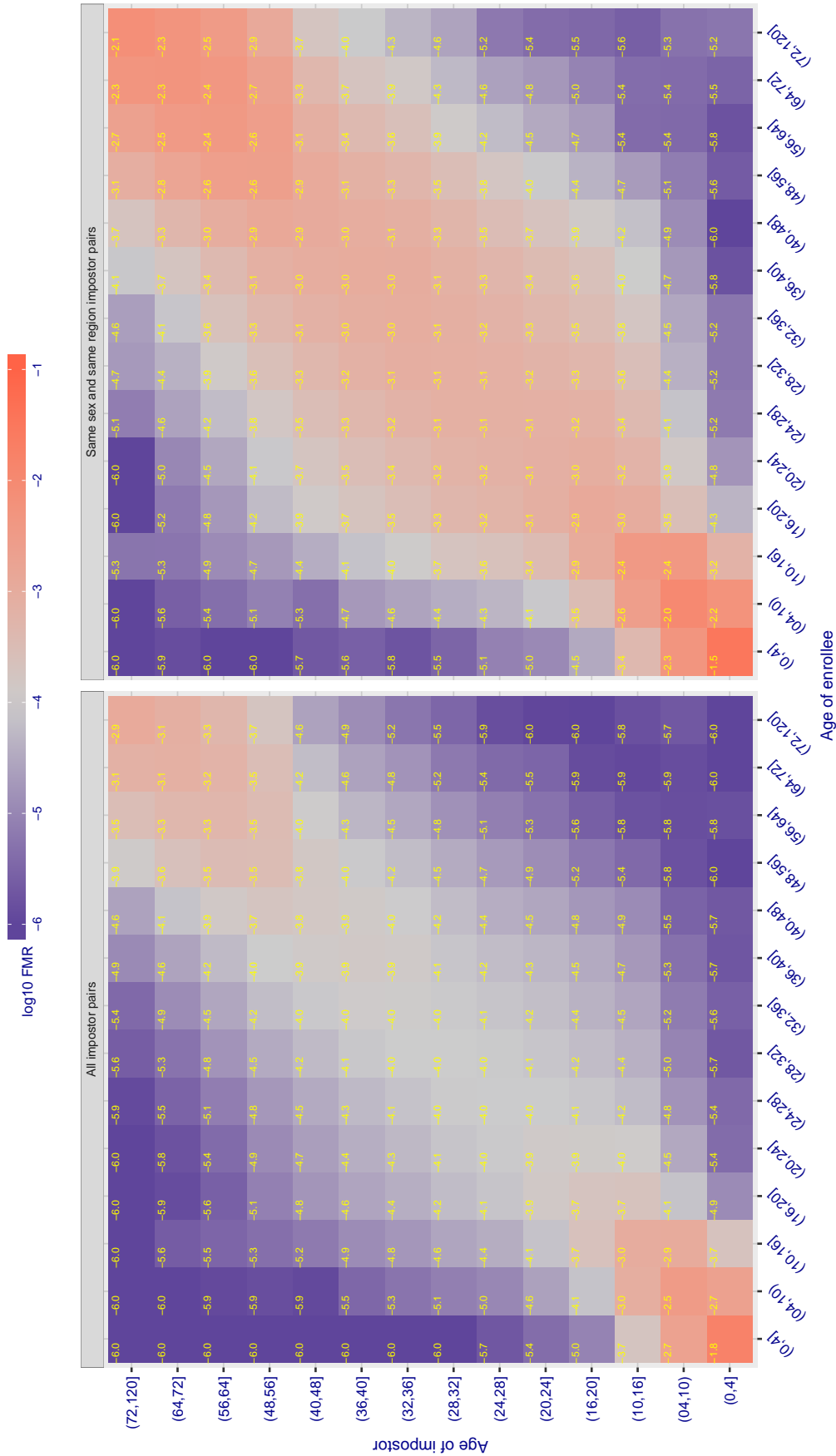


Figure 320: For algorithm anke-003 operating on visa images, the heatmap shows false match observed over impostor comparisons of faces from different individuals who have the given age pair. False matches are counted against a recognition threshold fixed globally to give $FMR = 0.001$ over all on the order of 10^{10} impostor comparisons. The text in each box gives the same quantity as that coded by the color: Light colors present a security vulnerability to, for example, a passport gate.

Cross age FMR at threshold $T = 1.526$ for algorithm anyvision_002, giving $FMR(T) = 0.0001$ globally.

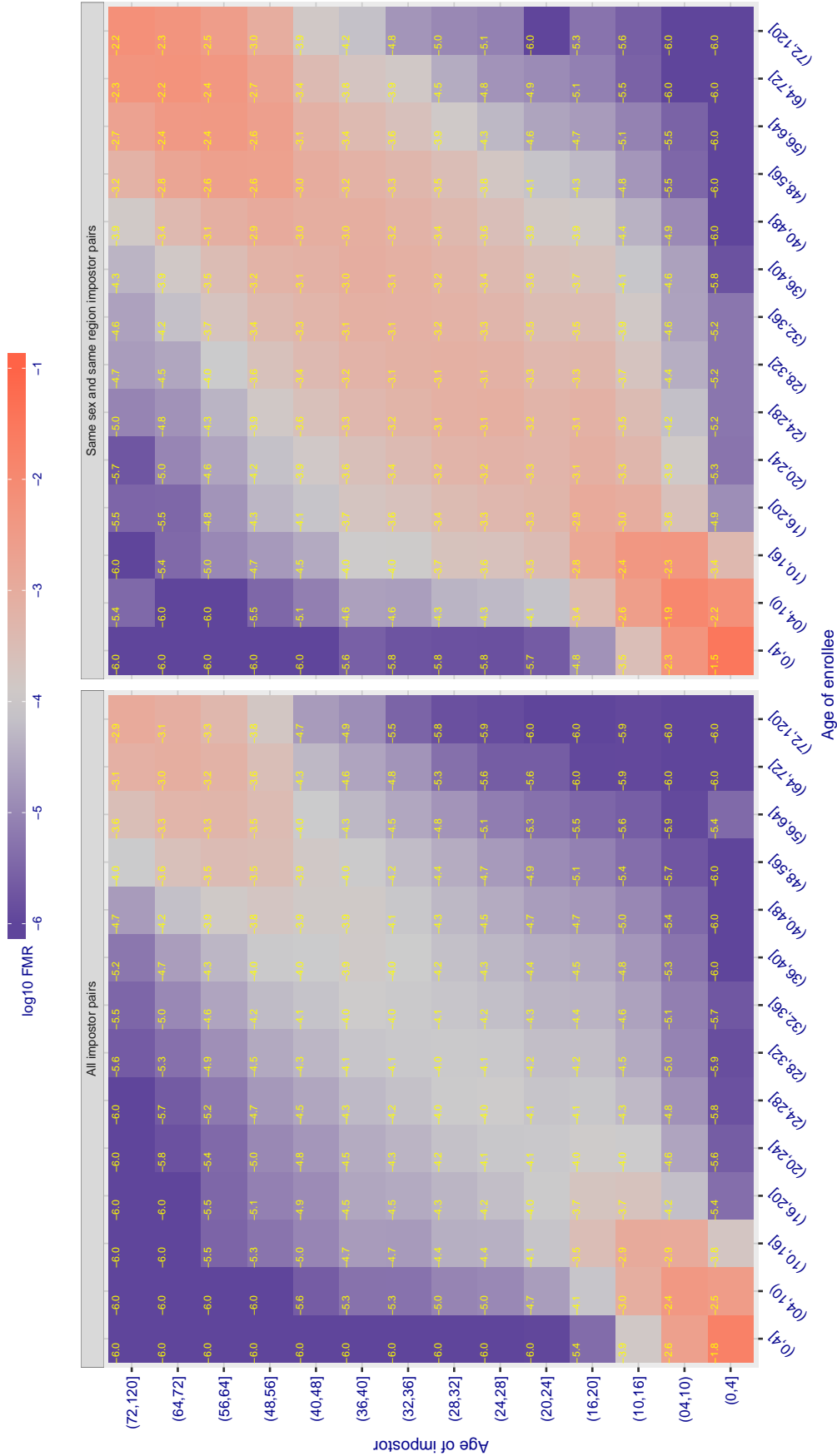


Figure 321: For algorithm anyvision-002 operating on visa images, the heatmap shows false match observed over impostor comparisons of faces from different individuals who have the given age pair. False matches are counted against a recognition threshold fixed globally to give $FMR = 0.001$ over all on the order of 10^{10} impostor comparisons. The text in each box gives the same quantity as that coded by the color. Light colors present a security vulnerability to, for example, a passport gate.

Cross age FMR at threshold $T = 1.375$ for algorithm anyvision_004, giving $FMR(T) = 0.0001$ globally.

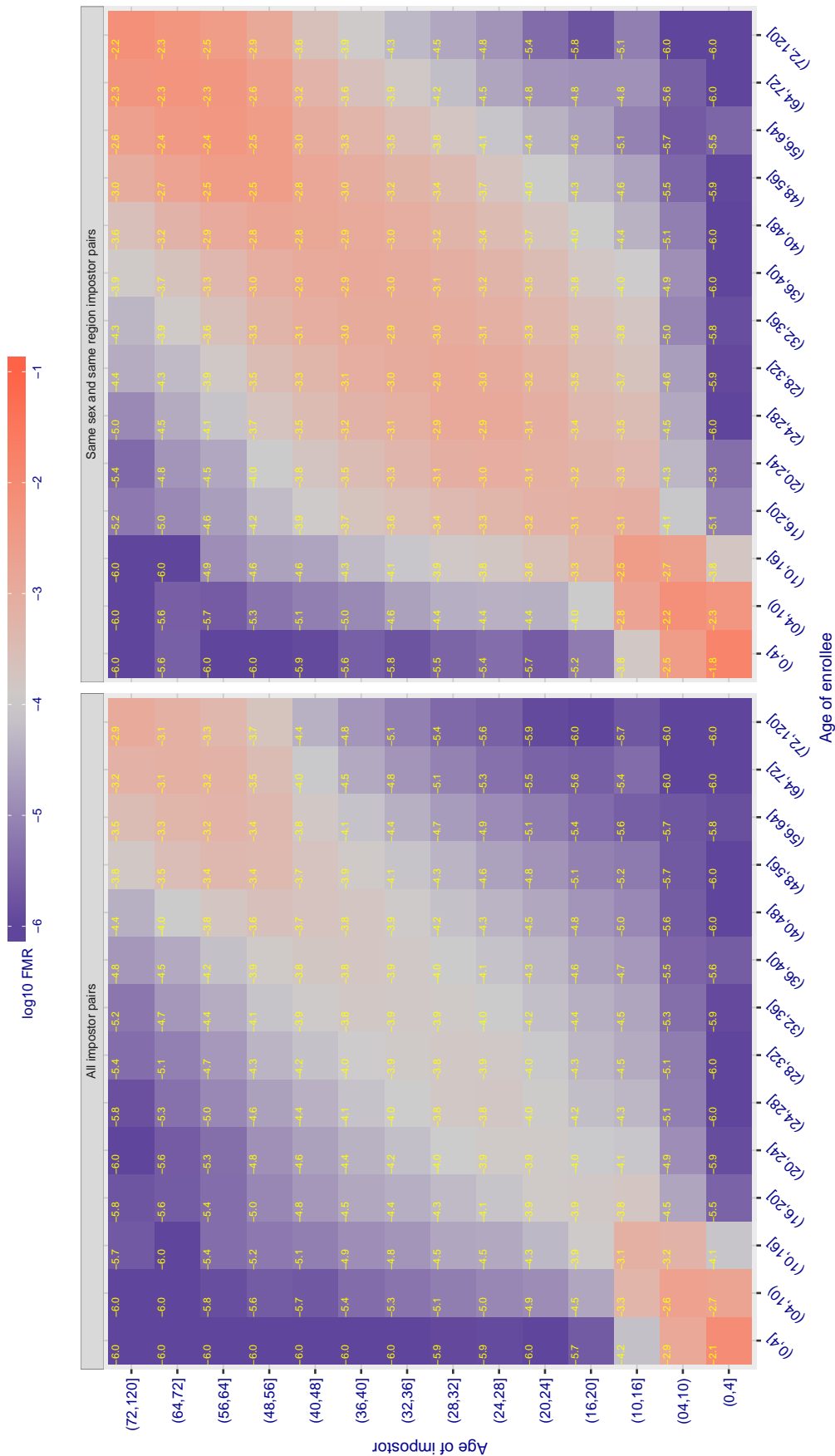


Figure 322: For algorithm anyvision-004 operating on visa images, the heatmap shows false match observed over impostor comparisons of faces from different individuals who have the given age pair. False matches are counted against a recognition threshold fixed globally to give $FMR = 0.001$ over all on the order of 10^{10} impostor comparisons. The text in each box gives the same quantity as that coded by the color. Light colors present a security vulnerability to, for example, a passport gate.

Cross age FMR at threshold $T = 3.868$ for algorithm aware_003, giving $FMR(T) = 0.0001$ globally.

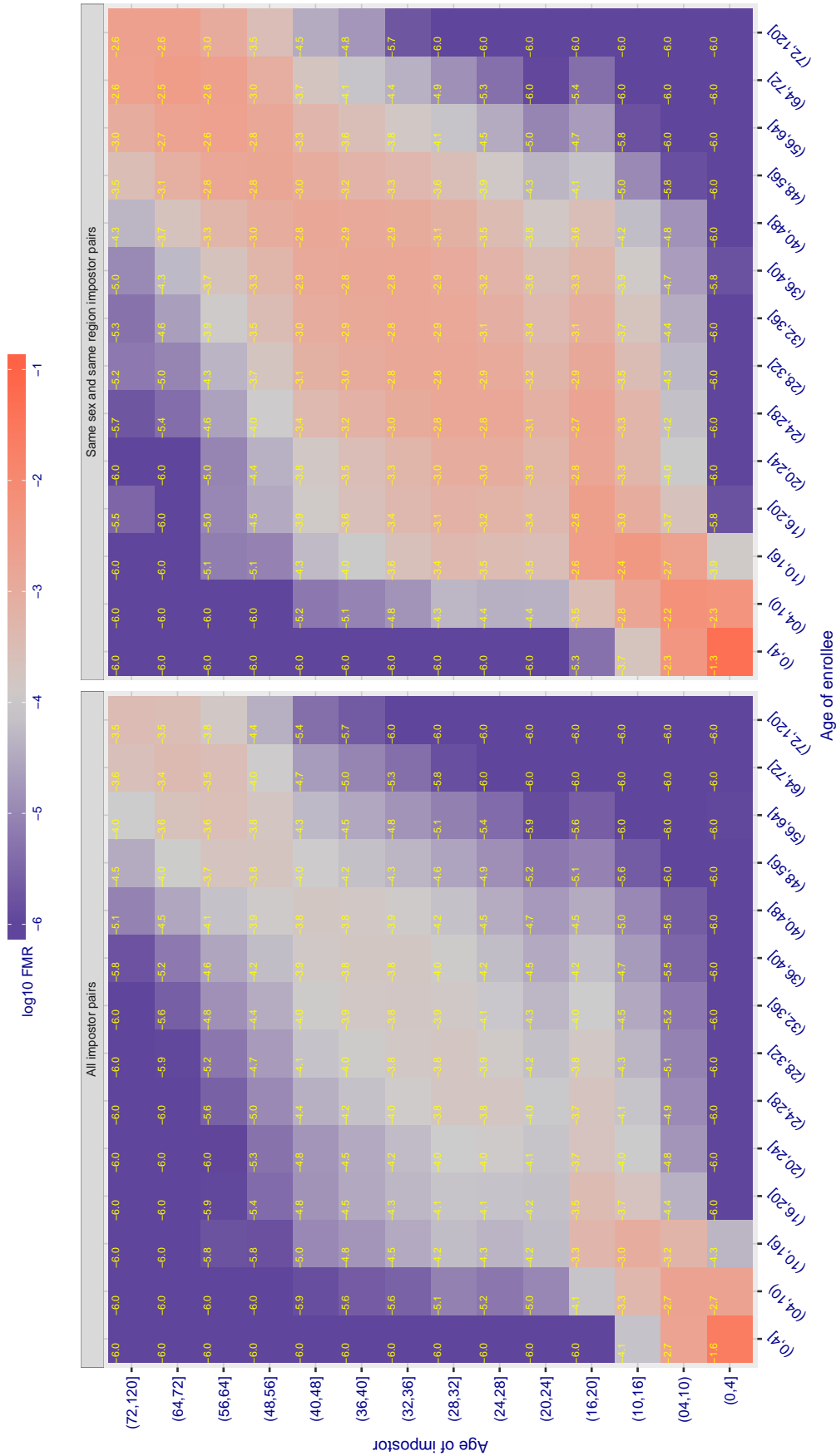


Figure 323: For algorithm aware-003 operating on visa images, the heatmap shows false match observed over impostor comparisons of faces from different individuals who have the given age pair. False matches are counted against a recognition threshold fixed globally to give $FMR = 0.0001$ over all on the order of 10^{10} impostor comparisons. The text in each box gives the same quantity as that coded by the color: Light colors present a security vulnerability to, for example, a passport gate.

Cross age FMR at threshold $T = 5.084$ for algorithm aware_004, giving $FMR(T) = 0.0001$ globally.

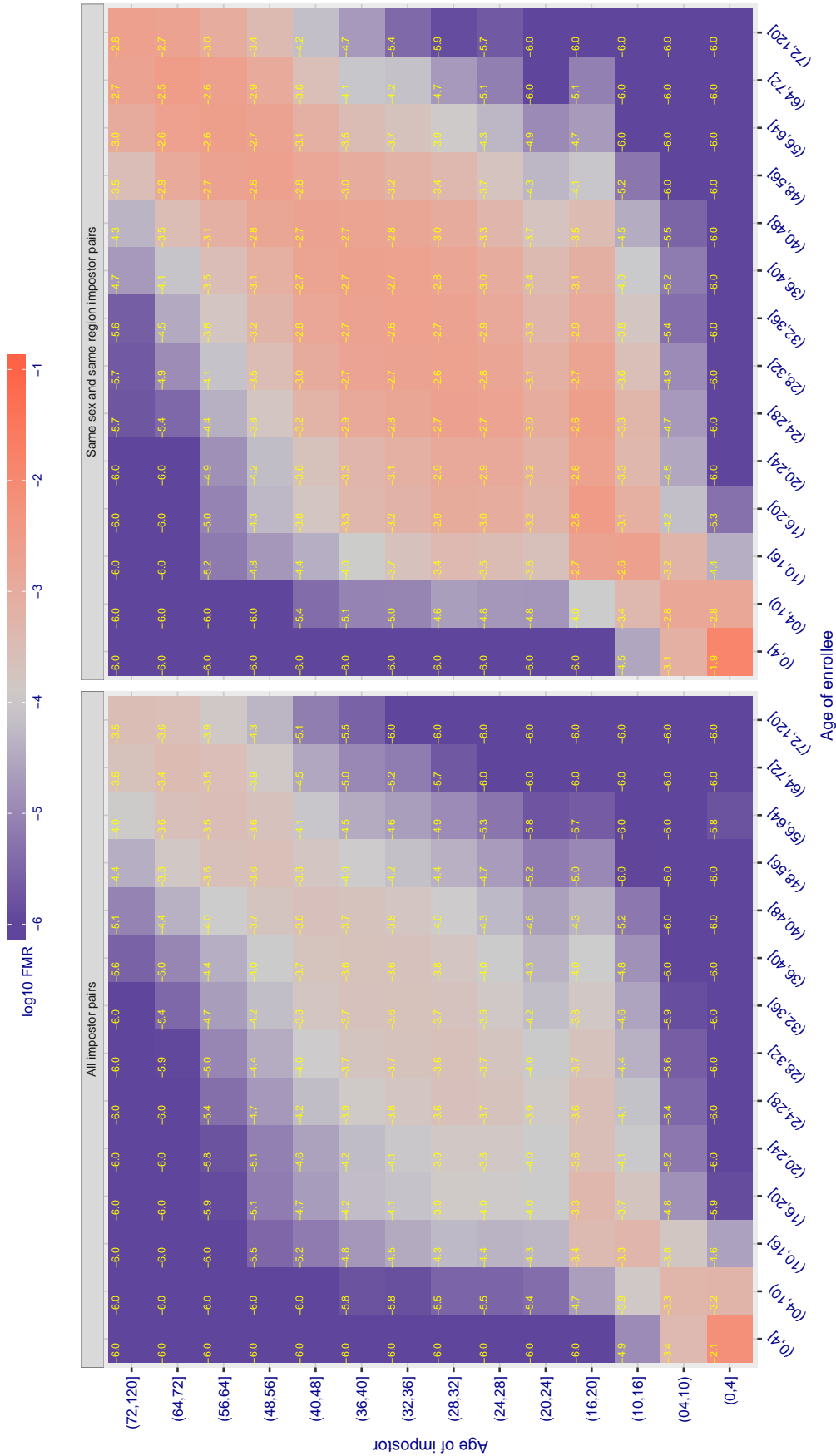


Figure 324: For algorithm aware-004 operating on visa images, the heatmap shows false match observed over impostor comparisons of faces from different individuals who have the given age pair. False matches are counted against a recognition threshold fixed globally to give $FMR = 0.001$ over all on the order of 10^{10} impostor comparisons. The text in each box gives the same quantity as that coded by the color: Light colors present a security vulnerability to, for example, a passport gate.

Cross age FMR at threshold $T = 0.919$ for algorithm ayonix_000, giving $FMR(T) = 0.0001$ globally.

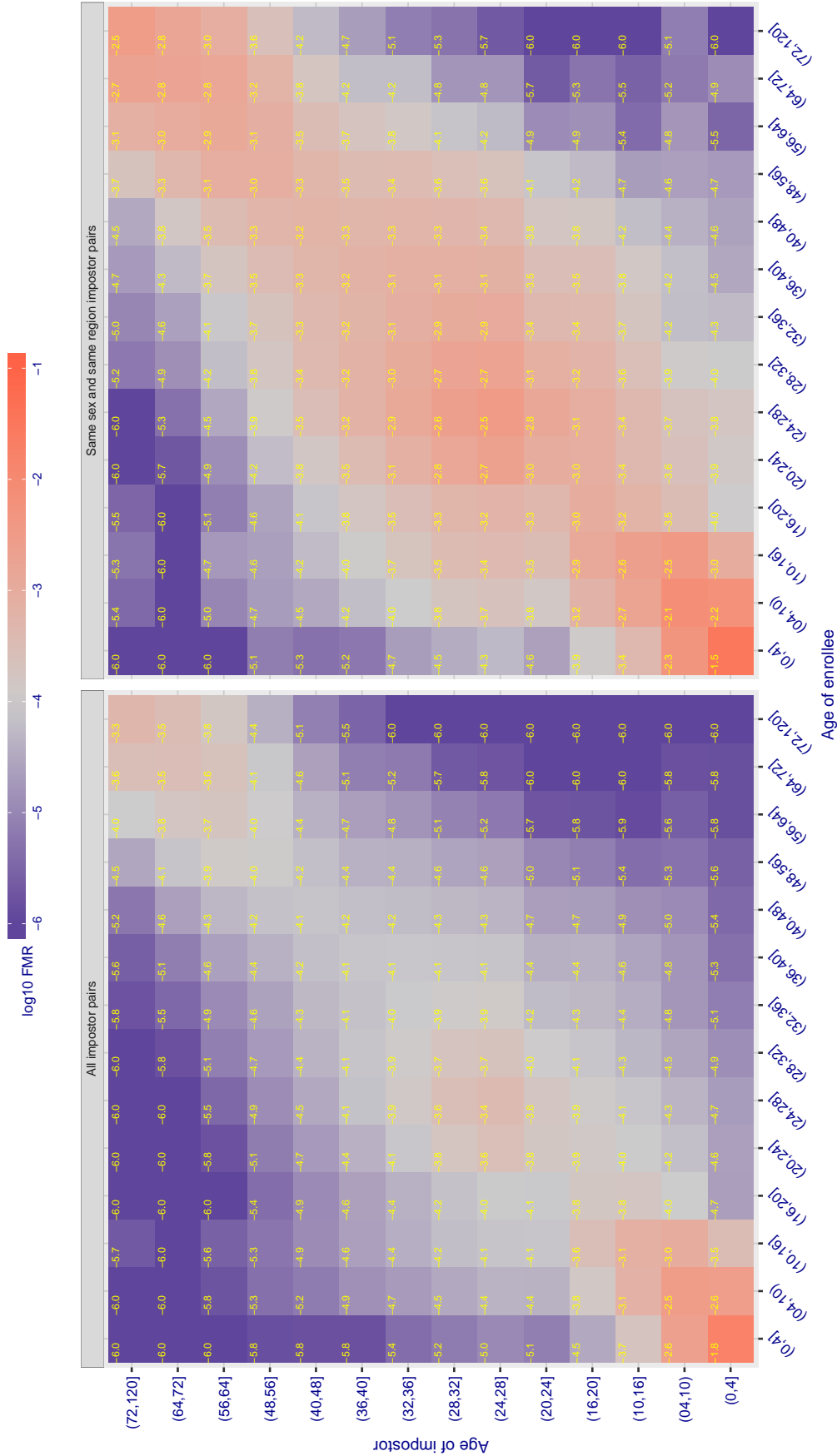


Figure 325: For algorithm ayonix-000 operating on visa images, the heatmap shows false match observed over impostor comparisons of faces from different individuals who have the given age pair. False matches are counted against a recognition threshold fixed globally to give $FMR = 0.0001$ over all on the order of 10^{10} impostor comparisons. The text in each box gives the same quantity as that coded by the color: Light colors present a security vulnerability to, for example, a passport gate.

Cross age FMR at threshold $T = 0.731$ for algorithm `bm_001`, giving $FMR(T) = 0.0001$ globally.

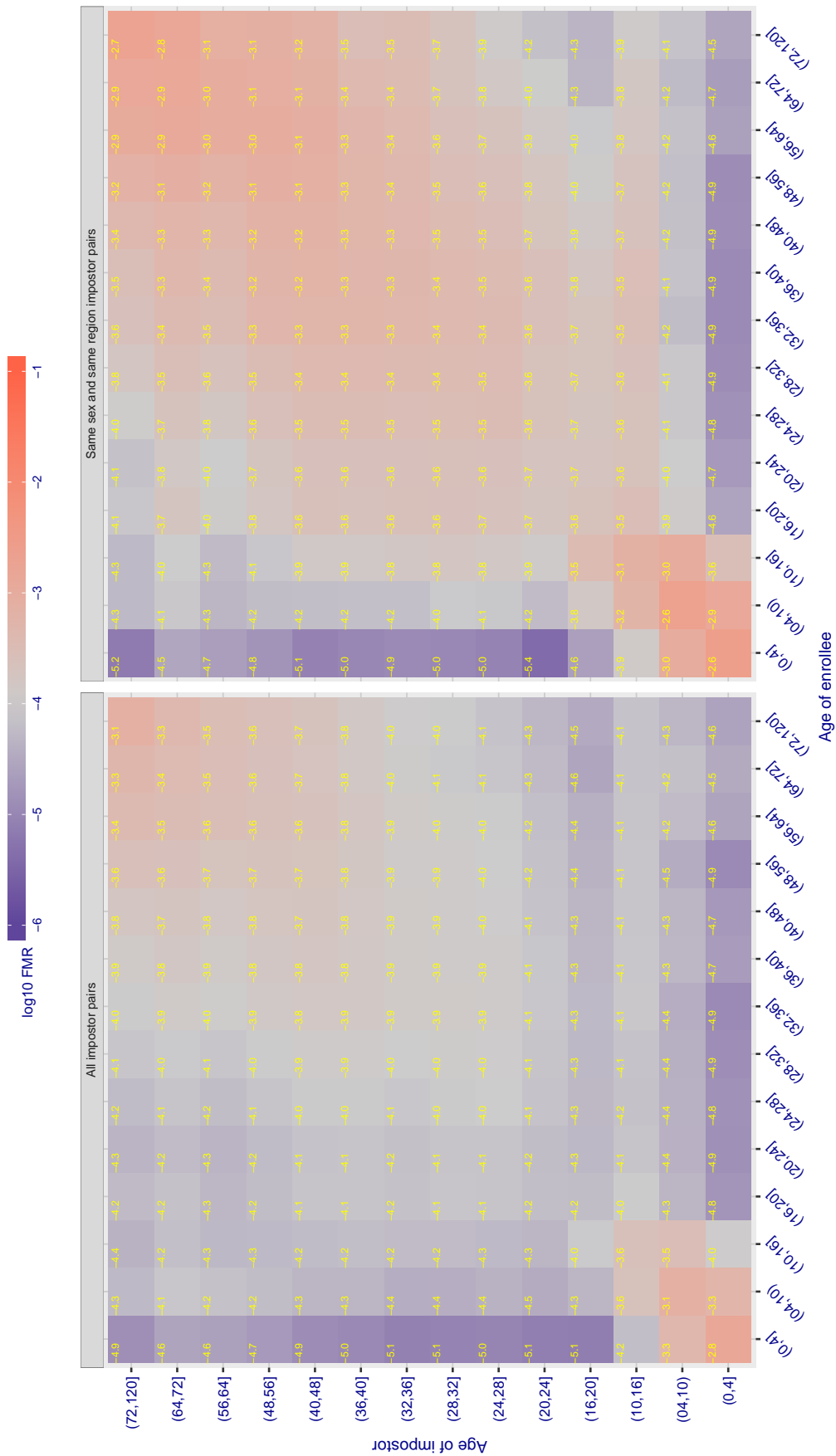


Figure 326: For algorithm `bm-001` operating on visa images, the heatmap shows false match observed over impostor comparisons of faces from different individuals who have the given age pair. False matches are counted against a recognition threshold fixed globally to give $FMR = 0.001$ over all on the order of 10^{10} impostor comparisons. The text in each box gives the same quantity as that coded by the color. Light colors present a security vulnerability to, for example, a passport gate.

Cross age FMR at threshold $T = 0.388$ for algorithm camvi_002, giving $FMR(T) = 0.0001$ globally.

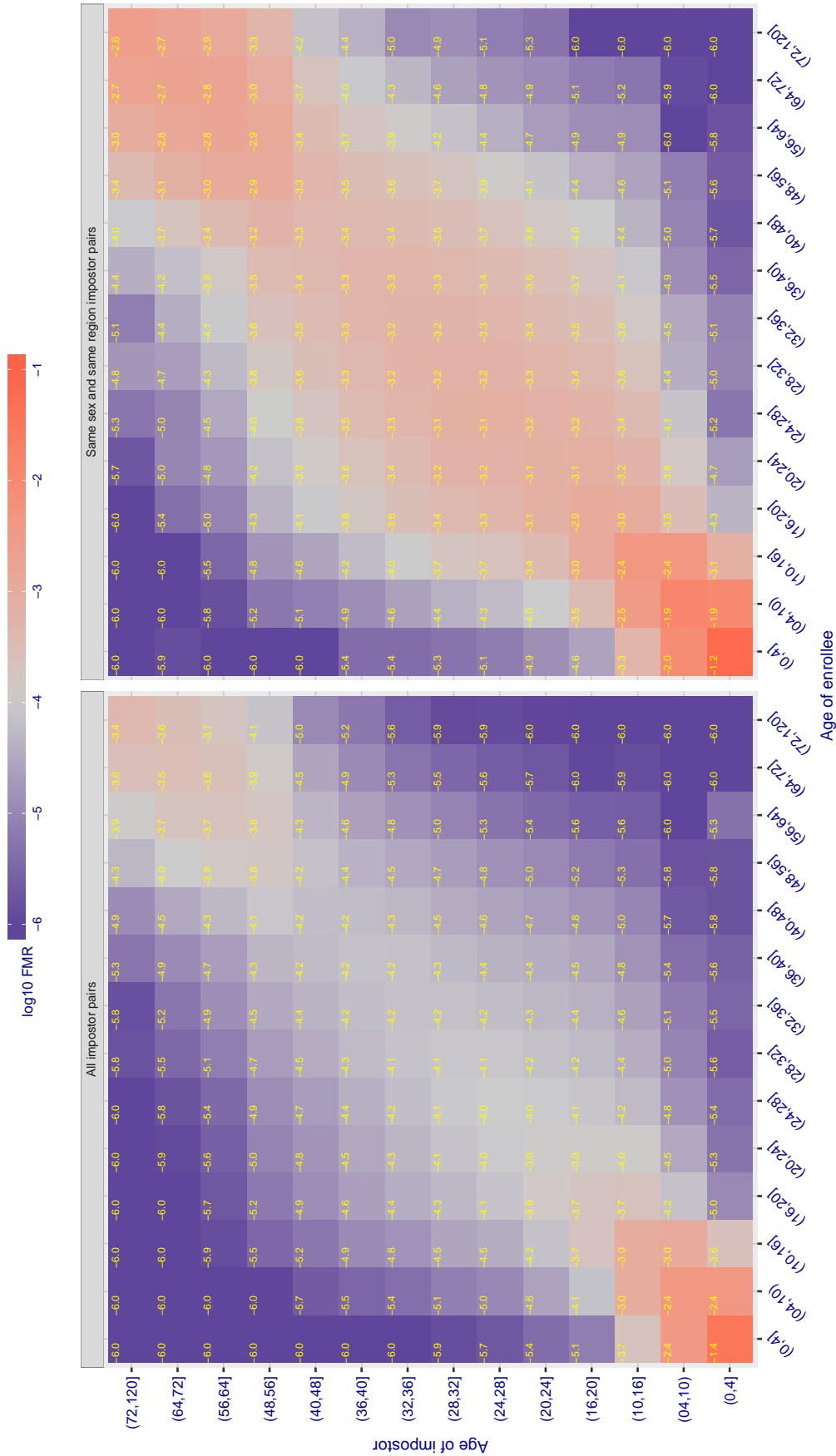


Figure 327: For algorithm camvi-002 operating on visa images, the heatmap shows false match observed over impostor comparisons of faces from different individuals who have the given age pair. False matches are counted against a recognition threshold fixed globally to give $FMR = 0.001$ over all on the order of 10^{10} impostor comparisons. The text in each box gives the same quantity as that coded by the color. Light colors present a security vulnerability to, for example, a passport gate.

Cross age FMR at threshold $T = 0.383$ for algorithm camvi_003, giving $FMR(T) = 0.0001$ globally.

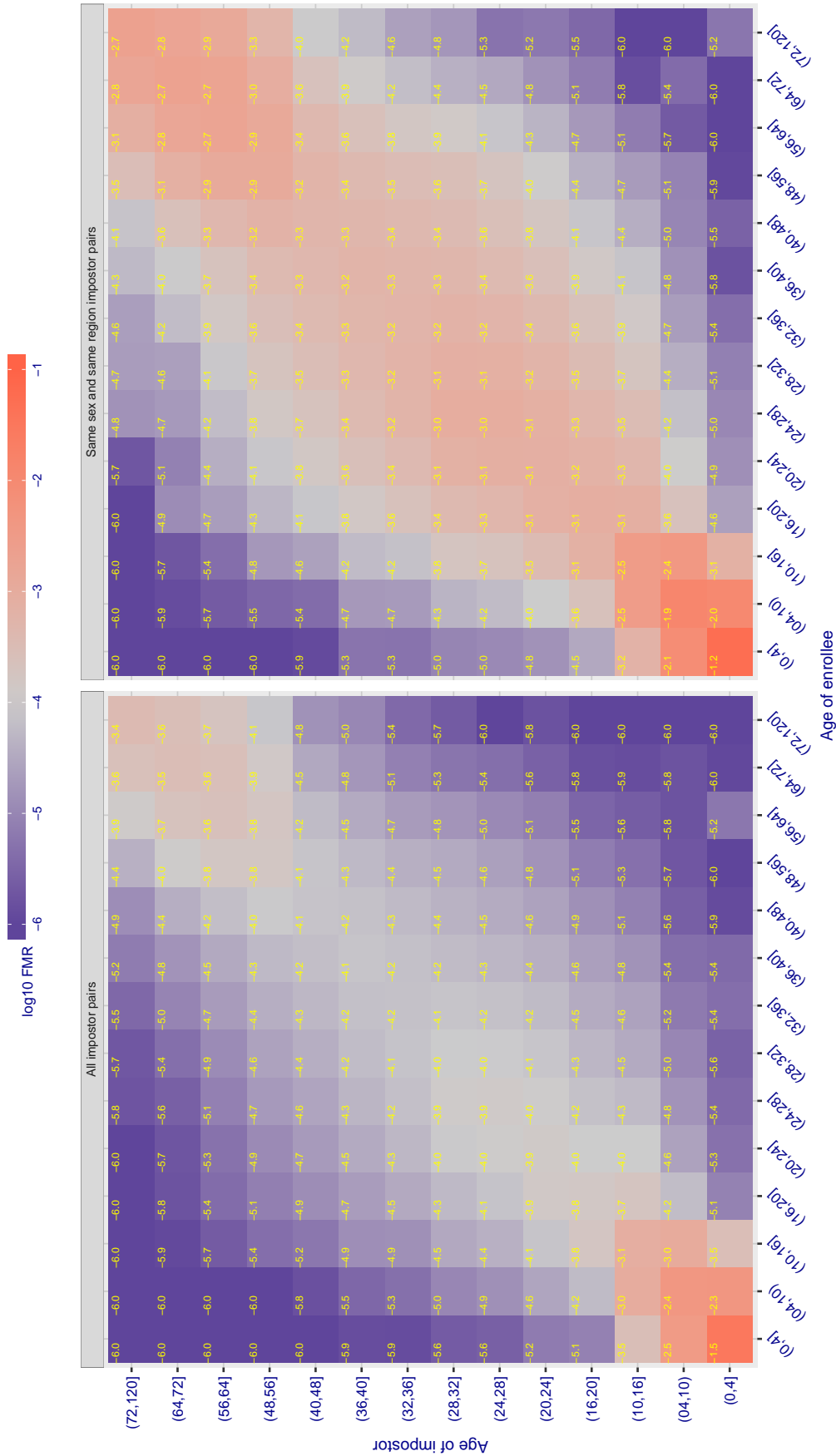


Figure 328: For algorithm camvi-003 operating on visa images, the heatmap shows false match observed over impostor comparisons of faces from different individuals who have the given age pair. False matches are counted against a recognition threshold fixed globally to give $FMR = 0.001$ over all on the order of 10^{10} impostor comparisons. The text in each box gives the same quantity as that coded by the color: Light colors present a security vulnerability to, for example, a passport gate.

Cross age FMR at threshold $T = 0.436$ for algorithm ceiec_001, giving $FMR(T) = 0.0001$ globally.

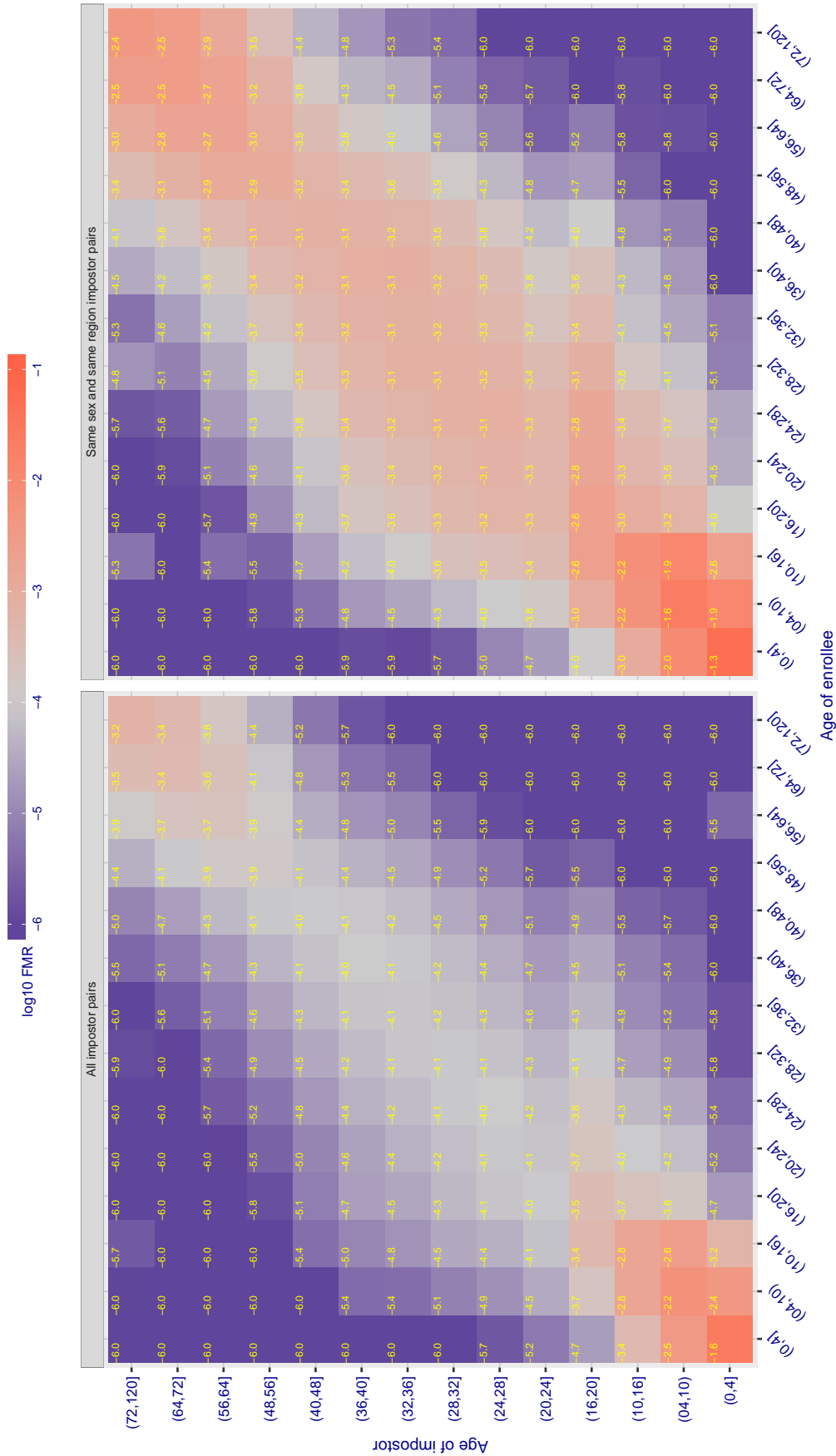


Figure 329: For algorithm ceiec-001 operating on visa images, the heatmap shows false match observed over impostor comparisons of faces from different individuals who have the given age pair. False matches are counted against a recognition threshold fixed globally to give $FMR = 0.001$ over all on the order of 10^{10} impostor comparisons. The text in each box gives the same quantity as that coded by the color. Light colors present a security vulnerability to, for example, a passport gate.

Cross age FMR at threshold $T = 3271.000$ for algorithm cogent_002, giving $FMR(T) = 0.0001$ globally.

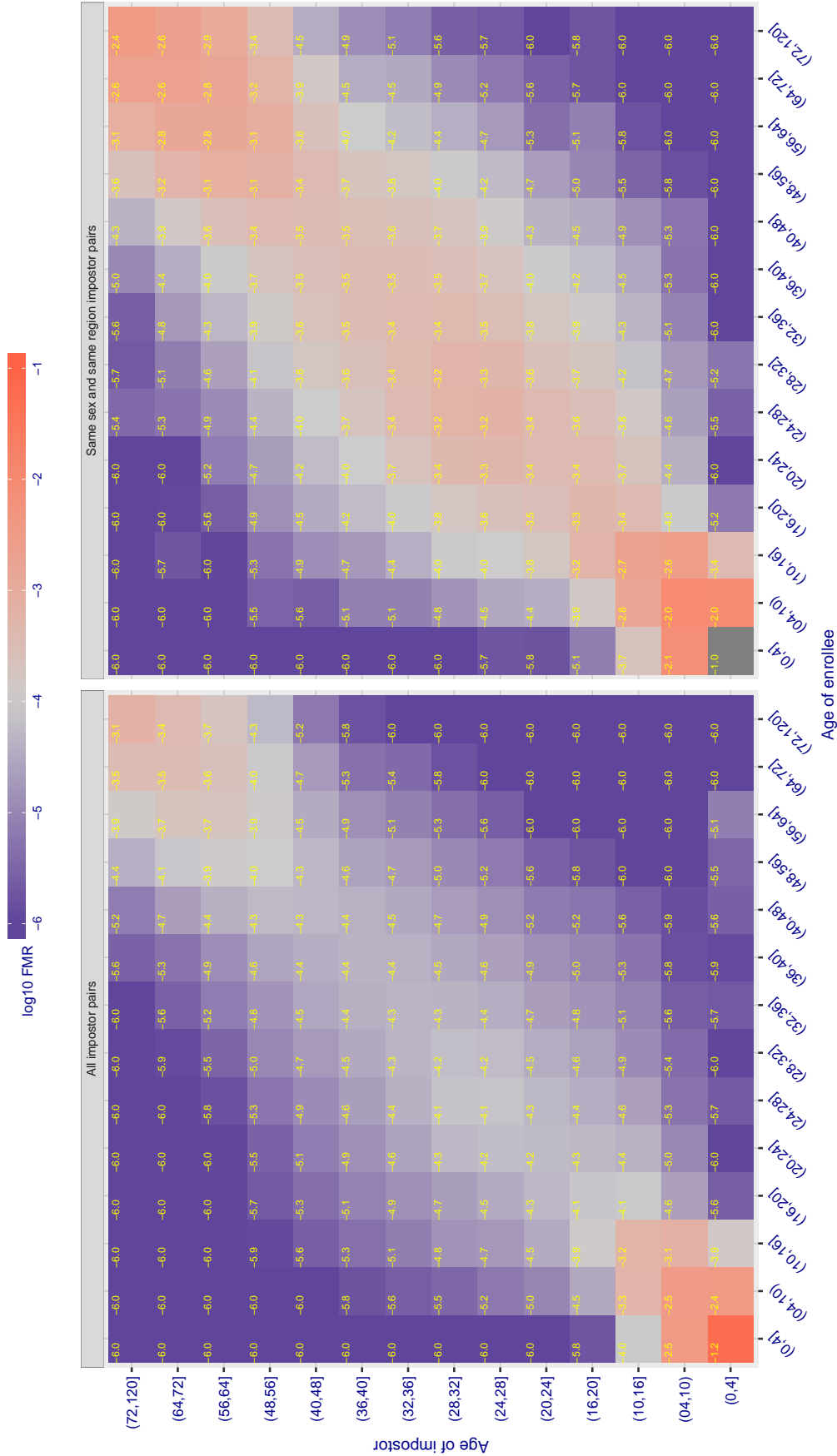


Figure 330: For algorithm cogent-002 operating on visa images, the heatmap shows false match observed over impostor comparisons of faces from different individuals who have the given age pair. False matches are counted against a recognition threshold fixed globally to give $FMR = 0.0001$ over all on the order of 10^{10} impostor comparisons. The text in each box gives the same quantity as that coded by the color. Light colors present a security vulnerability to, for example, a passport gate.

Cross age FMR at threshold $T = 2972.000$ for algorithm cogent_003, giving $FMR(T) = 0.0001$ globally.

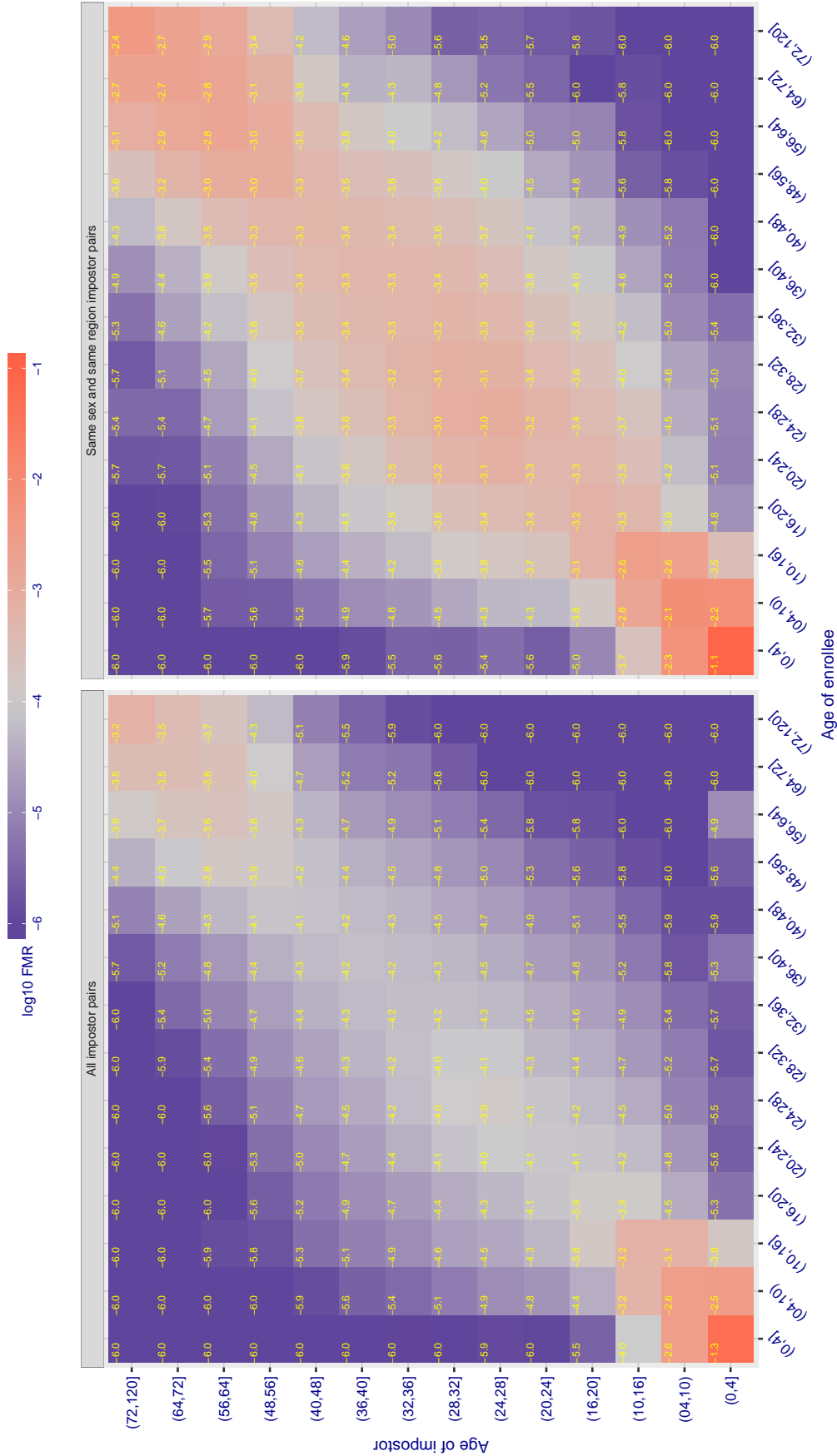


Figure 331: For algorithm cogent-003 operating on visa images, the heatmap shows false match observed over impostor comparisons of faces from different individuals who have the given age pair. False matches are counted against a recognition threshold fixed globally to give $FMR = 0.001$ over all on the order of 10^{10} impostor comparisons. The text in each box gives the same quantity as that coded by the color. Light colors present a security vulnerability to, for example, a passport gate.

Cross age FMR at threshold $T = 0.565$ for algorithm `cognitec_000`, giving $FMR(T) = 0.0001$ globally.

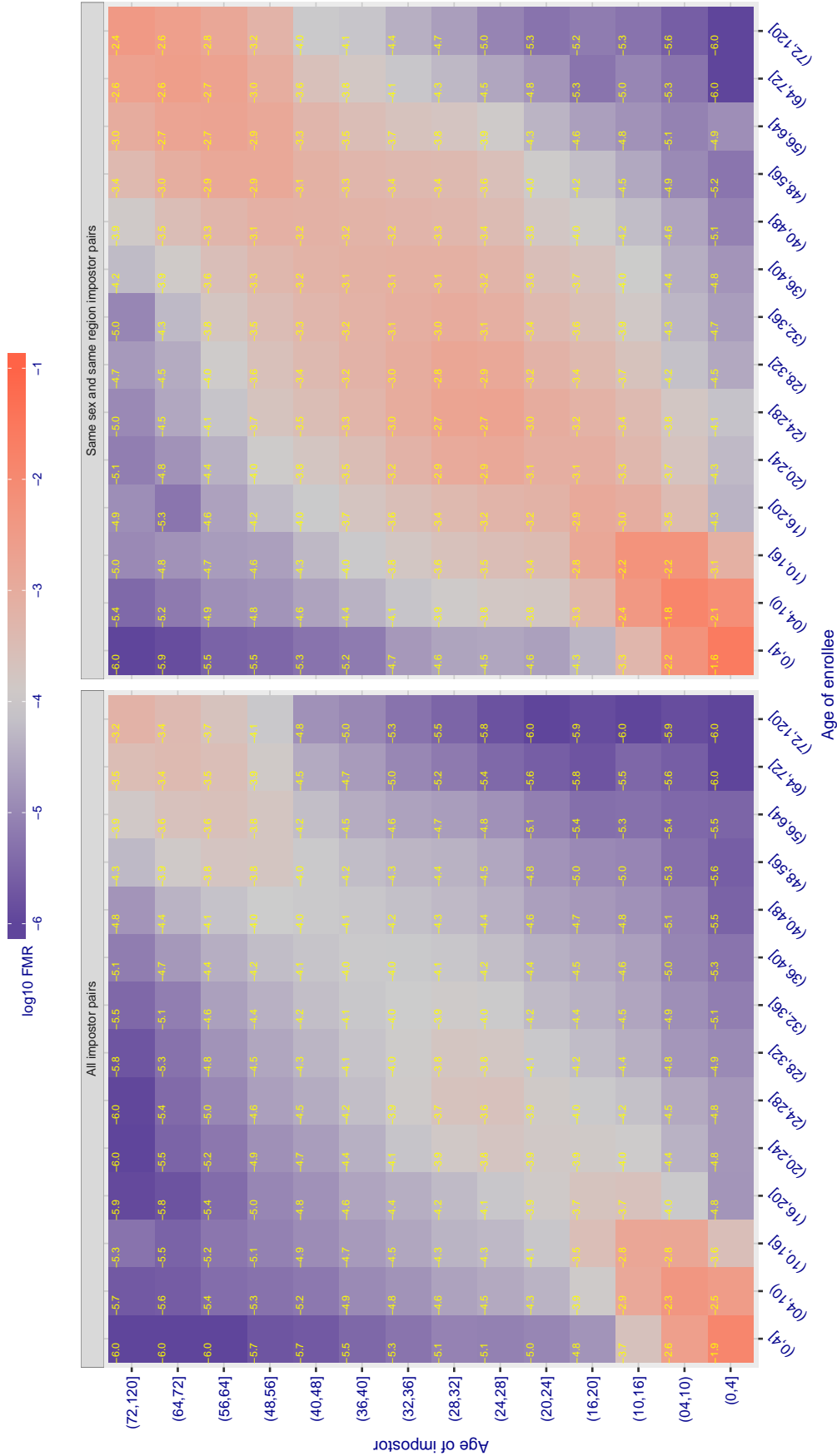


Figure 332: For algorithm `cognitec-000` operating on visa images, the heatmap shows false match observed over impostor comparisons of faces from different individuals who have the given age pair. False matches are counted against a recognition threshold fixed globally to give $FMR = 0.001$ over all on the order of 10^{10} impostor comparisons. The text in each box gives the same quantity as that coded by the color: Light colors present a security vulnerability to, for example, a passport gate.

Cross age FMR at threshold $T = 0.565$ for algorithm `cognitec_001`, giving $FMR(T) = 0.0001$ globally.

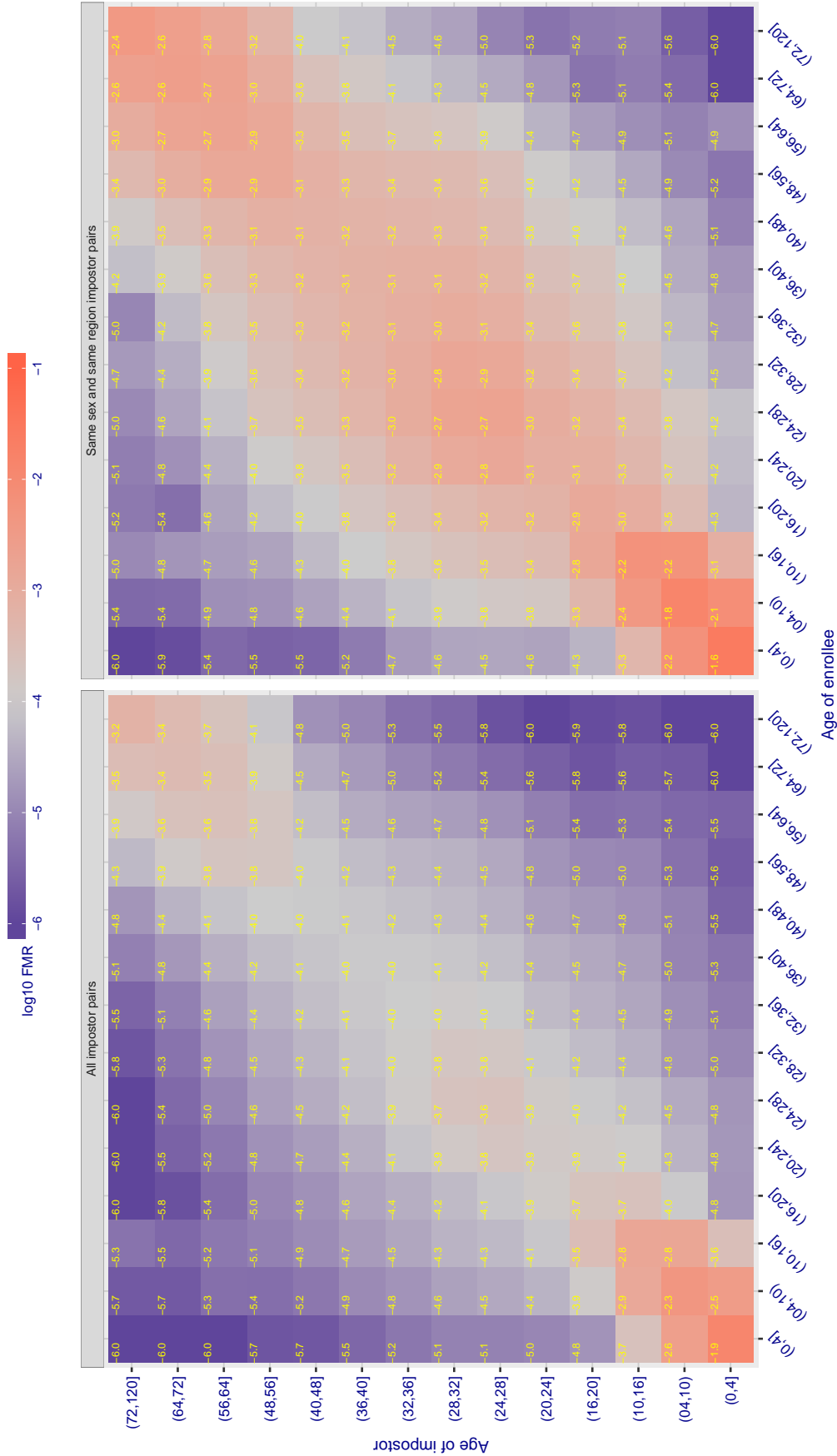


Figure 333: For algorithm `cognitec-001` operating on visa images, the heatmap shows false match observed over impostor comparisons of faces from different individuals who have the given age pair. False matches are counted against a recognition threshold fixed globally to give $FMR = 0.001$ over all on the order of 10^{10} impostor comparisons. The text in each box gives the same quantity as that coded by the color: Light colors present a security vulnerability to, for example, a passport gate.

Cross age FMR at threshold $T = 0.762$ for algorithm cyberextruder_001, giving $FMR(T) = 0.0001$ globally.

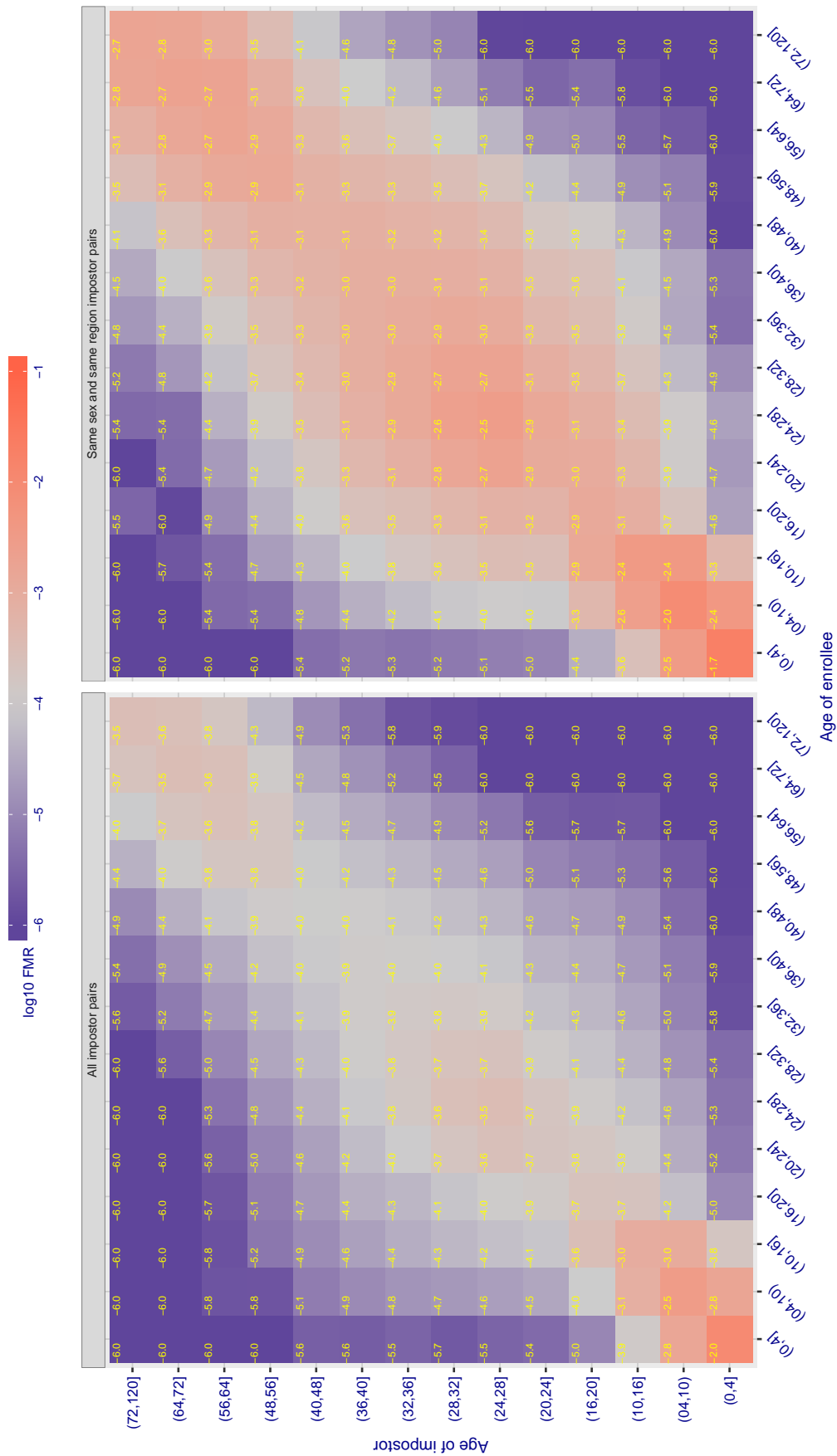


Figure 334: For algorithm cyberextruder-001 operating on visa images, the heatmap shows false match observed over impostor comparisons of faces from different individuals who have the given age pair. False matches are counted against a recognition threshold fixed globally to give $FMR = 0.001$ over all on the order of 10^{10} impostor comparisons. The text in each box gives the same quantity as that coded by the color. Light colors present a security vulnerability to, for example, a passport gate.

Cross age FMR at threshold $T = 0.500$ for algorithm cyberextruder_002, giving $FMR(T) = 0.0001$ globally.

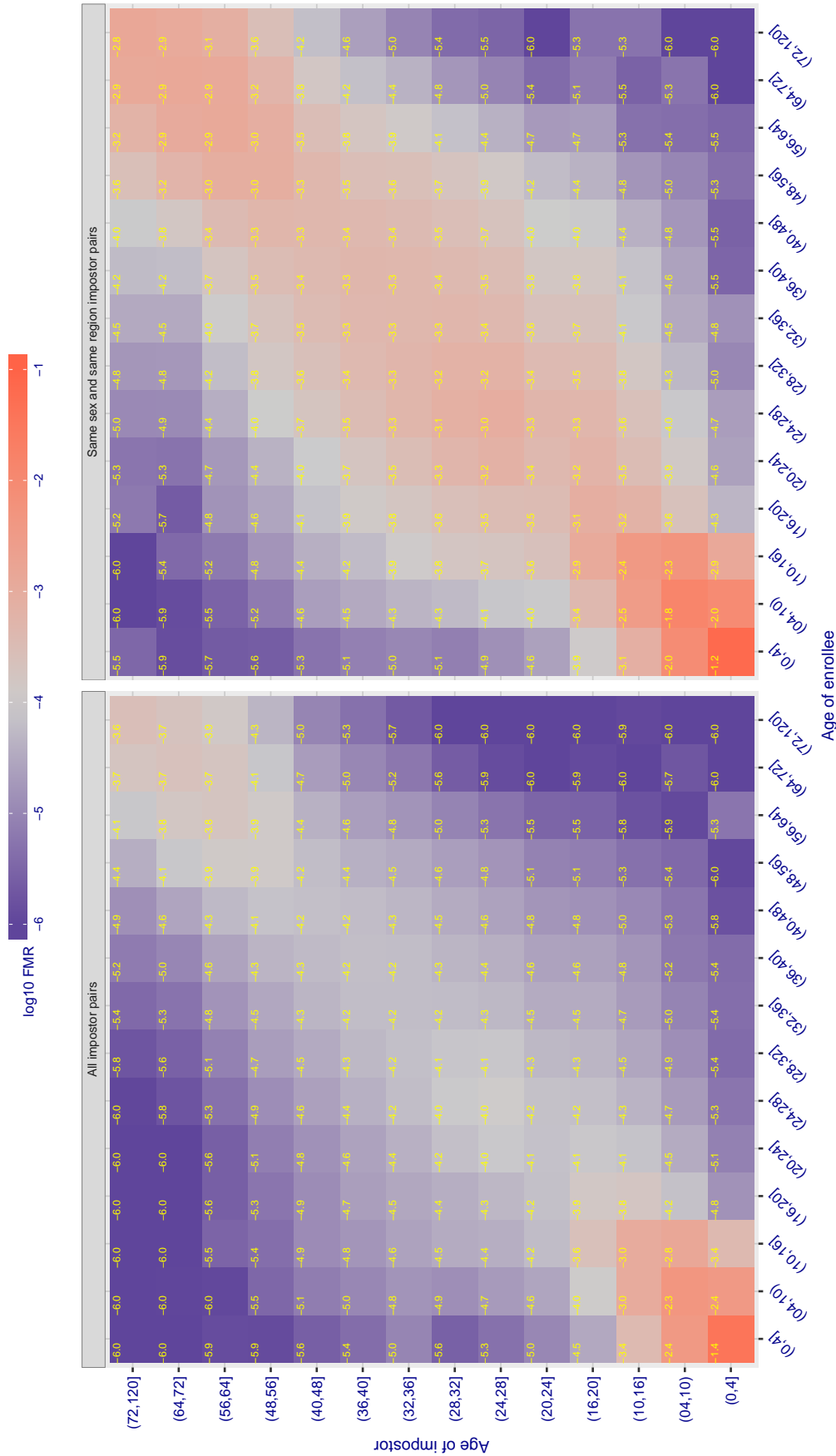


Figure 335: For algorithm cyberextruder-002 operating on visa images, the heatmap shows false match observed over impostor comparisons of faces from different individuals who have the given age pair. False matches are counted against a recognition threshold fixed globally to give $FMR = 0.001$ over all on the order of 10^{10} impostor comparisons. The text in each box gives the same quantity as that coded by the color. Light colors present a security vulnerability to, for example, a passport gate.

Cross age FMR at threshold $T = 1.409$ for algorithm cyberlink_000, giving $FMR(T) = 0.0001$ globally.

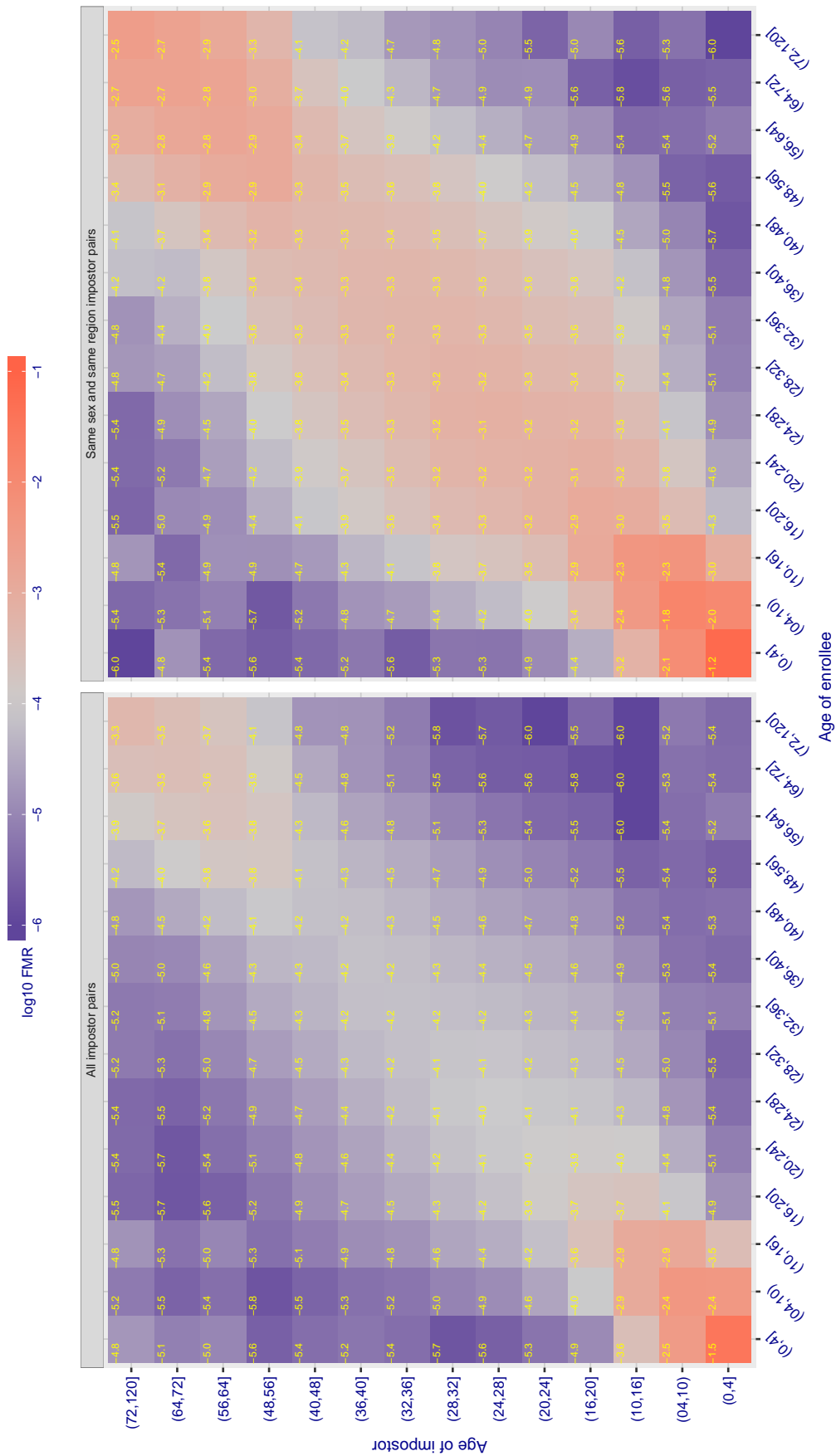


Figure 336: For algorithm cyberlink-000 operating on visa images, the heatmap shows false match observed over impostor comparisons of faces from different individuals who have the given age pair. False matches are counted against a recognition threshold fixed globally to give $FMR = 0.001$ over all on the order of 10^{10} impostor comparisons. The text in each box gives the same quantity as that coded by the color: Light colors present a security vulnerability to, for example, a passport gate.

Cross age FMR at threshold $T = 1.408$ for algorithm cyberlink_001, giving $FMR(T) = 0.0001$ globally.

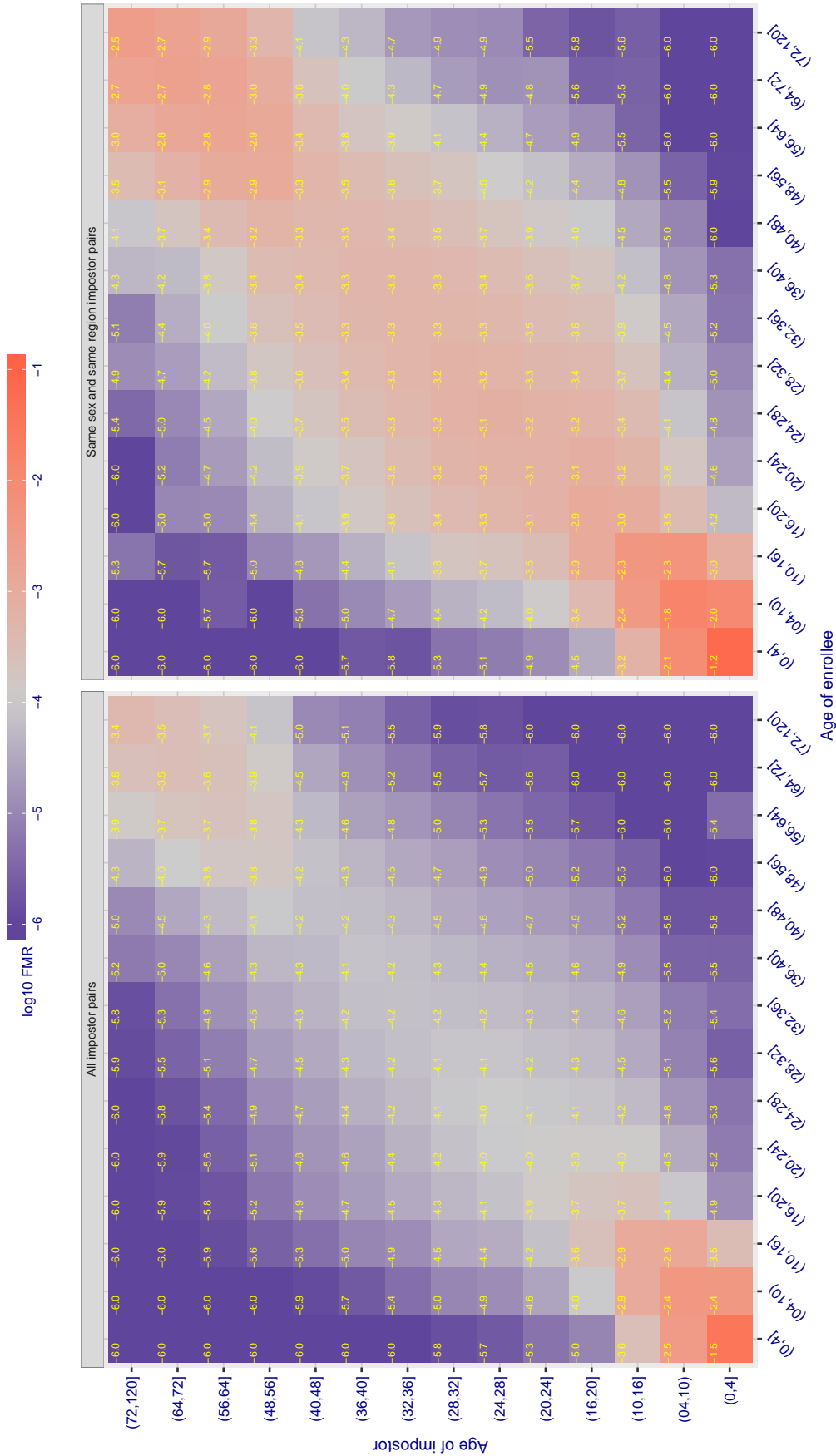


Figure 337: For algorithm cyberlink-001 operating on visa images, the heatmap shows false match observed over impostor comparisons of faces from different individuals who have the given age pair. False matches are counted against a recognition threshold fixed globally to give $FMR = 0.001$ over all on the order of 10^{10} impostor comparisons. The text in each box gives the same quantity as that coded by the color. Light colors present a security vulnerability to, for example, a passport gate.

Cross age FMR at threshold $T = 7630.000$ for algorithm dahua_001, giving $FMR(T) = 0.0001$ globally.

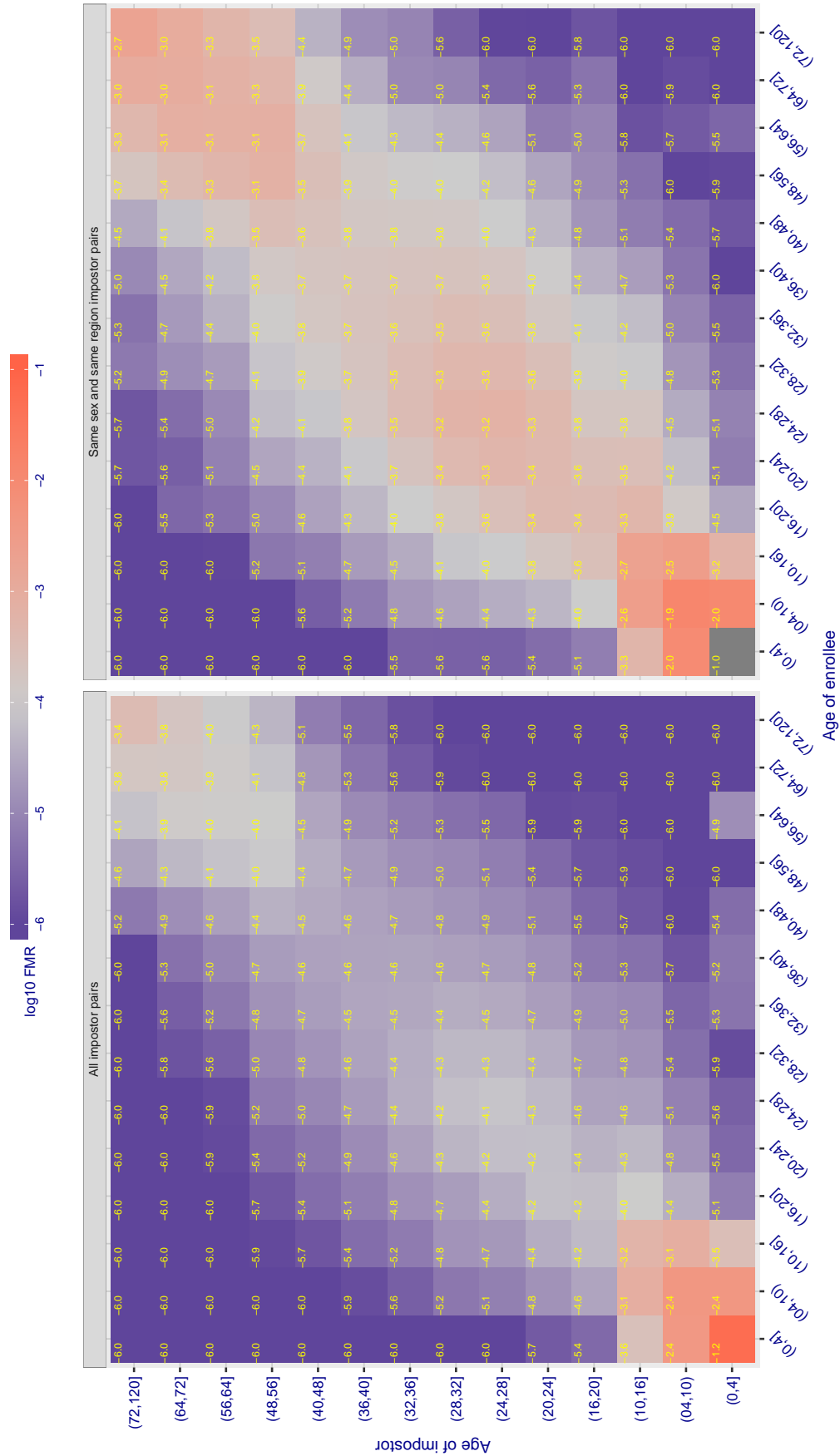


Figure 338: For algorithm dahua-001 operating on visa images, the heatmap shows false match observed over impostor comparisons of faces from different individuals who have the given age pair. False matches are counted against a recognition threshold fixed globally to give $FMR = 0.0001$ over all on the order of 10^{10} impostor comparisons. The text in each box gives the same quantity as that coded by the color. Light colors present a security vulnerability to, for example, a passport gate.

Cross age FMR at threshold $T = 6696.000$ for algorithm dahua_002, giving $FMR(T) = 0.0001$ globally.

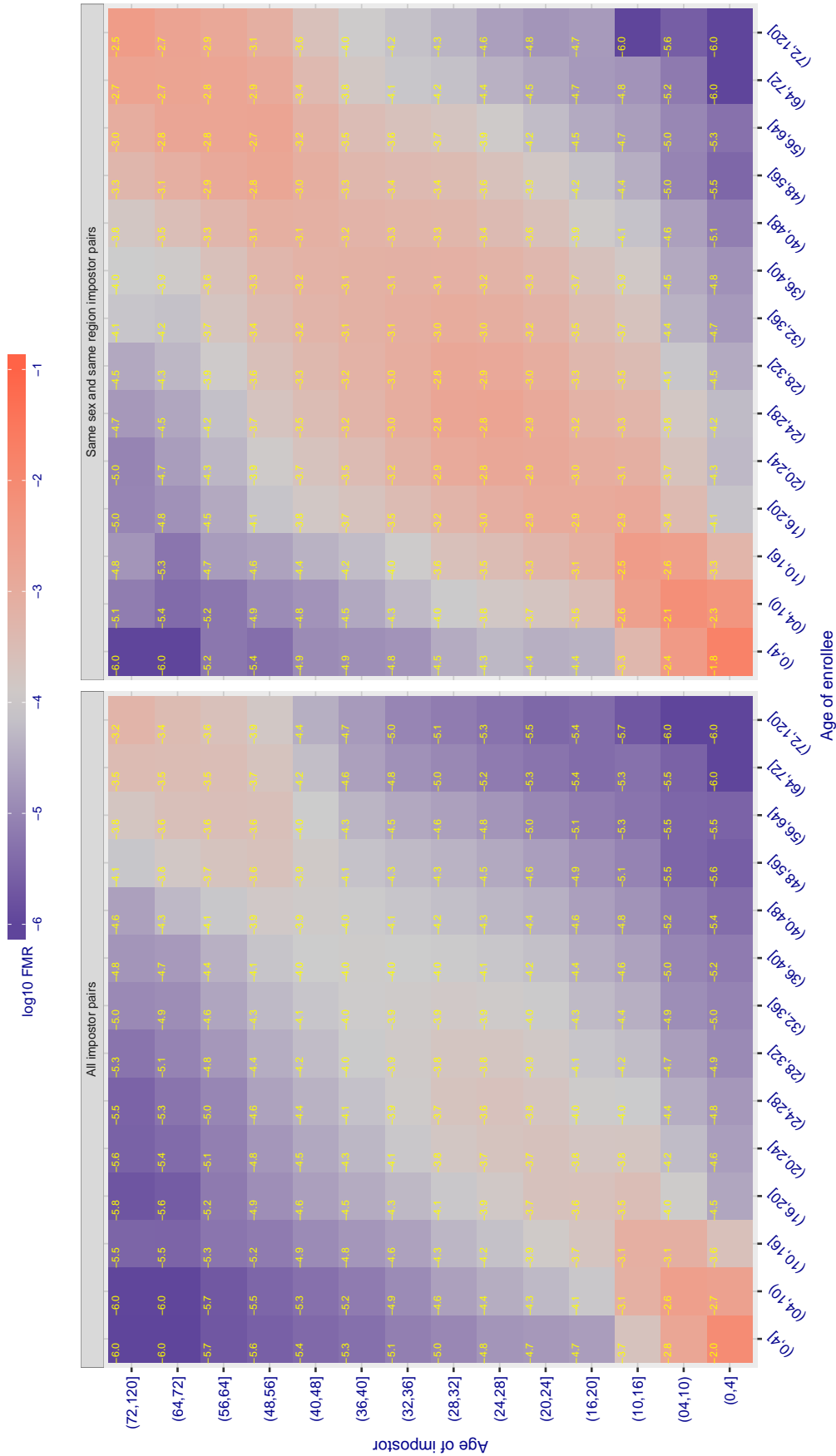


Figure 339: For algorithm dahua-002 operating on visa images, the heatmap shows false match observed over impostor comparisons of faces from different individuals who have the given age pair. False matches are counted against a recognition threshold fixed globally to give $FMR = 0.0001$ over all on the order of 10^{10} impostor comparisons. The text in each box gives the same quantity as that coded by the color. Light colors present a security vulnerability to, for example, a passport gate.

Cross age FMR at threshold $T = 79.344$ for algorithm dermalog_005, giving $FMR(T) = 0.0001$ globally.

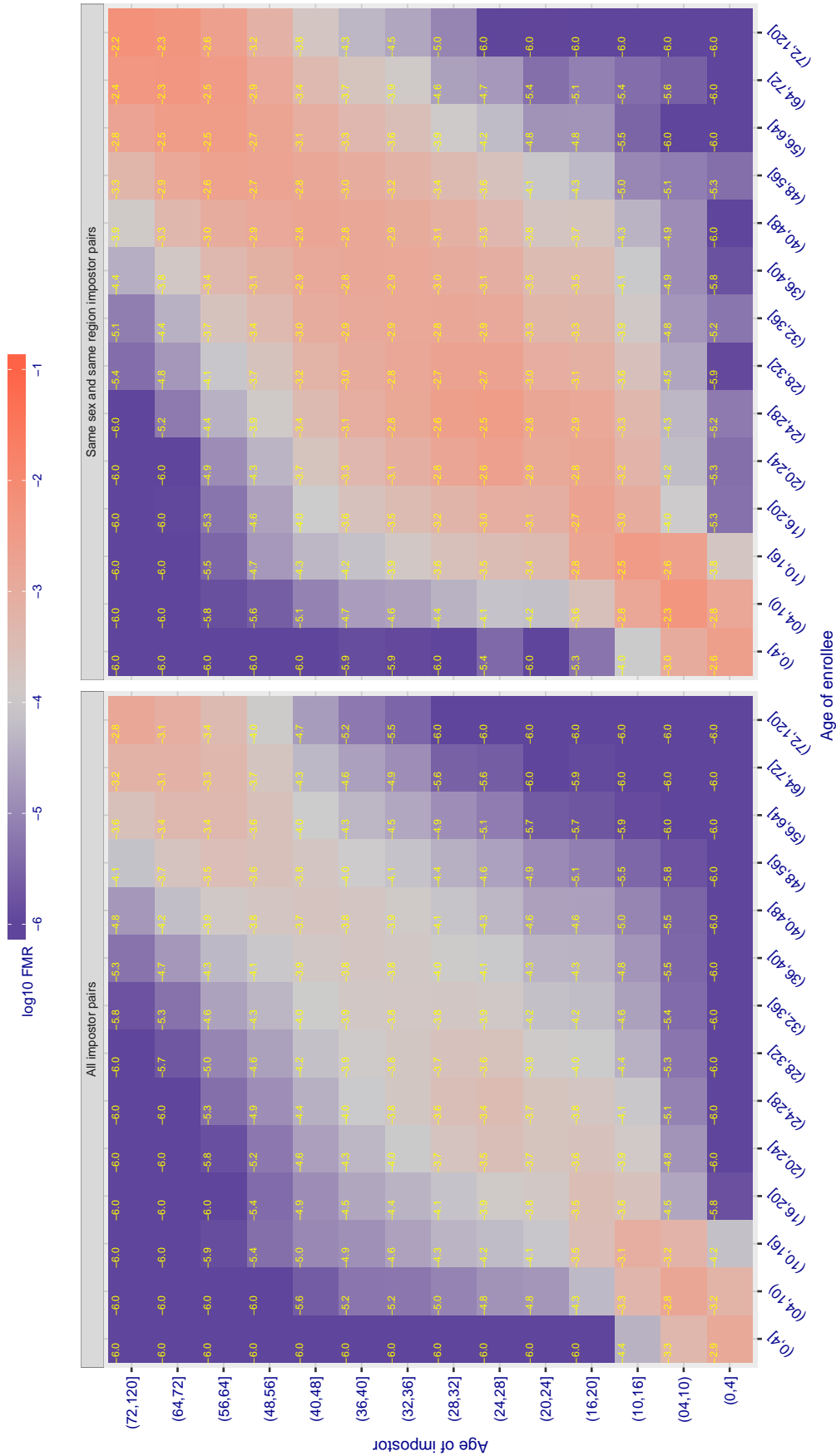


Figure 340: For algorithm dermalog-005 operating on visa images, the heatmap shows false match observed over impostor comparisons of faces from different individuals who have the given age pair. False matches are counted against a recognition threshold fixed globally to give $FMR = 0.001$ over all on the order of 10^{10} impostor comparisons. The text in each box gives the same quantity as that coded by the color. Light colors present a security vulnerability to, for example, a passport gate.

Cross age FMR at threshold $T = 79.670$ for algorithm dermalog_006, giving $FMR(T) = 0.0001$ globally.

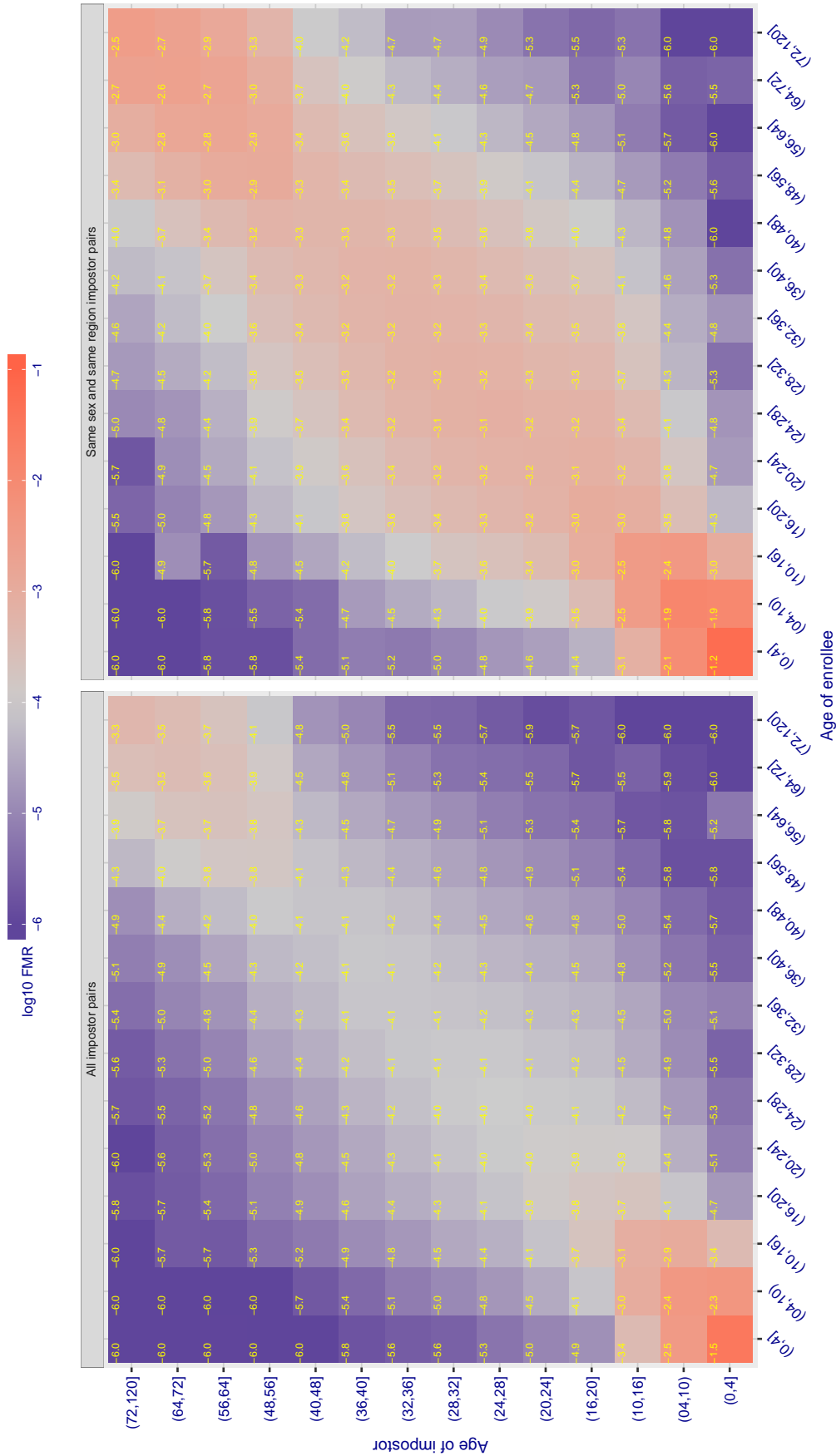


Figure 341: For algorithm dermalog-006 operating on visa images, the heatmap shows false match observed over impostor comparisons of faces from different individuals who have the given age pair. False matches are counted against a recognition threshold fixed globally to give $FMR = 0.001$ over all on the order of 10^{10} impostor comparisons. The text in each box gives the same quantity as that coded by the color. Light colors present a security vulnerability to, for example, a passport gate.

Cross age FMR at threshold $T = 0.675$ for algorithm digitalbarriers_002, giving $FMR(T) = 0.0001$ globally.

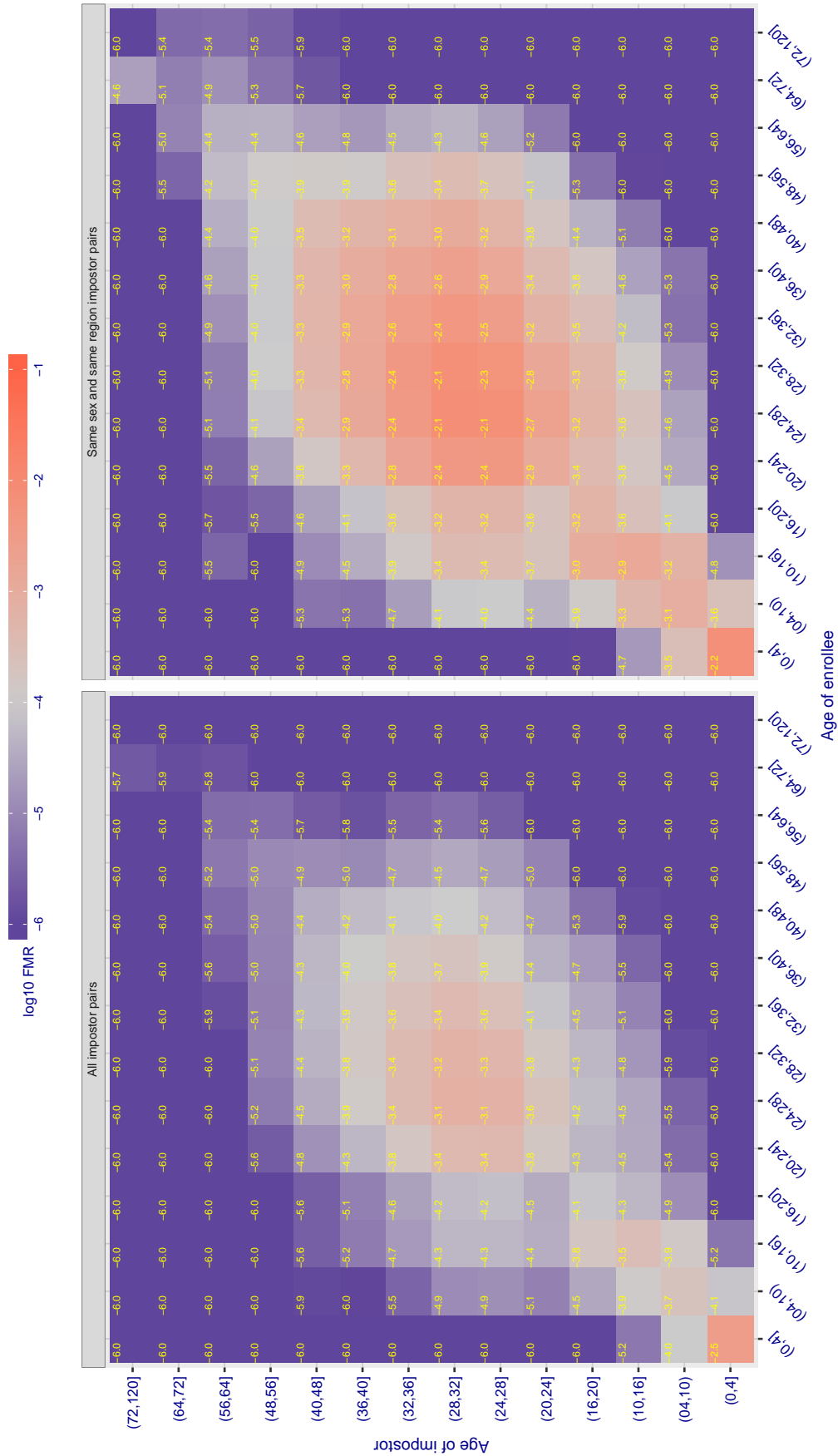


Figure 342: For algorithm digitalbarriers-002 operating on visa images, the heatmap shows false match observed over impostor comparisons of faces from different individuals who have the given age pair. False matches are counted against a recognition threshold fixed globally to give $FMR = 0.001$ over all on the order of 10^{10} impostor comparisons. The text in each box gives the same quantity as that coded by the color. Light colors present a security vulnerability to, for example, a passport gate.

Cross age FMR at threshold $T = 2.672$ for algorithm everai_001, giving $FMR(T) = 0.0001$ globally.

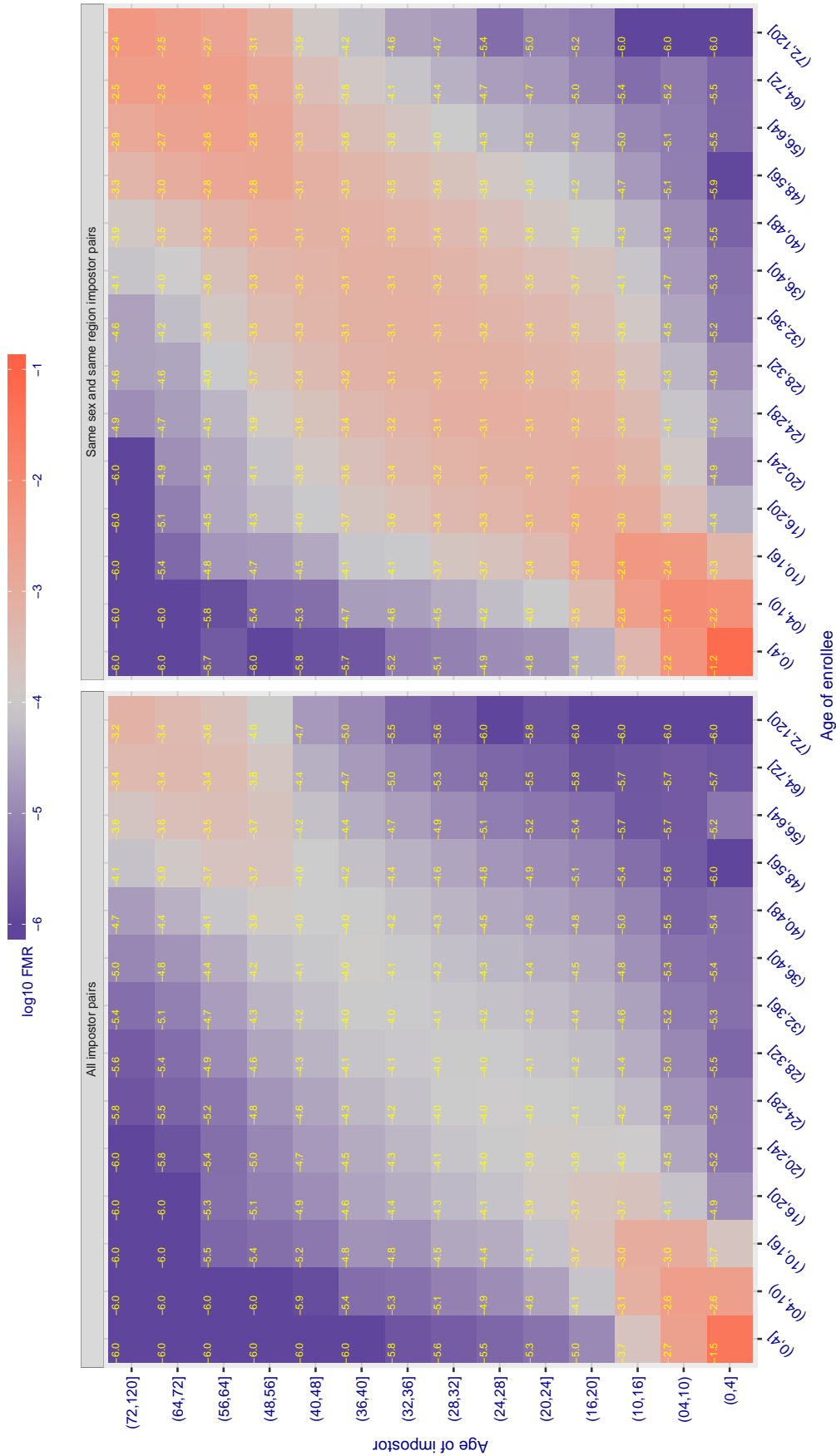


Figure 343: For algorithm everai-001 operating on visa images, the heatmap shows false match observed over impostor comparisons of faces from different individuals who have the given age pair. False matches are counted against a recognition threshold fixed globally to give $FMR = 0.001$ over all on the order of 10^{10} impostor comparisons. The text in each box gives the same quantity as that coded by the color. Light colors present a security vulnerability to, for example, a passport gate.

Cross age FMR at threshold $T = 2.589$ for algorithm everai_002, giving $FMR(T) = 0.0001$ globally.

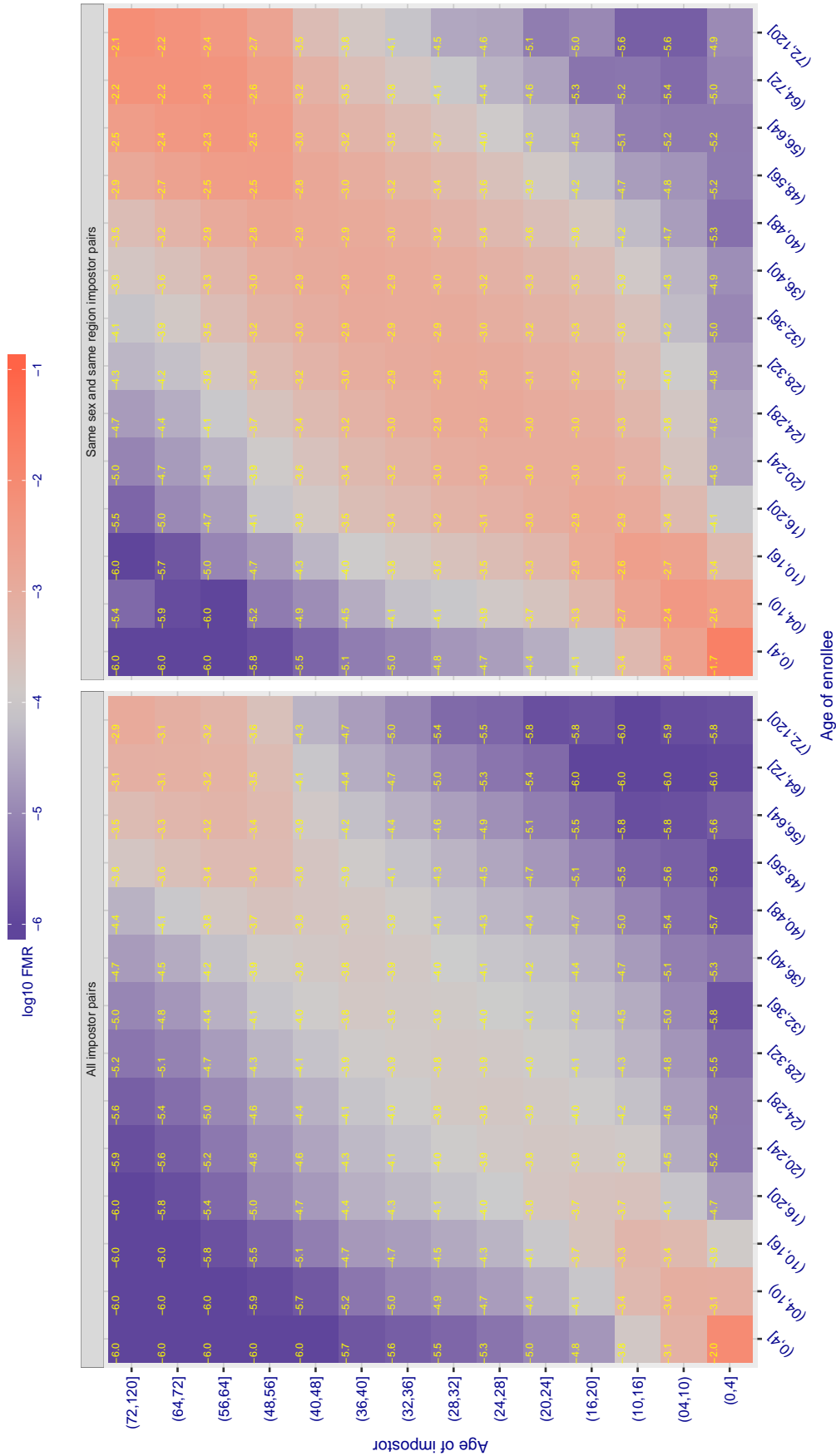


Figure 344: For algorithm everai-002 operating on visa images, the heatmap shows false match observed over impostor comparisons of faces from different individuals who have the given age pair. False matches are counted against a recognition threshold fixed globally to give $FMR = 0.001$ over all on the order of 10^{10} impostor comparisons. The text in each box gives the same quantity as that coded by the color. Light colors present a security vulnerability to, for example, a passport gate.

Cross age FMR at threshold $T = 0.618$ for algorithm glory_001, giving $FMR(T) = 0.0001$ globally.

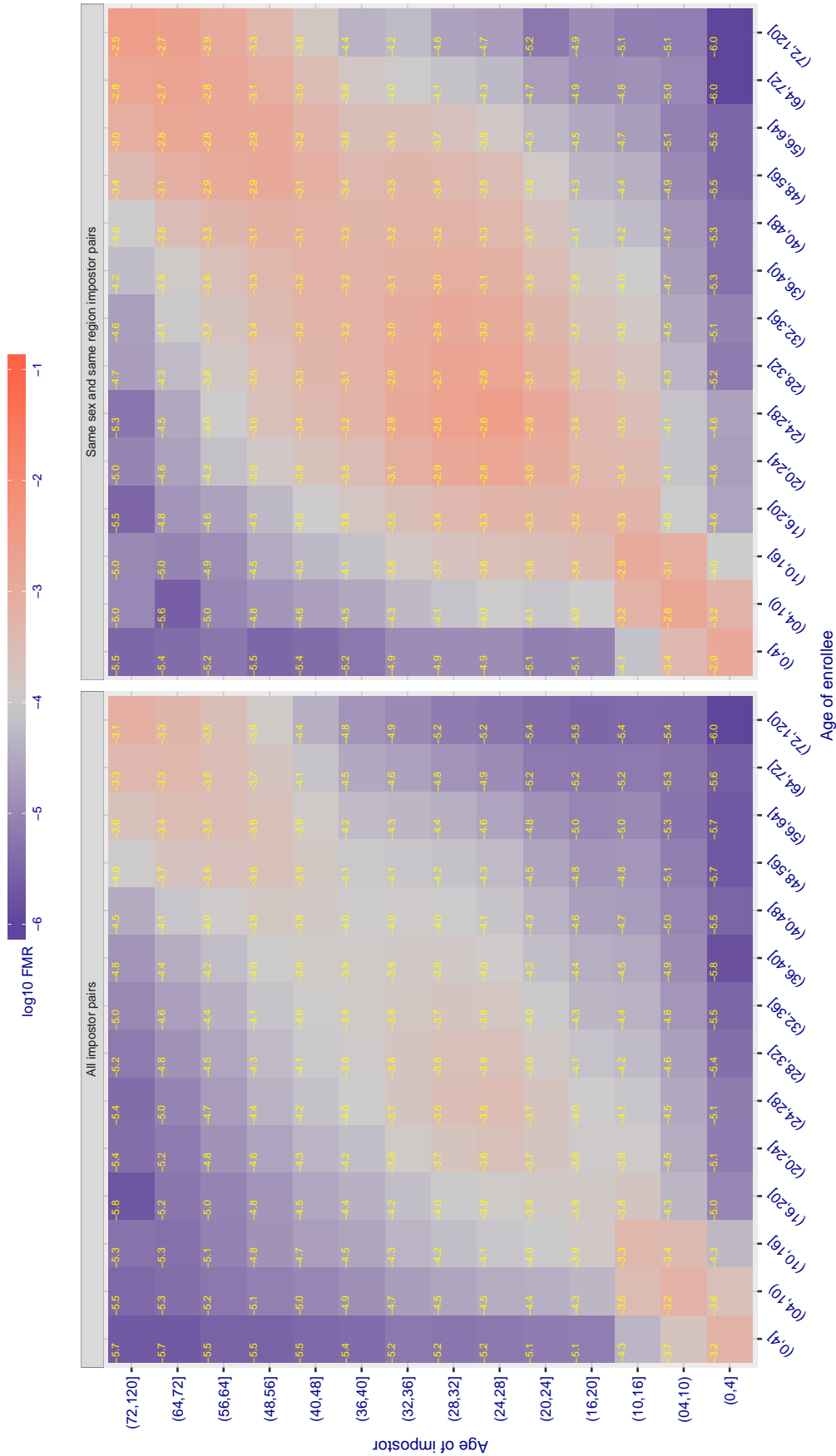


Figure 345: For algorithm glory-001 operating on visa images, the heatmap shows false match observed over impostor comparisons of faces from different individuals who have the given age pair. False matches are counted against a recognition threshold fixed globally to give $FMR = 0.001$ over all on the order of 10^{10} impostor comparisons. The text in each box gives the same quantity as that coded by the color: Light colors present a security vulnerability to, for example, a passport gate.

Cross age FMR at threshold $T = 0.559$ for algorithm gorilla_001, giving $FMR(T) = 0.0001$ globally.

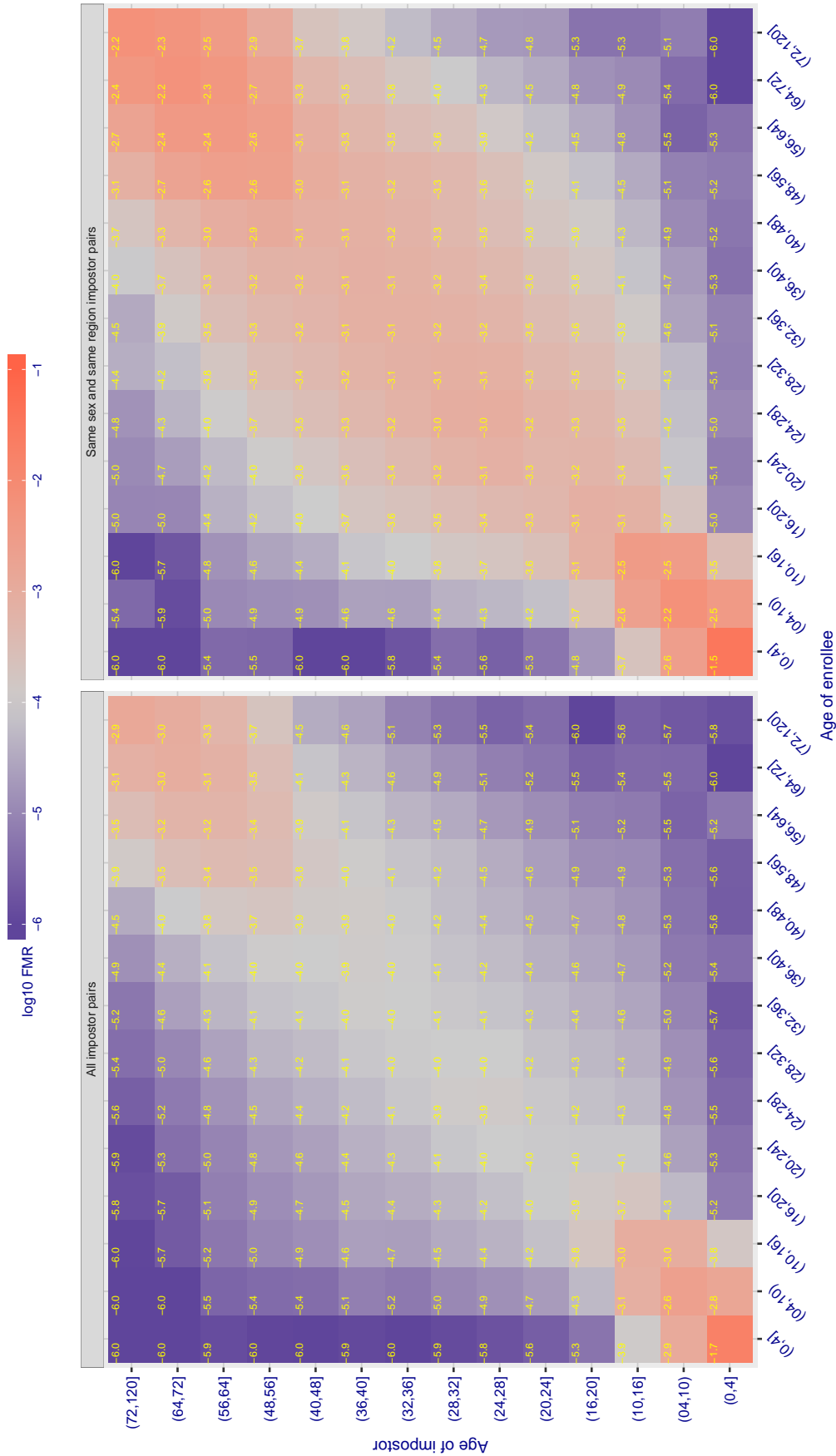


Figure 346: For algorithm gorilla-001 operating on visa images, the heatmap shows false match observed over impostor comparisons of faces from different individuals who have the given age pair. False matches are counted against a recognition threshold fixed globally to give $FMR = 0.001$ over all on the order of 10^{10} impostor comparisons. The text in each box gives the same quantity as that coded by the color: Light colors present a security vulnerability to, for example, a passport gate.

Cross age FMR at threshold $T = 0.483$ for algorithm gorilla_002, giving $FMR(T) = 0.0001$ globally.

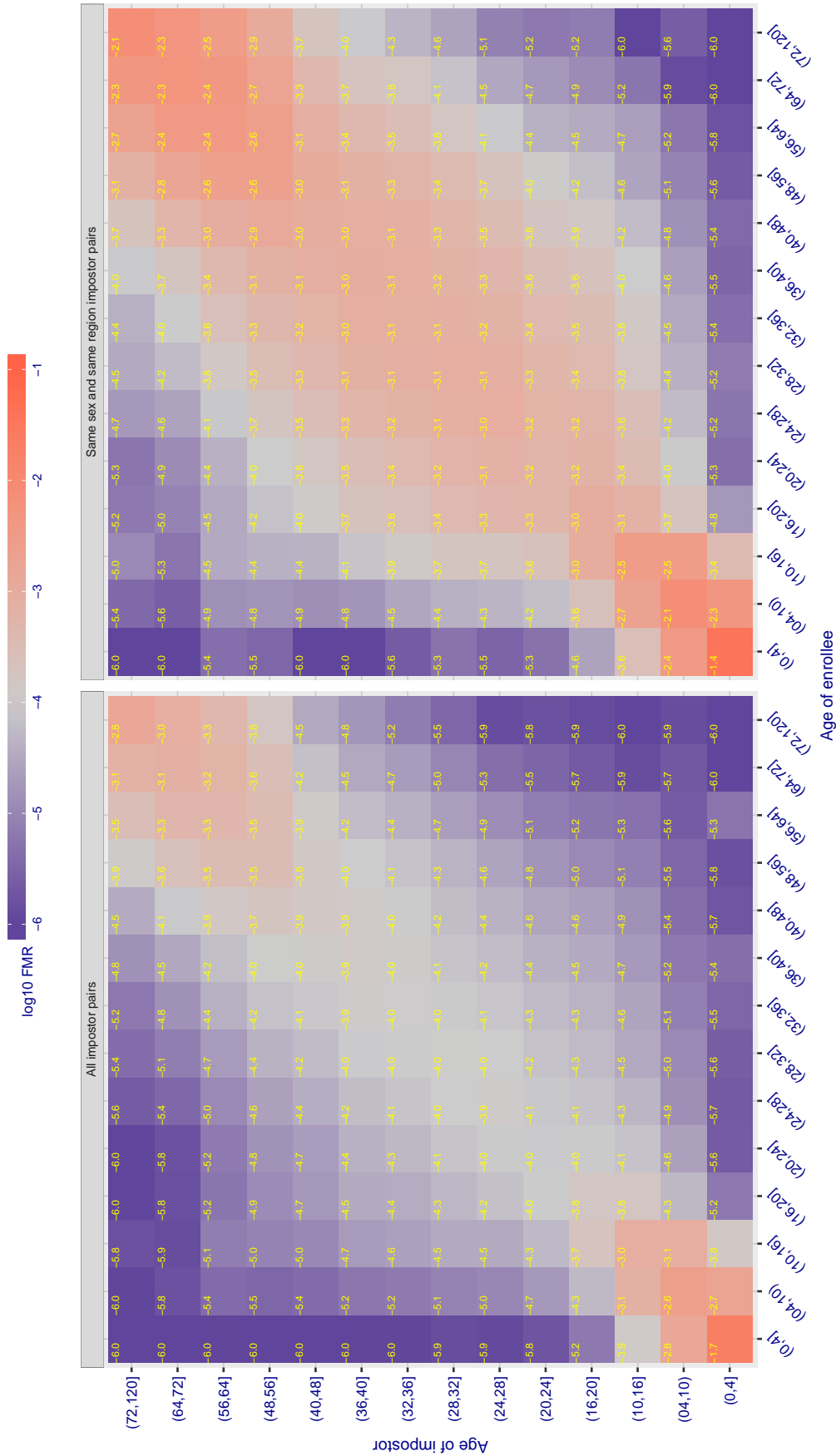


Figure 347: For algorithm gorilla-002 operating on visa images, the heatmap shows false match observed over impostor comparisons of faces from different individuals who have the given age pair. False matches are counted against a recognition threshold fixed globally to give $FMR = 0.0001$ over all on the order of 10^{10} impostor comparisons. The text in each box gives the same quantity as that coded by the color. Light colors present a security vulnerability to, for example, a passport gate.

Cross age FMR at threshold $T = 66.565$ for algorithm hik_001, giving $FMR(T) = 0.0001$ globally.

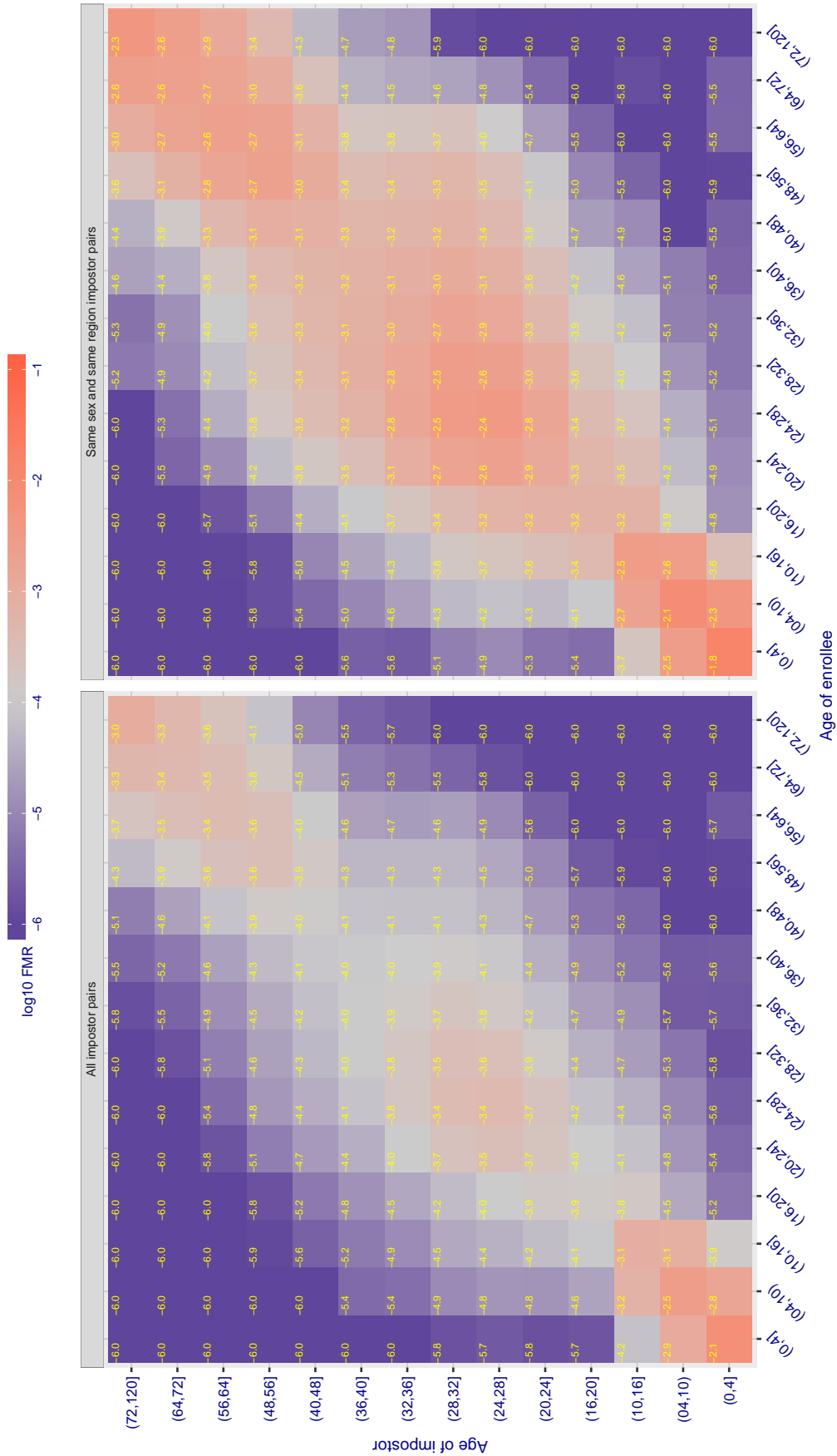


Figure 348: For algorithm hik-001 operating on visa images, the heatmap shows false match observed over impostor comparisons of faces from different individuals who have the given age pair. False matches are counted against a recognition threshold fixed globally to give $FMR = 0.001$ over all on the order of 10^{10} impostor comparisons. The text in each box gives the same quantity as that coded by the color. Light colors present a security vulnerability to, for example, a passport gate.

Cross age FMR at threshold $T = 0.971$ for algorithm hr_000, giving $FMR(T) = 0.0001$ globally.

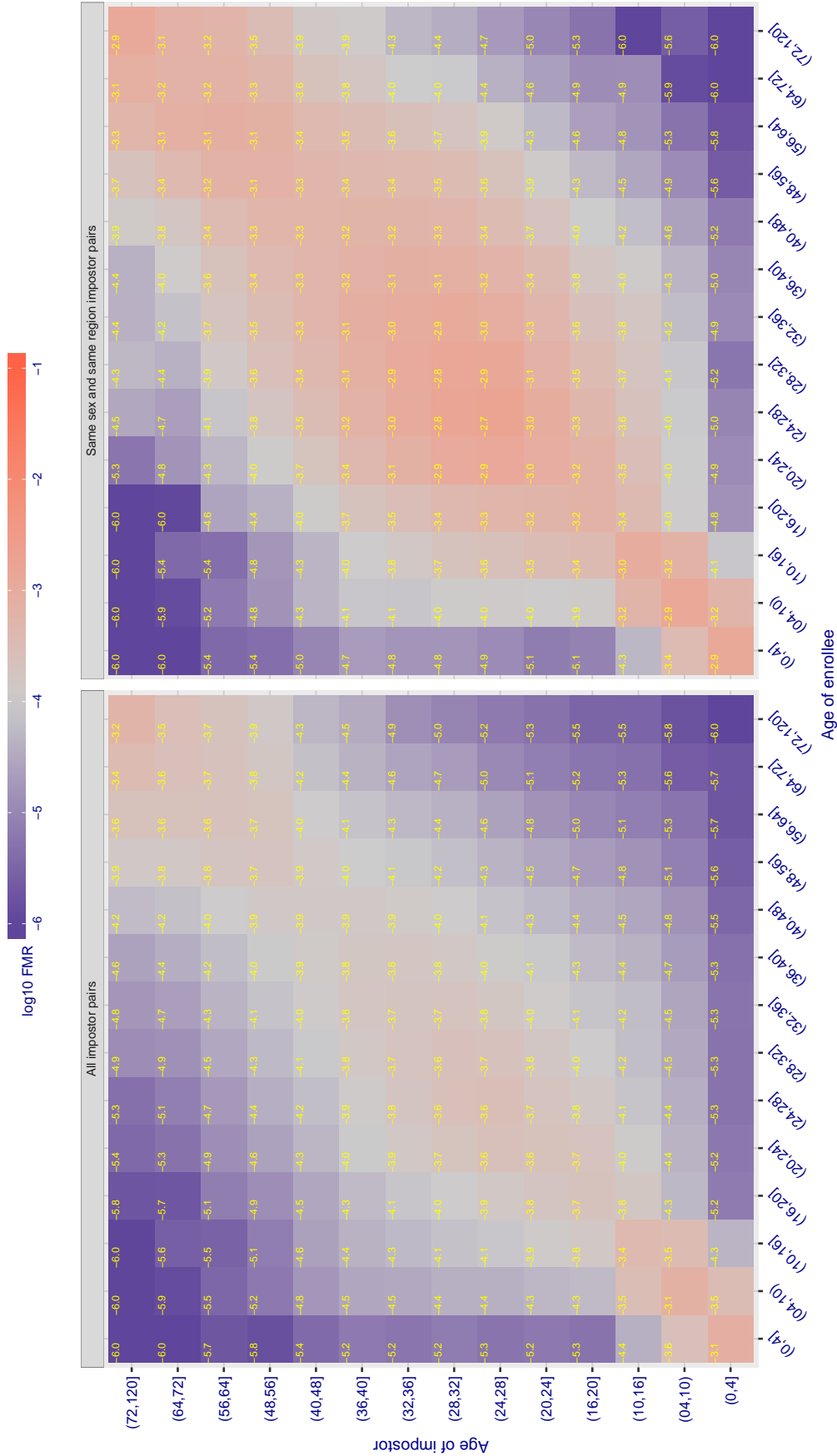


Figure 349: For algorithm hr-000 operating on visa images, the heatmap shows false match observed over impostor comparisons of faces from different individuals who have the given age pair. False matches are counted against a recognition threshold fixed globally to give $FMR = 0.0001$ over all on the order of 10^{10} impostor comparisons. The text in each box gives the same quantity as that coded by the color. Light colors present a security vulnerability to, for example, a passport gate.

Cross age FMR at threshold $T = 37645.000$ for algorithm id3_003, giving $FMR(T) = 0.0001$ globally.

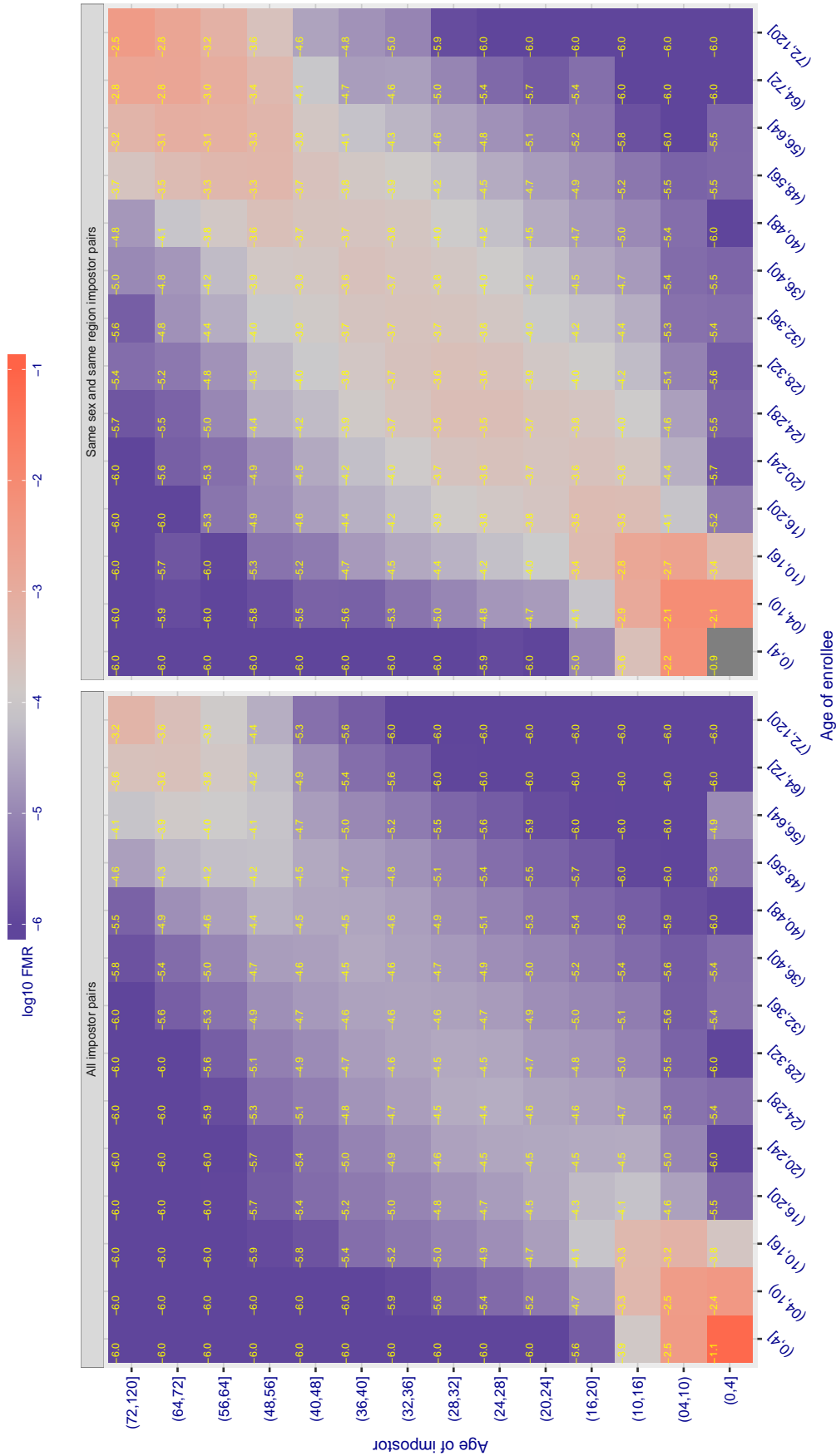


Figure 350: For algorithm id3-003 operating on visa images, the heatmap shows false match observed over impostor comparisons of faces from different individuals who have the given age pair. False matches are counted against a recognition threshold fixed globally to give $FMR = 0.0001$ over all on the order of 10^{10} impostor comparisons. The text in each box gives the same quantity as that coded by the color. Light colors present a security vulnerability to, for example, a passport gate.

Cross age FMR at threshold $T = 37001.000$ for algorithm id3_004, giving $FMR(T) = 0.0001$ globally.

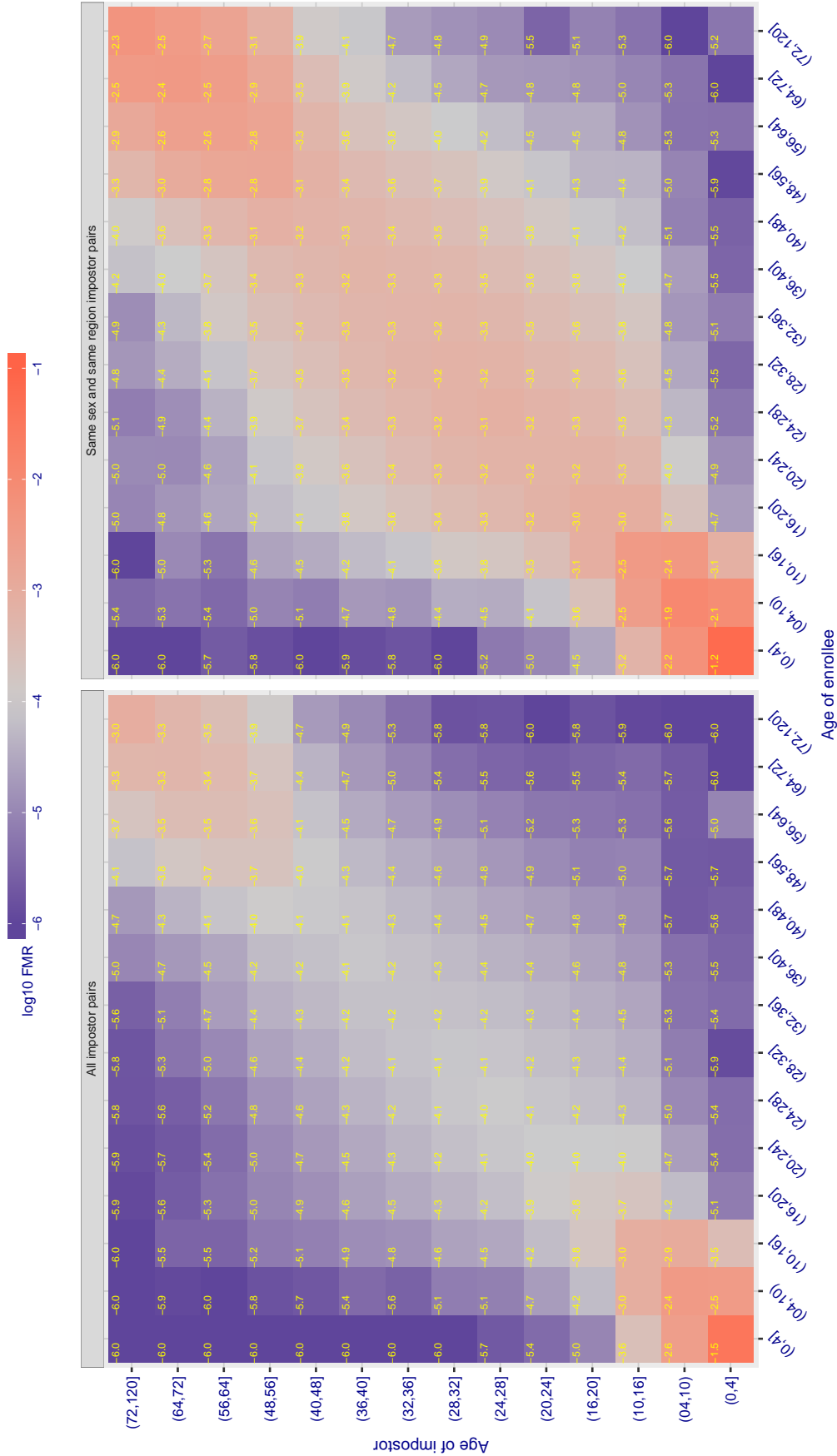


Figure 351: For algorithm id3-004 operating on visa images, the heatmap shows false match observed over impostor comparisons of faces from different individuals who have the given age pair. False matches are counted against a recognition threshold fixed globally to give $FMR = 0.001$ over all on the order of 10^{10} impostor comparisons. The text in each box gives the same quantity as that coded by the color. Light colors present a security vulnerability to, for example, a passport gate.

Cross age FMR at threshold $T = 3664.380$ for algorithm idemia_003, giving $FMR(T) = 0.0001$ globally.

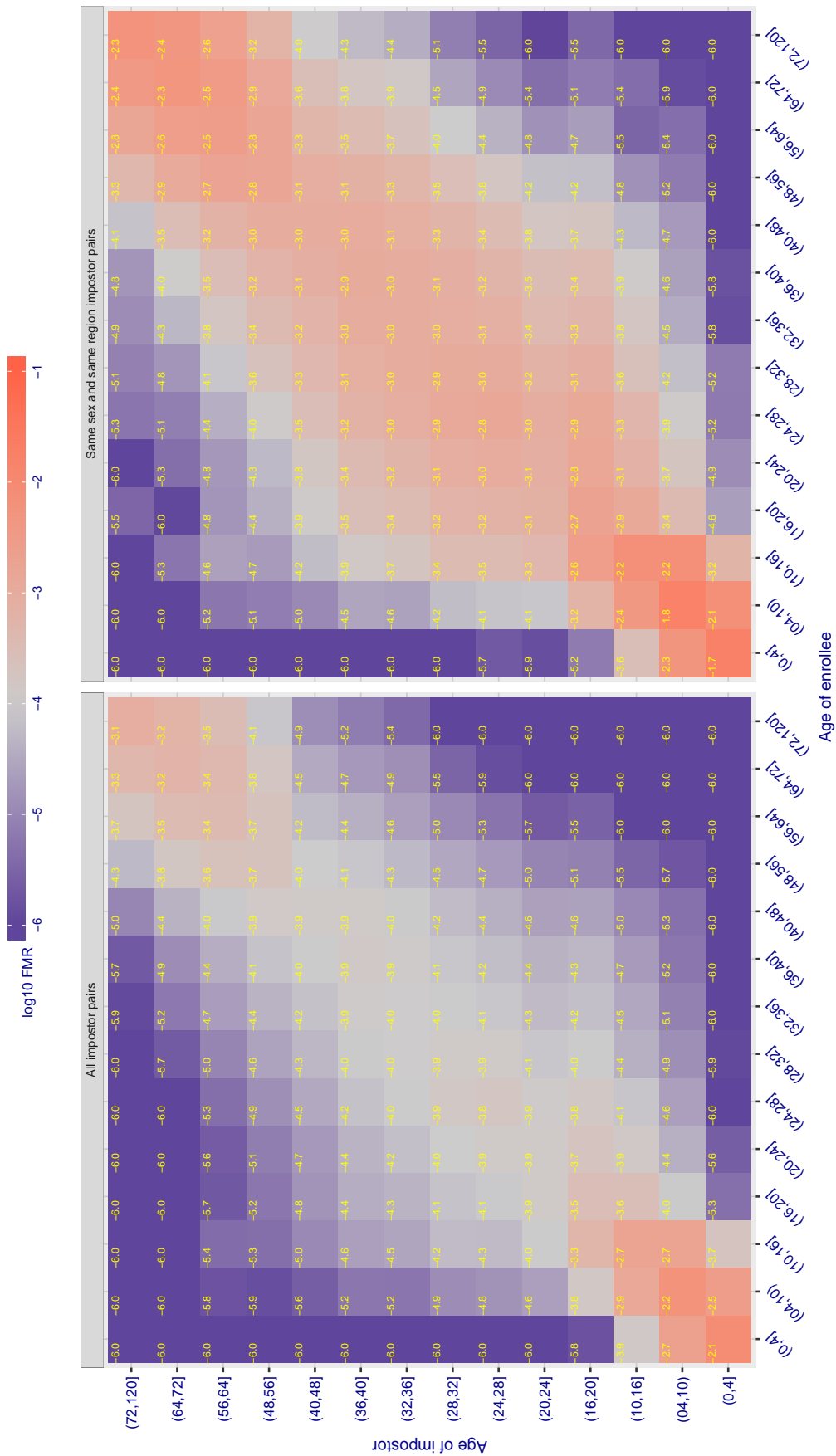


Figure 352: For algorithm idemia-003 operating on visa images, the heatmap shows false match observed over impostor comparisons of faces from different individuals who have the given age pair. False matches are counted against a recognition threshold fixed globally to give $FMR = 0.0001$ over all on the order of 10^{10} impostor comparisons. The text in each box gives the same quantity as that coded by the color. Light colors present a security vulnerability to, for example, a passport gate.

Cross age FMR at threshold $T = 3925.463$ for algorithm idemia_004, giving $FMR(T) = 0.0001$ globally.

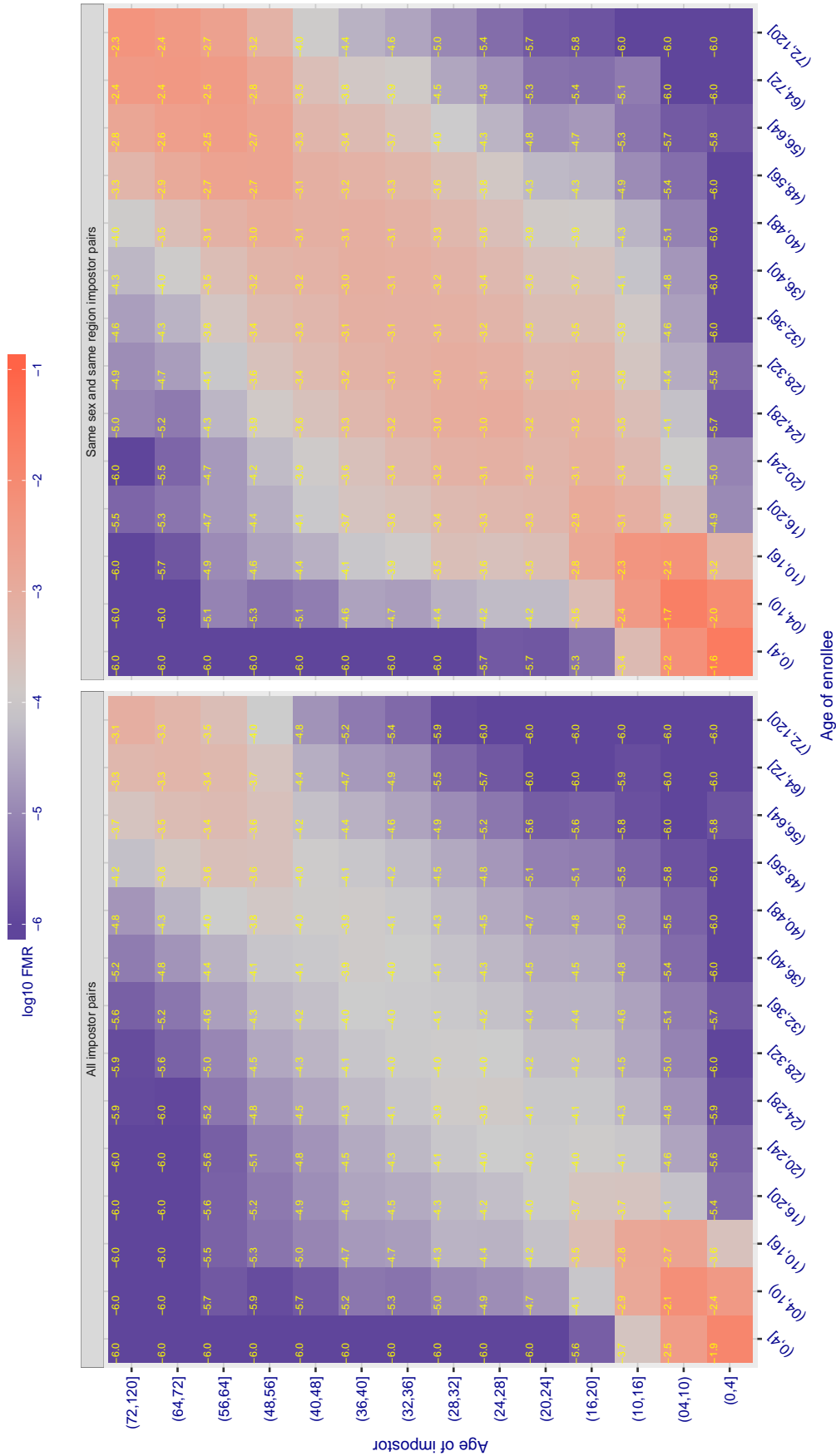


Figure 353: For algorithm idemia-004 operating on visa images, the heatmap shows false match observed over impostor comparisons of faces from different individuals who have the given age pair. False matches are counted against a recognition threshold fixed globally to give $FMR = 0.001$ over all on the order of 10^{10} impostor comparisons. The text in each box gives the same quantity as that coded by the color. Light colors present a security vulnerability to, for example, a passport gate.

Cross age FMR at threshold $T = 0.760$ for algorithm iit_000, giving $FMR(T) = 0.0001$ globally.

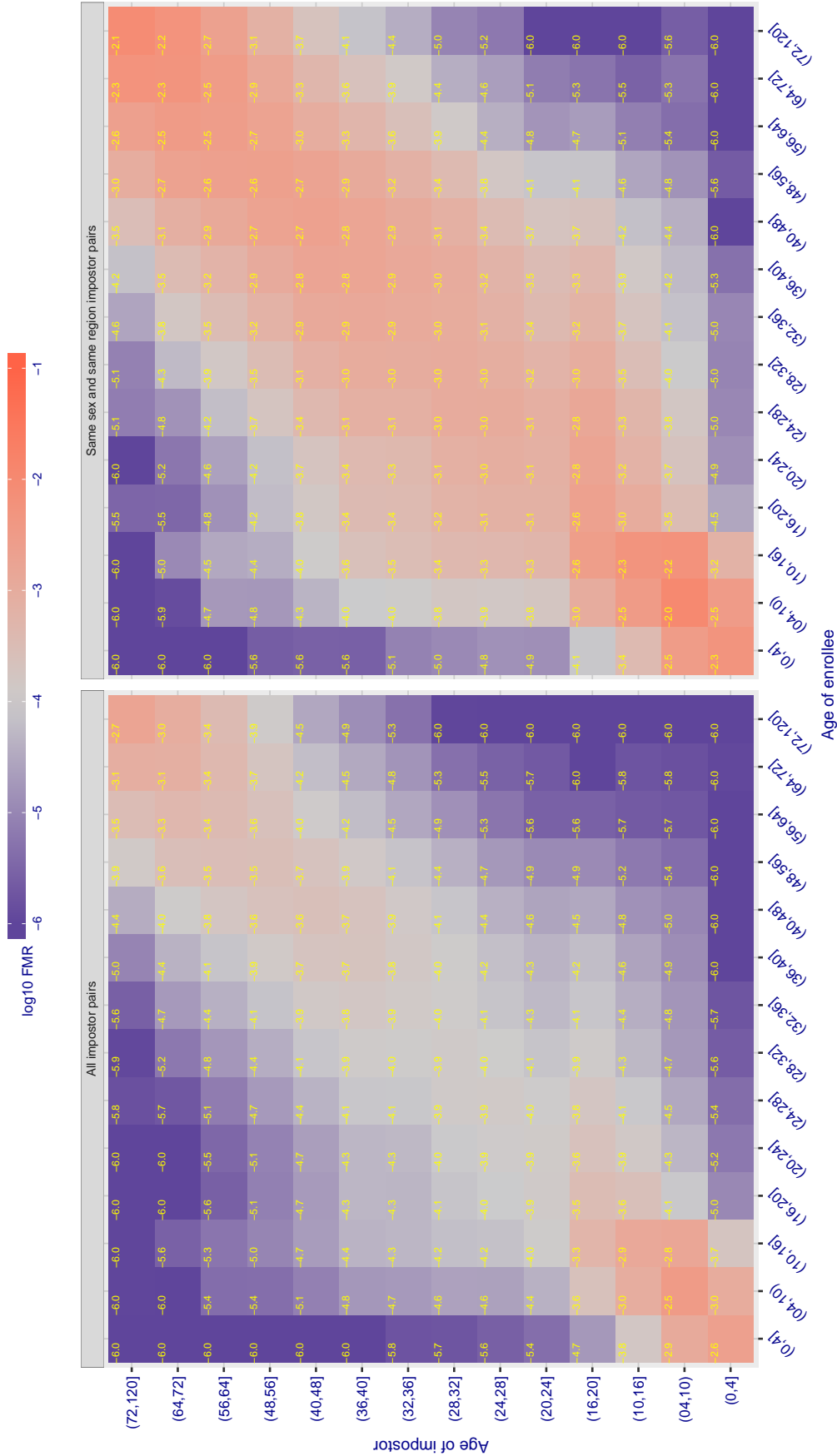


Figure 354: For algorithm iit-000 operating on visa images, the heatmap shows false match observed over impostor comparisons of faces from different individuals who have the given age pair. False matches are counted against a recognition threshold fixed globally to give $FMR = 0.0001$ over all on the order of 10^{10} impostor comparisons. The text in each box gives the same quantity as that coded by the color. Light colors present a security vulnerability to, for example, a passport gate.

Cross age FMR at threshold $T = 1.375$ for algorithm imperial_000, giving $FMR(T) = 0.0001$ globally.

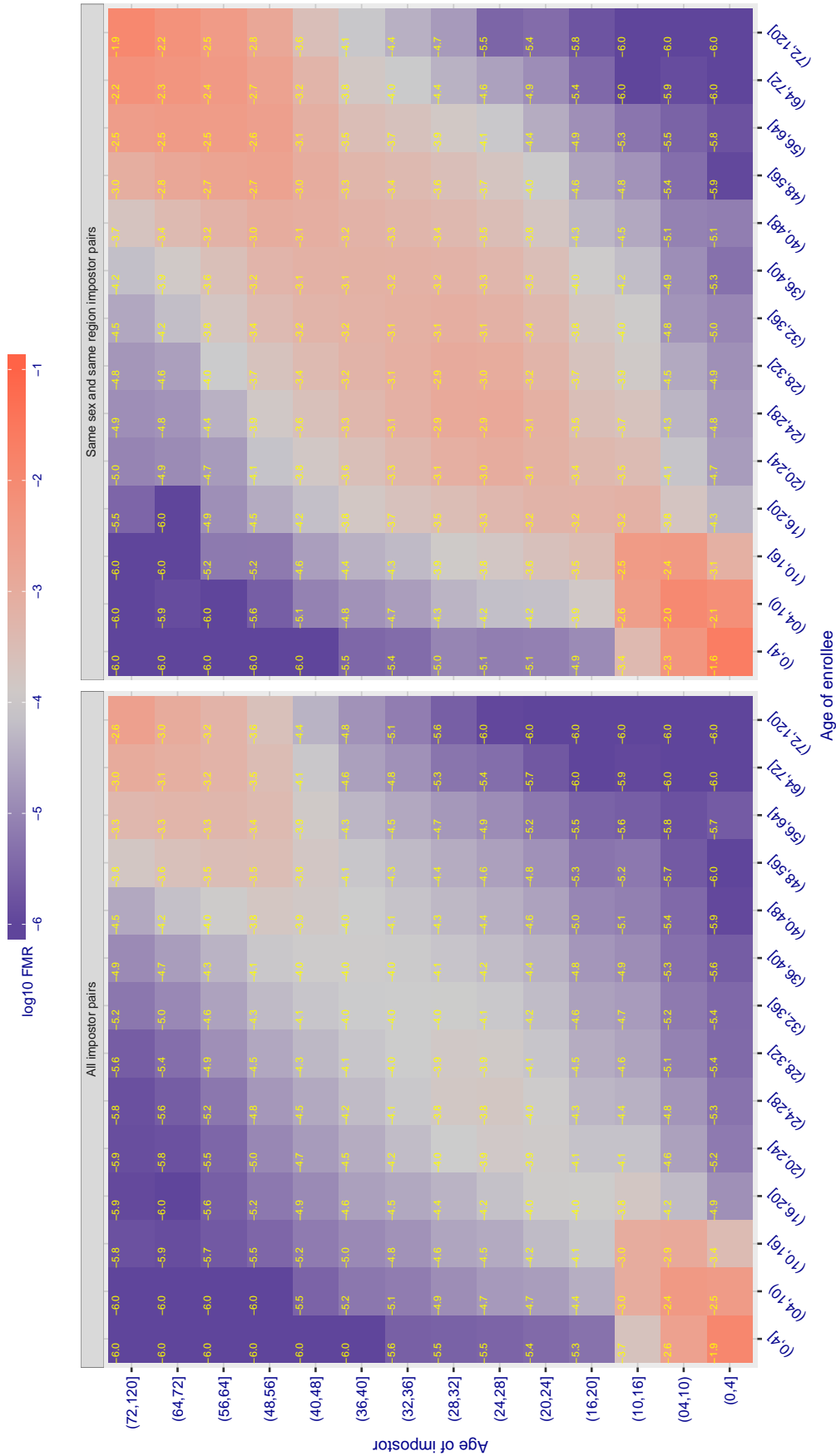


Figure 355: For algorithm imperial-000 operating on visa images, the heatmap shows false match observed over impostor comparisons of faces from different individuals who have the given age pair. False matches are counted against a recognition threshold fixed globally to give $FMR = 0.001$ over all on the order of 10^{10} impostor comparisons. The text in each box gives the same quantity as that coded by the color. Light colors present a security vulnerability to, for example, a passport gate.

Cross age FMR at threshold $T = 1.402$ for algorithm imperial_001, giving $FMR(T) = 0.0001$ globally.

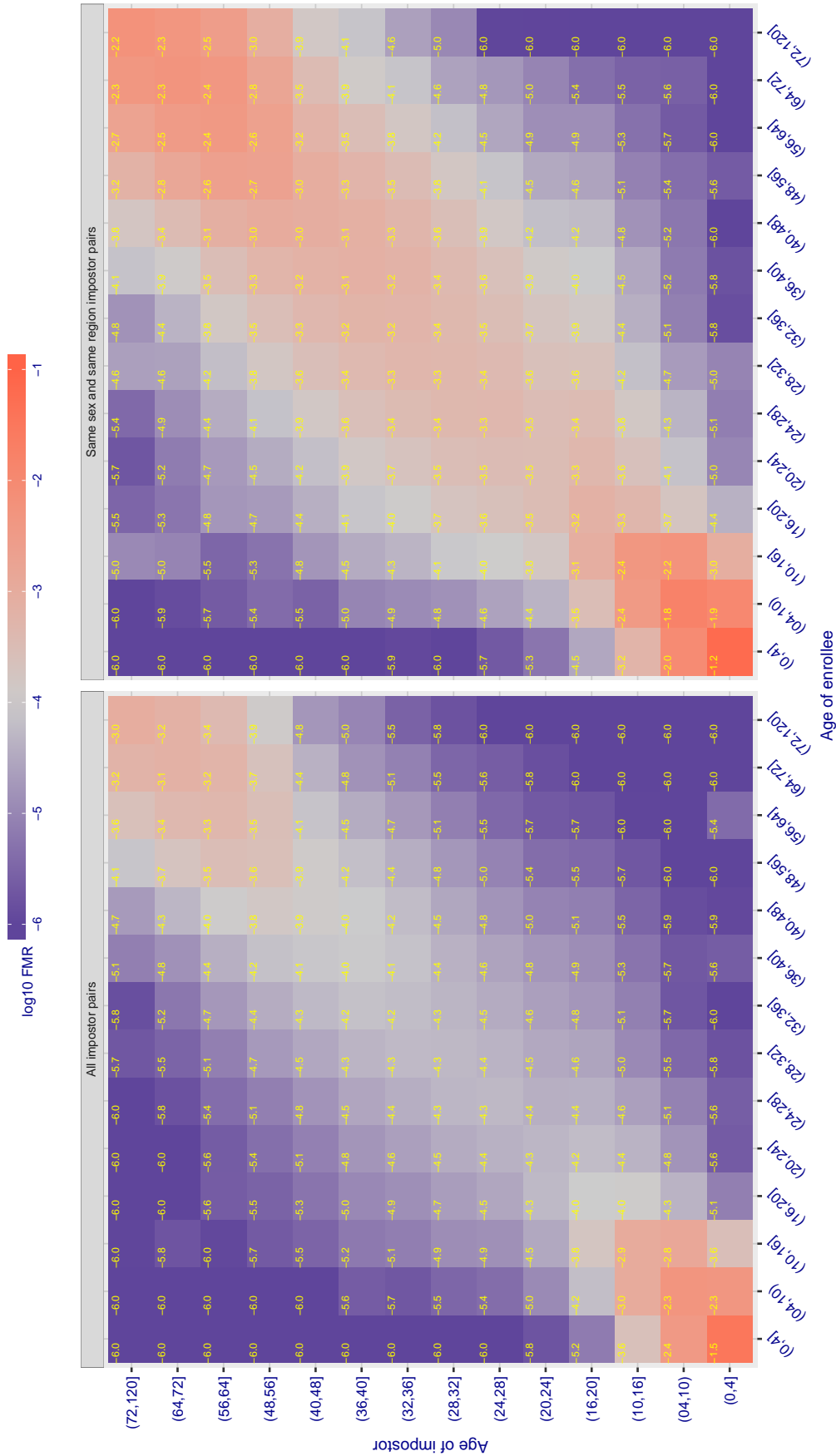


Figure 356: For algorithm imperial-001 operating on visa images, the heatmap shows false match observed over impostor comparisons of faces from different individuals who have the given age pair. False matches are counted against a recognition threshold fixed globally to give $FMR = 0.001$ over all on the order of 10^{10} impostor comparisons. The text in each box gives the same quantity as that coded by the color. Light colors present a security vulnerability to, for example, a passport gate.

Cross age FMR at threshold $T = 1.382$ for algorithm `incde_002`, giving $FMR(T) = 0.0001$ globally.

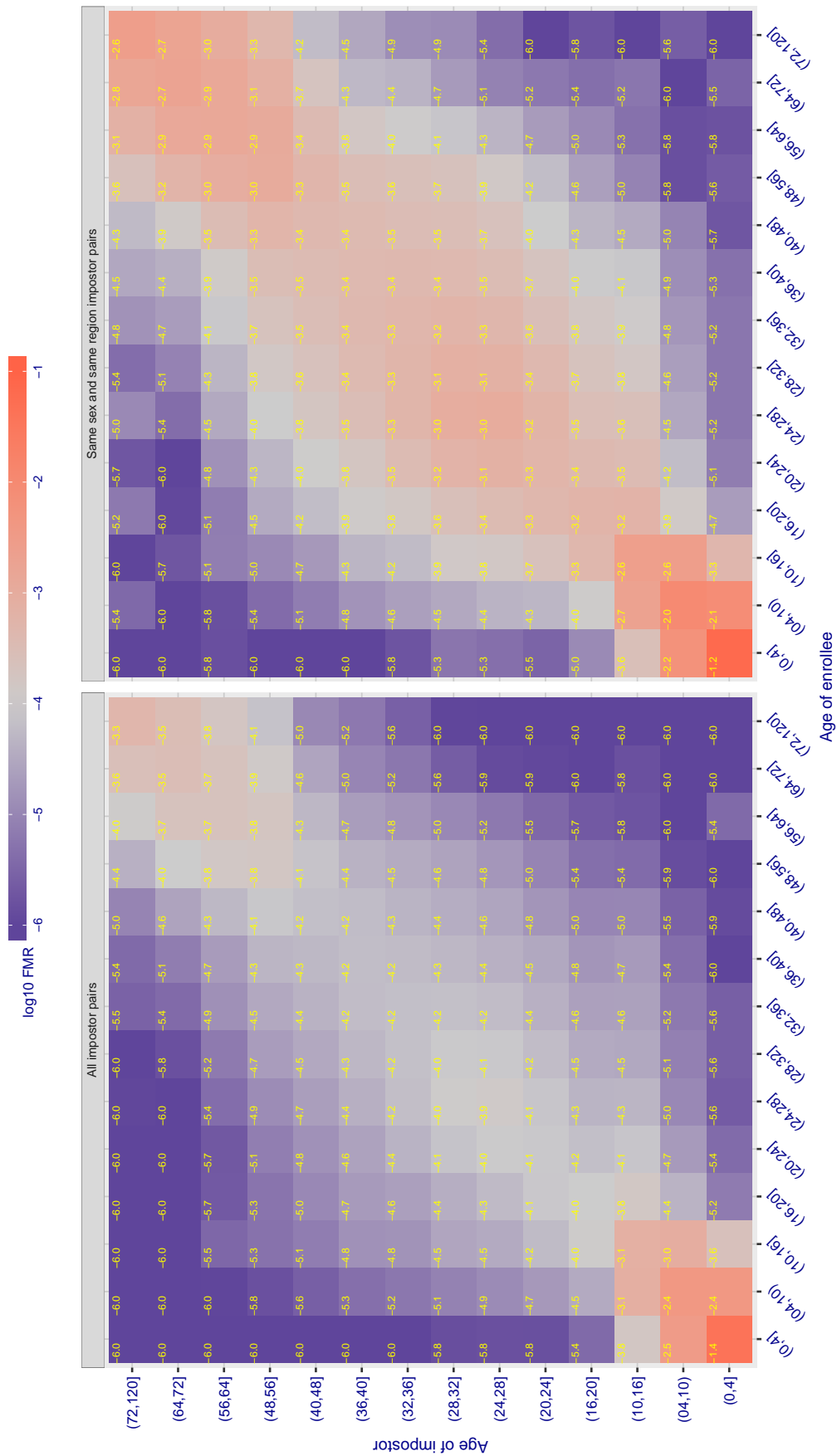


Figure 357: For algorithm `incde-002` operating on visa images, the heatmap shows false match observed over impostor comparisons of faces from different individuals who have the given age pair. False matches are counted against a recognition threshold fixed globally to give $FMR = 0.0001$ over all on the order of 10^{10} impostor comparisons. The text in each box gives the same quantity as that coded by the color. Light colors present a security vulnerability to, for example, a passport gate.

Cross age FMR at threshold $T = 1.427$ for algorithm `incode_003`, giving $FMR(T) = 0.0001$ globally.

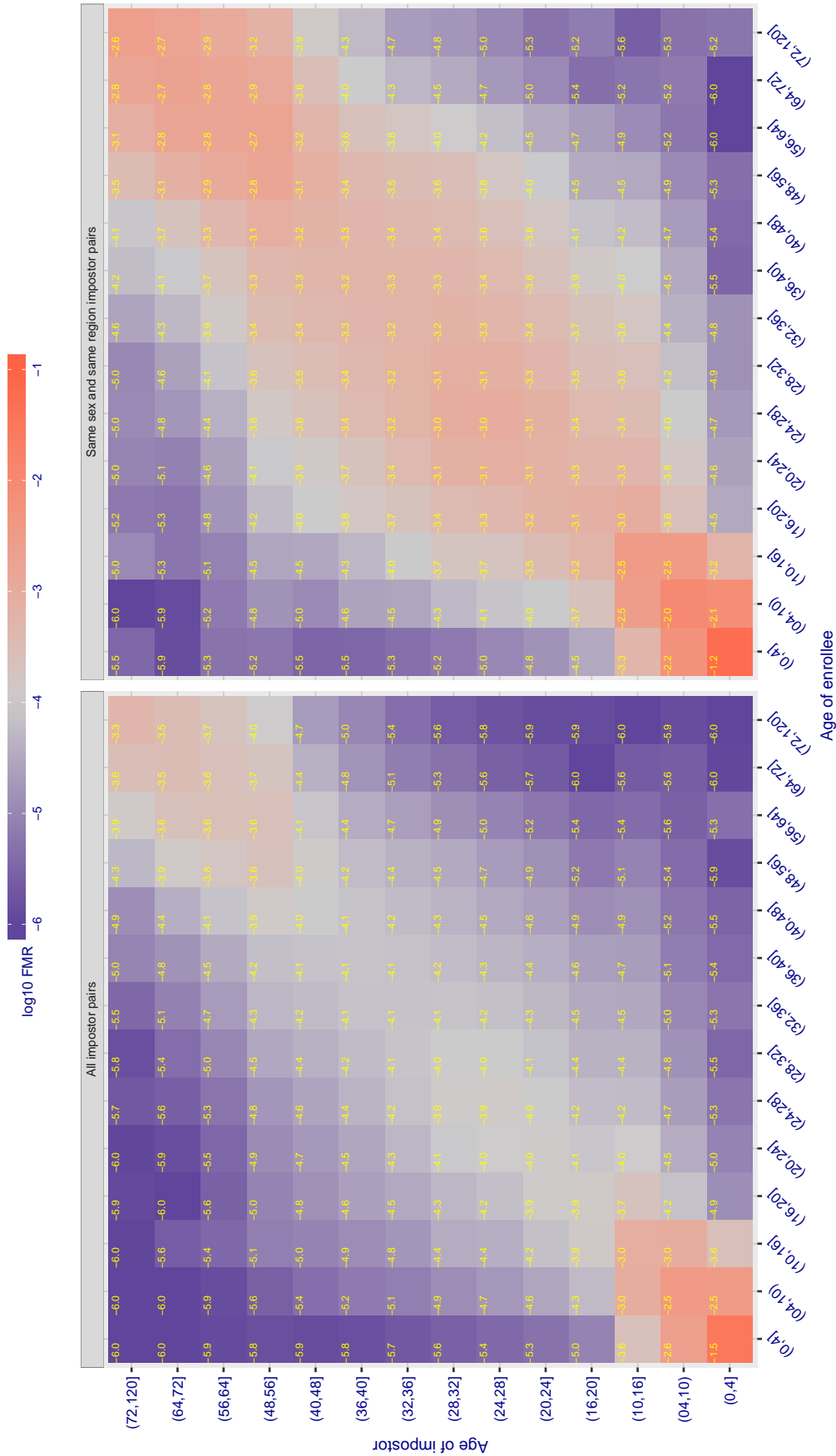


Figure 358: For algorithm `incode-003` operating on visa images, the heatmap shows false match observed over impostor comparisons of faces from different individuals who have the given age pair. False matches are counted against a recognition threshold fixed globally to give $FMR = 0.0001$ over all on the order of 10^{10} impostor comparisons. The text in each box gives the same quantity as that coded by the color: Light colors present a security vulnerability to, for example, a passport gate.

Cross age FMR at threshold $T = 29.232$ for algorithm innovatrics_004, giving $FMR(T) = 0.0001$ globally.

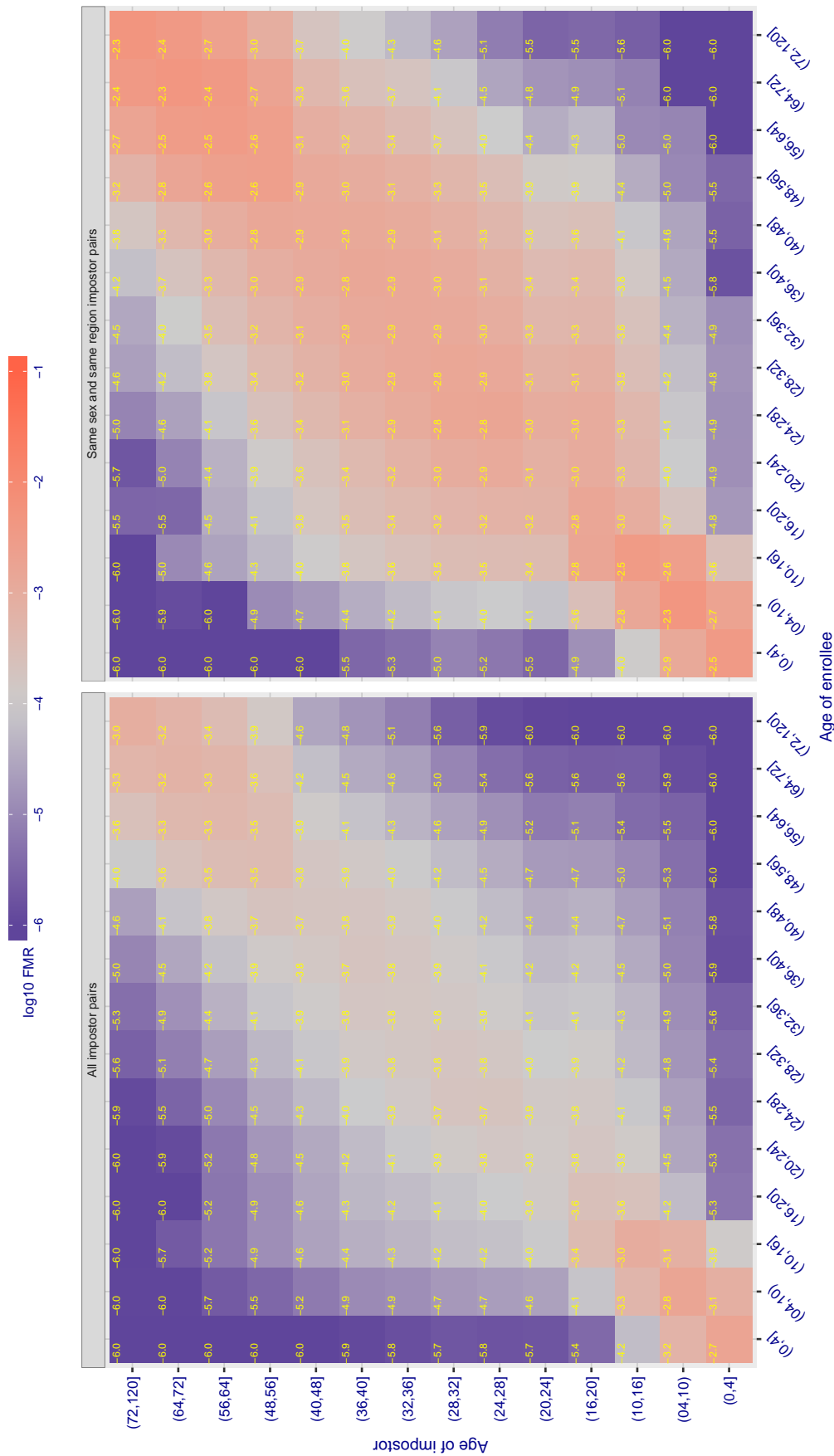


Figure 359: For algorithm innovatrics-004 operating on visa images, the heatmap shows false match observed over impostor comparisons of faces from different individuals who have the given age pair. False matches are counted against a recognition threshold fixed globally to give $FMR = 0.0001$ over all on the order of 10^{10} impostor comparisons. The text in each box gives the same quantity as that coded by the color. Light colors present a security vulnerability to, for example, a passport gate.

Cross age FMR at threshold T = 40.157 for algorithm innovatrics_005, giving FMR(T) = 0.0001 globally.

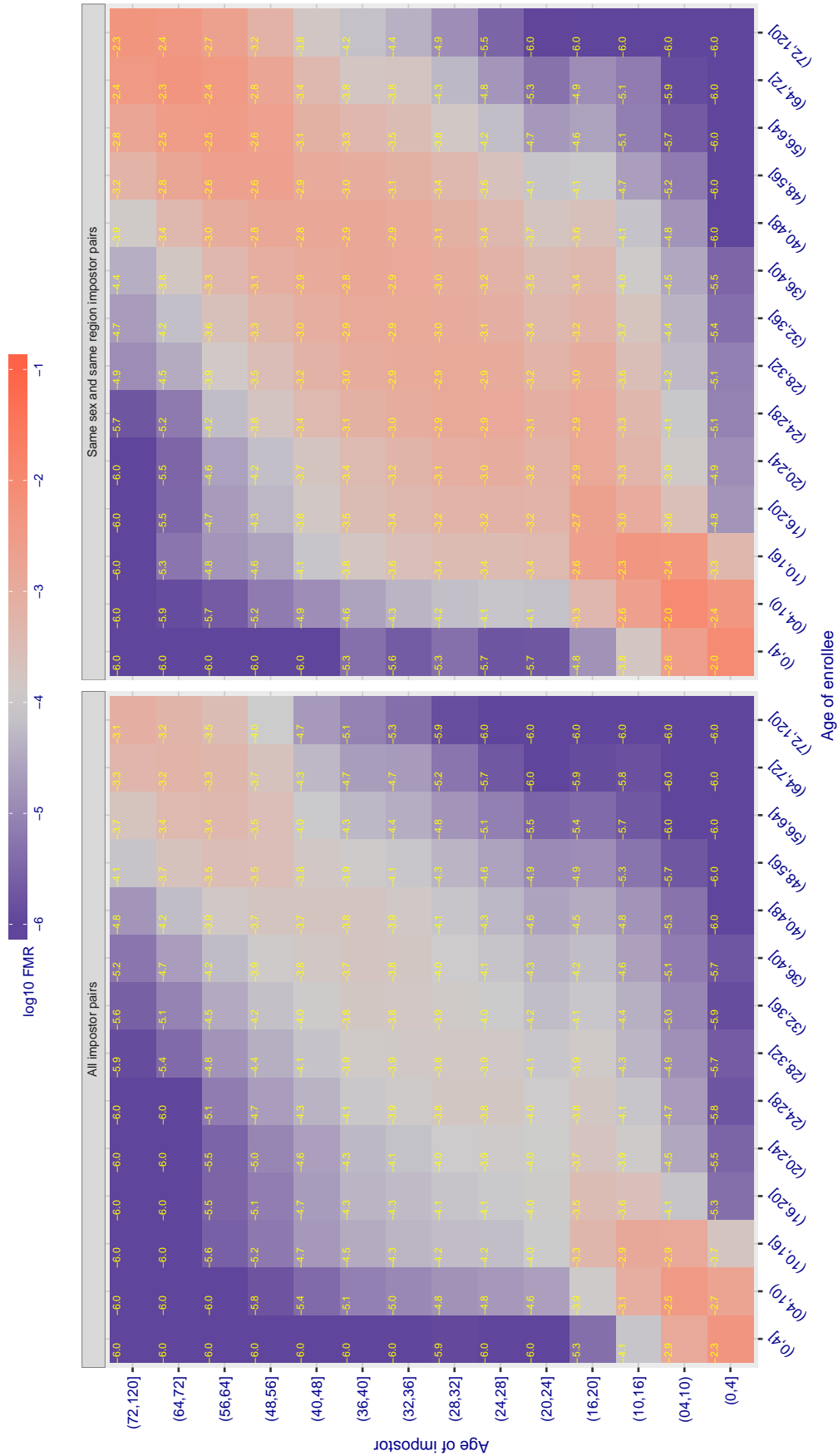


Figure 360: For algorithm innovatrics-005 operating on visa images, the heatmap shows false match observed over impostor comparisons of faces from different individuals who have the given age pair. False matches are counted against a recognition threshold fixed globally to give FMR = 0.001 over all on the order of 10¹⁰ impostor comparisons. The text in each box gives the same quantity as that coded by the color. Light colors present a security vulnerability to, for example, a passport gate.

Cross age FMR at threshold T = 49.664 for algorithm intellivision_001, giving FMR(T) = 0.0001 globally.

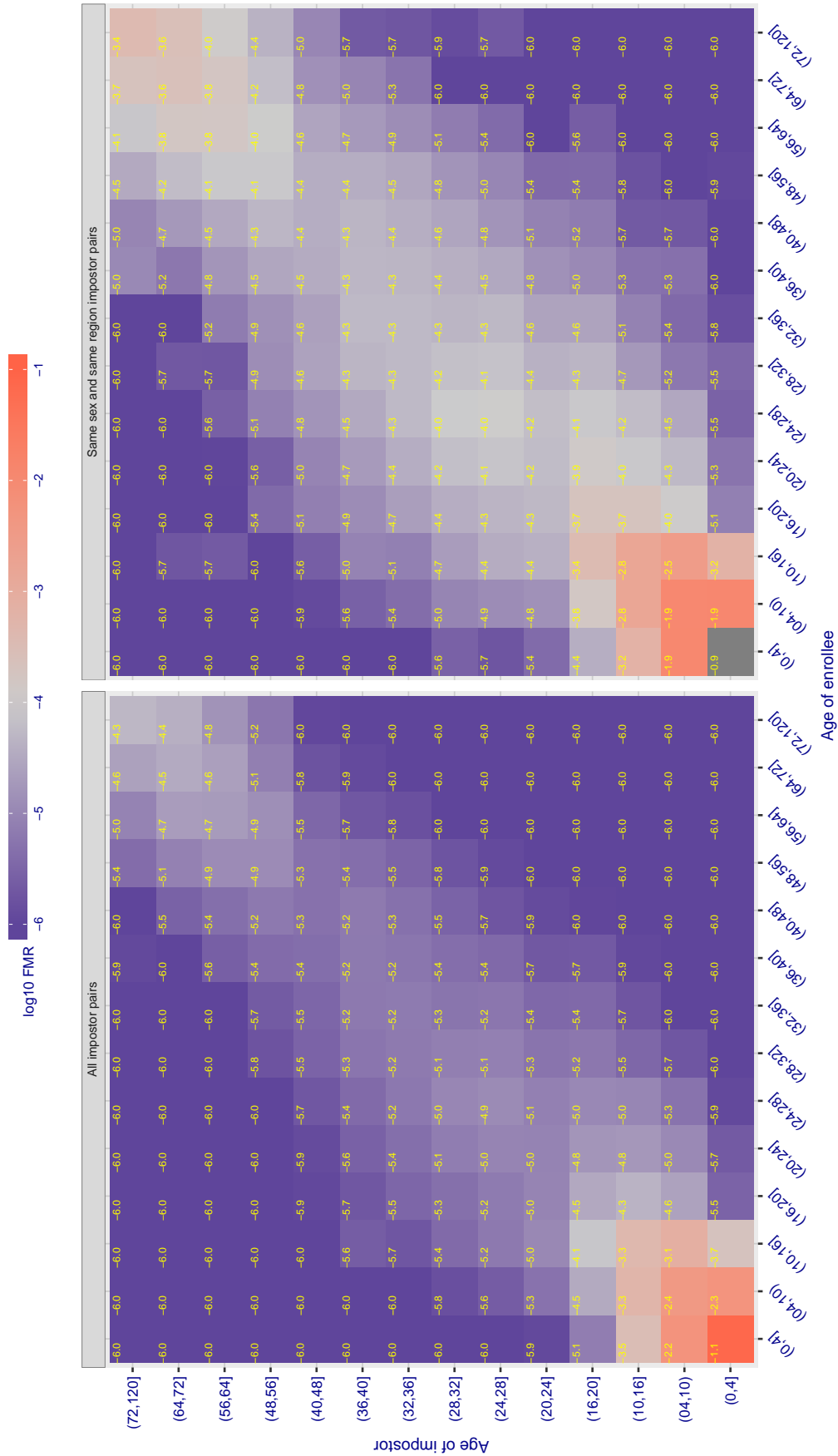


Figure 361: For algorithm intellivision-001 operating on visa images, the heatmap shows false match observed over impostor comparisons of faces from different individuals who have the given age pair. False matches are counted against a recognition threshold fixed globally to give FMR = 0.0001 over all on the order of 10¹⁰ impostor comparisons. The text in each box gives the same quantity as that coded by the color. Light colors present a security vulnerability to, for example, a passport gate.

Cross age FMR at threshold $T = 23.498$ for algorithm isityou_000, giving $FMR(T) = 0.0001$ globally.

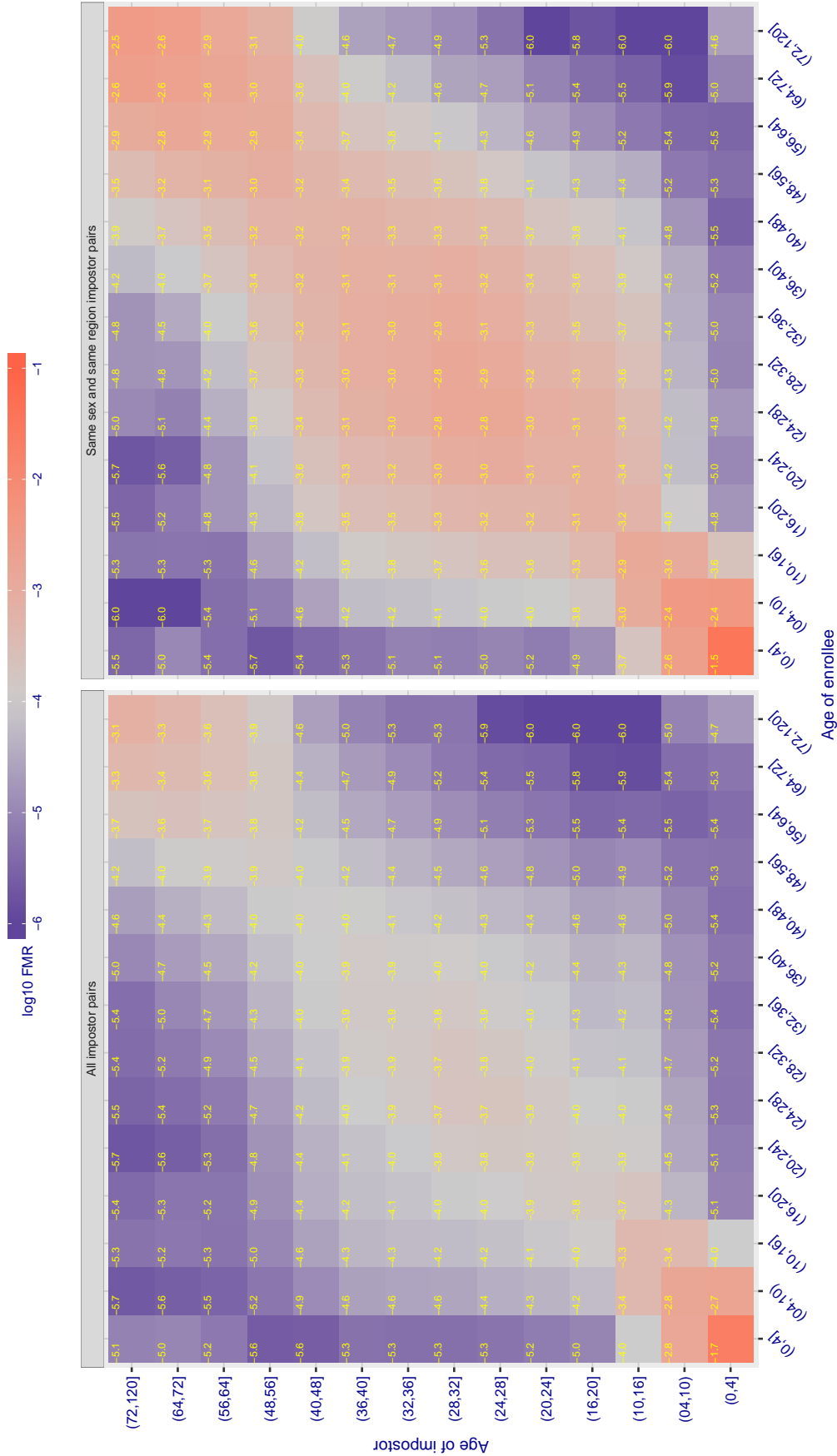


Figure 362: For algorithm isityou-000 operating on visa images, the heatmap shows false match observed over impostor comparisons of faces from different individuals who have the given age pair. False matches are counted against a recognition threshold fixed globally to give $FMR = 0.001$ over all on the order of 10^{10} impostor comparisons. The text in each box gives the same quantity as that coded by the color. Light colors present a security vulnerability to, for example, a passport gate.

Cross age FMR at threshold $T = 0.693$ for algorithm `isystems_001`, giving $FMR(T) = 0.0001$ globally.

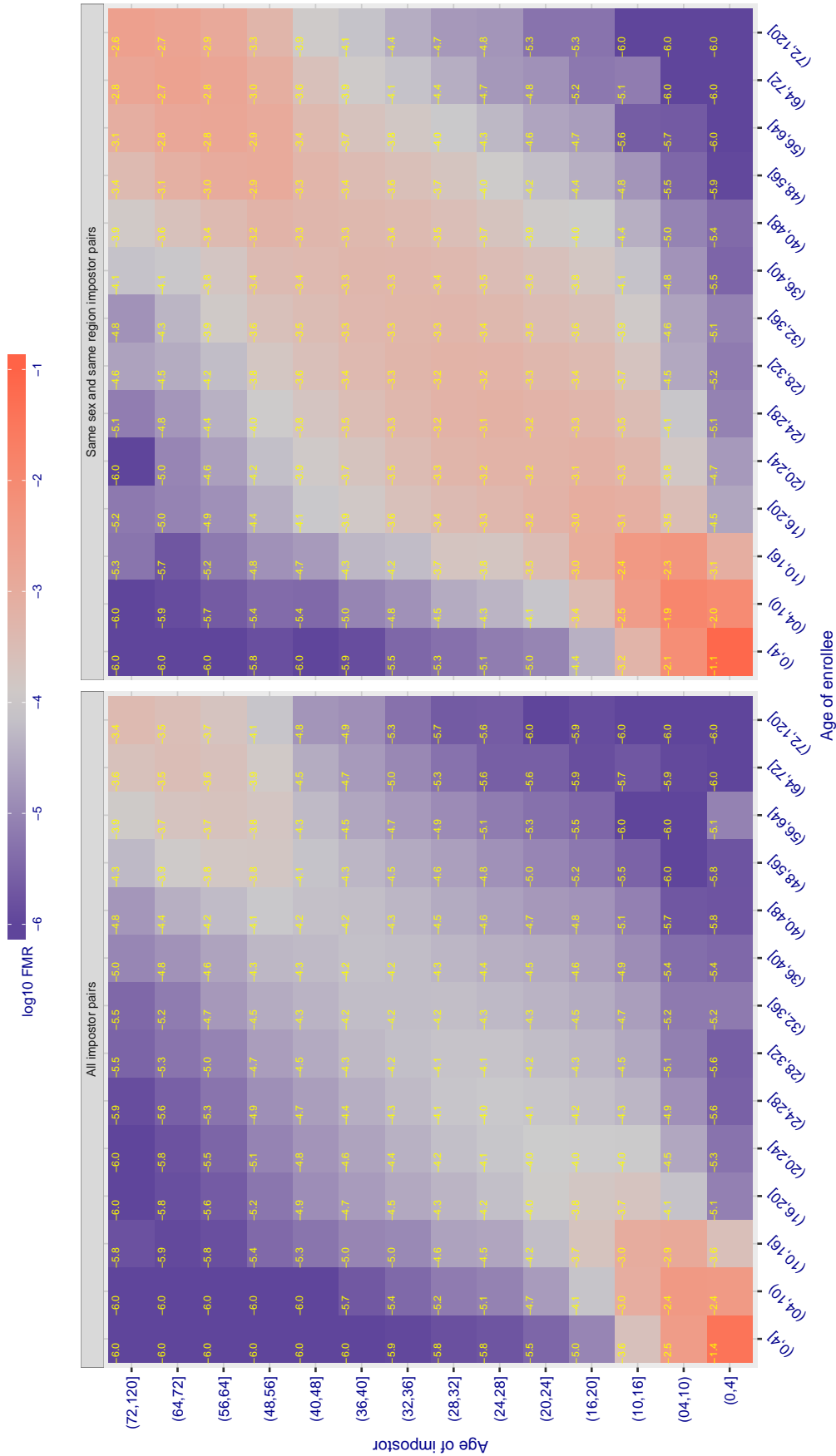


Figure 363: For algorithm `isystems-001` operating on visa images, the heatmap shows false match observed over impostor comparisons of faces from different individuals who have the given age pair. False matches are counted against a recognition threshold fixed globally to give $FMR = 0.001$ over all on the order of 10^{10} impostor comparisons. The text in each box gives the same quantity as that coded by the color. Light colors present a security vulnerability to, for example, a passport gate.

Cross age FMR at threshold $T = 0.690$ for algorithm `isystems_002`, giving $FMR(T) = 0.0001$ globally.

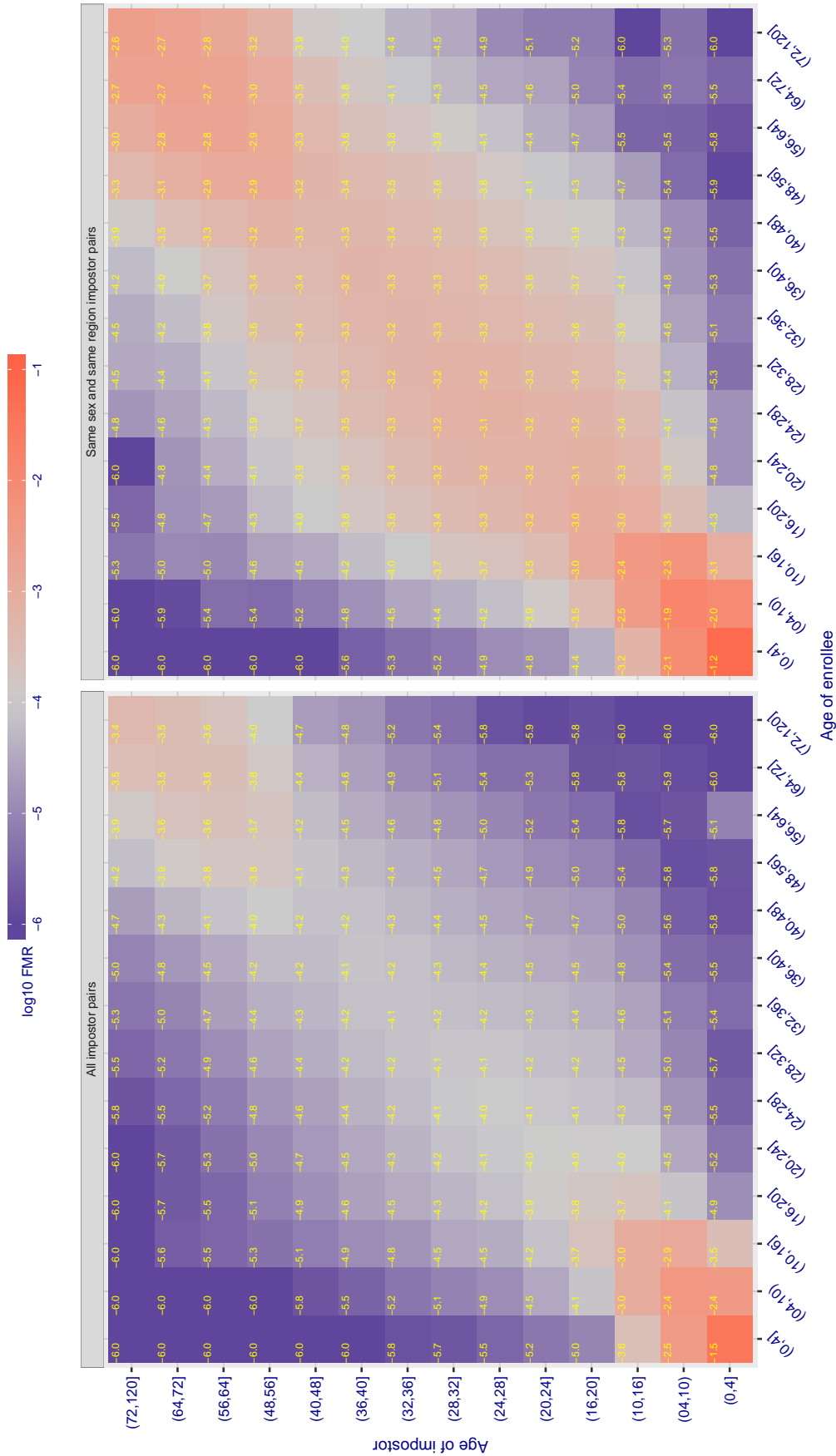


Figure 364: For algorithm `isystems-002` operating on visa images, the heatmap shows false match observed over impostor comparisons of faces from different individuals who have the given age pair. False matches are counted against a recognition threshold fixed globally to give $FMR = 0.001$ over all on the order of 10^{10} impostor comparisons. The text in each box gives the same quantity as that coded by the color. Light colors present a security vulnerability to, for example, a passport gate.

Cross age FMR at threshold $T = 49.879$ for algorithm itmo_005, giving $FMR(T) = 0.0001$ globally.

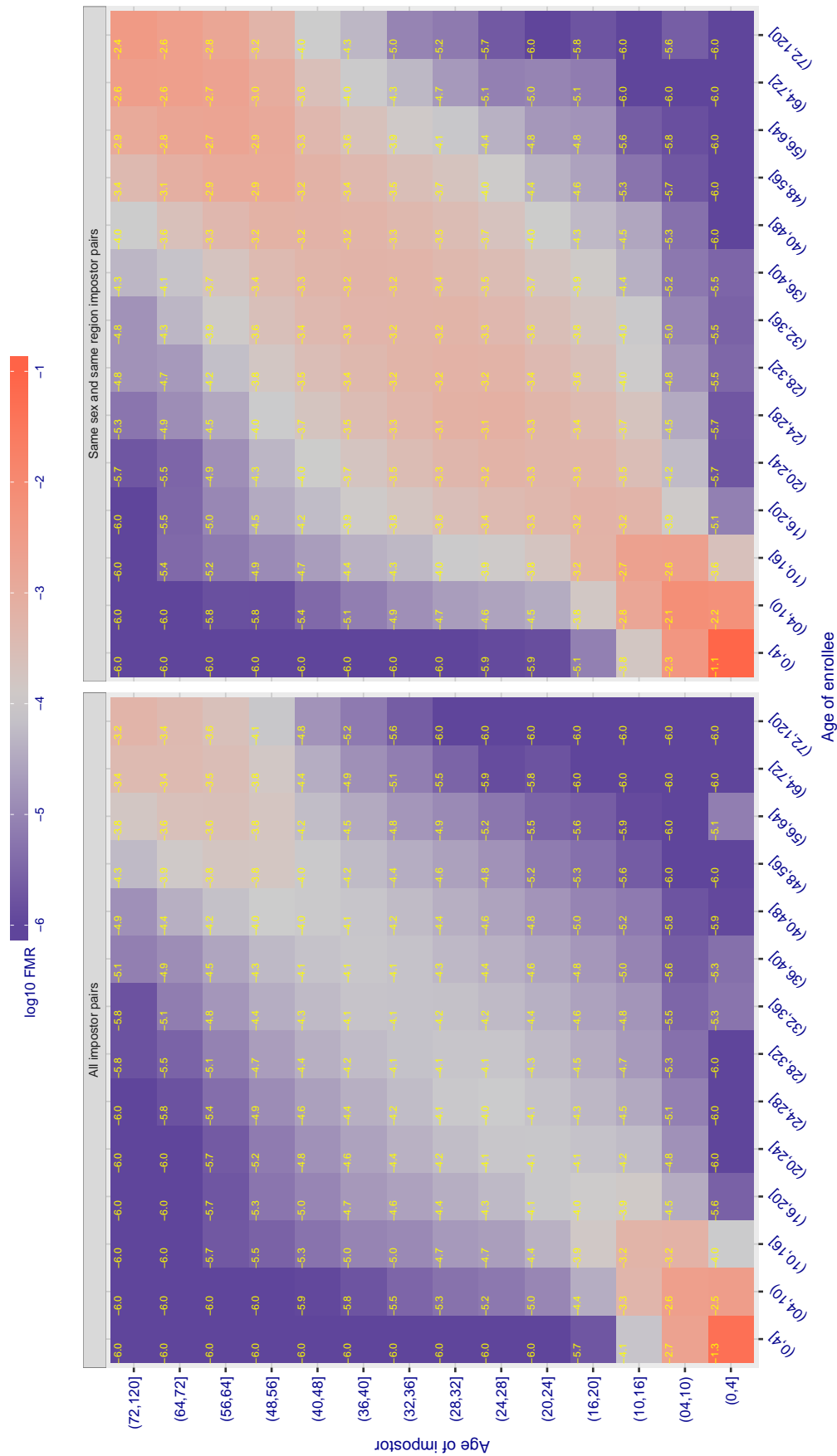


Figure 365: For algorithm itmo-005 operating on visa images, the heatmap shows false match observed over impostor comparisons of faces from different individuals who have the given age pair. False matches are counted against a recognition threshold fixed globally to give $FMR = 0.001$ over all on the order of 10^{10} impostor comparisons. The text in each box gives the same quantity as that coded by the color. Light colors present a security vulnerability to, for example, a passport gate.

Cross age FMR at threshold $T = 49.789$ for algorithm itmo_006, giving $FMR(T) = 0.0001$ globally.

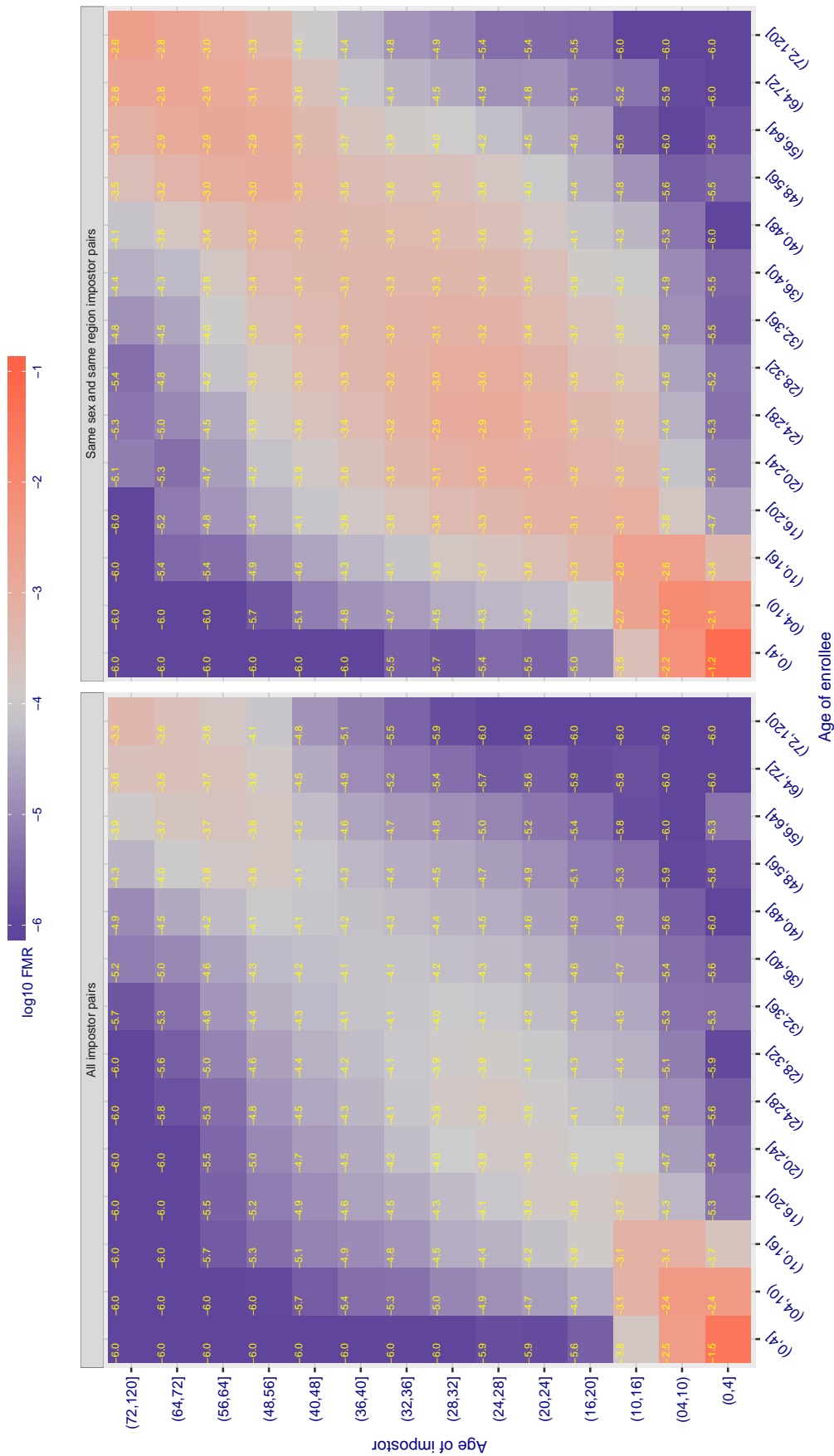


Figure 366: For algorithm itmo-006 operating on visa images, the heatmap shows false match observed over impostor comparisons of faces from different individuals who have the given age pair. False matches are counted against a recognition threshold fixed globally to give $FMR = 0.001$ over all on the order of 10^{10} impostor comparisons. The text in each box gives the same quantity as that coded by the color. Light colors present a security vulnerability to, for example, a passport gate.

Cross age FMR at threshold $T = 1.301$ for algorithm kakao_001, giving $FMR(T) = 0.0001$ globally.

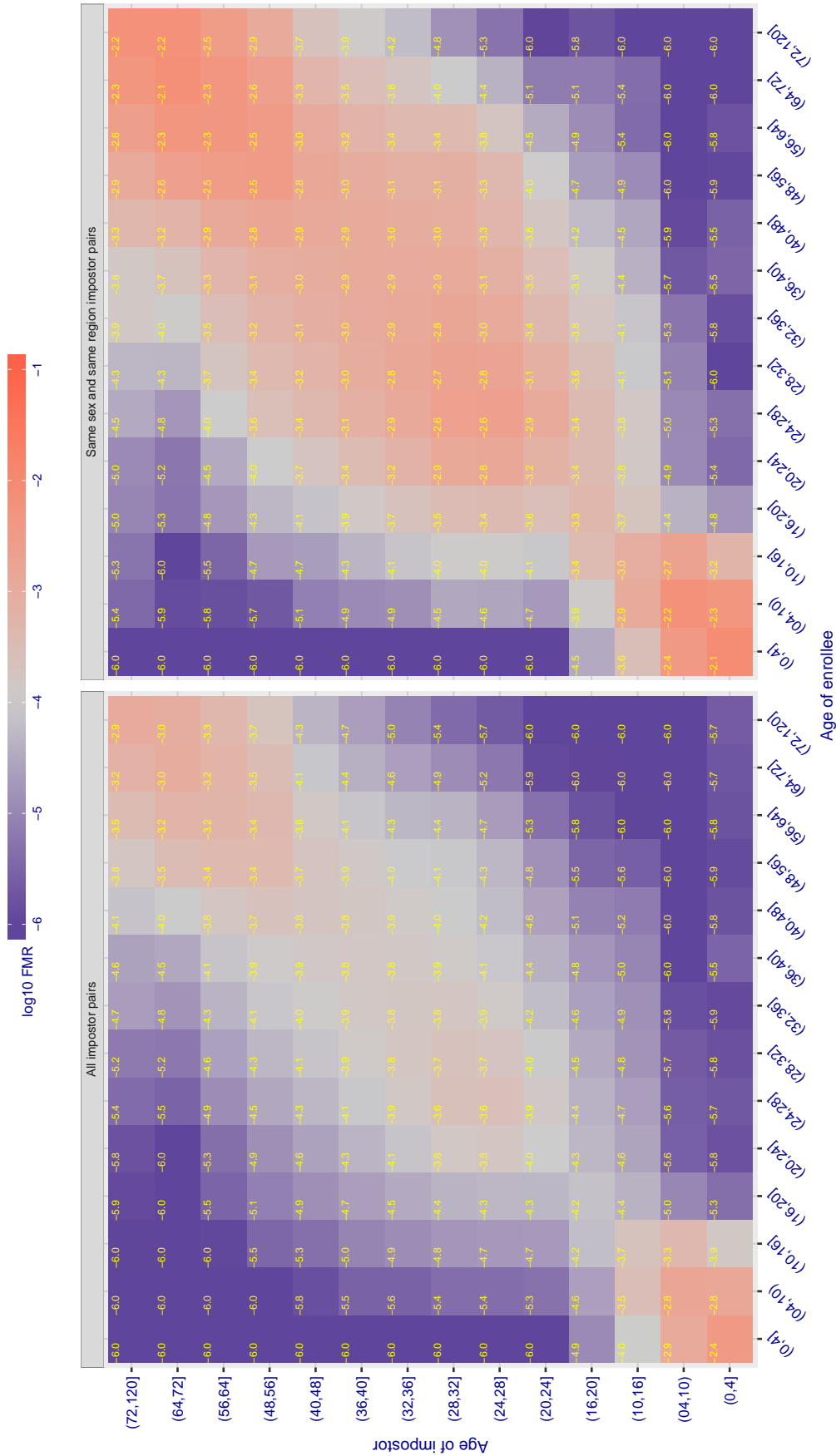


Figure 367: For algorithm kakao-001 operating on visa images, the heatmap shows false match observed over impostor comparisons of faces from different individuals who have the given age pair. False matches are counted against a recognition threshold fixed globally to give $FMR = 0.0001$ over all on the order of 10^{10} impostor comparisons. The text in each box gives the same quantity as that coded by the color. Light colors present a security vulnerability to, for example, a passport gate.

Cross age FMR at threshold $T = 0.701$ for algorithm lookman_002, giving $FMR(T) = 0.0001$ globally.

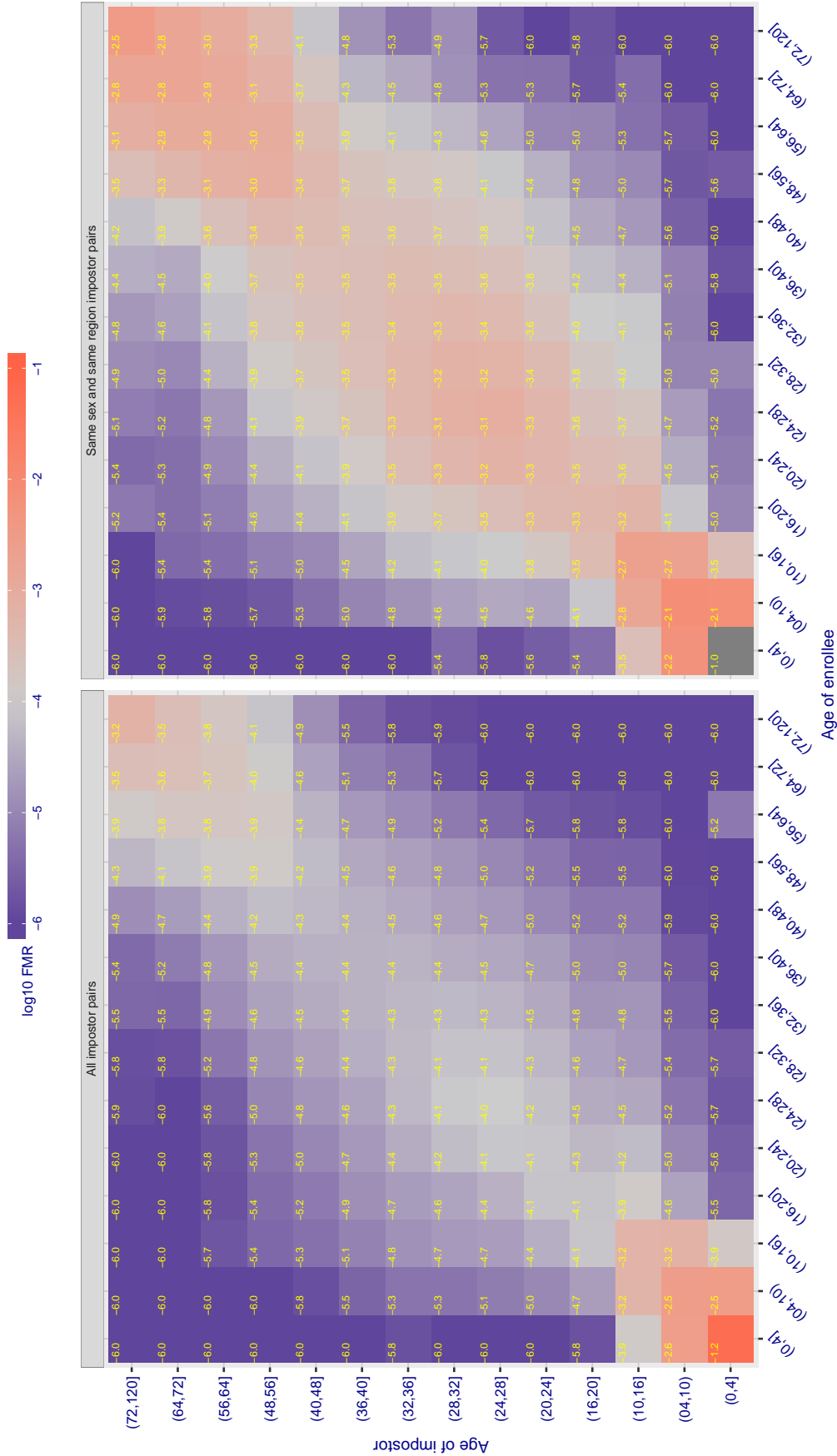


Figure 368: For algorithm lookman-002 operating on visa images, the heatmap shows false match observed over impostor comparisons of faces from different individuals who have the given age pair. False matches are counted against a recognition threshold fixed globally to give $FMR = 0.001$ over all on the order of 10^{10} impostor comparisons. The text in each box gives the same quantity as that coded by the color: Light colors present a security vulnerability to, for example, a passport gate.

Cross age FMR at threshold $T = 74.511$ for algorithm megvii_001, giving $FMR(T) = 0.0001$ globally.

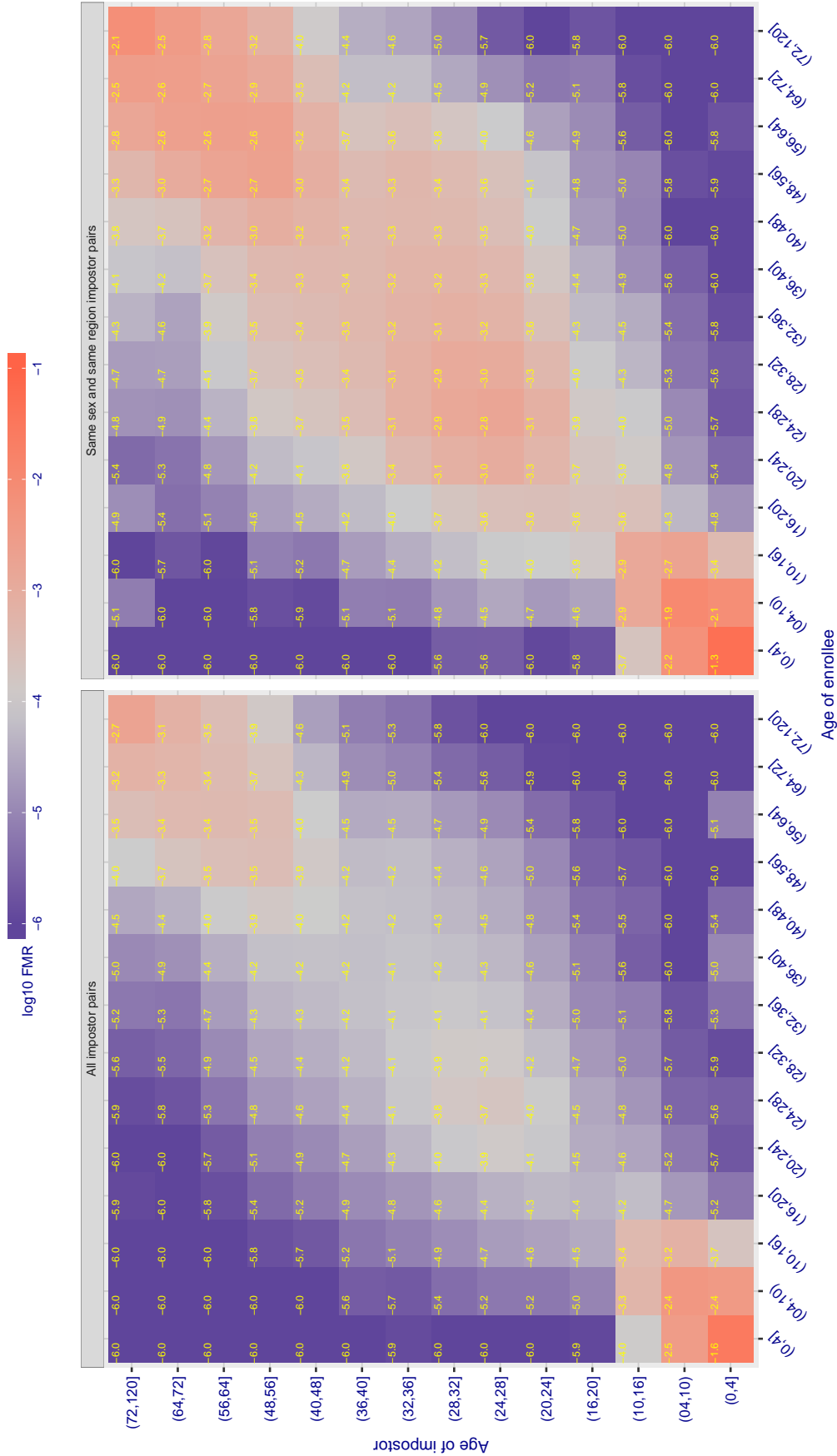


Figure 369: For algorithm megvii-001 operating on visa images, the heatmap shows false match observed over impostor comparisons of faces from different individuals who have the given age pair. False matches are counted against a recognition threshold fixed globally to give $FMR = 0.001$ over all on the order of 10^{10} impostor comparisons. The text in each box gives the same quantity as that coded by the color. Light colors present a security vulnerability to, for example, a passport gate.

Cross age FMR at threshold $T = 66.384$ for algorithm megvii_002, giving $FMR(T) = 0.0001$ globally.

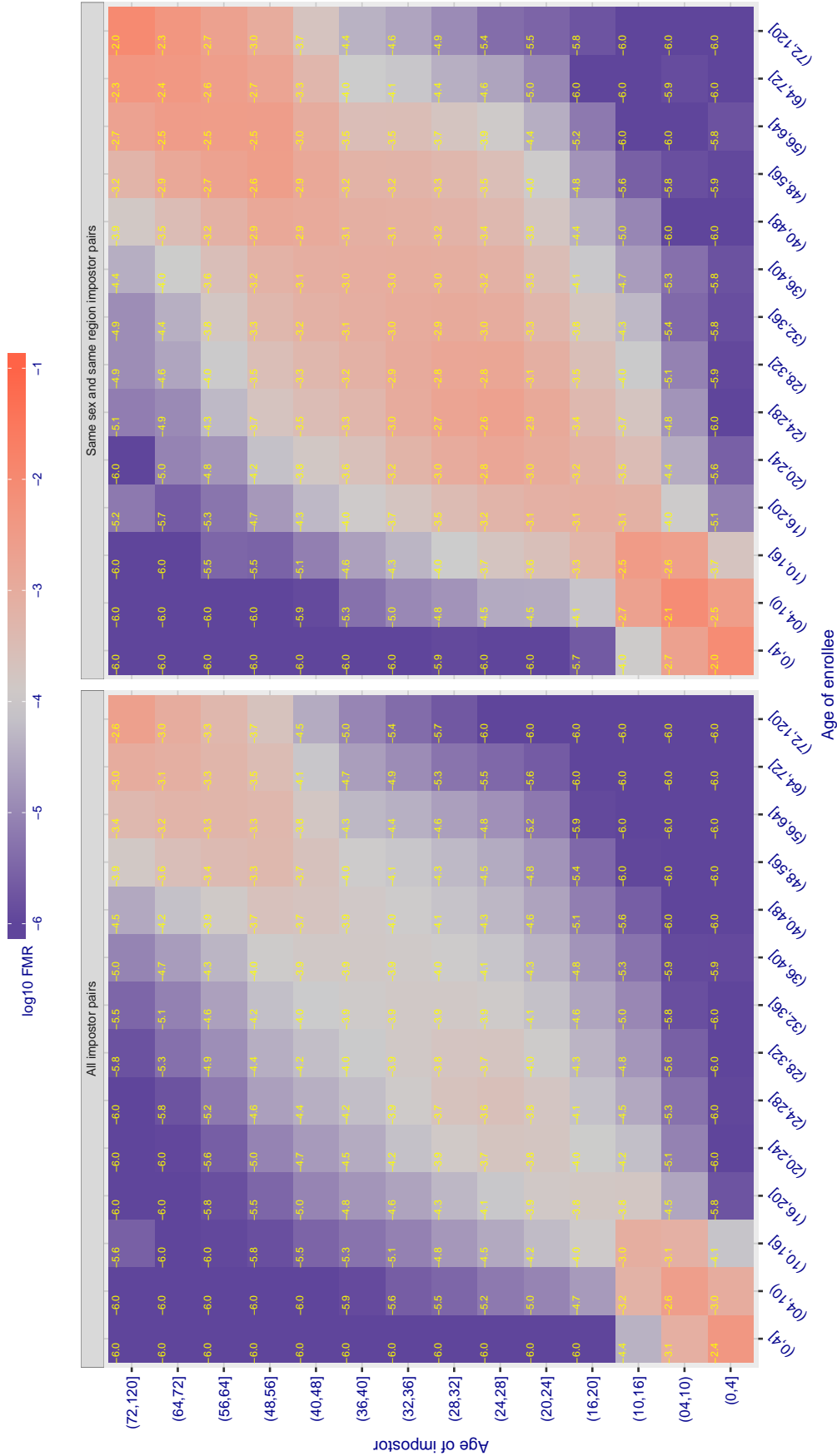


Figure 370: For algorithm megvii-002 operating on visa images, the heatmap shows false match observed over impostor comparisons of faces from different individuals who have the given age pair. False matches are counted against a recognition threshold fixed globally to give $FMR = 0.0001$ over all on the order of 10^{10} impostor comparisons. The text in each box gives the same quantity as that coded by the color. Light colors present a security vulnerability to, for example, a passport gate.

Cross age FMR at threshold $T = 0.425$ for algorithm meiya_001, giving $FMR(T) = 0.0001$ globally.

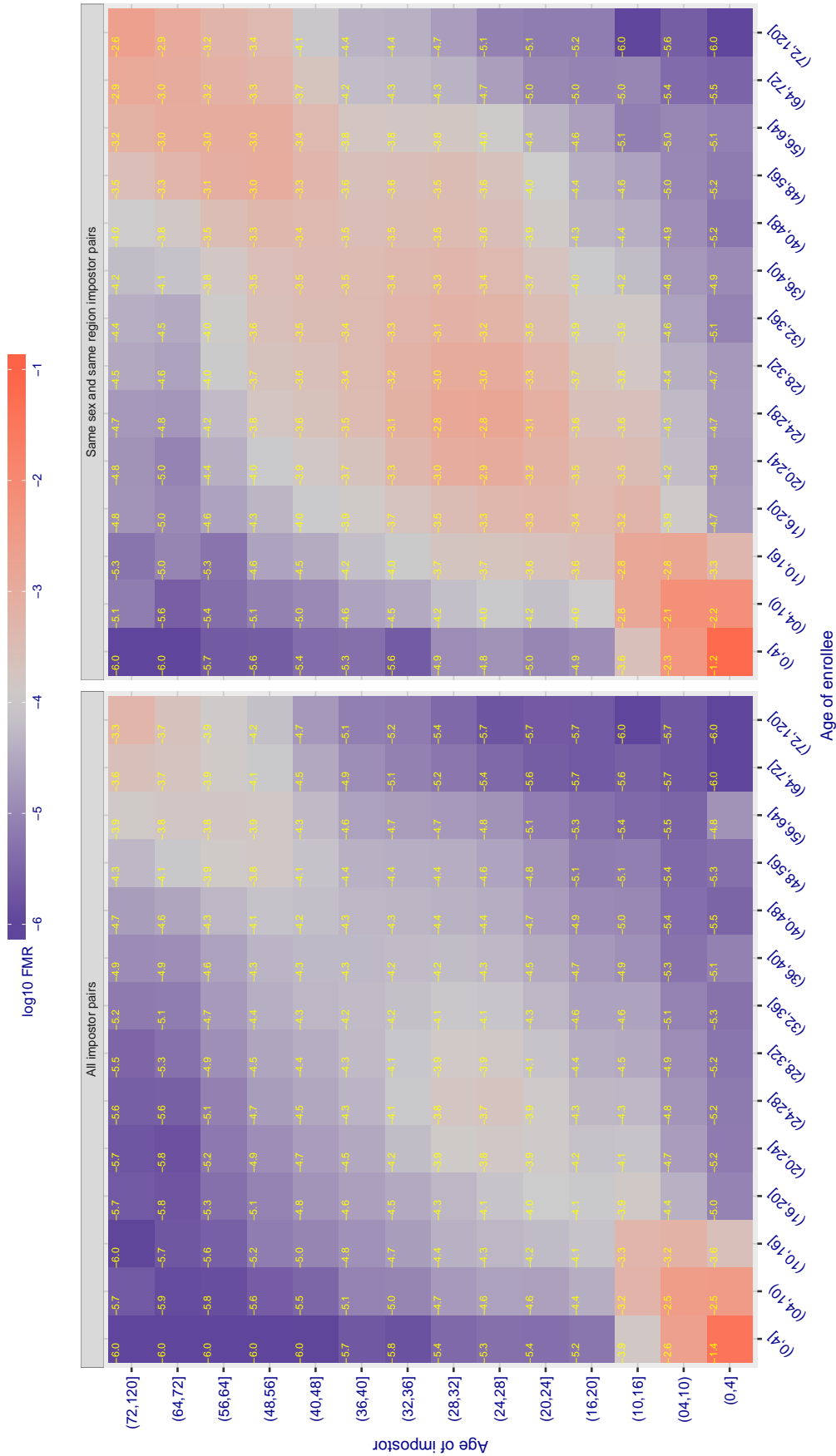


Figure 371: For algorithm meiya-001 operating on visa images, the heatmap shows false match observed over impostor comparisons of faces from different individuals who have the given age pair. False matches are counted against a recognition threshold fixed globally to give $FMR = 0.001$ over all on the order of 10^{10} impostor comparisons. The text in each box gives the same quantity as that coded by the color. Light colors present a security vulnerability to, for example, a passport gate.

Cross age FMR at threshold $T = 0.668$ for algorithm microfocus_001, giving $FMR(T) = 0.0001$ globally.

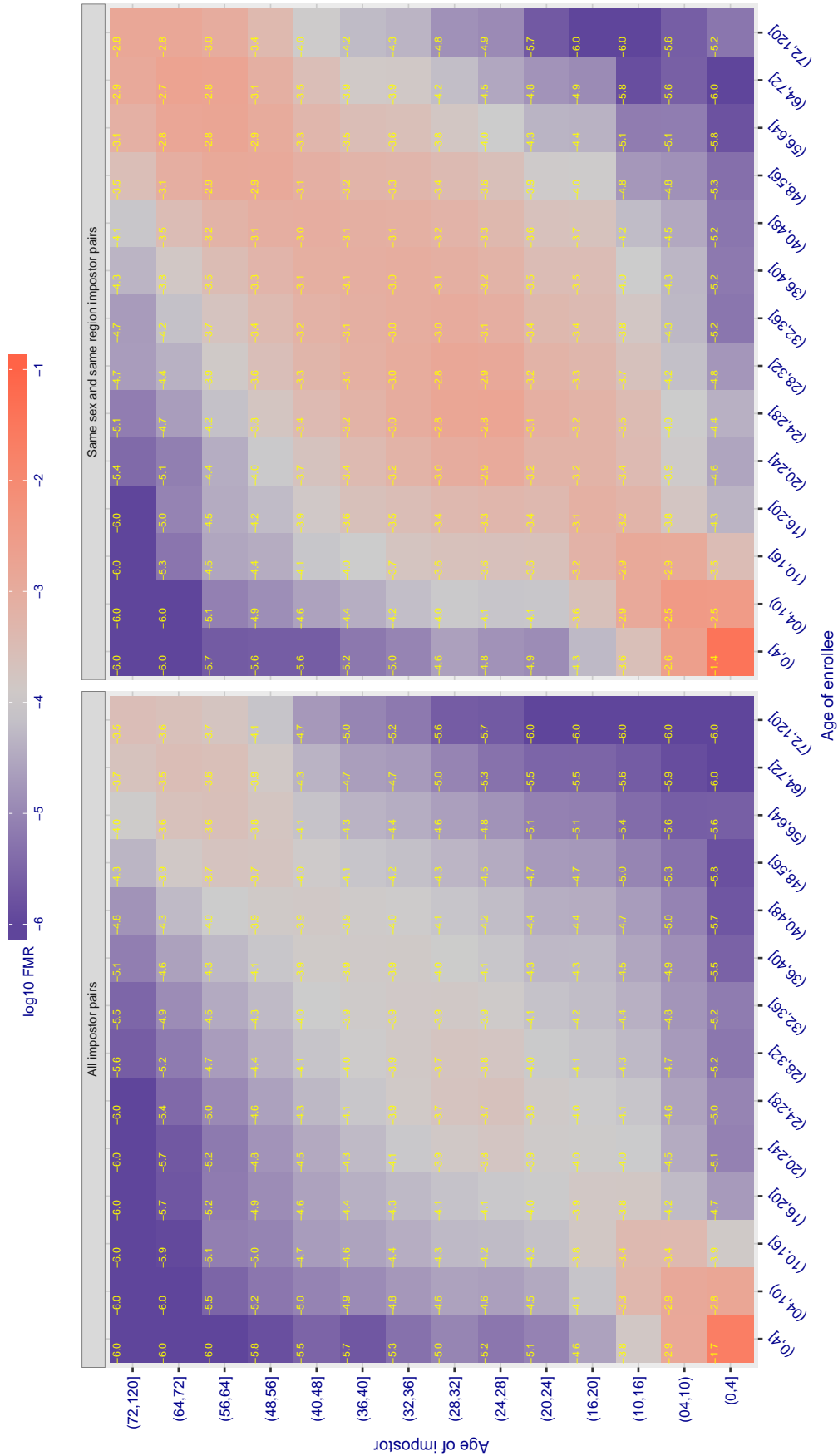


Figure 372: For algorithm microfocus-001 operating on visa images, the heatmap shows false match observed over impostor comparisons of faces from different individuals who have the given age pair. False matches are counted against a recognition threshold fixed globally to give $FMR = 0.001$ over all on the order of 10^{10} impostor comparisons. The text in each box gives the same quantity as that coded by the color. Light colors present a security vulnerability to, for example, a passport gate.

Cross age FMR at threshold $T = 0.602$ for algorithm microfocus_002, giving $FMR(T) = 0.0001$ globally.

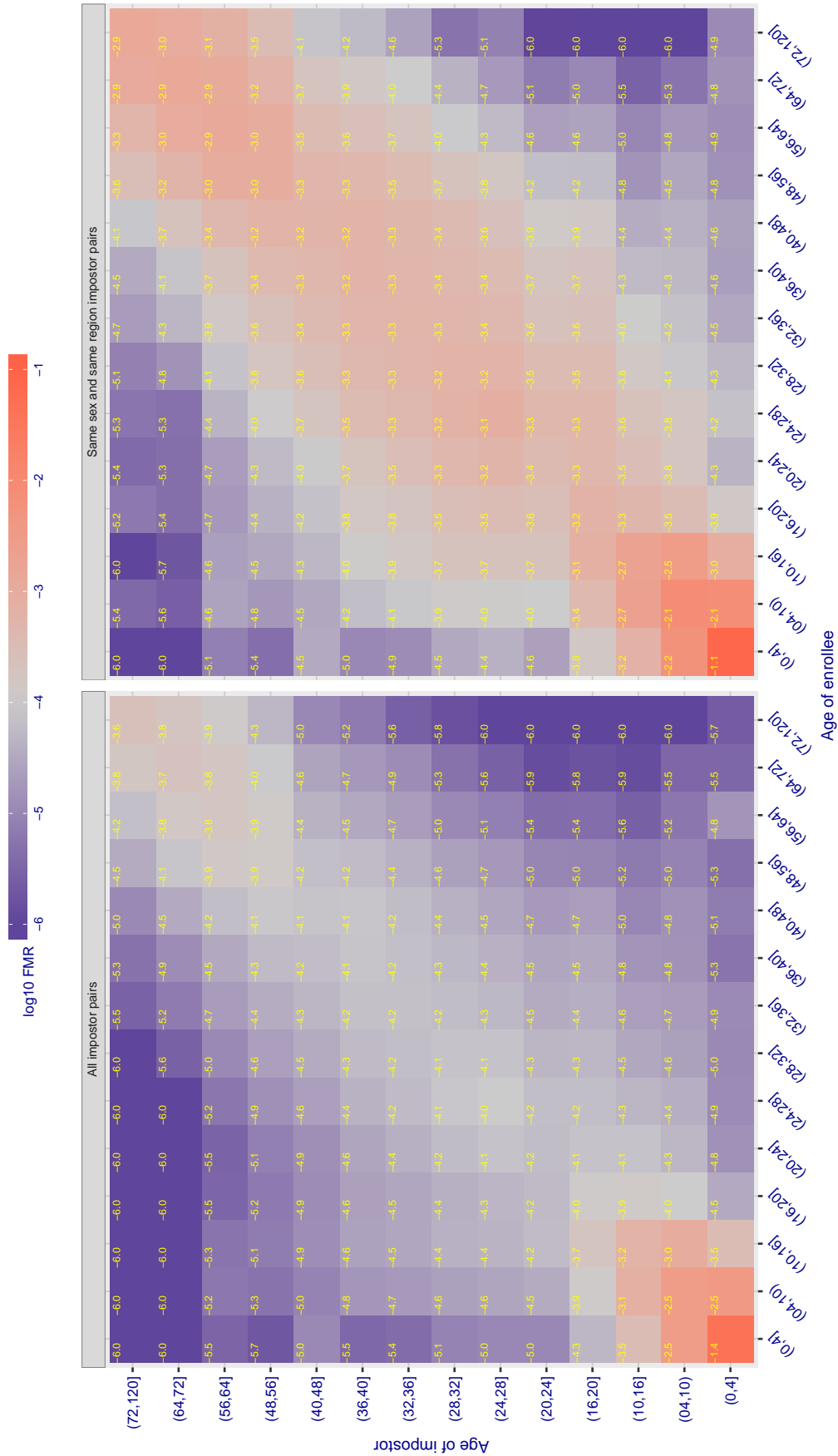


Figure 373: For algorithm microfocus-002 operating on visa images, the heatmap shows false match observed over impostor comparisons of faces from different individuals who have the given age pair. False matches are counted against a recognition threshold fixed globally to give $FMR = 0.0001$ over all on the order of 10^{10} impostor comparisons. The text in each box gives the same quantity as that coded by the color. Light colors present a security vulnerability to, for example, a passport gate.

Cross age FMR at threshold $T = 3859.000$ for algorithm neurotechnology_004, giving $FMR(T) = 0.0001$ globally.

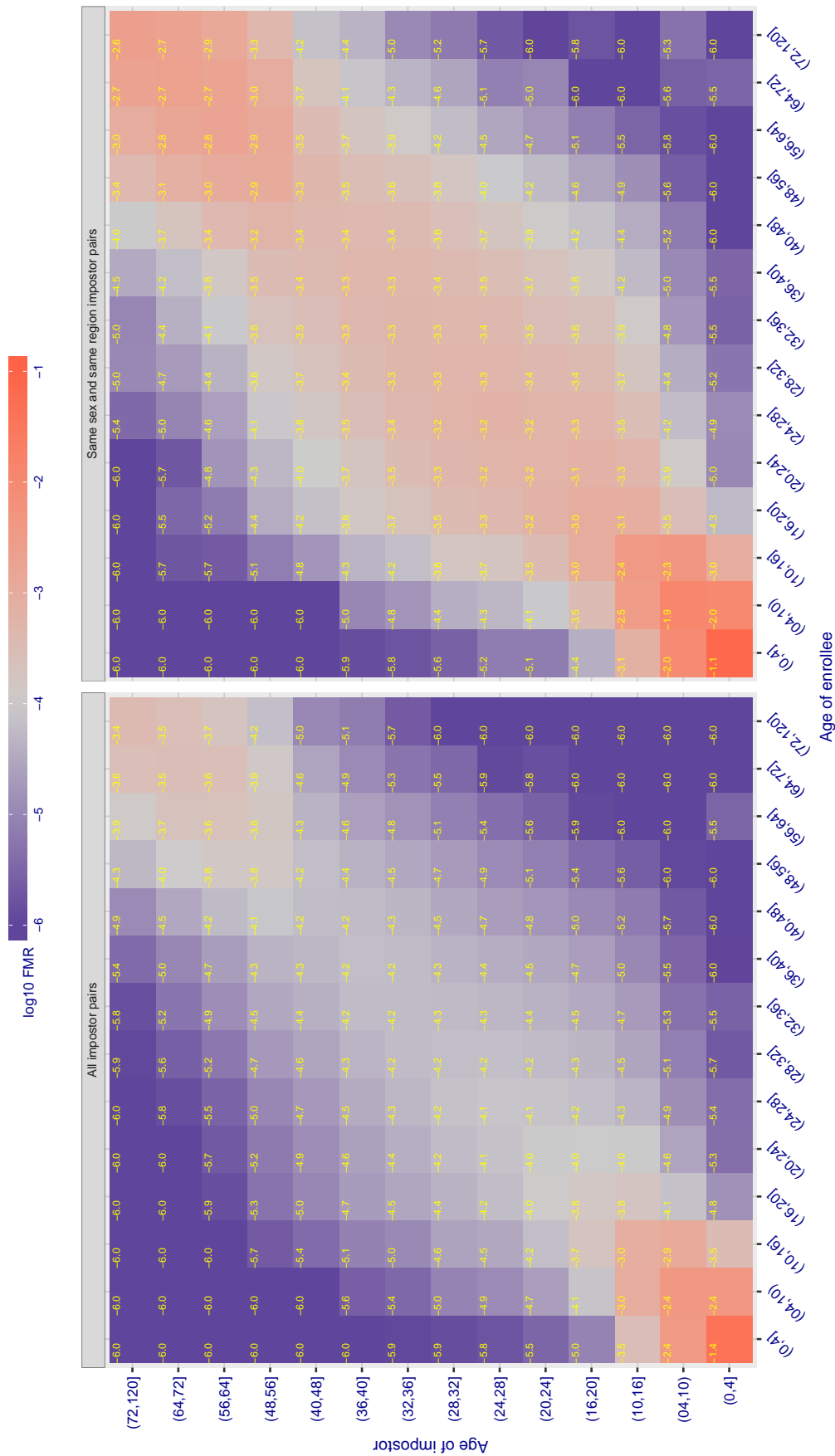


Figure 374: For algorithm neurotechnology-004 operating on visa images, the heatmap shows false match observed over impostor comparisons of faces from different individuals who have the given age pair. False matches are counted against a recognition threshold fixed globally to give $FMR = 0.001$ over all on the order of 10^{10} impostor comparisons. The text in each box gives the same quantity as that coded by the color. Light colors present a security vulnerability to, for example, a passport gate.

Cross age FMR at threshold $T = 1.000$ for algorithm `nodeflux_001`, giving $FMR(T) = 0.0001$ globally.

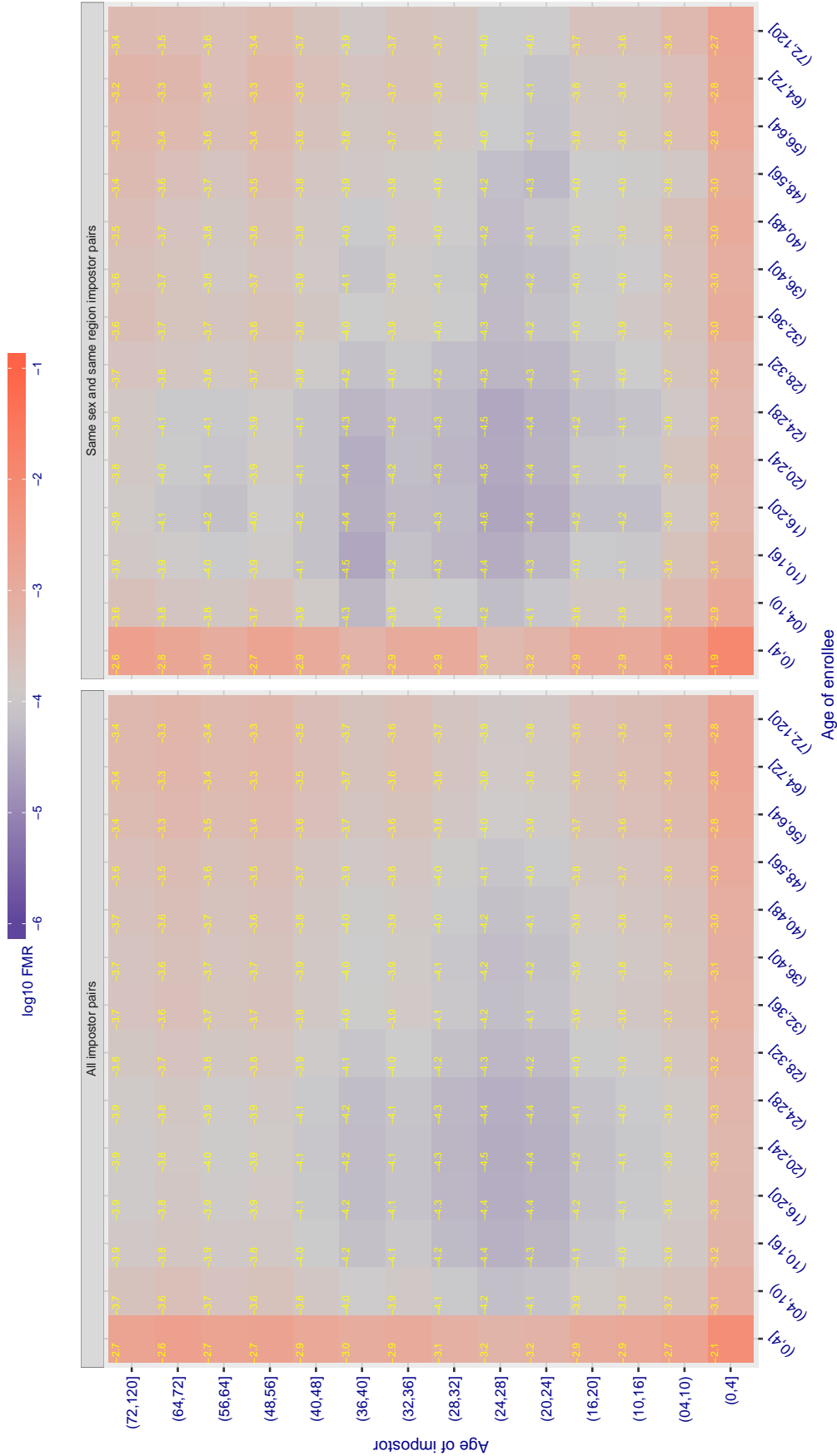


Figure 375: For algorithm `nodeflux-001` operating on visa images, the heatmap shows false match observed over impostor comparisons of faces from different individuals who have the given age pair. False matches are counted against a recognition threshold fixed globally to give $FMR = 0.001$ over all on the order of 10^{10} impostor comparisons. The text in each box gives the same quantity as that coded by the color. Light colors present a security vulnerability to, for example, a passport gate.

Cross age FMR at threshold $T = 1.487$ for algorithm ntechlab_005, giving $FMR(T) = 0.0001$ globally.

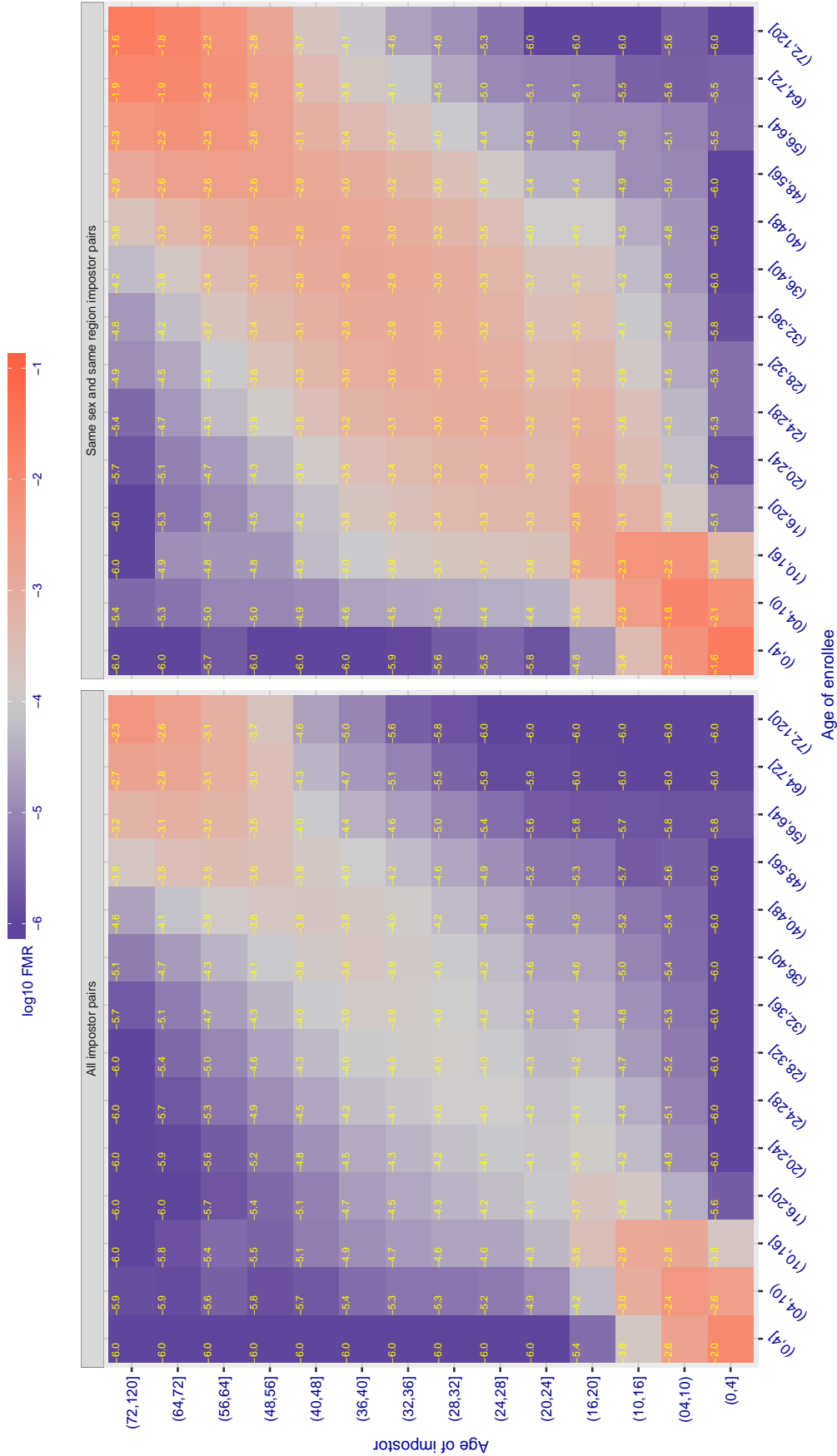


Figure 376: For algorithm ntechlab-005 operating on visa images, the heatmap shows false match observed over impostor comparisons of faces from different individuals who have the given age pair. False matches are counted against a recognition threshold fixed globally to give $FMR = 0.001$ over all on the order of 10^{10} impostor comparisons. The text in each box gives the same quantity as that coded by the color: Light colors present a security vulnerability to, for example, a passport gate.

Cross age FMR at threshold $T = 1.997$ for algorithm ntechlab_006, giving $FMR(T) = 0.0001$ globally.

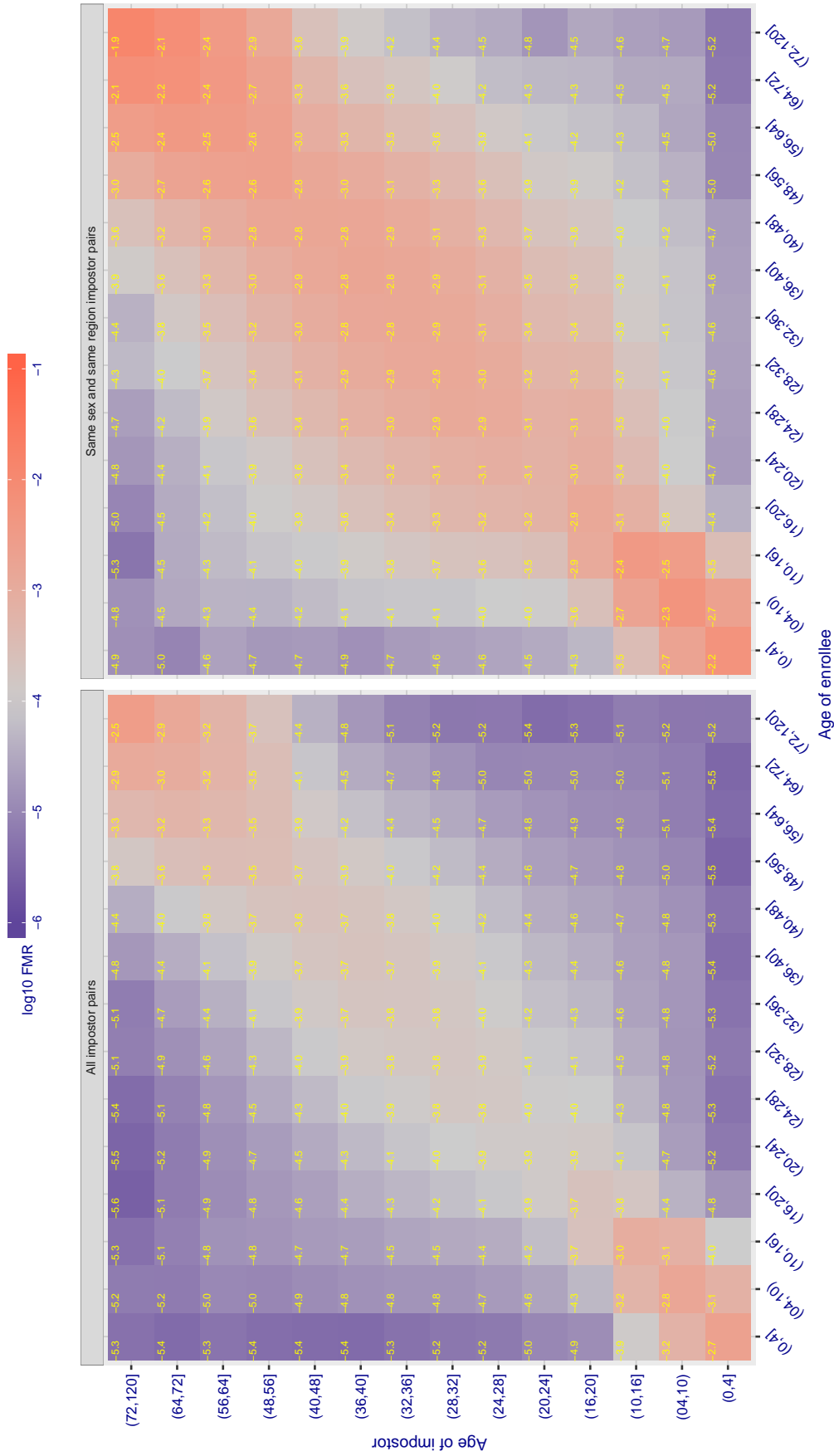


Figure 377: For algorithm ntechlab-006 operating on visa images, the heatmap shows false match observed over impostor comparisons of faces from different individuals who have the given age pair. False matches are counted against a recognition threshold fixed globally to give $FMR = 0.001$ over all on the order of 10^{10} impostor comparisons. The text in each box gives the same quantity as that coded by the color: Light colors present a security vulnerability to, for example, a passport gate.

Cross age FMR at threshold $T = 0.337$ for algorithm `psl_001`, giving $FMR(T) = 0.0001$ globally.

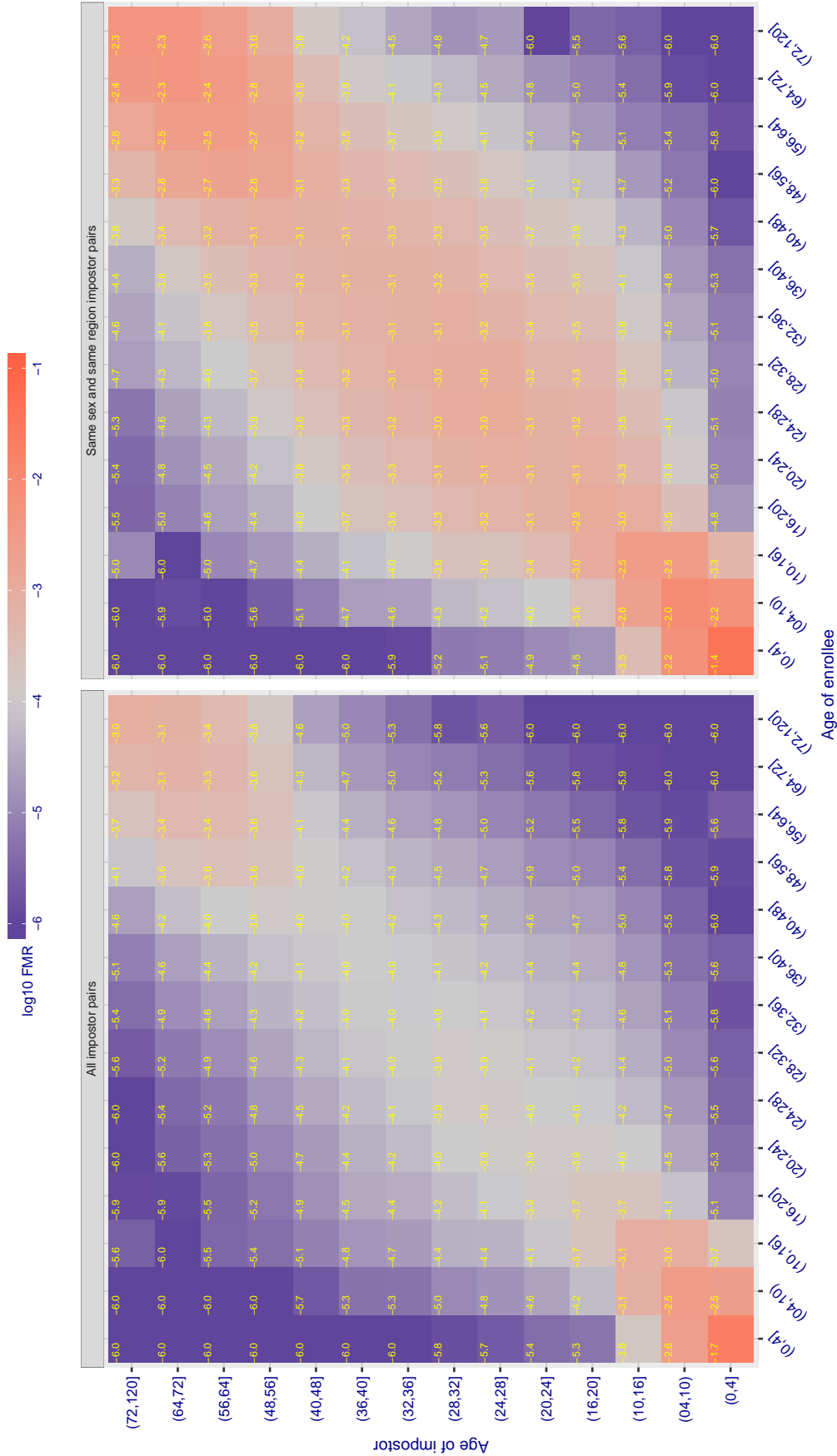


Figure 378: For algorithm `psl-001` operating on visa images, the heatmap shows false match observed over impostor comparisons of faces from different individuals who have the given age pair. False matches are counted against a recognition threshold fixed globally to give $FMR = 0.001$ over all on the order of 10^{10} impostor comparisons. The text in each box gives the same quantity as that coded by the color. Light colors present a security vulnerability to, for example, a passport gate.

Cross age FMR at threshold $T = 0.353$ for algorithm psl_002, giving $FMR(T) = 0.0001$ globally.

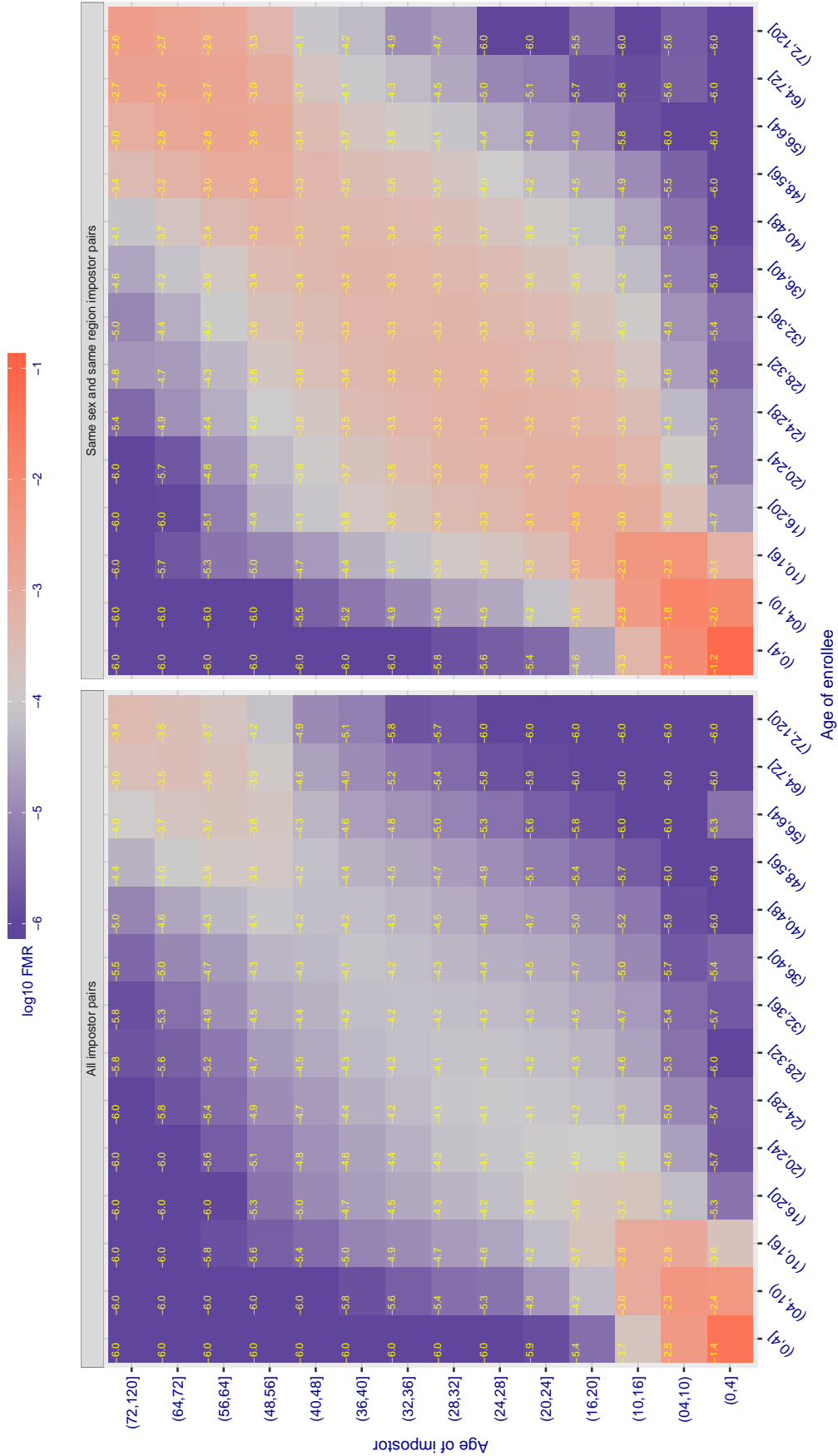


Figure 379: For algorithm psl-002 operating on visa images, the heatmap shows false match observed over impostor comparisons of faces from different individuals who have the given age pair. False matches are counted against a recognition threshold fixed globally to give $FMR = 0.001$ over all on the order of 10^{10} impostor comparisons. The text in each box gives the same quantity as that coded by the color. Light colors present a security vulnerability to, for example, a passport gate.

Cross age FMR at threshold $T = 0.750$ for algorithm rankone_005, giving $FMR(T) = 0.0001$ globally.

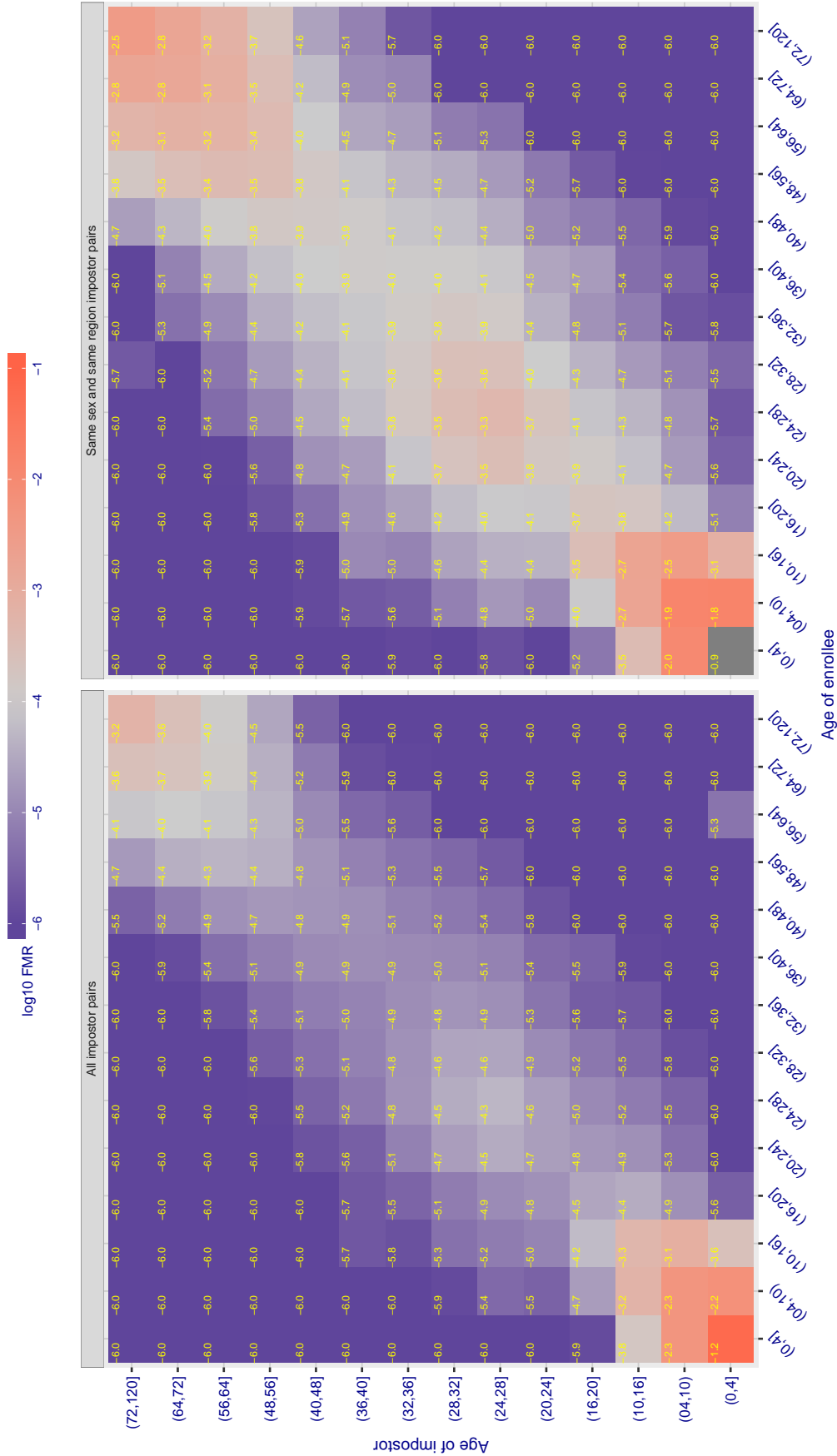


Figure 380: For algorithm rankone-005 operating on visa images, the heatmap shows false match observed over impostor comparisons of faces from different individuals who have the given age pair. False matches are counted against a recognition threshold fixed globally to give $FMR = 0.001$ over all on the order of 10^{10} impostor comparisons. The text in each box gives the same quantity as that coded by the color. Light colors present a security vulnerability to, for example, a passport gate.

Cross age FMR at threshold $T = 0.779$ for algorithm rankone_006, giving $FMR(T) = 0.0001$ globally.

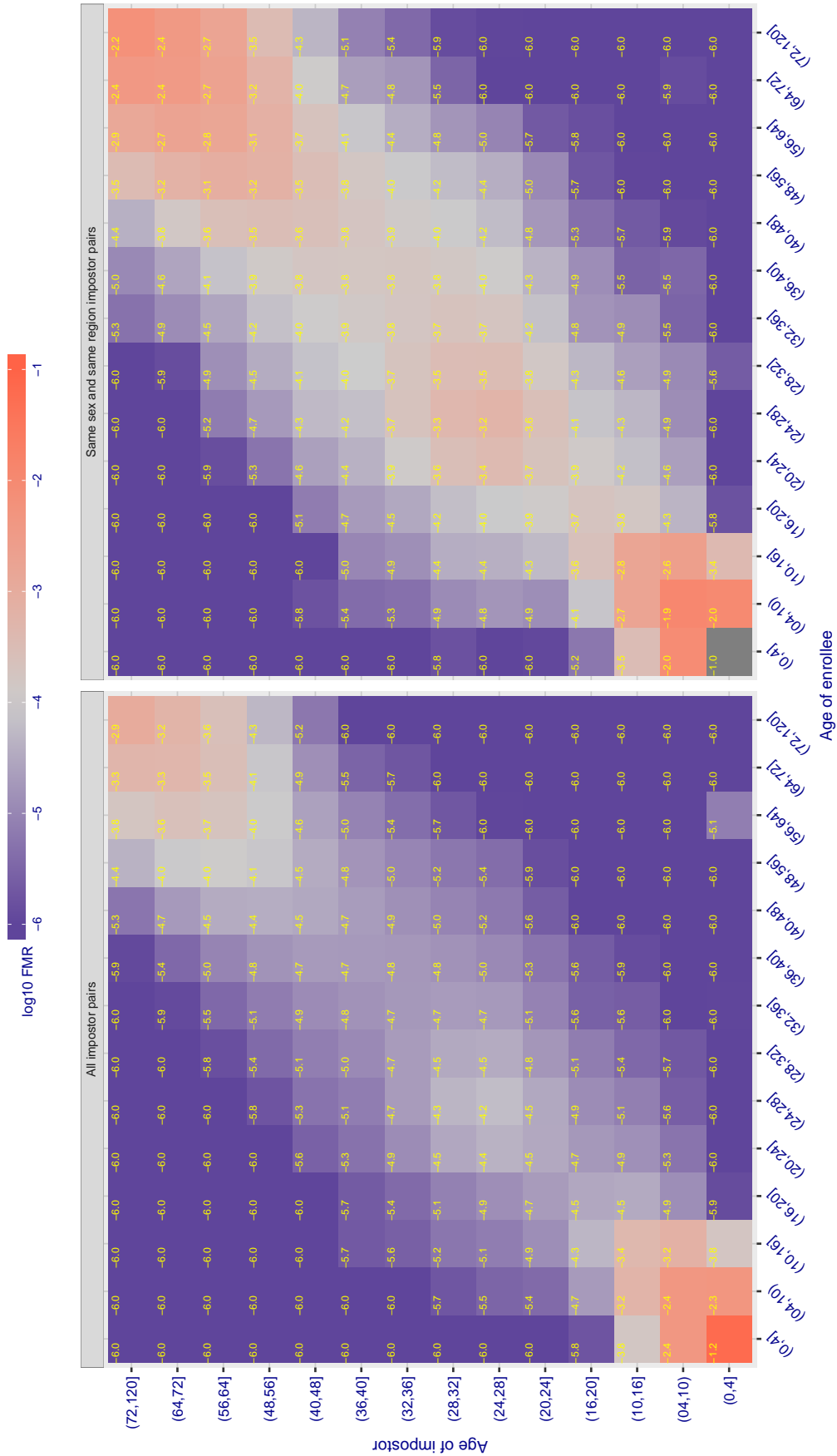


Figure 381: For algorithm rankone-006 operating on visa images, the heatmap shows false match observed over impostor comparisons of faces from different individuals who have the given age pair. False matches are counted against a recognition threshold fixed globally to give $FMR = 0.001$ over all on the order of 10^{10} impostor comparisons. The text in each box gives the same quantity as that coded by the color. Light colors present a security vulnerability to, for example, a passport gate.

Cross age FMR at threshold $T = 0.885$ for algorithm realnetworks_001, giving $FMR(T) = 0.0001$ globally.

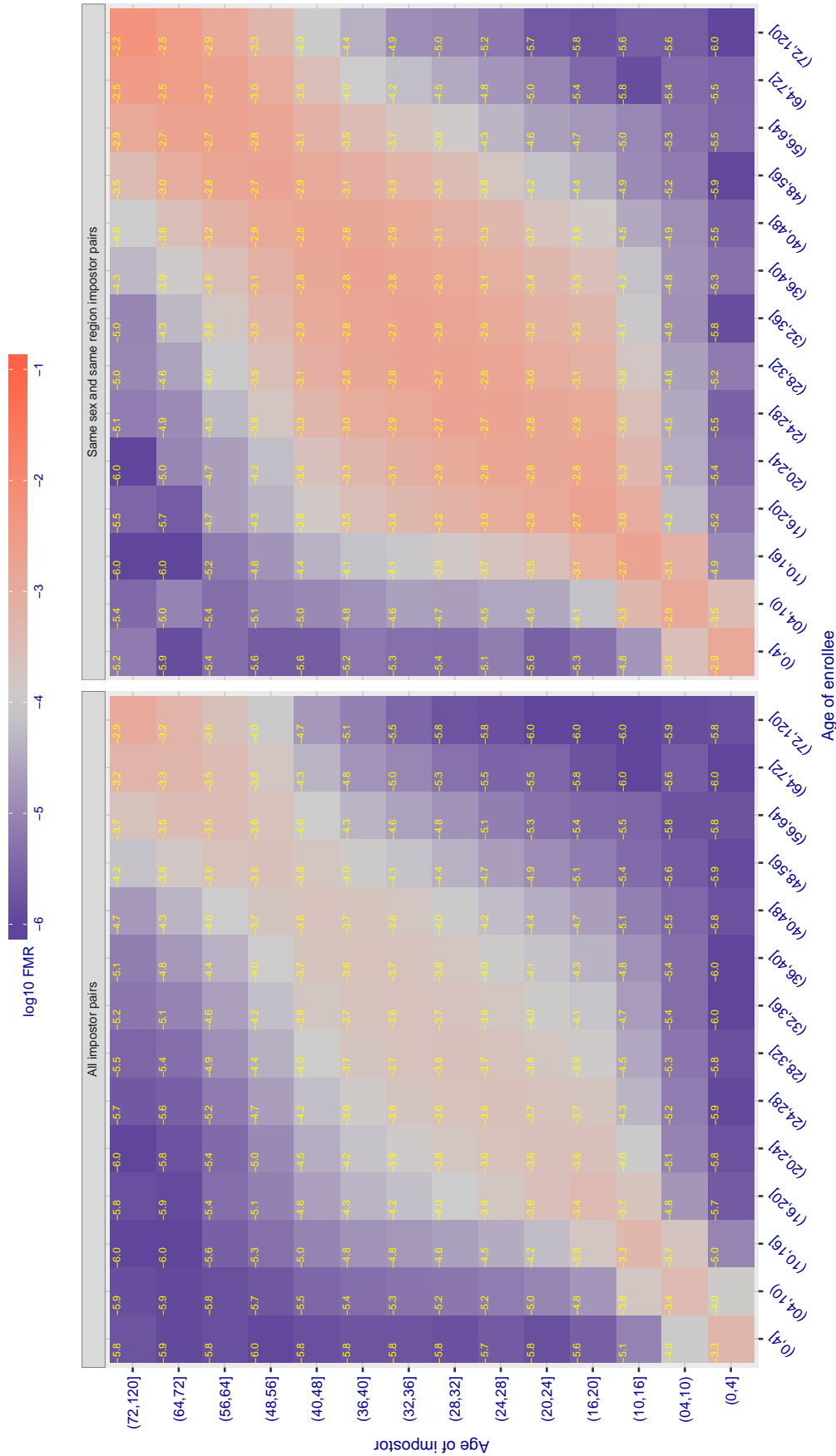


Figure 382: For algorithm realnetworks-001 operating on visa images, the heatmap shows false match observed over impostor comparisons of faces from different individuals who have the given age pair. False matches are counted against a recognition threshold fixed globally to give $FMR = 0.0001$ over all on the order of 10^{10} impostor comparisons. The text in each box gives the same quantity as that coded by the color. Light colors present a security vulnerability to, for example, a passport gate.

Cross age FMR at threshold $T = 0.883$ for algorithm realnetworks_002, giving $FMR(T) = 0.0001$ globally.

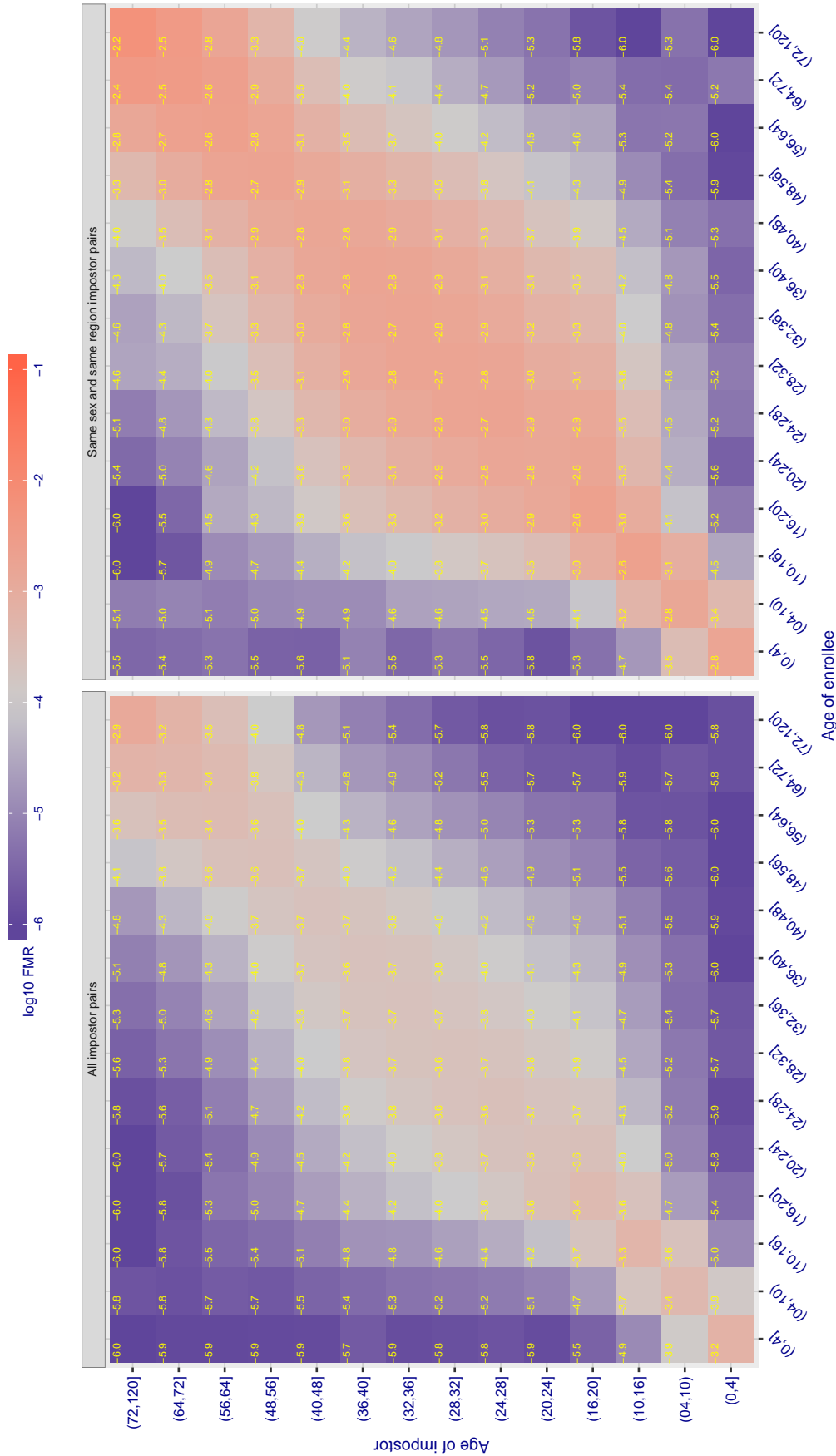


Figure 388: For algorithm realnetworks-002 operating on visa images, the heatmap shows false match observed over impostor comparisons of faces from different individuals who have the given age pair. False matches are counted against a recognition threshold fixed globally to give $FMR = 0.001$ over all on the order of 10^{10} impostor comparisons. The text in each box gives the same quantity as that coded by the color. Light colors present a security vulnerability to, for example, a passport gate.

Cross age FMR at threshold $T = 70.373$ for algorithm remarkai_000, giving $FMR(T) = 0.0001$ globally.

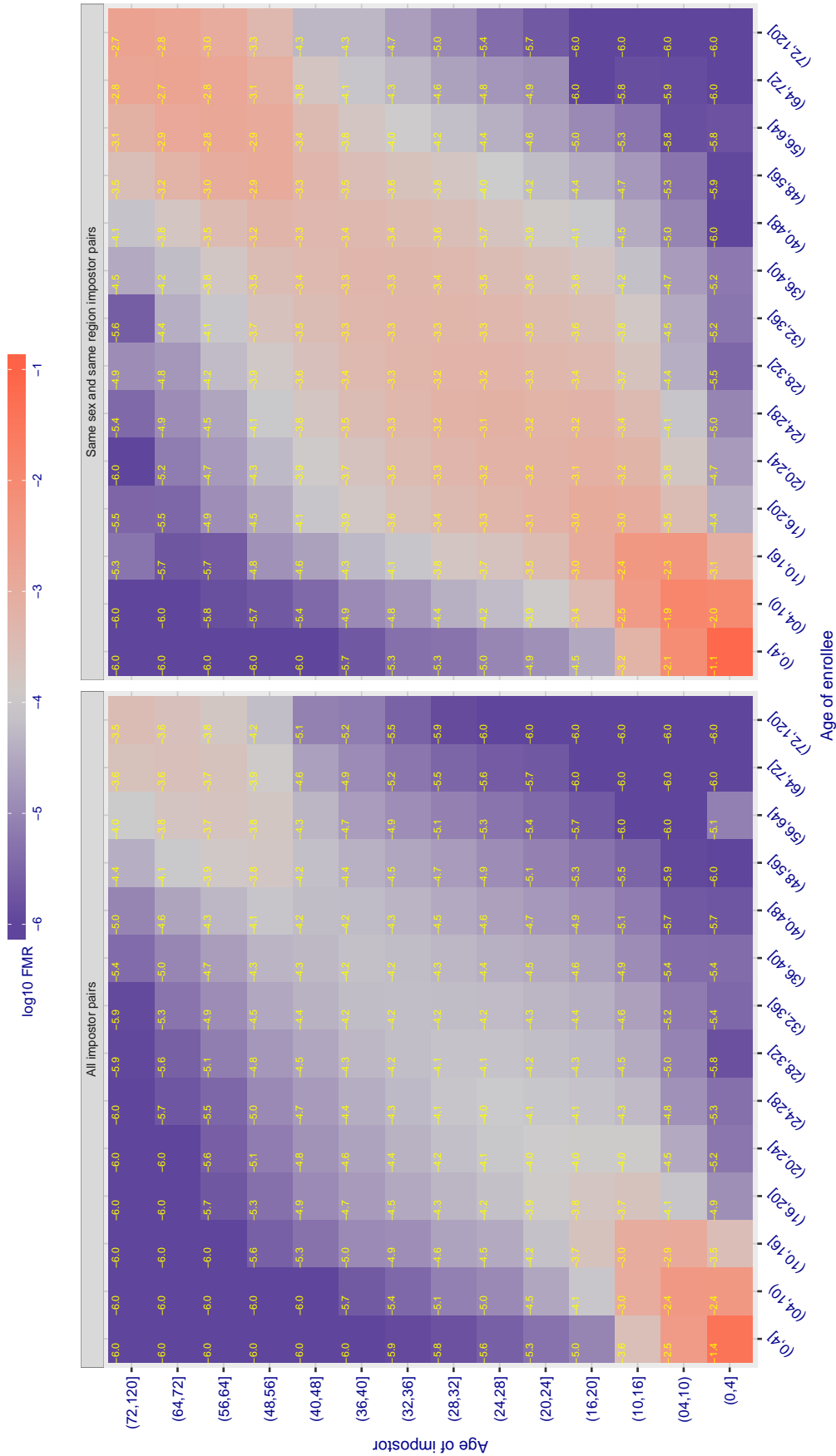


Figure 384: For algorithm remarkai-000 operating on visa images, the heatmap shows false match observed over impostor comparisons of faces from different individuals who have the given age pair. False matches are counted against a recognition threshold fixed globally to give $FMR = 0.001$ over all on the order of 10^{10} impostor comparisons. The text in each box gives the same quantity as that coded by the color. Light colors present a security vulnerability to, for example, a passport gate.

Cross age FMR at threshold $T = 70.384$ for algorithm remarkai_001, giving $FMR(T) = 0.0001$ globally.

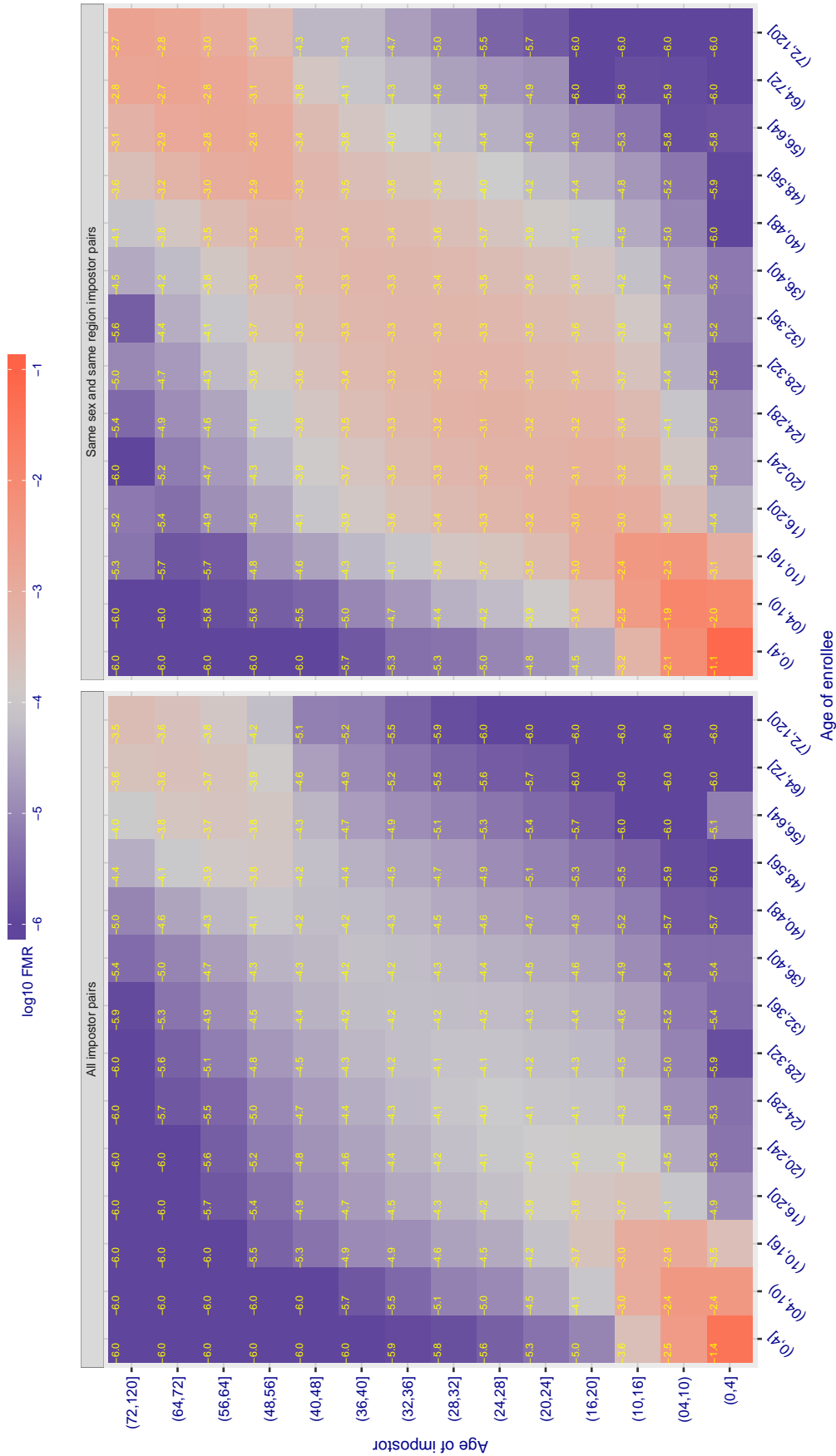


Figure 385: For algorithm remarkai-001 operating on visa images, the heatmap shows false match observed over impostor comparisons of faces from different individuals who have the given age pair. False matches are counted against a recognition threshold fixed globally to give $FMR = 0.001$ over all on the order of 10^{10} impostor comparisons. The text in each box gives the same quantity as that coded by the color. Light colors present a security vulnerability to, for example, a passport gate.

Cross age FMR at threshold $T = 0.682$ for algorithm `saffe_001`, giving $FMR(T) = 0.0001$ globally.

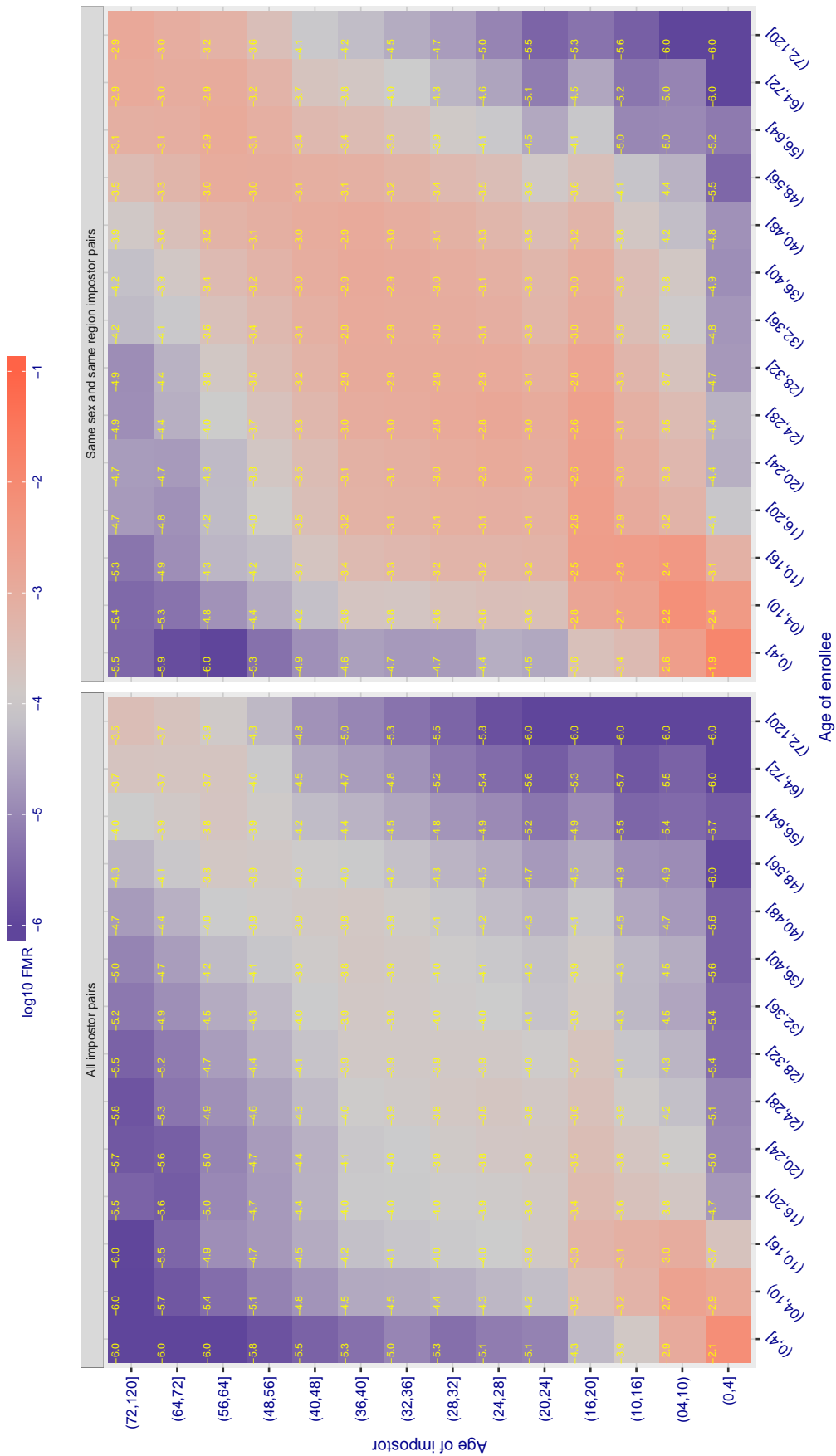


Figure 386: For algorithm `saffe-001` operating on visa images, the heatmap shows false match observed over impostor comparisons of faces from different individuals who have the given age pair. False matches are counted against a recognition threshold fixed globally to give $FMR = 0.001$ over all on the order of 10^{10} impostor comparisons. The text in each box gives the same quantity as that coded by the color: Light colors present a security vulnerability to, for example, a passport gate.

Cross age FMR at threshold $T = 0.383$ for algorithm `saffe_002`, giving $FMR(T) = 0.0001$ globally.

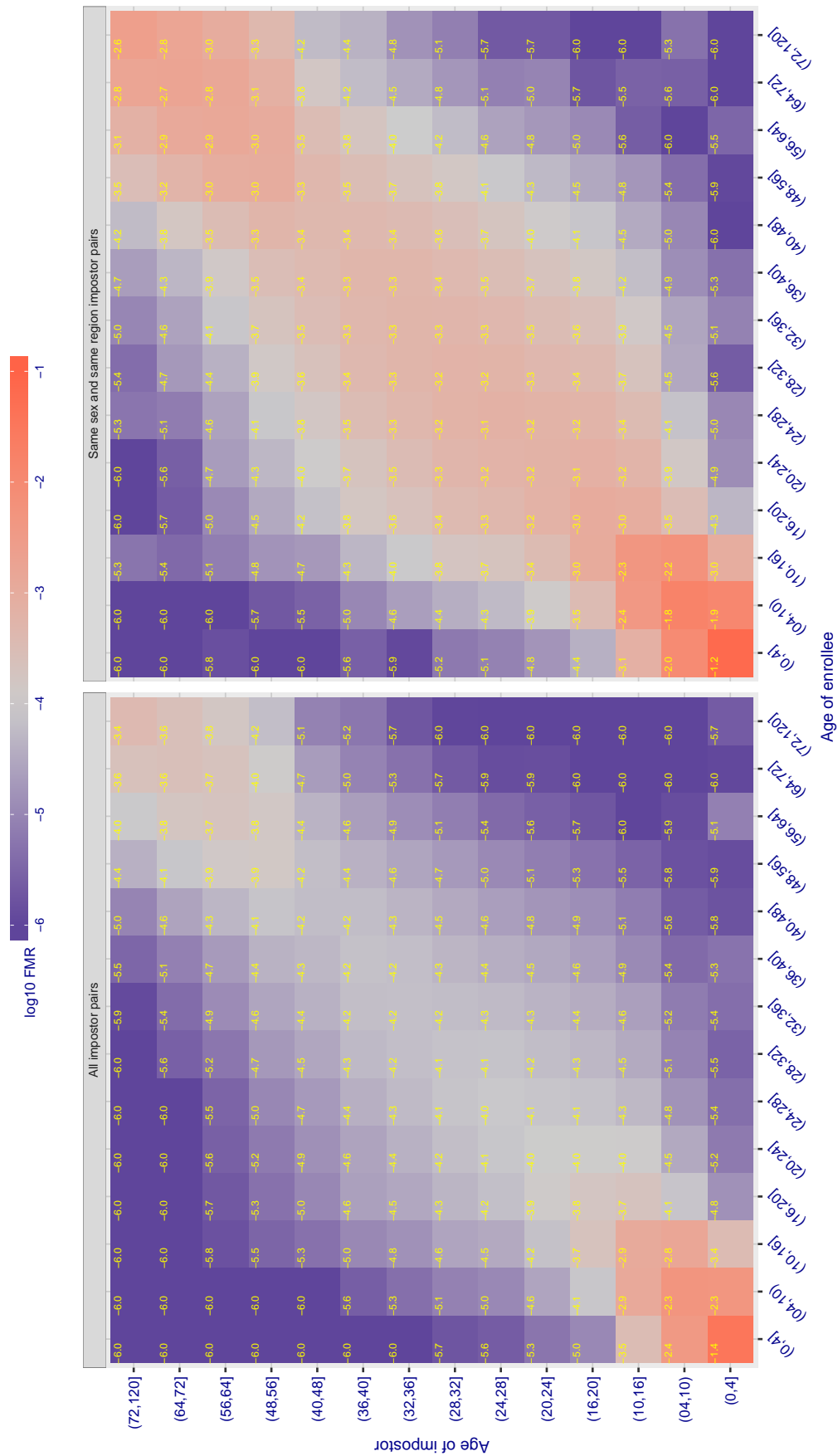


Figure 387: For algorithm `saffe-002` operating on visa images, the heatmap shows false match observed over impostor comparisons of faces from different individuals who have the given age pair. False matches are counted against a recognition threshold fixed globally to give $FMR = 0.001$ over all on the order of 10^{10} impostor comparisons. The text in each box gives the same quantity as that coded by the color: Light colors present a security vulnerability to, for example, a passport gate.

Cross age FMR at threshold $T = 0.390$ for algorithm `sensetime_001`, giving $FMR(T) = 0.0001$ globally.

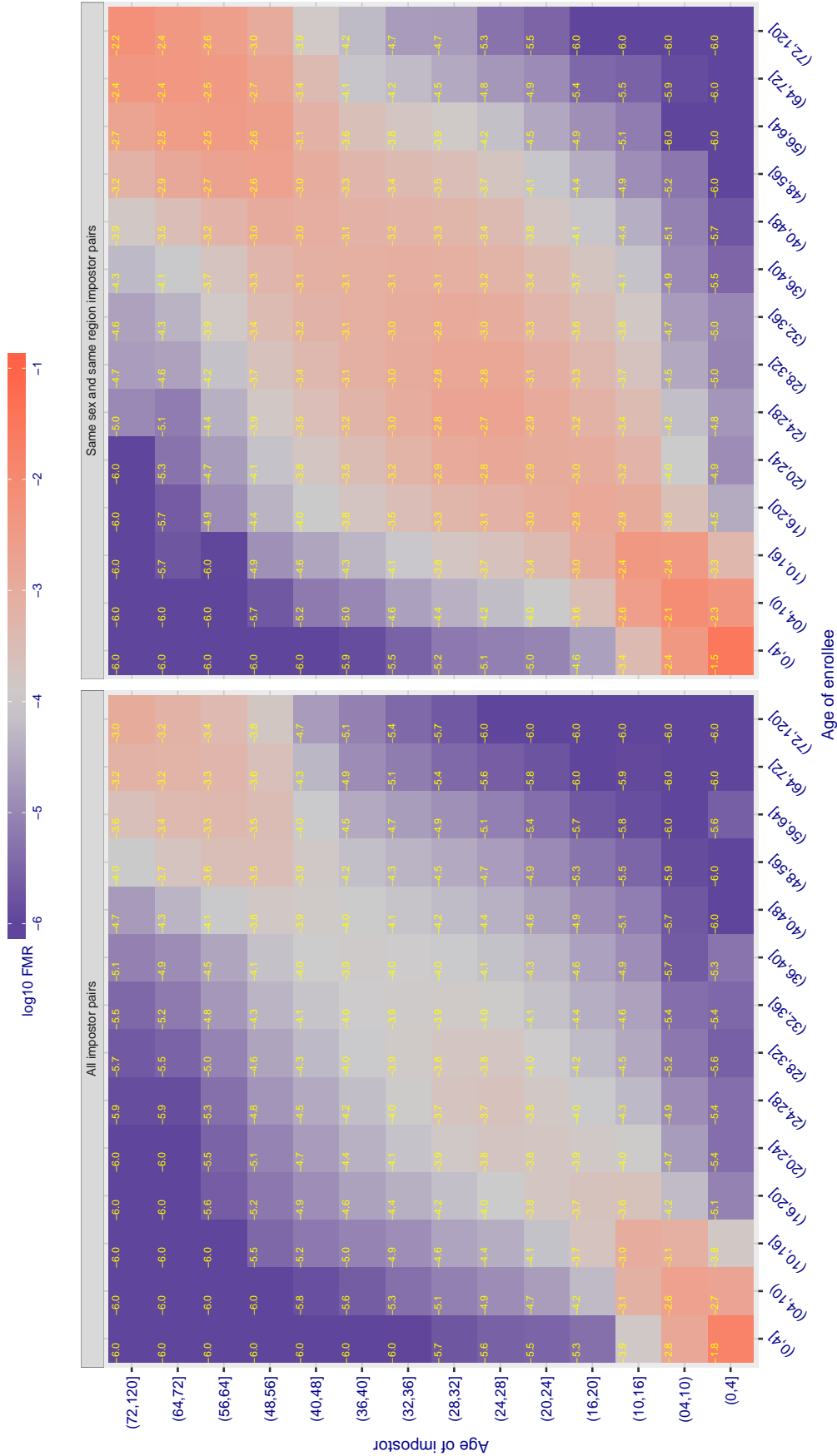


Figure 388: For algorithm `sensetime-001` operating on visa images, the heatmap shows false match observed over impostor comparisons of faces from different individuals who have the given age pair. False matches are counted against a recognition threshold fixed globally to give $FMR = 0.001$ over all on the order of 10^{10} impostor comparisons. The text in each box gives the same quantity as that coded by the color. Light colors present a security vulnerability to, for example, a passport gate.

Cross age FMR at threshold $T = 0.390$ for algorithm `sensetime_002`, giving $FMR(T) = 0.0001$ globally.

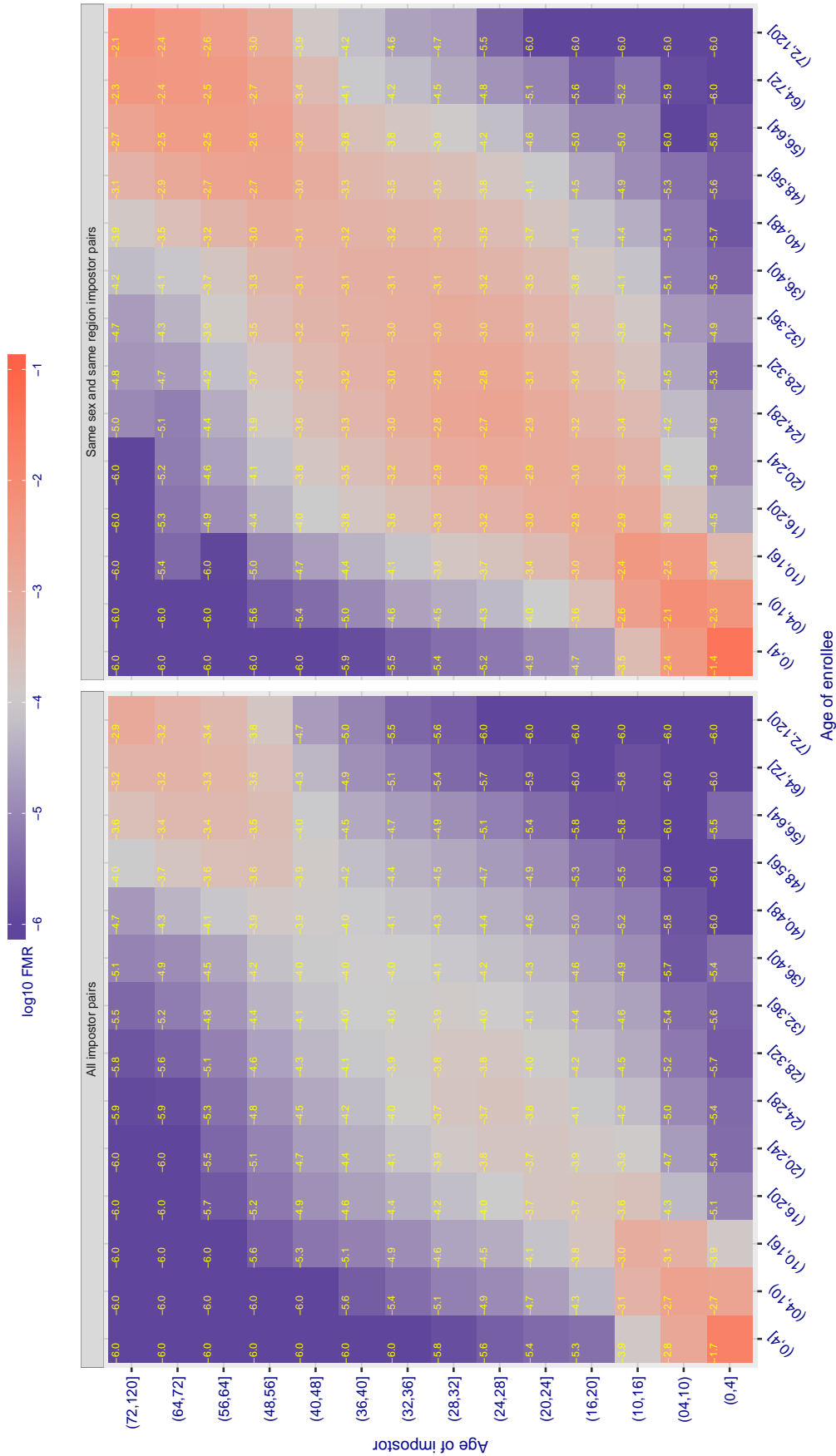


Figure 389: For algorithm `sensetime-002` operating on visa images, the heatmap shows false match observed over impostor comparisons of faces from different individuals who have the given age pair. False matches are counted against a recognition threshold fixed globally to give $FMR = 0.001$ over all on the order of 10^{10} impostor comparisons. The text in each box gives the same quantity as that coded by the color. Light colors present a security vulnerability to, for example, a passport gate.

Cross age FMR at threshold $T = 0.970$ for algorithm shaman_000, giving $FMR(T) = 0.0001$ globally.

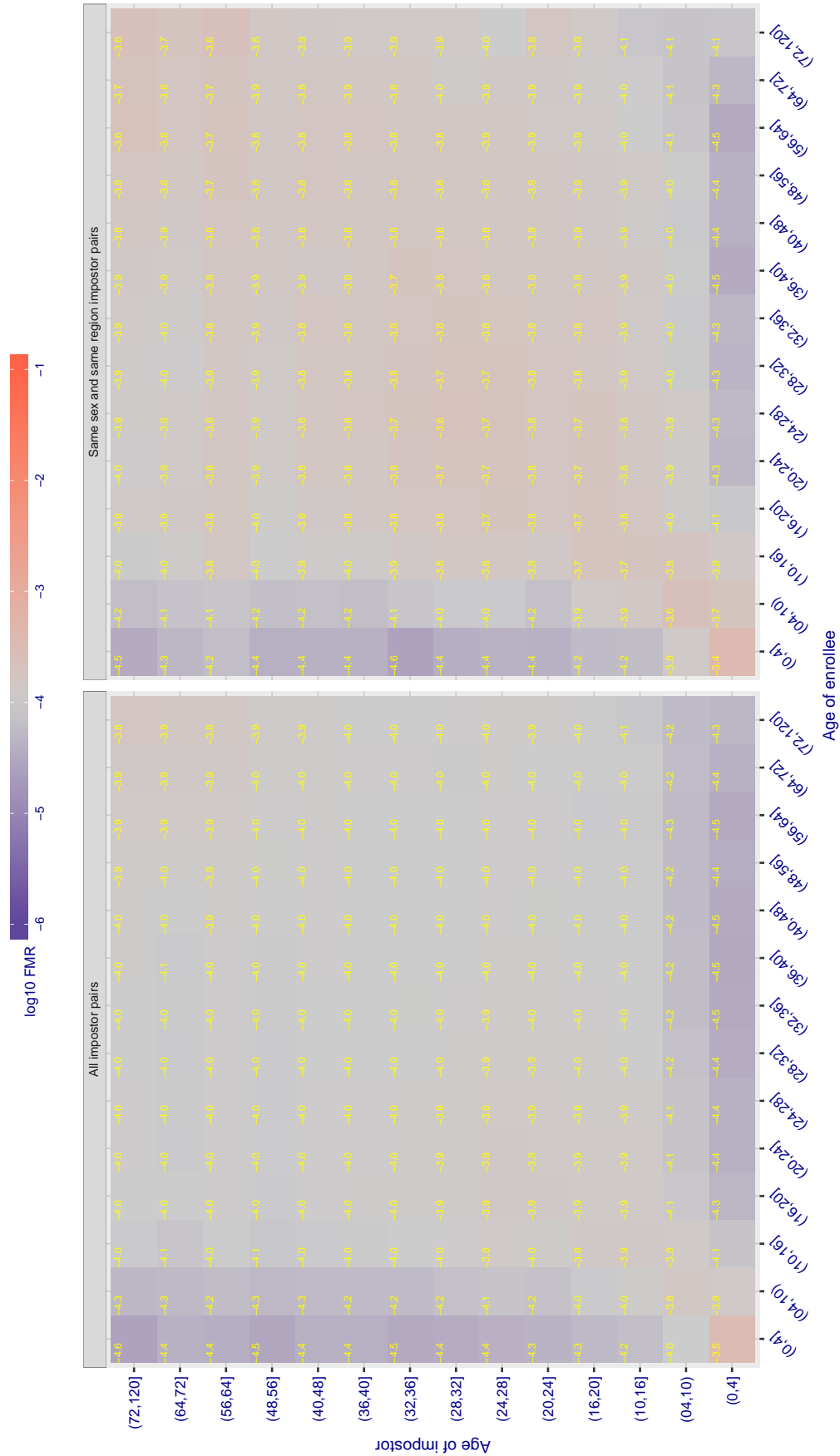


Figure 390: For algorithm shaman-000 operating on visa images, the heatmap shows false match observed over impostor comparisons of faces from different individuals who have the given age pair. False matches are counted against a recognition threshold fixed globally to give $FMR = 0.001$ over all on the order of 10^{10} impostor comparisons. The text in each box gives the same quantity as that coded by the color. Light colors present a security vulnerability to, for example, a passport gate.

Cross age FMR at threshold $T = 0.725$ for algorithm shaman_001, giving $FMR(T) = 0.0001$ globally.

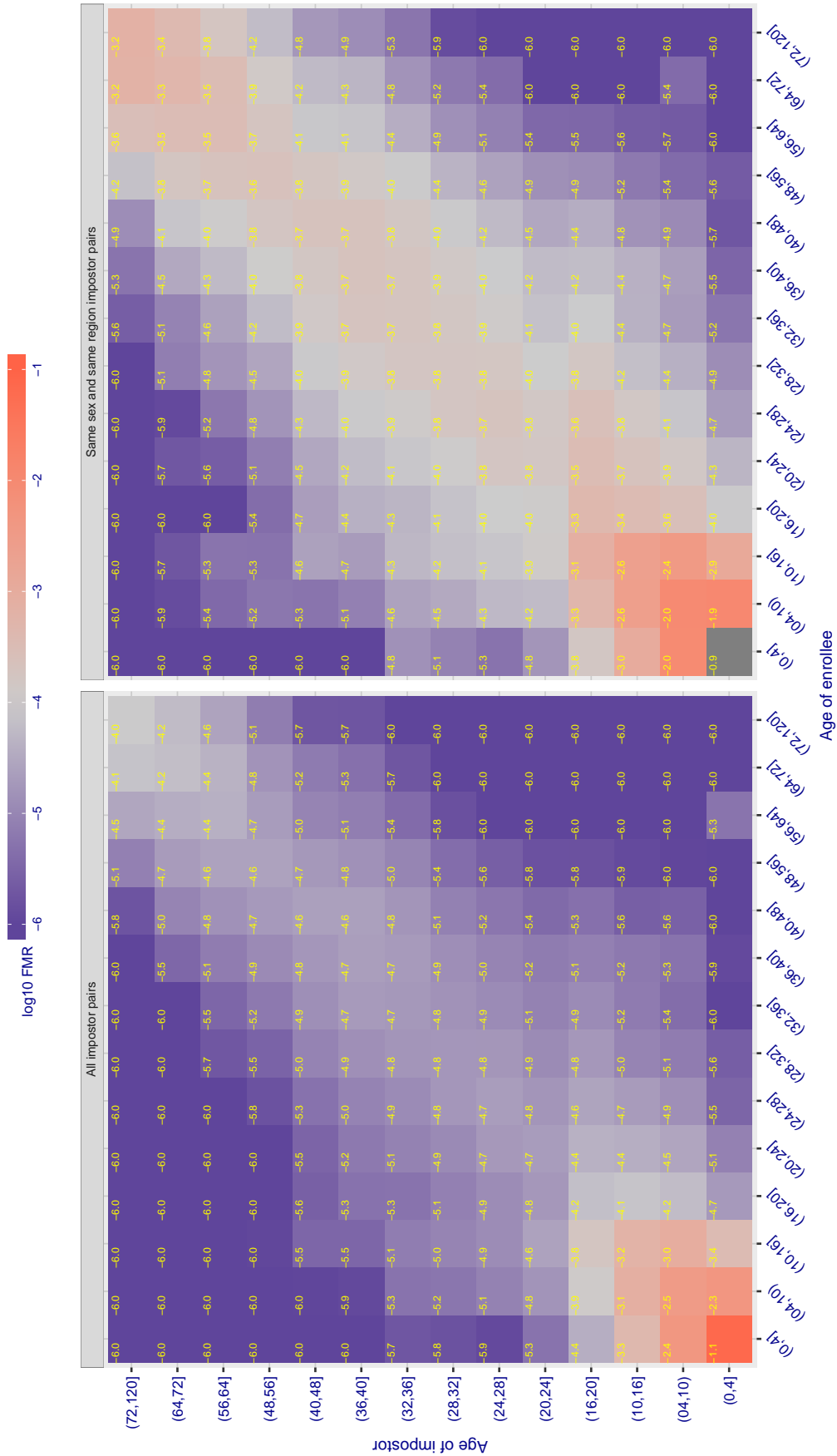


Figure 391: For algorithm shaman-001 operating on visa images, the heatmap shows false match observed over impostor comparisons of faces from different individuals who have the given age pair. False matches are counted against a recognition threshold fixed globally to give $FMR = 0.001$ over all on the order of 10^{10} impostor comparisons. The text in each box gives the same quantity as that coded by the color. Light colors present a security vulnerability to, for example, a passport gate.

Cross age FMR at threshold $T = 0.390$ for algorithm `siat_002`, giving $FMR(T) = 0.0001$ globally.

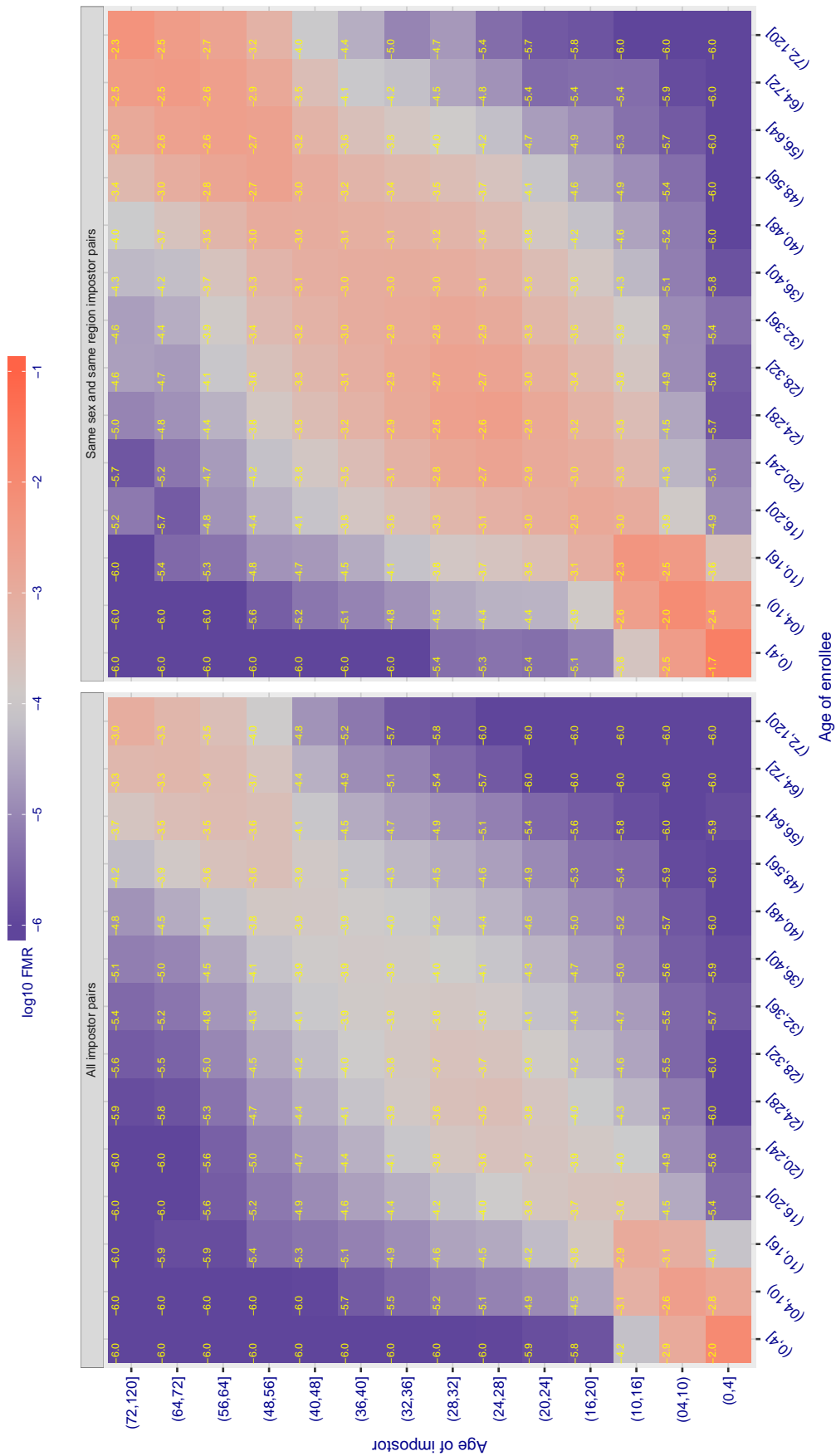


Figure 392: For algorithm `siat-002` operating on visa images, the heatmap shows false match observed over impostor comparisons of faces from different individuals who have the given age pair. False matches are counted against a recognition threshold fixed globally to give $FMR = 0.001$ over all on the order of 10^{10} impostor comparisons. The text in each box gives the same quantity as that coded by the color. Light colors present a security vulnerability to, for example, a passport gate.

Cross age FMR at threshold $T = 0.393$ for algorithm `siat_004`, giving $FMR(T) = 0.0001$ globally.

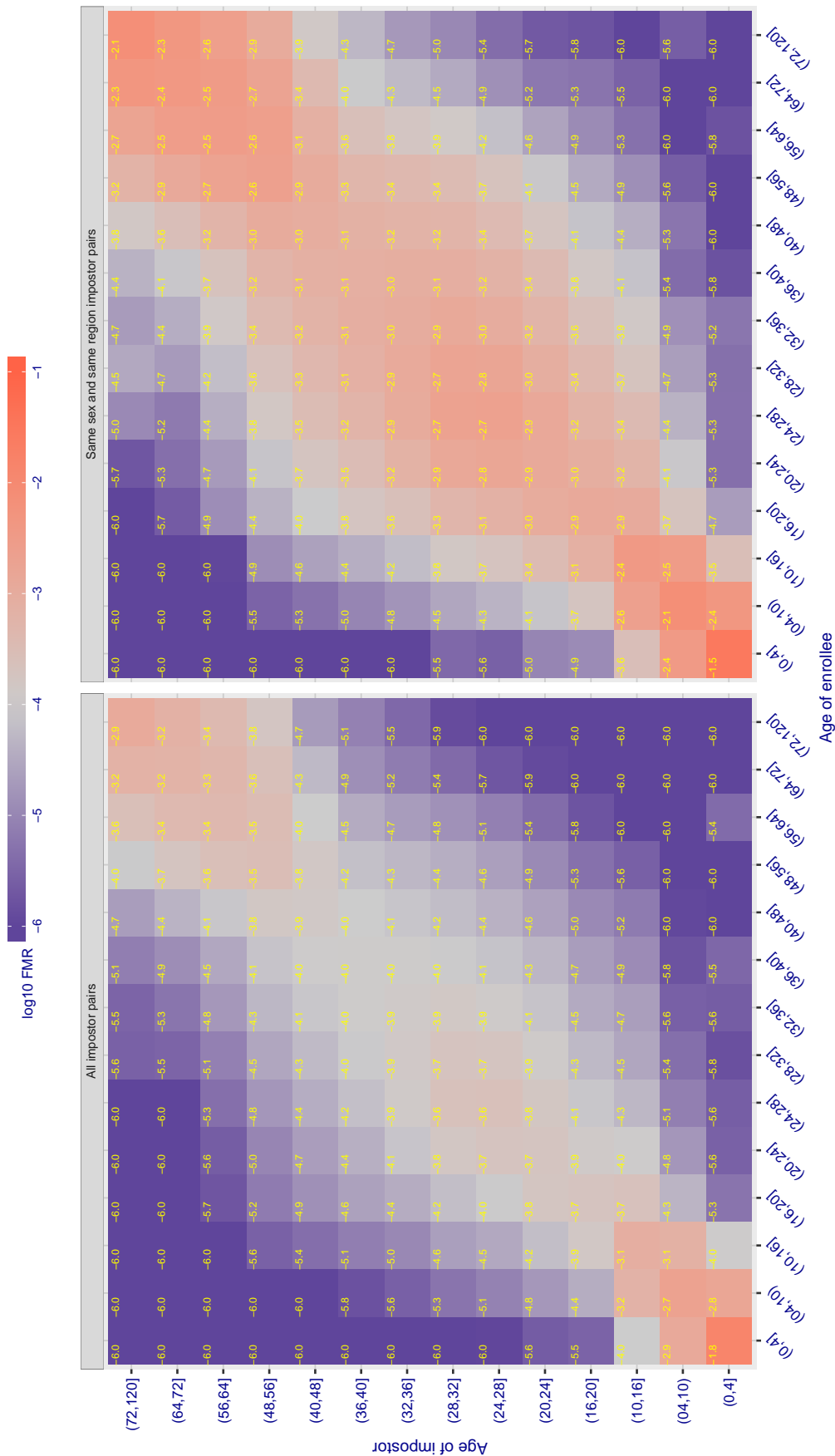


Figure 393: For algorithm `siat-004` operating on visa images, the heatmap shows false match observed over impostor comparisons of faces from different individuals who have the given age pair. False matches are counted against a recognition threshold fixed globally to give $FMR = 0.001$ over all on the order of 10^{10} impostor comparisons. The text in each box gives the same quantity as that coded by the color. Light colors present a security vulnerability to, for example, a passport gate.

Cross age FMR at threshold $T = 0.598$ for algorithm smilart_002, giving $FMR(T) = 0.0001$ globally.

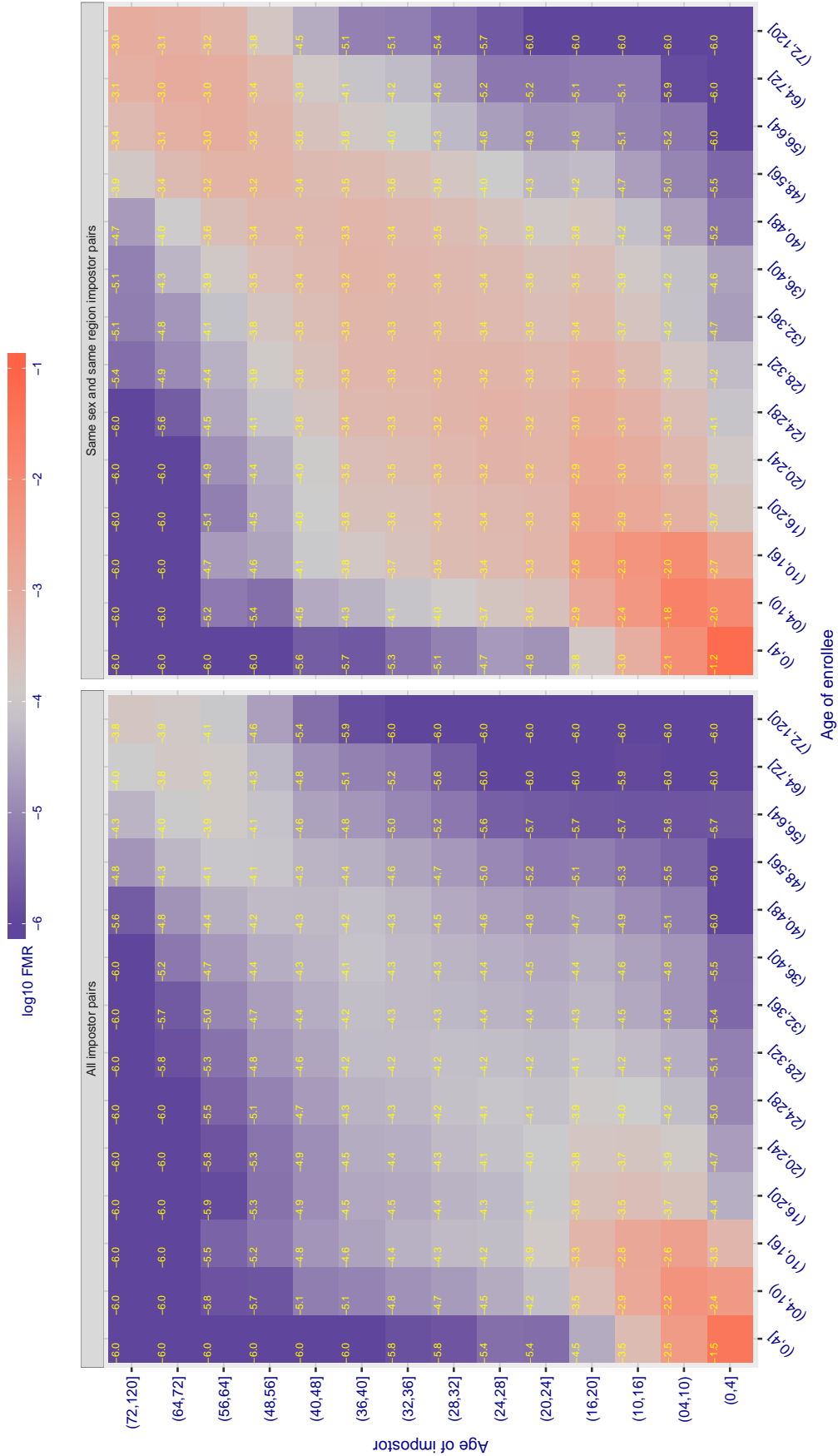


Figure 394: For algorithm smilart-002 operating on visa images, the heatmap shows false match observed over impostor comparisons of faces from different individuals who have the given age pair. False matches are counted against a recognition threshold fixed globally to give $FMR = 0.001$ over all on the order of 10^{10} impostor comparisons. The text in each box gives the same quantity as that coded by the color: Light colors present a security vulnerability to, for example, a passport gate.

Cross age FMR at threshold $T = 0.654$ for algorithm `smilart_003`, giving $FMR(T) = 0.0001$ globally.

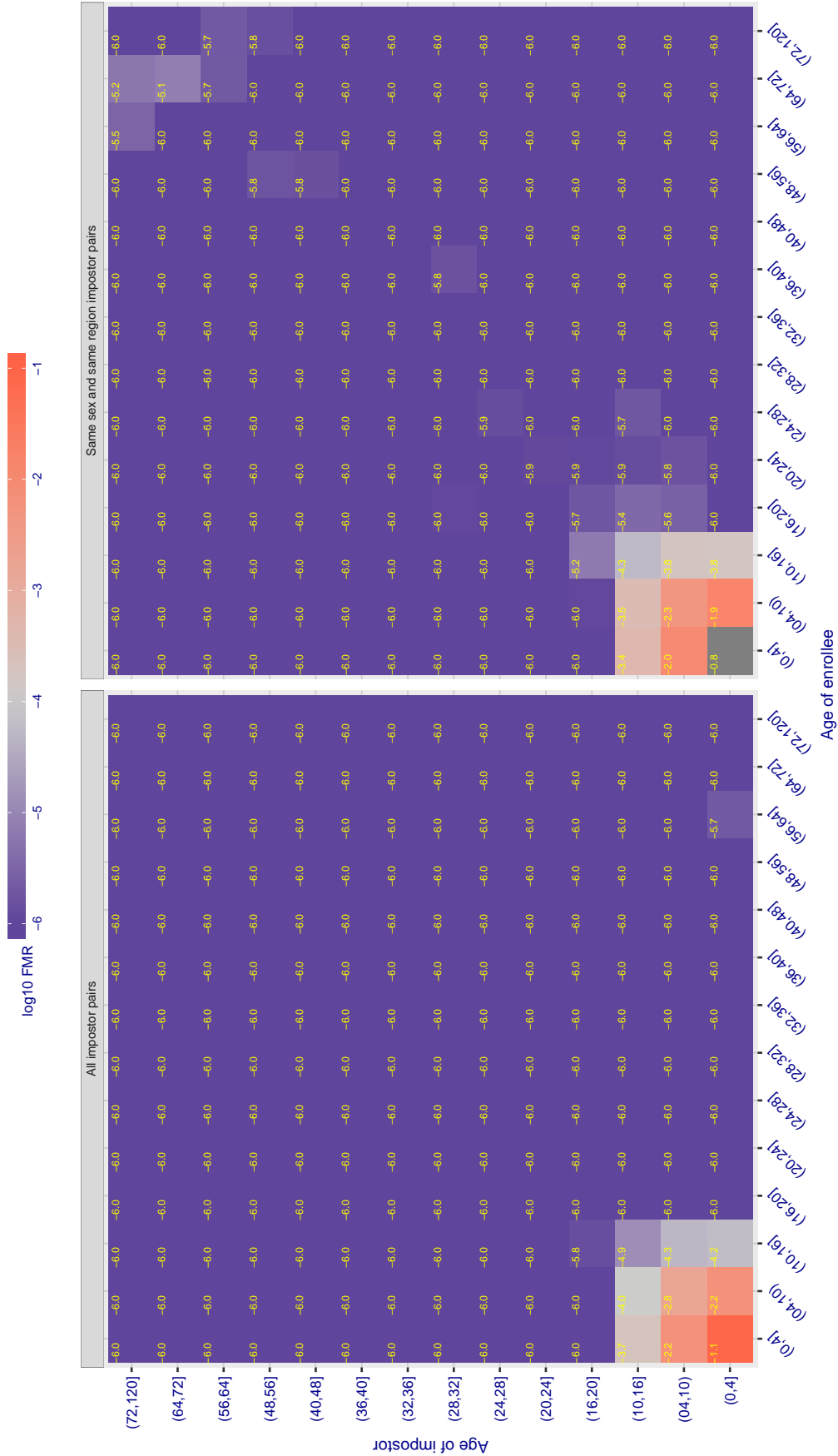


Figure 395: For algorithm `smilart-003` operating on visa images, the heatmap shows false match observed over impostor comparisons of faces from different individuals who have the given age pair. False matches are counted against a recognition threshold fixed globally to give $FMR = 0.001$ over all on the order of 10^{10} impostor comparisons. The text in each box gives the same quantity as that coded by the color: Light colors present a security vulnerability to, for example, a passport gate.

Cross age FMR at threshold $T = 0.881$ for algorithm `synesis_003`, giving $FMR(T) = 0.0001$ globally.

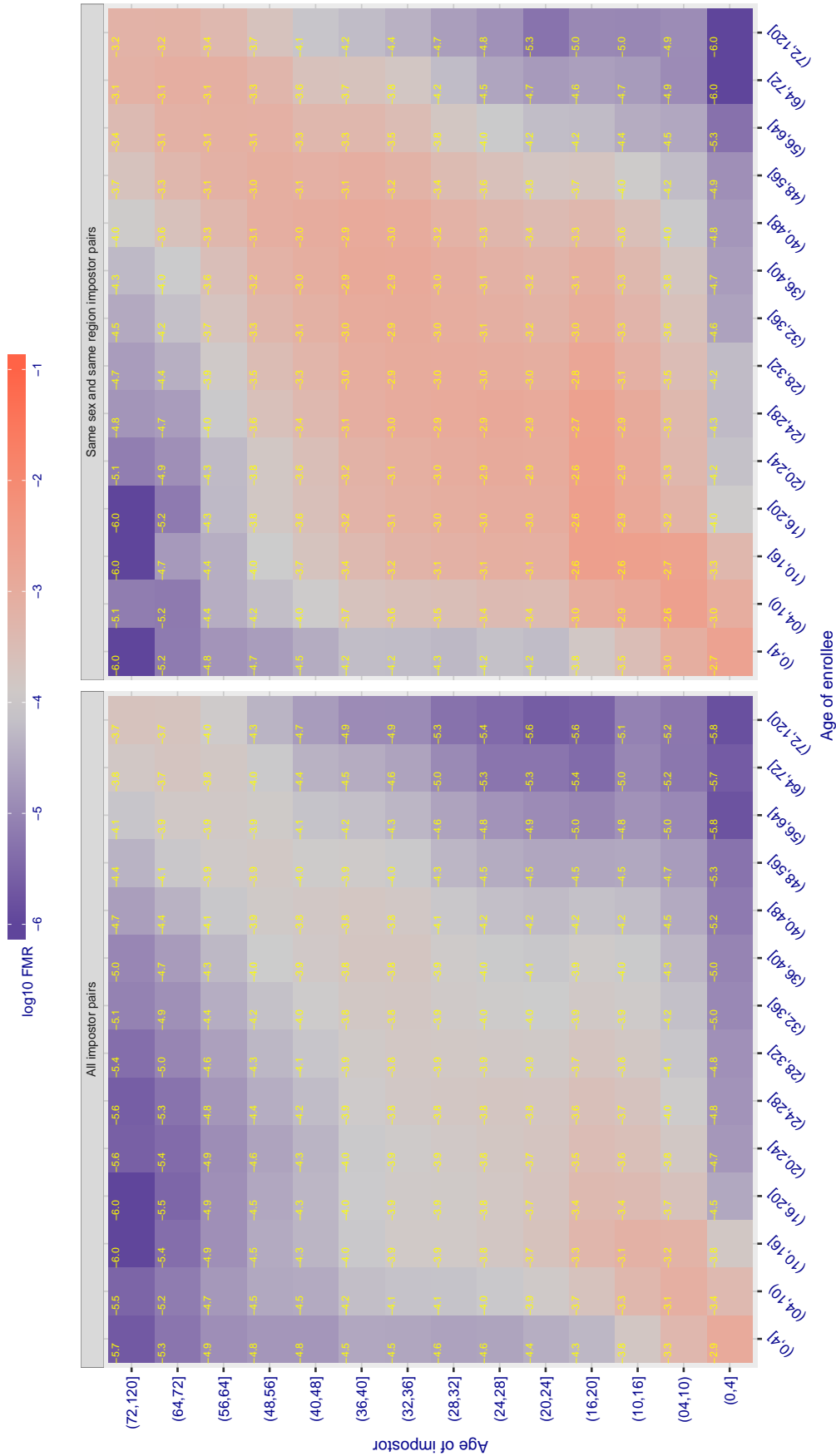


Figure 396: For algorithm `synesis-003` operating on visa images, the heatmap shows false match observed over impostor comparisons of faces from different individuals who have the given age pair. False matches are counted against a recognition threshold fixed globally to give $FMR = 0.001$ over all on the order of 10^{10} impostor comparisons. The text in each box gives the same quantity as that coded by the color. Light colors present a security vulnerability to, for example, a passport gate.

Cross age FMR at threshold $T = 0.221$ for algorithm `synesis_004`, giving $FMR(T) = 0.0001$ globally.

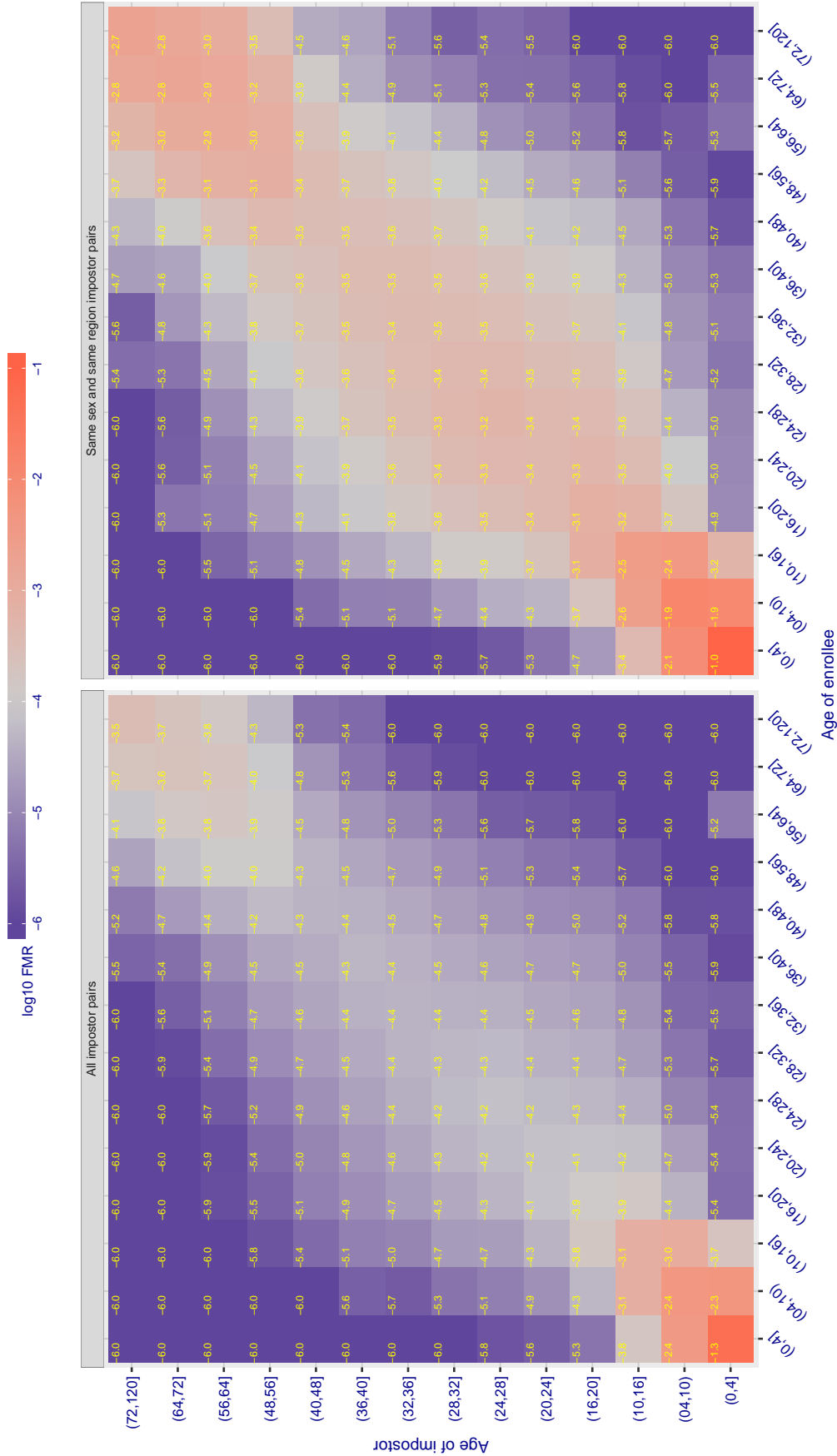


Figure 397: For algorithm `synesis-004` operating on visa images, the heatmap shows false match observed over impostor comparisons of faces from different individuals who have the given age pair. False matches are counted against a recognition threshold fixed globally to give $FMR = 0.001$ over all on the order of 10^{10} impostor comparisons. The text in each box gives the same quantity as that coded by the color: Light colors present a security vulnerability to, for example, a passport gate.

Cross age FMR at threshold $T = 148.416$ for algorithm tech5_001, giving $FMR(T) = 0.0001$ globally.

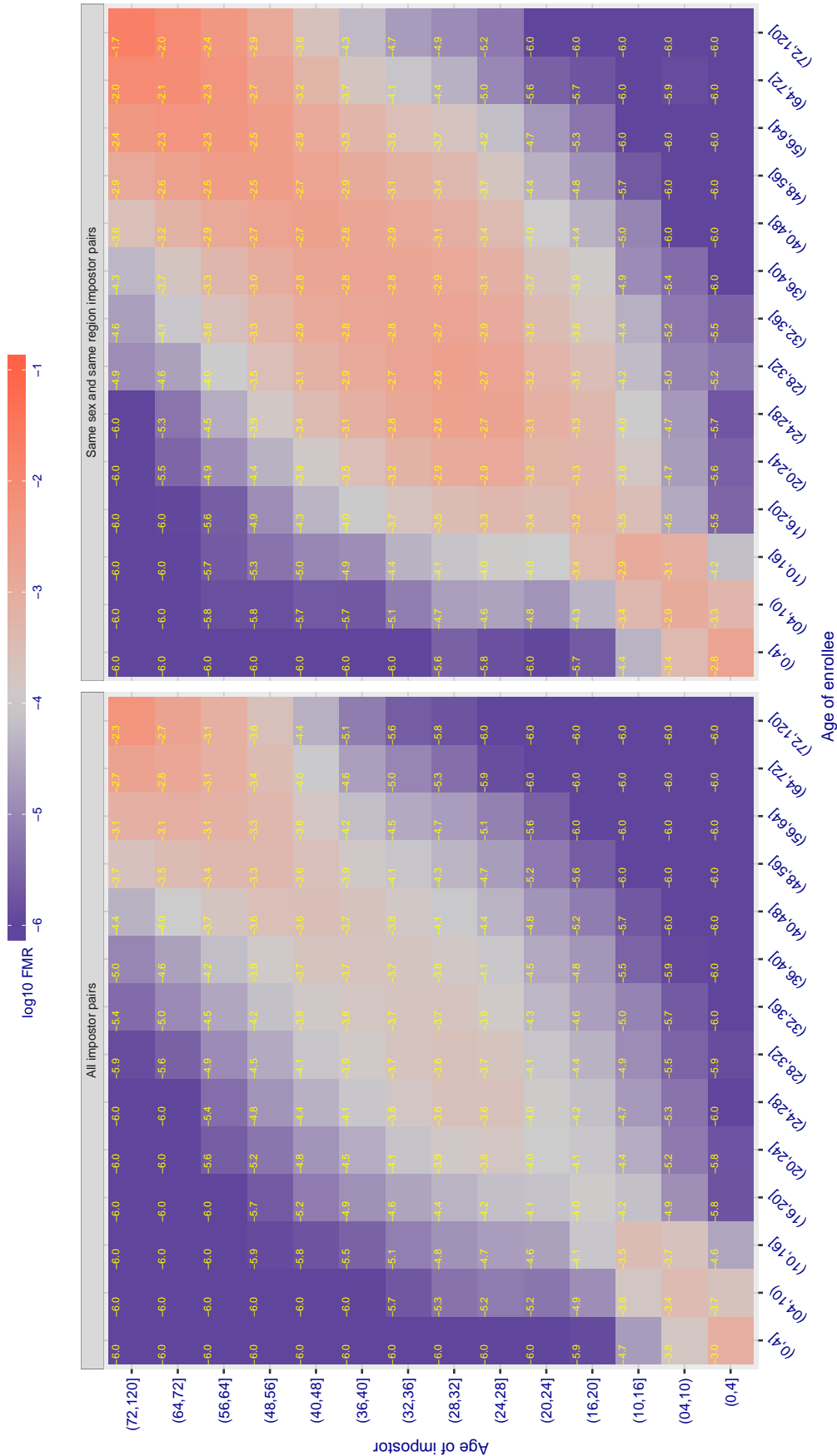


Figure 398: For algorithm tech5-001 operating on visa images, the heatmap shows false match observed over impostor comparisons of faces from different individuals who have the given age pair. False matches are counted against a recognition threshold fixed globally to give $FMR = 0.0001$ over all on the order of 10^{10} impostor comparisons. The text in each box gives the same quantity as that coded by the color: Light colors present a security vulnerability to, for example, a passport gate.

Cross age FMR at threshold $T = 147.661$ for algorithm tech5_002, giving $FMR(T) = 0.0001$ globally.

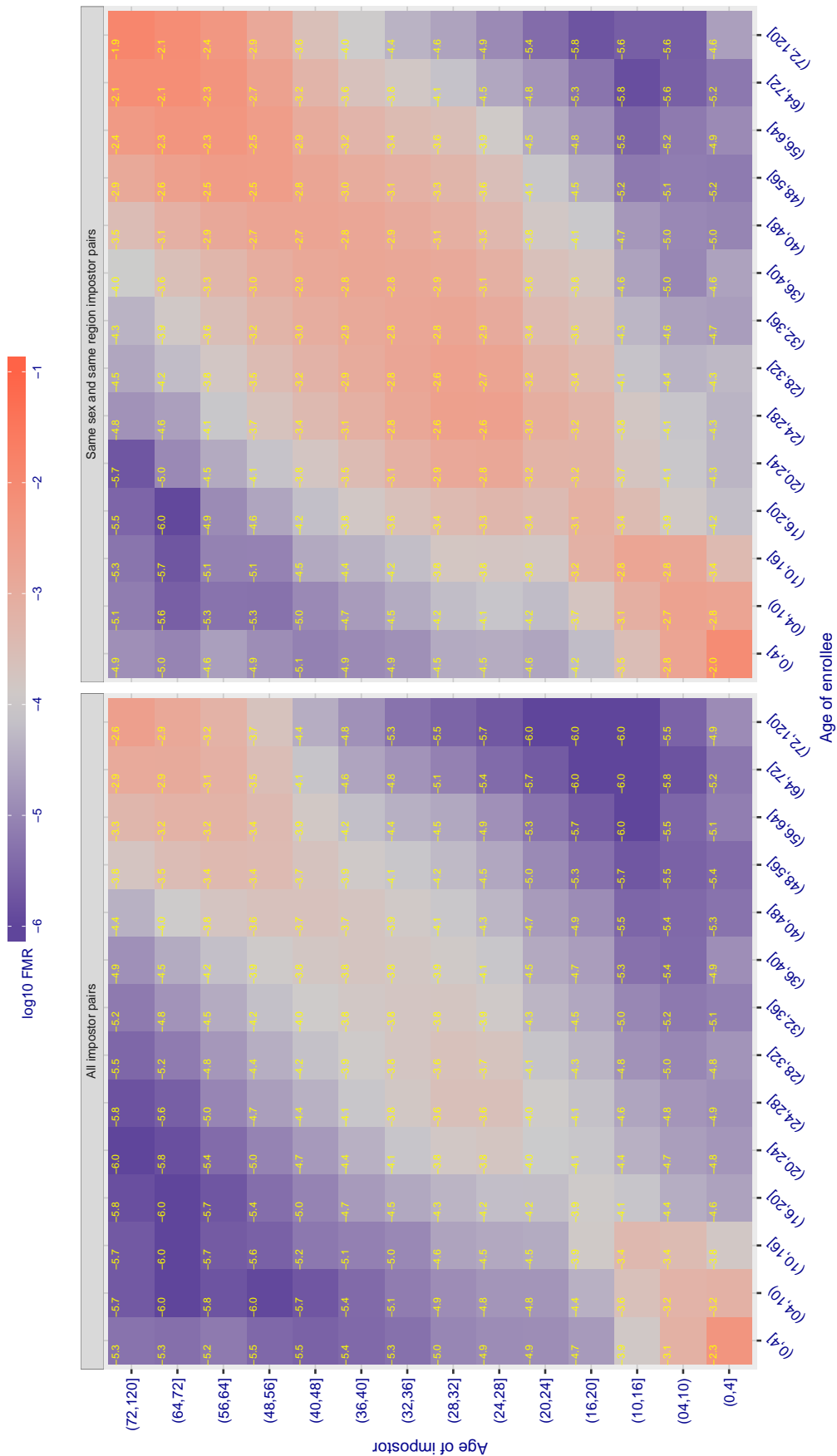


Figure 399: For algorithm tech5-002 operating on visa images, the heatmap shows false match observed over impostor comparisons of faces from different individuals who have the given age pair. False matches are counted against a recognition threshold fixed globally to give $FMR = 0.001$ over all on the order of 10^{10} impostor comparisons. The text in each box gives the same quantity as that coded by the color: Light colors present a security vulnerability to, for example, a passport gate.

Cross age FMR at threshold $T = 0.896$ for algorithm `tevia-003`, giving $FMR(T) = 0.0001$ globally.

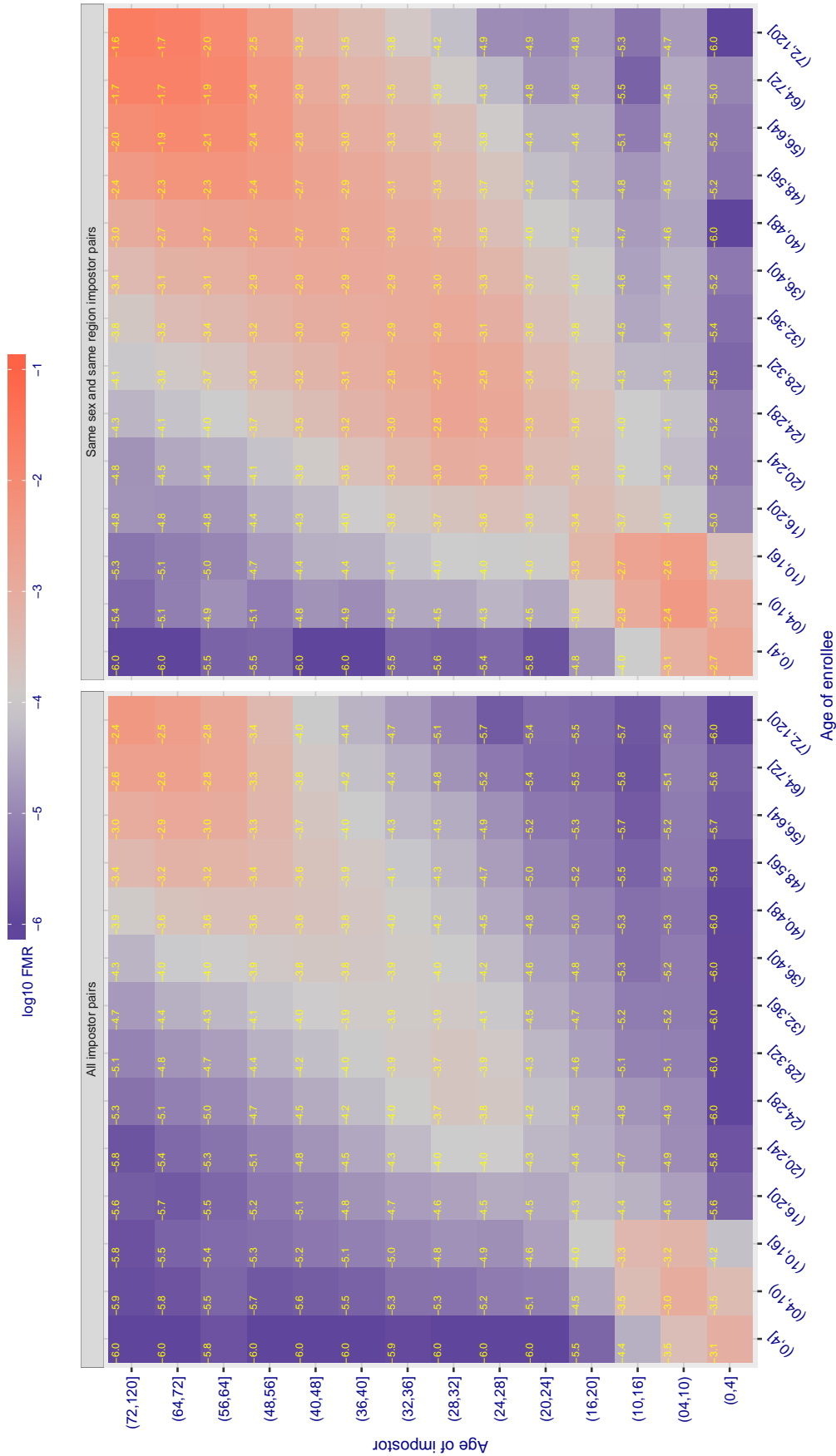


Figure 400: For algorithm `tevia-003` operating on visa images, the heatmap shows false match observed over impostor comparisons of faces from different individuals who have the given age pair. False matches are counted against a recognition threshold fixed globally to give $FMR = 0.001$ over all on the order of 10^{10} impostor comparisons. The text in each box gives the same quantity as that coded by the color: Light colors present a security vulnerability to, for example, a passport gate.

Cross age FMR at threshold $T = 0.896$ for algorithm `tevia_004`, giving $FMR(T) = 0.0001$ globally.

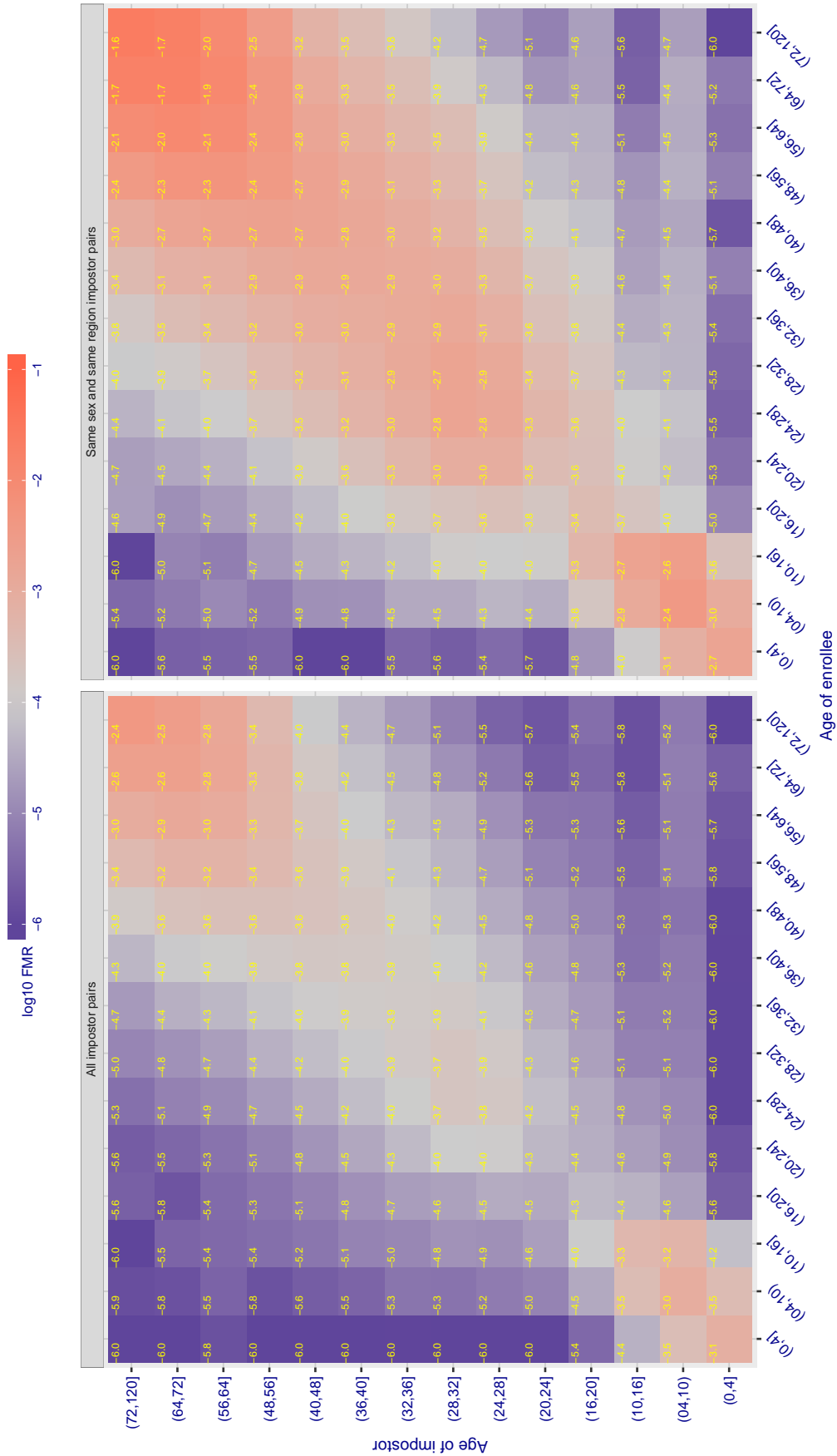


Figure 401: For algorithm `tevia_004` operating on visa images, the heatmap shows false match observed over impostor comparisons of faces from different individuals who have the given age pair. False matches are counted against a recognition threshold fixed globally to give $FMR = 0.001$ over all on the order of 10^{10} impostor comparisons. The text in each box gives the same quantity as that coded by the color: Light colors present a security vulnerability to, for example, a passport gate.

Cross age FMR at threshold $T = 151.011$ for algorithm tiger_002, giving $FMR(T) = 0.0001$ globally.

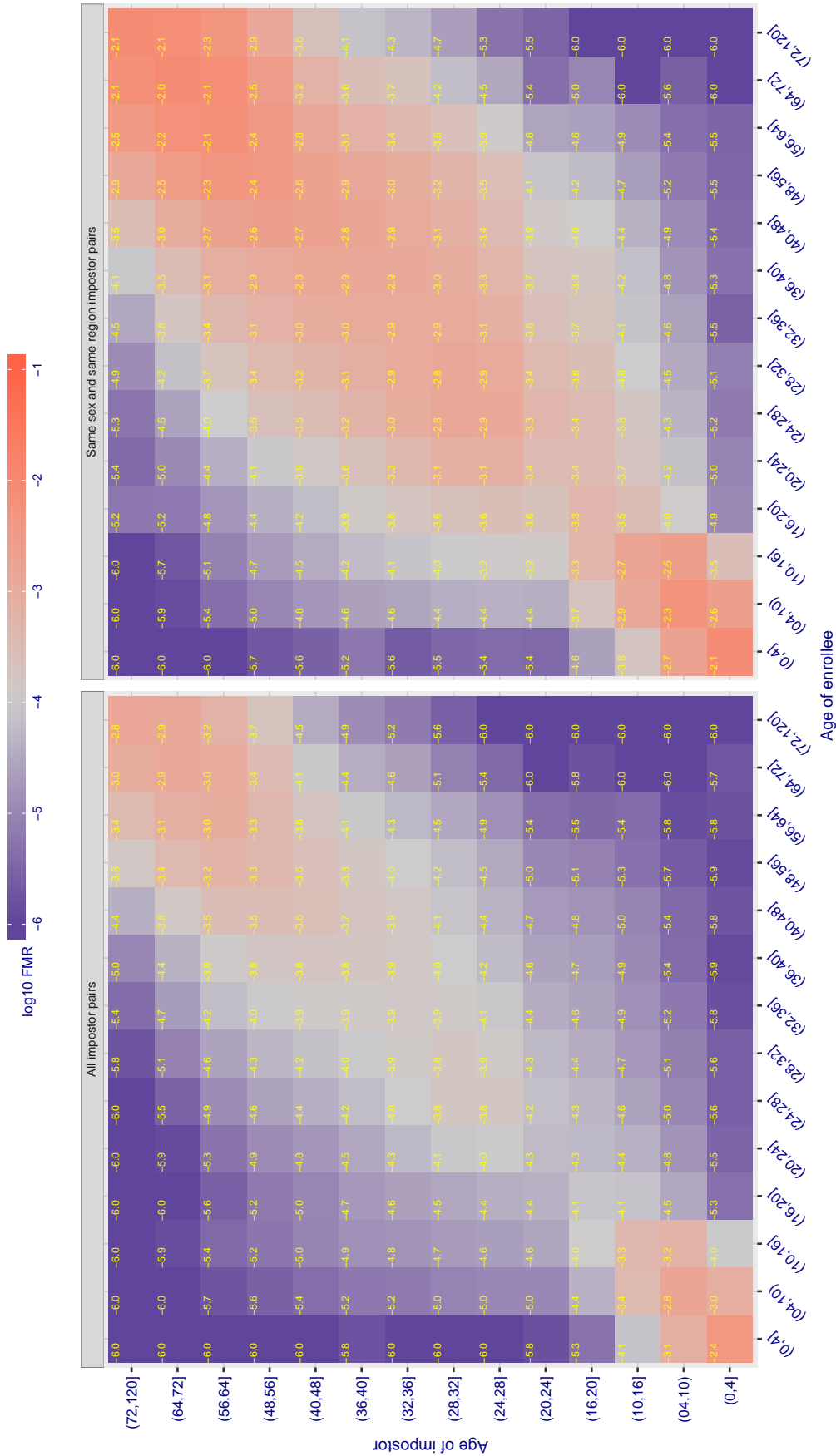


Figure 402: For algorithm tiger-002 operating on visa images, the heatmap shows false match observed over impostor comparisons of faces from different individuals who have the given age pair. False matches are counted against a recognition threshold fixed globally to give $FMR = 0.001$ over all on the order of 10^{10} impostor comparisons. The text in each box gives the same quantity as that coded by the color: Light colors present a security vulnerability to, for example, a passport gate.

Cross age FMR at threshold $T = 149.313$ for algorithm tiger_003, giving $FMR(T) = 0.0001$ globally.

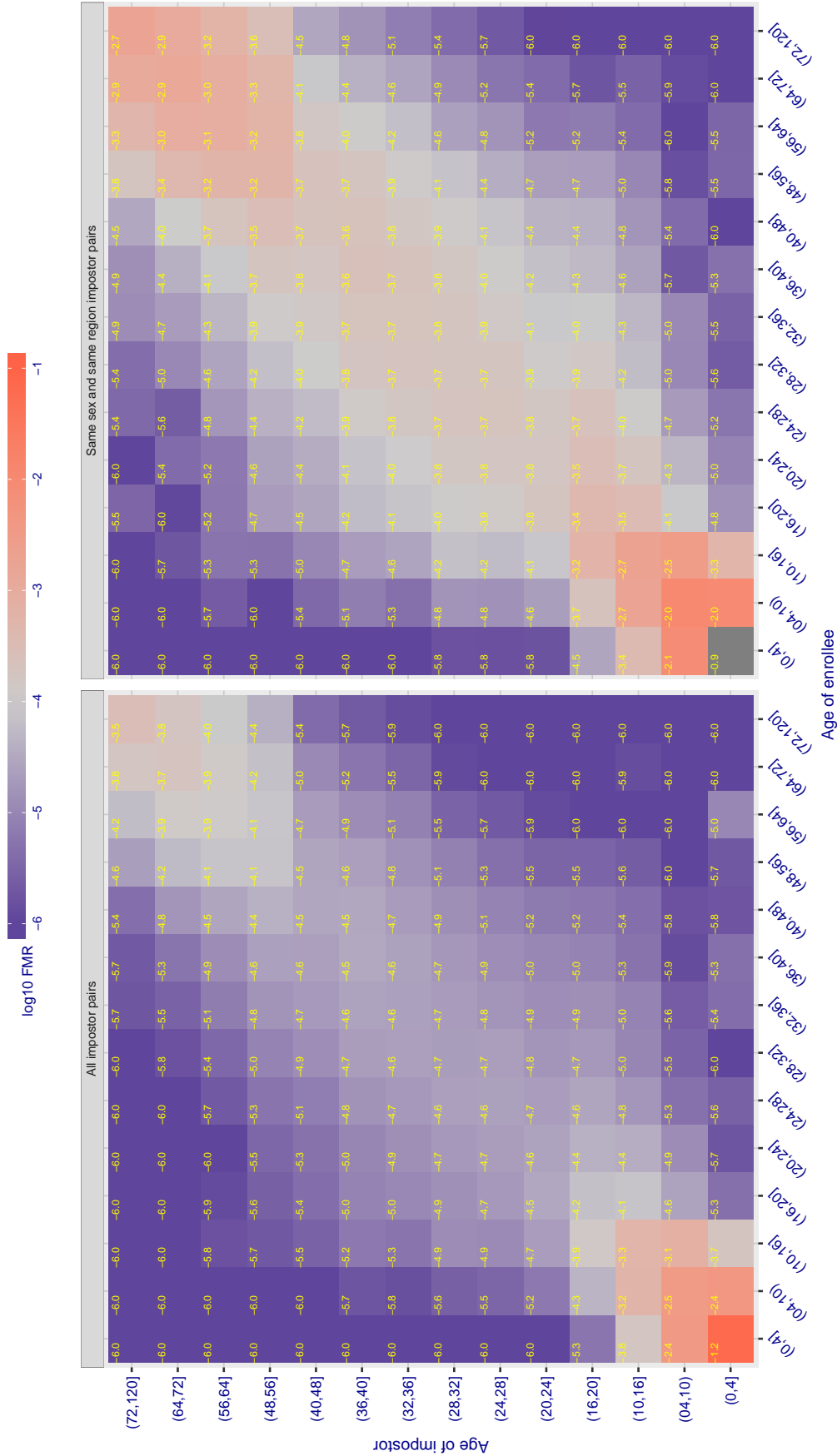


Figure 403: For algorithm tiger-003 operating on visa images, the heatmap shows false match observed over impostor comparisons of faces from different individuals who have the given age pair. False matches are counted against a recognition threshold fixed globally to give $FMR = 0.0001$ over all on the order of 10^{10} impostor comparisons. The text in each box gives the same quantity as that coded by the color. Light colors present a security vulnerability to, for example, a passport gate.

Cross age FMR at threshold $T = 0.628$ for algorithm toshiba_002, giving $FMR(T) = 0.0001$ globally.

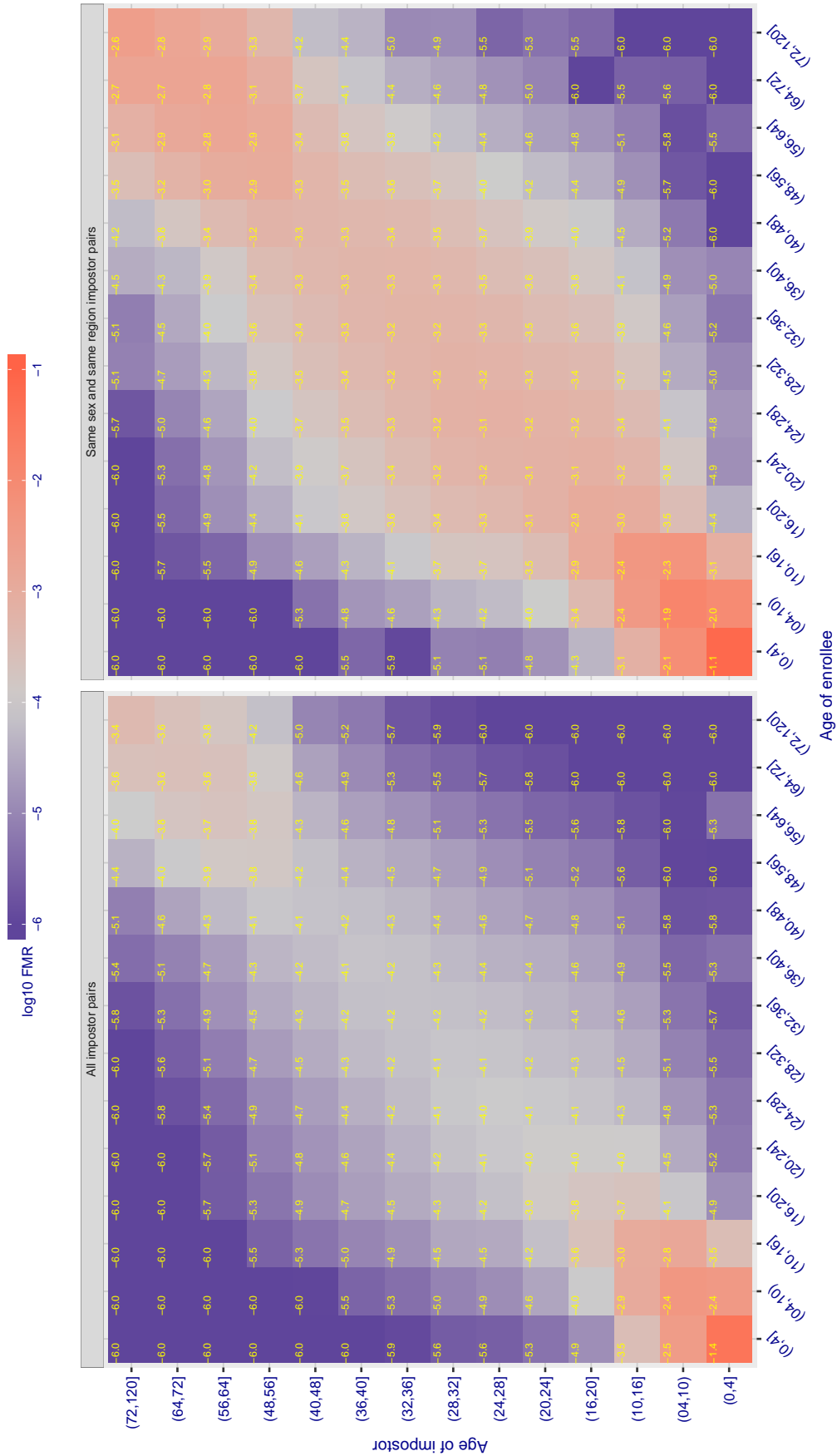


Figure 404: For algorithm toshiba-002 operating on visa images, the heatmap shows false match observed over impostor comparisons of faces from different individuals who have the given age pair. False matches are counted against a recognition threshold fixed globally to give $FMR = 0.0001$ over all on the order of 10^{10} impostor comparisons. The text in each box gives the same quantity as that coded by the color: Light colors present a security vulnerability to, for example, a passport gate.

Cross age FMR at threshold $T = 0.626$ for algorithm toshiba_003, giving $FMR(T) = 0.0001$ globally.

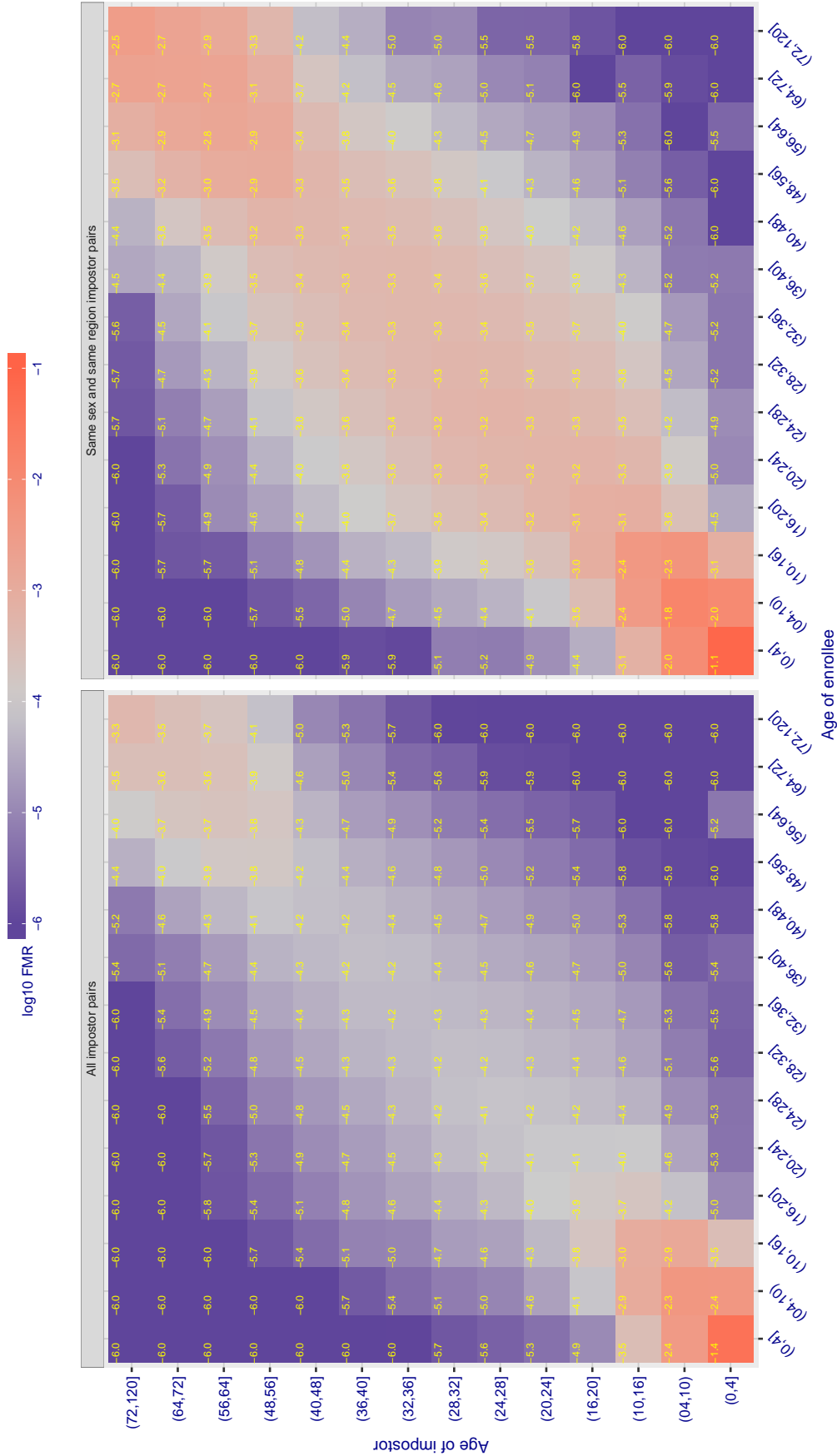


Figure 405: For algorithm toshiba-003 operating on visa images, the heatmap shows false match observed over impostor comparisons of faces from different individuals who have the given age pair. False matches are counted against a recognition threshold fixed globally to give $FMR = 0.001$ over all on the order of 10^{10} impostor comparisons. The text in each box gives the same quantity as that coded by the color: Light colors present a security vulnerability to, for example, a passport gate.

Cross age FMR at threshold $T = 0.428$ for algorithm vcog_002, giving $FMR(T) = 0.0001$ globally.

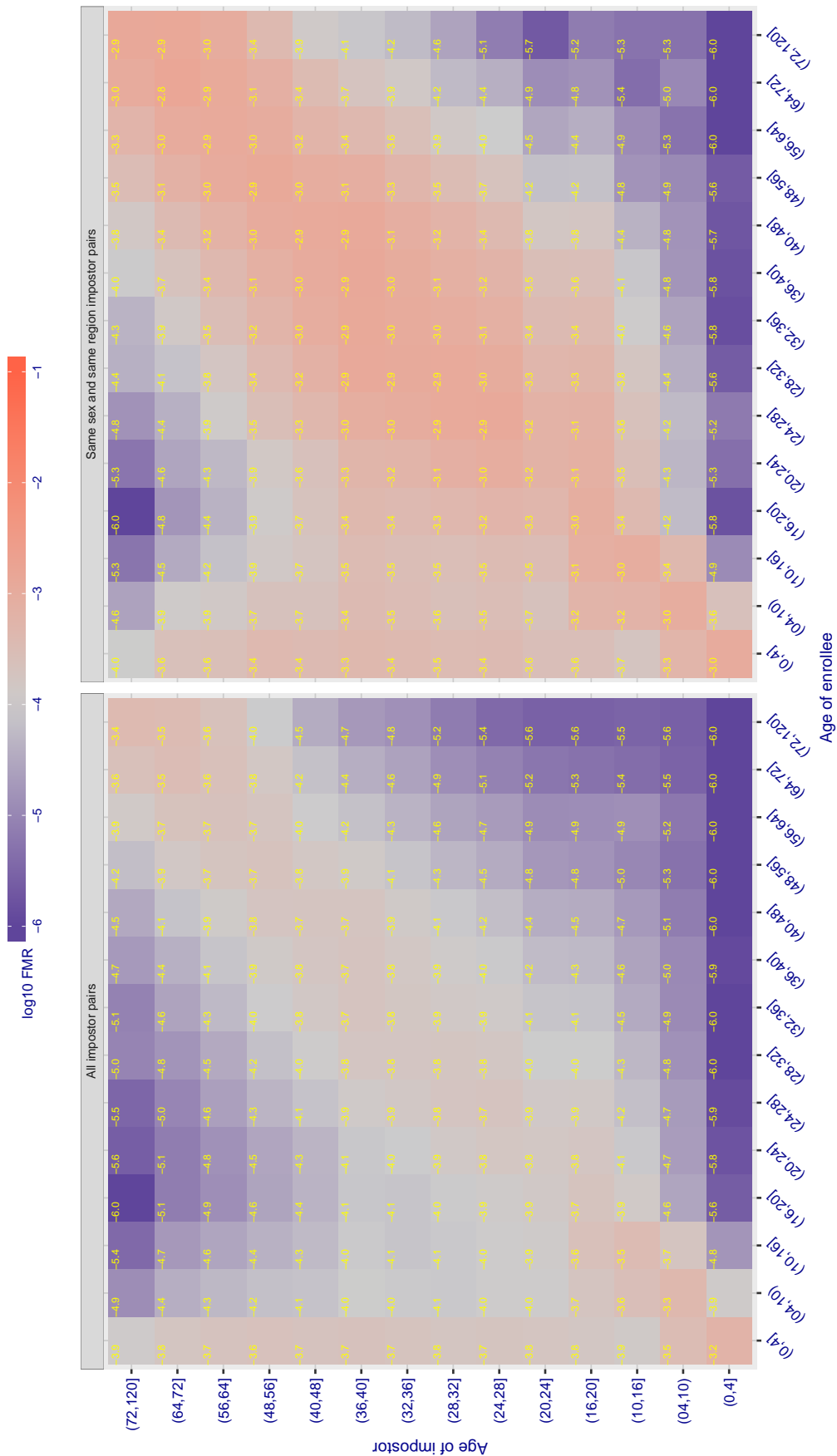


Figure 406: For algorithm vcog-002 operating on visa images, the heatmap shows false match observed over impostor comparisons of faces from different individuals who have the given age pair. False matches are counted against a recognition threshold fixed globally to give $FMR = 0.001$ over all on the order of 10^{10} impostor comparisons. The text in each box gives the same quantity as that coded by the color: Light colors present a security vulnerability to, for example, a passport gate.

Cross age FMR at threshold $T = 71.529$ for algorithm `vd_001`, giving $FMR(T) = 0.0001$ globally.

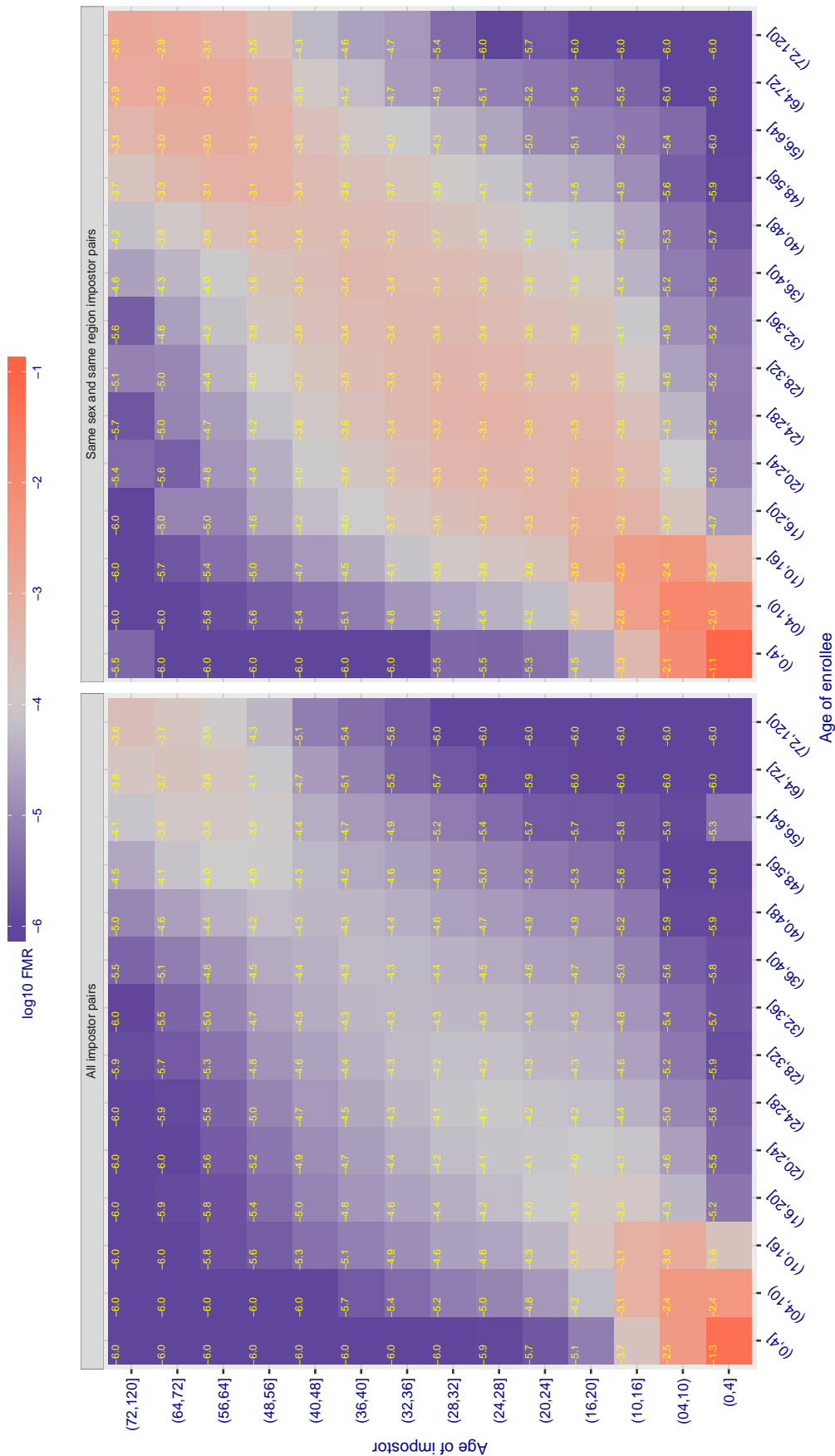


Figure 407: For algorithm `vd-001` operating on visa images, the heatmap shows false match observed over impostor comparisons of faces from different individuals who have the given age pair. False matches are counted against a recognition threshold fixed globally to give $FMR = 0.001$ over all on the order of 10^{10} impostor comparisons. The text in each box gives the same quantity as that coded by the color. Light colors present a security vulnerability to, for example, a passport gate.

Cross age FMR at threshold $T = 3.325$ for algorithm veridas_001, giving $FMR(T) = 0.0001$ globally.

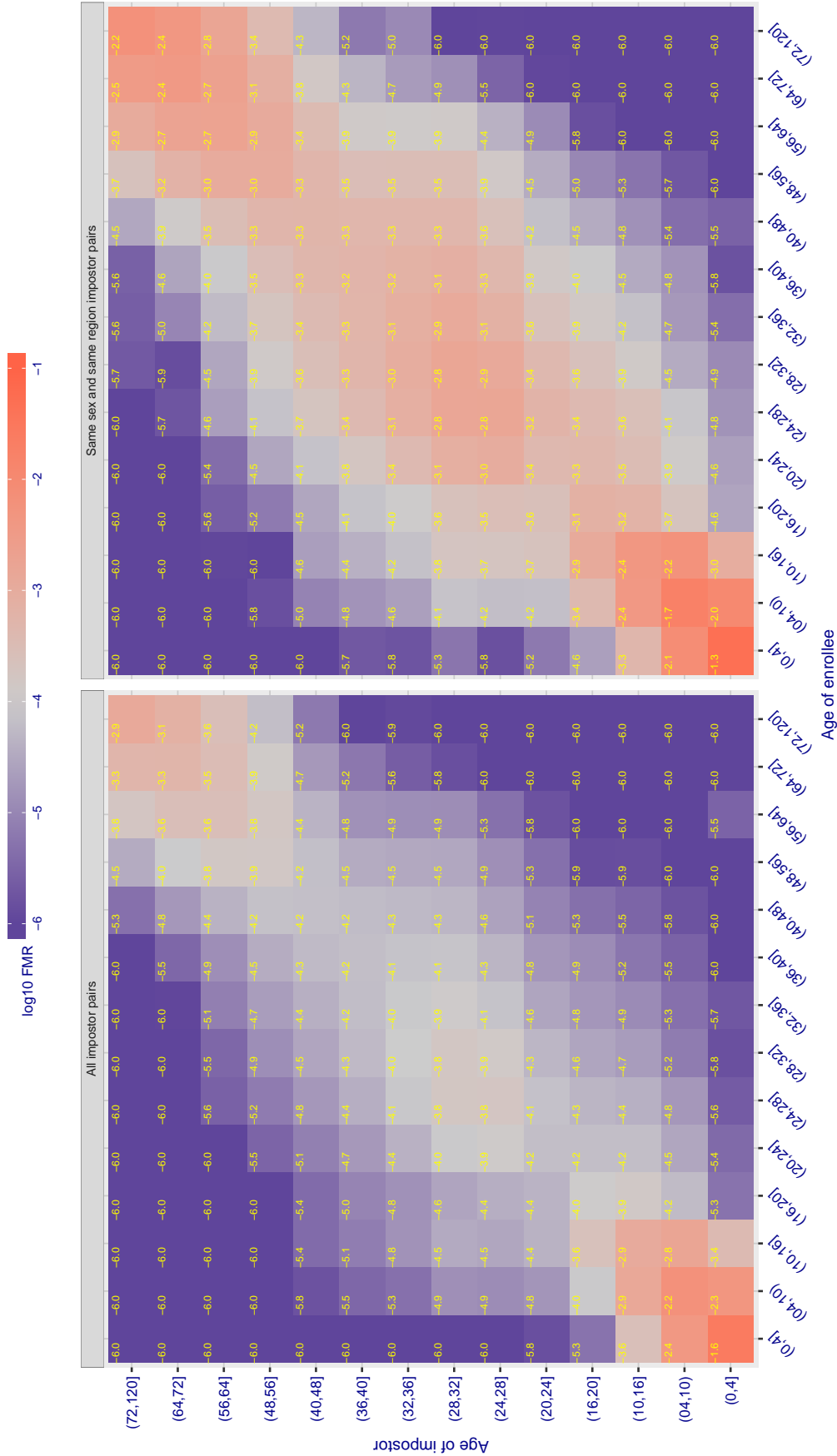


Figure 408: For algorithm veridas-001 operating on visa images, the heatmap shows false match observed over impostor comparisons of faces from different individuals who have the given age pair. False matches are counted against a recognition threshold fixed globally to give $FMR = 0.001$ over all on the order of 10^{10} impostor comparisons. The text in each box gives the same quantity as that coded by the color. Light colors present a security vulnerability to, for example, a passport gate.

Cross age FMR at threshold $T = 3.389$ for algorithm veridas_002, giving $FMR(T) = 0.0001$ globally.

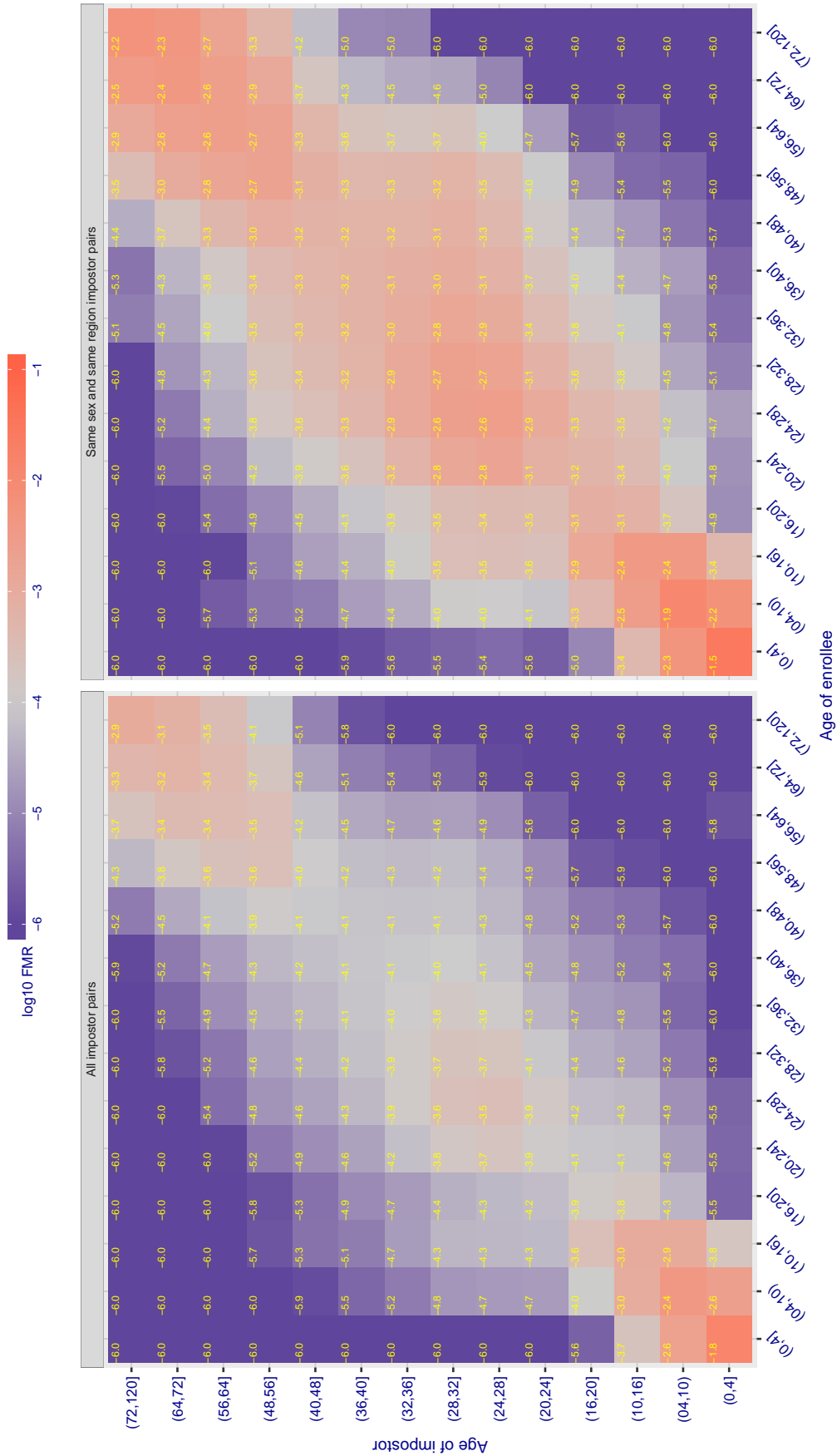


Figure 409: For algorithm veridas-002 operating on visa images, the heatmap shows false match observed over impostor comparisons of faces from different individuals who have the given age pair. False matches are counted against a recognition threshold fixed globally to give $FMR = 0.001$ over all on the order of 10^{10} impostor comparisons. The text in each box gives the same quantity as that coded by the color. Light colors present a security vulnerability to, for example, a passport gate.

Cross age FMR at threshold $T = 3.051$ for algorithm `vigilantsolutions_005`, giving $FMR(T) = 0.0001$ globally.

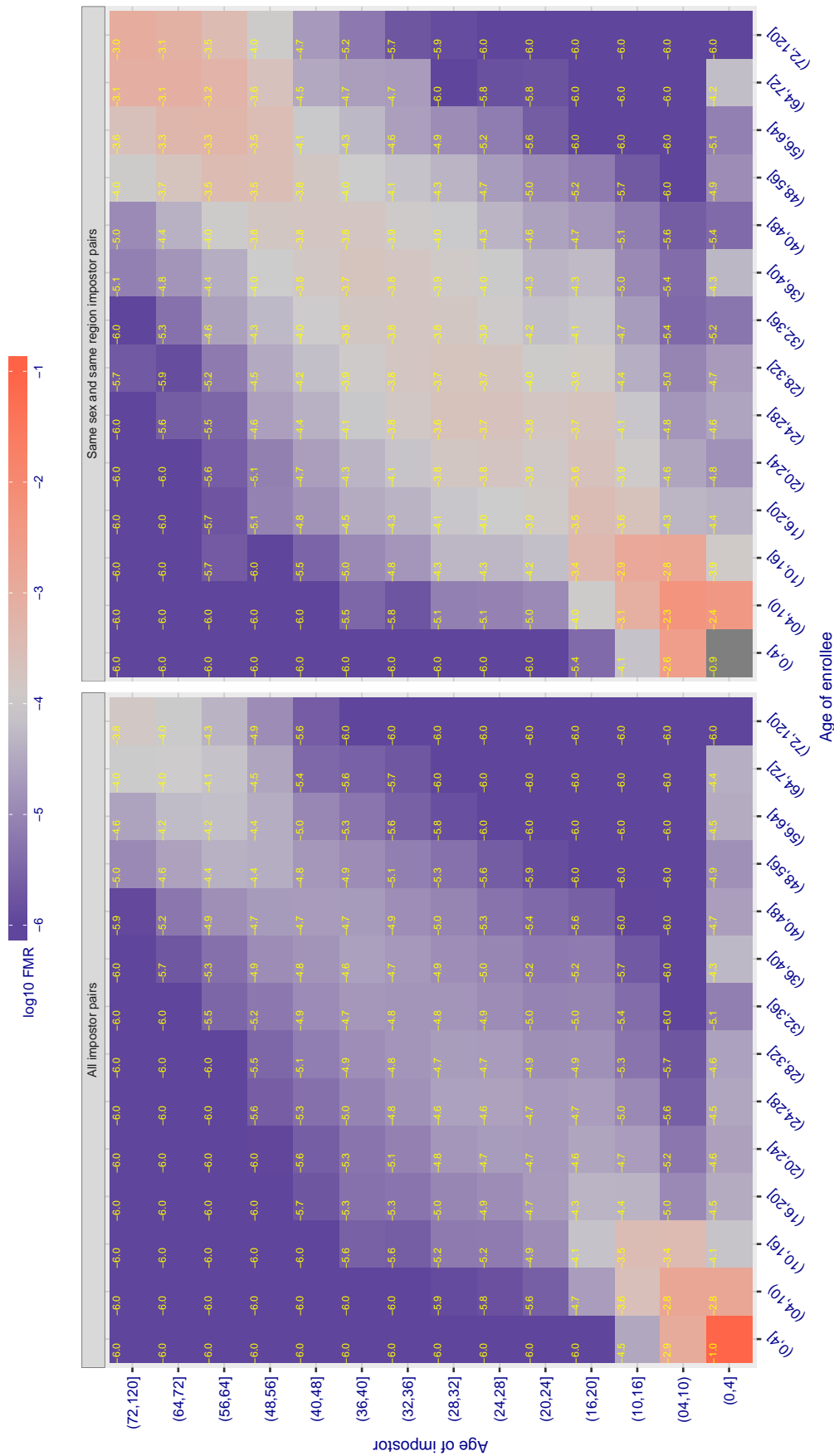


Figure 410: For algorithm `vigilantsolutions-005` operating on visa images, the heatmap shows false match observed over impostor comparisons of faces from different individuals who have the given age pair. False matches are counted against a recognition threshold fixed globally to give $FMR = 0.001$ over all on the order of 10^{10} impostor comparisons. The text in each box gives the same quantity as that coded by the color. Light colors present a security vulnerability to, for example, a passport gate.

Cross age FMR at threshold T = 3.057 for algorithm vigilantsolutions_006, giving FMR(T) = 0.0001 globally.

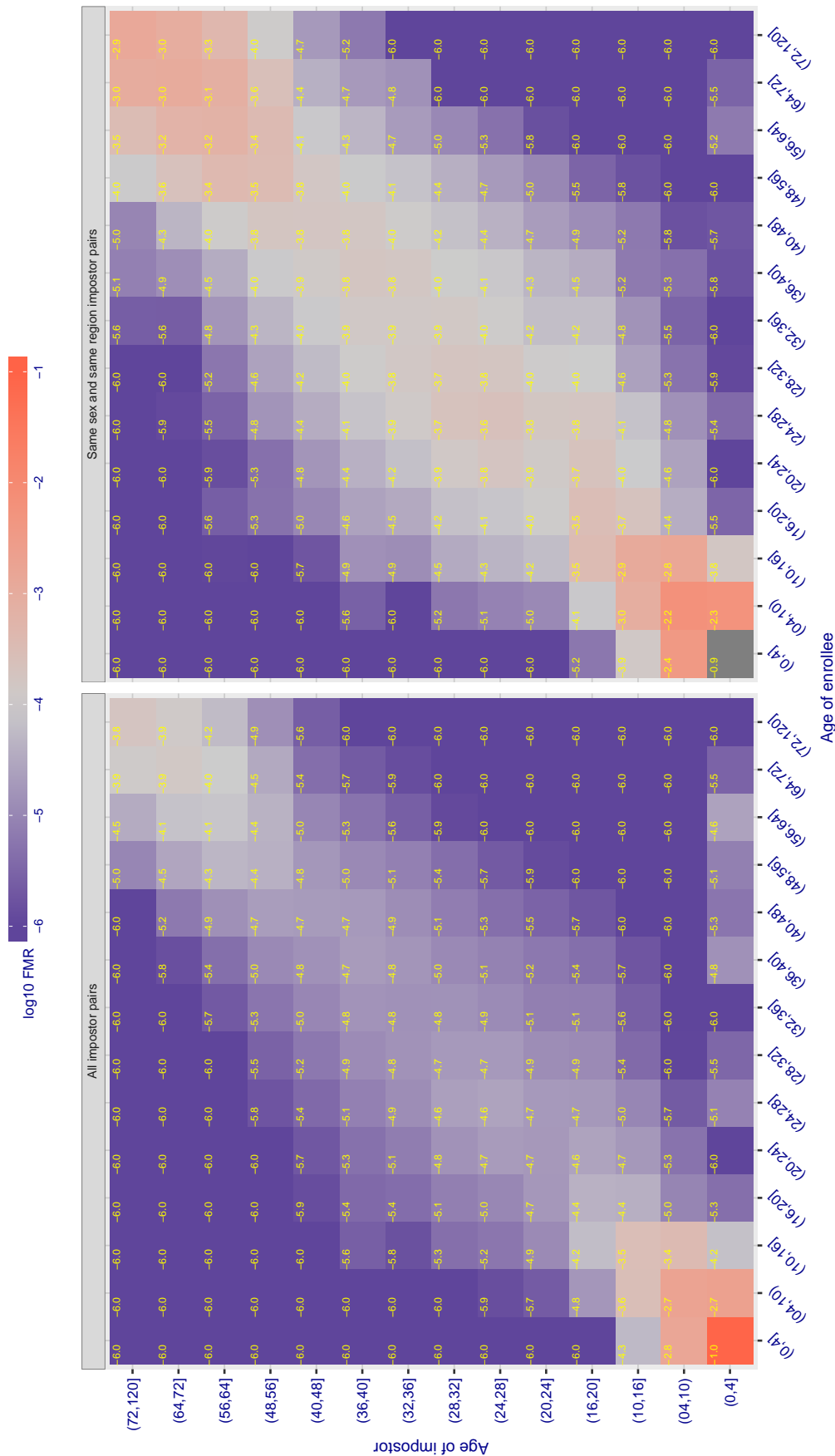


Figure 411: For algorithm vigilantsolutions-006 operating on visa images, the heatmap shows false match observed over impostor comparisons of faces from different individuals who have the given age pair. False matches are counted against a recognition threshold fixed globally to give FMR = 0.001 over all on the order of 10¹⁰ impostor comparisons. The text in each box gives the same quantity as that coded by the color. Light colors present a security vulnerability to, for example, a passport gate.

Cross age FMR at threshold $T = 0.432$ for algorithm `vion_000`, giving $FMR(T) = 0.0001$ globally.

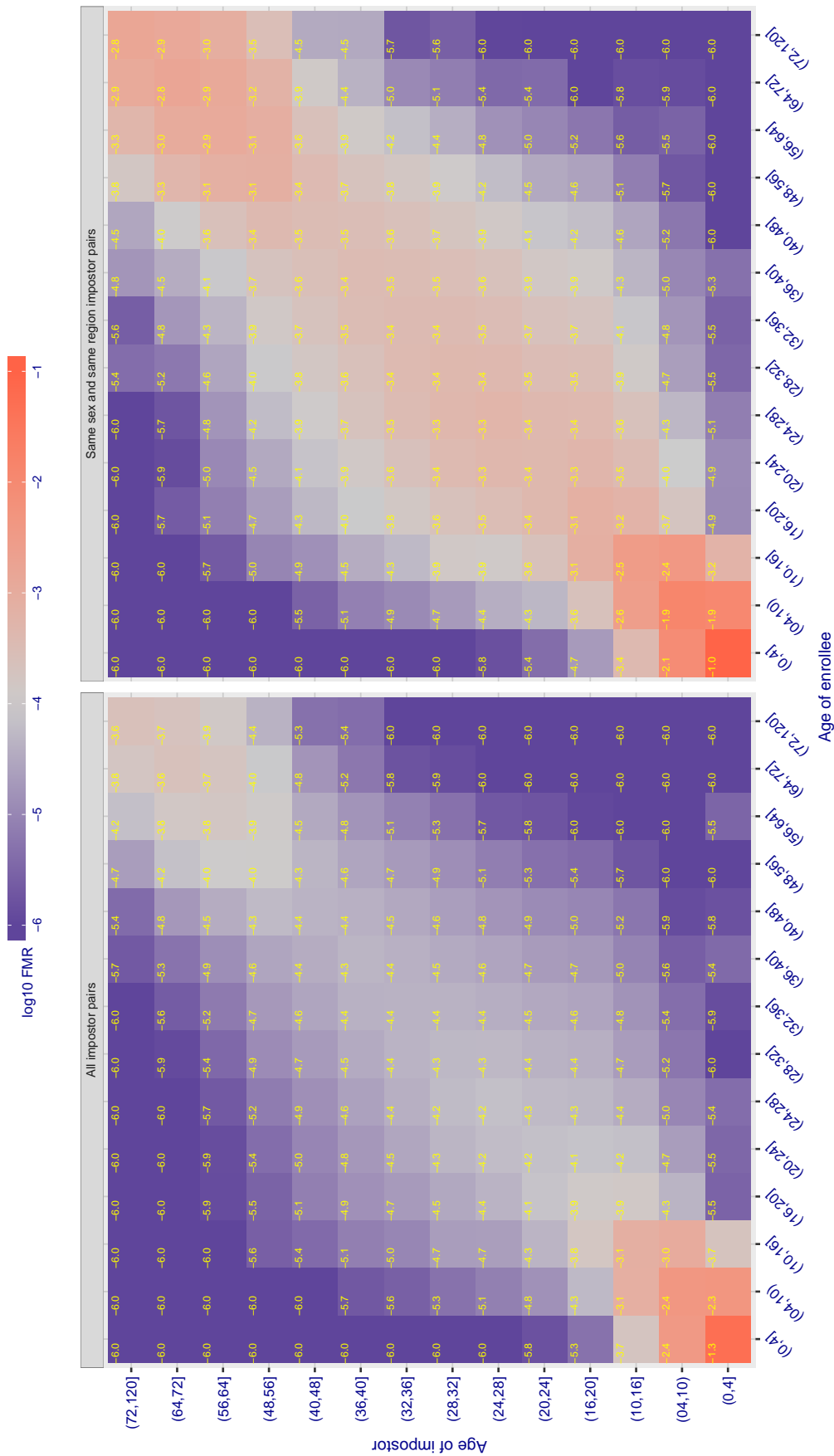


Figure 412: For algorithm `vion-000` operating on visa images, the heatmap shows false match observed over impostor comparisons of faces from different individuals who have the given age pair. False matches are counted against a recognition threshold fixed globally to give $FMR = 0.0001$ over all on the order of 10^{10} impostor comparisons. The text in each box gives the same quantity as that coded by the color: Light colors present a security vulnerability to, for example, a passport gate.

Cross age FMR at threshold $T = 0.433$ for algorithm visionbox_000, giving $FMR(T) = 0.0001$ globally.

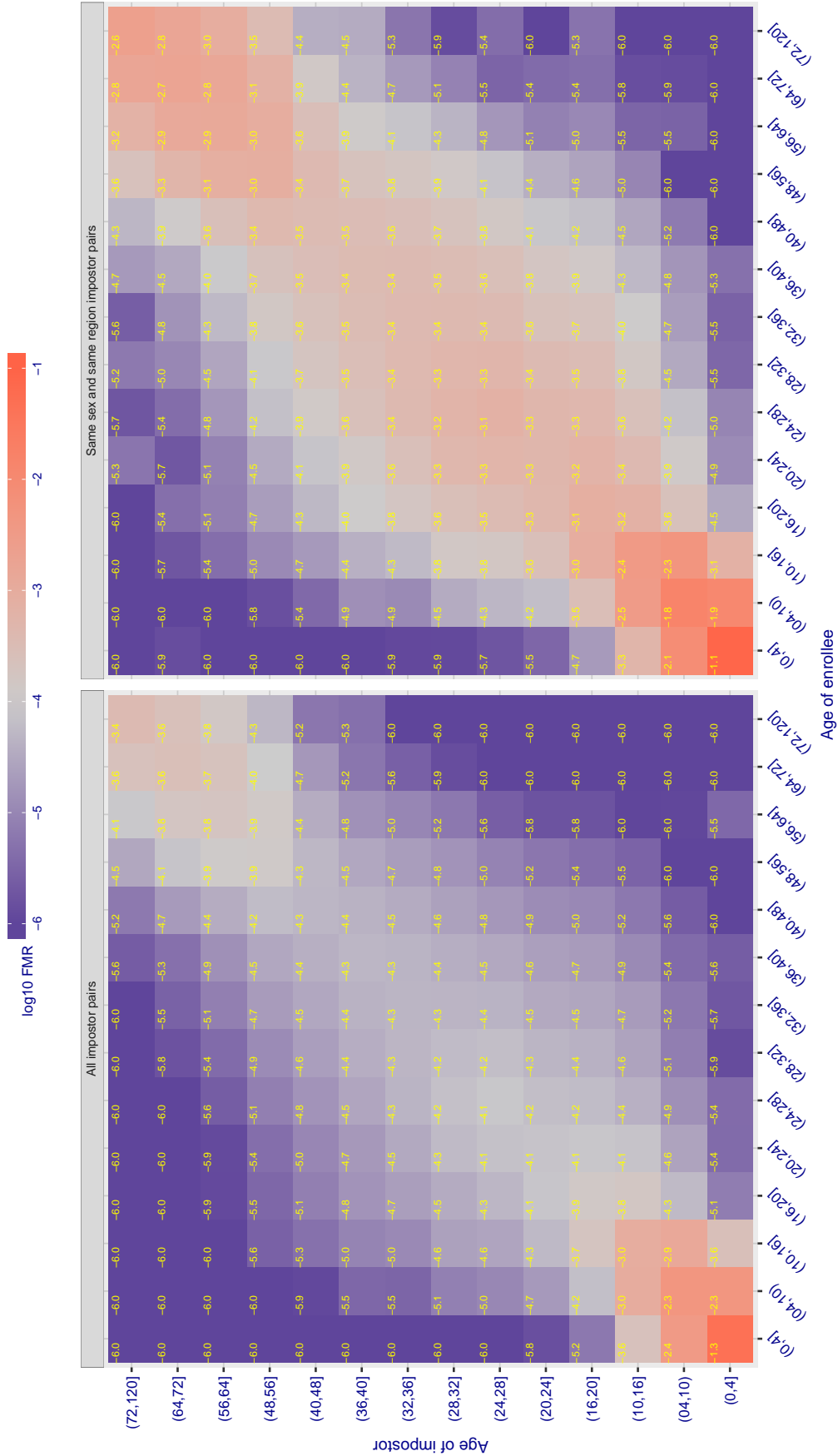


Figure 413: For algorithm visionbox-000 operating on visa images, the heatmap shows false match observed over impostor comparisons of faces from different individuals who have the given age pair. False matches are counted against a recognition threshold fixed globally to give $FMR = 0.0001$ over all on the order of 10^{10} impostor comparisons. The text in each box gives the same quantity as that coded by the color. Light colors present a security vulnerability to, for example, a passport gate.

Cross age FMR at threshold $T = 0.382$ for algorithm visionbox_001, giving $FMR(T) = 0.0001$ globally.

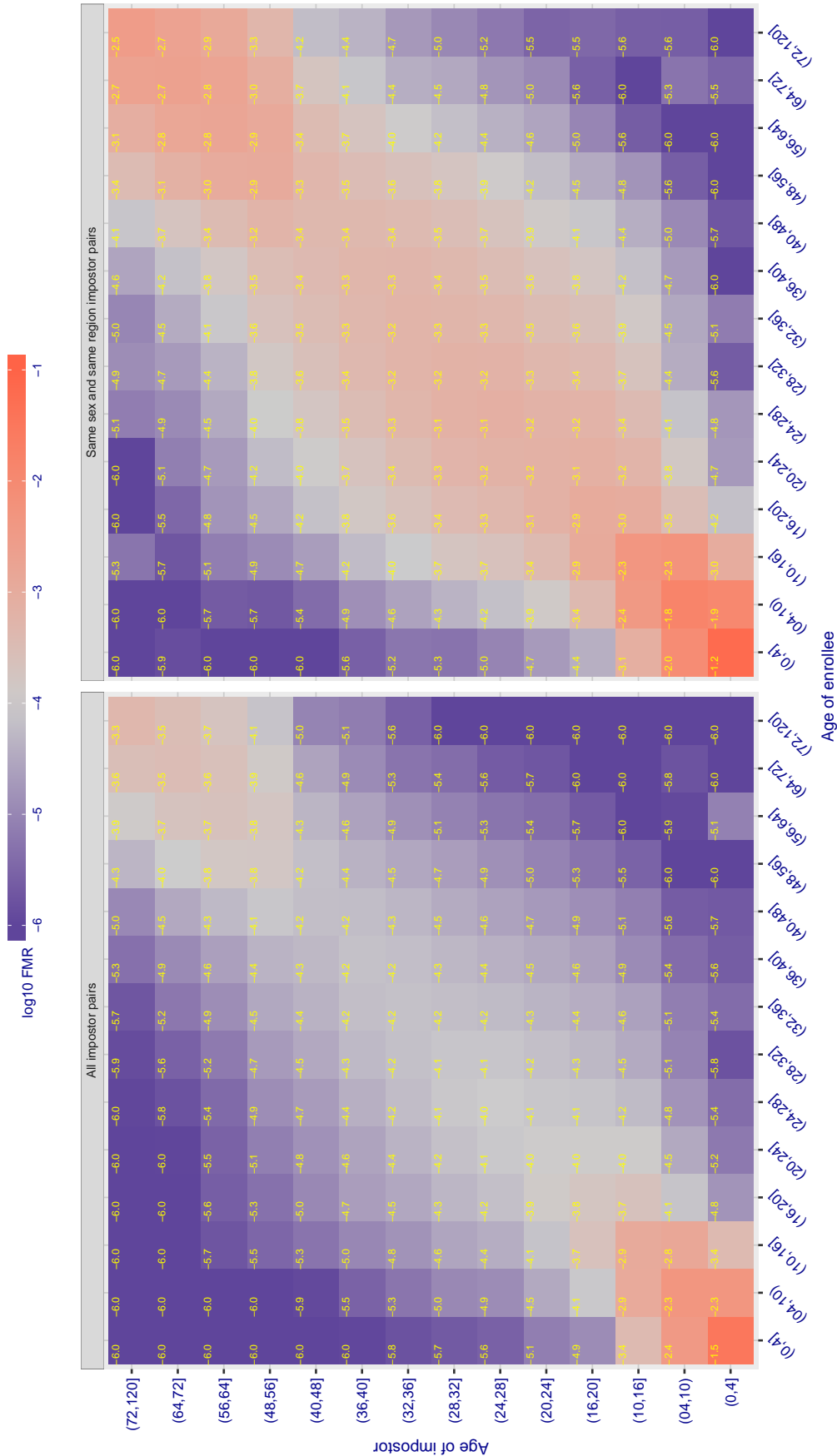


Figure 414: For algorithm visionbox-001 operating on visa images, the heatmap shows false match observed over impostor comparisons of faces from different individuals who have the given age pair. False matches are counted against a recognition threshold fixed globally to give $FMR = 0.001$ over all on the order of 10^{10} impostor comparisons. The text in each box gives the same quantity as that coded by the color. Light colors present a security vulnerability to, for example, a passport gate.

Cross age FMR at threshold $T = 0.000$ for algorithm visionlabs_005, giving $FMR(T) = 0.0001$ globally.

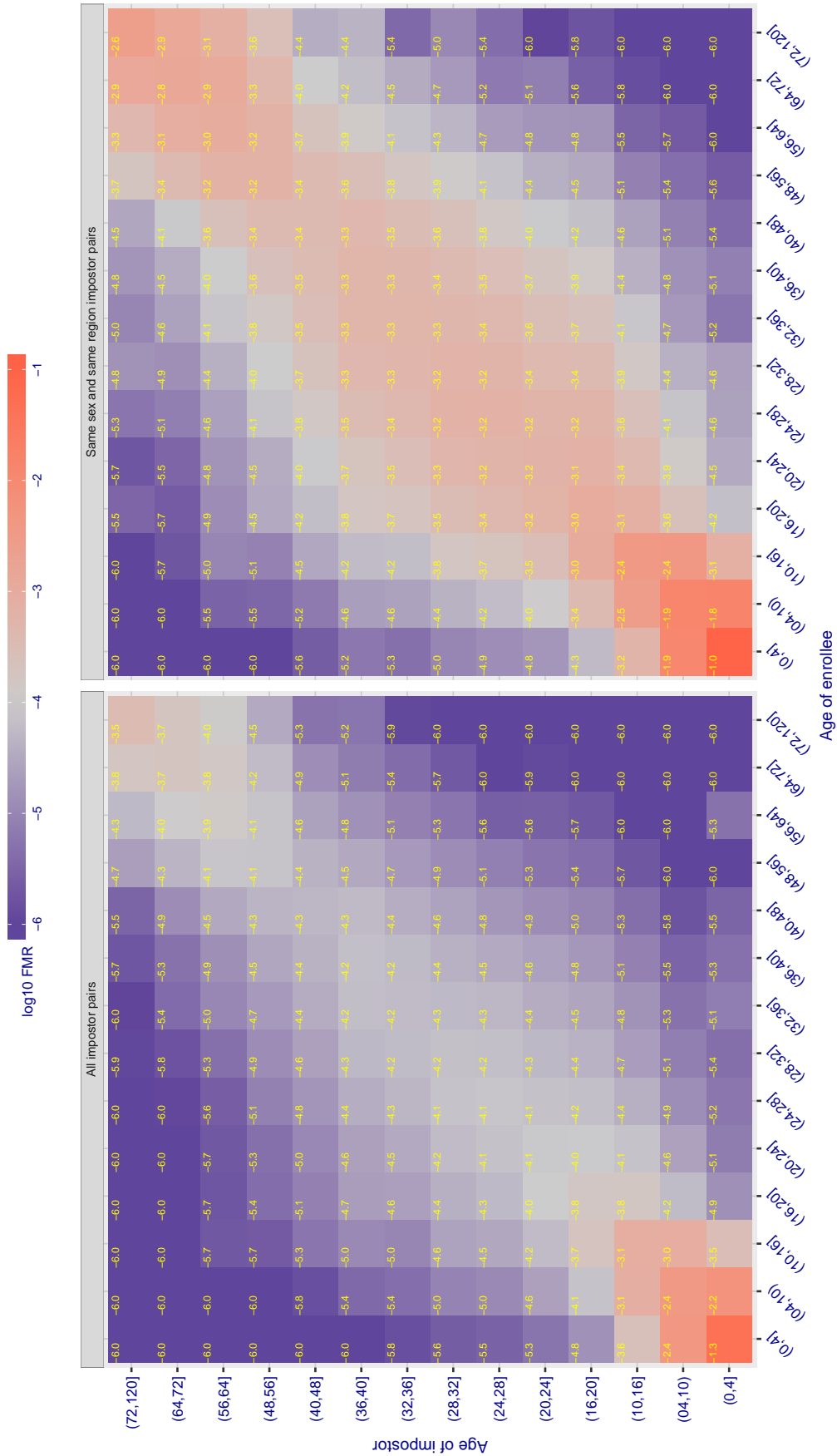


Figure 415: For algorithm visionlabs-005 operating on visa images, the heatmap shows false match observed over impostor comparisons of faces from different individuals who have the given age pair. False matches are counted against a recognition threshold fixed globally to give $FMR = 0.001$ over all on the order of 10^{10} impostor comparisons. The text in each box gives the same quantity as that coded by the color. Light colors present a security vulnerability to, for example, a passport gate.

Cross age FMR at threshold $T = 0.669$ for algorithm visionlabs_006, giving $FMR(T) = 0.0001$ globally.

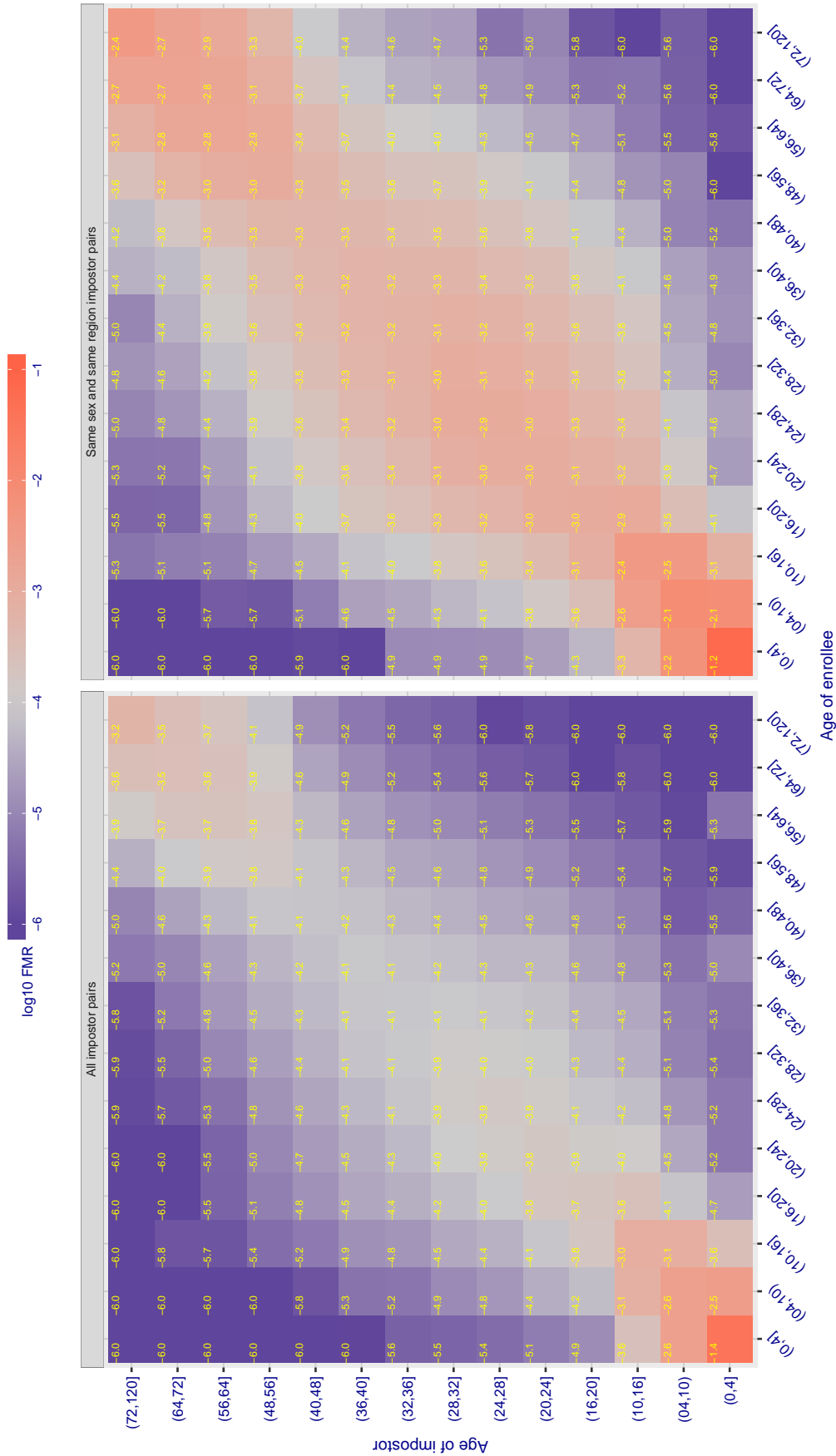


Figure 416: For algorithm visionlabs-006 operating on visa images, the heatmap shows false match observed over impostor comparisons of faces from different individuals who have the given age pair. False matches are counted against a recognition threshold fixed globally to give $FMR = 0.001$ over all on the order of 10^{10} impostor comparisons. The text in each box gives the same quantity as that coded by the color. Light colors present a security vulnerability to, for example, a passport gate.

Cross age FMR at threshold $T = 995.416$ for algorithm vocord_005, giving $FMR(T) = 0.0001$ globally.

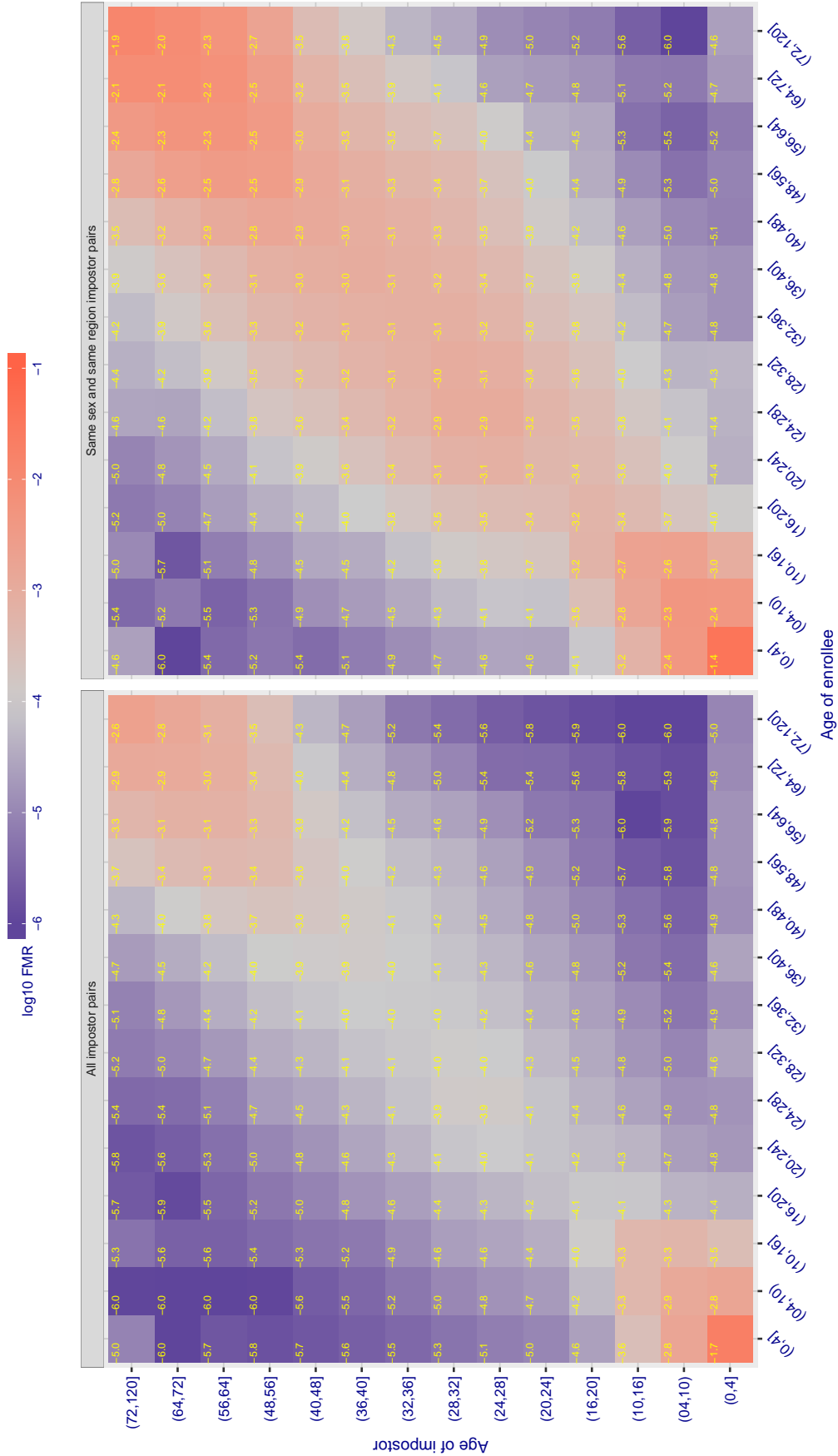


Figure 417: For algorithm vocord-005 operating on visa images, the heatmap shows false match observed over impostor comparisons of faces from different individuals who have the given age pair. False matches are counted against a recognition threshold fixed globally to give $FMR = 0.001$ over all on the order of 10^{10} impostor comparisons. The text in each box gives the same quantity as that coded by the color: Light colors present a security vulnerability to, for example, a passport gate.

Cross age FMR at threshold $T = 995.898$ for algorithm vocord_006, giving $FMR(T) = 0.0001$ globally.

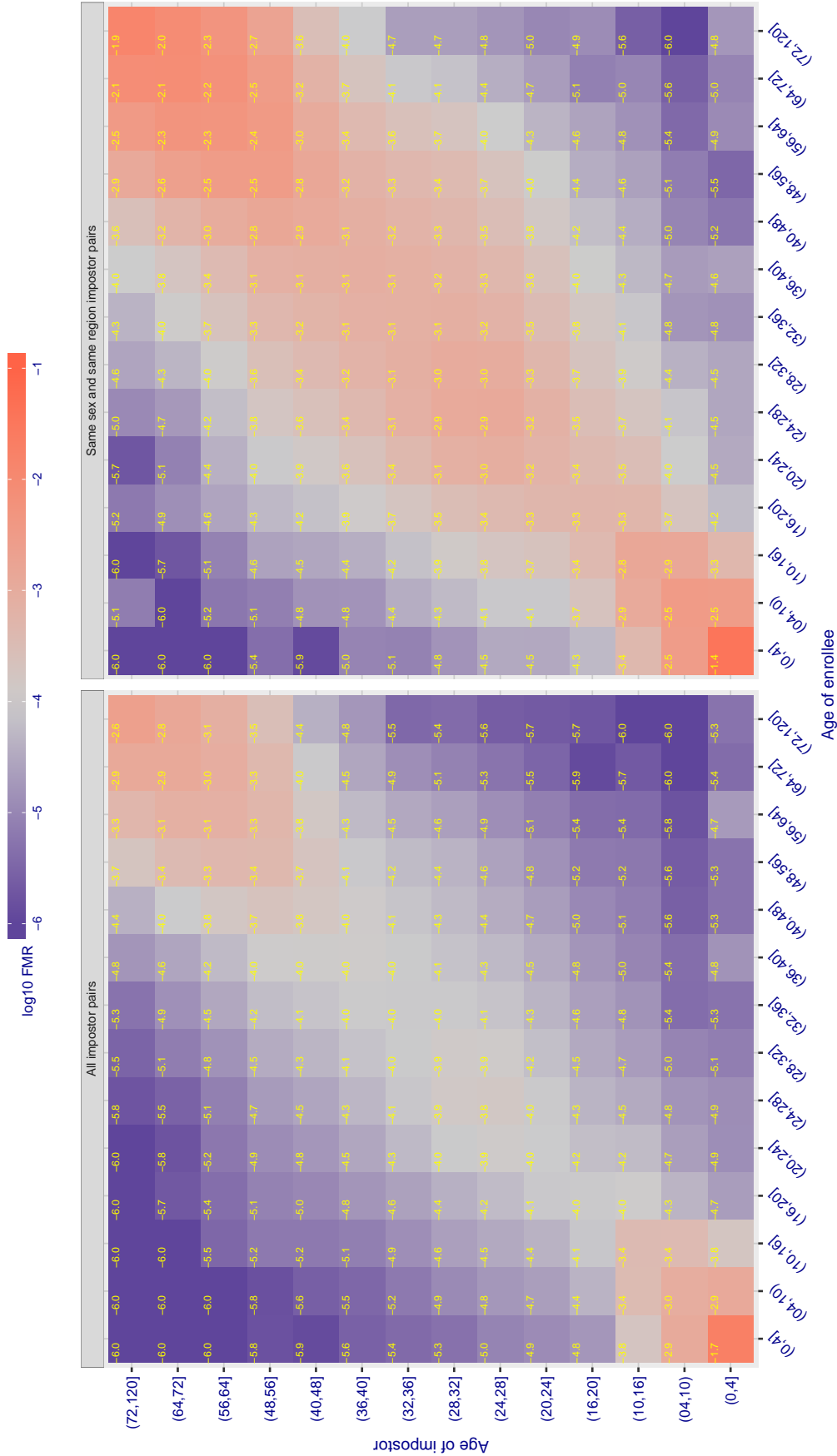


Figure 418: For algorithm vocord-006 operating on visa images, the heatmap shows false match observed over impostor comparisons of faces from different individuals who have the given age pair. False matches are counted against a recognition threshold fixed globally to give $FMR = 0.0001$ over all on the order of 10^{10} impostor comparisons. The text in each box gives the same quantity as that coded by the color. Light colors present a security vulnerability to, for example, a passport gate.

Cross age FMR at threshold $T = 5.544$ for algorithm yisheng_004, giving $FMR(T) = 0.0001$ globally.

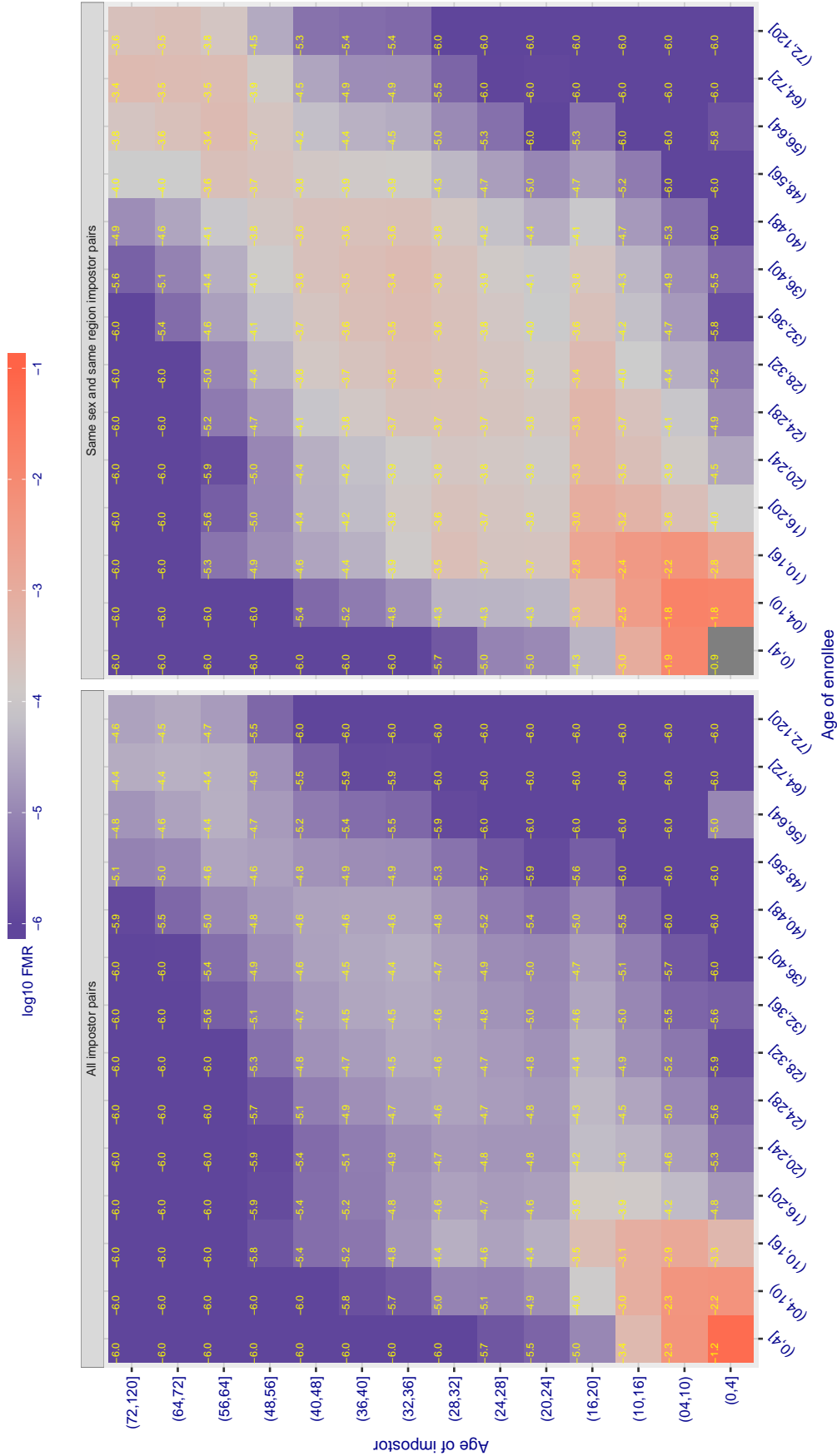


Figure 419: For algorithm yisheng-004 operating on visa images, the heatmap shows false match observed over impostor comparisons of faces from different individuals who have the given age pair. False matches are counted against a recognition threshold fixed globally to give $FMR = 0.001$ over all on the order of 10^{10} impostor comparisons. The text in each box gives the same quantity as that coded by the color. Light colors present a security vulnerability to, for example, a passport gate.

Cross age FMR at threshold $T = 37.698$ for algorithm yitu_003, giving $FMR(T) = 0.0001$ globally.

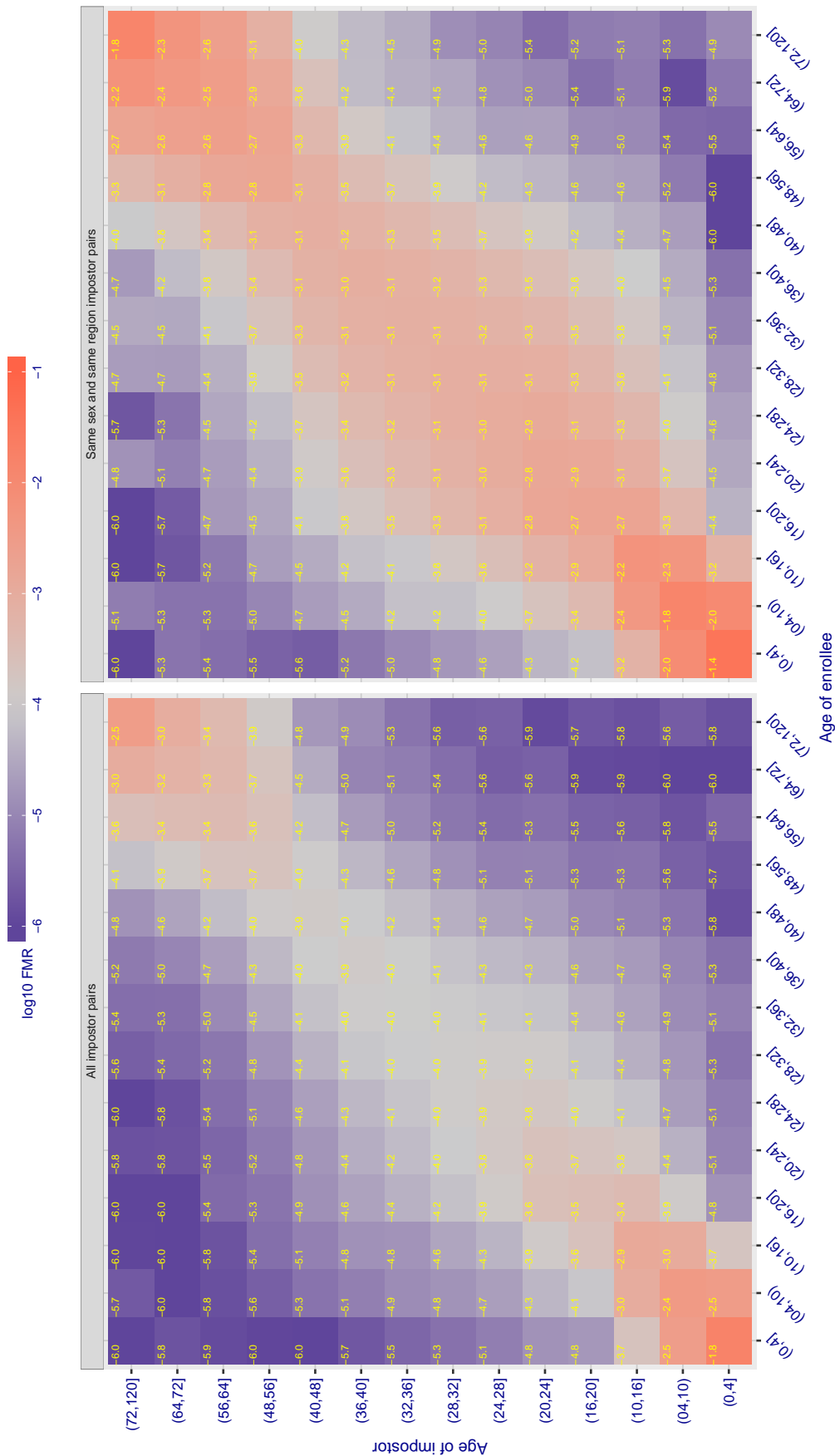


Figure 420: For algorithm yitu-003 operating on visa images, the heatmap shows false match observed over impostor comparisons of faces from different individuals who have the given age pair. False matches are counted against a recognition threshold fixed globally to give $FMR = 0.001$ over all on the order of 10^{10} impostor comparisons. The text in each box gives the same quantity as that coded by the color: Light colors present a security vulnerability to, for example, a passport gate.

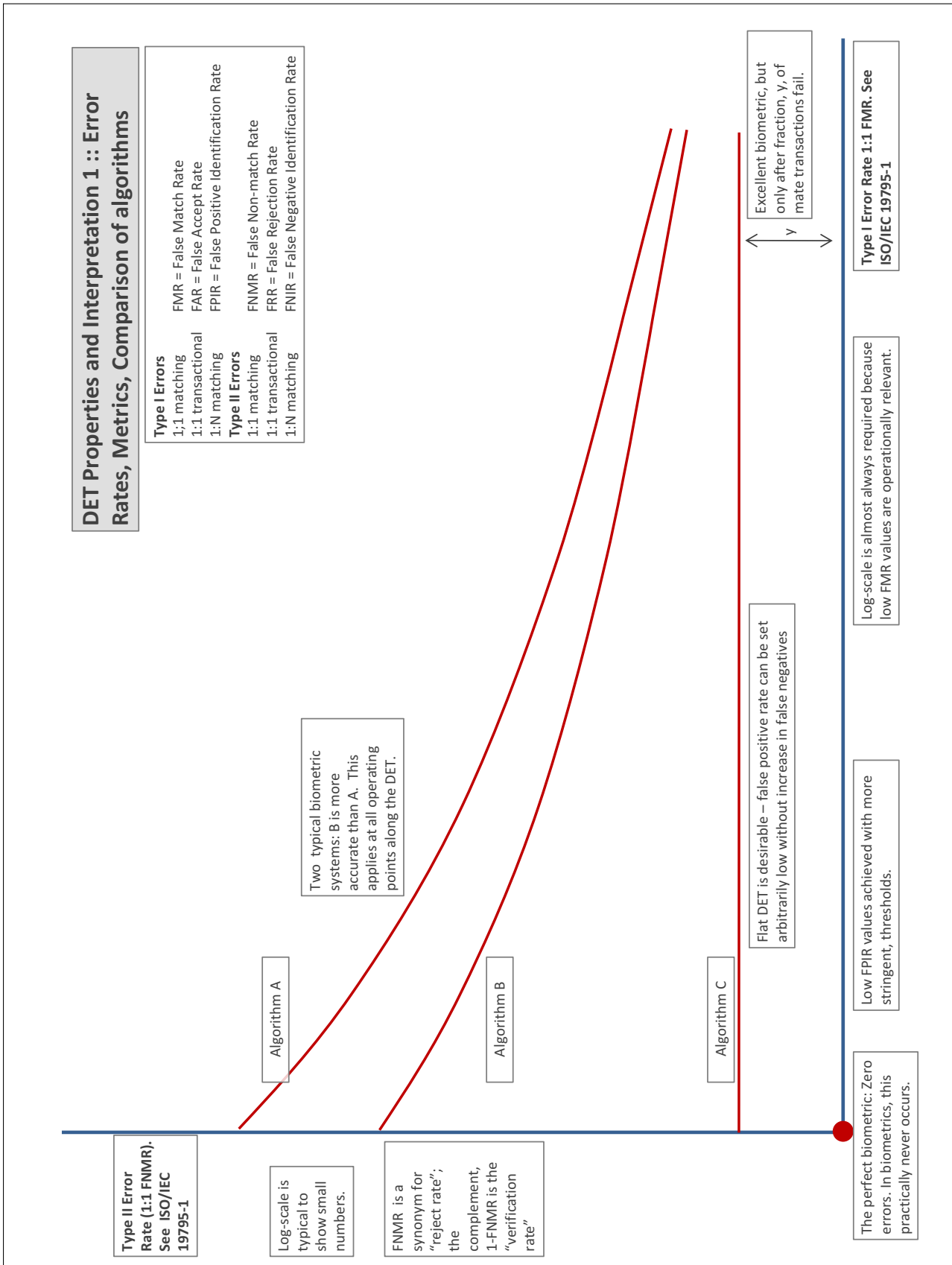
Accuracy Terms + Definitions

In biometrics, Type II errors occur when two samples of one person do not match – this is called a **false negative**. Correspondingly, Type I errors occur when samples from two persons do match – this is called a **false positive**. Matches are declared by a biometric system when the native comparison score from the recognition algorithm meets some **threshold**. Comparison scores can be either **similarity scores**, in which case higher values indicate that the samples are more likely to come from the same person, or **dissimilarity scores**, in which case higher values indicate different people. Similarity scores are traditionally computed by **fingerprint** and **face** recognition algorithms, while dissimilarities are used in **iris recognition**. In some cases, the dissimilarity score is a distance; this applies only when **metric** properties are obeyed. In any case, scores can be either **mate** scores, coming from a comparison of one person's samples, or **nonmate** scores, coming from comparison of different persons' samples. The words **genuine** or **authentic** are synonyms for mate, and the word **impostor** is used a synonym for nonmate. The words mate and nonmate are traditionally used in identification applications (such as law enforcement search, or background checks) while genuine and impostor are used in verification applications (such as access control).

A **error tradeoff** characteristic represents the tradeoff between Type II and Type I classification errors. For verification this plots false non-match rate (FNMR) vs. false match rate (FMR) parametrically with T.

The error tradeoff plots are often called **detection error tradeoff (DET)** characteristics or **receiver operating characteristic (ROC)**. These serve the same function but differ, for example, in plotting the complement of an error rate (e.g. $TMR = 1 - FNMR$) and in transforming the axes most commonly using logarithms, to show multiple decades of FMR. More rarely, the function might be the inverse Gaussian function.

More detail and generality is provided in formal biometrics testing standards, see the various parts of [ISO/IEC 19795 Biometrics Testing and Reporting](#). More terms, including and beyond those to do with accuracy, see [ISO/IEC 2382-37 Information technology -- Vocabulary -- Part 37: Harmonized biometric vocabulary](#)



DET Properties and Interpretation 1 :: Error Rates, Metrics, Comparison of algorithms

- Type I Errors**
- 1:1 matching
- 1:1 transactional
- 1:N matching
- Type II Errors**
- 1:1 matching
- 1:1 transactional
- 1:N matching
- FMR = False Match Rate
- FAR = False Accept Rate
- FPIR = False Positive Identification Rate
- FNMR = False Non-match Rate
- FRR = False Rejection Rate
- FNIR = False Negative Identification Rate

Type II Error Rate (1:1 FNMR). See ISO/IEC 19795-1

Log-scale is typical to show small numbers.

FNMR is a synonym for "reject rate"; the complement, 1-FNMR is the "verification rate"

Two typical biometric systems: B is more accurate than A. This applies at all operating points along the DET.

Algorithm A

Algorithm B

Algorithm C

Flat DET is desirable - false positive rate can be set arbitrarily low without increase in false negatives

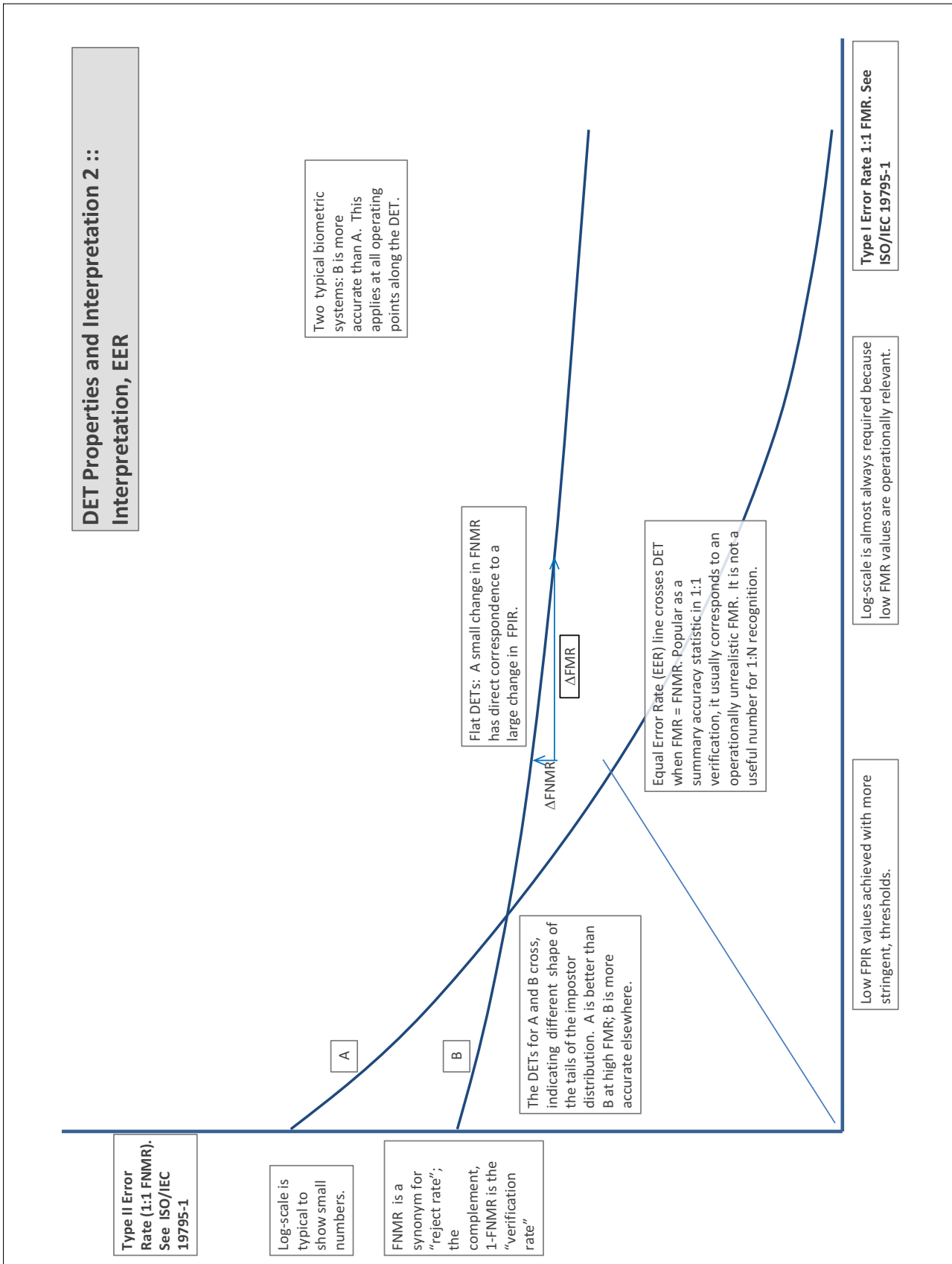
Excellent biometric, but only after fraction, y, of mate transactions fail.

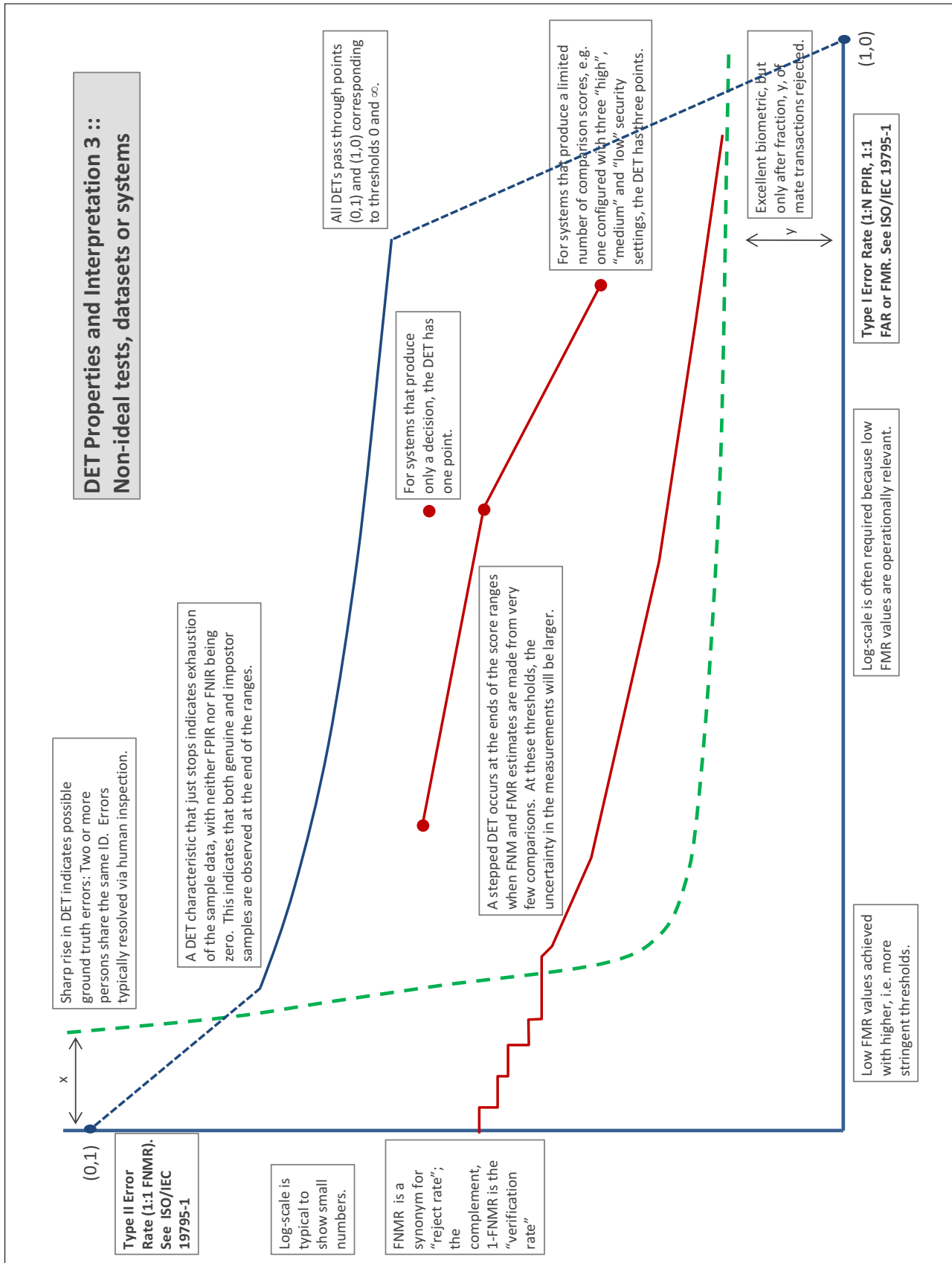
The perfect biometric: Zero errors. In biometrics, this practically never occurs.

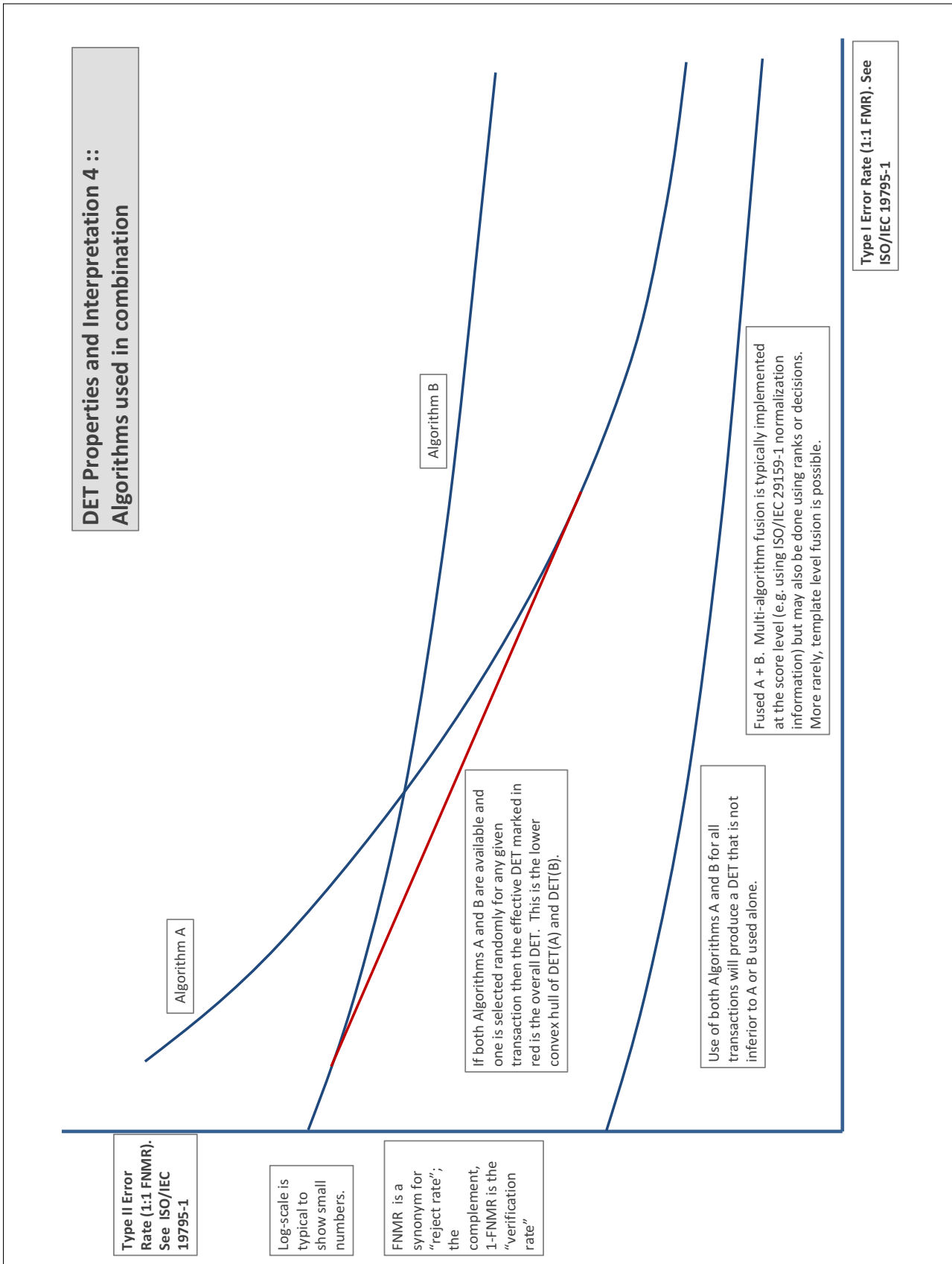
Low FPIR values achieved with more stringent, thresholds.

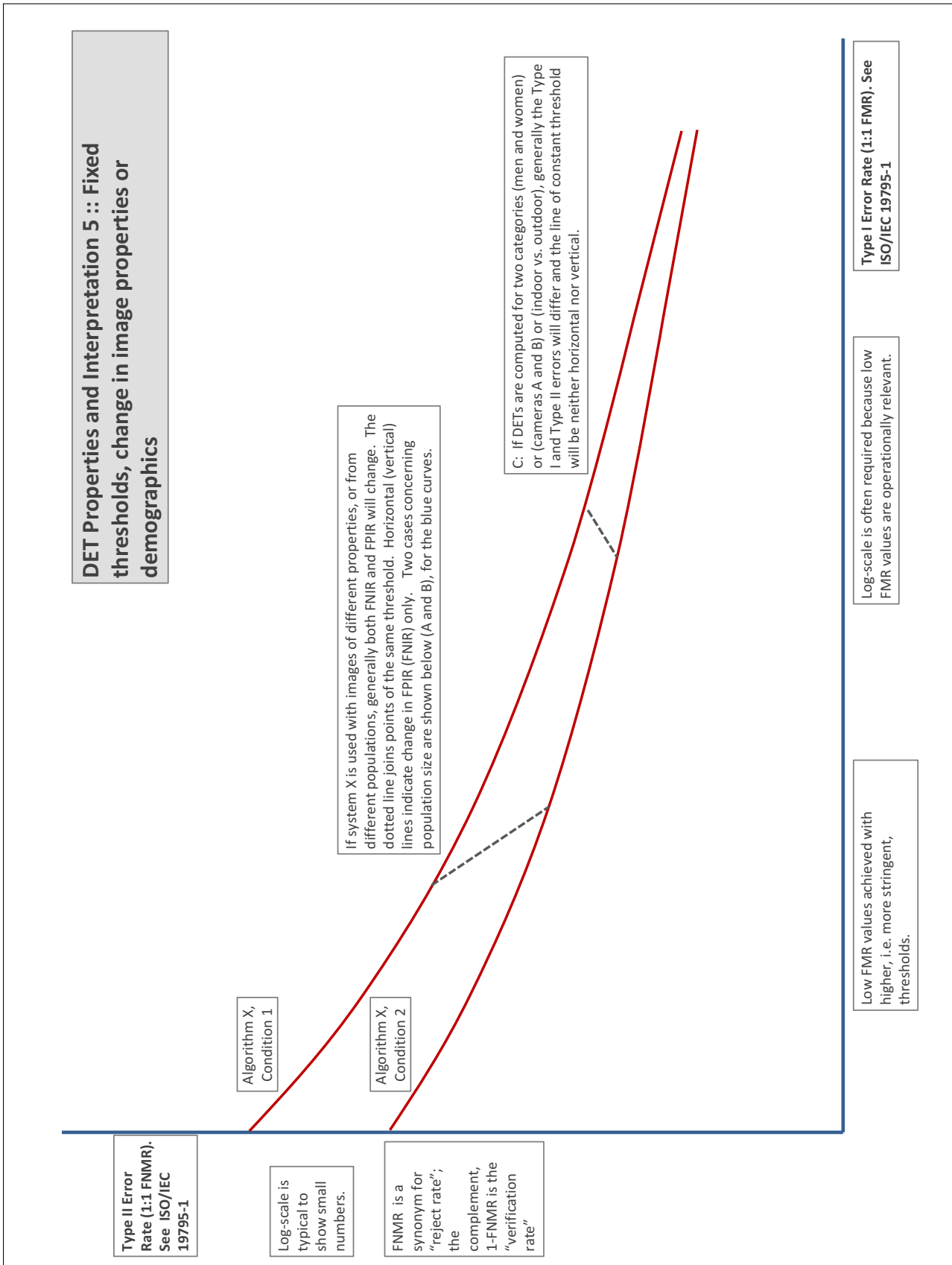
Log-scale is almost always required because low FMR values are operationally relevant.

Type I Error Rate 1:1 FMR. See ISO/IEC 19795-1









References

- [1] P. Jonathon Phillips, Amy N. Yates, Ying Hu, Carina A. Hahn, Eilidh Noyes, Kelsey Jackson, Jacqueline G. Cavazos, Géraldine Jeckeln, Rajeev Ranjan, Swami Sankaranarayanan, Jun-Cheng Chen, Carlos D. Castillo, Rama Chellappa, David White, and Alice J. O'Toole. Face recognition accuracy of forensic examiners, superrecognizers, and face recognition algorithms. *Proceedings of the National Academy of Sciences*, 115(24):6171–6176, 2018.